# NUCLEAR SCIENCE ABSTRACTS

Volume 32 Number 11

Abstracts 25496-27457

**December 15, 1975**

UNITED STATES
ENERGY RESEARCH AND DEVELOPMENT ADMINISTRATION

# REPORT COLLECTIONS IN THE UNITED STATES

The libraries listed below purchase and maintain microfiche collections of ERDA and foreign reports that are abstracted in *NSA*. Their collections also include *NSA* and its indexes, ERDA's Technical Progress Reviews, ERDA-sponsored translations, conference proceedings published by ERDA, and various bibliographic tools. Most of these libraries have microfiche reader-printers or other photocopy facilities with which to reproduce enlarged copies from microfiche. Charges for reproduction services vary.

Report collections of ERDA reports in countries other than the United States are listed on the inside back cover.

**ALABAMA**
Auburn, Auburn University
Tuskegee Institute, Tuskegee Institute
**ARIZONA**
Tucson, University of Arizona
**CALIFORNIA**
Davis, University of California
Los Angeles, University of California
Santa Barbara, University of California
**COLORADO**
Boulder, University of Colorado
**DISTRICT OF COLUMBIA**
Washington, Library of Congress
**FLORIDA**
Gainesville, University of Florida
**GEORGIA**
Atlanta, Georgia Institute of Technology
**HAWAII**
Honolulu, University of Hawaii
**IDAHO**
Pocatello, Idaho State University
**ILLINOIS**
Urbana, University of Illinois
**INDIANA**
Lafayette, Purdue University
**IOWA**
Ames, Iowa State University
**KANSAS**
Manhattan, Kansas State University
**KENTUCKY**
Lexington, University of Kentucky
**MARYLAND**
Baltimore, Johns Hopkins University
College Park, University of Maryland
**MASSACHUSETTS**
Cambridge, Massachusetts Institute of Technology
Worcester, Worcester Polytechnic Institute
**MICHIGAN**
Ann Arbor, University of Michigan
**MISSISSIPPI**
State College, Mississippi State University
**MISSOURI**
Columbia, University of Missouri
Kansas City, Linda Hall Library
**NEW JERSEY**
Princeton, Princeton University
**NEW MEXICO**
Albuquerque, University of New Mexico
**NEW YORK**
Albany, New York State Library
Albany, State University at Albany
Ithaca, Cornell University
New York, Columbia University
Rochester, University of Rochester
Syracuse, Syracuse University
**NORTH CAROLINA**
Raleigh, North Carolina State University
**OHIO**
Cincinnati, University of Cincinnati
Cleveland, Cleveland Public Library
Toledo, University of Toledo
**OKLAHOMA**
Norman, University of Oklahoma
**PENNSYLVANIA**
Philadelphia, University of Pennsylvania
Pittsburgh, Carnegie Library
University Park, Pennsylvania State University
**PUERTO RICO**
San Juan, University of Puerto Rico
**SOUTH CAROLINA**
Columbia, University of South Carolina
**TENNESSEE**
Knoxville, University of Tennessee
**TEXAS**
Austin, University of Texas
College Station, Texas A & M University
Houston, Rice University
**UTAH**
Salt Lake City, University of Utah
**VIRGINIA**
Blacksburg, Virginia Polytechnic Institute
Charlottesville, University of Virginia
**WASHINGTON**
Pullman, Washington State University
Seattle, University of Washington
**WEST VIRGINIA**
Morgantown, West Virginia University
**WISCONSIN**
Madison, University of Wisconsin

ERDA reports so indicated in *Nuclear Science Abstracts* are offered for sale by National Technical Information Service, U. S. Department of Commerce, Springfield, Virginia 22161.

Volume 32, Number 11, December 15, 1975

# NUCLEAR SCIENCE ABSTRACTS

*A semimonthly publication of the USERDA Office of Public Affairs*
*Published by the ERDA Technical Information Center*

*Nuclear Science Abstracts* provides the only comprehensive abstracting and indexing coverage of the international nuclear science literature. It covers scientific and technical reports of the U. S. Energy Research and Development Administration and its contractors, other U. S. Government agencies, other governments, universities, and industrial and research organizations. In addition, books, conference proceedings, individual conference papers, patents, and journal literature on a worldwide basis are abstracted and indexed. Each issue of *Nuclear Science Abstracts* includes four indexes: subject, personal author, corporate author, and report number.

The following organizations scan and abstract the nuclear science literature in their respective countries for input to the International Nuclear Information System of the International Atomic Energy Agency. By special agreement, the input to INIS is simultaneously sent to the ERDA Technical Information Center to enhance the timeliness of coverage of that literature in *Nuclear Science Abstracts*.

Atomic Energy of Canada Limited
Australian Atomic Energy Commission
Danish Atomic Energy Commission
Finnish Atomic Energy Commission
French Atomic Energy Commission
Japan Atomic Energy Bureau–Atomic Energy Research Institute
Commissie Nucleaire Informatieverzorging (Netherlands)
Institutt for Atomenergi (Norway)
Aktiebolaget Atomenergi (Sweden)
United Kingdom Atomic Energy Authority
Zentralstelle für Atomkernenergie-Dokumentation (West Germany)

Numerous organizations, societies, and publishers throughout the world provide *Nuclear Science Abstracts* with advance page-proof copy of their publications.

A list of the journals scanned regularly and the abbreviations used appears in the January 15 issue of *Nuclear Science Abstracts* and is supplemented in the July 15 issue. The January 15 issue also describes the scope and arrangement of the subject matter covered in *Nuclear Science Abstracts*. The subject matter covered is also described in TID-4552, *Subject Scope of Nuclear Science Abstracts*, available free from the USERDA Technical Information Center, P. O. Box 62, Oak Ridge, Tennessee 37830. An outline of the subject categories appears in the Contents of each issue.

## HOW TO OBTAIN NUCLEAR SCIENCE ABSTRACTS

*Nuclear Science Abstracts* is available to the public on a subscription basis from the Superintendent of Documents, U. S. Government Printing Office, Washington, D. C. 20402.

*NSA* is issued in two volumes per calendar year, one beginning January 15, the other July 15. Each volume consists of twelve issues.

For the two 12-issue volumes, the annual subscription rate is $121.05 for domestic subscribers and $151.35 for foreign subscribers. A single issue costs $5.05 domestic rates or $6.26 foreign rates. Domestic rates apply to the United States, Canada, Mexico, and Central and South American countries except Argentina, Brazil, Guyana, French Guiana, Surinam, and British Honduras.

Indexes are cumulated for each volume, i.e., on a six-month volume basis. If purchased on an annual subscription basis the two volume indexes are priced at $44.40 for domestic subscribers and $55.50 for foreign subscribers.

The volume indexes are also sold separately. Each volume index is priced on the basis of pagination at the time of publication.

Previous *NSA* cumulative indexes are available:

From Johnson Reprint Corporation, 111 Fifth Avenue, New York, N. Y. 10003:

**Vols. 1–4, Subjects and Authors (1948–1950), $30.00.**

From Technical Information Center, P. O. Box 62, Oak Ridge, Tennessee 37830:

**Vols. 5–10, Subjects and Authors (1951–1956), $5.25.**
**Vols. 11–15, Subjects (1957–1961), $19.00.**
**Vols. 11–15, Personal Authors (1957–1961), $14.25.**
**Vols. 11–15, Corporate Authors (1957–1961), $2.50.**

From Superintendent of Documents, U. S. Government Printing Office, Washington, D. C. 20402:

**Vols. 16–20, Subjects (1962–1966), $36.00.**
**Vols. 16–20, Personal Authors (1962–1966), $22.50.**
**Vols. 16–20, Corporate Authors (1962–1966), $3.75.**
**Vol. 26, Subjects and Authors (1972), $37.75.**
**Vol. 27, Subjects, Authors, and Report Numbers (Jan.–June 1973), $16.90.**
**Vol. 28, Subjects and Authors (July–Dec. 1973), $18.55.**
**Vol. 29, Subjects and Authors (Jan.–June 1974), $20.10.**
**Vol. 30, Subjects, Authors, and Report Numbers (Vols. 29 and 30) (July–Dec. 1974), $27.35.**
**Cumulative Report Number Index, Vols. 1–15 Revised, $4.00.**
**Cumulative Report Number Index, Vols. 16–20 Revised, $5.50.**
**Cumulative Report Number Index, Vols. 21–28, $9.35.**

From Xerox University Microfilms, 300 North Zeeb Road, Ann Arbor, Michigan 48106:

**Vols. 21–25, Subjects, Authors, and Corporate Authors (1967–1971), $195.00.**

*Nuclear Science Abstracts* is available on an exchange basis to universities, research institutions, industrial firms, and publishers of scientific information. Government agencies may obtain *NSA* free of charge. Inquiries should be directed to the USERDA Technical Information Center, P. O. Box 62, Oak Ridge, Tennessee 37830.

*Nuclear Science Abstracts* is also available on 16-mm and 35-mm microfilm in reel or cartridge from Princeton Microfilm Corporation, Alexander Road, Princeton, New Jersey 08540. The cost of Vols. 1–26 (1948–1972) including *Abstracts of Declassified Documents* (1947–1948) is $730.00. The indexes for *Nuclear Science Abstracts* Vols. 1–26 (1948–1972) are also available for $385.00. The cost of each volume (six months) of *NSA* and its indexes is $45.00.

# INDEXES TO *NSA*

Comprehensive indexes appear in each issue and are cumulated at the end of each volume. The report number indexes will be cumulated on both a volume and two-volume basis. Multivolume cumulations have been issued as indicated above.

All documents abstracted are indexed by subjects and personal authors. Report literature is indexed also by corporate author and report number. Each of these indexes in every issue is preceded by an introduction explaining in detail the organization of the index and the principles by which it is compiled. The reader is referred to these explanations for information not found in the brief summaries below.

## Personal Authors

Each author's name is indexed in the form appearing on the document abstracted, with the exception that given names are reduced to initials:

**HOLLOWAY, J.A.,** Survey of image processing methods for radiography, 31:16491
**HOLLWEG, J.V.,** Hydromagnetic waves in interplanetary space, 31:17953
**HOLMBERG, E.B.,** Distribution of clusters of galaxies as related to galactic absorption, 31:16040
**HOLMES, J.J.,** See BAYES, J.F., 31:17444

## Subjects

The subject index consisting of entries naming specific materials, objects, and processes is arranged alphabetically. Document titles, informative phrases, or both specific to these entries are arranged alphabetically under the entries.

Examples:

**NUCLEAR POWER PLANTS/REACTOR LICENSING**
Experience acquired in the design and construction of operating plants (German Federal Republic), 31:19104
**NUCLEAR POWER PLANTS/REACTOR SAFETY**
Conception of radiation safety in atomic electric power plants, 31:15032 (CONF-701074-P1)
**NUCLEAR POWER PLANTS/SITE SELECTION**
Safety-related site parameters for nuclear power plants, 31:19052 (WASH-1361)
Status and development of nuclear power in the Federal Republic of Germany, 31:19105
**NUCLEAR PROPERTIES/RESEARCH PROGRAMS**
Accelerator physics group progress report, July--December 1973 (Research summaries), 31:18544 (INS-R-139)

## Corporates

Technical report literature is indexed using the name of the organization or institution responsible for the issuance of the report.

17606 (ANL/HEP-7440, pp I.1-I.12) ACCELERATED POLARIZED PROTONS AT THE ZGS. Ratner, L. G. (Argonne National Lab., IL). Feb 1974.
From symposium on high energy physics with polarized beams; Argonne, Illinois, USA (8 Feb 1974).
In symposium on high-energy physics with polarized beams.

is indexed as:

**ARGONNE NATIONAL LAB., ILL. (USA)**
Accelerated polarized protons at the ZGS, 31:17606 (ANL/HEP-7440)
Acceleration of polarized protons in synchrotrons, 31:17692 (ANL/HEP-7440)
Analysis of population, birth, and death statistics in the counties surrounding the Big Rock Point Nuclear Power Station, Charlevoix County, Michigan, 31:16552 (ANL-8149)
Argonne polarized target facilities, 31:17762 (ANL/HEP-7440)
Calculation of transient fission-gas release from oxide fuels, 31:19031 (ANL-8143)

## Report Numbers

Technical report literature is also indexed using report numbers. This index includes information on where individual reports may be obtained. While not reports, patents and conference papers are indexed here as a matter of convenience.

| | | |
|---|---|---|
| **WASH-** | | |
| 1164 | 31:19025 | Dep. NTIS, $16.00 |
| 1359 | 31:16524 | Dep. NTIS, $10.60 |
| 1361 | 31:19052 | Dep. NTIS, $3.75 |
| **WCAP-** | (Misc.) | |
| 7906 | 31:19053 | Dep. NTIS, $5.50 |
| **XDC-** | | |
| 68-3-68 | 31:18463 | Dep. NTIS, $7.25 |
| **XN-** | (Non-ERDA) | |
| 74-21(Rev.1) | 31:19054 | |
| 209(Suppl.4) (Rev.1) | 31:18780 | Exxon, Richland, WA |
| **Y-** | | |
| 1966 | 31:19188 | Dep. NTIS, $4.00 |

# AVAILABILITY OF PUBLICATIONS ABSTRACTED

Public availability of all U. S. Energy Research and Development Administration reports is indicated in the report number indexes. The availability of other reports, when known, is also indicated. The availability of some unnumbered reports is given in the abstract.

Dissertations from *Dissertation Abstracts International, Part B* that are included in *Nuclear Science Abstracts* are available from Xerox University Microfilms, 300 North Zeeb Road, Ann Arbor, Michigan 48106.

Information on the availability of the published literature and unpublished conference papers abstracted in *Nuclear Science Abstracts* can be obtained from the USERDA Technical Information Center, P. O. Box 62, Oak Ridge, Tennessee 37830.

# TABLE OF CONTENTS

**Volume 32, Number 11, December 15, 1975**


| Category | Page |
|---|---|
| **CHEMISTRY** | 2523 |
| Analytical and Separations Chemistry | 2523 |
| *Activation and Nuclear Reaction Procedures* | 2523 |
| *Chemical and Spectral Procedures* | 2524 |
| *Radiometric and Radiochemical Procedures* | 2524 |
| *Separation Procedures* | 2525 |
| Inorganic, Organic, and Physical Chemistry | 2526 |
| *Chemical and Physicochemical Properties* | 2526 |
| *Isotope Effects* | 2527 |
| *Isotope Exchange and Isotope Separation* | 2529 |
| *Feed Materials Processing* | 2530 |
| Radiation Chemistry | 2530 |
| Radiochemistry and Nuclear Chemistry | 2535 |
| *Hot-Atom Chemistry* | 2536 |
| *Properties of Radioactive Materials* | 2536 |
| *Radioactive Waste Treatment* | 2537 |
| *Reactor Fuel Reprocessing* | 2538 |
| **CONTROLLED THERMONUCLEAR RESEARCH** | 2540 |
| Plasma Confinement and Heating | 2540 |
| Plasma Diagnostics | 2541 |
| Plasma Kinetics (General) | 2544 |
| Plasma Kinetics (Experimental) | 2544 |
| Plasma Kinetics (Theoretical) | 2544 |
| Plasma Production | 2545 |
| Plasma Stability | 2546 |
| Thermonuclear Engineering and Equipment | 2547 |
| Wave Phenomena | 2549 |
| **ENGINEERING** | 2552 |
| Facilities and Equipment | 2552 |
| *Lasers* | 2552 |
| *Cryogenic and Superconducting Equipment and Devices* | 2558 |
| Heat Transfer and Fluid Flow | 2559 |
| Materials Testing | 2560 |
| Nuclear Explosions | 2560 |
| Protective Structures and Equipment | 2561 |
| **ENVIRONMENTAL AND EARTH SCIENCES** | 2562 |
| Minerals and Ores | 2562 |
| Radioactivity Monitoring and Transport | 2564 |
| *Atmosphere* | 2564 |
| *Water* | 2565 |
| *Ecosystems and Food Cycles* | 2566 |
| Radiometric Techniques | 2566 |
| Site Surveys | 2566 |
| Thermal Effluents | 2566 |
| Chemical Effluents | 2567 |
| **INSTRUMENTATION** | 2568 |
| Radiation Detection Instruments | 2568 |
| *General Detectors and Monitors* | 2568 |
| *Radiation Dosimeters* | 2570 |
| *Nuclear Spectroscopic Instrumentation* | 2572 |
| *High Energy Physics Instrumentation* | 2573 |
| Radiometric Instruments | 2573 |
| Radiation Effects on Instrument Components, Instruments, or Electronic Systems | 2574 |
| Miscellaneous Instruments | 2574 |
| **ISOTOPE AND RADIATION SOURCE TECHNOLOGY** | 2576 |
| Isotope Separation (Industrial) | 2576 |
| Isotopic Power Sources | 2576 |
| Radiation Sources | 2576 |
| **LIFE SCIENCES** | 2578 |
| Radiation Effects on Biochemicals | 2578 |
| Radiation Effects on Cells | 2578 |
| Radiation Effects on Microorganisms | 2579 |
| Radiation Effects on Plants | 2580 |
| Radiation Effects on Animals | 2581 |
| *Man* | 2581 |
| *Vertebrates* | 2583 |
| *Invertebrates* | 2587 |
| Radionuclide Effects (Internal Source) | 2587 |
| *Man* | 2587 |
| *Animals* | 2589 |
| Nuclide Kinetics and Toxicology | 2589 |
| *Animals* | 2589 |
| New Tracer Techniques | 2590 |
| **MATERIALS** | 2596 |
| Ceramics and Cermets | 2596 |
| Metals and Alloys | 2598 |
| *Corrosion and Erosion* | 2598 |
| *Preparation and Fabrication* | 2600 |
| *Properties, Structure, and Phase Studies* | 2600 |
| *Radiation Effects* | 2608 |
| Other Materials | 2609 |
| **NUCLEAR MATERIALS AND WASTE MANAGEMENT** | 2612 |
| Accountability and Safeguards | 2612 |
| Disposal and Storage | 2612 |
| Handling Equipment and Procedures | 2612 |
| Transportation | 2612 |

# TABLE OF CONTENTS (continued)


| Category | Page |
|---|---|
| **PARTICLE ACCELERATORS** | 2613 |
| Design, Development, and Operation | 2613 |
| Auxiliaries and Components | 2613 |
| Ion Sources and Injection and Extraction Systems | 2613 |
| Ion Optics and Field Calculations | 2614 |
| Experimental Facilities | 2614 |
| **PHYSICS (ASTROPHYSICS AND COSMOLOGY)** | 2615 |
| Cosmic Radiation | 2615 |
| Stars | 2617 |
| Quasi-Stellar, Radio, and X-Ray Sources | 2627 |
| Solar Phenomena | 2630 |
| Galaxies | 2633 |
| Cosmology | 2639 |
| Planetary Phenomena | 2640 |
| **PHYSICS (ATMOSPHERIC)** | 2643 |
| Auroral and Ionospheric Phenomena | 2643 |
| Effects of Nuclear Detonations | 2649 |
| Magnetospheric Phenomena | 2649 |
| **PHYSICS (ATOMIC AND MOLECULAR)** | 2654 |
| Beams and Their Reactions | 2654 |
| Atomic and Molecular Properties | 2655 |
| Positronium, Muonium, and Muonic and Mesic Atoms and Molecules | 2657 |
| Collision Phenomena | 2657 |
| Atomic Theory | 2660 |
| **PHYSICS (ELECTROFLUID AND MAGNETOFLUID)** | 2661 |
| **PHYSICS (HIGH-ENERGY)** | 2664 |
| Particle Interactions and Properties (Experimental) | 2664 |
| *Electromagnetic* | 2664 |
| *Weak* | 2664 |
| *Strong (Baryon-induced)* | 2664 |
| *Strong (Meson-induced)* | 2665 |
| Particle Interactions and Properties (Theoretical) | 2666 |
| *General* | 2666 |
| *Electromagnetic* | 2668 |
| *Weak* | 2669 |
| *Strong (General)* | 2670 |
| *Strong (Baryon No. = 0)* | 2670 |
| *Strong (Baryon No. = 1)* | 2671 |
| *Strong (Baryon No. > 2)* | 2672 |
| Particle Invariance Principles and Symmetries | 2673 |
| *General* | 2673 |
| *Applications (Electromagnetic and Weak)* | 2673 |
| *Applications (Strong)* | 2674 |
| Scattering Theory | 2674 |
| **PHYSICS (LOW-TEMPERATURE)** | 2675 |
| Superconductivity | 2675 |
| **PHYSICS (NUCLEAR)** | 2677 |
| Neutron Interactions with Matter | 2677 |
| Nuclear Properties and Reactions, $A < 5$ | 2677 |
| **PHYSICS (NUCLEAR) (Cont'd.)** | |
| Nuclear Properties and Reactions, $6 < A < 19$ | 2678 |
| Nuclear Properties and Reactions, $20 < A < 38$ | 2680 |
| Nuclear Properties and Reactions, $39 < A < 58$ | 2681 |
| Nuclear Properties and Reactions, $59 < A < 89$ | 2683 |
| Nuclear Properties and Reactions, $90 < A < 149$ | 2684 |
| Nuclear Properties and Reactions, $150 < A < 189$ | 2687 |
| Nuclear Properties and Reactions, $190 < A < 219$ | 2688 |
| Nuclear Properties and Reactions, $A > 220$ | 2689 |
| Nuclear Theory | 2691 |
| **PHYSICS (RADIATION AND SHIELDING)** | 2695 |
| Radiation Physics | 2695 |
| Radiation Protection Standards | 2695 |
| Radiation Source Calibration and Standardization | 2695 |
| **PHYSICS (THEORETICAL)** | 2696 |
| General | 2696 |
| Quantum Field Theories | 2696 |
| Gravitation and General Relativity | 2699 |
| **REACTOR TECHNOLOGY AND REGULATION** | 2701 |
| Power Reactors, Non-Breeding, BWR-Type | 2701 |
| Power Reactors, Non-Breeding, PWR-Type | 2702 |
| Power Reactors, Non-Breeding, Graphite Moderated | 2703 |
| Power Reactors, Non-Breeding, Otherwise Moderated | 2706 |
| Power Reactors, Breeding | 2707 |
| Research, Test, and Experimental Reactors | 2709 |
| Production and Materials Testing and Processing Reactors | 2710 |
| Propulsion and Package Reactors | 2710 |
| Reactor Safety and Environmental Aspects | 2718 |
| Reactor Theory and Calculation | 2724 |
| Reactor Components and Accessories | 2724 |
| Reactor Fuels | 2725 |
| Reactor Control Systems | 2726 |
| Nuclear Power Plant Economics | 2727 |
| Reactor Licensing and Regulation | 2727 |
| **GENERAL AND MISCELLANEOUS** | 2729 |
| Information Handling | 2729 |
| Management | 2729 |
| Mathematics and Computers | 2729 |
| **CORPORATE INDEX** | INDEX-1 |
| **PERSONAL AUTHOR INDEX** | INDEX-9 |
| **SUBJECT INDEX** | INDEX-44 |
| **REPORT NUMBER INDEX** | INDEX-131 |

## STAFF OF NUCLEAR SCIENCE ABSTRACTS

**Editor and Production Manager**
David E. Bost

**Assistant Editor**
Lee M. Thompson

**Associate Editors**
M. Catherine Grissom
Robert C. Kelly
Sidney F. Lanier
Henry D. Raleigh
Charles E. Stuber

**Report Evaluators**
John H. Mitchell
Mary H. Newman

**Descriptive Cataloging Specialist**
J. Paul Meredith

**Subject Heading Specialist**
Dora H. Moneyhun

**Corporate Author Specialist**
Clara L. Fox

**Report Number Specialist**
Helen W. White

**Information Specialists**
P. Martin Alexander
E. Ray Bedford
Jane G. Buchanan
D. Lamar Cason
David C. Cunningham
Theodore F. Davis
James R. Dulaney
Stanley D. Frey
Darrell O. Galde
Martha W. Gerrard
Barbara J. Glenn
Everett J. Hoffman
Carolyn D. Houston
Lynda H. Kern
W. Hugh Kinser
Lisbeth C. Lieberman
William D. Matheny
Lorne T. Newman
Jean F. Peckham
Mona H. Raridon
Julia S. Redford
Stanley J. Rimshaw
Jessie W. Rushing
Robert W. Rutkowski
Francis L. Sachs
Lila B. Smith
Polly C. Summers
George H. Thoeming
Helen L. Ward
Lawrence T. Whitehead
Milton O. Whitson
Martha C. Wilson

**Publishing Coordinator**
Charles R. Bruce

**Computer Processing Coordinator**
Noboru Kawakami

**Communication concerning the editorial policy and content of *Nuclear Science Abstracts* should be addressed to the Editor, *Nuclear Science Abstracts*, USERDA Technical Information Center, P. O. Box 62, Oak Ridge, Tennessee 37830.**

---

*The Administrator of the Energy Research and Development Administration has determined that the publication of this periodical is necessary in the transaction of the public business required by law of this agency. Use of funds for printing this periodical has been approved by the Director of the Office of Management and Budget through June 30, 1978.*

Volume 32, Number 11 December 15, 1975

# NUCLEAR SCIENCE ABSTRACTS

## CHEMISTRY

**25496** (ANL-8085) PLANNING A NATIONAL CENTER FOR LARGE SCALE COMPUTATION IN CHEMISTRY RESEARCH. Report of a Workshop, Argonne National Laboratory, June 7–8, 1974. (Argonne National Lab., Ill. (USA)). 1974. Contract W-31-109-Eng-38. 90p. Dep. NTIS $5.45.

Recommendations prepared by the participants in a Workshop for Planning a National Center for Large Computation in Chemistry Research held at Argonne National Laboratory on June 7 and 8, 1974 are presented. The Workshop was sponsored jointly by Argonne National Laboratory and the Argonne Universities Association. The recommendations were prepared by five separate working groups on: (1) scientific projects; (2) support; (3) functions and staffing; (4) access and siting; and (5) scientific policy and management structure. Background material presented by invited speakers in plenary sessions preceding the workshop sessions is included in the report. A brief review of the development of the Center concept and a list of exemplary scientific projects, prepared by the working group on scientific projects, are also included. (auth)

## Analytical and Separations Chemistry

### *Activation and Nuclear Reaction Procedures*

*Refer also to abstracts 26290 and 26315.*

**25497** (CEA-R-4691) DETERMINATION OF IODINE 129 IN THYROIDS. Gros, R.; Cappellini, L.; Goujon de Beauvivier, M.; Jeanmaire, L.; Patti, F. (CEA Centre d'Etudes Nucleaires de Fontenay-aux-Roses, 92 (France). Dept. de Protection). Aug 1975. 18p. (In French). Dep. NTIS (US Sales Only) $4.00.

Activation analysis was used for the determination of $^{129}I$ in thyroids. Iodine is first extracted from the thyroid and irradiated as lead iodate, thus giving enough sensitivity and making it possible to use common laboratory material. The results showed that the present activity levels in France are between 1 and 50 pCi per gram of iodine; the values found in Argentina are clearly lower. (auth)

**25498** (CONF-751009-1) MERCURY AND CADMIUM CONCENTRATIONS IN MILK IN PUERTO RICO. Chellappan, S.; Pedersen, K. B.; Plaza, H. (Puerto Rico Nuclear Center, Mayaguez). 1975. 5p. Dep. NTIS $4.00.

Milk samples were analyzed statistically for Hg and Cd by thermal neutron activation (NAA). A Ge(Li) detector and a 4096 channel pulse-height analyzer were used. Mean values of the concentrations of Hg and Cd in milk are tabulated with their standard deviations. Observed variations in Cd and Hg concentrations were small; however NAA was found to be relatively insensitive for the determination of Cd. A significant peak was not observed in the energy range used for the determination. (JGB)

**25499** NONDESTRUCTIVE ACTIVATION ANALYSIS OF BROMINE. Yamadera, A.; Miyata, T.; Shiokawa, T. (Tohoku Univ., Sendai (Japan). Faculty of Science). Kakuriken Kenkyu Hokoku; 7: No. 1, 194-200(Jun 1974). (In Japanese).

The samples used were Japanese standard sea water, blood, and a standard solution of NaCl and NaBr. These samples were dried and irradiated with bremsstrahlung converted from 30 MeV electron beam accelerated with a Linac. After waiting for 2 hours the 37 keV $\gamma$ ray from $^{80m}Br$ was measured. After 10 days, 0.511 MeV $\gamma$ ray from $^{22}Na$, which is formed by $^{23}Na(\gamma, n)\ ^{22}Na$ reaction was measured. Biggest interference was given by $^{28}Mg$, which is formed by $^{30}Si(\gamma, 2p)\ ^{28}Mg$ reaction from Mg present in quartz ampoules, because the irradiation with bremsstrahlung was made to the samples sealed in the ampoules. The relation between the concentration of Br in samples and the area of the 37 keV photoelectric peak of $^{80m}Br$ was linear when the relation was plotted on a log-log graph. The gradient was 1. Therefore, the concentration of Br is proportional to the area of the photoelectric peak. The limit of detection was 10 $\mu$ g or 0.1 ppM for a sample of 100 mg. The accuracy below 1 ppM is not reliable, however, so far as quartz ampoules are used. (JA)

**25500** THE DISTRIBUTION OF SEVERAL TRACE ELEMENTS AND THEIR CHEMICAL BEHAVIOR IN THE HEAD-WATER AREA OF THE TAMA RIVER. Tanizaki, Y.; Nagatsuka, S. (Tokyo Metropolitan Isotope Research Center (Japan)). Nippon Kagaku Kaishi; 1974: No. 11, 2094-2098(Nov 1974). (In Japanese).

The distribution of trace elements and their chemical behavior in the head-water area of the Tama River were studied using activation analysis. The water samples were taken at 5 points in the main stream and 25 valleys flowing into it. Elements inducing long-life nuclides were prepared by evaporation to dryness and those inducing short-life nuclides by coprecipitation method with $Fe(OH)_3$ or $Al(OH)_3$. The activity of the irradiated samples was measured. Concentrations of Se, V, Co, As and Se were closely related to the geology of the areas through which the valley streams flow. Se content of streams which ran on the sedimentary rock formations was found to be 0.04 to 0.09 ppB, whereas in streams on the igneous rock formations Se was not detected. Arsenic content of each stream on the igneous rock formations or the Jurrasic formations was found to be 0.6 to 1.4 ppB, whereas in streams on the Cretaceous formations to be 1.7 to 2.3 ppB. Sb content had a close relation to the distance between the streams and the center of the metropolis rather than to the geology of the areas where the samples were taken, namely the shorter the distance, the higher became the Sb contents. (auth)

**25501** MONOSTANDARD ACTIVATION ANALYSIS OF ANCIENT PIGMENTS OF THE MURALS IN THE TAKAMATSUZUKA TUMULUS. Takeuchi, T. (Kyoto Univ., Kumatori, Osaka (Japan). Research Reactor Inst.); Shinogi, M.; Mori, I.; Yasuda, H. Annu. Rep. Res. Reactor Inst., Kyoto Univ.; 7: 20-28(Oct 1974).

Eight kinds of ancient pigments were analyzed instrumentally by neutron activation using standards containing only gold. A computer program was applied to processing of the data in qualitative and quantitative analyses. Element concentrations of each pigment are given and the relative values to iron, copper, or gold are compared with each other. Archaeological meanings of those concentrations are discussed. (auth)

**25502** APPLICATION OF RADIOACTIVATION ANALYSIS FOR THE DETERMINATION OF TRACE AMOUNTS OF ELEMENTS IN SEMICONDUCTOR MATERIALS. Kudo, K. (Nippon Telegraph and Telephone Public Corp., Tokai, Japan). J. Jap. Soc. Appl. Phys., Suppl.; 44: 319-327(Jan 1975).

From 6th conference on solid state devices; Tokyo, Japan (2 Sep 1974).

Radioactivation analysis is one of the most useful methods for the determination of trace impurities in semiconductor materials and of their distribution. Radioactivation analysis is classified into two methods. One is a nondestructive method and the other is a destructive one. The technique of $\gamma$ spectrometry using NaI detector or Li-drifted Ge-detector has been applied for the nondestructive method. On the other hand, a new method based on substoichiometry was proposed for the destructive method. The principle and characteristics of these methods and the application to the study of semiconductor materials are described. (auth)

**25503** DETERMINATION OF Ca, Mg, Ni, AND Si IN BIOLOGICAL MATERIALS BY NEUTRON ACTIVATION AND CHERENKOV COUNTING. Pietra, R.; Sabbioni, E.; Girardi, F. (EURATOM, Ispra, Italy). Radiochem. Radioanal. Lett.; 22: No. 4, 243-250(25 Aug 1975).

The analysis of Ca, Mg, Ni and Si in biological material has been carried out by neutron activation analysis and Cherenkov counting. The detection limits were 1 ng for Ca and Si, 5 ng for Mg and 50 ng for Ni. (auth)

**25504** DETERMINATION OF CARBON IN CHROMIUM BY PHOTON ACTIVATION. Fedoroff, M.; Loos-Neskovic, C.; Revel, G. (Centre d'Etudes de Chimie Metallurgique, Vitry-sur-Seine, France). Radiochem. Radioanal. Lett.; 22: No. 4, 283-288(25 Aug 1975).

Carbon is determined in chromium by activation in 35-MeV photons. The sample is dissolved by a fused $NaOH-NaNO_3$ bath. Carbon dioxide is then extracted by acid dissolution of the solidified bath. A limit of detection of 0.03 $\mu$g of carbon is achieved. (auth)

**25505** NEW METHOD OF DETERMINATION OF DEPTH DISTRIBUTION OF FLUORINE IN TEETH ENAMEL BY MEANS OF PROTON ACTIVATION ANALYSIS. Muller, J. Zobozdrav. Vestn.; 29: No. 3-4, 71-76(1974). (In Slovak).

The depth distribution of the fluorine concentration in tooth enamel can be readily and nondestructively measured by means of proton activation analysis. The author has studied teeth (in vitro) treated topically with 4% NaF in 0.1 mm $H_3PO_4$ (pH = 4.6), before washing and brushing. The results show a strong influence of this mechanical action on the removal of fluorine from surface layers of the enamel. These measurements were performed for various depths, by varying the proton energy. With certain changes in the measuring system the measurements can be performed also in vivo. (auth)

## Chemical and Spectral Procedures

*Refer also to abstracts 25977, 26231, 26242, and 26275.*

**25506** (UCRL-76743) STABLE ISOTOPE RATIO MEASUREMENTS IN HYDROGEN, NITROGEN, AND OXYGEN USING RAMAN SCATTERING. Harney, R. C.; Bloom, S. D.; Milanovich, F. P. (California Univ., Livermore (USA). Lawrence Livermore Lab.). 6 Aug 1975. 39p. (CONF-750806-3). Dep. NTIS $5.00.

From 170th American Chemical Society national meeting; Chicago, Illinois, USA (24 Aug 1975).

A method for measuring stable isotope ratios using laser Raman scattering was developed which may prove of significant utility and benefit in stable isotope tracer studies. Crude isotope ratio measurements obtained with a low-power laser indicate that with current technology it should be possible to construct an isotope ratio measurement system using laser Raman scattering that is capable of performing 0.1 percent accuracy isotope ratio measurements of $^{16}O/^{18}O$ in natural abundance oxygen gas or $^{14}N/^{15}N$ in natural abundance nitrogen gas in times less than two minutes per sample. Theory pertinent to the technique, designs of specific isotope ratio spectrometer systems, and data relating to isotope ratio measurements in hydrogen, nitrogen, and oxygen are presented. In addition, the current status of several studies utilizing this technique is discussed. (auth)

**25507** DETECTION OF $^{20}Na$ ATOMS AND MEASUREMENT OF SODIUM-VAPOR DENSITIES BY MEANS OF ATOMIC-RESONANCE FLUORESCENCE. Coolen, F.C.M.; Hagedoorn, H.L. (Eindhoven University of Technology, Eindhoven, Netherlands). J. Opt. Soc. Am. 65: No. 8, 952-955 (Aug 1975).

The method of atomic-resonance fluorescence has been applied to the detection of very small concentrations of radioactive $^{20}Na$ atoms ($< 3 \times 10^9$ m$^{-3}$). The $^{20}Na$ isotope is produced by the reaction $^{20}Ne(p,n)^{20}Na$ by passing a 20 MeV proton beam through a neon gas target of density $3.5 \times 10^{24}$ atoms/m$^3$. A beam of a continuous-wave dye laser tuned to the D2 line of sodium is transmitted through the production region and the fluorescence light is detected by means of photon counting. A digital synchronous-detection technique has been applied to measure the time-dependent behavior of the $^{20}Na$ atom density shortly after a proton irradiation. This behavior is determined both by radioactive decay and by diffusion of the atoms out of the production region. The absolute $^{20}Na$ atom density has been estimated, using Rayleigh scattering of the laser beam on the neon gas for calibration of the optical system. The density of neutral $^{20}Na$ atoms appeared to be an order of magnitude lower than the density produced. The detection method has also been used to measure the temperature dependence of saturated sodium-vapor density down to $3 \times 10^{11}$ atoms/m$^3$ (292 K). (auth)

**25508** SPECTROGRAPHIC DETERMINATION OF RARE EARTHS IN HIGH PURITY GADOLINIUM OXIDE USING STALLWOOD JET. Grampurohit, S. V.; Kaimal, V. N. P. (Bhabha Atomic Research Centre, Bombay (India). Spectroscopy Div.). Z. Anal. Chem.; 274: No. 2, 181-183(1975).

5 tabs.; 3 refs.

A spectrographic method is described for estimating trace rare earth impurities in high purity gadolinium oxide. The sample is mixed with graphite and excited in a d.c. arc using Stallwood Jet. The spectrum is recorded in the second order of 3.4 m Jarrell Ash grating spectrograph having a reciprocal linear dispersion of 1.2 Å/mm. The detection limit for Sm, Dy, and Y is 10 ppm and for Tb and Eu, 100 ppm. The precision of the method is ± 11%. (auth)

**25509** DETERMINATION OF DEUTERIUM IN HEAVY WATER BY GAS CHROMATOGRAPHY. Yishikawa, Y.; Shinozaki, A.; Arita, K. (Osaka Univ., Toyonaka (Japan). Coll. of General Education). Jpn. Anal.; 24: No. 1, 45-48(Jan 1975). (In Japanese).

Deuterium concentration in heavy water was determined by gas chromatographically. Heavy water was decomposed by using $LiAlH_4$. Heavy water reacted with $LiAlH_4$ in short time and both $H_2$ and HD were generated. $D_2$ was not formed in this reaction. When hydrogen was used as a carrier gas, only a peak corresponding to HD was observed and therefore deuterium concentration in heavy water was determined as HD. The plot of HD peak height against deuterium concentration in heavy water was found to be linear in the range of deuterium concentration from 0 to 42 atom%. The relative error was below 6.9%. This method can be applied to a small amount of water sample. It is relatively simple, and can work as a conventional method of analysis. (auth)

## Radiometric and Radiochemical Procedures

*Refer also to abstracts 25934, 25949, 25966, 25967, 25969, and 25970.*

**25510** RAPID METHOD FOR BACKGROUND CORRECTIONS IN TRACE ELEMENT ANALYSIS BY X-RAY FLUORESCENCE: AN EXTENSION OF REYNOLDS' METHOD. Wilband, J. T. (Univ. of Toledo). Am. Mineral.; 60: No. 3-4, 320-323(1975).

A method is described whereby a sample's background intensity in the Kalpha wavelength of an element can be obtained by reference to a calibration curve once its mass absorption coefficient was determined by the Reynolds' method. Data presented indicate that, in standards with mu/sub 0.9A/ ranging from 7 to 20 (most rocks and minerals), the reciprocal of the background intensity at the desired Kalpha line is linearly related to mu so long as the standards are free of the analyzed element. The relationship remains linear even though the analyzed element occurs in the target or other parts of the spectrometer. For routine analysis involving many samples, an accurate estimation of background can be obtained from the analyses of as few as four standards, foregoing the time spent measuring the background of each sample. Cu and Sr were determined in testing the method. (auth)

**25511** ANALYSIS OF $^3H$ AND $^{14}C$ LABELLED COMPOUNDS IN THE FORM OF DOUBLY LABELLED METHANE. Povinec, P. (Komenskeho Univerzita, Bratislava). Int. J. Appl. Radiat. Isot.; 26: No. 8, 465-469(Aug 1975).

A new method of simultaneous analysis of $^3H$ and $^{14}C$ labelled compounds is described. A doubly labelled sample is burned to form HTO and $^{14}CO_2$ which are used as reactants in the presence of the zinc dust and a ruthenium catalyst for preparation of doubly labelled methane. $^3H$ and $^{14}C$ activities of methane are counted simultaneously by means of an internal proportional counter. The method is very sensitive and may be used even for naturally labelled samples. The same apparatus may be used for preparation and counting of singly or doubly labelled samples. (auth)

**25512** CONVERSION OF WATER TO A COUNTING FOR LOW-LEVEL TRITIUM MEASUREMENTS BY MEANS OF ALUMINIUM CARBIDE. Siegenthaler, U.; Oeschger, H.; Schotterer, U.; Haenni, K. (Univ., Bern). Int. J. Appl. Radiat. Isot.; 26: No. 8, 459-464(Aug 1975).

A routine method for measuring tritium in natural water sam-

ples is described. The procedure is based on the reaction of water with $Al_4C_3$ which produces methane, then used as a counting gas for proportional counters with internal anticoincidence. With the present system, the blank count rate is 0.25 counts/min and the calibration factor around 75 TU/counts/min. A concentration of 21 TU can be measured with a standard deviation of 10% in 1300 min counting time without previous enrichment. Sample preparation is simple and needs little operating time. The method has been successfully used for over 3 years. (auth)

## Separation Procedures

*Refer also to abstracts 25563 and 25633.*

**25513** ADSORPTION BEHAVIOR OF METALS ON TEAE-CELLULOSE FROM HYDROCHLORIC ACID AND HYDROCHLORIC ACID-THIOCYANATE MEDIA. Kuroda, R.; Oguma, K.; Suzuki, M.; Fuchu, Y. (Chiba Univ. (Japan). Faculty of Engineering). Jpn. Anal.; 24: No. 1, 1-6 (Jan 1975). (In Japanese).

Ion-exchange adsorption behavior of a number of metals on a quaternary ammonium anion exchange cellulose (TEAE-cellulose) was surveyed in hydrochloric acid {(0.001 ~ 6)M} and hydrochloric acid (0.5 M)-ammonium thiocyanate {(0.003 ~ 1)M} media. The distribution coefficients were measured either by a column or batch equilibrium method. From dilute hydrochloric acid, V(V), Mo(VI), W(VI), Re(VII), platinum metals, Au(III), Hg(II), Se(IV) etc. are strongly adsorbed ($K_d$ > 100), their adsorption generally decreasing rapidly with increasing concentration of hydrochloric acid. Ca, Sr, Y, La, Ti(IV), Zr, V(IV), Mn(II), Fe(III), Co(II), Ni, Cu(II), Zn, Cd, Al, Ga(III), In(III), Ge(IV), As(III), Te(IV) and U(VI) do not favor the cellulose exchanger phase to any great extent over the acid concentration range tested. Therefore, unlike strong base resin, TEAE-cellulose exhibits a high selectivity for a limited number of metals. The adsorption of Pd(II) and Mo(VI) can be improved greatly by introducing thiocyanate to hydrochloric acid media, providing a basis for their selective separations. Favorable differences in the distribution coefficients allow many useful separations such as As(III)-W(VI), V(IV)-Mo(VI), Zn-Mo(VI)-Pd(II), Cu(II)-Au(III)-Pd(II) to be achieved. (auth)

**25514** SEPARATION OF ALKALI ELEMENTS WITH THE AID OF COMPLEX BISMUTH HALIDES. Plyushchev, V. E.; Septsova, N. M.; Stepina, S. B.; Vlasova, I. V. J. Appl. Chem. USSR (Engl. Transl.); 48: No. 2, 653-655(Mar 1975).

Translated from Zh. Prikl. Khim.; 48: No. 3, 637-640(Mar 1975).

Studies of solubility in systems of the type $MeHal-BiHal_3-H_2O$ (Me = Na, K, Rb, Cs; Hal = Cl, Br) at 25° showed that complex halides of bismuth with potassium, sodium, cesium, and rubidium can be isolated from neutral solutions with the aid of $BiCl_3$ or $BiBr_3$. Cesium halides can be isolated from mixtures with rubidium, potassium, and sodium halides, and rubidium can be separated from potassium and sodium, in the form of complex halides with bismuth; this applies to original solutions containing HCl or HBr, as well as to neutral solutions. (auth)

**25515** SEPARATION OF RHENIUM FROM MOLYBDENUM, CALCIUM, AND POTASSIUM BY ELECTRODIALYSIS. Zarinskii, V. A.; Borisova, L. V.; Prasolova, O. D.; Ermakov, A. N. (Inst. of Geochemistry and Analytical Chemistry, Moscow). J. Appl. Chem. USSR (Engl. Transl.); 48: No. 2, 663-665(Mar 1975).

Translated from Zh. Prikl. Khim.; 48: No. 3, 646-648(Mar 1975).

Electrodialysis was used for the separation of Rh from Mo in acid and neutral sulfate solution with the simultaneous removal of $K^+$ and $Ca^{2+}$ cations. A three-compartment electrodialyzer was used and pure perrhenic acid in high yield (over 98% extraction of Rh) was obtained from mixtures containing impurities in amounts comparable to the Rh content. The most favorable conditions are obtained with constant saturation of the anolyte and catholyte. For monitoring the separation of Rh from Mo, Ca, and K, the Rh and Mo were determined by spectrophotometry and K and Ca by flame spectrophotometry. (JSR)

**25516** CRYSTALLINE INSOLUBLE ACID SALTS OF TETRAVALENT METALS. XX. Forward and Reverse $Cs^+/H^+$ and $Rb^+/H^+$ Ion Exchange on Crystalline Zirconium Phosphate. Alberti, G. (Perugia Univ., Italy); Costantino, U.; Allulli, S.; Massucci, M. A. J. Inorg. Nucl. Chem.; 37: No. 7/8, 1779-1786(Jul 1975).

Forward and reverse $Cs^+/H^+$ and $Rb^+/H^+$ ion exchange were investigated by the batch-procedure in order to obtain both the titration and uptake curves, as well as x-ray diffractograms and water contents of the samples at the various $Cs^+$ or $Rb^+$ loadings. The interlayer distance of the exchanger increases discontinuously with increasing $Cs^+$ loading and three different phases, $ZrHCs(PO_4)_2 \cdot 2H_2O$, $ZrH_{0.5}Cs_{1.5}(PO_4)_2 \cdot 3H_2O$, and $Zr(CsPO_4)_2 \cdot 6H_2O$ with interlayer distances of 11.3, 11.7 and 14.2 Å, respectively, were found in the forward process. For the analogous $Rb^+$ ion exchange process the phases were $ZrH_{0.5}Rb_{1.5}2H_2O$ (10.6 Å) and $Zr(RbPO_4)_2 \cdot H_2O$ (9.2 Å). Reverse ion exchange processes both for $Cs^+$ and $Rb^+$ ions showed a considerable irreversibility especially in the range of 0 to 50% $Cs^+$ or $Rb^+$ loadings. It was concluded that the low apparent selectivity of crystalline zirconium phosphate towards large monovalent ions is due to steric hindrance and therefore enlarged phases of this exchanger, such as $Zr(HPO_4)_2 \cdot 8H_2O$ (10.4 Å), are expected to have a high selectivity towards $Cs^+$ or even larger cations. (auth)

**25517** USE OF THERMOCHROMATOGRAPHY FOR RAPID CHEMICAL SEPARATIONS. P. 2. Determination of Deposition Temperatures. Rudstam, G.; Grapengiesser, B. (Forskningsraadens Lab., Studsvik (Sweden)). Radiochim. Acta; 20: No. 3, 97-107(1973).

6 figs.; 6 tabs.; 8 refs.

The depostion temperatures of elemental states and/or chemical compounds of the elements Na, Co, Zn, Ge, As, Br, Rb, Ag, Cd, In, Sn, Sb, Te, I, Cs, and Ba have been determined. In the majority of cases the material on which the deposition takes place has been quartz, but some data for other materials have also been obtained. (auth)

**25518** LIQUID–LIQUID EXTRACTION OF HAFNIUM COMPLEX ION FROM AQUEOUS OXALIC ACID SOLUTIONS WITH HIGH MOLECULAR WEIGHT AMINE. Yakabe, K.; Minami, S. (Osaka Inst. of Tech.). J. Inorg. Nucl. Chem.; 37: No. 9, 1973-1976(Sep 1975).

Extraction of hafnium from aqueous oxalic acid solution with high molecular weight amine was studied. It was confirmed that the tetraoxalato complex ion of hafnium is extracted from aqueous oxalic acid solution with tri-n-octylamine in xylene solution. A mechanism for the extraction of hafnium complex ion was discussed on the basis of the results obtained. (auth)

**25519** SOLVENT EXTRACTION OF THORIUM FROM HYDROCHLORIC ACID SOLUTIONS BY SULPHOXIDES AND THEIR MIXTURES. Mohanty, S. R.; Reddy, A. S. (Utkal Univ., Bhubaneswar, India). J. Inorg. Nucl. Chem.; 37: No. 9, 1977-1982(Sep 1975).

The extraction of thorium from hydrochloric acid solutions by sulphoxides and their mixtures in various solvents has been investigated. The extraction increases with increase in the concentration of the acid and of the extractant. The species extracted are $ThCl_4.2DPSO.HCl$, $ThCl_4.2DOSO$ and $ThCl_4.3DPhSO$. Mixed complexes are formed with mixtures of extractants. The extraction of the metal is inversely dependent upon the dielectric constant of the solvent, the initial metal concentration and the temperature of the system. (auth)

**25520** SOLVENT EXTRACTION STUDIES WITH DINONYL NAPHTHALENE SULPHONIC ACID: SEPARATION OF PROTACTINIUM (V) FROM THE OTHER MIXED METAL IONS. Wang, S. M.; Chuang, H. C.; Tseng, C. L. (National Tsing Hua Univ., Taiwan, China). J. Inorg. Nucl. Chem.; 37: No. 9, 1983-1987 (Sep 1975).

From international congress on analytical chemistry; Kyoto, Japan (3 Apr 1972).

The use of dinonyl naphthalene sulfonic acid (HD) in the organic solvents as an extractant has been shown to be a simple and effective method for the separation of metallic ion from the others with the proper choice of acidic aqueous solution and with the aid of long-chain alcohols or some complexing agents. In the present paper, the method for the separation of $^{233}Pa$ from a mixture of various metal ions by the use of HD in n-hexane solution has been investigated. The average recovery of $^{233}Pr$ by this method was found to be more than 95%. (auth)

**25521** COMBINED MIXER-SETTLER FOR SOLVENT EXTRACTION MEASUREMENTS. Eccles, H.; Lawson, G. J.; Rawlens, D. J. (Univ. of Birmingham, Eng.). Chem. Ind. (London); No. 14, 616-617(19 Jul 1975).

It is stated that in order to establish parameters for solvent extraction processes small scale determinations of the distribution coefficient (D) of a metal ion between the two liquid phases are required. The extent of extraction depends on the pH of the aqueous phase, and distribution measurements are carried out to determine the log D/pH relationship. This is commonly done with the use of "shake flasks," the pH of the aqueous phase is affected, however, by the transfer of metal ions, and it is difficult to predict equilibrium pH values. Statistical variation between flasks also introduces error into the results. Alternatively, what is known as the "AKUFVE" instrument may be used, in which circulated phases are continuously mixed and separated and which provides automatic regulation of one aqueous phase pH and measurements of D; the disadvantage of this instrument is, however, its high cost. The apparatus described aims at combining the low cost of "shake flasks" with some of the advantages of the "AKUFVE." These advantages are described in detail.

The apparatus is stated to have proved very suitable for use with radioactive tracers for metal analysis. (UK)

**25522** EXTRACTION OF SCANDIUM WITH CAPRIC ACID. Yamada, H. (Gifu Univ., Japan); Tanaka, K.; Tanaka, M. J. Inorg. Nucl. Chem.; 37: No. 9, 2016-2018(Sep 1975).

The results of the extraction of scandium by capric acid are described and extraction constants are given. (UK)

# Inorganic, Organic, and Physical Chemistry

## Chemical and Physicochemical Properties

*Refer also to abstracts 25601, 25623, 25628, 25629, and 26272.*

**25523** (AED-CONF-75-080-007) HYBRIDIZATION OF NITROGEN IN ENAMINES. Ahlbrecht, H.; Papke, G. (Giessen Univ. (F. R. Germany). Inst. fuer Organische Chemie). 1975. 13p. (In German). INIS.

From meeting of lecturers in chemistry; Duesseldorf, F. R. Germany (7 Apr 1975).

4 figs.

The so far almost unknown hybridization of nitrogen in enamines was investigated. Analogous to the $^1J(^{13}C\text{-}H)$ coupling, a linear dependence between the coupling constant and the percent s-character of the nitrogen orbital can also be proved for the $^1J(^{15}N\text{-}H)$ coupling. A number of $^{15}N$-labelled imine-enamine tautomeric systems were produced, and the dependence of the $^{15}NH$ coupling on the electronic properties of the substituents is investigated. The result of measurements with N-phenyl enamines is discussed with regard to molecular theory. Some thought is given to the problem of hybridization of the lone-pair electrons at the nitrogen level in consideration of the hybridization index for the N-phenyl and vinyl coupling. (auth)

**25524** (DP-REPORT-734) TABLES OF THERMOPHYSICAL PROPERTIES OF HELIUM. Dragon Project Report. Petersen, H. (UKAEA Reactor Group, Winfrith. Atomic Energy Establishment). Jan 1971. 53p. Dep. NTIS (US Sales Only) $5.75.

The compressibility factor, density, thermal conductivity, and Prandtl number were calculated for He at different temperatures and pressures. The results are tabulated. (JSR)

**25525** (ERDA-50, pp 120-132) REVIEW OF ANL RESEARCH ON LITHIUM–HYDROGEN CHEMISTRY AND TRITIUM-CONTAINMENT TECHNOLOGY. Maroni, V. A.; Veleckis, E.; Van Deventer, E. H. (Argonne National Lab., IL). Jun 1975.

From symposium on technology related for fusion reactor systems; Miamisburg, Ohio, USA (1 Oct 1974).

In proceedings of the symposium on tritium technology related to fusion reactor systems. (Energy Research and Development Administration, Washington, D. C. (USA). Div. of Controlled Thermonuclear Research).

Experimental data on the thermodynamic properties of solutions of protium, deuterium, and tritium in liquid lithium are reported. The significance of the results is discussed with regard to problems that are pertinent to the development of controlled thermonuclear fusion reactors. Values are given for the equilibrium constants, free energies of formation, plateau dissociation pressures, and Sieverts' constants in the Li-LiH, Li-LiD, and Li-LiT systems. The observed isotope effects in these systems appear to reside predominantly in the gas phase. Results of studies of the distribution of tritium between liquid lithium and selected molten salts indicate that molten-salt extraction has potential utility as a means of recovering tritium from liquid lithium fusion reactor blankets. Other recent work at ANL has given evidence that multilayered bonded-metal composites could be useful in reducing tritium permeation rates through thermally hot structures (e.g., steam generator tubes) in fusion devices and power reactors. Hydrogen permeation data are presented for three bonded-metal composites (i.e., 316-SS/Cu/316-SS, 304-SS/Nb, and 304-SS/Cu/Nb) as well as for 304-SS and 316-SS. The data are compared to calculated permeabilities for the bonded-metal composites based on an electro-analog model. (auth)

**25526** (GERHTR-137) NEW CONCEPTIONS OF THE DEPOSITION MECHANISM OF PYROCARBON. Linke, J.; Nickel, H.; Luehleich, H.; Koizlik, K.; Pflaum, P.; Seeberger, D. Translation of JUL–1092-RW Aug 1974. 50p. Dep. NTIS $4.00.

Work performed under United States–German High Temperature Reactor Research Exchange Program.

An attempt is made to draw up a new model of the pyrolysis of gaseous hydrocarbons and of the deposition mechanism. After a short discussion of available models and their inadequacies, a new conception is put forward which can be characterized by the terms "Langmuir zone", "pyroaggregate hypothesis", and "droplet model". In this conception, the pyrolysis and subsequent carbon formation are transferred to a special zone of the gas chamber (Langmuir zone) which is a plasma. Results of new experiments confirm the assumptions. (45 references, 28 figures) (DLC)

**25527** (IRI-190-75-03) MEASUREMENT OF POLYDISPERSE AEROSOLS WITH THE SPIRAL CENTRIFUGE. Ferron, G. A.; Bierhuizen, H. W. J. (Interuniversitair Reactor Instituut, Delft (Netherlands)). Feb 1975. 42p. INIS.

The aerosol centrifuge designed by Stöber (1969) separates aerosol particles according to their aerodynamic size. When using this centrifuge to measure aerosol distributions, additional information concerning its operation is needed. Some important characteristics for the measurement of polydisperse aerosols are presented in this report. The mass of an aerosol deposited on a filter outside the centrifuge is measured with labelled NaCl aerosols. A computer program for the calculation of the mass distribution of an aerosol measured with the spiral centrifuge has been described. (NL)

**25528** (NP-20541) HEAVY WATER. Bibliography. (Ceskoslovenska Komise pro Atomovou Energii, Prague). 23 Jan 1975. 30p. (In Czech).

A bibliography from the international literature is presented on the production, economics, physical properties, analytical methods, purification of the water in reactors, and miscellaneous problems related to heavy water. An author index is appended. (JSR)

**25529** (Y-DA-6370) BIOLOGICAL DENITRIFICATION OF NITRATE WASTE SOLUTIONS. Napier, J. M.; Clark, F. E.; Strohecker, J. W. (Oak Ridge Y-12 Plant, Tenn. (USA)). Sep 1975. Contract W-7405-eng-26. 25p. Dep. NTIS $4.25.

The studies leading to the design of the Oak Ridge Y-12 plant biological denitrification system are briefly described. The system uses a flow-through stirred-bed reactor. Methanol and lime-neutralized acetic acid were evaluated as C sources. The acetic acid was selected because the calcium carbonate generated in the process is needed for neutralization of the acid wastes. Excess organic will be used to ensure maximum amount of nitrate destroyed. The system will generate solids in the form of calcium carbonate, aluminum hydroxide, and organic carbon and $N_2$ and $CO_2$ gases. (JSR)

**25530** THE HYDROTHERMAL SOLUBILITY OF BERYLLIUM OXIDE IN NaOH SOLUTIONS. Shindo, I. (National Inst. for Researches in Inorganic Materials, Sakura, Ibaraki (Japan)); Suzuki, H. Yogyo Kyokai Shi; 83: No. 953, 28-32(Jan 1975).

The hydrothermal solubility of beryllium oxide was measured between 300 and 600°C in NaOH solutions from 3.9 to 13.1 mol. The dissolution reaction changes from the equation (1) to the equation (2) at nearly 400°C. (1) $BeO + 3(OH)^- = BeO_2(OH)^{3-} + H_2O$ (below 350°C), (2) $BeO + 2(OH)^- = BeO_2^{2-} + H_2O$ (up to 400°C). And this transition temperature is varied with the concentration of basic solution. The other hand, the Van't Hoff equation is obeyed, the heat of solution is calculated as follows. (3) $2.7 \pm 0.1$ kcal/mol. (8.7 mol) (4) $5.0 \pm 0.1$ kcal/mol. (3.9 mol) These values are correlated to the equations (1) and (2). (auth)

**25531** RAMAN SPECTRUM OF THE $LaCl_6^{-3}$ OCTAHEDRON IN MOLTEN AND SOLID $Cs_2NaLaCl_6$, $Cs_3LaCl_6$, and $K_3LaCl_6$. Papatheodorou, G. N. (Univ. of Chicago). Inorg. Nucl. Chem. Lett.; 11: No. 7/8, 483-490(Jul 1975).

The Raman spectra of polycrystalline and molten $Cs_2NaLaCl_6$ from room temperature to 750° are reported. In addition, the Raman spectral changes on melting of the $Cs_3LaCl_6$ and the spectra of liquid $K_3LaCl_6$ are reported. (auth)

**25532** THERMOMETRIC STUDIES OF THE REDUCTION OF Mo(VI) BY Sn(II) IN 6 M-0.3 M HCl. Choi, B. C.; Jespersen, N. (Univ. of Texas, Austin). J. Inorg. Nucl. Chem.; 37: No. 9, 1945-1947(Sep 1975).

Reaction stoichiometry, kinetics, and thermochemistry for the reduction of Mo(VI) by Sn(II) have been studied in 6M to 0.3M HCl. Heats of reaction vary from -45 KJ/mole $e^-$ to -109 KJ/mole $e^-$ in this region. In all cases, Mo(V) is the product. In 0.3M HCl reduction yields molybdenum blue. Stoichiometrically, the species formed have the form $[Mo(VI)-Mo(V)_2]$. (auth)

**25533** KINETICS OF GASEOUS FLUORINE REACTIONS. Foon, R. (New South Wales Univ., Kensington, Australia); Kaufman, M. Prog. React. Kinet.; 8: 81-160(1975).

An extensive review of the subject of the kinetics of gaseous fluorine reactions is made covering thermochemistry and spectroscopy, experimental considerations (production and handling of

$F_2$, analysis of $F_2$ and HF, production of fluorine atoms, measurement of atomic fluorine concentration, determination of rate constants), rate data for elementary reactions of atomic fluorine (combination reactions, hydrogen abstraction reactions, halogen abstraction (and substitution), reactions of atomic fluorine, reactions of atomic fluorine with oxygen-containing molecules, reaction of atomic fluorine with compounds containing multiple bonds), rate data for elementary reactions of $F_2$, mechanisms of $F_2$ reactions (chain branching in $F_2$ reactions, $H_2-F_2$ explosions and flames–energy branching, the $Cl_2 + F_2$ reaction), molecular beam studies, chemiluminescence, (visible and ultraviolet, infrared), and theoretical molecular dynamics ($F + H_2$, $H + F_2$). (UK)

**25534** HEXAFLUOROPHOSPHATE AS A NON-COORDINATING ANION IN LANTHANIDE COMPLEXES. I. Dimethyl Sulfoxide Complexes. Kuya, M. K.; Serra, O. A.; Osorio, V. K. L. (Univ., Sao Paulo, Brazil). J. Inorg. Nucl. Chem.; 37: No. 9, 1998-1999(Sep 1975).

The preparation, analysis, and properties of complexes of the type LnX.xDMSO where Ln = La to Y and X = $PF_6^-$ is described. (UK)

**25535** LANTHANIDE COORDINATION IN DIMETHYL SULPHOXIDE AND ANTIPYRINE COMPLEXES OF RARE EARTH NITRATES. Bhandary, K. K. (Indian Inst. of Science, Bangalore); Manohar, H.; Venkatesan, K. J. Inorg. Nucl. Chem.; 37: No. 9, 1997-1998(Sep 1975).

It is well known that the size of the lanthanide ion goes on decreasing as the 4f sub-shell is filled. This contraction is correlated with the decrease in the coordination number and change in the crystal structure in a series of dimethyl sulphoxide (DMSO) complexes of lanthanide nitrates. These complexes have the general formula $Ln(NO_3)_3n(CH_3)_2SO$ where n = 4 for Ln = La to Gd and n = 3 for Ln = Tb to Yb. (UK)

**25536** KRYPTON FLUORIDE CHEMISTRY: A ROUTE TO $AuF_5$, $KrF^+AuF_6^-Xe_2F_3^+AuF_6^-$, AND $NO^+AuF_6^-$: THE $KrF^+/XeOF_4$ SYSTEM. Holloway, J. H.; Schrobilgen, G. J. (Univ. of Leicester, Eng.). J. Chem. Soc. (London), Chem. Commun.; No. 15, 623-624(1975).

Pyrolysis of newly prepared $KrF^+AuF_6^-$ gives $AuF_5$ which reacts with $XeF_2$ to produce $Xe_2F_3^+AuF_6^-$ and NOF to give $NO^+AuF_6^-$; $Kr^+AuF_6^-$ is a powerful oxidative fluorinating agent with respect to $O_2$ and Xe and the reaction of $KrF^+$ with excess $XeOF_4$ gives $XeOF_4.XeF_5^+$ and $O_2^+$ salts, not $XeOF_5^+$ as reported previously. (auth)

## Isotope Effects

*Refer also to abstracts 25595, 25596, 26202, 26233, 26760, 26761, and 26774.*

**25537** NITROSYLRHENIUM ($^{14}NO$ AND $^{15}NO$) COMPLEXES. Miki, E.; Mizumachi, K.; Ishimori, T. (Rikkyo Univ., Tokyo (Japan). Faculty of Science). Bull. Chem. Soc. Jpn.; 47: No. 12, 3068-3070(Dec 1974).

The $^{15}NO$-complexes for $M_2[ReX_5(NO)]$ (M=Rb, Cs, and pyH; X=Cl and Br) were prepared. The $^{15}N$-isotopic shift for their N-O stretching vibrations, ca. 40 $cm^{-1}$, supports the view that the oxidation state of the NO group is I, while that of the rhenium atom is II. The Re-(NO) stretching and the Re-(NO) bending vibrations were observed in the 610-620 $cm^{-1}$ region. A new compound, cis-(pyH) $[ReCl_4(NO)_2]$, was prepared, the oxidation state of its rhenium atom being considered to be I, and that of the NO group, I. (auth)

**25538** DEUTERIUM ISOTOPE EFFECTS ON THE REDEX DECOMPOSITION OF HYDROXYMERCURATED PROPENE AND 2-BUTENES IN AN AQUEOUS SOLUTION. Shinoda, S.; Saito, Y. (Tokyo Univ. (Japan). Faculty of Engineering). Bull. Chem. Soc. Jpn.; 47: No. 12, 2948-2952(Dec 1974).

Kinetic deuterium isotope effects on the redox decomposition of hydroxymercurated propene, cis-, and trans-2-butenes in an aqueous solution ($CH_3CH(OH)CHRHg^+ \rightarrow CH_3COCH_2R + Hg(O) + H^+$; R=H, $CH_3$) were determined by following the reaction in situ by means of PMR spectroscopy. Taking advantage of the PMR characteristics, the identity of the reaction conditions was confirmed by comparing the rates for the reactant mixtures (e.g., $CH_3CH(OH)CH_2Hg^+ + CH_3CD(OH)CH_2Hg^+$). The mercurials, deuterated on either $\beta$-carbon ($CH_3CD(OH)CH_2Hg^+$, $CH_3CD(OH)CHCH_3Hg^+$) or $\alpha$-carbon ($CH_3CH(OH)CDHHg^+$, $CH_3CH(OH)CDCH_3Hg^+$), gave primary and secondary deuterium isotope effects of 1.35–1.40 and 1.17–1.19 respectively. A possible structure of the activated complex was proposed in accord with the observed nature of the intra-molecular hydrogen shift. (auth)

**25539** CALCULATION OF THE ANHARMONICITY CONSTANTS FOR THE $H_2O$, $H_2S$, $H_2Se$ MOLECULES AND THEIR DEUTERIUM DERIVATIVES. Kapshtal, V.N. Opt. Spectrosc. (USSR) 38: No. 3, 285-286 (Mar 1975).

Equations for calculating the anharmonicity coefficients of molecules of the type $XY_2$ have been derived in general form. Numerical calculations carried out for the $H_2O$, $H_2S$, $H_2Se$ molecules and their deuterium derivatives have shown that it is necessary to take account of the off-diagonal anharmonicity constants in the potential function. (auth)

**25540** ISOTOPE SHIFT IN THE Cd I LINE 4678 Å ($5s5p\ ^3P_0$–$5s6s\ ^3S_1$) AND ODD–EVEN STAGGERING. Gagné, J.M.; Saint-Dizier, J.P. (Laboratoire d'optique et de spectroscopie, Département de Génie physique, Ecole Polytechnique, Campus de l'Université de Montréal, C. P. 6079, Succursale A, Montréal, Québec, Canada H3C 3A7). J. Opt. Soc. Am. 65: No. 8, 962-963 (Aug 1975). (auth)

**25541** INFRARED SPECTRA OF MONOMERIC GALLIUM TRIHALIDES IN SOLID ARGON. Pong, R.G.S.; Stachnik, R.A.; Shirk, A.E.; Shirk, J.S. (Department of Chemistry, Illinois Institute of Technology, Chicago, Illinois 60616). J. Chem. Phys. 63: No. 4, 1525-1532 (15 Aug 1975).

We have observed the infrared spectra of $GaCl_3$, $GaBr_3$, and $GaI_3$ in solid argon. Some absorptions due to the dimers are also reported. Isotopic shifts were partially resolved in several cases. The observed spectra are all consistent with a planar $D_{3h}$ structure for each of these molecules. (auth)

**25542** PHASE EQUILIBRIUM ISOTOPE EFFECTS IN MOLECULAR SOLIDS AND LIQUIDS. VAPOR PRESSURES OF THE ISOTOPIC NITROUS OXIDE MOLECULES. Yato, Y.; Lee, M.W.; Bigeleisen, J. (Department of Chemistry, University of Rochester, Rochester, New York 14627). J. Chem. Phys. 63: No. 4, 1555-1563 (15 Aug 1975).

The vapor pressures of three isotopic samples of $N_2O$ enriched in $^{15}N$ and $^{18}O$ have been compared with normal $N_2O$ over the temperature range 143–219 °K. Over the temperature range studied in the solid and in the liquid in the neighborhood of the triple point, the vapor pressures are in the sequence $^{14}N_2{}^{16}O > {}^{14}N^{15}N^{16}O > {}^{15}N^{14}N^{16}O > {}^{14}N_2{}^{18}O$. The crossover phenomena have been observed for $^{15}N^{14}N^{16}O/^{14}N_2{}^{18}O$ at 207 °K and for $^{14}N^{15}N^{16}O/^{14}N_2{}^{16}O$ at 215 °K. The experimental data confirm hindered translation in both the solid and the liquid as well as the potential energy coupling of the translation and rotation found in $CO_2$. Shifts in the internal stretching and bending modes on condensation lead to significant differences in the vapor pressures of the isomers $^{15}N^{14}N^{16}O$ and $^{14}N^{15}N^{16}O$. The latter has an abnormally large change in vapor pressure on melting compared with the other isotopic $N_2O$ molecules studied. This is associated with the coupling of the internal bend coordinate with the translation in the solid, which vanishes in the liquid. The isotope effect in the high temperature liquid is explained in terms of an anharmonicity of the external motions in addition to the temperature dependence of the stretching force constant. Model calculations of the logarithm of the reduced partition function ratios of the solid and liquid $\ln(f_c/f_g)$, are made in an anharmonic version of the Stern–Van Hook–Wolfsberg cell model. This model provides a good representation of the experimentally determined $\ln(f_c/f_g)$ for solid and liquid $N_2O$. (auth)

**25543** MASS SPECTROMETRIC DETERMINATION OF THE IONIZATION POTENTIAL AND DISSOCIATION ENERGY OF LiD. Ihle, H.R.; Wu, C.H. (Institute for Nuclear Chemistry, Kernforschungsanlage Jülich GmbH, Federal Republic of Germany). J. Chem. Phys. 63: No. 4, 1605-1608 (15 Aug 1975).

The ionization potential of LiD was determined as I.P.(LiD) $=7.7\pm0.1$ eV, from which a binding energy $\mathcal{D}_0(Lid^+) = 0.14\pm0.1$ eV results. From measurements of the gas equilibrium $Li_2(g)+D_2(g) \rightleftharpoons 2LiD(g)$ over dilute solutions of deuterium in liquid lithium a value for the dissociation energy $D^0(LiD) = 2.49\pm0.04$ eV was obtained. (auth)

**25544** DOMINANCE OF DIPOLE COUPLING OVER ISOTOPE SHIFT EFFECTS FOR INTERNAL CRYSTAL MODES: $\nu_3$ OF $KNO_3$ (III). Devlin, J.P. (Department of Chemistry, Oklahoma State University, Stillwater, Oklahoma 74074); Frech, R. J. Chem. Phys. 63: No. 4, 1663-1667 (15 Aug 1975).

The occurrence of well-separated and sharp transverse and longitudinal optic mode Raman features for the nitrate asymmetric stretching mode of $KNO_3$ (III) presents an exceptional opportunity to observe the effect of isotopic dilution on the dynamics of a crystal mode based on an intensely infrared active internal mode. It has been found that for most of the range of isotopic dilution with $^{15}N$, which is known to cause an $\sim$32 $cm^{-1}$ isotope shift for isolated $NO^-_3$ units, the $KNO_3$ (III) Raman spectrum for backscattering along the trigonal axis contains only two relatively sharp (TO and LO) features, as observed for the $^{14}N$ sample, but displaced in a regular manner towards the pure $^{15}N$ sample values. The sharpness of the Raman features relative to the $\nu_3$ features observed for the orientationally disordered $KNO_3$ (I), suggests that the spectra can be discussed as though the $k\simeq0$ selection rule is operating,

even though translational symmetry is clearly destroyed by isotopic mixing. It has also been shown that the atr $\nu_3$ infrared band of a 50:50 isotopic mixture behaves as though based on a single resonant mode. The results can be interpreted by assuming that dipole forces cause the nitrate units to vibrate with an "average" resonant frequency, a result that may have interpretive value in the analysis of vibrational spectra of disordered systems. (auth)

**25545** ENERGY PARTITIONING AND ASSIGNMENT OF EXCITED STATES IN THE ULTRAVIOLET PHOTOLYSIS OF HI AND DI. Clear, R.D.; Riley, S.J.; Wilson, K.R. (Department of Chemistry, University of California, San Diego, La Jolla, California 92037). J. Chem. Phys. 63: No. 4, 1340-1347 (15 Aug 1975).

Photofragment spectroscopy has been applied to the photolysis of hydrogen iodide and deuterium iodide at 37 550 $cm^{-1}$ (266.2 nm). The extent of excited $I(^2P_{1/2})$ atom production and the symmetry of the excited molecular states leading to dissociation are derived by measuring the translational energy and angular distributions of the recoiling H and D atoms. It is found that for HI, 36%±5% of the I atoms are formed in their excited state, while for DI the fraction is 26%±3%. In both cases, the transition leading to excited atoms is parallel, agreeing with Mulliken's spectral interpretation. These results, together with measurements reported by others at different wavelengths, are used to analyze the first absorption continuum of HI and DI. This continuum is found to be consistent with overlapping transitions to $^3\Pi_1$, $^3\Pi_{0+}$, and $^1\Pi$ excited states, as predicted by Mulliken. A nonlinear curve fitting technique is applied to the available data to separate each state's contribution to the total continuum absorption and to provide estimates of the shape of each excited state potential energy curve. (auth)

**25546** DEUTERON QUADRUPOLE COUPLING CONSTANTS IN $CD_3F$ AND 1,3,5-$C_6D_3F_3$. Bhattacharyya, P.K.; Dailey, B.P. (Department of Chemistry, Columbia University, New York, New York 10027). J. Chem. Phys. 63: No. 4, 1336-1339 (15 Aug 1975).

The deuteron quadrupole coupling constants in the deuterated methyl fluoride and 1,3,5-trifluorobenzene molecules have been determined from nematic phase studies using a pulsed FT NMR spectrometer. The values obtained in the molecular symmetry axis system are as follows: $\chi_{zz}$ = −47.8±1.5 kHz (in $CD_3F$) and $\chi_{zz}$ = −94.4±0.7 kHz (in 1,3,5-$C_6D_3F_3$). If the field gradient tensor is assumed to be diagonal in the C–D bond axis system, the values of the coupling constants referred to the C–D bond are given by $\chi_{CD}$ = 133±7 kHz (in $CD_3F$, $\eta$ = 0.03±0.03) and $\chi_{CD}$ = 180±3 kHz (in 1,3,5-$C_6D_3F_3$, $\eta$ = 0.05±0.01). (auth)

**25547** KINETIC ISOTOPE EFFECTS IN REDUCTIONS OF COBALT(III)--PENTAAMMINE COMPLEXES. Itzkowitz, M. M.; Nordmeyer, F. R. (Univ. of Rochester, NY). Inorg. Chem.; 14: No. 9, 2124-2129(Sep 1975).

Deuterium isotope effects arising in the rates of reduction of Co/sup III/$(NH_3)_5$L complexes were studied. Only the ammine ligands of the cobalt(III) were deuterated. Ratios of k/sub H// k/sub D/ were determined for L equals $OH^-$, $CN^-$, $SCN^-$, $N_3^-$, pyridine, nicotinamide, isonicotinamide, 4-pyridinecarboxylic acid, acetate ion, and fumarate ion. Reductions by $Cr^{2+}$ and $V^{2+}$ were included. Ratios of k/sub H//k/sub D/ near unity are consistent with a chemical mechanism for the $Cr^{2+}$ reductions of the isonicotinamide, 4-pyridinecarboxylic acid, and fumarate complexes. Ratios of k/sub H//k/sub D/ near unity are consistent with substitution-limited reductions for $V^{2+}$ reductions of the azido and isonicotinamide complexes. (auth)

**25548** INFRARED SPECTRA OF MATRIX ISOLATED DISULFUR MONOXIDE ISOTOPES. Hopkins, A. G.; Daly, F. P.; Brown, C. W. (Univ. of Rhode Island, Kingston). J. Phys. Chem.; 79: No. 17, 1849-1851(14 Aug 1975).

Infrared spectra of natural abundance and isotopically enriched $S_2O$ matrix isolated in Ar have been measured. The vibrational bands of $^{32}S_2{}^{16}O$, $^{32}S_2{}^{18}O$, $^{34}S_2{}^{16}O$, $^{34}S^{32}S^{16}O$, and $^{32}S^{34}S^{16}O$ have been assigned and the observed frequencies of these isotopes used to calculate the harmonic force constants of $S_2O$. (auth)

**25549** ARGON MATRIX INFRARED SPECTRA OF $CF_3OOF$ AND $CF_3OOOCF_3$ AND THEIR PHOTOLYSIS PRODUCTS. SPECTROSCOPIC EVIDENCE FOR THE $CF_3OO$ RADICAL. Smardzewski, R.R.; De Marco, R.A.; Fox, W.B. (Chemistry Division, U.S. Naval Research Laboratory, Washington, DC 20375). J. Chem. Phys. 63: No. 3, 1083-1089 (1 Aug 1975).

Ultraviolet photolysis of fluoroperoxytrifluoromethane, $CF_3OOF$, in argon matrices at 8 °K produced $CF_4$ and a new species, tentatively identified as the $CF_3OO$ radical, with infrared absorptions at 1173.7 and 1094.1 $cm^{-1}$. This species was also produced, along with $CF_4$, $CF_3OCF_3$, and $COF_2$, by photolysis of bistrifluoromethyl trioxide, $CF_3OOOCF_3$, at wavelengths below 300 nm. In the latter case, extensive isotopic labeling experiments with $CF_3{}^{16}O^{16}O^{16}OCF_3$, $CF_3{}^{16}O^{18}O^{16}OCF_3$, $CF_3{}^{18}O^{16}O^{18}OCF_3$, and $CF_3{}^{18}O^{18}O^{18}OCF_3$ led to the observation of four distinct isotopic absorptions for the O–O stretching vibration (1094.1 cm), thus confirming the nonequivalent oxygen atom structure of $CF_3OO$. (auth)

**25550** A RAMAN SPECTRAL STUDY OF AMORPHOUS SOLID WATER. Venkatesh, C.G.; Rice, S.A. (Department of Chemistry and The James Franck Institute, The University of Chicago, Chicago, Illinois 60637); Bates, J.B. J. Chem. Phys. 63: No. 3, 1065-1071 (1 Aug 1975).

Raman spectra of amorphous solid $H_2O$, [$H_2O$(as)], $D_2O$(as), and 12% $H_2O$ in $D_2O$(as) were measured over a temperature range from 30 to 120 °K. The spectra of $H_2O$(as) resemble those of liquid water more than they do those of ice Ic or ice Ih. The spectra suggest that the water molecules are located in two or three types of distinguishable environments depending on the details of the assignment. No structural changes were observed between 30 and 120 °K, but at ~160 °K the amorphous samples transformed rapidly and irreversibly to ice Ic. (auth)

**25551** $^{13}C$ CHEMICAL SHIELDING IN OXALIC ACID, OXALIC ACID DIHYDRATE, AND DIAMMONIUM OXALATE. Griffin, R.G. (Francis Bitter National Magnet Laboratory, Massachusetts Institute of Technology, Cambridge, Massachusetts 02139); Pines, A.; Pausak, S.; Waugh, J.S. J. Chem. Phys. 63: No. 3, 1267-1271 (1 Aug 1975).

$^{13}C$ chemical shielding tensors in three oxalates were investigated in order to determine the effects of protonation and conformation changes on the tensor elements and their orientations. The experimental results, together with those in the accompanying paper [R. G. Griffin and D. J. Ruben, J. Chem. Phys. 3, 1272 (1975)], indicate that, while neither of these factors seems to seriously affect the magnitudes $\sigma_{11}$ and $\sigma_{33}$, they do perturb $\sigma_{22}$ and the tensor orientation. Protonation produces an upfield shift (increased shielding) of $\sigma_{22}$ and in one case a concurrent rotation of the tensor about $\sigma_{33}$, the element which is perpendicular to the COO plane. On the other hand, the simple conformational change of the twisting of carboxyl groups relative to one another, which occurs in diammonium oxalate monohydrate, results in small rotation of the tensor around $\sigma_{11}$ and also may contribute to a decrease in the shielding of the $\sigma_{22}$ component in this molecule. The orientation of the $^{13}C$ tensor in oxalic acid dihydrate is different from that observed in other oxalate ions and carboxyl groups. The influence of a change in hydrogen bonding strength on tensor elements is discussed. (auth)

**25552** CARBON-13 CHEMICAL SHIELDING IN AMMONIUM HYDROGEN OXALATE HEMIHYDRATE. Griffin, R.G.; Ruben, D.J. (Francis Bitter National Magnet Laboratory, Massachusetts Institute of Technology, Cambridge, Massachusetts 02139). J. Chem. Phys. 63: No. 3, 1272-1275 (1 Aug 1975).

We have measured the two $^{13}C$ chemical shift tensors in single crystals of ammonium hydrogen oxalate hemihydrate, $NH_4HC_2O_4 \cdot (1/2)H_2O$, using solid state double resonance techniques. One of the two types of tensors in the unit cell, the one belonging to the ionic carboxyl group, is oriented with its least shield component $\sigma_{11}$ within 6° of the C–C bond, while the other tensor, belonging to the protonated carboxyl group, has its $\sigma_{11}$ twisted 24° off this bond. Both tensors have $\sigma_{33}$ perpendicular to the oxalate plane. Protonation of the carboxyl group does not affect the shifts of the $\sigma_{11}$ and $\sigma_{33}$ tensor elements, but it does move the $\sigma_{22}$ component in the direction of increased shielding. Implications of the orientation of these tensors to crystal and molecular structure determination are discussed. (auth)

**25553** STARK ENERGIES FOR MOLECULES WITH VIBRATIONALLY INDUCED DIPOLE MOMENTS. Muenter, A.A.; Dyke, T.R. (Department of Chemistry, Harvard University, Cambridge, Massachusetts 02138). J. Chem. Phys. 63: No. 3, 1224-1230 (1 Aug 1975).

For the various classes of molecules capable of having vibrationally induced electric dipole moments, explicit expressions for the resultant Stark energies are derived. In addition, the change in the vibrationally induced Stark effect with isotopic substitution of the B atoms in a tetrahedral $AB_4$ molecule is considered. (auth)

**25554** MOLECULAR BEAM ELECTRIC DEFLECTION OF THE TETRAHALIDES $CF_4$, $CCl_4$, $SiF_4$, $SiCl_4$, $GeCl_4$, $TiF_4$, $TiCl_4$, $VF_4$, AND $VCl_4$. Muenter, A.A.; Dyke, T.R. (Department of Chemistry, Harvard University, Cambridge, Massachusetts 02138); Falconer, W.E.; Klemperer, W. J. Chem. Phys. 63: No. 3, 1231-1236 (1 Aug 1975).

Using molecular beam electric deflection, the temperature dependence of polar behavior has been studied for the molecules $CF_4$, $CCl_4$, $SiF_4$, $SiCl_4$, $GeCl_4$, $TiF_4$, $TiCl_4$, $VF_4$, and $VCl_4$. A number of these molecules show polar behavior consistent with a vibrationally induced dipole moment for states with one or both of the triply degenerate vibrations excited. In four of the tetrachloride species, the presence of a vibrationally induced dipole moment was confirmed by the change in polar behavior with isotopic substituion of the Cl atoms. The deflection behavior of the transition metal tetrahalides varied from nonpolar in $VCl_4$ to very polar in $TiF_4$. (auth)

**25555** INTERNAL CATALYSIS IN IMINE FORMATION FROM ACETONE AND ACETONE-$d_6$ AND CONFORMATIONALLY CONSTRAINED DERIVATIVES OF N,N-DIMETHYL-1,3-PROPANEDIAMINE. Hine, J.; Li, W. S. (Ohio State Univ., Columbus). J. Org. Chem.; 40: No. 18, 2622-2626(5 Sep 1975).

The kinetics of the reactions of 3-exo-dimethylaminomethyl-2-endo-norbornanamine (1), cis-2-(dimethylaminomethyl)cyclohexylamine (2), and 3-endo-dimethylaminomethyl-2-endo-norbornanamine (3) with acetone, and of these three diamines, neopentylamine, and 2-endo-norbornanamine with acetone-$d_6$ to give imines were studied at 35° and various pH's by use of hydroxylamine to capture the imines as they are formed. Acetone-$d_6$ was more reactive than acetone in the reactions with hydroxylamine alone as well as in the reactions with each of the diamines; the average k/sup D//k/sup H/ was 1.2. The rate constants for the monoprotonated diamines were so large relative to those for the unprotonated diamines that reliable values for the latter could not be obtained. The dominant reaction mechanism appears to be a reversible formation of the carbinolamine derived from the tertiary-protonated form of the monoprotonated diamine followed by rate-controlling internal acid-catalyzed formation of the iminium ion. The rate constants are compared with those obtained as a by-product of deuterium exchange studies of reactions of 1, 2, 3, and five other monoprotonated diamines by the same mechanism. The comparisons show that structural features that destabilize conformations in which the two amino groups are far apart may decrease the reactivity by relative stabilization of a cyclic hydrogen-bonded form of the monoprotonated diamine as well as increasing the reactivity by relative stabilization of the transition state. Freezing the $H_2N–C–C–CH_2NMe_2$ dihedral angle of 1,3-diamines at values near 0, 60, and 120° does not give large differences in reactivity. Comparison of the rate constants for reactions of unprotonated neopentylamine and 2-endo-norbornanamine with those obtained previously for amines of the type $XCH_2CH_2NH_2$ gives no evidence for steric hindrance. (auth)

**25556** INVESTIGATIONS ON THE VAPOR PRESSURE ISOTOPE EFFECT OF n-PENTANE AND NEOPENTANE. Hoerner, C. Heidelberg; Heidelberg Univ. (1973). 76p. (In German). INIS.

Thesis.

The vapor pressure isotopic effect is treated phenomenologically and by quantum statistical methods. The apparatus and the preparation of the deuterated substances and the results of the measurements in the system n-pentane and in the system neopentane with the vapor pressure differences in $\alpha$-$D_1$-n-pentane, $\gamma$-$D_1$-n-pentane, perdeutero-n-pentane and monodeuteroneopentane as well as a consideration of the errors are described. (GE)

**25557** TEMPERATURE, ISOTOPE, AND SOLUTE EFFECTS ON THE NON-LINEAR ELECTRIC FIELD BEHAVIOR OF WATER. Bradley, P. A. (University Coll. of North Wales, Bangor); Jones, G. P.; Kolodziej, H. A. J. Chem. Soc. (London), Faraday Trans., II; 71: No. 6, 1200-1211(1975).

Measurements are reported on the non-linear electric field effect of the relative permittivity of aqueous systems at fields up to $10^7$ V $m^{-1}$. Over the range 273° to 293°K the Piekara factor ($\Delta\epsilon/E^2$) for water has the Langevin anticipated negative values but shows a distinct pattern with a minimum near 277°K. $H_2O$ and $D_2O$ liquids give indistinguishable values. Whilst acetone and pyridine show an essentially smooth variation of ($\Delta\epsilon/E^2$) over their complete concentration ranges in water, diozan and tetrahydrofuran show similar marked variations with a distinctive positive effect near the hemihydrate compositions. The influence of temperature on the sharp positive maxima with these two solutes is reported. t-Butyl alcohol, well known to give positive ($\Delta\epsilon/E^2$) values in the pure liquid, does so at all concentrations above mole fraction 0.25. In many cases it is clear that the Piekara factor shows far more detail than the $\epsilon_0$ against concentration plots as the measurements are sensitive to very small changes in permittivity due to the high fields. The observations are discussed with the aim of identifying the principal factors contributing to the newly observed effects. (auth)

**25558** DYNAMICS OF SOME HYDROGEN ISOTOPIC EXCHANGE REACTIONS AT HIGH ENERGIES. Malcolme-Lawes, D. J. (Cambridge Univ., Eng.). J. Chem. Soc. (London), Faraday Trans., II; 71: No. 6, 1183-1199(1975).

Classical trajectory studies have been performed using an empirical potential energy surface for the interactions H + $H_2$, D + $D_2$, T + $H_2$, T + $D_2$, H + $T_2$ and T + HD. Reaction and dissociation cross sections in each system are examined and a simple rule of thumb for estimating the low energy reaction efficiency is described. The integral reaction cross section ratios for the tritium atom reactions are found to be in good agreement with observed experimental isotope effects. The vibrational excitation of the product molecule and the centre of mass scattering distributions are also discussed. (auth)

**25559** ADDITION OF HOBr TO ALLENE. Secondary Deuterium Isotope Effects. Dolbier, W. R. Jr.; Al-Sader, B. H. (Univ. of Florida, Gainesville). Tetrahedron Lett.; No. 26, 2159-2162(Jun 1975).

Kinetic evidence is presented for the formation of a bromonium ion in the addition of HOBr to allene, evidence which also excludes the subsequent intervention of the 2-bromoallyl cation. (UK)

**25560** INFLUENCE OF THE DEUTERATION OF AROMATIC HYDROCARBONS ON THE RATE OF THE QUENCHING, BY OXYGEN, OF THEIR TRIPLET STATE IN SOLUTION. Ermolaev, V.L.; Tibilov, S.S. Opt. Spectrosc. (USSR) 38: No. 4, 470-471 (Apr 1975).

The rate of quenching of fluorescence of several aromatic hydrocarbons in solutions is reported. The changes in the quenching rate with deuteration of the aromatic hydrocarbon molecules are discussed. (AIP)

**25561** EFFECT OF HETEROVALENT IMPURITIES CODIFFUSING WITH MONOVALENT TRACERS IN IONIC CRYSTALS. Mitchell, J. L. Urbana, IL; University of Illinois (1974). 153p. University Microfilms Order No. 75-11,797.

Thesis (Ph. D.).

Tracer diffusion measurements were made for $^{45}Ca$ and $^{22}Na$ codiffusing into pure NaCl as a function of temperature, initial calcium concentration, and diffusion anneal time. The measured penetration profiles deviate markedly from the Gaussian dependence expected for diffusion from a thin source. The curvature is caused by each divalent Ca ion introducing an extra, "extrinsic," vacancy into the diffusion zone in order to maintain charge neutrality. In such cases, the limiting slope has been shown not to be a valid measure of the tracer diffusivity. Computer fits were generated by a model which corrects for the effect and is found to have excellent agreement with the data except for the most extreme cases. The model can find the initial concentration of the impurity and the diffusivity of the impurity within a factor of two from the penetration profile for the monovalent tracer. The effect enters to first order into the measurement of the isotope effect in ionic crystals and can result in major errors in the measured isotope effect for even small deviations from a Gaussian profile. The diffusion coefficients for $^{22}Na$ diffusing in NaCl over the temperature range of 575 to 775°C are given by D/sub Na/ equals 73 exp (–2.04 +- 0.02 eV/kT), and for $^{45}Ca$ D/sub Ca/ equals 0.23 exp (–1.61 +- 0.03 eV/kT). (Diss. Abstr. Int., B)

## *Isotope Exchange and Isotope Separation*

**25562** (AED-CONF-75-080-003) CHLORINE ISOTOPE EFFECTS IN INORGANIC EXCHANGE EQUILIBRIA. Heumann, K. G.; Hoffmann, R. 1975. 13p. (In German). INIS.

From meeting of lecturers in chemistry; Duesseldorf, F. R. Germany (7 Apr 1975).

8 figs.

Calculated equilibrium constants of exchange reactions with chlorine isotopes, the chloride isotope exchange in a heterogeneous system, the isotope ratio $^{35}Cl/^{37}Cl$ in the eluate fractions during the exchange of a strong basic anion exchanger, the calculated differences of the ionic radii of halogenide isotope pairs and the dependence of the isotope effect on the concentration of the elution solution on a basic anion exchanger are considered. (GE)

**25563** (ERDA-50, pp 113-119) SEPARATION OF HYDROGEN ISOTOPES FOR TRITIUM WASTE REMOVAL. Wilkes, W. R. (Mound Lab., Miamisburg, OH). Jun 1975.

From symposium on technology related for fusion reactor systems; Miamisburg, Ohio, USA (1 Oct 1974).

In proceedings of the symposium on tritium technology related to fusion reactor systems. (Energy Research and Development Administration, Washington, D. C. (USA). Div. of Controlled Thermonuclear Research).

A distillation cascade for separating hydrogen isotopes was simulated by means of a multicomponent, multistage computer code. A hypothetical test mixture containing equal atomic fractions of protium, deuterium and tritium, equilibrated to high temperature molecular concentrations was used as feed. The results show that a two-column cascade can be used to separate the protium from the tritium. Deuterium appears both in the protium and the tritium product streams. (auth)

**25564** SEPARATION OF SULFUR ISOTOPES WITH ENRICHMENT COEFFICIENT $>10^3$ THROUGH ACTION OF $CO_2$ LASER RADIATION ON $SF_6$ MOLECULES. Ambartsumyan, R.V.; Gorokhov, Yu.A.; Letokhov, V.S.; Makarov, G.N. (Spectroscopy Institute, USSR Academy of Sciences). JETP Lett. 21: No. 6, 171-172 (20 Mar 1975).

We report separation of sulfur isotopes by selective dissociation of $SF_6$ molecules in the strong field of a pulsed $CO_2$ laser. An enrichment coefficient 2800 was obtained in one cycle without cascading. (auth)

**25565** OPTICAL EXCITATION OF ISOTOPES THAT ARE SELECTIVE IN NUCLEAR SPIN. Zel'dovich, Ya.B.; Sobel'man, I.I.

(P. N. Lebedev Physics Institute, USSR Academy of Sciences). JETP Lett. 21: No. 6, 168-169 (20 Mar 1975).

We consider the possibility of atomic excitation that is selective in nuclear spin; this possibility is connected with lifting the hindrance to radiative transitions as a result of hyperfine interaction. (auth)

**25566** CHEMICAL-LASER-INDUCED ISOTOPICALLY SELECTIVE REACTION OF HCl. Arnoldi, D.; Kaufmann, K.; Wolfrum, J. (Max-Planck-Institut für Strömungsforschung, D 3400 Göttingen, Germany). Phys. Rev. Lett. 34: No. 26, 1597-1600 (30 June 1975).

A pulsed HCl chemical laser is used to excite HCl molecules vibrationally in the presence of Br atoms in a discharge-flow reactor. The rate of the reaction $Br+HCl(\nu) \rightarrow HBr+Cl$ increases by a factor of $10^{11}$ at room temperature if $HCl(\nu=0)$ is excited into $\nu=2$. Excitation occurs predominantly for $H^{35}Cl$. Cl atoms generated by the laser-stimulated reaction react with $Br_2$ to form BrCl, which is detected by time-resolved mass spectrometry and shows an enrichment of $^{35}Cl$ (90% $^{35}Cl$). (auth)

**25567** PROCEDURE AND DEVICE FOR THE SEPARATION OF GASEOUS OR VAPOROUS MATERIALS, PARTICULARLY ISOTOPES. Bley, P.; Ehrfeld, W.; Eisenbeiss, G. (to Gesellschaft fuer Kernforschung m.b.H., Karlsruhe (F. R. Germany)). German(FRG) Patent 2243730/S/. 4 Apr 1974. 10p. (In German).

The described procedure for the separation of gaseous and vaporous materials, particularly isotopes, with different molar weight and for different gas dynamic cross section, operates with nozzles which are passed by the gas or gas mixture as an expanding jet. The jet is separated into fractional jets by means of a skimmer blade edge which is placed in its flow route. A following deflection makes the separation of the fractional jet possible. Additional expansion renders post-acceleration possible. The partial jets which are lead away outwards are combined in a cascade if their material composition is equivalent. The skimmer blade edge itself is constructed as a deflection wall with respect to the surface which is turned towards the fractional jet. The particular advantages of the process and the separation nozzle device are the enhanced separation factor together with the reduced operational costs. (GE)

**25568** KINETICS OF THE EXCHANGE OF OXYGEN BETWEEN CARBON DIOXIDE AND CARBONATE IN AQUEOUS SOLUTION. Tu, C. K.; Silverman, D. N. (Univ. of Florida, Gainesville). J. Phys. Chem.; 79: No. 16, 1647-1651(31 Jul 1975).

A kinetic analysis of the exchange of oxygen between carbon dioxide and carbonate ion in alkaline, aqueous solutions is presented. The exchange was observed by placing $^{18}O$-labeled carbonate, not enriched in $^{13}C$, into solution with $^{13}C$-enriched carbonate, not enriched in $^{18}O$. The rate of depletion of $^{18}O$ from the $^{12}C$-containing species and the rate of appearance of $^{18}O$ in the $^{13}C$-containing species was measured by mass spectrometry. From these data, the second-order rate constant for the reaction between carbon dioxide and carbonate which results in the exchange of oxygen at 25° is $114 \pm 11\ M^{-1}\ sec^{-1}$. It is emphasized that this exchange of oxygen between species of $CO_2$ in solution must be recognized in studies using $^{18}O$ labels to determine the fate of $CO_2$ in biochemical and physiological processes. (auth)

**25569** SEPARATION OF URANIUM ISOTOPES BY URANIUM (IV)–URANIUM (VI) CHEMICAL EXCHANGE. Florence, T. M.; Batley, G. E.; Ekstrom, A.; Fardy, J. J.; Farrar, Y. J. (Australian Atomic Energy Commission Research Establishment, Lucas Heights). J. Inorg. Nucl. Chem.; 37: No. 9, 1961-1966 (Sep 1975).

The $^{235,238}U$ single stage isotopic separation factor ($\alpha$) was determined for the uranium (IV)–uranium (VI) exchange reaction in sulfuric acid, and found to be $\alpha = 1.0013 \pm 0.0004(1\sigma)$. The kinetics of the $H^+/UO_2^{2+}$ ion exchange reaction, and the $UO_2^{2+}/UO_2^{2+}$ and $U(IV)/UO_2^{2+}$ chemical exchange reactions on Dowex AG 50W cation exchange resin were studied in $H_2SO_4$ media. The possibility of developing a large scale process for uranium enrichment based on a U(IV)/U(VI) chemical exchange reaction was considered, and it was concluded that such a process would not be economical compared with established methods. (auth)

### *Feed Materials Processing*

*Refer also to abstract 26093.*

## Radiation Chemistry

*Refer also to abstracts 25618, 26004, 26021, 26297, 26299, 26304, 26310, and 26311.*

**25570** (AED-CONF-75-061-002) METHODS FOR REDUCING THE INFECTION HAZARD OF WASTEWATER SLUDGES. Farrell, J. B.; Stern, G. (National Environmental Research Center, Cincinnati, Ohio (USA). 1975. 12p. (SM–194/102). INIS.

From international symposium on the use of high-level radiation in waste treatment: status and prospects; Muenchen, F. R. Germany (17 Mar 1975).

In the United States, strong efforts are made to upgrade the quality of wastewater treatment. A schematic representation of a wastewater treatment plant with primary and secondary treatment is shown. The method chosen for disposal of sludge has a strong influence on the processing steps that sludge must undergo. The methods used for obtaining high pathogen reduction are demonstrated. The advantages and disadvantages of radiation treatment of sludge are enumerated. Radiation treatment seems to be one of the most effective procedures and to be rapidly approaching the cost-effective level. (GE)

**25571** (AED-CONF-75-061-010) SYNERGISTIC EFFECTS OF IRRADIATION OF WASTE WATER. Woodbridge, D. D.; Cooper, P. C.; Vandenburg, A. J.; Musselman, H. D.; Lowe, H. N. (Office of the Chief of Engineers, Washington, D. C. (USA)). 1975. 31p. (SM–194/304). INIS.

From international symposium on the use of high-level radiation in waste treatment: status and prospects; Muenchen, F. R. Germany (17 Mar 1975).

Theoretical considerations of the use of high-level radiation in the treatment of waste water have failed to consider the effects of the hydrated electron and the potential of possible synergistic effects of combining chlorine, oxygen, and irradiation. An extensive testing program at the University Center for Pollution Research of Florida Institute of Technology showed that irradiation of waste water samples immersed in an aqueous environment provide bacterial kill and reduction in organic pollution far greater than that obtained from theoretical considerations of G values and earlier experiments where the waste samples were not immersed in an aqueous environment. Tests on Staphylococcus aureus bacteria and fecal streptococcus bacteria indicate that the synergistic effects of oxygen observed for fecal coliform bacteria also apply to the pathogenic bacteria. A definite shielding factor due to the turbidity of the waste water was shown to exist. Synergistic effects were shown to significantly offset the shielding effects. Optimization of these synergistic effects can greatly increase the effectiveness of irradiation in the treatment of waste water. (auth)

**25572** (AED-CONF-75-061-013) AQUEOUS RADIATION CHEMISTRY IN RELATION TO WASTE TREATMENT. An Introductory Review. Hoigne, J. (Eidgenoessische Anstalt fuer Wasserversorgung, Abwasserreinigung und Gewaesserschutz, Duebendorf (Switzerland)). 1975. 18p. (SM–194/401). INIS.

From international symposium on the use of high-level radiation in waste treatment: status on prospects; Muenchen, F. R. Germany (17 Mar 1975).

1 fig.; 2 tabs.; 23 refs. With abstract. Available from ZAED.

The initiation of chemical reactions by irradiation, the yields and the reactions of the primary chemical species and competitions between solutes for these species, the role of secondary reactions and the role of oxygen for secondary reactions, the radiation-initiated oxidation of organic compounds, possibilities for chain reactions, and the competition between solutes and dispersed particles for reactive intermediates are reviewed. (GE)

**25573** (AED-CONF-75-061-014) RADIATION CHEMICAL DESTRUCTION OF PHENOL IN OXYGENATED AQUEOUS SOLUTIONS. Micic, O. I.; Nenadovic, M.T.; Markovic, V. M. (Institut za Nuklearne Nauke Boris Kidric, Belgrade (Yugoslavia)). 1975. 8p. (SM–194/402). INIS.

From international symposium on the use of high-level radiation in waste treatment: status and prospects; Muenchen, F. R. Germany (17 Mar 1975).

1 fig.; 1 tab.; 20 refs. With abstract. Available from ZAED.

The mechanisms of phenol degradation in irradiated aqueous solutions were studied. Irradiations were carried out using a $^{60}Co$ gamma source. The techniques of pulse radiolysis (Febetron 707) and kinetic absorption spectrophotometry were used for identification of transient species. For the dose rate 1.6 krad x $min^{-1}$ the phenol degradation yield, G(-phenol), remains constant in the range of phenol concentrations $5 \times 10^{-3}$ and $5 \times 10^{-5}$ M. Below 1.6 krad x $min^{-1}$, G(-phenol) depends on the dose rate, phenol concentration and the presence of oxygen in solution. Pulse radiolysis studies show that phenol peroxy radicals formed in irradiated solution are very unstable and decay rapidly by the first order reaction. It is the $O_2^-$ radical which reacts with phenol as a first step in the autodegradation chain. Special attention was paid to the determination of conditions under which G(-phenol) is constant and high. A comprehensive mechanism

is presented together with the absolute rate constants for the various radical reactions involved. (GE)

**25574** (AED-CONF-75-061-015) REMOVAL OF SOME CHEMICAL IMPURITIES FROM WASTE WATERS USING ELECTRON BEAM IRRADIATION. Fiti, M. (Institutul de Fizica Atomica, Bucharest (Romania)). 1975. 13p. (SM-194/403). INIS.

From international symposium on the use of high-level radiation in waste treatment: status and prospects; Muenchen, F. R. Germany (17 Mar 1975).

5 figs.; 2 tabs.; 21 refs. With abstract. Available from ZAED.

The radiolytic behavior of chromates and phenol in aqueous solution was studied in connection with their possible removal from waste waters. By radiolysis of their aqueous solutions the chromates (Cr sup(VI)) are reduced to Cr sup(III). The reduction yield is near 10 equiv/100 eV when in the solution a typical OH radicals scavenger is present. Using formic acid as OH scavenger in appropriate conditions of composition and irradiation, the Cr sup(VI) is reduced to Cr sup(III), which settles as $Cr(OH)_3$ during irradiation. The radiolytic oxidation of phenol in acid aqueous solution without aeration gives a polymeric material P sub(A), which separates from water at pH < 3. The P sub(A) product is formed with a yield corresponding to the G (-phenol) = 1-2 molec/100 eV. (GE)

**25575** (AED-CONF-75-061-016) EFFECTS OF GAMMA RADIATION FROM COBALT-60 ON DILUTE AQUEOUS SOLUTIONS OF LINEAR ALKYL SULFONATE SURFACTANTS AND OTHER ORGANIC POLLUTANTS. Rohrer, D. M. 1975. 13p. (SM-194/404). INIS.

From international symposium on the use of high-level radiation in waste treatment - Status and prospects; Muenchen, F. R. Germany (17 Mar 1975).

3 figs.; 17 refs. With abstract. Available from ZAED.

Operational experiences with the use of cobalt-60 for the treatment of waste water are reported. The purpose is to discuss the effects of cobalt-60 $\gamma$ radiation with regard to radiochemical destruction of specific organic pollutant species, specifically with the effects of gamma radiation from a 30,000 curie cobalt-60 source on aqueous solutions of linear alkyl sulfonate surfactants. Consideration is also given to similar effects of gamma radiation on pesticides and to the practical aspects of the use of gamma radiation for the treatment of waste water. (GE)

**25576** (AED-CONF-75-061-018) EFFECTS OF GAMMA RADIATION IN THE DEGRADATION OF DYES. Piccinini, N.; Ferrero, F. 1975. 18p. (SM-194/407). INIS.

From international symposium on the use of high-level radiation in waste treatment: status and prospects; Muenchen, F. R. Germany (17 Mar 1975).

4 figs.; 6 tabs.; 24 refs. With abstract. Available from ZAED.

To investigate the degradation kinetics of aqueous solutions of dyes of several classes, the effects of gamma radiation versus the dose (up to 80 krad), the dye concentration, the pH, and the oxygen content of these solutions were studied. For better outlining the influence of some of the above mentioned parameters, anthraquinonic dyes were irradiated in a wide range of doses (up to 5 Mrad). Experimental results agree with a first order kinetics for dye concentrations lower than 0.04 g/l, and with a zero order one for higher concentrations. The pH has a different influence according to the type of dye. Radiochemical degradation yields (Gsub(d)), never greater than a few units, show that the radical reactions, responsible for the decolorization effect, are limited to few transfer sequences. (GE)

**25577** (AED-CONF-75-061-019) POSSIBILITY OF THE USE OF HIGH-LEVEL RADIATION FOR THE DEGRADATION OF SOME SUBSTANCES PRESENT IN URBAN AND INDUSTRIAL WATERS. Cappadona, C.; Guarino, P.; Petruso, S.; Ardica, S. (Palermo Univ. (Italy). Istituto di Applicazioni e Impianti Nucleari). 1975. 25p. (SM-194/408). INIS.

From international symposium on the use of high-level radiation in waste treatment: status and prospects; Muenchen, F. R. Germany (17 Mar 1975).

2 figs.; 8 tabs.; 11 refs. With abstract. Available from ZAED.

Tests on representative solutions or suspensions of organic solvents, dyes, pesticides, and chlorophenols, were performed to investigate their behaviour by treatment with gamma radiation under static and aerated dynamic system. In most cases a notable degradation of these substances related to the pH to the oxigenation and composition of the medium and to the mixture of commercial products. (auth)

**25578** (AED-CONF-75-061-020) DEGRADATION OF PERSISTENT ORGANOCHLORINE POLLUTANTS BY GAMMA-RADIATION AND THE POSSIBLE USE FOR WASTE WATER TREATMENT. Vollner, L.; Rohleder, H.; Korte, F. 1975. 16p. (SM-194/409). INIS.

From international symposium on the use of high-level radiation in waste treatment: status and prospects; Muenchen, F. R. Germany (17 Mar 1975).

6 figs.; 2 tabs.; 12 refs. With abstract. Available from ZAED.

Some organochlorine pesticides, polychlorinated biphenyls, and related chemicals have become ubiquitous pollutants by their persistence and are common contaminants in waste waters. Since gamma-radiation represents a possible treatment for decontamination, radiation yield and degradation chemistry were investigated. The pattern of hexane extractable compounds obtained from acetone-water and from pure water solutions are not very different when compared by gas chromatographic analysis. Dechlorination and dehydrochlorination were found to be the most important mechanisms of the first attack. The complete destruction of chlorine pesticides and of other chlorinated hydrocarbons (as PCBs) at the ppM-level demand considerable radiation doses. G-values for dieldrin and its hexane extractable degradation products are $1 \times 10^{-3}$ in deionized water and $3.6 \times 10^{-3}$ in twice-distilled water. G-values for aldrin, lindane, chlordane and PCBs are in the same order of magnitude. (GE)

**25579** (AED-CONF-75-061-038) EXPERIENCE WITH A PILOT PLANT FOR SEWAGE SLUDGE: EXPERIMENTS ON THE INACTIVATION OF VIRUSES IN SEWAGE SLUDGE AFTER A RADIATION TREATMENT. Epp, C. 1975. 8p. (SM-194/607). INIS.

From international symposium on the use of high-level radiation in waste treatment: status and prospects; Muenchen, F. R. Germany (17 Mar 1975).

An experiment was devised in which defined virus quantities were packed into capsules and mixed with the digested sludge. At the end of the $\gamma$-induced hygienization process the capsules were removed from the sludge and examined for virus content. One volume (5.6 $m^3$) was infected with attenuated polio virus type I and the virus content was determined before and after the radiation treatment. In 33 sludge samples examined before hygienization, the presence of one or several viruses occurred in eight samples. With the 33 capsules examined after hygienization with 300 krad, only two showed presence of virus. Suspensions of attenuated polio virus type I packed into synthetic capsules with a medium virus dose of 10sup(6.92) JD 50/0.1 were immersed into sludge. In six experiments it was found that after hygienization, virus doses were reduced to an average value of 10sup(5.4) JD 50/0.1 ml. Radiation treatment reduced the exposed virus by more than 90%. Under natural conditions the investigation of the sewage sludge samples showed presence of virus four times less after hygienization than in the samples examined before hygienization. (auth)

**25580** (AED-CONF-75-061-041) EXPERIENCE WITH A PILOT PLANT FOR THE IRRADIATION OF SEWAGE SLUDGE. Analytical Studies on Sewage Sludge and Plant Material. Rosopulo, A.; Fiedler, I.; Staerk, H.; Suess, A. (Bayerische Landesanstalt fuer Bodenkultur, Pflanzenbau und Pflanzenschutz, Muenchen (F. R. Germany)). 1975. 9p. (SM-194/610). INIS.

From international symposium on the use of high-level radiation in waste treatment: status and prospects; Muenchen, F. R. Germany (17 Mar 1975).

9 tabs. With abstract. Available from ZAED.

Analyses of mineral nutrients and trace elements in sewage sludge over a one year period showed that there are relatively small differences in the content of inorganic constituents. A change was found in the ratio of $NH_4$-N to total N after a heat treatment; this means that the ammonium content increased in 70% of the analyzed samples compared to untreated sludge. After radiation treatment of sewage sludge no change can be observed up to a pH of 8. With an increase of the pH value ($\geq 8$) losses of $NH_4N$ can be observed. During the dewatering process of sewage sludge (which is influenced by sewage sludge treatment), potassium, sodium and ammonium are enriched in the filtering water. While there is a decrease of these alkali elements in the dewatered sewage sludge, almost no change in the other components can be observed. (auth)

**25581** (AED-CONF-75-061-045) RADIATION FIXATION OF VINYL CHLORIDE IN THE INSECTICIDE AEROSOL CONTAINER. Kagiya, V. T.; Takemoto, K. (Kyoto Univ. (Japan). Faculty of Engineering). 1975. 10p. (SM-194/705). INIS.

From international symposium on the use of high-level radiation in waste treatment: status and prospects; Muenchen, F. R. Germany (17 Mar 1975).

1 fig.; 5 tabs. With abstract. Available from ZAED.

Radiation fixation of vinyl chloride as poly(vinylchloride) powder by $\gamma$-induced polymerization in the aerosol container

is reported. An insecticide aerosol container containing vinyl chloride was irradiated at room temperature with γ rays from a cobalt-60 source. Vinyl chloride polymerized to a powdery polymer in the container. The polymerization conversion increased with the radiation dose, and after 10 Mrad irradiation, the sprayed gas did no longer contain vinyl chloride. This fact showed that vinyl chloride can be fixed by γ-irradiation in the aerosol container. In order to accelerate the reaction rate, the effect of various additives on the reaction was investigated. (GE)

**25582** (BMFT-FB-K-75-03) RADIATION CHEMICALLY INITIATED TELOMERIZATION OF FORMAMIDE AND ETHYLENE. Dederichs, B.; Saus, A.; Rath, H. P. (Bundesministerium fuer Forschung und Technologie, Bonn (F. R. Germany); Zentralstelle fuer Atomkernenergie-Dokumentation, Leopoldshafen (F. R. Germany)). Mar 1975. 40p. (In German). INIS.

11 figs.; 11 tabs.; 35 refs.

The radiation-initiated telomerization of formic acid amide and ethylene is possible by the use of pressure. The yield of prim. alkane carbonic acid amides is proportional to the absorbed dose. G-values are: G(amide) approximately 90, $G(-C_2H_4)$ approximately 260, with maximum yields at 60°C. The distribution of telomers corresponds to a geometrical progression. It is unaffected by the radiation dose. Within the range of 30 to 100 atm the reaction-pressure is of no influence upon the product yields, but there is linear connection between the consumption of ethylene and the molar ratio of ethylene solved in the reaction mixture. The small propagation constants (0.01 to 0.02) show that the relatively high amount of short-chain carbonic acid amides is due to the solubility of ethylene in formic acid amide (2 mol-% at 50 atm, 2.3 mol-% at 100 atm). Solvents generally lower the G-values, but the distribution of chain length is shifted to higher carbonic acid amides. With increasing dielectrical constants of the solvents with active hydrogen lead to uncontrolled side reactions. (auth)

**25583** (CALT-767P4-138) STUDIES IN CHEMICAL DYNAMICS AND RADIATION CHEMISTRY. Technical Progress Report, 1 July 1974--30 June 1975. Kuppermann, A. (California Inst. of Tech. Pasadena (USA)). 31 Jul 1975. Contract AT(04-3)-767. 179p. Dep. NTIS $12.00.

Research progress in the following areas is reported: low energy electron scattering; photoelectron spectrometry; elementary reactions by photolysis at variable wavelengths; collisions in crossed molecular beams; and, diffusion kinetics in the radiation chemistry of water. Publications related to the work are included. (JGB)

**25584** RATE CONSTANTS FOR THE REACTION OF OH RADICALS WITH A SERIES OF AROMATIC HYDROCARBONS. Hansen, D. A.; Atkinson, R.; Pitts, J. N. Jr. (Univ. of California, Riverside). J. Phys. Chem.; 79: No. 17, 1763-1766(14 Aug 1975).

Absolute rate constants for the reaction of OH radicals with a series of aromatic hydrocarbons have been determined at room temperature using a flash photolysis-resonance fluorescence technique. The rate constants ($k_1 \times 10^{12}$ $cm^3$ $molecule^{-1}$ $sec^{-1}$) obtained are as follows: benzene, 1.24 ± 0.12; toluene, 5.78 ± 0.58; o-xylene, 15.3 ± 1.5; m-xylene, 23.6 ± 2.4; p-xylene, 12.2 ± 1.2; 1,2,3-trimethylbenzene, 26.4 ± 2.6; 1,2,3-trimethylbenzen, 33.5 ± 3.4; 1,3,5-trimethylbenzene, 47.2 ± 4.8. These absolute rate constants are in good agreement with those determined recently for benzene and toluene and with those derived for a series of aromatic hydrocarbons from a relative rate study in an environmental chamber. (auth)

**25585** POLAROGRAPHIC AND OPTICAL PULSE RADIOLYSIS STUDY OF THE RADICALS FORMED BY OH ATTACK ON IMIDAZOLE AND RELATED COMPOUNDS IN AQUEOUS SOLUTIONS. Bansal, K. M.; Sellers, R. M. (Hahn-Meitner-Institut fuer Kernforschung, Berlin). J. Phys. Chem.; 79: No. 17, 1775-1780(14 Aug 1975).

Polarographic and optical pulse radiolysis studies of the radicals formed by OH attack on imidazole, 1-methylimidazole, 2-methylimidazole, and histidine have been performed. The absorption spectra of the radicals are characterized by peaks as 300 ± 15 and 390 ± 10 nm. The pK/sub a/ values of the radicals, measured from the pH dependence of the spectra, are ca. 1-2 units below those of the corresponding parent compound. At high pH's (greater than 11) a first-order, pH-dependent decay was observed with imidazole, 2-methylimidazole, and histidine, and is attributed to a water elimination reaction. The principal features of the polarograms are (i) a flat cathodic wave at potentials more negative than 0 V for the protonated radicals and (ii) for the unprotonated radicals a steep anodic wave extending up to ca. -0.5 V followed by a flatter cathodic wave. The polarographic data at high pH's (greater than 11) are consistent with the rearrangement reaction observed in the optical experiments. (auth)

**25586** ELECTRON SPIN RESONANCE SPECTRA OF CERTAIN FLUOROHYDRIDE RADICALS OF PHOSPHORUS, ARSENIC, AND ANTIMONY. Colussi, A. J.; Morton, J. R.; Preston, K. F. (National Research Council of Canada, Ottawa). J. Phys. Chem.; 79: No. 17, 1855-1858(14 Aug 1975).

Isotropic ESR spectra of a series of phosphorus fluorohydride radicals PH/sub n/F/sub 4 - n/, where n equals 0-4, have been observed in gamma-irradiated solid solutions of $PF_3$, $PF_2H$, and $PH_3$ in neopentane or $SF_6$. The spectra of $AsH_3F$ and $SbH_3F$ are also reported. The hyperfine interactions of these radicals are consistent with a totally symmetric semioccupied orbital in a framework possessing either C/sub 2v/ or C/sub s/ symmetry. The relative merits of Huckel and INDO molecular orbital calculations in predicting the various observed trends are discussed. (auth)

**25587** ELECTRON SPIN RESONANCE STUDY ON THE STRUCTURE OF RADICAL PAIRS IN IRRADIATED ORIENTED POLYETHYLENE. Fujimura, T.; Tamura, N. (Japan Atomic Energy Research Inst., Takasaki). J. Phys. Chem.; 79: No. 17, 1859-1863(14 Aug 1975).

A well-resolved DELTA M/sub s/ equals 1 ESR spectrum due to radical pairs was observed in oriented polyethylene irradiated at 77°K; this spectrum is ascribed to the pair of alkyl radicals. The change of the fine splitting with the angle between the magnetic field and the draw direction reveals that the radical pairs produced are intrachain type rather than interchain type. When the magnetic field is parallel to the chain axis, the maximum fine splitting, 371 G, is obtained. This splitting is due to interactions between members of the radical pair; interspin distance is calculated to be 5.31 A. The concentration of the paired radicals giving the observed DELTA M/sub s/ equals 1 spectrum is about 0.3 percent of that of the total radicals. On warming the sample above 77°K, the intensity of the DELTA M/sub s/ equals 1 spectrum due to the radical pair decreasing faster than that of the DELTA M/sub s/ equals 2 spectrum. Some evidence was also found for the existence of other types of radical pairs in irradiated polyethylene. (auth)

**25588** CHEMICAL BEHAVIOR OF RHODIUM(II)--AMMINE COMPLEXES GENERATED BY THE PULSE RADIOLYTIC ONE-ELECTRON REDUCTION OF RHODIUM(III) AMMINES. Lilie, J. (Hahn-Meitner-Institut fuer Kernforschung, Berlin); Simic, M. G.; Endicott, J. F. Inorg. Chem.; 14: No. 9, 2129-2133(Sep 1975).

The pulse radiolytic reduction of $Rh(NH_3)_5Cl^{2+}$, $Rh(NH_3)_5OH_2^{2+}$, $Rh(NH_3)_4Br_2^+$ by the hydrated electron was examined. The first two ligands of the product rhodium(II) complex are eliminated very fast (less than 1 mu sec), and the first intermediate identified is a $Rh(NH_3)_4^{2+}$ species. This further exchanges ammonia for water with k equals $3.5 \times 10^2$ $sec^{-1}$ for the first $NH_3$ and with k equals 40 $sec^{-1}$ for the second $NH_3$. In addition, $Rh(NH_3)_4^{2+}$ appears to disproportionate with k equals $1.4 \times 10^7$ $M^{-1}$ $sec^{-1}$. It reacts with oxygen with k equals $3.1 \times 10^8$ $M^{-1}$ $sec^{-1}$ forming a dioxygen adduct, $O_2Rh(NH_3)_4OH_2^{2+}$, which is relatively stable and has an absorption maximum at 265 nm with an absorptivity of 9200 $M^{-1}$ $cm^{-1}$. The $Rh(NH_3)_4^{2+}$ reduction of $Rh(NH_3)_4Br_2^+$ results in a chain reaction that catalyzes the exchange of $Br^-$ for $H_2O$ in the rhodium(III) substrate. (auth)

**25589** HYDROGEN BONDING. VI. Structural and Infrared Spectral Analysis of Lithium Hydroxide Monohydrate and Cesium and Rubidium Hydroxide Hydrates. Gennick, I.; Harmon, K. M. (Oakland Univ., Rochester, MI). Inorg. Chem.; 14: No. 9, 2214-2219(Sep 1975).

The infrared spectrum of $LiOH.H_2O$ shows, in addition to the stretching and bending modes of OH and $H_2O$ groups, seven bands in the 1000 to 300-$cm^{-1}$ region. Four of these bands give characteristic shifts upon deuterium substitution and confirm the presence of coordinated water and hydroxide ion in $LiOH.H_2O$. On the basis of internal coordinate analysis of the coordinated water and hydroxide subunits of the crystal structure, the various rocking and torsional vibrations of oxygen–hydrogen atoms and the lithium–oxygen lattice vibrations were assigned. Unlike other alkali metal hydroxide hydrates the water and hydroxide ions in $LiOH.H_2O$ form discrete, planar, hydrogen-bonded $[(OH^-)_2(H_2O)_2]$ anionic units rather than extended chains. RbOH and CsOH also form stable mono- and hemihydrates, the infrared spectra of which contain the rocking and wagging modes of strongly hydrogen-bonded, coordinated water. (auth)

**25590** MICROWAVE SPECTRUM AND DIPOLE MOMENT OF METHYLDIFLUOROPHOSPHINE--BORANE. Creswell, R. A.; Elzaro, R. A.; Schwendeman, R. H. (Michigan State Univ., East Lansing). Inorg. Chem.; 14: No. 9, 2256-2259(Sep 1975).

The microwave spectra of $CH_3PF_2.^{11}BH_3$, $CH_3PF_2.^{10}BH_3$, $CH_3PF_2.^{11}BD_3$, and $CH_3PF_2.^{10}BD_3$ were assigned. Stark effect measurements gave the following values for the dipole moment and its components: mu/sub a/ equals 3.52 (5) D, mu/sub b/ equals 1.76

(5) D, mu/sub c/ equals 0.0 D, and mu equals 3.94 (5) D. The absence of resolvable internal rotation splittings in the ground state yields lower limits of about 2000 cal/mol for the barriers to both $CH_3$ and $BH_3$ group internal rotation. By judicious transfer of structural parameters from related molecules r(P–B) was estimated to be 1.84 +- 0.02 A. (auth)

**25591** ESR SPECTRUM AND STRUCTURE OF $BrF_6$. Nishikida, K.; Williams, F.; Mamantov, G.; Smyrl, N. (Department of Chemistry, University of Tennessee, Knoxville, Tennessee 37916). J. Chem. Phys. 63: No. 4, 1693-1694 (15 Aug 1975).

The $BrF_6$ radical has been obtained by $\gamma$ irradiation of a mixture of $BrF_5$ in $SF_6$. The ESR spectrum was obtained and used to confirm the identity of the radical and to obtain hyperfine coupling constants. (AIP)

**25592** PROTON RADIOLYSIS OF $CHCl_3$ AND $CHBr_3$ AT HIGH DILUTION IN ARGON DURING CONDENSATION AT 15°K. INFRARED SPECTRA OF THE $CHX^+_2$, $CHX^-_2$, AND $CHX^-_3$ MOLECULAR IONS. Ault, B.S.; Andrews, L. (Chemistry Department, University of Virginia, Charlottesville, Virginia 22901). J. Chem. Phys. 63: No. 4, 1411-1418 (15 Aug 1975).

Matrix samples of chloroform and its deuterium and bromine analogs have been subjected to irradiation by a 2.0 keV proton beam during deposition, and the products trapped in an argon matrix at 15°K. Several infrared absorptions have been observed and assigned to a number of new molecular species. Extremely photosensitive bands observed at 652, 621, 593, and 570 $cm^{-1}$ have been assigned to the $CHCl^-_3$, $CHCl_2Br^-$, $CHClBr^-_2$, and $CHBr^-_3$ molecular anions, respectively. Absorptions at 998, 907, and 839 $cm^{-1}$, which were decreased by operating an exposed bulb filament, have been attributed to the isolated cations $CHCl^+_2$, $CHClBr^+$, and $CHBr^+_2$. Bands stable to the bulb filament at 1044, 988, and 898 $cm^{-1}$ were assigned to the $CHX^+_2$ ($X^-$) species and similar bands at 838, 795, and 735 $cm^{-1}$ were assigned to the $CHX_2^-$ anions. In addition, bands attributable to the species $CX_3$, $CX_2CX_3^+(X^-)$, $CHX_2$, and $HX^-_2$, which have been identified previously, were observed here as well. (auth)

**25593** SPIN DENSITY DISTRIBUTIONS IN PRIMARY OXIDATION AND REDUCTION PRODUCTS OF IRRADIATED NUCLEIC ACID CONSTITUENTS. Adams, S.M.; Box, H.C. (Department of Biophysics, Roswell Park Memorial Institute, Buffalo, New York 14263). J. Chem. Phys. 63: No. 3, 1185-1189 (1 Aug 1975).

Molecular orbital calculations of spin density at the INDO level of approximation have been performed for the primary oxidation and reduction products of irradiated nucleic acid constituents and for some related molecules. For the pyrimidine anions INDO spin densities are in qualitative agreement with experimentally obtained spin densities. INDO spin densities for certain of the neutral oxidation products do not agree with experimental results. (auth)

**25594** ESR, ENDOR, AND DOUBLE ENDOR AT 300°K OF DL-SERINE X IRRADIATED AT 340°K, A NEW RADICAL SPECIES. Hampton, D.A.; Moulton, G.C. (Department of Physics, Florida State University, Tallahassee, Florida 32306). J. Chem. Phys. 63: No. 3, 1078-1082 (1 Aug 1975).

When DL-serine single crystals are x rayed at 300°K or below, two stable radicals are observed at room temperature. One of these, IV, is of greater intensity than the other, V, and was previously identified. By irradiating at a slightly elevated temperature, ~340°K, the concentration of V becomes more intense than IV. In this work we report on a detailed study of V using ESR, ENDOR, and double ENDOR, all at room temperature. We have determined that V is

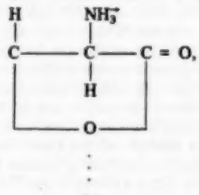

and have obtained five hyperfine tensors representing one $\alpha$-H, two $\beta$-H's, the rotating amino H's, and a fourth H which is probably in a neighboring molecule. We have also observed the ENDOR transition of the nitrogen. The $\alpha$-H tensor is somewhat unusual in that the isotropic term (−41.3 MHz) is considerably less than for a $2p\pi$ electron and of the same sign, but the anisotropic term is approximately the same (+31.9, +3.5, −35.4 MHz). This is consistent with our model since the bonding to the $\alpha$-carbon is strained and would not be expected to be pure $sp^2$. (auth)

**25595** SUBPICOSECOND RELAXATION OF LOCALIZED ELECTRONS IN LIQUID AMMONIA. Huppert, D.; Struve, W.S.; Rentzepis, P.M. (Bell Laboratories, Murray Hill, New Jersey 07974); Jortner, J. J. Chem. Phys. 63: No. 3, 1205-1210 (1 Aug 1975).

We report the results of an experimental study of the optical bleaching of the absorption spectrum of the solvated electron in dilute $Na–NH_3$ and $Na–ND_3(2\times10^{-4}\ M)$ solutions by a single 1.06 $\mu$ psec pulse (pulse duration 6 psec, pulse energy 30 mJ). The absorption spectrum of the solvated electron was monitored in the spectral range 1100–850 nm with the time resolution 20–3.3 psec. The line broadening of the solvated electron optical band originates from homogeneous broadening effects. The relaxation time of the excited state of the solvated electron was determined to be $\tau\simeq2\times10^{-13}$ sec. This ultrashort relaxation time favors relaxation between bound states of the solvated electron center. (auth)

**25596** DECAY MECHANISMS OF $CH_3$ IN 3-METHYLPENTANE AND 3MP-$d_{14}$ GLASSES AT 77°K AS INDICATED BY METHANE YIELDS. Neiss, M.A.; Sprague, E.D.; Willard, J.E. (Department of Chemistry, University of Wisconsin, Madison, Wisconsin 53706). J. Chem. Phys. 63: No. 3, 1118-1121 (1 Aug 1975).

The isotopic methane yields from $\gamma$ irradiation of 3-methylpentane, 3MP–1%$CH_3I$, 3MP-$d_{14}$–1%$CH_3I$, and 3MP-$d_{14}$–1%$CD_3I$ glasses confirm recent evidence from decay kinetics that thermal $CH_3$ radicals can abstract H from C–H bonds in hydrocarbon glasses at 77°K (plausibly by tunneling) and show that similar abstraction does not occur from C–D bonds. Also, in 3MP-$d_{14}$ the $CH_3$ (formed by the $CH_3I+e^- \rightarrow CH_3+I^-$ process) does not decay by radical combination processes ($CH_3+CH_3$ or $CH_3+C_6D_{13}$), implying that decay is by geminate recombination with the $I^-$ partner. In the $\gamma$ irradiation of 3MP-$d_{14}$–1%$CH_3I$ irradiated at 77°K, $G$ ($CH_3D$) from hot abstraction by $CH_3$ is 0.7; thermal $CH_3$ and $CD_3$ radicals are able to abstract H from low concentrations of C–H bond isotopic impurities; and the yields of scavengeable electrons and of radicals are substantially different than in 3MP-$h_{14}$. (auth)

**25597** YIELD OF SINGLET AND TRIPLET EXCITONS FROM X—RAY AND RUBY LASER EXCITATION OF ANTHRACENE SINGLE CRYSTALS. Hughes, R.C. (Sandia Laboratories, Albuquerque, New Mexico 87115); Soos, Z.G. J. Chem. Phys. 63: No. 3, 1122-1126 (1 Aug 1975).

A new method for determining the singlet:triplet yields for x-ray and ruby laser excited anthracene crystals is described. It was found that the ratio is higher than has been reported for x-ray excitation and lower than reported for ruby laser excitation. X-ray excitation produces roughly equal numbers of triplets and singlets. Ruby laser excitation indicates that the intersystem crossing rate from the first excited singlet is $1.5\pm0.5\times10^7$ $sec^{-1}$, which is larger than had been reported, but still smaller than for anthracene molecules in solution. The greater triplet yield produced by x irradiation is related to efficient spin–lattice relaxation in highly excited electronic states and neither spin–spin nor spin–lattice relaxation in the electron and hole ground states is important in the short time involved in geminate recombination. (auth)

**25598** ACTION OF $\gamma$-RADIATION ON COAL. Lebedev, V. V.; Cheredkova, K. I.; Golovina, G. S.; Krehkova, T. M.; Goroshko, V. D. (Inst. Goryuch. Iskop., Moscow). Khim. Tverd. Topl.; No. 1, 165-166(1975). (In Russian).

The molecular structure of the coal was greatly affected. The plot of relative electrical resistance dependence on radiation dose was minimum at 160 Mrd. Thermal destruction of the treated coal exhibited a tendency to a decrease in the yield of solid residue and to an increase in the yield of volatile products with increasing radiation doses. Yields of H and CO decreased, and that of $CH_4$ and $CO_2$ increased with increasing radiation doses of the preliminary treated coal. (LK)

**25599** SPECTRA OF ELECTRON PARAMAGNETIC RESONANCE OF NON-ORIENTED FREE RADICALS OF SULFUR-CONTAINING AMINO ACIDS. Dobryakov, S. N.; Krivenko, V. G.; Pulatova, M. K.; Sud'bina, E. N. (Inst. of Biological Physics, Pushchino, USSR). Biophysics (USSR) (Engl. Transl.); 18: No. 2, 230-235(Nov 1973).

Translated from Biofizika; 18: No. 2, 223-227(Nov 1973).

The authors have calculated the EPR spectra of randomly orientated sulfur-containing radicals of cystine and cysteine on the basis of the parameters of the EPR spectra of orientated paramagnetic centers observed in $\gamma$-irradiated monocrystals of cystine dihydrochloride and cysteine hydrochloride at temperatures of −196 and 20°C. The envelope of the EPR spectra was estimated with the M-20 computer for paramagnetic centers having three different values of the g factor ($g_{xx} \neq g_{yy} \neq g_{zz}$) and also for the particular case $g_{xx} = g_{yy} \neq g_{zz}$. Calculations of the EPR spectra were made for different values of the width of the line $\Delta H_k$. Comparison of the calculated and experimentally obtained EPR spectra established that in $\gamma$-irradiated sulfur-containing proteins at a temperature of −196°C the anion-radicals RSS-R form while at room temperature the radicals RS' or RSS' form. (auth)

**25600** ELECTRON NUCLEAR DOUBLE RESONANCE OF FREE RADICALS IN $\gamma$-IRRADIATED GLYCINE MONOCRYSTALS. Deigen, M. F.; Krivenko, V. G.; Pulatova, M. K.; Ruban, M. A.;

Teslenko, V. V.; Kayushin, L. P. (Inst. of Semiconductors, Kiev). Biophysics (USSR) (Engl. Transl.); 18: No. 2, 242-250(Nov 1973).

Translated from Biofizika; 18: No. 2, 235-242(Nov 1973).

The method of electron nuclear double resonance (ENDOR) has been used to investigate the ultrafine magnetic and quadrupole interaction of the unpaired electron of the $NH_3^+$ $\dot{C}HCOO^-$ radical with the nucleus of nitrogen at 77°K. The free radicals were obtained on γ-irradiation of the glycine monocrystal at 77°K and subsequent heating to 290°K. The angular relations of the lines of ENDOR of the nitrogen nucleus, the signs and the values of the constants of ultrafine magnetic and quadrupole interaction with this nucleus have been obtained. It is shown that the direction of the C−N chemical bond in the $NH_3^+$ $\dot{C}HCOO^-$ radical deviates from the direction of this bond in the undamaged molecule of glycine by 4°. (auth)

**25601** KINETIC STUDIES IN BILE ACID MICELLES. Chen, M.; Graetzel, M.; Thomas, J. K. (Univ. of Notre Dame, IN). J. Am. Chem. Soc.; 97: No. 8, 2052-2057(16 Apr 1975).

Kinetic processes in sodium taurocholate (NaTc) is studied by a pulse radiolysis investigation of the effect of micellization on the rate of reaction of e⁻/sub aq/ with the peptide group. Pyrene is solubilized in aqueous solutions of NaTC micelles and excited by a frequency doubled ruby laser pulse. The kinetics of the pyrene fluorescence decay are studied in the presence of nonionic and ionic quenchers. These data yield information about the permeability of the NaTC micelles with respect to various quenching solute molecules. While a neutral molecule such as oxygen readily penetrates into the micelle, the entry of iodide ions is inhibited by the negative micellar surface charge. Positively charged quenchers such as $Cu^{2+}$ and $Tl^+$ are strongly absorbed at the surface of NaTC micelles. The effect of additives on the permeability of NaTC micelles is also studied. The local viscosity in the interior of NaTC micelles is investigated by fluorescence depolarization measurement. The rotation of this probe within a NaTC micelle is strongly restricted and a microviscosity of 670 cP is derived. $Mg^{2+}$ ions, benzyl alcohol, and sodium lauryl sulfate (NaLS) decrease the microviscosity. NaLS exhibits the strongest effect. The 347.1 nm laser photolysis of pyrene also produces significant amounts of positive ions and hydrated electrons. While the photoionization cross section in NaTC and NaLS micelles is similar, the lifetime of pyrene cations is much shorter in the former than in the latter. In comicelles of NaLS and NaTC the lifetime of pyrene cations increases rapidly with increasing NaLS content of the micelle. The electrons which are photoejected from the pyrene in the interior of the micelle become hydrated in the surrounding aqueous phase. Hydrated electrons have a low reactivity toward monomer NaTC (kappa equals $10^9$ $M^{-1}$ $sec^{-1}$). The reactivity decreases further upon micellization. (auth)

**25602** REACTION OF OH WITH BENZOIC ACID. Isomer Distribution in the Radical Intermediates. Klein, G. W.; Bhatia, K.; Madhavan, V.; Schuler, R. H. (Carnegie-Mellon Univ., Pittsburgh). J. Phys. Chem.; 79: No. 17, 1767-1774(14 Aug 1975).

Products of the reaction of radiation-produced OH radicals with benzoic acid under conditions where the intermediate hydroxycyclohexadienyl radicals are quantitatively oxidized to hydroxybenzoic acids were examined by liquid chromatographic methods. In $N_2O$-saturated 1 mM benzoic acid solutions containing 0.5 mM ferricyanide as the radical oxidant the initial radiation chemical yields of o-, m-, and p-hydroxybenzoic acids are 1.7, 2.3, and 1.2, respectively. Decarboxylation contributes an additional phenol yield of 0.4 to give a total product yield of 5.6 which accounts for essentially all of the OH radicals produced in this system. Material balance considerations show that no major product is unaccounted for. The initially produced hydroxybenzoic acids are, however, not consumed to any important extent in the secondary processes so that the resultant phenoxyl radicals must, in this mixed-radical system, be reduced back to the original products rather than being oxidized further. A detailed model is described, which allows numerical integration methods to be used to take the competitive effects of the secondary processes into account and to describe the course of the reaction quite well up to conversions of approximately 25 percent. (auth)

**25603** ENHANCEMENT OF WATER RETENTION BY CROSS-LINKED CARBOXYMETHYLCELLULOSE THROUGH POLYSTYRENE GRAFTING OF GAMMA IRRADIATION. Bhattacharjee, S. S.; Perlin, A. S. (McGill Univ., Montreal). J. Polym. Sci., Polym. Lett. Ed.; 13: No. 2, 113-116(Feb 1975).

The absorbency and retention characteristics of crosslinked carboxymethylcellulose (CLCMC) with respect to water and saline can be substantially improved by two different treatments. One treatment involves gamma-radioinduced grafting of polystyrene onto fibers of CLCMC. At a critical level of grafting (approximately 25 percent) the retentive capacity of the fibers is almost doubled. Particularly noteworthy is the sharp increase that follows an initial drop in retentivity. It is concluded the polystyrene becomes associated preferentially with residual ordered regions of the CLCMC macromolecule, through the localization of free radicals in these regions. A second means for enhancing the water and saline retention value of CLCMC, consists of subjecting the material to gamma irradiation from a $^{60}Co$ source. Dosages used have ranged from 1.0 to 4.8 megarads (MR), depending on the degree of substitution of the initial carboxymethylcellulose. (JGB)

**25604** RADIOLYTIC OXIDATION OF IRON(II) IN A NEUTRAL AQUEOUS SOLUTION. Stuglik, Z.; Zagorski, Z. P. (Inst. of Nuclear Research, Warsaw). Radiochem. Radioanal. Lett.; 22: No. 4, 257-262(25 Aug 1975).

Radiolytic oxidation of Fe(II) in oxygen free neutral solution (starting pH 7.5) proceeds with a G value of 1−2 depending on the Fe(II) concentration or with 6.3 for $10^{-4}$−$10^{-1}$ M Fe(II) if $N_2O$ is present. Pulse radiolysis studies revealed the presence of a species during and after the pulse with $\epsilon = 2400 \pm 10\%$ and $\lambda_{max}$ of 300 nm, most probably identified as $FeOH^{2+}$. It slowly polymerizes into Fe(III) precipitate. (auth)

**25605** POST-DECRYSTALLIZATION RATES OF GRAFTED FIBERS AND THEIR EFFECT ON FIBER ELASTICITY. Piarik, M. (Slovak Technical Univ., Bratislava). Radiochem. Radioanal. Lett.; 22: No. 4, 263-268(25 Aug 1975).

Kinetics and details of the decrystallization process were examined in the zinc chloride solutions of 360% ethyl acrylate grafted rayon. (auth)

**25606** LUMINESCENCE OF γ-IRRADIATED SOLUTIONS OF SOME LUMINOPHORS IN PMMA. Adamska, J. (Technical Univ., Danzig); Gebicki, J.; Grodel, M.; Polacki, Z. Radiochem. Radioanal. Lett.; 22: No. 4, 251-256(25 Aug 1975).

The influence of γ-radiation on the luminescence spectra of anthracene, dichloroanthracene and POPOP in polymethyl methacrylate (PMMA) has been investigated. It has been found that $^{60}Co$ γ-irradiation at doses of 0.1 to 500 Mrad decreases quantum efficiency of scintillators and changes the energy distribution in the luminescence spectrum. The latter change can be used as the extent of radiation damages equally well as the change of the quantum efficiency. (auth)

**25607** ABSORPTION SPECTRUM, YIELD, AND DECAY KINETICS OF THE SOLVATED ELECTRON IN PULSE RADIOLYSIS OF LIQUID AMMONIA AT VARIOUS TEMPERATURES. Farhataziz; Perkey, L. M. (Univ. of Notre Dame, IN). J. Phys. Chem.; 79: No. 16, 1651-1664(31 Jul 1975).

The transient absorption spectrum of e/sub am/⁻ induced in neat liquid ammonia by nanosecond pulse radiolysis shifts to higher energies as temperature decreases. The transition energy at the absorption maximum increases from 0.67 to 0.88 eV as temperature decreases from 23 to −75°. The portion of bandwidth at half-maximum measured from the absorption maximum to the high-energy side of the spectrum is constant over the temperature range from 23 to −75°. For the same temperature range, the primary yield of e/sub am/⁻ is constant with a value and average deviation of 3.1 ± 0.3. The mechanism of decay of e/sub am/⁻ in pulse radiolysis of neat liquid ammonia is complex. (auth)

**25608** FORMATION AND DECAY OF THE BIPHENYL CATION RADICAL IN AQUEOUS ACIDIC SOLUTION. Sehested, K. (Danish Atomic Energy Commission, Roskilde); Hart, E. J. J. Phys. Chem.; 79: No. 16, 1639-1642(31 Jul 1975).

The biphenyl cation radical forms from the OH adduct of biphenyl in aqueous acidic medium. Its spectrum is similar to the established spectra of the biphenyl cation radical obtained in organic solvents and glasses. The OH adduct was shown to be the precursor by eliminating effects due to H atoms and by the use of OH radical scavengers. It forms from the OH adduct with a rate constant of $2 \times 10^4$ $M^{-1}$ $sec^{-1}$ and it decays with a first-order rate constant of $5.0 \times 10^3$ $sec^{-1}$. The hydrated electron forms the anion radical with a rate constant k equals $1.2 \times 10^{10}$ $M^{-1}$ $sec^{-1}$ by reaction with biphenyl. The OH and H radicals react with the biphenyl with rate constants of $9.0 \times 10^9$ and $5.0 \times 10^9$ $M^{-1}$ $sec^{-1}$, respectively. The mechanism of cation-radical formation is briefly discussed. (auth)

**25609** GAMMA-RAY AND ELECTRON PULSE RADIOLYSIS STUDIES OF AQUEOUS PEROXODISULFATE AND PEROXODIPHOSPHATE IONS. Levey, G.; Hart, E. J. (Argonne National Lab., IL). J. Phys. Chem.; 79: No. 16, 1642-1646(31 Jul 1975).

Pulse radiolysis and gamma radiolysis studies of solutions containing peroxodiphosphate anions were made. Rate constants for the reaction of the hydrated electron with $H_2P_2O_8^{2-}$, $HP_2O_8^{3-}$, and $P_2O_8^{4-}$ are $5.3 \pm 0.7 \times 10^9$, $1.6 \pm 0.2 \times 10^9$, and $1.8 \pm 0.3 \times 10^9$ $M^{-1}$ $sec^{-1}$, respectively. Spectra of transients were observed that are similar to those produced by pulse radiolysis of phosphate + $N_2O$ systems or by uv photolysis of phosphate systems.

Therefore it appears that the reaction of peroxodiphosphates with hydrated electrons results in –O–O– bond cleavage to yield a radical anion and an anion. G values for loss of peroxodiphosphate range from 1.5 to 5.9 as the pH is decreased from 10 to 4. The decomposition of 2 mM peroxodisulfate by gamma-rays yields $G(-S_2O_8^{2-})$ of about 2.5. The mechanism of the gamma-ray radiolysis of aqueous solutions of 2-propanol containing peroxodisulfate or peroxodiphosphate anions is similar to that of the uv photolysis of these anions. The peroxodisulfate plus 2-propanol system yields long-chain reactions which are very sensitive to the presence of dissolved oxygen. The peroxodiphosphate plus 2-propanol system yields chain reactions only at low pH. (auth)

**25610** DYNAMICS OF THE IRRADIATION DEFECT CENTERS IN POTASSIUM DIHYDROGEN PHOSPHATE OBSERVED BY EPR. Voelkel, G.; Windsch, W.; Urbanowitschius, W. (Karl-Marx-Universitaet, Leipzig). J. Magn. Resonance; 18: No. 1, 57-63 (Apr 1975).

X-irradiation of potassium dihydrogen phosphate forms paramagnetic defect centers with the structure $OPO_3H^-$. In the ferroelectric phase the principal axes of the radicals are dependent on the direction of the electric polarization of the crystal. In the paraelectric phase a dynamical exchange between the two polarization-dependent radical sites takes place that is connected with the proton tunneling in the hydrogen bonds. The lines collapse at $T = T_c + 17.5$ K. (UK)

**25611** STUDIES OF INTRINSIC LUMINESCENCE IN KCl. Purdy, A. E.; Murray, R. B. (Univ. of Delaware, Newark). Solid State Commun.; 16: No. 12, 1293-1296(15 Jun 1975).

Measurements have been made of the luminescence intensity, lifetime, emission spectra, and thermoluminescence associated with self-trapped exciton states in KCl, at temperatures of 7°K and above. These results indicate the presence of another exciton-like state in addition to the well-known state that decays by emission at 2.32 eV. Thermoluminescence glow peaks and spectra are correlated with $F + V_k$ and F + H recombination processes. (auth)

**25612** UNSTABLE INTERMEDIATES. CLIII. Electron Spin Resonance Spectra and Structure of Dichlorophosphoranyl Radicals. Nelson, D. J.; Symons, M. C. R. (Univ. of Leicester, Eng.). J. Chem. Soc. (London), Dalton Trans.; No. 12, 1164-1167(1975).

A range of dichlorophosphoranyl radicals $[(RO)P(O)Cl_2]^-$ have been prepared by exposure of the neutral molecules $(RO)P(O)Cl_2$, to $^{60}Co$ γ-rays at 77°K [R = Me, Et, Ph, $C_{10}H_7$ (-naphthyl), $MeOCH_2CH_2$, or $ClCH_2CH_2$]. Well resolved e.s.r. spectra obtained from $[(MeO)POCl_2]^-$ and $[(EtO)POCl_2]^-$ have enabled the components of the $^{31}P$ and $^{35,37}Cl$ hyperfine-coupling tensors to be derived. The results show that both tensors are nearly axial, but their principal axes are at right angles to each other. The two chlorine ligands must be nearly coaxial with the phosphorus atom and they share ca. 50% of the total spin density, the remainder being confined to 3s and 3p orbitals on phosphorus. (auth)

**25613** TUNNELLING RESONANCE IN ELECTRON SPIN-LATTICE RELAXATION. Clough, S.; Hill, J. R. (Univ. of Nottingham, Eng.). J. Phys., C (London); 8: No. 14, 2274-2282 (21 Jul 1975).

The time for the recovery after prolonged saturation of the electron spin resonance signal of free radicals in γ-irradiated 4-methyl-2, 6-ditertiarybutylphenol exhibits a remarkable peak in its magnetic-field dependence. At a temperature of 4.2°K it may be more than fifty times greater at a field of 0.34 T than at 0.27 T. At 0.34 T the electron Larmor frequency coincides with the frequency of tunnelling rotation of the 4-methyl groups of neighboring undamaged molecules with a consequent exchange of energy between the magnetic energy of the electron and the mechanical rotational energy of the methyl groups. The effect is to couple the electron Zeeman energy reservoir to a thermal system whose heat capacity is large and which is itself uncoupled to the lattice. The coupling can be switched on and off simply by changing the magnetic field, providing a simple means of studying the rate constants involved. The effect provides a new way of investigating quantum motions in molecular solids. (auth)

**25614** RADIATION YIELD OF IONS IN LIQUID DIELECTRICS AS A FUNCTION OF TEMPERATURE AND RADIATION ENERGY. Ivanov, V. I.; Kleshchenko, E. D.; Sukhanovskii, Yu. P.; Frolov, V. V. (Moscow Engineering Physics Inst.). Sov. Phys.–Tech. Phys.; 19: No. 11, 1468-1470(May 1975).

Translated from Zh. Tekh. Fiz.; 44: No. 11, 2383-2387(Nov 1974).

The Onsager theory is used to obtain the ion radiation yield G as a function of E the energy of the ionizing radiation and the temperature T in analytic form: $G(E, T) = \alpha T \exp[-b(E)/T]$, where $b(E) = c_1[c_2E - \sqrt{c_2E}]^{-1}$; α, $c_1$, and $c_2$ are constants. The radiation yield of ions in hexane at T = 217-233°K is measured. The theoretical and experimental functions G = G(T) are in satisfactory agreement, while the temperature dependence of the slope of the volt–ampere characteristic confirms the hypothesis. (auth)

**25615** INFLUENCE OF CYCLIC STRUCTURE ON THE RADIOLYSIS OF HYDROCARBONS. II. Radiolysis of Alkylcyclopentanes and Alkylcyclohexanes. Vojnarovits, L.; Foldiak, G. Acta Chim. Acad. Sci. Hung.; 82: No. 3, 285-303(1974).

Products formed via C–H and C–C bond fissions in the vicinity of the tertiary carbon atom of the molecule are predominant in the product spectrum of methyl- and ethylcyclopentane as well as methyl- and ethylcyclohexane irradiated in the liquid phase with $^{60}Co$ γ-radiation. Of the cyclic products 1-methyl and 1-ethylcycloalkenes are produced with highest yield from methyl- and ethylcycloalkanes. (Hung. Techn. Abstr.)

**25616** EFFECT OF POLYMERIZATION TEMPERATURE ON THE MORPHOLOGY OF AS-POLYMERIZED POLYETHYLENE PREPARED BY GAMMA-RAY-INDUCED POLYMERIZATION. Arai, H.; Wada, T.; Kuriyama, I. (Japan Atomic Energy Research Inst., Takasaki, Gunma. Takasaki Radiation Chemistry Research Establishment). Rep. Progr. Polym. Phys. Jap.; 17: 269-272(Jul 1974).

Polymerization was performed at 200 kg/cm² and 0 to 180°C for 10 to 120 minutes, and a dose rate of $1.5 \times 10^5$ rad/hr. The DSC melting curves of samples were recorded at a heating rate of 4°C/min in a nitrogen stream. Each sample was first melted at about 25°C above endothermic peak temperature, immediately recrystallized from the melt by cooling at the same rate to about 50°C, and then remelted under the same conditions. The molecular weight distribution of the samples was measured. No fibril structure was found in polyethylene formed at any polymerization temperature. However, the remarkable change in nascent morphology was observed at about 60°C. Below 55°C, the complex aggregates of small lamellar crystals with irregular growing faces were observed. From shadow length, their thickness was estimated to be about 60 to 100 Å. Above 60°C, the aggregates of large spherical particles were observed together with many semispherical particles. The polymers formed below 55°C showed a sharp single endothermic peak and bimodal molecular weight distribution, while the samples prepared above 60°C revealed double endothermic peaks and unimodal molecular weight distribution. These results indicate that the mechanism of crystallization during polymerization below 55°C is different from that above 60°C. It was further concluded that as-polymerized polyethylene prepared by γ-ray-induced polymerization is composed of folded chain crystals irrespective of reaction temperature. (JA)

## Radiochemistry and Nuclear Chemistry

**25617** PRODUCTION OF ULTRA HIGH ACTIVITY $^{11}C$-LABELED HYDROGEN CYANIDE, CARBON DIOXIDE, CARBON MONOXIDE, AND METHANE VIA THE $^{14}N(p, \alpha)^{11}C$ REACTION (XV). Christman, D. R.; Finn, R. D.; Karlstrom, K. T.; Wolf, A. P. (Brookhaven National Lab., Upton, NY). Int. J. Appl. Radiat. Isot.; 26: No. 8, 435-442(Aug 1975).

The use of $N_2$-$O_2$ or $N_2$-$H_2$ pressurized gaseous systems as targets in proton bombardment makes use of the $^{14}N(p, \alpha)^{11}C$ reaction and allows the facile, quantitative production of $H^{11}CN$, $^{11}CO_2$, $^{11}CO$ or $^{11}CH_4$ as needed. A system is described for the production of carrier-free, high activity (up to 2 Ci) $H^{11}CN$ in an on-line process in the effluent gas stream from a cyclotron target. The target gas is a mixture of 94.5% nitrogen, 5.5% hydrogen, run at a total pressure of 11 atmospheres. The primary products are converted to $^{11}CH_4$ in over 95% yield by radiolysis in the target, and this, along with $NH_3$ which is concurrently produced radiolytically, is converted quantitatively to carrier-free $H^{11}CN$ over platinum wire held at 1000°C. The radiation processes and dosimetry studies involved in the system are discussed. The product is available for use as gaseous $H^{11}CN$, or in base or carrier sodium cyanide, within 10 to 12 min after the end of an irradiation. It has been used as such in animal studies and also in the production of carrier-free dopamine-$^{11}C$ and norepinephrine-$^{11}C$ at levels up to 30 mCi at the time of delivery for medical use. An identical target, using tank $N_2$ with trace $O_2$ impurity as the target gas, can be used to produce carrier-free $^{11}CO_2$ at similar activity levels, and from this $^{11}CO$ or $^{11}CH_4$ can be made either on-line or by a rapid catalytic reduction. (auth)

## Hot-Atom Chemistry

**25618** (COO-3283-13) STUDIES IN HOT ATOM AND RADIATION CHEMISTRY. Progress Report, September, 1975. (Johns Hopkins Univ., Baltimore, Md. (USA). Dept. of Chemistry). 1975. Contract E(11-1)-3283. 10p. Dep. NTIS $4.00.

The cross sections of the ion-molecule reactions of $F^+(^3P)$ and $F^+(^1D)$ with molecular hydrogen and its stable isotopic variants were measured using a tandem mass spectrometer. The kinematics and differential cross sections for the reaction of $F^+(^3P)$ with $D_2$ were studied. The study of the exoergicity as a function of projectile ion energy showed that the bulk of the exothermicity of the reaction was converted into vibrational energy of the product ion. This data also indicated that at low energies (less than 2 eV) that the $FD^+$ product was produced in its ground state ($^2PI$) and at higher projectile energies the product was in the $^2SIGMA^+$ state. The energy and angular distribution of the ionic products in this reaction showed that at low energies the distribution showed a high degree of symmetry relative to +- $90^0$ although some forward peaking was detectable. At higher energies the distribution was asymmetric relative to +- $90^0$ indicating the presence of a direct mechanism. Failure to observe the reaction $F^+(D_2, FD)D^+$ was attributed to a violation of spin and symmetry conservation rules. Bombardment of $CF_4$ with near monochromatic electrons coupled with the use of coincidence mass spectrometer permitted the detection of the ion pair process $CF_4 + e$ yields $CF_3^+ + F + e$ for the first time. In addition a low level $CF_3^+$ ion was observed below the ionization potential of $CF_3$. This was attributed to the ionization of excited $CF_3$ radicals. The electronic states of $C^+$ produced by electron (100 eV) bombardment of halogenated methanes showed that in $CH_4$ 14 per cent of the $C^+$ product was in the first excited state ($^4P$) whereas in $CF_4$ 33 per cent of the $C^+$ was in this state. For other methane derivatives ($CCl_4$, $CBr_4$, $CI_4$, and $CHBr_3$) only ground state $C^+$ was produced. (auth)

**25619** PULSED-BEAM STUDY OF $^{111}$Cd NUCLEAR QUADRUPOLE INTERACTION WITH RECOIL-INDUCED LATTICE DEFECTS IN CUBIC PALLADIUM. Bertschat, H.; Haas, H.; Pleiter, F.; Recknagel, E.; Schlodder, E.; Spellmeyer, B. (Hahn-Meitner-Institut für Kernforschung Berlin GmbH, Bereich Kern- und Strahlenphysik, Berlin-West, Germany and Freie Universität Berlin, Fachbereich Physik, Berlin-West, Germany). Phys. Rev. B 12: No. 1, 1-3 (1 July 1975).

The quadrupole interaction of excited $^{111}$Cd nuclei with electric field gradients due to lattice defects in fcc palladium has been studied by the technique of time-differential observation of perturbed angular distribution of $\gamma$ rays. The lattice defects were induced by the recoiling ions following the nuclear reaction $^{108}Pd(\alpha, n)^{111}Cd$. A sharp frequency of 87(2) MHz is assigned to trapped interstitials. A broad temperature-dependent frequency distribution arising from various other lattice defects was found. A migration energy of 0.10(2) eV for free interstitials is deduced. (auth)

## Properties of Radioactive Materials

*Refer also to abstracts 25569 and 26094.*

**25620** (AED-CONF-75-080-006) STRUCTURE OF SELENIUM TETRAFLUORIDE: NEW PENTAFLUOR ORTHOCHALCOGENATES. Seppelt, K. (California Univ., Berkeley (USA). Dept. of Chemistry). 1975. 7p. (In German). INIS.

From meeting of lecturers in chemistry; Duesseldorf, F. R. Germany (7 Apr 1975).

13 figs. Available from ZAED.

It has been proved by nuclear resonance that selenium tetrafluoride has a structure analogous to sulfur tetrafluoride: two axially and two equatorially bonded fluorine atom pairs. The crystal structure was determined to be $Xe(OSeF_5)_2$. The compounds $CrO_2(OSeF_5)_2$, $VO(OSeF_5)_3$, $Ti(OTeF_5)_4$ and $CeW(OTeF_5)_5$ were prepared and fully characterized. Uranium chemistry: all compounds between $UF_6$ and $U(OTeF_5)_6$ [i.e., all UFsub(x)(OTeF$_5$)sub(6-x)] were synthesized. Individual members of this series may be of interest for isotope separation using lasers. $U(OTeF_5)_6$ is the heaviest non-polymeric inorganic molecule. (auth)

**25621** (ARH-SA-233) PARAMETERS FOR PLUTONIUM POLYMER FORMATION IN NITRIC ACID. Schuelein, V. L. (Atlantic Richfield Hanford Co., Richland, Wash. (USA)). May 1975. Contract AT(45-1)-2130. 16p. (CONF-750673-2). Dep. NTIS $4.00.

From 30th northwest regional meeting American Chemical Society; Honolulu, Hawaii, USA (12 Jun 1975).

The formation of plutonium polymer was determined at 20 to $100^0$C in 0.1 to 1.4M $HNO_3$ solutions containing 10 to 50 g/liter plutonium. Techniques for producing polymer and its detection are described. (auth)

**25622** (LBL-4070) RADIOPOLAROGRAPHY OF Am, Cm, Bk, Cf, Es AND Fm. Samhoun, K.; David, F. (California Univ., Berkeley (USA). Lawrence Berkeley Lab.). Jul 1975. Contract W-7405-ENG-48. 7p. (CONF-750913-11). Dep. NTIS $4.00.

From 4th international transplutonium elements symposium; Baden-Baden, F. R. Germany (13 Sep 1975).

The standard electrode potentials determined in this work are affected by the accuracy of determining delta $E_2$ and delta $E_3$, since these energies of amalgamation were estimated by correlation with those of some 4f elements. The accuracy on the measured half-wave potential itself is 5 mV for all elements, Bk and Cm excepted. Finally, we note that these standard potentials are in good agreement with those calculated by correlating the variation in P(M) function for 4f and 5f series. (auth)

**25623** RADIOTRACER STUDIES OF THE ADSORPTION OF AN AMPHOLYTIC SURFACTANT, N-DODECYL-$\beta$-ALANINE, AT THE AQUEOUS SURFACE. Okumura, T. (Kao Soap Co. Ltd., Tokyo (Japan). Household Goods Research Labs.); Nakamura, A.; Tajima, K.; Sasaki; Tsunetaka. Bull. Chem. Soc. Jpn.; 47: No. 12, 2986-2989(Dec 1974).

A tritiated ampholytic surfactant, N-dodecyl-$\beta$-alanine, $C_{10}H_{21}$-$(CHT)_2$-$NH_2^+$-$(CH_2)_2$-$COO^-$, was synthesized, and the amount of adsorption on an aqueous surface was measured directly by the radiotracer method. The adsorption isotherm near the neutral pH region showed a saturation value of $3.73 \times 10^{-10}$ mol/cm$^2$ above the concentration of about 1/5 of the critical micelle concentration in the absence of added salt, and a value of $4.74 \times 10^{-10}$ mol/cm$^2$ above the critical micelle concentration in the presence of 1 mol/1 NaCl. In the presence of 1 mol/1 NaCl, no effect of pH on the adsorption was found. The Gibbs adsorption isotherm applicable to the aqueous ampholytic surfactant was derived. The observed amounts of adsorption in the presence and absence of NaCl were in good agreement with the values calculated from the Gibbs adsorption isotherm, using the surface tension data measured by the Wilhelmy plate method. (auth)

**25624** MOESSBAUER SPECTROSCOPIC STUDIES OF THE EFFECT OF ANIONS IN THE SECOND COORDINATION SPHERE IN THE EC-DECAY. Sano, H.; Ohnuma, T. (Tokyo Metropolitan Univ. (Japan). Faculty of Science). Bull. Chem. Soc. Jpn.; 48: No. 1, 266-269(Jan 1975).

The $^{57}$Fe-Mössbauer emission spectra of $^{57}$Co-labelled $[Co(NH_3)_6](NO_3)_3$, $[Co(en)_3](NO_3)_3$, $K_3[Co(CN)_6]$, $K_3[Co(NO_2)_6]$, $[Co(NH_3)_6]_2C_2O_4)_3 4H_2O$, $[Co(en)_3]_2(C_2O_4)_3.9H_2O$, $[Co(NH_3)_6][Fe(CN)_6]$, $[Co(NH_3)_6][Cr(C_2O_4)_3]\cdot 3H_2O$, and $[Co(NH_3)_6][Fe(C_2O_4)_3]\cdot 3H_2O$ sources were determined. Oxalate anions and trisoxalatochromate and trisoxalatoferrate complex anions located outside the first coordination sphere of the decayed atom are still involved in the local radiolytic processes initiated by the EC-decay. The yields of $^{57}$Fe species found in the ferrous-charge state were interpreted by using the data of $\gamma$-radiolysis and hot-atom chemistry of the $^{59}Co(n,\gamma)^{60}Co$ reaction. (auth)

**25625** INTERPRETATION OF LOW-TEMPERATURE LUMINESCENCE SPECTRA OF RUBIDIUM URANYL NITRATE AND SODIUM URANYL ACETATE. Abramov, A.P.; Razumova, I.K. Opt. Spectrosc. (USSR) 38: No. 3, 318-320 (Mar 1975).

Luminescence spectra and kinetics of rubidium uranyl nitrate and sodium uranyl acetate crystals were studied at 4.2 °K. The spectra were interpreted using a model that involves the presence of various types of emitting centers in the crystals. (auth)

**25626** STANDARD ELECTRODE POTENTIALS AND ENTHALPIES OF FORMATION OF SOME LANTHANIDE AND ACTINIDE AQUO-IONS. Nugent, L. J. (Oak Ridge National Lab., TN). J. Inorg. Nucl. Chem.; 37: No. 7/8, 1767-1770(Jul 1975).

Polarographic first half-wave amalgamation potentials for many of the lanthanide and actinide aquo-ions M(III) aq were reanalyzed according to recent interpretations of the amalgamation mechanisms. The analysis yields new values for some of the standard electrode potentials $E^0M(O-III)$ and $E^0M(O-II)$ and the standard enthalpy of formation $\Delta H_f^0(M(III)aq)$. The lanthanide metals La, Ce, Sm, Eu, Gd, Tb, Ho, Yb and Lu, and the actinide metals Ac, U, Am, Cm, Bk, Cf, Es and Fm, are treated. (auth)

**25627** PREPARATION, CRYSTAL, AND MOLECULAR STRUCTURE OF $/UO_2(o-OC_6H_4-CH=N(CH_2)_2NH(CH_2)_2N(CH_3)_2NO_3/\cdot CH_2Cl_2$. Bandoli, G. (Consiglio Nazionale delle Richerche, Padua); Clemente, D. A.; Cingi, M. B. J. Inorg. Nucl. Chem.; 37: No. 7-8, 1709-1714(Jul 1975).

The crystal and molecular structure of $|UO_2(o-OC_6H_4-CH=N(CH_2)_2NH(CH_2)_2N(CH_3)_2)NO_3|\cdot CH_2Cl_2$ has been determined from 3-dimensional x-ray data collected by counter methods. The structure has been refined by least-squares techniques to a final conventional R factor of 8.2%. The material crystallizes in space group Pbc $2_1$ of the orthorhombic system, with four molecules in a cell of dimensions a = 9.298(6), b = 20.541(9) and c = 10.925(8) Å.

The crystal consists of discrete monomeric molecules interspersed with $CH_2Cl_2$ molecules which do not interact with the "inner core" of the complex. The coordination around uranium is approximately pentagonal bipyramidal with uranyl oxygens in axial positions; four equatorial sites are occupied by the tetradentate Schiff base, nitrate group occupying the fifth site. The bond distances and angles reveal no surprises when compared with other analogous uranyl-Schiff bases complexes. (auth)

**25628** BERKELIUM AND CERIUM OXIDATION BY SODIUM PERXENATE IN NITRATE SOLUTIONS. Lebedev, I. A.; Chepovoil, V. I.; Myasoedov, B. F. (Inst. of Geochemistry and Analytical Chemistry, Moscow). Radiochem. Radioanal. Lett.; 22: No. 4, 239-242(25 Aug 1975).

With the addition of sodium perxenate to solutions of Ce(III) and diluted $HNO_3$, cerium can be oxidized to Ce(IV) forming a precipitate. This precipitate coprecipitates indicator amounts of $^{249}Bk$, but not $^{155}Eu$ and $^{244}Cm$ which indicate berkelium oxidation to Bk(IV). (auth)

**25629** OXIDATION OF MICROAMOUNTS OF Bk(III) AND Ce (III) BY OZONE IN NITRATE SOLUTIONS. Myasoedov, B. F.; Chepovoil, V. I.; Lebedev, I. A. (Inst. of Geochemistry and Analytical Chemistry, Moscow). Radiochem. Radioanal. Lett.; 22: No. 4, 233-238(25 Aug 1975).

Indicator amounts of $^{249}Bk$ and $^{144}Ce$ ($10^{-9}-10^{-6}$M) in 1-9M $HNO_3$ are oxidized by ozone to the tetravalent state for 0.5-1 min. The degree of oxidation of Bk increases with the decrease of $HNO_3$ concentration, while that of Ce decreases. The completeness of Bk(III) and Ce(III) oxidation to Bk(IV) and Ce(IV) was tested by coprecipitation with zirconium phosphate. (auth)

**25630** ELECTROLYTIC REDUCTION OF URANYL ION USING AN ION EXCHANGE MEMBRANE. Hsiang, C. C.; Chang, C. T. (National Tsing Hua Univ., Taiwan, China). J. Inorg. Nucl. Chem.; 37: No. 9, 1949-1950(Sep 1975).

A kinetic investigation of the reduction of uranyl ion was carried out. The electrolytical cell was divided by a cation exchange membrane into a cathode and an anode compartment. The uranium solution in the former was virtually kept constant during electrolysis by continuously supplying hydrogen ion from the latter via the membrane. The reaction rate was found to be directly proportional to the concentration of uranyl ion, but independent of acidity above 0.3N HCl. (auth)

**25631** CRYSTAL AND MOLECULAR STRUCTURE OF URANYL ACETATE DIHYDRATE. Howatson, J. (Univ. of Wyoming, Laramie); Grev, D. M.; Morosin, B. J. Inorg. Nucl. Chem.; 37: No. 9, 1933-1935(Sep 1975).

The crystal structure and atomic arrangement of uranyl acetate dihydrate, $UO_2(CH_3COO)_2.2H_2O$, have been determined by a single-crystal x-ray diffraction study. The crystal is orthorhombic, space group Pnam, with Z = 4, a = 9.622, b = 14.833, and c = 6.808Å. The structure was solved by Fourier methods and refined to R = 0.041 for 821 observed reflections. The coordination sphere of the uranium contains seven oxygen atoms approximating a pentagonal bipyramid. One-half of the acetate ions link adjacent bipyramids to form chains, while the remaining acetate ions are chelated to individual uranium atoms. Only one of the water molecules is bonded directly to the uranium. (auth)

**25632** INVESTIGATIONS ON CESIUM URANATES. III. Crystal Structures of $Cs_2U_4O_{12}$. von Egmond, A. B. (Stichting Reaction Centrum Nederlands, Petten). J. Inorg. Nucl. Chem.; 37: No. 9, 1929-1931(Sep 1975).

The crystal structures of three $Cs_2U_4O_{12}$ phases have been investigated by x-ray diffraction methods. The positions of the uranium and cesium atoms of the rhombohedral $\alpha$-phase were obtained from single crystal x-ray analysis. The positions of the uranium and cesium atoms in the monoclinic $\beta$-phase and the cubic $\gamma$-phase could be obtained from x-ray powder analysis. Furthermore the oxygen atoms in the $\gamma$-phase could be located. The structures of $Cs_2U_4O_{12}$ are closely related to the crystal structure of $UO_2$. (auth)

**25633** ELECTRODEPOSITION OF PLUTONIUM AT TRACER CONCENTRATIONS FROM A MIXED $NH_4Cl/NH_4I$ SYSTEM. Irlweck, K.; Veselsky, J. C. (International Atomic Energy Agency, Seibersdorf, Australia). Int. J. Appl. Radiat. Isot.; 26: No. 8, 481-483(Aug 1975).

Electrodeposition of minute quantities of Pu from ammonium iodide liquors, based on the method of Mitchell, has been developed. The method is described. The dependence of Pu recovery on the duration of electrolysis and the time function of the Pu deposition with electrolytes of different composition were investigated. (UK)

**25634** PROTACTINIUM (V) AND URANIUM (V) TROPOLONATES. Bagnall, K. W. (Univ. of Manchester, Eng.).; Bhandari, A. M.; Brown, D.; Lidster, P. E.; Whittaker, B. J. Chem. Soc. (London), Dalton Trans.; No. 13, 1249-1252(1975).

Penta(tropolonato)-protactinium(v) and -uranium(v), $[Pa(trop)_5]$ and $[U(trop)_5]$, have been prepared by reactions involving tropolone and the appropriate pentaethoxide in anhydrous benzene. Reactions between uranium pentachloride and an excess of tropolone in non-aqueous solvents have yielded chlorotetra(tropolonato) uranium(v), $[U(trop)_4Cl]$. Some physical and chemical properties of these complexes are reported and the $UCl_5$-tropolone reaction is discussed. (auth)

**25635** SULPHOXIDE COMPLEXES OF THE ACTINOID (IV) NITRATES. Alvey, P. J. (Univ. of Manchester, Eng.); Bagnall, K. W.; Lopez, O. V.; Brown, D. J. Chem. Soc. (London), Dalton Trans.; No. 13, 1277-1280(1975).

Complexes of the actinoid tetranitrates with sulphoxides, $M(NO_3)_4.xR_2SO$ [R = Et (deso), M = Th, U, or Np, x = 3; R = Ph (dpso), M = Th, U, or Np, x = 3 and M = Th, U, Np, or Pu, x = 4; R = $\alpha$ -$C_{10}H_7$(naphthyl, dnso), M = Th, x = 3] have been prepared. The ir, Raman, and electronic spectra of the complexes are discussed. (auth)

## Radioactive Waste Treatment

**25636** (INIS-mf-1640, pp 483-488) EXPERIENCE WITH IODINE FILTERS IN THE PRODUCTION OF IODINE TAGGED COMPOUNDS ON THE CURIE SCALE. Schulze-Pillot, G. (Farbwerke Hoechst A. G., Frankfurt am Main). Mar 1974. (In German).

From seminar on the testing of iodine filters; Karlsruhe, F. R. Germany (4 Dec 1973). (Commission of the European Communities, Brussels (Belgium)).

During the production of iodine-tagged compounds, iodine is released in the form of pure iodine, iodide and organic compounds. The order of activity concentration in the treated solutions used is Ci/ml and the amount of radioactive material released can be as high as 100πCi. This may all be released instantaneously or over periods of up to one hour. The work is carried out in cells from which the exhaust air passes over activated charcoal iodine filters at two levels. Under operating conditions the decontamination factor of the two-level filtering measured over a period of 24 hours lies between $10^4$ and $10^5$. This figure is lower than expected from the retention efficiency of each individual filter. The retention efficiency as a function of the time after release of the radioactive substance was therefore also measured. (INIS)

**25637** (KFK-2162) EXPERIMENTAL STUDIES ON THE POSSIBILITY OF USING A CERAMIC MATRIX FOR FIXING THE HIGH LEVEL RADIOACTIVE WASTES. Husain, S. R.; Rudolph, G.; Hild, W. (Gesellschaft fuer Kernforschung m.b.H., Karlsruhe (F. R. Germany)). Jun 1975. 31p. Dep. NTIS (US Sales Only) $4.75.

A ceramic product was developed to fix high-level radioactive wastes for storage and final disposal. In the present experiments some of the properties (e.g., visual change, change in size or shape, change in weight, change in structure, density and leachability) are studied for the long-term stability of the product under heat and radiation treatment. The properties are not severely affected by radiation or by heat treatment. The leaching property is slightly affected due to heating. From the results it appears that the heating has a dominant effect over the radiation on the properties of the ceramic product. (auth)

**25638** (SAND-75-0255, pp 10-15) NEW SOLIDIFICATION PROCESS FOR NUCLEAR WASTE. Lynch, R. W.; Dosch, R. G. Aug 1975.

In Sandia technology. (Sandia Labs., Albuquerque, N. Mex. (USA)).

A new process involving ion exchange can be used to solidify nuclear wastes. It is named the Sandia Solidification Process. (auth)

**25639** FLOCCULATION TREATMENT OF RADIOACTIVE CONTAMINATED SEA WATER, (2). Operational Performance with Real Wastes. Sakurai, A.; Nagaoka, Y.; Morishita, S.; Wadachi, Y. (Japan Atomic Energy Research Inst., Tokai, Ibaraki. Tokai Research Establishment). Nippon Genshiryoku Gakkaishi; 17: No. 1, 27-30(Jan 1975). (In Japanese).

Low-level radioactive contaminated sea water containing $^{137}Cs$, $^{60}Co$, and $^{144}Ce$, of an amount of 64 $m^3$, brought from the Marine Radioecological Research Station of the National Institute of Radiological Sciences to the Tokai Establishment of the Japan Atomic Energy Research Institute, was treated with two-stage flocculation. The first stage of the flocculation was performed

to remove $^{137}Cs$ with copper ferrocyanide floc, and the ensuing second stage was applied to remove $^{60}Co$ and $^{144}Ce$ with calcium phosphate floc in alkaline solution. The results obtained revealed that the radioactive contamination was substantially reduced by the first-stage flocculation, while the second stage further lowered it to a level amply meeting expectations. As a result of the two-stage flocculation, the overall decontamination factor was indicated to be approximately 10. The sludge remaining from the flocculation was dewatered to 90% water content under reduced pressure. Then for the purpose of storage, the product was solidified with cement in a steel container, of a volume of 200 liters. (auth)

**25640** REPROCESSING AND THE PROBLEM OF PUBLIC ACCEPTANCE. Imai, Y. (Japan Atomic Industrial Forum, Inc., Tokyo). At. Jpn.; 18: No. 5, suppl.1, 78-86(May 1974).

Comparison was made between Japan and overseas on nuclear fuel reprocessing plants by a study team of Japan Atomic Industrial Forum, Inc. (JAIF). The object was to study the public acceptance problem on the establishment of fuel reprocessing industry and to learn its policy from the USAEC and other organizations. The report covers 1) the reprocessing of spent fuel, 2) public acceptance problems overseas, 3) U.S. attitude on the preservation of environment, 4) problems concerning the treatment of wastes, 5) reprocessing consignment overseas and public acceptance, 6) trends in reprocessing technology, and 7) public acceptance and development of technology. Specifically, attention was paid to "as-low-as-practicable" concept adopted by the USAEC for the preservation of environment, and the zero release of low-level radioactive liquid wastes and the solidification of high level radioactive liquid wastes. Underground storage reduces the amount of monitoring and maintenance. The trend of transformation is transformation of uranium into $UF_6$ and plutonium into $PUO_2$ at reprocessing sites. It is necessary to clarify the range of possibility and feasibility of research for the removal of tritium. (JA)

**25641** BITUMINIZATION OF RADIOACTIVE WASTES, 1. Mixing Properties of Bitumen and Simulated Wastes. Ono, T.; Mizuochi, H. (Central Research Inst. of Electric Power Industry, Komae, Tokyo (Japan). Technical Lab. No. 1). Denryoku Chuo Kenkyusho Gijutsu Daiichi Kenkyusho Hokoku; No. 73111, 1-26(Jul 1974). (In Japanese).

The mixing examination of several kinds of bitumen and simulated radioactive wastes such as concentrated refreshment solution, spent ion-exchange resins and filter sludges, and releases from nuclear power station, were carried out. Bitumen and wastes were well mixed and dispersed each other to form uniform solidified wastes by heating. Maximum mixing ratios of wastes were 50-70 wt% for concentrated solution or resins and 10 wt% for filter sludges. The specific gravity of solidified wastes was more than 1.2 for concentrated solution and less than 1.2 for resins and filter sludges. The penetration of the solidified wastes decreased and the softening point of them increased with the increase of mixing ratio of the wastes. (auth)

**25642** VOLUME REDUCTION OF RADIOACTIVE SOLID WASTES BY INCINERATION, 1. Study on Incineration of Radioactive Solid Wastes. Ono, T.; Suzuki, J. (Central Research Inst. of Electric Power Industry, Komae, Tokyo (Japan). Technical Lab. No. 1). Denryoku Chuo Kenkyusho Gijutsu Daiichi Kenkyusho Hokoku; No. 73117, 1-34(Aug 1974) (In Japanese).

In the volume reduction by incineration of radioactive solid wastes, it is necessary to completely remove dusts containing radioactive material. In usual incinerating method, a lot of dust enters a dust collector. The possibility in incineration of restraining the amount of dust entering the collector and an incineration method are considered. Surface combustion is able to restrain the production of dust such as soot, and incineration of carbonized material dry distilled at somewhat higher temperature works well for surface combustion. It is necessary to carbonize slowly, controlling the yielding velocity of heat dissolved gas so that the gas does not carry away particles in carbonization. The process of incineration system is: when dried wastes are carbonized, poisonous gases together with combustible gas are dissolved and produced, carbonized material obtained thereby is incinerated by surface burning; after removing poisonous gas from dissolved gas by gas treatment, the mixed combustion of combustible gas is performed. (auth)

**25643** PROCESS FOR CLEANING RADIOACTIVELY CONTAMINATED METAL SURFACES. Mihram, R. G.; Snyder, G. A. (to Halliburton Co.). US Patent 3,873,362. 25 Mar 1975. Filed date 29 May 1973. 14p.

A process is described for removing radioactive scale from a ferrous metal surface, including the steps of initially preconditioning the surface by contacting it with an oxidizing solution (such as an aqueous solution of an alkali metal permanganate or hydrogen peroxide), then, after removal or decomposition of the oxidizing solution, the metallic surface is contacted with a cleaning solution which is a mixture of a mineral acid and a complexing agent (such as sulfuric acid and oxalic acid), and which preferably contains a corrosion inhibitor. A final step in the process is the treatment of the spent cleaning solution containing radioactive waste materials in solution by adding a reagent selected from the group consisting of calcium hydroxide or potassium permanganate and an alkali metal hydroxide to thereby form easily recovered metallic compounds containing substantially all of the dissolved metals and radioactivity. (auth)

**25644** DECONTAMINATION PROCESS FOR RADIOACTIVE LIQUIDS. Peeters, K. J. A.; Van de Voorde, N. L. C. (to Belgonucleaire S. A.). US Patent 3,896,045. 22 Jul 1975. Priority date 29 Aug 1972, F. R. Germany. 8p.

Radioactive liquids and the products thereof are decontaminated by contacting the radioactive liquid with a sorbent in a sulfate-containing medium selected from the group consisting of a barium salt and a barium salt mixed with up to 50 percent of a metal ferrocyanide. (auth)

## *Reactor Fuel Reprocessing*

*Refer also to abstract 25905.*

**25645** (INIS-mf-1640, pp 175-184) IODINE RETENTION IN REPROCESSING PLANTS. Herre, F. (Gesellschaft zur Wiederaufarbeitung von Kernbrennstoffen mbH, Leopoldshafen, Ger.). Mar 1974. (In German).

From seminar on the testing of iodine filters; Karlsruhe, F. R. Germany (4 Dec 1973). (Commission of the European Communities, Brussels (Belgium)).

A description is given of the iodine filtering equipment at the reprocessing plant at Karlsruhe (WAK), together with details of preliminary test results and operating experience in the two years to date. The problems of iodine retention in large-scale plants are listed. (INIS)

**25646** (INIS-mf-1640, pp 185-198) IODINE TRAPPING FROM THE EXHAUST AIR OF REPROCESSING PLANTS. Furrer, J.; Wilhelm, J. G. (Gesellschaft fuer Kernforschung mbH, Karlsruhe, Ger.). Mar 1974.

From seminar on the testing of iodine filters; Karlsruhe, F. R. Germany (4 Dec 1973). (Commission of the European Communities, Brussels (Belgium)).

Reprocessing plants are at present being planned for a fuel throughput of 1500t/a. Assuming that the fuel comes from light water reactors, is discharged after 2 years of full power operation and reprocessed after a cooling period of 160 days, a total decontamination factor of 1800 must be achieved, to prevent emission in excess of 0.1mCi/h $^{131}I$ through the exhaust stack of the reprocessing plant. In addition, approx. 280 kg $^{129}I$ with a total activity of 46 Ci $^{129}I$ are produced during one year's operation. It would seem advisable to bind, immediately at the beginning of reprocessing, the $^{129}I$ to solid sorption materials, which can be permanently stored. This would eliminate all problems presented by the occurrence of $^{129}I$ in the waste solutions from the reprocessing plant. The retention behavior of iodine sorption material in laboratory tests with air-$NO_2$ mixtures as carrier gas is described. In addition the efficiency of the material in the tank and solvent exhaust gases of a reprocessing plant is discussed. (INIS)

**25647** MULTIVARIABLE CASCADE CONTROL OF PUREX PROCESS. Kotoh, N.; Kiyose, R.; Yamamoto, Y. (Tokyo Univ. (Japan). Faculty of Engineering). J. Nucl. Sci. Technol. (Tokyo); 12: No. 1, 53-60(Jan 1975).

A differential-difference equation model is introduced, which can describe the dynamics of any type of extractor, whether mixer-settler, pulsed column, or rapid contactor. The differential or difference equation models used by several investigators prove to be particular cases of this model. From the results calculated by this model, it is shown that there exist an optimal stage and an optimal component for monitoring the performance in the control of extractors. A computer control system for the solvent extraction step of the Purex process is devised with use made of a generalized version of the classical cascade control law, which the authors have named the Multivariable Cascade Control Law. This law can easily be extended for application to the control of the Purex process as a whole. (auth)

**25648** BUGS IN THE NUCLEAR FUEL CYCLE. Kaplan, G. IEEE (Inst. Electr. Electron. Eng.) Spectrum; 12: No. 9, 56-64 (Sep 1975).

In March 1975 ERDA published a report (ERDA-33) which concluded that unless prompt and effective actions are taken for the

safeguarding and handling of nuclear fuels, the use of nuclear fission energy is limited. If nuclear power development is to continue fuel reprocessing plants must become operational, acceptable safeguards systems for separated Pu must be established, and the safe permanent disposal of high-level radioactive wastes must be demonstrated. The problems and risks involved in the storage of spent reactor fuel, the reprocessing of the spent fuel for the recovery of Pu and unused U, the disposal of high-level radioactive waste, and the shipment of nuclear material, mainly that of spent fuel and high-level waste, are discussed. (LCL)

# CONTROLLED THERMONUCLEAR RESEARCH

## Plasma Confinement and Heating

*Refer also to abstracts 25710, 25711, and 26730.*

**25649** (AED-CONF-75-043-020) COLLISION DAMPING OF THE ELECTROSTATIC ION WAVES AND TURBULENT HF HEATING. Harms, K. D. (Kernforschungsanlage Juelich G.m.b.H. (F. R. Germany). Inst. fuer Plasmaphysik). 1975. 5p. (In German). INIS.

From spring meeting of the Fachausschuesse Kurzzeitphysik and Plasma- und Gasentladungphysik of the DPG; Duesseldorf, F. R. Germany (4 Mar 1975).

The collision-induced linear damping rate $\gamma(c)$ for electrostatic ion Bernstein waves was calculated with the aid of a more realistic model, namely under consideration of the Fokker-Planck equation. It is shown that in turbulent HF heating of fusion plasmas a) the parametric excitation of ion Bernstein wave turbulence is impracticable, and b) that destabilization of electrostatic ion waves at the lower hybrid frequency seems to be a highly promising method. (GG/AK)

**25650** (CONF-750905-19) CONFINEMENT AND NEUTRAL INJECTION EXPERIMENTS IN ORMAK. The ORMAK Group. Lyon, J. F. (Oak Ridge National Lab., Tenn. (USA)). 1975. 23p. Dep. NTIS $4.25.

From 7th European conference on controlled fusion and plasma physics; Lausanne, Switzerland (1 Sep 1975).

The ORMAK operating regime was extended to higher toroidal fields, discharge currents and neutral injection power. Confinement studies have concentrated on anomalous electron transport through scaling studies at constant q and the effects of MHD instabilities (through soft x-ray fluctuations) and impurities [through Z/sub eff/(r) comparisons]. Ion heating increases linearly with coinjection power and counterinjection heating efficiency increases with discharge current. (auth)

**25651** (Y-1988) CONTROL STRATEGY FOR PLASMA EQUILIBRIUM IN A TOKAMAK. Miskell, R. V. (Oak Ridge Y-12 Plant, Tenn. (USA)). Aug 1975. Contract W-7405-eng-26. 75p. Dep. NTIS $5.45.

Dynamic control of the plasma position within the torus of a TOKAMAK fusion device is a significant factor in the development of nuclear fusion as an energy source. This investigation develops a state variable model of a TOKAMAK thermonuclear device, suitable for application of modern control theory techniques. (auth)

**25652** CONCERNING THE ARTICLE BY L. P. ZAKATOV AND A. G. PLAKHOV "MECHANISM OF PLASMA HEATING BY AN ELECTRON BEAM IN A PROBKOTRON MACHINE". Demirkhanov, R.A.; Gevorkov, A.K.; Popov, A.F.; Kolmakov, O.A. JETP Lett. 21: No. 7, 189-190 (5 Apr 1975).

We compare the experimental results obtained in [1] with the model proposed in [2,3] for plasma heating under the condition of two-stream instability in a probkotron. It is shown that the experimental data given in [1] can be qualitatively explained by the model stochastic cyclotron heating. (auth)

**25653** HEATING OF A DENSE PLASMA BY A POWERFUL BEAM OF RELATIVISTIC ELECTRONS. Breizman, B.N.; Ryutov, D.D. (Nuclear Physics Institute, Siberian Division, USSR Academy of Sciences). JETP Lett. 21: No. 7, 192-193 (5 Apr 1975).

We indicate the conditions under which dissipation of the energy of Langmuir oscillations excited in a plasma by a relativistic electron beam leads to an effective heating of the bulk of the plasma electrons. These conditions can be realized in experiments on beam heating of a dense plasma. (auth)

**25654** OPTIMAL PLASMA COMPRESSION IN Z AND Θ PINCHES. Zhdanov, S.K.; Trubnikov, B.A. (Moscow Engineering Physics Institute). JETP Lett. 21: No. 6, 169-170 (20 Mar 1975).

The feasibility of adiabatic compression of a uniform plasma, not accompanied by the development of shock waves, is demonstrated. The laws governing the optimal growth of the external magnetic field (Θ pinch) and of the longitudinal current (Z pinch) are obtained. (auth)

**25655** THE NUMBER OF FAST IONS IN A LASER PLASMA. Silin, V.P. (P. N. Lebedev Physics Institute, USSR Academy of Sciences). JETP Lett. 21: No. 6, 152-153 (20 Mar 1975).

It is demonstrated that the number of high-energy ions produced when a powerful laser beam acts on a target can be determined if one assumes a rapid establishment of the electromagnetic field in the plasma and a rapid density-profile deformation due to the plasma acceleration in a small region with growing field. (auth)

**25656** DEPENDENCE OF THE RADIATION LOSSES OF A THERMONUCLEAR PLASMA ON THE ATOMIC NUMBER OF THE IMPURITY AND THE TEMPERATURE. Gervids, V.I.; Kogan, V.I. JETP Lett. 21: No. 6, 150-151 (20 Mar 1975).

We calculate the dependence of the radiation losses of a thermonuclear plasma on the atomic number Z of the impurity and on the electron temperature $T_e$ and also the Z dependence of the "lethal" relative impurity concentration in a DT reactor. (auth)

**25657** PROGRESS AND FUTURE TRENDS OF RESEARCHES ON HIGH β PLASMA. Tamaru, T.; Ogawa, K. (Electrotechnical Lab., Tanashi, Tokyo (Japan). Tanashi Branch). Denshi Gijutsu Sogo Kenkyusho Iho; 38: No. 3-5, 226-232 (Jul 1974). (In Japanese).

The present status of high β plasma researches in the world has been surveyed and reviewed. The high β plasma confinement researches are taking place theoretically and experimentally in a very wide scope of the toroidally symmetric and asymmetric configurations. Future plans aiming at the realization of fusion reactor by the high β approach are not yet definite except for the theta-pinch approach. "Scyllac" in Los Alamos, which is an unaxisymmetric high β torus, is an example of this approach. Several types of axisymmetric high β torus are proposed for next generation experiments in fusion research; they are the high β tokamak, torus screw pinch and torus reversed field pinch. A very brief review of researches on the high β plasma production and heating is also given. (auth)

**25658** HEATING OF PLASMA BY NEUTRAL BEAM INJECTION. Matsuda, S. (Japan Atomic Energy Research Inst., Tokai, Ibaraki. Tokai Research Establishment). Nippon Genshiryoku Gakkaishi; 16: No. 9, 459-466 (Sep 1974). (In Japanese).

Problems concerning the heating of plasma by neutral particle beam are discussed. Confinement and heating of plasma are necessary for realizing a fusion reactor. Heating is performed by plasma current, but in order to surmount the limitation of joule heating, the heating with injected neutral particle beam is necessary. The neutral beam is obtained by the neutralization of accelerated ion beam with a gas cell. Impurities in neutral gas make serious disturbance in reactors. High density, pure gas is required. The injection hole for the neutral beam is small, and the collimation of the beam is one of requirements. Characteristics of the neutral beam are good heating efficiency, easy injection into magnetic field, well known mechanism of heating process, and feasibility to use for other purpose than heating. The neutral beam is ionized in a torus system and captured. The efficiency of capture depends on the energy of the neutral beam and the linear density of plasma. The beam escaping capture hits the wall of system and produces impurities in plasma. In case of low beam energy, the instability of plasma may arise, and the staying time of fast ions in plasma becomes short. Then, the energy of the beam is determined by upper and lower limits. The instability due to the injection of neutral beam has not been observed at the present level. The efficiency of neutralization of accelerated ions from ion sources is reduced at high energy. Molecular ions or negative ions are considered to increase the neutralizing efficiency. The ions are initially produced by ion sources. Requirements for the ion sources are high plasma density, high electron temperature, low ion temperature, uniform distribution on electrode surface, and good efficiency of plasma production. Characteristics of the ion sources developed at LBL and ORNL are presented in this paper. Experiments of neutral beam injection have been made since 1973 at various institutes. (JA)

**25659** EXPERIMENTAL INVESTIGATION OF THE INTERACTION BETWEEN LASER RADIATION AND AN ARGON PLASMA. Bakeev, A.A.; Vas'kovskii, Yu.M.; Vorob'eva, N.N.; Nikolashina, L.I.; Orlov, V.K.; Rovinskii, R.E.; Sedov, A.K.; Shirokova, I.P. Sov. J. Quantum Electron. 5: No. 1, 40-42 (July 1975).

An investigation was made of the processes which accompanied the passage of high-power laser radiation ($\lambda = 1.06$ μ) through an argon plasma generated in a plasmatron. Interaction of a laser beam of over $10^7$ W/cm² power density with a plasma whose initial temperature was 9500 °K and in which the electron density was $\sim 10^{16}$ cm$^{-3}$ produced a perturbed region whose expansion during the first 10 μsec was of detonation type and which changed subsequently to a slow-combustion regime maintained throughout the passage of the laser beam. The plasma temperature rose to 19 000 °K in the perturbed region although the absorption of the laser radiation was less than the experimental error ($\eta_\lambda \leq 0.04$ cm$^{-1}$). (auth)

**25660** PARAMETRICALLY INDUCED ELECTRON HEATING NEAR THE PLASMA FREQUENCY. Mizuno, K.; DeGroot, J.S. (Department of Applied Science, University of California, Davis, California 95616). Phys. Rev. Lett. 35: No. 4, 219-223 (28 July 1975).

The nonlinear saturation and evolution of the parametric instability which occurs near the critical density (microwave frequency, $\omega_0$, equals plasma frequency, $\omega_{pe}$) is studied experimentally. A strong anomalous heating of electrons is observed after the instability saturates. For high powers, a large fraction of the absorbed energy is given to suprathermal electrons. The results may be explained in terms of quasilinear diffusion of electrons in parametrically induced turbulence. (auth)

**25661** PLASMA LEAKAGE THROUGH A LOW-$\beta$ LINE CUSP. Hershkowitz, N.; Leung, K.N.; Romesser, T. (Department of Physics, University of California, Los Angeles, California 90024). Phys. Rev. Lett. 35: No. 5, 277-280 (4 Aug 1975).

The half-width of the leakage aperture of plasma through a low-$\beta$ line cusp is found to be twice the hybrid gyroradius $(r_e r_i)^{1/2}$ with $r_e$ and $r_i$ as the electron and ion gyroradii. This steady-state width is shown to develop in a time less than the ion gyroperiod. (auth)

**25662** OBSERVATION OF FLAT-TOP VELOCITY DISTRIBUTIONS OF ELECTRONS IN TURBULENTLY HEATED PLASMAS. Adati, K.; Iguchi, H.; Ito, Y.; Kawabe, T.; Kondo, K.; Mitarai, O.; Muraoka, K.; Sugihara, R. (Institute of Plasma Physics, Nagoya University, Nagoya, 464 Japan). Phys. Rev. Lett. 35: No. 5, 280-284 (4 Aug 1975).

Velocity distributions of the electrons have been measured by a Thomson-scattering method with an eight-channel polychoromator in the initial stage of a linear turbulent-heating experiment. Flat-top distributions were observed associated with high-frequency fluctuations ($\omega \lesssim \omega_{pi}$) just before the onset of fast heating of the electrons. Those results were compared with computer simulations and theoretical analysis based on quasilinear process. (auth)

**25663** SYSTEM FOR RAPID INJECTION OF METAL ATOMS INTO PLASMAS. Marmar, E.S.; Cecchi, J.L.; Cohen, S.A. (Plasma Physics Laboratory, Princeton University, Princeton, New Jersey 08540). Rev. Sci. Instrum. 46: No. 9, 1149-1154 (Sept 1975).

A system for producing 300-μsec bursts of $10^{17}$ metal atoms with 3-eV average energy is described. It is shown that this system can be successfully used to introduce impurities into CTR-oriented tokamaks for transport and confinement studies. (auth)

**25664** BEHAVIOR OF SOME SINGLY IONIZED, HEAVY-ION IMPURITIES DURING COMPRESSION IN A THETA-PINCH PLASMA. Jalufka, N.W. (National Aeronautics and Space Administration, Langley Research Center, Hampton, Virginia 23665). Phys. Fluids 18: No. 8, 1051-1055 (Aug 1975).

The introduction of a small percentage of an impurity gas containing a desired element into a theta-pinch plasma is a standard procedure used to investigate the spectra and atomic processes of the element. This procedure assumes that the mixing ratio of impurity to fill gas remains constant during the collapse and heating phase. Spectroscopic investigations of the constant mixing ratio assumption for a 2 % neon and argon impurity verifies the assumption only for the neon impurity. However, for the 2 % argon impurity, only 20 to 25 % of the argon is in the high-temperature compressed plasma. It is concluded that the constant mixing ratio assumption is not applicable to the argon impurity. (auth)

**25665** HEATING OF END REGION PLASMA IN A THETA PINCH. Hess, R.A.; Griem, H.R. (Department of Physics and Astronomy, University of Maryland, College Park, Maryland 20742). Phys. Fluids 18: No. 8, 1056-1058 (Aug 1975).

Rapid heating of the plasma in the end region of a turbulent, collisionless theta pinch has been observed by spectroscopic methods. Nonclassical energy transport from the hot central plasma is the most probable explanation for this heating. (auth)

**25666** COLLISIONAL LOSSES FROM A MIRROR MACHINE WITH AN END STOPPER. McHarg, B.B. Jr.; Oakes, M.E. (Department of Physics, University of Texas, Austin, Texas 78712). Phys. Fluids 18: No. 8, 1059-1065 (Aug 1975).

Collisional losses from the ends of a mirror machine place substantial restrictions on the confinement time of a plasma in such a device. One method proposed to improve the viability of a mirror machine reactor is to reduce the end losses by some means other than the magnetostatic field. Such a device is called an end stopper and it has the effect of changing the loss cone of the usual mirror machine into a loss hyperboloid (two sheet). The end losses from a mirror machine with an ideal, perfectly reflecting end stopper are studied by numerically solving the Fokker–Planck equation with appropriate mirror-end stopper boundary conditions. The mirror and end stopper are assumed to be a square well system and only decay of the ions from the system is considered. (auth)

**25667** TRANSVERSE DIFFUSION OF PARTICLES AND ENERGY IN A LASER-HEATED PLASMA COLUMN. Bethe, H.A. (University of Washington, Seattle, Washington 98195); Vlases, G.C. Phys. Fluids 18: No. 8, 982-990 (Aug 1975).

In a laser-heated magnetically confined column of plasma separated from material walls by a vacuum field, laser energy absorption near the center leads to a "light pipe" effect essential to the concept of heating long columns to fusion temperatures. Outward diffusion of particles at the vacuum-plasma boundary tends to move the position of maximum density inward, and hence to narrow the light pipe, while over-all expansion of the heated column against the field tends to widen it. A model is formulated to describe these effects and is treated analytically and numerically. The results indicate that for conditions of interest, the light pipe will persist long enough to permit heating of reactor-scale columns. (auth)

**25668** ION CYCLOTRON-RESONANCE HEATING IN A TOROIDAL OCTUPOLE. Barter, J.D.; Sprott, J.C. (University of Wisconsin, Madison, Wisconsin 53706). Phys. Rev. Lett. 34: No. 26, 1607-1609 (30 June 1975).

rf power near the ion cyclotron-resonance frequency has been used to produce a hundredfold increase (from $\lesssim 1$ to $\sim 100$ eV) in the ion temperature in a toroidal octupole device. The heating produces no noticeable instabilities or other deleterious effects except for a high reflux of neutrals from the walls. The heating rate is consistent with theory and the limiting ion temperature is determined by charge-exchange losses. (auth)

**25669** ION HEATING BY EXPANSION OF BEAM-HEATED PLASMA. Chu, K.R. (Science Applications, Incorporated, McLean, Virginia 22101); Clark, R.W.; Lampe, M.; Liewer, P.C.; Manheimer, W.M. Phys. Rev. Lett. 35: No. 2, 94-98 (14 July 1975).

A column of plasma whose electrons are rapidly heated by an electron beam or laser will expand against the external magnetic field, setting up large-amplitude magnetosonic oscillations. We study the dissipation of these oscillations by anomalous resistance, ion Landau damping, and ion counterstreaming, and show that much of the initial $T_e$ can be converted into $T_i$. (auth)

**25670** BEAM SELF-TRAPPING AND DYNAMICS OF LASER-INDUCED MAGNETOPLASMAS. Loter, N.G.; Cohn, D.R.; Halverson, W.; Lax, B. (Francis Bitter National Magnet Laboratory, Massachusetts Institute of Technology, Cambridge, Massachusetts 02139). J. Appl. Phys. 46: No. 8, 3302-3309 (Aug 1975).

Spatially and temporally resolved measurements of transmitted laser radiation, radial density profiles, and plasma dynamics indicate beam self-trapping in $CO_2$ laser-induced helium plasmas in strong longitudinal magnetic fields. Trapping is observed for the cases of $\beta > 1$, $\beta \simeq 1$, and $\beta < 1$. Longitudinal plasma growth occurs principally by breakdown waves and weak radiation-supported detonation waves. (auth)

**25671** CURRENT FILAMENTATION IN PARALLEL-FIELD TURBULENT PLASMAS. Biskamp, D. (Max-Planck Institut für Plasmaphysik, Garching, West Germany); Horton, W. Jr. Phys. Rev. Lett. 35: No. 1, 39-42 (7 July 1975).

An electromagnetic instability leading to filamentation of the current flowing along a magnetic field in a highly resistive plasma is investigated. The instability provides a possible explanation of the discrepancy that exists between turbulent-heating experiments and numerical simulations of the electrostatic parallel-field current-driven instability. (auth)

**25672** KINETIC PROCESS OF PLASMA HEATING DUE TO ALFVÉN WAVE EXCITATION. Hasegawa, A.; Chen, L. (Bell Laboratories, Murray Hill, New Jersey 07974). Phys. Rev. Lett. 35: No. 6, 370-373 (11 Aug 1975).

We elucidate the kinetic process of plasma heating by the resonant excitation of the shear Alfvén wave. The heating occurs as a result of the damping of the modified (by the finite ion Larmor radius and electron inertia) Alfvén wave which is excited by mode conversion at the resonant layer. The heating rates of ions and of electrons are comparable in the collisional regime; otherwise electrons are predominantly heated. (auth)

## Plasma Diagnostics

*Refer also to abstract 25930.*

**25673** (AED-CONF-74-085-010) THOMSON SCATTERING IN A STATIONARY H ARC WITH A cw-Ar ION LASER STABILIZED BY A MAGNETIC FIELD. Hirsch, K.; Doebele, H. F. (Stuttgart Univ. (TH) (F. R. Germany). Inst. fuer Plasmaforschung). 1974. 7p. (In German). INIS.

From spring meeting of the Deutsche Physikalische Gesellschaft e. V. of the Fachausschuesse: Atomphysik, Kurzzeitphysik, Molekularphysik, Plasmaphysik; Stuttgart, F. R. Germany (4 Mar 1974).

The paper discusses stationary and quasistationary scattering with in-face detection—a fairly new method of plasma diagnostics—

and its advantages. The signal-to-noise ratio is the most important quantity in in-phase detection. It was measured as a function of electron density as well as of measuring time with different laser power as parameter. The parameters of the magnetic-field stabilized light arc are given, and the experimental arrangement is described. Also measured were electron density and electron temperature with magnetic induction and plasma pressure as parameters. (GE)

**25674** (AED-CONF-74-005-011) POSSIBILITIES OF LASER SCATTERING DIAGNOSTICS IN PLASMAS. Doebele, H. F. (Stuttgart Univ. (TH) (F. R. Germany). Inst. fuer Plasmaforschung). 1974. 36p. (In German). INIS.

From spring meeting of the Deutsche Physikalische Gesellschaft e. V. of the Fachausschuesse: Atomphysik, Kurzzeitphysik, Molekularphysik, Plasmaphysik; Stuttgart, F. R. Germany (4 Mar 1974).

The laser has opened many new possibilities for plasma diagnostics. Intensive monochromatic light sources with higher precision and better time resolution have helped to improve such well-known techniques as interferometry and Schlieren method. At the same time, the range of applicability was extended into the infrared range. Due to the wave length dependence of the plasma diffraction index, the effects increase approximately lambda in interferometry and approximately lambda$^2$ in the Schlieren methods. The laser also helped to develop entirely new methods such as utilization of the Faraday effect in the electrons of a plasma in a magnetic field which allows the calculation of the product $n_e \times B$ from the rotation of the polarization plane of monochromatic light with linear polarization. Here, too, the effect increases approximately lambda$^2$, and measurements have been carried out up to FIR (HCN,337 $\mu$). The best diagnostic possibilities are offered by the Thomson scattering diagnostics. Electron and ion temperatures, electron densities, drift velocities, magnetic fields, wave propagation and dissipation can be measured by this method. (auth)

**25675** (AED-CONF-75-043-018) MEASUREMENTS OF ELECTRON DENSITY AND HEAT CONDUCTION IN A DECAYING ARC DISCHARGE IN AIR. Arning, F.; Haesing, W.; Stojanoff, C. G. (Technische Hochschule Aachen (F. R. Germany). 1975. 5p. (In German). INIS.

From spring meeting of the Fachausschuesse Kurzzeitphysik and Plasma- und Gasentladungphysik of the DPG; Duesseldorf, F. R. Germany (4 Mar 1975).

Spectroscopic measurements were carried out at the NI 4,935 line of a decaying air arc. These measurements provide the basis for a space-time picture of the electron density for the first 200 $\mu$sec after interruption of the energy supply. In order to avoid a measurement of the whole line profile, the correlation between line maximum and total line intensity was calculated as a function of electron density and temperature and was then compared with the measured correlation. The electron densities thus obtained were compared with the electron densities calculated from the absolute line intensities on the assumption of thermal equilibrium. The temperature distribution is used to calculate the radial velocities. In the region of 7,000 K - 12,000 K, the thermal conductivity determined by instationary measurements is compared with results of stationary measurements. (auth)

**25676** (AED-CONF-75-043-026) MEASUREMENT OF PLASMA VELOCITIES BY DOPPLER-SHIFTED SPECTRAL LINES WITH SHIFTS OF FAR LESS THAN LINE WIDTH. Doebele, H. F.; Massig, J. H. (Stuttgart Univ. (TH) (F. R. Germany). Inst. fuer Plasmaforschung). 1975. 5p. (In German). INIS.

From spring meeting of the Fachausschuesse Kurzzeitphysik and Plasma- und Gasentladungsphysik; Duesseldorf, F. R. Germany (4 Mar 1975).

The new method for which the experimental arrangement is described is distinguished from similar methods by the fact that a high signal-to-noise ratio, Stark shifts of spectral lines or accidental disadjustment of the spectral filter do not affect the measured values. Plasma velocities were measured as a function of the so-called cold gas velocity which provides a measure for the rate of gas flow through the plasma torch. The lower threshold of sensitivity amounted to shifts of 1 mA for spectral lines of a width of about 1 A. (GG/AK)

**25677** (AED-CONF-75-043-027) STATIONARY LASER SCATTERING MEASUREMENTS IN A H-ARC STABILIZED BY A MAGNETIC FIELD: TEMPERATURE MEASUREMENT OF EXCITED H-ATOMS. Doebele, H. F.; Hirsch, K. (Stuttgart Univ. (TH) (F. R. Germany). Inst. fuer Plasmaforschung). 1975. 10p. (In German). INIS.

From spring meeting of the Fachausschuesse Kurzzeitphysik and Plasma- und Gasentladungsphysik of the DPG; Duesseldorf, F. R. Germany (4 Mar 1975).

The main advantages of stationary scattering diagnostics with gas lasers are shown, and the experimental arrangement for 90° scattering experiments is described. The Thomson scattering profile of free electrons measured at the magnetic-field stabilized light arc hydrogen plasma with the 5,145 A line of an Ar ion laser was used to determine $n_e = 2 \times 10^{15}/cm^{-3}$ and $T_e = 1.6$ eV. The blue 4,880 A line of the Ar ion laser near the H$\beta$ line was then used to measure the scattering profile of excited H atoms and to calculate the Doppler temperature of $T_2$ approximately 1.5 eV. The authors explain why a continuous Ar ion laser influences the arc plasma and induces plasma fluctuations. (GE)

**25678** (AED-CONF-75-043-030) SPACE- AND TIME-RESOLVED MEASUREMENTS OF SOFT X-RAY EMISSION IN THE PLASMA FOCUS. Nahrath, B. (Stuttgart Univ. (TH) (F. R. Germany). Inst. fuer Plasmaforschung). 1975. 5p. (In German). INIS.

From spring meeting of the Fachausschuesse Kurzzeitphysik and Plasma- und Gasentladungsphysik of the DPG; Duesseldorf, F. R. Germany (4 Mar 1975).

1 fig.

A deuterium plasma was diagnosed in the NESSI plasma focus facility with the aid of a pulsed channel plate. The time-dependence of the neutron yield of the electron temperature and of the intensity of the soft and hard X-rays was also determined. (GE)

**25679** (IPF-74-3) NEUTRON RADIOGRAPHY IN THE PLASMA FOCUS. Ruffner, D. (Stuttgart Univ. (TH) (F. R. Germany). Inst. fuer Plasmaforschung). May 1974. 86p. (In German). INIS.

46 figs.; 39 refs.

Starting with some theoretical considerations, the paper describes the experimental basis for neutron radiography in the plasma focus. With an appropriate combination of scintillator and image converter, average optical density can already be reached at neutron density of about $5 \times 10^4$ n/cm$^2$. Contrast studies near the plasma focus with the aid of neutrons have thus become possible for the first time. (auth)

**25680** (IPP-2/227) COMPUTING THE ELECTRON DENSITY PROFILE FROM MICROWAVE INTERFEROMETER MEASUREMENTS. Baker, K. (Max-Planck-Institut fuer Plasmaphysik, Garching/Muenchen (F. R. Germany)). Nov 1974. 27p. INIS. 3 refs. With figs. and tabs.

The plasma electron density profile can be deduced by measuring the phase change PSI over the plasma length using a multichannel microwave interferometer. An APL program originally developed by J. G. Wegrove to calculate this density and which is used on WIIB by E. Wuersching has been changed to provide a faster calculation time as well as modified to allow one to simulate the plasma numerically. The program was also enlarged to investigate various beam properties. The stellarator geometry prohibits the use of parallel probing beams which can be used with tokamaks. Moreover, the plasma cross section is closer to an ellipse than a circle which further complicates evaluation techniques. With the APL program, profiles can be produced quickly while experimental measurements are being taken. However, a FORTRAN translation primarily for use in Grenoble with Wega was made as the programs were further developed to include an error evaluation and an iteration technique in searching for an optimum beam spacing. Calculations using the geometrical configuration foreseen for Wega indicate that mathematical techniques used to deduce the density profile from a numerically simulated plasma yielded reasonable profiles even when 20% experimental error on phase measurements was included. There was found to be no unique optimum beam configuration. Dealing with each individual beam, it was found exact focusing is not critical. Assuming a fan-shaped microwave beam instead of an infinitely thin one, introduced an error of approximately 10%. The programs and their uses are described in detail here. All are related to the FORTRAN program PROFILE with experimental input values of phase change PSI or PSI values deduced from an assumed density. It gives as output an approximation of the density profile. (auth)

**25681** (N-73-23756) CURRENT EXTENSION FROM A QUASI-STEADY MPD ARCJET. Kuriki, K.; Inutake, M. (Tokyo Univ. (Japan). Inst. of Space and Aeronautical Science). Mar 1973. 17p. (ISAS-490). NTIS $3.00.

Experimental studies were made on the properties of a plasma stream emanating from a pulsed MPD arcjet. From diagnostic measurements, a large fraction of the discharge current was found to extend in the plasma downstream of the electrodes. This extending current was found to be desirable in the quasi-steady operation of an MPD arcjet. The quasi-steadiness should be inferred from the properties of the plasma flow as well as the current and voltage of the arc discharge. The current extension is strongly affected by the working gas injected before the arc dis-

charge, initial tank pressure and applied magnetic field. An instability was found to be induced by the extending current in the plasma plume. (auth)

**25682** (UCRL-50025-75-2, pp 13-18) THOMSON SCATTERING OF LASER LIGHT FROM A PLASMA. Peratt, A. L. 1 May 1975.

In Electronics Engineering Department quarterly report No. 2, 1975. (California Univ., Livermore (USA). Lawrence Livermore Lab.).

The incoherent scattering of laser light from an electromagnetic plasma forms the basis of a powerful diagnostics tool. This article describes an experiment designed to extract information about plasma densities, temperatures, and magnetic fields in a dynamic pinch plasma by means of ruby laser light. In addition, techniques involving the heterodyne detection of longer wavelength lasers are discussed, providing for the diagnostics of plasmas with densities ranging from $10^{11}$ cm$^{-3}$ through those associated with dense plasma focus and with temperatures of a few eV to several keV. (auth)

**25683** DISTRIBUTIONS OF CURRENT DENSITY AND HEAT FLUX AROUND A CYLINDRICAL PROBE IN AN ATMOSPHERIC PRESSURE PLASMA. Kanazawa, A. (Tokyo Inst. of Tech. (Japan). Faculty of Engineering); Nonouchi, S. Kagaku Kogaku; 38: No. 9, 643-648 (Sep 1974). (In Japanese).

The current density and heat flux distributions around circular cylinder immersed in an atmospheric pressure argon plasma flow of which temperature is 13,240°K and stream velocity is 230 m/sec were measured, and the applicability of a bare cylindrical probe to the dense plasma flow was investigated. It was found from the experimental and numerical studies that the current to the cylindrical probe is centered at the front stagnation region (the current density at the front stagnation point is 2,000 times as much as that at the rear stagnation point) because the front boundary layer is near the frozen state and the rear one is near thermal equilibrium. These matters show that the bare cylindrical probe can be used for study of the dense plasma flow with the aid of the analysis in the front stagnation region. (auth)

**25684** EIGENVALUES OF A PARALLEL-PLATE PLASMA WAVEGUIDE. Hashimoto, T.; Aoki, K. (Kyushu Univ., Fukuoka (Japan). Faculty of Engineering). Kyushu Daigaku Kogaku Shuho; 47: No. 4, 493-500 (Sep 1974). (In Japanese).

As one of the methods to measure plasma parameters, there is plasma diagnosis by microwaves, which utilizes the fact that the reflection and permeation characteristics of the microwaves vary according to plasma parameters. A simplest model of this plasma diagnosis method is a parallel-plate plasma waveguide system laterally oscillated by a parallel-plate waveguide. The problem of this oscillation system can be analysed by integral transformation as the boundary value problem of electromagnetic field. In advance of the analysis, it is necessary to know every eigenvalue of a parallel-plate plasma waveguide. The equation for the determination of the eigenvalues of a parallel-plate plasma waveguide is a transcendental equation, so that it is not easy to investigate the eigenvalues analytically. In this paper, the regions in which the eigenvalues can exist are decided analytically, and electromagnetic waves are classified. The eigenvalues were investigated in each region on the Allis diagram, and several eigenvalues were numerically indicated. These analytical results led to the fact that the behavior of the eigenvalues of a parallel-plate plasma waveguide to plasma parameters was almost the same as that of the eigenvalues of axis symmetrical mode in a circular plasma waveguide. (JA)

**25685** EFFECT OF THE FORM OF THE ELECTRON-ENERGY DISTRIBUTION FUNCTION ON THE VOLT-AMPERE RESPONSE CURVE OF A DOUBLE PROBE AND THE POTENTIAL OF A NULL CURRENT IN A PLASMA. Vasil'eva, I.A. (Institute of High Temperatures, Academy of Sciences of the USSR). High Temp. 12: No. 6, 1014-1018 (July 1975).

An approximate analytical expression for the volt-ampere response curve of a double probe is obtained using electron-energy ($\epsilon$) distribution functions of the form $f \sim \sqrt{\epsilon} \exp[(\epsilon/\alpha)^k]$, where $\alpha$ and k are positive constants. Relationships are derived by which one can determine the mean energy of the electrons from the derivative of the volt-ampere response curve at the origin and the saturation ion current. It is shown that the utilization of the standard method of analyzing the double-probe response curve, accurate only in the case of the Maxwell distribution ($k=1$), results in a large error in the determination of the characteristic energies of the electrons when $k \neq 1$. It is established that the form of the distribution function strongly affects the potential of a null current in a plasma. (auth)

**25686** HIGH-PRESSURE DISCHARGES. Asinovskii, É.I.; Zeigarnik, V.A. (Institute of High Temperatures, Academy of Sciences of the USSR). High Temp. 12: No. 6, 1120-1135 (July 1975).

This article discusses the main trends in investigations of high-pressure discharges and indicates the regions of permissible parameters; it takes note of the principal methods for the diagnosis of a gas-discharge plasma. (auth)

**25687** DIAGNOSTICS OF A STATIONARY MPD-TYPE PLASMA JET WITH A HCN LASER INTERFEROMETER. Graser, W.; Hoffmann, P. (DFVLR-Institut für Plasmadynamik, 7 Stuttgart 80, Pfaffenwaldring 38, West Germany). Appl. Phys. Lett. 27: No. 5, 273-275 (1 Sept 1975).

A HCN laser interferometer of the Ashby-Jephcott type operating at a wavelength of 337 μm was used to measure spatially resolved electron densities in a stationary MPD-type plasma jet with non-LTE behavior. Experiments were performed with and without superimposed magnetic fields up to 0.1 T at the exit of the plasma accelerator. Electron densities were obtained within the limits of $5\times10^{12}$ and $10^{15}$ cm$^{-3}$ with an accuracy better than 10%. Within the axially symmetric expanding plasma of about 15-cm average diameter and 50-cm length the radial resolving power came to less than 1 cm. So this technique has proved to be suitable to fill a gap in the diagnostics of stationary magnetized plasmas in the mean range of electron densities. (auth)

**25688** TIME-RESOLVED PINHOLE CAMERA FOR OBSERVATION OF NANOSECOND-DURATION X—UV PLASMA EMISSION. Johnson, D.J.; Stephanakis, S.J.; Boller, J.R. (Naval Research Laboratory, Washington, DC 20375). Rev. Sci. Instrum. 46: No. 9, 1155-1157 (Sept 1975).

A vacuum diode with a rear-mounted Pilot-B scintillator has been coupled with a conventional evacuated pinhole camera. The cathode of the diode is fabricated from 2-μ thick polycarbonate (Kimfol) with a 200-Å aluminum layer on the rear surface. Incident photons with energies above the carbon *K* edge (284 eV) are highly absorbed in the polycarbonate, but photons with energies below the *K* edge are absorbed in the aluminum and produce photoelectrons. This yields a photoelectron sensitivity which is peaked at approximately 275 eV. The photoelectrons are accelerated by a 10-kV cathode potential to an aluminum anode coating on the scintillator, and scintillation photons are observed with an image converter camera. Streak photographs of exploded-wire x–uv radiation taken with this system are presented. (auth)

**25689** DYNAMICS OF THE DENSE PLASMA FOCUS AS DETERMINED FROM AN ANALYSIS OF LASER SCATTERING SPECTRA. Downing, J.N. (Los Alamos Scientific Laboratory, University of California, Los Alamos, New Mexico 87544); Eisner, M. Phys. Fluids 18: No. 8, 991-1001 (Aug 1975).

Time resolved 90° scattering spectra have been observed from a dense plasma focus illuminated by a pulse of laser light, for two axial positions, 0.6 cm and 1.3 cm from the face of the center electrode. Scattered laser light was observable in the time interval from 10 nsec prior to the arrival of the collapse on axis until the time when the visible light bremsstrahlung from the dense pinch decreased below the background illumination of the plasma sheath. The frequency spectrum was markedly asymmetric about the laser frequency, and a model has been postulated which attributes the asymmetry to the effects of a nonisotropic velocity distribution. Analysis of the data based on this model has given the radial collapse velocity ($\simeq3.5\times10^7$ cm/sec), density ($2\text{–}4\times10^{19}$ cm$^{-3}$), and ion temperature ($\simeq70$ eV) in the plasma sheath. No scattering from the dense pinch region was observed, and an *implied* axial flow velocity of $> 10^8$ cm/sec was inferred from the experimental results. (auth)

**25690** ANODE PHENOMENA IN A COLLISION-DOMINATED PLASMA. Biblarz, O.; Dolson, R.C.; Shorb, A.M. (Naval Postgraduate School, Monterey, California 93940). J. Appl. Phys. 46: No. 8, 3342-3346 (Aug 1975).

Anodes display either a glow mode or a constricted mode in plasmas of interest for MHD generator applications. The purpose of this paper is to outline the conditions underlying the existence of anode constrictions or anode spots in conjunction with criteria governing the anode glow. A steady current flowing through velocity and thermal boundary layers is investigated. The sheath and the ambipolar region are considered from an approximation theory viewpoint, and then the nonexistence of a one-dimensional Cartesian or diffuse mode for a nonreacting anode region is shown using the continuum equations for electrostatic probes. (auth)

**25691** ELECTROSTATIC POTENTIAL DUE TO A FINITE NUMBER OF DOUBLE LAMINAE IN FREE SPACE. Pasha, M.L. (Department of Petroleum and Natural Gas, Mineral Industries Building, Pennsylvania State University, University Park, Pennsylvania 16802). J. Appl. Phys. 46: No. 8, 3368-3375 (Aug 1975).

The potential problems due to a finite number of double laminae in the form of disks and spherical caps are considered. The solution of each problem is reduced to the solution of some Fredholm integral equations of the second kind and Volterra integral equations of the first kind which are easily invertible. Detailed solutions are presented for the particular case of a pair of double laminae and the expressions for some

physical quantities such as the total charge on the laminae are derived. Even some of the limiting results obtained from the analysis of the particular case seem to be new. At the end of the paper some numerical solutions of the problem are obtained. (auth)

**25692** MEASUREMENT OF THE WIDTH AND THE SHIFT OF NOBLE GAS SPECTRAL LINES IN A SHOCK TUBE. Klein, P. Duesseldorf; Duesseldorf Univ. (1975). 94p. (In German). INIS.

Thesis.

Plasma generation and plasma state values are discussed along with the measurement of line width and line shift which are caused by the Stark effect of the microfields of a plasma and play an important part in plasma diagnostics. An apparatus for measuring these values as a factor of the electron density was developed, and investigations were carried out with Ar, Kr, and Xe. (GE)

**25693** EXPERIMENTAL SET-UP FOR OBTAINING TIME-RESOLVED SPECTRAL LINE PROFILES. Iordanescu, S.; Ionescu-Bujor, T. (Inst. of Physics, Bucharest). Rev. Roum. Phys.; 20: No. 1, 11-15(1975).

The electronic system designed for obtaining time-resolved line profiles using an oscillating Fabry-Perot interferometer is described. This system ensures a better than 1% linear correspondence between the oscilloscope time axis and wavelength scale and makes possible the investigation of transient plasmas at any instant of time in a range of 0 to 10 μsec starting from the discharge onset. (auth)

**25694** DETERMINATION OF THE OPTICAL THICKNESS OF AN INHOMOGENEOUS PLASMA USING THE DISPERSION WINGS OF SELF-REVERSED LINES. Luizova, L.A. Opt. Spectrosc. (USSR) 38: No. 4, 362-363 (Apr 1975).

A method for treating experimental data obtained by observing the self-reversed line profile recorded with and without a mirror behind the discharge tube is described. The method allows one to find the optical thickness of a plasma and the radial distribution of the absorbing atoms without using data on the mirror reflectance. (auth)

## Plasma Kinetics (General)

**25695** (IPP-0/26) TRANSVERSE COLLECTIVE BEAM FORCES AND SELF-INFLECTION OF A RELATIVISTIC ELECTRON BEAM IN AXISYMMETRIC MAGNETIC FIELDS. Hofmann, I.; Luccio, A. U.; Nielsen, C. E. (Max-Planck-Institut fuer Plasmaphysik, Garching/Muenchen (F. R. Germany)). Dec 1974. 33p. INIS.

12 figs.; 1 tab.; 8 refs.

The results of an analytical and numerical study of some effects of collective fields upon transverse oscillations of a REB in an axisymmetric magnetic field are presented. Intra-beam and beam-beam effects in multiturn systems are included and the various forms of space charge induced coupling investigated. The situation described is relevant to the first revolutions after injection of intense beams. Special account is given to self-inflection of a REB in an Electron Ring Accelerator. (auth)

**25696** (RISO-320, pp 61-68) PLASMA PHYSICS. Dec 1974.

In Physics Department annual progress report, 1 January–31 December 1974.

Brief discussions are given for the following topics: (1) solid $H_2$ film, (2) theory for pellet refuelling, (3) rotating plasma measurements, (4) spectra of rotating pellet-plasma interaction, (5) Farley instability in the Q-machine, (6) Kelvin-Helmholtz instability, (7) electron heating at the cyclotron resonance, and (8) ion beam instability. (MOW)

**25697** RADIATIVE ENERGY LOSSES IN A NONEQUILIBRIUM LITHIUM PLASMA. Potapov, A.V.; Tsvetkova, L.E. Opt. Spectrosc. (USSR) 38: No. 3, 253-255 (Mar 1975).

The results of a theoretical investigation into the radiative energy losses in a nonequilibrium lithium plasma are reported. (auth)

## Plasma Kinetics (Experimental)

**25698** EMISSION IN THE VACUUM UV BY A MOLECULAR-GAS PLASMA. Vargin, A.N.; Golubev, O.A.; Malkin, O.A. (Moscow Engineering Physics Institute). High Temp. 12: No. 5, 825-830 (May 1975).

Vacuum UV spectra have been recorded for nitrogen, oxygen, and carbon monoxide at about 10⁴°K and atmospheric pressure; absolute measurements have been made of the radiation energy distribution in the range 2500–1100 Å. The measured radiation intensities are compared with the theoretical results of [1–3], from which estimates were made of contributions from various radiation processes. The proportion of the radiation due to electron attachment giving the ions $N^-$, $O^-$, and $C^-$ has been determined, and the photodetachment cross sections have been determined for these ions. (auth)

**25699** TURBULENCE IN IMPLODING CYLINDRICAL ELECTROSTATIC ION-ACOUSTIC SHOCKS. Hershkowitz, N.; Christensen. T.E. (Department of Physics and Astronomy, University of Iowa, Iowa City, Iowa 52242). Phys. Rev. Lett. 35: No. 4, 216-219 (28 July 1975).

"Turbulent" electrostatic shocks with imploding cylindrical wave fronts were produced in a modified double-plasma device. The growth rate of turbulence is found to be less than for planar shocks produced in the same device. This behavior is attributed to the fact that for sufficiently small radii of curvature only cylindrically symmetric ion-acoustic modes will exhibit substantial growth while in the planar case maximum growth can occur for off-axis (three-dimensional) modes. (auth)

**25700** CENTRAL STRUCTURE OF LOW-$n$ BALMER LINES IN DENSE PLASMAS. Hey, J.D.; Griem, H.R. (Department of Physics and Astronomy, University of Maryland, College Park, Maryland 20742). Phys. Rev. A 12: No. 1, 169-185 (July 1975).

Stark-broadened profiles of the Balmer lines $H_\alpha$ and $H_\beta$ have been measured by means of a high-pressure electromagnetically driven shock tube, at electron densities $N_e \sim 10^{17}$ cm$^{-3}$ and temperatures $\kappa T \sim 1.5$ eV. The measured profiles of $H_\alpha$, down to ~5% of peak intensity, are in much better agreement with the theoretical profiles of Kepple and Griem than with the results of more recent computations by Vidal, Cooper, and Smith. This suggests that for hydrogen lines with significant upper- and lower-state broadening, only *elastic* scattering contributions to the upper-lower state interference term should be included in the line-broadening operator. For $H_\beta$, agreement is obtained with both theories except within the central dip, the discrepancies between measured and predicted modulations being somewhat larger than those obtained in recent arc experiments. Our results for $H_\beta$ can be interpreted as indicating the presence of a transition layer of much lower electron density near the walls rather than the necessity for including the effects of ion dynamics in the calculations. The first-order dynamical correction to the Holtsmark profile for a single Stark component is considered in analogy with stellar dynamics, and found to be of negligible importance under our conditions. Additional measurements of the central structure of $D_\beta$ and the He I 4471-Å line are consistent with these conclusions. (auth)

**25701** PLASMA SHEATH PROPAGATION IN A COAXIAL ACCELERATOR. Ionescu-Bujor, T.; Iordanescu, S.; Mandache, N.; Zaharescu, M.; Zoita, A.; Zoita, V. (Inst. of Physics, Bucharest). Rev. Roum. Phys.; 20: No. 1, 51-58(1975).

The propagation of plasma sheath produced in a low-energy, gas-triggered, coaxial accelerator is studied using light guides and photomultipliers. The mass of the accelerated plasma increases during propagation and the total mass accelerated during one pulse depends on the operating voltage. Sheath velocities of the order of 5 cm/μsec have been obtained at the end of the accelerator. (auth)

## Plasma Kinetics (Theoretical)

**25702** (SAI-74-629-LJ) TRANSPORT AND ENERGY BALANCE STUDIES IN TOKAMAK CONFINEMENT SYSTEMS: A STATUS REPORT. Byrne, N.; Klein, H.; McBride, J.; Stuart, G.; Tamor, S. (Science Applications, Inc., La Jolla, Calif. (USA)). 20 Sep 1974. 130p. Dep. NTIS $9.50.

This report describes the results of a four-month program on fluid-numerical analysis of transport properties in Tokamak-type confined plasmas. Results presented include: (1) a one-dimensional transport code (G1M) to integrate fluid equations on either the Alfven-wave time scale or the diffusion time scale, and in slab, cylinder, or general 1-D metric geometry, (2) a survey of conditions for current and gradient driven instabilities to exist in the Tokamak skin phase, (3) application of the code to skin-phase studies using classical toroidal transport, (4) comparison of code results with conditions required for microinstabilities, (5) a Monte Carlo code which integrates the cyclotron radiation transfer equations for an arbitrary axisymmetric system in the absence of reflectors, (6) convergence studies on the radiation code, using Doublet III parameters, (7) a survey of possible operating points in TCT systems for fairly arbitrary values of magnetic field and beam current, and (8) a demonstration of the existence of multi-valued solutions to the equations for TCT operating points over a restricted range of beam current. (auth)

**25703** (TID-26860) SECOND QUARTERLY PROGRESS REPORT ON PLASMA COMPUTATIONAL RESEARCH. (California Univ., Berkeley (USA). Electronics Research Lab.). 1 Jul 1975. Contract E(04-3)-34. 35p. Dep. NTIS $4.75.

Summaries are given of research progress on the following areas: (1) one-dimensional diffusion code, ESIDIF, (2) simulation of cross field diffusion in the presence of an electrostatic wave, (3) nonphysical effects in quiet start computer simulations, (4) cold beam nonphysical instabilities and cures, (5) drift cyclotron instability theory, (6) diffusion model using an external wave and Coulomb collision operator, and (7) stability study of two-component plasmas by the extended Penrose criterion. (MOW)

**25704** CONTINUOUS EMISSION SPECTRUM OF A LOW-TEMPERATURE XENON PLASMA. Zemtsov, Yu.K.; Skorokhod, E.P. Opt. Spectrosc. (USSR) 38: No. 3, 250-252 (Mar 1975).

The absorption coefficient and emissivity of a xenon plasma are calculated at initial pressures of hundreds of Torr and temperatures of 5000–15 000 °K. (auth)

**25705** PSEUDOPOTENTIAL MODEL OF A NONIDEAL MULTIPLE IONIZED PLASMA, INVESTIGATED BY THE MONTE CARLO METHOD. Valuev, A.A.; Norman, G.É.; Filinov, V.S. (Institute of High Temperatures, Academy of Sciences of the USSR). High Temp. 12: No. 5, 818-824 (May 1975).

A pseudopotential model is proposed for a two-component plasma consisting of electrons and z-fold ions. Equations of state and correlation functions for z=2 and 4 are calculated in a wide range of the nonideality parameter by the Monte Carlo method. Results are also presented in reduced form, allowing determination of the charactericitics of the z dependence. The differences between electron-electron and ion-ion correlation functions are explained. Comparison is made with the linear and nonlinear Debye—Hückel approximations. (auth)

**25706** ONE-DIMENSIONAL FLOW OF A NONISOTHERMAL PLASMA. Mikulin, A.I. High Temp. 12: No. 6, 1058-1064 (July 1975).

An examination is made of quasi-one-dimensional flow of a two-component strongly nonisothermal plasma in a channel of variable cross section, allowing for heat transfer of the components. It is shown that the plasma flow regimes in the supersonic part of the channel depend appreciably on the heat transfer regimes for the plasma components in the subsonic part of the channel. Particular and numerical solutions are presented to illustrate these regimes. (auth)

**25707** FINITE HEAT CONDUCTION EFFECTS ON ION CYCLOTRON AND DRIFT CYLOTRON MODES. Hudson, M.K. (Space Sciences Laboratory, University of California, Berkeley, California 94720). Phys. Fluids 18: No. 8, 1077-1078 (Aug 1975).

Finite heat conduction effects on the ion cyclotron and drift cyclotron instabilities are investigated, and found to be destabilizing in certain regions of parameter space ($\nu \gg \omega$). (auth)

**25708** PLASMA SIMULATION STUDIES OF STIMULATED SCATTERING PROCESSES IN LASER-IRRADIATED PLASMAS. Forslund, D.W.; Kindel, J.M.; Lindman, E.L. (University of California, Los Alamos Scientific Laboratory, Los Alamos, New Mexico 87544). Phys. Fluids 18: No. 8, 1017-1030 (Aug 1975).

The behavior of stimulated Brillouin and Raman scattering is studied by a number of periodic and aperiodic plasma simulations. The one-dimensional studies at low power, roughly defined by the oscillating velocity of an electron being less than its thermal velocity, tend to support the spatial theory. Typically, in the aperiodic simulations trapping nonlinearities of the electrostatic wave and electron heating can saturate the amount of backscatter at a reasonable level. At high powers in both periodic and aperiodic simulations an x-type breaking or wave collapse phenomenon occurs after saturation which leads to an equilibration between pondermotive force, electron pressure, and ion pressure. Simulations of a random frequency modulated laser are discussed. Two-dimensional simulations and their relationship to the one-dimensional results are briefly mentioned. (auth)

**25709** TWO-DIMENSIONAL AND THREE-DIMENSIONAL ENVELOPE SOLITONS. Kaw, P.K.; Nishikawa, K.; Yoshida, Y. (Faculty of Science, Hiroshima University, Hiroshima, Japan); Hasegawa, A. Phys. Rev. Lett. 35: No. 2, 88-91 (14 July 1975).

We have obtained symmetric envelope solitons in two and three dimensions in a medium with a saturated nonlinear susceptibility given by $\chi_{NL} \sim \exp(-|\phi|^2)-1$, where $\phi$ is an appropriately normalized field amplitude. Examples for an electromagnetic wave and an electrostatic wave trapped in a plasma are presented. (auth)

**25710** ENERGY DEPOSITION INTO DENSE COLLISIONLESS PLASMAS BY ROTATING BEAMS. Chu, K.R. (Science Applications, Incorporated, 1651 Old Meadow Road, McLean, Virginia 22101); Kapetanakos, C.A.; Clark, R.W. Appl. Phys. Lett. 27: No. 4, 185-187 (15 Aug 1975).

A nonturbulent mechanism is proposed whereby a rotating electron or ion beam pulse rapidly deposits energy on the ions of a dense, magnetized, weakly collisional plasma through excitation of the compressional Alfvén mode. (auth)

**25711** CONDUCTIVITY OF IONIZED FLOWING GASES. Lee, J.J. (Laboratory of Plasmas Studies, Cornell University, Ithaca, New York 14850). Appl. Phys. Lett. 27: No. 4, 187-189 (15 Aug 1975).

In a previous paper, the electron distribution function for a weakly ionized flowing gas in an electric field has been derived. The distribution function is used to calculate the conductivity of the flow. First, the gas molecules are considered as hard spheres. The resulting formula is identical in form to that obtained by Margenau, except that a correction term due to the flow speed is included in the temperature. Next, the gas is treated as Maxwell molecules. In this case, when the field is perpendicular to the flow, the expression reduces to the familiar form $ne^2/m\ (\nu+i\omega)$, independent of the temperature and the flow speed. (auth)

**25712** ENERGY BALANCE IN A TWO-TEMPERATURE DEUTERIUM PLASMA. Ionescu-Pallas, N.; Visinescu, M.; Dorabantu, I. A. (Inst. of Atomic Physics, Bucharest). Rev. Roum. Phys.; 20: No. 1, 43-49(1975).

The energy transfer between the electron and deuteron components of a hot fully ionized deuterium plasma is studied under the following circumstances: (a) the prevailing mechanism is the elastic Coulombian scattering, (b) each charged particle is screened by the surrounding particles of opposite charge at the so-called "Debye radius", (c) Born approximation is used for estimating the collision cross-section, (d) local thermodynamic equilibrium and Maxwell-like velocity distribution do hold separately for electrons and deuterons. The rate of energy transfer is finally given as an analytical expression in terms of temperatures, particle densities and atomic constants. (auth)

# Plasma Production

**25713** OPTICS IN LASER-PRODUCED PLASMAS. Giovanielli, D.V.; Godwin, R.P. (University of California, Los Alamos Scientific Laboratory, Los Alamos, New Mexico 87544). Am. J. Phys. 43: No. 9, 808-817 (Sept 1975).

The concepts of linear optics are applied to the physics of energy coupling into laser-produced plasmas currently of interest in laser-initiated fusion research. The effects of polarization and angle of incidence upon reflection and refraction are recalled. Singular behavior occurs in the region of the plasma where the real part of the dielectric constant vanishes, the so-called "critical density" region. The effective generation of Langmuir waves at the surfaces of bounded plasmas through the optical resonance of obliquely incident electromagnetic radiation is heuristically discussed. Enhanced electric fields, enhanced "collisionless" damping, harmonic generation, the presence of energetic electrons, and density profile modifications which result near the critical density from the excitation of these plasma waves are described. While more complex plasma processes may occur, they are not within the scope of this review. (auth)

**25714** ELECTROSTATICALLY DRIVEN OVERDENSE RF PLASMA SOURCE. Motley, R.W.; Bernabei, S.; Hooke, W.M.; Jassby, D.L. (Plasma Physics Laboratory, Princeton University, Princeton, New Jersey 08540). J. Appl. Phys. 46: No. 8, 3286-3292 (Aug 1975).

We describe a radio-frequency plasma generator consisting of two collinear cylinders surrounding a magnetically confined plasma column, excited by up to 7 kW of power at 155 MHz. The source is capable of generating plasma densities of the order of $m_i/m_e$ times the critical density $n_c = m_e\omega^2/4\pi e^2$. The plasma density, the efficiencies of plasma heating, and the ion and electron heating associated with this generator are described in detail. (auth)

**25715** A STEADY-STATE HIGH-DENSITY MAGNETIZED ARCJET PLASMA COLUMN. Tang, J.T.; Luhmann, N.C. Jr.; Turechek, J. (University of California, Los Angeles, California 90024); Jassby, D.L. J. Appl. Phys. 46: No. 8, 3376-3380 (Aug 1975).

A four-stage differentially pumped arcjet system generates a fully ionized current-free 1-m-long plasma column of uniform density $10^{13} \lesssim n_e \lesssim 10^{15}$ cm$^{-3}$ and temperature $T_i \sim T_e \sim 1$–7 eV confined by an axial magnetic field up to 9 kG. The first three stages consist of an arc chamber, a separation chamber, and an experimental chamber. The addition of a fourth stage converts the device into a double-ended differentially pumped system; it ensures the uniformity of the plasma column in high-density plasma operation. The properties of the four-stage differentially pumped plasma system are reported. (auth)

**25716** SECOND-HARMONIC LIGHT FROM THE INTERACTION OF A NANOSECOND $CO_2$ LASER PULSE WITH THE PLASMA PRODUCED FROM POLYETHYLENE SHEET. Baldis, H.A.; Pépin, H.; Johnston, T.W.; Parbhakar, K.J. (Institut National de la Recherche Scientifique-Energie, Université du Québec, Varennes, Québec, Canada JOL 2PO). Phys. Rev. Lett. 35: No. 1, 37-39 (7 July 1975).

A 4-$J$, 10.6-$\mu$m, pulsed (2 nsec), $CO_2$ laser has produced small amounts ($4\times10^{-7}$ of incident fundamental) of second-harmonic back

emission (5.3 μm) with a definite threshold at about 1 *J*. Any three-halves frequency emission (7.07 μm) is at least 50 times fainter than the second harmonic. This is consistent with theoretical concepts. (auth)

**25717** TWO MODES OF OPERATION OF AN ARC PLASMA SOURCE IN AN EXTERNAL MAGNETIC FIELD. Korsun, A. G.; Meshcheryakov, S. A. Sov. Phys.-Tech. Phys.; 19: No. 11, 1500-1501 (May 1975).

Translated from Zh. Tekh. Fiz.; 44: No. 11, 2423-2425 (Nov 1974).

Two different modes of operation are found for a plasma source with an external axial magnetic field. In the 'cathode' the predominant axial voltage drop occurs near the axis. In this case the source produces an electron flux which carries a high proportion of the discharge power. As the discharge current and working gas flow rate increase, a transition to an "anode" mode occurs, in which the voltage drop is concentrated in a sheath near the anode, where an ion flux is formed. (auth)

# Plasma Stability

**25718** MULTIWAVE DECAY INTERACTIONS. Kol'chugina, I.A.; Litvak, A.G.; Khazanov, I.V. (Radiophysics Research Institute). JETP Lett. 21: No. 6, 147-148 (20 Mar 1975).

The stabilization of parametric instability of coherent plasma oscillations is investigated in the case when the energy transfer from the instability region into the dissipation region is effected by dynamic decay processes. (auth)

**25719** SELF-MODULATION OF HIGH-FREQUENCY ELECTRIC FIELD AND FORMATION OF PLASMA CAVITIES. Ikezi, H. (Nagoya Univ. (Japan). Inst. of Plasma Physics); Nishikawa, K.; Mima, K. J. Phys. Soc. Jpn.; 37: No. 3, 766-773 (Sep 1974).

Self-modulation of the oscillating electric field is observed when its frequency is near the electron plasma frequency. The localized field due to the self-modulation is found to make depressions in the plasma density, and to move in unison with the density dip with approximately the ion-acoustic speed. The maximum amplitudes of the high-frequency field and the density dip are linearly proportional to each other, but the former shows a phase jump at the bottom of the density dip. All these features are qualitatively explained by the results of the recent theory of coupled electron-plasma and ion-acoustic solitary waves. The self-modulation occurs in the overdense region, the parametric decay instability is observed in the underdense region. (auth)

**25720** EFFECT OF A MICROWAVE FIELD ON THE ION-ACOUSTIC INSTABILITY OF A HOMOGENEOUS PLASMA. Vokhmin, P.A.; Klimovskii, I.I. (Institute of High Temperatures, Academy of Sciences of the USSR). High Temp. 12: No. 6, 1154-1155 (July 1975).

Using a hydrodynamic approximation, the dispersion relations are derived for the question of stabilizing the ion-acoutic instability of a homogeneous weakly ionized plasma subjected to a microwave electric field. (AIP)

**25721** INCREASING THE EFFICIENCY OF A GASDYNAMIC LASER. Breev, V.V.; Kukharenko, A.T.; Napartovich, A.P.; Sharkov, V.F. (I. V. Kurchatov Atomic Energy Institute). High Temp. 12: No. 6, 1181-1182 (July 1975).

The results of calculations concerning the efficiency of carbon dioxide lasers are given. The possibility of improving the efficiency of the gasdynamic laser by mixing cold $CO_2$ into the wake behind the nozzle assembly is considered. (AIP)

**25722** LOWER-HYBRID BEAM-PLASMA INSTABILITY. Chang, R.P.H. (Bell Laboratories, Murray Hill, New Jersey 07974). Phys. Rev. Lett. 35: No. 5, 285-288 (4 Aug 1975).

Experimental and theoretical studies of the nonresonant lower-hybrid beam-plasma instability have been carried out. The instability has a maximum growth rate when the phase velocity of the wave along the magnetic field lines is comparable to the electron thermal velocity. Electron heating associated with this instability has also been observed. (auth)

**25723** THEORY OF RELATIVISTIC SELF-FOCUSING OF LASER RADIATION IN PLASMAS. Hora, H. (Photon Physics Group, Dept. Eng. Physics, Australian National University, Canberra and School of Physics, University of New South Wales, Kensington-Sydney, Australia). J. Opt. Soc. Am. 65: No. 8, 882-886 (Aug 1975).

Propagation into a homogeneous plasma of a laser beam at irradiances higher than 1/500 of the relativistic threshold can result in self-focusing due to the highly sensitive relativistic dependence of the optical constants on laser irradiance. Electron densities slightly less than the relativistic-cutoff densities are required. Simultaneously with the self-focusing, it is also possible to achieve a dielectric increase (swelling) of laser energy density in the plasma that could reach 1/3 of its maximum value. In prepulsed plasmas, generated by Nd-glass-laser pulses of $3\times10^{16}$ W/cm$^2$, relativistic diffraction-limited self-focusing can generate relativistic electron-oscillation energies and hence pair production. (auth)

**25724** STABILITY OF LARGE ASPECT RATIO DIFFUSE PROFILE TOKAMAKS WITH CIRCULAR FLUX SURFACES. Vahala, G. (Courant Institute of Mathematical Sciences, New York University, New York, New York 10012). Phys. Fluids 18: No. 8, 1034-1039 (Aug 1975).

It is shown that the stability of axisymmetric diffuse profile tokamaks is always governed by that of the straight cylindrical screw pinch if one assumes small deviations from circular flux surfaces and small inverse aspect ratio $\epsilon$, regardless of the ordering of $\beta$ in $\epsilon$. Unstable modes with very small growth rates or those which are very highly localized are excluded from this treatment. Suydam-type modes are included. The sharp boundary and diffuse profile results are compared and commented on. (auth)

**25725** INFLUENCE OF SELF-FIELDS ON THE FILAMENTATION INSTABILITY IN RELATIVISTIC BEAM-PLASMA SYSTEMS. Davidson, R.C. (Los Alamos Scientific Laboratory, University of California, Los Alamos, New Mexico 87544); Hui, B.H.; Kapetanakos, C.A. Phys. Fluids 18: No. 8, 1040-1044 (Aug 1975).

The influence of equilibrium self-fields on the filamentation instability in relativistic beam-plasma systems is investigated within the framework of a macroscopic cold-fluid description. For a low-density beam ($k_b<k_e$) propagating through a nonrelativistic plasma background, the instability criterion for ordinary-mode propagation perpendicular to $B^0_z\hat{e}_z$ is shown to be (assuming perturbations with $\partial/\partial\theta\approx0\approx\partial/\partial z$) $(\omega^2_{pb}\beta^2_{bz}/\omega^2_{cb})\{1+(2\omega^2_{pb}/\omega^2_{cb})\,[\beta^2_{bz}(1-f_M)-(1-f_q)]\}^{-1}>1$, where $\omega_{pb}$ is the beam plasma frequency, $\omega_{cb}$ is the beam cyclotron frequency, $\beta_{bz}c$ is the axial velocity of the beam, and $f_M$ and $f_q$ are the fractional current neutralization and fractional charge neutralization, respectively, by the background plasma. The azimuthal self-magnetic field has a stabilizing influence for $f_M<1$, whereas the radial self-electric field has a destabilizing influence for $f_q<1$. (auth)

**25726** ELECTROMAGNETIC ION CYCLOTRON INSTABILITY DRIVEN BY ION ENERGY ANISOTROPY IN HIGH-BETA PLASMAS. Davidson, R.C. (Los Alamos Scientific Laboratory, University of California, Los Alamos, New Mexico 87544); Ogden, J.M. Phys. Fluids 18: No. 8, 1045-1050 (Aug 1975).

Low frequency ($\omega\simeq\omega_{ci}=e_iB_0/m_ic$) transverse electromagnetic perturbations propagating parallel to a confining magnetic field $B_0\hat{e}_z$ are shown to exhibit instability in the presence of ion energy anisotropy with $T_{i\perp}>T_{i\parallel}$. The characteristic maximum growth rate for $T_{i\perp}>T_{i\parallel}$ is $\gamma_M\simeq(\beta_{i\perp}/2)^{1/2}\omega_{ci}$, where $\beta_{i\perp}=8\pi n_iT_{i\perp}/B^2_0$, and the wavelengths corresponding to instability are of order $c/\omega_{pi}$, where $\omega_{pi}$ is the ion plasma frequency. Within the context of a quasi-linear model, it is shown that the characteristic time scale for energy isotropization through nonlinear response of the ions to the instability is several $\gamma^{-1}_M$. Since $\gamma^{-1}_M<\tau_{i\parallel}$ (the ion-ion binary collision time) in typical high-density pinch experiments, this instablity appears to provide a viable collective mechanism for ion energy isotropization during the implosion or post-implosion phases of these experiments. It is also shown that the instability persists in the limit of weakly magnetized ions ($|\omega+i\gamma|>\omega_{ci}$, $k^2_zr^2_{Li}>1$) and strongly magnetized electrons ($|\omega+i\gamma|<\omega_{ce}$, $k^2_zr^2_{Le}<1$) provided $\beta_{i\perp}>1$. The instability also has applications to astrophysical plasmas with $T_{i\perp}>T_{i\parallel}$ as well as laboratory plasmas heated by neutral-particle injection perpendicular to $B_0$. (auth)

**25727** NONLINEAR EVOLUTION OF STIMULATED RAMAN BACKSCATTER IN COLD HOMOGENEOUS PLASMA. Koch, P.; Albritton, J. (Laboratory for Laser Energetics, College of Engineering and Applied Sciences, University of Rochester, Rochester, New York 14627). Phys. Rev. Lett. 34: No. 26, 1616-1620 (30 June 1975).

We present an analytic solution for Raman backscatter in a cold homogeneous plasma, valid until saturation by breaking of the longitudinal waves, or by self-consistent depletion of the pump. We give quantitative values for the pump strength necessary for the former to occur first, and the transmission at saturation. Nonlinear particle bunching causes growth of electromagnetic sidebands. In quarter-critical plasma, a sideband at $\omega=3/2\omega_0$ reaches 8% of the pump intensity at wave breaking. (auth)

**25728** LOW-FREQUENCY STABILITY OF ASTRON CONFIGURATIONS. Lovelace, R.V. (School of Applied and Engineering Physics and Laboratory of Plasma Studies, Cornell University, Ithaca, New York 14853). Phys. Rev. Lett. 35: No. 3, 162-164 (21 July 1975).

A sufficient condition is obtained for stability of low-frequency kink perturbations of an astron-type particle ring embedded in a dense low-temperature plasma. (auth)

**25729** A SIMPLE MODEL FOR HIGH-CURRENT ARCS STABILIZED BY FORCED CONVECTION. Lowke, J.J.; Ludwig, H.C. (Westinghouse Research Laboratories, Pittsburgh, Pennsylvania 15235). J. Appl. Phys. 46: No. 8, 3352-3360 (Aug 1975).

Using a one-dimensional analysis investigations are made of properties of arcs stabilized by forced convection in a nozzle. For the current regime where arc diameters are large enough so that conduction and turbulence losses can be neglected at the arc center, yet small enough so that axial pressure and velocity distributions are determined by the nozzle shape, a simple model yields the following analytic properties: (i) Electric field $E(z)$ and temperature distributions $T(z)$ are independent of current, $I$; (ii) arc area is proportional to arc current and is given approximately by a simple formula; (iii) $T(z)$ is approximately independent of $p_0$, but $E(z) \propto p_0^{1/2}$ and arc area $\propto 1/p_0^{1/2}$, where $p_0$ is the tank pressure; and (iv) the Cassie equation for the time variation of arc conductance is valid. It is assumed that the effective radiation-emission coefficient $U(T)$ is independent of arc radius. We have made measurements of arc area as a function of current in sulfur hexafluoride. These results, together with similar measurements of other investigators using also air and nitrogen, are in good agreement with the theoretical predictions. (auth)

**25730** PREDICTION OF PROPERTIES OF ARCS STABILIZED BY FORCED CONVECTION. Tuma, D.T.; Lowke, J.J. (Westinghouse Research Laboratories, Pittsburgh, Pennsylvania 15235). J. Appl. Phys. 46: No. 8, 3361-3367 (Aug 1975).

A one-dimensional arc model has been used to calculate the central temperature, arc radius, and electric field as a function of axial position for steady-state arcs in forced convection in nozzles. Calculations indicate that the axial distributions of pressure, plasma velocity, and gas velocity are sensitive to the degree of gas heating by the arc of the surrounding gas, significant differences being obtained between assumptions of the gas being isothermal or expanding adiabatically. Despite the fact that turbulence effects are omitted in the model, good agreement is obtained with experimental results of arc temperature, radius, and electric field for a 2000-A arc in nitrogen. Calculations as a function of current indicate regimes of low, intermediate, and high current where arc voltage respectively decreases, is constant, and increases with increase of current. In the latter regime, the increase in voltage is caused by the arc "clogging" or restricting the gas flow in the nozzle. (auth)

**25731** STABILIZATION OF TWO-STEAM INSTABILITIES. Buts, V. A. (Physicotechnical Inst., Kharkov). Sov. Phys.; Tech. Phys.; 19: No. 11, 1496-1497 (May 1975).

Translated from Zh. Tekh. Fiz.; 44: No. 11, 2419-2420 (Nov 1974).

It is shown that two-stream instabilities can be stabilized by electromagnetic waves or by variation of the beam velocity. (auth)

# Thermonuclear Engineering and Equipment

*Refer also to abstracts 25525, 25563, 25777, 25802, 26203, 26290, and 26291.*

**25732** (CONF-750723-14) CONSIDERATIONS OF TEST FACILITY REQUIREMENTS FOR CTR SURFACE SCIENCE EXPERIMENTS. Kaminsky, M. (Argonne National Lab., Ill. (USA)). 1975. Contract W-31-109-Eng-38. 34p. Dep. NTIS $4.75.

From international conference on radiation test facilities for the CTR surface and materials program; Argonne, Illinois, USA (15 Jul 1975).

During the operation of large size plasma facilities and future controlled thermonuclear fusion reactors the surfaces of such major components as container walls, beam limiters, diverter walls and beam-dump walls of the injector region will be exposed to particle and photon bombardment from primary plasma radiations and from secondary radiations. Such plasma radiations can cause, for example, physical and chemical sputtering, blistering, particle- and photon-impact induced desorption, secondary electron and x-ray emission, backscattering, nuclear reactions, photo-decomposition of surface compounds, photocatalysis, and vaporization. Such surface effects in turn can (a) seriously damage and erode the bombarded surface and (b) release major quantities of impurities which will contaminate the plasma. For a determination of the plasma impurity concentrations and the surface erosion rates it is necessary to know the yield values of the various particle emission phenomena. The need for radiation test facilities is described which will allow the study of individual surface processes with various types of single radiation sources. The subsequent need for multiple-component radiation sources that will allow in a controlled way the assessment of surface effects due to the simultaneous bombardment of surfaces by various combinations of specified types of particles and photons is also described. Finally, the need for plasma-radiation test facilities that will simulate more closely the plasma-radiation environment to be expected is considered. (auth)

**25733** (ERDA-50) PROCEEDINGS OF THE SYMPOSIUM ON TRITIUM TECHNOLOGY RELATED TO FUSION REACTOR SYSTEMS, MIAMISBURG, OHIO, OCTOBER 1-2, 1974. Smith, W. H.; Wilkes, W. R.; Wittenberg, L. J. (eds.). (Energy Research and Development Administration, Washington, D. C. (USA). Div. of Controlled Thermonuclear Research). Jun 1975. 171p. (CONF-741050-). Dep. NTIS $7.60.

From symposium on technology related for fusion reactor systems; Miamisburg, Ohio, USA (1 Oct 1974).

Separate abstracts were prepared for 12 of the included papers. (MOW)

*For abstracts of individual papers see: 25525, 25563, 25734-25742, and 26203.*

**25734** (ERDA-50, pp 5-14) ENVIRONMENTAL CONSIDERATIONS FOR ALTERNATIVE FUSION REACTOR BLANKETS. Johnson, A. B. Jr.; Young, J. R. (Battelle Pacific Northwest Labs., Richland, WA). Jun 1975.

From symposium on technology related for fusion reactor systems; Miamisburg, Ohio, USA (1 Oct 1974).

In proceedings of the symposium on tritium technology related to fusion reactor systems. (Energy Research and Development Administration, Washington, D. C. (USA). Div. of Controlled Thermonuclear Research).

Comparisons of alternative fusion reactor blanket/coolant systems suggest that environmental considerations will enter strongly into selection of design and materials. Liquid blankets and coolants tend to maximize transport of radioactive corrosion products. Liquid lithium interacts strongly with tritium, minimizing permeation and escape of gaseous tritium in accidents. However, liquid lithium coolants tend to create large tritium inventories and have a large fire potential compared to flibe and solid blankets. Helium coolants minimize radiation transport, but do not have ability to bind the tritium in case of accidental releases. (auth)

**25735** (ERDA-50, pp 15-29) TRITIUM DIFFUSION IN FUSION REACTOR MATERIALS. Elleman, T. S.; Verghese, K. (North Carolina State Univ., Raleigh). Jun 1975.

From symposium on technology related for fusion reactor systems; Miamisburg, Ohio, USA (1 Oct 1974).

In proceedings of the symposium on tritium technology related to fusion reactor systems. (Energy Research and Development Administration, Washington, D. C. (USA). Div. of Controlled Thermonuclear Research).

Measured grain boundary diffusion coefficients for tritium in 304-stainless steel are observed to be many orders of magnitude above the measured bulk diffusion coefficients. Application of standard grain boundary diffusion models to these data suggest that grain boundary diffusion should be the principal transport mechanism for tritium in stainless steel. Niobium is proposed as a structural material for fusion reactors and as a possible membrane for the diffusion separation of tritium from the lithium blanket. Experiments on tritium release from niobium at low tritium concentrations show that release is controlled by a surface film, presumably an oxide layer, over the studied temperature range 20 to 900°C. Results above 500°C give tritium release rates consistent with bulk diffusion coefficients, but release results remain anomalous at lower temperatures. Available information on hydrogen diffusion in metal oxides suggests that ceramic materials may be useful as barriers to tritium diffusion. Calculations on the steady-state tritium transport in the torus of the Los Alamos theta-pinch fusion reactor show that the tritium migration is influenced by the tritium diffusion rates assumed for the ceramic insulators. Experiments on tritium diffusion in single-crystal alpha-alumina are underway in which the tritium is injected through neutron transmutation of a surface blanket of a $^6$Li salt, followed by measurement of the tritium release rate from the specimen. (MOW)

**25736** (ERDA-50, pp 30-40) DIFFUSION AND AUTORADIOGRAPHIC INVESTIGATIONS OF THE TRITIUM-304 STAINLESS STEEL SYSTEM. Downs, G. L.; Braun, J. D.; Chaney, K. F.; Powell, G. W. (Mound Lab., Miamisburg, OH). Jun 1975.

In proceedings of the symposium on tritium technology related to fusion reactor systems. (Energy Research and Development Administration, Washington, D. C. (USA). Div. of Controlled Thermonuclear Research).

The diffusion coefficient of tritium in 304-stainless steel at low temperatures (100 to 300°C) was determined. Autoradiography was used to establish the concentration as well as the distribution of tritium in the alloy. The autoradiographic study shows that tritium is distributed heterogeneously at room temperature in the cold-

worked alloy and also in the fusion zone of weldments. Tritium partitions preferentially to the delta ferrite in weldments and to martensite produced by the cold working of 304-stainless steel. (auth)

**25737** (ERDA-50, pp 50-59) TRITIUM EFFLUENT CONTROL PROJECT AT MOUND LABORATORY. Kershner, C. J. (Mound Lab., Miamisburg, OH). Jun 1975.

From symposium on technology related for fusion reactor systems; Miamisburg, Ohio, USA (1 Oct 1974).

In proceedings of the symposium on tritium technology related to fusion reactor systems. (Energy Research and Development Administration, Washington, D. C. (USA). Div. of Controlled Thermonuclear Research).

Tritium control technology and philosophies that have been developed at the various weapons complex sites can be drawn upon for the design and operation of fusion research facilities and Controlled Thermonuclear Reactor fuel cycle and tritium confinement systems. Historically, tritium control has been based on high volume air flows and dilution of effluent systems. As a consequence of the "as low as practical" criterion, control philosophies were reevaluated and control efforts intensified. It is the results of these recent efforts that are most applicable to the CTR program. At Mound Laboratory the tritium control development efforts are centered around an advanced technology project. The philosophy and goals of this project and a nearly completed pilot scale effluent control laboratory are described. (auth)

**25738** (ERDA-50, pp 60-75) CURRENT SANDIA PROGRAMS AND LABORATORY FACILITIES FOR TRITIUM RESEARCH. Swansiger, W. A.; West, L. A. (Sandia Labs., Livermore, CA). Jun 1975.

From symposium on technology related for fusion reactor systems; Miamisburg, Ohio, USA (1 Oct 1974).

In proceedings of the symposium on tritium technology related to fusion reactor systems. (Energy Research and Development Administration, Washington, D.C. (USA). Div. of Controlled Thermonuclear Research).

Currently envisioned fusion reactor systems will contain substantial quantities of tritium. Strict control of the overall tritium inventory and environmental safety considerations require an accurate knowledge of the behavior of this isotope in the presence of Controlled Thermonuclear Reactor (CTR) materials. A 14,000 $ft^2$ laboratory for tritium research is currently under construction at Sandia Laboratories in Livermore. Details about the laboratory in general are provided. Results from studies of hydrogen isotope diffusion in surface-characterized metals will be presented. Details of two permeation systems (one for hydrogen and deuterium, the other for tritium) will be discussed. Data will also be presented concerning the gettering of hydrogen isotopes and application to CTR collector designs. (auth)

**25739** (ERDA-50, pp 76-86) TRITIUM PROBLEMS IN FUSION REACTOR SYSTEMS. Hickman, R. G. (Univ. of California, Livermore). Jun 1975.

From symposium on technology related for fusion reactor systems; Miamisburg, Ohio, USA (1 Oct 1974).

In proceedings of the symposium on tritium technology related to fusion reactor systems. (Energy Research and Development Administration, Washington, D. C. (USA). Div. of Controlled Thermonuclear Research).

A brief introduction is given to the role tritium will play in the development of fusion power. The biological and worldwide environmental behavior of tritium is reviewed. The tritium problems expected in fusion power reactors are outlined. A few thoughts on tritium permeation and recent results for tritium cleanup and $CT_4$ accumulation are presented. Problems involving the recovery of tritium from the breeding blanket in fusion power reactors are also considered, including the possible effect of impurities in lithium blankets and the use of lithium as a regenerable getter pump. (auth)

**25740** (ERDA-50, pp 89-104) METAL TRITIDE TECHNOLOGY. Bowman, R. C.; Carlson, R. S.; Attalla, A.; Wiedenheft, C. J.; DeSando, R. J. (Mound Lab., Miamisburg, OH). Jun 1975.

From symposium on technology related for fusion reactor systems; Miamisburg, Ohio, USA (1 Oct 1974).

In proceedings of the symposium on tritium technology related to fusion reactor systems. (Energy Research and Development Administration, Washington, D. C. (USA). Div of Controlled Thermonuclear Research).

Tritide forming metals and alloys may function as convenient and efficient collectors and storage materials for deuterium and tritium. These materials could effectively store the tritium recovered from the blanket or collected from other parts of the reactor. In view of the tritium storage capacity of metal tritides, these systems could function as effective tritium pumps. Tritium could also be regenerated from the metal tritide to be reclaimed as a fuel. Several metal tritides have been investigated at Mound Laboratory in recent years with emphasis on evaluating their physical characteristics and radiation damage behavior. This paper briefly summarizes some of these results on pressure-composition-temperature relations, gas release annealing behavior, and pulse nuclear magnetic resonance (NMR) studies of radiation damage properties for selected metal tritides. (auth)

**25741** (ERDA-50, pp 105-112) ENGINEERING STUDIES OF TRITIUM RECOVERY FROM CTR BLANKETS AND PLASMA EXHAUST. Watson, J. S. (Holifield National Lab., Oak Ridge, TN). Jun 1975.

From symposium on technology related for fusion reactor systems; Miamisburg, Ohio, USA (1 Oct 1974).

In proceedings of the symposium on tritium technology related to fusion reactor systems. (Energy Research and Development Administration, Washington, D. C. (USA). Div. of Controlled Thermonuclear Research).

Engineering studies on tritium handling problems in fusion reactors have included conceptual and experimental studies of techniques for recovery of tritium bred in the reactor blanket and conceptual designs for recovery and processing of tritium from plasma exhausts. The process requirements and promising techniques for the blanket system depend upon the materials used for the blanket, coolant, and structure and on the operating temperatures. Process requirements are likely to be set in some systems by allowable loss rates to the steam system or by inventory considerations. Conceptual studies have also been made for tritium handling equipment for fueling, recovery, and processing in plasma recycle systems of fusion reactors, and a specific design has been prepared for "near-term" Tokamak experiments. (auth)

**25742** (ERDA-50, pp 133-155) PRELIMINARY DESIGN OF THE TRITIUM HANDLING FACILITIES FOR THE PROPOSED LOS ALAMOS FUSION TEST REACTOR. Vier, D. T.; Anderson, J. L.; Krakowski, R. A. (Los Alamos Scientific Lab., CA). Jun 1975.

From symposium on technology related for fusion reactor systems; Miamisburg, Ohio, USA (1 Oct 1974).

In proceedings of the symposium on tritium technology related to fusion reactor systems. (Energy Research and Development Administration, Washington, D. C. (USA). Div. of Controlled Thermonuclear Research).

The proposed Los Alamos Fusion Test Reactor is a theta-pinch machine with a major radius of 40 m and a minor radius of 10.5 cm. The reactor will be designed for 40-50 shots per day of which four may be D-T shots and the rest D-D shots. The tritium handling facilities include a gas injector system, vacuum system, a tritium waste treatment system for vacuum pump effluents and a large, cell cleanup system. The injector system will use a uranium bed as the tritium source. The vacuum system is an ultraclean, all-cryogenic system using an array of cryo-pumps and cryosorption pumps. The tritium waste treatment system will effectively remove all tritium from vacuum pump exhausts prior to their release to the atmosphere. A larger system will be used to clean up tritium from the air in the reactor cell if a major failure occurs, thus contaminating the cell with tritium. The entire system is being designed to keep the maximum credible tritium release during such a major failure to approximately 0.3 g. Both cleanup systems will remove tritium from air by the conversion of all hydrogen isotopes to water followed by adsorption of the water on molecular sieve. (MOW)

**25743** (LA-5980) XPECT: A MONTE CARLO PROGRAM TO PREDICT THE EXPECTED-TIME-TO-NEXT-FAILURE IN CONTROLLED THERMONUCLEAR RESEARCH SYSTEMS. Boicourt, G. P. (Los Alamos Scientific Lab., N. Mex. (USA)). Aug 1975. 36p. Dep. NTIS $4.00.

The ability to predict failure rates is of increasing importance in controlled thermonuclear research (CTR) engineering as the systems increase in size. If a large CTR system is assembled without an examination of failure rates, its usefulness may be limited by insufficient time between failures. The usual mean-time-between-failure calculation does not apply here. Instead, an analogous quantity, the expected-time-to-next-failure, is defined and a Monte Carlo program (XPECT) is given for its computation. The computation takes advantage of the fact that failures in present CTR systems occur predominantly in developmental components being used in large quantities. (auth)

**25744** (LA-UR-75-636) MICROSPHERICAL LASER TARGETS BY CHEMICAL VAPOR DEPOSITION. McCreary, W. J. (Los Alamos Scientific Lab., N. Mex. (USA)). Sep 1975. 13p. (CONF-750921-1). Dep. NTIS $4.00.

From 5th international conference on chemical vapor deposition; London, UK (22 Sep 1975).

Apparatus and process conditions are described for the chemical vapor deposition (CVD) of thin (0.5 to 5 mu m) metal shells onto hollow microspheres to alter their physical characteristics and to increase their strength. The metals, including Ni, Mo, Re and Mo-Re are deposited from the pyrolysis of their carbonyls onto the substrates in small volume (0.2 to 10 ml) fluid beds at reduced pressures, usually from 50 to 400 torr (6.6 kPa to 53.3 kPa). The substrates, ranging in size from approximately 40 mu m to 200 mu m, have very low mass and high surface to mass ratios and do not form conventional fluid beds. The procedures for coating these substrates have been modified to permit coating and recovering a few (approximately 20 particles) very carefully selected microspheres. Techniques developed to form freestanding thin wall metal microspheres by leaching soluble substrates through porous CVD shells which are then overcoated to close the pores and to increase the wall thickness are discussed. Some of the destructive and nondestructive tests used to evaluate the coated and gas filled microspheres are described. Some of the CVD Mo/Re coatings proved to be superconducting. (auth)

**25745** (ORNL-TM-4990) NUMERICAL SIMULATION FOR AXIALLY SYMMETRIC BEAMLETS IN THE DUOPIGATRON ION SOURCE. Jaeger, E. F.; Whitson, J. C. (Oak Ridge National Lab., Tenn. (USA)). Aug 1975. 47p. Dep. NTIS $5.50.

A convergent 2-D numerical model for cylindrically symmetric beamlets in the duoPIGatron ion source was developed. The model includes space charge of both ions and electrons, finite ion temperature at the source plasma, and a method of selecting the self-consistent emitter shape. Results show well focused beamlets for a sample problem which approximates the 25 keV ion source used for neutral injection in ORMAK. (auth)

**25746** (UCID-16874) DT FUSION NEUTRON IRRADIATION OF WRDC ELECTRON MICROSCOPY SAMPLES. MacLean, S. C. (California Univ., Livermore (USA). Lawrence Livermore Lab.). 18 Jul 1975. Contract W-7405-Eng-48. 11p. Dep. NTIS $4.00.

The experimental parameters for irradiating the above specimens with 14-MeV neutrons from the LLL Rotating Target Neutron Source are described. No test results are given. (MOW)

**25747** (UCID-16876) USSR IMPLODING LINER PROGRAM. Shearer, J. W. (California Univ., Livermore (USA). Lawrence Livermore Lab.). 6 Aug 1975. Contract W-7405-Eng-48. 16p. Dep. NTIS $4.00.

A summary is given of the history and rationale of the USSR program to implode metallic liners for the fusion program. The explosive driven, magnetic drive, and compressed gas driven research is reviewed. (MOW)

**25748** EFFECT OF THE CONDUCTING SHELL AND ITS GAP ON GENERATION OF THE VERTICAL MAGNETIC FIELD IN A TOKAMAK DEVICE. Matsuda, S.; Suzuki, N.; Ohga, T.; Itoh, S. (Japan Atomic Energy Research Inst., Tokai, Ibaraki. Tokai Research Establishment). Jpn. J. Appl. Phys.; 13: No. 10, 1604-1609 (Oct 1974).

The equilibrium of a plasma confined in tokamak devices with an iron core is obtained by a superposition of the vertical magnetic fields generated by the image current flowing in the conducting shell, by the external coils and by the leakage magnetic field from the iron core. Among these the field by the shell plays the most significant role. However, it has been known theoretically that the existence of the shell gap decreases the vertical magnetic field by the shell, and it has been also suggested that the leakage magnetic field from the iron core is useful for compensating the dips of the vertical field near the shell gap. These vertical field distributions are investigated experimentally by using a special pick up coil and a simulated plasma current system to obtain the absolute intensity and the effect of the shell gap. The results give an effective gap width which is compared with the approximate theories. (auth)

**25749** NUMERICAL CALCULATIONS OF SCREW AND REVERSED FIELD PINCH PLASMAS. Hirano, Y.; Kiyama, S.; Shimada, T.; Ogawa, K. (Electrotechnical Lab., Tanashi, Tokyo (Japan). Tanashi Branch). Denshi Gijutsu Sogo Kenkyusho Iho; 38: No. 3-5, 156-172 (Jul 1974). (In Japanese).

A numerical calculation code for the linear screw and reversed field pinches is developed. A fully ionized plasma is assumed. To this plasma cylindrically-symmetric magnetic fields are applied, thus causing a pinch collapse. The plasma is treated in hydromagnetic approximation including the electric and thermal conductivity. Separated temperatures are assigned to the electrons and ions. External current circuits are considered so as to satisfy self-consistently the boundary conditions for the axial and azimuthal magnetic fields. The results of the numerical calculations are in good agreement with experimental results, such as those obtained on the diamagnetic signal, the period of the radial oscillation of plasma, the electron temperature and density measured by the laser-scattering and the magnetic fields in the plasma measured with the magnetic probes. A numerical study of the screw pinch plasma is made in the range of the initial density, $5 \times 10^{14} \sim 10^{16}/cm^3$; initial temperature of the plasma, 0.1 ~ 5 eV; maximum value of the magnetic field, 10 ~ 20 kG; and bias field for the axial magnetic field 0.25 ~ 1 kG; and using some other parameters. An interesting result is that the beta value of the plasma decreases when the positive bias field is applied, or the initial temperature of the plasma is relatively low. The positive bias field makes a deep pitch minimum of the magnetic lines of force. Therefore the magnetohydrodynamic stability is seriously affected by the positive bias field. This condition of the stability is improved by starting the Z-discharge shortly before the theta-discharge. The stable configuration of the reversed field pinch proposed by Robinson, et al. is numerically examined. (auth)

**25750** ESTIMATION OF TEMPERATURE AND HEAT FLUX IN A PULSED ELECTROMAGNETIC PLASMA ACCELERATOR. Rushailo, A.M. High Temp. 12: No. 6, 1115-1119 (July 1975).

A theoretical model is presented for the thermal processes in an extended accelerator [1−3] with the following characteristic parameters: current density j about 200 $A/cm^2$, temperature at core of flow $t_* \sim 2.5 \cdot 10^{4\circ}K$, wall temperature $t_w \sim 10^{3\circ}K$, plasma density $\rho \sim 10^{-7}$ $g/cm^3$ ($n \sim 10^{16} - 10^{17}$ $cm^{-3}$), speed at start of the channel $v_0 \sim 10^6$ cm/sec, at the exit $v \sim 7 \cdot 10^6$ cm/sec, and $Pr \sim 10^{-2}$ and $Re \sim 10^3$. The mechanism is considered for transfer of Joule dissipation from the plasma to the walls by electron conduction incorporating the variability in the transfer coefficients and the presence of a relatively cold layer near the electrodes. (auth)

**25751** PLASMA-CATHODE ELECTRON GUN. Bayless, J.R. (Hughes Research Laboratories, 3011 Malibu Canyon Road, Malibu, California 90265). Rev. Sci. Instrum. 46: No. 9, 1158-1160 (Sept 1975).

The plasma-cathode electron gun is a new type of electron source which is suitable for applications requiring a large area, high-energy electron beam. It employs a plasma generated within a cold low-voltage, hollow-cathode discharge as the source of electrons. Plasma cathode devices are characterized by their simplicity and versatility, and they offer a number of advantages over other designs. An electron gun producing a beam with dimensions of 5×125 cm has been developed for use with high-power cw gas lasers. This device has been operated at beam energies of 150 keV and cw beam current densities of 0.1–0.2 $mA/cm^2$. (auth)

**25752** TECHNIQUE FOR SAMPLING GASES IN HOLLOW MICROSPHERES. Ebner, M.A.; Rensel, W.B. (KMS Fusion, Inc., Ann Arbor, Michigan 48106). Rev. Sci. Instrum. 46: No. 9, 1290-1291 (Sept 1975).

A simple technique is described for inserting single gas-filled laser fusion pellets into high-vacuum systems for qualitative gas analysis. (auth)

**25753** NEUTRON CAPTURE IN LASER-FUSION PELLETS. Henley, J.; Meldner, H.W. (Department of Physics and Institute for Pure and Applied Physical Sciences, University of California at San Diego, La Jolla, California 92037). Phys. Rev. C 12: No. 2, 407-412 (Aug 1975).

Investigating the feasibility of obtaining slow neutron fluencies sufficient for multiple-capture nucleosynthesis, we have applied a Monte Carlo technique to determine the moderation of neutrons in a superdense laser-energized fusion pellet. We studied pellets of varying chemical composition and structure ranging in size from $\rho R \sim 1$ to 50 $g/cm^2$ and found our results to be rather insensitive to the parametrization of the hydrodynamic motion. That is, the neutron spectra were largely unaffected by reasonable variations of peak density, time of disassembly, and shape of the density profile. A useful method of improving the ratio of moderated to unmoderated neutrons was to dilute the thermonuclear fuel with hydrogen and/or the addition of a beryllium reflector. We also calculated the ratio of fission, neutron capture, and $(n,p)$ reactions in pellets seeded with traces of $^{238}U$ target material. (auth)

## Wave Phenomena

*Refer also to abstracts 25649 and 25709.*

**25754** (IPP-4/82) COUPLING AND ABSORPTION OF LOWER-HYBRID WAVES IN A THERMONUCLEAR PLASMA. Puri, S.; Tutter, M. (Max-Planck-Institut fuer Plasmaphysik, Garching/Muenchen (F. R. Germany)). 1975. 56p. (AED-CONF-75-045-003). INIS.

From 2nd international congress on waves and instabilities in plasmas (SICWIP); Innsbruck, Austria (17 Mar 1975).

24 figs.; 2 tabs.; 56 refs. With abstract.

The three important aspects, namely 1) accessibility, 2) matching and 3) absorption of the lower-hybrid waves in a thermonuclear plasma are studied under idealized but physically pertinent conditions within the framework of linearized theory. (auth)

**25755** "ANOMALOUS" EFFECTS IN THE APPEARANCE OF A DETONATION WAVE AT A FREE SURFACE. Fortov, V.E.; Musyankov, S.I.; Yakushev, V.V.; Dremin, A.N. (Branch of the Institute of Chemical Physics, Academy of Sciences of the USSR, Chernogolovka). High Temp. 12: No. 5, 840-846 (May 1975).

Experimental results and estimates are presented for the thermodynamic, optical, electrical, gasdynamic, and mechanical properties of a plasmoid formed during the appearance of a detonation wave at a free surface. It is shown that the effects observed in the experiments are caused by the shock wave that is generated during expansion of the detonation products of a condensed explosive. (auth)

**25756** AN IONIZATION WAVE IN A TURBULENT GAS FLOW. Golubev, V.S.; Malikov, M.M. (I. V. Kurchatov Institute of Atomic Energy). High Temp. 12: No. 5, 831-834 (May 1975).

Propagation of the ionization front is considered for an electrical discharge in a turbulent gas flow; the basic mechanism for ionization energy transport through the wave front is transfer of plasma by turbulent velocity pulsations in the neutral gas. There is qualitative agreement between the calculated velocity for the ionization front and the available experimental evidence. (auth)

**25757** CREATION AND ANNIHILATION OF POSITIVE AND NEGATIVE PULSES IN AN UNSTABLE MACROPLASMA. Sato, T. (Geophysics Research Laboratory, University of Tokyo, Tokyo, 113, Japan). Phys. Rev. Lett. 35: No. 4, 223-226 (28 July 1975).

Repeated creation and annihilation of positive and negative pulses of spatially trapped particles are numerically observed as a result of nonlinear interactions in an extremely unstable macroplasma. Positive and negative pulses are successively created at opposite trapping boundaries and propagate toward each other with nearly constant speeds. Each pair of pulses collides and disappears at the center. New pulses are generated at shorter spacing, but propagate faster so that the time interval is nearly conserved. (auth)

**25758** EVALUATION OF PLASMA-WAVE SPECTRAL DENSITY FROM CROSS-POWER SPECTRA. Ilić, D.B.; Harker, K.J. (Institute for Plasma Research, Stanford University, Stanford, California 94305). Rev. Sci. Instrum. 46: No. 9, 1197-1200 (Sept 1975).

The plasma-wave spectral density is evaluated by performing a spatial Fourier transform on experimental cross-power spectra of ion acoustic waves. The cross-power spectra are recorded on analog magnetic tape, converted to digital form, transferred to digital magnetic tape, and Fourier transformed on a digital computer. The important effects of sampling, finite data strings, and data smoothing on the end results are discussed and illustrated. The results indicate the usefulness of the spectral density method for the study of nonlinear wave phenomena. (auth)

**25759** THIRD HARMONIC GENERATION FROM LASER-PRODUCED PLASMA. Baldis, H.A.; Pépin, H. (INRS-Energie, Université du Québec, Varennes, P.Q., JOL 2PO, Canada); Grek, B. Appl. Phys. Lett. 27: No. 5, 291-292 (1 Sept 1975).

Third harmonic emission has been observed from a laser-created plasma, using a nanosecond TEA $CO_2$ laser. The observed threshold for this emission is $6\times10^{12}$ W cm$^{-2}$. (auth)

**25760** NONLINEAR THIRD-HARMONIC GENERATION IN A PLASMA BY A GAUSSIAN ELECTROMAGNETIC BEAM: EFFECT OF SELF-FOCUSING. Sodha, M.S.; Khanna, R.K.; Tripathi, V.K. (Department of Physics, Indian Institute of Technology, New Delhi-110029, India). Phys. Rev. A 12: No. 1, 219-224 (July 1975).

With the use of expressions for the nonlinear current density derived previously, the generation of the third harmonic in a collisional plasma by a Gaussian electromagnetic beam has been studied when the power of the beam exceeds the critical power for self-focusing. The self-focusing is caused by the nonuniform heating and redistribution of electrons. It is seen that the self-focusing of the main beam enhances the power of harmonic output by about three orders of magnitude in a typical case in the paraxial-ray approximation. The treatment is applicable after a time on the order of the energy relaxation time [$\sim (2m\nu/M)^{-1}$]. (auth)

**25761** FOCUSING OF FAST PLASMA SHOCK WAVES. Sandel, F.L.; Niimura, M.; Robertson, S.H.; Gross, R.A. (Plasma Physics Laboratory, Columbia University, New York, New York 10027). Phys. Fluids 18: No. 8, 1075-1076 (Aug 1975).

Plasma shock waves have been focused by reflection from an appropriately shaped end wall of a coaxial electromagnetically driven shock tube. The duration of the hot, dense focus, its spatial location, and the plasma properties at the focus are compared with computer simulation predictions. (auth)

**25762** EFFECT OF TRAPPING ON THE SATURATION OF THE RAMAN BACKSCATTER INSTABILITY. Klein, H.H.; Ott, E.; Manheimer, W.M. (Naval Research Laboratory, Washington, D.C. 20375). Phys. Fluids 18: No. 8, 1031-1033 (Aug 1975).

The criterion for whether the Raman backscatter instability saturates by electron trapping or by pump depletion is determined and tested by computer simulation. (auth)

**25763** THEORY OF STIMULATED SCATTERING PROCESSES IN LASER-IRRADIATED PLASMAS. Forslund, D.W.; Kindel, J.M.; Lindman, E.L. (Theoretical Division, University of California, Los Alamos Scientific Laboratory, Los Alamos, New Mexico 87545). Phys. Fluids 18: No. 8, 1002-1016 (Aug 1975).

Analytic theory of the linear and nonlinear behavior of the one-dimensional Brillouin and Raman scattering instabilities is given. Results are presented for the problems of an infinite homogeneous plasma and of a finite inhomogeneous plasma. Nonlinear fluid equations can predict backscatter energies the order of the incident laser energy; however, the size of the interaction region and nonlinear effects on the excited electrostatic wave are very important in determining the amount of backscatter. In many cases of contemporary interest for a high power laser incident on a target plasma, the latter effects can play a crucial role in reducing backscatter to a tolerable level. (auth)

**25764** OBSERVATION OF NONLINEAR LANDAU DAMPING OF BROAD-BAND PLASMA OSCILLATIONS. Matthieussent, G. (Laboratoire de Physique des Plasmas, Université de Paris Sud, Centre d'Orsay, 91 Orsay, France); Olivain, J. Phys. Rev. Lett. 34: No. 26, 1610-1613 (30 June 1975).

Nonlinear damping of a broad-band spectrum of plasma waves has been observed. Frequencies lower than the spectrum are growing from background noise. A shift of the entire spectrum towards lower frequencies results. The evolution of the spectrum is in good agreement with the predictions of weak-turbulence theory. Measurements of the electron velocity distribution are presented. (auth)

**25765** STOCHASTIC ACCELERATION BY A SINGLE WAVE IN A MAGNETIC FIELD. Smith, G.R.; Kaufman, A.N. (Department of Physics and Lawrence Berkeley Laboratory, University of California, Berkeley, California 94720). Phys. Rev. Lett. 34: No. 26, 1613-1616 (30 June 1975).

The nature of a particle orbit in an electrostatic plasma wave is modified by a magnetostatic field, because there exists a set of resonant parallel velocities $(\omega+l\Omega)/k_z$. If the wave amplitude $\Phi_0$ is sufficiently large, neighboring resonant regions overlap, and the particle motion becomes stochastic; the threshold condition is $k^2{}_r(e/m)\Phi_0|J(k_r\rho)|\simeq\Omega^2/16$. As an application, a weakly damped intermediate-frequency ion-acoustic wave may be used to heat the tail of an ion distribution. (auth)

**25766** SELF-FOCUSING AND SELF-DISTRIBUTION OF ELECTROMAGNETIC WAVES IN A PLASMA DUE TO COLLISION-INDUCED NONLINEARITY. Chandra, P.; Tripathi, V.K. (Department of Physics, Indian Institute of Technology, New Delhi-110029, India). J. Appl. Phys. 46: No. 8, 3320-3325 (Aug 1975).

In this paper we have investigated the nonlinear dielectric constant of a slightly ionized plasma showing the Ramsaver effect. Within the approximation of the Harp model for collisions (i.e., taking the collision frequency for electrons to be small below the speed $v=v_0$ and infinitely large above $v=v_0$) the heating of low-speed-domain electrons by the field of an electromagnetic wave and their subsequent transfer to the high-speed domain is the source of nonlinearity. The nonlinearity is seen to be a saturating function of the intensity of the beam. For a Gaussian beam this type of nonlinearity results in the self-made oscillatory waveguide propagation of the beam. The critical power for self-focusing is much smaller than that predicted by Stenflow and Yu. For a typical case of a plasma with $\omega^2{}_p/\omega^2\simeq0.2$, the self-focusing length of a beam of 400 W, $\omega\sim10^{14}$ sec$^{-1}$, $r_0=10c/w$, comes out to be 0.2 cm. However, below certain critical values of the initial beam radius ($r_0<r_0$ min), focusing cannot be obtained regardless of the power of the beam. For amplitude-modulated uniform plane waves, the nonlinearity results in the distortion of the amplitude envelope and the frequency broadening of the wave. (auth)

**25767** TRANSMISSION OF A TRANSIENT ELECTROMAGNETIC PLANE WAVE INTO A LOSSY HALF-SPACE. Papazoglou, T.M. (Department of Nuclear Engineering, University of Arizona, Tucson, Arizona 85721). J. Appl. Phys. 46: No. 8, 3333-3341 (Aug 1975).

The problem of a causal transient plane wave incident at an arbitrary angle on a lossy half-space is considered. The frequency domain solution is inverted to the time domain through a detailed analysis of its features in the complex frequency plane. Previously derived results for the interface are extended to include the interior of the dissipative medium. The effect of frequency dependence of the conductivity and permittivity of the lossy medium is considered. The Debye dispersion model is

adopted and is shown to be compatible with the analytical method employed. Numerical applications are provided for each case. (auth)

**25768** GENERATION AND BEHAVIOR OF LARGE-AMPLITUDE ION-ACOUSTIC WAVES. Karatzas, N.T.; Anastassiadis, A.J. (Plasma Physics Laboratory Nuclear Research Center "Democritus", Athens, Greece); Papadopoulos, K. Phys. Rev. Lett. 35: No. 1, 33-36 (7 July 1975).

Excitation of ion-acoustic waves by a current due to the dissipative effect of electron-neutral collisions is studied experimentally. The ion waves grow to a very large amplitude ($\delta n/n \sim 1$) where ion-trapping phenomena and sideband formation are expected to be important. (auth)

**25769** HELIUM BLAST-WAVE MEASUREMENTS OF LASER-HEATED MICROSHELL TARGETS. Leonard, T.A.; Mayer, F.J. (KMS Fusion, Incorporated, P. O. Box 1567, Ann Arbor, Michigan 48106). J. Appl. Phys. 46: No. 8, 3562-3565 (Aug 1975).

Measurements of blast waves produced by laser heating of spherical glass-shell targets in an atmosphere of 20 Torr helium are described. These measurements made use of a streak camera, monitoring the self-luminosity of the strong shock, a blast probe detecting the ionization behind the shock front, and a piezoelectric pressure probe recording the pressure pulse of the shock. The time history of the blast wave is used to determine the kinetic energy of target dissembly via a simple model which is applicable in both the strong-shock and acoustic regions. These measurements show that the inferred blast-wave energy increases for larger radius-time-shock coordinates. This anomalous effect is ascribed to "fast" ion preheating of the ambient helium gas in front of the shock wave. (auth)

**25770** LOSS OF NEUTRALIZATION FOR A STABLE NEUTRALIZED ION BEAM. Gabovich, M. D. (Inst. of Physics, Kiev). Sov. Phys.–Tech. Phys.; 19: No. 11, 1502-1503 (May 1975).

Translated from Zh. Tekh, Fiz.; 44: No. 11, 2425-2428 (Nov 1974).

The view is developed that the achievable degree of neutralization of an ion beam passing through a rarefied gas is associated with the transfer of energy to neutralizing electrons in Coulomb collisions with beam ions and in the excitation of electron plasma oscillations by the beam. (auth)

**25771** NONLINEAR BEHAVIOR OF MONOCHROMATIC SURFACE WAVES EXCITED BY A BEAM. Kitsenko, A. B.; Pankratov, I. M.; Stepanov, K. N. Sov. Phys.–Tech. Phys.; 19: No. 11, 1505-1506 (May 1975).

Translated from Zh. Tekh. Fiz.; 44: No. 11, 2430-2432 (Nov 1974).

The motion of a charged particle in the electric field of a monochromatic electrostatic surface wave of small but finite amplitude in an external magnetic field is analyzed by the method of averaging. The amplitude of a monochromatic surface wave excited by a monoenergetic low-density beam of particles is estimated in the saturation stage, in which the oscillation frequency of the trapped particles is of the same order as the linear growth rate. (auth)

**25772** METHOD FOR OPTICAL MODULATION OF AN ELECTRON BEAM. Sotnikov, V. I. (Moscow Physical-Technical Inst.). Sov. Phys.–Tech. Phys.; 19: No. 11, 1510-1511 (May 1975).

Translated from Zh. Tekh. Fiz.; 44: No. 11, 2436-2438 (Nov 1974).

It is proposed to modulate an electron beam by nonlinear transformation of an electromagnetic wave into a charge-density wave. Expressions are obtained for the modulation depth for a modified decay relation and the usual decay relation. (auth)

**25773** PROPAGATION OF SHOCK WAVES IN INHOMOGENEOUS MEDIA. Glatman, R. A. (Design and Research Inst., Leningrad). Sov. Phys.–Tech. Phys.; 19: No. 11, 1390-1392 (May 1975).

Translated from Zh. Tekh. Fiz.; 44: No. 11, 2250-2254 (Nov 1974).

A new model is proposed for an approximate solution of the problem of shock-wave propagation in an inhomogeneous medium which makes it possible to interpret the method developed by Whitham physically and to establish its region of applicability. General conditions are given for which use of the Whitham method gives good results. Particular cases of shock-wave motion in media with stationary inhomogeities are studied in hydrodynamics and magnetohydrodynamics; the propagation of weak shock waves is analyzed. (auth)

**25774** RESONANCE BROADENING FOR WAVE-PARTICLE AND WAVE-WAVE TURBULENCE. Fisch, N.J.; Bers, A. (Research Laboratory of Electronics and Department of Electrical Engineering and Computer Science, Massachusetts Institute of Technology, Cambridge, Massachusetts 02139). Phys. Rev. Lett. 35: No. 6, 373-376 (11 Aug 1975).

We propose an approximate but simple and general procedure for treating resonance broadening in weak-turbulence interactions. The resonance-broadening corrections to the wave-particle, wave-wave, nonlinear-Landau-damping, and four-wave weak-turbulence equations are computed as examples. The procedure may be used to predict at the outset whether resonance broadening occurs in a specific higher-order process. (auth)

# ENGINEERING

## Facilities and Equipment

**25775** (UCRL-50025-75-2) ELECTRONICS ENGINEERING DEPARTMENT QUARTERLY REPORT NO. 2, 1975. (California Univ., Livermore (USA). Lawrence Livermore Lab.). 1 May 1975. Contract W-7405-eng-48. 33p. Dep. NTIS $4.00.

Separate abstracts were prepared for ERA for the eight sections included. Only five sections were abstracted for NSA since the remaining three sections were not in scope for NSA. (WHK)

*For abstracts of individual sections see: 25682, 25878, and 25929–25931.*

### Lasers

*Refer also to abstract 26784.*

**25776** (SAND-75-0255) SANDIA TECHNOLOGY. Weber, J.; Mead, P. (eds.). (Sandia Labs., Albuquerque, N. Mex. (USA)). Aug 1975. Contract AT(29-1)-789. 39p. Dep. NTIS $4.00.

Significant development activities of Sandia Laboratories are reported in six sections. A separate abstract was prepared for each section for Energy Research Abstracts (ERA). Two sections were also in scope for NSA. (RCK)

*For abstracts of individual sections see: 25638 and 25777.*

**25777** (SAND-75-0255, pp 16-20) ELECTRON-BEAM INITIATED HF LASERS. Gerber, R. A.; Patterson, E. L. Aug 1975. In Sandia technology. (Sandia Labs., Albuquerque, N. Mex. (USA)).

Electron beams were used to ignite hydrogen/fluorine mixtures, producing laser energies up to 4.2 kJ, and giving hope that this approach may soon produce energy levels suitable for laser-fusion studies. (auth)

**25778** DEPENDENCE OF MOLECULAR-LASER EFFICIENCY ON THE EMISSION SPECTRUM. Igoshin, V.I.; Oraevskii, A.N. (P. N. Lebedev Physics Institute, USSR Academy of Sciences). JETP Lett. 21: No. 6, 148-150 (20 Mar 1975).

It is concluded that the efficiency of a molecular laser increases when the stimulated emission is shifted from the transition characterized by the maximum gain to higher rotational states. Methods of realizing this effect are proposed. (auth)

**25779** $CO_2$ LASER INITIATED BY A GLIDING DISCHARGE. Andreev, S.I.; Belousova, I.M.; Dashuk, P.N.; Zaroslov, D.Yu.; Zobov, E.A.; Karlov, N.V.; Kuz'min, G.P.; Nikiforov, S.M.; Prokhorov, A.M.; Sidorov, A.N.; Chelnokov, L.L.; Yarysheva, M.D. (P. N. Lebedev Physics Institute, USSR Academy of Sciences). JETP Lett. 21: No. 7, 194-195 (5 Apr 1975).

We report initiation of an autonomous volume discharge in the working mixture of a $CO_2$ laser by the radiation of a gliding discharge. Lasing is obtained at working-mixture pressures up to 105 atm. At an energy input to the volume discharge up to 150 J/liter atm, the output radiation energy amounted to 10 J/liter atm. (auth)

**25780** RUBY RING LASER SUBJECTED TO AN EXTERNAL SIGNAL. Antsiferov, V.V.; Derzhi, N.M.; Kuch'yanov, A.S.; Pivtsov, V.S.; Ugozhaev, V.D.; Folin, K.G. (Institute of Physics of Semiconductors, Siberian Branch, USSR Academy of Sciences, Novosibirsk). Sov. J. Quantum Electron. 5: No. 1, 30-32 (July 1975).

A superregenerative amplification scheme was used to obtain unidirectional stimulated emission from a ruby ring laser under free-oscillation and *Q*-switched conditions. The duration of external control pulses was either $t_i > L/c$ or $t_i < L/c$. The carrier frequency of giant pulses could be tuned within a range of 0.25 nm when the spectrum was $6\times10^{-5}$ nm wide. Reproducible generation of short high-coherence light pulses was achieved. (auth)

**25781** ELECTRON-BEAM-PUMPED $Al_xGa_{1-x}Sb$ SEMICONDUCTOR LASER. Akimov, Yu.A.; Burov, A.A.; Zagarinskii, E.A.; Kryukova, I.V.; Petrushenko, Yu.V.; Stepanov, B.M. (All-Union Scientific-Research Institute of Optophysical Measurements). Sov. J. Quantum Electron. 5: No. 1, 37-39 (July 1975).

Stimulated emission from $Al_xGa_{1-x}Sb$ solid solutions, excited by an electron beam and cooled with liquid nitrogen, was observed for the first time. This emission was observed throughout the direct-gap range of compositions and the emission wavelength was within the range 1.1–1.6 μ. The dependence of the forbidden-band width $E_g$ on the solid-solution composition $x$ was determined and the point of transition from the direct- to the indirect-gap structure was found ($x_c \simeq 0.25$, $E_{gc} \simeq 1.145$ eV). A discrepancy between the experimental results and a graphical determination of the dependence $E_g(x)$ was due to the influence of donor levels ($E_d \simeq 20$ meV) below the indirect $L$ minimum. The parameters of a sealed electron-beam-pumped laser made of such a material were determined. (auth)

**25782** INFLUENCE OF THE REFLECTION OF THE OUTPUT SIGNAL ON THE STABILITY OF THE FREQUENCY AND POWER OF A CARBON DIOXIDE LASER. Domanov, M.S.; Shcherbatykh, V.D. Sov. J. Quantum Electron. 5: No. 1, 55-58 (July 1975).

The results are given of calculations and an experimental investigation of the influence of the reflection of the output on the frequency and power of a single-frequency carbon dioxide laser. It is shown that, in the case of weak reflection, the dependences of the frequency and power on the distance from a reflecting object are sinusoidal and the maximum change in the frequency is proportional to the amplitude reflection coefficient of this object. In the case of strong reflection, the frequency exhibits a hysteresis and this results in hopping of the emission frequency from one branch of the frequency curve to another. The power may be modulated by 100% under these conditions. (auth)

**25783** POSSIBILITY OF CONSTRUCTING A FAR-ULTRAVIOLET LASER UTILIZING TRANSITIONS IN MULTIPLY CHARGED IONS IN AN INHOMOGENEOUS PLASMA. Vinogradov, A.V.; Sobel'man, I.I.; Yukov, E.A. (P. N. Lebedev Physics Institute, USSR Academy of Sciences, Moscow). Sov. J. Quantum Electron. 5: No. 1, 59-63 (July 1975).

Radiative characteristics of a laser plasma are considered. It is shown that a considerable proportion of the absorbed laser energy may be converted into resonance lines of multiply charged ions. Two methods for the utilization of resonance x-ray radiation in the population inversion in a two-component plasma are discussed. In one method, the resonance radiation of one component in the dense core of the plasma is used for selective resonance pumping of some level in the other component in the outer rare region. In the second method, the radiation of ions in the outer layer is used to photoionize ions in the inner core; this produces conditions analogous to those in a supercooled plasma and a population inversion is established. In all cases, the gain may be of the order of $10^3$ $cm^{-1}$. (auth)

**25784** SOME FEATURES OF THE KINETICS OF THE EMISSION SPECTRUM OF A LASER WITH A MOVING RUBY ROD. Tursonov, A.T. (Samarkand State University). Sov. J. Quantum Electron. 5: No. 1, 64-66 (July 1975).

An experimental investigation was made of the influence of the motion of a ruby laser rod, relative to standing waves in the resonator, on the kinetics of the emission spectrum. Two main types of change in the emission spectrum resulted from the motion of the ruby rod: In one case the emission frequency periodically increased and in the other it periodically decreased. A possible mechanism of these effects was considered. A kinematic modulation of the intensities of the individual modes, which appeared because of the scattering of light on inhomogeneities in the ruby rod, was also observed. (auth)

**25785** EXPERIMENTAL INVESTIGATION OF A GASDYNAMIC LASER UTILIZING MIXTURES OF CARBON MONOXIDE AND AN INERT GAS. Gavrikov, V.F.; Dronov, A.P.; Orlov, V.K.; Piskunov, A.K. Sov. J. Quantum Electron. 5: No. 1, 69-70 (July 1975).

Stimulated emission was obtained from mixtures of CO molecules with inert gases (He, Ne, Ar, Kr) expanding supersonically in a planar nozzle 4 cm long (the expansion ratio at the edge of the nozzle was 100). The influence of the nature of the inert gas and of the initial pressure of the mixture on the output power of the stimulated radiation was investigated. The effects observed in the CO gasdynamic laser could be explained by considering the vibration-vibrational ($\nu$-$\nu$) and vibration-translational ($\nu$-$T$) processes as the rotation-translational interaction. (auth)

**25786** FREQUENCY SCANNING IN A LASER WITH AN ACTIVE NEGATIVE FEEDBACK. Makogon, M.M.; Serdyukov, V.I. (Institute of Optics of the Atmosphere, Siberian Branch, USSR Academy of Sciences, Tomsk). Sov. J. Quantum Electron. 5: No. 1, 79-80 (July 1975).

The emission frequency of a laser with an active negative feedback was scanned. An interferometer with a piezoelectric ceramic element was used to control the frequency during stimulated emission. The frequency jumps during scanning were considerably smaller than under free-oscillation conditions and this was attributed to the elimination of the inhomogeneity of the population inversion. (auth)

**25787** CHEMICAL LASER UTILIZING A MIXTURE OF CARBON DISULFIDE AND SULFUR TRIOXIDE. Gerasimov, Yu.A.; Kashnikov, G.N.; Orlov, V.K.; Piskunov, A.K.; Romanenko, Yu.V.; Taran, A.V. Sov. J. Quantum Electron. 5: No. 1, 83-84 (July 1975).

Photoinitiated stimulated emission was obtained from a mixture of $CS_2$

and $SO_3$. The output energy was higher and the optimal pressure of $CS_2$ considerably lower than in the case of the $CS_2+O_2$ mixture. A qualitative explanation was provided of this increase in the efficiency of $CS_2$. (auth)

**25788** RESONANT ENHANCEMENT OF THE OUTPUT POWER OF A He–Ne LASER DUE TO MODULATION OF THE DISCHARGE CURRENT. Tuchin, V.V.; Akchurin, G.G. (N. G. Chernyshevskii State University, Saratov). Sov. J. Quantum Electron. 5: No. 1, 87-88 (July 1975).

It was found experimentally that the output power of an He–Ne laser ($\lambda=0.63$ μ) increased resonantly when the discharge current was modulated at a frequency $f_m \simeq 60$ kHz. This was attributed to a redistribution of the electrical properties of the gas-discharge plasma as a result of an artificial excitation of striae in the discharge. The possibility of using this phenomenon in the control of the output power of gas lasers was considered. (auth)

**25789** CALCULATION OF THE ENERGY CHARACTERISTICS OF A THERMALLY EXCITED CARBON DIOXIDE LASER. Anan'kin, A.I. Sov. J. Quantum Electron. 5: No. 1, 89-90 (July 1975).

The results are given of calculations of the output power of a thermally excited $CO_2$ laser. The influence of the initial pressure and temperature of the gas mixture on the specific power characteristics is discussed. (auth)

**25790** SEALED COPPER VAPOR LASER. Bokhan, P.A.; Nikolaev, V.N.; Solomonov, V.I. (Institute of the Optics of the Atmosphere, Siberian Branch, USSR Academy of Sciences, Tomsk). Sov. J. Quantum Electron. 5: No. 1, 96-98 (July 1975).

A description is given of the construction and power supply of a sealed copper vapor laser generating pulses at a repetition frequency of 6–10 kHz and producing an average power of 2 W. (auth)

**25791** SEMICONDUCTOR LASER WITH A DISTRIBUTED FEEDBACK. Luk'yanov, V.N.; Shelkov, N.V.; Yakubovich, S.D. Sov. J. Quantum Electron. 5: No. 1, 99-100 (July 1975).

Stimulated emission was obtained from an optically pumped gallium arsenide laser with a distributed feedback. The feedback was produced by a diffraction grating formed on the surface of a *p*-type GaAs layer prepared by the diffusion of zinc into an *n*-type substrate. The grating was in optical contact with the active layer and its period satisfied the Bragg condition for a guided mode within the gain band of the laser. For the selected Bragg scattering order, the radiation was extracted at right angles to the grating surface. The far-field distribution consisted of a single lobe with a divergence of 5–20′, which corresponded to the emission from one to five randomly distributed modes whose frequencies depended on the position of the excited region in the laser. (auth)

**25792** MODEL OF PULSATIONS OF THE RADIATION EMITTED BY A SOLID-STATE LASER. Kazantsev, A.P.; Krivoshchekov, G.V.; Semibalamut, V.M.; Smirnov, V.S. (Institute of Semiconductor Physics, Siberian Branch, USSR Academy of Sciences, Novosibirsk). Sov. J. Quantum Electron. 5: No. 1, 101-102 (July 1975).

A simple model is proposed for the description of pulsations (spiking) of the radiation emitted by a solid-state laser. The model is based on rate equations with random forces. When the noise level reaches a certain small critical value, the emission becomes quasiperiodic. Spiking is observed at a higher noise level. Experimental results obtained in studies of the amplitude stabilization are interpreted. (auth)

**25793** ORGANIC DYE LASER PUMPED BY IFP-40000 PULSE-DISCHARGE LAMPS. Strizhnev, V.S. (Institute of Physics, Belorussian SSR Academy of Sciences, Minsk). Sov. J. Quantum Electron. 5: No. 1, 119-120 (July 1975).

Solutions of complex organic compounds were used as the active medium in a high-power laser with an output energy of 27 J and an efficiency of 0.7%. The duration of the output pulses was 102 μsec. The angular and energy characteristics of the output radiation were determined. A strong influence of the homogeneity of the active solution on the stimulated emission was observed. (auth)

**25794** CONTINUOUSLY OPERATING $CO_2$ LASER WITH A NON-SELF-MAINTAINED DISCHARGE. Anokhin, A.V.; Babaev, I.K.; Blinov, N.A.; Grachev, A.F.; Dolgov-Savel'ev, G.G.; Mikhailov, M.D.; Orlov, V.K.; Razumtsev, V.F.; Savel'ev, V.V.; Cheburkin, N.V. Sov. J. Quantum Electron. 5: No. 1, 133-134 (July 1975).

A non-self-maintained gas discharge was used to excite the active medium of a cw carbon dioxide laser. Preionization was produced by an electron beam of 150 keV energy. The specific output power from a mode volume was 3 W/cm and the efficiency was 7%. A study was made of the influence of the processes occurring in the cathode region on the stability of the discharge and on the energy characteristics of the laser. (auth)

**25795** ELECTRON-BEAM-CONTROLLED PULSE LASER WITH AN OUTPUT ENERGY OF 500 J. Dolgov-Savel'ev, G.G.; Kon'kov, I.D.; Leont'ev, I.A.; Lyakishev, V.G.; Orlov, V.K.; Telepin, S.N.; Cheburkin, N.V. Sov. J. Quantum Electron. 5: No. 1, 135-136 (July 1975).

The results are given of an investigation of the energy characteristics of an electron-beam controlled $CO_2$ laser with a working volume of 10 liter kept at a gas pressure of 1 atm. A cold-cathode electron gun was used to generate the electron beam which preionized the active medium. A study was made of the operation of the electron accelerator in the case of different systems of supplying the voltage to the electron gun. Measurements were made of the magnitude, duration, and uniformity of the electron-beam current which passed through Ti and Al foils on its way to the discharge chamber. The parameters of the output radiation of the laser were determined. (auth)

**25796** LASER ACTION IN SOLUTIONS OF RHODAMINE 6G IN MIXED AQUEOUS-ORGANIC SOLVENTS. Smirnov, V.S.; Zabiyakin, Yu.E.; Bakhshiev, N.G. Opt. Spectrosc. (USSR) 38: No. 3, 334-335 (Mar 1975).

The spectral luminescence and lasing properties of solutions of rhodamine 6G in binary aqueous-organic solvents is investigated. It is shown that when the amount of the organic component in the solution is 30% or higher, the aggregation process of the dye is expressed only weakly and, in practice, does not have any effect on the spectral luminescence and lasing characteristics of the solvent. Moreover, the large total content of water in the solution favors a reduction of the induced, nonselective losses. All of this leads to an increase in the output energy of rhodamine 6G in comparison with that of the purely organic mixture by more than a factor of 2. (auth)

**25797** USE OF LUMINESCENCE CONVERTER IN A LAMP LASER BASED ON RHODAMINE 6G IN ETHANOL. Levin, M.B.; Cherkasov, A.S.; Shirokov, V.I. Opt. Spectrosc. (USSR) 38: No. 3, 336-338 (Mar 1975).

In a lamp laser based on rhodamine 6G in ethanol with the better of two experimental luminescence converters for the pump light with $10^{-3}$-$M$ solutions of the luminophor in ethanol, an increase in the output energy was achieved only for relatively small concentration $C_a$ of rhodamine 6G. But, in comparison with a nonluminous filter, which provided the same protection from photochemical damage for the active medium, the converter gives an energy increase over the whole experimental range of $C_a$, since, even for very large concentrations, $C_a=5\times10^{-5}M$, the output energy inceases by a factor 1.4. (auth)

**25798** SPECIAL FEATURES OF QUASICONTINUOUS LASING CONDITIONS OF A RUBY LASER WITH PLANE MIRRORS. Antsiferov, V.V.; Kuchyanov, A.S.; Pivtsov, V.S.; Ugozhaev, V.D.; Molin, K.G. Opt. Spectrosc. (USSR) 38: No. 3, 339-343 (Mar 1975).

A method for obtaining quasicontinuous $TEM_{00q}$ output in a ruby laser with plane mirrors is described. The possibility of reducing the effectiveness of mechanical perturbations to an insignificant level (without using specialized stabilization techniques) in lasing under conditions where the spatial inhomogeneities of the inversion are smoothed out has been experimentally demonstrated. The dynamics of the spectrum corresponding to a particular case are discussed for spiked laser conditions, which occur at the cessation of such smoothing: a regular gradual change in the frequency during lasing toward the long wavelength region at a rate of twice that of the thermal drift of the gain curve. Based on the experimental results, a comparison of the dynamics mode shift was carried out for the various operating regimes as well as a refinement of their classification according to this feature. (auth)

**25799** THEORY OF A RING LASER WITH AN INHOMOGENEOUS RESONATOR. Birman, A. Ya.; Savushkin, A.F. Opt. Spectrosc. (USSR) 38: No. 3, 348-350 (Mar 1975).

The equations for the complex amplitude of the oppositely traveling waves in a ring laser are formulated. The resonator is comprised of a transparent set of reflecting, focusing, absorbing, scattering, and anisotropic elements that are nonuniform in the transverse direction, with the parameters of active medium, located in a magnetic field also being distributed nonuniformly in the resonator. (auth)

**25800** RUBY LASER WITH VARIABLE RESONATOR LENGTH. Makogon, M.M. Opt. Spectrosc. (USSR) 38: No. 3, 351-352 (Mar 1975).

Measurements of the operation parameters of the ruby laser were made under varying resonator lengths in order to minimize random spiking. (AIP)

**25801** THEORY OF HIGH-SPEED FLOW GAS LASER. Vedenov, A.A.; Napartovich, A.P. (I. V. Kurchatov Institute of Atomic Energy). High Temp. 12: No. 5, 835-839 (May 1975).

The problem of determining the efficiency of a resonator through which an active laser medium flows is considered. An approximate approach is postulated by means of which answers can be obtained in real situations by simple calculations. An expression for the resonator efficiency is obtained in explicit form for certain realistic models of the $CO_2$ laser. The dependence of laser performance on many parameters is taken into account, and the problem of optimizing the output power with respect to these parameters can thus be set. (auth)

**25802** ONE NANOSECOND $CO_2$ LASER CHAIN FOR LASER–TARGET INTERACTION STUDIES. Rheault, F.; Lachambre, J.; Lavigne, P. (Defense Research Establishment, Valcartier,

P.O. Box 880, Courcelette, P.Q., Canada G0A 1R0); Pépin, H.; Baldis, H.A. Rev. Sci. Instrum. 46: No. 9, 1244-1248 (Sept 1975).

A $CO_2$ oscillator–amplifier laser system generating short pulses of radiation in the gigawatt range is described. Emphasis is laid upon self-oscillation problems associated with a high-gain amplifier chain. The insertion of $SF_6$, Freon, and $C_2H_5OH$ cells between the amplifier modules is found efficient in suppressing any oscillation in the presence of a polyethylene target. The characteristics of the output radiation are given together with the reflection measurements of the target during the interaction with the laser pulse. (auth)

**25803** Q—SWITCHING OF LASER CAVITY WITH AN OPEN-AIR SPARK GAP. Ishii, S.; Ahlborn, B. (Department of Physics, University of British Columbia, Vancouver, B.C. V6T 1W5, Canada). Rev. Sci. Instrum. 46: No. 9, 1287-1288 (Sept 1975).

A laser cavity has been Q-switched using a spark plasma as the optically active element. (auth)

**25804** EFFICIENT ELECTRICAL INITIATION OF AN HF CHEMICAL LASER. Mangano, J.A.; Limpaecher, R.L.; Daugherty, J.D.; Russell, F. (Avco Everett Research Laboratory, Incorporated, Everett, Massachusetts 02149). Appl. Phys. Lett. 27: No. 5, 293-295 (1 Sept 1975).

Efficient electron-beam initiation of an atmospheric-pressure HF chain-reaction laser has been demonstrated. Intrinsic electrical efficiencies of up to 875% have been observed with laser output energy densities of up to 51 J/liter atm at low initiation levels. This result was obtained for a laser mixture containing $H_2$:$F_2$:He:$O_2$ at mole fractions of 0.08:0.30:0.61:0.01. Laser output energy was extracted from a volume of 104 $cm^3$. (auth)

**25805** HIGH GAIN AT 10.6 mu m FROM AN ELECTRON-BEAM-CONTROLLED PULSED DISCHARGE. Carmichael, C. H. H.; Garnsworthy, R. K.; Mathias, L. E. S. (Australian Defence Science Service, Maribymong). Appl. Phys. Lett.; 24: No. 12, 608-610(15 Jun 1974).

$CO_2$-$N_2$ gas mixtures were held at pressures up to 300 kPa and brief ionizing pulses from a gas-discharge electron gun and a low inductance energy supply circuit were used. The experimental arrangement is described. Using a probe beam from a $CO_2$ laser a high gain may be achieved, and an even higher gain if an admixture of $H_2$ to the gas mixture is made. Gains of up to $10m^{-1}$ with a decay time constant of 100 ns may be achieved, so that nanosec. pulses of radiation may be amplified. (Elect. Electron. Abstr.)

**25806** PROPERTIES OF HIGH-ORDER TRANSVERSE MODES IN ASTIGMATIC LASER CAVITIES. Chao, S.L.; Forsyth, J.M. (The Institute of Optics, University of Rochester, Rochester, New York 14627). J. Opt. Soc. Am. 65: No. 8, 867-875 (Aug 1975).

A theory of the modes in a resonator bounded by the surface of a triaxial ellipsoid was given previously by Weinstein. We have applied this theory to characterize the modes observed in a large-aperture Brewster-window laser. Recognizing that Brewster windows impart astigmatism to the laser cavity, we can find an equivalent ellipsoidal cavity with which to associate the modes. The theory predicts various forms of mode structure, depending on the total astigmatism present. We have verified the theory experimentally and show that high-order modes having rectangular symmetry may be obtained even though a circular aperture is used in the cavity.

**25807** COMPACT CONTINUOUS HF MICROWAVE-DISCHARGE MIXING LASER. Gagné, J.M.; Bertrand, L.; Conturie, Y.; Mah, S.Q.; Monchalin, J.P. (Laboratoire d'optique et de spectroscopie, Département de Génie physique, Ecole Polytechnique, Campus de l'Université de Montréal, C. P. 6079, Succursale A, Montréal, Québec, Canada H3C 3A7). J. Opt. Soc. Am. 65: No. 8, 876-881 (Aug 1975).

The performance of a continuous chemical laser is discussed. Fluorine atoms are produced in a $SF_6$ + He mixture by means of a microwave-discharge apparatus that operates in a continuous mode. A maximum output power of 4 W is obtained for a 5 cm length of amplifying medium; this power output is primarily due to $P$ transitions from the 1-0 and 2-1 bands. Weak transitions in the 3-2 band are also observed. The maximum value of measured gain is 0.11 $cm^{-1}$; good agreement is obtained between theoretical and experimental values of gain. (auth)

**25808** PERIODIC GIANT—PULSE RUBY LASER WITH LOW INTERMITTENT INSTABILITY. Gruzdev, V.V.; Zhuravel', V.A.; Lavrov, V.I.; Lebedev, V.B.; Kornilov, N.A. Sov. J. Opt. Technol. 41: No. 11, 522-524 (Nov 1974).

The factors determining the delay time instability of the radiation pulses relative to the trigger pulses of a giant—pulse ruby laser, Q switched by means of an electro—optic shutter unit, were examined. Means are suggested for reducing this parameter. (auth)

**25809** THE OPERATION OF TYPE GOS—1000 LASERS UNDER SHORT—PULSE CONDITIONS. Kirsanov, V.P.; Rybal'skii, V.V.; Tolkunov, L.I.; Troshkin, S.V. Sov. J. Opt. Technol. 41: No. 11, 540-541 (Nov 1974).

Pulses with a duration of $\sim 10^{-4}$ second and an energy of $\sim 300$ J at an efficiency of $\sim 1\%$ are obtained in GOS—1000B and GOS—1001 lasers in the free—running mode of operation. The lasing pulse is shortened by a forced mode of pump lamp operation with a change in their filling and an appropriate choice of discharge circuit parameters. (auth)

**25810** OUTPUT COUPLING AND DISTRIBUTED FEEDBACK UTILIZING SUBSTRATE CORRUGATIONS IN DOUBLE-HETEROSTRUCTURE GaAs LASERS. Scifres, D.R.; Burnham, R.D.; Streifer, W. (Xerox Palo Alto Research Center, Palo Alto, California 94304). Appl. Phys. Lett. 27: No. 5, 295-297 (1 Sept 1975).

Conventional double-heterostructure lasers with a thin $n$-$Ga_{1-y}Al_yAs$ layer grown on a periodically corrugated $n$-GaAs substrate have been operated at room temperature. The evanescent tail of the guided mode interacts with the substrate corrugation to produce both distributed feedback and output coupling perpendicular to the waveguide. A single polarized low-divergence ($0.65°\times10°$) output beam at 8825 Å radiated normal to the waveguide was obtained from such a diode with cleaved end facets at a threshold current of 4.1 $kA/cm^2$. (auth)

**25811** PROPOSED ATOMIC MERCURY ANTI-STOKES FREQUENCY CONVERTER. Komine, H.; Byer, R.L. (Microwave Laboratory, W. W. Hansen Laboratories of Physics, Stanford University, Stanford, California 94305). Appl. Phys. Lett. 27: No. 5, 300-302 (1 Sept 1975).

We propose to use population stored in the radiatively trapped $6^2P_1^\circ$ atomic mercury resonant level (1850 Å) for frequency conversion by an anti-Stokes or two-photon process. Inversion is with respect to the lower-lying $6^3P^\circ_{0,1,2}$ levels which are assumed empty following selective quenching or rapid conversion to the mercury dimer. Photon conversion gains of $2.5\times10^{-2}$ cm/MW for 1.06-μm and $8.7\times10^{-5}$ cm/MW for 10.6-μm input wavelengths with corresponding 0.4157- and 0.9116-μm output wavelengths are calculated at a $10^{16}$-$cm^{-3}$ inversion density. (auth)

**25812** INFRARED MOLECULAR LASERS PUMPED BY ELECTRONIC-VIBRATIONAL ENERGY TRANSFER FROM Br($4^2P_{1/2}$): $CO_2$, $N_2O$, HCN, AND $C_2H_2$. Petersen, A.B.; Wittig, C. (Electrical Engineering Department, University of Southern California, University Park, Los Angeles, California 90007); Leone, S.R. Appl. Phys. Lett. 27: No. 5, 305-307 (1 Sept 1975).

Infrared lasers pumped by electronic-vibrational (E-V) energy transfer are reported. Gas mixtures containing electronically excited Br atoms ($^2P_{1/2}$) are prepared by flash photolyzing $Br_2$ in the presence of a polyatomic molecule. The ensuing E-V process is selective and pumps the polyatomic molecule into specific energy states. In addition to obtaining gain and/or stimulated emission at $CO_2$ and $N_2O$ laser frequencies, we have obtained stimulated emission from HCN at 3.85, 7.25, and 8.48 μm, and from $C_2H_2$ in the region 7–8 μm. Extension of the principles involved to other polyatomic molecules is straightforward, and a number of applications are suggested by our results to date. (auth)

**25813** DEVELOPMENT OF AN EFFICIENT 9-kW 496-μm $CH_3F$ LASER OSCILLATOR. Cohn, D.R.; Fuse, T.; Button, K.J.; Lax, B.; Drozdowicz, Z. (Francis Bitter National Magnet Laboratory, Massachusetts Institute of Technology, Cambridge, Massachusetts 02139). Appl. Phys. Lett. 27: No. 5, 280-282 (1 Sept 1975).

A 496-μm $CH_3F$ cavity laser characterized by an average power of 9 kW and predominant single longitudinal mode operation with a linewidth of 28 MHz has been constructed. The power conversion efficiency of the laser ($CH_3F$ power out/$CO_2$ pump power in) is on the order of $1.5\times10^{-3}$. The $CH_3F$ gas is pumped in a zig-zag fashion by the $CO_2$ laser radiation. (auth)

**25814** A SIMPLE PULSED LASER SYSTEM TUNABLE IN THE ULTRAVIOLET. Atkinson, G.H. (Department of Chemistry, Syracuse University, Syracuse, New York 13210); Schuyler, M.W. Appl. Phys. Lett. 27: No. 5, 285-287 (1 Sept 1975).

A flashlamp-pumped dye laser, operating with a 55-nsec (FWHM) pulsed output, has been used in conjunction with a 90° phase-matched nonlinear optical crystal (ADA) to generate tunable radiation in the 290–300-nm region at power levels greater than 1 kW. (auth)

**25815** MODE CALCULATIONS IN UNSTABLE RESONATORS WITH FLOWING SATURABLE GAIN. 2: FAST FOURIER TRANSFORM METHOD. Sziklas, E.A. (Pratt & Whitney, Florida Research & Development Center, West Palm Beach, Florida 33403); Siegman, A.E. Appl. Opt. 14: No. 8, 1874-1889 (Aug 1975).

We present further calculations of the three-dimensional mode patterns and power outputs from a high-power gas-dynamic laser, including a nonuniform flowing, saturable gain medium plus index inhomogeneities (shocks) inside the laser. The calculations are carried out using a plane-wave or k-space expansion together with the fast Fourier transform. A new expanding-beam coordinate transform converts all diverging or converging sections of the resonator mode into equivalent collimated beam sections. The resulting FFT propagation code is significantly faster than earlier propagation codes using other eigenmode expansions. (auth)

**25816** HELIUM—NEON LASER STABILIZED ON IODINE: DESIGN AND PERFORMANCE. Tuma, W.; van der Hoeven, C.J. (National Physical Research Laboratory, CSIR, P.O. Box 395, Pretoria 0001, South Africa). Appl. Opt. 14: No. 8, 1896-1897 (Aug 1975).

A helium—neon laser operating at 633 nm was frequency stabilized on a hyperfine component of $^{127}I_2$ with saturated absorption. The stability achieved was $2.5\times10^{-12}$ at an averaging time of 400 sec. The frequency was reproducibie to $5\times10^{-11}$. (auth)

**25817** POTENTIAL ELECTRONIC TRANSITION CHEMICAL LASER: PARAMETRIC EVALUATION. Sutton, D.G.; Suchard, S.N. (The Aerospace Corporation, P.O. Box 92957, Los Angeles, California 90009). Appl. Opt. 14: No. 8, 1898-1910 (Aug 1975).

Through the utilization of a generalized computer code that calculates the minimum reactive branching ratio required for a species to display optical gain, a parametric study was performed to ascertain which properties of the electronic potential curves of a heteronuclear diatomic molecule have the greatest effect on the suitability of that molecule as a potential electronic transition laser. The results of this study demonstrate that diatomic systems separate into different classes when the question of the minimum required reactive branching ratio is confronted. This separation of molecular systems was translated through the use of compiled molecular constants into a determination of which vibrational-level distribution class is most favorable for specific heteronuclear diatomic molecules to display optical gain; potential laser candidates were pointed out. In addition, a generalized gain equation for electronic transitions heteronuclear diatomic molecules that takes into account both rotational and vibrational partitioning was derived. (auth)

**25818** PHYSICS OF DYE LASERS. Shank, C.V. (Bell Laboratories, Holmdel, New Jersey 07733). Rev. Mod. Phys. 47: No. 3, 649-657 (July 1975).

The physical mechanisms important to the operation of tunable lasers utilizing organic dyes are discussed. The uniqueness of organic dyes as a tunable laser medium is reviewed by investigating the optical properties of two broadened energy levels. The complete energy level system is investigated and gain and efficiency are calculated. The wide variety of practical laser configurations possible for optically pumped dye lasers are examined. New topics of interest such as dye vapor lasers and short pulse generation are discussed. (auth)

**25819** LOW-THRESHOLD LPE $In_{1-x}Ga_xP_{1-z}As_z$/$In_{1-x}Ga_xP_{1-z}As_z$/$In_{1-x}Ga_xP_{1-z}As_z$ YELLOW DOUBLE-HETEROJUNCTION LASER DIODES ($J<10^4$ A/cm$^2$, $\lambda\simeq5850$ A, 77 °K). Hitchens, W.R.; Holonyak, N. Jr.; Wright, P.D.; Coleman, J.J. (Department of Electrical Engineering and Materials Research Laboratory, University of Illinois at Urbana-Champaign, Urbana, Illinois 61801). Appl. Phys. Lett. 27: No. 4, 245-247 (15 Aug 1975).

Liquid phase epitaxial (LPE) $In_{1-x}Ga_xP_{1-z}As_z$/$In_{1-x}Ga_xP_{1-z}$/$In_{1-x}Ga_xP_{1-z}As_z$ ($x\sim0.66$, $z\sim0.005$; $x\sim0.71$, $z\sim0.10$) double-heterojunction laser diodes that operate in the yellow at relatively low current densities ($J<10^4$ A/cm$^2$, $\lambda\sim5850$ Å, 77 °K) are reported. The lattice-matched LPE quaternary growth process, employing $GaAs_{1-y}P_y$ substrates, and the double-heterojunction laser diode properties are described. (auth)

**25820** STIMULATED EMISSION AT 281.8 NM FROM XeBr. Searles, S.K.; Hart, G.A. (Laser Physics Branch, Optical Sciences Division, Naval Research Laboratory, Washington, D. C. 20375). Appl. Phys. Lett. 27: No. 4, 243-245 (15 Aug 1975).

Xenon with 0.10–4% $Br_2$ was excited by an e-beam device over the range 10–3000 Torr. Stimulated emission was observed on the transition $XeBr^*\rightarrow Xe+Br+h\nu$ (281.8 nm). Proof of laser emission and mechanistic details are discussed. (auth)

**25821** INTEGRATED GaAs-AlGaAs DOUBLE-HETEROSTRUCTURE LASERS. Hurwitz, C.E.; Rossi, J.A.; Hsieh, J.J.; Wolfe, C.M. (Lincoln Laboratory, Massachusetts Institute of Technology, Lexington, Massachusetts 02173). Appl. Phys. Lett. 27: No. 4, 241-243 (15 Aug 1975).

Integrated structures consisting of a double-heterostructure GaAs-AlGaAs etched-mesa Fabry-Perot laser coupled to a high-purity GaAs waveguide have been fabricated and tested. Room-temperature threshold current densities as low as 7.5 kA/cm$^2$ for 1-μm-thick active layers were measured. (auth)

**25822** LASER-EXCITED PHOTOLUMINESCENCE OF THREE-LAYER GaAs DOUBLE-HETEROSTRUCTURE LASER MATERIAL. Nash, F.R.; Dixon, R.W.; Barnes, P.A.; Schumaker, N.E. (Bell Laboratories, Murray Hill, New Jersey 07974). Appl. Phys. Lett. 27: No. 4, 234-237 (15 Aug 1975).

The successful fabrication of high-quality DH GaAs lasers from a simplified three-layer structure is reported. A major asset of this structure is the transparency of its final layer to recombination radiation occurring in the active layer, thus permitting the use of nondestructive photoluminescent techniques for material evaluation prior to device fabrication. In the course of photoluminescence investigations on this material the additional important observation has been made that indirect excitation (in which photocarriers are generated in the top ternary layer) has significant advantages over direct excitation (in which photocarriers are generated directly in the active layer). These include (i) the direct measurement of Al concentrations in both upper layers, (ii) the measurements of the minority-carrier diffusion length in the upper layer, (iii) an easily obtained indication of taper in the thickness of the upper layer, and (iv) surprisingly effective excitation of the active layer. By combining direct and indirect excitation it is shown that a clearer understanding of the location and detrimental influences of defects in the GaAs laser structure may be obtained. For example, the width of the region of reduced luminescence associated with many defects is found to be very excitation dependent and is confirmed to arise from reduced active region luminescence. The photoluminescent excitation techniques described should be useful in the study of other heterostructure devices and material systems. (auth)

**25823** CO CHAIN-REACTION CHEMICAL LASER. Jeffers, W.Q.; Ageno, H.Y. (McDonnell Douglas Research Laboratories, McDonnell Douglas Corporation, St. Louis, Missouri 63166). Appl. Phys. Lett. 27: No. 4, 227-229 (15 Aug 1975).

The operation of a CO chemical laser fueled by carbon monosulfide (CS) and oxygen and pumped by a chain-reaction mechanism is reported. For CS-to-$CS_2$ mole ratios of 2.0, the chain length is 8.5. The optical performance of this chain-reaction laser, producing specific energies of 67 kJ/lb$_m$, is superior to the performance of previous CO chemical lasers. (auth)

**25824** TRANSFORM-LIMITED PICOSECOND PULSE GENERATION IN A SYNCHRONOUS MODE-LOCKED DYE LASER PUMPED BY DOUBLED Nd:YAG. Goldberg, L.S.; Moore, C.A. (Naval Research Laboratory, Washington, D. C. 20375). Appl. Phys. Lett. 27: No. 4, 217-219 (15 Aug 1975).

Synchronous mode locking of a dye laser longitudinally pumped by the second-harmonic pulse train from a passively mode-locked, repetitively pulsed Nd:YAG laser has been studied. The dye laser, incorporating Fabry-Perot tuning elements, has produced intense $TEM_{00}$ pulses as short as 12 psec in duration with a transform-limited bandwidth of 2 cm$^{-1}$. The mode-locked dye pulses are time synchronizable with the intense Nd:YAG pulses and have been tuned from 549–727 nm using several laser dyes. Both lasing efficiency and pulse duration exhibit pronounced cavity length dependences that result from processes of gain depletion and population recycling during a pumping pulse. Pulses shorter than the pump are generated under cavity length conditions for which only gain depletion effects occur. (auth)

**25825** IMPROVED PERFORMANCE OF AN ELECTRIC-DISCHARGE $N_2$-CO MIXING LASER. Brunet, H.; Mabru, M. (Laboratoires de Marcoussis, Centre de Recherches de la Compagnie Generale d'Electricite, Division Lasers, Section Sources d'Ondes Cohérentes, 91460 Marcoussis, France). J. Appl. Phys. 46: No. 8, 3683-3684 (Aug 1975).

An electric-discharge CO mixing laser is described in which $N_2$ is vibrationally excited in a discharge and then mixed with cold CO providing laser action between 5.0 and 5.8 μ in a low-pressure high-Mach-number channel. Results of experiments with a 21-cm-wide 1.3-cm-high channel are described. Maximum laser power obtained is 720 W corresponding to an efficiency of 7% and a specific power of about 21 kW (kg/s)$^{-1}$. (auth)

**25826** ROTATIONAL RELAXATION IN A LINE-SELECTED CONTINUOUS HF CHEMICAL LASER. Skifstad, J.G.; Chao, C.M. (School of Mechanical Engineering, Purdue University, West Lafayette, Indiana 47907). Appl. Opt. 14: No. 7, 1713-1718 (July 1975).

Rotational relaxation effects in a cw chemical laser amplifier or a line-selected oscillator are examined in terms of a simple analytical model. Three rotational levels in each vibrational level of the lasing transition are taken to have finite rotational relaxation rates. The results indicate the effects are likely to be significant, lowering the available power and leading to an optimum level of the line intensity for maximum power output, apart from consideration of optical losses at mirrors, windows, etc. While the model accounts for $\Delta j=\pm1$ transitions only, the collisional transition probability was augmented in the computations in an attempt to provide high estimates for the rotational relaxation rates, including factors such as $\Delta j>1$ transitions. (auth)

**25827** LASER BASED ON ELECTROCHEMILUMINESCENCE. Keszthelyi, C.P. (Chemistry Department, Louisiana State University, Baton Rouge, Louisiana 70803). Appl. Opt. 14: No. 7, 1710-1712 (July 1975).

The specific points raised here augment the full paper on this same subject by Measures [Appl. Opt. 13, 1121 (1974)]. In support of the feasibility of such a laser, an electrochemiluminescent system with $\phi_{ecl}\sim0.2$ is cited from the literature (vs$\phi_{ecl}\sim1.4\times10^{-2}$); and in relation to the feasibility calculations, the incompleteness of the Feldberg model is noted. Various other topics are also discussed. (auth)

**25828** TUNABILITY CHARACTERISTICS OF WAVEGUIDE $CO_2$ LASERS WITH INTERNAL ETALONS. Leeb, W.R. (NASA

Goddard Space Flight Center, Greenbelt, Maryland 20771). Appl. Opt. 14: No. 7, 1706-1709 (July 1975).

We investigate the possibility of increased tuning range of waveguide $CO_2$ lasers by using a longer discharge and a tilted intracavity etalon as axial mode selector. Taking into account etalon losses, the tuning range was calculated as a function of laser gain, pressure, and discharge length. Improvements depend strongly on the index of refraction and the absorbtivity of the etalon material. The comparison with a length-restricted laser without mode selection shows that the use of a CdTe etalon in a laser with 25-cm active length could increase the tuning range from 1.5 GHz to 2.2 GHz. However, an air etalon reduces the bandwidth due to higher tilting losses. (auth)

**25829** PREALIGNMENT OF GAS LASER CAVITIES. Hernqvist, K.G.; Firester, A.H. (RCA Laboratories, Princeton, New Jersey 08540). Rev. Sci. Instrum. 46: No. 8, 1040-1042 (Aug 1975).

A method of coarse alignment and fine tuning of the cavity of a gas laser is presented. The laser cavity to be aligned is treated as a Fabry–Perot cavity, and its transmission of a frequency-swept laser is maximized. An experiment is described showing that this fine-tuning procedure results in maximum power output when the laser is operated. The method is particularly well-suited to laser manufacturing. (auth)

**25830** SIMPLE AND RELIABLE SUBSONIC HF CHEMICAL LASER WITH 40 W POWER OUTPUT (16 W DF). Proch, D.; Pummer, H.; Kompa, K.L. (Max-Planck-Institut für Plasmaphysik (Euratom Association), 8046 Garching, Germany); Wanner, J. Rev. Sci. Instrum. 46: No. 8, 1101-1104 (Aug 1975).

The design and performance of a transverse flow subsonic chemical laser with a total power output of 40 W for HF and 16 W for DF are presented. Laser operation has been observed in the wavelength range 2.6–3.0 $\mu$ for HF and 3.6–4.0 $\mu$ for DF resulting from $v=2-1$ and $1-0$ transitions of the HF molecule and from $v=3-2$, $2-1$, and $1-0$ transitions of DF. The range of the participating rotational states in the emission spectra can be controlled to some extent by a variation of the gas temperature in the optical cavity region. The observed total power levels correspond to an electrical efficiency of 1.3% for HF and 0.9% for DF. (auth)

**25831** CURRENT-REGULATED, HIGH-VOLTAGE POWER SUPPLY FOR CW GAS LASERS. Maxson, D.; Seiler, D.G.; Tipton, L. (Department of Physics, North Texas State University, Denton, Texas 76203). Rev. Sci. Instrum. 46: No. 8, 1110-1112 (Aug 1975).

An economical, high-voltage, highly stable, current-regulated power supply with less than 0.1% rms ripple is described. The dynamic capabilities of 0–30 kV and 0–30 mA provide a versatile instrument for use with many cw gas lasers. (auth)

**25832** EXPERIMENTAL AND THEORETICAL ELECTRON-BEAM-SUSTAINED $CO_2$ LASER OUTPUT AT ~200 AND ~300 °K. Douglas-Hamilton, D.H.; Feinberg, R.M.; Lowder, R.S. (Avco Everett Research Laboratory, Incorporated, Everett, Massachusetts 02149). J. Appl. Phys. 46: No. 8, 3566-3575 (Aug 1975).

A six-temperature kinetic model of the $He:He_2Co_2:N_2:CO$ laser system is developed, in which five temperatures describe the vibrational excitation of the three $CO_2$ modes, $N_2$, and CO, while the sixth refers to the kinetic temperature. Theoretical predictions of gain and laser output are compared with experiments performed on an electron-beam sustainer laser used at atmospheric pressure. Gain and laser measurements have been made with initial gas temperature near 200 and 300 °K. A stable discharge can be produced in this type of laser in gas mixtures containing no He, and successful electric laser operation has been demonstrated using $H_2$ as $CO_2\nu_2$ deactivant. Various gas mixtures have been investigated experimentally and theoretically; specific output $J>100$ J/liter atm was obtained both in $He:N_2:CO_2:H_2$ 3:2:1:0 and 0:3:1:0.08, with efficiencies near 30%. While the gain measured appears to peak later and decay later than predicted, in all laser output measurements there is good agreement between theoretical prediction and experiment. (auth)

**25833** LASER FOCAL SPOT MEASUREMENTS. Brannon, P.J.; Anthes, J.P.; Cano, G.L.; Powell, J.E. (Sandia Laboratories, Albuquerque, New Mexico 87115). J. Appl. Phys. 46: No. 8, 3576-3579 (Aug 1975).

The focal spot size for a high-powered neodymium laser has been determined by measuring the energy passing through pinholes of various sizes and also, by photographing the focused spot. A comparison of the two methods indicated that the photographic method could give misleading results. The spot size was also determined by measuring the absorbed energy by target pellets of various sizes. This method always gave a smaller value than the pinhole method. The difference was attributed to plasma effects. (auth)

**25834** ANISOTROPY IN THE LASER PERFORMANCE OF $NdP_5O_{14}$. Huber, G.; Krühler, W.W.; Bludau, W.; Danielmeyer, H.G. (Max-Planck-Institut für Festkörperforschung, 7 Stuttgart 1, Postfach 1099, Federal Republic of Germany). J. Appl. Phys. 46: No. 8, 3580-3584 (Aug 1975).

We report, for the first time in a biaxial laser material, on the distribution of fluorescence cross sections in the index ellipsoid. The largest effective fluorescence cross section of pure $NdP_5O_{14}$ at room temperature $(2.0\pm0.1)\times10^{-19}$ cm$^2$ for light at 1.0512 $\mu$ wavelength polarized parallel to the 2 axis which coincides with the crystallographic $b$ axis. We predict from the cross sections the cw thresholds and polarizations of the four highest-gain laser transitions and verify the results quantitatively by operating one crystal in all major polarizations. We measured the major phase and group refractive indices and the thermal expansion coefficient of the optical lengths near 1.05 $\mu$ wavelength. We also discuss the twin domains which have different orientations of the crystallographic and optic axes. In imperfect crystals they can easily be created by thermal stresses which can drastically increase the laser threshold. (auth)

**25835** FAST ACOUSTO-OPTIC LENS $Q$ SWITCH. Scott, M.L.; Jernigan, J.; Hutcheson, L.; Gould, D. (Physics Division, Research Department, Naval Weapons Center, China Lake, California 93555). J. Appl. Phys. 46: No. 8, 3483-3488 (Aug 1975).

A fast acousto-optic $Q$ switch has been demonstrated which relies on a linear FM pulse of acoustic energy to act as a moving lens. While one coordinate of the focus of the lens is fixed by the rate of frequency sweep, the other coordinate is "swept" in time by the frequency variation of the pulse. The on time of the switch is proportional to the reciprocal of the pulse bandwidth. Experiments have been conducted which verify the characteristics of this technique. A $TeO_2$ Bragg cell was used in a successful attempt to $Q$ switch a Nd/YAG laser with the acousto-optic lens approach. (auth)

**25836** HETEROJUNCTION LASER OPERATION OF N—FREE AND N—DOPED $GaAs_{1-y}P_y$ ($y$=0.42–0.43, $\lambda\sim6200$ Å, 77 °K) NEAR THE DIRECT-INDIRECT TRANSITION ($y\sim y_c\simeq0.46$). Coleman, J.J.; Holonyak, N. Jr.; Ludowise, M.J.; Wright, P.D. (Department of Electrical Engineering and Materials Research Laboratory, University of Illinois at Urbana-Champaign, Urbana, Illinois 61801); Groves, W.O.; Keune, D.L.; Craford, M.G. J. Appl. Phys. 46: No. 8, 3556-3561 (Aug 1975).

The successful LPE growth of $In_{1-x}Ga_xP_{1-y}As_y$/ $GaAs_{1-y}P_y$ single heterojunction on VPE substrates makes possible the study of stimulated emission in N-free and N-doped $GaAs_{1-y}P_y$ in a region ($y$=0.42–0.43) much closer to the direct-indirect transition ($y\equiv y_c=0.46$, 77 °K) than previously. Laser operation in N-free $GaAs_{1-y}P_y$ on the $\Gamma$-Zn ($E_\Gamma$-$E_{Zn}$) recombination transition has been achieved at energies as high as 2.00 eV ($\lambda=6200$ Å), and some line narrowing has been observed at energies as high as 2.01 eV ($\lambda=6170$ Å, $y=0.43$). In contrast to diodes made on lower composition substrates, the diodes of this work do not change their threshold current densities in the range 77–4.2 °K, indicating that laser operation occurs on direct transitions lying within ~kT of the indirect donor states (Te) associated with the $X$ conduction-band minima. From $E_\Gamma + kT\sim E_X - E_d$ ($y=0.42$–$0.43$), the depth of indirect Te donor states in $GaAs_{1-y}P_y$ is estimated to fall in the range $E_d=22$–$32$ meV. Nitrogen doping in these laser diodes increases the threshold current densities since the N impurity is an efficient trap and introduces competing indirect recombination. For $y=0.42$–$0.43$ $GaAs_{1-y}P_y$ heterojunction laser operation on the N trap lies ~10 meV lower in energy than on the $\Gamma$-Zn transition. Beyond $y=0.42$–$0.43$, the N trap may be required for stimulated emission, but in this range diode operation at high currents becomes difficult because of the large change in carrier mobility. (auth)

**25837** TUNABLE-WAVELENGTH, SINGLE TRANSVERSE AND LONGITUDINAL MODE, $Nd^{3+}$ GLASS $Q$-SWITCHED LASER. Petite, G. (Service de Physique Atomique, Centre d'Etudes Nucléaires de Saclay, BP N°2-91190 Gif-sur-Yvette, France). J. Appl. Phys. 46: No. 8, 3462-3464 (Aug 1975).

A new tunable-wavelength, single transverse and longitudinal mode, $Nd^{3+}$ glass $Q$-switching laser is described. Single-longitudinal-mode operation is achieved by using saturable absorber $Q$ switching and intracavity resonators. Tunability is achieved over a 50-Å range by means of a birefringent filter, consisting of a single calcite plate and a polarizer. The energy is about 25 mJ, obtained in a 17-ns pulse. (auth)

**25838** DIODE LASER PUMPING. Skagerlund, L. E. (to AB Bofors). US Patent 3,898,588. 5 Aug 1975. Priority date 3 Jul 1972, Sweden. 8p.

A diode laser is pumped or pulsed by a repeated capacitive discharge. A capacitor is periodically charged from a dc voltage source via a transformer, the capacitor being discharged through the diode laser via a controlled switching means after one or more charging periods. During a first interval of each charging period the transformer, while unloaded, stores a specific amount of energy supplied from the dc voltage source. During a subsequent interval of the charging period said specific amount of energy is transmitted from the transformer to the capacitor. The discharging of the capacitor takes place during a first interval of a charging period. (auth)

**25839** MULTIPLE-SOURCE PLASMA-OVERLAP LASER. Brinkman, W. F. Jr.; Silfvast, W. T.; Wood, O. R. II. (to Bell

Telephone Labs., Inc.). US Patent 3,898,587. 5 Aug 1975. Filed date 25 Jan 1974. 6p.

There are disclosed lasers employing lithium–indium ion mixtures or beryllium–gallium ion mixtures, in which the active medium is produced by overlap of two plasmas derived from optical or electron beam vaporization of material from two separated metallic sources extending parallel to the intended laser axis. Typically, a pulsed vaporization process produces ionized plasmas that can produce a Penning collision energy transfer in the plasma overlap region to produce the laser population inversion. Superradiant lasing action is the simplest mode of stimulated emission of the coherent radiation. A charge transfer system employing two species of atoms, either one or both being in an ionized state, also can produce the population inversion. (auth)

**25840** LASER STABILIZATION TECHNIQUE. Shuey, D. R. (to Xerox Corp.). US Patent 3,898,583. 5 Aug 1975. Filed date 28 Dec 1973. 10p.

The output power level of a laser is stabilized at a predetermined set point by a feedback control circuit. The light emitted from one end of a laser is detected and converted into an electrical current by a photodetector. This current is then amplified and converted into a proportional voltage by a buffer amplifier and the resultant voltage is compared to a reference voltage to provide an error signal. The error signal is integrated and fed back to correctively adjust the driving current for the laser, thereby compensating for any tendency of the power level of the light beam emitted from the other end of the laser to drift from a predetermined set point. (auth)

**25841** GAS DYNAMIC LASER DEVICE AND METHOD OF OPERATING SUCH A DEVICE. Born, G. (to Messerschmitt-Boelkow-Blohm GmbH). US Patent 3,898,584. 5 Aug 1975. Priority date 9 Nov 1972, F. R. Germany. 8p.

The invention relates to a gas dynamic laser device such as a $CO_2$-transmitter or amplifier wherein auxiliary pressure means are provided for maintaining the pressure in the combustion chamber at a substantially constant level even during outflow of the gas from the combustion chamber. The pressure control and thus the concomitant temperature control in the combustion chamber may be accomplished, for example, by adjusting or reducing the volume of the combustion chamber during the gas outflow, by introducing air under pressure into the combustion chamber, or by employing a specially constructed and arranged solid fuel pack which will sustain a strong gas flow into said combustion chamber. (auth)

**25842** SELF-PULSING IN MEDIUM-POWER He--Ne LASERS. Chow, C.N.Y. Minneapolis; Univ. of Minnesota (1974). 165p. University Microfilms Order No. 75-12,188.

Thesis (Ph. D.).

An analytical model is developed to describe self-pulsing in medium-power He-Ne laser. The numerical results show that the oscillating modes can be coupled by population pulsation such that the resonant dispersion can be linearized as required for undistorted pulse propagation while simultaneously satisfying the uniform gain condition across the inhomogeneous bandwidth. The analyses also predict an increase in pulse velocity as well as power output as the laser becomes locked. Experimental measurements indeed show that when the laser is switched from partially unlocked to fully self-locked operation, the pulse velocity increases by about 9 parts in $10^6$ and the average output power increases by about 0.5 percent. (Diss. Abstr. Int., B)

**25843** BURIED-HETEROSTRUCTURE INJECTION LASERS. Tsukada, T. (Hitachi Ltd., Kokubunji, Tokyo). J. Jap. Soc. Appl. Phys., Suppl.; 44: 33-37(Jan 1975).

From 6th conference on solid state devices; Tokyo, Japan (2 Sep 1974).

Buried-heterostructure injection lasers which have the filamentary GaAs active regions completely surrounded by GaAlAs have been proposed and successfully fabricated. The active regions of these new lasers can be made extremely small and do not have dimensional unbalances in the cross sections usually encountered in conventional lasers. Due to the small active region of this laser, the threshold current has been reduced to a value as low as 15 mA. The removal of the dimensional unbalance has brought about the improvements of the optical characteristics such as Gaussian beam profile, fundamental mode operation, mode reproducibility, and mode stability. Moreover, owing to good thermal properties of these lasers, cw operation was easily obtained. (auth)

**25844** DISTRIBUTED FEEDBACK LASER IN CdS UNDER ELECTRON BEAM EXCITATION. Aoyagi, Y.; Namba, S. (Inst. of Physical and Chemical Research, Wako, Japan). Jap. Soc. Appl. Phys., Suppl.; 44: 39-43(Jan 1975).

From 6th conference on solid state devices; Tokyo, Japan (2 Sep 1974).

Distributed feedback laser was observed in CdS with a simple DFB structure under electron beam excitation. The lasing characteristics such as the temperature dependence and the time dependence of the laser were examined. The line width of the laser spectrum was found to be less than 0.8 Å. Compared to a conventional laser, the lasing wavelength was insensitive to temperature. The dependence of the lasing wavelength on temperature is explained by the change of the refractive index. In some samples the DFB lasing was observed to occur only at the start of the excitation pulse and the pulse width was much shorter than that of a conventional laser. This phenomenon is explained by a gain switching mechanism. (auth)

**25845** STIMULATED EMISSION IN InSb UNDER THE TWO-PHOTON EXCITATION. Yoshida, T.; Miyazaki, K.; Fujisawa, K. (Univ., Osaka). J. Jap. Soc. Appl. Phys., Suppl.; 44: 45-49(Jan 1975).

From 6th conference on solid state devices; Tokyo, Japan (2 Sep 1974).

Both spontaneous and stimulated emissions (about 5.3 $\mu$m) were observed in n-InSb, which was cooled by a closed cycle refrigerator, and pumped by the selected line output from a TE $CO_2$ laser. The stimulated emission was observed for the temperature between 20 and 40°K, and the spontaneous emission up to about 150°K. The emission intensity was proportional to the square of the pumping laser intensity below the threshold. Above the threshold, it increased very rapidly. The emission intensity and photoconductance change depend on the pumping laser wavelength drastically. From these facts, it is certain that these emissions are due to the two-photon excitation. With samples of different carrier densities, the emission wavelength changed. The wavelength tuning by means of magnetic field was also observed. (auth)

**25846** ELECTRON ENERGY DISTRIBUTION FUNCTION IN THE POSITIVE COLUMN OF A HELIUM–CADMIUM LASER. Ciobanu, M. I.; Ciura, A. I.; Cojocaru, E.; Popescu, I. M. (Inst. of Atomic Physics, Bucharest). Rev. Roum. Phys.; 20: No. 1, 29-41(1975).

Experimental determination of the electron energy distribution function in the positive column of the He–Cd laser is reported. The distribution function is obtained from the second derivative of the probe characteristic. The electron temperature and density are deduced as function of working conditions. (auth)

**25847** SELF-MODE-LOCKING OF AN ARGON ION LASER WITH A NONLINEAR ABSORBER. Boriseva, M.S.; Muravev, V.M. Opt. Spectrosc. (USSR) 38: No. 4, 437-438 (Apr 1975).

The results of an experimental investigation are presented of the effects of the location of active media in the resonator of an argon ion laser 4880-Å wavelength with a nonlinear absorber operating in the wideband (to 9 GHz) self-mode-locked regime. (auth)

**25848** TUNABLE SINGLE-FREQUENCY XENON LASER OPERATING AT THE TWO INFRARED TRANSITIONS $\lambda = 5.57$ $\mu$m AND 3.51 $\mu$m. Aleksandrov, E.B.; Kulyasov, V.N.; Kharnang, K. Opt. Spectrosc. (USSR) 38: No. 4, 439-440 (Apr 1975).

This paper describes a tunable single-frequency laser based on the $Xe^{136}$ isotope that lases at the two ir transitions at wavelengths $\lambda = 5.57$ $\mu$m and 3.51 $\mu$m. Values of the homogeneous widths of the two transitions $5d[7/2]_4 \rightarrow 6p[5/2]_3 (\lambda = 5.57$ $\mu$m) and $5d[7/2]_3 \rightarrow 6p[3/2]_2 (\lambda = 3.51$ $\mu$m) were obtained from the width of the Lamb dip in the dependence of the laser output power on tuning frequency. The shift of the hyperfine components $F = 9/2 \rightarrow F = 7/2$ of the 5.57-$\mu$m line relative to the center of the $Xe^{136}$ line are determined with the aid of an amplifying cell containing the isotope $Xe^{129}$. (auth)

**25849** EFFECT OF THE LIFETIME OF METASTABLE NEON ATOMS ($1s_5$) ON THE FREQUENCY MODULATION OF A He-Ne LASER ($\lambda = 6323$ A). Melnikov, L.A.; Sedelnikov, V.A.; Tuchin, V.V. Opt. Spectrosc. (USSR) 38: No. 4, 448-449 (Apr 1975).

The effects of the long lifetime of metastable states of neon on the frequency modulation of a He–Ne laser lasing at 6328 Å is investigated. (AIP)

**25850** ONE SOURCE OF ERROR IN THE MEASUREMENT OF THE GAIN PROFILE OF A LASER LINE. Rotar, S.V.; Solovev, V.S.; Telegin, B.V. Opt. Spectrosc. (USSR) 38: No. 4, 451-452 (Apr 1975).

Errors in the measurement of the gain profile of a laser are investigated. (AIP)

**25851** POLARIZATION OF THE EMISSION OF A GAS LASER WITH A NONLINEAR ABSORPTION CELL. Smirnov, V.S.; Tumaikin, A.M. Opt. Spectrosc. (USSR) 38: No. 4, 457-458 (Apr 1975).

The polarization of the emission of gas lasers with nonlinear absorbers in the lasing cavity is investigated. (AIP)

**25852** MOLECULAR HYDROGEN LASER PUMPED BY A RELATIVISTIC ELECTRON BEAM. Kim, J. J. Madison, WI; University of Wisconsin (1974). 112p. University Microfilms Order No. 75-9981.

Thesis (Ph. D.).

The pumping mechanism of stimulated emission of radiation from molecular hydrogen pumped by a high-power electron beam was studied. A fast rising, 10 nsec pulse of $10^4$ A of 700 keV electrons was guided by a pulsed magnetic field of 2 to 15 kG through the hydrogen gas of pressure from 5 to 200 torr. Intense lasing action was observed in the vacuum ultraviolet region of the molecular hydrogen spectrum, i.e., in the Lyman band (approximately 1600 A) and the Werner band (approximately 1100 A) transitions similar to the previous molecular hydrogen laser experiments. There exist discrepancies in the pressure dependence of the laser output among the various reports, and it is explained in terms of the energy distribution of plasma electrons produced in the breakdown of the gas due to the high electric field induced by the fast-rising current pulse. Comparison is made between the transverse discharges and e-beam excitations, and favors the plasma electron hypothesis. The effect of cooling has been studied. The optical gain is increased by liquid nitrogen cooling, but the gain does not simply depend on 1/root T due to the Doppler broadening. It is explained in terms of the redistribution of the rotational levels, which is restricted by the prohibition of intercombination between the symmetric and antisymmetric states. The intensity alternation in each rotational branch of a vibrational progression is preserved in the lasing action, and is understood in terms of the distribution of molecules in the rotational levels, the selection rules, and the symmetry properties. The influence of foreign gases, such as He, Ar, and $N_2$, in the molecular hydrogen laser was examined and results interpreted in terms of the electron temperature in the various gases. This is also shown to be consistent with the plasma electron theory. The influence of preionization was studied, but the lasing action was destroyed until the e-beam was delayed by approximately a millisecond. It is attributed to the plasma in the gas that causes a rapid magnetic neutralization on the e-beam, causing the cancellation of the induced back emf. (Diss. Abstr. Int., B)

## *Cryogenic and Superconducting Equipment and Devices*

**25853** (JINR-P13-8790) FORM OF A SIGNAL OF A SUPERCONDUCTING QUANTUM INTERFEROMETER IN HYSTERESIS MODE. Vasil'ev, B. V.; Danikov, V. V.; Likharev, K. K. (Joint Inst. for Nuclear Research, Dubna (USSR)). 1975. 19p. (In Russian). Dep. NTIS (US Sales Only) $4.00.

The form of a signal of a superconducting quantum interferometer was investigated. It is shown that the signal is of a usual triangular form in the region of positive and small negative detuning whereas in the region of great negative detuning the signal form becomes rectangular. (auth)

**25854** EFFECT OF TRANSVERSE MAGNETIC FIELDS ON dc JOSEPHSON CURRENT. Rosenstein, I.; Chen, J.T. (Department of Physics, Wayne State University, Detroit, Michigan 48202). Phys. Rev. Lett. 35: No. 5, 303-305 (4 Aug 1975).

We have observed diffraction patterns in critical dc Josephson tunnel current versus magnetic field applied perpendicular to the junction plane. The patterns can be explained by assuming that the perpendicular field penetrates the edge of each film and channels through the junction parallel to the films. An "edge penetration depth," $\lambda_1$, gives a quantitative description of the patterns and their dependence on the angle of field direction. We have found $\lambda_1(T) \propto (1 - T/T_c)^{-1/2}$. (auth)

**25855** LIMITING FLUX-PASSAGE TIME IN NARROW SUPERCONDUCTORS. Rachford, F.J.; Wolf, S.A.; Nisenoff, M. (Naval Research Laboratory, Washington, D. C. 20375); Huang, C.Y. Phys. Rev. Lett. 35: No. 5, 305-307 (4 Aug 1975).

A limiting value for the supercurrent response of narrow superconductors upon flux passage has been deduced from measurements of the 9.2-GHz impedance of thin cylindrical films. The observed times are in good agreement with the predicted relation $\tau_1 \simeq h/2\Delta\ (T)$, where $2\Delta\ (T)$ is the BCS energy gap for the material. (auth)

**25856** SIMPLE, LOW-NOISE UHF SQUID MAGNETOMETER. Clark, T.D.; Jackel, L.D. (School of Applied and Engineering Physics and Laboratory for Atomic and Solid State Physics, Cornell University, Ithaca, New York 14853). Rev. Sci. Instrum. 46: No. 9, 1249-1252 (Sept 1975).

We describe the development of a simple, rugged, low-noise SQUID magnetometer, biased in the uhf range, and constructed around the extensively used two-hole SQUID ring. This design is novel, both in the manner in which rf is coupled to the SQUID ring, and in the ability of the magnetometer system to couple strongly to an external signal or a flux transformer cell. (auth)

**25857** OPERATING CHARACTERISTICS OF THIN-FILM RF—BIASED SQUID's. Falco, C.M.; Parker, W.H. (Department of Physics, University of California, Irvine, Irvine, California 92664). J. Appl. Phys. 46: No. 8, 3238-3243 (Aug 1975).

Operating characteristics of rf-biased thin-film SQUID's of diameter as large as 1 cm are reported. Observation on these SQUID's have experimentally verified several of their conventionally assumed properties such as the dependence of the quantum interference signal on critical current of the weak link, total inductance of the SQUID, inductive coupling between drive coil and the SQUID, and random magnetic flux noise. A simple technique of lowering the inductance, and hence increasing the signal, of large-diameter SQUID's is reported. (auth)

**25858** JOSEPHSON TUNNELING: AN EXAMPLE OF STEADY-STATE SUPERRADIANCE. Rogovin, D. (Department of Physics, and Optical Sciences Center, University of Arizona, Tucson, Arizona 85721). Phys. Rev. B 12: No. 1, 130-133 (1 July 1975).

We demonstrate that the self-oscillations of a Josephson junction can be regarded as an example of steady-state superradiance. (auth)

**25859** SUPERCONDUCTIVE AC DYNAMOELECTRIC MACHINES HAVING TWO ROTORS. Wedman, L. N. (to Westinghouse Electric Corp.). US Patent 3,898,490. 5 Aug 1975. Filed date 24 Sep 1973. 6p.

An ac dynamoelectric machine is constructed with a stator and a pair of rotors. The inner rotor is connected to the drive shaft of the machine and has an induction winding, such as a squirrel cage winding. Between the inner rotor and the stator there is located a second rotor that is essentially free floating. The second or intermediate rotor is provided with a superconducting field winding. (auth)

**25860** RELIABLE DC SQUID MADE WITH TUNNEL JUNCTIONS. Clarke, J.; Goubau, W. M.; Ketchen, M. B. (Univ. of California, Berkeley). IEEE (Inst. of Electr. Electron. Eng.) Trans. Magn.; MAG-11: No. 2, 724-727(Mar 1975).

D. C. SQUIDs of cylindrical geometry have been fabricated using Nb–NbO/sub x/–Pb tunnel junctions. The SQUIDs can be thermally cycled repeatedly and cooled in the earth's magnetic field without significant loss of performance. Flux resolution of 3 x $10^{-5}$ $phi_0$/root Hz above a frequency of 1 Hz has been achieved through optimization of electronic circuitry and careful shielding. Fluctuations and drift in the temperature of the helium bath are found to be the major source of long-term SQUID noise. With a simple temperature stabilizer, drift has been reduced to less than 8 x $10^{-6}$ $phi_0$/hr over a three hour period. (auth)

**25861** SUPERCONDUCTING SAMPLING SYSTEM. Bond, A. J. Lafayette, IN; Purdue Univ. (1974). 117p. University Microfilms Order No. 75-17,161.

Thesis (Ph. D.).

The ability to store a persistent current in a superconducting loop has been used to develop a superconducting sampling system. In this system a persistent current loop stores a sample of an input signal and applies it to the input stage of a crossed film cryotron (CFC) amplifier. A theoretical analysis based on an improved electrical equivalent circuit for superconducting switching element is included. It is shown that the switching speed of the sampling cryotrons determines the upper cutoff frequency of the system. The experimental results agree qualitatively with the theoretical analysis. These results show that the effective bandwidth of the sampling system represents at least an order of magnitude increase over that of the CFC amplifier operating in its normal mode. The product of minimum detectable energy with the response time of the superconducting sampling system is $10^{-30}$ J · sec. It is possible that in a properly designed system of this type the energy-response time produced would be of the order $10^{-33}$ J · sec which approaches the quantum limit of 6.6 x $10^{-34}$ J · sec. (Diss. Abstr. Int. B)

**25862** PREPARATION OF JOSEPHSON JUNCTION BY dc ANODIZATION. Koyanagi, M.; Koga, S.; Endo, T.; Yonezaki, G.; Nakamura, A. (Electrotechnical Lab., Tokyo). J. Jap. Soc. Appl. Phys., Suppl.; 44: 135-140(Jan 1975).

From 6th conference on solid state devices; Tokyo, Japan (2 Sep 1974).

Lead-oxide-lead junction is prepared by vacuum deposition and by dc anodization for the determination of 2e/h at 1 mV level. In order to investigate the fundamental properties of suitable junction for the purpose, two experiments are performed. The first is the magnetic field dependence of the Josephson critical current but it does not contain any special indication about the suitable junction. The second is the microwave power dependence of the normal tunneling current. Two typical behaviors are observed corresponding to the junction resistance above and below 20 mΩ. It is found that the junction of lower resistance than 20 mΩ is suitable for the determination of 2e/h at 1 mV level. The behavior of the junction having the resistance higher than 20 mΩ can be explained by the theory of single particle photon assisted

current assuming the space variation of rf field in the junction, but that of lower resistance junction can not be explained. (auth)

**25863** PHENOMENON NEWLY FOUND IN SUPERCONDUCTING-NORMAL CROSSINGS. Iguchi, I. (Tokyo Univ.). J. Jap. Soc. Appl. Phys., Suppl.; 44: 141-146(Jan 1975).

From 6th conference on solid state devices; Tokyo, Japan (2 Sep 1974).

A new phenomenon was observed in superconducting-normal (S-N) crossings. It appears in any type of S-N junctions tested so far. The phenomenon is considered to be a property of superconductor that arises from an inhomogeneous current distribution near S-N boundary. As a consequence of this effect, a new critical current was defined in addition to the usual critical current of the superconducting film, and many strange I-V characteristics were observed. The effect can be used as a three terminal device. (auth)

**25864** 50 Hz LOSS MEASUREMENTS ON SUPERCONDUCTING NIOBIUM COAXIAL CONDUCTORS. Grigsby, R.; Rogers, E. C. (British Callender's Cables Ltd., London). Cryogenics; 13: No. 2, 100-102(Feb 1973).

A method is described for the measurement of ac losses in a cylindrical conductor forming part of a coaxial superconducting pair. Results given for 25 $\mu$m niobium are substantially lower than previous values obtained for this material when tested in the form of narrow strips, and show that, if used as the conductor in a superconducting power cable, the material could carry a peripheral current density of 360 A $cm^{-1}$ with tolerable losses ($< 10\ \mu W\ cm^{-2}$) at temperatures of up to 7°K. (auth)

**25865** HIGH PRECISION CURRENT SUPPLY. Bloyet, D.; Gonord, P.; Varoquaux, E. J. A.; Vibet, C. (Paris Univ., Orsay, France). J. Phys., E (London); 8: No. 8, 636-638(Aug 1975).

Using a commercial dc voltmeter, a current supply for a superconducting magnet with a stability of a few parts/million can easily be built. A slow sweep mode is also included in the feedback circuitry. (auth)

**25866** TEMPERATURE DISTRIBUTION ALONG SUPERCONDUCTING POWER TRANSMISSION LINES. Keilin, V. E.; Kovalev, I. A.; Pozonkov, M. M. (Inst. of Atomic Energy, Moscow). Cryogenics; 15: No. 6, 323-326(Jun 1975).

A system of equations, describing the refrigerant's parameters (temperature and pressure) change, during its flow along a heated pipeline, for example, along a superconducting power transmission line (SPTL), is derived. The possibility of a temperature maximum existing in the SPTL is found. The possibility, in principle, of "isothermal" SPTL (with constant temperature, along its length) is shown. The most favorable refrigerant parameters' region for SPTL is determined. (auth)

**25867** ACTION OF GLOW DISCHARGE ON LEAD FILMS WHEN MAKING SUPERCONDUCTIVE MICRO-CIRCUITS. Larikov, L. N.; Voytovich, I. D.; Krasil'nikov, V. W.; Lobodyuk, A. A.; Sosnitskii, V. N.; Shmatko, O. A. Radiotekhnika (Moscow); No. 3, 65-77(1974). (In Russian).

When making superconductive microcircuits by the photolithographic technique, the most effective method of removing oxides and products of photolithography from sections of film layers subjected to chemical processing is purification by ions of inert gas in a high-frequency glow discharge. In the process of such cleaning, bulges are frequently formed on the treated sections of lead, leading to impairment of homogeneity, peeling, destruction of the circuit layer, and disturbance of the conditions necessary for creating a tunnel junction. An investigation is made of the influence of the surface state of the substrate and the conditions of film sputtering on the formation of bulges, and methods are proposed for preventing them. It is established that the degree of bulging of lead films during processing in a glow discharge depends on a number of factors: the conditions of film deposition and treatment; adhesion of the film to the substrate; the material and surface state of the substrate and so forth. When making superconductive microcircuits, the most useful method for preventing film peeling is to deposit the film on a stationary substrate in a vacuum no worse than $10^{-5}$ mm Hg at the maximum possible rate. The most effective measure for eliminating bulges when discharge-treating lead films is to use a negative photoresist as a sublayer. While the photoresist can be automatically produced (direct scheme) in the sublayer of ordinary cryotronic microcircuits, this is not possible in circuits on tunnel cryotrons. In this case the lead should be applied to an underlayer of another metal such as indium. (Ref. Zh.)

## Heat Transfer and Fluid Flow

*Refer also to abstract 27285.*

**25868** (KFKI-75-52) AXIAL DISTRIBUTION OF VOID FRACTION IN SUBCOOLED BOILING. Maroti, L. (Kozponti Fizikai Kutato Intezet, Budapest (Hungary)). 1975. 30p. Dep. NTIS (US Sales Only) $4.50.

A theoretical approach to the axial distribution of liquid temperature, vapor quality and void fraction in subcooled boiling is presented. The model is based on the temperature distribution of the thermal boundary layer which can be considered as a measure of deviation from equilibrium condition. It is shown that wall-superheat and subcooling are convenient tools for expressing the vapor generation and the condensation rate in the process. The model is compared with experimental data taken from the available literature and the agreement is found to be surprisingly good, in spite of the fact that the model does not use any empirical constant except those of the applied correlations like void, convective and boiling heat transfer correlations. (auth)

**25869** (RT/ING-(75)6) TWO-PHASE THERMAL BOUNDARY LAYERS ALONG HEATED WALLS. Cumo, M.; Farello, G. E.; Ferrari, G.; Nozzi, P.; Montanari, M. (Comitato Nazionale per l'Energia Nucleare, Rome (Italy)). 1975. 45p. Dep. NTIS (US Sales Only) $5.25.

The present research is an attempt to provide an experimental insight on the development of two-phase thermal boundary layers. An exponential trend was found of the overall boundary layer thickness with length along the heated strip. Flowrate and pressure influences on the thickness of boundary layer appear to be rather weak. (auth)

**25870** (RT/ING-(75)7) DESIGN CORRELATION FOR PRESSURE DROPS IN COILED, ONCE-THROUGH STEAM GENERATORS. Campolunghi, F.; Cumo, M.; Ferrari, G.; Techy, Z.; Vaccaro, G. (Comitato Nazionale per l'Energia Nucleare, Rome (Italy)). 1975. 28p. Dep. NTIS (US Sales Only) $4.50.

A two-phase pressure drop correlation for once-through coiled steam generators is suggested on the basis of a set of experimental data. The correlation employs the results of the well-known homogeneous model, corrected for both specific mass flowrate and pressure. Experimental results are reproduced within a ±10% error. (auth)

**25871** DETERMINATION OF THE INITIAL POINT OF NET VAPOR GENERATION IN FLOW BOILING SYSTEMS. Unal, H. C. (Nijverheidsorganisatie TNO, Apeldornzuid, Netherlands). Int. J. Heat Mass Transfer; 18: No. 9, 1095-1099(Sep 1975).

A correlation to determine the initial point of net vapor generation for water and Refrigerant-22 is given. The range of data correlated is as follows: geometry: circular tubes, rectangular channels and annuli; pressure: 0.1 to 15.8 $MN/m^2$; hydraulic diameter: 0.004 to 0.020 m; subcooling: 3.2 to 42 K; heat flux: 0.02 to 1.92 $MW/m^2$; mass velocity: 132 to 2818 $kg/m^2s$; accuracy: 30%. A scaling law to predict this point for other liquids than those mentioned above has also been established. Experimental determination of the initial point of net vapor generation for water has been carried out with a high-speed photographic technique at 13.9 and 15.8 $MN/m^2$. (auth)

**25872** CRITICAL HEAT FLUXES FOR CURVED AND STRAIGHT SURFACES DURING SUBCOOLED FLOW BOILING. Hughes, T. G. University Park, PA; Pennsylvania State University (1974). 157p. University Microfilms Order No. 75-19,773.

Thesis (Ph. D.).

An analytical and experimental investigation of the critical heat flux on concave, convex and straight heated surfaces has been carried out for subcooled, flow boiling in Freon 113. A total of 274 experiments have been conducted at five mean velocities and four subcoolings. The analytical study and the experimental data indicate that for equal velocity and subcooling, concave surfaces sustain larger critical heat fluxes than straight surfaces which, in turn, sustain larger critical heat fluxes than convex surfaces. The analytical results are compared with the experimental results of this and other work. An idealized vapor bubble cycle has been defined and is used as the basis for a critical heat flux model. In the model, vapor bubbles are assumed to depart from the heated surface when they have grown to the edge of the hydrodynamic sublayer. The frequency of the idealized vapor bubble cycle has been derived and combined with expressions for the energy associated with each vapor bubble cycle and the number of active sites present to produce a critical heat flux expression. The resulting expression contains only one empirical constant. Expressions for the ratio of the critical heat flux between concave and convex surfaces, and between straight and convex surfaces have been derived. These expressions contain no empirical constants and predict that for the conditions of this study, the concave surface will sustain critical heat fluxes of between 1.5 and 2.0 times those for the convex surface, depending upon the radial acceleration and sub-

cooling of the bulk fluid. The straight surface was predicted to sustain between 1.0 and 1.2 times the critical heat flux magnitudes accommodated by the convex surface. An experimental, closed loop boiling apparatus with interchangeable curved and straight test sections was constructed for this study. Details of the apparatus design and operating procedures for the experimental program are given. Tabular summaries of the experimental data are presented for all surfaces, along with graphical comparison of the experimental and analytical results. (Diss. Abstr. Int., B)

## Materials Testing

**25873** DETECTABLE WELD DEFECTS BY CURRENT NDT CODE. Miyoshi, S. (Fuji Electric Co. Ltd., Tokyo (Japan)). pp 3-8 of Significance of Defects in Welded Structures. Kanazawa, T. (Tokyo Univ. (Japan). Faculty of Engineering); Kobayashi, A. S. (eds.). Tokyo, Japan; University of Tokyo Press (1974).

From Japan-U.S. seminar on significance of defects in welded structures; Tokyo, Japan (15 Oct 1973).

Integrity of a weld is assessed on the basis of information obtained by nondestructive examination (NDE); reliability of the assessment is then influenced by the accuracy of the NDE information. As a code in this field, there is ASME Boiler and Pressure Vessel Code Sec. III specifying various nondestructive examination methods, which is widely used. The influences of the ASME code are extensive in Japan, because nuclear industry derives its support from various other industries. However, results of the studies made on nondestructive examination techniques differ somewhat from those of the ASME code. Comments are presented concerning the examination techniques, radiography and magnetic particle examination in particular, and the acceptance standards in production inspection and in-service inspection of weld defects in the ASME Boiler and Pressure Vessel Code Sect. III. (JA)

**25874** ACOUSTIC EMISSION RESEARCH IN JAPAN FOR FLAW DETECTION IN WELD. Onoe, M. (Tokyo Univ. (Japan), Inst. of Industrial Science). pp 22-47 of Significance of Defects in Welded Structures. Kanazawa, T. (Tokyo Univ. (Japan). Faculty of Engineering); Kobayashi, A. S. (eds.). Tokyo, Japan; University of Tokyo Press (1974).

From Japan-U.S. seminar on significance of defects in welded structures; Tokyo, Japan (15 Oct 1973).

Acoustic emission (AE) is transient elastic waves generated by the rapid release of energy within a material; this occurs during plastic deformation, crack initiation and propagation. A highly stressed region near a defect or a crack is thus a good source of AE; the elastic waves can be detected with an ultrasonic sensor attached on the surface of a material. The research works reported at the meetings of Japan Committee on Acoustic Emission (JCAE) are reviewed, with particular attention paid to the detection of delayed cracking in high strength steel weldments. The use of AE for material testing has become standard practice in Japan. Flaw detection in welds, i.e., because of the difficulty in its application to welding process, the works on the AE technique have been concentrated in detecting the delayed cracking in welds. It is useful for locating defects and estimating their seriousness in a reactor vessel with many welds, using sensors. (JA)

**25875** RECENT DEVELOPMENTS IN ACOUSTIC EMISSION AS APPLIED TO WELDING DEFECTS. Ono, K. (California Univ., Irvine (USA)). pp 48-57 of Significance of Defects in Welded Structures. Kanazawa, T. (Tokyo Univ. (Japan). Faculty of Engineering); Kobayashi, A. S. (eds.). Tokyo, Japan; University of Tokyo Press (1974).

From Japan-U.S. seminar on significance of defects in welded structures; Tokyo, Japan (15 Oct 1973).

Extensive research and development efforts during the past decade have raised acoustic emission (AE) testing to the rank of the practical methods of nondestructive evaluation. Intensive development work is under way in several countries in order to monitor large welded structures for the detection of incipient failure. The scientific basis of AE testing is still very poor however. Three phases of AE techniques are described, i.e., signal characterization, mechanisms of AE during fracture processes, and flaw location schemes. In the first phase, the potential analysis methods that may establish the origin of AE signal are examined, and in the second phase, the basis is formed for the AE testing of welding defects. Finally, in the third phase, a best example of practicality of the AE technique is presented, and a representative testing system and its characteristics are examined. (JA)

**25876** TREND OF LARGE GENERATOR ROTOR FORGINGS. Watanabe, J. (Japan Steel Works Ltd., Muroran, Hokkaido. Muroran Plant). Karyoku Genshiryoku Hatsuden; 25: No. 9, 881-884(Sep 1974). (In Japanese).

The unit capacity of steam turbine generators, especially the four pole type ones for nuclear power generation, has increased remarkably in recent years. Along with this, the generator rotor forgings used are also increasing in both size and weight, and it presents the problems in manufacturing. The size, weight, and quality of generator rotor forgings are reviewed. With the advance of supersonic flaw detection techniques, model representation and quantification of defects are now possible, and on the other hand, mechanical properties in the central part of shaft forgings are being revealed. While the forgings of few defects and sufficient mechanical properties are available, quantitative evaluation of their safety aspect can also be done by linear fracture mechanics. There is now prospect for the supply of the shaft forgings for generators up to 2,000 MW with 50 Hz. (JA)

**25877** IMAGE RECORDING WITH NEUTRONS. Robertson, T. J. M. (United Kingdom Atomic Energy Authority, Harwell, Eng.). Br. J. Non-Destr. Test.; 17: No. 4, 114-117 (Jul 1975).

A description is given of the methods of image recording in use at present: neutron converter foils used with photographic film; scintillator screens and their applications; and track-etch systems. The advantages and disadvantages of each method are described. The enhancement of patterns by auto-radiography and possible use of statically-charged surfaces for image recording with neutrons are discussed. (auth)

## Nuclear Explosions

*Refer also to abstracts 25981, 25997, and 26688.*

**25878** (UCRL-50025-75-2, pp 21-23) LSI DEVELOPMENT FOR MICROCOMPUTER APPLICATION TO WEAPON CONTROL. Huen, T. 1 May 1975.

In Electronics Engineering Department quarterly report No. 2, 1975. (California Univ., Livermore (USA). Lawrence Livermore Lab.).

The concept of the secure PAL (permissive-action link) system has been proposed for the control of nuclear weapons. Essential to the successful application of this system is the design of a miniature, all-LSI (large-scale-integration), secure PAL coded switch (SPCS). Two prototypes have been constructed to demonstrate the feasibility of a coded switch that occupies a volume of less than 0.5 $cm^3$. Engineering development work on this system since 1972 is discussed, as is current activity. (auth)

**25879** (UCRL-52000-75-7, pp 13-17) NATIONAL SECURITY. Nuclear Silo Counterforce: Calculating the Soviet-U. S. Balance. Jul 1975.

In Lawrence Livermore Laboratory energy and technology review. (California Univ., Livermore (USA). Lawrence Livermore Lab.).

In recent months the nuclear counterforce work of Kosta Tsipis of the Stockholm International Peace Research Institute and the Massachusetts Institute of Technology has gained wide circulation. His arguments are grounded on comparing, for the Soviet Union and the U. S., the lethality (or K factor), rather than numbers of missiles or throw weight. The latter parameters, he claims, are irrelevant to a counterforce capability against ICBM silos, whereas K, which is a function of yield and accuracy, is a valid measure of potential counterforce performance. Using K factors, he reaches a number of conclusions indicating that the U. S. has and will continue to have counterforce superiority over the U.S.S.R. We have analyzed the counterforce situation also using K factors, but taking into account several parameters and arguments not included by Dr. Tsipis. Although some of the conclusions of our analysis agree with his, there are significant differences. In particular, we find that by 1985 the Soviet Union could equal the U. S. in counterforce lethality and could have a first-strike countersilo capability. (auth)

**25880** NOTE ON THE DURATION OF EARTHQUAKE AND NUCLEAR-EXPLOSION GROUND MOTIONS. Hays, W. W. (Geological Survey, Denver). Bull. Seismol. Soc. Am.; 65: No. 4, 875-883(Aug 1975).

The duration of ground acceleration, an important engineering seismology parameter, was determined for a subset of nuclear explosion and earthquake accelerograms. The nuclear-explosion, ground-motion data sample consisted of accelerograms derived from velocity recordings of high-yield events, MILROW and CANNIKIN, which have been assigned surface-wave magnitudes of 5.3 and 5.7, respectively. The earthquake-data sample consisted pri-

marily of the Richter magnitude 6.6 San Fernando earthquake accelerograms. The criterion used to define duration of ground acceleration was the amount of time that the absolute acceleration is equal to or greater than 5 percent g, an approximate index of the strong phase of ground shaking. On the basis of this criterion and the data subset used, the duration of earthquake ground acceleration differs from that of nuclear explosions. The difference, which is not as great as has generally been thought in the past, is small inside 20 km. Earthquake durations are greater beyond 20 km. The scatter in the duration data was analyzed and found to be sensitive to local site amplification phenomena. These preliminary conclusions need to be validated by further research. (auth)

**25881** (AD-783181) NORSAR LOCATION CALIBRATIONS AND TIME DELAY CORRECTIONS. Scientific Report on Phase 3. Berteussen, K. A. (Norges Teknisk-Naturvitenskapelige Forskningsraad, Kjeller. NORSAR). 3 Jan 1974. Contract F44620-74-C-0001. 46p. NTIS $3.25.

Deviations from theoretical expected values are observed for slowness and travel time for P-signals crossing the array. These observed anomalies are presented. At NORSAR these are corrected for both when performing beamforming and when locating events. The method used is explained and the effect of these corrections both on signal detectability and event location is shown to be quite profound. Some simple crust models, plane dipping moho and a moho which is a curved interface, are tested and found to be able to explain as a maximum 25% of the observed squared deviations. (auth)

## Protective Structures and Equipment

**25882** CONCEPTS OF DESIGN, OPERATION AND SAFETY ON HOT LABORATORIES. Nippon Genshiryoku Gakkaishi; 17: No. 3, 107-114(Mar 1975). (In Japanese).

A description is given on the basic concepts of hot laboratory design and operation, forming part of the results of the work carried out by the Research Committee of Hot Laboratory, Atomic Energy Society of Japan. (auth)

# ENVIRONMENTAL AND EARTH SCIENCES

## Minerals and Ores

**25883** (CONF-740587-1) POSSIBLE METALLOTECTONIC CLASSIFICATION OF URANIUM DEPOSITS. Ziegler, V. May 1974. Translation of SM-183/16. 22p. Dep. NTIS $4.25.

From symposium on the formation of uranium ore deposits; Athens, Greece (6 May 1974).

The primary distribution of uranium and thorium is closely associated with the structural history of the sialic crust and hence with sialic magmatism. Accordingly, far from being distributed homogeneously, uranium should be associated preferentially with certain structural elements of the continental crust. Economic or subeconomic concentrations of uranium deriving for the most part from the primary distribution through hypogenic or supergenic remobilization should also be distributed in fairly close association with these structural elements. The author proposes a metallotectonic classification in the form of a table in which the deposits are grouped according to both the metallogenic type to which they belong and to the main structural elements with which they are associated; the relative ages of the minerals are also indicated. From this table, which is based on the principal known occurrences of uranium in the world, it is possible to see the main characteristics of the distribution of uranium deposits. The chief purpose of the table is to indicate the principles of a method for studying the distribution of uraniferous deposits. Drawn up for a particular region, with appropriate structural and metallogenic distinctions, such a table should make it possible to discern the far more detailed regional patterns which are called for in the search for deposits. (auth)

**25884** (STI/PUB-391) RADON IN URANIUM MINING. Proceedings of a Panel Held in Washington, D. C., 4-7 September 1973. Panel Proceedings Series. (International Atomic Energy Agency, Vienna (Austria)). 1975. 180p. (In English and French). (CONF-7309134-). IAEA $11.00.

From panel on radon in uranium mining; Washington, District of Columbia, USA (4 Sep 1973).

Nine papers were presented in three sessions on effects of radiological and waste management legislative controls on uranium costs and ore reserves, technical problems of uranium mine ventilation, and research on mode of radon release by different types of ore bodies. Separate abstracts were prepared for each paper. (LK)

*For abstracts of individual papers see: 25886-25894.*

**25885** FORMATION OF URANIUM ORE DEPOSITS FROM GROUNDWATER. Hirono, S. (Power Reactor and Nuclear Fuel Development Corp., Tokai, Ibaraki (Japan). Tokai Works). Onsen Kagaku; 25: No. 2, 55-57(Oct 1974). (In Japanese).

Sedimentary uranium deposits in Japan occur in the Tertiary formation granitic rocks. The uranium seems to be dissolved in groundwater from these rocks and deposited under various physico-chemical and mineralogical conditions, then concentrated in special parts or minerals of sediments. The importance of the adsorption of uranium by zeolite and carbonaceous matters is examined. From analysis of uranium ores and observation it was found that the concentration of uranium solution from which uranium was adsorbed by zeolite should be high compared with that of groundwater. From this and the presence of sulfur in the form of pyrite or gypsum in ores, it was postulated that the uranium solution of high concentration would have been formed through the dissolution of the adsorbed uranium in zeolite by the sulphuric acid produced by the oxidation of pyrite partially contained in sediments. Through repeated reactions, some enriched ores would have been formed under favorable conditions. Fine carbonaceous matters usually found in most detrital sediments would have played the similar part to zeolite in the enrichment of such uranium deposits, according to the author. (JA)

**25886** EFFECT OF RADIOLOGICAL PROTECTION STANDARDS ON THE URANIUM MARKET. Francois, Y.; Pradel, J.; Zettwoog, P. (CEN, Fontenay-aux-Roses, France). pp 15-36 of Radon in uranium mining. Vienna; International Atomic Energy Agency (1975). (In French).

From panel on radon in uranium mining; Washington, District of Columbia, USA (4 Sep 1973). See STI/PUB-391; CONF-7309134-. (International Atomic Energy Agency, Vienna (Austria)).

On the basis of concrete results obtained in the CEA's uranium mines over a period of 15 years, the authors determine in the first part of the paper to what extent the costs of radiological protection, which are based on current EURATOM standards, affect the price of uranium. The principles on which radiological protection is organized in the CEA mines are mentioned (independence of the radiological protection service from the mining services, constant presence in the workings of radiological protection officers, multiple sampling). Emphasis is placed on the precautions which have to be taken in order to ensure that radioactivity measurements are representative despite the extreme complexity and the variability of conditions in the workings and so that not just lip service is paid to the standards. A description is given of the way in which the operation of the ventilation system is varied on the basis of radioactivity measurements as the workings are extended. The authors reach the conclusion that in the CEA mines, where the uranium content in the ores frequently exceeds one per cent, it is possible to ensure that the current standard ($3 \times 10^{-10}$ Ci Rn/litre, the equilibrium factor for radon and its daughters being taken as 0.5) is actually adhered to and that nevertheless the cost of radiological protection remains marginal. In the second part of the paper the possible effects of increasing the stringency of the standards are examined. The considerations are based on several thousands of measurements carried out in various workings and galleries. It is shown that the correlation between radon concentration and ore content is weak, which rules out the possibility of being able to calculate in a simple way what the reduction in uranium reserves would be if it were necessary to reduce the acceptable concentrations in the air of the workings. It is concluded that the introduction of slightly stricter standards - by a factor of three, for example - would in the short term have only a slight effect on the price of uranium from existing mines, and this effect would undoubtedly be absorbed in future mines, provided that operations were geared to these new standards from the outset. In the long term the uranium market would not be affected and the effect on world reserves would be negligible. On the other hand, stricter standards going beyond a certain threshold might make mining impossible and reduce world reserves to the amounts obtainable by quarrying. (LK)

**25887** EFFECTS OF RADIOLOGICAL AND WASTE-MANAGEMENT LEGISLATIVE CONTROLS ON URANIUM PRODUCTION COSTS WITH SPECIFIC REFERENCE TO THE BEAVERLODGE OPERATION OF ELDORADO NUCLEAR LIMITED. Bell, D. D. (Eldorado Nuclear Limited, Ottawa, Ont.). pp 37-48 of Radon in uranium mining. Vienna; International Atomic Energy Agency (1975).

From panel on radon in uranium mining; Washington, District of Columbia, USA (4 Sep 1973). See STI/PUB-391; CONF-7309134-. (International Atomic Energy Agency, Vienna (Austria)).

Within 10 years, up to 1973, the cost of reducing the radiation exposure in uranium mines from 1 working level (W. L.) to <0.3 W. L., in constant (1973) dollars, has been $1.07 per ton of ore milled. The cost of waste management has added $0.19 per ton. Factors which may vary these costs are location, geological occurrence of the ore, and imposition of regulations not foreseen at the inception of the mine. Improvements were accomplished by a major increase in volume of ventilation and a general cooperation in the application of controls. The sampling of all working areas is done by plan, and the results are announced monthly, including an underground exposure summary giving cumulative exposures since 1966. Waste management was improved by re-routing of effluents, by construction of secondary and tertiary dams to increase the retention time and afford emergency safeguards, and by chemical treatment to render certain pollutants insoluble. The sum of these added costs may significantly affect the mine cut-off grade, and hence the published data on reserves throughout the uranium mining industry may become invalid. (auth)

**25888** RADON IN URANIUM MINING: EFFECT OF PROTECTIVE CONTROLS ON URANIUM RESOURCES IN SOUTH AFRICAN MINES. Haasbroek, A. C.; Du Toit, R. S. J. (Department of Mines, Pretoria). pp 49-60 of Radon in uranium mining. Vienna; International Atomic Energy Agency (1975).

From panel on radon in uranium mining; Washington, District of Columbia, USA (4 Sep 1973). See STI/PUB-391; CONF-7309134-. (International Atomic Energy Agency, Vienna (Austria)).

The past and the current situation with respect to the radiation levels of working atmospheres in South African gold/uranium mines is reviewed. The effect of ventilation on the radiation levels in the uranium section of a gold mine is summarized. Legislation currently applicable to the ventilation of the under-

ground working places of South African mines is dealt with and the effect of protective controls on uranium resources is discussed. (auth)

**25889** VENTILATION AND OTHER PROBLEMS IN CONTROLLING RADON DAUGHTERS IN URANIUM MINES. Yourt, G. R. pp 63-72 of Radon in uranium mining. Vienna; International Atomic Energy Agency (1975).

From panel on radon in uranium mining; Washington, District of Columbia, USA (4 Sep 1973). See STI/PUB-391; CONF-7309134-. (International Atomic Energy Agency, Vienna (Austria)).

In many respects the control of alpha radioactivity in mine atmospheres can be achieved by applying the same methods used for other airborne contaminants such as dust, diesel exhausts, blasting gases and methane. This is done by suppressing, confining, diluting and removing the contaminants. Some additional and special methods and problems encountered are discussed. (auth)

**25890** VENTILATION OF URANIUM MINES. Francois, Y.; Pradel, J.; Zettwoog, P.; Dumas, M. (CEN, Fontenay-aux-Roses, France). pp 73-109 of Radon in uranium mining. Vienna; International Atomic Energy Agency (1975). (In French).

From panel on radon in uranium mining; Washington, District of Columbia, USA (4 Sep 1973). See STI/PUB 391; CONF-7309134-. (International Atomic Energy Agency, Vienna (Austria)).

Ventilation of French mines is described in terms of the primary ventilation system, which brings the outside air close to the working places using the overall structure of the mine to form the airways, and the secondary ventilation system, which is for the distribution of the primary air or for the ventilation of the development drifts and blind tunnels. Brief mention is made of the French regulations on the ventilation of mines in general and uranium mines in particular. The authors describe the equipment used and discuss the installed capacities and air flow per man and per working place. The difficulties encountered in properly ventilating various types of working places are mentioned, such as sublevel development drifts, reinforced stopes, and storage chambers with an artificial crown. The second part of the paper is devoted to computer calculations of the primary ventilation system. Emphasis is given to the layout of the ventilation system and to air flow and negative pressure measurements at the base of the mine. The authors show how calculations can be applied to new heading operations, a change in resistance, the replacement or addition of a ventilator, and a new air inlet or outlet. The authors come to the conclusion that since ventilation is at present the most reliable way of avoiding the pollution of mines, a thorough knowledge of the capabilities in this respect can often help improve working conditions. Despite the progress made, however, constant surveillance of the ventilation systems in uranium mines by a separate team with no responsibility for production problems is still necessary if high efficiency is to be maintained. (LK)

**25891** MINE ENGINEERING AND VENTILATION PROBLEMS UNIQUE TO THE CONTROL OF RADON DAUGHTERS. Rock, R. L. (EMS-Denver Technical Support Center). pp 111-126 of Radon in uranium mining. Vienna; International Atomic Energy Agency (1975).

From panel on radon in uranium mining; Washington, District of Columbia, USA (4 Sep 1973). See STI/PUB-391; CONF-7309134-. (International Atomic Energy Agency, Vienna (Austria)).

Quality and quantity of ventilation are the two interrelated but key factors in any radon-daughter control programme. The better the intake air quality (little or no contamination from radon and its daughters), the less are the total air requirements for ventilation of active mining areas. Engineering principles for quantity distribution of air through underground working areas are straightforward and the formulae and theories governing forced ventilation are not within the scope of this paper. Rather, this paper discusses the principal methods of utilizing mine planning to facilitate radon-daughter control and also treats the more subtle features of mine ventilation which are especially critical in the ventilation of mines where radon gas constitutes an environmental contamination problem. (auth)

**25892** RADON-222 EMANATION CHARACTERISTICS OF ROCKS AND MINERALS. Barretto, P. M. C. (National Nuclear Energy Commission, Rio de Janeiro). pp 129-150 of Radon in uranium mining. Vienna; International Atomic Energy Agency (1975).

From panel on radon in uranium mining; Washington, District of Columbia, USA (4 Sep 1973). See STI/PUB-391; CONF-7309134-. (International Atomic Energy Agency, Vienna (Austria)).

The activity, emanation rate and percentage of radon-222 escape were investigated for a variety of rocks and minerals using alpha scintillation counting techniques. Rocks show a wide range of leakage with values ranging from 1 to 20% and an activity of 2 to 80 x $10^{-4}$ pCi/h·g under identical laboratory conditions. The stronger emanations were found among granitic rocks and conglomerates whereas basic and calcareous rocks showed the lowest values. Accessory minerals, although rich in uranium, show very low radon emanation, i.e. less than 1 to 2%. The lack of dependence of emanation on parent uranium concentrations was clearly established. Also a positive correlation was observed between weathering and radon escape and between natural alpha dose and emanation. High-temperature experiments (up to 1200°C) on minerals demonstrated a progressive decrease in the percentage of radon loss. This phenomenon appears to be the result of annealing of natural radiation damage. As expected, an increasing radon loss with decreasing particle size was observed. The temperature dependence of radon emanation in the range of -80°C to +250°C was investigated and showed a strong adsorption for temperatures below -20°C. (auth)

**25893** LABORATORY STUDY OF RADON EMANATION FROM DOMESTIC URANIUM ORES. Austin, S. R. (Denver Mining Research Center). pp 151-163 of Radon in uranium mining. Vienna; International Atomic Energy Agency (1975).

From panel on radon in uranium mining; Washington, District of Columbia, USA (4 Sep 1973). See STI/PUB-391; CONF-7309134-. (International Atomic Energy Agency, Vienna (Austria)).

Laboratory measurements of radon emanation were made by a slightly modified sealed-can gamma-only method of radiometric assaying for equivalent uranium. When a sample is sealed in a container, the percentage build-up of gamma activity of the radon daughters, lead-214 and bismuth-214, from sealing time to equilibrium is equal to the percentage build-up of radon-222 and thus to the percentage emanation and may be calculated from two measurements at suitable times. The use of drill-core samples allows the partial assessment of radon problems before mining begins. The measured radon emanation from individual samples ranges from less than 1% to 91%. The average values of samples from various domestic mining areas range from 8% to 57%. Factors appearing to affect emanation are: (1) porosity and permeability; (2) ore grade; (3) uranium mineral species (seldom controlling); (4) crystal or particle size; (5) lithology (coalified wood emanates less than sandstone, mudstone emanates more); (6) radium mineralogy; (7) geologic age; (8) mobility of deposits; and (9) moisture content. The dominance of one or more of these factors determines the effectiveness of specific control measures. (auth)

**25894** EFFECTS OF STRICTER RADIATION EXPOSURE STANDARDS ON URANIUM COSTS AND ORE RESERVES. McGinley, F. E. (Atomic Energy Commission, Grand Junction, CO). pp 3-14 of Radon in Uranium Mining. Vienna; International Atomic Energy Agency (1975).

From panel on radon in uranium mining; Washington, District of Columbia, USA (4 Sep 1973). See STI/PUB-391; CONF-7309134-. (International Atomic Energy Agency, Vienna (Austria)).

The radon daughter products found in uranium mine atmospheres have been assumed as the cause of the higher-than-expected incidence of lung cancer among underground uranium miners. Although radon-daughter measurements have been made in United States uranium mines since about 1950, it was not until 1960 that regulatory standards were adopted and systematic monitoring began. The Federal Radiation Council (FRC) in 1967 recommended that occupational exposure be controlled so that no individual miner received an exposure of more than 6 working level months (WLM) in any consecutive 3-month period and an exposure of more than 12 WLM in any consecutive 12-month period. For the next few years there was considerable controversy over the need for a reduced exposure standard. Ultimately, upon recommendation of the FRC, a standard of 4 WLM per year was adopted, effective 1 July 1971. All standards required records to be maintained of individual miners' cumulative radon-daughter exposure. The economic impact of the adoption of the standard of 4 WLM per year on 1 July 1971 has been difficult to evaluate. Certainly, mining costs have increased and many of the small high-cost and marginal mines have shut down, but this may reflect the recent market condition as much as the reduction in the exposure standard. As for the impact of a further reduction in the exposure standard, undoubtedly costs would rise, additional mines would shut down, and reserves minable by underground methods would decrease significantly. It is hoped that the results of a continuing review of epidemiological data, which showed a decrease in the incidence of lung cancer among uranium miners, will obviate the necessity for recommending a further reduction in the exposure standard. (LK)

**25895** LITHOLOGY AND URANIUM POTENTIAL OF JURASSIC FORMATIONS IN THE SAN YSIDRO–CUBA AND MAJORS RANCH AREAS, NORTHWESTERN NEW MEXICO. Santos, E. S. Geological Survey Bulletin 1329. Washington, DC; Geological Survey (1975). 22p. GPO $1.60.

The aggregate thickness of sedimentary rocks of Jurassic age near the eastern and southeastern margin of the San Juan Basin in Sandoval County, N. Mex., is about 1150 feet (350 metres). The Entrada Sandstone at the base is overlain successively by the Todilto, Summerville, and Morrison Formations. The Entrada Sandstone, 97 to 227 feet (30 to 69 m) thick, consists of a lower, silty member composed of red and brown siltstone and fine-grained sandstone, and an upper, sandy member composed of brown and white sandstone. The Todilto Formation, 5 to 125 feet (1.5 to 38 m) thick, consists of a lower, limestone unit about 5 feet (1.5 m) thick, and an upper, massive white gypsum unit. The Summerville Formation, 0 to 50 feet (0 to 15 m) thick, consists of variegated, interstratified mudstone, claystone, siltstone, and sandstone. The Morrison Formation, 750 to 870 feet (229 to 265 m) thick, is divided into three members; the Recapture Member at the base, 200 to 350 feet (61 to 107 m) thick, is overlain successively by the Westwater Canyon Member, 0 to 240 feet (0 to 73 m) thick, and the Brushy Basin Member, 200 to 350 feet (61 to 107 m) thick. The Recapture Member consists mainly of red and white color-banded fine-grained sandstone. The Westwater Canyon and Brushy Basin Members consist mainly of red and green mudstone interstratified with grayish-orange arkosic sandstone. The upper unit of the Brushy Basin Member is called the Jackpile sandstone, a name of economic usage. It is 0 to 165 feet (0 to 50 m) thick and consists of white and grayish-orange fine-, medium-, and coarse-grained arkosic sandstone. A comparison of ore-bearing sandstone units in the Ambrosia Lake and Laguna mining districts with equivalent sandstone units in the area studied reveals many similarities, in color, texture, mineral composition, and minor-element distribution. Differences are minor and most of the sandstone in the Morrison Formation above the Recapture Member in the area studied is considered to be a potential host for uranium ore deposits. (auth)

## Radioactivity Monitoring and Transport

*Refer also to abstracts 25914, 25915, 26094, and 26316.*

**25896** (COO-3132-20) ORIGINS OF THE DEEP-SEA SEDIMENTS AND THEIR VARIATIONS WITH TIME. Annual Progress Report No. 6, May 1975. Biscaye, P. E. (Columbia Univ., Palisades, N. Y. (USA). Lamont-Doherty Geological Observatory). May 1975. Contract AT(11-1)-3132. 52p. Dep. NTIS $5.75.

Techniques for studying water mass mixing and sediment transport in the benthic layer of the deep sea and the effects of these processes on the continental shelf specifically in the New York Bight were studied. Results are presented for the first major combined geochemistry-physical oceanography cruise. Data on the nature of the bottom sediments are presented principally in context of their potential as sources of both radon and methane in the lower water columa. Preliminary data on the nature and composition of suspended particulates also indicate potential for tracing the mechanisms of solids dispersal in the Bight. (PCS)

**25897** (ERDA-54(Vol.2)(74)) ENVIRONMENTAL MONITORING AT MAJOR U. S. ENERGY RESEARCH AND DEVELOPMENT ADMINISTRATION SITES, CALENDAR YEAR 1974. (Energy Research and Development Administration, Washington, D. C. (USA). Div. of Operational Safety). Aug 1975. 577p. Dep. NTIS $16.60.

The purpose of this compendium is to present, in a central reference document, all of the annual reports summarizing the results of the environmental monitoring programs conducted at each of the Energy Research and Development Administration (ERDA) sites which have a potential for environmental impact or which release a significant quantity of radioactivity or nonradioactive pollutants. The individual reports comprising this compendium were prepared in accordance with ERDA Manual Chapter 0513, "Effluent and Environmental Monitoring and Reporting." Each contains data on the levels of radioactivity and nonradioactive pollutants in effluents and the environs at each site, and an interpretation of effluent and environmental measurements and sampling results in relation to the appropriate standards for environmental protection, including estimates of potential radiation exposures offsite. It is noteworthy that, in most cases, these potential offsite exposures are so low they cannot be determined by direct measurement methods but must be estimated by calculational techniques. All offsite exposures from routine effluent releases were less than one percent of the radiation protection guidelines for the public in 1974. (auth)

**25898** (TID-3910-S11) TERRESTRIAL AND FRESHWATER RADIOECOLOGY. A Selected Bibliography. Klement, A. W. Jr.; Shultz, V. (Washington State Univ., Pullman (USA). Dept. of Zoology). 1975. 167p. Dep. NTIS $7.60.

This compilation of data on terrestrial and freshwater radioecology contains some 1400 references and is based on publications for which abstracts appeared in Volumes 29 and 30 of Nuclear Science Abstracts and references obtained from other sources. Many were obtained from reviews and other publications. A number of more general references have been included which are not basically on ecology but may be related, and it is hoped of interest to ecologists, e.g. use of tracers in pesticide studies. While compilation of a list in an area broad in scope is often somewhat arbitrary, an attempt was made to reference publications which were related to field or laboratory studies of wild species of plants and animals with respect to radiation effects or metabolic studies involving radionuclides, including parasites. Studies of laboratory or domestic organisms have not in general been included unless such studies are ecological in nature, e.g., on population growth or synergistic. References are included to brackish water and brackish water organisms. Environmental monitoring was included only when natural waters and wild animals or plants were involved. Other kinds of material are included such as nuclear power plant thermal pollution and reports concerning organisms at nuclear energy installations even though the particular study did not involve research on radiation effects or cycling of radionuclides. (CH)

**25899** SYSTEMATIZED NUCLEAR RADIATION MONITORING NEEDED. At. Jpn.; 18: No. 8, 24-27(Aug 1974).

The optimum system of environmental radiation monitoring with reference to items, frequency, and limits of area for measurement is considered. As subjects of environmental radiation monitoring, it is appropriate to choose such as are directly related to human exposure; for example, air dose, air, water, agricultural and aquatic foods, etc. The critical pathways, critical foods, and critical nuclei become effective items. Measuring should be done from fixed points, which are decided considering dispersal of radioactive substances and environmental conditions in the highly populated areas. The air dose, air, water, etc., should be checked not less than or on an averge of every three months, and agricultural and aquatic products should be measured during the harvest and the fishing season. The limits of areas for monitoring will be determined by the pattern of dispersal of radioactivity, the amounts discharged, the kinds of radioactivity, etc., as well as the natural environmental conditions, the meterological conditions, the topography, and the social environmental conditions where nuclear facilities are located. Environmental radiation monitoring should begin about two years before the commencement of operation of nuclear energy facilities for obtaining necessary information, and for training. In addition, it is also important to review the monitoring plan and its results from time to time to meet with changes in the natural and social environment. (JA)

### Atmosphere

*Refer also to abstracts 25884, 25886–25894, 26035, 26093, and 27160.*

**25900** (COO-3425-10) MEASUREMENT OF AIRBORNE RADIOACTIVITY AND ITS METEOROLOGICAL APPLICATION. Part IV. Annual Report, 1 April 1972–31 March 1973. Reiter, R.; Sladkovic, R.; Kanter, H. J.; Carnuth, W.; Poetzi, K. (Fraunhofer-Gesellschaft zur Foerderung der Angewandten Forschung e.V., Garmisch-Partenkirchen (F. R. Germany). Inst. fuer Atmosphaerische Umweltforschung). Jan 1975. Contract AT(11-1)-3425. 119p. Dep. NTIS $9.00.

Results obtained by a previously described method of studying the exchange of air masses between stratosphere and troposphere are reported. Continuous data on the ratio of $^{7}Be$, $^{32}P$, $^{33}P$, and $^{35}S$ and of fallout radioisotopes are given for the entire period reported. First measurements with a Rawinsonde station and with a lidar system are described. An intrusion of stratospheric air into the troposphere is described by a detailed meteorological analysis. The transport between place of intrusion and observation could be reconstructed with all details over a distance of about 12,000 km. Subsidence has been observed only during the first part of the course of transport. Over more than half the distance of the transport was maintained by advection. A case of horizontal mixing observed could be described by two corresponding trajectories on the same plane. Radionuclides with a short life-time originating from a Chinese nuclear test were determined in fallout by gamma-spec-

trometry. Solar flares increase the frequency of intrusions of stratospheric air into the troposphere. (auth)

**25901** (HASL-296) DATA SET FOR NOBLE GAS PLUME EXPOSURE MODEL VALIDATION. Gogolak, C. V. (Energy Research and Development Administration, New York (USA). Health and Safety Lab.). Jul 1975. 15p. Dep. NTIS $4.00.

A data set for calculations of exposure to radioactive plumes from light water power reactors was assembled using measurements made with continuously-monitoring ionization chambers at seven sites in the vicinity of a boiling water power reactor. Each record consists of an hourly measurement of wind speed, wind direction, and temperature at three heights, solar radiation, the gamma exposure rate recorded at the seven locations and the average release rate. The set consists of 9504 such records corresponding to continuous data gathered over 13 months. (auth)

**25902** (KFK-2172) CALCULATION OF THE GAMMA-DOSE RATE FROM A CONTINUOUSLY EMITTED PLUME. Huebschmann, W.; Papadopoulos, D. (Kernforschungszentrum Karlsruhe (F. R. Germany). Abt. Strahlenschutz und Sicherheit). Jun 1975. 42p. (In German). Dep. NTIS (US Sales Only) $5.25.

A computer model is presented which calculates the long term gamma dose rate caused by the radioactive off-gas continuously emitted from a nuclear reactor stack. The statistical distribution of the wind direction and velocity and of the stability categories is taken into account. The emitted activity, distributed in the atmosphere according to the statistics, is assumed to be concentrated at the mesh points of a three-dimensional grid. The grid spacing and the integration limits determine the accuracy as well as the computer time needed. When calculating the dose rate in a given wind direction, the contribution of the activity emitted into the neighboring sectors is evaluated. This influence is demonstrated in the results, which are calculated with an error below 3 per cent and compared to the dose rate distribution curves of the models. (auth)

**25903** (NCRP-44) KRYPTON-85 IN THE ATMOSPHERE: ACCUMULATION, BIOLOGICAL SIGNIFICANCE, AND CONTROL TECHNOLOGY. (National Council on Radiation Protection and Measurements, Washington, D. C. (USA)). 1 Jul 1975. 86p.

The projected rapid growth of the nuclear power industry necessitates a careful assessment of any related potential for environmental pollution. $^{85}Kr$ releases deserve special attention because of the inherent difficulty in their control and their essentially nonreactive and mobile nature in the atmosphere. The purpose of this report is to estimate the future global concentrations of $^{85}Kr$, their potential significance, and possible techniques for their control. Projections of $^{85}Kr$ accumulations are made to the year 2000, as this is now sufficiently close to permit reasonable approximations to be made of the world's energy requirements and the extent to which they will then be fulfilled by nuclear power reactors. On the other hand, the year 2000 is sufficiently far off to allow for periodic reappraisal of the projections of $^{85}Kr$ accumulation in relation to developing information about the biological effects of this nuclide and the technology for control of $^{85}Kr$ releases. In addition to the global projections, the present report also includes estimates of $^{85}Kr$ concentrations near nuclear fuel chemical reprocessing plants. (auth)

**25904** (ORNL-tr-2976) ATOMIC POWER STATIONS AS A SOURCE OF $14^0C$ DISCHARGE. Rublevskii, V. P.; Zykova, A. S.; Turkin, A. D. Translation by Martha Gerrard of Russian Report. 5p. (CONF-730907-26). Dep. NTIS $4.00.

From 3rd international congress of the International Radiation Protection Association meeting; Washington, District of Columbia, USA (9 Sep 1973).

Carbon-14 is produced in nuclear reactors by neutron reactions in $^{14}N$, $^{17}O$, and $^{13}C$. The expanding use of nuclear reactors for power production will contribute additional amounts of $^{14}C$ to the existing background levels due to atmospheric testing of nuclear devices and natural production by neutrons in the upper atmosphere. This report considers the problem of environmental $^{14}C$ contamination from increasing use of nuclear reactors for power production. Experimental data on $^{14}C$ production at different types of nuclear power stations in the USSR are presented. Future $^{14}C$ production at nuclear power stations will be some 12,000 Ci/day to the year 2010. The $^{14}C$ concentration in the terrestrial biosphere will reach 1050 percent of its natural level by this year. These estimates are compared with existing equilibrium levels of naturally occurring $^{14}C$ and with the decreasing inventory of $^{14}C$ from atmospheric nuclear tests. (auth)

**25905** DOSE ESTIMATION MODEL FOR GASEOUS FISSION PRODUCTS FROM NUCLEAR FACILITIES. Yamamoto, Y.; Mishiro, M.; Maekawa, M. (Tokyo Univ. (Japan). Faculty of Engineering). J. Fac. Eng., Univ. Tokyo, Ser. B; 32: No. 4, 589-636(Dec 1974).

A model for the calculation of activities of individual fission product nuclides, total activity, gamma radiation and beta particles, available for reactors of any type, is presented. Using this model, the fission product's activity produced in all reactors in Japan based on the Japanese nuclear electricity generating schedule was calculated for several decades in units of months. The concentration distribution of fission products in the atmosphere and exposure rates from released gaseous radionuclides arising from the stack of either reactors or reprocessing plants were calculated on the basis of Pasquill's Equation. (auth)

**25906** DEPOSITION RATE OF AEROSOL PARTICLES FROM TURBULENT FLOW THROUGH VERTICAL ANNULI. Kitamoto, A.; Takashima, Y. (Tokyo Inst. of Tech. (Japan)). Bull. Tokyo Inst. Technol. (Engl. Ed.); No. 121, 67-82(Mar 1974).

Particle deposition rate in a smooth annular tube was theoretically estimated by means of the aerosol transport model according to Wells and Chamberlain. Three kinds of aerosol particles were used for experiment: 1) droplets of tricresyl phosphate, 2) polystyrene solid spheres and 3) Aitken nuclei. The diameter of the droplets was determined from the rate of sedimentation in a Schaefer cell. The polystyrene spheres of 5 $\mu$m diameter tagged with $^{51}Cr$ were used. The polystyrene spheres were monodisperse solid particles, whereas tricresyl phosphate particles were droplets. In order to measure the deposition rate of submicron particles, the Aitken nuclei were tagged with ThB ($^{212}Pb$). The Aitken nuclei, nonspherical aggregate of very small particles, were measured by their diffusivity in laminar flow with a diffusion box. The deposition surface of the apparatus was a brass rod of 1.27 cm diameter placed axially in a copper tube of 3.81 cm internal diameter. The activity of the particles in air stream was determined from the average value of activity caught in the samplers fitted with membrane filters (Millipore filter) at either end of the tube. Isokinetic sampling speed was used for sampling 5 $\mu$m particles, but for 2 $\mu$m and smaller particles, sampling velocity was less than isokinetic. The most reliable results as compared with experimental data were predicted in case of the particle diameter from 0.1 to 5 $\mu$m by the numerical analysis based on the effective eddy diffusivity model of particles, defined by the equation of deposition velocity for monodisperse particle system. (JA)

**25907** RADIOACTIVITY OF THE AIR AND SOME FOODS IN MOSCOW IN 1971 AND 1972. Zykova, A. S.; Telushkina, E. L.; Erfremova, G. P.; Kuznetsova, G. A.; Kiselev, V. V. Gig. Sanit.; No. 3, 53-55(1975). (In Russian).

The article reports the results of systematic monitoring of the density of radioactive fallout and concentrations of artificial radioactive aerosols in the ground layer of air in Moscow and vicinity in 1971 and 1972. It also presents data on the amount of $^{90}Sr$ and $^{137}Cs$ in milk, potatoes, and cabbage sampled in three different places in Moscow Oblast. The amount of radioactive fallout in 1971 was about the same as in 1970 but was approximately 50% less in 1972. The $^{90}Sr$ content of all the foods tested was practically the same in 1971 and 1972, but the $^{137}Cs$ content of milk and potatoes was somewhat lower in 1972 than in 1971. 1972 was a year in which global fallout and concentration of radionuclides in the air diminished appreciably. (JPRS)

**25908** ENVIRONMENTAL RADIOACTIVITY. Report of the Federal Government. Bundesrat - Drucksache; No. 7/2510, 1-21 (Aug 1974). (In German).

15 figs.; 3 tabs.

The evaluation of more than 50 official points of measurement for the control of environmental radioactivity in the German Federal Republic showed a marked decrease of activity concentration in the surveyed fields of precipitation, air, water, milk, and humans as compared to 1972. This decrease can be attributed to the stopping of above-ground nuclear weapons tests effected in 1963. In 1973, a survey of the environment of nuclear power stations did not show any significant difference between these regions and others. The mean genetic radiation exposure in the year 1973 is given in a chart. Selected data from different places of measurement give mean values and annual balances of the radionuclides $^{137}Cs$ and $^{90}Sr$ for men, women, and children, as well as for cistern water, milk, and hospital food. Finally, a balance of the import and export of radionuclides in 1973 is given. (GE)

## Water

*Refer also to abstract 25912.*

### Ecosystems and Food Cycles

*Refer also to abstract 25907.*

**25909** (PRNC-183-A) PUNTA HIGUERO ENVIRONMENTAL STUDIES. Supplementary Report. Parrish, J. D. (Puerto Rico Nuclear Center, Mayaguez). 1 May 1975. Contract E(40-1)-1833. 20p. Dep. NTIS $4.00.

For the Puerto Rico Water Resources Authority.

Data are presented on the number and species of fish and invertebrates in shallow waters near shore at the Punta Higuero proposed power plant site in Puerto Rico. (CH)

## Radiometric Techniques

*Refer also to abstract 25900.*

**25910** DISCORDANT IO-AGES AND THE URANIUM AND THORIUM DISTRIBUTION BETWEEN ZIRCON AND HOST ROCKS. Fukuoka, T.; Kigoshi, K. (Gakushuin Univ., Tokyo (Japan). Faculty of Science). Geochem. J. (Nagoya); 8: No. 3, 117-122 (Sep 1974).

Io-ages obtained for glass-zircon pairs which were not consistent with expected ages were discussed on the basis of uranium and thorium distribution between zircon and glass. Uranium and thorium distribution between zircon and host rocks from dacites and granites were also discussed. Discordant Io-ages obtained for glass-zircon pairs with normal $(TH/U)_{zircon}/(Th/U)_{glass}$ ratio are explained by early stage crystallization of the zircon in the magma. Discordant Io-ages with abnormal $(Th/U)_{zircon}/(Th/U)_{glass}$ ratios suggest that the zircon was captured in the magma as xenocryst. The discrepancy between $(Th/U)_{zircon}/(Th/U)_{glass}$ ratios (about 0.19) for dacites and $(Th/U)_{zircon}/(Th/U)_{whole\ rock}$ ratios (about 0.12) for granites could be explained by crystallization of granitic zircon from liquid having chemical composition different from that of the whole rock of granite. (auth)

**25911** IONIUM DATING OF ACIDIC VOLCANIC ROCKS. Fukuoka, T. (Gakushuin Univ., Tokyo (Japan). Faculty of Science). Geochem. J. (Nagoya); 8: No. 3, 109-116(Sep 1974).

Concentrations of uranium, and concentrations and isotopic ratios of thorium in zircon and glass were determined for pyroclastic dacite pumices in southern Kyushu, Japan, and Io-ages were calculated. Uranium and thorium distributions in other minerals were also determined. Uranium and thorium contents of minerals were highest for zircon and decreased in the order, zircon-apatite-glass-mafic minerals-plagioclase. Zircons showed the highest U/Th activity ratios compared with other minerals. Io-ages obtained by glass-zircon pair for pyroclastic flows in southern Kyushu, except for Ata pyroclastic flow were consistent with $^{14}C$ and fission track ages and the stratigraphic sequence. Comparison of uranium and thorium concentrations in mineral constituents of acidic volcanic rocks showed that the glass-zircon pair is the most preferable for ionium dating. (auth)

## Site Surveys

**25912** (LA-5998-MS) WATER SUPPLY AT LOS ALAMOS DURING 1974. Purtymun, W. D. (Los Alamos Scientific Lab., N. Mex. (USA)). Jun 1975. Contract W-7405-ENG-36. 20p. Dep. NTIS $4.00.

The Los Alamos water supply for 1974 consisted of $1624 \times 10^6$ gal from 16 wells in three fields, with an additional $35 \times 10^6$ gal from a gallery in Water Canyon. Water-level trends are as anticipated under current pumpage practices. Recommendations for a new well in the Pajarito field and a replacement well in the Guaje field are still valid. An exceedingly dry spring and summer, or an outage of a high-yield well, could result in a shortage of supply for an indefinite period of time. Monthly pumping and production data are presented for the years 1972, 1973, and 1974 for each of the 16 wells and the Water Canyon gallery. (auth)

**25913** DETAILS OF MICROEARTHQUAKE SWARMS IN THE COLUMBIA BASIN, WASHINGTON. Malone, S. D.; Rothe, G. H.; Smith, S. W. (Univ. of Washington, Seattle). Bull. Seismol. Soc. Am.; 65: No. 4, 855-864(Aug 1975).

Three microearthquake swarms in the Columbia River basin of eastern Washington were studied by means of a small portable seismic network. Earthquakes in this area typically occur in swarms, concentrated both temporally and spatially. One unusual characteristic of the three swarms studied was the shallow focal depths of all events. Most events located had depths less than 1 km; none were deeper than 2 km. Composite focal mechanism solutions indicate that more than one fault surface is active in any one swarm. All events had some thrust component with the axis of maximum compression oriented roughly in a north-south direction. (auth)

## Thermal Effluents

*Refer also to abstract 27404.*

**25914** (AECL-5108) BIOLOGY AND HEALTH PHYSICS DIVISION PROGRESS REPORT, OCTOBER 1 TO DECEMBER 31, 1974. (Atomic Energy of Canada Ltd., Chalk River Nuclear Labs.). 1974. 114p. Dep. NTIS (US Sales Only) $8.75. AECL $3.00.

Separate abstracts were prepared for three sections of this report. (CH)

*For abstracts of individual sections see: 25915, 25951, and 26048.*

**25915** (AECL-5108, pp 41-72) ENVIRONMENTAL RESEARCH BRANCH. Ophel, I. L. (Chalk River Nuclear Labs., Ont.). 1974.

In Biology and Health Physics Division progress report, October 1 to December 31, 1974. (Atomic Energy of Canada Ltd., Chalk River, Ontario. Chalk River Nuclear Labs.).

Progress is reported on studies of the effects of thermal effluents from the Gentilly reactor on temperature distribution in the St. Lawrence River and biological effects on plants and molluscs in the discharge area. Radiation monitoring activities in the vicinity of the Chalk River Nuclear Laboratories during the period included a preliminary study of the hydrology of Perch Lake and of the Gentilly-2 reactor site; measurements of the uptake of tritium by trees in the Perch Lake disposal area; measurements of the content of $^{60}Co$ and $^{90}Sr$ in Perch Lake; measurements of the distribution of natural deuterium in water of the St. Lawrence River and its tributaries; measurements of the content of various radionuclides in liquid effluents; and measurements of the $\gamma$ dose rate at the boundary of the Chalk River area. (CH)

**25916** (DP-MS-75-12) THERMAL EFFECTS ON GROWTH AND RESPIRATION RATES OF THE MAYFLY, DOLANIA AMERICANA (EPHEMEROPTERA). Harvey, R. S. (Du Pont de Nemours (E. I.) and Co., Aiken, S. C. (USA). Savannah River Lab.). 1975. Contract AT(07-2)-1. 38p. (CONF-750838-1). Dep. NTIS $4.50.

From annual meeting of the Ecological Society of America with the American Institute of Biological Sciences; Corvallis, Oregon, USA (17 Aug 1975).

The mayfly Dolania Americana, common in the sand of Upper Three Runs Creek, Savannah River Plant, was studied to determine the effects of seasonal changes in temperature on population growth rates and to determine the effects of slight elevations in water temperature on respiration rates of this benthic species. Growth of the population increased with stream temperature until peak emergence of adults in June and July. There was a strong inverse correlation between body weight and respiration rates of immature nymphs. Respiration rates at 2.5, 5, and $10^0C$ above ambient creekwater temperatures were not significantly higher than those measured at ambient creekwater temperatures. (auth)

**25917** (PB-221498) ANALYSIS OF ENGINEERING ALTERNATIVES FOR ENVIRONMENTAL PROTECTION FROM THERMAL DISCHARGES. Environmental Protection Technology Series. (Environmental Protection Agency, Las Vegas, Nev. (USA). Environmental Monitoring and Support Lab.). Mar 1973. 236p. GPO $2.60.

A decision tree framework was used to integrate engineering decisions concerned with the control of environmental impacts from stationary thermal power plants. The engineering costs and the ecological response of fish communities to any sequence of decisions in the tree can be computed with the models developed in this study. A series of formulations were also developed to describe the environmental impact of siting a series of power plants in a region. Both the static and dynamic models require verification before they are applied. Impacts of thermal and chemical discharges to the receiving waters and mechanical damage from screening devices are modeled. (USGRDR)

**25918** (UCSD-10P20-202) RESEARCH ON THE MARINE FOOD CHAIN. Progress Report, July 1974--June 1975. Part I. Introduction and Account of Work in Progress. Part II. Manuscript Reports of Work Concluded. Part III. Cruise Summaries. (California Univ., La Jolla, San Diego (USA). Inst. of Marine Resources). 1975. Contract AT(11-1)-GEN-10. 921p. (IMR-75-5). Dep. NTIS $49.25.

The all-group field program during 1971-74 was on plankton dynamics in the central gyre of the North Pacific. Cruises to this area were completed, and the resultant manuscripts for the 1974-75 period are included in Part II of the report. During the past year the major field program was a series of four quarterly cruises in the Southern California Bight designed to evaluate the possible local and far-field effects of the cooling water system and thermal plume of the San Onofre Nuclear Power plant. Additional field programs included a cruise to the Gulf of California (R/V Alpha Helix) concerned with problems in marine photobiology, a cruise in Antarctic waters south of Buenos Aires (Islas Orcadas, formerly U.S.N.S. Eltanin) concerned with phytoplankton productivity, and a cruise in the Atlantic off northwestern Africa (F. S. Meteor) concerned with sediment microbiology. (auth)

**25919** PRESENT STATUS AND FUTURE ASPECTS OF WARM DISCHARGE IN THERMAL AND NUCLEAR POWER PLANTS. Saito, M. (Tokyo Electric Power Co., Inc. (Japan)). Doboku Gakkaishi; 59: No. 12, 2-8(Nov 1974). (In Japanese).

The objects of modern civil engineering are not only to promote investigation and planning for power source development but also to solve the warm discharge problem in thermal and nuclear power plants in cooperation with the research workers in the fields of oceanography and meteorology as well as marine production and biology. The execution of preliminary investigations on the meteorology, ground configuration, tidal current, and temperature and quality of water in peripheral sea has become possible in cooperation with prefectural research institute and fishermen's unions since 1965. According to the administrative regulation, nuclear power plants and the thermal power plants over 150,000 KW must submit to the MITI a report concerning the effects of the construction on natural and social environment. Present status in foreign countries is briefly reviewed for reference. Measures for the regulation of warm discharge in Japan are explained. For elucidating the actual state of the diffusion of warm discharge, for investigating the effects of warm discharge on marine lives and for promoting the utilization of warm discharge, it is desirable to establish the future measures to counter the warm discharge. Elucidation of the actual state of diffusion of a large quantity of warm discharge, reduction of its effects and promotion of investigation of the effects on marine lives are urgent matters to be realized. (JA)

**25920** LEGAL ASPECTS OF THERMAL DISCHARGES. Martin, A. J. J. Hydraul. Div., Am. Soc. Civ. Eng.; 100: No. HY 7, 1059-1072(Jul 1974).

An overview of those legal areas which directly affect technical and planning decisions is presented in the form of 2 legal approaches which constrain the indiscriminate release of thermal discharges to receiving waters. One takes the form of private remedies which have traditionally been available to aggrieved parties who are in some way damaged by the harmful discharge. The 2nd approach utilizes the various statutory constraints leading to direct governmental action. It appears that statutory law is playing the prominent role in restricting the temperature to which receiving waters may be raised as a result of such discharges by using effluent limitations and water quality standards. (Water Resour. Abstr.)

## Chemical Effluents

*Refer also to abstracts 25500, 25529, 25897, and 25918.*

# INSTRUMENTATION

## Radiation Detection Instruments

*Refer also to abstracts 26354 and 26401.*

**25921** OBSERVATIONAL TECHNIQUES. Gursky, H.; Schwartz, D. (Center for Astrophysics, Cambridge, MA). pp 25-98; 389-394 of X-ray Astronomy. Giacconi, R. (ed.). Dordrecht, Netherlands; Reidel (1974).

Techniques for detecting X radiation are reviewed. The following topics are discussed: cosmic X-ray sources, scanning and pointing experiments, vehicle considerations, and X-ray detectors. (BJG)

### General Detectors and Monitors

*Refer also to abstract 25877.*

**25922** (CONF-750935-2) BOUNDS FOR INTEGRAL RESPONSES OBTAINED FROM NEUTRON ACTIVATION MEASUREMENTS. Stallmann, F. W.; Kam, F. B. K. (Tennessee Univ., Knoxville (USA); Oak Ridge National Lab., Tenn. (USA)). 1975. 7p. Dep. NTIS $4.00.

From 1st ASTM-Euratom symposium on reactor dosimetry; developments and standarization; Petten, Netherlands (22 Sep 1975).

A method for obtaining good approximations to the integral responses for evaluating neutron flux spectra from activation detector data is discussed. (WHK)

**25923** (COO-1105-220) MODULATION AND CODING DETECTION OF ENERGY ABSORPTION. Moran, P. R. (Wisconsin Univ., Madison (USA). Medical Physics Labs.). [nd]. 10p. Dep. NTIS $4.00.

This report discusses the theory of modulation and coding detection schemes. Applications of these techniques in active radiation dosimetry measurements would appear to be particularly promising. Modern integrated circuits provide ready made modulation and coding detection electronics so that the circuit design problems for such systems are already worked out and the circuits available as off the shelf devices. The applications to real time measurement of fast neutrons in a hostile environment of high gamma ray background using either a gaseous or solid state ionization chamber are described. (auth)

**25924** (JINR-E13-8920) TIMING IN FISSION FRAGMENT DETECTION AT HIGH ALPHA-BACKGROUND. Andert, K.; Banifatov, A. E.; Gansoring, D.; Kalinin, A. I.; Krogulski, T.; Zorin, G. N. (Joint Inst. for Nuclear Research, Dubna (USSR)). 1975. 13p. Dep. NTIS (US Sales Only) $4.00.

The ionisation multi-plate fission chamber working together with the fast, low-noise level preamplifier, is described. Fission fragments were registered with the efficiency of about 50% at the background of $10^3$ $\alpha sec^{-1}$. The timing characteristics are illustrated by the time distributions of fission events measured at the $\mu^-$-beam of the 680 MeV synchrocyclotron, JINR, Dubna. (auth)

**25925** (JINR-P13-8915) UNIVERSAL CAMAC-COINCIDENCE CIRCUIT. Gabriel, F.; Shuravin, V. N.; Andert, K. (Joint Inst. for Nuclear Research, Dubna (USSR)). 1975. 13p. (In Russian). Dep. NTIS (US Sales Only) $4.00.

A universal CAMAC-coincidence circuit is described. All basic parameters are controlled in a wide range from the CAMAC-dataway: the coincidence resolving time ($2\tau$) from 1 nsec to 10 $\mu$ sec and the anticoincidence resolving time from 10 nsec to 10 $\mu$ sec. (auth)

**25926** (JINR-P13-8919) SOME PECULIARITIES OF THE SURFACE-BARRIER DETECTORS MADE OF HIGH-IMPEDANCE HOLE SILICON. Kushniruk, V. F.; Nikitina, R. A.; Kharitonov, Yu. P. (Joint Inst. for Nuclear Research, Dubna (USSR)). 1975. 11p. (In Russian). Dep. NTIS (US Sales Only) $4.00.

Anomalous spectrum lines and the decrease of the c.v. characteristic slope were observed by means of the detectors made of high-impedance p-silicon. These peculiarities are explained by the assumption about the existence of the positive charge localized on the surface. Various mechanisms leading to the distortion of the spectrum line form are discussed. (auth)

**25927** (JINR-P13-8989) INVESTIGATION OF THE TIMING PROPERTIES OF SERIAL COAXIAL Ge(Li) DETECTORS OF LARGE VOLUME. Banifatov, A. E.; Zorin, G. N.; Sabirov, B. M.; Skakodub, V. A.; Sokolov, A. D.; Ortlepp, Kh. G.; Reznikov, R. S.; Shcherbakov, G. M. (Joint Inst. for Nuclear Research, Dubna (USSR)). 1975. 9p. (In Russian). Dep. NTIS (US Sales Only) $4.00.

The time resolutions of serial coaxial circular wraparound Ge(Li) detectors of large volume (30 to 90 $cm^3$) were determined to meet the requirements of a whole series of experiments in nuclear physics. (auth)

**25928** (JINR-P13-9001) CONTROL SYSTEM FOR AUTOMATIC CALIBRATION OF AN EXPERIMENT WITH SCINTILLATION AND CHERENKOV COUNTERS. Kollar, D.; Kollarova, L.; Horvath, P. (Joint Inst. for Nuclear Research, Dubna (USSR)). 1975. 20p. (In Russian). Dep. NTIS (US Sales Only) $4.00.

The control system, consisting of various programming units and executive controller, which allows one to provide control up to max. 4 CAMAC crates according to the program provided by the programming units or by the computer, is described. The control system is intended for autonomous control of fast logic modules for time measurement with a resolving time of about 1 ns, for high voltage control of the photomultipliers and so on in the physical experiments with scintillation and Cherenkov counters. The control system was designed at the Laboratory of Nuclear Problems. (auth)

**25929** (UCRL-50025-75-2, pp 1-4) TUMOR IMAGING GAMMA-RAY CAMERAS. Ewins, J. H. 1 May 1975.

In Electronics Engineering Department quarterly report No. 2, 1975. (California Univ., Livermore (USA). Lawrence Livermore Lab.).

The Engineering Research, Biomedical, and Radiochemistry Divisions of LLL, the University of California Medical Center (San Francisco), and the Lawrence Berkeley Laboratory (LBL) are collaborating to produce the next generation of nuclear medicine cameras. Characterized by an order-of-magnitude finer spatial resolution than present-day cameras, a 100-picture-element prototype has been developed by use of high-purity germanium, grown and fabricated at LLL. (auth)

**25930** (UCRL-50025-75-2, pp 18-21) SILICON DETECTOR SYSTEM FOR X-RAY PULSE CALORIMETRY OF LASER-PRODUCED PLASMAS. McQuaid, J. H.; Violet, C. E.; Petruzzi, J. 1 May 1975.

In Electronics Engineering Department quarterly report No. 2, 1975. (California Univ., Livermore (USA). Lawrence Livermore Lab.).

A new type of calorimeter has been developed for measuring x-ray yields from laser-produced plasma. The calorimeter, which consists of silicon detector, a charge-sensitive preamplifier, and an analog-to-digital readout scheme, can take signals from a number of detector outputs simultaneously. X rays interacting with the detector produce hole-electron pairs in proportion to the total energy lost in the detector (approximately $10^{12}$ eV). In this application, the detector can be characterized as a solid-state ionization chamber. The detector signal is fed to a charge-sensitive preamplifier which generates a voltage pulse proportional to the x-ray energy absorbed. In this way the x-ray energy is measured by "direct conversion," rather than by temperature rise due to an energy flux. (auth)

**25931** (UCRL-50025-75-2, pp 23-27) MOS TIME-RESOLVED RADIATION DETECTORS. Balch, J. W.; McConaghy, C. 1 May 1975.

In Electronics Engineering Department quarterly report No. 2, 1975. (California Univ., Livermore (USA). Lawrence Livermore Lab.).

Time-resolved radiation detectors, incorporating metal-oxide-semiconductor (MOS) transistors as both detectors and nonvolatile memory, have been developed at LLL for detecting low-energy x rays, electrons, and protons. These detectors, which rely upon the semipermanent radiation effects of ionizing radiation on MOS transistors, are capable of detecting single pulse irradiations with 1-ns time resolutions. Their nonvolatile memory is very useful for recovering data after the noise of pulsed radiation environments has subsided. Development of these detectors required the fabrication of a custom MOS transistor array with an extremely high breakdown voltage. (auth)

**25932** (UCRL-Trans-10889) THERMAL NEUTRON SOURCE AND PROBLEMS OF CALIBRATING THERMAL-, INTERMEDIATE-, AND FAST-NEUTRON RADIOMETERS. Vasilev,

R. D.; Dorofeev, G. A.; Mordovskaya, T. C.; Petrov, B. I.; Pemenov, M. I. 1962. Translation of Russian Report. (CONF-621201-1). 16p. Dep. NTIS $4.00.

From symposium on neutron detection, dosimetry, and standardization; Harwell, UK (10 Dec 1962).

The method of calibrating thermal neutron radiometers with a paraffin sphere having an $\alpha$-$\beta$e source in its center is described in detail. (WHK)

**25933** SYSTEMS OF NUCLEAR INSTRUMENT. Nishino, O. (Kogakuin Univ., Tokyo (Japan)). Genshiryoku Kogyo; 20: No. 10, 9-11(Oct 1974. (In Japanese).

The followings are examples of systematized nuclear instruments: radiation measurement system, radiation control system, monitoring system of environmental radiation, data processing in liquid scintillation counting, pattern recognition of scintigraphy in nuclear medicine and well-known $\gamma$-ray spectroscopy. Standardization of hardwares increases the flexibility of composing systems and makes modification and expansion easy. The CAMAC system should be paid more interest than before in Japan. (JA)

**25934** SYSTEMS IN LIQUID SCINTILLATION COUNTING. Ikeda, M. (Tokyo Metropolitan Isotope Research Center (Japan)). Genshiryoku Kogyo; 20: No. 10, 25-29(Oct 1974). (In Japanese).

The remarkable research results by using radioisotope tracers in biochemical and nuclear medical fields owe much to the liquid scintillation counting technique (LSC). It is needless to say that LSC is an excellent measuring means. But also the contribution of effort toward systematizing the measuring procedure can not be overlooked. Here, the data processing system is described. Elementary data obtained by LSC are rather simple. These are (1) sample number, (2) measuring time, (3) counts in each channel, (4) counts in each channel by external source, and others. The final data are obtained through the first and second step processing. At present, the system up to the first step processing is incorporated in most equipment and put in practical use. The use of computers is of significance indeed if the second step processing is included. Therefore such a system should be designed considering data processing procedures. Only one example of LSC data processing system is introduced. However, many other applications are found in references listed. (JA)

**25935** PROBLEMS OF COSMIC GAMMA-RAY OBSERVATION. Makino, F. (Nagoya Univ. (Japan). Faculty of Science). pp 152-156 of Symposia on the Cosmic Observations for the Fiscal Year 1973. Tokyo, Japan; Tokyo Univ., Inst. of Space and Aeronautical Science (Mar 1974). (In Japanese)

From symposia on the cosmic observations for the fiscal year 1973; Tokyo, Japan (10 Dec 1973). (Tokyo Univ. (Japan). Inst. of Space and Aeronautical Science).

Problems concerning the measurement of the low energy isotropic component of cosmic gamma-ray are discussed. Observation of the isotropic component has been carried out with man-made satellites and balloons. The detectors used were CsI(Tl) or NaI(Tl) crystals. The difficulty in the measurement is to distinguish the gamma-ray to be measured from other particles and secondary gamma-ray. The gamma-ray produced by the main body of satellites can be measured, while the gamma-ray from long-life (more than 10 $\mu$ sec) activity produced in the crystal itself can hardly be corrected. Fishman, and Dyer and Morfill investigated into the spectra of radioactivity. In the observation with balloons, the separation from atmospheric component is a matter of concern. An extrapolation method of altitude variation has been made for this purpose, however, it is hard to use this method for non-directional detectors. Downward gamma-rays were measured by opening and closing a shutter. Existence of primary component was suggested from the measurement, and more precise measurement is planned. The measurement with satellites on the orbits near the earth is affected by the intensity variation of cosmic rays owing to latitude, background due to radiation band and so on. Therefore, it is hard to draw conclusion from the measurement. Finally, it should be mentioned that the spectra measured are energy loss spectra and not photon spectra. (JA)

**25936** GENERAL RECOMBINATION IN IONIZATION CHAMBERS WITH SPATIALLY NON-UNIFORM IONIZATION INTENSITY: TWO SPECIAL CASES. Boag, J. W. (Inst. of Cancer Research, Stutton, Eng.). Int. J. Radiat. Phys. Chem.; 7: No. 2/3, 243-249 (Apr 1975).

The proportion of general recombination which occurs in an ionization chamber with non-uniform distribution of ionization has been examined for two cases of practical interest: (1) when the ionization intensity declines exponentially through the gas layer, and (2) when the ionization is concentrated in cylindrical columns which retain their form as they drift to the electrodes. In both these cases, it is shown that the simple formula for general recombination based on the average ionization intensity over the whole volume of the chamber is a good first approximation in the near-saturation region and the extent of correction necessary for extremely non-uniform distribution is investigated. (auth)

**25937** MONITORING SURFACE CONTAMINATION. Gale, H. J. (Univ. of Nottingham, Eng.). Phys. Med. Biol.; 20: No. 4, 656-657 (Jul 1975).

Monitoring equipment based on a scintillation system has been suggested as an improved means of monitoring permitted levels (derived working limits, DWL) of beta-gamma emitting isotopes, and particularly of electron capture nuclides (Bush, D., and Hundal, R. C., 1971, Health Phys., 21, 651). The responses of two instruments (MXl 23 GM tube, mica end window, and Mini-Instruments' NaI(Tl) crystal, 1 mm × 2.3cm, with thin beryllium window) have therefore been compared, using small area sources uniformly contaminated with the electron capture nuclides $^{125}$I, $^{51}$Cr, $^{85}$Sr, $^{54}$Mn, and $^{65}$Zn. The scintillation system brought about a satisfactory improvement in signal-to-background ratio for $^{125}$I. The improvement was not very marked for the other nuclides, and for $^{51}$Cr in particular there was difficulty in obtaining a satisfactory response. More consistent responses were obtained when the measurements were based on 'effective' microcuries, although the sensitivity of the scintillation system was still only just adequate. It was concluded that in order to be able to measure satisfactorily at the DWL the best approach is to use DWLs calculated for individual isotopes (Gibson, J. A. B., Webb, G. A. M., and Wrixon, A.D., 1974, in Proc. SRP Int. Symp. on Radiation Protection - Philosophy and Implementation, Aviemore, Scotland). (UK)

**25938** HIGH-SENSITIVITY APPEARANCE POTENTIAL SPECTROMETER FOR THE DETECTION OF PHOTONS, ELECTRONS, AND IONS. Kluge, A. (Fa. Leybold-Heraeus, Cologne, West Germany). Rev. Sci. Instrum. 46: No. 9, 1179-1181 (Sept 1975).

A versatile appearance potential spectrometer has been developed to detect photons and electrons, emitted during electron bombardment, for determining the binding energies of the electrons of surface atoms. Primary currents down to 50 $\mu$A yield good signals for the detection of electrons. Furthermore, the detection of desorbed ions can be used for measuring the threshold energy of ion emission. A special preamplifier is used for a high signal-to-noise ratio. (auth)

**25939** COUNTING RATE DEPENDENT GAIN SHIFTS IN FLOW PROPORTIONAL COUNTERS. Spielberg, N.; Tsarnas, D.I. (Department of Physics, Kent State University, Kent, Ohio 44242). Rev. Sci. Instrum. 46: No. 8, 1086-1091 (Aug 1975).

The counting rate dependent shift of pulse height distributions in cylindrical (flow) proportional counters has been studied. The effects of various counter tube constructional and operational parameters on this shift were investigated. Certain of these parameters also introduce time dependent features into the shift phenomenon. Space charge effects are not major causes of the shifts except under extreme operating conditions. Direct intervention of adsorbed molecules or molecular ions in the multiplication process may also be eliminated as major factors. It is hypothesized that the primary mechanism for the shift is the buildup on the anode wire of a loosely adherent sheath of polarizable molecules or molecular fragments of quench gas, which effectively increases the diameter of the anode wire, thereby decreasing the gas gain for a fixed applied voltage. The equilibrium thickness of the sheath is a function of counting rate, photon energy, gas gain, gas pressure, and wire diameter and surface condition. Calculation of the thickness of this sheath gives a reasonable result. By proper choice of anode wire diameter, material, and heat treatment, the shift can be made negligible. There is also some hope that a proper choice of quench gas can also reduce or eliminate the effect. (auth)

**25940** DESIGN AND PROPERTIES OF POSITION-SENSITIVE PROPORTIONAL COUNTERS USING RESISTANCE-CAPACITANCE POSITION ENCODING. Borkowski, C.J.; Kopp, M.K. (Oak Ridge National Laboratory, Oak Ridge, Tennessee 37830). Rev. Sci. Instrum. 46: No. 8, 951-962 (Aug 1975).

The construction and signal processing methods of several experimental gas-filled, position-sensitive proportional counters (PSPCs) using resistance-capacitance (*RC*) position encoding are described, and guidelines for the design and operation of these counters are given. Using these guidelines, we were able to improve the spatial resolution and shorten the signal processing time; for example, the intrinsic spatial uncertainty in the position measurement was reduced to 28 $\mu$ FWHM for alpha particles and 100 $\mu$ FWHM for low-energy x rays (2–6 keV). Also, the signal processing time was reduced to 0.6 $\mu$sec without seriously degrading the spatial resolution. These results have widened the field of application of the *RC* position encoding method for position measurements of low-energy photons, neutrons, and charged particles in a wide variety of nuclear physics experiments, in nuclear medicine imaging, and in low-dose, medium-resolution radiography. (auth)

**25941** STABILIZATION OF PHOTOMULTIPLIERS IN LIQUID SCINTILLATION COUNTERS. Soini, E. (Wallac Oy, Research Department, P.O. Box 10, 20101 Turku 10, Finland). Rev. Sci. Instrum. 46: No. 8, 980-984 (Aug 1975).

A special stabilization system has been constructed to control the overall gain of photomultiplier tubes in a liquid scintillation counter. The system uses GaAsP light emitting diodes in the measurement chamber to produce separate reference light pulses for each photomultiplier tube. The system has provided a significant improvement in both short and long term stability and in operational reliability. (auth)

**25942** PERFORMANCE OF SEM SCINTILLATION MATERIALS. Pawley, J. B. (Univ. Coll., London). pp 27-34 of Scanning Electron Microscopy, 1974. Johari, O.; Corvin, I. (eds.). Chicago; Illinois Institute of Technology, SEM Symposia Office (1974).

From proceedings of the scanning electron microscopy; Chicago, Illinois, USA (8 Apr 1974).

The standard SEM secondary electron detector is only marginally free from statistical noise introduced when the number of photo-electrons per incoming secondary is less than about four because of inefficiencies in the scintillator, the PMT photocathode and the optical path between them. This estimate has been confirmed using a fixed current primary beam of varying voltage applied to various types of scintillators attached to a light pipe normally used to detect transmitted electrons. The signal to noise ratio (S/N) of the PMT output was measured, and the results for various materials were plotted as a function of beam voltage. Although plastic scintillation material could not be measured directly in this way because of its rapid degradation during the measurements, comparative measurements of its relative luminescent efficiency indicated that when used in a standard detector a decrease in efficiency of as little as 50 percent below that of a new scintillator would be expected to produce a measurable decrease in the S/N of the detector. Additional experiments indicated that plastic scintillators in a standard detector lose 50 percent of their efficiency after collecting a current of $5 \times 10^{-9}$ A for slightly less than 1 hour. Several alternate materials examined included plastic coated on quartz light pipes, lithium doped glass, P-47 powdered phosphor and single crystals of P-46 and $CaF_2$ (Eu). These were compared on the basis of light output, decay time, S/N obtainable, resistance to radiation damage and stability in the intermittent vacuum environment of the SEM specimen chamber. On the basis of these criteria, P-47 and P-46 seemed most suitable. (auth)

**25943** MEASURING DEVICE FOR ANGULAR DEPENDENCE OF SCATTERED RADIATION. Moser, H. (to Gesellschaft fuer Kernforschung m.b.H., Karlsrune (F. R. Germany)). German(FRG) Patent 2338481/8/. 13 Feb 1975. 9p. (In German).

2 figs.

A measuring device for angular dependence of stray radiation with high time resolution (nanosecond region) is claimed. Possible uses are particle size measurements, aerosol particle control, and production control in fiber and dye production. (GE)

**25944** CALIBRATION FIGURES FOR THE TYPE 1383A IONIZATION CHAMBER. Woods, M. J.; Lucas, S. E. M. (National Physical Lab., Teddington, Eng.). Int. J. Appl. Radiat. Isot.; 26: No. 8, 488(Aug 1975).

Following the earlier publication of a comprehensive list of calibration figures for the NPL standard 1383A ionization chamber (Woods, M. J., Int. J. Appl. Radiat. Isotop.: 21; 752 (1970)) figures for $^{7}Be$, $^{18}F$, $^{43}K$, $^{56}Co$, $^{67}Ga$, $^{68}Ga$, $^{125}I$, $^{131}Cs$, $^{169}Yb$ have now been obtained and are given. (UK)

**25945** CALIBRATION OF THE 1383A IONIZATION CHAMBER FOR $^{125}I$. Woods, M. J.; Lucas, S. E. M. (National Physical Lab., Teddington, Eng.). Int. J. Appl. Radiat. Isot.; 26: No. 8, 488-490(Aug 1975).

The radioactive concentration of solutions of $^{125}I$ have been measured and the standardised solutions used to determine a calibration figure for $^{125}I$ in the NPL standard 1383A ionization chamber. The standardisation was carried out by three methods; the convential $4\pi$ $\beta$-$\gamma$ coincidence technique, a method in which the source was sandwiched between two cooled Si detectors to give approximately $4\pi$ counting geometry, and a method in which the sources were placed in a large high pressure $4\pi$-proportional counter, the two halves of which were used as the two detectors. The results of the calibration measurements and a summary of the calibration factors are tabulated. (UK)

**25946** CHARACTERISTICS OF A NaI(Tl) SCINTILLATION CHAMBER. Bruninx, E. (Philips Gloeilampenfabrieken N. V., Eindhoven, Netherlands). Int. J. Appl. Radiat. Isot.; 26: No. 6-7, 429-430(Jun 1975).

The response characteristics of a NaI(Tl) scintillation chamber, used for the stoichiometric analysis of chemical compounds by means of neutron activation, have been investigated. The total $\gamma$-ray detection efficiency, and the variation of counter response for axial and for radial source displacements are shown graphically. Measurement of the overall stability of the counting chain indicated a standard deviation of the single observation of 0.04%. (UK)

**25947** SATURATION CHARACTERISTICS OF IONIZATION CHAMBERS AT LOW PRESSURES. Varma, M. N.; Baum, J. W. (Brookhaven National Lab., Upton, NY). Health Phys.; 29: No. 3, 399-405(Sep 1975).

Mesh wall ionization chambers are useful for determining the radial distribution of dose around a moving charged particle, by measuring the saturation ionization current. In order to evaluate and understand the saturation curves of the mesh wall ionization chamber, ionization current vs voltage curves were studied at pressures from 0.017 to 2 Torr in a large ionization chamber and in a small mesh wall ionization chamber located within the large chamber. Results indicate that saturation in the internal mesh wall chamber (probe) depends on (a) competition between collection in the probe and large ionization chamber, (b) recombination at very low voltages, (c) gas amplification at higher voltages, and (d) probe position. Saturation in the large chamber depends on recombination at low voltages and on gas amplification at higher voltages. For both the probe and large ionization chamber, collection of positive ions proved best; however, saturation voltages had to be chosen carefully at each pressure in order to achieve optimum balance of the above mentioned effects. (auth)

**25948** SIGNAL-TO-NOISE RATIO OF NUCLEAR TRACK EMULSIONS EXPOSED TO ELECTRONS. Coleman, C. I. (Imperial Coll. of Science and Tech., London). J. Photogr. Sci.; 23: No. 2, 50-58(Mar 1975).

Methods of recording photoelectron images in nuclear track emulsions ("electronography") are described, and the theory of the process is discussed. Parameters affecting the detective quantum efficiency (DQE) of electronography are examined in detail, and the DQE is shown to be higher than that of unaided photography, and almost independent of exposure level. Practical aspects of the development and subsequent analysis of electronographs are considered and several experimental results are presented. (auth)

**25949** INSTABILITY OF LIQUID SCINTILLATION COUNTING DUE TO SAMPLE SORPTION OF THE COUNTING VIAL. Tykva, R. (Ceskoslovenska Akademie Ved, Prague); Podracka, E. Int. J. Appl. Radiat. Isot.; 26: No. 8, 495-498(Aug 1975).

It is reported that in experiments performed with the $^{3}H + ^{32}P$ pair, activity measurements on aqueous solutions in a liquid scintillation spectrometer are accompanied by instability of working parameters due to a permanent increase of counting rates in the $^{3}H$-channel and a simultaneous decrease of counting rates in the $^{32}P$-channel. Changes in counting rates of $^{32}P$-labelled samples in $^{3}H$-, $^{14}C$- and $^{32}P$-channels, as recorded for 0 to 14 days after the sample preparation, are tabulated. The experimental data suggest that the spectral shift of amplitudes of the recorded counting rates is due to sorption of the labelled substances on to the inner surface of vials and to interactions of emitted electrons with the vial. Consequently, the present effect asserts itself especially with nuclides emmitting $\beta$ particles of a higher initial kinetic energy and particularly in cases when tritium is detected simultaneously since in the $^{3}H$-channel, there are recorded counts due to interactions of electrons of a higher kinetic energy with the vial. (UK)

**25950** RADIATION DETECTOR. (To Stichting Reactor Centrum Nederland). Netherlands Patent 7,314,253/A/. 16 Oct 1973. 5p. (In Dutch).

A new configuration is described for a radiation detection system that reduces the dead time problem by measuring the duration of the pulse current. It is particularly suitable for providing digital readout. (auth)

## *Radiation Dosimeters*

**25951** (AECL-5108, pp 11-39) HEALTH PHYSICS BRANCH. Cowper, G. (Chalk River Nuclear Labs., Ont.). 1974.

In Biology and Health Physics Division progress report, October 1 to December 31, 1974. (Atomic Energy of Canada Ltd., Chalk River, Ontario. Chalk River Nuclear Labs.).

Developments in radiation monitoring for health physics are reported. Much effort has gone into the analysis of typical radiation exposure situations to provide relationships between neutron flux and dose for a variety of neutron detectors having a limited energy response and a range of probable neutron spectra likely to be encountered in real situations where the primary neutron source either from an accelerator or a fission process is shielded or scattered to some extent by materials such as water,

heavy water, concrete or iron. In another situation where the handling of plutonium could result in a contaminated puncture wound and it would be a matter of some urgency to determine the amount of plutonium present, recently developed amplifying semiconductor junction detectors show considerable promise. These detectors developed in industry under contract have been found capable of resolving the L X-rays of plutonium so that by comparing the magnitudes of the measured X-ray intensities an estimate of the thickness of tissue covering the activity could be made. The unambiguous detection of one source of radiation or radioactivity in the presence of others of less critical effect is another important requirement in health physics. This situation is well represented in the requirement to detect tritium which may escape from a heavy water power reactor into an environment which is contaminated also with radioactive rare gases and is subject to external gamma radiation fields. Instruments now being completed for tritium monitoring at the Bruce Generating Station have been designed to meet these requirements. (auth)

**25952** (CEA-R-4687) SENSITIVITY OF RTL, RPL AND PHOTOGRAPHIC DETECTORS TO 14.7-MeV NEUTRONS. Spurny, F.; Medioni, R.; Portal, G. (CEA Centre d'Etudes Nucleaires de Fontenay-aux-Roses, 92 (France). Dept. de Protection). Aug 1975. 21p. (In French). Dep. NTIS (US Sales Only) $4.25.

The sensitivity of various types of $\gamma$ detectors to neutrons should be known for a better dosimetry of electromagnetic radiations in neutron fields. The sensitivity of various types of detectors to 14.7 MeV neutrons was studied using RTL ($^{nat}$LiF, $^{7}$LiF, Ca $SO_4$: Dy, $Al_2O_3$), RPL (C.E.C. glasses), and photographic detectors (KODAK-PATHE dosemeters). The methods used for the determination of the neutron and photon mixed field are described and the effect of containers and packing on the accuracy of results was investigated. For each detector studied the specific sensitivity to neutrons (sensitivity of the product alone) and the apparent sensitivity in usual operating conditions (action of surrounding materials) is given. (auth)

**25953** (CEA-R-4688) SENSITIVITY OF VARIOUS THERMOLUMINESCENT, RADIOPHOTOLUMINESCENT, AND PHOTOGRAPHIC DETECTORS TO NEUTRONS EMITTED BY A $^{252}$Cf SOURCE. Spurny, F.; Medioni, R.; Chapuis, A. M.; Portal, G. (CEA Centre d'Etudes Nucleaires de Fontenay-aux-Roses, 92 (France). Dept. de Protection). 1975. 17p. (In French). Dep. NTIS (US Sales Only) $4.00.

The specific sensitivity of various thermoluminescent, radiophotoluminescent and photographic detectors to the neutron spectrum of a $^{252}$Cf source was measured and the effect of the size and composition of the containers in which they might be put was investigated. PB 33 radiophotoluminescent glasses, radiothermoluminescent alumina and calcium sulfate were less sensitive to fission neutrons whereas photographic emulsions were more sensitive. The former should be used for $\gamma$ detection in mixed fields of photons and fission neutrons. (auth)

**25954** (CONF-750935-4) DOSIMETRY MATERIALS FOR HIGH-TEMPERATURE APPLICATIONS. Kerr, H. T.; Adair, H. L.; Allen, E. J. (Oak Ridge National Lab., Tenn. (USA)). 1975. 15p. Dep. NTIS $4.00.

From 1st ASTM-Euratom symposium on reactor dosimetry; developments and standardization; Petten, Netherlands (22 Sep 1975).

Conventional neutron threshold dosimetry materials originally developed for low-temperature applications are not usually suited for applications above 600°C because of material compatibility considerations. Insulator materials and encapsulation techniques are available to extend the useful range of many conventional materials, and some new dosimeter materials have been identified and developed specifically for high-temperature applications. The vanadium alloys and vanadium encapsulated materials can be used with beryllium-oxide insulators up to 1000°C. Uniform ceramic wires can be produced from oxide materials so the amount of dosimeter material present can be controlled. A technique is available for coating dosimeters such as the oxide wires with carbon and silicon carbide for extremely high-temperature applications. The basic criteria for high-temperature dosimetry are presented. (WHK)

**25955** (COO-1105-226) TL RESPONSE TO 1–30 kV ELECTRONS OF TLD-100 AND TLD-100 DIFFUSED WITH VARIOUS ELEMENTS. Lasky, J. B.; Moran, P. R. (Wisconsin Univ., Madison (USA). Medical Physics Labs.). 1973. 16p. Dep. NTIS $4.00.

The TL response of LiF TLD-100 has been examined as a function of diffusional dopings of the dosimeter surface layers. The glow curve shapes and TL response for irradiations with Cs gamma-rays compared with electrons in the 1 to 30 kV energy range provide a good diagnostic and suggest some interesting practical applications. (auth)

**25956** (COO-1105-228) PHOTO-TL IN $CaSO_4$:Dy: HIGH EXPOSURE DOSIMETRY. Caldas, L. V. E.; Mayhugh, M. R. (Instituto de Energia Atomica, Sao Paulo (Brazil); Wisconsin Univ., Madison (USA). Dept. of Physics). 1974. 20p. Dep. NTIS $4.00.

$CaSO_4$:Dy exposed to $10^3$ to $10^8$R then annealed in the range 280 to 400°C displays little TL in the major dosimetry peak near 200°C. Subsequent illumination with 250 nm light reinduces the 200°C TL. This radiation-enabled photo-TL is roughly proportional to the square root of the enabling exposure at least to $10^8$R. (auth)

**25957** (COO-1671-62) RESPONSE OF NUCLEAR EMULSIONS TO IONIZING RADIATIONS. Katz, R.; Pinkerton, F. E. (Nebraska Univ., Lincoln (USA)). 1975. 33p. (CONF-750927-2). Dep. NTIS $4.75.

From 5th symposium on microdosimetry; Varbania Pallanza, Italy (22 Sep 1975).

Heavy ion tracks in Ilford K-2 emulsion are simulated with a computer program which makes use of the delta-ray theory of track structure, and the special assumption that the response of this emulsion to gamma-rays is 8-or-more hit. The Ilford K-series of nuclear emulsions is produced from a parent stock called K.0 emulsion, sensitized to become K.1 to K.5, and desensitized to become K-1 to K-3. Our simulations demonstrate that the emulsions K.5 through K.0 to K-1 are 1-or-more hit detectors, while K-2 is an 8-or-more hit detector. We have no data for K-3 emulsion. It would appear that emulsions of intermediate hittedness might be produced by an intermediate desensitization, to mimic or match the RBE-LET variations of biological cells, perhaps to produce a "rem-dosimeter". In the K-2 emulsion no developable gains are produced by stopping H, He, and Li ions. The emulsion has "threshold-like" properties, resembling etchable track detectors. It should prove useful in the measurement of high LET dose in a strong low LET background, as for pions or neutrons. Since it can be expected to accumulate and repair "sublethal damage", to display the ion-kill and gamma-kill inactivation modes, the grain-count and track width regimes, it may serve to model biological effects. (auth)

**25958** ENERGY DEPENDENCE OF THE RESPONSE OF LITHIUM FLUORIDE TLD RODS IN HIGH ENERGY ELECTRON FIELDS. Holt, J. G.; Edelstein, G. R.; Clark, T. W. (Memorial Hospital, New York). Phys. Med. Biol.; 20: No. 4, 559-570 (Jul 1975).

The energy dependence of lithium fluoride dosemeters is a complicated function of energy as well as of cavity size. In the application of TLD to charged particle dosimetry, a cavity perturbation effect may exist even though the ratios of the mass stopping powers are constant over the energies encountered. This effect was investigated for lithium fluoride rods in electron fields ranging in energy from 2.5 to 20 MeV. A 13% change of TL response per unit of absorbed dose was measured over that energy range. A semi-empirical theory was developed to account for the cavity effect, using Burlin cavity theory as a starting point. The agreement between theory and measurement is satisfactory. (auth)

**25959** APPLICATIONS OF CAVITY THEORIES FOR ELECTRONS TO LiF DOSEMETERS. Paliwal, B. R.; Almond, P. R. (Anderson (M. D.) Hospital and Tumor Inst., Houston, TX). Phys. Med. Biol.; 20: No. 4, 547-558 (Jul 1975).

A tabulation of the existing data on the response of LiF to electrons measured by various authors is presented. Theoretical calculations were carried out using the Burlin et al. theory (Burlin, T. E., Snelling, R. J., and Owen, B., 1969, in Proc. 2nd Symp. on Microdosimetry, Stresa, Italy (Brussels: Commission of European Communities) p.455) and its modified version by Almond and McCray (Almond, P. R., and McCray, K., 1970, Phys. Med. Biol., 15, 335). Experimentally measured response by the authors is also reported. It was concluded that the predictions made by the two approaches differ significantly. (auth)

**25960** MECHANISM OF THE FRICKE DOSIMETER. Jayson, G. G.; Parsons, B. J.; Swallow, A. J. (Liverpool Polytechnic). Int. J. Radiat. Phys. Chem.; 7: No. 2/3, 363-370 (Apr 1975).

An amplified mechanism is given for the response of the Fricke dosimeter to radiation. OH radicals react with $Cl^-$ to give stepwise, Cl atoms and $Cl_2^-$, both of which oxidize $Fe^{2+}$ and $FeSO_4$. Hydrated electrons and H atoms give rise to $HO_2$ radicals which form $Fe^{3+}HO_2^-$. Part of this complex dissociates to give $Fe^{3+}$ and $H_2O_2$, while part reacts with $SO_4^{2-}$ to give $Fe^{3+}HO_2^-SO_4^{2-}$. Part of this dissociates giving $FeSO_4^+$, while part forms $Fe^{3+}HO_2^-(SO_4^{2-})_2$, which dissociates giving $Fe(SO_4)_2^-$. Hydrogen peroxide reacts with $Fe^{2+}$ and $FeSO_4$ to give respectively, $Fe^{3+}$ and $FeSO_4^+$. Equilibrium

proportions of $Fe^{3+}$, $FeSO_4^+$ and $Fe(SO_4)_2^-$ are attained through reaction of $Fe^{3+}$ with $SO_4^{2-}$ and $FeSO_4^+$ with $SO_4^{2-}$. (auth)

**25961** RESPONSE OF THE HEXAHYDROXYETHYL PARA-ROSANILINE CYANIDE DOSIMETER TO 3.0-MeV PROTONS. Rosenstein, M. (Bureau of Radiological Health, Rockville, MD); Eisen, H.; Roush, M. L.; Silverman, J. Int. J. Radiat. Phys. Chem.; 26: No. 6-7, 423-426 (Jun 1975).

Experiments carried out on radiochromic dye-film dosimeters consisting of 8.6% by weight of the colorless dye precursor, hexahydroxyethyl pararosaniline cyanide, dissolved in nylon, are reported. The experiments were designed to determine the response of the dosimeters to radiations with a LET significantly greater than those used in previous work and also to verify that the response to the degraded electron spectrum near the end of the electron range was not significantly different from that at the surface or at other depths in the absorber. A 33% reduction in the response of the dosimeter for 3.0 MeV protons (LET = 135 MeV $cm^2$ $g^{-1}$) over that of $\gamma$ rays and electrons (LET < 4 MeV $cm^2$ $g^{-1}$) was observed. This is in close agreement with the 30% reduction predicted by the particle track theory. The magnitude of reduction in dosimeter response due to the variation in LET noted indicates that the dosimeter response is independent of depth in the absorber within the error limits of the experiments. (UK)

**25962** MEASUREMENT OF SMALL DOSES USING RADIO-PHOTOLUMINESCENT SILVER-ACTIVATED METAPHOSPHATE GLASSES. Barthe, J.; Bouvard, G.; Commanay, L. (Univ., Toulouse). Health Phys.; 29: No. 1, 213-216(Jul 1975).

A new recording principle for dose measurement using radio-photoluminescent (RPL) silver-activated metaphosphate glasses is described. The method, based on the measurement of RPL decay times instead of the usual RPL intensity measurement, allows one in principle to measure doses as low as 0.1 mR. The predose is abnormally low ( a few $\mu$R). By the method it is possible to distinguish more easily between photon and neutron doses in those doses where there are differences in the nature of RPL centers as a function of LET. The initial results also show a pronounced effect of small differences in glass composition and its thermal history, which may be usable as a tool in RPL glass quality control. (UK)

**25963** FEASIBILITY OF A NEUTRON SENSITIVE POCKET IONIZATION DOSIMETER WITH BUILT IN GAMMA RAY COMPENSATION. Tymons, B. J.; Cooper, P. N. (Univ. of Birmingham, Eng.). Health Phys.; 29: No. 1, 137-141(Jul 1975).

A fast neutron sensitive ionisation chamber which has compensation for $\gamma$ radiation has been tested with $^{241}Am/Be$ and $^{60}Co$ sources and found to have a response proportional to the biological dose of both fast neutrons and $\gamma$ rays. The device consists of two ionisation chambers, one predominantly fast neutron sensitive and the other predominantly $\gamma$ ray sensitive. These are connected in series and a linking capacitor is connected in parallel. By a suitable choice of lining materials for the chambers, chamber volumes, and capacities of the chambers and linking capacitor it is possible to achieve $\gamma$ ray compensation from the partial recharging of the neutron sensitive chamber by the linking capacitor. It is concluded that with improved dielectric materials the device could be produced as a self-contained personnel dosimeter. (auth)

**25964** PULSE RADIATION DOSIMETRY OF 4 MeV BREMSSTRAHLUNG WITH A THERMISTOR BRIDGE. White, P. H.; Gobbett, R. H. (United Kingdom Atomic Energy Authority, Aldermaston, Eng.). J. Phys., E (London); 8: No. 8, 684-687(Aug 1975).

A thermistor bridge has been constructed which will measure relative pulsed deposited dose in similar spectra which is reproducible from shot to shot to within approximately 5%. The absolute dose measured is consistent with that measured by LiF thermoluminescent dosimeters in a 4 MeV bremsstrahlung spectrum if photon absorption and electron scattering are fully taken into account. (auth)

## *Nuclear Spectroscopic Instrumentation*

**25965** (ARH-CD-276) NAMES AND DESCRIPTIONS OF CHEMICAL TECHNOLOGY LABORATORY DETECTOR SYSTEMS. Zimmer, W. H. (Atlantic Richfield Hanford Co., Richland, Wash. (USA)). Mar 1975. 106p. Dep. NTIS $8.50.

Gamma and x-ray detector systems providing spectral information for analysis in the Gamma, X-ray Data Reductions (GXDR) system are identified by an alphabetic name. Rather than provide a full page description of a detector system every time one is mentioned, this document is presented for reference. One page detector descriptions will be provided as the detector systems are placed in service. Each type of detector system is pictured, followed by a one page description of the system and of its applications. All of these detectors are semiconductor detectors which must be cooled to the boiling of liquid nitrogen and evacuated to a maximum pressure of $10^{-5}$ Torr in order to operate. (auth)

**25966** (ARH-ST-114-1) GAMMA, X-RAY DATA REDUCTION SYSTEM. Volume I, Gamma. Zimmer, W. H. (Atlantic Richfield Hanford Co., Richland, Wash. (USA)). Dec 1974. Contract AT(45-1)-2130. 87p. Dep. NTIS $4.75.

The Gamma, X-Ray, Data Reduction (GXDR) system performs automatic gamma energy analysis data reductions including the calculation of activity with or without time correction, activation analysis, precision, limits of detection, peak interference correction, sorption correction, and random summing correction. Reports are assembled on magnetic tape. All of this is done quickly by the GXDR with 8K x $2^{16}$ computer core, 8K x $2^{24}$ hard-wired core, and two cassette magnetic tape systems. (auth)

**25967** (BM-RI-7907) FAST PULSE PROCESSING FOR GAMMA-RAY SPECTROSCOPY. Fasching, G. E.; Patton, G. H. (Energy Research and Development Administration, Morgantown, W. Va. (USA). Morgantown Energy Research Center). 1974. 14p.

A pulse-counting system is described that improves the energy resolution of less-precise gamma-radiation detectors [e.g., NaI(Tl)] by minimizing pulse-pile-up distortion. A pile-up detector selects either a fast or a slow processing channel, depending on whether more than one pulse is recorded during the resolving time of the system. This system has been used for determinations of of S in a continuous flow of coal (cf. Stewart et al., Analyt. Abstr.; 27: 3315(1974)). (Anal. Abstr.)

**25968** (EMI-4-74) MAGNETIC ENERGY ANALYSER FOR SLOW ELECTRONS. Limberg, W. (Fraunhofer-Gesellschaft zur Foerderung der Angewandten Forschung e.V., Freiburg (F. R. Germany). Ernst-Mach-Inst.; Technische Hochschule Aachen (F. R. Germany)). Aug 1974. 48p. (In German). INIS. Thesis.

A differential spectrometer with high time and energy resolution has been developed using the principle of energy analysis with a longitudinal homogeneous magnetic field. This way it is possible to measure the energy distribution of low energy electrons (eV-range) in the presence of high energy electrons without distortions by secondary electrons. The functioning and application of the analyzer is demonstrated by measuring the energy distributions of slow electrons emitted by a filament. (auth)

**25969** (UCRL-76699) PRECISE ANALYSES BY GAMMA SPECTROMETRY. Gunnink, R.; Niday, J. B. (California Univ., Livermore (USA). Lawrence Livermore Lab.). 14 Aug 1975. 31p. (CONF-750806-5). Dep. NTIS $4.75.

From 170th American Chemical Society national meeting; Chicago, Illinois, USA (24 Aug 1975).

An important application of Ge(Li) gamma-ray spectrometry is its use in nondestructive analysis. Highly precise results can be obtained by computer reduction of the data even though the spectra may be very complicated. However, this successful computer reduction requires a thorough understanding of the principles involved in the detection and acquisition techniques. Some of the more important parameters that are involved in the making of accurate measurements are discussed. Included are discussions of proper methods for delineation of the background under the peaks and for precise characterization of the peak shapes, problems related to detector calibrations, and methods for quantitative interpretation of peak intensities. Examples of gamma-ray analysis of plutonium on a small computer system are used to demonstrate that properly implemented techniques can give results to within 1 percent for the various isotopic constituents. (auth)

**25970** DATA PROCESSING TECHNIQUES FOR GAMMA SPECTROSCOPY. Okamura, M. (Nippon Atomic Industry Group Co. Ltd., Tokyo). Genshiryoku Kogyo; 20: No. 10, 12-16 (Oct 1974). (In Japanese).

In spectrometers of comparatively many channels, the problem is their drift, but it can be solved by the method of closed loop feedback stabilization. It is meaningless to print out all the data. Readout should be carried out by selecting truly necessary parts. Magnetic tapes, capable of high density recording, involves a problem of having no standard. Selection of multichannel analyzers is discussed. (JA)

**25971** INTERACTIVE VIDEO-GRAPHIC DISPLAY SYSTEM FOR USE WITH CATHODE RAY TUBE SCANNING DEVICES. Menzies, G.; O'Donnell, H. A.; Perry, A. J.; Robinson, C. J. (Univ. of Glasgow). J. Phys., E (London); 8: No. 8, 676-681 (Aug 1975).

The design principles of a 24 in. diameter interactive display system are discussed, the display being refreshed from a buffer. This part of the design is quite general. Its particular use when attached to the department's "POLLY" bubble chamber film measuring device provides a new facility that should be of great value with difficult film. It could also provide a far greater flexibility of scan pattern for "POLLY" than can be obtained by other techniques. The principle of a video data set which is introduced can be applied to any of the CRT scanning devices currently in use. (auth)

### *High Energy Physics Instrumentation*

**25972** (JINR-P13-8987) TOTAL ABSORPTION CHERENKOV γ-SPECTROMETER. Bunyatov, S. A.; Zalikhanov, B. Zh.; Kurbatov, V. S.; Khalbaev, A. (Joint Inst. for Nuclear Research, Dubna (USSR)). 1975. 16p. (In Russian). Dep. NTIS (US Sales Only) $4.00.

The spectrometric and time characteristics of five Cherenkov γ-spectrometers of total absorption in the electron beam of 30 to 300 MeV have been investigated. Use of a radiator of enhanced transmittance and thorough choosing of potential dividers for photomultiplier-49 provide better energy and time characteristics for a given type of spectrometers. The energy resolution of γ-spectrometers for 100 MeV electrons is equal on the average to $(28.0 \pm 2.6)\%$. The energy dependence of resolution is well described by the formula $\Delta E/E = A/\sqrt{E}$. The time resolutions of γ-spectrometers are in the range of 4 to 5 ns. The efficiency of the electron recording from 30 to 300 MeV is 100%. (auth)

**25973** (ORNL-TM-5040) PRELIMINARY DESIGN CALCULATIONS FOR AN IONIZATION SPECTROMETER FOR USE IN COLLIDING BEAM EXPERIMENTS. Gabriel, T. A.; Amburgey, J. D.; Santoro, R. T. (Oak Ridge National Lab., Tenn. (USA)). Sep 1975. Contract W-7405-eng-26. 15p. Dep. NTIS $4.00.

The calculated response of an ionization spectrometer containing NaI, Fe, and Ar to charged pions and kaons in the 0.1- to 1.0-GeV/c momentum range is presented. (auth)

**25974** (RL-75-090) MULTIPROGRAMMED COMPUTER SYSTEM FOR THE INTERACTIVE EXAMINATION OF EXPERIMENTAL DATA. Hand, R. P.; Hutton, J. S.; Maden, D.; Rosner, R. A. (Science Research Council, Chilton (UK). Rutherford High Energy Lab.). May 1975. 13p. Dep. NTIS (US Sales Only) $4.00.

The paper describes a facility, based on a 32K Honeywell DDP 516 computer, for general interactive functions associated with the analysis of the raw data from experiments in high energy physics, consisting of the tracks of charged particles recorded either photographically or electronically. The main features of its compact and modular operating system are discussed and the use of a fast data link to an IBM 360/195 is described. (auth)

**25975** EFFECTS DUE TO STREAMER SHAPE. Lozanskii, E. D.; Pontekorvo, D. B. (Joint Inst. for Nuclear Research, Dubna, USSR). Sov. Phys. - Tech. Phys.; 19: No. 11, 1432-1433 (May 1975).

Translated from Zh. Tekh. Fiz.; 44: No. 11, 2322-2325(Nov 1974).

A model of streamer development is proposed. The difference between the shape of the streamer surface and an ellipsoid of revolution is taken into account. Calculations based on the model agree with the experimental data. (auth)

## Radiometric Instruments

**25976** (AED-CONF-75-085-001) RADIOMETRIC LEVEL MEASURING. Heier, K. (Laboratorium Prof. Dr. Berthold, Wildbad (F. R. Germany)). 1975. 22p. (In German). INIS.

From meeting on level-measuring technology; Duesseldorf, F. R. Germany (10 Apr 1975).

22 figs. Available from ZAED. Shortened version to be published in VDI-Bericht no. 231.

The article gives a survey of limiting quantities, detectors and measuring instruments, measuring amplifiers, measuring arrangements and radiation sources suitable for the absorption and backscattering methods. The fully automatic filling level control in coil production for spark-ignition engines and the quantitative filling level measuring in continuous steel casting are lined as examples. (GE)

**25977** (LBL-4248) ENERGY DISPERSIVE X-RAY FLUORESCENCE SPECTROMETRY USING PULSED X-RAY EXCITATION. Jaklevic, J. M.; Landis, D. A.; Goulding, F. S. (California Univ., Berkeley (USA). Lawrence Berkeley Lab.). Aug 1975. Contract W-7405-ENG-48. 14p. (CONF-750831-2). Dep. NTIS $4.00.

From 24th annual conference on applications of x-ray analysis; Denver, Colorado, USA (6 Aug 1975).

An energy dispersive X-ray fluorescence spectrometer using pulsed X-ray excitation has been developed for use in large-scale environmental analysis programs. A grid controlled X-ray tube is coupled with variable secondary fluorescence targets to analyze for a wide variety of elements with almost optimum sensitivity. The operation of the pulsed tube in a feedback loop with the semiconductor detector spectrometer results in a substantial increase in output counting rates without pile-up. The loop functions by turning off the excitation immediately upon detection of an event by the spectrometer. Pile-up events are virtually eliminated and the X-ray tube's available anode power is better utilized. The electronic control of this feedback mode results in some unique features in the response of the system to varying sample mass. These features are discussed in detail. Experimental results for sensitivity and accuracy over the range of elements measured are presented. Early operating experience with the unit indicates increases of counting rates of a factor of five compared with similar conventional systems. (auth)

**25978** SYSTEMS ON INDUSTRIAL APPLICATION OF NUCLEAR GAUGES. Shimizu, M. (Fuji Electric Co. Ltd., Tokyo (Japan)). Genshiryoku Kogyo; 20: No. 10, 17-20(Oct 1974). (In Japanese).

Radiometric gages for industrial uses are reviewed. A profile integrating type β thickness gauge for the measurement and control of unevenness of thickness (profile) not only in the direction of run but also in the transverse direction, required in plastic film processing, is described. Gamma level gauges for the level control of continuous casting molds and beta thickness gauges for the process control of sheet paper making are other examples of application to industrial process control systems. The gamma level gauges are adopted due to its fast response and noncontacting operation. In the sheet paper making process, since base weight and moisture content are important factors for product quality, β thickness gauges and moisture gauges are combined together with computers, and perform feedback control in large systems. Here the β gauges operate only one of the components of the total system. (JA)

**25979** IMPROVED IN SITU GAMMA-RAY TRANSMISSION DENSITOMETER FOR MARINE SEDIMENTS. Hirst, T. J. (Lehigh Univ., Bethlehem, PA); Perlow, M. Jr.; Richards, A. F.; Burton, B. S.; van Sciver, W. J. Ocean Eng.; 3: No. 1, 17-27(Jun 1975).

The first-generation University of Illinois gamma-ray transmission densitometer, designed for the in situ measurement of sediment bulk density, was modified by incorporating in the detector probe (1) an Americium-241 alpha particle pulser and an anti-walk gain stabilization control to maintain better temperature stability and (2) a small power supply and an IC preamplifier to eliminate the need for a high-voltage coaxial cable between the detector and external signal conditioning electronics package. This second-generation Lehigh University system has been successfully deployed since 1971 in routine use from ships and submersibles in the Atlantic and Pacific Oceans and the Gulf of Mexico. Results are presented of system operations to (1) measure bulk density over the range of 1.2–1.8 $Mg/m^3$ in the Hudson Canyon, (2) penetrate 1.9 m into the seafloor in the San Diego trough and, (3) be lowered to a water depth of 3.6 km in the Gulf of Mexico. (auth)

**25980** RELEASE OF RADIOACTIVITY FROM A SCANDIUM TRITIDE ELECTRON CAPTURE DETECTOR USED IN GAS CHROMATOGRAPHY. Carlton, W. H.; Braselton, W. E. Jr.; Bransome, E. D. Jr. (Medical Coll. of Georgia, Augusta). Health Phys.; 29: No. 3, 411-413(Sep 1975).

An assessment of the radiation hazard to laboratory personnel, using a commercially available scandium tritide ($Sc^3H$) electron capture detector for gas chromatography, is presented. Data show that there is a significant $^3H$ build-up in the laboratory environment of the gas chromatograph and even in a mailing container. This second phenomenon has so far been ignored in the literature but represents a significant contamination of laboratory facilities (especially if they are to be used for other analytical work with tritium) and an opportunity for inadvertent ingestion of tritium by laboratory personnel. (UK)

## Radiation Effects on Instrument Components, Instruments, or Electronic Systems

**25981** (UCRL-76568) COMPARATIVE EMP DESIGN PRACTICES. Martin, L. C. (California Univ., Livermore (USA). Lawrence Livermore Lab.). 11 Jul 1975. 8p. (CONF-751021-1). Dep. NTIS $4.00.

From EEE international symposium on electromagnetic compatibility; San Antonio, Texas, USA (7 Oct 1975).

A large amount of effort is devoted to the hardening of systems against various effects. The nuclear electromagnetic pulse (EMP) creates potentially severe protection problems in hardening against electromagnetic effects. Each hardening effort is usually supported through development or application of sets of rules, practices, constraints, etc., which aid in decision-making throughout the design process. Several excerpts from a few sets of EMP design rules and practices taken from relatively independent sources are presented for comparison of essential features and mode of expression. A general objective is to clarify some of the EMP practices present in general EMC work and to encourage further interchange of relevant information. (auth)

**25982** MEASUREMENT OF THE QUANTUM EFFICIENCY OF AN ELECTRON MULTIPLIER AS A FUNCTION OF INCIDENT PROTON ENERGY. Cho, Z.H.; Singh, M.; Mohabbatizadeh, A.; Chai, J.; Cheung, H. (Laboratory of Nuclear Medicine and Radiation Biology and Electrical Science and Engineering Department, University of California, Los Angeles, California 90024); Sackerlotzky, O.H. Rev. Sci. Instrum. 46: No. 9, 1273-1274 (Sept 1975).

The quantum efficiency (QE) of an electron multiplier tube with oxidized Cu–Be dynodes was measured for incident protons over the energy region of 0.5–2 MeV at beam currents of 0.1–0.5 nA. The QE is relatively constant with energy up to 1.4 MeV. At higher energy the QE is inverse proportionally to incident energy, dropping to about half the peak value at 2.0 MeV. The proton beam was obtained from a Van de Graaff accelerator at UCLA. (auth)

**25983** LARGE SIGNAL S-PARAMETERS: MODELING AND RADIATION EFFECTS IN MICROWAVE POWER TRANSISTORS. Graham, E. D. Jr.; Chaffin, R. J.; Gwyn, C. W. (Sandia Labs., Albuquerque, NM). pp 87-99 of Microwave Semiconductor Devices, Circuits, and Applications. Ithaca, NY; Cornell University (1973).

From microwave semiconductor devices, circuits and applications conference; Ithaca, New York, USA (14 Aug 1973). See CONF-730828-.

Microwave power transistors are usually characterized by measuring the source and load impedances, efficiency, and power output at a specified frequency and bias condition in a tuned circuit. These measurements provide limited data for circuit design and yield essentially no information concerning broadbanding possibilities. Recently, a method using large signal S-parameters has been developed which provides a rapid and repeatable means for measuring microwave power transistor parameters. These large signal S-parameters have been successfully used to design rf power amplifiers. Attempts at modeling rf power transistors have in the past been restricted to a modified Ebers-Moll procedure with numerous adjustable model parameters. The modified Ebers-Moll model is further complicated by inclusion of package parasitics. In the present paper an exact one-dimensional device analysis code has been used to model the performance of the transistor chip. This code has been integrated into the SCEPTRE circuit analysis code such that chip, package and circuit performance can be coupled together in the analysis. Using this computational tool, rf transistor performance has been examined with particular attention given to the theoretical validity of large-signal S-parameters and the effects of nuclear radiation on device parameters. (auth)

**25984** EFFECTS OF GAMMA IRRADIATION ON LSA OSCILLATOR PERFORMANCE. Wilson, W. E. (Sandia Labs., Albuquerque, NM). pp 135-145 of Microwave Semiconductor Devices, Circuits, and Applications. Ithaca, NY; Cornell University (1973).

From microwave semiconductor devices, circuits and applications conference; Ithaca, New York, USA (14 Aug 1973). See CONF-730828-.

Circuit modeling of the LSA relaxation oscillator is discussed. Computer simulations of the circuit model are given, and results of a more realistic diode model are compared with the diode model used here. Oscillator preradiation characteristics are described, and the permanent and transient effects of gamma irradiation on the device are discussed. The final section summarizes the results and gives general conclusions. (WHK)

**25985** INVESTIGATION OF RADIATION DEFECTS IN SILICON $p^+$–n JUNCTIONS IRRADIATED WITH $\gamma$ QUANTA. Berman, L.S.; Vitman, R.F.; Shuman, V.B. (A. F. Ioffe Physicotechnical Institute, Academy of Sciences of the USSR, Leningrad). Sov. Phys.—Semicond. 9: No. 2, 202-204 (Aug 1975).

A comprehensive study was made of radiation defects in silicon $p^+$–n junctions irradiated with $Co^{60}$ $\gamma$ rays. The capacitance method was used in combination with measurements of the minority-carrier lifetime. The rates of introduction of radiation defects were determined and their energy levels as well as recombination properties were found. The kinetics of the isothermal annealing of radiation defects was investigated. (auth)

## Miscellaneous Instruments

*Refer also to abstracts 25775, 26961, and 27337.*

**25986** (CONF-750840-1) COMPUTER UTILITY FOR INTERACTIVE INSTRUMENT CONTROL. Day, P. (Argonne National Lab., Ill. (USA)). Aug 1975. 24p. Dep. NTIS $4.25.

From symposium on computer networking and chemistry; Chicago, Illinois, USA (24 Aug 1975).

A careful study of the ANL laboratory automation needs in 1967 led to the conclusion that a central computer could support all of the real-time needs of a diverse collection of research instruments. A suitable hardware configuration would require an operating system to provide effective protection, fast real-time response and efficient data transfer. An SDS Sigma 5 satisfied all hardware criteria, however it was necessary to write an original operating system; services include program generation, experiment control real-time analysis, interactive graphics and final analysis. The system is providing real-time support for 21 concurrently running experiments, including an automated neutron diffractometer, a pulsed NMR spectrometer and multi-particle detection systems. It guarantees the protection of each user's interests and dynamically assigns core memory, disk space and 9-track magnetic tape usage. Multiplexor hardware capability allows the transfer of data between a user's device and assigned core area at rates of 100,000 bytes/sec. Real-time histogram generation for a user can proceed at rates of 50,000 points/sec. The facility has been self-running (no computer operator) for five years with a mean time between failures of 10 days and an uptime of 157 hours/week. (auth)

**25987** (IRI-131-74-01) INFLUENCE OF DEAD TIME ON THE STOCHASTICS OF PULSE DETECTION SYSTEMS. de Vries, J. W. (Interuniversitair Reactor Instituut, Delft (Netherlands)). May 1974. 47p. (In Dutch).

**25988** (JINR-P13-8913) CAMAC-CABLE DELAY FOR ANALOG SIGNALS. Gabriel, F.; Shuravin, V. N.; Tyupikov, V. K.; Andert, K. (Joint Inst. for Nuclear Research, Dubna (USSR)). 1975. 9p. Dep. NTIS (US Sales Only) $4.00.

The construction and performance of a computer controlled CAMAC delay is described. The delay can be changed from 1 to 63 nsec. (auth)

**25989** (JINR-P13-8914) UNIVERSAL CAMAC PULSE SHAPER. Gabriel, F.; Shuravin, V. N.; Andert, K. (Joint Inst. for Nuclear Research, Dubna (USSR)). 1975. 16p. (In Russian). Dep. NTIS (US Sales Only) $4.00.

A high-stable CAMAC pulse shaper is described. The pulse length is controlled from the CAMAC-dataway and can be changed in steps of about 3.5% from 20 nsec to 150 μsec. This single-width-module operates in two modes: the "normal" mode and the "updating" one. The double pulse resolution of the "updating" mode is 20 nsec. (auth)

**25990** (JINR-P13-8916) CAMAC MATRIX FOR DISTRIBUTING FAST LOGIC. Gabriel, F.; Shuravin, V. N.; Andert, K. (Joint Inst. for Nuclear Research, Dubna (USSR)). 1975. 13p. (In Russian). Dep. NTIS (US Sales Only) $4.00.

Construction and the parameters of a CAMAC-module for fast logic signals are described. This unit allows a computer controlled connection of its 8 inputs with its 8 outputs in any possible combination. Examples of application of the CAMAC-matrix in the field of high energy and nuclear physics are given. (auth)

**25991** SHIMADZU ELECTROMAGNETIC FLOWMETER FOR LIQUID SODIUM. Komori, Y.; Someyama, T. (Shimadzu Seisakusho Ltd., Kyoto (Japan)); Iwamoto, S.; Yamada, K.; Kobayashi,

H. Shimadzu Hyoron; 31: No. 4, 163-169(Dec 1974). (In Japanese).

A 300 A bore electromagnetic flowmeter for liquid sodium has been developed to be used for a fast breeder reactor and its heat transmission flow test loop. An electromagnetic flowmeter having saddle type coils has been developed on the orthodox theory of circular transverse-field electromagnetic flowmeter; though the theory naturally has some limitations in practice. The accuracy obtained in the calibration test of the two flowmeters with liquid sodium was comparable to that of a test loop. The test was carried out in the dry-calibration method which could not provide a high accuracy in flow measurement of liquid sodium. The method of magnetic field calculation, the field measuring method and the dry-calibration technique are described. The problems involved in the flowmeters of larger bores, such as non-uniform fluid velocity and magnetic field distortion, are discussed, and a simple method to solve them described. (auth)

**25992** PRESENT STATUS AND TREND OF MULTI-CHANNEL ANALYZERS. Murata, Y. (Musashi Inst. of Tech., Kawasaki, Kanagawa (Japan). Atomic Research Lab.). Nippon Genshiryoku Gakkaishi; 16: No. 8, 411-417(Aug 1974). (In Japanese).

In Japan, multi-channel analyzers were used in radiation measurements about 1960, since then their market has increased very rapidly due to the needs of precise measurement, increase of the data processing capability of computers, and the development of semiconductor detectors. For Willkinson type ADC, the clock signal frequency mainly used is 50 to 100 MHz, the fastest one of 200 MHz being commercially available. In addition, upgrading in resolution, linearity and stability (including digital stabilizer), and improvement by adding an off-set function have been performed, while the resolution deterioration due to high input rate and the complaints on the catalog expressions for single channel function are recognized. The analyzers involve three systems mainly composed of hardware, mini-computers and the system belonging to the mini-computers. In the future, ADC with the clocks of higher speed and resolution will grow, and clock frequency may be several hundreds MHz. The analyzers will be improved further, and the type with built-in microcomputers will be put into practice. (JA)

**25993** SCANNING ELECTRON MICROSCOPY, 1974. Proceedings of the Conference Held at Chicago, Illinois, April 8-11, 1974. Johari, O.; Corvin, I. (eds.). Chicago; Illinois Institute of Technology, SEM Symposia Office(1974). 1180p. (CONF-7404103-). $26.50.

Three separate abstracts were prepared for NSA and one abstract was prepared for ERA from the 126 papers presented. (WHK)

*For abstracts of individual papers see: 25942, 26084, and 26256.*

**25994** SOLID STATE DEVICES. Proceedings of the 6th Conference, Tokyo, Japan, September 2-3, 1974. Journal of the Japan Society of Applied Physics, Volume 44, Supplement, 1975. Tokyo; Japan Society of Applied Physics (1975). 361p. (CONF-7409119-).

Forty-five papers are presented under the following headings: optoelectronic devices, acoustic devices, cryoelectronic devices, GaAs devices, charge transfer devices, MOS memory devices, field effect devices, and device technology. Separate abstracts were prepared for 7 papers; one other paper was selected for EDB. (DLC)

*For abstracts of individual papers see: 25502, 25843-25845, 25862, 25863, and 26258.*

**25995** SYSTEM FOR THE DETECTION OF THE CHANGE OF PLACE OF A RADIATION SOURCE. Paul, B. (to Siemens A. G., Muenchen (F. R. Germany); Siemens A. G., Berlin (F. R. Germany)). German(FRG) Patent 2335261/S/. 30 Jan 1975. 7p. (In German).

2 figs.

A method for detection of the change of place of a radiation source—especially an infra-red source—is described. Radiosensitive resistances connected in a bridge circuit serve as receptors. The change of place of a radiation source can thus be monitored in two dimensions at right angle to the direction of observation. (GE)

**25996** MICROWAVE SEMICONDUCTOR DEVICES, CIRCUITS, AND APPLICATIONS. Proceedings of the Fourth Biennial Cornell Electrical Engineering Conference Held at Ithaca, New York, August 14-16, 1973. Ithaca, NY; Cornell University (1973). 432p. (CONF-730828-).

From microwave semiconductor devices, circuits and applications conference; Ithaca, New York, USA (14 Aug 1973).

Separate abstracts were prepared for 2 of the 44 papers presented. The remaining 42 papers were not within the scope of NSA. (WHK)

*For abstracts of individual papers see: 25983 and 25984.*

# ISOTOPE AND RADIATION SOURCE TECHNOLOGY

## Isotope Separation (Industrial)

*Refer also to abstract 25565.*

**25997** (UCRL-52000-75-7) LAWRENCE LIVERMORE LABORATORY ENERGY AND TECHNOLOGY REVIEW. Carr, R. B.; Barnett, J. M.; Berlo, R. C.; McCaleb, C. S.; Prono, J. K. (eds.). (California Univ., Livermore (USA). Lawrence Livermore Lab.). Jul 1975. Contract W-7405-Eng-48. 29p. Dep. NTIS $4.00.

Energy perspectives, lasers and laser applications, national security, and fossil energy are reviewed. Separate abstracts were prepared for the 4 sections. Two of these are announced in NSA and all 4 in ERA. (LK)

*For abstracts of individual sections see: 25879 and 25998.*

**25998** (UCRL-52000-75-7, pp 9-12) LASERS AND LASER APPLICATIONS. Laser Isotope Separation of Uranium. Jul 1975.

In Lawrence Livermore Laboratory energy and technology review. (California Univ., Livermore (USA). Lawrence Livermore Lab.).

U. S. capacity to produce isotopically enriched uranium for nuclear power generation is thought to be adequate to meet demands through the early 1980's. However, if additional enrichment facilities are not available then, the projected demand will sharply exceed supply. U. S. plants currently supply 12,000 tonnes of separative work per year. Based on the projected demand for electrical power, their annual output will need to be 100,000 tonnes by the turn of the century. At that time the U. S. will be spending approximately $10 million per day for uranium enrichment. Thus the economic motivation for developing less costly processes than those currently in use is very great. LLL is investigating new enrichment processes involving laser excitation of the uranium-235 atoms in a stream of natural uranium vapor, followed by separation of the excited uranium-235 from the unexcited uranium-238 atoms. Thus far, natural uranium containing 0.7 percent uranium-235 has been enriched to reactor-grade uranium containing 3 percent uranium-235. Initial experiments have yielded 4 mg of enriched material and established the basic principles for future large-scale operations. (auth)

**25999** ANALYTICAL SOLUTION FOR REAL CASCADE EQUATION IN STEADY STATE. Yamamoto, I.; Kanagawa, A. (Nagoya Univ. (Japan). Faculty of Engineering). J. Nucl. Sci. Technol. (Tokyo); 12: No. 2, 120-127(Feb 1975).

Steady state real cascades are analyzed. The method adopted is based on two difference equations representing the conservation of the total flow and the desired material flow, respectively. Introducing what is termed the "desired material flow cut" as a stage parameter corresponding to the "total flow cut" or "cut", the flow relations of the desired material flow are reduced to the same form as that of the total flow rate. The flow rate is not subject to any restrictive assumption except the conservation of mass flow, so that the method can be applied to almost any type of real cascade with side flows and losses. Adoption of a suitable iterative calculation will permit this treatment to deal with cascades constituted of separators with large values of separation factor without resorting to approximation, because the "desired material flow cut" of each stage is described exactly by the separation factors of each stage. The difference equations are solved analytically, for which the determinants B(i,j) and D(i,j) are introduced, which are the functions of stage parameters from the i-th to the j-th stage. With these determinants, explicit relations are obtained between the flow rate of each stage and the stage parameters of the whole cascade. The determinants are calculated by the recurrence formula. (auth)

**26000** SEPARATIVE PROPERTIES OF COUNTER-CURRENT BEAMS TYPE CENTRIFUGE. I. Three Different Flow Schemes. Todo, F. (Kawasaki Heavy Industries, Ltd., Kobe (Japan). Technical Research Lab.). Nippon Genshiryoku Gakkaishi; 17: No. 2, 81-85(Feb 1975). (In Japanese).

The separative properties of counter-current Beams-type gas centrifuge are studied for three different flow schemes (enriching, stripping and one-time through). The diffusion equation is solved by assuming thin cylindrical counter-current streams. The relations of the gas feed rate to both separation factor and separative power are given. The more important results of the analysis are that: (1) The enriching centrifuge should produce higher separative efficiencies at values of cut below 0.5, while values above 0.5 should produce a similar effect on the stripping centrifuge. (2) When the cut is 0.5, the Beams-type centrifuge requires a large gas flow rate to obtain high efficiency. (auth)

**26001** CONSTRUCTION OF 13-STAGE DIFFUSION CASCADE AND SEPARATION OF URANIUM AND ARGON ISOTOPES. Isomura, S.; Watanabe, T.; Nakane, R. (Institute of Physical and Chemical Research, Wako, Saitama (Japan)). Rikagaku Kenkyusho Hokoku; 50: No. 6, 211-227(Dec 1974). (In Japanese).

A small-scale plant of gaseous diffusion with thirteen identical stages, which forms a square cascade, has been built to measure the separation efficiency of the barrier for the uranium isotopes over a wide range of operating conditions. The regulation of cascade is made by automatic control of both high and low pressures at each stage. The separation of uranium and argon isotopes is carried out under the condition of total reflux. The results show that the observed values of the separation efficiency for both isotopes can be well correlated with the theoretical curves calculated by the Present and de Bethune theory. (auth)

**26002** INTERNATIONAL CONFERENCE ON URANIUM ISOTOPE SEPARATION, 5-7 MARCH 1975. Ferguson, A. T. G. (United Kingdom Atomic Energy Authority, Harwell, Eng.). J. Br. Nucl. Energy Soc.; 14: No. 3, 213-218(Jul 1975).

A report is presented of the International Conference on Uranium Isotope Separation held in London and jointly organized by the British Nuclear Energy Society and Kerntechnische Gesellschaft. There were five main sessions of review and original papers, followed by a concluding session devoted to summing-up and questions. The main sessions dealt with the following subjects: nozzle and laser processes; rotating plasma and other new processes; gaseous diffusion and centrifuge plants; analyses, optimizations, and comparisons of technologies. (UK)

## Isotopic Power Sources

**26003** DEVELOPMENT OF A NUCLEAR-POWERED ARTIFICIAL HEART. Mott, W. E.; Cole, D. W. Jr. (Atomic Energy Commission, Washington, DC). Trans., Am. Soc. Artif. Intern. Organs.; 18: 152-158(1972).

Of the few known methods of furnishing power for a completely implantable artificial heart one of the most promising involves the conversion of the thermal energy from the decay of man-made radioisotopes. Serious consideration of radioisotopic, or nuclear, heat sources for implantable power supplies began in early 1964. Since then there have been some notable accomplishments on the road to a nuclear-powered system but a large number of important and difficult problems remain to be clarified. The overall objective of the Atomic Energy Commission's current program is to examine critically these problems and to provide information so that the reasonableness and practicability of the nuclear approach can be assessed at an early date. Research and development projects are underway on radioisotope heat source fuel and containment materials, on a highly reliable, long-life thermal energy conversion system and its requisite high performance thermal insulation package, on the coupling of the converter output power to the diaphragm of a suitable blood pump in such a manner that the system is fully responsive to the needs of the body, and on the radiobiological implications of large-scale heat source implantation. (auth)

## Radiation Sources

*Refer also to abstracts 25572, 25574, 25575, 25577, 25578, 25580, and 25932.*

**26004** (AED-CONF-75-061-034) SOME APPROACHES AND INVESTIGATIONS: THE WASTE-WATER AND SLUDGE REUTILIZATION PROJECT BY GAMMA-IRRADIATION AT THE CITY OF KECSKEMET, HUNGARY. Simon, J.; Gacs, F.; Urban, A. 1975. 5p. (SM-194/603). INIS.

From international symposium on the use of high-level radiation in waste treatment: status and prospects; Muenchen, F. R. Germany (17 Mar 1975).

2 tabs.; 19 refs. Available from ZAED.

Within the framework of the increasing efforts made by the Hungarian Government, to increase the effectivity of the environmental control, a plan was drawn up to find a solution for the sterilization of waste water of communal origin. Kecskemet, the selected town, has 80,000 inhabitants and a waste water production of 10 to 12,000 $m^3$/d. After determination of the bacteriological and parasitological characteristics of the waste water,

the effect of 150 to 600 krad of gamma radiation on the microflora was studied. Tables are given of the rate of diminution expressed in percent values showing the most conspicuous reduction in the case of mycobacteria after 150 krad (100%). Furthermore, the alteration of the chemical components, the oxygen consumption, as well as the oil content was studied. The technical concept for the gamma irradiation facility is described. (GE)

**26005** RADIOISOTOPES IN INDUSTRIAL PROCESSING ENGINEERING. Vogg, H. (Kernforschungszentrum Karlsruhe (F. R. Germany). Lab. fuer Isotopentechnik). Chem.-Ing.-Tech.; 47: No. 7, 316-318(Apr 1975). (In German).

From 2nd workshop of the Fachunterauschuss Radioisotope in der Verfahrenstechnik of the VDI-Gesellschaft Verfahrentechnik und Chemieingenieurwesen; Stuttgart, F. R. Germany (25 Apr 1974).

Residence time measurements in the chemical industry, residence time spectrum and reactor models for a pipe reactor with stirring device, application of radioisotopes for the investigation of the axial mixing in a rotary tube, experimental investigations on a production rotary tube furnace, intermixing studies and quantitative analysis with radioactive indicators, applicability of radioisotopes in the aluminium industry, pneumatic homogenization, possible applications of the radionuclide technique to investigate stationary and non-stationary multiphase flows, flow investigation in the chemical industry, and the determination of the flow rates in a vibrating muffle furnace for hardening and tempering of screws are dealt with. (GE)

# LIFE SCIENCES

## Radiation Effects on Biochemicals

*Refer also to abstracts 26049, 26050, and 26083.*

**26006** (ERDA-tr-38, pp 1-9) RADIOTHERMOLUMINESCENCE OF DNA AND THE NATURE OF THE PRIMARY ACTIVE PARTICLES IN GAMMA-IRRADIATED DNA. Skvortsov, V. G.; Milinchuk, V. K.; Pshezhetskii, S. Ya. Jul 1975. Translated from Radiobiologiya; 15: No. 1, 3-9(1975).

In Radiobiology.

The radiothermoluminescence (RTL) of dry and moistened preparations of double-stranded and single-stranded DNA of thymus origin was investigated. The results of RTL are considered together with the data obtained by the ESR method. It was shown that the primary products of low-temperature radiolysis in DNA are electron-cation pairs, the predominant sites of stabilization of which are the nitrogen bases and phosphate groups of DNA. The spectral composition of the RTL of DNA is characterized by the presence of two bands with lambda/sub max/ equals 410 and 470 m mu, the spectral contribution of which depends on the temperature. The RTL of DNA is considered as phosphorescence of the thymine and evidently adenine bases. The possible factors leading to the predominant localization of radiation damages in DNA—the formation of free radicals on thymine—are discussed. (tr-auth)

**26007** (ERDA-tr-38, pp 24-31) OXYGEN-DEPENDENT EFFECT OF THE DOSE RATE IN THE GAMMA IRRADIATION OF PROTEINS. Kharchenko, L. I.; Pavlovskaya, T. E. (Inst. of Biochemistry, Moscow). Jul 1975. Translated from Radiobiologiya; 15: No. 1, 21-26(1975).

In Radiobiology.

The number of oxygen atoms bound during the gamma irradiation of a 10 per cent aqueous solution of human serum albumin at the maximum of the doses used (1000 kR) and dose rates 400, 200, 100, and 50 R/sec, is 2.24, 2.62, 3.15, and 3.90 atoms per protein molecule, respectively. The observed decrease in the effectiveness of irradiation with increasing dose rate is explained by the rapid absorption of oxygen in radiation chemical reactions and by the creation of a state of hypoxia in the irradiated objects. It is suggested that the oxygen-dependent dose rate effect can be detected for all objects with a suitable selection of the radiation intensity and value of the total dose of irradiation. (tr-auth)

**26008** (ERDA-tr-38, pp 32-38) MECHANISM OF THE CHANGE IN THE HETEROGENEOUS SYSTEM OF HEMOGLOBIN UNDER CONDITIONS OF RADIATION PATHOLOGY. Starodub, N. F. (Inst. of Molecular Biology and Genetics, Kiev). Jul 1975. Translated from Radiobiologiya; 15: No. 1, 27-31(1975).

In Radiobiology.

In a study of the basic principles of the disruption of the fractional composition of rat hemoglobin after x irradiation under in vitro and in vivo conditions, together with the similarity in the damage to the heterogeneous system of this hemoprotein, substantial differences were also detected. Moreover, changes in the fractional composition of hemoglobin during irradiation are nonspecific; analogous deviations are also noted under other influences on hemoglobin. Possible factors determining the quantitative changes in the heterogeneous system of hemoglobin in the peripheral blood erythrocytes of irradiated animals are discussed. (tr-auth)

**26009** (ERDA-tr-38, pp 130-133) INFLUENCE OF POLYVINYL SULFATE ON THE NUCLEIC ACID METABOLISM DURING IRRADIATION. Kharitanovich, N. P.; Dokshina, G. A.; Pegel, V. A.; Yartsev, E. I.; Yashunskii, V. G. (Tomsk Univ., Moscow). Jul 1975. Translated from Radiobiologiya; 15: No. 1, 104-107 (1975).

In Radiobiology.

Polyvinyl sulfate (PVS) was used as an inhibitor of nucleases in order to protect endrogenous nucleic acids from degradation by depolymerases activated during irradiation. Noninbred male white rats were irradiated using a strong flux betatron at doses of 700 and 1000 rad. The PvS, prepared in physiological solution, was injected intravenously in doses of 25 and 50 mg/kg body weight 30 min after irradiation. The data indicate that PVS is a strong inhibitor of nucleases. (ERB)

**26010** (ERDA-tr-38, pp 134-138) NATURE OF THE TERMINAL GROUPS OF BREAKS INDUCED BY IONIZING RADIATION IN DNA IN VIVO. Gaziev, A. I. (Inst. of Biological Physics, Pushchino, USSR). Jul 1975. Translated from Radiobiologiya; 15: No. 1, 107-111(1975).

In Radiobiology.

Single-stranded breaks with 5'OH, 5'$PO_4$, and 3'OH ends, determined by the phosphatase, polynucleotide kinase, and DNA ligase reactions, are recorded in the DNA of gamma-irradiated cells of E. coli. The number of breaks with 5'ends corresponds to breaks recorded by the method of sedimentation in an alkaline sucrose gradient. The yield of breaks with different ends varies with the dose. Most (70 to 40 percent at doses of 10 to 30 krad) of the single-stranded breaks of 5'$PO_4$ and 3'OH ends are repaired by ligase. (tr-auth)

**26011** (TID-26867) JOINT RADIATION SURVEY RESULTS, 1973. Gileadi, M. (Puerto Rico Nuclear Center, Mayaguez). 1973. 222p. Dep. NTIS $14.25.

Data are presented on the radiation dose to patients in Puerto Rico during diagnostic x-ray examinations in 1973. Data are included on the type of diagnostic examination, sex and age of the patient, type of facility and type of x-ray unit used for the examinations. Detailed dosimetric studies were made in the major facilities to determine the radiation dose to the gonads taking into account various techniques of positioning patients, collimation and filtration of the x-ray beam, and other parameters affecting dose. (CH)

**26012** INVESTIGATION OF THE EFFECT OF ULTRAVIOLET RADIATION ON BIOLOGICAL MEMBRANES. II. Effect of Irradiation on Chemiluminescence of the Mitochondria. Marzoyev, A. I.; Roshchupkin, D. I.; Vladimirov, Yu. A. (Moscow State Medical Inst.). Biophysics (USSR) (Engl. Transl.); 18: No. 2, 265-271(Nov 1973).

Translated from Biofizika, 18: No. 2, 258-263(Nov 1973).

The $Fe^{2+}$-activated chemiluminescence of the native and ultraviolet irradiated mitochondria isolated from rat liver was investigated. In the samples irradiated in air at the moment of introduction of iron a rapidly attenuating burst of luminescence is observed which as shown by experiments with extraction, is generated in the lipids of the membranes. Ultraviolet radiation stimulates the development (shortens the period of induction) of the slow burst of chemiluminescence associated with the process of slow chain oxidation of the lipids. From analysis of the possible causes it is assumed that this phenomenon is due to the acceleration of the generation of chains through breakdown into radical of the peroxides formed during irradiation and ultraviolet inactivation of the anti-oxidants. The role of the reactions of photo-oxidation of the lipids in ultraviolet damage to the physiological functions of the mitochondria is discussed. (auth)

**26013** SEMI-IN VITRO REPAIR OF DNA IN GERMINATING SPORES OF BACILLUS SUBTILIS IRRADIATED WITH GAMMA-RAY. Terano, H.; Fujita, Y.; Komano, T.; Kadota, H. (Kyoto Univ. (Japan). Faculty of Agriculture). Agric. Biol. Chem. (Tokyo); 38: No. 11, 2157-2160(Nov 1974).

DNA repair synthesis was studied in germinating spores of Bacillus subtilis made permeable to deoxyribonucleoside triphosphates by treatment with Brij 58. The synthesis is dependent on the presence of all four deoxyribonucleoside triphosphates, but does not require adenosine triphosphate. Repair synthesis in the γ-ray irradiated and Brij 58 treated germinating spores was observed in wild type strain 168Tt, but not in DNA polymerase I-deficient mutant strain D22. Furthermore, the single-strand breaks of DNA in the germinating spores of strain 168Tt induced by γ-ray irradiation were rejoined during postirradiation incubation in the presence of four deoxyribonucleoside triphosphates, nicotinamide adenine dinucleotide, and magnesium ion. In the case of a mutant D22, the γ-ray induced DNA single-strand breaks were not rejoined. (auth)

## Radiation Effects on Cells

**26014** (ERDA-tr-38, pp 68-75) MOLECULAR MECHANISM OF THE DAMAGE TO CELLS AND PROTECTION FROM THE ACTION OF IONIZING RADIATIONS. Communication 3. Relationship of the Protective Effect to the Development of the Nonspecific Response. Veksler, A. M.; Ermekova, V. M.; Kozlovich, L. I.; Korystov, Yu. N.; Kublik, L. N.; Eidus, L. Kh. (Inst. of Biological Physics, Pushchino, USSR). Jul 1975. Translated from Radiobiologiya; 15: No. 1, 51-56(1975).

In Radiobiology.

The dynamics of the development of a reversible nonspecific response (NR) of cells under the influence of hypothermia and with the administration of cysteamine was studied on an asyn-

chronous culture of Chinese hamster fibroblasts. A correlation of the development of the NR and radioresistance was established. It was shown that when cysteamine is administered at various periods after irradiation, the postradiation protection shows a wave-like variation. This is explained by the superposition of two processes: the realization of latent damages, slowed down as a result of the development of the NR, and the repair of these damages by the enzyme system with an activity that also varies periodically as a result of the development of the NR. (tr-auth)

**26015** (ERDA-tr-38, pp 108-113) COMBINED ACTION OF TAURINE AND CATIONS OF CERTAIN METALS ON THE POST-RADIATION SURVIVAL OF A SOC CELL CULTURE. Yartsev, E. I.; Aldonyasov, V. I.; Yakovlev, V. G.; Novosel'tseva, S. D.; Kolesnikov, Yu. A.; Goryacheva, V. N. Jul 1975. Translated from Radiobiologiya; 15: No. 1, 83-87(1975).

In Radiobiology.

In a study of the combined action of taurine and metals (potassium, magnesium, calcium, zinc), it was established for the first time at the cellular level that the use of taurine and potassium and zinc salts in various concentrations increases the survival of irradiated SOC cells to 40 percent; the addition of magnesium and calcium salts does not change the effectiveness of taurine. The greatest effectiveness is possessed by potassium and taurine in the case of addition to the incubation medium in equimolar ratios. (tr-auth)

**26016** ON CODING OF PEDIGREES OF DIVIDING CELLS. Sakka, M. (Tohoku Univ., Sendai (Japan). School of Medicine). Nippon Igaku Hoshasen Gakkai Zasshi; 34: No. 9, 704-708(Sep 1974). (In Japanese).

Time lapse cinemicrograms of cultured hepatoma cells of the rat (Katsuta and Takaoka) were analyzed and pedigrees of dividing cells were constructed. There were two types of pedigrees, full and fragmentary. Full pedigrees were divided into two classes and coded as in table. Ar, cell in a pedigree, viable or lethal, is identified by combination of 0 and 1. Lethal pedigrees were coded. Frequency distribution of pedigrees after irradiation (400 to 800 R) was given in table. Viable pedigrees were listed in table. The number of generations in which post-irradiation (400 to 800 R) cell death took place is given in tables. The full paper will appear elsewhere in the near future. (auth)

**26017** CHANGES IN THE ORGANIZATION OF CHROMOSOMES DURING THE CELL CYCLE: RESPONSE TO ULTRAVIOLET LIGHT. Schor, S. L.; Johnson, R. T.; Waldren, C. A. (Cambridge Univ., Eng.). J. Cell Sci.; 17: No. 3, 539-565(May 1975).

Fusion between mitotic and interphase cells results in the premature condensation of the interphase chromosomes into a morphology related to the position in the cell cycle at the time of fusion. These prematurely condensed chromosomes (PCC) have been used in conjunction with uv irradiation to examine the interphase chromosome condensation cycle of HeLa cells. The following observations have been made: there is a progressive decondensation of the chromosomes during $G_1$ which is accentuated by uv irradiation; the chromosomes become more resistant to uv-induced decondensation during $G_2$ and mitosis; there is a close correlation between the degree of chromosome decondensation and the amount of unscheduled DNA synthesis induced by uv irradiation during $G_1$ and mitosis; and hydroxyurea enhances the ability of uv irradiation to promote the decondensation of chromosomes during $G_1$, $G_2$, and mitosis. Hydroxyurea also potentiates the lethal action of uv irradiation during mitosis and $G_1$. These data are discussed in relation to the suggestion that chromosomes undergo a progressive decondensation during $G_1$ and condensation during $G_2$. (auth)

**26018** THE MODIFYING EFFECTS OF STRAIN AND AGE ON THE MUTAGENIC SPECIFICITY OF ULTRAVIOLET LIGHT IN NEUROSPORA CRASSA. Kilbey, B. J.; Purdom, S. (Edinburgh Univ. (UK). Dept. of Genetics). Mol. Gen. Genet.; 135: No. 4, 295-307(1974).

4 figs.; 1 tab.; 17 refs.

Two derivatives of Neurospora crassa are described which show opposite specific reversional responses to UV. Both derivatives carry the same two auxotrophic alleles and appear to differ only in a single gene which influences the pattern of mutagen specificity. The differences between the derivatives only develop after the cultures have been aged for two to four weeks. Various possible explanations are considered. (GE)

**26019** MICROWAVES IN RADIOTHERAPY OF TUMORS—ALTERNATIVE TO HEAVY PARTICLES. Dietzel, F.; Ringleb, D.; Schneider, U.; Wricke, H. (Giessen Univ. (F. R. Germany). Wilhelm-Conrad-Roentgen-Klinik; Giessen Univ. (F. R. Germany). Zentrum fuer Radiologie). Strahlentherapie; 149: No. 4, 438-441(Apr 1975).

1 fig.; 13 refs.

An increase of the radiosensitivity can be obtained by means of microwave use in combination with sparsely ionizing radiation. Comparing the therapeutic effect on the model of a euoxic tumor (mice testicles) with a tumor that contains important parts of hypoxic cells (solid tumor of Ehrlich) it appears that the sensitization evidently is seen in the hypoxic tumor first of all. No sensitization can be obtained on the euoxic proliferation tissue of the testicles. The temperature enhancement ratio (TER) does not increase linearly with increasing temperature, but is the greatest within the scope of 41°C. The mere heat effect appears in the foreground with high temperatures (43°C and more). The high frequency application holds promise for a solution of the oxygen problem in radiotherapy and could substitute for heavy particles (high LET). (GE)

## Radiation Effects on Microorganisms

*Refer also to abstracts 26010 and 26013.*

**26020** (AED-CONF-75-061-005) SURVEYS ON RADIATION-RESISTANT ASPOROGENIC BACTERIA IN NATURAL ENVIRONMENTS. Yano, K.; Cho, B.; Yoshinaka, T.; Yamaguchi, H. (Tokyo Univ., (Japan). 1975. 16p. (SM-194/202). INIS.

From international symposium on the use of high-level radiation in waste treatment: status and prospects; Muenchen, F. R. Germany (17 Mar 1975).

Surveys on aerobic and asporogenic radioresistant bacteria in nature have been done with over 200 samples which included rice grains, feces of animals, water, muds, and soils. Non-spore forming survivors after gamma irradiation at a dose of $8.1 \times 10^5$ rad were pigmented yellow, pink, and red. Only spore formers were obtained from soil. Aqueous samples often contained survivors. Except Pseudomonas radiora isolated from rice grains, all were Gram positive. An isolate similar to Micrococcus radiodurans was obtained from puddle water. Arthrobacter radiotolerans isolated from wells at Misasa, Japan, which are famous as a Rn-containing springs, exhibited extreme resistance with shoulder dose and $D_0$ value calculated to be $6 \times 10^5$ and $1 \times 10^6$ rad, respectively. Notably, the samples from two wells at Misasa always contained high and/or extremely resistant strains and those from another well sometimes had a high resistance. Some ecological aspects and the incidence of the resistant in specific areas are discussed. (GE)

**26021** RADIATION CHEMICAL STUDY ON RADIOSENSITIZATION OF E. COLI BY SODIUM CHLORIDE. Shih Chen, S. J.; Arai, S.; Matsuyama, A. (International Atomic Energy Agency, Vienna (Austria)). Sci. Pap. Inst. Phys. Chem. Res. (Jap.); 68: No. 1, 21-29(Mar 1974). (In Japanese).

Radiation chemical basis of NaCl radiosensitization was investigated for the decrease in $G(H_2O_2)$ and the kinetic behavior of the $Cl_2^-$ transients in concentrated neutral aqueous NaCl solutions. The decrease of $G(H_2O_2)$ with increasing NaCl concentrations according to the cube-root correlation was observed at NaCl concentrations greater than about $8 \times 10^{-3}$ M. This may be an indirect evidence for the formation of atomic chlorine in a spur as a precursor of the $Cl_2^-$. Scavenging activities of sodium thioglycolate and potassium ferrocyanide for the $Cl_2^-$ did not quantitatively correlate with their protective effects on E. coli B/r against NaCl radiosensitization. The presence of L-valine during irradiation did not so much affect the formation and decay of the $Cl_2^-$, while it was appreciably effective to remove the radiosensitizing action of NaCl. These results suggest a possibility that the mechanism for NaCl radiosensitization may involve damages in some cellular sites or biochemical processes which can be protected by valine and perhaps thioglycolate. (auth)

**26022** EFFECTS OF DISCRETE NUCLEAR UV-MICROBEAM IRRADIATION ON HERPES VIRUS AND SV40 INFECTION. Deak, I. I.; Defendi, V. (Oxford Univ.). J. Cell Sci.; 17: No. 3, 531-538(May 1975).

The requirement for a nucleolus in the expression of structural genes of nuclear viruses was examined by means of experiments in which the nucleolus or other parts of the nucleus were inactivated by a microbeam of ultraviolet light. These experiments showed that the expression of such genes is not dependent on nucleolar function. This conclusion is discussed in the light of previous experiments in which similar inactivation of the nucleolus was shown to prevent the expression of cellular structural genes. (auth)

**26023** LACK OF CHEMICALLY INDUCED MUTATION IN REPAIR-DEFICIENT MUTANTS OF YEAST. Prakash, L. (Univ. of Rochester, NY). Genetics; 78: 1101-1118(Dec 1974).

Two genes, rad6 and rad9, that confer radiation sensitivity in

the yeast Saccharomyces cerevisiae also greatly reduce the frequency of chemically-induced reversions of a tester mutant cyc1-131, which is a chain initiation mutant in the structural gene determining iso-1-cytochrome c. Mutations induced by ethyl methanesulfonate (EMS), diethyl sulfate (DES), methyl methanesulfonate (MMS), dimethyl sulfate (DMS), nitroquinoline oxide (NQO), nitrosoguanidine (NTG), nitrogen mustard (HN2), beta-propiolactone, and tritiated uridine, as well as mutations induced by ultraviolet light (UV) and ionizing radiation were greatly diminished in strains homozygous for either the rad6 or rad9 gene. Nitrous acid and nitrosoimidazolidone (NIL), on the other hand, were highly mutagenic in these repair-deficient mutants, and at low doses, these mutagens acted with about the same efficiency as in the normal RAD strain. At high doses of either nitrous acid or NIL, however, reversion frequencies were significantly reduced in the two rad mutants compared to normal strains. Although both rad mutants are immutable to about the same extent, the rad9 strains tend to be less sensitive to the lethal effect of chemical mutagens than rad6 strains. It is concluded that yeast requires a functional repair system for mutation induction by chemical agents. (auth)

**26024** TRANSFORMING MARKER THAT PRODUCES MERODIPLOIDS WITH HIGH EFFICIENCY AND STABLE TRANSFORMANTS WITH LOW EFFICIENCY IN STREPTOCOCCUS. Ravin, A. W.; Ma, M. (Univ. of Chicago). Genetics; 80: No. 3, 421-443(Jul 1975).

A mutation (ery-r8) conferring a high level of resistance to erythromycin in the Challis strain of Streptococcus sanguis can be transferred to wild-type erythromycin-sensitive recipients via single molecules of donor DNA. The transformants thus produced are of two types: cells slightly more resistant to erythromycin than wild-type and capable of segregating (at a frequency of 2 x $10^{-4}$/bacterium/generation) either wild-type or highly-resistant cells like the original donor type; cells phenotypically and genotypically identical to the original donor type. The unstable diploids (ery-r8/+) occur with a frequency equivalent to that obtained with high-efficiency (HE) markers, whereas the stable donor-type (ery-r8) transformants occur with about five hundred times lower frequency. Penetration of the wild-type recipient by more than one molecule of DNA bearing the ery-r8 marker increases by as much as seven times the incidence of stable transformants. uv-irradiation of molecules bearing the ery-r8 marker diminishes their ability to cooperate in producing a stable transformant, although the uv sensitivity of stable transformant production by a single DNA molecule is not different from that of diploid production. Hence, stable transformants do not appear to be produced by a process typical of low efficiency (LE) markers, which are generally highly sensitive to ultraviolet irradiation. Moreover, stable ery-r8 transformants are produced with equally low frequencies in strains of S. pneumoniae that discriminate (hex+) and fail to discriminate (hex-) between HE and LE markers. (auth)

## Radiation Effects on Plants

*Refer also to abstract 26049.*

**26025** (ERDA-tr-38, pp 124-129) MODIFICATION OF THE INJURIOUS EFFECT IN THE GAMMA IRRADIATION OF SEEDS OF RADIOSENSITIVE AND RADIORESISTANT CROPS. Kaplan, I. S.; Tikhomirov, F. A.; Khvostova, V. V. (Moscow State Univ.). Jul 1975. Translated from Radiobiologiya; 15: No. 1, 98-103 (1975).

In Radiobiology.

It was shown that the influence of low and high temperatures during the irradiation of seeds produces a decrease in the general injurious effect, both for a comparatively radiosensitive crop (kidney beans) and for radioresistant crops (flax, mustard). It is suggested that the removal of the injurious effect is due to the action of such supplementary treatment (ST) on short-lived radicals, which is confirmed by experiments with storage of irradiated seeds. Supplementary treatment permits the production of a high frequency of mutations, both in radioresistant and in radiosensitive crops. (tr-auth)

**26026** (ERDA-tr-38, pp 199-202) EFFECTIVENESS OF 0.2 MeV NEUTRONS IN THE IRRADIATION OF SEEDS OF ARABIDOPSIS THALIANA (L.) HEYNH. Ginter, T. N.; Ivanov, V. I.; Troitskii, N. A.; Drozd, G. G. (Scientific Research Inst. of Medical Radiology, Obninsk, USSR). Jul 1975. Translated from Radiobiologiya; 15: No. 1, 158-161(1975).

In Radiobiology.

The effects of 0.2 MeV neutrons on the survival, growth, development, fertility, and mutation process in Arabidopsis thaliana was studied as part of an investigation of the relative effectiveness of neutrons of various energies on biological materials. For all of the characteristics studied, the effectiveness of neutrons of different energies in the irradiation of dormant seeds of Arabidopsis thaliana coincides. Consequently, the multiple differences in the concentration of tracks of neutron recoil nuclei in the tissues and in the length of the ranges, like the differences in the LET and the relative role of different mechanisms of the absorption of the energy of 0.2, 2.0, and 5.6 MeV neutrons, have no significant effect on their biological effectiveness, which in Arabidopsis thaliana within the range of energies considered depends only on the absorbed dose. (ERB)

**26027** STUDIES ON THE EFFECT OF GAMMA RAYS ON TRIGONELLA FOENUM-GRAECUM L. Raghuvanshi, S. S.; Singh, A. K. (Lucknow Univ. (India)). Cytologia (Tokyo); 39: No. 3, 473-482(Sep 1974).

Trigonella foenum-graecum is a legume used for fodder, vegetables, and green manuring while seeds are used as condiments. Different aspects of this species are under investigation in our laboratory for several years (Raghuvanshi and Joshi 1964, 1965 a, b, 1967, Raghuvanshi and Singh 1974). The paper presents the study of the effect of gamma radiation on this species. Dry seeds of Trigonella foenum-graecum were irradiated at 10 to 60 kR. Germination percentage, rate of growth, pollen fertility, and seed setting were investigated in $M_1$. Chromosomal aberration and chromosomal mosaicism were noted at 40 kR. Lethals, steriles, semisteriles, dwarfs, and some promising variants were isolated in $M_2$. (auth)

**26028** STUDIES ON VARIETAL DIFFERENCES OF RADIOSENSITIVITY IN SOYBEAN. Takagi, Y. (Institute of Radiation Breeding, Omiya, Ibaraki (Japan)). Hoshasen Ikushujo Kenkyu Hokoku; No. 3, 45-87(Mar 1974). (In Japanese).

Several hundreds of cultivated and wild soybean varieties were subjected to $\gamma$-ray irradiation, and their radiosensitivity in dormant seed irradiation was estimated. A wide range of radiosensitivity was found among the varieties, and some correlation between the radiosensitivity and some agronomic characters was observed. Difference of the radiosensitivity among the varieties exposed chronically to $\gamma$-field was observed, and it was found that cultivated varieties showed higher resistance to radiation than wild types in chronic irradiation, while the cultivated varieties showed more sensitivity than the wild types in seed irradiation. The $F_2$ plants of the hybrid between Tachisuzunari (radioresistant group) and Shinmejiro (radiosensitive group) were divided clearly into two groups, radioresistant and radiosensitives, by the ratio of 3:1. The $F_2$ populations of hybrid were also investigated on the frequency of generating the cells with chromosome bridge in the first mitosis of root tips after seed irradiation. Clear phenotypic segregation ratio of 3 (low frequency) to 1 (high frequency) was also recognized. Correlative investigation between radiosensitivity and flower color (white, purple, and violet) was carried out with 609 varieties throughout the experiment. The difference of radiosensitivity in soybean varieties was mostly controlled by a single gene pair $rs_t^+$ and $rs_t$. Goishishirobana (the type sensitive to seed irradiation) was crossed with Tachisuzunari and shinmejiro. All $F_1$ plants by the cross showed similar radiosensitivity to that of Tachisuzunari. In the $F_2$ generation of the hybrid between Goishishirobana and Tachisuzunari, radioresistant and radiosensitive plants appeared at the ratio of 3:1 only in seed irradiation, while in the $F_2$ generation of the hybrid between Goishishirobana and shinmejiro, four phenotypes of radiosensitivity, radioresistant in both seed and plant irradiation, radiosensitive in both irradiation, radiosensitive in seed irradiation and radioresistant in plant irradiation, and extremely sensitive regardless of irradiation method, were observed by the proportion of 9:3:3:1. (JA)

**26029** THEORETICAL CONSIDERATIONS ON THE PROBLEMS OF SCREENING OF MUTANTS, 1. Methods for Selection of a Mutant in the Presence of Chimera in $M_1$-Spikes. Ukai, Y.; Yamashita, A. (Institute of Radiation Breeding, Omiya, Ibaraki (Japan)). Hoshasen Ikushujo Kenkyu Hokoku; No. 3, 1-44(Mar 1974).

Following the mutagenic treatment of seeds or plants at a vegetative stage of self-pollinating crop plants, desirable mutants are usually selected in the second generation after the treatment on the basis of the lines, each of which is derived from a single spike or plant. In such situation, the number of plants per line is one of the most important factors determining the efficiency for the selection of mutants. By the use of an electronic computer, the number of plants per line, which minimizes the total number of $M_2$-plants required to screen a desirable mutant line under fixed probability, was determined with special reference to the chimeric structure of $M_1$-spikes. In case of an easily detectable type of mutant, the number of required total $M_2$-plants is at minimum when n = 1, and increases with the increase of

the number of plants per line irrespective of chimera size and segregation ratio. With the model for an indiscernible mutant, the number of plants per line minimizing the required total number of plants strikingly increases as the number of sectors increases and/or segregation ratio decreases. If the expenditure of land and labor required for raising $M_1$-plants is not negligible, the number of plants per line should be determined on the basis of the combination of the expenditure needed for raising both $M_1$-and $M_2$-populations. The number of plants per line minimizing required total plants depends on the number of sectors. The minimum total required expenditure decreases as the number of sectors increases. In contrast to generally believed thoughts, in most cases, the presence of sectors in $M_1$-spikes does not lead to disadvantage in the selection of a desirable mutant, whether the mutant is of easily detectable type or not. If the mutant aimed at is not an easily detectable one, and/or the expenditure needed for growing $M_1$-plants is negligible, the estimation of the number of sectors is essential to determine the most adequate number of plants per line. (JA)

**26030** VARIATIONS IN CHROMOSOMAL DAMAGE IN PLANTS AND ANIMALS. Pankova, N. V. (Laboratory of Experimental Cardiology, Moscow). Priroda; No. 4, 78-82 [nd]. (In Russian).

The exact character of chromosomal damage is of great importance to biologist-researchers, since it would reveal the mechanism of formation of the damage (which might, in turn, throw some light on the submicroscopic structural nature of the chromosome), and might also supply definite information on the radiation danger threatening all living things. M. A. Arsen'yevaya and G. G. Tinyakov in 1958 showed the high radiation sensitivity of monkey reproductive cells; their work was the basis of United Nation recommendations the following year. The author's work has concerned chromosomal changes observed at various stages of development, following the action of ionizing radiation and other agents. Root cells of Crepis capillaries and frog lymphocytes were taken as samples. Irradiation resulted in damage to the genetic elements, which varied strongly in its type (deletion, duplication, realignment) depending on the developmental stage ($G_0$, $G_1$, $G_2$, S). (JPRS)

**26031** PRELIMINARY STUDIES ON THE GENETIC AND BREEDING BEHAVIOR OF RADIATION INDUCED MACROMUTANTS IN BARLEY. Goswami, B. I. (Gauhati Univ., Italy). Curr. Sci. (India); 44: No. 17, 644-646(5 Sep 1975).

Dry barley seeds of cultivar $K_{12}$ were γ-irradiated at doses of 10, 15, 20, 25, or $30 \times 10^3$ R. The genetic characteristics and breeding behavior of the resultant mutants were determined. (ERB)

## Radiation Effects on Animals

**26032** (SAAS-176) STATE AND TENDENCIES OF CHEMICAL PROTECTION AGAINST IONIZING RADIATION. A Literature Survey, 1973. Siegel, G.; Tapp, E.; Haehn, J.; Hannig, H.; Diaske, R.; Scheefeld, E. (Staatliches Amt fuer Atomsicherheit und Strahlenschutz, Berlin (German Democratic Republic)). Apr 1975. 78p. (In German). Dep. NTIS (US Sales Only) $7.00.

Papers published in 1973 in the field of chemical protection against ionizing radiation are reviewed. Protection studies in vitro and in vivo, the biochemical, pharmacological, and toxic effects of radioprotective agents, the mechanisms of protective action, and the trends in this field of research are described. (auth)

### Man

*Refer also to abstracts 25915 and 27160.*

**26033** (DHEW/FDA-75-8024) GONAD SHIELDING IN DIAGNOSTIC RADIOLOGY. (Bureau of Radiological Health, Rockville, Md. (USA)). Jun 1975. 20p. GPO.

The importance of gonad shielding during diagnostic radiography for protection of patients against harmful effects of radiation is discussed. The value of training programs for medical personnel is stressed. (CH)

**26034** (NTIS/PS-75/173) RADIOLOGY, A Bibliography with Abstracts, Period Covered by Report, 1967-October 1974. (National Technical Information Service, Springfield, Va. (USA)). 1974. 143p. NTIS $25.00.

Research reports on the use of x rays and gamma rays in diagnostic and therapeutic procedures are cited. Data are included on radiation protection and population exposure. Current x-ray equipment and facilities are discussed. The bibliography contains 102 references and covers the period 1967 to October 1974. (auth)

**26035** (ORNL-TM-4781) EXAMPLE OF THE APPLICATION OF THE CUEX METHODOLOGY: THE CALCULATED EXPOSURE RESULTING FROM ROUTINE STACK RELEASES FROM THE HADDAM NECK NUCLEAR POWER PLANT. Sweeton, F. H. (Oak Ridge National Lab., Tenn. (USA)). Sep 1975. Contract W-7405-eng-26. 29p. Dep. NTIS $4.00.

The CUEX (Cumulative Exposure Index) relates the concentrations of various nuclides in the environment to assigned annual dose limits. A computer code has been written to calculate this index for stack releases of radioactivity. This report is written to illustrate how the code in its present form can be applied to a particular reactor. The data used here are from the Haddam Neck (Connecticut Yankee) Nuclear Power Plant, a relatively large plant that has been in operation for 6 years. The results show that the highest exposure expected from the actual releases of gaseous $^{85}Kr$, $^{133}Xe$, $^{131}I$, and $^{3}H$ is about 0.2 percent of the as low as practicable limits set by the Nuclear Regulatory Commission. Of the nuclides considered, $^{133}Xe$ is by far the most important; the chief mode of exposure to this nuclide is submersion in air. In the case of $^{131}I$ the main exposure route is external irradiation from the activity on the ground except for the special case of the thyroid for which about 70 percent of the exposure arises from ingestion. (auth)

**26036** FUNCTION AND METABOLISM OF IRRADIATED HUMAN PLATELETS. Basic Study for Radioprotection from Fatal Bleeding. Kuramoto, A.; Taketomi, Y.; Ihara, A.; Uchino, H. (Hiroshima Univ. (Japan). Research Inst. for Nuclear Medicine and Biology). Hirosaki Igaku; 27: No. 6, 527-535(Jun 1974). (In Japanese).

Aimed at examining morphologic changes and functional disturbances of the platelets irradiated, as a basic study of radioprotection from fatal bleeding, morphologic changes of the human platelets by irradiation to 1000 to 50,000 R of x-ray were examined under electron microscope with special reference to platelet aggregation. The ADP aggregation was well maintained, the SH base in the membrane was modified by the activated ATPase, and prostaglandin inhibited the aggregation of irradiated platelets. The morphologic changes observed were transfer of α granules to the periphery and increase of platelets, and lysosome enzyme activity was observed in the granules. Although the lipid peroxide production in platelet was increased, the serotonin uptake showed only a tendency to slight decrease. Thus, the energy metabolism of irradiated platelets, the glycolytic activity in particular, showed no abnormality. (JA)

**26037** RADIATION MYELOPATHY. Nagase, T.; Tanaka, Y.; Yoshioka, T.; Kan, S.; Watabe, T. (Keio Univ., Tokyo (Japan). School of Medicine). Rinsho Hoshasen; 19: No. 6, 451-462(Jun 1974). (In Japanese).

Of the patients with malignant tumor who had received radiation therapy for the past six years, 1966 to 1971, we experienced eight patients with radiation myelopathy as one of the side effects of radiation therapy. Of eight patients, two patients belonged to the transient type, and six patients to the chronic progressive type. The incidence was about 1.6%. The latent time from completion of the radiation therapy to the occurrence of this symptom ranged from 3 to 38 months with average of 14 months. Tumor doses were 6,000 to 12,000 rads. Irradiation was divided into 32 to 57 times. Assumed exposure doses to the spinal cord were 5,000 to 10,000 rads. The patients with transient type had paralysis in the terminal end of the extremities and Lehrmitte's sign. All patients with chronic progressive type had sensory and motor disturbance, of which four patients had Brown-Sequard symptom. In the patients with transient type, the symptoms naturally disappeared after 5 to 6 months. However, no recovery was observed in those with chronic progressive type. It is difficult to accurately diagnose radiation myelopathy. Therefore, in due consideration of the assumption that the spinal cord was irradiated, irradiation dose, over-all treatment time, number of fractions, symptoms, latent period, amount of protein in the spinal fluid laboratory findings, and myelography are decided as standards of diagnosis. There were many factors in radiation myelopathy. As supported by Boder and Pallis, there seemed to be a relationship between time and dose. In addition, when irradiation was done by the conventional method, it was considered that the tolerance dose was generally 4,000 to 5,000 rads or 1,400 to 1,500 rets, although there were individual differences. (JA)

**26038** INTRACAVITARY IRRADIATION OF EARLY RECTAL CANCER FOR CURE. A Series of 186 Cases. Papillon, J. (Univ., Lyon). Cancer, Suppl.; 36: No. 2, 696-701(Aug 1975).

From conference on advances in cancer management, Part I; New York, NY (25 Nov 1974).

If radical surgery is the only rational policy for most cases of rectal cancer, the problem of local treatment in poor surgical risk patients should be discussed in selected cases. Only limited,

fairly-well-differentiated tumors, still confined to the rectal wall may have a sufficiently low probability of lymphatic spread to be amenable to local treatment. Rectal cancer, usually regarded as being slightly radiosensitive when treated by external irradiation, proves to be highly radiosensitive in the case of early cancer treated by intracavitary irradiation. This method is able to control a large amount of limited polypoid and ulcerative adenocarcinomas. In a series of 133 cases followed more than 5 years, the rate of death from cancer is only 9 percent, and the 5-year survival rate is 78 percent. As compared with local excision or electrocoagulation, intracavitary irradiation has several advantages. It does not require colostomy nor anesthesia. Contact x-ray therapy is an ambulatory treatment applicable even to elderly and fragile patients. There is no danger of fistula in the case of tumor of the anterior wall in female patients. It preserves all the chances of cure by subsequent surgery in case of failure. (auth)

**26039** COMBINATION OF PERCUTANEOUS $^{60}$Co γ TELETHERAPY AND $^{32}$P ENDOLYMPHATIC THERAPY FOR THE TREATMENT OF SUPRADIAPHRAGMATICALLY LOCALIZED LYMPHOGRANULOMATOSIS. Strietzel, M.; Hennig, K. Radiobiol. Radiother.; 16: No. 2, 197-202(1975). (In German).

Endolymphatic therapy offers some convincing advantages from the radiotherapeutic aspect. The reliability of its effect, however, is connected with presuppositions which are frequently not fulfilled in the manifest supradiaphragmatical involvement in lymphogranulomatosis. Therefore, the only endolymphatic therapy of subdiaphragmatical lymph-node stations proves to be problematic. It should always be followed by an additional percutaneous $^{60}$cobalt irradiation. These experiences and earlier examinations of patients with Hodgkin's disease form the basis of a randomized study. They should clarify, whether endolymphatic therapy is suited to prevent craniocaudal spreading of lymphogranulomatosis and thus to improve the quote of success in the long run. All patients with supradiaphragmatically localized lymphogranulomatosis of stage I and II primarily receive a percutaneous $^{60}$cobalt teletherapy to all supradiaphragmatic lymphnodes with doses of at least 4000 R tumour dose. The patients with even-numbered year of birth were then exposed to an endolymphatic therapy (on the average 2.1 mCi $^{32}$P-tri-octyl-phosphate); those with odd-numbered year of birth form the collective for comparison. In the group without endolymphatic therapy $^{9}/_{18}$ (=50%) were free of recurrences, in the group with endolymphatic therapy $^{17}/_{25}$ (=68%) were free of recurrences. Supradiaphragmatic recurrences were observed in $^{4}/_{18}$ (=22%) and $^{8}/_{25}$ (=32%), respectively. Subdiaphragmatic recurrences occurred in $^{6}/_{18}$ (=33%) and $^{2}/_{25}$ (=8%), respectively. In view of questioning, the latter value is especially important as it can point to an effect of endolymphatic therapy. Totally $^{16}/_{18}$ (=89%) survived up to now after an average observation period of 34.4 months and $^{23}/_{25}$ (=92%), respectively, after 33.5 months. (auth)

**26040** NUCLEAR MEDICINE IN CLINICAL PEDIATRICS. Conference Held at San Francisco, California, February 16–17, 1973. Handmaker, H.; Lowenstein, J. M. (eds.). Acton, MA; Publishing Sciences Group, Inc. (1975). 307p. (CONF-730235-).

From symposium on nuclear medicine in pediatrics; San Francisco, California, USA (16 Feb 1973).

Separate abstracts were prepared for the 19 chapters. (CH)

*For abstracts of individual chapters see: 26095–26097 and 26125–26140.*

**26041** RADIATION SAFETY IN THE SOVIET UNION. Radiobiol. Radiother.; 16: No. 2, 235-240(1975). (In German).

The state system of radiation safety in the Soviet Union is described and a detailed characteristic is given of the valid sanitary standards, radioprotective regulations, and of the problems for the administration of institutions and works, for authorities, and scientific institutes. Based on their own observations and on literature about radiation doses to individual population groups and to the staff the authors conclude that at the present stage of development of the society the state system of radiation protection of the USSR guarantees a high safety for the whole population and its individual groups. Simultaneously the development of atomic industry and the peaceful use of radiation sources necessitate the further study of the following problems: further scientific establishment and legal sanction of standards regulating radiation doses to the staff working with ionizing radiation sources for different purposes; further elaboration of means for complex radiation protection of the workers and of the technical staff as well as precautionary measures for the protection of the population; further improvement of the individual protective means for the professionally radiation exposed persons; elaboration of a safe system of individual dosimetry of the staff; and study of influence of radiation effects of low intensity on the population by means of epidemiological methods of examination. (auth)

**26042** POSSIBILITIES TO DECREASE SKIN LESION IN STATIONARY-FIELD X-IRRADIATION BY ALTERING THE ACTUAL pH OF THE SKIN. Spies, H. (Univ., Greifswald, Ger.). Radiobiol. Radiother.; 16: No. 2, 161-164(1975). (In German).

Starting from the hitherto ineffective methods to decrease skin lesions in stationary-field x-ray deep therapy a new method is tested. By abolition of the acid film from the irradiated skin parts sensitivity can be considerably increased by thoroughly cleaning the irradiation fields with soap and water and thereafter drying them well 30 minutes before exposure. Five considerable advantages are obtained by this simple method: radiation response of the skin is decreased; daily radiation dose can be increased; stay in the clinic is reduced by one third; and improvement of subjective well-being. (auth)

**26043** CHANGES OF RADIOLOGICAL RESPONSE BY RADIATION THERAPY OF CANCER PATIENTS. Ghilezan, N. (Aus dem Onkologischen Institut, Cluj). Radiobiol. Radiother.; 16: No. 2, 142-151(1975). (In German).

The immunological, antitumor power of resistance with its two components, humoral and cellular immunity, is described. T-lymphocytes play the most important part in the determination of antitumor power of resistance. The problem of an undesired immunosuppressive effect of radiation therapy arises. The influence of radiation therapy on the immunological reactivity of organisms in the following situations is discussed: irradiation of primary tumours and of regional neoplastic lymph-nodes; prophylactic irradiation of regional lymph-nodes; and the unavoidable and undesired irradiation of the thymus the morphofunctional integrity of which being absolutely necessary for the recovery of the lymphoreticular system after radiation therapy. The antitumor effect of radiation therapy is incontestable. Certain conditions, however, are to be avoided: overdosage, combination with immunosuppressive therapeutics as to cytostatics, and steroid hormones. (auth)

**26044** OCCUPATIONAL SKIN CANCER: A REVIEW. Emmett, E. A. (Univ. of Cincinnati). J. Occup. Med.; 17: No. 1, 44-49(Jan 1975).

The following causes of skin cancer in industry are reviewed: ultraviolet radiation, polycyclic aromatic hydrocarbons, ionizing radiation, arsenic, trauma, heat, burns and chronic irritation. Measures for prevention of various types of carcinogenesis are discussed. (HLW)

**26045** SEARCH FOR RADIOPROTECTIVE AGENTS. XXVII. Synthesis of Some Trithiocarbonates. Tulecki, J.; Golus, B. (Inst. Of Chemistry and Analytics, Poznan, Poland). Pol. J. Pharmacol. Pharm.; 25: 259-261(1973).

The following novel trithiocarbonates were obtained in the reaction of exchange of potassium trithiocarbonate and appropriate halogenated compounds: di-(4-bromobenzyl)-, di-(4-cyanobenzyl)-, di-(1-carbethoxybenzimidazolyl-2-methyl-, and di-(1-carbmethoxybenzimidazolyl-2-methyl)-trithiocarbonates. The compounds will be tested for their radioprotective properties. (auth)

**26046** MODERN RADIOBIOLOGICAL ASPECTS OF TUMOR THERAPY. Hug, O. (Univ., Munich). Arch. Klin. Exp. Ohren-, Nasen- Kehlkopfheilkd.; 205: 37-48(1973). (In German).

On the basis of experimental data concerning the cytological effects of ionizing radiation the various repair and recovery processes are discussed on which the effectiveness of dose fractionation depends. The increasing knowledge of cell kinetics of normal and malignant tissues allows the interpretation of clinical experience on the fraction effect. Futhermore it may favour the development of tumorspecific and perhaps even individual schedules of treatment. (auth)

**26047** INCREASED CLINICALLY SYMPTOMATIC PULMONARY RADIATION REACTIONS WITH ADJUVANT CHEMOTHERAPY. Lamoureux, K. B. (National Cancer Inst., Bethesda, MD). Cancer Chemother. Rep.; 58: No. 5, 705-708 (1974).

It appears reasonable to warn those engaged in combination therapy involving radiation therapy and chemotherapy of the possibility of increased radiation reactions. With respect to radiation pneumonitis, this warning is not intended to discourage aggressive therapy. The institution of unnecessary or incorrect therapy and the possible discontinuation of effective chemotherapy should be prevented. Skin reaction to radiation is increased after numerous cycles of chemotherapy with the MOPP program as described by DeVita et al, although this has yet to be evaluated completely. These conclusions and the report by Byfield on the possible synergistic effect of vincristine and radiation therapy leading to radiation myelitis at a much lower dose than would be

expected, highly suggest that increased reactions be looked for in all organ systems that are irradiated during combination studies. With respect to a patient showing symptoms of chest pathology, including fever, severe cough, dyspnea, the possibility of acute symptomatic radiation pneumonitis should be considered in the differential diagnosis if the patient has recently received radiotherapy to the chest, especially if it was given after or coincident with chemotherapy. (auth)

## Vertebrates

*Refer also to abstracts 25914, 26008, 26009, and 26030.*

**26048** (AECL-5108, pp 75-88) HEREDITARY CHANGES AND TUMOUR INDUCTION IN VERTEBRATES AND METHODS FOR DERIVING HUMAN DATA ON DISEASES LIKELY TO BE INCREASED BY IRRADIATION. McGregor, J. F.; Smith, M. E. (Chalk River Nuclear Labs., Ont.). 1974.

In Biology and Health Physics Division progress report, October 1 to December 31, 1974. (Atomic Energy of Canada Ltd., Chalk River, Ontario. Chalk River Nuclear Labs.).

Preliminary results are reported from studies on rats to determine whether exposure to $\beta$ radiation at doses from 1,600 to 12,800 rads in combination with cigarette tar or 2-anthramine results in a yield of skin tumors substantially greater than the sum of the yields expected for the two agents separately. Methods used for the compilation of data on human populations for use in a long-term epidemiological study on the possible genetic and carcinogenic effects of medical exposures to radiation are presented. Computer methods used for the linkage of vital and health records with individual and family histories to be used for studies relating to the prevention, etiology, and treatment of ill-health are discussed. (CH)

**26049** (ERDA-tr-38) RADIOBIOLOGY, VOL. 15, NO. 1, 1975. Translation of Radiobiologiya; 15: No. 1, 3-168(1975). 212p. Dep. NTIS $7.60.

Separate abstracts were prepared for each of the 38 papers presented in this issue. (ERB)

*For abstracts of individual papers see: 26006-26010, 26014, 26015, 26025, 26026, 26050-26076, 26091, and 26102.*

**26050** (ERDA-tr-38, pp 10-17) RECOVERY OF DNA IN MAMMALIAN CELLS IN LONG-TERM PERIODS AFTER IRRADIATION. Laneeva, N. I.; Sverdlov, A. G. (Leningrad Inst. of Nuclear Physics). Jul 1975. Translated from Radiobiologiya; 15: No. 1, 10-15(1975).

In Radiobiology.

It was shown that for a period of two days after irradiation of rats at a dose of 900 R there is a sharp decrease in the intrinsic viscosity and rate of sedimentation of the nuclear DNA of the spleens of the irradiated animals. On the third and fourth days after irradiation, the polymerization of the nuclear DNA is restored to a substantial degree. In experiments with labeled precursors $^{14}$C-formate and 2$^{14}$C-thymidine, it was shown that the restoration of the polymerization occurs under conditions of profound suppression of the basic synthesis of DNA. (tr-auth)

**26051** (ERDA-tr-38, pp 18-23) RADIORESISTANCE OF MAMMALS AND THE REACTIONS OF DEAMINATION OF CERTAIN NITROGEN COMPOUNDS. Zeinalov, T. A.; Kulygina, A. A.; Ryazanov, V. M.; Kudryashov, Yu. B.; Gorkin, V. Z. (Inst. of Biological and Medical Chemistry, Moscow). Jul 1975. Translated from Radiobiologiya; 15: No. 1, 16-20(1975).

In Radiobiology.

Disturbances in the reactions of deamination of nitrogen bases in the mitochondrial fractions of the liver and small intestine have already been noted 2 h after irradiation of white rats or mice with X rays at a dose of 700 rad and guinea pigs at a dose of 300 rad. The irradiation of Mongolian gerbils at a dose of 1500 rad does not cause the appearance either of histamine deaminase or of adenylate deaminase activity. Increasing the radioresistance of the animals as a result of feeding the animals the assortment of grasses comprising the fodder of Mongolian gerbils or administering aminoethylisothiuronium prevents the development of the disturbances of deamination reactions characteristic of radiation sickness in the mitochondrial fractions of the liver and small intestine. (tr-auth)

**26052** (ERDA-tr-38, pp 47-54) INHIBITION OF THE TRANSPORT OF PHOSPHOLIPIDS AMONG THE ORGANELLES OF LIVER CELLS OF IRRADIATED RATS. Kaznacheev, Yu. S.; Kolomiitseva, I. K. (Inst. of Biological Physics, Pushchino, USSR). Jul 1975. Translated from Radiobiologiya; 15: No. 1, 37-41(1975).

In Radiobiology.

The exchange of phosphatidylcholine (PC) and phosphatidylethanolamine (PET) among various subcellular fractions of the liver in the normal state and 1 hr after the irradiation of rats at a dose of 1200 R was investigated. It was shown that the rate of transport of PC is 1.5 to 2 times as high as the rate of transport of PET in the systems microsomes-mitochondria and microsomes-nuclei. In the early periods after irradiation, the rate of transport for PC and PET in the systems microsome-mitochondria and microsomes-nuclei decreases. (tr-auth)

**26053** (ERDA-tr-38, pp 55-60) EFFECTS OF THREE AND FIVE REPEATED EXPOSURES TO SMALL DOSES OF X RAYS ON THE CARBOHYDRATE-ENERGY METABOLISM OF THE BRAIN. Mironova, T. M.; Cherkasova, L. S.; Fomichenko, V. G. (Inst. of Physiology, Minsk). Jul 1975. Translated from Radiobiologiya; 15: No. 1, 42-45(1975).

In Radiobiology.

The rats were subjected to three whole-body X irradiations at intervals of two and three days at a summary dose of 40 R and five irradiations at three-day intervals at a summary dose of 50 R. During the first day after the end of the third irradiation, an increase in the biologically active complex of glycogen with proteins, a decrease in G-1-P, and an increase in creative phosphate were detected in the cerebrum; after the end of the fifth irradiation the changes were insignificant, although the corticosterone level in the blood was elevated in both cases. The discoordination of the processes of the initial stage of glycogenolysis was detected on the 9th to 15th days after the end of the fifth irradiation, against a background of a decrease in the level of corticosterone in the blood. A tendency for a restoration of metabolism was observed in the presence of a normal level of the hormone. The glycogen-lipid complex evidently plays an adaptive role. (tr-auth)

**26054** (ERDA-tr-38, pp 61-67) EFFECTIVENESS OF HIGH-POLYMER DNA UNDER CONDITIONS OF COMPLEX THERAPY OF ACUTE RADIATION SICKNESS. Ivannik, B. P.; Dorofeev, V. M.; Murzaev, V. I.; Ryabchenko, N. I. (Scientific Research Inst. of Medical Radiology, Obninsk, USSR). Jul 1975. Translated from Radiobiologiya; 15: No. 1, 46-50(1975).

In Radiobiology.

Rats of the Wistar line were irradiated with the gamma rays of $^{60}$Co at a dose of 750 R, dose rate 2500 R/min. After 30 days the survival of the irradiated animals was 3.4 per cent. The intraperitoneal injection of thymus DNA (3 mg/100 g of weight) 24 hrs after irradiation increased the survival of the animals to 21.3 per cent. Treatment of the irradiated animals with antibiotics (I), vitamins (II), and amino acids (III), conducted from the fourth to the 20th day, increased the survival to 55.5 per cent. The administration of DNA 24 hrs after irradiation, together with treatment with I, II, and III, conducted from the fourth to the 20th day, increased the survival of the irradiated animals to 89.9 per cent. (tr-auth)

**26055** (ERDA-tr-38, pp 76-81) INFLUENCE OF HUMORAL FACTORS FROM THE CALF THYMUS ON THE IMMUNOLOGICAL STATUS AND PROCESSES OF HEMATOGENESIS OF THE IRRADIATED ORGANISM. Communication 3. Influence of the Factor from the Thymus (FT-3) on the Postradiation Restoration of Hemopoiesis. Skobel'tsyna, E. S.; Kendysh, I. N.; Grinberg, S. M.; Samuleva, S. V. (Kharkov Inst. of Medical Radiology). Jul 1975. Translated from Radiobiologiya; 15: No. 1, 57-61 (1975).

In Radiobiology.

It was shown that the factor from the thymus FT-3 promotes a more rapid restoration of hematogenesis in rats irradiated at a dose of 650 R, determined according to the number of leukocytes in the peripheral blood and the number of myelokaryocytes in the femur. FT-3 promotes a restoration of the weight of the thymus and does not influence the restoration of the weight of the spleen. (tr-auth)

**26056** (ERDA-tr-38, pp 82-86) EFFECTS OF IONIZING RADIATION ON THE ACTIVE TRANSPORT OF SODIUM IN MULTICELLULAR BIOLOGICAL MEMBRANES. Communication 2. Radiation Changes in the Properties of the Basal and Apical Membranes of Epithelial Cells of Frog Skin. Nadareishvili, K. Sh.; Sanaya, T. V.; Sandodze, V. Ya.; Tevdoradze, V. V. (Inst. of Physiology, Tbilisi, USSR). Jul 1975. Translated From Radiobiologiya; 15: No. 1, 62-65(1975).

In Radiobiology.

The constants of the permeability of the membranes of the epithelial cells of frog skin after irradiation were determined in the work. It was found that irradiation at a dose of 300 kR sharply inhibits the selectivity of the apical membranes with respect to $Na^+$ ions and intensifies the work of the mechanism of active transport of $Na^+$ in the basal membrane. It is suggested that the passive sodium channels in the apical and basal membranes of epithelial cells are expanded immediately after irradiation, while

the intensification of the work of the sodium pump is a compensatory response, the mechanism of which will require special investigation. (tr-auth)

**26057** (ERDA-tr-38, pp 87-90) EARLY APPEARANCE OF TISSUE ANTIGENS IN THE BLOOD SERUM OF IRRADIATED ANIMALS. Nevinnaya, A. P.; Klemparskaya, N. N.; Ivanov, A. A. Jul 1975. Translated from Radiobiologiya; 15: No. 1, 66-68 (1975).

In Radiobiology.

The appearance of tissue antigens during the first hour and day after irradiation was noted in the blood serum of animals (rats and rabbits) irradiated at lethal and sublethal doses of gamma rays. (tr-auth)

**26058** (ERDA-tr-38, pp 91-95) MODIFICATION OF THE RADIOPROTECTIVE ACTION OF HYPOXIC HYPOXIA BY ARTIFICIAL HIBERNATION OF THE ORGANISM. Ovakimov, V. G.; Yarmonenko, S. P. (Inst. of Labor Hygiene and Occupational Diseases, Moscow). Jul 1975. Translated from Radiobiologiya; 15: No. 1, 69-73 (1975).

In Radiobiology.

In a study of the radioprotective effect of hypoxic hypoxia under conditions of resistance of the organism to the action of an acute oxygen deficiency artificially created by means of hibernation (hypothermia under conditions of neuroplegia), data were obtained on a substantial weakening of the radioprotective effect of hypoxic hypoxia in hibernated mice. The dose reduction factor for hypoxic hypoxia in hibernated animals is equal to approximately 1.27, and for the nonhibernated animals equal to approximately 2.5. (tr-auth)

**26059** (ERDA-tr-38, pp 96-101) CHEMICAL PROTECTION OF MICE FROM THE REPEATED ACTION OF NEUTRON RADIATION. Kavukchyan, T. V.; Sverdlov, A. G. (Leningrad Inst. of Nuclear Physics). Jul 1975. Translated from Radiobiologiya; 15: No. 1, 74-78 (1975).

In Radiobiology.

The radioprotective action of chemical compounds in the case of repeated neutron-irradiation of mice at a dose of 100 rad x 3 at two and four-day intervals between influences was investigated. With such a system of irradiation, a higher survival and effectiveness of chemical protection (cystaphos 44.8 percent, cystamine 32 percent, mexamine 21 percent) were observed than in the case of a single influence at the same dose, which is associated with recovery processes in the critical organs--the intestines and bone marrow. (tr-auth)

**26060** (ERDA-tr-38, pp 102-107) RADIOPROTECTIVE EFFECTIVENESS OF CYSTAPHOS IN THE CASE OF INTRAGASTRIC ADMINISTRATION IN EXPERIMENTS ON MONKEYS. Znamenskii, V. V.; Zherebchenko, P. G.; Terekhov, A. V.; Dikovenko, E. A.; Zeitunyan, K. A.; Semenov, L. F. (Inst. of Biophysics, Moscow). Jul 1975. Translated from Radiobiologiya; 15: No. 1, 79-82 (1975).

In Radiobiology.

The work was devoted to a study of the radioprotective effectiveness of cystaphos in the case of intragastric administration at various doses in experiments on monkeys. It was shown that this sulfur-containing radioprotector exhibits a pronounced radioprotective effect both with respect to survival of the animals and with respect to degree of protection of the organs of hematogenesis. (tr-auth)

**26061** (ERDA-tr-38, pp 114-118) NEUROPHYSIOLOGICAL ANALYSIS OF THE CONSEQUENCES OF EARLY POSTNATAL IRRADIATION OF RATS. Airapetyants, M. G.; Kolomeitseva, I. A. (Journal of Higher Nervous Activity and Neurophysiology, Moscow). Jul 1975. Translated from Radiobiologiya; 15: No. 1, 89-92 (1975).

In Radiobiology.

In sexually mature rats, irradiated on the first to second day of postnatal life, a predominance of synchronized rhythms in the background EEG and an intensification of the responses of the visual cortex to the action of a light stimulus were established. Against a background of hypersynchronized rhythms, the appearance of conditioned reflex responses is reduced. The results of special tests are evidence not so much of a defect of the formation of motor conditioned reflexes in the irradiated animals as of a difficulty of their implementation against a background of the intensified synchronization of the EEG. (tr-auth)

**26062** (ERDA-tr-38, pp 119-123) ANALYSIS OF THE STATE AND REACTIVE PROPERTIES OF THE CHOLINERGIC SYSTEM OF REGULATION UNDER CONDITIONS OF TOTAL BODY AND LOCAL (HEAD, BODY) IRRADIATION OF RATS. Nuzhyni, V. P. (First Moscow Medical Inst.). Jul 1975. Translated from Radiobiologiya; 15: No. 1, 93-97 (1975).

In Radiobiology.

It was shown that the increase in the cholinergic activity of the tissues of the heart and the diencephalic region of the brain of rats subjected to whole-body irradiation at a dose of 350 rad is due to irradiation of the body of the animals. The sensitivity of the cholinoreceptors of the rat heart is increased in the case of all variations of irradiation, becoming most pronounced in the case of total-body irradiation and irradiation of the head of the animals. (tr-auth)

**26063** (ERDA-tr-38, pp 139-142) INFLUENCE OF RADIATION ON THE SYNTHESIS OF CATALASE BY THE RAT LIVER. Komov, V. P.; Strelkova, M. A. (Chenmicopharmaceutical Inst., Leningrad). Jul 1975. Translated from Radiobiologiya; 15: No. 1, 111-113 (1975).

In Radiobiology.

The effect of whole-body x irradiation on the rate of synthesis of rat liver catalase was studied. It was found that as a result of the irradiation of rats at a dose of 800 rad, within the interval from 22 to 144 hours of the course of radiation sickness, the accelerated rate of catalase synthesis in the liver was reduced 2.6-fold in comparison with the controls. (ERB)

**26064** (ERDA-tr-38, pp 143-146) PECULIARITIES OF RADIOSENSITIVITY ASSOCIATED WITH SEX. Communication 4. Effects of Ionizing Radiation on the Sexual Cycles of Female Mice and Guinea Pigs. Alekseeva, L. V.; Kudryavtseva, A. A. (Inst. of Biological Physics, Pushchino, USSR). Jul 1975. Translated from Radiobiologiya; 15: No. 1, 114-117 (1975).

In Radiobiology.

The changes in the sexual cycles of female mice and guinea pigs under the influence of gamma radiation were studied. Irradiation at doses of 500 to 750 R resulted in disturbances of the sexual cycles as early as 1 hour after irradiation. No restoration of the cycles was noted for a period of two months or more. (ERB)

**26065** (ERDA-tr-38, pp 147-150) CONTENT OF COENZYME A AND ACTIVITY OF DEHYDROGENASES IN THE CASE OF PROLONGED X IRRADIATION IN SMALL DOSES. Cherkasova, L. S.; Novik, V. A.; Tsykhun, G. F. (Inst. of Physiology, Minsk). Jul 1975. Translated from Radiobiologiya; 15: No. 1, 117-120 (1975).

In Radiobiology.

The influence of chronic x irradiation on the content of coenzyme A in the brain and liver, the activity of a number of redox enzymes of the mitochondria of the brain and cardiac muscle, and the content of glucocorticoids in the blood was studied using sexually mature Wistar white rats. The substantial stability of the Co A metabolism of the brain and liver under conditions of chronic x irradiation was noted, on the other hand, the pronounced lability of the enzymes of the tricarboxylic acid cycle and the pyruvate dehydrogenase of the brain was noted. The cardiac muscle and liver were more radioresistant to the chronic influence of ionizing radiation at low doses. The changes noted in the corticosterone content of the peripheral blood are evidence of the inclusion of the hypothalamo-pituitary-adrenal system in the response to the action of chronic irradiation with small doses, one of the possible mechanisms of compensation. (ERB)

**26066** (ERDA-tr-38, pp 151-155) STUDY OF THE ACTIVITY OF CERTAIN ENZYMES OF THE GASTROINTESTINAL TRACT AND THEIR INHIBITORS IN THE CASE OF RADIATION LESION AND THE ACTION OF THIOPHOSPHAMIDE. Savitskii, I. V.; Karpovich, G. A. (Odessa Medical Inst.). Jul 1975. Translated from Radiobiologiya; 15: No. 1, 120-124 (1975).

In Radiobiology.

The activity of trypsin and pepsin and their inhibitors at various stages of development of the radiation effect and under the influence of the radiomimetic thiophosphamide was studied in whole-body x-irradiated (600 R) rats. It was found that pepsin activity in the stomach and blood serum decreases in the early periods following irradiation followed by a substantial increase. Thiophosphamide did not produce a significant change in the activity at any time following treatment. One of the causes of the late rise in pepsin activity following irradiation could be a change in the blood level of pepsin inhibitor. A sharp rise in the activity of trypsin in the pancreas is noted following both irradiation and thiophosphamide treatment. Simultaneous with this, a rise in the level of the trypsin inhibitor in the blood serum is observed. (ERB)

**26067** (ERDA-tr-38, pp 156-158) CHANGES IN THE ACTIVITY OF BLOOD CARBOANHYDRASE AFTER THE INFLUENCE OF INCREASED OXYGEN PRESSURE ON THE IRRADIATED ORGANISM. Ivanov, K. V.; Dmitriev, A. I. Jul 1975. Translated from Radiobiologiya; 15: No. 1, 124-127 (1975).

In Radiobiology.

The variation of the activity of blood carboanhydrase was studied in rabbits that were placed under conditions of increased oxygen pressure directly after x irradiation (1000 R). In the control animals (irradiation only), a decrease in the carboanhydrase

activity was observed in the early period of the primary response to irradiation, followed by a slight increase in activity, while at the height of the radiation response, a sharp decrease was noted. The effects of breathing oxygen under increased pressure following irradiation were to increase and prolong the indicated responses. (ERB)

**26068** (ERDA-tr-38, pp 159-161) RADIOIMMUNOLOGICAL STUDY OF THE SECRETION OF INSULIN DURING ACUTE RADIATION SICKNESS. Barkalaya, A. I. Jul 1975. Translated from Radiobiologiya; 15: No. 1, 127-129(1975).

In Radiobiology.

The secretory activity of the insular apparatus during acute radiation sickness was studied by a radioimmunological method. The rats received whole-body acute gamma irradiation (750 R; 310 to 281 R/min) and the insulin content of the plasma assayed by radioimmunoassay using $^{125}I$. The results obtained indicate that the postradiation dynamics of the insulin content of the blood are of a phase nature. It is entirely possible that the fluctuations of insulin secretion noted are associated to a definite degree with the phase activity of the adrenals and repeated glycemic reactions of the irradiated organism. (ERB)

**26069** (ERDA-tr-38, pp 162-166) TISSUE CATECHOLAMINES AND RADIOSENSITIVITY OF RODENTS. Graevskaya, B. M.; Zolotareva, N. N. (Inst. of the Evolutionary Morphology and Ecology of Animals, Moscow). Jul 1975. Translated from Radiobiologiya; 15: No. 1, 129-132(1975).

In Radiobiology.

A comparison is made of the radiosensitivity of rodents of different species and mice of different lives with the content of catecholamines in certain tissues and biological fluids. The organisms used included moles, rats, mice, golden hamsters, and guinea pigs. Catecholamine content was determined in adrenals, spleen, liver, blood, and urine. Radiosensitivity was estimated according to the 30-day mortality after a single whole-body x irradiation. The data presented permit the conclusion that an extremely satisfactory correlation is observed between the radiosensitivity of rodents of different species and lives, on the one hand, and the content of adrenaline and noradrenaline in their tissues and biological fluids, on the other. It is direct for the catecholamine content in the adrenals, urine, and blood and universe for the relative content of adrenaline and noradrenaline in the tissues of the spleen and liver; for adrenaline it is somewhat more pronounced than for noradrenaline. (ERB)

**26070** (ERDA-tr-38, pp 167-170) CONTENT OF BETA-MERCAPTOETHYLAMINE IN THE TISSUES OF MICE IN THE CASE OF JOINT USE OF CYSTAMINE AND 5-METHOXYTRYPTAMINE. Mordukhovich, V. V. (Military-Medical Academy, Leningrad). Jul 1975. Translated from Radiobiologiya; 15: No. 1, 132-136(1975).

In Radiobiology.

Data are cited on the content of MEA in the tissues of mice following the administration of cystamine alone and in combination with 5-methoxytryptamine (5-MOT). The data were obtained using the method of isotopic dilution ($^{35}S$). It was found that in the long-term period (2 to 3 hours) following the administration of both protectors, in all the investigated tissues a sharp increase in the concentration of MEA was detected in comparison with the values detected after the use of cystamine alone. (ERB)

**26071** (ERDA-tr-38, pp 171-175) INFLUENCE OF 6-METHYLTHIOURACIL ON THE MORPHOLOGICAL AND HISTOCHEMICAL CHANGES IN THE TISSUES OF THE LIVER AND SPLEEN OF IRRADIATED ANIMALS. Smirnov, G. P. (Orenburg Medical Inst., USSR). Jul 1975. Translated from Radiobiologiya; 15: No. 1, 136-140(1975).

In Radiobiology.

In order to determine the mechanism of the radioprotective action of 6-methylthiouracil (6-MTU), the structural and biochemical changes in the liver and spleen of x-irradiated rats were investigated. From the results obtained, it can be assumed that one of the leading factors in the mechanism of the protective effect of 6-MTU is the early tissue dystrophy of the liver and spleen of the animals. The destruction of the tissues in turn promotes the formation and accumulation of factors stimulating the regeneration of hematogenic and other tissues of the irradiated organism. (ERB)

**26072** (ERDA-tr-38, pp 176-179) TRANSKETOLASE ACTIVITY OF THE BRAIN, LIVER, AND SPLEEN DURING RADIATION SICKNESS. Sokolov, I. I.; Kuksin, E. M. (Dnepropetrovsk State Univ., USSR). Jul 1975. Translated from Radiobiologiya; 15: No. 1, 140-142(1975).

In Radiobiology.

The influence of lethal doses of x radiation on the transketolase activity in the brain, liver, and spleen of rats during the dynamics of the development of radiation sickness was investigated. At the height of radiation sickness, the transketolase activity in the brain, liver, and spleen increased 102.8, 87.7, and 156.7 percent respectively. (ERB)

**26073** (ERDA-tr-38, pp 180-182) FREE RADICAL STATES OF THE ORGANS AND TISSUES OF WHITE RATS AFTER THE INFLUENCE OF FAST NEUTRONS AND THE ADMINISTRATION OF 1-p-CHLOROPHENYLTETRAZOLE-2-THIONE. Chebotarev, E. E.; Kulyabko, P. N.; Kuz'menko, V. A.; Fedorchenko, V. I. (Inst. of Molecular Biology and Genetics, Kiev). Jul 1975. Translated from Radiobiologiya; 15: No. 1, 143-145(1975).

In Radiobiology.

The influence of 1-p-chlorophenyltetrazole-2-thione, which exhibits a strong radioprotective action, on the level of free radicals in the tissues of rats following neutron irradiation was investigated and the results compared to previous results for x-irradiated rats. Tissues of the brain, heart, lungs, liver, spleen, kidneys, muscles, and blood were extracted and analyzed by electron spin resonance. A decrease in the free radical activity in almost all of the tissues was observed not only at 0.5 and 3 hours, but also at 24 hours following irradiation and administration of the radioprotector. Free radical activity in the brain tissues differed somewhat from that of the other tissues. The absence of normalization of the level of free radical after the administration 1-p-chlorophenyltetrazole-2-thione to the animals before irradiation with fast neutrons is evidence that the neutrons probably more profoundly damage the metabolic processes, which cannot be normalized by chemoprotectors. (ERB)

**26074** (ERDA-tr-38, pp 186-190) INFLUENCE OF THYMIDINE ON THE FREQUENCY OF PATHOLOGICAL PROCESS IN THE LONG-TERM PERIODS AFTER IRRADIATION OF RATS. Bukhtoyarova, Z. M. Jul 1975. Translated from Radiobiologiya; 15: No. 1, 148-151(1975).

In Radiobiology.

The effects of thymidine, one of the basic precursors of DNA, on the survival of gamma-irradiated rats and on the frequency of the appearance of pathological changes in the irradiated animals. It was found that the administration of thymidine one day after irradiation at a dose of 450R did not change the average lifetime of the animals, nor were any differences noted either in the total number of rats with tumors or in the frequency of osteosarcomas and soft-tissue tumors. The absence of a therapeutic effect following the administration of thymidine at the optimum time, when recovery begins and when the administration of DNA has a clear therapeutic effect, is evidence that the molecular mechanism of the repair of radiation damages with the aid of DNA is rather complex and cannot be explained by any single mechanism. (ERB)

**26075** (ERDA-tr-38, pp 191-193) COMPARATIVE EVALUATION OF THE RADIOVULNERABILITY OF THE INTESTINE IN LABORATORY ANIMALS WITH VARIOUS RADIOSENSITIVITIES. Fedotova, M. I.; Belousova, O. I. Jul 1975. Translated from Radiobiologiya; 15: No. 1, 151-154(1975).

In Radiobiology.

The change in the number of cells in the duodenum of rats, guinea pigs, and rabbits, exhibiting dose and time differences in the development of the gastrointestinal syndrome was studied. The intestinal devastation developed most rapidly and substantially in rats and more slowly and to a lesser degree in rabbits and especially in guinea pigs. However, the subsequent recovery processes occurred more rapidly in rats. (ERB)

**26076** (ERDA-tr-38, pp 194-198) RADIOPROTECTIVE ACTION OF CYSTAPHOS IN THE IRRADIATION OF MICE AT VARIOUS PERIODS OF POSTNATAL DEVELOPMENT. Timoshenko, S. I.; Bogatyrev, A. V. (Inst. of Nuclear Physics, Leningrad). Jul 1975. Translated from Radiobiologiya; 15: No. 1, 154-158(1975).

In Radiobiology.

Variations in the radioprotective action of cystaphos during the process of postnatal development were studied and the factors that influence the expression of the radioprotective properties of the preparation were determined. The mice were x-irradiated at either one week, two weeks, three weeks, four weeks, or sexually mature stages of development at doses of 300 to 1000R at 100R intervals. The data obtained show that in all of the age periods cystaphos distinctly protects the animals at doses of radiation producing damage to both the hematogenic system and the gastrointestinal tract. However, the physiological state of the critical system, especially the gastrointestinal tract (in four-week-old mice) is of vital significance in the manifestation of the protective action of cystaphos. (ERB)

**26077** (GSF-K-56(3.ed.)) ACUTE AND CHRONIC RADIATION SYNDROME IN DOMESTIC ANIMALS. Nuessel, M. (Ges-

ellschaft fuer Strahlen- und Umweltforschung m. b. H., Neuherberg/Muenchen (F. R. Germany). Inst. fuer Strahlenschutz). Nov 1974. 47p. (In German). INIS.

13 figs.; 3 tabs.; 41 refs.

The paper reports on the incidence and the clinical picture of the radiation syndrome in domestic animals, especially in pigs which are often used in animal experiments. The following parameters which influence the radiation reaction are discussed: type of irradiation (whole-body, partial-body and local irradiation), mean lethal radiation dose, radiation quality and RBE, age, and individual radiosensitivity. The various symptoms of the radiation syndrome and the lesions which lead to death (death due to intestinal lesions, death following changes in the central nervous system) are described. The symptoms manifested after chronic and internal irradiation are discussed. The paper closes with some remarks on the usability of irradiated animals for human consumption. (GE)

**26078** (NP-20566) REPORT ON THE INADEQUACY OF EXISTING RADIATION PROTECTION STANDARDS RELATED TO INTERNAL EXPOSURE OF MAN TO INSOLUBLE PARTICLES OF PLUTONIUM AND OTHER ALPHA-EMITTING HOT PARTICLES. Dolphin, G. W. (National Radiological Protection Board, Harwell (UK)). 14 Feb 1974. 3p. Dep. NTIS (US Sales Only) $4.00.

Data are summarized from a number of studies on the induction of neoplasms in experimental animals following exposure to various doses of internal or external ionizing radiations. Data on the incidence of skin cancers in human patients following exposure to therapeutic doses of x radiation are included. It is pointed out that no cases of human cancer associated with exposure to insoluble particles or soluble compounds of Pu have been documented. (CH)

**26079** EXPERIMENTAL STUDIES OF FACTORS INFLUENCE LUNG COLONY FORMATION. Tanaka, Y. (Tenri Hospital, Nara (Japan)). Nippon Igaku Hoshasen Gakkai Zasshi; 34: No. 10, 769-774(Oct 1974). (In Japanese).

El-LP-12 cells (Lung passaged subline of Ehrlich carcinoma) injected intravenously into dd Y mice result in the formation of visible lung colonies which are introduced as a model for pulmonary metastases. Various factors affecting lung metastases such as anticoagulant, HR cells and localized irradiation of the lungs prior to cell injection were examined and the following results were obtained. The relationship between the number of tumor nodules injected was found to be linear from $1 \times 10^6$ to $4 \times 10^6$ cells. Administration of heparin or dextran sulfate prior to the intravenous injection resulted in a significant decrease in pulmonary metastases. The number of lung colonies observed has been found to be affected by the simultaneous intravenous injection of a large number of heavily-irradiated cells (HR cells). Localized irradiation prior to tumor cell inoculation significantly increased the incidence of pulmonary metastases in the irradiated lungs only. From the study of vascular permeability of the lung, dilatation of capillaries or increased permeability may be one of the main mechanisms of this phenomenon. (auth)

**26080** MODIFICATION OF RADIATION EFFECT BY SHOWDOMYCIN ON HAIR ROOTS OF THE MOUSE. Egawa, J.; Ishioka, K. (Teikyo Univ., Tokyo (Japan). Faculty of Medicine). Nippon Igaku Hoshasen Gakkai Zasshi; 34: No. 10, 763-768(Oct 1974). (In Japanese).

Radiosensitizing effect of Showdomycin on Escherichia coli B/r in aerated and anoxic conditions was reported by Y. Titani. This report concerns experimental results of modification of radiation effect on hair roots of the mouse by Showdomycin. The mouse skin was irradiated by 29 KVp x-ray 8 days after initial plucking. Irradiation of growing hair results in the damage of hair bulb, thus dysplastic hair is produced. The incidence of dysplastic hair is related to radiation dose. Six administrations of 300 μg of Showdomycin intraperitoneally during 3 days or 6 days combined with the irradiation of 500 R x rays results in approximately 50% increase in the incidence of dysplastic hair. The influence of the time interval between the last administration of Showdomycin and irradiation on the incidence of dysplastic hair was studied. There is no difference in the results from 2 to 6 hours of administration time before irradiation. Further study in the mechanism of radiosensitizing effect seems to be valuable. (auth)

**26081** PHARMACOLOGICAL STUDIES ON CHEMICAL PROTECTORS AGAINST RADIATION, 13. Influence of X-Irradiation on Various Organ Weights of Mouse and Effect of Radioprotective Substances. Shinoda, M.; Ohta, S.; Chiba, C. (Hoshi Coll. of Pharmacy, Tokyo (Japan)); Takagi, Y.; Akaboshi, S. Yakugaku Zasshi; 94: No. 10, 1206-1211(Oct 1974). (In Japanese).

X irradiation of mice in the range of 50 to 600 R results in rapid decrease in weight of the spleen and thymus until 3 days after the irradiation but the weight recovers thereafter. Testis weight decreases gradually from about 7 days after the irradiation and this decrease continues for about 30 days. This decrease in organ weight is in significant linear correlation with the irradiated dose. There was no specific irradiation on the seminal vesicle, submaxillary gland, and kidneys. S-2-aminoethylisothiuronium-Br-HBr, 2-mercaptoethylamine-HCl, serotonin, epinephrine, and ethylisothiourea were ineffective against the specific decrease in the weight of the spleen, thymus, and testis by 400 R x-ray irradiation. (auth)

**26082** RECOVERY OF THE B-CELL POPULATION IN ADULT THYMECTOMIZED, LETHALLY-IRRADIATED AND BONE MARROW-RECONSTITUTED MICE. van Muiswinkel, W. B.; van Beek, J. J.; van Soest, P. L. (Erasmus Univ., Rotterdam). Immunology; 29: No. 2, 327-336(Aug 1975).

The recovery of the B-cell population in adult thymectomized, irradiated, and bone marrow-reconstituted mice (T × BM mice) was studied. The number of B cells in the spleen of T × BM mice was estimated at various times after bone marrow transplantation. The spleen cells to be tested were mixed with dexamethasone-resistant thymocytes (DRT) and sheep red blood cells (SRBC) and transferred to irradiated recipients. The number of plaque-forming cells (PFC) in the spleen of the recipients was determined 7 days later. Using this functional B-cell assay a sequential appearance of the precursors of IgM-, IgG-, and IgA-PFC in the spleen of T × BM mice was observed. The precursors of IgM-PFC (IgM-B cells) were present immediately after transplantation. The first IgG-B cells could be detected at 13 to 16 days after transplantation and the IgA-B cells finally appeared at 22 days after transplantation. The number of B cells reached a constant and normal level at 30 days after transplantation. The IgM-, IgG-, and IgA-B cell development in sham-thymectomized irradiated and bone marrow-reconstituted mice (ST × BM mice) was virtually the same as in T × BM mice. (auth)

**26083** CHANGE IN THE ANTI-OXIDATIVE ACTIVITY OF MOUSE LIVER LIPIDS DURING EXPERIMENTAL CARCINOGENESIS. Burlakova, E. B.; Molochkina, E. M. (Inst. of Chemical Physics, Moscow). Biophysics (USSR) (Engl. Transl.); 18: No. 2, 302-308(Nov 1973).

Translated from Biofizika; 18: No. 2, 293-298(Nov 1973).

Changes in the anti-oxidative activity (a.o.a.) of mouse liver lipids on exposure to the carcinogenic action of o-amino azotoluene, 3,4-benzpyrene and γ-radiation were investigated. It was found that in different forms of carcinogenesis the change in a.o.a. is of the same phasic character: fall in the first stage to a certain minimum (to 0.6 of the normal value), then rise to a level 2 to 3 times the normal. A connection was established between these changes and the morphological stages of carcinogenesis. The directed change of anti-oxidative activity using inhibitors of radical reactions in different stages of carcinogenesis correspondingly alters the course of the process, accelerates it or slows it down depending on the dose and time of administration of the inhibitor. This indicates the important role of this physicochemical characteristic of the lipids for the process of carcinogenesis. (auth)

**26084** EFFECT OF RADIATION, INSULIN, CONCANAVALIN A, AND TRYPSIN ON THE SURFACE TOPOLOGY OF RAT THYMOCYTES. Lin, P. S.; Kwock, L.; Ehrhart, C. (Tufts New England Medical Center, Boston). pp 691-696 of Scanning Electron Microscopy, 1974. Johari, O.; Corvin, I. (eds.). Chicago; Illinois Institute of Technology, SEM Symposia Office (1974).

From proceedings of the scanning electron microscopy; Chicago, Illinois, USA (8 Apr 1974).

Radiation doses as low as 100 rads cause significant decreases in the transport of alpha-aminoisobutyric acid (AIB) in rat thymocytes in vitro. Since amino acid transport is a membrane phenomenon, a search was made for alteration in the surface topology of normal and irradiated thymocytes by scanning electron microscopy (SEM), as a function of time after irradiation. All specimens were prepared by critical point methods. Thymocyte membranes deteriorate with increasing time in vitro, but the cell membranes of irradiated cells appear to change faster than their non-irradiated counterparts. Membrane breakdown starts focally and with time spreads over the entire cell surface. Concanavalin A, insulin, and trypsin protect the sodium-dependent AIB transport against the adverse effects of ionizing radiation in rat thymocytes. The effects of these agents on the surface topology of these cells were studied by SEM. Untreated thymic cells generally appear to be spherical with a smooth topology. In contrast, the majority of treated cells exhibit wrinkly surface irregularities. Cells treated with insulin and then irradiated do not deteriorate as fast as the control irradiated cells. The radiation insult to a transport system linked to sodium permeation leads to a focal extrusion of macromolecules, observed by SEM. (auth)

**26085** INVESTIGATIONS OF THE METABOLISM OF NAD IN EMBRYONIC NEURAL TISSUE OF MICE AFTER IRRADIATION WITH X-RAYS. van Beuningen, M. Freiburg i. B.; Freiburg Univ. (1974). 57p. (In German). INIS.

Thesis.

The NAD content and protein content in embryonic neural tissue of embryo mice increased from the 10th to 11th day after removal by caesarian section. The relationship between NAD quantity and increase in size measured by the protein content was investigated. (GE)

**26086** CYTOLOGICAL EFFECTS OF THERAPY WITH TETRAHYDROFOLIC ACID AND CYSTEIN TO BONE-MARROW AND PERIPHERAL BLOOD-PICTURE OF WHOLE-BODY IRRADIATED RATS. Schuenzel, G.; Ruethrich, H. L.; Schmidt, W. Radiobiol. Radiother.; 16: No. 2, 173-180(1975). (In German).

One postradiation application of tetrahydrofolic acid combined with cystein moderates initial plasia of rats in the range of LD 90/30 and favours repopulation of bone-marrow with nucleated cells in the examination period of 14 days following the single total irradiation with 800 R for the first time significantly from the 10th day after irradiation. The accelerated regeneration of marrow likewise applies to granulopoiesis and to erythropoiesis but at different times. Due to the different lifespan and function of white and red blood cells the different effects depending on the condition of the peripheral blood-picture in connection with complexity of acute radiation syndrome are overshadowed as well as intensified. Significant differences in the numerical values of leukocytes and erythrocytes per $mm^3$ of circulating blood generally appeared between treated animals and controls from the 10th day after irradiation. (auth)

**26087** RADIATION EFFECTS ON TESTES. VI. 5′ Nucleotidase and Adenosine Triphosphatase Following Partial-Body Gamma Irradiation. Gupta, G. S.; Bawa, S. R. (Panjab Univ., India). Radiobiol. Radiother.; 16: No. 2, 221-234(1975). (In German).

Five-prime nucleotidase is localized in both exocrine and endocrine parts of the testis. At subcellular levels, it seems to be distributed in nuclear, mitochondrial and microsomal fractions. The enhanced activity of the enzyme after first week has been related to the secondary effect of radiation due to stimulation of the pituitary and adenosine triphosphate (ATP) esters which seem to be involved in the control mechanisms of 5′ nucleotidase. The Km (1.25 mM) and energy of activation for the hydrolysis of (AMP) (17,000 cals/deg/mol) by normal and radiated testicular enzymes are comparable. The subcellular distribution studies suggest that 5′ nucleotidase is enhanced in the nuclei of testicular cells. Effect of radiation on testicular ATPase seems to depend upon the dose and the environmental temperature. At low environmental temperature ATPase declines followed by stimulation, whereas at high environmental temperature, the activity of ATPase is enhanced without showing the point of minima. Enhanced activity of ATPase of rat testis seems to be associated with mitochondria and seems to be related to the effect of radiation, the altered testis pituitary axis and the loss of gonial cells in seminiferous tubules. Inability of stimulation of testicular ATPase to Na/K during early period of radiation injury indicates the loss of membrane ATPase of the radiosensitive germ cells. Ability of Na/K to stimulate ATPase in atrophied testis suggests that nongerminal cells are endowed with Na/K ATPase whereas normal adult testis is predominantly rich in mitochondrial ATPase. (auth)

**26088** FOUR R's OF RADIOTHERAPY. Withers, H. R. (Univ. of Texas, Houston). Adv. Radiat. Biol.; 5: 241-247(1975).

Radiotherapy given as multiple doses can be effective in sterilizing cancers, but the processes whereby the neoplasm is eradicated and the normal tissues are preserved are not fully understood. The differential between normal tissue and tumor response is enhanced by dose fractionation, single doses resulting in severe normal tissue injury when the dose is sufficient to control a proportion of treated tumors. Data are reviewed from radiobiological studies on laboratory animals and cultured cells that have thrown some light on four of the phenomena that influence the outcome of fractionated-dose radiotherapy, one or more of which may account for the relative sparing of normal tissues. These are repair of sublethal injury in normal and neoplastic cells, reoxygenation of the tumor, redistribution through the division cycle, and regeneration of surviving normal and malignant cells between dose fractions. These have been called the four R's of fractionated radiotherapy. Other factors are involved in the outcome of multifraction radiotherapy, including maintenance of the architectural integrity of the normal tissues, the volume of tissue irradiated, the tumor bed, and the immunocompetence of the host. (90 references) (CH)

**26089** DEFENSE OF CUTANEOUS CELLS AGAINST UV IRRADIATION. II. Restricted Photomediated Binding of Trimethyl Psoralen to Pigmented Skin In Vivo. Carter, D. M.; Jegasothy, B. V.; Condit, E. S. (Yale Univ., New Haven). J. Invest. Dermatol.; 60: No. 5, 274-277(May 1973).

Distinct differences in grain distribution were seen in autoradiographs of pigmented and nonpigmented skin from spotted guinea-pig ears subjected to photosensitizing conditions by the topical application of tritiated trimethyl psoralen ($^3H$ TMP) and exposure to uv irradiation at 365 nm. Grains were localized over cells throughout the epidermis in nonpigmented skin, but they were not seen beneath the stratum corneum in pigmented skin. Since TMP covalently binds to epidermal nucleic acids only after irradiation, these experiments demonstrate that the compacted melanized cells of the outer epidermis shield the DNA of underlying cells by severely restricting the penetration of uv light into the skin. (auth)

### *Invertebrates*

*Refer also to abstract 26120.*

**26090** TEMPERATURE-SENSITIVE CELL-LETHAL MUTANTS OF DROSOPHILA: ISOLATION AND CHARACTERIZATION. Arking, R. (Univ. of California, Irvine). Genetics; 80: No. 3, 519-537(Jul 1975).

One hundred and twenty-one temperature-sensitive (ts) sex-linked lethals were screened by means of x-ray-induced somatic crossing over to determine if any were ts cell-lethal mutants. Cell-lethal mutations were identified by their ability to block the development of homozygous clones when raised under restrictive conditions (29 degrees). Twenty-two ts cell-lethal mutants were isolated and categorized into three classes, depending upon the patterns of damage observed in larval and imaginal tissues. The phenotypes produced by these mutations ranged from those which affected only a limited set of structures (i.e., genital discs only) to those which affected diverse tissues at all stages of the life cycle. Each mutation has its own characteristic time-dependent pattern, frequency, and type of damage. All the mutations affect imaginal tissue, but only one-third of the mutations affect both larval and imaginal tissue. The fastest-acting lethals need 15 hours at the restrictive temperature to kill the cells and the slowest-acting lethals require at least 48 hours. By choosing the appropriate mutant and by manipulating the times of exposure to the restrictive temperature, it has proven possible to produce duplications and deficiencies in specific structures of the adult. A mechanism by which lethality might yield such structures is suggested. In addition, 15 of the mutants are ts female sterile mutants. Only one of these 15 mutants can recover its fertility when shifted back down to the permissive temperature (22 degrees). (auth)

## Radionuclide Effects (Internal Source)

**26091** (ERDA-tr-38, pp 39-46) EVALUATION OF THE MUTAGENIC EFFECTIVENESS OF THE ISOTOPE $^{14}C$. Golenetskii, G. P.; Suskov, I. I.; Stepanok, V. V. Jul 1975. Translated from Radiobiologiya; 15: No. 1, 32-36(1975).

In Radiobiology.

In the course of the formulation of the problem and proposals for discussion, a formal calculated estimate of the total mutagenic effectiveness of the radiocarbon isotope $^{14}C$ in the case of its uniform distribution in the carbon of the organism is given. The value obtained for the RGE of $^{14}C$ is no less than 4000, which is two to three orders of magnitude greater than the values obtained by other authors experimentally. Possible causes for this discrepancy are indicated. The hypothesis of a possible role of natural radiocarbon as one of the basic natural mutagens and sources of supplementation of the gene pool is advanced. It is suggested that $^{14}C$ be used as an effective mutagen in radiation selection. (tr-auth)

### *Man*

*Refer also to abstracts 26035, 26041, and 26078.*

**26092** (RFP-2363) CONSIDERATION OF THE EFFECT OF LYMPH-NODE DEPOSITION UPON THE MEASUREMENT OF PLUTONIUM AND AMERICUM IN THE LUNGS. Falk, R.B.; Lagerquist, C. R. (Atomics International Div., Golden, Colo. (USA)). 19 Aug 1975. Contract E(29-2)-3533. 20p. Dep. NTIS $4.00.

Measurement of an inhaled radionuclide by external photon counting includes quantities which may be contained in lymph nodes, as well as quantities in the lungs. An overestimate of the lung burden can result, if a portion of the radionuclide were

present in the lymph nodes. This problem is analyzed with respect to the measurement of inhaled plutonium containing plutonium-241 and americium-241, when americium-241 has been used as a tracer for the plutonium. Equations are derived which yield the amounts of americium and of plutonium in the lungs and in the lymph nodes as a function of time after exposure and for various translocation and retention parameters. Count histories (count profiles) of actual exposure cases are compared with calculated count profiles in order to gain insight into possible values of the translocation and retention parameters. Comparison is also made with calculated count profiles using values of translocation and retention parameters recommended by the International Commission on Radiological Protection (ICRP) for use with the Task Group Lung Model. The magnitude of the possible overestimate (error factor) was calculated for combinations of parameters which yielded matches to the observed count histories. (auth)

**26093** (Y-1992) ANALYSIS OF LONG-TERM DATA ON URANIUM IN AIR. Sanders, M. (Oak Ridge Y-12 Plant, Tenn. (USA)). Sep 1975. Contract W-7405-eng-26. 14p. Dep. NTIS $4.00.

The main function of the Oak Ridge Y-12 Plant uranium processing areas is to convert raw materials to rough shapes suitable for machining and finishing to an exact configuration. The Plant also recycles waste materials generated by the various manufacturing processes. The processes which have been selected for discussion are those where long-term experience has demonstrated that positive engineering techniques are required for effective control of uranium airborne activity in the working environment and in the outside environs. These operations are reduction of $UF_4$ to metal, casting, rolling and forming, machining, wet chemistry recycle, and $UF_4$ extraction. In the work with depleted uranium, the rolling and forming and foundry operations are of primary concern. Data are presented on the radioactivity in gaseous and liquid effluents discharged to the environment, size of airborne particles, and in vivo monitoring and urine analysis of personnel to determine internal exposure levels during the past seven years. (CH)

**26094** BEHAVIOR OF $^{210}$Pb ($^{210}$Bi) $^{210}$Po IN NATURAL ENVIRONMENT AND ITS DOSE CONTRIBUTION, 1. Introduction. Abe, S.; Abe, M. (National Inst. of Radiological Sciences, Chiba (Japan)). Hoshasen Kagaku; 17: No. 7, 121-126(Jul 1974). (In Japanese).

Explanation is made on the behavior of $^{210}$Pb, $^{210}$Bi, and $^{210}$Po in natural environment, the position of these isotopes in uranium series, the radioactive properties of the isotopes of these elements, maximum permissible concentration of these isotopes, the properties of metallic polonium and its compounds, and the characteristic behavior of polonium compounds. The element polonium has oxidation states of −2, +2, +4, and +6 valent. Polonium is well known for the property to form many volatile compounds. Many of carbonyls, hydrides, halides, and organic compounds have boiling points around 100°C. Also, $^{210}$Po emits $\alpha$ rays, which are much shorter in flight range. In the human body, the $\alpha$ ray is completely absorbed and causes various hazards. Therefore, strict care must be paid in the handling of $^{210}$Po. All of more than 30 isotopes of polonium are radioactive. Only three of these, $^{210}$Po, $^{208}$Po, and $^{209}$Po have a long half decay period. Metallic polonium is easily formed when Ag, Te, Ni, or Cu, which is more basic than Po, is immersed in the aqueous solution of polonium salts. Polonium is also easily deposited by electrolysis. A number of data are tabulated for the compounds of the title elements. (JA)

**26095** RADIOBIOLOGY AND DOSIMETRY. Saenger, E. L.; Kereiakes, J. G. (Univ. of Cincinnati). pp 209-229 of Nuclear Medicine in Clinical Pediatrics. Handmaker, H.; Lowenstein, J. M. (eds.). Acton, MA; Publishing Sciences Group, Inc. (1975).

From symposium on nuclear medicine in pediatrics; San Francisco, California, USA (16 Feb 1973). See CONF-730235-.

A brief review of radiobiology is presented that should indicate the reasonable limits of pediatric nuclear medicine. Together with the dosimetric information and the few caveats of laboratory procedure, the use of nuclear medicine as clinically indicated, maintaining doses as low as practicable, should be readily applied to pediatrics. In discussing benefits versus risks in nuclear medicine, the conscience guide (CG) was introduced as a unit, being defined as the referral rate to better qualified centers from a laboratory where expertise in a given test is lacking versus the total number of examinations done in that laboratory. When considering procedures in the pediatric age group, the physician is urged to use the CG to do only those procedures for which he and his staff have adequate equipment and experience. In this way, the best interests of the patient and physician can be insured. (auth)

**26096** NEW INSTRUMENTATION. Powell, M. R.; Perez-Mendez, V. pp 231-241 of Nuclear Medicine in Clinical Pediatrics. Handmaker, H.; Lowenstein, J. M. (eds.). Acton, MA; Publishing Sciences Group, Inc. (1975).

From symposium on nuclear medicine in pediatrics; San Francisco, California, USA (16 Feb 1973). See CONF-730235-.

A rather wide variety of approaches are available toward improving pediatric nuclear medicine imaging. Hopefully, some that have been described in this brief paper and many other combinations will become available in useful commercial instrumentation to more closely approach the ideal situation where maximum use is made of the available gamma photons to obtain improved images with further decrease of patient radiation exposure. (auth)

**26097** COMPUTER IMAGING PROCEDURES. Budinger, T. F. (Univ. of California, Berkeley). pp 243-260 of Nuclear Medicine in Clinical Pediatrics. Handmaker, H.; Lowenstein, J. M. (eds.). Acton, MA; Publishing Sciences Group, Inc. (1975).

From symposium on nuclear medicine in pediatrics; San Francisco, California, USA (16 Feb 1973). See CONF-730235-.

The advantages of computer imaging procedures for radioisotope scanning of pediatric patients are reviewed. (CH)

**26098** EARLY DETECTION OF LUNG CANCER IN HIGH RISK POPULATIONS. Brooks, S. M. (Univ. of Cincinnati). J. Occup. Med.; 17: No. 1, 19-22(Jan 1975).

Early detection of lung cancer is discussed with regard to chest x ray and spectrum cytology as screening tests, the use of fiberoptic bronchoscopy, and recommendations for evaluation of high risk populations. The following environmental carcinogens are considered; uranium, asbestos, chromate, cigarette smoke, and benzo(a)pyrene. Carcinogenic effects of host factors are discussed; an example is the increased activity of aryl hydrocarbon hydroxylase, an enzyme found in many tissues, following exposure to benzo(a)pyrene. (HLW)

**26099** HISTOSTRUCTURAL PECULIARITIES AND RADIATION RESISTANCE OF THE TISSUE OF DIFFUSE TOXIC GOITER UNDER THERAPY WITH $^{131}$I. Livergant, J. E.; Kolesnikova, G. S. Radiobiol. Radiother.; 16: No. 2, 165-172(1975). (In German).

The results of examinations of the histostructure of goiter of 10 patients are reported who had thyreotoxicosis with complications of the heart and circulatory system and of the liver and who died during the treatment with $^{131}$I. Radiation injury to the thyroid tissue was most pronounced in preponderantly parenchymal and microfollicular, respectively, structures, whereas such lesions could be demonstrated only to a low extent or not at all in colloid goiter as well as in cystic degeneration. The dependence of radiation resistance of the tissue of toxic goiter on histostructural peculiarities of the preponderant parts of the functionally stimulated thyroid epithelium is discussed. (auth)

**26100** $^{35}$S THERAPY OF CHONDROSARCOMA. Loebe, J. Radiobiol. Radiother.; 16: No. 2, 207-213(1975).

The application of a high dose of $^{35}$S for interstitial therapy to a patient with chondrosarcoma of the pelvis, sacrum, and lumbar portion of the spine after non-radical operation is reported. In an interval of 4 weeks 250 mCi $^{35}$S ($Na_2SO_4$) each were intravenously administered; total activity after 7 treatments was 1.75 Ci. Excretion of $^{35}$S in the urine was 75% after the first injection, 90% of the applied activity after the last treatment. Within the first 24 hours excretion of $^{35}$S is especially high; after all injections already between 80 and 90% of the totally expected activity was demonstrated during this time. The activity decrease in the blood is correspondingly steep after $^{35}$S application. The limiting factor for this therapy type is the behaviour of hematopoiesis so that thorough hematological controls of the course are necessary during and after treatment. (auth)

**26101** INTERSTITIAL RADIATION THERAPY USING RADIOACTIVE CESIUM. Spoljar, M.; Bulic, N. (Inst. of Oncology and Radiotherapy, Zagreb). Radiobiol. Radiother.; 16: No. 2, 203-206(1975).

Based on their longstanding experience with radium the authors hold that the interstitial application of radioactive sources has in certain cases some advantages over other types of radiotherapy. Such a therapy is indicated in the first place in cancers of the oral cavity, the lower lip, and the skin. Due to the adverse properties of radium the authors replaced radium by radioactive cesium. They treated by interstitial application 15 patients with cancer of the lower lip, 6 skin cancers, 6 cancers of the tongue, 1 cancer of the buccal mucosa, and 1 case of breast cancer. The size of the tumours ranged from 1.5 to 16 $cm^2$. The total applied doses ranged from 4,100 rad administered in 82 h, to 7000 rad in 252 h. In all radically treated patients a primary cure could be recorded. (auth)

### Animals

**26102** (ERDA-tr-38, pp 183-185) CHANGE IN THE PHOSPHOLIPID METABOLISM IN RAT LUNGS AFTER TREATMENT WITH PLUTONIUM. Surina, A. G. Jul 1975. Translated from Radiobiologiya; 15: No. 1, 145-147(1975).

In Radiobiology.

An investigation was conducted of the content and biosynthesis of individual phospholipids in the lungs of rats at various periods after a single inhalation of a nitrate solution of polymeric plutonium. The inhalation led to substantial ionization doses in the lungs; 712 rads at 2 weeks and 2554 rads after seven months. The change in the phospholipid metabolism in lungs injured by plutonium was manifested in an increase in the content and inhibition of the synthesis of these substances. In view of the fact that biosynthesis was inhibited, the increased content may be due to inflammatory infiltration of the lungs with lymphocytes, macrophages, histiocytes, and neutrophils or to a decrease in the activity of phospholipases. (ERB)

**26103** EXPERIMENTAL STUDIES ON THE PRODUCTION OF OSTEOSARCOMA BY BERYLLIUM AND ON THE EFFECT OF IRRADIATION ON IT. Matsuura, K. (Jikei Univ., Tokyo (Japan). School of Medicine). Nippon Seikei Geka Gakkai Zasshi; 48: No. 7, 403-418(Jul 1974). (In Japanese).

The author attempted to produce osteosarcoma of the femur in a series of 211 rabbits using various Be compounds, $BeCO_3$, Be-acetate, Be-acetylacetonate, Be-laurate, and Be-stearate. In another experiment, a chronological study was made of the genesis of $BeCO_3$-induced osteosarcoma by means of $^{87m}Sr$-scintiscanning to explore the possibility of early detection both qualitatively and quantitatively with the aid of a computer. Furthermore, $BeCO_3$-induced osteosarcoma was given $^{60}Co$ irradiation, 500 R at a time up to a total dose of 20,000 R in an attempt to investigate the radiosensitivity of the malignancy both radiologically and histologically. These experiments yielded the following results. The incidence of tumor in the $BeCO_3$ group, 38%, would probably become higher, since 21 of 55 rabbits surviving for long time might also have developed malignancy. The time span of induced tumor development was radiologically between 10 and 21 months. Histological findings were those of typical osteosarcoma with prominent osteoid formation. In the Be-acetylacetonate group, one case (surviving 13 months) developed osteosarcoma, which contained portions suggestive of reticulum cell sarcoma and of Ewing's sarcoma. Strontium-87m scintiscanning permitted the detection of the tumor 4 to 6 months earlier than routine roentgenography. The computer analysis of bone scintigrams permitted the quantitative observation of the process of $BeCO_3$-induced osteosarcoma, hopefully being of value in the discovery of otherwise undetectable small lesions as well as in the quantitative assessment of the malignancy. Radiotherapy was given to the $BeCO_3$-induced osteosarcoma in a total dose up to 20,000 R. Immediately after exposure to this tumorigenic agent, the massive dose of 20,000 R failed to cause a complete destruction of the tumor tissues. However, marked generative changes in the tumor cells were found following a dose of 10,000 R. (auth)

## Nuclide Kinetics and Toxicology

### Animals

*Refer also to abstract 25898.*

**26104** INTRAMUSCULAR RETENTION OF $UO_3$ AND $UO_2$. Beiter, H.; Gibb, F. R.; Marrow, P. E. (Rochester Univ., NY). Health Phys.; 29: No. 2, 273-277(Aug 1975).

Uranium dioxide ($UO_2$) and uranium trioxide ($UO_3$), in biological terms, are prototype $U^{4+}$ and $U^{6+}$ compounds, respectively. The intramuscular injection studies performed in rats described in this report were designed to complement previously reported inhalation studies in dogs and certain in vitro solubility assessments of these same materials. The intramuscular retention functions of the two $^{235}U$ enriched uranium oxides were found to resemble closely those determined for the lungs; specifically, for $UO_3$: $R_{(muscle)} = A_0e^{-0.183t} + B_0e^{-0.017t}$ versus $R_{(lung)} = A_0e^{-0.147t} + B_0e^{-0.023t}$; and for $UO_2$: $R_{(muscle)} = A_0e^{-0.0041t}$ versus $R_{(lung)} = A_0e^{-0.0038t}$, where $A_0$ and $B_0$ represent fractional retentions whose sum is 1.0 and t is expressed in days. A single rabbit study with intramuscular $UO_2$ gave a confirmatory retention half-time of 172 days. (auth)

**26105** EFFECTIVENESS OF AMINOALKYL PHOSPHONIC ACIDS IN REMOVING URANIUM FROM THE BODY. Ivannikov, A. T. Gig. Tr. Prof. Zabol.; No. 5, 45-46(1975). (In Russian).

The effectiveness of several aminoalkyl phosphonic acids (DTPP, EDDIP, ETPP) in removing uranyl nitrate from rats was studied in relation to the time and route of administration of the complexing agents (subcutaneous, intravenous, peroral, intragastric). They proved to be most effective when given before (they persist in the body for 9 hours) or immediately after the intake of uranium. Parenteral injection was the most effective route of administration. It was 8 to 16 times more effective than the peroral route because of their low absorbability from the gastrointestinal tract. (JPRS)

**26106** EFFECTS OF STIMULATION OF THE CENTRAL NERVOUS SYSTEM WITH PHYSICAL AGENTS ON THE PERMEABILITY OF THE PLEURAL CAVITY TO RADIOACTIVE PHOSPHORUS. Faytel'berg-Blank, V. R.; Kovalenko, L. I. (Odessa Agricultural Inst.). Fiziol. Zh. SSSR; No. 2, 261-266(1975). (In Ukrainian).

Evaluations were made of the rates of absorption of $^{32}P$ from the pleural cavities of 299 cats following stimulation of the left sincipital, right temporal, both occipital and both orbital areas of the cerebral cortex with ultrasound (0.2, 0.6, 1.0 and 1.6 W/cm$^2$; 5 min) and diathermic currents (1625 Hz; 500 and 750 mA/cm$^2$; 35 min), and its accumulation in internal organs. Both forms of treatment were found to result in enhanced absorption of $^{32}P$ from the pleural cavities, with the highest amounts accumulating in the liver and the kidneys, and lesser amounts in the spleen and the lungs. 0.2 W/cm$^2$ ultrasound and 500 mA/cm$^2$ diathermic current represented the most effective stimulant for each category of physical agent in enhancing permeability. The areas of the cerebral cortex that were found most selective in promoting permeability, and on that basis most susceptible to ultrasound and diathermy, could generally be ranked in the following order: orbital, left sincipital, and right occipital. (JPRS)

**26107** INHIBITION OF THE ISOPROTERENOLE-INDUCED NET $^{45}Ca$ UPTAKE INTO THE VENTRICULAR MYOCARDIUM OF RATS BY ORGANIC $Ca^{2+}$ ANTAGONISTS OR $K^+$ AND $Mg^{2+}$ IONS. Bernsmeier, H. Freiburg i. B.; Freiburg Univ. (1974). 27p. (In German). INIS.

Thesis.

Infarct-similar or disseminated myocardial necroses in rats can especially be produced by high doses of isoproterenole (aludrine) which stimulates the decomposition of energy-rich phosphate to a maximum. As a result of an isoproterenole-caused increase of the transmembranary $Ca^{++}$ influx, there is an inundation of the myocardium with $Ca^{++}$ ions which initiate the breakdown of the ATP and creatine phosphate fraction by the activation of the myofibril ATP-ase and by harming the mitochondria function. Physiological $Ca^{++}$ antagonists like $K^+$ and $Mg^{++}$ salts evidently inhibit the disappearance of energy-rich phosphate which results in a protection against necroses. A new group of organic $Ca^{++}$ antagonists (isoptine, substance D600, segontine) are even more effective. These substances in suitable doses can largely prevent the isoproterenole-induced $Ca^{++}$ inundation of the myocardium, so that the breakdown of the ATP and creatine phosphate fraction and thus the morphological comprehensible structure decomposition no longer occurs. The findings enable the conclusion that the $Ca^{++}$ ions take on a key position in the occurrence of myocardial necroses which had not previously been considered. (GE)

**26108** ATTEMPT TO ACCELERATE EXCRETION OF YTTRIUM-91 FROM THE ORGANISM BY MEANS OF COMBINED APPLICATION OF EDTA AND DIURETICS. Arkhipova, T. P.; Sukhacheva, E. I. Tr. Inst. Ekol. Rast. Zhivotn., Ural. Nauchn. Tsentr, Akad. Nauk SSSR; 89: 53-56(1974). (In Russian).

Rats were administered $^{91}YCl_3$ (3 $\mu$Cl) I/V, 2 hrs after administration of novurite (I; 1.75 mg, im.) or dehydratine (II; 0.4 mg, po.); 2 to 3 min after $^{91}YCl_3$ the rats were given $^{14}C$-tagged Ca-EDTA (20 $\mu$ moles, I/V). I and II accelerated excretion of $^{91}Y$ in urine in 24 hrs; II lowered deposition of $^{91}Y$ in liver, while I increased its deposition in the skeleton. I and II increased the excretion of Ca-EDTA in urine during the first 2 hrs, but in combined administration with Ca-EDTA it slightly retarded excretion of $^{91}Y$, so that it is believed to be necessary to use I and II for the elevation of the effectiveness of the complexon. (Ref. Zh.)

**26109** RELATIONSHIP OF THE EXTENT OF THE EXCRETION OF YTTRIUM-91 FROM THE ORGANISM AND THE DOSE AND DURATION OF THE ADMINISTRATION OF Ca-EDTA. Bashenov, A. V.; Men'shikova, G. A. Tr. Inst. Ekol. Rast. Zhivotn., Ural. Nauchn. Tsentr, Akad. Nauk SSSR; 89: 37-42(1974). (In Russian).

A solution of $^{91}Y$ chloride (40 $\mu$Cl) and—after 3, 8, 32, 64, or 128 days—Ca-EDTA (10 to 200 $\gamma$-moles) were administered to rats via the tail vein. Yttrium-91 excretion proceeds most intensely in the first days, then decreases (especially through the kidneys; from the 6th day excretion is primarily via the feces). The $^{91}Y$ content in the organism decreases due to its mobilization

from the soft tissues, while its content in the skeleton remains constant throughout the experiment. Administration of Ca-EDTA intensifies $^{91}Y$ excretion; administration of Ca-EDTA is more effective in the earlier periods after $^{91}Y$ administration. For all doses and at all periods of the experiment, the fraction of $^{91}Y$ in the organism, which is accessible to the Ca-EDTA, decreases more slowly than that for natural mechanisms of mobilization. (Ref. Zh.)

**26110** DYNAMICS OF THE DISTRIBUTION OF CESIUM-137 IN RESPECT TO POTASSIUM IN VARIOUS ORGANS AND SYSTEMS. Dubrovina, Z. V.; Otlygin, V. A.; Malkin, P. M.: Sokov, L. A. Tr. Inst. Ekol. Rast. Zhivotn., Ural. Nauchn. Tsentr, Akad. Nauk SSSR; 89: 33-36(1974). (In Russian).

A completely analogous distribution of Cs and K has been shown in individual organs and systems of rats, with consistently higher fixation coefficient of Cs as compared to K. In blood plasma and in some tissue (liver, kidneys) the equilibrium content of $^{137}Cs$ is reinstated rapidly. (Ref.Zh.)

**26111** ALTERING IODINE METABOLISM IN THE CALF BY FEEDING IODINE-BINDING AGENTS. Miller, J. K.; Swanson, E. W.; Lyke, W. A.; Byrne, W. F. (Comparative Animal Research Lab., Oak Ridge, TN). Contract AT(40-1)-GEN-242. J. Dairy Sci.; 58: 931-937(Jun 1975).

Effects of feeding cottonseed meal and anion-exchange resin on iodine absorption and excretion by calves were investigated. Each additional amount of resin fed from 0.3 to 3.5 g/kg body weight further increased fecal excretion from single oral iodine-131 and intravenous iodine-125 doses. By feeding 3 to 10 g cottonseed meal/kg body weight, excretion of oral iodine-131 given daily was increased 7 to 94 percent in feces and reduced as much as 35 percent in urine, but plasma iodine-131 was not changed. Introducing 1 g resin/kg body weight daily into the diet increased fecal iodine-131 excretion three to five times that with cottonseed meal alone and reduced both plasma and urinary iodine-131. The same amount of resin fed daily had similar effects on excretion of iodine-131 injected subcutaneously each day. Although iodine depletion by a highly efficient iodine binder (resin) in the gastrointestinal tract is probable, iodine binding by a natural feed constituent (cottonseed meal) was relatively inefficient. (auth)

## New Tracer Techniques

*Refer also to abstracts 26068, 26095, 26096, and 26103.*

**26112** DISTURBED CSF CIRCULATION AMONG GERIATRIC PATIENTS. Significance of delayed CSF Circulation. Yamamoto, M.; Chiba, K.; Tanno, M.; Yamada, H.; Matsui, K. (Tokyo Metropolitan Geriatric Medical Center (Japan)). Kaku Igaku; 11: No. 6, 625-635(Dec 1974). (In Japanese).

Cerebrospinal fluid (CSF) circulation has yet to be studied in aged people. So far our results indicate the delay of CSF circulation time being correlate with deterioration of the central nervous system. Radioisotope cisternography was performed in 74 cases (45 male cases, 29 female cases, with an average age of 66) with $^{169}Yb$-DTPA injected into the subarachnoid space via lumbar puncture. Counts over the lumbar region, thoracic region and the head were recorded using PHO/Gamma HP $\gamma$-camera, sequentially after injection, and images of these regions were obtained. Cases with peak value of the brain counts after 24 hours are considered to be the case with delayed circulation. In order to compare degree of the delay of CSF circulation with brain symptoms (mental dullness, gait disturbance, incontinence of urine, mutism), ratio of counts at 6 hours and 24 hours ($C_{24}/C_6$) was used. Out of 54 cases over 50 years old, 37 cases (69%) showed delayed circulation of CSF. Among them, three cases showed transient ventricular filling, four cases showed persistent ventricular filling, and 30 cases showed only delayed circulation. In cases without brain symptom the $C_{24}/C_6$ was below 0.92, however, the more the number of brain symptoms increases the higher this ratio becomes. These ratios also increase with aging. In summary, high incidence of abnormal CSF circulation was observed among aged patients. The CFS circulation related well with the degree of disturbance in brain function. (auth)

**26113** MEASUREMENT OF PLASMA RENIN ACTIVITY BY RADIOIMMUNOASSAY. Tagawa, H.; Maehata, E. (Mitsui Memorial Hospital, Tokyo (Japan)); Ishii, M.; Ikeda, S. Kaku Igaku; 11: No. 6, 657-663(Dec 1974). (In Japanese).

A modified method of radioimmunoassay of angiotensin I for measurement of plasma renin activity (PRA) was reported. Standard angiotensin I was pipetted to tubes containing tris acetate buffer ( H7.4), $^{125}I$-angiotensin I and antiserum (supplied by Dainabot RL Lab), and they were kept overnight at 4°C. Dextran-coated charcoal was used for separation of B and F. Standard curve was depicted by plotting the difference of B/T% between each angiotensin standard and 0-standard containing no angiotensin. This procedure seemed to eliminate the possible error occurring especially in low-renin samples, which might be caused by the presence of factors in plasma. Both intra- and inter-assay variations were small. Recovery and dilution experiments gave excellent results. This method gave results correlated well with bioassay (r = 0.905) and with two commercially available radioimmunoassay kits (r = 0.941 and 0.971). In normotensive controls, PRA showed a tendency of inverse correlation with sodium excretion; when sodium excretion was 50-200 mEq/day, however, PRA fell within a relatively small range, which was 1.10 ± 0.58 ng/ml/hr (m ± SD) in the fasting state during recumbency. (ERB)

**26114** IMPROVEMENT OF THE MEASUREMENT OF ALPHA-FETOPROTEIN BY RADIOIMMUNOASSAY. Fukushima, T.; Sato, T.; Saito, M.; Asano, K. (Fukushima Medical Coll. (Japan)). Nippon Sanka Fujinka Gakkai Zasshi; 26: No. 6, 527-528(Jun 1974). (In Japanese).

The quantitative determination of $\alpha$-fetoprotein by radioimmunoassay was improved from the previous method with much variation. The samples used were sera of pregnant females, fetal extracts, and placental extracts, and the reagent was $\alpha$-feto protein-$^{125}I$. The following points in the measurement were modified: the previous method measured precipitates (bound matters) but the present method measures the supernatant (nonbound matters); while the kit was added in the first reaction, it is added 24 hours later; and the horse serum added for the preparation of the standard curve is replaced by the normal human serum. As a result, in comparison with the previous method, the standard curve for reading arises slightly more rapidly, and the higher the concentration, the greater the difference is. The precision of the supernatant % is smaller than the precipitate % in 80 of coefficient of variability and the concentration of 200 mg/ml. The recovery rate of the modified method produced more satisfactory results than the previous one. (JA)

**26115** MEASUREMENT OF ESTROGEN IN AMNIOTIC FLUID BY RADIOIMMUNOASSAY. Sasaki, T.; Fujiwara, A. (Hiroshima Univ. (Japan). School of Medicine). Nippon Sanka Fujinka Gakkai Zasshi; 26: No. 6, 531-532(Jun 1974). (In Japanese).

The three fractional measurements of estrogen in amniotic fluid by radioimmunoassay were examined and were confirmed to be excellent in precision and recovery rate, allowing accurate measurements of small amounts. Samples were fractionated estrone, estradiol, and estriol, to which a $^{3}H$-labeled substance was added for radioimmunoassay. Since it was confirmed on five cases of normal pregnancy that estriol was of binding type in more than 95% after the middle stage of pregnancy, it was measured as the total estrogen in clinical cases. It was gradually increased with the course of pregnancy in normal pregnancies, and the value of the terminal stage was 10 to 20 times higher than that of the former and middle stages. It was very low in placental death and anencephalic babies. The present method was valuable in diagnostic application. (JA)

**26116** DIAGNOSIS OF ADRENAL DISEASE BY VISUALIZATION OF HUMAN ADRENAL GLANDS WITH $^{131}I$-19-IODOCHOLESTEROL. Fukuchi, S.; Nakajima, K.; Takenouchi, T.; Nishisato, K.; Nakamura, M. (Tohoku Univ., Sendai (Japan). School of Medicine). Kaku Igaku; 11: No. 5, 553-559(Oct 1974). (In Japanese).

Iodine-131-labeled 19-iodocholesterol was used in visualizing the adrenal glands of 36 patients including 13 patients with primary aldosteronism, 10 with Cushing's syndrome, one with pheochromocytoma, two with 17$\alpha$-hydroxylase deficiency, and nine with normally functioning adrenal tissue. Six to 9 days after the intravenous administration of the dose, the patient's adrenal glands were imaged with a 5 inch crystal rectilinear photoscanner. Normally functioning adrenal glands were readily visualized after administration of $^{131}I$-19-iodocholesterol. In 13 patients with primary aldosteronism, the photoscan gave a positive indication of the size of the lesion in a gland containing an adenoma, with a normal radioactivity concentration in the opposite gland. Seven patients with Cushing's syndrome due to ACTH excess showed adrenal glands approximately equal in size and radioactivity concentration. An adrenal adenoma in three patients with Cushing's syndrome definitely visualized on scan, with no uptake in the opposite gland. In a patient with a large pheochromocytoma, the involved gland was not imaged, but normal adrenal image of the normal contralateral glands was shown. In two patients with 17$\alpha$-hydroxylase deficiency, both demonstrated bilaterally equal sized adrenal glands. The biological half-life of the $^{131}I$-19-iodocholesterol was 2.2 to 52.60 days, and by calculation, the effective half-life was 1.77 to 1.98 days. (auth)

**26117** STUDIES ON RADIOIMMUNOASSAY OF 2,5-DIMETHOXY-4-METHYLAMPHETAMINE. Kido, Y.; Nagamatsu, K.; Ishizeki, C. (National Inst. of Hygienic Sciences, Tokyo (Japan)). Yakugaku Zasshi; 94: No. 10, 1290-1295(Oct 1974). (In Japanese).

A method of radioimmunoassay of 2,5-dimethoxy-4-methylamphetamine (DOM), a hallucinogen, was studied. In order to use for immunization, DOM-glutaraldehyde-human serum albumin conjugate was prepared from DOM, glutaraldehyde, and human serum albumin, followed by purification by dialysis. Anti-DOM antiserum was obtained by repeated injection of the prepared antigen to guinea pig. The method of radioimmunoassay established after some experiments was as follows: To an aliquot of the test serum or sample solution, a definite amount of DOM labeled with $^3H$ and anti-DOM antiserum were added, then the globulin fraction was isolated by salting out as a precipitate, which contains the bound DOM coming from the test serum or sample solution, and labeled DOM. Radioactivity of the precipitate was measured, and the amount of DOM in the test serum or sample solution was determined from a calibration curve, which was prepared with various known amounts of standard DOM. The sensitivity of this radioimmunoassay was 1 to 100 ng/ml, and the specificity to DOM was so sufficient that several pharmaceuticals such as ephedrine, dopamine, and epinephrine showed no disturbance to this method. (auth)

**26118** STUDIES ON A RADIOIMMUNOASSAY FOR PLASMA TESTOSTERONE. Konno, M.; Hosaka, M.; Mamiya, T.; Nishimura, R. (Yokohama City Univ. (Japan). Faculty of Medicine). Nippon Hinyokika Gakkai Zasshi; 65: No. 10, 637-647(Oct 1974). (In Japanese).

Using one step of Sephadex LH-20 micro column chromatography with the solvent system of hexane, benzene, methanol (90 : 5 : 5), complete separation of testosterone from 5α-dihydrotestosterone (DHT) was developed. The antiserum against testosterone-3 oxime-bovine serum albumin was supplied by the Department of Pharmacological Research, Teikoku Hormone Mfg. Co., Ltd. and was used at a dilution of 1 : 20,000. The antiserum has high affinity for testosterone and DHT (Cross reaction: testosterone 100, DHT 117%). It is possible to determine simultaneously testosterone and DHT concentrations in plasma by this method. Plasma of 0.05 ml from men and 0.5 ml from women was used for analysis. Following extraction with ether and chromatography on Sephadex LH-20, the dried purified extract was incubated with antiserum at room temperature for 30 min. $(NH_4)_2SO_4$ was used to separate free from bound testosterone. Various factors affecting the method blank, accuracy, sensitivity, and precision were investigated. The mean blank was 9.0 ± 5.9 (M ± SD) pg per sample. The mean recovery of testosterone-$^3H$ added to 21 samples was 83.6 ± 6.3%. The accuracy and precision of the method were satisfactory. The concentration of testosterone in plasma from men was 559 ± 170 ng/dl, and in the sample collected from women 32 ± 12 ng/dl, and in plasma from patients with carcinoma of the prostate who were treated by synthetic estrogenic agents for 1 to 7 years 19 ± 6 ng/dl. Our values for plasma testosterone concentration in women were lower than those reported previously. To determine plasma testosterone concentration by the use of radioimmunoassay, complete separation of testosterone from other steroids is quite essential. (auth)

**26119** STUDIES ON LUNG SCANNING IN PATIENTS WITH PULMONARY TUBERCULOSIS. Relations of Lung Scintigram as Well as Pulmogram with Chest Roentgenogram. Chia, S. (Hirosaki Univ., Aomori (Japan). School of Medicine). Nippon Kyobu Rinsho; 33: No. 7, 478-491(Jul 1974). (In Japanese).

Lung scintigram and pulmogram were carried out simultaneously by means of $^{131}I$-macroagglutinated albumin (MAA) in 73 patients with pulmonary tuberculosis having no heart disease and undergoing no surgical treatment for lung and in 27 controls without cardiopulmonary disease. The relation of the lung scintigram and pulmogram to the findings of routine dorsoventral chest x-ray film was investigated in this study. The findings of chest x-ray-film were classified according to NTA criterion. On 126 pulmonary lesions in 73 patients with pulmonary tuberculosis, 60 showed abnormal findings of both scintigram and chest x-ray film, these being mostly sclerotic changes. Forty eight showed abnormal findings of scintigram and slightly abnormal of x-ray film, these being pleural changes, large cavities etc; 15 showed normal finding of scintigram and slightly abnormal of x-ray film, all being medium-size disseminated changes. Three showed abnormal of scintigram and normal of x-ray film, two of them being protracted productive change. Pulmograms were taken in the entire lung field, upper lung field, and lower lung field. By these pulmograms in each field, the abnormality was more often observed in the percentage and difference of pulmonary blood flow between right and left in the groups of more advanced findings of chest x-ray film classified according to NTA. It is concluded as follows: Lung scintigram and pulmogram, expressing pulmonary hemodynamics, do not always demonstrate the same findings as shown in chest x-ray film. Therefore, these scanning methods are useful for medical practice of pulmonary tuberculosis, furthermore of pulmonary diseases, besides chest x-ray film. (auth)

**26120** RADIOISOTOPE LABELING OF MOSQUITOES. Lur'ye, A. A. (Inst. of Medical Parasitology and Tropical Medicine, Moscow). Usp. Sovrem. Biol.; 79: No. 1, 64-77(1975). (In Russian).

The current status of methods of labeling mosquitoes with radioisotopes for the purpose of determining their dispersion, numbers, viability, behavioral characteristics, and biology was reviewed. The disadvantages and advantages of the various labeling methods are compared with those of other methods used. Techniques for labeling larvae and imagos are considered in detail. Problems related to the danger of radioisotope damage to the insects and to the possible loss of the label or transfer of it to a nonlabeled insect are discussed. Promising means of further improving the radioisotope labeling technique are considered. (JPRS)

**26121** AUTOMATED IMMUNORADIOMETRIC ASSAY FOR FERRITIN. Jones, B. M.; Worwood, M. (Welsh National School of Medicine, Cardiff). J. Clin. Pathol.; 28: No. 7, 540-542(Jul 1975).

A semi-automated method for the immunoradiometric assay of ferritin has been developed. Results obtained with serum samples showed excellent correlation between this method and the previously described assay. A further useful reduction in the assay time may be achieved by incubating for 3 hours at 37°C instead of 24 hours at 4°C. (auth)

**26122** BIOLOGICAL TEST OF DAMAGE CAUSED BY IgC BY SEVERAL METHODS OF IODINATION. Hemmings, W.A. (University Coll. of North Wales, Bangor); Redshaw, M. Int. J. Appl. Radiat. Isot.; 26: No. 6-7, 426-429(Jun 1975).

Experiments are described whereby the relative damage caused by five different methods of protein iodination were compared using the system of IgG transport in the suckling mouse. Having been fed a mixture of an $^{125}I$ and a $^{131}I$ preparation of mouse IgG the mice were killed after 3 hr and heart blood collected. The protein precipitated from the serum was counted and the correction of the apparent $^{125}I$ count rate for cross talk due to $^{131}I$ was made. The results are expressed as concentration quotients (C.Q.) that is the ratio young mouse serum count rate/fed protein count rate. The results show that the lactoperoxidase technique gives rise to an outstandingly high C.Q.; thus, this is the mildest procedure of those tested available for the iodination of proteins. (UK)

**26123** RADIORECEPTOR ASSAY FOR EVALUATION OF THE PLASMA GLUCOCORTICOID ACTIVITY OF NATURAL AND SYNTHETIC STEROIDS IN MAN. Ballard, P. L.; Carter, J. P.; Graham, B. S.; Baxter, J. D. (Univ. of California, San Francisco). J. Clin. Endocrinol. Metab.; 41: No. 2, 290-304(Aug 1975).

An assay for plasma glucocorticoid activity has been developed using specific glucocorticoid receptors. Unlike other assays for cortisol and certain synthetic corticosteroids, this radioreceptor assay measures the glucocorticoid activity of all natural and synthetic steroids. Steroids extracted from as little as 0.05 ml of plasma are incubated with $^3H$-dexamethasone and cytosol receptors from cultured rat hepatoma cells. From 0.5 to 50 ng of cortisol are accurately detected. Glucocorticoid activities of adult plasmas determined by the assay correlate closely with corticoid levels obtained in the CBG-isotope and fluorometric assays. Other steroids are measured in proportion to both concentration and potency as glucocorticoids. Relative activities include: cortisol 100, dexamethasone 940, prednisolone 230, prednisone 3, estradiol 1 and androstenedione 1. A similar ranking of steroids was found using receptors from a human source (fetal lung). The assay has been useful in detecting glucocorticoid activity in unidentified medications and in measuring plasma glucocorticoid levels after administration of synthetic corticosteroids. (auth)

**26124** THREE-DETECTOR GAMMA-RAY ENCEPHALOGRAPHY. Radiobiol. Radiother.; 16: No. 2, 182-195(1975). (In German).

Essential aspects of the development of 3-detector measuring technique were to overcome the defects and to complete the advantages of gamma-ray encephalography following the administration of $^{197}Hg$- or $^{99m}Tc$-labeled compounds. In one examination a left and a right lateral as well as a craniocaudal parallel projection each of cerebral activity distribution was made. The detector holder allows an easy and rapid adjustment of the measuring probes directly at the surface of the head. The exact and reproducible fixation of the detectors which are equipped with highly sensitive segment collimators over the centres of fields to be measured is obtained by means of a special adjustment tech-

nique. The fields to be measured of each projection are arranged in a matrix of 7 lines and 4 columns. Caudally the lateral matrix ends at the skull-base. According to the head-size of the patients (including children) the size of measuring fields ranges from 2.2 $cm^2$ to 2.9 $cm^2$. The limitation to 26 and 24, respectively, measuring fields per projection and detector allows a satisfactory localization of cerebral activity concentrations on the one hand and enables the registration of relatively high pulse rates in a shortened duration of examination compared to cerebral scintigraphy thus bringing the presupposition for a high sensitivity of detection on the other. Essential part of quantitative data processing is the comparison of normalized pulse rates of the measuring fields to normal values of measuring fields determined for persons with healthy cerebral organs. The difference of measured value and standard value given in units of its average error yields a statement of probability about a pathological deviation being present or not. Using the sums of pulse rates of opposite lateral measuring fields the statistical significance of detection in the median sagittal area of the brain is increased. The percentage pulse rate differences of the right-left measuring field couples are also used for evaluation. The results obtained by means of electronic data processing are clearly represented according to the topographic arrangement of the measuring fields. Pathological values are especially marked in order to facilitate findings. Comparative measurements on a head phantom with model tumours yielded a higher sensitivity of detection of 3-detector gamma-ray encephalography comapred to computer cerebroscintigraphy. By clinical testing expectations connected with the development of the method were met concerning localization as well as concerning the detection of median and parasagittal tumours. (auth)

**26125** CENTRAL NERVOUS SYSTEM: BRAIN. Mishkin, F. S. (Martin Luther King General Hospital, Los Angeles). pp 7-22 of Nuclear Medicine in Clinical Pediatrics. Handmaker, H.; Lowenstein, J. M. (eds.). Acton, MA; Publishing Sciences Group, Inc. (1975).

From symposium on nuclear medicine in pediatrics; San Francisco, California, USA (16 Feb 1973). See CONF-730235-.

Present radiopharmaceuticals and detector systems have provided nuclear medicine physicians with tools capable of detecting a variety of brain abnormalities with little radiation exposure to pediatric patients. It is essential that the referring physician as well as the physician performing the procedure recognize both the limitations and virtues of these techniques. Appropriate selection of brain imaging procedures in each specific case must be the rule. Brain scintigraphy reliably solves certain problems, such as detecting or excluding intracranial tumors and identifying early cerebral inflammatory disease, cerebral ischemic disease, and a variety of congenital anomalies. Other situations, such as seizures without a focal neurologic deficit, acute meningitis, and hydrocephalus, are less often benefited by these studies. The role of these procedures in acute trauma and its sequelae is at the present time limited in pediatric practice. (auth)

**26126** CENTRAL NERVOUS SYSTEM: CEREBROSPINAL FLUID. James, A. E. Jr. (Johns Hopkins Medical Inst., Baltimore); Campeau, R.; Udvarhelyi, G. B. pp 23-43 of Nuclear Medicine in Clinical Pediatrics. Handmaker, H.; Lowenstein, J. M. (eds.). Acton, MA; Publishing Sciences Group, Inc. (1975).

From symposium on nuclear medicine in pediatrics; San Francisco, California, USA (16 Feb 1973). See CONF-730235-.

Radionuclide imaging studies provide clinically useful information in children with abnormalities of CSF movement and absorption. Not only are the diagnostic considerations different from adults, but the technical ones are also. Further use of this diagnostic test in children with neurological problems is anticipated. (auth)

**26127** THYROID. Fisher, D. A.; Johnson, D. E. (Harbor General Hospital, Torrance, CA). pp 45-56 of Nuclear Medicine in Clinical Pediatrics. Handmaker, H.; Lowenstein, J. M. (eds.). Acton, MA; Publishing Sciences Group, Inc. (1975).

From symposium on nuclear medicine in pediatrics; San Francisco, California, USA (16 Feb 1973). See CONF-730235-.

In vivo thyroid function testing is conducted with isotopes of iodine, the rate-limiting substrate for thyroidal hormonogenesis, or with pertechnetate, an anion which the thyroid follicular cells will concentrate or trap similarly to iodide, but will not organify. The physical characteristics of these isotopes, their advantages or indications, their disadvantages, and the average radiation dose to the thyroid in the infant, child, and adult are reviewed. The latter is expressed as estimated dose in rads per microcurie administered assuming an uptake of 27 percent and a biological half-life of 68 days. For many years the standard isotope for thyroid studies has been $^{131}I$. This isotope, however, has the disadvantage of a high radiation dose to the gland, especially in infants and children. Furthermore the high-energy gamma ray (364 keV) requires low-efficiency, thick septal collimators for scanning. More recently $^{123}I$, $^{123}I$, and $^{99}$/sup m/Tc-pertechnetate have been used. (auth)

**26128** LUNG. DeNardo, G. L. (Univ. of California, Davis); Blankenship, W. J.; Burdine, J. A. Jr.; DeNardo, S. J. pp 57-68 of Nuclear Medicine in Clinical Pediatrics. Handmaker, H.; Lowenstein, J. M. (eds.). Acton, MA; Publishing Sciences Group, Inc. (1975).

From symposium on nuclear medicine in pediatrics; San Francisco, California, USA (16 Feb 1973). See CONF-730235-.

At present no simple statement can be made relative to the role of radionuclidic lung studies in the pediatric population. It is safe to assume that they will be used with increasing frequency for research and clinical applications because of their sensitivity and ready applicability to the pediatric patient. Methods comparable to those used in adults can be used in children older than 4 years. In younger children, however, a single injection of $^{133}Xe$ in solution provides an index of both regional perfusion and ventilation which is easier to accomplish. This method is particularly valuable in infants and neonates because it is rapid, requires no patient cooperation, results in a very low radiation dose, and can be repeated in serial studies. Radionuclidic studies of ventilation and perfusion can be performed in almost all children if the pediatrician and the nuclear medicine specialist have motivation and ingenuity. Spontaneous pulmonary vascular occlusive disease which occurs in infants and pulmonary emboli in children are easily detected using radionuclides. The pathophysiologic defects of pulmonary agenesis, bronchopulmonary sequestration, and foreign body aspiration may be demonstrated by these techniques. These techniques also appear to be useful in following patients with bronchial asthma, cystic fibrosis, congenital emphysema, and postinfection pulmonary abnormalities. (auth)

**26129** CARDIOVASCULAR: RADIOISOTOPIC ANGIOCARDIOGRAPHY. Kriss, J. P. (Stanford Medical Center, CA). pp 69-79 of Nuclear Medicine in Clinical Pediatrics. Handmaker, H.; Lowenstein, J. M. (eds.). Acton, MA; Publishing Sciences Group, Inc. (1975).

From symposium on nuclear medicine in pediatrics; San Francisco, California, USA (16 Feb 1973). See CONF-730235-.

Radioisotopic angiocardiography, performed after the intravenous injection of $^{99}$/sup m/Tc-labeled pertechnetate or albumin, is a simple, rapid, and safe procedure which permits identification and physiologic assessment of a wide variety of congenital and acquired cardiovascular lesions in infants and children. These include atrial and ventricular septal defect, tetralogy of Fallot, pulmonic stenosis, aortopulmonary window, transposition of the great vessels, valvular stenosis and/or insufficiency, myocardial lesions, and lesions of the great vessels. The simplicity of the procedure lends itself to repeated measurements to assess the effects of therapy or to follow the course of the disease. A wide spectrum of congenital and acquired cardiovascular diseases have been studied which have particular application to the pediatric age group. (auth)

**26130** CARDIOVASCULAR: SHUNT QUANTITATION. Ashburn, W. L. (Univ. of California, San Diego); Alazraki, N. P. pp 81-88 of Nuclear Medicine in Clinical Pediatrics. Handmaker, H.; Lowenstein, J. M. (eds.). Acton, MA; Publishing Sciences Group, Inc. (1975).

From symposium on nuclear medicine in pediatrics; San Francisco, California, USA (16 Feb 1973). See CONF-730235-.

It is clear that the use of radionuclide techniques in left-to-right shunt detection is relatively new and that many more patients must be studied to accumulate a reliable experience with these methods in order to select the best approach. Even so, it appears that radionuclide methods may prove to be excellent screening procedures for pediatric patients with heart murmurs of undetermined etiology as well as a tool for following pre- and postoperative shunt patients. We would not presume that these techniques will in any way replace cardiac catheterizations for complete diagnostic evaluation but rather they may be used to indicate the need for this more definitive, but necessarily more expensive and traumatic, procedure. (auth)

**26131** LIVER. Handmaker, H. (Children's Hospital of San Francisco). pp 89-101 of Nuclear Medicine in Clinical Pediatrics. Handmaker, H.; Lowenstein, J. M. (eds.). Acton, MA; Publishing Sciences Group, Inc. (1975).

From symposium on nuclear medicine in Pediatrics; San Francisco, California, USA (16 Feb 1973). See CONF-730235-.

Liver imaging techniques with presently available equipment can provide the pediatrician with valuable information about the size, shape, and integrity of the liver, and assist in assessing extent of abdominal masses. A variety of diseases have characteristic patterns, and these should be appreciated, particularly that of branching, dilated intrahepatic radicals. Cautious use of the $^{131}I$-RB study

can assist in further evaluation, particularly in the jaundiced child. Correlation with the clinical problem is essential to maximize the effectiveness of these studies. (auth)

**26132** SPLEEN. Freedman, G. S. (Yale Univ., New Haven). pp 103-116 of Nuclear Medicine in Clinical Pediatrics. Handmaker, H.; Lowenstein, J. M. (eds.). Acton, MA; Publishing Sciences Group, Inc. (1975).

From symposium on nuclear medicine in pediatrics; San Francisco, California, USA (16 Feb 1973). See CONF-730235-.

Careful examination of the left upper quadrant of the pediatric patient will usually disclose the presence or absence of an enlarged spleen. Although the spleen has a wide variation in weight and mobility, the normal spleen rarely extends below the left costal margin. While the presence of a palpable spleen is usually of pathological significance, the wide variation in splenic weight and position may make the detection of splenomegaly difficult on routine physical examination. When present, it may be difficult to differentiate the enlarged spleen from other palpable masses in the left upper quadrant. For these reasons, radionuclide imaging of the spleen has become a simple and valuable method for precisely locating and establishing the accurate size of functioning splenic tissue. The size and weight of the spleen can be approximated by direct measurement from the scan; normal values have been established based on the splenic length and the age and weight of the child. The diagnostic usefulness of radionuclide scanning of the spleen in lymphoma, leukemia, other malignancies, anemia and other blood dyscrasias, infectious diseases, granuloma, and cysts is discussed. (CH)

**26133** KIDNEY. Conway, J. J.; Filmer, R. B. (Children's Memorial Hospital, Chicago). pp 117-131 of Nuclear Medicine in Clinical Pediatrics. Handmaker, H.; Lowenstein, J. M. (eds.). Acton, MA; Publishing Sciences Group, Inc. (1975).

From symposium on nuclear medicine in pediatrics; San Francisco, California, USA (16 Feb 1973). See CONF-730235-.

An attempt is made to define the definitive indications for the use of renal imaging, renography, and radionuclide cystography in children. Limitations of space prohibit a comprehensive discussion of all of the criteria for such studies. The more common indications and uses of radionuclide scintiscanning are discussed. It is of importance to recognize the simplicity of these examinations which require no preparation, offer a minimum morbidity to the child, and in most instances produce less radiation burden than comparable roentgenographic techniques. The potential for research in the field of pediatric urology with such techniques is unlimited. Recognition of the usefulness of nuclear medicine techniques by the pediatrician and practicing clinician will increase as these studies become more available. (auth)

**26134** BONE. Bell, E. G. (Crouse-Irving Memorial Hospital, Syracuse, NY); Mahon, D. F. pp 133-148 of Nuclear Medicine in Clinical Pediatrics. Handmaker, H.; Lowenstein, J. M. (eds.). Acton, MA; Publishing Sciences Group, Inc. (1975).

From symposium on nuclear medicine in pediatrics; San Francisco, California, USA (16 Feb 1973). See CONF-730235-.

Bone scanning provides information on the extent of primary bone tumors, on possible metastatic disease, on the presence of osteomyelitis prior to observation of roentgenographic changes so that earlier therapy is possible, on the presence of collagen diseases, on the presence of fractures not disclosed by x-ray films, and on the evaluation of aseptic necrosis. However, the total effect and contribution of bone scanning to the diagnosis, treatment, and ultimate prognosis of pediatric skeletal diseases is, as yet, unknown. (auth)

**26135** TUMOR. Morita, E. T. (Mount Zion Hospital and Medical Center, San Francisco). pp 149-156 of Nuclear Medicine in Clinical Pediatrics. Handmaker, H.; Lowenstein, J. M. (eds.). Acton, MA; Publishing Sciences Group, Inc. (1975).

From symposium on nuclear medicine in pediatrics; San Francisco, California, USA (16 Feb 1973). See CONF-730235-.

In addition to the actual staging procedure in childhood tumors and the search for metastases at a later date, radionuclide studies are useful in patients who are predisposed to certain tumors. Imaging procedures offer a relatively noninvasive means by which a primary tumor and evidence of nodal or distant metastasis can be assessed. Nodal involvement is difficult to assess except for those which take up material actively such as $^{131}I$ in thyroid carcinoma and $^{67}Ga$-citrate in lymphomas. Those patients in whom tumors have a familial relationship or predisposition can be evaluated. (auth)

**26136** HEMATOLOGY. Price, D. C.; Ries, C. (Univ. of California, San Francisco). pp 157-185 of Nuclear Medicine in Clinical Pediatrics. Handmaker, H.; Lowenstein, J. M. (eds.). Acton, MA; Publishing Sciences Group, Inc. (1975).

From symposium on nuclear medicine in pediatrics; San Francisco, California, USA (16 Feb 1973). See CONF-730235-.

This paper reviews the wide variety of radioisotopic techniques available to pediatricians in hematologic evaluation of their patients, with comments on the tracer techniques, and an indication of some new territory in splenic evaluation and nonradioactive tracers which may prove to be of considerable interest in the future. The only differences in applying these techniques to the pediatric population, compared with the adult population, lie in the different spectrum of hematologic diseases under consideration in this age group and the greater sensitivity to problems of radiation exposure which the pediatrician and the nuclear medicine physician must have in administering the isotopes in vivo. With these considerations in mind, the usefulness of such radioisotopic techniques in the evaluation of pediatric hematologic disease remains unquestionable. Radiopharmaceuticals and the radiation doses associated with the various procedures are listed. It is hoped in the future that fluorescent excitation techniques will replace at least some of the radioisotope techniques, obviating all considerations of patient irradiation in such instances. (auth)

**26137** IN VITRO STUDIES: DIGOXIN. Lowenstein, J. M. (Pacific Medical Center, San Francisco). pp 187-191 of Nuclear Medicine in Clinical Pediatrics. Handmaker, H.; Lowenstein, J. M. (eds.). Acton, MA; Publishing Sciences Group, Inc. (1975).

From symposium on nuclear medicine in pediatrics; San Francisco, California, USA (16 Feb 1973). See CONF-730235-.

Radioimmunoassay is an ideal application of nuclear medicine to pediatrics, making it possible to measure nanogram and picogram quantities of compounds in the serum. The digoxin RIA is illustrative of the problems and applications of the technique. Both dose and serum levels of digoxin are higher (on a weight basis) in infants and children than in adults. Because of the narrow therapeutic range of digoxin and its dangerous toxicity, and with the variability introduced with age, metabolic factors, absorption, and compliance, digoxin RIA has become indispensable to the cardiologist. (auth)

**26138** IN VITRO STUDIES: ENDOCRINOLOGICAL. Kaplan, S. L. (Univ. of California, San Francisco). pp 193-201 of Nuclear Medicine in Clinical Pediatrics. Handmaker, H.; Lowenstein, J. M. (eds.). Acton, MA; Publishing Sciences Group, Inc. (1975).

From symposium on nuclear medicine in pediatrics; San Francisco, California, USA (16 Feb 1973). See CONF-730235-.

The availability of sensitive radioimmunoassays for protein and steroid hormones which require small volumes of plasma (50 mu l 1 ml) have provided a means to assess a variety of endocrine disorders in children. All radioimmunoassay procedures are based on the interaction of radioactive-labeled and unlabeled hormone with a hormone-specific antiserum. Iodine-131 or $^{125}I$ are used for labeling protein hormones and $^{3}H$ for steroid hormones. (auth)

**26139** CLINICAL EXPERIENCE IN A CHILDREN'S HOSPITAL. Gliday, D. L. (Hospital for Sick Children, Toronto). pp 203-208 of Nuclear Medicine in Clinical Pediatrics. Handmaker, H.; Lowenstein, J. M. (eds.). Acton, MA; Publishing Sciences Group, Inc. (1975).

From symposium on nuclear medicine in pediatrics; San Francisco, California, USA (16 Feb 1973). See CONF-730235).

Experience indicates that there is a much higher information yield from integrated, rather than separate, interpretations of radiological and nuclear medical procedures. Daily review of this integrated material by the resident staff has facilitated a continuous critical appraisal and rapid accumulation of a pool of relevant experience. This has permitted us to quickly develop the criteria necessary to make accurate and significant nuclear medical diagnoses in pediatric patients. (auth)

**26140** NEW HORIZONS. Handmaker, H. (Children's Hospital of San Francisco). pp 261-267 of Nuclear Medicine in Clinical Pediatrics. Handmaker, H.; Lowenstein, J. M. (eds.). Acton, MA; Publishing Sciences Group, Inc. (1975).

From symposium on nuclear medicine in pediatrics; San Francisco, California, USA (16 Feb 1973). See CONF-730235-.

The diagnostic value of radionuclide scintiscanning in pediatric patients is discussed and new diagnostic advances are predicted. (CH)

**26141** GALLIUM CITRATE Ga 67 SCANS IN FEBRILE PATIENTS. Habibian, M. R.; Staab, E. V.; Matthews, H. A. (Univ. of North Carolina, Chapel Hill). J. Am. Med. Assoc.; 233: No. 10, 1073-1076(8 Sep 1975).

Scanning with gallium citrate Ga 67 is a sensitive technique for the detection of localized inflammatory disease. In a group of 22 febrile patients, 17 had one or more abnormal areas of radioactive gallium localization. Eight patients showed localized areas of inflammation; five showed no area of local inflammation within the field of the scan. The remaining patients had excellent clinical and laboratory confirmation of neoplastic or inflammatory disease. These cases illustrate the usefulness of radioactive gallium in

febrile patients in whom the cause of the fever cannot be otherwise determined. (auth)

**26142** TUMOR SCANNING WITH GALLIUM 67. Andrews, G. A.; Edwards, C. L. (Oak Ridge Associated Universities, TN). J. Am. Med. Assoc.; 233: No. 10, 1100-1103(8 Sep 1975).

A brief history of the medical uses of $^{67}Ga$ is given. The scanning procedure is described and the concentration of the isotope in various tissues and organs is discussed. The usefulness of $^{67}Ga$ in studying various types of clinical situations, including cancer, is discussed. The advantages of $^{67}Ga$ over other radioisotopes in whole-body scanning are emphasized. (HLW)

**26143** SIMPLE RADIOIMMUNOASSAY FOR UNCONJUGATED ESTRIOL IN PREGNANCY PLASMA. Kao, M.; Braunstein, G.; Rasor, J.; Horton, R. (Univ. of California, Los Angeles). J. Lab. Clin. Med.; 86: No. 3, 513-520(Sep 1975).

A simple and specific radioimmunoassay (RIA) for the measurement of plasma or serum unconjugated estriol ($E_3$) in pregnancy is described for general laboratory use. Two different antibodies utilized had low cross-reaction to estrone ($E_1$) and estradiol-17 beta ($E_2$). With either of these antibody reagents, a method was designed that requires only an extraction step using a specific solvent mixture of ethyl acetate and n-hexane (3:2, v/v), one-hour incubation with working antibody, and separation of bound from free $E_3$ by ammonium sulfate. Standard curves useful in the range of 0 to 2000 pg were obtained. This assay, requiring only 0.05 ml of plasma, can be completed within 4 hours. The sensitivity of this RIA was 10 pg. The intra- and interassay coefficients of variation (CV) were 5.0 and 9.4 percent, respectively. When $E_3$ determinations by this method are compared with RIA values by a more complicated technique using Celite column chromatography, the results are not significantly different. There was a good correlation between our RIA and a standard urine $E_3$ determination (n equals 137, r equals 0.82, p less than 0.001). Using our simplified method, the mean plasma $E_3$ during pregnancy was 1.0 +- 0.6 ng. per milliliter at 10 weeks, 2.3 +- 0.6 ng. per milliliter at 20 weeks, 6.5 +- 1.4 ng. per milliliter at 30 weeks, and 16.5 +- 5.1 ng. per milliliter at term. Since the serum RIA reflects changes in free $E_3$ which has a shorter half-life than conjugated $E_3$, this rapid and simple method is attractive as an approach to monitor fetal-placental function. (auth)

**26144** INTERLABORATORY REPRODUCIBILITY OF GASTRIN MEASUREMENTS BY RADIOIMMUNOASSAY. Rayford, P.; Reeder, D. D.; Thompson, J. C. (Univ. of Texas, Galveston). J. Lab. Clin. Med.; 86: No. 3, 521-527(Sep 1975).

A collaborative study was conducted to determine interlaboratory variations in the measurement of gastrin by radioimmunoassay (RIA). A kit containing reagents for a communal RIA method, as well as test samples containing different amounts of human synthetic gastrin (SHG I) and test samples of serum from a fasting normal patient admixed with varying volumes of serum from a patient with the Zollinger-Ellison syndrome, was sent to each collaborating investigator. Each investigator was requested to measure the gastrin concentrations in test samples by means of the communal RIA method, as well as the RIA method utilized in his or her laboratory. Use of the communal RIA method resulted in no significant interlaboratory variation in the determination of gastrin concentration in SHG I test samples and a maximum two- to threefold variation in determination of gastrin serum test samples. In contrast, when individual RIA methods were used to measure gastrin concentrations, the amount of SHG I in test samples reported by one laboratory was significantly different than that reported by the other three. In addition, use of different RIA methods resulted in a 2- to 19-fold interlaboratory variation in serum gastrin measurements and the maximum variation was found when the gastrin in normal fasting serum was measured. Increased variations in results, when different RIA methods were used, may be due to differences in preparation and purification of labeled antigen, to differences in separation of bound from free hormone, and to differences in the antibodies themselves. (auth)

**26145** HEART SCANNING WITH $^{99m}Tc$-LABELED ALBUMIN MICROAGGREGATES. Chazov, E. I.; Kramer, A. A.; Malyshev, Yu. M.; Kulikov, L. M.; Mazaev, A. V.; Ivanov, K. M.; Ruda, M. Ya. (Inst. of Cardiology, Moscow). Kardiologiya; 13: No. 1, 11-16(Jan 1973). (In Russian).

The present paper is devoted to the study of possibilities of clinical use of the heart scanning with albumin microaggregates to assess the blood supply of myocardium. The authors used albumin microaggregates 45 ± 5 microns in diameter labelled with $^{99m}Tc$ which were introduced through a catheter into the coronary arteries of the heart. The experiments have been carried out on four dogs. Absence of ECG changes after intracoronary administration of albumin microaggregates and good informative data on scanograms permitted the authors to pass over to clinical investigations. During coronography, eight patients received $^{99m}Tc$-labeled albumin microaggregates into coronary arteries of the heart, which was then scanned. The authors succeeded in showing the safety of intracoronary administration of $^{99m}Tc$-labeled albumin microaggregates. Distribution of AMA corresponds to the blood flow in the arterial capillary bed of myocardium and permits to detect such areas as are poorly supplied. The method pro- . vides a visual idea of presence, amplitude localization of ischemic areas, and even of the degree of ischemization. (auth)

**26146** DIFFERENTIAL DIAGNOSIS OF TUMORS OF THE SALIVARY GLANDS WITH RADIOACTIVE ISOTOPES. Garcia, R. R. (Clinica Puerto de Hierro de la Seguridad Social, Madrid). Int. J. Oral Surg.; 3: No. 5, 330-334(1974).

The paper describes the author's experience using citrate of $^{67}Ga$ to diagnose malignant tumorous diseases, specifically those of the salivary glands. Present theories of the mechanism by which the $^{67}Ga$ deposit is produced are evaluated. Using 2 mCi intravenously and performing the study after 48 hours, 7,090 positive results were obtained in the malignant tumors, but it must be stated that positive results were also obtained in benign tumors as well as in non-tumorous malignant and benign diseases. Scintigraphy with $^{67}Ga$ was combined with gammagraphy with $^{99m}Tc$, and cols nodules or empty areas were revealed by the latter radioisotope, while malignant tumors were detected by $^{67}Ga$. (auth)

**26147** PEG TEST: A NEW RADIOIMMUNOASSAY FOR THE DETECTION OF HEPATITIS B ANTIGEN. Lambert, P. H.; Triboilet, E.; Knoepfel, M.; Madalinski, K.; Miescher, P. A. Schweiz. Med. Wochenschr.; 104: 128-129(26 Jan 1974).

A new radioimmunoassay for hepatitis B antigen (HBAg) is described. Test sera are mixed with $^{125}I$-Fab fragments isolated from purified anti HBAg antibody. Free $^{125}I$-Fab was separated from HBAg-bound $^{125}I$-Fab by precipitation with polyethylene glycol (PEG) at 10%. This method proved very sensitive and applicable to the detection of HBAg even in presence of antibody excess. It is not susceptible to the effect of anti-Fc antiglobulins. (auth)

**26148** FOUR-HOUR DOUBLE ANTIBODY RADIOIMMUNOASSAY FOR HUMAN LH: STUDY OF THE KINETICS OF THE REACTIONS. Vekemans, M.; Robyn, C. (Univ. Libre, Brussels). Eur. J. Obstet., Gynecol. Reprod. Biol.; 4: No. 3, 111-123(1974).

The dynamics of the immunological reactions involved in a double antibody radioimmunoassay for HLH were investigated in order to set up a rapid assay. Classically, assays are conducted in 5 or 6 days at 4°C. Shortening the incubation of unlabelled HLH with anti-HCG serum decreases the sensitivity of the assay, whereas reduction of the second incubation with labelled HCG enhances it. However, a too short second incubation results in insufficient binding of the labelled hormone. With first and second incubations of 2 and 1 hours respectively, 10mIU of HLH decrease the amount of labelled hormone bound to the antibody by 35%. Immunoprecipitation of the hormone antihormone complexes by the second antibody was faster in buffer containing 20% human serum than in buffer alone: respectively 80 to 10% of precipitation are obtained within 1 hour. A rapid radioimmunoassay was standardized, reducing the three incubations to 2, 1, and 1 hours, respectively. All incubations were conducted at 37°C. Sensitivity varied around 1.5 mIU. Index of precision was 0.19. Within and between assay variations were 13.0 and 14.6%. Results obtained with classical and rapid assays were highly correlated. (auth)

**26149** RADIOISOTOPE STUDIES IN PRIMARY HYPOTHYROIDISM. Sheiretova, E.; Peshev, N.; Ivanov, Zh. Vutr. Boles.; 13: No. 4, 58-61(1974). (In Russian).

Fifty patients with primary myxedema after radio-iodine treatment and operative intervention are examined. The following radioisotope methods were used in making the diagnosis: $^{131}I$ cummulation, protein bound radio-iodine in serum and conversion index, Hamolsky test, and thyroscintigraphy. The high diagnostic value of the complex investigation of the organic and non-organic phase of iodine metabolism is underlined. An accelerated hormonesynthesis was established in 15 per cent of the patients examined, that might be explained as a manifestation of a compensatory reaction due to elevated endogenic thyrotropic stimulation and radical reconstruction of the intrathyroid iodine metabolism in cases of residual thyroid parenchyma. (auth)

**26150** DETERMINATION OF DIGOXIN LEVELS IN BLOOD BY THE RADIOIMMUNOASSAY METHOD. Maitre Azcarate, M. J.; de Artaza Andrade, M.; Marquez Montes, J.; Martin Judez, V.; Fernandez de Miguel, J. M.; Valles Belsue, F.; Arnaiz, A.; Botello, A. (Clinica Puerta de Hierro, Spain). Rev. Esp. Cardiol.; 27: No. 3, 245-250(1974). (In Spanish).

Using radioimmunoassay techniques with tagged digoxin, the digoxin levels were determined in blood samples from three groups of patients: A) patients with a good response to digitalis

treatment; B) patients with signs of digitalis intoxication, and C) patients in whom the digitalis treatment was insufficient to obtain a good clinical response. We found that the blood digoxin levels were from 1 to 2 μg/ml in group A, above 2 μg/ml in group B, and from 0.5 to 0.9 μg/ml in group C. Since these patients were selected excluding any factors that might alter glycoside metabolism, we assume that the figures in group A are optimal for proper myocardial impregnation and that levels above 2 μg/ml are capable of producing digitalis intoxication. These values are in good correlation with those obtained by other authors. (auth)

# MATERIALS

**26151** (RISO-320, pp 12-60) SOLID STATE PHYSICS (NEUTRON SCATTERING). Dec 1974.

In Physics Department annual progress report, 1 January–31 December 1974.

Studied were: spin waves in terbium (magnetic anisotropy, magnon–phonon interaction); molecular field calculation of magnetic structures in Er; theory of exchange interaction and magnon spectrum in Gd, magnetic moments in Tb–Tm alloys; magnetic ordering in dhcp Pr and in Pr–Nd alloys; critical temperature of alloys with two order parameters, magnetic excitations and excitons in Pr, coupling between magnetic excitations and phonons in Pr, magnetic form factor of Pr–26% Nd; crystal fields in Er–96% Y, ErSb, NdN, $REAl_2$; magnetic properties of $LiTbF_4$; antiferromagnetism in $HoPO_4$; magnetic properties of $MnNb_2O_6$; canonical bands of bcc metals; electronic structure of metals; lattice dynamics of $Cu_2O$; phase transition in $C_{10}F_8$; neutron scattering in $C_2F_6$; phase transition in solid DCN; structure and dynamics of $H_2$ adsorbed on graphite; neutron scattering in solid $H_2$ under pressure and in liquid $H_2$ and $N_2$; convective fluctuations in nematic para-azoxyanisol; structure of amorphous solid $D_2O$; structure of the high-pressure $TeO_2$ phase; pressure dependence of the Neel temperature of Cr; structure of Se crystals; Debye–Waller factor of MgO; and neutron slowing-down by Bragg reflection from a moving single crystal. (DLC)

## Ceramics and Cermets

*Refer also to abstracts 25735, 26185, 26203, 26242, 26266, 26300, 26941, 26942, 26946, 26950, 26952, 26953, 27244, 27259, 27298, 27423, 27427, 27432–27434, and 27436.*

**26152** (CONF-701074-P2, pp 292-307) ANALYSIS OF SINTERING OF URANIUM DIOXIDE AT LOW TEMPERATURES. Marion, I.; Daskelu, G. 1970. Translated from Trudy Nauchno-Tekhnicheskoi Konferentsii "Atomnaya Energetika, Toplivnye Tsikly, Radiatsionnoe Materialovedenie", Ul'yanovsk, 5–10 Oktyabrya 1970 G. Vol. II.

From conference on atomic power, fuel cycles, and radiation study of materials; Ul'yanovsk, USSR (5 Oct 1970).

In proceedings of the scientific-technical conference "atomic power, fuel cycles, radiation study of materials".

The effects of sintering on the properties of $UO_2$ fuel pellets were examined. It was found that uranyl nitrate concentration in the ADU precipitation solution should be no more than 140 g/l. The optimum calcination and reduction temperature for the ADU is 550°C. The optimum O/U ratio is 2.3. Additions of $TiO_2$ at 0.01 to 0.06% promote sintering and high density using these processing guidelines, $UO_2$ pellets can be sintered to a density of 10.4 to 10.5 g/cm³ at 1300°C. (JRD)

**26153** (DP-Report-752) HIGH TEMPERATURE GRAPHITE IRRADIATION CREEP EXPERIMENT IN THE DRAGON REACTOR. Dragon Project Report. Manzel, R.; Everett, M. R.; Graham, L. W. (UKAEA Reactor Group, Winfrith. Atomic Energy Establishment). May 1971. 34p. Dep. NTIS (US Sales Only) $7.00.

The irradiation induced creep of pressed Gilsocarbon graphite under constant tensile stress has been investigated in an experiment carried out in FE 317 of the OECD High Temperature Gas Cooled Reactor "Dragon" at Winfrith (England). The experiment covered a temperature range of 850°C to 1240°C and reached a maximum fast neutron dose of $1.19 \times 10^{21}$ n cm$^{-2}$ NDE (Nickel Dose DIDO Equivalent). Irradiation induced dimensional changes of a string of unrestrained graphite specimens stressed to 40%, 58% and 70% of the initial ultimate tensile strength of pressed Gilsocarbon graphite. Total creep strains ranging from 0.18% to 1.25% have been measured and a linear dependence of creep strain on applied stress was observed. Mechanical property measurements carried out before and after irradiation demonstrate that Gilsocarbon graphite can accommodate significant creep strains without failure or structural deterioration. Total creep strains are in excellent agreement with other data, however the results indicate a relatively large, temperature-dependent, primary creep component which at 1200°C approaches a value three times larger than the normally assumed initial elastic strain. Secondary creep constants derived from the experiment show a temperature dependence and are in fair agreement with data reported elsewhere. A possible interpretation of the results is given. (auth)

**26154** ELECTRON-DIFFRACTION AND X—RAY DIFFRACTION STUDY OF RARE EARTH METAL OXIDES IN THIN FILMS. Kashaev, A.A.; Ushchapovskii, L.V.; Il'in, A.G. (Irkutsk State Pedagogical Institute). Sov. Phys.—Crystallogr. 20: No. 1, 114-115 (July 1975).

A number of rare earth metal oxide thin films were investigated via electron diffraction and x-ray diffraction. An fcc phase was found which upon heating transformed to bcc. (AIP)

**26155** ENHANCEMENT OF THE EXCHANGE INTERACTION IN $Eu_{1-x}Sm_xS$ SOLID SOLUTIONS WITH SEMICONDUCTING CONDUCTION. Samokhvalov, A.A.; Arbuzova, T.I.; Afanas'ev, A.Ya.; Babushkin, V.S.; Loshkareva, N.N.; Morozov, Yu.N.; Simonova, M.I.; Bamburov, V.G.; Lobachevskaya, N.I. (Institute of Metal Physics, Ural Scientific Center, Academy of Sciences of the USSR, Sverdlovsk). Sov. Phys.—Solid State 17: No. 1, 26-28 (July 1975).

An investigation was made of the magnetic, electrical, and optical properties of $Eu_{1-x}Sm_xS$ solid solutions. Measurements of the magnetization, paramagnetic susceptibility, electron spin resonance, electrical conductivity, and diffuse reflection yielded information on the exchange interaction and electron conduction in $Eu_{1-x}Sm_xS$. Possible causes of the observed enhancement of the exchange interaction in $Eu_{1-x}Sm_xS$ were considered. The $Eu_{1-x}Sm_xS$ solid solutions were used as an example to demonstrate the possibility of increasing the Curie temperature of europium chalcogenides while retaining their semiconducting properties. (auth)

**26156** X—RAY K EMISSION SPECTRA OF VANADIUM IN ITS OXIDES. Cherkashenko, V.M.; Kurmaev, É.Z.; Fotiev, A.A.; Volkov, V.L. (Institute of Metal Physics, Institute of Chemistry, Ural Scientific Center, Academy of Sciences of the USSR, Sverdlovsk). Sov. Phys.—Solid State 17: No. 1, 167-170 (July 1975).

An investigation was made of the $K\beta'$ and $K\beta_5$ emission bands of vanadium in the oxides VO, $V_2O_3$, $VO_2$, and $V_2O_5$, in the series $V_nO_{2n-1}$ (n=3, 4, 6) and $V_nO_{2n+1}$ (n=3, 6), and in amorphous vanadium pentoxide. The maxima of the $K\beta'$ and $K\beta_5$ bands shifted in the direction of higher energies with increasing degree of oxidation of vanadium. Broadening of these bands exhibited by some of the $V_nO_{2n-1}$ oxides (n=3, 4, 6) indicated that vanadium ions existed in two oxidation states: $V^{3+}$ and $V^{4+}$. This band broadening was not observed for the oxides $V_6O_{13}$ and $V_3O_7$. (auth)

**26157** THE CHANGE IN THE STRUCTURE OF ZINC SULFIDE FILMS DUE TO ELECTRON BOMBARDMENT AND LASER RADIATION. Amigud, Z.G.; Bolotov, I.E.; Bragin, F.I.; Rabinovich, L.V.; Fisheleva, S.B. Sov. J. Opt. Technol. 42: No. 1, 37-39 (Jan 1975).

The different stages in the destruction of zinc sulfide films, subjected to electron bombardment (~60 keV) and laser radiation, are examined. Under the action of laser radiation destruction begins with the formation of isolated microcraters, located in a recrystallized amorphous film. Bombardment of the films with an electron beam of sufficient intensity also causes recrystallization and subsequent destruction. (auth)

**26158** CHEMICAL EFFECT ON X-RAY K-ABSORPTION EDGES OF MANGANESE, CHROMIUM, AND VANADIUM. Asada, E. (National Chemical Lab. for Industry, Tokyo (Japan)). Chem. Lett. (Tokyo); No. 12, 1467-1472 (Dec 1974).

The narrow absorption peak appearing on the lower energy side of the K-absorption edges of manganese, chromium, and vanadium in the form of oxides was specially investigated. The appearance of this peak depends on the oxidation number of metal atoms, rather than on their coordination number. (auth)

**26159** ESR STUDIES ON PARAMAGNETIC DEFECT CENTERS PRODUCED IN GaP BY $N^+$-ION IMPLANTATION. Matsumori, T.; Miyazaki, K. (Tokai Univ., Tokyo (Japan). Faculty of Engineering). Tokai Daigaku Kiyo Kogakubu; 1974: No. 1, 35-48 (Nov 1974). (In Japanese).

$N^+$ ions are implanted in p-type GaP crystals grown up from the liquid phase and resulting defect centers are measured by use of an ESR spectrometer. Implantation of $N^+$ ions is made in the A-(111) and B-($\bar{1}\bar{1}\bar{1}$) faces on the substrates with $10^{16}$ ions/cm² at 200 keV at room temperature. The ESR spectra are measured at 77°K using an X-band microwave spectrometer. Before annealing, the g-value takes $2.0032 \pm 0.0004$, the half-width of the signal about 7 gauss, and the spin density $4.5 \times 10^{18}$ spins/cm³. This center disappears after annealing at 450°K. The annealing behavior has two stages, which take the activation energies of about 0.23 eV and 0.30 eV, respectively. (auth)

**26160** YOUNG'S MODULI OF COMPACT MATRICES FOR HTGR FUEL. Kikuchi, A.; Iwamoto, K. (Japan Atomic Energy Research Inst., Tokai, Ibaraki. Tokai Research Establishment). J. Nucl. Sci. Technol. (Tokyo); 12: No. 3, 174-180 (Mar 1975).

Young's moduli of matrices of compacted graphite samples were determined from measured values of ultrasonic-wave propagation through the sample at room temperature. The results were analyzed with particular interest directed to the effects of differences in matrix density and graphite orientation on the propa-

gation velocity, from which the modulus was calculated. The value of Young's modulus increased with binder content in the matrices constituted uniquely of one kind of graphite material, while in the case of composite matrices embodying a mixture of petroleum coke graphite and natural graphite, the modulus decreased with increasing natural graphite content. The velocity of ultrasonic-wave propagation—from which the value of Young's modulus is derived—depends on the density alone in isotropic matrices prepared from milled isotropic coke graphite, whereas in anisotropic matrices embodying needle coke graphite it depends on graphite orientation as well as on density. The contributions of density ($\rho$) and of reflective intensity ratio (IR) to the propagation velocity (V) are expressed $\Delta V = a(\Delta\rho)^n$ and $\Delta V = b(\Delta IR)$, where the symbol $\Delta$ indicates increment, while a, b and n are constants depending upon the characteristics of the compact matrix. (auth)

**26161** STUDIES ON THERMAL SHOCK RESISTANCE OF SEVERAL KINDS OF GRAPHITE. Sato, S.; Imamura, Y. (Ibaraki Univ., Hitachi (Japan). Faculty of Engineering); Sato, K.; Kon, J. Zairyo; 24: No. 258, 221-226(Mar 1975). (In Japanese).

A technique is presented to determine the thermal shock resistance of graphite by the basic analysis of nonsteady thermal stress in a circular disk heated by an arc discharge at its central area. The thermal shock resistance, defined as $\Delta = \sigma_\theta k/E\alpha$, ($\sigma_\theta$: circumferential tensile thermal stress, k: thermal conductivity, E: Young's modulus, $\alpha$: thermal expansion coefficient), can be determined en bloc only by measuring the arc discharge electric power using the specific nondimensional thermal stress $S_*$ which is calculated theoretically as the maximum saturation stress in the non-dimensional diffusion time $\tau > 1/4$. This technique is also applicable to measure simultaneously the thermal diffusivity $\kappa = k/c\rho$ (c: specific heat, $\rho$: density). The experimental studies for several kinds of graphite were carried out and the results were compared with the values of $\sigma_\theta k/E\alpha$ and $k/c\rho$ estimated indirectly from these individual mechanical and physical properties. (auth)

**26162** PHASE TRANSITION AND SWITCHING IN PYROLYTIC $VO_2$ FILMS. Serbinov, I. A.; Ryabova, L. A.; Savitskaya, Ya. S. (Inst. of Radio Engineering and Electronics, Moscow). Thin Solid Films; 27: No. 1, 171-176 (May 1975).

$VO_2$ films about 3,000 Å thick were prepared by the pyrolysis of vanadile acetylacetonate $(C_5H_7O_2)_2VO$. The changes in the electrical, optical and structural properties of the films during the phase transition have been investigated. Various switching effects in $VO_2$ films were also studied. (auth)

**26163** OPTICAL PROPERTIES OF PRASEODYMIUM OXIDE FILMS. Goswami, A.; Goswami, A. P. (National Chemical Lab., Poona). Thin Solid Films; 27: No. 1, 123-128 (May 1975).

The refractive index $n_f$, absorption index $k_f$ and absorption coefficient $\alpha$ of vacuum-deposited films of praseodymium oxide prepared under different conditions have been evaluated from the transmittance T data at different wavelengths in the visible region. The optical energy gap was estimated to be approximately 3.40 eV. (auth)

**26164** "SELECTION RULE" FOR IRREDUCIBLE REPRESENTATIONS INDUCING SECOND-ORDER PHASE TRANSITIONS IN MAGNETIC STRUCTURES. Michelson, A. (Department of Physics, Technion-Israel Institute of Technology, Haifa, Israel). Phys. Rev. B 12: No. 3, 1071-1075 (1 Aug 1975).

Besides the restrictions imposed on the possible symmetry changes occurring in magnetic second-order phase transitions by the Landau theory, an additional restriction exists due to the specific form of the density function involved in these transitions. This restriction is presented as a "selection rule" for irreducible representations of the space group of the high-symmetry phase inducing the phase transitions. A general mathematical form of this selection rule is derived differing from that obtained by Kovalev. The role of crystal structure type in this rule is investigated, and results concerning some particular structure types are obtained. Prediction of magnetic symmetry of ferromagnetic Eu compounds is made. (auth)

**26165** ACOUSTIC-SURFACE-WAVE VELOCITY DECREASE PRODUCED BY ION IMPLANTATION IN LITHIUM NIOBATE. Hartemann, P. (Thomson-CSF Research Center, Domaine de Corbeville, 91401 Orsay, France). Appl. Phys. Lett. 27: No. 5, 263-265 (1 Sept 1975).

Ion implantation was found to reduce the velocity of an acoustic surface wave propagating in lithium niobate. This frequency-dependent decrease may be mainly attributed to a reduction of the effective electromechanical coupling coefficient as reported in this letter. The impedance of 138-MHz interdigital transducers deposited on implanted niobate substrates has been determined versus ion dose. (auth)

**26166** NEW OSCILLATION PHENOMENA IN $VO_2$ CRYSTALS. Taketa, Y.; Kato, F.; Nitta, M.; Haradome, M. (The Physical Science Laboratories, Nihon University at Narashino, 7-24-1 Narashino-Dai, Funabashi, Chiba-Ken, Japan). Appl. Phys. Lett. 27: No. 4, 212-214 (15 Aug 1975).

New oscillation phenomena in $VO_2$ crystals were observed. The oscillation is generated in the temperature region of the crystal transition, and its voltage and frequency depend upon the ambient temperature. The waveform of the oscillation is a rectangular pulse. (auth)

**26167** TUNNELING CONDUCTIVITY IN 4*Hb*-$TaS_2$. Wattamaniuk, W.J.; Tidman, J.P.; Frindt, R.F. (Department of Physics, Simon Fraser University, Burnaby, British Columbia, Canada V5A 1S6). Phys. Rev. Lett. 35: No. 1, 62-65 (7 July 1975).

A $T^2$ behavior for the conductivity across the layers is observed in 4*Hb*-$TaS_2$ crystals below 35 *K*. This indicates that tunneling occurs between metallic layers separated by an insulating layer. Evidence for thermally activated hopping is observed at higher temperatures. (auth)

**26168** THE EFFECTS OF RADIATION-INDUCED DISPLACEMENT DAMAGE ON IMPURITY CONDUCTION IN GALLIUM ARSENIDE. Berg, N.J. (Harry Diamond Laboratories, Washington, D. C. 20438); Lieberman, A.G. J. Appl. Phys. 46: No. 8, 3475-3482 (Aug 1975).

The effects of $^{60}$Co $\gamma$-ray and high-energy neutron displacement damage on impurity conduction in epitaxial gallium arsenide were investigated. The activation energy ($\epsilon_2$) associated with the transition regime of the impurity conduction process was found to increase by a factor of 5 as a result of $^{60}$Co $\gamma$ irradiation, and only by a factor of 1.6 for a comparable neutron irradiation. In addition, the ratio of the Hall carrier density at low and high temperatures, $(n_H)_4\,_K/(n_H)_{300\,K}$, decreased by a larger amount for $^{60}$Co $\gamma$ irradiation than for neutron irradiation. The effects of neutron irradiation are explained in terms of increased compensation. For the case of $^{60}$Co $\gamma$ irradiation, it is postulated that a new donor level is introduced which does not participate in the impurity conduction process. In addition, with respect to the impurity conduction process, it is found that $\epsilon_2$ is proportional to $\epsilon_1$ (the conduction-band activation energy) and varies inversely with neutral donor spacing in accord with the model proposed by Mikoshiba. Also $\rho_{3\epsilon}$, the hopping regime resistivity, is found to vary inversely with the square of the free-carrier concentration and exponentially with the quantity $0.6/N_D^{1/3}a$. (auth)

**26169** ELECTRON-ENERGY LOSSES IN SILICON: BULK AND SURFACE PLASMONS AND ČERENKOV RADIATION. Chen, C.H.; Silcox, J.; Vincent, R. (School of Applied and Engineering Physics, Clark Hall, Cornell University, Ithaca, New York 14850). Phys. Rev. B 12: No. 1, 64-71 (1 July 1975).

Characteristic electron-energy-loss processes in crystalline silicon foils are examined for scattering angles less than $2.5 \times 10^{-4}$ rad. The relatively high energy of the electron beam (75 keV), combined with a low angular divergence ($8 \times 10^{-6}$ rad), allows identification of retardation effects in both volume and surface excitations. The results are consistent with complete probability distribution maps, calculated as a function of energy loss $\hbar\omega$ and scattering angle $\theta$, using recent optical data for the dielectric constants of Si. The half-width of the angular intensity distribution in the volume plasmon ($\hbar\omega_p = 16.6$ eV) agrees with the theoretical value to within 3%. Below 4 eV ($\epsilon_1 > 10$), a dispersive peak in the loss spectrum is observed which is interpreted as a volume loss due to Čerenkov radiation for $\theta \geq 5 \times 10^{-5}$ rad, and which, at small angles, transforms into multiple surface modes propagating parallel to the specimen surface in a waveguide fashion. Between 4.3 eV and $\hbar\omega_p = 16.6$ eV ($\epsilon_1$ negative), the prominent excitation is the surface plasmon in which the wave fields decay exponentially on both sides of the surface. The dispersion follows the light line and then approaches an asymptotic energy (8.2 eV) which is less than the energy calculated for a clean Si surface ($\hbar\omega_s = 11.0$ eV), but dispersion curves calculated for 20- and 50-Å $SiO_x$ ($x \simeq 1.5$) approximately fit the data. (auth)

**26170** FREE-TO-BOUND TRANSITION IN $\beta$-SiC DOPED WITH BORON. Kuwabara, H.; Yamada, S. (Shizuoka Univ., Hamamatsu, Japan). Phys. Status Solidi (a); 30: No. 2, 739-746(16 Aug 1975).

There are two series of infrared emission bands in $\beta$-SiC doped with boron. One of them is predominant at lower temperatures and has already been assigned to be due to the nitrogen donor–boron acceptor pair recombination. The other one, designated as A emission, is investigated in detail. It is shown that both the spectral shape of the zero-phonon band of the A emission and its temperature dependence are well described by the free-to-bound transition model. The recombination of electrons in the conduction band with holes trapped at the boron acceptors will be responsible for the mechanism of the A emission. The ionization energies of the nitrogen donor and the boron acceptor are estimated to be about 0.055 and 0.735 eV, respectively. (9 fig) (auth)

**26171** STUDY OF THE CONTRASTS IN ELECTRON MICROSCOPY (FROM 100 keV TO 1 MeV) IN THE CASE OF SYMMETRICAL POSITION AND APPLICATIONS. Pardo, B.; Marraud, A.; Renard, D. (C. N. R. S., Orsay, France). Phys. Status Solidi (a); 30: No. 2, 577-586(16 Aug 1975). (In French).

The channeling properties of individual Bloch waves are studied when the crystal orientation is just at the symmetry position. When the two Bloch waves are equivalent, the transmitted intensity varies very quickly with the specimen thickness. It follows that defects or very weak local variations of thickness can be observed. Calculations for any specific condition yield the accelerating voltage and the crystal orientation which lead to the maximum sensitivity. As an example, thin films were observed: $Nd_2O_3$ at 100 kV and Au at 1 MeV. (auth)

**26172** FACETING OF $UO_2$ SINGLE CRYSTAL SURFACES. Krasevec, V.; Navinsek, B. (Univ. of Ljubljana, Yugoslavia). Phys. Status Solidi (a); 30: No. 2, 501-509(16 Aug 1975).

The thermal behaviour of $UO_2$ thin foils of ⟨110⟩, ⟨001⟩, and ⟨111⟩ orientation was observed by transmission electron microscopy using pulse beam heating. It is shown that the striations which appeared after such heat treatment represent {111} facets elongated in ⟨110⟩ directions. A possible relation between faceting and surface reduction of $UO_2$ is discussed. (auth)

**26173** INDIRECT EXCHANGE INTERACTIONS IN $EuB_6$. Glaunsinger, W. S. (Arizona State Univ., Tempe). Phys. Status Solidi (b); 70: No. 2, K151-K155(1 Aug 1975).

The Bloembergen–Rowland and RKKY interactions in bulk $EuB_6$ are examined, and EPR evidence is given which favors the latter. (DLC)

**26174** SINTERING OF SOLID ALLOYS IN VACUO AND IN HYDROGEN. Senchikhin, V. K.; Pikunov, D. V.; Tret'yakov, V. I. Tsvetn. Met.; No. 3, 71-73(Mar 1975). (In Russian).

On the basis of laboratory and industrial studies, the possibility was demonstrated of increasing the quality of (Ti, W) C–WC–Co alloys by use of vacuum sintering and sintering in hydrogen. Operational durability of the alloys sintered in a vacuum was 20 to 60% higher. (tr-auth)

**26175** PHOTOCONDUCTIVITY OF INDIUM PHOSPHIDE DOPED WITH IRON AND NICKEL. Grushko, N.S.; Russu, É.V.; Slobodchikov, S.V. (A. F. Ioffe Physicotechnical Institute, Academy of Sciences of the USSR, Leningrad). Sov. Phys.–Semicond. 9: No. 2, 224-225 (Aug 1975).

The photoionization energy of levels in InP:Fe and InP:Ni were studied. The temperature dependence of the photoconductivity as well as the infrared quenching spectra were examined. (AIP)

**26176** PHOTOCONDUCTIVITY OF EuO. Nikolaev, V.I.; Samokhvalov, A.A.; Sever, G.N. (M. V. Lomonosov State University, Moscow). Sov. Phys.–Semicond. 9: No. 2, 251-252 (Aug 1975).

The photoconductivity along with the photo-emf spectra of EuO were investigated at room temperature. (AIP)

**26177** ELASTIC AND MAGNETOELASTIC PROPERTIES OF ERBIUM ORTHOFERRITE UNDER SPIN REORIENTATION CONDITIONS. Belov, K.P.; Kadomtseva, A.M.; Krynetskii, I.B.; Kovtun, N.M.; Milov, V.N.; Khokhlov, V.A. (M. V. Lomonosov State University, Moscow). Sov. Phys.–Solid State 17: No. 2, 416-417 (Aug 1975).

Data are presented on the magnetostriction, the thermal expansion, and the temperature dependence of $ErFeO_3$ crystals. (AIP)

**26178** SPECIFIC HEAT OF $Pr_3Te_4$ AND $La_3Te_4$. Mitarov, R.G.; Tikhonov, V.V.; Vasil'ev, L.N.; Oskotskii, V.S.; Golubkov, A.V.; Smirnov, I.A. (A. F. Ioffe Physicotechnical Institute, Academy of Sciences of the USSR, Leningrad). Sov. Phys.–Solid State 17: No. 2, 310-312 (Aug 1975).

The specific heats of $La_3Te_4$ and $Pr_3Te_4$ have been investigated in a vacuum adiabatic calorimeter over the specific heat $C_{Sch}$ associated with the transfer of 4*f* electrons to the higher energy levels formed as a result of the splitting of the ground state of the ion $Pr^{3+}(^3H_4)$, has been found and isolated. The results are interpreted in terms of the point-ion model. Values of the energy levels are given. Agreement between theory and experiment lies in the range 0.4–0.6%. It is concluded that no other anomalies, apart from the Schottky effect, exist in $Pr_3Te_4$ in the temperature range investigated. (auth)

**26179** SPECTRAL AND MAGNETOOPTICAL INVESTIGATION OF THE MAGNETIC ANISOTROPY OF ERBIUM IRON GARNET. Belyaeva, A.I.; Eremenko, V.V.; Silaev, V.I.; Vaishnoras, R.A.; Potakova, V.A. (Physicotechnical Institute of Low Temperatures, Academy of Sciences of the Ukrainian SSR, Khar'kov). Sov. Phys.–Solid State 17: No. 2, 233-236 (Aug 1975).

Spectral and magnetooptical investigations have been used to study the magnetic anisotropy of erbium iron garnet at T=4.2 °K. The part played by the trivalent erbium in producing the anisotropy at low temperatures is discussed. The axis of easy magnetization [100] of $Er_3Fe_5O_{12}$ is determined. A unique relation is established between the polarization of the absorption bands of the rare earth ion and the direction of the magnetic moment of the crystal. (auth)

**26180** SUPERCONDUCTING AND NORMAL STATE PROPERTIES OF SEVERAL TERNARY TITANIUM OXIDES. Johnston, D. C. San Diego, CA; University of California (1975). 209p. University Microfilms Order No. 75-11,230.

Thesis (Ph. D.).

$LiTi_2O_4$ is one end member of the homogeneity range of the superconducting spinel phase Li/sub 1 + x/Ti/sub 2-x/$O_4$ (0 less than or equal to x less than or equal to 1/3), with transition temperatures of up to approximately 14°K. X-ray structure analysis, electrical resistivity, magnetic susceptibility, dielectric constant, and heat capacity measurements were carried out in order to characterize the superconducting and normal state properties of $LiTi_2O_4$ and of other compositions within the homogeneity range of the spinel phase. These measurements establish $LiTi_2O_4$ as a weak-coupling, d-band superconductor with superconducting state properties well-described by the BCS theory of superconductivity. They also show that in the vicinity of the composition $LiTi_2O_4$, the transition temperature of spinel phase samples is independent of composition, but that a sudden disappearance of superconductivity occurs for composition parameters (x) greater than about 0.1. This is attributed to a composition-induced metal–insulator transition. Reasons for the metallic character of $LiTi_2O_4$ and for the metal–insulator transition are discussed. A study of the physical properties of several other ternary oxides containing titanium showed that none of these compounds are superconducting. $YTiO_3$ was found to exhibit ferromagnetic ordering at 29°K, and is therefore the first example of a ferromagnetic compound containing titanium cations as the only magnetic species present. High-temperature magnetic susceptibility measurements on compounds in the system (Sc/sub 1-x/Ti/sub x/)$_2O_3$ confirm the dominant antiferromagnetic interaction between the spin-only $d^1$ titanium cations. However, low-temperature measurements revealed weak ferromagnetic ordering at 3°K for samples with composition parameters x greater than tilde 0.7. (Diss. Abstr. Int., B)

**26181** FIELD ION MICROSCOPY OF TRANSITION METAL CARBIDES AND COMPUTER SIMULATION. Ko, F. Y. Providence; Brown University (1974). 187p. University Microfilms Order No. 75-9193.

Thesis (Ph. D.).

Several transition metal carbides (especially in the molybdenum–carbon system) are studied by means of field ion microscopy. The field ion micrographs of alpha MoC, alpha $Mo_2C$, as well as other carbides, are presented. A computer technique is used to simulate the ion image formation process for these carbides. Both the geometrical degree of protrusion of a surface atom on a field ion microscopic specimen and nearest neighbor interactions of that atom are considered in various simulation models. A best-fit model is then chosen by comparing the simulated patterns with the observed field ion micrographs. A mechanism of field ion image formation is proposed, and qualitative explanations are given for the characteristic features of the carbide images. (Diss. Abstr. Int., B)

# Metals and Alloys

**26182** RECOMA MAGNETS USED IN MOTORS AND BEARINGS. Wiesmann, H. Brown Boveri Rev.; 62: No. 5, 215-218 (May 1975).

Recoma magnets have a wide range of potential applications because of their magnetic properties. A prerequisite for their full realization is, amongst other things, a project optimization based on these magnetic properties. Associated problems in motors and bearings are pointed out and comparison is made with traditional magnetic materials. (auth)

## *Corrosion and Erosion*

*Refer also to abstracts 25628 and 25629.*

**26183** (AECL-4582) SOLUBILITY OF NICKEL AND COBALT FERRITE IN WATER UP TO 300°C. Von Massow, R. E.; Sullivan, G. R.; Waugh, G. N. (Atomic Energy of Canada Ltd., Pinawa, Manitoba. Whiteshell Nuclear Research Establishment). Jun 1975. 80p. NTIS (US Sales Only) $7.00. AECL $2.00.

Thermodynamic data in the literature are used to compute metal ion concentrations in aqueous solution in equilibrium with the spinels $NiFe_2O_4$ and $CoFe_2O_4$ at temperatures up to 300°C as a function of pH and dissolved $H_2$. Results are discussed in relation to the transport of corrosion products in nuclear power plants. (14 tables) (auth)

**26184** ELECTRO-TRANSPORT OF HYDROGEN IN ZIRCONIUM. Mishima, Y.; Ishino, S.; Miyazaki, N. (Tokyo Univ. (Japan). Faculty of Engineering). Tokyo Daigaku Kogakubu Kiyo, A; No. 11, 46-47(Dec 1973). (In Japanese).

Movement of hydrogen in zirconium under applying electric field was studied at 300°C with a direct current density of 7.5 $A/mm^2$. Change in hydrogen concentration was determined metallographically by counting total length of hydride precipitates in a specimen slowly cooled under current following electromigration treatment for long periods at 300°C. Hydrogen migrates to an anode side of the specimen, indicating that the "effective charge" of hydrogen is negative. More detailed experiment will be necessary to correlate the results with fundamental quantities. (auth)

**26185** FORMATION OF VOID IN OXIDE SCALE ON NIOBIUM WITH HIGH TEMPERATURE OXIDATION. Yamawaki, M. (Tokyo Univ. (Japan)). Denki Kagaku; 42: No. 12, 612-616(Dec 1974).

A mode of formation of void in oxide scale on niobium with oxidation was studied in the temperature range 585 to 760°C using an observation-in-polarized-light technique. The voids formed in this temperature range have typically the shape of a circular cone with a concaved bottom. Using the above technique reflection from the surfaces of the voids could be clearly observed from outside of the scale. In an early short period of less than 5 or 10 min an initial group of voids are formed and their diameters are expanded with oxidation according to a parabolic time law. After the formation of the initial group of voids, new void formation ceases up to about 30 min. Thereafter, a second group of voids begin to form in the oxide/metal interface region of the specimen. The density of the initial group of voids is highly affected by the surface roughness of the specimen as well as the reaction temperature. (auth)

**26186** INFLUENCE OF ALLOYING ELEMENTS ON THE SOLUBILITY OF HYDROGEN IN VANADIUM. Eguchi, T. (Tohoku Univ., Sendai (Japan)); Morozumi, S. J. Jpn. Inst. Met.; 38: No. 11, 1025-1030(Nov 1974). (In Japanese).

Solubility of hydrogen in vanadium and its binary alloys containing titanium, chromium, iron, and cobalt, respectively, was measured in the temperature range between 600 to 1200°C under one atmosphere pressure of hydrogen gas. The influence of alloying elements on the solubility, and the correlation between hydrogen solubility and electronic structure of alloys were discussed. The following results were obtained: (1) The solubility decreased with increase in amount of each alloying element, with the exception of titanium. (2) The lattice strain induced by alloying did not affect the solubility. (3) Relative partial molar entropy and enthalpy increased linearly with increase in electron/atom ratio from 4.9 to 5.4. (4) Variation in entropy was correlated to that in the electronic specific heat coefficient of alloy. (5) Variation in enthalpy was explained by that in density of state at the Fermi surface in the alloys. (auth)

**26187** TANTALUM ANODIC OXIDATION. I. Evidence for Surface Heterogeneity and Roughness. Brambilla, P.; Cerofolini, G. F. Thin Solid Films; 27: No. 1, 1-15 (May 1975).

A model based on the hypothesis that heterogeneity and roughness play an important role in the anodization of tantalum is proposed. It is shown that the roughness can be described by a well-behaved decreasing function of the oxide thickness, and that the heterogeneity is characterized by the distribution of the prototropic exchange potential. Application to a particular case, the anodization of a $\beta$-tantalum film sputtered onto glazed ceramic, shows the result that the surface is formed by two zones, each heterogeneous. The same qualitative behavior is shown by tantalum nitride films, although for these films the prototropic exchange potential distributions have not been explicitly evaluated. (auth)

**26188** INHIBITION OF HYDROGEN ENVIRONMENT EMBRITTLEMENT BY $SO_2$. Jacobs, A. J.; Chandler, W. T. (Rockwell International, Canoga Park, CA). Scr. Metall.; 9: No. 7, 767-769 (Jul 1975).

Results of tensile tests conducted on SAE 4340 steel and Inconel 718 exposed to $H_2/SO_2$ mixtures are presented. The tests were conducted to determine if small ($\leq$1.5%) amounts of $SO_2$ could effectively inhibit hydrogen environment embrittlement (HEE) over a wide range (20 to 7000 psi) of hydrogen pressures. The tensile tests were conducted at a strain rate of 0.05 in./in.-min on notched round specimens having a $K_t$ of 8.4. The test conditions and results are summarized in tables for SAE 4340 steel and Inconel 718. Considering the Inconel 718 test results, 0.5% $SO_2$ is a less effective inhibitor of HEE than an order-of-magnitude smaller concentration of $O_2$, which gives complete inhibition. A 0.5% concentration of $SO_2$ is a better inhibitor at low (20 psi) than at elevated (7000 psi) hydrogen pressure. At ~1 atm total pressure, 0.5% $SO_2$ was able to arrest crack growth in a compact tension specimen, whereas tensile specimens exposed to the same concentration of $SO_2$ underwent a 17% loss in tensile strength. The difference in inhibition can be attributed to differences in crack growth rates between the two types of tests. Results of calculations show that crack arrest due to inhibition occurred at a stress intensity of approximately 32 ksi $\sqrt{\text{in.}}$ The stress intensity in the tensile specimen tested in this program was higher, for example, the stress intensity calculated for the maximum load and the initial notch geometry is approximately 63 ksi $\sqrt{\text{in.}}$ With a crack formed, the stress intensity would be higher yet. Thus, during much of its growth period the crack in the tensile specimen would be growing at a faster rate than in a precracked specimen with a reduced opportunity for inhibition by the $SO_2$. (auth)

**26189** CORROSION OF A 50Cr--50Ni ALLOY IN LIQUID VANADATE SYSTEMS IN THE TEMPERATURE RANGE 750 TO 950°C. Dooley, R. B. (Queen's Univ., Kingston, Ont.); Wilson, J. R. ASME Publication 74-WA/CD-2. New York; American Society of Mechanical Engineers (1975). 7p. $3.00.

From winter annual meeting; New York, NY (17 Nov 1974).

A 50Cr–50Ni commercial alloy was corroded in pure $V_2O_5$ and in vanadate melts containing sodium, sulphate, and chloride in the temperature range 750–950°C in a rotating disk apparatus. Results are discussed in terms of the material's capability of forming a protective barrier layer and the subsequent dissolution of this layer into the liquid vanadate melt. Marked internal oxidation of a chromium-rich phase was noted throughout the temperature range. At 750 and 810°C this is associated only with chloride containing melts, but at 950°C the attack, while enhanced by chloride, also occurs in nonchloride melts. (auth)

**26190** CORROSION WEEK '74. Volume II. 74th Manifestation of the European Federation of Corrosion, Budapest, Hungary, October 14–20, 1974. Farkas, T.; Straner, G.; Wagner, M. (eds.). Budapest; OMKDK-Technoinform (1974). 470p. (In Several Languages). (CONF-741099-P2).

Fifty-four papers presented at the conference are included. Topics covered include corrosion problem in energy-related industries, corrosion of various metals, methods of inhibiting corrosion, and weathering of paints and resins. (MCG)

**26191** CORROSION WEEK '74. Volume I. 74th Manifestation of the European Federation of Corrosion, Budapest, Hungary, October 14–20, 1974. Farkas, T.; Straner, G.; Wagner, M. (eds.). Budapest; OMKDK-Technoinform (1974). 583p. (In Several Languages). (CONF-741099-P1).

Fifty papers presented at the conference are included. Topics covered include: corrosion problems in industry, corrosion inhibitors, corrosion mechanisms, and properties of coatings for corrosion protection. Separate abstracts were prepared for three papers. (MCG)

*For abstracts of individual papers see: 26192, 26193, and 26197.*

**26192** STUDY OF CORROSION RESISTANCE OF ALUMINUM CONVERSION LAYER BY THE RADIO–CHEMICAL METHOD. Badacsonyi; Maleczki; Varga. pp 239-246 of Corrosion Week '74. Vol. I. Farkas, T.; Straner, G.; Wagner, M. (eds.). Budapest; OMKDK-Technoinform (1974). (In German).

From 74th meeting of the European Federation of Corrosion; Budapest, Hungary (14 Oct 1974). See CONF-741099-P1.

A testing method applying the radioactive isotope technique was worked out whereby the conversion layers preventing corrosion were examined. Prior to the forming of a layer by the green chromatic process the treatment baths were labelled with $^{51}Cr$ isotopes and the process leading to the formation of the layer was observed. The readiness of dissociation of the layers from the surface at various storing time in the solvent bath were determined on the basis of the increase of the counting rate. The dependence of the conversion layer on the circumstances under which the dying takes place, indicated by the chrome content and the intensity of the radioactive isotope, was also examined. The optimum parameters for treatment baths can be stated with relative ease by utilising the radiochemical testing method whereby the radiation intensity is measured; furthermore, the corrosion resistance of the protective layer and the rate of corrosion and the dissociation of the layer is worked out. (auth)

**26193** RESULTS OBTAINED WITH THE RADIOCHEMICAL METHODS DURING THE EXAMINATION OF THE FORMATION OF THE CONVERSION LAYER OF ALUMINUM. Maleczki, E. pp 281–288 of Corrosion Week '74. Vol. I. Farkas, T.; Straner, G.; Wagner, M. (eds.). Budapest; OMKDK-Technoinform (1974). (In French)

From 74th meeting of the European Federation of Corrosion; Budapest, Hungary (14 Oct 1974). See CONF-741099-P1.

In the study of the conversion layers formed chemically on Al during chemical treatment of the surface, the use of radio-

active isotopes has made it possible to determine exactly the various phases of formation of these layers. The quantities of the layers formed in various chemical baths were determined with the use of radioisotopes. Conclusions were made on the mechanism of formation of these layers. The incorporation of components into the metallic surface begins within the first second. (tr-auth)

## Preparation and Fabrication

*Refer also to abstracts 27328 and 27356.*

**26194** WELDING METALLURGY OF STAINLESS AND HEAT-RESISTING STEELS. Castro, R.; de Cadenet, J. J. Cambridge, Eng.; Cambridge University Press (1975). 200p.

The subject is covered in chapters, entitled: stainless and heat-resisting steels; the welding operation; application of the fusion welding processes to stainless and heat-resisting steels; the welding of stainless and heat-resisting martensitic steels; the welding of stainless and heat resisting semi-ferritic and ferritic steels; the welding of austenitic or austenitic-ferritic stainless and heat-resisting steels; the welding of corrosion-resistant and high temperature nickel-base alloys; the welding of age-hardening stainless and heat-resisting steels; dissimilar metal welding using austenitic filler metals; application of weldability tests to stainless and heat-resisting steels. (UK)

**26195** GROWTH OF MULTINEEDLES OF TUNGSTEN CAUSED BY REACTION OF TUNGSTEN OXIDE WITH ACETONE. Okuyama, F. (Department of Fine Measurements, Nagoya Institute of Technology, Gokiso-cho, Syowa-ku, Nagoya, Japan). J. Appl. Phys. 46: No. 8, 3255-3259 (Aug 1975).

The growth of crystalline needles of tungsten on the tungsten substrate through chemical reaction between vacuum-deposited tungsten oxide and acetone vapors of (3–5) $\times 10^{-6}$ Torr was investigated with the aid of a field emission and a transmission electron microscope. A large number of tungsten needles were found to be grown by heating the substrate, onto which tungsten oxide had been deposited, initially at a temperature in the range ~1500–1800°K in acetone and then at a temperature between ~2300 and ~2600°K in acetone-free vacuum. The needles were mostly [110] oriented and their number density amounted to $\sim 10^7/cm^2$. It is believed that the needle growth was closely related to the reduction of the oxide by carbon provided from acetone through the thermal cracking. (auth)

**26196** MULTIFILAMENTARY NIOBIUM–TIN ($Nb_3Sn$) FOR SUPERCONDUCTING GENERATOR APPLICATIONS. Scanlan, R. M.; Fietz, W. A. (General Electric Corp., Schenectady, NY). IEEE (Inst. Electr. Electron. Eng.) Trans. Magn.; 11: No. 2, 287-290(1975).

The cable approach for producing a $Nb_3Sn$ conductor is evaluated and results of bend and tensile tests for various cables presented. Fabrication methods for producing long lengths of multifilamentary $Nb_3Sn$ superconductor are discussed and test data for several small coils presented. (DLC)

**26197** CRACKFREE AND HIGHLY CORROSION RESISTANT Co–Mo ALLOY ELECTROPLATES. Saurat, M.; Chassaing, E.; Vu Quang Kinh. pp 63-70 of Corrosion Week '74. Vol. I. Farkas, T.; Straner, G.; Wagner, M. (eds.). Budapest; OMKDK-Technoinform (1974).

From 74th meeting of the European Federation of Corrosion; Budapest, Hungary (14 Oct 1974). See CONF-741099-P1.

Thick and crack free Co-Mo coatings containing 12 to 20 wt% of molybdenum can be electroplated on some metal substrates from aqueous citrate baths of suitable compositions, under proper plating conditions. These deposits show a columnar microstructure with a hardness of about 400 V.H.N. They have a close packed hexagonal structure. The tensile stress in the deposits does not change very much with the molybdenum content, but decreases when cathodic current density is increased. Their resistance in concentrated hydrochloric acid is satisfactory. It is highly improved by an adequate heat treatment of the coatings. (auth)

**26198** APPLICATION OF TUNGSTEN COATINGS BY ELECTROLYSIS OF SALT MELTS. Balikhin, V. S.; Pavlovskii, V. A. Tsvetn. Met.; No. 3, 70(Mar 1975). (In Russian).

The possibility was shown of electrolytic precipitation of dense tungsten layers, with a thickness of from several microns to several millimeters, from a $NaCl–NaF–WO_3$ melt onto nickel and molybdenum substrates. The recommended electrolysis regime is T = 900 ± 20°C and $D_K$ = 0.01 to 0.1 $A/cm^2$. (tr-auth)

**26199** DECARBONIZATION OF TUNGSTEN AND MOLYBDENUM POWDERS. Chizhikov, D. M.; Savin, A. V.; Safonov, V. I.; Vodop'yanova, L. S.; Fedorova, G. A. Tsvetn. Met.; No. 3, 73-75(Mar 1975). (In Russian).

The effect of oxygen on decarbonization and of this process on changes in density of metals was demonstrated. From porosity changes it is possible to monitor the decarbonization. Various degrees of purity of the carbon were investigated, and it was shown that the purer the metallic powder with respect to carbon, under the same stable equal conditions, the higher its sinterability. (tr-auth)

## Properties, Structure, and Phase Studies

*Refer also to abstracts 25735, 25736, 25776, 25876, 26725, 26943, 26946, 26950, 26953, 27277, and 27426.*

**26200** (AECL-4761) STRAIN INDUCED BY THERMAL CYCLING OF HYDRIDED OZHENNITE 0.5. Bell, L. G.; Sawatzky, A. (Atomic Energy of Canada Ltd., Pinawa, Manitoba. Whiteshell Nuclear Research Establishment). May 1975. 30p. NTIS (US Sales Only) $4.50. AECL $1.00.

A creep program on annealed zirconium alloy Ozhennite 0.5 was undertaken to investigate the effect of various variables on thermal cycle-induced strain steps. Tests mainly at a stress of 63 MPa and at 425°C with periodic cycles to a lower temperature showed that strain steps of the order of 0.1 to 0.3% readily occur for each thermal cycle which would precipitate zirconium hydride. A hydrogen-free specimen did not exhibit any measurable strain steps and deformed only about 0.3%. Hydrided specimens deformed as much as 7.3% mainly as a result of strain steps. The step size decreased gradually with increased number of cycles and was a function of hydrogen concentration. At 100 μg/g and 300 μg/g hydrogen, the step size was about the same but it then decreased with increasing hydrogen concentration. The effects of changing stress and temperature cycle size were briefly investigated. A theory to explain strain steps is described. In short, dislocations are generated by precipitation of hydrides and are made free to move by re-solution of the hydrides. (auth)

**26201** (AWRE-O-16/75) SURVEY OF THE HEAT TREATMENT AND MECHANICAL PROPERTIES OF URANIUM/LOW TITANIUM ALLOYS. McCarthy, G. P. R. (UKAEA Weapons Group, Aldermaston. Atomic Weapons Research Establishment). Aug 1975. 28p. Dep. NTIS (US Sales Only) $4.50. UK 50 pence.

A survey of the heat treatment and mechanical properties of uranium alloys containing up to 1.6 wt% titanium was made. The amount of information available in the literature is somewhat limited. One trend that was observed was that increasing the titanium content up to 0.8 wt% gave increasing elongation for a given strength level. There was no information on alloys above 0.8 wt% titanium to indicate to what extent this trend continues. (17 tables, 7 fig, 12 references) (auth)

**26202** (DP-MS-74-74) HYDROGEN TRANSPORT IN IRON AND STEEL. Louthan, M. R. Jr.; Derrick, R. G.; Donovan, J. A.; Caskey, G. R. Jr. (Du Pont de Nemours (E. I.) and Co., Aiken, S. C. (USA). Savannah River Lab.). 1975. Contract AT(07-20-1. 11p. (CONF-750925-4). Dep. NTIS $4.00.

From conference on effects of hydrogen on behavior of materials; Jackson, Wyoming, USA (7 Sep 1975).

The permeabilities of protium, deuterium, and tritium in iron and T-1 steel at temperatures as low as 260°K are in agreement with the equation proposed by Gonzalez. However, the permeabilities of HP-9-4-20 and 4130 steel to hydrogen are typically lower than predicted. The present data also show that, within experimental accuracy, the isotope effect on the permeability of hydrogen in HP-9-4-20, 4130 and T-1 steel, and high purity iron can be estimated by an inverse square root of mass correction. Trapping effects prevent the development of diffusivity and solubility equations. (auth)

**26203** (ERDA-50, pp 41-49) CURRENT TRITIUM CHEMICAL STUDIES AT OAK RIDGE NATIONAL LABORATORY. Smith, F. J.; Redman, J. D.; Strehlow, R. A.; Bell, J. T. (Oak Ridge National Lab., TN). Jun 1975.

From symposium on technology related for fusion reactor systems; Miamisburg, Ohio, USA (1 Oct 1974).

In proceedings of the symposium on tritium technology related to fusion reactor systems. (Energy Research and Development Administration, Washington, D. C. (USA). Div. of Controlled Thermonuclear Research).

The equilibrium pressures of hydrogen isotopes in the Li-LiH-$H_2$, Li-LiD-$D_2$ and Li-LiT-$T_2$ systems are being measured. The solubility of hydrogen in lithium was studied and the data are in reasonable agreement with the literature values. The Li-LiD-$D_2$ system is now being studied. The first experimental measurements of the equilibrium pressures of tritium between 700 and 1000°C as a function of the LiT concentration in the Li-LiT-$T_2$ system have also been completed. The permeation of tritium through clean metals and through metals under simulated steam generator conditions is being investigated. Measurements of tritium permeation through clean nickel at temperatures between 636 and 910°K were made using a mixed isotope technique. The

tritium permeability, DK/sub s/', as a function of temperature was determined to be ln DK/sub s/' [cc(NTP).mm.min$^{-1}$.torr/sup -1/2/.cm$^{-2}$] equals -0.906 - 6360/T(°K). The measured permeation activation energy was 12.6 ± 0.4 kcal/mole. (MOW)

**26204** (ORNL-tr-2921) TUNGSTEN HEAVY-METAL ALLOYS. Jangg, G.; Kieffer, R.; Childeric, B.; Ertl, E. Translated by R. G. Mansfield from Planseeber. Pulvermet.; 22: 15-28 (1974). 11p. Dep. NTIS $4.00.

Studies on tungsten heavy metal alloys with cobalt-iron-nickel binder showed that a small cobalt addition has a positive effect on the ductility and hardness; the favorable influence on the ductility is greater than that on the hardness decrease. At binder metal compositions of about 5 Ni, 3 Co, 2 Fe, an optimum compromise between hardness and elongation is attained. The studies have also shown that further improvements are possible by a suitable choice of sintering temperatures and sintering times. The sintering temperature should only be high enough to provide sufficient liquid phase during sintering. The sintering time should not exceed 30 to 60 minutes. Longer sintering, particularly at excessively high temperatures, cause an undesirable grain growth in the tungsten grains within the heavy metal structure which reduces the elongation. (As value the torsion rupture angle on rods is measured.) (auth)

**26205** (ORO-3262-40) DEFORMATION PROCESSES IN REFRACTORY METALS. Progress Report, 1 December 1974–30 November 1975. Donoso, J. R.; Reed-Hill, R. E. (Florida Univ., Gainesville (USA)). 1975. Contract AT(40-1)-3262. 46p. Dep. NTIS $5.50.

Work in progress is mostly concerned with the stress-strain behavior of niobium, as affected by dynamic strain aging. An investigation of the aging phenomena in nickel containing carbon as the major interstitial impurity was also conducted. Some aspects of the deformation behavior of the hexagonal metals titanium and zirconium still warrant investigation and are also being considered. (auth)

**26206** (SAND-75-5119) HYDROGEN TRANSPORT IN 4130 STEEL. Kass, W. J. (Sandia Labs., Albuquerque, N. Mex. (USA)). 1974. 22p. (CONF-750925-6). Dep. NTIS $4.25.

From conference on effects of hydrogen on behavior of materials; Jackson, Wyoming, USA (7 Sep 1975).

Solubility data indicate that under glow discharge conditions, hydrogen entering the lattice is already dissociated in the gas phase. Since one expects subsequent diffusion to be no longer limited by a surface process, the remaining anomalous low temperature diffusion behavior may be related to a bulk process such as trapping. The normal permeation behavior is consistent with a trapping mechanism since the steady state permeation rate is not affected by trapping. Consequently, in normal permeation measurements it appears that both perturbations to simple diffusion occur, the hydrogen dissociation is influenced by a slow surface step and the bulk diffusion is perturbed by trapping sites. (auth)

**26207** (SAND-75-8712) EFFECT OF COPPER ON CRACK PROPAGATION IN BERYLLIUM SINGLE CRYSTALS. Aldinger, F.; Wilhelm, M. (Max-Planck-Institut fuer Metallforschung, Stuttgart (F.R. Germany). Inst. fuer Werkstoffwissenschaften). Aug 1974. Translation of Einfluss des Kupfers auf die Rissausbreitung in Beryllium-Einkristallen. 86p. Dep. NTIS $7.50.

The effect of copper additives on the fracture energy and the development of cracks parallel to the basal plane was studied in zone-refined single crystalline beryllium. At 77°K the cleavage planes are very smooth, so the crack propagation energy, which is independent of copper content (less than 2 at. percent Cu) in the range of measurement accuracy, is only a little higher than the surface energy of the basal plane. At room temperature, due to intense plastic processes taking place in front of the crack tip, the fracture energy is an order of magnitude higher than at low temperatures. The effect of copper on the plastic processes can be divided into two regions. In region I (less than 1.2 at. percent Cu), in which the crack propagation energy increases sharply with increasing copper content, crack propagation is controlled by prism slips. The decrease in crack propagation energy in region II (greater than 1.2 at. percent Cu) can be attributed to a reduction of beryllium twinning energy with increasing copper content. (auth)

**26208** PHOTOCONDUCTIVITY IN COMPENSATED N—TYPE InSb UNDER CYCLOTRON RESONANCE CONDITIONS. Gulyaev, Yu.V.; Popov, V.A.; Potapov, V.T.; Strakhov, V.A.; Chusov, I.I.; Yaremenko, N.G. (Institute of Radio Engineering and Electronics, Academy of Sciences of the USSR, Moscow). Sov. Phys.—Solid State 17: No. 1, 173-177 (July 1975).

An experimental investigation was made of the photoconductivity of strongly compensated n-type InSb under cyclotron resonance conditions at wavelengths $\lambda = 0.75-1.2$ mm. At liquid-nitrogen temperature the phase of the photoresponse $\Delta E$ changed rapidly in a narrow range of magnetic fields near cyclotron resonance. When the temperature was lowered, the dependence of the response on the magnetic fields H assumed a definite two-humped shape. At sufficiently low temperatures the dependence $\Delta E(H)$ began to reproduce qualitatively the cyclotron absorption line. These features of the photoconductivity of compensated *n*-type InSb under cyclotron resonance conditions were attributed to a considerable influence of the sacttering of electrons by polar optical phonons and to the relatively long electron momentum relaxation time. A theoretical solution was obtained to the problem of the photoconductivity in the case of inelastic scattering of electrons by optical phonons and frequent collisions between electrons. (auth)

**26209** MAGNETIC SUSCEPTIBILITY AND THERMAL CONDUCTIVITY OF METALLIC SAMARIUM AT HIGH TEMPERATURES. Vedernikov, M.V.; Kizhaev, S.A.; Petrov, A.V.; Moreva, N.I. (A. F. Ioffe Physicotechnical Institute, Academy of Sciences of the USSR, Leningrad). Sov. Phys.—Solid State 17: No. 1, 212-213 (July 1975).

We report the first measurements of the thermal conductivity of samarium in the temperature range 100—1000 °K. The presence of a magnetic phase transition in this region is confirmed. (AIP)

**26210** IMPEDANCE OF INDIUM ANTIMONIDE IN A TRANSVERSE MAGNETIC FIELD. Dobrovol'skii, V.N.; Uzhva, V.I. (T. G. Shevchenko State University, Kiev). Sov. Phys.—Solid State 17: No. 1, 226-227 (July 1975).

The dependence on electric field of the impedance of indium antimonide in a transverse magnetic field was studied. The magnetic field varied from 0 to 6525 Oe. While the temperature was 77 °K. (AIP)

**26211** TANTALUM ANODIC OXIDATION. II. Demonstration that a Constant Current Density Must Be the Response to a Linear Ramp of the Anodization Potential. Cerofolini, G. F. (Laboratori Componenti Integrati, Milan). Thin Solid Films; 27: No. 1, 17-18 (May 1975).

It is demonstrated mathematically that a constant current density must be the response to a linear ramp of the anodization potential. (auth)

**26212** CHANGE IN STRUCTURE OF FILMS OF SPUTTERED Ta DURING STABILIZATION OF DEPOSITION CONDITIONS. Christensen, O.; Marhic, C.; Klein, B. J.; Barbezat, S. (CNRS, Meudon, France). Thin Solid Films; 27: No. 1, 39-47 (May 1975). (In French).

The structure of sputtered tantalum films deposited by dc biased dc diode sputtering has been studied. $\beta$ tantalum is observed under equilibrium deposition conditions, when consistent and reproducible results are obtained. The structure of the films sputtered during the period of stabilizing deposition develops from the bcc phase to the $\beta$ phase through mixtures of the two. Based on the assumption that $\beta$ tantalum is impurity stabilized, it is concluded that the source of impurities in the system is the thick film of tantalum grown on the discharge electrodes, collector, and anode. (auth)

**26213** INFLUENCE OF FILM THICKNESS ON THE FORMATION OF $\beta$—Ta AND BCC-Ta. Schauer, A.; Peters, W. (Siemens AG, Munich, Ger.). Thin Solid Films; 27: No. 1, 95-99 (May 1975).

Ta films of various thicknesses were deposited under very clean conditions in a sputtering system with an electrodeless ring discharge. The resistivity, temperature coefficient, and structure of films on $Ta_2O_5$-coated glass substrates were studied. The results show that $\beta$-Ta is formed predominantly in the nucleation step; there is a transition to bcc-Ta in the growth stage, and finally in thick films only very pure bcc-Ta is detected. Impurity atoms are necessary not only for the nucleation but also for the growth of $\beta$-Ta. (auth)

**26214** DIELECTRIC PROPERTIES OF ANODIZED Al—Ta ALLOY FILMS WITH HIGH Al CONTENT. Schauer, A.; Roschy, M.; Juergens, W. (Siemens AG, Munich, Ger.). Thin Solid Films; 27: No. 1, 111-121 (May 1975).

At 1 mA cm$^{-2}$ the anodization voltage of sputtered Al—Ta alloy films with about 7 at.% Ta content rises linearly with time at a rate of 0.45 V s$^{-1}$. The Al—Ta thickness-anodization voltage ratio and the oxide growth constant have been determined, for 7 to 14 at.% Ta in the films with 1% citric acid electrolyte, to be 1.03 to 0.94 nm V$^{-1}$ and 1.42 to 1.5 nm V$^{-1}$, respectively. The permittivity was found to range from 10.0 to 11.4, corresponding to a capacitance density of about 330 pF mm$^{-2}$ for an anodization voltage of 200 V. The temperature coefficient of capacitance (tcc) was 500 ppM K$^{-1}$. The capacitance between 400 Hz and 1 MHz remained constant within ±1%. At 1 kHz the dissipation factor tan $\delta$ was 0.6%. Nearly all leakage currents were between 0.1 and 0.5 nA using 5.6 nF test capacitors and 50 V as the test voltage. This corresponds to an insulation resistance R of $10^{11}$ Ω or more, or a time constant $\tau$(=RC) of approximately 1000 s.

For the 50 V test the yield was about 90% and at least 80% of the capacitors had no short circuits after step stress tests up to 90 V. The current-voltage characteristics of capacitors made from Al–Ta (7 at.% Ta) films showed non-destructive breakdown voltages greater than 100 V. A small deviation from symmetry was noticed whether the Al–Ta electrode was positive or negative, indicating that the capacitors were virtually nonpolar. In some cases non-shorting breakdown was observed. (auth)

**26215** INFLUENCE OF SUBSTRATE TEMPERATURE ON THE ELECTRICAL PROPERTIES OF THIN InSb FILMS FLASH-EVAPORATED ONTO GLASS. Burvenich, X. M. (Ghent State Univ.). Thin Solid Films; 27: No. 1, 129-134 (May 1975).

The results of resistivity and Hall voltage measurements on InSb films 1000 Å thick, flash-evaporated onto glass substrates over a wide range of substrate temperatures, are reported. From the experimental curves obtained, an optimum substrate temperature is deduced. The position of a sharp peak observed in the mobility versus substrate temperature curve is explained in terms of a stoichiometric interval associated with the pressure-temperature diagram of the In–Sb binary system. (auth)

**26216** NITROGEN-DOPED TANTALUM THIN FILM CAPACITORS WITH IMPROVED TEMPERATURE STABILITY. Anders, W. (Siemens AG, Munich). Thin Solid Films; 27: No. 1, 135-140 (May 1975).

The changes in capacitance, temperature coefficient of capacitance (tcc) and dissipation factor (tan δ) of tantalum thin film capacitors subjected to heat treatment depend significantly on the nitrogen content of the Ta and the $Ta_2O_5$. If tantalum films deposited by reactive sputtering contain between 5 and 15 at.% nitrogen, the tan δ and tcc of the finished capacitors can be reduced to constant values of $1.5 \times 10^{-3}$ and 135 ppM $K^{-1}$ respectively (test frequency 1 kHz) by heat treatment at temperatures between 250 and 350°C. However, if the nitrogen content is smaller or greater, or if β-Ta is used, both the tcc and tan δ increase sharply with rising temperature and prolonged heat treatment. (auth)

**26217** INVESTIGATION OF THE VAPORIZATION OF MOLYBDENUM IN AN ULTRAHIGH VACUUM. Dekhtyar, I. Ya.; Kolesnik, V.N.; Patoka, V.I.; Silant'ev, V.I. (Institute of Metal Physics, Academy of Sciences of the Ukrainian SSR). High Temp. 12: No. 5, 870-874 (May 1975).

A study was made of the vaporizability of molybdenum, as well as of the character of the effect of preliminary annealing and of dissolved gases on its vaporizability under conditions of an ultrahigh vacuum. One variant of the Langmuir differential methods was used to measure the vapor pressure of molybdenum. The experiments were made in an ultrahigh-vacuum unit having oil-free means of evacuation, which made it possible to attain a rarefaction of $1 \cdot 10^{-12}$ mm Hg. The spectrum of the residual gases was analyzed using an IPDO-1 mass-produced omegatron device for measuring partial pressures. The parameters of preliminary annealing, after which reliable data on vaporization rates are obtained, are established. A study was made of the effect of dissolved gases on the vaporizability of molybdenum. A comparison is made between the results of the present work and the data of other authors. (auth)

**26218** DETERMINATION OF THE THERMAL CONDUCTIVITY OF TUNGSTEN BY THE METHOD OF INDIRECT HEATING OF A HEATED FILAMENT IN A VACUUM. Fedosov, V.A.; Paleev, I.I. (D. I. Mendeleev All-Union Scientific-Research Institute of Meterology). High Temp. 12: No. 5, 880-885 (May 1975).

Formulas are derived for determining the thermal conductivity by the method of indirect heating of a heated filament in a vacuum. Relationships are obtained which take account of the variability of the thermal conductivity and the degree of blackness of the investigated sample as a function of the temperature. The article gives the construction of the instrument and a schematic diagram of the unit in which the thermal conductivity of tungsten was determined in the range 1700–2500 °K. (auth)

**26219** INVESTIGATION OF THE THERMAL EXPANSION OF TUNGSTEN-RHENIUM ALLOYS IN THE REGION OF SOLID SOLUTIONS AT TEMPERATURES OF 200–900 °C. Zaichenko, V.M.; Mints, R.G.; Petukhov, V.A.; Chekhovskoi, V.Ya. (High Temperature Institute, Academy of Sciences of the USSR). High Temp. 12: No. 5, 889-891 (May 1975).

A study was made of the mean coefficient of thermal expansion of tungsten-rhenium alloys in the interval 200–900 °C. An anomalous concentration dependence of the mean coefficient of thermal expansion of the alloys under study is disclosed. A theoretical explanation of the effect is proposed. (auth)

**26220** THE EMISSION INHOMOGENEITY OF MOLYBDENUM. Gerashchenko, S.S.; Dogadaev, R.V.; Martynov, V.L. (I. V. Kurchatov Institute of Atomic Energy). High Temp. 12: No. 5, 892-898 (May 1975).

A thermoemission microscope ($P_{res}$, $1.0–4.0 \cdot 10^{-7}$ mm Hg) was used to investigate the emission characteristics of different sorts of molybdenum: an alloy based on molybdenum with industrial impurities of Ti and Zr within the limits of 1%, MChVP molybdenum, and single-crystal molybdenum, (111) face. Histograms are constructed of the distribution function of the work function with respect to the emission surface for the alloy, and for MChVP molybdenum in the starting state and after heat treatments. The article discusses the effect of carbon-containing components of the residual gas as a possible reason for the low value of the work function for the alloy. The effect of residual gases on the numerical value of the work function is confirmed for single-crystal molybdenum, (111) face. The determining mechanisms in the change in the emission picture as a result of high-temperature heat treatment of the alloy, MChVP molybdenum, and single-crystal molybdenum, (111) face are discussed. (auth)

**26221** DECOMPOSITION OF AUSTENITE IN AN IRON–COBALT–MOLYBDENUM ALLOY. Musiol, C.; Brook, R. (Univ. of Sheffield, Eng.). Scr. Metall.; 9: No. 7, 693-696 (Jul 1975).

The heat treatment characteristics and mechanical properties of an Fe–20 percent Co–5 percent Mo were investigated. Two laboratory melts were made in which a difference in deoxidation procedure resulted in differences in residual C and O content. The similar transformation characteristics of the melts are described along with the effects of C content. The melt containing the greater C content showed lower martensitic transformation temperature, higher yield strength, and greater toughness. (JRD)

**26222** INTERNAL FRICTION OF Nb AFTER DEFORMATION AT LOW TEMPERATURE. Ferron, G.; Riviere, A.; Quintard, M.; Petit, J.; de Fouquet, J. (CNRS, Poitiers, France). Scr. Metall.; 9: No. 7, 697-704 (Jul 1975). (In French).

The behavior of the internal friction peaks P alpha and P beta of Nb after deformation at –180°C and without intermediary reheating was examined during successive temperature increases to 80°C. A very sharp evolution of the peaks was found in this temperature region. The experimental observations show that the identification of the relaxation peaks observed after cold working must take into consideration the effect of the deformation temperature and possible intermediary anneals below 50°C. An increase of the peak P alpha and the progressive elimination of different beta effects between -120 and 50°C was detected on metal cold worked at -180°C. An evolution of the configuration of the dislocations and their immediate environment, caused by relatively mobile defects, was proposed. (JSR)

**26223** DIRECT OBSERVATION OF (110) [110] SLIP IN FCC SINGLE CRYSTALS OF A NICKEL BASE SUPERALLOY. Carry, C.; Strudel, J. L. (Ecole des Mines de Paris). Scr. Metall.; 9: No. 7, 731-736 (Jul 1975).

Elementary slip mechanisms during creep at 850°C were studied in single crystals of Ni-base superalloys. It was found that although in pure fcc metals the unusual glide mode appears only after large deformations have taken place or by shock-loading, in all nickel base superalloys because of their high threshold stress, this mechanism is triggered directly from the beginning. The need for high temperature and high stress for (110) [anti 110] activated slip is confirmed by these observations. Experiments are underway to investigate the activation of [110] glide at various strain-rates. (auth)

**26224** DIFFUSION OF /sup 114m/In IN NiAl. Lutze-Birk, A.; Jacobi, H. (Max-Planck-Institut fuer Eisenforschung, Duesseldorf). Scr. Metall.; 9: No. 7, 761-765 (Jul 1975).

The mobility of Al and Ni atoms in NiAl was studied by measuring the diffusivity of /sup 114m/In in this compound. From a comparison with the diffusivities of the transition metal atoms it may be concluded that the mobilities of both species are controlled by both lattice defects V/sub Ni/ and Ni/sub Al/ in a correlated diffusion mechanism. As in the diffusion studies of the transition metal atoms a maximum in the activation energy was observed near stoichiometry for the diffusion of In. This is explained by an increasing concentration of structural defects upon deviation from stoichiometry which reduces the total activation energy by a term equal to the formation energy of thermal defects. (auth)

**26225** ACOUSTIC EMISSION DUE TO DEFORMATION TWINNING IN TITANIUM AND Ti–6Al–4V ALLOY. Tanaka, H.; Horiuchi, R. (Tokyo Univ.). Scr. Metall.; 9: No. 7, 777-780 (Jul 1975).

Deformation slip and twinning in Ti–Al–V alloys were studied using acoustic emission. It was found that acoustic emission during plastic deformation of titanium and Ti–6Al–4V alloy were accompanied by twin formation. Furthermore, it is important that acoustic emission technique is an effective method for detecting twinning. (auth)

**26226** MODEL FOR ANOMALOUS SELF-DIFFUSION IN GROUP-IV*B* TRANSITION METALS. Sanchez, J.M.; de Fontaine, D. (Materials Department, School of Engineering and Applied Science, University of California, Los Angeles, California 90024). Phys. Rev. Lett. 35: No. 4, 227-230 (28 July 1975).

A model for anomalous diffusion in the bcc phase of group IV*B* transition metals is proposed, based on the identity of structure of the activated complex for diffusion and the basal plane of the low-temperature metastable $\omega$ phase. An expression for the diffusion coefficient is derived from a phenomenological free energy of formation of an $\omega$ embryo. Excellent agreement is obtained with experimental data for bcc Zr. (auth)

**26227** CRITICAL BEHAVIOR AT A VALENCE INSTABILITY. Lawrence, J.M.; Croft, M.C.; Parks, R.D. (Department of Physics and Astronomy, University of Rochester, Rochester, New York 14627). Phys. Rev. Lett. 35: No. 5, 289-292 (4 Aug 1975).

The isomorphic phase transition in the system $Ce_{1-x}Th_x$, which is characterized by a delocalization of the 4*f* electron and a concomitant volume change, has been studied through measurements of the density and resitivity. For samples near the critical composition ($x \simeq 0.264$) derivatives of these quantities diverge with mean-field exponents. Such mean-field behavior implies a long-force range, and suggests that electroelastic coupling dominates the critical behavior. (auth)

**26228** HIGH-PRESSURE EFFECTS ON THE SUPERCONDUCTING TRANSITION TEMPERATURE OF ALUMINUM. Gubser, D.U.; Webb, A.W. (Naval Research Laboratory, Washington, D. C. 20375). Phys. Rev. Lett. 35: No. 2, 104-107 (14 July 1975).

The superconducting transition temperature $T_c$ of aluminum has been measured as a function of pressure to 62 kbar, at which point $T_c$ was reduced to 0.075 *K* from its zero pressure value of 1.18 *K*. These data cover ranges of temperature and pressure which allow differentiation between theoretical and empirical predictions. The data clearly obey the empirical relation of Smith and Chu and suggest a new volume dependence for the electron-phonon interaction. (auth)

**26229** SUPERCONDUCTING PROPERTIES OF THE SINGLET—GROUND-STATE SYSTEM (*La*Pr)$Sn_3$. McCallum, R.W.; Fertig, W.A.; Luengo, C.A.; Maple, M.B. (Institute for Pure and Applied Physical Sciences, University of California, San Diego, La Jolla, California 92037); Bucher, E.; Maita, J.P.; Sweedler, A.R.; Mattix, L.; Fulde, P.; Keller, J. Phys. Rev. Lett. 34: No. 26, 1620-1623 (30 June 1975).

The depressions of the superconducting transition temperature $T_c$ as a function of Pr concentration and the specific-heat jump $\Delta C$ at $T_c$ as a function of $T_c$ have been measured for the singlet-ground-state system (LaPr)$Sn_3$. The results are well represented by numerical calculations based on the Pr energy-level scheme determined from separate measurement of the Schottky heat-capacity anomaly and the Van Vleck paramagnetic susceptibility contributed by the Pr ions. (auth)

**26230** EXPERIMENTAL CONTRIBUTION TO THE SUMMATION PROBLEM OF PINNING FORCES IN TYPE-II SUPERCONDUCTORS. Antesberger, G.; Ullmaier, H. (Institut für Festkörperforschung der Kernforschungsanlage, D 517 Jülich, Germany). Phys. Rev. Lett. 35: No. 1, 59-62 (7 July 1975).

The pinning-force density $P_v$ in Nb single crystals containing platelike $Nb_2N$ precipitates shows a strong dependence on the orientation of the precipitates with respect to the flux-line direction. Using purely geometrical arguments this anisotropy can be quantitatively explained by assuming that $P_v \propto K^2_0$, where $K_0$ is the individual flux-line-defect interaction force. This points to a summation process which is governed by the elastic behavior of the flux lattice. (auth)

**26231** MASS-SPECTROGRAPHIC ANALYSIS OF HIGH-$T_c$ Nb-Ge SPUTTERED FILMS. Santhanam, A.T.; Gavaler, J.R. (Westinghouse Research Laboratories, Pittsburgh, Pennsylvania 15235). J. Appl. Phys. 46: No. 8, 3633-3636 (Aug 1975).

Secondary ion mass spectroscopy (SIMS) has been used to determine the concentration profiles of niobium and germanium in high-$T_c$ (22 K) Nb-Ge films which were deposited onto polished sapphire substrates by a low-energy sputtering technique. X-ray lattice parameter data on such films indicate that in some cases their average composition is Nb-rich nonstoichiometric $Nb_3Ge$. The SIMS analysis reveals a nonuniform composition within these sputtered films. The Ge concentration increases with film thickness but at least a portion of the film has the stoichiometric $Nb_3Ge$ composition. The occurrence of high critical temperatures in such films is thus still compatible with the hypothesis that the highest $T_c$'s in the Nb-Ge system are due to the presence of the stoichiometric or near-stoichiometric $Nb_3Ge$ compound. (auth)

**26232** EFFECT OF IMPURITIES AND STRAIN AMPLITUDE ON SLIP IN FATIGUE OF NIOBIUM SINGLE CRYSTALS. Nine, H.D. (Research Laboratories, General Motors Corporation, Warren, Michigan 48090). J. Appl. Phys. 46: No. 8, 3260-3265 (Aug 1975).

The type of slip deformation and the fatigue life in torsional fatigue of niobium single crystals were found to depend on both the cyclic strain amplitude and the interstitial impurity content. Two different slip-type populations were observed. At low strain amplitude, one population showed persistent slip bands, but the other, fatigued under identical conditions, showed asymmetric slip and asymmetric deformation. Differences in the two populations were related to interstitial impurity content. It is suggested that interstitial impurities affect the slip type by inhibiting cross-slip of dislocations. (auth)

**26233** LATTICE CONSTANTS OF $\beta$-$PdH_x$ AND $\beta$-$PdD_x$ WITH $x$ NEAR 1.0. Schirber, J.E.; Morosin, B. (Sandia Laboratories, Albuquerque, New Mexico 87115). Phys. Rev. B 12: No. 1, 117-118 (1 July 1975).

Lattice constants of the $\beta$ phase of $PdH_x$ and $PdD_x$ for the concentration range $0.8 < x < 0.98$ have been measured at 77 K using a powder x-ray diffraction technique. The lattice constant $a_0$ of $PdH_x$ is slightly larger ($\sim 0.1\%$) than of $PdD_x$ and $d \ln a_0/dx = 0.044$ for both $PdH_x$ and $PdD_x$; extrapolated $a_0$ values for $x = 1.0$ are 4.090 and 4.084 Å for PdH and PdD, respectively. This study shows that the inverse isotope effect in the superconducting transition temperature is not simply a result of the relative volume of $PdH_x$ and $PdD_x$. (auth)

**26234** NUCLEAR ACOUSTIC RESONANCE IN SINGLE-CRYSTAL HYDROGEN-FREE TANTALUM. Sundfors, R.K.; Wang, T.H.; Bolef, D.I.; Fedders, P.A. (Laboratory for Ultransonics, Physics Department, Washington University, St. Louis, Missouri 63130); Westlake, D.G. Phys. Rev. B 12: No. 1, 26-30 (1 July 1975).

Nuclear-acoustic-resonance studies have been made of single-crystal 99.99% pure tantalum metal from which all hydrogen has been removed (hydrogen concentration much less than 7 at. ppm or 0.04 wt ppm). The shapes and widths of the $^{181}Ta$ $\Delta m = \pm 1$ and $\pm 2$ absorption lines can be explained as due to quadrupole broadening caused by a random distribution of charged impurities. Unlike hydrogenated Ta, the $\Delta m = \pm 2$ line shape and linewidth for the hydrogen-free specimen are independent of magnet angle and temperature between 78 and 300 K. The measured $^{181}Ta$ Knight shift is $(1.14 \pm 0.02)$ % relative to $^{181}Ta$ in $KTaO_3$. The magnitudes and relative signs of the components of the tensor relating electric field gradient to elastic strain are $S_{11} = \pm 26 \times 10^{15}$ statcoulomb $cm^{-3}$ and $S_{44} = -29 \times 10^{15}$ statcoulomb $cm^{-3}$. (auth)

**26235** THEORY OF NUCLEAR SPIN DIFFUSION IN A SPATIALLY VARYING MAGNETIC FIELD. Genack, A.Z.; Redfield, A.G. (Columbia University, New York, New York 10027 and IBM Thomas J. Watson Research Center, Yorktown Heights, New York 10598). Phys. Rev. B 12: No. 1, 78-87 (1 July 1975).

Spin diffusion driven by either a magnetization gradient or a field gradient is viewed as a flow of magnetization current. An expression for this current in a nonuniform field is derived. The magnetization current is the vehicle for a cross relaxation between the nuclear dipole-dipole energy and the spin energy of interaction with the inhomogeneous part of the magnetic field. From a measurement of the decay rate of dipole energy in the presence of large field gradients, which are present in type-II superconductors or at normal-superconductor interfaces, the spin-diffusion coefficient can be determined. Coupled differential equations describing magnetization and dipole energy densities are deduced and their solution is discussed. (auth)

**26236** SPIN WAVES IN TERBIUM. I. TWO-ION MAGNETIC ANISOTROPY. Jensen, J.; Houmann, J.G.; Møller, H.B. (Danish Atomic Energy Commission, Research Establishment Risø, Roskilde, Denmark). Phys. Rev. B 12: No. 1, 303-319 (1 July 1975).

The energies of spin waves propagating in the *c* direction of Tb have been studied by inelastic neutron scattering, as a function of a magnetic field applied along the easy and hard directions in the basal plane, and as a function of temperature. From a general spin Hamiltonian, consistent with the symmetry, we deduce the dispersion relation for the spin waves in a basal-plane ferromagnet. This phenomenological spin-wave theory accounts for the observed behavior of the magnon energies in Tb. The two $\hat{q}$-dependent Bogoliubov components of the magnon energies are derived from the experimental results, which are corrected for the effect of the direct coupling between the magnons and the phonons, and for the field dependence of the relative magnetization at finite temperatures. A large $\hat{q}$-dependent difference between the two energy components is observed, showing that the anisotropy of the two-ion coupling between the magnetic moments in Tb is substantial. The $\hat{q}$-dependent anisotropy deduced at 4.2 K is of the same order of magnitude as the isotropic part, and depends strongly on the orientation of the moments in the basal plane. The rapid decrease of both the axial- and the basal-plane anisotropy with increasing temperatures implies that the two-ion coupling is effectively isotropic above $\sim 150$ K. We present arguments for concluding that, among the mechanisms which may introduce anisotropic two-ion couplings in the rare-earth metals, the modification of the indirect exchange interaction by the spin-orbit coupling of the conduction electrons is of greatest importance. (auth)

**26237** SPIN WAVES IN TERBIUM. II. MAGNON-PHONON INTERACTION. Jensen, J.; Houmann, J.G. (Danish Atomic Energy Commission Research Establishment, Risø, Roskilde, Denmark). Phys. Rev. B 12: No. 1, 320-331 (1 July 1975).

The selection rules for the linear couplings between magnons and phonons propagating in the *c* direction of a simple basal-plane hcp ferromagnet are determined by general symmetry considerations. The acoustic-optical magnon-phonon interactions observed in the heavy-rare-earth metals have been explained by Liu as originating from the mixing of the spin states of the conduction electrons due to the spin-orbit coupling. We find that this coupling mechanism introduces interactions which violate the selection rules for a simple ferromagnet. The interactions between the magnons and phonons propagating in the *c* direction of Tb have been studied experimentally by means of inelastic neutron scattering. The magnons are coupled to both the acoustic- and optical-transverse phonons. By studying the behavior of the acoustic-optical coupling, we conclude that it is a spin-mixed-induced coupling as proposed by Liu. The coupled magnon–transverse-phonon system for the *c* direction of Tb is analyzed in detail, and the strengths of the couplings are deduced as a function of wave vector by combining the experimental studies with the theory. (auth)

**26238** SPIN WAVES IN TERBIUM. III. MAGNETIC ANISOTROPY AT ZERO WAVE VECTOR. Houmann, J.G.; Jensen, J. (Danish Atomic Energy Commission Research Establishment Risø, Roskilde, Denmark); Touborg, P. Phys. Rev. B 12: No. 1, 332-344 (1 July 1975).

The energy gap at zero wave vector in the spin-wave dispersion relation of ferromagnetic Tb has been studied by inelastic neutron scattering. The energy was measured as a function of temperature and applied magnetic field, and the dynamic anisotropy parameters were deduced from the results. The axial anisotropy is found to depend sensitively on the orientation of the magnetic moments in the basal plane. This behavior is shown to be a convincing indication of considerable two-ion contributions to the magnetic anisotropy at zero wave vector. With the exception of the sixfold basal-plane anisotropy of the unstrained lattice, the dynamic anisotropy parameters deduced from our results agree with macroscopic measurements both with respect to the magnitudes (at zero temperature) and the temperature dependences. The deviations observed cannot be explained by existing theories which include the effects of zero-point deviations from the fully aligned ground state, and we tentatively propose polarization-dependent two-ion couplings as their origin. (auth)

**26239** STUDIES OF TIN JOSEPHSON JUNCTIONS OF ANOMALOUSLY HIGH SUPERCURRENT. Paley, S.; Wilson, J.; Gayley, R.I. (State University of New York, Buffalo, New York 14214). Phys. Rev. B 12: No. 1, 157-162 (1 July 1975).

We have studied tin Josephson junctions that have unusually high supercurrents and which exhibit bulk values for superconducting energy gap and critical temperature. We find good agreement with the BCS theory for the temperature dependence of the energy gap and the maximum supercurrent. Our results agree with the prediction, based on strong-coupling theory, that the ratio of gap to critical temperature should be slightly higher than the BCS value. For the maximum supercurrent we find the BCS value in disagreement with the strong-coupling prediction that the supercurrent should not exceed 91% of the BCS value. (auth)

**26240** MAGNETIZATION OF AMORPHOUS Gd-Co-Ni FILMS. Hasegawa, R.; Taylor, R.C. (IBM Thomas J. Watson Research Center, Yorktown Heights, New York 10598). J. Appl. Phys. 46: No. 8, 3606-3608 (Aug 1975).

The temperature dependence of magnetization from 4.2 to 500 °K for amorphous Gd-Co-Ni films obtained by evaporation is found to be satisfactorily described by a two-sublattice model in which the two 3*d* transition metals form one sublattice interacting antiferromagnetically with the Gd sublattice. The unique magnetization behavior observed is attributed to an intersublattice exchange interaction which is small in comparison to the transition-metal intrasublattice exchange interaction. (auth)

**26241** STRUCTURE AND SUPERCONDUCTIVITY OF METASTABLE PHASES IN LIQUID-QUENCHED Zr-Rh ALLOYS. Togano, K.; Tachikawa, K. (National Research Institute for Metals, 2-3-12 Nakameguro, Meguro-Ku, Tokyo, Japan). J. Appl. Phys. 46: No. 8, 3609-3613 (Aug 1975).

Using the liquid-quenching technique adapted to an arc furnace, Zr-Rh alloys containing 0–36 at.% Rh were rapidly quenched from the liquid state. Body-centered cubic solid solution of Zr is retained up to 17 at.% Rh beyond the maximum equilibrium solubility limit of 8 at.% Rh. Broad maxima in the x-ray and electron diffraction patterns, indicative of a noncrystalline structure, are obtained for alloys containing 18–27 at.% Rh. The noncrystalline phase shows a sharp superconducting transition at 4.1 K. The annealing behaviors of the metastable phases were investigated by continuous observations in the hot stage of an electron microscope and electrical resistivity measurements. The metastable phases transform to equilibrium phases on heating at temperatures above 500 °C and very fine structures are produced by the transformation. (auth)

**26242** DETECTION OF SURFACE NITROGEN IN HIGH-$T_c$ $Nb_3Ge$ FILMS BY AUGER ANALYSIS. Shen, L.Y.L. (Bell Laboratories, Murray Hill, New Jersey 07974). J. Appl. Phys. 46: No. 8, 3614-3618 (Aug 1975).

Auger electron spectroscopy was applied to $Nb_3Ge$ films that possessed $T_c$'s above 20 K. The surface composition was determined from the Auger spectra. A considerable amount of nitrogen was detected on the surface. This amount, which varied by a factor of 3 across the surface, was 100 times higher than the nitrogen concentration in the film. The discrepancy is tentatively assigned to the effect of argon-ion sputter cleaning prior to the Auger measurements. (auth)

**26243** NEW MAGNETIC MATERIALS. Nagel, H. Brown Boveri Rev.; 62: No. 5, 210–214(May 1975).

Properties of permanent magnet materials recently developed at Brown Boveri and based on the rare earth elements are described. These new types of magnets markedly extend the current range of Recoma magnets. The diversity of available magnetic properties will allow Recoma magnets to be introduced into many fields of application. The materials include alloys of Co with RE = Sm, misch metal, Y and Fe and Cu. (DLC)

**26244** TWO PHONON SCATTERING OF X RAYS IN BODY CENTERED CUBIC METALS. Lahti, A. V.; Laehteenkorva, E. E. (Oulu Univ., Finland). J. Phys., F (London); 5: No. 7, 1249–1256 (Jul 1975).

Calculations of two phonon scattering intensities for vanadium at 300 °K show that the approximation in which the Brillouin zone is replaced by the Debye sphere overestimates the intensity in a wide region around the zone center and underestimates it near the outermost zone corners. The deviations seem to be directly related to zone geometry. Their contribution to the total diffuse intensity is comparatively small. In a geometrically correct approximation, which is independent of experimental dispersion data, the two phonon intensities are calculated from the elastic constants. This method is applicable to all bcc metals. (auth)

**26245** LOW TEMPERATURE RESISTANCE ANOMALIES IN SINGLE CRYSTALS OF Tb AND Dy. Tindall, D. A.; Jericho, M. H. (Dalhousie Univ., Halifax, Nova Scotia). J. Phys., F (London); 5: No. 7, 1359–1364(Jul 1975).

The electrical resistivity of Dy and Tb single crystals was investigated between 4 °K and 60 mK. Instead of being temperature independent the resistance decreased by about 1.3% when the temperature was lowered to 60 mK. The effect is isotropic in Dy but seems to be anisotropic in Tb, where for a c axis sample the resistance increased again below 0.8 °K, after an initial decrease. The suggested interpretation of the effect is a splitting of impurity levels, which can modify the elastic and inelastic scattering of the conduction electrons. (auth)

**26246** MOESSBAUER SPECTROSCOPY OF RARE EARTH IMPURITIES IN HEXAGONAL HOST METALS: ZrEr. Stoehr, J.; Cashion, J. D.; Wagner, W. (Technische Univ., Munich). J. Phys., (London); 5: No. 7, 1417–1425(Jul 1975).

The Moessbauer effect can be used to obtain information on the electronic ground state of rare earth impurities in hexagonal host metals. It is shown that the properties of the electronic ground state may in general be determined unambiguously and it is pointed out that for Moessbauer studies polycrystalline samples are sufficient. Experimentally the system ZrEr is considered, where the data indicate that an error was made in the analysis of previous Moessbauer data. The CEF ground state of Er impurities in Zr is found to be a $\Gamma_7$ Kramers' doublet with $g_{\parallel} = +13.8 \pm 0.4$ and $|g_{\perp}| = 2.8 \pm 0.2$. The exchange coupling constant is derived to be $|J_{sf}| = 3.5 \times 10^{-2}$ eV. (auth)

**26247** POSSIBLE PREFERENTIAL ORDER-DISORDER IN A15($\beta$-W TYPE) COMPOUNDS. Wand, F. E.; Holden, J. R. (Naval Surface Weapons Center, Silver Spring, MD). Solid State Commun.; 17: No. 2, 225–227(15 Jul 1975).

A possible existence of preferential disorder in the B sites in $A_3B$($\beta$-W type) compounds is demonstrated. This appears to support the "A-chain integrity" recognized in these compounds. Therefore, the correlation between the order–disorder parameters and the superconducting critical temperatures, investigated in the past, should be reexamined. (auth)

**26248** AC QUANTUM INTERFERENCE IN SUPERCONDUCTING FILMS WITH PERIODICALLY MODULATED THICKNESS. Martinoli, P.; Daldini, O.; Leeman, C.; Stocker, E. (Eidgenoessische Technische Hochschule, Zurich). Solid State Commun.; 17: No. 2, 205–209(15 Jul 1975).

Alternating current quantum interference has been observed in type II superconducting films with periodic thickness modulation. Marked supercurrent steps appear at well defined voltages in the current-voltage characteristics when vortex motion is induced by superimposed dc and rf currents. An essential condition for the observation of the effect is matching of the vortex lattice to the periodic pinning structure due to the thickness modulation. (auth)

**26249** TUNNELING EXPERIMENTS ON SUPERCONDUCTING PALLADIUM–DEUTERIUM ALLOYS. Eichler, A.; Wuehl, H.; Stritzker, B. (Kernforschungsanlage, Juelich, Ger.). Solid State Commun.; 17: No. 2, 213-216(15 Jul 1975).

Superconducting tunneling experiments on D/Pd ≃ 0.9 samples show that this Pd–D alloy is a weak coupling superconductor ($2\Delta/kT_c = 3.6$). The tunneling characteristics prove the optical phonon modes of the deuterium to play an important role for superconductivity. (auth)

**26250** NMR OF Dy NUCLEI IN FERROMAGNETIC $DyAl_2$ AND Dy METAL. Berthier, Y. (Grenoble Univ., France); Barak, J.; Barbara, B. Solid State Commun.; 17: No. 2, 153-155(15 Jul 1975).

The NMR spin echo of Dy nuclei in ferromagnetic $DyAl_2$ yields for the $^{161}$Dy hyperfine field constant, $a = -845.2 \pm 0.3$ MHz and quadrupolar splitting. $2P = 420.0 \pm 0.3$ MHz compared with $a = -830.0 \pm 0.5$ MHz and $2P = 387.8 \pm 0.5$ MHz in ferromagnetic Dy metal. The different contributions to these parameters are discussed. A line, observed at 1273 MHz in Dy metal, is attributed to $\Delta m_I = 2$ transition. (auth)

**26251** LATTICE DISTORTIONS DUE TO DEUTERIUM IN NIOBIUM. Bauer, G.; Seitz, E.; Horner, H.; Schmatz, W. (Kernforschungsanlage, Juelich, Ger.). Solid State Commun.; 17: No. 2, 161-165(15 Jul 1975).

The quasielastic diffuse scattering of neutrons from deuterium interstitials in niobium has been measured and compared with data calculated from a Kanzaki force model with central forces acting on nearest and next-nearest neighbors. It is found that the cubic symmetry of the long range distortion field of H in Nb is already established in the immediate neighborhood of the defect. (auth)

**26252** NEW MAGNETOELECTRIC COMPOUND: $DyCoO_3$. Velleaud, G.; Mercier, M. (Institut Universitaire de Technologie, Montlucon, France). Solid State Commun.; 17: No. 2, 237-239 (15 Jul 1975).

A first order magnetoelectric effect with $\alpha = 10^{-2}$ is measured on a powder sample of $DyCoO_3$, due to the $Dy^{3+}$ ions. The metamagnetic behavior is demonstrated. (auth)

**26253** ULTRASONIC ATTENUATION IN PURE AND Gd-DOPED SUPERCONDUCTORS: $LaSn_3$ AND $LaAl_2$. Herrmann, G.; Boemmel, H. E. (Konstanz Univ., Ger.). Solid State Commun.; 17: No. 2, 241-244(15 Jul 1975).

The ultrasonic attenuation (UA) has been investigated in the pure and magnetically doped superconductors $LaSn_3$ and $LaAl_2$, the latter being an ideal Abrikosov–Gorkov system. The UA of pure $LaSn_3$ and $LaAl_2$ agrees well with BCS prediction. The experiments in doped $LaSn_3$ proved difficult due to high background attenuation. The results in $La_{1-n}Gd_nAl_2$ (n = 0.377 at. %), though, show a significant discrepancy with the theories which is not understood. (auth)

**26254** NEW INTERPRETATION OF SURFACE STATES IN W AND Mo. Kasowski, R. V. (Du Pont de Nemours (E. I.) and Co., Wilmington, DE). Solid State Commun.; 17: No. 2, 179-183(15 Jul 1975).

The linear combination of muffin tin orbitals (LCMTO) technique has been used to calculate surface states in the s, $dz^2$ band gap of W and Mo. These states are found to be very sensitive to surface reconstruction effects in that they become more localized and their energies shift by ~0.08 Ry. Furthermore, reconstruction reduces the dangling bond charge density in the vacuum region. (auth)

**26255** COMMENT ON POSSIBLE CORRELATION BETWEEN T/sub c/ AND THE NUMBER OF STABLE ISOTOPES OF SUPERCONDUCTING ELEMENTS. Ottinsen, T.; Parr, H. (Univ., Oslo). Solid State Commun.; 17: No. 2, 137-138(15 Jul 1975).

Recently a correlation between $T_c$ and the number of naturally occurring isotopes (N) of the superconducting elements has been claimed. It is proposed that this merely reflects the connection between $T_c$ and the valence: odd valence means odd Z and few stable isotopes. (auth)

**26256** INVESTIGATION OF THE RELATIONSHIP BETWEEN FRACTURE TOPOGRAPHY AND MICROSTRUCTURE OF THREE TITANIUM ALLOYS. Chesnutt, J. C.; Williams, J. C. (Rockwell International, Thousand Oaks, CA). pp 895-902 of Scanning Electron Microscopy, 1974. Johari, O.; Corvin, I. (eds.). Chicago; Illinois Institute of Technology, SEM Symposia Office (1974).

From proceedings of the scanning electron microscopy; Chicago, Illinois, USA (8 Apr 1974).

The microstructures and mechanical properties of two commercial alpha + beta titanium alloys (Ti–6Al–4V and Ti–6Al–2Sn–4Zr–6Mo) and one metastable beta alloy (Ti–11.5Mo–4Sn–6Zr) were varied over a wide range by thermal and thermomechanical treatment. A total of nine microstructural conditions including the beta-phase, (beta + omega) phases and (alpha + beta) phase were analyzed. In the alpha + beta alloys, these conditions include variations in volume fraction primary alpha from 0 to 50 percent and variations in yield strength from 100 to 180 ksi. The fracture surfaces examined represent both fatigue and monotonic loading, the latter being in either plane stress or plane strain. Wide variations in fracture topography, including flat, fatigue fracture of primary alpha, intergranular fracture along prior beta grain boundaries, and ductile tearing are observed. These variations are related to various differences. (auth)

**26257** REMARKS ON SOME EXCEPTIONS TO THE ENGEL–BREWER RULES. Hill, H. H. (Los Alamos Scientific Lab., NM). J. Phys. Chem. Solids; 36: 830-831(1975).

A simple expression for extrapolating measured shear moduli to very high pressures was compared with the modulus G/sup TF/ calculated using the Thomas–Fermi model. Previously reported experimental measurements on metals and semimetals were compared with G/sup TH/ and only Be exceeded this value significantly and only Ti, Zr, and Nb were significantly lower. The shear modulus G was calculated for Al using the simple expression and compared with G/sup TH/. (JSR)

**26258** ENHANCEMENT OF THE SUPERCONDUCTING TRANSITION TEMPERATURE BY ION IMPLANTATION. Meyer, O. (Kernforschungszentrum, Karlsruhe, Ger.). J. Jap. Soc. Appl. Phys., Suppl.; 44: 23-29(Jan 1975).

From 6th conference on solid state devices; Tokyo, Japan (2 Sep 1974).

$T_c$ is increased if Al, Mo, and Re films are implanted with ions able to form intermetallic compounds but otherwise of low solubility in Al, Mo, and Re. For Al, the $T_c$ increase is pronounced for large electronegativity values except Au; Cs increases $T_c$. For Mo, a change transfer mechanism is responsible for the $T_c$ increase. $T_c$ of Re is increased by Zr, N, and S implants. (DLC)

**26259** PRESSURE DEPENDENCE OF THE MAGNETIC ORDERING TEMPERATURE OF $Gd_3Co$ AND $Tb_3Co$. Parviainen, S. (Univ., Turku, Finland). Phys. Status Solidi (a); 30: No. 2, K173-K176(16 Aug 1975).

The temperature variation of the low-field mutual inductance was measured at 1 to 3500 bar. The max at the Neel transition decreased with pressure and shifted to lower temperatures. Results are treated using the RKKY model. (DLC)

**26260** TRANSFERRED HYPERFINE FIELDS AT THE TIN SITE IN THE HEUSLER-TYPE ALLOYS $Co_2YSn$ (Y = Ti, Zr, Hf, V). Gorlich, E. A.; Kmiec, R.; Latka, K.; Matlak, T.; Ruebenbauer, K.; Szytula, A.; Tomala, K. (Jagiellonian Univ., Krakow). Phys. Status Solidi (a); 30: No. 2, 765-770(16 Aug 1975).

The hyperfine magnetic fields at the tin site in ferromagnetic Heusler type alloys $Co_2YSn$ (Y = Ti, Zr, Hf, V) were measured by the Moessbauer effect using the 23.9-keV γ-line in $^{119m}$Sn. The samples were checked by x-ray diffraction analysis, magnetization measurements, and neutron diffraction (for $Co_2TiSn$ only). Results were interpreted in terms of the Blandin–Campbell formalism and qualitative agreement with the experimental data was obtained for a number of conduction electrons per atom of about 0.5. (auth)

**26261** MAGNETIC ANISOTROPY OF SINGLE CRYSTALS OF INTERMETALLIC $R_2Co_{17}$ (R = Tb, Dy, Ho, Lu) COMPOUNDS. Deryagin, A. V.; Kudrevatykh, N. V. (Ural State Univ., Sverdlovsk, USSR). Phys. Status Solidi (a); 30: No. 2, K129-K133 (16 Aug 1975).

The temperature dependence of the spontaneous magnetization and the magneto crystalline anisotropy field and constants was determined at 77 to 1000°K. (DLC)

**26262** ANALYTICAL SOLUTION FOR THE AVALANCHE BREAKDOWN VOLTAGE OF $p^+$-n JUNCTIONS AND SCHOTTKY DIODES. Lerach, L.; Albrecht, H. (Univ., Munich). Phys. Status Solidi (a); 30: No. 2, 625-636(16 Aug 1975).

A new analytical expression for the avalanche breakdown voltage of $p^+$-n and Schottky diodes as a function of the net doping concentration was derived based on a power function approximation for the charge carrier ionization rates. The breakdown voltage decreases with increasing doping concentration, N, until a minimum is reached corresponding to a doping concentration $N_{min}$. Further increase of N leads to an anomalous behaviour. The breakdown voltage increases with N exceeding $N_{min}$. Normally this effect cannot be measured because the tunneling mechanism dominates the breakdown characteristic in this doping region. The observation is limited therefore to low energy bandgap high-mobility semiconductors, e.g. InSb which is discussed in detail. For this semiconductor the minimum avalanche breakdown voltage has been calculated to be $U_{min} = 1.2$ V occurring at a corresponding doping concentration $N_{min} = 0.7 \times 10^{13}$ cm$^{-3}$. The temperature dependence resulting from this model shows anomalous behaviour

in the doping range $N > N_{min}$. The breakdown voltage decreases with increasing temperature. This is known from published measurements. (auth)

**26263** BULK MAGNETIC BEHAVIOR AND METAMAGNETISM OF SOME RARE EARTH-ZINC ($RZn_2$; R = Eu, Dy, Er, AND Tm) INTERMETALLICS. Debray, D.; Wortmann, B. F.; Methfessel, S. (Ruhr-Univ., Bochum, Ger.). Phys. Status Solidi (a); 30: No. 2, 713-720(16 Aug 1975).

Magnetic measurements on polycrystalline samples of $EuZn_2$, $DyZn_2$, $ErZn_2$, and $TmZn_2$ are reported as functions of temperature and applied field. All the compounds show a Curie-Weiss behaviour in the paramagnetic region characterized by a positive paramagnetic Curie temperature and effective moments which are close to tripositive free-ion values for $DyZn_2$ and $ErZn_2$, and markedly different for $EuZn_2$ and $TmZn_2$. In $EuZn_2$, Eu is in a divalent state and the observed higher effective moment of 8.22 Bohr magnetons is attributable to conduction electron polarization due to s–f exchange interaction. The effective moment of 6.48 Bohr magnetons for $TmZn_2$ is considerably smaller than the tripositive free-ion value and suggests an intermediate valence state for Tm. The observed positive sign of the paramagnetic Curie temperatures is explained in terms of a modified RKKY interaction which takes into account interelectron interaction between the conduction electrons. All the four compounds order magnetically at low temperatures. $EuZn_2$, $DyZn_2$, and $TmZn_2$ order antiferromagnetically, whereas $ErZn_2$ shows a ferromagnetic ordering. Field-induced metamagnetic transitions are observed in $EuZn_2$, $DyZn_2$, and $TmZn_2$. In $EuZn_2$, a first-order type "spin-flop" transition from the antiferromagnetic state (AF–SF) is observed. On the contrary, both $DyZn_2$ and $TmZn_2$ show a first-order type direct transition from the antiferromagnetic to a paramagnetic phase (AF–P). The different behaviour of $EuZn_2$ as compared to that of $DyZn_2$ and $TmZn_2$ is due to the very low magnetocrystalline anisotropy of Eu in its all-spin divalent state. (auth)

**26264** MAGNETIC PROPERTIES, MAGNETIC STRUCTURE, AND CRYSTAL FIELD IN PrZn AND NdZn. Morin, P.; Pierre, J. (C. N. R. S., Grenoble, France). Phys. Status Solidi (a); 30: No. 2, 549-559(16 Aug 1975).

The magnetic properties of PrZn and NdZn compounds are studied by magnetic measurements and neutron diffraction. Both compounds are antiferromagnetic below 52 and 70°K, respectively. The ordered moments are reduced to 2.35 and 2.55 $\mu_B$ at low temperatures by crystal field effects. Dilatometric measurements reveal a large tetragonal distortion, arising at the Néel temperature and reaching 1.4% at 4.2°K in PrZn. The crystal field parameters are found coherent in sign with those of the heavy rare earth compounds. In PrZn, the magnetostriction is sufficient to explain the fourfold direction of the moment. The ambiguities on the magnetic structure are discussed. (auth)

**26265** OPTICAL PROPERTIES OF BERYLLIUM. Taut, M.; Skokan, R. (Univ., Dresden). Phys. Status Solidi (b); 70: No. 2, K157-K160(1 Aug 1975).

The frequency dependent dielectric constant $\epsilon(\omega) = \epsilon_1(\omega) + i\epsilon_2(\omega)$ is calculated. The imaginary part $\epsilon_2(\omega)$ was calculated directly, while the real part $\epsilon_1(\omega)$ was obtained by means of the Kramers–Kronig relation. (DLC)

**26266** $L_I$, $L_{II}$, AND $L_{III}$ ABSORPTION EDGES OF YTTERBIUM METAL AND ITS OXIDE. Nigam, A. K.; Gupta, M. K.; Gupta, R. K. (Indian Telephone Industries Ltd., Lucknow). Phys. Status Solidi (b); 70: No. 2, K173-K177(1 Aug 1975).

Measurements on the position and structure of $L_I$, $L_{II}$, and $L_{III}$ absorption edges in Y are reported along with the shift of the edge in its oxide. White lines accompanying $L_{II}$ and $L_{III}$ on the high energy side are assigned to the transitions $L_{II} \rightarrow O_{IV}$ and $L_{III} \rightarrow O_{IV,V}$. The energies of the $O_{IV}$ and $O_{IV,V}$ levels were determined. (DLC)

**26267** ESR INVESTIGATION OF LOCALIZED STATES IN AMORPHOUS BORON. Gewinner, G.; Kubler, L.; Koulmann, J. J.; Jaegle, A. (Univ. of Haut-Rhin, Mulhouse, France). Phys. Status Solidi (b); 70: No. 2, 595-599(1 Aug 1975).

ESR signals of amorphous boron samples are observed between 1.5 and 800°K. The samples are found to yield a large signal at $g = 2.0028 \pm 2 \times 10^{-4}$ corresponding to a spin density as high as $5 \times 10^{19}$ spins/cm$^3$. This ESR line is attributed to a true bulk effect and the study of line width versus temperature gives direct evidence for the localized nature of the involved electronic states. Diffusion of carriers in these states is observed and the hopping frequency versus temperature determined. The contribution of these singly occupied states to the electric conductivity is estimated to be $\sigma \approx 10^{-4}$ $(\Omega\ cm)^{-1}$ at 300°K. Spin–lattice relaxation times are measured below 77°K and a consistent model for line width and line shape proposed. The intrinsic or extrinsic nature of the observed line is also discussed. (auth)

**26268** SURFACE ENERGIES OF SIMPLE METALS. II. Hietschold, M.; Paasch, G.; Ziesche, P. (Univ., Dresden). Phys. Status Solidi (b); 70: No. 2, 653-662(1 Aug 1975).

The simple model for the electronic structure of surfaces of simple metals given in part I is used to investigate three problems: (1) possibility and physical background for systematization of surface energies, (2) anisotropy, and (3) temperature dependence of surface energies, dipole barriers, and relative lattice relaxation. It is shown that the surface energies show a characteristic dependence from the density parameter $r_s$ and from the valency Z which seems to be most pronounced for valencies one and two. The model is reliable for closed-packed surfaces up to a value of the surface packing fraction of 0.7. The static electronic part of surface energy considered yields only a very small temperature dependence. (auth)

**26269** PSEUDOPOTENTIAL METHOD AND THERMODYNAMICS OF ALLOYS. I. Disordered Solid Solutions. Fuks, D. L.; Zhorovkov, M. F.; Panin, V. E. (Physico-Technical Inst., Tomsk, USSR). Phys. Status Solidi (b); 70: No. 2, 793-798(1 Aug 1975).

A pseudopotential method is applied to construct the thermodynamical potential of a binary solid solution. The state equation is solved for a disordered solid solution. The mixing energy is shown to be a complex concentration function depending on the type of the crystalline lattice. The influence of a uniform compression on the solubility of alloy components is investigated, the enthalpy and work function under adiabatic compression are determined. The numerical calculations are carried out for Mg–Zn and Ba–Cd systems. (auth)

**26270** ELECTRON CONFIGURATION AND MAGNETIC MOMENT OF 3d TRANSITION METAL ATOMS. Galperin, F. M. (State Univ. of the Mordov, Saransk, USSR). Phys. Status Solidi (b); 70: No. 2, K133-K137(1 Aug 1975).

Ferromagnetic criteria are given which show that Ni, Co, Fe but not V, Ti, Sc are ferromagnetic. Atomic magnetic moments are calculated for these metals and for Mn. (DLC)

**26271** MORPHOTROPIC AND ISOMORPHIC SERIES AND TRENDS IN BAND STRUCTURE. Altshuler, A. M.; Vekilov, Yu. Kh.; Umarov, G. R. (Moscow Inst. of Steel and Alloys). Phys. Status Solidi (b); 70: No. 2, K147-K149(1 Aug 1975).

An analysis was made of the band structure of the following two morphotropic series: InP, InAs, InSb, InBi; GaSb, InSb, TlSb; and for the isomorphic series ZnTe, CdTe, HgTe. Their energy gaps are tabulated. (DLC)

**26272** DRAG EFFECT IN INDIUM ANTIMONIDE. Kosarev, V.V.; Tamarin, P.V. (A. F. Ioffe Physicotechnical Institute, Academy of Sciences of the USSR, Leningrad). Sov. Phys.–Semicond. 9: No. 2, 172-175 (Aug 1975).

New information is reported on the size effect in the thermoelectric power of n-type InSb single crystals and an analysis is made of the temperature dependences of the phonon components of the thermoelectric power $\alpha_f(T)$ of n- and p-type samples with different dopant concentrations. The theory of the drag effect is developed for a nonparabolic conduction band and two types of phonon-electron interaction (due to piezoelectric and deformation potential). This theory describes qualitatively the experimental data on the drag effect in n- and p-type indium antimonide. However, the anomalies found in the temperature dependence of $\alpha_f(T)$ cannot be explained by the "classical" theory. It is therefore suggested that these anomalies may be due to special features of the phonon—electron interaction in a field of charged impurities. (auth)

**26273** COMPARATIVE CHARACTERISTICS OF CURRENT INSTABILITIES AND RECOMBINATION RADIATION EMITTED BY AN IMPACT-IONIZED PLASMA IN n-TYPE InSb SUBJECTED TO AN EXTERNAL MAGNETIC FIELD. Grishechkina, S.P.; Luchinin, S.D. (Institute of Semiconductor Physics, Siberian Branch, Academy of Sciences of the USSR, Novosibirsk). Sov. Phys.–Semicond. 9: No. 2, 153-155 (Aug 1975).

A comparative study was made of the characteristics of the integrated intensity of the recombination radiation emitted by an impact-ionized plasma in n-type InSb subjected to an external magnetic field and a similar study was made of current instabilities, which were recorded simultaneously with the recombination radiation. The threshold fields for the excitation of the recombination radiation were always lower than the threshold fields for the appearance of the current instabilities throughout the sample. The distributions of the intensity of the recombination radiation and of the amplitude of the current oscillations along a sample were similar: Both had a minimum in the central part of the sample, which was in good agreement with the distribution of the total electric field along the sample. A qualitative study was made of the influence of an external magnetic field on the recombination radiation intensity and on the amplitude of the current oscillations. Moreover, the dependence of the oscillation amplitude on the current through the sample was investigated. (auth)

**26274 FERROMAGNETIC PROPERTIES OF THE RARE EARTH ELEMENTS.** Druzhinin, V.V.; Zapasskii, S.P.; Povyshev, V.M. (Moscow Engineering Physics Institute). Sov. Phys.—Solid State 17: No. 2, 330-331 (Aug 1975).

The magnetization of the metals Tb, Dy, Ho, Er, and Tm has been calculated in the molecular field approximation taking account of all terms in the one-ion anisotropy of the hexagonal lattice. The external magnetic field is assumed to be in the easy direction, i.e., with H||c for Tb, Dy, and Ho and with H⊥c for Er and Tm. It is assumed that the change of the exchange interaction and the parameters of the anisotropy field from one metal to another is due to the quantum numbers S, L, and J and that the radial integrals do not change. Calculations were made of the magnetization curves for all five metals in different fields, the paramagnetic Curie temperature for the easy direction, and the magnetic moments at low temperatures. The results of the calculation are compared with experiment and discussed. (auth)

**26275 INTERPRETATION OF THE EMISSION SPECTRUM OF LANTHANUM IN THE ULTRASOFT X—RAY REGION.** Kabachnik, N.M.; Sazhina, I.P. (M. V. Lomonosov State University, Moscow). Sov. Phys.—Solid State 17: No. 2, 249-252 (Aug 1975).

The intensities of the emission lines of lanthanum in the $N_{IV,V}$ threshold region are calculated. All the main radiative and nonradiative transitions which arise during the bombardment of La by high-energy electrons have been taken into account in the calculations. The calculation was made on the basis of the many electron theory of the atom within the framework of a diagonalization method. The results of the calculations are compared with the experimental results and the identification of the lines is discussed. (auth)

**26276 HIGH-TEMPERATURE TRANSPORT PROPERTIES OF THULIUM, YTTERBIUM, AND LUTETIUM.** Zinov'ev, V.E.; Gel'd, P.V.; Sokolov, A.L. (S. M. Kirov Ural Polytechnic Institute, Sverdlovsk). Sov. Phys.—Solid State 17: No. 2, 259-260 (Aug 1975).

Measurements are reported of the temperature dependences of the electrical resistivity (from 290 to 1200 °K), thermal diffusivity, and thermal conductivity (from 550 to 1400 °K) of polycrystalline thulium, ytterbium, and lutetium. Near 600 °K ytterbium was found to have a strong anomaly in the transport properties, associated with a phase transition. The results obtained are compared with those for the gadolinium subgroup of rare earth metals and the similarity of the temperature dependences of their thermophysical properties is discussed. (auth)

**26277 LOW TEMPERATURE ANOMALIES IN NIOBIUM, VANADIUM, AND TANTALUM.** Sellers, G. J. Urbana, IL; University of Illinois (1975). 175p. University Microfilms Order No. 75-14,169.

Thesis (Ph. D.).

Specific heats of superconducting Nb, V, and Ta and of normal Ta were measured at 0.05 to 2°K in an outgassed condition and with H or D added as interstitial solutes. The presence of H or D in these bcc transition metals produces an isotope-dependent specific heat anomaly, which can dominate the normal lattice contribution and which appears to be related to a displacive motion of the interstitial H or D. No evidence is found in these metals which would be suggestive of a second superconducting energy gap. Thermal conductivities of superconducting Nb and Ta samples were also measured at 0.04 to 4°K, both outgassed and with dissolved H or D. Presence of H or D results in a decrease of the thermal conductivity. In Nb doped with D, the phonon mean free path exhibits a minimum which occurs at the same temperature at which a deuterium-related anomaly was observed in the specific heat. Phonon scattering caused by the addition of H to Nb or Ta is complicated by the presence of resonant scattering from dislocations produced by precipitation of the beta-phase hydride. A technique was developed which permits the accurate measurement of heat capacities to very low temperatures without the use of a heat-switch. As a test of this technique, the specific heat of Cu, with and without hydrogen impurities, was measured at 0.04 to 1°K. Presence of hydrogen increases the specific heat by approximately 1 percent. Above 0.3°K, the data for hydrogen-free copper are in good agreement with the copper reference equation. At lower temperatures, there is an additional contribution to the heat capacity which might be associated with oxygen impurities. (Diss. Abstr. Int., B)

**26278 TEMPERATURE DEPENDENT RESISTIVITIES OF LEAD AND $Pb_{1-x-y}Bi_xTl_y$ ALLOYS FROM 7 TO 300°K.** Benford, S. M. Kent, OH; Kent State University (1974). 157p. University Microfilms Order No. 75-7080.

Thesis (Ph. D.).

Resistivities of $Pb_{0.9}Bi_{0.1}$, $Pb_{0.9}Tl_{0.1}$, $Pb_{0.9}Bi_{0.5}Tl_{0.05}$, and pure lead were measured between 7 and 300°K by an ac mutual inductance technique. Anharmonic effects as large as 12 percent in lead and nearly 9 percent in Pb—Bi were observed at room temperature, with smaller values for the other alloys. The temperature dependent resistivities exhibited deviation from Matthiesson's rule at all temperatures. (auth)

**26279 PROPERTIES OF SUPERCONDUCTING Cu-RICH COMPOSITES CONTAINING $V_3Si$ OR $V_3Ga$.** Chen, W. Y. K. Pasadena, CA; California Institute of Technology (1975). 164p. University Microfilms Order No. 75-9519.

Thesis (Ph. D.).

Superconducting Cu-rich composites containing the A-15 compounds $V_3Si$ or $V_3Ga$ were made by the "Tsuei" process (melting into ingots followed by cold working and heat treatment). Superconducting transition temperatures of the composites were measured. X-ray diffraction analyses were performed. Microstructures were studied using both the optical metallograph and the scanning electron microscope. For some composites containing $V_3Ga$, the critical current densities as functions of transverse magnetic field up to 60 kG, and as functions of temperature from 4.2 to 12°K were measured. It was found that the Tsuei process does not work for the composites containing $V_3Si$, but works satisfactorily for $V_3Ga$; reasons are discussed. Relations between measured properties and various metallurgical factors such as alloy compositions, cross-section reduction ratios, and heat treatment are discussed. The mechanism for the observed superconductivity in the materials is also discussed. It was also found that the Tsuei composites are expected to have high inherent magneto-thermal stability based on the stability theory of superconducting composites. (DLC)

**26280 PROXIMITY EFFECT IN Ag—Pb ALLOYS.** Sun, Y. S. E. Pasadena, CA; California Institute of Technology (1975). 145p. University Microfilms Order No. 75-9541.

Thesis (Ph. D.).

The superconducting properties and the microstructure of the Ag/sub 100-x/Pb/sub x/ alloys (1 less than or equal to x less than or equal to 5) prepared by rapid quenching from the liquid state with and without subsequent heat treatments, were studied. X-ray diffraction shows that supersaturated solid solutions of Pb in Ag can be obtained up to 3.2 at. percent Pb. By suitable heat treatment, it is possible to vary the size and distribution of the Pb precipitates in the Ag matrix and reproducible superconducting properties in the alloy can be observed. The superconducting transition temperature of these samples can be qualitatively explained by the Silvert and Singh's theoretical calculation. The critical current versus field behavior of these alloys can be explained by the modification of the Josephson effect. It was concluded that the three-dimensional proximity effect is the main mechanism for the superconductivity in the Ag—Pb alloys. Based on the Hilsch empirical formula which was based on experimental results obtained on layer structures, the experimental data show that the electron—phonon—electron interaction in silver is attractive. The interaction parameter NV obtained is approximately 0.06, which would lead to a value of $10^{-8}$ °K for the superconducting transition temperature of Ag. These values are in agreement with other determinations which were done on vapor-deposited metallic film sandwiches. Hence, the Hilsch empirical relation valid for layer structures is also valid in the three-dimensional case. Because the transition temperature and the critical current can be varied in a wide range by controlling the heat treatments, the Ag—Pb superconductors might have some useful applications. (Diss. Abstr. Int., B)

**26281 SURFACE STUDIES OF COBALT ALLOYS IN ULTRA HIGH VACUUM UTILIZING CONTACT RESISTANCE.** Catalano, J. F. Syracuse, NY; Syracuse University (1974). 83p. University Microfilms Order No. 75-9723.

Thesis (Ph. D.).

The utilization of the contact resistance in an ultra high vacuum environment as an experimental observable, which is capable of yielding information concerning surface phenomena, is explored from theoretical, electrical, and mechanical foundations to applications in the prediction of adhesion and friction properties. The classical crossed rod experiment was used to obtain the contact resistance versus applied load plots for three cobalt—rhenium alloy systems. Thus, the effect of alloying on the contact resistance was also investigated. This work was supported by scanning electron microscopy surface studies. Since these experiments were done in ultra high vacuum, $10^{-9}$ torr, and on ultra clean surfaces, the effectiveness of various surface cleaning techniques was explored via the contact resistance. A discrepancy between ac and dc sensing potentials on the resulting contact resistance was found under particular conditions. (Diss. Abstr. Int., B)

**26282 CHEMICAL BOND APPROACH TO METALS AND ALLOYS.** Gualtieri, D. M. Syracuse, NY; Syracuse University (1974). 143p. University Microfilms Order No. 75-10,543.

Thesis (Ph. D.).

The BCS theory of superconductivity was extended to the transition elements and their alloys by a chemical bond approach based on the electronic configurations of the Engel—Brewer theory of alloys. The net attractive potential between electrons in Cooper pairs, V/sub BCS/, for the late transition series elements and

alloys is shown to arise mainly from a generalized electron–electron interaction related to bonding of electrons on the d level alone, the phonon-induced attraction being nearly zero. A mechanism is proposed in which a scattering of superconducting d electrons into nonsuperconducting s and p states is responsible for a predictable reduction in V/sub BCS/. The electron-per-atom ratio and a new chemical parameter, the average atomic radius for coordination twelve, were applied successfully to the prediction of the maximum energy product of multiphase commercial permanent magnets. The correlations developed for the maximum energy product with these two parameters can be applied to optimize the compositions of existing permanent magnets or suggest hypothetical alloy mixtures of possibly better magnetic properties. Heats of reaction of the pseudo-binary alloys Fe Al/sub 3-X/(Ag;Zn;Pt;Au)/sub X/ were measured by DTA calorimetry. Data suggest an enhancement in bond formation at a critical concentration of the electron donor consistent with a simple valence bond model for these alloys. (Diss. Abstr. Int., B)

**26283** SUPERCONDUCTING PENETRATION DEPTH IN THIN FILMS OF LEAD. Kerchner, H. R. Urbana, IL; University of Illinois (1974). 174p. University Microfilms Order No. 75-11,794.

Thesis (Ph. D.).

Attenuation of an axial magnetic field by cylindrical thin films of superconducting lead and their normal-state resistance were measured. From the temperature dependence of the normal-state resistance, the film thickness and the electron mean free path were determined. From the field attenuation, the film thickness, and the mean free path, the superconducting conductivity, the London penetration depth lambda/sub L/, and penetration depth lambda, were derived. In order to interpret the field-attenuation measurements, the coherence length and the superconducting conductivity at finite temperatures were calculated by using the strong-coupling theory of superconducting lead. The experimental results for the superconducting conductivity at zero temperature and its temperature dependence agree well with theoretical and zero-temperature results. The bulk zero-temperature penetration depth lambda (0) should be 453 +- 8 A. (DLC)

**26284** NUCLEAR MAGNETIC RESONANCE STUDY OF DILUTE COPPER—VANADIUM ALLOYS. Follstaedt, D. M. Urbana, IL; University of Illinois (1975). 167p. University Microfilms Order No. 75-14,109.

Thesis (Ph. D.).

$^{51}V$, $^{63}Cu$, and $^{65}Cu$ nuclear resonances were used to obtain information on the relative amounts of dissolved and undissolved vanadium, on the magnetic nature of the dissolved vanadium atom, on the magnetization of the copper host in the vicinity of this dissolved atom, and on the electric field gradients produced in the host when the atom is dissolved. The Knight shift of the dissolved $^{51}V$ resonance is +0.14 +- 0.02 percent at 4.2°K, and increases to +0.21 +- 0.02 percent at 300°K. Estimated characteristic temperatures for the impurity susceptibility are theta equals 1100, 4300°K for quadratic and Curie–Weiss forms of temperature dependence. These are approximately the same as obtained for Cu–Co and are larger than that of Au–V (theta equals 290°K), in agreement with current theoretical understanding of magnetic impurities. An assumed copper satellite was observed to have a magnetic splitting at high fields (up to 58 kgauss) with a splitting relative to the pure copper Knight shift given by DELTA K/K equals −0.662 +- 0.015. It is thought to be due to copper nuclei, which are second nearest neighbors to dissolved vanadium atoms. A magnetization broadening of the $^{63}Cu$ main line at 58 kgauss was observed. Low-field (less than 10 kgauss) satellite studies give a second-order quadrupole satellite, believed due to first neighbor copper nuclei to dissolved vanadium atoms. Its quadrupole coupling constant is estimated to be nu/sub Q/ approximately 3.7 Mc. It is concluded that the magnetic nature of vanadium atoms in copper is similar to that of cobalt, but the electric fields are much stronger around vanadium atoms. (Diss. Abstr. Int., B)

**26285** ULTRASONIC RESONANCE AND NON-RESONANCE STUDIES OF SINGLE CRYSTAL TANTALUM WITH KNOWN HYDROGEN IMPURITIES. Wang, T. H. Seattle; Washington University (1974). 105p. University Microfilms Order No. 75-14,912.

Thesis (Ph. D.).

Tantalum single crystals charged with low hydrogen concentrations C (C equals H/Ta, ranging from 0.000 to 0.0267) were studied using nuclear acoustic resonance (NAR) techniques and background ultrasonic attenuation measurement at 78 to 300°K. Acoustic waves of 10MHz and 5MHz were propagated along the cylindrical axes of the samples, which were the [110] axes. The polarization direction was along the [1$\bar{1}$0] or the [001] axis for 10MHz transverse waves and was along the [1$\bar{1}$0] axis for 5MHz transverse waves. Longitudinal waves of 10MHz were also used. In the NAR experiments, the magnetic field was rotated either in the (110) or the (1$\bar{1}$0) plane. For the dehydrogenated sample, the widths and shapes of the $^{181}Ta$ NAR DELTA m equals +-2 and DELTA m equals +-1 absorption lines can be explained as due to quadrupole broadening caused by a random distribution of static electric field gradients. The elastic constant C' equals $\frac{1}{2}$ ($C_{11} - C_{12}$) increased with decreasing temperature down to 78°K. For the hydrogenated samples, the DELTA m equals +-2 linewidth depends not only linearly on hydrogen concentration (from C equals 0.00488 to C equals 0.0167) at room temperature but also on temperature for each of the two samples with C equals 0.00488 and C equals 0.0115. The activation energy of hydrogen motion in the solid solution phase is measured to be 8.8 +-0.9 KJ/mole and the critical temperature of hydrogen precipitation is 190°K for C equals 0.0115. Thermal hysteresis of this critical temperature is found during warming. The estimated average net strain in the crystal caused by hydrogen precipitation is $3 \times 10^{-4}$ at 78°K where virtually all of the hydrogen are precipitated out as hydride particles. From the measured increases in background ultrasonic attenuation and in $^{181}Ta$ NAR linewidth, it is suggested that the low temperature cycled, hydrogenated samples contain some residual dislocations which are associated with hydrogen precipitation. (Diss. Abstr. Int., B)

**26286** THEORETICAL MAGNON DISPERSION CURVES FOR Gd. Lindgård, P. (Department of Physics, Danish Atomic Energy Commission Research Establishment, Risø, 4000 Roskilde, Denmark); Harmon, B.N.; Freeman, A.J. Phys. Rev. Lett. 35: No. 6, 383-386 (11 Aug 1975).

The magnon dispersion curve of Gd metal has been determined from first principles by use of augmented-plane-wave energy bands and wave functions. The exchange matrix elements $I(\vec{k},\vec{k})$ between the $4f$ electrons and the conduction electrons from the first six energy bands were calculated under the assumption of an unscreened Coulomb interaction. The results are in good overall agreement with experiment provided the $I(\vec{k},\vec{k})$ are diminished by a constant scale factor of about 2 which may be caused by screening. (auth)

**26287** ANISOTROPY OF THE HOT-ELECTRON CONDUCTIVITY IN *n*-TYPE Ge AT LIQUID-HELIUM TEMPERATURE. Movchan, E.A.; Bondar', N.N.; Zinchenko, V.A. (Institute of Semiconductors, Academy of Sciences of the Ukrainian SSR, Kiev). Sov. Phys.—Semicond. 9: No. 2, 227-228 (Aug 1975).

Antimony-doped Ge crystals oriented by the x-ray method were studied at low temperature. We report results of measurements of the field dependence of the electrical conductivity. (AIP)

## Radiation Effects

*Refer also to abstracts 25619, 27419, and 27435.*

**26288** (COO-1198-1137) RECOVERY OF LEAD AFTER ELECTRON IRRADIATION AT 1.5 K. Birtcher, R. C. (Illinois Univ., Urbana (USA). Materials Research Lab.). May 1975. Contract AT(11-1)-1198. 64p. Dep. NTIS $6.25.

The low-temperature recovery of lead following an electron irradiation at 1.5°K shows the same features observed for all fcc metals except for gold. Stage I occurs below 5.5°K. The I/sub D/ recovery substage occurs at 4.15 K +- 0.05°K with an activation energy of 0.010 eV +- 0.001 eV. The I/sub E/ substage shifts with defect concentration in lead as it does in copper. The I/sub E/ activation energy is 0.010 eV +- 0.001 eV. Since platinum and lead anneal in Stage I in the normal fashion, the strange behavior of gold is not clearly determined by its position in the periodic table. (auth)

**26289** IONIZATION MECHANISM OF STRUCTURE DEFECT FORMATION IN INDIUM ANTIMONIDE. Abdullaev, A.; Vitovskii, N.A.; Mashovets, T.V.; Morozov, Yu.G. (A. F. Ioffe Physicotechnical Institute, Academy of Sciences of the USSR, Leningrad). Sov. Phys.—Semicond. 9: No. 1, 43-47 (July 1975).

An analysis is made of the possible mechanism of the formation of structure defects in indium antimonide by irradiation with photons whose energy is insufficient for the generation of Frenkel' pairs in elastic scattering processes. It is shown that the proposed mechanism explains the observed changes in the concentration of electrically active impurities and in the mobility of carriers during irradiation and annealing. (auth)

**26290** IMPLANTATION PROFILES OF LOW-ENERGY HELIUM IN NIOBIUM AND THE BLISTERING MECHANISM. Behrisch, R.; Bøttiger, J.; Eckstein, W.; Littmark, U.; Roth, J.; Scherzer, B.M.U. (Max-Planck-Institut für Plasmaphysik, EURATOM-Association, D 8046 Garching bei München, Federal Republic of Germany). Appl. Phys. Lett. 27: No. 4, 199-201 (15 Aug 1975).

The depth profiles of 1.5–15-keV $^3He$ ions implanted into a Nb single crystal at doses of $5\times10^{16}$–$7\times10^{17}$/cm$^2$ have been measured using the $^3He$ $(d,p)$ $^4He$ reaction. A comparison of the results with theoretical predictions for the range and the damage distribution of $^3He$ in amorphous material shows reasonable agreement. Furthermore, the

Deckeldicke (i.e., thickness of the covers of the blisters) was determined by Rutherford backscattering in double alignment. The results indicate that stress release rather than explosion of gas bubbles is the dominant mechanism in blister formation. (auth)

**26291** REDUCTION OF SURFACE EROSION CAUSED BY HELIUM BLISTERING: MICROSTRUCTURAL EFFECTS. Das, S.K.; Kaminsky, M. (Argonne National Laboratory, Argonne, Illinois 60439); Rossing, T.D. Appl. Phys. Lett. 27: No. 4, 197-199 (15 Aug 1975).

An attempt has been made to determine if a suitable microstructure (e.g., grain size, dispersion of oxide particles in a metal matrix) of a material can be found to reduce the helium buildup and subsequent blistering in near-surface regions. A comparison of the surface erosion due to helium blistering in aluminum and sintered aluminum powder (SAP) has been made for irradiation at room temperature with 100-keV $He^+$ ions to a dose of 1.0 C/cm². The results show high reduction in erosion rate in SAP by more than 3 orders of magnitude as compared to the erosion rate in pure aluminum. (auth)

**26292** SUPERCONDUCTIVITY AND ATOMIC ORDERING IN NEUTRON-IRRADIATED $Nb_3Al$. Sweedler, A.R.; Cox, D.E. (Brookhaven National Laboratory, Upton, New York 11973). Phys. Rev. B 12: No. 1, 147-156 (1 July 1975).

We have utilized the technique of neutron-induced disorder to study the effect of atomic ordering on the superconducting transition temperature $T_c$ of the *A*-15 compound $Nb_3Al$. Large depressions in $T_c$ are observed when $Nb_3Al$ is irradiated with high-energy neutrons ($E > 1$ MeV) at 140°C. For samples whose value of $T_c$ before irradiation was 18.7 K no superconductivity was observed to 1.4 K after irradiation to a fluence of $1.4 \times 10^{19}$ $n/cm^2$. The widths of the transition temperatures remain constant as $T_c$ is depressed and $T_c$ is recovered by annealing at 750°C after irradiation. The Bragg-Williams long-range-order parameter $S$ was determined by least-squares analysis of neutron-diffraction data from powdered samples both before and after irradiation. A reduction in $S$ of 18% is observed for samples irradiated to a fluence of $1.2 \times 10^{19}$ $n/cm^2$. For the same fluence $T_c$ is depressed to 52% of its value before irradiation. The lattice parameter $a_0$ of the *A*-15 phase expands upon irradiation, increasing from 5.183 Å for unirradiated samples to 5.200 Å for samples irradiated to $5.0 \times 10^{19}$ $n/cm^2$. The results are discussed in terms of *A*-site occupation in the $A_3B$ *A*-15 structure and extrapolations of $T_c$ for complete order are considered. (auth)

**26293** V CENTERS IN SINGLE CRYSTALS $Al_2O_3$. Turner, T. J.; Crawford, J. H. (North Carolina Univ., Chapel Hill). Solid State Commun.; 17: No. 2, 167-169(15 Jul 1975).

From optical and thermal bleaching experiments it is concluded that the 400 nm absorption band which appears in $Al_2O_3$ after γ-irradiation is a composite V band. One of its components is attributed to the $V_{OH}^-$ center which also is responsible for a localized vibrational band at 3316 $cm^{-1}$ analogous to the one observed for the $V_{OH}$ center in MgO. The irradiation also results in electron trapping at $Cr^{3+}$ impurity ions to produce a band at 227 nm. Annealing at 170°C destroys the $V_{OH}^-$ center by releasing holes which convert the $Cr^{2+}$ to $Cr^{3+}$ with an attendant thermoluminescence. (auth)

**26294** PREDICTION OF IRRADIATION CREEP FROM MICROSTRUCTURAL DATA. Wolfer, W. G. (Oak Ridge National Lab., TN). Scr. Metall.; 9: No. 7, 801-802(Jul 1975).

Measured densities of radioinduced dislocations, loops, as a function of dose, are used in a model for deriving irradiation creep from stress-dependent bias factors. Predictions using the model with low fluence data result in creep rates that are much too low. However, with high fluence data an irradiation creep behavior is predicted which agrees with in-pile measurements and shows an increase within the temperature range of swelling that is similar to the swelling-enhanced creep in slit stainless steel tubes. (JRD)

**26295** ELECTRON IRRADIATION AND ANNEALING OF GOLD-DOPED p-TYPE GERMANIUM. Boyarkina, N.I.; Smirnov, L.S.; Stas', V.F. (Institute of Semiconductor Physics, Siberian Branch, Academy of Sciences of the USSR, Novosibirsk). Sov. Phys.—Semicond. 9: No. 2, 249-250 (Aug 1975).

Germanium doped with gold was irradiated with electrons. Carrier density and mobility was studied as a function of temperature and the annealing process. (AIP)

**26296** FORMATION OF STRUCTURE DEFECTS IN INDIUM ANTIMONIDE AS A RESULT OF γ-RAY BOMBARDMENT. Abdullaev, A.; Vitovskii, N.A.; Mashovets, T.V.; Mustafakulov, D. (A. F. Ioffe Physicotechnical Institute, Academy of Sciences of the USSR, Leningrad). Sov. Phys.—Semicond. 9: No. 2, 184-186 (Aug 1975).

An investigation was made of the energy spectra, kinetics of formation, and annealing of defects generated in n- and p-type indium antimonide by bombardment with $Co^{60}$ γ rays at 77°K. Irradiation of undoped n-type crystals caused donors to form electrically inactive complexes; after the n–p conversion, defects appeared which gave rise to acceptor states at $E_V + 40 \pm 2$ meV. Acceptor states at $E_V + 34 \pm 1$ meV appeared in InSb:Ge and InSb:Mn. The nature of the defects and the mechanisms of their formation were analyzed. (auth)

# Other Materials

*Refer also to abstracts 25526, 25985, 26190, 26191, and 27348.*

**26297** INFLUENCE OF GAMMA-RAY IRRADIATION AND FILLERS OF SOLID LUBRICANTS ON FRICTION AND WEAR OF POLYETHYLENE. Nishiura, T.; Miki, M.; Awatani, J. (Osaka Univ., Suita (Japan). Inst. of Scientific and Industrial Research). Mem. Inst. Sci. Ind. Res., Osaka Univ.; No. 31, 37-44(Mar 1974).

High-density polyethylene was filled with solid lubricants ($MoS_2$, graphite carbon) and irradiated to $10^9$ r dose by $^{60}Co$. The friction and wear properties were examined under severe and dry conditions against mild steel. The wear properties of the irradiated polymer are improved remarkably. On the other hand, the effect of fillers is not significant on either irradiated or unirradiated polyethylene. The critical temperature described in the previous paper is almost constant for the unirradiated polyethylene, but the temperature for the irradiated one increases with the increase of the sliding speed. (auth)

**26298** ON THE CARRIER DEPTH DISTRIBUTION IN ION IMPLANTED SILICON LAYERS. Maekawa, H.; Matsumori, T. (Tokai Univ., Tokyo (Japan). Faculty of Engineering). Tokai Daigaku Kiyo Kogakubu; 1974: No. 1, 27-34(Nov 1974). (In Japanese).

A study was made on the carrier depth distribution in boron- and phosphorus-ion implanted silicon layers. In case of boron-implanted layers, the carrier depth distribution is slightly wider than that calculated by LSS theory, but in case of phosphorus-implanted layers the carrier profile exhibits an exponential tail at the position considerably deeper than that expected straggling depth. Experimental results suggest that this phenomenon would be due to the interstitial diffusion of phosphorus atoms. Furthermore, experimental formula for this actual carrier profile is presented. (auth)

**26299** MECHANICAL PROPERTIES OF POLYMER IMPREGNATED CONCRETE POLYMERIZED BY GAMMA-RAYS. Ohgishi, S. (Nagoya Inst. of Tech. (Japan)); Ono, H.; Tanahashi, I.; Araki, K.; Kasahara, Y. Zairyo; 23: No. 255, 1050-1056(Dec 1974). (In Japanese).

The relationship between the strength of PIC and the total exposure dosage of gamma-rays was discussed for the mortar specimens containing MMA monomer cured by irradiation at the dose rate of (1.25, 2.5, 5 and 10) $\times 10^5$ Roentgen/hr. In addition, the effects of the turning irradiation, wrapping and annealing were examined, and the strength of PIC polymerized by the radiation method was compared with that of PIC polymerized by the thermal catalytic initiation method. The results show that the total radiation dosage for polymerization to obtain the desirable MMA-PIC strength is 4MR at $10^6$R/hr dose rate, 3 MR at $5 \times 10^5$ R/hr, about 2.5 MR at $2.5 \times 10^3$ R/hr and 2 MR at $1.25 \times 10^3$ R/hr. These values change depending upon the ambient temperature in the radiation cave. If the polymerization is carried out under an appropriate condition, the characteristics of PIC, obtained by both the thermal catalytic initiation method and the radiation polymerizing method, are the same. The effect of annealing on PIC strength is negligibly small in the temperature range lower than 100°C. Therefore, it is necessary to make the annealing temperature higher than 100°C. No effect of the turning irradiation was found out. (auth)

**26300** CONTROLLED ATMOSPHERE ELECTRON MICROSCOPY STUDIES OF GRAPHITE GASIFICATION: THE CATALYTIC INFLUENCE OF VANADIUM PENTOXIDE. Baker, R. T. K.; Thomas, R. B.; Wells, M. (United Kingdom Atomic Energy Authority, Harwell, Eng.). Carbon; 13: No. 2, 141-145 (Apr 1975).

CAEM was used to examine the behavior of V and $V_2O_5$ as catalysts in the graphite-oxygen reaction. The similarities in both quantitative effects indicate that the same reactive species is operative in both systems. The pronounced activity of these catalysts is attributed to their ability to wet and spread over the graphite surface at moderately low temperatures. It is also shown that $V_2O_5$ has the ability to penetrate into graphite and that catalytic attack occurs mainly by a channeling mode, although it is possible that the intercalated material may exert a catalytic influence on the reaction. (auth)

**26301** GALVANOMAGNETIC EFFECTS IN NARROW-GAP $Cd_xHg_{1-x}Te$ AT LIQUID-HELIUM TEMPERATURES. Bovina, L.A.; Savchenko, Yu.N.; Stafeev, V.I. Sov. Phys.—Semicond. 9: No 1, 15-18 (July 1975).

An investigation was made of the influence of transverse and longitudinal magnetic fields ($B \leq 4.5$ kG) on the S-type current–voltage characteristics of homogeneous diode structures based on $Cd_xHg_{1-x}Te$ ($x \sim 0.2$) at 4.2°K. The changes in the characteristics were found to be due to a considerable magneto-resistance. The samples were divided into three groups in accordance with the magnetoresistance, Hall coefficient, and electrical resistivity. One of these groups exhibited anomalously high transverse and longitudinal magnetoresistances: The ratio $\Delta\rho$ (B)/$\rho_0$ reached 60 for B=4.3 kG. The galvanomagnetic effects in $Cd_xHg_{1-x}Te$ at liquid-helium temperatures were explained using a band model postulating the presence of an impurity acceptor band located near the bottom of and overlapping the conduction band. (auth)

**26302** FLUCTUATIONS AND ORDER IN A ONE-DIMENSIONAL SYSTEM. A SPECTROSCOPICAL STUDY OF THE PEIERLS TRANSITION IN $K_2Pt(CN)_4Br_{0.3} \cdot 3(H_2O)$. Brüesch, P.; Strässler, S.; Zeller, H.R. (Brown Boveri Research Center, CH 5401 Baden, Switzerland). Phys. Rev. B 12: No. 1, 219-225 (1 July 1975).

Using optical spectroscopy in the energy range 1 meV–6 eV as a tool we have studied the Peierls transition in $K_2Pt(CN)_4Br_{0.3} \cdot 3(H_2O)$. We find a pseudogap at 0.2 eV at room temperature which transforms into a real gap as $T \to 0$ without significantly changing the gap energy. From this we infer that although no long-range order exists at room temperature the rms order parameter has already reached its zero temperature value. At $T \simeq 0$ we find a strong structure in $\sigma$ ($\omega$) at $\omega \sim 15$ cm$^{-1}$ which is assigned to an oscillation of the pinned charge-density wave (CDW). A simple phenomenological model allows us to estimate the contribution of the thermally unpinned CDW to the dc conductivity at $T > 0$. We conclude that the contribution is 50% or less of the total conductivity. (auth)

**26303** RADIATION PROTECTION OF FIBER OPTIC MATERIALS: EFFECT OF CERIUM DOPING ON THE RADIATION-INDUCED ABSORPTION. Friebele, E.J. (Naval Research Laboratory, Washington, D.C. 20375). Appl. Phys. Lett. 27: No. 4, 210-212 (15 Aug 1975).

High-numerical-aperture lead silicate and barium crown glass unclad fibers have been doped with cerium to decrease their radiation sensitivity. The radiation-induced optical loss in both the visible and near-infrared in these core materials has been studied as a function of time ($10^{-1}$–$10^4$ sec) after pulsed irradiation and cerium concentration (0–1 wt%). It has been determined that cerium is effective in decreasing the loss at a given time and increasing the decay rate of absorption. (auth)

**26304** SELF-TRAPPED HOLE AND THERMOLUMINESCENCE IN $KmgF_3$. Alcala, R.; Koumvakalis, N.; Sibley, W. A. (Oklahoma State Univ., Stillwater). Phys. Status Solidi (a); 30: No. 2, 449-456(16 Aug 1975).

A luminescence band at 380 nm (3.26 eV) resulting from the recombination of electrons with $[X_3^-]$ centers is identified by means of polarization studies. In addition, the thermoluminescence from electron-irradiated $KMgF_3$ both pure and doped with $Ni^{2+}$, $Co^{2+}$, $Mn^{2+}$, and $Li^+$ is reported. (auth)

**26305** CARRIER LIFETIME MEASUREMENTS ON ELECTRON-IRRADIATED SILICON CRYSTALS. Graff, K.; Pieper, H. (AEG-Telefunken, Heilbronn, Ger.). Phys. Status Solidi (a); 30: No. 2, 593-599(16 Aug 1975).

Experimental results of carrier lifetime measurements on dislocation-free, swirl-free, float-zoned, p-type silicon crystals are reported before and after electron irradiation, strong illumination of the specimen, and annealing processes. An experimental arrangement is presented to determine even small values of minority carrier lifetime following the photoconductive-decay-method with application of a boxcar averager in combination with a waveform eductor. It can be shown that strong illumination of the silicon specimen after electron irradiation decreases the carrier lifetime even on as-grown crystals in dependence on still unknown crystal properties. Thus the photon-induced solar cell degradation can be explained by properties of the as-grown silicon single crystal. (auth)

**26306** MECHANISMS OF RADIATION-STIMULATED INTERSTITIAL DIFFUSION IN SEMICONDUCTORS. Kiv, A.E.; Iskanderova, Z.A. (Krivorog State Pedagogical Institute). Sov. Phys.–Semicond. 9: No. 2, 211-213 (Aug 1975).

It is shown that the application of the model of localized electron excitations to interstitital diffusion in semiconductors not only does not reduce the barriers but even inverts the potential relief. Various possible deformations of the potential relief as a result of localization of electron excitations in the vicinity of a saddle point are considered for a diffusing atom. The discussion includes also the possibility of an increase in the barrier height, resulting in the slowing down of diffusion. A comparison is made of the conditions for the realization of the charging mechanism and of the localization of electron excitations. (auth)

**26307** ELECTRICAL PROPERTIES OF SILICON IRRADIATED WITH 660 MeV PROTONS. Konopleva, R.F.; Novikov, S.R.; Rubinova, É.É. (B. P. Konstantinov Leningrad Institute of Nuclear Physics, Academy of Sciences of the USSR, Gatchina). Sov. Phys.–Semicond. 9: No. 2, 214-216 (Aug 1975).

The temperature dependences of the Hall effect and of the electrical resistivity of silicon were studied for a sample irradiated by 600 MeV protons. (AIP)

**26308** HIGH-TEMPERATURE ANNEALING OF SILICON IRRADIATED WITH 660 MeV PROTONS. Rubinova, É.É.; Konopleva, R.F.; Novikov, S.R. (B. P. Konstantinov Leningrad Institute of Nuclear Physics, Gatchina). Sov. Phys.–Semicond. 9: No. 2, 159-162 (Aug 1975).

An investigation was made of high-temperature ($T_{ann}$=70–650°C) isochronous and isothermal annealing of n- and p-type Si irradiated with 660 MeV proton doses from $9 \cdot 10^{11}$ to $1 \cdot 10^{15}$ cm$^{-2}$. The radiation defects were annealed in three stages in p-type Si and in two stages in n-type Si. The activation energy of stage I (70–300°C) was 1.1 and 1.45 eV for n and p-type Si, respectively. The activation energy of negative annealing stage II in p-type Si (300–400°C) was $E_a$ = 1.3–1.9 eV. Stage II in n-type Si(300–650°C) was characterized by an energy $E_a$ = 3.7 eV and stage III in p-type Si(400–650°C) by $E_a \simeq 6$ eV. The radiation defects were found to be thermally stable and a great proportion of them (~80%) were annealed at $T_{ann} > 400$°C; they were destroyed almost completely at $T_{ann}$=650°C. The results of isochronous and isothermal annealing were used in the determination of the kinetics of annealing of radiation defects generated in Si by 660 MeV protons. The processes occurring during annealing were found to be complex and they involved dissociation of radiation defects and formation of new defects. An analysis of the results indicated that disordered regions and complexes composed of primary radiation defects and lattice imperfections were generated by protons in the lattice of Si. (auth)

**26309** INVESTIGATION OF ONE-DIMENSIONAL CONDUCTING SYSTEMS: SCREENING AND EXCITONIC SUPERCONDUCTIVITY IN ORGANOMETALLIC COMPOUNDS. Davis, D. H. Stanford, CA; Stanford University (1974). 166p. University Microfilms Order No. 75-6831.

Thesis (Ph. D.).

The superconducting transition temperature was calculated for a model linear conducting system consisting of a metal-atom chain surrounded by an excitonic medium. The gap equation is calculated numerically using the dielectric response method which allows the details of the electron-electron effective interaction to be taken into account. Parameters are derived from a model consisting of a platinum atom spine to which cyanine dye molecules have been complexed. The Thomas-Fermi method is applied to the problem of screening due to an electron gas confined to a filament and a coaxial infinite cylinder. Using parameters derived for $K_2Pt(CN)_4Cl_{0.32}.2.6H_2O$, the potential in the region between the filament and cylinder due to a source charge in the filament is evaluated > and found to vary approximately as e/sup -kappa/sub eff/sup r//r with an effective screening length about ten times that of metallic platinum. The electronic band structure of the platinum atom chain is taken to be a simple cosine function with band width appropriate to the partially oxidized platinum cyanide complexes. The Fermi level is also chosen based on these complexes. The numerical solution to the gap equation, determined by iteration, is stable and converges to a unique set of solutions for a wide variety of input parameters. Transition temperatures were determined from the value of the gap at the Fermi level using the BCS law of corresponding states. Transition temperatures of the order of $10^3$ °K were found under optimum conditions. (Diss. Abstr. Int., B)

**26310** RADIATION DAMAGE IN ALKALI HALIDE CRYSTALS. Thompson, P. E. Newark, DE; University of Delaware (1975). 169p. University Microfilms Order No. 75-14,976.

Thesis (Ph. D.).

The correspondence between the depth of F-centers produced by energetic protons bombarding a KCl single crystal and the range of the protons in the crystal is investigated. A photomicrographic technique was developed to obtain the depth of the color centers. The range of the protons in KCl was interpolated from the results of prior investigators who reported the range of protons in argon. A correspondence between the depth of the F centers and the range of the protons was established. The radiation damage produced during a channeled backscattering experiment is investigated. The formation of radiation damage was monitored by measuring the change in the dechanneling length of the incident 15-MeV $^{16}O^{3+}$ which were aligned along the (100) plane of a KI(Tl) scintillation crystal. The formation of this damage was compared to the formation of F centers in a KI(Tl) crystal with 0.95-MeV H, which have the same energy to mass ratio as the 15-MeV $^{16}O$. It was found that although the oxygen ions lose forty times more energy per unit distance than the protons, the damage was formed at the same rate. This lack of particle identity in the formation of radiation

damage is due to the saturation of F centers within particle tracks during irradiation. (Diss. Abstr. Int., B)

**26311** COLOR-CENTER AND RADIATION-DAMAGE EFFECTS IN ALKALI HALIDES IRRADIATED TO HIGH PARTICLE FLUENCE. Wardle, M. R. W. Newark, DE; University of Delaware (1975). 134p. University Microfilms Order No. 75-6394.

Thesis (Ph. D.).

Alkali metal halide crystals were examined photographically after bombardment to a high dose (greater than $10^{16}/cm^2$) of high-energy (typically 1.5-MeV) protons. The crystals showed a minimum in the F- and M-center profile at the end of the proton range immediately after irradiation. During storage in the dark at room temperature, this minimum became deeper and a peak of absorption appeared within the minimum. These effects were explained using reasonable physical processes involving color-center diffusion and aggregation and energy-loss-radiation-damage correlations. (Diss. Abstr. Int., B)

**26312** EFFECTS OF NUCLEAR RADIATION ON LOW TEMPERATURE TRANSPORT PROPERTIES OF EPITAXIALLY-GROWN GALLIUM ARSENIDE. Berg, N. J. Baltimore; University of Maryland (1974). 182p. University Microfilms Order No. 75-14,298.

Thesis (Ph. D.).

The effects of $^{60}Co$ gamma-ray and high-energy neutron displacement damage upon the low-temperature transport properties of epitaxial gallium arsenide were investigated. The activation energy ($epsilon_2$) associated with the transition regime of the impurity conduction process increased by a factor of 5 as a result of $^{60}Co$ gamma radiation, and only by a factor of 1.6 for a comparable neutron irradiation. In addition the ratio of the Hall carrier density at low and high temperatures, $(n_H)_{4^0K}/(n_H)_{300^0K}$, decreased by a larger amount for $^{60}Co$ gamma irradiation than for neutron irradiation. The breakdown field increased with irradiation and this is a result of radiation-induced changes in compensation and, for transition regime specimens, a lowering of the trap depth. Specimens for which the donor impurity concentration is less than $5 \times 10^{15}$ $cm^{-3}$ are governed by discrete level statistics, while the phenomenon of decreasing activation energy with increasing impurity concentration is due to conduction band tailing. For specimens having donor impurity concentrations exceeding $5 \times 10^{15}$ $cm^{-3}$ a continuum of donor states forms in the forbidden gap and band statistics predominate. Nevertheless for concentrations up to about $3 \times 10^{16}$ $cm^{-3}$ the conduction and impurity bands are separated by a virtual gap in the sense that the two bands have separate mobilities and that an activation energy is required to excite electrons from the impurity band to conduction band. (Diss. Abstr. Int., B)

# NUCLEAR MATERIALS AND WASTE MANAGEMENT

**26313** (AECL-5136) MANAGING NUCLEAR WASTES. Dyne, P. J. (Atomic Energy of Canada Ltd., Pinawa, Manitoba. Whiteshell Nuclear Research Establishment). May 1975. 19p. Dep. NTIS (US Sales Only) $4.00

The discussion is presented under the following section headings: nuclear power in Canada's future economy; nuclear wastes; nuclear waste management; how much nuclear waste?; storing spent fuel; fuel reprocessing and waste management; reactor wastes; alternatives for the long term; the safety of waste management schemes; waste management plans; and, the risk and the benefit. An appendix on radioactivity and its hazards is included.

## Accountability and Safeguards

**26314** (GAT-T-2334) MATERIAL SURVEILLANCE AND VERIFICATION PROGRAM AT A URANIUM ENRICHING PLANT. DeVito, V. J. (Goodyear Atomic Corp., Piketon, Ohio (USA)). 21 Aug 1975. Contract E(33-2)-1. 16p. (CONF-751017-2; SM-201/23). Dep. NTIS $4.00.

From symposium on safeguards of nuclear materials; Vienna, Austria (20 Oct 1975).

A license for a nuclear facility in the United States is approved only after a licensee demonstrates by procedure or practice that an adequate material control system exists. A license can specify acceptable material control practices. Therefore, processors in the United States receiving uranium hexafluoride ($UF_6$) from a U. S. Government-owned enriching plant can accept shipper's values for nuclear material accounting purposes if: there is surveillance during withdrawal of the $UF_6$, an independent sample is obtained, and certain measurement verification is subsequently performed by the receiver or the receiver's agent. Because of the high equipment and operating costs, essentially all $UF_6$ processors have adopted a surveillance and verification program. A resident observer is employed to perform surveillance, obtain samples, and tamper-safe the shipping cylinders. Samples are analyzed by the receiver or by an independent laboratory. The observer determines by surveillance that withdrawals, or transfers of material, weighings, and sampling are accomplished in accordance with accepted procedures. Surveillance of the withdrawals includes observing the transfer of $UF_6$ from the enriching plant cylinder to the shipping cylinder(s) and the withdrawal of samples. In addition, it includes observing the weighing of all cylinders associated with a sample lot of $UF_6$. Following the surveillance of withdrawals, weighings, and sampling, the cylinders are made tamper-safe by the application of tamper-indicating devices. Statistics for the verification program have shown shipper and receiver measurements to be within the limits acceptable for adequate material control. (auth)

**26315** (REG/G-5.53(8-75)) QUALIFICATION, CALIBRATION, AND ERROR ESTIMATION METHODS FOR NONDESTRUCTIVE ASSAY. (Nuclear Regulatory Commission, Washington, D. C. (USA). Office of Standards Development). Aug 1975. 7p. NUREG.

This guide describes methods and procedures acceptable to the NRC staff for meeting the provisions of paragraph 70.58(f) of 10 CFR Part 70 as it relates to the use of nondestructive assay. (LK)

## Disposal and Storage

*Refer also to abstracts 25648, 25887, and 25905.*

**26316** (JUL-1163) ULTIMATE STORAGE OF SPENT FUEL ELEMENTS OF THE AVR TEST POWER STATION IN THE ASSE SALT MINE. Wolf, J. (Kernforschungsanlage Juelich G.m.b.H. (F. R. Germany). Inst. fuer Chemische Technologie; Technische Hochschule Aachen (F. R. Germany)). Feb 1975. 142p. (In German). INIS.

Thesis.

With regard to the ultimate storage of irradiated AVR pebble-bed reactor carbide fuel elements in the salt of Asse, a number of tests and calculations are presented to demonstrate that there is no credible possibility of the MCA (maximum credible accident) defined for the salt. Some 1,000 fuel elements at a time are packed in gas-tight containers, which are stacked in boreholes. The boreholes are then sealed with concrete. Lay-out and functions of the special airlock and transportation systems are described with special reference to aspects of the safety of the overall procedure. Possible accidents in the mine are discussed in detail. $^{85}Kr$ and T release rates are determined in laboratory tests by heating of the spherical fuel elements. Tests with fuel elements embedded in salt or stagnant brine were carried out at various temperatures to investigate their behavior in final storage. Kr and T release, extraction of fission products, mechanical resistance and corrosion were examined in these tests. Finally, the permeability of salt and salt-concrete to radioactive gases were investigated in a special experimental arrangement. The diffusion and permeability coefficients obtained for $^{85}Kr$, HT, and HTO allow an estimation of the gas discharge of the stored fuel element. (GE)

**26317** TREATMENT AND DISPOSAL OF LOW-LEVEL RADIOACTIVE SLUDGES BY SOLAR EVAPORATION. Lee, S. H. (Atomic Energy Research Inst. Seoul). J. Korean Nucl. Soc.; 4: No. 3, 194-202(1972).

Solar evaporation can reduce the water content of radioactive sludge produced from the clay absorption liquid waste treatment process from 60% to 25 to 30% in 15 days. (auth)

## Handling Equipment and Procedures

*Refer also to abstracts 27454 and 27455.*

**26318** NUCLEAR FUEL PELLET LOADING MACHINE. Kee, R. W.; Denero, J. V. (to Westinghouse Electric Corp.). US Patent 3,897,673. 5 Aug 1975. Filed date 3 Aug 1973. 6p.

An apparatus for loading nuclear fuel pellets on trays for transfer in a system is described. A conveyor supplies pellets from a source to a loading station. When the pellets reach a predetermined position at the loading station, a manual or automatically operated arm pushes the pellets into slots on a tray and this process is repeated until pellet sensing switches detect that the tray is full. Thereupon, the tray is lowered onto a belt or other type conveyor and transferred to other apparatus in the system, such as a furnace for sintering, and in some cases, reduction of $UO_{2.1}$ to $UO_2$. The pellets are retained on the tray and subsequently loaded directly into fuel rods to be used in the reactor core. (auth)

## Transportation

*Refer also to abstract 25648.*

**26319** (LA-5834-MS) ROVER SHIPPING CASK. Lobb, B.; Noyes, H. E.; Smith, D. R. (Los Alamos Scientific Lab., N. Mex. (USA)). Aug 1975. Contract W-7405-ENG-36. 53p. Dep. NTIS $5.45.

A large well-shielded shipping container, commonly known as the Rover cask, has been designed to accommodate fuel elements from the Rover and TORY IIC reactors in compliance with existing regulatory requirements. Background material and approvals are given in the Appendixes. (auth)

# PARTICLE ACCELERATORS

## Design, Development, and Operation

**26320** (ORNL-TM-4942) TECHNICAL SPECIFICATION FOR A 25 MV TANDEM ELECTROSTATIC ACCELERATOR. Jones, C. M.; Biggerstaff, J. A.; Blair, J. K.; Ball, J. B.; Larson, J. D.; Martin, J. A.; McConnell, J. W.; Milner, W. T.; Murray, J. A.; Ziegler, N. F. (Oak Ridge National Lab., Tenn. (USA)). Aug 1975. Contract W-7405-eng-26. 152p. Dep. NTIS $10.75.

Specifications are given for an accelerator system to consist of a 25 MV tandem electrostatic accelerator and specified ancillary equipment, including an injector, a beam transport system, a vacuum system, a control system, and a system for storage of the insulating gas and transport of the gas to and from the accelerator. The insulating gas shall be $SF_6$. The tandem electrostatic accelerator shall be vertical in orientation and of folded construction, and shall be installed in a new structure adjacent to the Oak Ridge Isochronous Cyclotron. (auth)

**26321** LOW VOLTAGE ACCELERATORS AS NEUTRON GENERATORS. Hannappel, L.; Schneider, H. (Giessen Univ. (F. R. Germany). Abt. Grossgeraete (Angewandte Kernphysik)). Kerntechnik; 17: No. 2, 74-80(Feb 1975). (In German).

5 figs.; 15 refs.

The nuclear reaction, $^3H(d, n)\ ^4He$, with a cross-section maximum at about 100 keV deuteron energy, has prompted the development and construction of low voltage ion accelerators (a few 100 kV), with high current ion sources (up to 1 A), as well as the development of a special target technology. As a result, it is possible at present to build neutron generators with source strengths of up to $10^{14}\ s^{-1}$. A distinction is drawn between pumped neutron machines with a vacuum system, and generators with sealed tubes. The individual components of these generator types are described, possible variants are compared, and yields and other data are presented. The advantages and particular features of neutron generators with sealed tubes are discussed. The necessity of shielding neutron sources is stressed. (auth)

**26322** LINEAR ACCELERATORS: THE DEMAND AND THE RESPONSE. Atherton, L. (M.E.L. Equipment Co. Ltd. Manor Royal, Sussex, Eng.). Medicamundi; 20: No. 1, 2-11(1975).

A commercial 20 MeV electron linear accelerator is described, including the automation, beam bending, stabilization, and display features. The control system is effective in regulating the beam profile over the field within +-2 percent at 100 MeV. (PMA)

## Auxiliaries and Components

**26323** (JINR-P13-8934) SYSTEM FOR CONTROLLING AND MEASURING OF TIME PULSE STRAGGLING OF MODULATORS OF A LINEAR ACCELERATOR SILUND. Gleibman, E. M.; Inkin, V. D.; Nikolaev, V. P. (Joint Inst. for Nuclear Research, Dubna (USSR)). 1975. 14p. (In Russian). Dep. NTIS (US Sales Only) $4.00.

A system on-line with the computer, used to control and measure the time pulse straggling of modulators of a linear accelerator, is described. The time-to-digital converter is used for time analysis, and simultaneity of modulator operation for each acceleration cycle is controlled by a hodoscope register. The measuring devices are connected with the computer by means of the CAMAC crate. (auth)

**26324** (RL-75-097) INITIAL SURVEY OF EPIC LATTICE CONFIGURATIONS USING TRIPLET DAMPING. Maidment, J. R. M. (Science and Technology Agency, Tokyo (Japan). Atomic Energy Bureau). 25 Aug 1975. 4p. (EPIC/MC-85). Dep. NTIS (US Sales Only) $4.00.

The use of combined function triplet units to provide the required degree of damping adjustment in EPIC is considered. The results of a numerical survey of possible EPIC configurations indicate that reverse bend triplets provide an extremely flexible method of damping adjustment. (PMA)

**26325** SHIELDING OF HIGH ENERGY ACCELERATORS. Kato, K. (National Lab. for High Energy Physics, Oho, Ibaraki (Japan)). Genshiryoku Kogyo; 20: No. 12, 32-37(Dec 1974). (In Japanese).

Shielding research for high energy accelerators is rather in the background, in contrast with spectacular high energy physics experiments performed with them. High energy accelerators can be divided broadly into those for electrons and those for protons; in both cases, with the acceleration energy exceeding about 10 MeV, neutrons become a predominant component for shielding requirements. The shielding for high energy accelerators is described as follows: historical background for the shielding of high energy accelerators; features of the high energy accelerator shielding; shielding calculations for high energy accelerators including scaling method, Moyer's method and O'Brien's technique, and the future trend in shielding. Finally, some topics in this field encountered in the West are mentioned briefly. (JA)

**26326** INTERFERENCE PHENOMENON IN OPTICAL TRANSITION RADIATION AND ITS APPLICATION TO PARTICLE BEAM DIAGNOSTICS AND MULTIPLE-SCATTERING MEASUREMENTS. Wartski, L. (Institut d'Electronique Fondamentale, Laboratoire Associé au CNRS, Université Paris-XI, Bâtiment 220, 91405 Orsay, France); Roland, S.; Lasalle, J.; Bolore, M.; Filippi, G. J. Appl. Phys. 46: No. 8, 3644-3653 (Aug 1975).

The optical transition radiation emitted by electron-irradiated aluminum, silver, gold-coated plates, and self-supported aluminum and Mylar films has been investigated experimentally. The investigation was made with an electron beam incident at 45°, having a mean intensity of 1 μA, and an energy which was varied from 35 up to 72 MeV ($68.5 < \gamma < 140.9$). The study of the angular distribution and degree of polarization has shown that the high-directivity radiation is emitted around the direction of specular reflection and that the contribution of the optical bremsstrahlung is negligible. When two parallel foils are used, the resulting angular distribution exhibits an oscillating behavior arising from the interference of the fields emitted at both interfaces. This interference phenomenon is strongly related to the so-called formation zone in a vacuum, introduced by Garibyan. The intensity of light integrated in a small aperture at the center of the interference pattern presents a strong $\gamma$ dependence (of the form $\gamma^4$) which was exploited in the optimization of the phase adjustment of the electron bunches in the accelerating sections of the machine. In such a device using the interference phenomena in transition radiation, the possibility of measurements of the beam energy with a precision of about 1% has also been shown. On the basis of the visibility of fringes, the angular spread of the electron beam and the mean-square scattering angle in a given material were also estimated. (auth)

## Ion Sources and Injection and Extraction Systems

**26327** (GSI-PB-1-75) UNILAC PROJECT REPORT NO. 15. (Gesellschaft fuer Schwerionenforschung m.b.H., Darmstadt (F. R. Germany)). Apr 1975. 33p. (In German). INIS.

35 figs.; 2 tabs.; 7 refs.

Results are reported on: (1) the development of a duoplasmatron ion source for the production of multiply charged silver ions; (2) the development of a B(max) anode duoplasmatron ion source with direct cooling; (3) first measurements with a duopigatron ion source; and (4) the constructional layout of Faraday cups. (GE)

**26328** (JINR-P9-8921) ELECTROSTATIC SYSTEM FOR BEAM EXTRACTION FROM THE PHASOTRON WITH THE MAGNETIC FIELD VARIATION. Vasilenko, A. T.; Glazov, A. A.; Denisova, L. G.; Dmitrievskii, V. P.; Denisov, Yu. N.; Kol'ga, V. V.; Polumordvinova, N. I.; Sidorova, V.I.; Treibal, E. (Joint Inst. for Nuclear Research, Dubna (USSR)). 1975. 17p. (In Russian). Dep. NTIS (US Sales Only) $4.00

The design and calculation results are presented for an electrostatic beam extraction system with magnetic field spatial variations. The design includes a remote control system and a high radioactivity preventive inspection procedure. (auth)

**26329** (JINR-P9-9023) SELECTION OF THE PARAMETERS OF THE ELEMENTS OF A BEAM EXTRACTION SYSTEM OF A PHASOTRON WITH A SPACE VARIATION OF A MAGNETIC FIELD USING THE IRON CURRENT EXTRACTION CHANNEL. Zaplatin, N. L.; Samsonov, E. V.; Chesnov, A. F. (Joint Inst. for Nuclear Research, Dubna (USSR)). 1975. 24p. (In Russian). Dep. NTIS (US Sales Only) $4.25.

Magnetic fields are calculated for a beam extraction and deflection system which uses an iron current channel. The iron current section of the channel, with a power supply of ~90 kW, provides a magnetic field dropoff of 4700 Oe for the input part of the section (septum thickness 0.4 cm) and of 4500 Oe for the output section

(septum thickness 1.0 cm). In this case the magnetic field perturbations due to the channel weakly affect the extraction efficiency. (auth)

## Ion Optics and Field Calculations

**26330** (RL-75-093) EFFECT OF COUPLING ON VARIABLE DAMPING IN EPIC. Rees, G. H. (Science Research Council, Chilton (UK). Rutherford Lab.). May 1975. 3p. (EPIC/MC-84). NTIS (US Sales Only) $4.00.

The horizontal beam size is varied in EPIC by adjusting the damping of the radial betatron oscillations. There is less damping of the radial than of the vertical betatron motion, so the possibility arises that coupling between the two transverse motions may readjust the damping ratios. It is shown that for coupling introduced by skew quadrupole fields, the effect on the damping is generally small. (auth)

## Experimental Facilities

*Refer also to abstract 27161.*

**26331** (LA-6008-MS) BEAM INTENSITY MONITORING FOR THE EXTERNAL PROTON BEAM AT LAMPF. Barrett, R. J.; Anderson, B. D.; Willard H. B.; Anderson, A. N.; Jarmie, N. (Los Alamos Scientific Lab., N. Mex. (USA)). Jul 1975. Contract W-7405-ENG-36. 6p. Dep. NTIS $4.00.

Three different intensity monitors were tested in the external proton beam at LAMPF, and together cover the entire range of beam currents available. A 800 kg Faraday cup was installed and used to measure the absolute intensity to better than 1 percent for beam currents up to several nanoamperes. A high gain ion chamber was used as part of the calibration procedure for the Faraday cup, and was found to be useful when monitoring very small beam intensities, being reliable down to the few picoampere level. A secondary emission monitor was also tested, calibrated, and found to be trustworthy only for beams of greater than 50 pA intensity. (auth)

# PHYSICS (ASTROPHYSICS AND COSMOLOGY)

## Cosmic Radiation

*Refer also to abstracts 25935 and 26620.*

**26332** PROBLEMS OF COSMIC GAMMA-RAY OBSERVATION, 2. Nakagawa, S.; Tsukuda, M.; Okudaira, K.; Hirasima, Y.; Yoshimori, M. (Rikkyo Univ., Tokyo (Japan). Faculty of Science). pp 157-171 of Symposia on the Cosmic Observations for the Fiscal Year 1973. Tokyo, Japan; Tokyo Univ., Inst. of Space and Aeronautical Science (Mar 1974). (In Japanese)

From symposia on the cosmic observations for the fiscal year 1973; Tokyo, Japan (10 Dec 1973). (Tokyo Univ. (Japan). Inst. of Space and Aeronautical Science).

The low energy diffuse component of continuous gamma-rays was measured with a man-made Satellite. The origin of the gamma ray between 0.5 and 5 MeV may be the inverse Compton effect of cosmic background black-body radiation and high energy electrons. Some doubts exist in electron density and the existence of a metagalactic component. The energy region between 5 and 30 MeV has hardly been observed. Many observations were made for the energy region up to 100 MeV, and the information on energy spectra is obtained. The gamma ray in this region may be produced by the decay of $\pi^0$ mesons. Continuous gamma rays from point sources were observed by many people. Discrepancies among the observed results are seen. Pulses of x rays and $\gamma$ rays from NP0532 were investigated. The mechanism of gamma-ray pulse generation was studied by using synchrotron radiation or the inverse Compton effect. The existence of the gamma ray with line spectrum is conceivable. Annihilation gamma ray and the gamma ray due to the deexcitation of excited nuclei are considered. At present, the improvement of detectors is necessary. Recently, phenomena of cosmic gamma-ray burst were observed. The origin of this burst is a future problem. Precise measurement of solar burst gamma-ray is also requested. The present project is to continue the observation of line gamma ray and to develop a gamma-ray spectrometer for the energy region around 10 MeV. (JA)

**26333** ON THE COMPONENT OF COSMIC RAY PARTICLES. On the Life of Cosmic Ray in Galaxy. Nishimura, J. (Tokyo Univ. (Japan). Inst. of Space and Aeronautical Science). pp 172-180 of Symposia on the Cosmic Observations for the Fiscal Year 1973. Tokyo, Japan; Tokyo Univ., Inst. of Space and Aeronautical Science (Mar 1974). (In Japanese)

From symposia on the cosmic observations for the fiscal year 1973; Tokyo, Japan (10 Dec 1973). (Tokyo Univ. (Japan). Inst. of Space and Aeronautical Science).

The components of primary cosmic ray were studied, and various nuclear components from helium to lead were discovered. The components and their abundance give information concerning the generating mechanism of cosmic ray. The spallation reaction of nuclei such as C, N or O collided with interstellar material produces light nuclei such as Li, Be or B. In order to explain observed quantity with the cross section of the spallation reaction, it must be assumed that cosmic ray has run through the space corresponding to the amount of the interstellar material. In relation with these points, energy spectra of nuclei in primary cosmic ray, isotopes in cosmic ray, superheavy nuclei and primary electrons are discussed. The energy spectra of nuclei in cosmic ray depend on the nuclei. The result of balloon observation in U. S. A. indicated the energy dependence of the life of nuclei in the galaxy. Direct estimate of the life in the galaxy can be made by observing the abundance of the radioisotopes with finite life in cosmic ray. The most important nucleus in $^{10}$Be. The heavy nuclei with atomic number more than iron was little observed. However, there is some possibility of the existence of transuranium elements at the time of the explosion of supernova. Development of large volume detectors is required for this sort of experiment. The origin of galaxy electromagnetic waves is synchrotron radiation emitted by electrons in cosmic ray being curved owing to the galaxy magnetic field. The electrons lose their energy by inverse Compton scattering. These effects affect the energy spectra of electrons. Then, the observation of energy spectra gives information on the life of electrons in galaxy. Groups of U. S. A., India and Japan are making the observation of electron spectra. At present, it is hard to derive a unified result from the results by these groups. Finally, the balloons for these observations are explained. (JA)

**26334** FUTURE OF THE OBSERVATION OF HEAVY PRIMARY COSMIC RAY. pp 200-202 of Symposia on the Cosmic Observations for the Fiscal Year 1973. Tokyo, Japan; Tokyo Univ., Inst. of Space and Aeronautical Science (Mar 1974). (In Japanese)

From symposia on the cosmic observations for the fiscal year 1973; Tokyo, Japan (10 Dec 1973). (Waseda Univ., Tokyo (Japan). Science and Engineering Research Lab.).

The data on electric charge distribution and energy distribution of the nuclei heavier than iron in cosmic rays were accumulated. Two methods of observation are now in use. One is a method to use an electric signal from the detectors with small effective area carried by man-made satellites, and the other is the method to use the solid state track detectors with large area on balloons. If the space shuttle plan is realized, the method to use an electric signal will be absolutely advantageous. At present, the track detectors are practical. The energy distribution was observed in case of $Z > 35$ and energy of 5 GeV/n. For $Z > 60$, the energy distribution was measured by Price et al. up to 2 GeV/n. It is planned to measure the flux in the energy range more than 5 GeV/n, because it can be carried out easily. The expected number of events to be detected are estimated for a detector of 50 m$^2$ and 20 hr exposure. A schematic drawing of the detector system is presented. (JA)

**26335** PROBLEMS OF THE OBSERVATION OF HEAVY PRIMARY COSMIC RAY ISOTOPE, AND A FUTURE PLAN. Yoshimori, M.; Okudaira, K.; Hirasima, Y.; Murakami, H.; Tsukuda, M. (Rikkyo Univ., Tokyo (Japan). Faculty of Science). pp 193-199 of Symposia on the Cosmic Observations for the Fiscal Year 1973. Tokyo, Japan; Tokyo Univ., Inst. of Space and Aeronautical Science (Mar 1974). (In Japanese)

From symposia on the cosmic observations for the fiscal year 1973; Tokyo, Japan (10 Dec 1973). (Tokyo Univ. (Japan). Inst. of Space and Aeronautical Science).

Heavy isotopes in cosmic rays were studied in order to investigate the origin of the cosmic ray, the life of the cosmic ray in the galaxy, and the thickness of interstellar materials through which the cosmic ray passed. The abundance ratio of $^{12}$C and $^{13}$C was measured with nuclear plates, and the ratio $^{13}$C/$^{12}$C was about 0.08. The abundance ratio of $^{7}$Be, $^{9}$Be, and $^{10}$Be was observed with a counter telescope comprising a solid-state and a scintillation detector. It was impossible by this method to determine the time of stay of cosmic rays in galaxy. Observation of heavy isotopes with $Z = 3 \sim 26$ was made with a telescope comprising plastic and Cherénkov counters. The resolving power of the telescope was not enough to obtain a decisive result. A telescope with large area silicon semiconductor detectors is designed for the observation with higher mass resolving power than before. A preliminary experiment was carried out. (JA)

**26336** FOR THE OBSERVATION OF GALACTIC COSMIC RAY FROM NEIGHBOURHOOD OF INTERSTELLAR SPACE. Kuge, A. (Rikkyo Univ., Tokyo (Japan). Faculty of Science). pp 181-192 of Symposia on the Cosmic Observations for the Fiscal Year 1973. Tokyo, Japan; Tokyo Univ., Inst. of Space and Aeronautical Science (Mar 1974). (In Japanese)

From symposia on the cosmic observations for the fiscal year 1973; Tokyo, Japan (10 Dec 1973). (Tokyo Univ. (Japan). Inst. of Space and Aeronautical Science).

The energy spectra of cosmic ray and the related topics are discussed. The observed spectra showed a broad maximum around several hundreds MeV/n and linear decrease in higher energy range than 10 GeV/n. Solar modulation theory was presented for the explanation of the broad maximum. Recently, a broad minimum was observed in the energy range around several tens MeV/n, and it became the origin of the solar modulation theory. Therefore, it is necessary to use the solar modulation theory for the interpretation of interstellar cosmic ray spectra. Then, the observation of cosmic ray with energy more than 10 GeV/n is required for the direct investigation of cosmic ray origin. Various detection systems for this high energy cosmic ray were designed and constructed. Observed spectra are power functions of energy. The ratio of light nuclei ($3 \leq Z \leq 5$) to medium weight nuclei ($6 \leq Z \leq 9$) showed the tendency of decrease with increasing energy. The energy dependence of the age of cosmic rays was proposed from the observed energy spectra. The data concerning the cosmic rays from interstellar space give information for the origin and propagation of cosmic rays. (JA)

**26337** FOKKER-PLANCK THEORY FOR COSMIC RAY DIFFUSION IN THE PRESENCE OF ALFVEN WAVES 1. THEORY. Hollweg, J.V.; Skadron, G. (NCAR High Altitude Observatory, Boulder, Colorado 80303). J. Geophys. Res. 80: No. 19, 2701-2707 (1 July 1975).

Using the standard quasi-linear Fokker-Planck approach and an

expansion of the cosmic ray distribution function in Legendre polynomials, we derive a complete set of Fokker-Planck coefficients and expressions for the complete cosmic ray diffusion tensor due to linearly polarized planar Alfvén waves propagating at an angle to the average magnetic field. We find that although an off-diagonal term formally appears in the diffusion tensor, it is identically zero. In addition, the cross-field diffusion coefficient is identically the same as that found for wave propagation exactly parallel to the average magnetic field. (auth)

**26338** AURORAL ELECTRONS AND THE OPTICAL EMISSIONS OF NITROGEN. Feldman, P.D.; Doering, J.P. (Johns Hopkins University, Baltimore, Maryland 21218). J. Geophys. Res. 80: No. 19, 2808-2812 (1 July 1975).

The differential flux of auroral primary and secondary electrons and the emission of the 1 PG and 2PG (first and second positive) systems of $N_2$ and the 1 NG (first negative) system of $N_2^+$ were measured in a rocket experiment during a steady IBC II$^+$ aurora. The electron data indicate that the incident auroral electrons were nearly monoenergetic with energy of about 25 keV. A single power law of the form $F=F_0E^\alpha$ cannot accurately describe the secondary electron spectrum in the energy range of 3–85 eV. However, the spectrum may be approximated by using $\alpha=-3.2$ between 7 and 20 eV and $\alpha=-0.9$ between 25 and 85 eV. The measured intensity and altitude profile of the $N_2$ 1 PG (5,2) band at 6685 Å agree well with the values calculated by using the measured electron flux and laboratory cross-section data. About 40% of the $N_2^+$ 1 NG(0,0) band emission at 3914 Å is excited by electrons with energy below 85 eV. (auth)

**26339** SEARCH FOR COSMIC-RAY ANTIMATTER. Smoot, G.F.; Buffington, A.; Orth, C.D. (Space Sciences Laboratory and Lawrence Berkeley Laboratory, University of California, Berkeley, California 94720). Phys. Rev. Lett. 35: No. 4, 258-261 (28 July 1975).

In a sample of $1.5\times10^4$ helium and $4.0\times10^4$ higher-charged nuclei, obtained with balloon-borne superconducting magnetic spectrometers, we find the ratio of antinuclei to nuclei in the cosmic rays to be less than $8\times10^{-5}$ for rigidities (momentum/charge) between 4 and 33 GV/$c$ and less than $10^{-2}$ between 33 and 100 GV/$c$, at the 95% confidence level. (auth)

**26340** HIGH-ENERGY GALACTIC GAMMA RADIATION FROM COSMIC RAYS CONCENTRATED IN SPIRAL ARMS. Bignami, G.F.; Fichtel, C.E.; Kniffen, D.A.; Thompson, D.J. (NASA/Goddard Space Flight Center, Greenbelt, Maryland). Astrophys. J. 199: No. 1, 54-60 (1 July 1975).

A model for the emission of high-energy (>100 MeV) γ-rays from the galactic disk has been developed and compared with recent SAS-2 observations. In the calculation, it is assumed that (1) the high-energy galactic γ-rays result primarily from the interaction of cosmic rays with galactic matter, (2) on the basis of theoretical and experimental arguments the cosmic-ray density is proportional to the matter density on the scale of galactic arms, and (3) the matter in the Galaxy, atomic and molecular, is distributed in a spiral pattern consistent with density wave theory and the experimental data on the matter distribution that is available, including the 21-cm H I line emission, continuum emission from H II regions, and data currently being used to estimate the $H_2$ density. The calculated $^{\pi}$γ-ray distribution is in good agreement with the SAS-2 observations in relative shape and absolute flux. As a corollary, the nonuniform cosmic-ray distribution of this model tends to support the galactic origin of the fraction of the cosmic rays which are important in the production of high-energy photons. Modifications of the basis model show that the γ-ray flux is relatively sensitive to large variations of the assumed distribution of molecular hydrogen in the Galaxy. (auth)

**26341** MOTION OF CHARGED PARTICLES NORMAL TO AN IRREGULAR MAGNETIC FIELD. Jokipii, J.R. (Departments of Planetary Sciences, and Astronomy, University of Arizona). Astrophys. J. 198: No. 3, 727-732 (15 June 1975).

The motion of charged particles is considered in a fluctuating magnetic field which varies only in directions normal to its mean direction. Such a field would be produced, for example, by an ensemble of magnetosonic waves propagating normal to an ambient magnetic field. The appropriate generalization of gradient drift motion is derived in terms of the magnetic fluctuation spectrum, and an effective diffusion coefficient is derived. (auth)

**26342** A STUDY OF FAST TIME STRUCTURE WITHIN COSMIC GAMMA-RAY BURSTS. Imhof, W.L.; Nakano, G.H.; Johnson, R.G.; Kilner, J.R.; Reagan, J.B. (Lockheed Palo Alto Research Laboratory); Klebesadel, R.W.; Strong, I.B. Astrophys. J. 198: No. 3, 717-725 (15 June 1975).

Data taken with a fast resolution germanium spectrometer surrounded by a large area plastic scintillator, on board the low-altitude polar orbiting satellite 1972-076B, and with γ-ray sensors on the *Vela* satellite system have been used to study the fine time structure of two cosmic γ-ray bursts. For the 1972 December 18 event, both energy spectra and intensity measurements were obtained, whereas due to depletion of the cryogen for the germanium sensor, only intensity information was obtained for the 1973 July 21 event, all on a fast time scale. Several microbursts with time widths of the order of 60 ms or less occurred at various times during each of these γ-ray bursts. The observed microburst structure was even more pronounced in the 1973 July 21 burst. During the early portions of the 1972 December 18 event the spectrum was observed to increase in hardness. However, during the microbursts, when the intensities were higher, the spectra were not significantly different than at neighboring times. There is no evidence for narrow (~0.02 to ~3 ms) spikes with $\gtrsim$15 percent of the number of photons in the first 60-ms microburst. (auth)

**26343** ORIGIN OF COSMIC RAYS. Stecker, F.W. (Theoretical Studies Group, National Aeronautics and Space Administration, Goddard Space Flight Center, Greenbelt, Maryland 20771). Phys. Rev. Lett. 35: No. 3, 188-191 (21 July 1975).

With the use of recent observations of the galactic gas and γ-ray distributions, the galactic cosmic-ray distribution is deduced. This distribution is identical to that of supernova remnants (within experimental error), strongly supporting the hypothesis that most observed cosmic rays are produced by supernovae in our own galaxy. The average age of the cosmic-ray sources is suggested from the character of their distribution to be about 30 million years. (auth)

**26344** HYDROMAGNETIC WAVES AND COSMIC-RAY DIFFUSION THEORY. Lee, M.A.; Völk, H.J. (Enrico Fermi Institute, University of Chicago). Astrophys. J. 198: No. 2, 485-491 (1 June 1975).

Pitch-angle (and energy) diffusion of cosmic rays in hydromagnetic wave fields is considered. The treatment remains strictly within the quasi-linear approximation. It is shown that the popular assumption of an isotropic power spectrum tensor of magnetic fluctuations requires in this case equal forms and magnitudes of Alfvén and magnetosonic wave spectra—a situation which is generally unlikely. The relative contribution to the pitch-angle diffusion coefficient from the cyclotron resonances and Landau resonance due to the different types of waves are evaluated for a typical situation in the solar wind. Since in this approximation also the Landau resonance does not lead to particle reflections, a proper consideration of the nonlinear particle orbits is indeed necessary to overcome the well-known difficulties of quasi-linear scattering theory for cosmic rays near 90° pitch angle. (auth)

**26345** A MEASUREMENT OF COSMIC-RAY POSITRON AND NEGATRON SPECTRA BETWEEN 50 AND 800 MV. Daugherty, J.K. (University of Maryland); Hartman, R.C.; Schmidt, P.J. Astrophys. J. 198: No. 2, 493-505 (1 June 1975).

A balloon-borne spark chamber magnetic spectrometer has been used to measure the spectra of cosmic-ray positrons and negatrons at energies between 50 and 800 MV. The data reported here were obtained during two flights from Fort Churchill, Manitoba, in 1972 July. The present results indicate that the dominance of negatrons from primary sources, found in earlier experiments above 200 MV, extends down to at least 50 MV. Solar modulation of the positron component is found to be consistent with that of the total electron spectrum, assuming that the positron component is entirely attributable to collisions between cosmic-ray nuclei and the interstellar gas. (auth)

**26346** ON EMISSION LINES IN THE COSMIC GAMMA-RAY BACKGROUND. Clayton, D.D.; Ward, R.A. (Department of Space Physics and Astronomy, Rice University). Astrophys. J. 198: No. 2, 241-244 (1 June 1975).

We calculate the composite spectrum of γ-rays resulting from the decay of $^{56}$Ni to $^{56}$Co to $^{56}$Fe throughout the history of the universe. The results for several cosmological models are presented and compared with the *Apollo* 15 measurements at low resolution of the cosmic background. The radioactivity background is a significant fraction of the total, and several of its features may be detectable. (auth)

**26347** DISTORTIONS OF THE MICROWAVE BACKGROUND RADIATION SPECTRUM IN THE SUBMILLIMETER WAVELENGTH REGION. Chan, K.L. (Princeton University, Department of Physics); Jones, B.J.T. Astrophys. J. 198: No. 2, 245-248 (1 June 1975).

Our numerical calculation shows that the linear approximation of the Compton-distorted radiation spectrum fails seriously in the submillimeter range. Numerical results agree with the Zel'dovich, Illarionov, and Sunyaev approximation in the limiting case when the matter temperature $T_e$ is much higher than the initial radiation temperature $T_0$. With a certain modification on the ZIS approximation, we use it to estimate the amplitude of Compton effect and perform a $\chi^2$ test on the possible combinations of $T_0$ and $Y_{eff}$ (cf. Appendix for notations) allowed by observations. (auth)

**26348** A SIMPLE METHOD TO EXTRACT INFORMATION ON ANISOTROPY OF PARTICLE FLUXES FROM SPIN-MODULATED COUNTING RATES OF COSMIC RAY TELESCOPES. Hsieh, K.C.; Lin, Y.C. (Department of Physics, University of Arizona, Tucson, Arizona 85721); Sullivan, J.D. J. Geophys. Res. 80: No. 16, 2305-2308 (1 June 1975).

A simple method to extract information on anisotropy of particle fluxes from data collected by cosmic ray telescopes on spinning spacecraft but without sectored accumulators is presented. Application of this method to specific satellite data demonstrates that it requires no prior assumption on the form of angular distribution of the fluxes; furthermore, self-consistency ensures the validity of the results thus obtained. The examples show perfect agreement with the corresponding magnetic field directions. (auth)

**26349** ORIGIN OF ULTRA HIGH ENERGY COSMIC RAYS. Kiraly, P.; Osborne, J. L.; White, M.; Wolfendale, A. W. (Durham Univ., Eng.). Nature (London); 255: No. 5510, 619-620(19 Jun 1975).

Evidence for large and small scale anisotropies in the directional distribution of very high energy cosmic ray particles is discussed, and it is concluded that it is not significant enough to be considered a strong argument in the controversy about galactic versus extragalactic origin. The authors state that caution should be exercised in interpreting the data for two reasons: firstly because of the weakness of the evidence for anisotropy, and secondly because of ambiguities of interpretation even if the "observed" anisotropies represent a genuine effect. (UK)

**26350** ANISOTROPY OF COSMIC RADIATION IN THE GALAXY. Gombosi, T. (Kozponti Fizikai Kutato Intezet, Budapest); Kota, J.; Somogyi, A. J.; Varga, A.; Betev, B.; Katsarsky, L.; Kaviakov, S.; Khirov, I. Nature (London); 255: No. 5511, 687-689 (26 Jun 1975).

The existence of cosmic ray anisotropy in the Galaxy had not been shown experimentally, but measurements are here reported that prove the existence of an anisotropy in galactic cosmic radiation. It was detected in the examination of extensive air showers produced by cosmic ray primaries of energies $6 \times 10^{13}$ eV, which are not affected by solar modulation. The apparatus employed was situated on the Bulgarian mountains at an altitude of 2925 m, and was of conventional Geiger counter type. Measurements were made over the period 1968 to 1972, and over 11,000 hours' running time about $10^8$ showers were recorded. The mathematical method used in the data analysis is described, and the results are discussed. The anisotropy observed appears to indicate that at least some cosmic ray primaries with energies about $6 \times 10^{13}$ eV are of galactic origin. (UK)

**26351** STRUCTURE OF IRREGULAR GALACTIC MAGNETIC FIELDS. Somogyi, A. J. (Kozponti Fizikai Kutato Intezet, Budapest). Nature (London); 255: No. 5511, 689-690(26 Jun 1975).

A method is here described that, assuming that the diffusion approximation for cosmic ray propagation is valid, is suitable for determining the structural composition of "random" galactic fields from cosmic ray measurements. The method is claimed to be suitable down to structures of characteristic lengths ~0.001 to 1 pC. The energy range of the cosmic ray particles considered is $10^{12}$ eV $\lesssim E \lesssim 10^{15}$ eV, and for simplicity it is assumed that the galactic cosmic radiation comprises only protons. (UK)

**26352** HALO-DISK REPENETRATION OF THE COSMIC PARTICLES. Suh, P. K. (Grumman Aircraft Engineering Corp., Bethpage, N. Y. (USA). Research Dept.). Astron. Astrophys.; 35: No. 3, 339-344(Oct 1974).

2 figs.; 29 refs.

There is emerging evidence that the cosmic particles actively exchange positions between the disk and halo domains. The cosmic electron is used as a probe for the halo-disk repenetration probability, and various physical implications of the possible physical halo formation are examined. (auth)

**26353** LIGHT OF THE UNIVERSE. Henry, R. C. (Johns Hopkins Univ., Baltimore). Astronaut. Aeronaut.; 13: No. 7, 16-20(1975).

The Universe's background radiation, including radio waves, microwaves, infrared radiation, ultraviolet radiation, X-rays, and gamma rays, is examined in relation to its cosmological significance. (BJG)

**26354** X-RAY ASTRONOMY. Volume XLIII. Giacconi, R.; Gursky, H. (eds.). Dordrecht, Netherlands; Reidel (1974). vp.

Separate abstracts were prepared for the 10 papers included. (BJG)

*For abstracts of individual papers see: 25921, 26355, 26426, 26427, 26492–26494, 26517, 26578, and 26659.*

**26355** COSMIC X-RAY BACKGROUND. Schwartz, D.; Gursky, H. (Center for Astrophysics, Cambridge, MA). pp 359-388 of X-ray Astronomy. Giacconi, R. (ed.). Dordrecht, Netherlands; Reidel (1974).

Observations of background X radiation are reviewed. Mechanisms of the production of cosmic X radiation and sources in the X-ray background are discussed. (BJG)

**26356** SURFACE STRUCTURE AND CHEMICAL COMPOSITION. Kopal, Z. (Univ. of Manchester, Eng.). pp 143-170 of Moon in the Post-Apollo Era. Vol. VII. Dordrecht, Netherlands; Reidel (1974).

A survey is given of Earth-based observations and additional data rendered by space flight photography which gives a fairly complete picture of the surface structure of the Moon. The results of analysis of the soil samples brought back by astronauts are presented and the consequences discussed. The radioactive concentrations measured from $\alpha$ and $\gamma$ spectra appear to show interesting anomalies. Chemical and nuclear reactions caused by cosmic-ray impact and the yield of artificial radioactive elements are discussed as well as the effects of the continuous irradiation to which the Moon surface is exposed. (auth)

**26357** ALMOST COMPLETE SURVEY OF 21 CM LINE RADIATION FOR $|b| \geq 10°$. IV. The HI Column Density as a Function of Position of the Sky. Heiles, C. (Univ. of California, Berkeley). Astron. Astrophys., Suppl. Ser.; 29: No. 1, 37-55 (Apr 1975).

A contour map of HI column density for velocities between $-93$ to $+75$ kms$^{-1}$ is presented. (auth)

**26358** FOKKER-PLANCK THEORY FOR COSMIC RAY DIFFUSION IN THE PRESENCE OF ALFVÉN WAVES, 1, THEORY. Hollweg, J.V.; Skadron[1], G. (NCAR High Altitude Observatory, Boulder, Colorado 80303). J. Geophys. Res. 80: No. 22, 2701-2707 (1 Aug 1975).

Using the standard quasi-linear Fokker-Planck approach and an expansion of the cosmic ray distribution function in Legendre polynomials, we derive a complete set of Fokker-Planck coefficients and expressions for the complete cosmic ray diffusion tensor due to linearly polarized planar Alfvén waves propagating at an angle to the average magnetic field. We find that although an off-diagonal term formally appears in the diffusion tensor, it is identically zero. In addition, the cross-field diffusion coefficient is identically the same as that found for wave propagation exactly parallel to the average magnetic field. (auth)

**26359** *PIONEER* 10 MEASUREMENTS OF THE CHARGE AND ENERGY SPECTRUM OF SOLAR COSMIC RAYS DURING 1972 AUGUST. Webber, W.R.; Roelof, E.C. (Physics Department, University of New Hampshire, Durham); McDonald, F.B.; Teegarden, B.J.; Trainor, J. Astrophys. J. 199: No. 2, 482-493 (15 July 1975).

We have measured the energy spectrum and charge composition of solar cosmic rays integrated over the giant events of 1972 August on the *Pioneer* 10 spacecraft located at 2.2 AU. Within the energy range 8–50 MeV nucleon$^{-1}$, the individual nuclei from He to Si appear to have average differential spectra of the form $dN/dE \sim E^{-2.7}$, except for carbon, which exhibits a slightly steeper spectrum with $\gamma = 3.1$. The average charge composition in this energy range is similar in most respects to that measured in other recent flare events using counters, emulsions, and plastic detectors, although it differs significantly, for $Z = 10$-14 nuclei, from some earlier emulsion abundances. These data provide further evidence that the He abundance relative to C and N and O nuclei is variable from event to event, and also that this ratio is energy-dependent. The abundance of Na and Al nuclei was determined for the first time in solar cosmic rays. In the light of these data, the question of the relative abundances of solar cosmic rays and solar atmospheric abundances in the $Z = 10-14$ range is reexamined. Results are also presented for the $^3$He flux. (auth)

## Stars

*Refer also to abstracts 26354, 26474–26476, 26478, 26499, 26505, 26556, 26557, and 26567.*

**26360** CAN SUPERNOVAE EXPLAIN THE R-PROCESS ELEMENTAL ABUNDANCES. Ohnishi, T. (Kyoto Univ., Uji (Japan). Inst. of Atomic Energy). Tech. Rep. Inst. At. Energy, Kyoto Univ.; No. 154, 1-18(Nov 1971).

The possibility of the formation of heavy neutron rich nuclides in the universe is investigated by comparing the r-process time scale with the exploding or the cooling time scales of various types of stars. It becomes clear from the study of time scales that the r-process nuclides except the mass region of $70 \leq A \leq 120$ can not be produced in the expanding shells of type-I supernovae, but the heavier nuclides than $A \simeq 120$ can be easily synthesized in the cooling shells of neutron stars or in the expanding shells of supermassive stars. The time dependent treatments of the r-process in the exploding shells are made. (auth)

**26361** THE ROLE OF DELAYED NEUTRONS IN THE R-PROCESS. Ohnishi, T.; Nishi, T. (Kyoto Univ., Uji (Japan). Inst. of Atomic Energy). Tech. Rep. Inst. At. Energy, Kyoto Univ.; No. 158, 1-11(Dec 1972).

The effect of delayed neutron emission in the cooling period

of the r-process is investigated. The delayed neutron emission is assumed to follow the negaton decay cascade in the cooling period and seems to be the most efficient decay mode except the negaton decay. Two types of level density are assumed for the excited states of a daughter nuclide to which negaton decays feed: the one is the constant level density without dependence on the excitation energy, and the other is the level density of the equidistant spacing model. It has become clear that the half-widths of the r-process abundance peaks are explained by the effect of the delayed neutrons. Though the delayed neutrons considerably smooth out the odd-even structure of the r-abundances, the observed odd-even relation of N(even) > N(odd) in the off-magic nuclear region is not reproduced by this effect alone. Here N(A) is the abundance of the nuclide of mass A. The most effective mechanism possibly leading the observed odd-even relation may be the neutron recapture reaction during the cooling. (auth)

**26362** WAVELENGTH DEPENDENCE OF POLARIZATION. XXVIII. CIRCUMSTELLAR SCATTERING: POLARIZATION AND REDDENING MODELS. Shawl, S.J. (Department of Physics and Astronomy, University of Kansas, Lawrence, Kansas 66045). Astron. J. 80: No. 8, 595-601 (Aug 1975).

Results of calculations of the polarization and reddening produced by circumstellar scattering envelopes are presented. Models are given for scattering by spherical silicate, graphite, and iron grains and by the hydrogen molecule. Various geometries, density distributions, and particle size distributions are included. The following paper contains a comparison of the results of this paper with observation. (auth)

**26363** ON THE EVIDENCE FOR CIRCUMSTELLAR OBSCURATION OF OB STARS. Bohannan, B. (Joint Institute for Laboratory Astrophysics, University of Colorado and National Bureau of Standards, Boulder, Colorado 80302). Astron. J. 80: No. 8, 625-636 (Aug 1975).

Reddish found a strong increase of color excess with increasing stellar luminosity—here referred to as the Reddish Effect—in ten young galactic clusters and associations. New photometric and spectroscopic observations drawn from the literature are combined with data used by Reddish to reconsider the color excess versus intrinsic magnitude diagrams of the same ten stellar groups. The reality of the Effect is questioned in all but one of the systems; this was accomplished by identifying possible foreground stars and by recognizing some of the brightest stars as supergiants, then applying correct intrinsic color indices. After careful reanalysis, the one stellar group to retain an indication of the Reddish Effect is Cygnus OB2. No correlation of reddening with luminosity was found for five additional very young stellar groups in the southern hemisphere; these groups should exhibit the Effect if it is a natural consequence of stellar evolution. Reddish ascribed the correlation to massive circumstellar remnants of material from which the stars formed. However, a peculiar dispersion in color excess could also be attributed to patchy dust within the stellar group. In several stellar systems previously identified as displaying the Reddish Effect, a correlation of observed color excess with dust and gas concentrations is noted on Palomar Sky Survey prints. If present, circumstellar dust clouds should manifest their existence in modes other than a correlation of color excess with luminosity. The following possibilities are considered and all show negative results: correlation of color excess with spectral type; correlation of reddening slope $E_{U-B}/E_{B-V}$ with spectral type; observable infrared excess. The preceding astrophysical arguments strongly imply that circumstellar dust remnants from stellar formation do not remain around stars during their main-sequence lifetimes. (auth)

**26364** PARALLAXES OF 18 DWARF MEMBERS OF THE HYADES CLUSTER. Klemola, A.R.; Harlan, E.A.; McNamara, B.; Wirtanen, C.A. (Lick Observatory, Board of Studies in Astronomy and Astrophysics, University of California, Santa Cruz, California). Astron. J. 80: No. 8, 642-646 (Aug 1975).

Trigonometric parallaxes measured for 18 dwarf members of the Hyades with magnitudes 9–13 in 16 fields lead to a weighted mean parallax of 0.0230±0.0015 (m.e.) arcsec and distance modulus of 3.19±0.15 (m.e.) mag. (auth)

**26365** ASTROMETRIC STUDIES OF THE REGIONS BD +17°4946, BD −5°3071, AND ROSS 730−1. Russell, J.; Gatewood, G. (Allegheny Observatory, University of Pittsburgh, Pittsburgh, Pennsylvania 15214). Astron. J. 80: No. 8, 652-654 (Aug 1975).

Positions, proper motions, and absolute parallaxes were found for 46 stars in the regions of BD +17°4946, BD −5°3071, and Ross 730−1. BD +17°4946 showed some evidence of irregular variations in position and magnitude. The residuals for Ross 730−1 were used in a preliminary study to test for an appropriate weighting system; a weak weighting system was indicated. (auth)

**26366** ASTROMETRIC ORBIT, ECLIPSING PERIOD CHANGES, AND PARALLAX OF VW CEPHEI. Hershey, J.L. (Sproul Observatory, Swarthmore College, Swarthmore, Pennsylvania). Astron. J. 80: No. 8, 662-667 (Aug 1975).

Six hundred ten plates taken from 1942 to 1974 with the 61−cm Sproul refractor have been analyzed for parallax and orbital motion. An orbital period of 30.45 y and a photocentric semimajor axis of 0.″130 have been found, indicating the presence of a third body which has subsequently been observed visually according to prediction. The photographic and visual data yield a direct determination of the mass of the eclipsing pair and of the third star. The variations in the times of minimum which prompted astrometric surveillance as possible orbital light-time effects are found to be due to period changes in the eclipsing pair, although a small light-time effect is detectable. VW Cephei and Ross 614 are the only cases where a stellar companion has been seen as a result of prediction from a photographic astrometric orbit. An absolute parallax of 0.″041 ± 0.″002 has been found for VW Cephei. (auth)

**26367** DETECTION OF INTERSTELLAR SiS AND A STUDY OF THE IRC+10216 MOLECULAR ENVELOPE. Morris, M. (University of Chicago); Gilmore, W.; Palmer, P.; Turner, B.E.; Zuckerman, B. Astrophys. J. Lett. 199: No. 1, L47-L51 (1 July 1975).

Microwave emission in the $J=6\rightarrow5$ and $J=5\rightarrow4$ transitions of $^{28}Si^{32}S$ has been detected toward IRC+10216. The $J=2\rightarrow1$ line of $^{28}Si^{16}O$ and several rotational lines of $HC_3N$ were also detected in the envelope of this unusual carbon star. The SiS/SiO abundance ratio in IRC+10216 is greater than unity, as expected for the atmosphere of a carbon star. Observations of eight linear molecules in IRC+10216 can be explained by a collisional excitation mechanism if the envelope is massive ($\gtrsim 1$ $M_\odot$). However, a more likely excitation mechanism involves the absorption of near-infrared photons into excited vibrational states. Then the observed line intensities can be accounted for with an envelope of much smaller mass ($2\text{–}35 \times 10^{-3}$ $M_\odot$). The Sgr B2 molecular cloud is probably another source of SiS emission. (auth)

**26368** RED GIANTS AND SUPERGIANTS WITH DEGENERATE NEUTRON CORES. Thorne, K.S. (California Institute of Technology); Żytkow, A.N. Astrophys. J. Lett. 199: No. 1, L19-L24 (1 July 1975).

A new type of stellar model is constructed. It is related to neutron stars as ordinary red giants are related to white dwarfs. Its external appearance is similar to that of an ordinary M supergiant, but its evolutionary lifetime is 10 times longer. Our models are constrained to be relativistic but nonrotating, and to contain a degenerate neutron core of mass 1 $M_\odot$ and radius 10 km, surrounded by a nondegenerate, massive, diffuse envelope. The core and envelope turn out to be separated by a thin (~40 m) energy-generation layer. The envelope convects from this layer all the way out to the photosphere. The effective temperatures and radii are ~ 2700 K and ~ 1000 $R_\odot$. Within a fairly narrow range of effective temperatures and radii, two families of models were found: "red giants" and "red supergiants" with luminosities and masses less than and greater than ~ 65,000 $L_\odot$ and ~ 10 $M_\odot$, respectively. The luminosity of a giant comes 97 percent from gravitational contraction and 3 percent from nuclear burning. That of a supergiant is 5 percent from gravitational contraction and 3 percent from nuclear burning. That of a supergiant is 5 percent from gravitational contraction and 95 percent from hydrogen burning by nonequilibrium, hot CNO reactions. The CNO reaction products are convected directly from the hydrogen-burning shell out to the photosphere of the supergiant, where they should be observable. (auth)

**26369** RELATIVISTIC EFFECTS IN THE BINARY PULSAR PSR 1913+16. Barker, B.M.; O'Connell, R.F. (Department of Physics and Astronomy, Louisiana State University, Baton Rouge). Astrophys. J. Lett. 199: No. 1, L25-L26 (1 July 1975).

The relativistic precession of both the spin and the periastron of the pulsar 1913+16, in the gravitational field of its companion, are analyzed. (auth)

**26370** LINEAR POLARIZATION VARIATIONS MODULO 5.6 DAYS IN HDE 226868. Nolt, I.G.; Kemp, J.C.; Rudy, R.J.; Southwick, R.G.; Radostitz, J.V.; Caroff, L.J. (Department of Physics, University of Oregon, Eugene, Oregon 97403). Astrophys. J. Lett. 199: No. 1, L27-L29 (1 July 1975).

We have found linear-polarization variations in the ultraviolet ($U$ filter) in HDE 226868, as folded on the $^d$.6 orbital period. The amplitudes are $\Delta p$ =0.25 percent and $\Delta\theta$=2°.7. (auth)

**26371** A COOL DEGENERATE DWARF WITH A METAL-RICH ATMOSPHERE. Hintzen, P.; Tapia, S. (Steward Observatory, University of Arizona). Astrophys. J. Lett. 199: No. 1, L31-L33 (1 July 1975).

G165−7, a recently discovered cool degenerate dwarf ($B-V$=0.84), displays a very rich spectrum containing absorption features due to Ca II, Ca I, Mg I, Fe I, and probably CH and Mn I. (auth)

**26372** ULTRAVIOLET PHOTOMETRY FROM THE ORBITING ASTRONOMICAL OBSERVATORY XX. THE ULTRAVIOLET EXTINCTION BUMP. Savage, B.D. (Space Astronomy Laboratory, Washburn Observatory, University of Wisconsin, Madison). Astrophys. J. 199: No. 1, 92-109 (1 July 1975).

Interstellar extinction curves over the wavelength region 1800–3600 Å are presented for 36 stars. The stars have $E(B-V)$ in the range 0.03 to 0.55, and are mostly confined to the brighter OB associations distributed along the plane of the Galaxy. Every extinction curve exhibits a broad extinction bump peaking near 2175 Å (4.6 $\mu^{-1}$). The position of the peak and the profile of the feature appear remarkably constant among the sample of stars. With only a few exceptions, $E(\lambda_{max}-3320)$, a measure of the strength of the feature, correlates very well with $E(B-V)$, implying that the bump has an interstellar rather than a circumstellar origin. The observation that the bump position and shape are constant, or very nearly constant, places severe restrictions on the grain geometrical parameters if the feature is to be explained by classical scattering theory employing bulk optical constants. In fact, the restrictions are so severe that an alternate explanation seems to be required unless the dust grains that exist in widely separated regions of space and under very different physical conditions have nearly identical size and shape distributions. Three extinction curves that extend to 1100 Å are also presented. These curves show the same general extinction characteristics reported earlier. The curve for 22 Sco provides another example of a star that is physically associated with nebulosity and that also has abnormally low far-ultraviolet extinction. We have searched the extinction curves for fine structure such as abrupt slope changes or new diffuse interstellar features. Unfortunately, there is no convincing evidence for such structure over the interval 1800–3600 Å. (auth)

**26373** OBSERVATIONS OF THE Mg II LINES NEAR 2800 Å FROM *COPERNICUS*. Kondo, Y. (Lyndon B. Johnson Space Center, Houston); Modisette, J.L.; Wolf, G.W. Astrophys. J. 199: No. 1, 110-119 (1 July 1975).

Observations of the Mg II resonance doublet lines at 2795 and 2802 Å, and their respective subordinate lines at 2797 and 2790 Å, have been made for some 40 stars in the spectral region O8–B8 employing the Princeton telescope-spectrometer on the *Copernicus* satellite. Equivalent-width measures, determined by a new approach, are in agreement with the recent theoretical predictions made by Snijders and Lamers for most of the stars. Deviations from the theoretical predictions have been found for the earliest spectral types, where the rotational velocity effects, discussed recently by Collins, appear to make the equivalent widths greater. Evidence of emission has been found in a few stars of earliest and latest spectral types studied. (auth)

**26374** THE SPECTRUM OF HD 125823 (a CENTAURI). Underhill, A.B.; Fahey, R.P.; Klinglesmith, D.A. (Laboratory for Optical Astronomy, Goddard Space Flight Center, Greenbelt, Maryland). Astrophys. J. 199: No. 1, 120-126 (1 July 1975).

Equivalent widths and profile observations of representative lines in the spectrum of the helium variable HD 125823 (a Centauri) are presented around one cycle of 8.814 days. European Southern Observatory Camera III spectrograms (3.3 Å $mm^{-1}$) covering the region 3350–4950 Å, and Camera II spectrograms covering the region 4800–6600 Å at 12.4 Å $mm^{-1}$, are used. The equivalent widths of the hydrogen lines and lines of C II, O II, Mg II, Si II, and Ca II do not vary in a systematic way by a significant amount during the He I cycle, while lines of N II, Si III, and Fe III vary in antiphase to the He I lines. The projected rotational velocity is estimated to be 17 Km $s^{-1}$ from the cores of the sharp lines, but the wings of these lines are broader than that. Representative profiles are presented of the weak, shallow Fe I lines which appear between phases 0.9 and 0.3 of the He I variation. The origin of these lines is not understood. (auth)

**26375** ON THE EVOLUTION AND COMPOSITION OF SIRIUS AND PROCYON. Hartmann, L.; Garrison, L.M. Jr.; Katz, A. (Washburn Observatory, University of Wisconsin-Madison). Astrophys. J. 199: No. 1, 127-130 (1 July 1975).

Stellar models are calculated and compared to the new observational data available for Sirius and Procyon. Sirius can be fitted by normal compositions ($X=0.7$, $Z=0.02$) very near the zero-age main sequence. Procyon is more evolved, hence more ambiguous; an anomalous composition (high $X$ or $Z$) or a smaller mass than the astrometric mass is necessary to fit its position in the H-R diagram. (auth)

**26376** LONG-PERIOD VARIABLES: FURTHER WORK ON THE CORRELATION OF PERIOD WITH OH RADIAL-VELOCITY PATTERN. Dickinson, D.F. (Center for Astrophysics, Harvard College Observatory and Smithsonian Astrophysical Observatory); Kollberg, E.; Yngvesson, S. Astrophys. J. 199: No. 1, 131-134 (1 July 1975).

Recent radio observations at 18 cm have found a number of new OH stars, all of which exhibit the double-peaked spectrum characteristic of these objects. They confirm the correlation between stellar period and the velocity separation of the two emission peaks. A less stringent correlation seems to exist between the $I$–$K$ color index and the velocity separation. (auth)

**26377** DISTANCES AND LUMINOSITIES OF IRREGULAR VARIABLES OF TYPE N. Peery, B.F. Jr. (Department of Astronomy, Indiana University). Astrophys. J. 199: No. 1, 135-144 (1 July 1975).

Near-infrared photometric data of Baumert are shown to suggest that the variety in the observed (0.78 – 1.08) $\mu$ color index of N irregular variables (L*b* and Sr*b*) is primarily a consequence of interstellar reddening. On this hypothesis, color excesses are used to estimate distances of 60 N irregulars. Luminosities follow from photometry relative to Vega and the observed flux distribution of 19 Psc out to 14 $\mu$; the latter star is taken as the prototype N irregular. Derived distances are supported by the Oort double-sine distribution of radial velocities, by some apparent association with galactic spiral features, and by agreement with bolometric corrections of Mendoza and Johnson. Within a Keenan-Morgan C subclass there is a dispersion in $M_{bol}$ of ~ 1 mag or more. $M_{bol}$ increases from $\langle M_{bol}\rangle = -4.4$ in C4 to $\langle M_{bol}\rangle = -5.6$ in C7. Near-infrared CN bands do not correlate with luminosity, but the Merrill-Sanford bands emerge as negative luminosity indicators. (auth)

**26378** OBSERVATIONS OF NEAR-INFRARED $C_2$ BANDS IN THE SPECTRA OF CARBON STARS. Gilra, D.P. (Department of Astronomy, University of California, Berkeley, California 94720). Astrophys. J. 199: No. 1, 145-147 (1 July 1975).

It is pointed out that features due to the (3,0) Phillips band of $C_2$ in the 7715–7750 Å region can be used to identify carbon stars at moderate dispersion. Also, the first observations are reported of the (2,0) Ballik-Ramsay band of $C_2$ at 1.1726 $\mu$. (auth)

**26379** P CYGNI STARS AND MASS LOSS. Kuan, P.; Kuhi, L.V. (Department of Astronomy, University of California, Berkeley). Astrophys. J. 199: No. 1, 148-165 (1 July 1975).

The Sobolev approximation is used to compute line profiles formed in rapidly expanding atmospheres. Twelve levels of hydrogen are used in determining the level populations in the envelope under statistical equilibrium. The results are compared to observed hydrogen Balmer series profiles of P Cygni and other stars of similar type. It is found that a decelerating envelope can most adequately account for the observed profiles. Mass loss rates and mechanical momentum fluxes are determined for these stars and correlated with infrared excesses. It is found that low momentum flux favors the presence of dust in the envelope, as indicated by the presence of large infrared excess, whereas high momentum fluxes are found for stars having a free-free infrared emission spectrum. (auth)

**26380** PATTERNS OF CONVECTION IN THE EVOLUTION OF MASSIVE STARS. Schlesinger, B.M. (Astronomy Department, Indiana University, Bloomington). Astrophys. J. 199: No. 1, 166-172 (1 July 1975).

Models for stars of $30\mathfrak{M}_\odot$ have been computed with an algorithm that assumes every point in the star to be radiative or fully convective. The ordinary Schwarzschild criterior is used. Semiconvection is not treated explicitly. In the resulting models, detached convective shells with superadiabatic inner boundaries appear instead of semiconvection. Since these boundaries travel inward by overshoot more rapidly than the core recedes, such detached convective zones would not persist in an actual star but would mix with the core. Inward of the detached convection, the hydrogen profile is insensitive to the treatment of convection if mass points are frequently redistributed in regions with a steep gradient of chemical composition. Treatment of overshoot will be necessary if radiative and convective zones are to represent semiconvection. During shell hydrogen burning, a convective region outside the nuclear burning shell and a semiconductive region farther outside will arise independent of overshoot. The $^{14}N+\alpha$ reaction may precede triple-$\alpha$ ignition in the core ins tars of $30\mathfrak{M}_\odot$. (auth)

**26381** STELLAR RATES FOR SOME REACTIONS OF INTEREST IN ASTROPHYSICS. Rios, M. (California Institute of Technology); Schweitzer, J.S.; Anderson, B.D. Astrophys. J. 199: No. 1, 173-178 (1 July 1975).

Experimental cross sections for the $^{46}Ti(p,\gamma)^{47}V$, $^{50}Cr(p,\gamma)^{51}Mn$, and $^{58}Ni(\alpha,p)^{61}Cu$ reactions have been numerically integrated over a Maxwell-Boltzmann velocity distribution to determine thermonuclear reaction rates in the temperature range $2 \leq T_9 \leq 10$ and for the $^{58}Ni(\alpha,\gamma)^{62}Zn$ reaction in the range $3 \leq T_9 \leq 5$. Appropriate analytic expressions for the experimental rates and for stellar rates in which the target nuclei are in a thermal distribution of excited states are presented. Experimental rates are compared with theoretical calculations. (auth)

**26382** UPPER MASS LIMITS FOR STABLE ROTATING WHITE DWARFS. Durisen, R.H. (Theoretical Studies Branch, Space Science Division, NASA-Ames Research Center, Moffett Field, California). Astrophys. J. 199: No. 1, 179-183 (1 July 1975).

Models of nonmagnetic, axisymmetric, differentially rotating, zero-temperature white dwarfs are constructed and tested for stability. Upper mass limits, beyond which models become secularly and dynamically unstable to growth of nonaxisymmetric perturbations, are found at 2.5 $M_\odot$ and 4.6 $M_\odot$, respectively. The upper mass limit for secular stability is practically the same for the two angular momentum distributions considered. Crude growth rates due to gravitational radiation and degenerate-electron viscosity are calculated for the secularly unstable

models. Except for a narrow parameter range, gravitational radiation is the dominant destabilizing mechanism. For $3.5\,M_\odot \lesssim M \lesssim 4.6\,M_\odot$, the secular instability grows on a time scale $\sim 10^3$ to $10^1$ years; for $M \gtrsim 4.6\,M_\odot$, the dynamic instability grows on a time scale ~seconds. Implications of these results for mass transfer binary star systems and degenerate stellar cores are discussed. (auth)

**26383** SPECTRAL TURNOVERS OF GALACTIC SUPERNOVA REMNANTS. Dulk, G.D. (Department of Astro-Geophysics, University of Colorado, Boulder); Slee, O.B. Astrophys. J. 199: No. 1, 61-68 (1 July 1975).

High-resolution observations of 14 galactic supernova remnants have been made at 80 and 160 MHz with the Culgoora radioheliograph. The spectra of 7 to 10 of the sources exhibit a turnover at $\lesssim 100$ MHz, which we attribute to free-free absorption taking place in the inner regions of the Galaxy. The absorption could occur in large ($\gtrsim 20$ pc), low-density ($n \simeq 10$ cm$^{-3}$) H II regions created by O5 to O8 stars. Alternatively, absorption could occur in cold dense clouds which are a feature of the steady-state model of the interstellar medium, or, more likely, in cold, partly ionized regions of moderate density which are a feature of the time-dependent model. (auth)

**26384** THE CIRCULARIZATION OF CLOSE BINARY ORBITS: CENTAURUS X-3. Chevalier, R.A. (Kitt Peak National Observatory). Astrophys. J. 199: No. 1, 189-195 (1 July 1975).

If the neutron star in Cen X-3 resulted from a normal supernova explosion, the resulting binary system must have had considerable eccentricity. As the present eccentricity is small, mechanisms for circularizing the orbit are examined with the aim of setting constraints on the evolution of the binary system. Tidal interaction in an unstable decaying orbit allows only small initial eccentricities, since there are observational limits on changes in the semimajor axis. Using similar arguments, tidal interaction in which the primary rotates synchronously with the binary period is consistent wtih any initial eccentricity. Tidal interaction does not yield an explanation for the observed period changes in Cen X-3. Thus it may be necessary to go to a combination of mass loss and mass transfer as the circularization mechanism, although a delicate balance between the two is required. (auth)

**26385** MASS TRANSFER IN BINARY X—RAY SYSTEMS. McCray, R.; Hatchett, S. (Department of Physics and Astrophysics, University of Colorado). Astrophys. J. 199: No. 1, 196-205 (1 July 1975).

The influence of X-ray heating on gas flows in binary X-ray systems is examined. A simple estimate is obtained for the evaporative wind flux from a stellar atmosphere due to X-ray heating that agrees with numerical calculations by Alme and Wilson but disagrees with calculations by Arons and Basko and Sunyaev for the Her X-1—HZ Her system. The wind flux is sensitive to the soft X-ray spectrum. The self-excited wind mechanism does not work. Mass transfer in the Hercules system probably occurs by flow of the atmosphere of HZ Her through the gravitational saddle point of the system. The accretion gas stream is probably opaque with atomic density $n \gtrsim 10^{15}$ cm$^{-3}$ and is confined to a small fraction of $4\pi$ steradians. Other binary X-ray systems are briefly discussed. (auth)

**26386** GROUND STATE OF ELECTRON MATTER IN HIGH MAGNETIC FIELDS. Glasser, M.L. (Department of Applied Mathematics, University of Waterloo, Waterloo, Ontario, Canada). Astrophys. J. 199: No. 1, 206-207 (1 July 1975).

It is shown that for a dense electron plasma, Coulomb interactions, which are negligible in weak magnetic fields, can in strong magnetic fields profoundly modify the properties of the system. They should therefore be considered in speculations regarding the surface properties of pulsars. (auth)

**26387** THE SURFACE OF A NEUTRON STAR IN SUPERSTRONG MAGNETIC FIELDS. Glasser, M.L. (Department of Applied Mathematics, University of Waterloo, Waterloo, Ontario); Kaplan, J.I. Astrophys. J. 199: No. 1, 208-219 (1 July 1975).

We study the effects of electron interactions in the structure of matter in extreme ($B \gtrsim 10^{12}$ gauss) magnetic fields. It is found that intere'lectronic repulsion tends to produce an anisotropic crystalline structure. (auth)

**26388** ON THE IMPLICATIONS OF THE NONEXISTENCE OF UNSTABLE OUTGOING NORMAL MODES FOR THE STABILITY OF SPHERICAL STELLAR MODELS TO NONRADIAL PERTURBATIONS IN GENERAL RELATIVITY. Ipser, J.R. (University of Chicago). Astrophys. J. 199: No. 1, 220-226 (1 July 1975).

This paper studies whether, without tackling the question of completeness of the normal modes, one can relate the question of the nonexistence of unstable normal modes having purely outgoing waves at large radii to the question of the stability of systems to perturbations involving gravitational radiation in general relativity. An affirmative conclusion is established for the case of nonradial perturbations of spherical relativistic stellar models; that is, it is shown that a model is stable to small nonradial perturbations essentially if and only if it does not possess an unstable outgoing normal mode. This result is combined with those of an earlier paper to show that a relativistic model is stable to nonradial perturbations if its density decreases outward monotonically and if its relativistic Schwarzschild discriminant is positive. (auth)

**26389** COARSE PHOTOSPHERIC CONVECTION AND THE EJECTION OF DUST BY R CORONAE BOREALIS. Wdowiak, T.J. (Marshall Space Flight Center, Huntsville, Alabama). Astrophys. J. Lett. 198: No. 3, L139-L140 (15 June 1975).

It is suggested that 10 to 100 convection cells exist in a coarse structure across the surface of R CrB and are responsible for the formation of dust patches that are ejected asymmetrically by radiation pressure. (auth)

**26390** NOVAE, SUPERNOVAE, AND NEUTRON SOURCES. Starrfield, S. (Department of Physics, Arizona State University); Truran, J.W.; Sparks, W.M. Astrophys. J. Lett. 198: No. 3, L113-L117 (15 June 1975).

We have evolved thermonuclear runaways in 1.1 $M_\odot$ and 1.25 $M_\odot$ white dwarfs where we have assumed extremely enhanced $^{12}$C in the envelope. A "super" nova-type outburst results, in which peak temperatures exceeding $2\times10^9$ K and peak burning rates of $3\times10^{24}$ ergs g$^{-1}$ s$^{-1}$ are achieved. A shock forms and ejects more than $10^{29}$ g moving with speeds up to 90,000 km s$^{-1}$. The subsequent $\beta^+$ decays provide enough additional energy to eject nearly $2\times10^{30}$ g. The peak luminosity is $10^{10}\,L_\odot$ at an effective temperature of nearly $3\times10^5$ K. One model produces a substantial neutron flux for a short time, sufficient to drive an intermediate neutron-capture process. (auth)

**26391** TYPE I SUPERNOVAE I. THE He II, He I, H I SPECTRUM, 30 DAYS AFTER THE EXPLOSION. Gordon, C. (IBM Thomas J. Watson Research Center, Yorktown Heights, New York). Astrophys. J. 198: No. 3, 765-773 (15 June 1975).

We have computed the He II, He I, and H I spectra (lines and continuum) for a model of Type I supernovae consisting of a spherically expanding shell with a stratification of ionization. We have assumed three different laws for the variation of the density $\rho$ ($v$) with the expansion velocity $v$ in the shell [$\rho\simeq\rho_0(w/v)^2$; $p\simeq\rho_1$, and $\rho\simeq\rho_2(v_0/v)^2$], and have determined $\rho_0$, $\rho_1$, or $\rho_2$ by comparison of our theoretical spectrum with the observed spectrum of SN 1972 in NGC 5253 corresponding to the same stage of evolution. Helium is the most abundant element, but hydrogen must be present in the bulk of the ejected material if we want to explain the observed stratification of ionization. The relative abundance of H and He varies with the density law adopted. For all the density models the temperature $T_e$ in the inner layers of the shell must be close to 20,000 K. The expansion of the shell cannot be adiabatic, and our model requires the presence of a neutron star inside the shell. (auth)

**26392** THE LIGHT OF THE SUPERNOVA OUTBURST. II. THE CASE OF SUPERNOVA 1972e. Chiu, B.C.; Morrison, P. (Department of Physics and Center for Space Research, Massachusetts Institute of Technology); Sartori, L. Astrophys. J. 198: No. 3, 617-628 (15 June 1975).

The optical output of the bright Type I supernova 1972e is best studied of any, both for quantitative spectrophotometry (Hale Observatories) and for the range of spectral band measured. We examine it in detail as a test of the fluorescence theory of supernova light. The observed light curve and spectra allow the partition of the output into two distinct portions: one, the rather red quasi-Planckian continuum with its accompanying emission and absorption lines which comes directly from the expanding gas shell ejected in the explosion; the other, wide fluorescent emission lines and a weak blue two-photon continuum. The direct light dominates the observed spectrum at earlier times, but fades more rapidly. The form of the prolonged light-curve tail and the two identifiable lines of He II support the fluorescence model. The 10124 Å line of He II predicted in 1969 is present in the correct position, with roughly the intensity given by the simplest fluorescent model. The shifts of the He II lines vary with time about as predicted by that model, while Ca II lines associated with the direct shell emission show a different redshift evolution. Other strong lines of fluorescent origin seem present but are not identified. The fluorescence model implies a much greater energy output in XUV light than in all optical emission, so that the early optical dominance of the direct shell radiation in this case does not affect the main conclusion: the total radiative output of a Type I explosion supernova explosion is at least tens of times greater than all we observe in the infrared and visible bands. (auth)

**26393** THE WEAK INTERACTION AND GRAVITATIONAL COLLAPSE. Schramm, D.N. (University of Chicago, Department of Astronomy and Astrophysics, and the Enrico Fermi Institute); Arnett, W.D. Astrophys. J. 198: No. 3, 629-639 (15 June 1975).

Recent developments in weak interaction physics as well as a more careful examination of previously known phenomena should yield a much clearer picture of the gravitational collapse of an evolved stellar core than has previously been possible. It is shown that the dominant neutrino-emitting process throughout much of the collapse is ordinary electron capture. The effects of neutral currents and the coherent

scattering of neutrinos is discussed. A modified neutrino transport supernova model, whereby momentum transfer from neutrino scattering blows off the outer part of a star while leaving a dense remnant, may be quite reasonable. The boundary between collapse and ejection is near $\rho \sim 2 \times 10^{11}$ g cm$^{-3}$. Possible implications for origin of the cosmic rays and the heavy elements in the interstellar medium are discussed. (auth)

**26394** ON THE ORIGIN OF λλ4640–4650 EMISSION IN X–RAY STARS. McClintock, J.E.; Canizares, C.R. (Department of Physics and Center for Space Research, Massachusetts Institute of Technology); Tarter, C.B. Astrophys. J. 198: No. 3, 641-652 (15 June 1975).

A prominent and rapidly variable emission feature near λλ4640–4650 has been observed in six of the eight optical counterparts of compact galactic X-ray sources. It appears very likely that the emission is generated in the vicinity of the compact source by the interaction of X-rays with nearby gaseous matter. Three likely sources of the emission are the ions C III, N III, and O II. The results of a detailed computational model of an X-ray source surrounded by a uniform distribution of matter are presented. The computed temperature, ionization structure, electron density, and radiation fields are used to discuss three possible origins of the λλ4640–4650 emission: (1) nonselective emission by one or more of the ions C III, N III, and O II; (2) selective emission of the N III λλ4634–4641 in the "Of star process"; (3) selective emission of N III λλ4634–4641 in the Bowen fluorescence process. The results of the model X-ray source computation indicate that processes (1) and (2) are unlikely to be effective, whereas it appears likely that the Bowen fluorescence mechanism is an important source of N III λλ4634–4641 emission in celestial X-ray sources. The hypothesis can be tested most directly by looking for a selected set of O III emission lines which lie shortward of ~ 3800 Å, and which are created in the Bowen process. (auth)

**26395** OPTICAL PULSATIONS IN HZ HERCULIS. III. DISCOVERY OF PULSED EMISSION LINES. Davidsen, A. (Astronomy Department and Space Sciences Laboratory, University of California, Berkeley); Margon, B.; Middleditch, J. Astrophys. J. 198: No. 3, 653-660 (15 June 1975).

We have detected periodic optical pulses from HZ Herculis in a 100 Å band containing the emission features He II λ4686 and the N III λ4640 multiplet. On two nights when broad-band pulses were detected with ~0.3 percent modulation, the narrow-band data reveal coherent pulses at the same phase, with amplitude ~2.5 percent. About one-third of the total pulsed component of optical emission is contained within this 100 Å band and is therefore undoubtedly associated with the emission lines. We infer that one or more of these lines must be strongly pulsed, with amplitude exceeding 25 percent, which implies an extremely high efficiency of X-ray optical pulse reprocessing. The observed pulse frequency and its time derivative yield the velocity (±2 km s$^{-1}$) rather than near the compact X-ray source or in the gas stream as suggested by other observers. We propose that radiative recombinations of He II and dielectronic recombinations of N III can explain the observed pulsed emission line strengths and that the pulsed lines are formed in a dense region of the HZ Her atmosphere. The occurrence of optical pulses before X-ray turn-on proves that pulsed X-rays are at times present in the HZ Her system even when they are unobservable at Earth. (auth)

**26396** OBSERVATIONS OF PULSAR RADIO EMISSION. III. STABILITY OF INTEGRATED PROFILES. Helfand, D.J.; Manchester, R.N.; Taylor, J.H. (Department of Physics and Astronomy, University of Massachusetts, Amherst). Astrophys. J. 198: No. 3, 661-670 (15 June 1975).

An investigation of the manner in which individual pulsar pulses combine to form a stable integrated profile is presented. The stabilization time is found to be closely related to pulsar type, with sources that exhibit drifting subpulses stabilizing most rapidly and the multicomponent sources requiring the largest number of pulses to establish a constant profile shape. The mode-changing phenomenon is investigated in detail for PSR 0329+54 over the frequency range 150–1400 MHz. Evidence for mode changes with a short memory time scale is presented for other multicomponent sources. Secular changes in integrated profile shape over periods of days to years were searched for but not found. (auth)

**26397** ACCRETION ONTO NEUTRON STARS UNDER ADIABATIC SHOCK CONDITIONS. Shapiro, S.L.; Salpeter, E.E. (Center for Radiophysics and Space Research, Cornell University). Astrophys. J. 198: No. 3, 671-682 (15 June 1975).

The accretion of gas onto a neutron star is examined for the case in which a strong, adiabatic shock front forms above the stellar surface to decelerate the incident plasma stream. Steady-state, spherically symmetric flow is considered, all magnetic fields are ignored, and rapid thermalization by plasma instabilities in the shock front is assumed. The dynamical and thermal structure of the emission zone between the surface and the shock front is determined, and the emergent radiation spectrum is calculated. In many cases an appreciable fraction (about one-quarter) of the total energy is emitted in the form of γ-ray photons between 1 and 10 MeV. The possible relevance of the model calculations to observations of galactic X-ray sources and γ-ray bursts is discussed. (auth)

**26398** COMPOSITION OF THE NEUTRON STAR SURFACE IN PULSAR MODELS. Michel, F.C. (Space Physics and Astronomy Department, Rice University). Astrophys. J. 198: No. 3, 683-685 (15 June 1975).

We examine the question of whether ions are available from the neutron star surface to provide the relativistic stellar winds from pulsars. Although Ruderman and Sutherland suggest that ions are *not* available, we are unable to find firm support for that conclusion. The rate at which the ions would be lost is compatible with the total number of ions (helium, we assume) estimated by Rosen and Cameron to be available and is compatible with the observed distribution of pulsar periods and ages. Consequently it would appear that ion availability from the surfaces of pulsars continues to be a plausible assumption, albeit certainly not an obligatory one. (auth)

**26399** A MULTIPLE PULSAR MODEL FOR QUASI-STELLAR OBJECTS AND ACTIVE GALACTIC NUCLEI. Arons, J. (Department of Astronomy, University of California, Berkeley); Kulsrud, R.M.; Ostriker, J.P. Astrophys. J. 198: No. 3, 687-707 (15 June 1975).

We assume that there have existed small ($\sim 10^0$ pc) central regions in galaxies where the rate of pulsar-forming supernova events is high ($10^0$–$10^2$ yr$^{-1}$). The supernova remnants in these regions largely overlap and constitute ideal environments for the production of and radiation from high-energy particles. Certain aspects of active galactic nuclei—luminosity (thermal and nonthermal fractions, fluctuations, cosmical dispersion), geometry (size, structure, apparent expansion rates), evolution (with redshift) —can be treated naturally with any such supernova remnant model. We calculate in the context of the specific magnetic dipole model of pulsars, expected distributions of electromagnetic fields, particle energies, and emitted radiation, and find that, within the accuracy of the calculations, there is rough agreement between computed quantities and observed properties of active galactic nuclei and QSOs. Filaments of thermal gas created during the supernova explosions will be both contained and accelerated by the pressure of the nonthermal gas. Assuming an element size of $10^{30}$ g, we find that emission and absorption lines will be successively produced (in rough agreement with observations) by gas elements as they are accelerated out of the nucleus and reach final velocities of approximately $10^4$ km s$^{-1}$. Large excursions in total luminosity will occur when strong new pulsars are formed. The temporal behavior (rapid rise, slower decay) and polarization characteristics (maximum polarization at maximum light) of these fluctuations are again consonant with present, very limited, observational material. Because the new pulsar's field triggers the release of the stored particles' energy, large outbursts can contain energy exceeding that of an individual pulsar. (auth)

**26400** STATISTICAL ACCELERATION OF RELATIVISTIC PARTICLES IN AN ASSEMBLY OF SPHERICAL ELECTROMAGNETIC WAVES. Kulsrud, R.M. (Plasma Physics Laboratory, Princeton University); Arons, J. Astrophys. J. 198: No. 3, 709-715 (15 June 1975).

It is shown that if a charged particle moves among a large number of antennae, each of which radiates an electromagnetic wave, the energy and momentum of the particle is increased in a stochastic manner. This acceleration is a resonant process: at various points on its orbit, the particle encounters regions in which the phase of the beats between a pair of waves encounters the frame in which the particle is, on average, at rest. The energy and momentum of a particle change in a secular manner at points, and this phenomenon, when summed over all resonances, leads to a stochastic acceleration if the antennae are randomly located. This process may be significant in models of quasi-stellar objects and active galactic nuclei which rely upon strong electromagnetic waves as the basic energy input. (auth)

**26401** PHASE-CONTRAST DETECTION OF TELESCOPE SEEING ERRORS AND THEIR CORRECTION. Dicke, R.H. (Joseph Henry Laboratories, Physics Department, Princeton University). Astrophys. J. 198: No. 3, 605-615 (15 June 1975).

The technique of phase-contrast microscopy applied to a telescope permits the detection and correction of phase errors in real time. These corrections can be made separately for two or more levels of the atmosphere. It may be possible to correct the seeing errors in a circular patch up to 2′ in diameter about a reference star $m_v \sim 11$ or brighter. (auth)

**26402** THE INTERSTELLAR LINES OF THE FEIGE STARS. Cohen, J.G.; Meloy, D.A. (Kitt Peak National Observatory, Tucson, Arizona). Astrophys. J. 198: No. 3, 545-549 (15 June 1975).

New measurements of the equivalent widths and radial velocities of the interstellar lines of Ca II and Na I in the spectra of Feige stars are presented. The upper limits to the Na I interstellar line imply that the gas in the halo has a much larger value of the ratio of the column density of Ca II to that of Na I than does the plane, and that this

ratio is larger than the intermediate value obtained previously from a group of brighter halo stars. From this we deduce that there is gas up to at least 1 kpc above the plane, and that this gas has much more Ca II relative to Na I than does the plane. The interstellar equivalent width corresponding to looking out of the Galaxy from the plane at $b^{II} = 90°$ is about 300 mÅ for the stronger of the Ca II lines. The velocity measurements imply that this gas is moving slowly toward the plane in a time scale such that replenishment of the halo gas is necessary. (auth)

**26403** HELIUM λ10830 IN ALPHA VIRGINIS A AND B. Meisel, D.D. (Department of Physics and Astronomy, State University of New York College at Genesco); Berg, R.A. Astrophys. J. 198: No. 3, 551-553 (15 June 1975).

Line profiles and velocities of He I λ10830 obtained at maximum velocity separation of the spectroscopic binary Spica (α Vir) are presented. We derive a mass ratio, $M_A/M_B$, of 1.4 and an equatorial velocity of 88 km $s^{-1}$ for α Vir A. A meaningful discussion of observed equivalent widths of the He I λ10830 line awaits a more certain determination of the spectral classification of α Vir B. (auth)

**26404** HEAVY ELEMENTS IN THE PECULIAR A STAR HD 25354. Pyper, D.M. (University of Wisconsin-Parkside); Hartoog, M.R. Astrophys. J. 198: No. 3, 555-559 (15 June 1975).

The spectrum of the Sr-Cr-Eu Ap star HD 25354 shows strong lines of Eu II, Dy II, Ce II, Nd II, and Sm II. Lines of Hg II and PT II are probably present, and U II is possibly present but very weak. Our results disagree with an earlier line identification of HD 25354 by Jaschek and Brandi in that we find no Th, Am, or Cm lines, and in that Ho lines are not unusually strong on our spectrograms. The apparent overabundances of Hg and Pt in HD 25354 as well as in several other Ap stars of the Cr-Eu type may imply that these stars represent a a transition between two groups: Ap stars having abundance anomalies in Si, Fe-peak elements, and the rare earth elements; and the Hg-Mn Ap stars. (auth)

**26405** ON THE EFFECTIVE TEMPERATURE OF ALPHA HERCULIS A. Knapp, S.L.; Currie, D.G.; Liewer, K.M. (Department of Physics and Astronomy, University of Maryland, College Park). Astrophys. J. 198: No. 3, 561-562 (15 June 1975).

Measurements of α Her A with the amplitude interferometer yield a uniform disk angular diameter of $0''.058 \pm 0''.009$. The fundamental effective temperature, 2450 K, obtained from this measurement is in good accord with those of luminous stars of neighboring spectral types, and differs markedly from previous determinations. (auth)

**26406** ON THE POSSIBILITY OF MAGNETIC STARSPOTS ON THE PRIMARY COMPONENTS OF W URSAE MAJORIS TYPE BINARIES. Mullan, D.J. (Bartol Research Foundation of the Franklin Institute). Astrophys. J. 198: No. 3, 563-573 (15 June 1975).

We examine the hypothesis that magnetic starspots occur in W UMa stars. Crude estimates of toroidal field strength in these rapidly-rotating stars suggest that the fields may be large enough (2–10 kilogauss) to permit spots to form. The probability of spot formation is larger on the primary component than on the secondary, especially in the Rucinski's W type systems. It is shown that the existence of starspots on the *primary* component in W UMa systems can account for the apparent temperature excess of the secondary relative to the primary in W type systems, and for the much smaller variations in the light curve exhibited by Rucinski's A type systems. We predict upper limits on the amplitude of the distortions which can occur in the light curve of these systems due to starspot activity. The presence of starspots leads to flare activity, but flares with amplitudes as large as $\Delta m_v = 1$ mag are expected to occur very rarely, only once every few years in W UMa. Flares of amplitude 0.01 mag, may, however, occur sufficiently frequently to explain short-term deviations from mean light curves occurring within a single night's observations. Cycles of starspot activity appear to have periods of 5–10 years in two of these systems. Tidal effects may be important in determining preferred starspot longitudes. (auth)

**26407** THE *COPERNICUS* OBSERVATIONS: INTERSTELLAR OR CIRCUMSTELLAR MATERIAL?. Steigman, G. (Yale University Observatory); Strittmatter, P.A.; Williams, R.E. Astrophys. J. 198: No. 3, 575-582 (15 June 1975).

It is suggested that the sharp absorption lines observed in the ultraviolet spectra of early-type stars by the *Copernicus* satellite may be entirely accounted for by the circumstellar material in the H II regions and associated transition zones around the observed stars. If this interpretation is correct, the *Copernicus* results yield little information on the state of any interstellar (as opposed to circumstellar) gas, and in particular shed little light on the degree of element depletion in interstellar space. (auth)

**26408** RADIATION PRESSURE ON GRAINS AS A MECHANISM FOR MASS LOSS IN RED GIANTS. Kwok, S. (School of Physics and Astronomy, University of Minnesota, Minneapolis). Astrophys. J. 198: No. 3, 583-591 (15 June 1975).

A quantitative model is constructed for the process of radiation pressure on dust to explain the mass loss observed in cool giants. Results are given for six sample stars, demonstrating the effects of stellar luminosity, mass and effective temperature on the mass loss rate. The envelope expansion velocity and average grain size related to the fraction of grain material condensed and the gas density is found to be the key factor in determining the feasibility of mass ejection under this mechanism. (auth)

**26409** ANALYTIC STELLAR MODELS IN GENERAL RELATIVITY. Adams, R.C. (Physics Department, University of Pennsylvania); Cohen, J.M. Astrophys. J. 198: No. 2, 507-512 (1 June 1975).

In this paper we describe a method for deriving analytic stellar models in general relativity. The models are exact solutions to Einstein's equations. By inverting the usual procedure in astrophysics, we reduce Einstein's static field equations to one first-order linear differential equation. Such an equation can always be reduced to quadratures. Two new exact solutions are presented and the rotational properties explored. (auth)

**26410** ON THE PASSAGE OF RADIATION THROUGH INHOMOGENEOUS, MOVING MEDIA. XII. POLARIZED WAVES IN A PLANE, SHEARED MEDIUM. Lee, M.A.; Lerche, I. (Enrico Fermi Institute, University of Chicago). Astrophys. J. 198: No. 2, 477-484 (1 June 1975).

Using the complete set of Maxwell equations, we follow the ray paths and Stokes parameters of a polarized wave which passes through a slab of differentially shearing material of variable refractive index. We relate the polarization state of the signal leaving the top of the slab to the polarization state of the initial wave. In general the two are not the same. We have done these calculations to illustrate the point that the polarization properties of observed pulsar signals may be very different from those of the emitted signals due to propagation effects in the differentially shearing magnetospheres that most pulsars are believed to possess. And while we recognize that the precise amount of polarization variation is model dependent, out calculations show that even for simple situations a noticeable polarization variation occurs. Accordingly the calculations reported here are an educative device: they show that it is, perhaps, unwise to assume that the observed polarization properties of pulsar signals are the same as the emitted signals. (auth)

**26411** THE ULTRAVIOLET SPECTRUM OF BETA LYRAE. Hack, M. (Osservatorio Astronomico, Trieste); Hutchings, J.B.; Kondo, Y.; McCluskey, G.E.; Plavec, M.; Polidan, R.S. Astrophys. J. 198: No. 2, 453-465 (1 June 1975).

Details are presented of low-resolution (0.2–0.4 Å) scans of the spectrum of β Lyrae in the region 1000–3000 Å, obtained from the *Copernicus* OAO. The continuous spectrum appears to correspond to type B5 or later while the line spectrum is largely dominated by very strong emission of lines characteristic of earlier spectral types. Small velocity variations, similar to those of the shell lines in the visible spectrum, are seen. Consideration of the intensity variations and profiles of the lines suggests that the ultraviolet emission lines originate in a large rotating, expanding volume, probably centered on the secondary star. No features can be identified with the secondary star itself. A discussion of models for the system is given, and it is considered that present evidence suggests that the second object is a mass-accreting black hole. (auth)

**26412** THE EVOLUTION OF SUPERNOVA REMNANTS. III. THERMAL WAVES. Chevalier, R.A. (Kitt Peak National Observatory). Astrophys. J. 198: No. 2, 355-359 (1 June 1975).

The effect of heat conduction on the evolution of supernova remnants is investigated. A thermal wave, or electron conduction front, can travel more rapidly than a shock wave during the first thousand years of the remnant's evolution. A self-similar solution describing this phase has been found by Barenblatt. Numerical computations verify the solution and give the evolution past the thermal wave phase. While shell formation is not impeded, the interior density and temperature profiles are smoothed by the action of conduction. (auth)

**26413** A SEARCH FOR $H^-$ IN THE SHELL SURROUNDING χOPHIUCHI. Snow, T.P. Jr. (Princeton University Observatory). Astrophys. J. 198: No. 2, 361-367 (1 June 1975).

We have explored some of the consequences of a recent suggestion that the infrared excesses in a specific class of Be stars, called extreme Be stars, are produced by $H^-$ free-bound emission. The star χ Oph is shown to have an infrared flux distribution typical of extreme Be stars, and we have estimated that the observed infrared excess that the column density of $H^-$ in the shell surrounding χ Oph should be on the order of a few times $10^{15}$ $cm^{-2}$. We have used ultraviolet spectrophotometric data obtained with the Princeton telescope-spectrometer aboard the satellite *Copernicus* to search for a predicted autoionizing absorption feature due to $H^-$ at 1129.54 Å, and we place an upper limit on the column density of $H^-$ of $2 \times 10^{14}$ $cm^{-2}$. The discrepancy between the observed and expected column densities does not necessarily imply that the adopted interpretation of the infrared excesses in extreme Be stars is incorrect, although this is a possibility. Other explanations may be that the line of sight through the shell surrounding χ Oph does not intersect the relatively cool, dense regions where the infrared excess originates, or that the theoretical calculations

describing the predicted $H^-$ absorption line in the ultraviolet are incorrect. (auth)

**26414** THE CIRCUMSTELLAR SHELL OF ALPHA ORIONIS FROM A STUDY OF THE Fe II EMISSION LINES. Boesgaard, A.M. (Institute for Astronomy, University of Hawaii); Magnan, C. Astrophys. J. 198: No. 2, 369-378 (1 June 1975).

Nine spectrograms exposed for the 3100–3300 Å region $\alpha$ Orionis at 3.4 and 6.7 Å $mm^{-1}$ have been obtained to study the Fe II emission lines. Information on the radial velocities, line widths, intensities, and shapes of the 17 Fe II emission lines from multiplets 1, 6, and 7 comprise the basic data. The Fe II lines appear to follow the motions of the photosphere but are redshifted by an average of 5 km $s^{-1}$. The line widths vary from about 20 to about 80 km $s^{-1}$ from the weakest (relative intensity $=1$) to the strongest line (relative intensity $=5.5$). The stronger emission lines show self-reversed absorption centers. All the lines are asymmetric in that the shortward side is more intense. A model of a spherical envelope moving with a uniform velocity, which gives an effective velocity gradient of geometrical origin, has been derived to explain the observed features. It is found that the Fe II lines arise in regions of infalling material with a radius of $\sim 2.5\ R_*$ and a Doppler broadening of 14 km $s^{-1}$. This model accounts fairly well for the observed redshifts, asymmetries, widths, intensities, and shapes of most of the lines. The velocity field of the model appears to be too crude to explain all the phenomena, but the random motions which give rise to the broad lines and are intimately associated with the mean motion of the infalling material. This can perhaps be explained by motions of large-scale bubbles or convective cells. (auth)

**26415** GAS DYNAMICS OF SEMIDETACHED BINARIES. Lubow, S.H.; Shu, F.H. (University of California, Berkeley). Astrophys. J. 198: No. 2, 383-405 (1 June 1975).

We analyze the gas dynamics of semidetached binary systems within the context of the Roche model. With the adoption of the assumptions that the contact component rotates synchronously and that the flow occurs isothermally with the thermal speed being a small fraction $\epsilon$ of the relative orbital speed, $\Omega d$, of the two stars, we show that the steady flow can be formulated in terms of a problem with multiple length scales. Using this concept, we demonstrate the following by semianalytical methods. (1) The escape of material from the surface of the contact component is accomplished by a highly nonisotropic stellar wind which reaches sonic velocities in a neighborhood of the inner Lagrangian point, L1, of size $\epsilon$ in comparison with the orbit separation $d$. (2) This wind throttles into a narrow stram of material which makes a prescribed angle with respect to the line joining the stellar centers ranging from 19°.5 to 28°.4 for the full range of possible stellar mass ratios. (3) The width of the stream scales $\epsilon d$ while its density scales with $\epsilon^{-2}\dot{M}/\Omega d^2$, where $\dot{M}$ is the mass transfer rate.(4) The stream width remains nearly constant over the part of the stream which is nearly straight, and narrows somewhat as the stream curves toward the detached component. (5) If the detached component is smaller than a certain specified size, the stream results in the formation of a disk of material of prescribed size orbiting the detached component in a direct sense. A subsidiary issue examined briefly in this paper is the flow mechanism responsible for moving material to the equator of the contact component, and from there to the L1 region where it is lost by the directed stellar wind. The mechanism of mass loss is not straightforward because the gas cannot proceed directly from high pressures to low since the strong Coriolis forces produce deflections similar to those associated with the geostrophic wind in the Earth's atmosphere. Comparisons of our work are made with previous theoretical studies, and some applications are indicated for a variety of observed astronomical systems. (auth)

**26416** STELLAR EVOLUTION AT HIGH MASS WITH SEMICONVECTIVE MIXING ACCORDING TO THE LEDOUX CRITERION. Stothers, R.; Chin, C. (Institute for Space Studies, Goddard Space Flight Center, NASA). Astrophys. J. 198: No. 2, 407-417 (1 June 1975).

Semiconvective mixing has been included in new evolutionary sequences of models for stars of 10, 15, and 30 $M_\odot$, with four different initial chemical compositions. The models have been constructed with the help of the Ledoux criterion both for the definition of convective instability and for the state of convective neutrality that is assumed to be attained in regions with a gradient of mean molecular weight. Allowance for convective overshooting has also been made. Semiconvection is found to be almost nonexistent at 10 $M_\odot$ and of minor importance at 15 $M_\odot$. But at 30 $M_\odot$ semiconvection covers most of the intermediate zone and develops into full convection if the initial hydrogen and metal abundances are both high. If the initial metals abundance is low, a "blue loop" phase follows the early red-supergiant phase during core helium burning, just as it does for all initial chemical compositions at 10 and 15 $M_\odot$, when the new $3\alpha$ reaction rate is adopted. If the initial hydrogen abundance is low, the star goes directly into a "blue hook" phase without first becoming a red supergiant. The critical importance of the depths of the semiconvective zone and of the outer convective envelope in promoting a blue loop and in determing the maximum effective temperature attained on the loop is demonstrated. The thermally stable stages of the blue-loop phase cover an amount of log $T_e$ and a fraction of the helium-burning lifetime that are almost independent of stellar mass, although the maximum effective temperature attained on the loop is hotter at higher stellar masses. The effective temperature ranges agree roughly with observational data, but the predicted blue-to-red ratios for masses higher than about 15 $M_\odot$ do not. (auth)

**26417** ON THE TREATMENT OF CONVECTION AS A NONRADIAL STELLAR PULSATION. Deupree, R.G. (David Dunlap Observatory). Astrophys. J. 198: No. 2, 419-423 (1 June 1975).

The problem of nonlinear, nonadiabatic, nonradial stellar pulsation has been examined by a computational approach. The difficulties of such an approach are discussed in detail, and the limitations of the present method of solution are listed. A test calculation with a particular RR Lyrae model pulsating in the fundamental mode reveals that convection is present in the second helium ionization zone only when the luminosity amplitude becomes large and even then is present during only part of the pulsation cycle. The convective motion, measured by the nonradial velocity component, grow during rising luminosity, reaches a maximum after maximum luminosity, and decays during the other parts of the cycle. The possible consequences of this phenomenon are briefly discussed. (auth)

**26418** DOUBLE-SHELL-SOURCE EVOLUTION AT 2 $M_\odot$. Gingold, R.A. (Mount Stromlo and Siding Spring Observatory, Research School of Physical Sciences, Australian National University). Astrophys. J. 198: No. 2, 425-429 (1 June 1975).

A 2 $M_\odot$ Population I star was evolved from the core helium-burning phase to the ninth strong helium shell flash. The intershell convective zone did not reach the hydrogen-containing layers, and thus no neutron production by the $^{13}C(\alpha, n)^{16}O$ reaction was possible. Mixing is unlikely to occur during later relaxation cycles. The temperatures are too low for neutron production the $^{22}Ne(\alpha,n)^{25}Mg$ reaction in the intershell convective zone. The convective envelope fails by a wide margin to reach regions containing processed material. The results indicate that there are difficulties with the suggestion that helium shell flashes explain the existence of low-mass stars having unusual surface abundances. (auth)

**26419** SPECTROPHOTOMETRIC STUDIES OF GASEOUS NEBULAE. XXIV. THE AMORPHOUS LOW-EXCITATION PLANETARY IC 4593. Czyzak, S.J.; Buerger, E.G. (Perkins Observatory, The Ohio State and Ohio Wesleyan Universities); Aller, L.H. Astrophys. J. 198: No. 2, 431-433 (1 June 1975).

Photoelectrically calibrated line intensity measurements are presented for IC 4593, whose spectrum has also been observed photographically (Mount Wilson) and with the Wampler-Robinson super-scanner device (Lick). This relatively homogeneous nebula shows little evidence of clumpiness as illustrated by the characteristic radiations of [O I], [S II], and [N II]. An estimate of the chemical composition from ionic concentrations, based on extrapolation procedures of the type suggested by Seaton, is compared with results of a model calculation by Buerger. For most elements the agreement is reasonably good, but there is an order of magnitude discordance for [N II]. It is suggested that great caution must be used with extrapolation of [N II] lines to estimate nitrogen abundance in gaseous nebulae. It is concluded that nitrogen abundances estimated from extrapolation of [N II] line data can sometimes be in error. (auth)

**26420** ULTRASHORT-PERIOD BINARIES. III. THE ACCRETION OF HYDROGEN-RICH MATTER ONTO A WHITE DWARF OF ONE SOLAR MASS. Taam, R.E.; Faulkner, J. (Lick Observatory, Board of Studies in Astronomy and Astrophysics, University of California, Santa Cruz). Astrophys. J. 198: No. 2, 435-438 (1 June 1975).

We have followed the thermonuclear runaways which develop when white dwarfs of 1 $M_\odot$ accrete hydrogenrich material at $10^{-10}$ $M_\odot$ per annum, a canonical rate of accretion which would accompany the emission of gravitational radiation in ultrashort-period binaries. The existence of such thermonuclear effects is a necessary but not sufficient criterion for gravitational radiation to play an important role in the evolution of these binaries. (auth)

**26421** AXISYMMETRIC QUASISTATIONARY STABILITY OF A CHARGED KERR BLACK HOLE. Wang, M.Y. (Center for Theoretical Studies, University of Miami, Coral Gables, Florida 33124). Phys. Rev. D 11: No. 12, 3392-3394 (15 June 1975).

The stability of a charged Kerr black hole under axisymmetric quasistationary perturbation is proved. (auth)

**26422** SPECTRUM AND POLARIZATION OF X—RAYS FROM ACCRETION DISKS AROUND BLACK HOLES. Lightman, A.P.; Shapiro, S.L. (Center for Radiophysics and Space Research, Cornell University). Astrophys. J. Lett. 198: No. 2, L73-L75 (1 June 1975).

The emergent radiation spectrum and polarization of X-rays from accretion disks around black holes are calculated. A linear polarization of a few percent should be observed above $\sim 1$ keV from compact binary X-ray sources containing black holes if a disk exists. The

observed, hard X-ray component of the Cyg X-1 spectrum cannot be explained by the standard, instability-free accretion disk model. (auth)

**26423** HYPOTHESIS FOR THE TYPE I SUPERNOVA LIGHT CURVE. Leventhal, M.; McCall, S. L. (Bell Telephone Labs., Murray Hill, NJ). Nature (London); 255: No. 5511, 690-692 (26 Jan 1975).

Changes in the observed luminosity of type I supernova events are described and a model involving $^{56}$Ni in white dwarfs is suggested to explain these changes. Because of its exponential nature it has been suggested that the light curve is associated with decay in the remnant of explosively produced radioactive species, such as $^{254}$Cf and $^{56}$Ni. Such hypotheses have, however, fallen into disfavor. Attention has been refocused on such a possibility by observations made of the supernova in IC4182 by Van Hise. This author, from half life measurements, pointed out an interesting relationship to the decay sequence of $^{56}$Ni, and also that the light curve looks very much like the $^{56}$Ni-$^{56}$Fe decay curve, but with an enhanced rate. Furthermore nucleosynthesis calculations indicate that the most abundant radioactive element produced by type I supernovae may be $^{56}$Ni. It is proposed that a type I supernova event leads to the formation of a fully convective white dwarf star containing ~0.2 $M_\odot$ of $^{56}$Ni with a ~1 $M_\odot$ remnant expanding away with a velocity of ~20,000 km/sec and containing a smaller amount of $^{56}$Ni. This hypothesis leads in a simple way to an understanding of the data. (UK)

**26424** ON THE HISTORY OF CEN X-3. Meyer-Hofmeister, E. (Max-Planck-Institut fuer Physik und Astrophysik, Muenchen (F. R. Germany)). Astron. Astrophys.; 36: No. 2, 261-265(Nov 1974).

3 figs.; 2 tabs.; 15 refs.

It is assumed that the x-ray binary Cen X-3 has evolved from an initial system of which one component was a massive star through a phase of mass transfer and a following supernova explosion. What possible initial systems lead to an evolved system of which the masses are in agreement with the mass function of Cen X-3 are investigated. For a complete sample of initial configurations a lower limit of 3 days for the final periods is found. Since the observed period of Cen X-3 is 2.087 days it is concluded that further mass loss has taken place. Maximal and minimal rates of mass loss are derived. (auth)

**26425** MASSIVE BLACK HOLES AS GRAVITATIONAL LENSES. Silvestro, G. (Turin Univ. (Italy). Istituto di Fisica; Consiglio Nazionale delle Ricerche, Turin (Italy). Lab. di Cosmo-Geofisica). Astron. Astrophys.; 36: No. 1, 41-48(Nov 1974).

5 figs.; 3 tabs. 18 refs.

A dense stellar system is considered containing a massive collapsed object. When an orbiting star goes behind the black hole, gravitational deflection of light in the hole's gravitational field may considerably increase its apparent luminosity, giving rise to a short light pulse. Such a "gravitational focussing" effect is analyzed for a Newtonian spherically symmetric stellar system containing at its center a Schwarzschild black hole; counting rate, pulse length, and amplitude distributions are evaluated assuming a steady-state distribution of stars in a characteristic region near the black hole. The effect, which depends mainly on the fraction of collapsed mass in the system, appears to provide a possible observational test for massive black holes. Its detection should be feasible with present techniques for a compact globular cluster containing a collapsed object of some thousandths the total mass. (auth)

**26426** COMPACT X-RAY SOURCES. Tananbaum, H. (Center for Astrophysics, Cambridge, MA); Tucker, W. H. pp 207-266 of X-ray Astronomy. Giacconi, R. (ed.). Dordrecht, Netherlands; Reidel (1974).

The evolution of close binaries into X-ray stars is discussed. Several cosmic X-ray sources are examined individually. (BJG)

**26427** SUPERNOVA REMNANTS. Gorenstien, P. (Center for Astrophysics, Cambridge, MA); Tucker, W. H. pp 267-297 of X-ray Astronomy. Giacconi, R. (ed.). Dordrecht, Netherlands; Reidel (1974).

Observational features of X-ray emission from supernova remnants are reviewed. Individual supernova remnants are discussed. (BJG)

**26428** ULTRAVIOLET SPECTRA OF $\epsilon$ ORI, B0 IA, AND $\kappa$ ORI, B0.5 IA. Stalio, R.; Selvelli, P. L. (Astronomical Institute, Utrecht). Astron. Astrophys., Suppl. Ser.; 21: No. 2, 241-277 (1975).

The ultraviolet spectra of the supergiant stars $\epsilon$ and $\kappa$ Ori are described. The observations were made by the Copernicus Satellite and cover the spectral ranges 1000-1540 Å and 1620-3200 Å. According to the classification in the visible, the spectral features of the two stars appear very similar. Table 4 gives the identifications and the equivalent widths. The resonance lines of highly ionized elements are seen to be shifted toward shorter wavelengths and the resonance doublets of N V and Si IV present P Cyg profiles. In the figures are reported the profiles of the most interesting spectral features. (auth)

**26429** NARROW-BAND PHOTOMETRY OF 31 AND 32 CYG. Cester, B.; Pucillo, M. (Astronomical Observatory Trieste, Italy). Astron. Astrophys., Suppl. Ser.; 21: No. 2, 189-192 (Aug 1975).

Photoelectric observations of 31 and 32 Cyg made at Trieste during the international campaigns 1971 and 1972 with three interferential filters are reported. The magnitudes for the components of 31 Cyg are deduced. (auth)

**26430** TWO-COLOR PHOTOMETRY OF THE SHORT PERIOD RR LYRAE STAR DY PEG. Geyer, E. H.; Hoffmann, M. (Univ., Bonn). Astron. Astrophys., Suppl. Ser.; 21: No. 2, 183-188 (Aug 1975).

By photoelectric photometry in B and V with a double beam photometer two resp. four consecutive cycles have been observed of the $RR_s$-star DY Peg. The non-periodic light curve changes suggest overtone pulsation of this c-type variable. (auth)

**26431** PHOTOMETRIC STUDY OF THE $RR_s$-STAR CY AQR. Geyer, E. H.; Hoffmann, M. (Univ., Bonn). Astron. Astrophys., Suppl. Ser.; 21: No. 2, 178-182(Aug 1975).

Fairly high-speed photoelectric photometry in B and V has been carried out of the ultra-short period RR Lyrae star CY Aqr for five consecutive cycles. The observations cannot be reconciled either by the beat period given by Elst (1972) or by Fitch (1973). The beat phenomenon in this star may therefore be fictitious. (auth)

**26432** UBV PHOTOMETRY OF THE ALGOL SYSTEM RX GEM. Hall, D. S.; Walter, K. (Univ., Tubingen, Germany). Astron. Astrophys., Suppl. Ser.; 20: No. 227-235(May 1975).

We present UBV observations of this eclipsing binary obtained between 1967 and 1971 at three different observatories: 325 in V, 316 in B, 182 in U. Normal points of the individual observations are also presented: 72 in V, 74 in B, 46 in U. (auth)

**26433** PERIODS AND PERIOD VARIATIONS OF SOME ECLIPSING VARIABLES. Guarnieri, A.; Bonifazi, A.; Battistini, P. (Univ., Bologna). Astron. Astrophys., Suppl. Ser.; 20: No. 2, 119-225(May 1975).

For the eclipsing binaries AR Aur, BF Aur, AH Cep, EK Cep, V1143 Cyg, u Her, AR Lac available data have been collected and discussed with regard to period study. Seventeen new times of minimum are given. For AR Aur, BF Aur, AH Cep, AR Lac period changes are put into evidence. 1672 photoelectric measurements of these systems are listed at the end of the paper. (auth)

**26434** LINE IDENTIFICATION LIST OF 3 HYA. Hensberge, H.; de Loore, C. (Vrije Univ., Brussels). Astron. Astrophys., Suppl. Ser.; 20: No. 2, 183-197(May 1975).

Line identifications, equivalent widths and atomic data used in another study of 3 Hya are given. (auth)

**26435** SOUTHERN OPEN STAR CLUSTERS. VI. UBV-H$\beta$ PHOTOMETRY OF 18 CLUSTERS FROM CENTAURUS TO SAGITTARIUS. Moffat, A. F. J.; Vogt, N. (Ruhr-Univ., Bochum, Germany). Astron. Astrophys., Suppl. Ser.; 20: No. 2, 155-182(May 1975).

The photoelectric photometry reveals the reality of 14 clusters of which 2 were previously uncatalogued, 9 have spectral types earlier than B3 and 8 contain 10 supergiants. The distances range out to 2.3 kpc from the sun. One cluster coincides with a Cepheid variable. (auth)

**26436** SOUTHERN OPEN STAR CLUSTERS. V. UBV-H$\beta$ PHOTOMETRY OF 20 CLUSTERS IN CARINA. Moffat, A. F. J.; Vogt, N. (Ruhr-Univ., Bochum, Germany). Astron. Astrophys., Suppl. Ser.; 20: No. 2, 125-153(May 1975).

The photoelectric photometry reveals the reality of 16 clusters of which 4 were previously uncatalogued, 12 have spectral types earlier than B3 and 6 contain 7 supergiants. The distances range out to 5 kpc from the sun. Two clusters coincide with 2 Cepheid variables. (auth)

**26437** SOUTHERN OPEN STAR CLUSTERS. IV. UBV-H$\beta$ PHOTOMETRY OF 26 CLUSTERS FROM MONOCEROS TO VELA. Moffat, A. F. J.; Vogt, N. (Ruhr-Univ., Bochum, Germany). Astron. Astrophys., Suppl. Ser.; 20: No. 2, 85-124(May 1975).

Photoelectric photometry reveals the reality of 21 clusters of which 7 were previously uncatalogued. Eleven have spectral types earlier than B3, and 8 contain 9 supergiants. The distances range out to 6 kpc from the sun. Four clusters coincide with interesting stars: 2 Cepheids, 1 Wolf-Rayet, 1 U Gem type. (auth)

**26438** CAPTURE OF STARS BY ROTATING HOMOGENEOUS SPHERICAL CLUSTERS. Baranov, A. S. (Inst. of Theoretical Astronomy, Leningrad). Celestial Mech.; 11: No. 4, 517-528 (Jun 1975).

Changes of the orbit of a star passing through a homogeneous spherical cluster have been estimated. Before entering the cluster the star is supposed to move in a Keplerian parabolic orbit. When passing through the cluster the star is subject both to the attraction of the smoothed-out distribution of matter in the cluster and to dynamical friction. Due to dynamical friction the energy of the star becomes negative which leads to the elliptic-type motion of the star after leaving the cluster and to capturing the star by the cluster. The formulae for the changes of the star orbit in the cluster are given. Numerical estimation shows that open clusters transform star orbits more noticeably than do globular clusters. (auth)

**26439** EMISSION LINES AND RADIAL VELOCITIES OF THE VV CEPHEI TYPE STAR BD +63°3. Barbier, M. (Observatoires de Marseille). Astron. Astrophys., Suppl. Ser.; 20: No. 3, 305-312(Jun 1975).

Three spectrographic plates at a dispersion of 20 Å $mm^{-1}$ and one spectrographic plate at a dispersion of 12 Å $mm^{-1}$ have been obtained for the VV Cephei type star BD +63°3. We identify 93 emission lines, principally of [FeII] and also of H, OII, [SII], SII, [CrII], FeII [NiII], NiII, CuII. From the emission [FeII] lines a mean temperature of 6300 + 1500° K has been derived. The radial velocity of the emission lines of the various elements differs by 6 km $s^{-1}$ from the velocity determined for the absorption lines of the late type component. An upper limit for the absolute magnitude of BD +63°3 has been determined on the basis of the velocity of the interstellar calcium line: $M_v > -7.9$. (auth)

**26440** NATURE OF THE PUPPIS CLUSTER NGC 2483. Fitzgerald, M. P.; Moffat, A. F. J. (Ruhr-Univ., Bochum, Germany). Astron. Astrophys., Suppl. Ser.; 20: No. 3, 289-304(Jun 1975).

The photographic UBV photometry ($V \leq 15.7$) and the spectral types presented here for NGC 2483 and a nearby field do not support the suggestion of Lindoff and Johansson (1968) that NGC 2483 is a unified cluster with pre-main sequence evolution. At best the slight excess of stars over the field consists of: (1) ~17 probable G-K giants at ~2 kpc, $E_y \sim 0.4$; (2) 6 B3-5 stars at ≃4 kpc, $E_y \simeq 0.5$; (3) 8 b1-3 stars at ≃0.9 kpc; (4) ~15 fainter stars probably belonging to (2) and (3); (5) 2 OB stars at ≃4.5 kpc, $E_y \simeq 0.6$. In an appendix photoelectric UBV photometry to V = 15.7 for 103 stars in a 4° × 4° field centred on NGC 2483 is presented. Objective prism classification for 95 of these is also given. (auth)

**26441** STELLAR GROUPS BA 12, BA 13, BA 14, AND BA 15. Hassan, S. M. (Univ. of Basel). Astron. Astrophys., Suppl. Ser.; 20: No. 3, 255-267(Jun 1975).

A three color photometric study of four stellar groups (Ba 12, Ba 13, Ba 14 and Ba 15) in the UBV system is represented. The color magnitude diagrams of the four groups indicate the existence of a main sequence and of a giant branch in contrast to groups of stars produced by random fluctuations in a star field. The distances, the color excesses, and other parameters are determined for the four groups. (auth)

**26442** SPECTRAL SURVEY OF THE SOUTHERN MILKY WAY II. O-B5 Stars l = 237° to 281°. Nordstrom, B. (Stockholm Observatory, Saltsjobaden). Astron. Astrophys., Suppl. Ser.; 21: No. 2, 193-239(Aug 1975).

A catalogue, part II of the Stockholm Observatory Southern Milky Way Survey, is presented, based on objective prism plates with a dispersion of 240 Å $mm^{-1}$ at $H_\gamma$ as well as blue and visual direct plates. The catalogue contains spectral types, blue magnitudes, positions and finding charts for 562 O-B5 stars and emission-line objects to a limiting magnitude of about 12.5m. The region covered is a 3° wide belt along the galactic equator, l = 237°-281°. (auth)

**26443** VISTAS IN ASTRONOMY. Volume 16. Beer, A. (ed.). New York; Pergamon Press (1974). 344p. $48.50.

A series of papers dealing with theoretical and experimental work in solar, planetary, and stellar astronomy, including stellar spectroscopy, photometry, and radio astronomy. The topics covered include: solar flares, the historical development of solar theories, the intrinsic light variation and the reflection effect in very close eclipsing binary systems with distorted components, spectroscopic binaries, early-type stars with abnormal spectra, photometric classification of the O-B stars, the nova DQ Herculis, emission nebulas at radio wavelengths, and the planetary nebulas as radio sources. (IAA)

**26444** GAS DISTRIBUTION IN TYPE I AND II SUPERNOVA ENVELOPES NEAR MAXIMUM LIGHT. Chugai, N.N. (Astronomical Council, Academy of Sciences of the USSR). Sov. Astron.—AJ 19: No. 1, 119-120 (July 1975).

There is a substantial difference in the time dependence of the Doppler shifts of absorption lines in the spectra of type I and II supernovae. The distinction is attributed to a differing density distribution in type I and II supernova envelopes. (auth)

**26445** KINEMATICS OF STARS GROUPED BY GALACTIC ORBITAL ELEMENTS. Karimova, D.K.; Pavlovskaya, E.D. (Shternberg Astronomical Institute, Moscow). Sov. Astron.—AJ 19: No. 1, 123-124 (July 1975).

The velocity-ellipsoid parameters are independent of spectral type for stars grouped by e and i. The values of $V_\odot$, $\sigma_1$, $\sigma_2$, $\sigma_3$, and $\sigma_1/\sigma_3$ increase with e and i. The percentage of nearly circular orbits within the galactic plane is greater for emission-line stars. (auth)

**26446** KINEMATIC PARAMETERS OF THE HYADES–PRAESEPE STAR STREAM. Nezhinskii, E.M.; Osipkov, L.P. (Leningrad University). Sov. Astron.—AJ 19: No. 1, 125-126 (July 1975).

The kinematic parameters of the Hyades–Praesepe stream are determined and compared with the values derived by Ogorodnikov and Latyshev. (auth)

**26447** POSSIBLE MECHANISM OF GAMMA-RAY FLARE FORMATION ON UV CETI TYPE STARS. Karitskaya, E.A. (P.K. Shternberg State Astronomical Institute). Sov. Astron.—AJ 19: No. 1, 112-114 (July 1975).

It is suggested that the γ-ray flares recorded on the "Vela" satellites are associated with flare activity of UV Ceti type stars. It is also suggested that these flares are similar to solar chromospheric flares by their physical nature but differ from them by higher energy release, which also causes the great difference. A possible model of γ-ray flare formation is proposed; the intense convection in red dwarfs generates strong magnetic fields ~ $6 \cdot 10^4$ G. During annihilation, the energy of this field changes into the energy of a large number of more energetic paticles than in the case of solar flares. These particles penetrate deeper into the dense atmospheric layers and heat the plasma to a temperature of $10^9$ °K. The high density provides rapid thermal radiation loss of the energy obtained (during 0.015 sec), which predominates over other mechanisms of energy transfer. It is shown that several tenths of the energy of fast particles incident on the photosphere is radiated away in the γ-ray range, and the emission in the optical range can be less by four orders of magnitude. The parameters of the emission region and of the region of magnetic field annihilation are estimated. One can explain the characteristic times, power, and also the observed spectrum of γ-ray flares in the framework of the given model. (auth)

**26448** STATISTICS OF γ-ray BURSTS. Usov, V.V.; Chibisov, G.V. (P. N. Lebedev Physics Insitute, Academy of Sciences of the USSR). Sov. Astron.—AJ 19: No. 1, 115-116 (July 1975).

The dependence of the number of recorded γ-ray bursts on the sensitivity of the detectors is discussed. It is shown that observations of γ bursts with already existing detectors having sensitivity of the order of $10^{-6}$–$10^{-7}$ erg/cm². sec taken over a period of the order of one year may elucidate the nature of the sources of γ bursts. (auth)

**26449** SUPERNOVA REMNANTS AS OPTICAL NEBULAE. Lozinskaya, T.A. (Shternberg Astronomical Institute, Moscow). Sov. Astron.—AJ 19: No. 1, 21-28 (July 1975).

Detailed interferometry of the very faint optical nebulae identified with the supernova remnants VRO 42.05.01 and HB 9 was carried out in 1970–1973. Two possible values for the expansion velocity of VRO 42.05.01 are obtained: 13±5 or 35±km/sec. Its filaments are 0.3—0.6 pc thick, according to monochromatic Hα photographs; the half-width of the Hα line emitted by individual filaments corresponds to 60—70 km/sec. For HB 9, the diffuse filamentary system is expanding at 70±10 km/sec; the Hα half-width reaches ≃60 km/sec. The age and kinetic energy of the envelope ejected in the outburst are $3 \cdot 10^5$ yr and $10^{50}$ erg for VRO 42.05.01, and $10^5$ yr and $10^{50}$ erg for HB 9. In a second section of the paper a survey is given of nebular supernova remnants having a reliably measured expansion velocity. These nebulae form an evolutionary sequence of kindred objects expanding into regions of the interstellar medium of different densities. The type of supernovae responsible for the remnants is discussed. (auth)

**26450** SPECTROPHOTOMETRY OF NOVA DELPHINI 1967. Babaev, M.B. (Shemakha Astrophysical Observatory, Academy of Sciences of the Azerbaidzhan SSR). Sov. Astron.—AJ 19: No. 1, 29-33 (July 1975).

The nova that appeared in Delphinus early in July 1967 was observed spectroscopically from October 1967 to November 1969. About 300 spectrograms of the nova were obtained with a 35° objective prism on the 350 mm Shemakha AST-452 meniscus telescope (dispersion 116 Å/mm at $H_\gamma$) and with the 2 m telescope (dispersions: 10, 30, 75, 90 Å/mm.) Multiple absorption and emission components of the spectral lines have been found; the relative shifts and multiplicity of the

components are determined. Variations with time during the development of the nova are established for the equivalent width $W_\lambda$ and halfwidth $\Delta\lambda$ [km/sec] of the H$\beta$–H9 lines as well as the central intensity I relative to the continuum. A negative Balmer discontinuity is observed at $\lambda \simeq 3730$ Å. The amplitude of the discontinuity increases in the late evolutionary phase of the nova spectrum, reaching $2-3^m$. The sharpening of the discontinuity is correlated with the forbidden-line intensities. The discontinuity varies rapidly with time and its position in the spectrum changes; as the radiation excess increases it shifts toward longer wavelengths. (auth)

**26451** SUPERNOVAE IN BINARY SYSTEMS. Khabazin, Y.G. (Lebedev Physics Institute, Academy of Sciences of the USSR). Sov. Astron.–AJ 19: No. 1, 34-37 (July 1975).

Previous calculations for the evolution of close binary systems in which one component experiences an outburst show that the exploding component should be considerably less massive than the other star; at the time of the outburst the second component should be a massive young main-sequence star. A detailed analysis is made of the variations in a binary-system orbit that are induced by an outburst of one component. If the outburst is nearly spherically symmetric, the orbit will be approximately circular afterward. The values for the orbital eccentricity are consistent with those inferred from observations of x-ray sources. A limit is set on the asymmetry of the outburst such that there will be an insignificant departure from the results obtained assuming spherical symmetry. It is known that a system can be disrupted by a spherically symmetric outburst if more than half of its mass is lost. An allowance for capture of part of the envelope by the normal component does not alter this result appreciably. The orbital eccentricity of the Cygnus X-1 system considerably exceeds that of massive close binaries, a circumstance which may indicate that an outburst did occur in the Cyg X-1 system. (auth)

**26452** POSSIBLE ROLE OF PLASMA TURBULENCE IN THE RADIATION FROM ACCRETING GAS. Kaplan, S.A.; Lamb, F.K.; Pines, D.; Pethick, C.J.; Tsytovich, V.N. (Scientific Research Radiophysics Institute, Gor'kii). Sov. Astron.–AJ 19: No. 1, 38-42 (July 1975).

It is shown that the excitation of plasma turbulence during the accretion of gas onto dense objects significantly enhances the electromagnetic radiation (increases the efficiency of the accretion) and accelerates electrons to ultrarelativistic energies. Accretion onto nonmagnetized objects leads to the generation of radiation with a sharp peak in the infrared range, while in the case of accretion with a strong magnetic field the maximum of the spectral density lies in the x-ray range. (auth)

**26453** POLARIZATION IN ZEEMAN-SPLIT ABSORPTION LINES. Sazonov, V.N. (P. N. Lebedev Physics Institute, Academy of Sciences of the USSR). Sov. Astron.–AJ 19: No. 1, 42-46 (July 1975).

A study is made of polarization in an absorption line formed under conditions of local thermodynamic equilibrium in a magnetic field B without allowance for scattering but with allowance for normal and anomalous dispersion and, in particular, Faraday rotation of the plane of linear polarization in a magnetoactive plasma in the atmosphere of a star. In the case of strong Faraday rotation in a homogeneous magnetic field the expressions (17) are obtained for the profiles of the blue ($-\sigma$), central ($\pi$), and ($+\sigma$) components of a normal Zeeman triplet on a spectrogram in circularly polarized light. These expressions differ from the expressions (17'), which are obtained without allowance for dispersion. As an example, the narrow-band spectropolarimetric observations of the line λ 4254 in the spectrum of the star $\beta$ CrB are considered. (auth)

**26454** PHOTOMETRIC ELEMENTS OF THE ECLIPSING BINARY V444 CYGNI, AND THE NATURE OF THE WOLF-RAYET COMPONENT. Cherepashchuk, A.M. (Shternberg Astronomical Institute, Moscow). Sov. Astron.–AJ 19: No. 1, 47-53 (July 1975).

The Wolf–Rayet star in the V444 Cyg system is shown to be a helium star that has left main sequence and reached a terminal evolutionary phase. (auth)

**26455** OBSERVATIONS OF VARIABLE X–RAY SOURCES IN GLOBULAR CLUSTERS. Clark, G.W.; Markert, T.H.; Li, F.K. (Physics Department and Center for Space Research, Massachusetts Institute of Technology). Astrophys. J. Lett. 199: No. 2, L93-L96 (15 July 1975).

Observations with the MIT detectors on the OSO-7 satellite have revealed a previously unreported variable hard X-ray source at midgalactic latitude in the globular cluster NGC 1851. The source, designated MX 0513–40, varied in intensity by a factor $\gtrsim 5$ in 16 days and had a peak 12-day average energy flux of $4.7\times10^{-10}$ ergs cm$^{-2}$ s$^{-1}$ in the energy range 1–10 keV, with $dN/dE \sim E^{-1.4}$. Observations of the X-ray sources 3*U* 2131+11 and 3*U* 1746–37 are also reported which confirm their locations in globular clusters NGC 7078 (M15) and NGC 6441, respectively, and demonstrate that they too are variable. (auth)

**26456** THE RELATIONSHIP BETWEEN HD 87892 AND NGC 3132. Méndez, R.H. (Instituto de Astronomía y Física del Espacia, Buenos Aires). Astrophys. J. 199: No. 2, 411-417 (15 July 1975).

The observations suggest that the central star of NGC 3132 is a double system, the visually brighter component being HD 87892. The nebula is ionized by a very hot object whose characteristics are briefly discussed. The assumption that NGC 3132 lies at the same distance as HD 87892 leads to a very small ionized nebular mass. (auth)

**26457** THE DISTRIBUTION OF STARS IN GALACTIC NUCLEI: LOADED POLYTROPES. Huntley, J.M. (Department of Astronomy, University of Virginia, Charlottesville); Saslaw, W.C. Astrophys. J. 199: No. 2, 328-335 (15 July 1975).

We consider the structure of a galactic nucleus in which a compact supermassive object (e.g., a black hole or spinar) is embedded. The surrounding stars are assumed to satisfy a polytropic or isothermal equation of state. The density distribution of these loaded polytropes has a sharp central spike in which the time scale for stellar collisions can be short. Other properties of loaded polytropes, such as their masses, radii, projected density distribution, relaxation times, and stability, can also differ significantly from those of normal polytropes. (auth)

**26458** THERMODYNAMIC STABILITY OF RELATIVISTIC STELLAR CLUSTERS. Katz, J.; Horwitz, G.; Klapisch, M. (The Racah Institute of Physics, The Hebrew University of Jerusalem, Jerusalem, Israel). Astrophys. J. 199: No. 2, 307-321 (15 July 1975).

Equilibrium configurations of *isothermal* relativistic stellar clusters with truncated isotropic Maxwell-Boltzmann distribution of energies have been studied. An argument is given, showing that the energy cutoff should be equal to the gravitochemical potential as seen from infinity. Solutions of Einstein's equations are obtained for a wide range of values of temperature *and* chemical potential as seen from infinity. Conditions of stability are determined by thermodynamic criteria. It is shown that the (temperature, chemical potential) -plane contains two possible regions of stability in the limits of our calculations. One region is related to the stable configurations found by dynamical means. The second zone is new and is associated with values of the central redshift ranging from 1 to 4. (auth)

**26459** *Skylab* ULTRAVIOLET STELLAR SPECTRA: VARIATION OF INTENSITY AND STRUCTURE OF STRONG LINES WITH TEMPERATURE AND LUMINOSITY. Henize, K.G.; Wray, J.D.; Parsons, S.B.; Benedict, G.F.; Bruhweiler, F.C.; Rybski, P.M. (Department of Astronomy, University of Texas at Austin); O'Callaghan, F.G. Astrophys. J. Lett. 199: No. 2, L119-L121 (15 July 1975).

Objective-prism spectra at ultraviolet wavelengths extending to 1300 Å were photographed during the three *Skylab* missions in a survey covering 9 percent of the sky. Several spectral features, notably resonance lines of C IV and Si IV, show striking variations with stellar temperature and luminosity. Marked P Cygni profiles in C IV and Si IV, indicative of significant outflow of mass, appear in the spectra of all stars with $M_{bol}$ brighter then $-8.4$. (auth)

**26460** OBSERVATIONS OF A BRIGHT, VARIABLE X–RAY SOURCE IN A GLOBULAR CLUSTER. Canizares, C.R.; Neighbours, J.E. (Department of Physics and Center for Space Research, Masschusetts Institute of Technology). Astrophys. J. Lett. 199: No. 2, L97-L99 (15 July 1975).

The source 3*U* 1820–30 in NGC 6624 has been observed with the OSO-7 satellite. It shows variability of up to a factor of 5 in intensity over days and months and of a factor of 2 in ~5–10 minutes, but there are no evident periodicities. The luminosity of the source is $1.0\times10^{38}$ ergs s$^{-1}$ (1–10 keV). We review arguments which suggest that mass accretion onto a neutron star or black hole provides the most likely mechanism of X-ray production. (auth)

**26461** SOFT X–RAY EMISSION FROM HERCULES X–1. Shulman, S.; Friedman, H.; Fritz, G.; Henry, R.C.; Yentis, D.J. (E. O. Hulburt Center for Space Research, Naval Research Laboratory). Astrophys. J. Lett. 199: No. 2, L101-L104 (15 July 1975).

A rocket observation of Her X-1 has detected an intense flux of X-rays at energies below 1 keV. The 0.18–0.28 keV flux was $2\times10^{-9}$ ergs cm$^{-2}$ s$^{-1}$ compared with a 1–10 keV flux of $3.3\times10^{-9}$ ergs cm$^{-2}$ s$^{-1}$. The low-energy flux was pulsating with the 1.24 period, although the pulse profile differed markedly from that at higher energies. A subsequent rocket observation, during that portion of the 35-day cycle when the 1–10 keV X-rays were not detectable, failed to detect any low energy X-rays. An upper limit in the 0.18–0.28 energy band of $2\times10^{-10}$ ergs cm$^{-2}$ s$^{-1}$ was obtained for this observation. (auth)

**26462** PION CONDENSED MATTER AT HIGH DENSITIES: EQUATION OF STATE AND STELLAR MODELS. Hartle, J.B.; Sawyer, R.F.; Scalapino, D.J. (Department of Physics, University of California, Santa Barbara). Astrophys. J. 199: No. 2, 471-481 (15 July 1975).

Equations of state for the ground state of matter at nuclear densities and above are derived, including the effects of a condensed charged pion wave. Nonrotating neutron star models are constructed using these

equations of state, and their observational significance is discussed. (auth)

**26463** LIGHT AND COLOR VARIATIONS OF THE FLARE STAR BY DRACONIS: A CRITIQUE OF STARSPOT PROPERTIES. Vogt, S.S. (Department of Astronomy, University of Texas at Austin McDonald Observatory). Astrophys. J. 199: No. 2, 418-426 (15 July 1975).

Periodic light and color variations of the now quiescent flare star BY Dra are presented and shown to be inconsistent with a thermal dark spot model at the present time. The present observations are explained in terms of persistent Ca II emission regions or plages. From a discussion of past photometric data for BY Dra it is concluded that :(1) The spot of 1965 was dark, covering at least 12 percent of the stellar surface at an effective temperature of at least 300 K cooler than the surrounding photosphere, and lasted for at least two years. (2) Period changes in the BY Dra light curves indicate the presence of differential stellar rotation. (3) There is no observational evidence for the existence of a starspot cycle on this system. (4) Spotted regions are elongated in the longitude direction, and are most likely composed of an assemblage of small spots, rather than of a single spot or several large spots. This elongation suggests that dynamo-generated magnetic fields and not residual primeval fields are responsible for spot formation. (auth)

**26464** HIGH-RESOLUTION PROFILES OF SODIUM AND POTASSIUM LINES IN ALPHA ORIONIS. Goldberg, L.; Ramsey, L.; Testerman, L.; Carbon, D. (Kitt Peak National Observatory). Astrophys. J. 199: No. 2, 427-431 (15 July 1975).

Profiles of the K I resonance line at 7698.98 Å and of the $D_1$ and $D_2$ lines of Na I in the spectrum of $\alpha$ Ori have been recorded photoelectrically using the main beam of the McMath solar telescope at KPNO. The Na lines were observed in the fourth order of the spectrograph and the K I line in the third order, providing a resolving power of approximately 50 mA. The observed profiles are consistent with a model in which radiation from the stellar photosphere is scattered and reemitted by an expanding envelope or envelopes of radius large compared with that of the photosphere. Each blueshifted absorption core appears to consist of two components of approximately the same intensity. The first has a heliocentric radial velocity of $+11-13$ km s$^{-1}$, which agrees very well with measurements of other resonance lines by other observers, whereas the second is in the range $+4-6$ km s$^{-1}$ and appears not to have been detected previously. (auth)

**26465** THE LIGHT CURVE OF CV SERPENTIS, THE SOMETIMES-ECLIPSING WOLF-RAYET STAR. Schild, R.; Lillier, Wm. (Center for Astrophysics, Harvard College Observatory). Astrophys. J. 199: No. 2, 432-435 (15 July 1975).

New photoelectric observations of the *B*-magnitude of CV Ser made in 1973 and 1974 show no clear evidence of an eclipse, but they establish night-to-night variablity of several percent, a systematic brightness change of 0.035 mag during a portion of the single orbit observed in 1973, and irregular flaring in 1974. We made iris photometer measurements of Harvard patrol plates taken between 1905 June and 1953 July, and find no evidence of a very deep eclipse such as observed by Hjellming and Hiltner. We present several new light curves and discuss them in the light of the recent results of Cowley *et al.* (auth)

**26466** THE $^{12}C/^{13}C$ RATIO IN STELLAR ATMOSPHERES. IV. ELEVEN G AND K TYPE GIANTS. Tomkin, J.; Lambert, D.L.; Luck, R.E. (McDonald Observatory and Department of Astronomy, The University of Texas, Austin). Astrophys. J. 199: No. 2, 436-442 (15 July 1975).

High-resolution photoelectric scans of portions of the 4-0, 5-1, 2-0, 3-1, and 4-2 bands of the CN red system in the spectra of 11 late-type giants have been obtained. Analysis of the $^{12}CN$ and $^{13}CN$ line intensities gives the folowing $^{12}C/^{13}C$ abundance ratios: $20\pm3$ ($\epsilon$ Vir), $22\pm3$ ($\zeta$ Cyg), $19\pm2$ ($\beta$ Cet), $11.5\pm1.5$ ($\epsilon$ Cyg), $22\pm4$ (46LMi), $17\pm4$ ($\zeta$ Cep), $19\pm3$ ($\alpha$ Ari), $6.5\pm1$ ($\gamma$ Leo A), $18\pm3$ ($\alpha$ Hya), $13\pm2$ ($\gamma$ Dra), and $13\pm3$ ($\gamma$ Sge). Revised $^{12}C/^{13}C$ ratios of 14 and 9 are derived for $\alpha$ Ser and $\alpha$ Tau, respectively. The low $^{12}C/^{13}C$ ratios of $\epsilon$ Cyg and $\alpha$ Ser are interpreted as evidence that they have been extensively mixed during the core helium flash. (auth)

**26467** THE TRIPLE-ALPHA RATE, SCREENING FACTORS, AND THE HELIUM FLASH. Tarbell, T.D.; Rood, R.T. (California Institute of Technology). Astrophys. J. 199: No. 2, 443-447 (15 July 1975).

A simple but accurate stability analysis is presented for a degenerate stellar core containing a temperature-sensitive nuclear fuel. It is used to study the dependence of the helium core mass at the helium flash $M_{cf}$ on the triple-$\alpha$ rate and its screening factor. Updated values of $M_{cf}$ are computed, and a sizable discrepancy between the results of different workers is removed. (auth)

**26468** HYDRODYNAMIC MODELS OF A CEPHEID ATMOSPHERE. I. DEEP ENVELOPE MODELS. Karp, A.H. (Astronomy Program, University of Maryland, College Park). Astrophys. J. 199: No. 2, 448-461 (15 July 1975).

The implicit hydrodynamic code of Kutter and Sparks has been modified to include radiative transfer effects. This modified code has been used to compute deep envelope models of a classical Cepheid with a period of $12^d$. It is shown that in this particular model the hydrogen ionization region plays only a small role in producing the observed phase lag between the light and velocity curves. The cause of the bumps on the model's light curve is examined, and a mechanism is presented to explain those Cepheids with two secondary features on their light curves. This mechanism is shown to be consistent with the Hertzsprung sequence only if the evolutionary mass-luminosity law is used. (auth)

## Quasi-Stellar, Radio, and X-Ray Sources

*Refer also to abstracts 25921, 26354, 26382, 26384, 26385, 26394, 26395, 26422, 26426, 26443, 26451, 26455, 26457, 26460, 26461, 26543, 26546, 26560, 26578, and 26585.*

**26469** STUDY OF THE BRIGHTNESS AND POLARIZATION STRUCTURE OF EXTRAGALACTIC RADIO SOURCES. Stull, M.A.; Price, K.M.; D'Addario, L.R.; Wernecke, S.J.; Graf, W.; Grebenkemper, C.J. (Radio Astronomy Institute, Stanford, California 94305). Astron. J. 80: No. 8, 559-580 (Aug. 1975).

We have determined the brightness and linear polarization structure of 19 extended extragalactic radio sources at a frequency of 10.7 GHz and with a synthesized beam $17\times17$ arcsec csc $\delta$. Compact components with self-absorption spectra coincident with the nucleus of an associated galaxy are fairly common, while many sources display regions of high percentage polarization, sometimes greater than 40%. Comparison of our results with other studies, all at lower frequencies (generally 5 GHz), has yielded information on spectra, depolarization rates, and Faraday rotation of the polarization plane in various source regions. We can identify at least four distinct classes of extragalactic radio source. These classes form a sequence along which the prominence of the compact central component declines relative to that of the extended outer regions, while those outer regions become more ordered in their structure and assume specific polarization characteristics. We speculate that this sequence is in fact an evolutionary sequence. (auth)

**26470** OPTICAL STUDIES OF 10 HIGH GALACTIC LATITUDE X—RAY SOURCES. Bahcall, J.N. (Institute for Advanced Study); Bahcall, N.A.; Murray, S.S.; Schmidt, M. Astrophys. J. Lett. 199: No. 1, L9-L11 (1 July 1975).

Optical studies are reported for a representative sample of 10 unidentified high galactic latitude ($|b|\geq20°$) X-ray sources that are north of declination $-25°$ and that have 3U error boxes less than or of the order of 0.5 square degrees. The source 3U 1410-03 is identified with a peculiar emission-line spiral galaxy, NGC 5506, and a distance group 4 rich cluster of galaxies, Abell 2142, is suggested as a possible identification for 3U 1555+27. It is shown that very few of the unidentified high galactic latitude sources are quasi-stellar sources brighter than 17.5 mag, although one possible X-ray quasar, NAB 0137-01, is reported. (auth)

**26471** THE REDSHIFTS OF 3C 129 AND 3C 129.1, THE RADIO-TAIL GALAXIES. Spinrad, H. (Department of Astronomy, University of California, Berkeley). Astrophys. J. Lett. 199: No. 1, L1-L1 (1 July 1975).

The average redshift of the "head-tail" radio galaxies 3C 129 and 3C 129.1 is found to be $+6400$ km s$^{-1}$; the projected length of the radio tail for 3C 129 is then derived as at least 625 kpc. (auth)

**26472** FURTHER OBSERVATIONS OF CYGNUS X-3 WITH The *UHURU* SATELLITE. Leach, R.W.; Murray, S.S.; Schreier, E.J.; Tananbaum, H.D.; Ulmer, M.P. (Center for Astrophysics, Harvard College Observatory); Parsignault, D.R. Astrophys. J. 199: No. 1, 184-188 (1 July 1975).

We present observations of the periodically varying X-ray source Cygnus X-3 made with the *Uhuru* satellite between 1970 December 27 and 1973 January 16. Our results are: 1. A value for the period. $P=0^d.1996811\pm0^d.0000016$; the 2 $\sigma$ upper limit to a continuous change in the period is $P^{-1}dP/dt\leq2\times10^{-12}$ s$^{-1}$. 2. No systematic change is observed in the effective low energy absorption across the $0^p.2$ cycle. 3. Cyg X-3 exhibits different average intensity levels which have been seen to persist for as long as 9 days at a time. The hardest spectra (in the 2–10 keV range) are derived from the times of lowest 2–6 keV intensity. 4. Cygnus X-3 was observed with *Uhuru* during the large radio outburst first noted on 1972 September 3. The spectral parameter $kT$ for thermal bremsstrahlung emission increases systematically from $\sim$ 2 keV to $\sim$3 keV from $\sim$ August 30 to $\sim$ September 3, and then decreased back to $\sim$2 keV by September 7. During this time, the 2–6 keV intensity of Cygnus X-3 fluctuated by a factor of 4 ranging from $\sim$150 cnt s$^{-1}$ to $\sim$600 cnt s$^{-1}$ which is the highest intensity yet observed for this source. (auth)

**26473** COMPTON-SYNCHROTRON MODELS FOR THE NUCLEUS OF CENTAURUS A (NGC 5128). Grindlay, J.E. (Center for Astrophysics, Harvard College Observatory and Smithsonian Astrophysical Observatory). Astrophys. J. 199: No. 1, 49-53 (1 July 1975).

Compton-synchrotron models are constructed to account for the observed microwave through X-ray spectrum and the recently reported flux of $\gamma$-rays with $E_\gamma \gtrsim 3 \times 10^{11}$ eV from NGC 5128 (Cen A). The spectrum suggests a double source structure in the nucleus of NGC 5128. The $\gamma$-rays arise from inverse Compton scattering of a synchrotron photon spectrum that must extend through X-ray energies. The observed $\gamma$-ray flux and the self-absorbed synchrotron spectra determine the source angular sizes, energy densities, and magnetic fields. Such parameters for the sources in the nuclei of active galaxies may enable the eventual description of the source mechanisms. Further implications of the model and possible observations are discussed. (auth)

**26474** PULSARS AND HIGH DENSITY PHYSICS. Hewish, A. (Cavendish Laboratory, Cambridge CB3 0HE, England). Rev. Mod. Phys. 47: No. 3, 567-572 (July 1975).

The discovery of pulsars and their interpretation as neutron stars are recounted in the 1974 Nobel Prize acceptance address. (AIP)

**26475** HIGH-RESOLUTION OBSERVATIONS OF THE RADIO EMISSION FROM BETA PERSEI. Clark, B.G.; Kellermann, K.I. (National Radio Astronomy Observatory); Shaffer, D. Astrophys. J. Lett. 198: No. 3, L123-L124 (15 June 1975).

The angular size of the radio emission from $\beta$ Persei (Algol) was measured during a flare and found to be about 4 milli-arcsec equivalent Gaussian diameter, corresponding to linear dimensions of 0.1 AU and mean brightness temperature $4\times10^8$ K. The observed change in the interferometer fringe visibility in a few hours corresponds to a mean apparent expansion velocity of 500–1000 km $s^{-1}$, or to a stationary, slightly elliptical source. (auth)

**26476** CYGNUS X-1: DISCOVERY OF VARIABLE CIRCULAR POLARIZATION. Michalsky, J.J.; Swedlund, J.B.; Stokes, R.A. (Battelle Observatory, Battelle-Northwest Laboratories). Astrophys. J. Lett. 198: No. 3, L101-L104 (15 June 1975).

HDE 226868, the optical counterpart of Cyg X-1, has been observed for circular polarization during 1974. Observations in five colors suggest that circular polarization results from an interstellar effect. Measurements of the blue polarization reveal circular polarization variations synchronous with the $5^d.6$ orbital period. The circular polarization variation appears to be similar to the blue intensity variation. (auth)

**26477** EVIDENCE FOR LONG-PERIOD SPORADIC PULSATIONS IN THE HARD X—RAY FLUX OF CYGNUS X-1. Frontera, F.; Fuligni, F. (Laboratorio Tecnologie e Studio Radiazioni Extraterrestri, Consiglio Nazionale Ricerche, Bologna, Italy). Astrophys. J. Lett. 198: No. 3, L105-L108 (15 June 1975).

Power spectral density estimates performed on the data of three balloon observations of Cyg X-1 show a peak at a frequency of $5.75\times10^{-2}$ Hz. This is interpreted as evidence for the presence of strong correlations in the hard X-ray flux of the source. That peak, however, appears to be present, in the single observation, only for limited periods of time, outside which it tends to disappear or to be displaced. Pulsations of limited duration, about 1 hour, cannot be excluded as a possible cause of the detected phenomenon. (auth)

**26478** MODES OF MASS TRANSFER AND CLASSES OF BINARY X—RAY SOURCES. van den Heuvel, E.P.J. (Institute for Advanced Study). Astrophys. J. Lett. 198: No. 3, L109-L112 (15 June 1975).

It is shown that if one assumes that compact stars (neutron stars or black holes) can be born as companions to main-sequence stars of any mass $M$, powerful ($L_x = 10^3-10^5\,L_\odot$) binary X-ray sources with lifetimes $\gtrsim 10^9$ yr are preferably expected to occur for $M < 2.1\,M_\odot$ and $M \gtrsim 20\,M_\odot$. Systems in the first mass range become X-ray sources when the normal star overflows its Roche lobe due to evolutionary expansion. Systems in the second mass range become X-ray sources when the normal star becomes a blue supergiant or an Of star, and develops a strong stellar wind before it overflows its Roche lobe. In the mass range $2.1 \lesssim M/M_\odot \lesssim 20$ practically no long-lived X-ray binaries are expected since evolutionary stages with strong winds are absent and the accretion rates resulting from Roche-lobe overflow are in general so large ($10^{-6}$ to $10^{-3}\,M_\odot$ $yr^{-1}$) that any X-ray emission from a companion will soon be extinguished. (auth)

**26479** SLOWLY ROTATING RELATIVISTIC STARS. V. STATIC STABILITY ANALYSIS OF $n$=3/2 POLYTROPES. Hartle, J.B. (Department of Physics, University of California, Santa Barbara); Munn, M.W. Astrophys. J. 198: No. 2, 467-476 (1 June 1975).

The static stability analysis of slowly and uniformly rotating relativistic stars is applied to the $n$-3/2 Tooper polytropes corresponding to an ideal nonrelativistic neutron gas. The method tests the stability of a sequence of stellar models against the modes of oscillation which correspond to radial modes in a nonrotating star. It involves a comparison of the uniformly rotating models to be tested with a sequence of models having a specified differential rotation. The equations of structure of these differentially rotating stars are derived and integrated, and the critical central density dividing the stable models from the unstable models is determined. (auth)

**26480** ELECTROMAGNETIC PULSE FROM SUPERNOVAE. Colgate, S.A. (New Mexico Institute of Mining and Technology, Socorro). Astrophys. J. 198: No. 2, 439-445 (1 June 1975).

We have calculated the upper and lower limits to the radiated electromagnetic pulse from a supernova assuming that the mass fraction of the matter expanding inside the dipole magnetic field shares energy and maintains pressure balance in the process. Although the surface layer of the star of thickness 1 g $cm^{-3}$ may be shock-accelerated to $(\Gamma-1) \simeq 100$, where $\Gamma = (1-B_r^2)^{-1/2}$ and $c\beta_r$ is the fluid velocity behind the shock, and expand into vacuum with $(\Gamma-1) \to 10^5$, the equatorial magnetic field retards this expansion so that the inner, more massive layers of the ejected matter effectively accelerate the presumed canonical dipole magnetic field to greater velocities than would be the case by the surface layer alone. This results is a pulse of $10^{46}$ ergs in a width of $\lambda/2 \simeq 150$ cm. Circumstellar matter like a corona would not affect the pulse. Similarly, electron self-radiation effects appear to be small. The principal attenuation of the pulse occurs due to interstellar matter. If the ions are *not* dragged along by charge separation, then the ion attenuation of the wave essentially ceases at the point where $\eta = (eB\lambda)/(2\pi mc^2) \simeq 1$, and $R = 2\times10^{16}$ cm. At this point, the wave has not been significantly attenuated. On the other hand, free electrons will attenuate the wave so that $\eta \to 1$ at $R \simeq 5.5\times10^{13}$ cm and a pulse of $3\times10^{34}$ ergs should escape further nonlinear relativistic particle attenuation. Charge separation effects may allow more pulse energy to escape. (auth)

**26481** OBSERVATIONS OF THE CIRCINUS X-1 REGION. Baity, W.A.; Ulmer, M.P. (University of California, San Diego); Peterson, L.E. Astrophys. J. 198: No. 2, 447-452 (1 June 1975).

THE UCSD X-ray telescope on board the OSO-7 satellite has provided observations of the Cir X-1 region for over 110 days between 1971 December and 1973 March. Although statistically significant fluctuations in the 7–11 keV flux were measured, no periodicities in the range between 5 hours and 100 days were found, to an upper limit of ~40 percent amplitude. Intensities in the 7–57 keV range show variability by a factor of approximately 25, and changes in the spectral shape reflected by a number spectral index $\alpha$ varying from $1.1\pm0.1$ to $3.0\pm0.5$. There is a positive correlation between intensity and spectral shape, with a steeper spectrum at times of peak intensity. Although power-law, exponential, and blackbody spectral shapes are equally good fits to our data alone, examination of all the available data appears to rule out a simple blackbody spectrum, at least at times of maximum intensity. (auth)

**26482** THE ABSORPTION-LINE SPECTRUM OF THE QUASI-STELLAR OBJECT PHL 957. Wingert, D.W. (Princeton University Observatory). Astrophys. J. 198: No. 2, 267-279 (1 June 1975).

Six new high-dispersion spectra of the quasi-stellar object PHL 957($z_{em}$=2.69) have been obtained with the Princeton integrating television system at the coudé focus of the 200-inch (5 m) telescope. Together with earlier data, 179 absorption lines were found, mostly between 3550 and 4500 Å. The absorption redshift system at $z = 2.3099$ is most prominent, with 26 lines, including a very strong L$\alpha$ line. Another system, close to the emission redshift, was found to be double, with $z$=2.6638 and 2.6624. Many lines were identified as L$\alpha$–L$\beta$ pairs. For the major redshift systems and the L$\alpha$–L$\beta$ pairs, column densities and velocity dispersions were obtained from curves of growth. The redshift system at $z$=2.3099 resembles interstellar material in ionization and abundance ratios, and constitutes strong evidence for absorption originating in a galaxy along the line of sight to the quasar. The double system at $z$=2.663 has higher ion states and most likely is associated with the quasar. (auth)

**26483** VARIABILITY OF THE X—RAY SOURCES IN THE MAGELLANIC CLOUDS. Tuohy, I.R.; Rapley, C.G. (University College London, Mullard Space Science Laboratory). Astrophys. J. Lett. 198: No. 2, L69-L72 (1 June 1975).

We have conducted further *Copernicus* observations of the SMC and LMC X-ray sources. The SMC X-1 data provide an improved X-ray period of $3^d.89217\pm0^d.00012$ and establish a new phase of JD $2{,}442{,}276.15\pm0.04$ for the eclipse center. Several aspects of source variability are discussed. Our LMC data confirm the variability of LMCX-1, LMCX-2, and LMCX-3. In addition we review recent data concerning optical counterparts of these sources. (auth)

**26484** A COMPARISON OF SOME RADIO AND OPTICAL PROPERTIES OF QUASI-STELLAR SOURCES AND BL LACERTAE OBJECTS. Usher, P.D. (Astronomy Department, The Pennsylvania State University, University Park, PA 16802). Astrophys. J. Lett. 198: No. 2, L57-L60 (1 June 1975).

An empirical relation between radio spectral index and amplitude of optical variability for quasi-stellar sources with continuous, featureless

optical spectra (QC sources) is extended to include sources with optical spectral lines. The radio spectral index at 5 GHz is found to correlate with the ratio of radio to optical luminosity in a clear-cut fashion when optical and radio variability is taken into account. QC sources are found to represent a tightly knit group *vis-à-vis* the general population. The predictive capabilities of the correlations are discussed. The properties of the weak-line N galaxy 3C 371 are very similar to those of the QC source population. When optical variability is taken into account, the Hubble diagram provides further evidence for a cosmological interpretation of redshift. (auth)

**26485** COMMENTS ON GOTT AND GUNN'S SOLUTION OF DOUBLE QUASARS. Barnothy, J.M. (Evanston, Illinois). Astrophys. J. Lett. 198: No. 2, L61-L62 (1 June 1975).

The explanation offered by Gott and Gunn for the double quasar 1548+115—namely, that the gravitational lens brightening of faraway quasars by foreground quasars increases the chance of finding more pairs of quasars—is examined and shown to be incorrect. (auth)

**26486** OPTICAL CONDENSATIONS AND FILAMENTS IN THE NORTHEAST RADIO LOBE OF NGC 5128. Blanco, V.M.; Graham, J.A.; Lasker, B.M.; Osmer, P.S. (Cerro Tololo Inter-American Observatory, La Serena, Chile). Astrophys. J. Lett. 198: No. 2, L63-L64 (1 June 1975).

Extended diffuse and filamentary optical features are shown to exist in the outer northeast component of the radio source associated with NGC 5128. Some spectroscopic observations are reported, and preliminary remarks are made about the nature of these features. (auth)

**26487** VARIABILITY AND OPTICAL-RADIO PROPERTIES OF BL LACERTAE OBJECTS. Pollock, J.T. (Center for Astrophysics, Harvard College Observatory and Smithsonian Astrophysical Observatory). Astrophys. J. Lett. 198: No. 2, L53-L56 (1 June 1975).

The optical variability of new candidates for the BL Lacertae class of objects and of two known members of this class has been examined using the Harvard plate collection. A correlation is indicated between the maximum known range of optical variability and the observed radio spectral index at 5 GHz. Light curves for PKS 0735+17 and 2254+07 (OY 091) are presented. (auth)

**26488** THE NEBULOSITY AROUND 3C 48. Wampler, E.J.; Robinson, L.B. (Anglo-Australian Telescope Board, Epping, New South Wales 2121, Australia); Burbidge, E.M.; Baldwin, J.A. Astrophys. J. Lett. 198: No. 2, L49-L52 (1 June 1975).

Spectrophotometric measurements of the nebulosity around 3C 48 have been made with the Lick image-tube scanner on the 3-m telescope. The forbidden emission lines [O III] λλ5007, 4959, [Ne II] λ3869, and [O II] λ3727 were detected in the nebulosity on the north side, while the Balmer lines were absent. The forbidden lines are narrower but have larger equivalent widths than those present in the spectrum of the central QSO, and have a slightly larger redshift, 0.370, than that of the QSO (0.368), thus ruling out the gravitational redshift hypothesis for this object. No emission lines were detected in the nebulosity on the south side. The continuum on the north was dominated by scattered continuum from the central object. We have no evidence concerning the presence or absence of a galaxy of stars associated with 3C 48. The hot gas giving rise to the emission lines could either be part of a rotating shell or disk about the QSO or be gas ejected from it. (auth)

**26489** POSSIBLE MODELS FOR SOME TRANSIENT X-RAY SOURCES. Pacini, F.; Shapiro, S. L. (Cornell Univ., Ithaca, NY). Nature (London); 255: No. 5510, 618-619(19 Jun 1975).

Reference is made to a transient x-ray source that flared up in Centaurus during December 1974 and was observed by the satellite Ariel V in the energy interval 3 to 30 keV. Within a few days the source increased in intensity to a peak of 0.02 photons/cm$^2$/sec/keV, then decreased, until after about one month the intensity had fallen by a factor of about 5. The source showed a definite periodicity of 6.75 ± 0.03 min. It is thought that investigations of this source may throw some light on its nature and possibly that of other transient sources. Two alternative models are proposed, and it is suggested that the source may flare again in the near future, although there is no clear evidence for repetitive outbursts. In the first model the periodicity is attributed to the intrinsic rotation of a compact star, such as a white dwarf or a neutron star. In the second model the periodicity is attributed to the orbital period of a binary system containing a compact object. A mathematical analysis is made of these two models. (UK)

**26490** OPTICAL IDENTIFICATIONS OF RADIO SOURCES SELECTED FROM THE B2 CATALOGUE. IV. Grueff, G.; Vigotti, M. (Univ., Bologna). Astron. Astrophys., Suppl. Ser.; 20: No. 1, 57-82(Apr 1975).

An attempt has been made to push the optical identifications of radio sources beyond the limit of the Palomar Sky Survey. A total of 115 fields, which were empty on the Palomar Sky Survey, have been photographed with the 48" Schmidt Telescope, and 200" telescope of Hale Observatories. Reliable indentifications are proposed for 44 radio sources, or 38% of the starting sample. Some implications of these results are discussed briefly. In particular, it is found that the number of identifications with galaxies increases very sharply when one goes deeper than $M_v \sim 19.5$, while almost no quasars are found fainter than 20.5m. (auth)

**26491** RADIO AND OPTICAL DATA ON A COMPLETE SAMPLE OF RADIO FAINT GALAXIES. Colla, G. (Univ., Bologna); Fanti, C.; Gioia, I.; Lari, C.; Lequeux, J.; Lucas, R.; Ulrich, M. H. Astron. Astrophys., Suppl. Ser.; 20: No. 1, 1-36(Apr 1975).

Radio sources from the B2 catalogue have been identified with galaxies in the "Catalogue of Galaxies and of Clusters of Galaxies." 54 ellipticals, 3 peculiar galaxies and 10 spiral galaxies were found. All these objects have been observed at 1415 MHz at Nançay, 42 have been observed at Westerbork and a few at Nançay at 5000 MHz. These observations allow the determination of the radio spectrum and a study of the radio structure. Spectroscopic observations have also been made at McDonald Observatory and Kitt Peak National Observatory providing redshifts for 41 galaxies and as a result the redshifts are known for all the galaxies except 3 spirals. The results of the radio and optical observations are given in the present paper; the interpretation of the data is discussed elswhere. (auth)

**26492** MECHANISMS FOR THE PRODUCTION OF X-RAYS IN A COSMIC SETTING. Blumenthal, G. R. (Univ. of California, Santa Cruz); Tucker, W. H. pp 99-153 of X-ray Astronomy. Giacconi, R. (ed.). Dordrecht, Netherlands; Reidel (1974).

A brief review of classical radiation theory is given. Mechanisms for X-ray production in cosmic X-ray sources are discussed. (BJG)

**26493** X-RAYS SKY. Giacconi, R. pp 155-168; 397-442 of X-ray Astronomy. Giacconi, R. (ed.). Dordrecht, Netherlands; Reidel (1974).

Various sources of cosmic X-rays are discussed. A catalog of X-ray sources is included. (BJG)

**26494** EXTRA GALACTIC X-RAY SOURCES. Kellogg, E. M. (Center for Astrophysics, Cambridge, MA). pp 321-357 of X-ray Astronomy. Giacconi, R. (ed.). Dordrecht, Netherlands; Reidel (1974).

Several extragalactic X-ray sources are discussed. X-ray emission mechanisms are reviewed. (BJG)

**26495** RELATIVISTIC-ELECTRON HEATING BY INDUCED COMPTON SCATTERING. Dedkov, G.V. (P. K. Shternberg State Astronomical Institute). Sov. Astron.—AJ 19: No. 1, 117-118 (July 1975).

An equation is obtained for relativistic-electron heating by induced Compton scattering of unpolarized, isotropic electromagnetic radiation. For a definite electron density in quasars and nuclei of Seyfert galaxies, the initial radiation spectrum is distorted due to this effect. The absence of distortions in the observed spectra allows us to estimate the upper limit of relativistic-electron density, and also the heating efficiency in corresponding sources. (auth)

**26496** SPACE DISTRIBUTION OF OH ABSORPTION IN THE SOURCE NGC 6334. Slysh, V.I. (Observatoire de Meudon). Sov. Astron.—AJ 19: No. 1, 14-17 (July 1975).

The neighborhood of NGC 6334 has been mapped in the 1667 MHz OH line in both circular polarizations, and in the 1665 MHz line in left-circular polarization. Right-ascension scans through the center of the source have been made in the 1612 and 1720 MHz satellite OH lines. The two absorption features in the OH spectrum of the source NGC 6334 have a different space distribution. The narrow feature at 5.5 km/sec radial velocity has a constant optical depth over the source, and is formed in a rarefied cloud of large angular size located between the sun and the source. A second (broad and deep) spectral feature has a radial velocity of −4 km/sec, the same as the radial velocity of the continuum source; it arises in two or three compact OH clouds 1−2 pc across. The two OH maser emission centers NGC 6334N and 6334S are located inside the clouds. These clouds have a high total hydrogen density, possibly in molecular form, with a value typical for dense dust clouds. The absorption in the satellite lines is anomalous. In the 1720 MHz line the absorption is about twice that expected, while in the 1612 MHz line the absorption is abnormally weak and is observed only in cloud 3, which surrounds the maser source NGC 6334S. (auth)

**26497** STUDIES OF CLUSTER X—RAY SOURCES. ENERGY SPECTRA FOR THE PERSEUS, VIRGO, AND COMA CLUSTERS. Kellogg, E.; Baldwin, J.R. (Center for Astrophysics, Harvard College Observatory and Smithsonian Astrophysical Observatory); Koch, D. Astrophys. J. 199: No. 2, 299-306 (15 July 1975).

We present the final *Uhuru* X-ray differential-energy spectra for the Perseus, Virgo, and Coma clusters of galaxies. The power-law and isothermal bremsstrahlung model forms, both with a low-energy cutoff, are given. For bremsstrahlung, the energy-dependent Gaunt factor is

calculated by an improved method. The spectra, best fits to the *Uhuru* 2-10 keV data, are also compared with other observations of these sources in the energy range 0.1–100 keV. For Perseus, the data above 20 keV favor the bremsstrahlung fit marginally. For Virgo, the data of Catura *et al.* between 0.25 and 1.0 keV clearly favor the bremsstrahlung curve. For Coma, the weakest of the three sources, the data are less precise, but there is some evidence for a low-energy turnover or cutoff. The implications of such a cutoff are discussed briefly. In the course of describing our data-fitting procedure, we discuss the problem of parameter estimation for this situation, where we are fitting a nonlinear function containing three parameters—normalization, slope, and low-energy cutoff—with two of the parameters strongly correlated. A framework for presenting the results is described, equivalent to giving all the elements of the covariance matrix, but more readily useful in this case. We quote 68 percent confidence error bars for the *independently* determined slope and cutoff parameters, corresponding to the diagonal terms of the covariance matrix. We also plot the 68 percent confidence limits for the fitted spectral functions, which correspond to giving both the diagonal and the off-diagonal terms of the covariance matrix. (auth)

**26498** TIME VARIATIONS IN SOURCES OF SILICON MONOXIDE EMISSION AT 7 MILLIMETERS. Spencer, J.H.; Schwartz, P.R. (E. O. Hulburt Center for Space Research, Naval Research Laboratory). Astrophys. J. Lett. 199: No. 2, L111-L113 (15 July 1975).

Time variations in SiO $J=1$–0, $v=1$ and $v=2$ intensity with a time scale which probably corresponds to the infrared light curve have been observed in $o$ Cet and $R$ Cas. A short time scale variation of about 1 hour has been detected in the emission of SiO from the Orion infrared source. (auth)

**26499** PERIOD CHANGES IN CENTAURUS X-3. Sparks, W.M. (NASA Goddard Space Flight Center, Greenbelt, Maryland 20771). Astrophys. J. 199: No. 2, 462-466 (15 July 1975).

A number of mechanisms which can change the orbital period are applied to various models of Cen X-3. Only four models which give rise to feasible mechanisms are found. Possible observations which could distinguish between these models are suggested. (auth)

**26500** RADIO OBSERVATIONS OF CYGNUS X-3 FROM 1973 DECEMBER TO 1974 JUNE. Gregory, P.C. (Physics Department and Institute of Astronomy, University of British Columbia, Vancouver); Seaquist, E.R.; Hughes, V.A.; Woodsworth, A. Astrophys. J. 199: No. 2, 467-470 (15 July 1975).

Observations of Cygnus X-3 on 79 days during the period 1973 December to 1974 June at 10.5 or 22 GHz are presented. During this period several large outbursts (>5 Jy) were recorded, together with many smaller ones. From an analysis of a total of 253 days of observations, we find that the flux density of Cygnus X-3 at centimeter wavelengths exceeded 10 Jy on ~2 percent of the days and exceeded 1 Jy on about one-third of the days observed. (auth)

# Solar Phenomena

*Refer also to abstracts 26344, 26354, 26359, 26443, 26453, 26628, 26653, 26655, 26659, 26661, and 26827.*

**26501** COLUMNAR CONTENT MEASUREMENTS OF THE SOLAR-WIND TURBULENCE NEAR THE SUN. Callahan, P.S. (Jet Propulsion Laboratory, California Institute of Technology). Astrophys. J. 199: No. 1, 227-236 (1 July 1975).

The solar-wind turbulence near the Sun is investigated with data obtained near the superior conjunctions of *Mariners* 6, 7, and 9. The data are time histories of the change in the electron columnar content between the Earth and the spacecraft. It is found that the comoving turbulence spectrum is well represented by a power law $[P(\nu)\ \alpha\nu^{-\beta}]$ of index $\beta=3.9\ \pm0.2$. Comparison of the average spectral amplitude near the Sun ($r\simeq0.15$ AU) with that near 1 AU shows that the turbulence declines with heliocentric distance as $\Delta n\ (r)\ \alpha r^{-2.36\pm0.11}$, ignoring time variations. In the region near the Sun ($0.07 \lesssim r \lesssim 0.22$ AU), $\Delta n\ (r)$ declines more slowly. It is suggested that there is a region of enhanced turbulence near the Sun. The *Mariner* 9 spectral amplitudes correlate with Zurich sunspot number. The relationship of the present observations to theories of solar-wind heating is discussed. (auth)

**26502** ON THE VARIATION OF THE SOLAR WIND VELOCITY FOLLOWING SOLAR FLARES. Huang, Y. (Telecommunication Laboratories, Chung-Li, Taiwan, Republic of China); Lee, Y. J. Geophys. Res. 80: No. 19, 2863-2865 (1 July 1975).

By use of the superposed epoch method, changes in the solar wind velocity following solar flares have been investigated by using the solar wind velocity data obtained by Pioneer 6 and 7 and Vela 3, 4, and 5 satellites. A significant increase of the solar wind velocity has been found on the second day following importance 3 solar flares and on the third day following importance 2 solar flares. No significant increase of the solar wind velocity has been found for limb flares. (auth)

**26503** THE 1640.4 Å Hα LINE OF He II OBSERVED FROM *Skylab*. Feldman, U.; Doschek, G.A.; VanHoosier, M.E.; Tousey, R. (E. O. Hulburt Center for Space Research, Naval Research Laboratory). Astrophys. J. Lett. 199: No. 1, L67-L70 (1 July 1975).

Profiles obtained from NRL *Skylab* solar spectra of the 1640.4 Å feature identified as the Hα line of He II re discussed and compared with theoretical profiles derived assuming (*a*) collisional excitation and (*b*) radiative recombination as the dominant excitation mechanism. Relative intensities of this line as a function of altitude above and below the solar white-light limb (from −12″ to +8″) are also given for a representative quiet Sun region and for a polar coronal hole. (auth)

**26504** ON THE ROTATION OF GAS AND MAGNETIC FIELDS AT THE SOLAR PHOTOSPHERE. Foukal, P. (Center for Astrophysics); Jokipii, J.R. Astrophys. J. Lett. 199: No. 1, L71-L73 (1 July 1975).

We point out that observations of a 5 percent velocity difference between photospheric gas and magnetic structures at a given latitude may simply result from angular momentum conservation by fluid elements in the convection zone. Estimates of the viscosity and magnetic drag are considered, and we conclude that they probably are not large enough to enforce strictly rigid rotation. (auth)

**26505** THE HELIUM CHROMOSPHERE, CORONAL HOLES, AND STELLAR X—RAYS. Zirin, H. (Big Bear Solar Observatory, Hale Observatories). Astrophys. J. Lett. 199: No. 1, L63-L66 (1 July 1975).

The solar chromosphere at the limb seen in D3 is an irregular bright band 1000 km thick with a dark band 1000 km thick beneath. The D3 chromosphere disappears in coronal holes. We demonstrate how the D3 emission, as well as the other He I and He II lines, can be explained quantitatively by photionization by coronal back-radiation. A Chapman layer with $N$ (He) $H=5\times10^{17}$ is formed near $\tau=1$ in the He I and He II continua. The chromospheric He emission or absorption is weak in coronal holes because there is no coronal back-radiation. Based on this model, the soft X-ray flux from stars with He λ10830 absorption lines is estimated as proportional to the 10830 equivalent width and the apparent area. (auth)

**26506** MORPHOLOGICAL EVOLUTION OF X—RAY FLARE STRUCTURES FROM THE RISE THROUGH THE DECAY PHASE. Kahler, S.W.; Krieger, A.S. (American Science and Engineering, Inc.); Vaiana, G.S. Astrophys. J. Lett. 199: No. 1, L57-L61 (1 July 1975).

The morphological evolution of 12 solar X-ray subflares from onset through the decay phase has been studied using photographic X-ray images obtained from *Skylab*. The spatial configurations are found to vary widely from flare to flare, but they appear to be composed of two basic kinds of structures. The first, which we have termed "X-ray kernels," are brightest during the rise phase; and the second, looplike structures, appear during the maximum and decay phases of the event. The X-ray kernels are small pointlike structures (typically 10″ or less) which may be related to the nonthermal phases of flares. (auth)

**26507** HEATING OF CORONAL MATERIAL AT X—RAY BRIGHT POINTS. Glencross, W.M. (Mullard Space Science Laboratory, Department of Physics and Astronomy, University College London). Astrophys. J. Lett. 199: No. 1, L53-L56 (1 July 1975).

Golub *et al.* have described the development of bright X-ray features associated with localized enhancements in the magnetic field at the solar surface. Since the radiating plasma is no hotter than that in fainter coronal features, the increased flux must be due to an enhancement in the number density of particles. This *Letter* suggests that the magnetic ropes present might be constructed of twisted braids which are wrapped one around the other. These components would be separated by current sheets where the density of material can be far higher than that normally considered appropriate for the corona. If the plasma in these sheets is maintained above $10^6$ K, the flux radiated could exceed that from the rest of the magnetic rope. This material would account for the enhanced brightness of the X-ray regions. The conversion of magnetic energy during merging of braids is shown to provide sufficient thermal energy to maintain the dense plasma at coronal temperatures throughout the lifetimes observed, while the development of instabilities in this process accounts for the "flarelike" brightenings. Conditions met where bright points develop should differ only in magnitude from those encountered elsewhere in coronal magnetic fields. This suggests that the same energy conversion process could be important in determining the energy balance of this part of the solar atmosphere. (auth)

**26508** DYNAMICS OF SOLAR MAGNETIC FIELDS. VI. FORCE-FREE MAGNETIC FIELDS AND MOTIONS OF MAGNETIC FOOT-POINTS. Low, B.C.; Nakagawa, Y. (High Altitude Observatory, National Center for Atmospheric Research). Astrophys. J. 199: No. 1, 237-246 (1 July 1975).

A mathematical model is developed to consider the evolution of force-free magnetic fields in relation to the displacements of their foot-points. For a magnetic field depending on only two Cartesian coordinates and time, the problem reduces to solving a nonlinear elliptic partial differential equation. As illustration of the physical process, two specific

examples of evolving force-free magnetic fields are examined in detail, one evolving with rising and the other with descending field lines. It is shown that these two contrasting behaviors of the field lines correspond to sheared motions of their foot-points of quite different characters. The physical implications of these two examples of evolving force-free magnetic fields are discussed. (auth)

**26509** TEMPERATURE DEPENDENCE OF EMISSION MEASURE IN SOLAR X—RAY PLASMAS. I. NONFLARING ACTIVE REGIONS. Phillips, K.J.H. (Laboratory for Solar Physics Astrophysics, NASA-Goddard Space Flight Center, Greenbelt, Maryland). Astrophys. J. 199: No. 1, 247-254 (1 July 1975).

Previous determinations of the form of the emission measure distribution function $\phi$ ($T$) for solar active regions are examined. It is found that two analyses in particular are affected by low quality of either observational or atomic data. An alternative, *ab initio* method of analysis is discussed. (auth)

**26510** DUAL-FREQUENCY MEASUREMENT OF THE SOLAR GRAVITATIONAL MICROWAVE DEFLECTION. Weiler, K.W.; Ekers, R.D. (Kapteyn Astronomical Institute, University of Groningen, Groningen, The Netherlands); Raimond, E.; Wellington, K.J. Phys. Rev. Lett. 35: No. 3, 134-137 (21 July 1975).

The Westerbork synthesis radio telescope was used to measure the solar gravitational deflection of radio waves over a period of 10 days, in October 1973, centered on the occultation of the quasar 3C279 by the sun. Simultaneous measurements at two frequencies (5.0 and 1.4 GHz) allowed the removal of the effects of refraction in the solar corona. The gravitational bending measured was $1.038 \pm 0.033$ times that predicted by general relativity. As a by-product of these observations, values for the parameters at a model of the coronal electron density were also obtained. (auth)

**26511** SOLAR ROTATION AS MARKED BY EXTREME-ULTRAVIOLET CORONAL HOLES. Wagner, W.J. (Sacramento Peak Observatory, AFCRL). Astrophys. J. Lett. 198: No. 3, L141-L144 (15 June 1975).

Spectroheliograms produced in the light of Fe XV $\lambda$284 by the Goddard Space Flight Center experiment on OSO-7 are used to determine solar rotational periods for low-emission coronal hole features. From 1972 May to 1973 October, daily measures were obtained of the coronal hole area appearing at the central solar meridian. Autocorrelations of the coronal-hole-area time series in seven latitutde zones provide synodic rotation periods which indicate a close to rigid rotation by such features for lag lengths of only one rotation. For latitudes below about 50°, both the autocorrelation functions for short-lived coronal holes and analyses of more persistent features over these 18 months suggests a quadrupolar distribution of coronal hole longitudes. (auth)

**26512** CONFIRMATION OF KNOWN NUMERICAL SOLUTIONS FOR THE QUIET SOLAR WIND EQUATIONS. Cuperman, S. (CIRES, University of Colorado); Metzler, N.; Spiegelglass, M. Astrophys. J. 198: No. 3, 755-759 (15 June 1975).

A detailed comparison of two integration methods for the quiet solar wind, namely, starting at the "singular critical point" and proceeding outward and then inward (Method I) and starting at "infinity" and proceeding inward (Method II), is given. No consideration is given to interaction with interstellar gas. It is found that (i) in the domain where both methods provide physical solutions (e.g., from 1 $R_\odot$ to a few AU heliocentric distance) the results coincide within less than 1 percent (this confirms the validity of the results obtained so far by the authors using Method I); (ii) Method II provides physical solutions over all the interplanetary range, which represents an advantage over Method I; and (iii) while for solutions within 1–2 AU heliocentric distance the two methods consume comparable computer time, for solutions up to very large heliocentric distances, Method II is preferable. (auth)

**26513** THE RELATIVE ABUNDANCES AND ENERGY SPECTRA OF SOLAR-FLARE-ACCELERATED DEUTERIUM, TRITIUM, AND HELIUM-3. Anglin, J.D. (Enrico Fermi Institute and Department of Physics, The University of Chicago). Astrophys. J. 198: No. 3, 733-753 (15 June 1975).

The relative abundances and energy spectra of $^2$H, $^3$H, and $^3$He have been studied in energetic solar particle events with the University of Chicago IMP-5 charged-particle telescope. The outstanding result of these observations is the remarkable scarcity of $^2$H and $^3$H in several flares which have extremely large abundances of $^3$He. For example, we find in the 1970 July 30 solar particle event $\Gamma$ ($^3$He/$^4$He) $= 0.54 \pm 0.09$ between 10.5 and 22.1 MeV nucleon$^{-1}$, while at the same time $\Gamma$ ($^2$H/$^3$He) $\leq 0.05$. (The symbol $\Gamma$ is used to represent the ratio of the integral fluxes of two species in the same energy-per-nucleon interval.) Since these normally rare isotopes are thought to be the products of $^4$He fragmentation during particle acceleration, it is not clear how one could be observed without the others. Yet the data clearly show that $^2$H and $^3$H are extremely rare. In a large sum composed of 75 solar flare events, we find $\Gamma$ ($^3$H/$^1$H) $= (5.4 \pm 2.4) \times 10^{-5}$ between 10.5 and 13.5 MeV nucleon$^{-1}$. A detailed comparison of these observations with different nuclear production models is undertaken in this paper. It is shown that neither the isotropic production models developed in this paper, nor the model of Ramaty and Kozlovsky, in which $^3$He is preferentially produced in the backward direction by a beam of protons directed downward into the photosphere, provides an adequate explanation of all the observational data. (auth)

**26514** SOLAR RADIATION INDUCED ROTATIONAL BURSTING OF INTERPLANETARY PARTICLES. Sparrow, J.G. (Space Astronomy Laboratory, State University of New York at Albany, Albany, New York 12203). Geophys. Res. Lett. 2: No. 6, 255-257 (June 1975).

It is suggested that the magnitudes of the two radiation induced rotational bursting mechanisms have been overestimated and that they do not work significantly faster than the Poynting-Robertson effect in removal of interplanetary particles. (auth)

**26515** MEAN-FREE-PATH DEPENDENCE OF $\kappa_2$ IN CLEAN SUPERCONDUCTORS. Ostenson, J.E.; Finnemore, D.K. (Ames Laboratory and Department of Physics, Iowa State University, Ames, Iowa 50010). Phys. Rev. B 12: No. 1, 114-116 (1 July 1975).

The slope of the magnetization curve near the upper critical field $H_{c2}$ has been measured for *Nb*Ta alloys in order to study systematically the deviations from the Eilenberger theory in the clean limit. $\kappa$ values determined from these slopes, $\kappa_2$, agree well with the theory for $\kappa$ greater than 1.0, but the measurements lie well above the theory for $k < 1.0$. A study of pure V, as well as these alloys, shows that $\lambda/\xi$ rather than $\xi/l_{tr}$ is the important parameter governing the magnitude of the deviation. (auth)

**26516** SPECTRAL CHARACTERISTICS OF SOLAR RADIO BURSTS ASSOCIATED WITH SHORTWAVE FADEOUTS. Babcock, R. R. (Air Force 12th Weather Squadron, Hamilton, MA). J. Atmos. Terr. Phys.; No. 9, 1227-1230(Sep 1975).

Spectral characteristics of centimeter wavelength solar radio bursts as measured at the Sagamore Hill Radio Observatory were correlated with shortwave fadeouts (SWF). It was found that there is a definite relation between the intensity and shape of the spectrum of a solar radio burst and the occurrence of a SWF. These results imply "threshold" values for the cm-$\lambda$ component of the radio spectrum if the accompanying x-ray emissions are to be intense enough to cause a SWF. (auth)

**26517** SOLAR X-RAY EMISSION. Vaiana, G. (American Science and Engineering, Inc., Cambridge, MA); Tucker, W. H. pp 169-205 of X-ray Astronomy. Giacconi, R. (ed.). Dordrecht, Netherlands; Reidel (1974).

A review of the structure of the solar atmosphere is given. Solar activity is discussed in the context of X-ray emission. (BJG)

**26518** STUDIES ON SOME ASPECTS OF ENHANCED SOLAR MICROWAVE RADIATION. Das Gupta, M. K. (Center of Advanced Study in Radio Physics and Electronics, Calcutta); Sarkar, S. K. Indian J. Radio Space Phys.; 2: No. 3, 196-198(Sep 1973).

Data on disturbed sun emission at different microwave frequencies observed at Sagamore Hill Solar Radio Observatory for a period of about 4 years have been examined in relation to their occurrences, peak flux values, energy excesses and spectral distributions. Important results obtained from the statistical analyses are: (i) spectrum of the average S-component shows a maximum at 4995 MHz and is independent of the phase of the 27-day cycle, (ii) occurrences of both the "simple" bursts ("simple impulsive" and "gradual rise and fall") are maximum at 4995 MHz, and (iii) spectra of majority of the "inverted U" type of microwave bursts have the peak at 4995 MHz. The analysis suggests that for the study of solar terrestrial phenomena the solar flux observation at 4995 MHz would serve as a better index instead of at 2800 MHz assumed till now to be a reliable index. (auth)

**26519** COMPILATION OF NORMALIZED SOLAR WIND DENSITIES AND VELOCITIES (1965/1971). Diodato, L.; Moreno, G.; Signorini, C. (C. N. R., Frascati, Italy). Astron. Astrophys., Suppl. Ser.; 20: No. 3, 314-362(Jun 1975).

Measurements of the solar wind bulk speed and density performed at 1 AU by the spacecraft Vela-3, Explorers-33-34-35 and HEOS-1, in the period from July 1965 to June 1971, are normalized to similar conditions. The resulting three-hour averages are shown in tabular form. (auth)

**26520** GEOMAGNETIC Sq AND $S_D$ AT SABHAWALA (DEHRA DUN) AND ALIBAG DURING 1964–65. Srivastava, B. J.; Abbas, H. (National Geophysical Research Inst., Hyderabad, India). Indian J. Radio Space Phys.; 2: No. 3, 173-176(Sep 1973).

A comparative study of the solar quiet daily magnetic variation Sq and the disturbance daily variation $S_D$, recorded at Sabhawala

(Dehra Dun) and Alibag during the quiet-sun years 1964 and 1965, is presented and the seasonal characteristics discussed. The mean Sq (H), Sq (Z), Sq (D) ranges at Sabhawala are found to be 18γ, 17γ, 3.5′ as against 35γ, 21γ, 2.7′ at Alibag. The mean $S_D$ (H), $S_D$ (Z), $S_D$ (D) ranges at Sabhawala work out as 24γ, 6γ, 0.9′ as against 21γ, 8γ, 0.8′ at Alibag. While at Alibag, the peak in Sq (H) variation is observed around 1130 LT in all the three seasons, at Sabhawala, it occurs around 1030 LT in winter, 1300 LT in equinoxes and 1400 LT in summer months. These values are also compared with the already published results of Hyderabad for 1965. The differences in Sq arise from the latitudinal separation between Alibag-Hyderabad and Sabhawala, the proximity of Sabhawala to the northern hemispheric Sq current system focus, and the coastal character of Alibag. The $S_D$ variations at the three stations show similar seasonal characteristics. (auth)

**26521 RELATIVISTIC LIGHT DEFLECTION IN ASTROMETRY.** Arifov, L.Ya.; Kadyev, R.K. (Institute of Nuclear Physics Academy of Sciences of the Uzbek SSR). Sov. Astron.—AJ 19: No. 1, 97-100 (July 1975).

A discussion is given of the influence of the relativistic effect of light deflection in the sun's gravitational field upon the results of astrometric observations. The relativistic corrections to the star coordinates and the variation of latitude are determined. A fundamentally new method is proposed for measuring absolute annual parallaxes, and a new procedure for investigating the Einstein effect by means of a physical clock. (auth)

**26522 DYNAMICS OF PARTIALLY IONIZED GAS IN THE GRAVITATIONAL FIELD OF THE SUN.** Gidalevich, E.Ya. (Ural Scientific Center, Academy of Sciences of the USSR). Sov. Astron.—AJ 19: No. 1, 54-56 (July 1975).

In this article the dynamics of the interstellar gas, partially ionized by ultraviolet solar radiation in the gravitational field of the sun, is examined. It is shown that the role of gas ionization consists in the appearance of an additional partial pressure of the ionized component of the gas side by side with the pressure of the neutral component. This leads to acceleration and, correspondingly, a cooling of the gas flow at distances on the order of 10 a.u. from the sun. A pressure curve for the interstellar gas is found. A suggestion is offered regarding the possible role of this process in in the deceleration of the solar wind. (auth)

**26523 DIRECTIVITY OF RADIATION OF LOCAL SOURCES OF THE SLOWLY VARYING COMPONENT OF SOLAR RADIO EMISSION AT 3.2 CM.** Borovik, V.N.; Gel'freikh, G.B.; Lubyshev, B.I. (Main Astronomical Observatory, Academy of Sciences of the USSR). Sov. Astron.—AJ 19: No. 1, 57-61 (July 1975).

The directivity of the radiation of 18 local sources (LS) of the sun's radio emission at 3.2 cm was studied using the Large Pulkovo radiotelescope. For eight LS connected with relatively stable sunspot groups (mainly of classes J and H of Waldmeier's classification) the dependence of the LS flux on the angular distance from the center of the disk has the nature of a cosine curve with a "cutoff" top. An east-west asymmetry is observed, manifested in the rising of the LS about a day earlier than the sunspot in the absence of an analogous afterglow at the western limb. Analogous but less clearly expressed properties of the LS are noted for unstable sunspot groups. The nature of the directivity curve found is in qualitative agreement with the theory of the thermal gyroresonance radiation of the S component of the sun's radio emission if allowance is made for the effect of the dependence of the emission coefficient on the direction and for certain properties of the model of the generation region. (auth)

**26524 MECHANISM OF FORMATION OF QUIESCENT SOLAR PROMINENCES.** Sasorov, P.V. (Moscow Physicotechnical Institute). Sov. Astron.—AJ 19: No. 1, 62-65 (July 1975).

Further study of the mechanism of formation of quiescent solar prominences suggested by Pikel'ner[1] is presented. A prominence is formed from gas flowing from the chromosphere into a region of troughs in the arches of magnetic field lines. The estimated flow of material into the prominences is $2 \cdot 10^{14}$ cm$^{-2}$sec$^{-1}$. The establishment of such a flow is studied. The mechanism given provides an explanation for the observed phenomenon of "depletion" of the corona in the neighborhood of quiescent prominences. (auth)

**26525 HYDROGEN EMISSION IN A DISINTEGRATING PROMINENCE WITH A BRIGHT BALMER CONTINUUM.** Yakovkin, N.A.; Zel'dina, M.Yu.; Rakhubovskii, A.S. (Astronomical Observatory of Kiev State University). Sov. Astron.—AJ 19: No. 1, 66-69 (July 1975).

The Balmer lines H α-H38, many metal and helium lines, and the bright Balmer continuum starting near H32 are seen in the spectrum of the prominence. The electron density $n_e = 10^{11}$ cm$^{-3}$ and the effective length $l = 3 \cdot 10^9$ cm are determined from the Stark effect and from the Saha equation for higher levels, respectively. The electron temperature $T_e = 7200$ °K is obtained by nine methods. The degree of ionization of hydrogen is less than 10%. It is shown that 80% of the emission in the Hα line is caused by scattering of photospheric radiation. The radiation temperature is determined in the Hα line (4750 °K), the *La* line (6950 °K), the Lyman continuum (6100 °K), and the Balmer continuum (2950 °K). (auth)

**26526 SYSTEMS OF LATITUDINAL STRUCTURES ON THE SUN.** Kozhevnikov, N.I. (P. K. Shternberg State Astronomical Institute). Sov. Astron.—AJ 19: No. 1, 70-73 (July 1975).

Distributions in heliographic latitude of a number of activity parameters connected with sunspots are treated by methods of spectral analysis in order to bring out periodic structures in these distributions. It is found that these distributions contain periodic components with periods on the order of 2, 4, 8, 16, and 32°. (auth)

**26527 TIME VARIATIONS IN EXTREME-ULTRAVIOLET EMISSION LINES AND THE PROBLEM OF CORONAL HEATING.** Vernazza, J.E.; Foukal, P.V.; Huber, M.C.E.; Noyes, R.W.; Reeves, E.M.; Schmahl, E.J.; Timothy, J.G.; Withbroe, G.L. (Center for Astrophysics, Harvard College Observatory and Smithsonian Astrophysical Observatory). Astrophys. J. Lett. 199: No. 2, L123-L126 (15 July 1975).

We have analyzed the time structure of the intensity of solar chromospheric and coronal extreme-ultraviolet lines, obtained by the Harvard College Observatory spectrometer aboard *Skylab*. We find changes in the intensity of up to 50 percent in times as short as 1 minute, but not periodic oscillations. Some evidence is found for the presence of shock waves in the chromosphere and the transition region. It is suggested that the solar chromosphere and corona are heated by nonperiodic waves. (auth)

**26528 THE LOCATION OF THE SITE OF ENERGY RELEASE IN A SOLAR X—RAY SUBFLARE.** Petrasso, R.D.; Kahler, S.W.; Krieger, A.S.; Silk, J.K. (American Science and Engineering, Inc., Cambridge, Massachusetts); Vaiana, G.S. Astrophys. J. Lett. 199: No. 2, L127-L130 (15 July 1975).

A rapid sequence of high-resolution X-ray photographs was obtained by the S-054 X-ray Telescope Experiment on *Skylab* on 1973 September 1. During the course of this observation, photographs were obtained of a flarelike brightening in a simple, bipolar active region. Analysis reveals the following facts. The event had the form of a small, elongated bright feature whose narrowest dimension was less than 4″ (~3000 km). The brightness peak of the flarelike brightening was located within 3″ (~2200 km) of the center of brightness of a preexisting loop structure that crossed the magnetic neutral line. This loop was observed to brighten gradually beginning approximately 10 minutes prior to the flarelike event. During the rise of the event, the 2–17 Å X-ray brightness of the center of the subflare core rose by over a factor of 10 in a time period of 196 seconds or less. If the flarelike brightening is assumed to be spatially associated with the loop, then only a restricted segment of the loop emits a substantial fraction of the total soft X-ray energy of the event. (auth)

**26529 COMMENTS CONCERNING THE PHOTOIONIZATION MODEL FOR EXCITATION OF RESONANCE LINES OF He I AND He II IN THE SOLAR CHROMOSPHERE.** Milkey, R.W. (Kitt Peak National Observatory). Astrophys. J. Lett. 199: No. 2, L131-L132 (15 July 1975).

Recently there has been much discussion of the production of the solar resonance lines of He I and He II by extreme-ultraviolet photons impinging on the upper chromosphere photoionizing He I and He II with the subsequent recombinations producing the emission lines. In this paper the consequences of this model for the emergent line profiles are examined and are shown to lead to an apparent contradiction with the observed profiles. (auth)

**26530 ON THE VARIATION OF THE SOLAR WIND VELOCITY FOLLOWING SOLAR FLARES.** Huang, Y. (Telecommunication Laboratories. Chung-Li, Taiwan, Republic of China); Lee, Y. J. Geophys. Res. 80: No. 22, 2863-2865 (1 Aug 1975).

By use of the superposed epoch method, changes in the solar wind velocity following solar flares have been investigated by using the solar wind velocity data obtained by Pioneer 6 and 7 and Vela 3, 4, and 5 satellites. A significant increase of the solar wind velocity has been found on the second day following importance 3 solar flares and on the third day following importance 2 solar flares. No significant increase of the solar wind velocity has been found for limb flares. (auth)

**26531 SOLAR MODELS OF LOW NEUTRINO-COUNTING RATE: THE DEPLETED MAXWELLIAN TAIL.** Clayton, D.D.; Dwek, E.; Newman, M.J.; Talbot, R.J. Jr. (Department of Space Physics and Astronomy, Rice University). Astrophys. J. 199: No. 2, 494-499 (15 July 1975).

We present evolutionary sequences for the Sun which confirm that the $^{37}$Cl counting rate will be much reduced if the high-energy tail of the Maxwellian distribution of relative energies is progressively depleted. If the depletion is characterized by $\exp[-\delta\,(E/kT)^2]$, the counting rate falls below 1 SNU for $\delta \geq 10^{-2}$. Observational tests of these ideas are discussed. (auth)

**26532** RADIATION PHENOMENA IN TYPE II SOLAR RADIO BURSTS AND LABORATORY SHOCK-WAVE EXPERIMENTS. Krall, N.A. (Laboratory for Applied Plasma Studies, Science Applications, Inc., La Jolla, California); Smith, D.F. Astrophys. J. 199: No. 2, 500-503 (15 July 1975).

The known spectrum of turbulence in and behind a collisionless shock wave is used to compute the relaxation of the electron distribution function in the presence of that turbulent spectrum. It is concluded that a nonthermal tail of the sort required to explain Type II solar burst radiation does not develop from the turbulent environment of a collisionless shock wave. Alternate mechanisms for the radiation are proposed, based on similar observations in laboratory experiments. (auth)

# Galaxies

*Refer also to abstracts 26333, 26336, 26340, 26350, 26383, 26399, 26400, 26442, 26456–26458, 26470, 26471, 26483, 26484, 26486–26488, 26491, 26495, and 26497.*

**26533** (IFKKI-75/5) POSSIBLE EXPLANATION FOR THE ORIGIN OF THE MAGNETIC FIELDS IN THE GALACTIC SPIRAL ARM. Bagge, E. (Kiel Univ. (F. R. Germany). Inst. fuer Reine und Angewandte Kernphysik). Apr 1975. 26p. (In German). INIS.

From 13th international conference on cosmic rays; Denver, Colo. (17 Aug 1973).

8 figs.; 5 refs.

A theory for the movement of the interstellar gas under the influence of the gravitational field in the neighbourhood of the galactic arms is developed. If this gas bears electric charges of one sign (ωsub(e) approximately 3,000 electrons/gramm) a system of electric currents is produced by the relative velocity of the galactic gas and the spiral arms for which the streamlines are concentrated a little more to the galactic plane than above and below it. By this way a large spaced magnetic field along the galactic arms is generated with opposite directions of the magnetic field vectors on the two sides of the galactic plane. (orig.)

**26534** COLLECTIVE INSTABILITIES OF SELF-GRAVITATING SYSTEMS. Infinite Homogeneous Case. Ikeuchi, S.; Nakamura, T.; Takahara, F. (Kyoto Univ. (Japan). Dept. of Physics). Prog. Theor. Phys. (Kyoto); 52: No. 6, 1807-1818(Dec 1974).

The instability modes of self-gravitating systems were investigated in comparison with electron oscillations in a plasma for the following four cases: one system of a collisionless or a hydrodynamical decription, two systems with a relative velocity of a collisionless and a hydrodynamical one, two collisionless ones, and two hydrodynamical ones. The fundamental unstable mode is the Jeans instability, but for the coexistence of two systems, the critical Jeans length becomes longer due to the stabilization effect of relative velocity. Moreover, when the relative velocity is higher than a certain value, each system becomes independently unstable for the Jeans mode and they appear as overstable modes. On the other hand, the Landau instability occurs only in the system of a collisionless and hydrodynamical description, in contrast with a plasma case where the Landau mode appears in a two-collisionless system as well. The condition for the occurrence of the Landau mode is obtained as the existence of the distribution function with velocity dispersion and the repulsive force (or effect). In relation to the density wave theory of spiral arms, the Landau growing mode in a stellar and gaseous system is discussed. (auth)

**26535** HEAT BALANCE STATE OF THE INTERSTELLAR GAS. Dependences on the Amount of Cooling- and Heating-Agencies. Sato, T. (Kyoto Univ. (Japan). Dept. of Physics). Prog. Theor. Phys. (Kyoto); 52: No. 4, 1174-1187(Oct 1974).

The properties of the interstellar gas in which the heating balances the cooling (the heat balance state) are investigated for the temperature range $30K < T < 10^8K$ taking the abundance of heavy elements and the flux of low energy cosmic rays as parameters. The temperature and the pressure of the gas in a heat balance state are investigated as functions of the density for various values of these parameters, and it is found that the interstellar medium can take the so-called two-phase structure for wide ranges of these parameters and almost all stages of the galactic evolution. The growth time of the thermal instability is investigated and found to be short enough to realize the two-phase structure except for the case of a very small flux of low energy cosmic rays with the ionization rate of hydrogen less than $10^{-19}$ sec$^{-1}$. The gas without heavy elements can also have a two-phase structure if more than 0.1 per cent of its hydrogen is in molecular form. This may be significant for star formation at very early stages of galactic evolution. The phase transition between the two stable phases driven by variation of the flux of low energy cosmic rays is discussed and it is suggested that this phase transition controls the star formation in a galaxy. (auth)

**26536** HARD X—RAY OBSERVATIONS OF NGC 4151. Baity, W.A.; Jones, T.W.; Wheaton, W.A.; Peterson, L.E. (University of California, San Diego). Astrophys. J. Lett. 199: No. 1, L5-L8 (1 July 1975).

The X-ray source 3U 1207+39, associated with the Seyfert galaxy NGC 4151, has been scanned repeatedly by the UCSD X-ray telescope on board the OSO-7 satellite. A weak source with a hard spectrum has been unambiguously detected in this region in 1972 October, and with lesser statistical significance at other times between 1971 November and 1973 May. The photon spectrum in the 7- keV range is best fitted by a power law of the form $dN/dE=0.012\ E^{-1.1\pm0.2}$ photons cm$^{-2}$ s$^{-1}$ keV$^{-1}$, consistent with the *Uhuru* measurement in the 2–6 keV range. The hard spectrum observed and very short electron lifetimes implied severely constrain nonthermal models for the emission. An extremely hot gas, $T \geq 10^9$ K, is also consistent with the observations. (auth)

**26537** LIMITS TO THE NEUTRAL HYDROGEN CONTENT OF ELLIPTICAL GALAXIES. Shostak, G.S.; Roberts, M.S. (National Radio Astronomy Observatory, Charlottesville, Virginia 22901); Peterson, S.D. Astron. J. 80: No. 8, 581-583 (Aug 1975).

Upper limits to the H I content of 15 elliptical galaxies are presented. These limits are typically $\sim 10^8$ $M_\odot$, assuming a rectangular 21-cm profile with 330-km sec$^{-1}$ width. The effects of alternative line shapes and widths on the derived hydrogen mass are considered, and explanations for the lack of detected H I are reviewed. (auth)

**26538** COMPARISON OF NEW 12-cm RADIAL VELOCITIES WITH VVO OPTICAL RADIAL VELOCITIES OF GALAXIES. Dickel, J.R. (Department of Astronomy, University of Illinois, Urbana, Illinois 61801); Rood, H.J. Astron. J. 80: No. 8, 584-586 (Aug 1975).

21-cm radial velocities ($V_{21}$) are given for nine galaxies with optical radial velocities ($V_{CR}$) published by Chincarini and Rood (1972a,b). The statistic, $V_{CR}-V_{21}$, has an average value of $4\pm19$ km sec$^{-1}$ and a standard deviation of $52\pm13$ km sec$^{-1}$. The 21-cm radial velocity for NGC 4670 is 106 km sec$^{-1}$ smaller than the optical radial velocity derived by Kintner (1971). (auth)

**26539** INTERSTELLAR MEDIUM: UV COMPLEX INDEX OF REFRACTION OF SEVERAL CANDIDATE MATERIALS. Egan, W.G.; Hilgeman, T. (Research Department, Grumman Aerospace Corporation, Bethpage, New York 11714). Astron. J. 80: No. 8, 587-594 (Aug 1975).

Ultraviolet determinations have been made of the optical complex index of refraction of augite, bytownite, enstatite, diopside, troilite, pyrrhotite, and the Bruderheim meteorite and the results have been used in a Mie scattering program. From this analysis, bytownite and meteorite particles of radii between 0.1 and 0.001 μm could account for the interstellar extinction peak at 0.22 μm; however, both of these materials would produce a double peak at 0.22 μm. The splitting for the meteoritic material is stronger than that of the bytownite, and thus harder to reconcile to the interstellar extinction. Enstatite is improbable because the absorption maximum occurs at ~0.26 μm. The other samples also do not have appropriate absorption curves and are ruled out. (auth)

**26540** ON THE ORION INFRARED NEBULA/MOLECULAR CLOUD. Zuckerman, B. (University of California, Berkeley); Palmer, P. Astrophys. J. Lett. 199: No. 1, L35-L38 (1 July 1975).

Observational and theoretical studies of the Orion Nebula and the associated molecular clouds have greatly increased our understanding of this and other regions in which star formation is taking place. Fundamental questions remain unanswered; and in this *Letter* we address three of them: (1) the chemical composition of the molecular cloud, (2) its internal motions, and (3) the role of magnetic fields in its evolution. We show that the gas phase chemistry and internal motions in one part of the cloud are distinctly different from those in the rest of the cloud, and two recent estimates of the magnetic field strengths are very uncertain. (auth)

**26541** FURTHER EVIDENCE FOR MAGNETISM IN THE ORION REGION. Chaisson, E.J. (Center for Astrophysics, Harvard College Observatory and Smithsonian Astrophysical Observatory); Beichman, C.A. Astrophys. J. Lett. 199: No. 1, L39-L42 (1 July 1975).

Observations of two transitions ($F=1\rightarrow1$, 1665 MHz, and $F=1\rightarrow2$, 1612 MHz) within the $^2\Pi_{3/2}$, $J=3/2$ state of interstellar OH illustrate near classic Zeeman patterns strongly suggestive of a magnetic field of several milligauss, at least within the vicinity of the Orion maser source. (auth)

**26542** OBSERVATIONS OF STARLIGHT-EXCITED LINES IN THE ORION NEBULA. Grandi, S.A. (Steward Observatory, University of Arizona). Astrophys. J. Lett. 199: No. 1, L43-L46 (1 July 1975).

Image tube spectra have been obtained of the Orion Nebula for wavelengths between 5000 and 9000 Å. Permitted lines of N I and O I are identified and are explained by direct starlight excitation. (auth)

**26543** 3C 123: A DISTANT FIRST-RANKED CLUSTER GALAXY AT $z$=0.637. Spinrad, H. (Department of Astronomy, University of California, Berkeley). Astrophys. J. Lett. 199: No. 1, L3-L4 (1 July 1975).

Spectra of the very faint cluster galaxy and radio source 3C 123 yield a redshift $z$=0.637. The optical spectrum, morphological type, approximate absolute magnitude, and cluster membership strongly suggest 3C 123 to be an optical object more distant, but very similar to, 3C 295. The radio source is a little larger and intrinsically more powerful than Cgynus A. (auth)

**26544** THE INFRARED SPECTRUM OF NGC 1068. Rieke, G.H.; Low, F.J. (Steward Observatory and Lunar and Planetary Laboratory, University of Arizona). Astrophys. J. Lett. 199: No. 1, L13-L17 (1 July 1975).

New infrared photometry of NGC 1068 shows that the spectrum continues to rise smoothly through 34 μ and that there is a shallow absorption feature near 10 μ. The total infrared flux from the nuclear source is about $2.3\times10^{-11}$ W m$^{-2}$, which corresponds to a luminosity of $10^{11}$ $L_\odot$ at a distance of 11 Mpc. (auth)

**26545** REDSHIFTS AND MORPHOLOGY OF GALAXIES IN THE COMA CLUSTER. Gregory, S.A. (Steward Observatory). Astrophys. J. 199: No. 1, 1-9 (1 July 1975).

By new observations of redshift and morphology, a sample of galaxies brighter than $m_p$=15.8 is nearly completed out to radial distance of 2.79 from the center of the Coma cluster. The redshift results show that the line-of-sight velocity dispersion first decreases and then increases again with distance from the cluster center with a mean value of $\sigma_r$=896 km s$^{-1}$. A marginally positive test for solid body rotation of 85±66 km s$^{-1}$ degree $^{-1}$ is also found. These results are consistent with numerical models of partially relaxed systems. The morphological study shows that the relative number of spiral and irregular galaxies increases with radial distance. This seems consistent with the existence of a hot intracluster medium. However, an alternative view, that the elliptical and spiral galaxies form independent systems, cannot be excluded at this time. (auth)

**26546** RADIO GALAXIES IN THE COMA CLUSTER. Tifft, W.G.; Tarenghi, M. (Steward Observatory, University of Arizona, Tucson). Astrophys. J. 199: No. 1, 10-15 (1 July 1975).

Redshifts for 23 possible radio galaxies with $m_p<17$ in the field of the Coma cluster are reported and discussed. Of the 16 most likely cluster members, half are nonelliptical galaxies with emission lines in their spectra, and the remainder are non-emission-line for E or S0 galaxies. Except for the two of the weakest sources, the galaxies have redshifts which average 600 km s$^{-1}$ greater than the cluster mean. The excess redshift does not appear to depend upon emission-line properties or distance from the cluster center. The non-emission-line galaxies are brighter both optically and at radio wavelengths than the emission-line objects. A direct correlation of radio magnitude and redshift appears to exist for the non-emission-line radio sources. (auth)

**26547** THE NGC 507 CLUSTER OF GALAXIES. Tifft, W.G.; Hilsman, K.A. (Steward University, University of Arizona, Tucson); Corrado, L.C. Astrophys. J. 199: No. 1, 16-18 (1 July 1975).

Redshifts and accurate positions for galaxies in the core of the NGC 507 group are presented. The group is shown to be closely similar to other groups of galaxies located nearby, including the Perseus cluster. A conventional viral analysis shows the usual excess kinetic energy. The redshift-magnitude diagram is consistent with the presence of bands. (auth)

**26548** EMISSION-LINE LUMINOSITIES OF SEYFERT GALAXIES. Adams, T.F. (Yerkes Observatory, The University of Chicago); Weedman, D.W. Astrophys. J. 199: No. 1, 19-30 (1 July 1975).

New observations of emission-line intensities are presented for 32 Seyfert galaxies. On the basis of correlations among these intensities and continuum properties inferred from *UBV* photometry, we conclude that class 1 Seyfert galaxies (those with broad Balmer line wings) are ionized by a strong radiative source and are not significantly reddened by dust. The intrinsic Hα luminosities of the nuclei range from $10^{42}$ to $10^{43}$ ergs s$^{-1}$, corresponding to a range in $M_U$ from -16 to -22.5, and a range in $M_V$ from −16 to −22. Other properties of the nuclei do not seem to be dependent on luminosity. For class 2 Seyfert galaxies (those resembling NGC 1068), the intrinsic $L$ (Hα) after correction for dust reddening are comparable to those of class 1, but the forbidden line luminosities are typically 30 times stronger in class 2. We conclude that the properties of class 2 nuclei could be explained by the presence of large numbers of very hot, luminous stars substantially reddened by dust. However, it is still not possible to explain class 1 nuclei in this manner, and we make no progress in explaining the intense sources of radiation in these nuclei. (auth)

**26549** INTERSTELLAR FORMALDEHYDE NEAR STARS OF THE ORION POPULATION. Dieter, N.H. (Radio Astronomy Laboratory, University of California, Berkeley). Astrophys. J. 199: No. 1, 289-296 (1 July 1975).

Interstellar formaldehyde absorption lines have been detected in the direction of 100 Orion-population stars. The low angular resolution of this survey prevents discerning any *direct* connection between these young stars and the gas surrounding them, but does allow establishing that the dust clouds in which they have formed are different from quiescent clouds. In these regions of recent star formation, there is a higher percentage of relatively strong $H_2CO$ lines, which can be explained by a difference in their density and/or temperature gradients. A further indication of the effect on the dust clouds of the formation of stars lies in the velocity dispersion of the formaldehyde lines. Dust clouds containing very young clusters (with no visible early-type stars) have broader lines. The Orion Nebula region show a significant difference in the dispersions measured near the center and at the periphery. (auth)

**26550** OBSERVATIONS OF NGC 6764, A BARRED SEYFERT GALAXY. Rubin, V.C.; Thonnard, N.; Ford, W.K. Jr. (Department of Terrestrial Magnetism, Carnegie Institution of Washington). Astrophys. J. 199: No. 1, 31-38 (1 July 1975).

Spectra of NGC 6764, a previously unstudied barred spiral galaxy, reveal strong asymmetrical emission lines from the semistellar nucleus. Permitted and forbidden lines are about 750 km s$^{-1}$ wide, which identify the galaxy as a Seyfert galaxy. Spectra in several position angles suggest that discrete gas clouds just outside the nucleus have both tangential and radial components of motion. (auth)

**26551** EVIDENCE FOR CONTRACTION IN THE NUCLEAR RING OF THE BARRED SPIRAL GALAXY NGC 3351. Rubin, V.C.; Ford, W.K. Jr.; Peterson, C.J. (Department of Terrestrial Magnetism, Carnegie Institution of Washington). Astrophys. J. 199: No. 1, 39-48 (1 July 1975).

The nucleus of the barred spiral galaxy NGC 3351 consists of a ring of low-excitation H II regions. Line-of-sight velocities around the ring indicate a well-defined sinusoid, but with maximum and minimum velocities displaced about 20° from that predicted from the geometry of the outer galaxy. One simple interpretation is that the nuclear ring is a circle in the plane of the galaxy which is rotating and contracting with $V_{rot}$=126±16 km s$^{-1}$ and $V_{con}$=34±11 km s$^{-1}$ at $R$=340 pc. Other possible interpretations are also discussed. (auth)

**26552** CARBON MONOXIDE IN COLLAPSING INTERSTELLAR CLOUDS. de Jong, T.; Chu, S.; Dalgarno, A. (Center for Astrophysics, Harvard College Observatory). Astrophys. J. 199: No. 1, 69-78 (1 July 1975).

We have calculated the energy loss rates, the brightness temperatures and the profiles of lines of carbon monoxide in collapsing interstellar clouds. The most recent data for the $H_2$—CO collision rates have been used in the calculations; a useful extrapolation of these data to high $j$ levels is given. The density distribution and the velocity field inside the cloud are varied, one model applying to a cloud of uniform density that is collapsing in free fall, and a second to a cloud in isothermal collapse. Analytical relations for total CO cooling at low and high densities are derived. The effects of varying the cross sections and the density distribution, the velocity field, and the geometry of the clouds are discussed. The line profiles are a sensitive tool for testing the models against the observations. The observed CO lines can be explained by collapsing models in which both density and velocity gradients occur. The intensity ratio of the $j$=2→1 and the $j$=1→0 CO lines in Orion is consistent with such models. We predict that CO infrared line from dense interstellar clouds should be observable with instruments of high spectral resolution at wavelengths longward of 200 microns. (auth)

**26553** CO, CS, AND HCN IN A CLUSTERING OF REFLECTION NEBULAE IN MONOCEROS. Kutner, M.L. (Physics Department, Columbia University); Tucker, K.D. Astrophys. J. 199: No. 1, 79-85 (1 July 1975).

Carbon monoxide line emission at λ=2.6 mm has been observed over an area of ~3 1/2°×3 1/2° in L1646, a diffuse dust cloud containing a grouping of reflection nebulae. The $H_2$ mass is estimated from the CO observations to be $>3.2\times10^4$ $M_\odot$. Five CO emission peaks are observed, each apparently associated with at least one reflection nebula, with the strongest peak at α (1950) = 6$^h$05$^m$20$^s$, δ (1950) = −6°22′30″. Around this position, extended (10′×10′) emission is observed from HCN and CS, suggesting a core with $H_2$ density $\lesssim 8\times10^4$ cm$^{-3}$. This core appears to be rotating with $\Omega \geq 7.4\times10^{-14}$ s$^{-1}$. There is also evidence for self-absorption in the CO line in this direction, suggestive of a collapsing cloud. (auth)

**26554** OBSERVATIONS OF THE POLARIZATION CHARACTERISTICS OF GALACTIC $H_2O$ SOURCES. Bologna, J.M.; Johnston, K.J.; Knowles, S.H.; Mango, S.A.; Sloanaker, R.M. (E. O. Hulburt Center for Space Research, Naval Research Laboratory, Washington, D.C.). Astrophys. J. 199: No. 1, 86-91 (1 July 1975).

Twenty-four $H_2O$ sources associated with H II regions have been examined for circular and linear polarization. No circular polarization

was found in any source. Approximately 25 percent have been found to show linear polarization in at least some features. The percent polarization in W75 S varied in the same sense as the intensity, while the position angle of the polarized radiation remained constant. This, together with the fact that 25 percent of the sources show linear polarization, indicates that the cross-relaxation rate of maser-level degenerate substates via infrared line radiation is almost equal to the stimulated emission rate in many $H_2O$ sources. (auth)

**26555** MICROWAVE DETECTION OF INTERSTELLAR HDO. Turner, B.E. (National Radio Astronomy Observatory, Charlottesville, Virginia 22901); Zuckerman, B.; Fourikis, N.; Morris, M.; Palmer, P. Astrophys. J. Lett. 198: No. 3, L125-L128 (15 June 1975).

The $1_{11}$–$1_{10}$ transition of singly deuterated water has been detected in emission at the wavelength of 3.72 mm toward the Kleinmann-Low nebula (KL) in Orion A. This is probably the first observation of nonmaser (i.e., low brightness temperature) emission from interstellar water molecules. Analysis indicates that most of the oxygen in KL is probably contained in water molecules if $[HDO]/[H_2O] \simeq [D]/[H]$, but not if $[HDO]/[H_2O] > [D]/[H]$. The HDO line shape is different from that of other molecules previously observed toward KL. (auth)

**26556** STUDIES OF THE INFRARED SOURCE CRL 2688. Ney, E.P. (School of Physics and Astronomy, University of Minnesota); Merrill, K.M.; Becklin, E.E.; Neugebauer, G.; Wynn-Williams, C.G. Astrophys. J. Lett. 198: No. 3, L129-L134 (15 June 1975).

Infrared, optical, and radio observations are described of a newly discovered galactic infrared source. Most of the radiation comes from 1.″5 diameter infrared source at a temperature of about 150 K, but some visible emission in the form of a symmetrical highly polarized reflection nebulosity is also seen. The object could represent either a very early or a very late stage in stellar evolution. (auth)

**26557** SPECTROSCOPIC OBSERVATIONS OF CRL 2688. Crampton, D.; Cowley, A.P. (Dominion Astrophysical Observatory); Humphreys, R.M. Astrophys. J. Lett. 198: No. 3, L135-L137 (15 June 1975).

Spectra of the visible objects at the position of the infrared source CRL 2688 indicate that these are nebulosities reflecting the light of an obscured F5 Ia star. Apart from this apparently normal spectrum, strong absorption features identified as molecular $C_3$ and emission lines identified as molecular $C_2$ and [S II] are observed. Our observations suggest that an F5 Ia star surrounded by a dense shell is at the position of the infrared source. (auth)

**26558** TIME VARIATIONS AND SPECTRAL STRUCTURE OF THE METHANOL MASER IN ORION A. Barrett, A.H.; Ho, P.; Martin, R.N. (Department of Physics and Research Laboratory of Electronics, Massachusetts Institute of Technology). Astrophys. J. Lett. 198: No. 3, L119-L122 (15 June 1975).

Temporal variations have been detected in the $CH_3OH$ emission from Orion A over the period from 1973 December to 1974 December, in the $J=4$, 5, 6, and 7 transitions. Temporal variations are one of the classical symptoms of astrophysical masers. Observations with a resolution of 0.12 km s$^{-1}$ show that these transitions are composed of at least six features. (auth)

**26559** THE CORONA OF THE GIANT SPIRAL GALAXY NGC 253. Freeman, K.C.; Carrick, D.W.; Craft, J.L. (Mount Stromlo and Siding Spring Observatory, Research School of Physical Sciences, Australian National University). Astrophys. J. Lett. 198: No. 3, L93-L96 (15 June 1975).

Giant spirals may have coronae with masses of order $10^{12}$ to $10^{13}$ $M_\odot$ and radii up to about 1 Mpc. Deep surface photometry of the giant spiral NGC 253 shows that the total photographic luminosity $L$ of its corona is unlikely to exceed $3.10^9$ $L_\odot$. If its corona is typical of those postulated by Ostriker *et al.*, then its $M/L$ ratio exceeds 600. If the picture proposed by Einasto *et al.* is more appropriate, then its $M/L$ exceeds 5800. (auth)

**26560** SOUTHERN GALAXY CLUSTERS INDENTIFIED WITH 3U X—RAY SOURCES. Melnick, J. (Departamento de Astronomía, Universidad de Chile, Santiago, Chile); Quintana, H. Astrophys. J. Lett. 198: No. 3, L97-L99 (15 June 1975).

Plate inspection of fields within the error boxes of three high-latitude sources have been made. For two fields, more than one cluster of galaxies might be associated with the source. A morphology-luminosity criterion recently proposed is not sufficient to discriminate between the candidates. (auth)

**26561** PHYSICAL CONDITIONS AND STRUCTURE IN NGC 7293, "THE HELIX". Warner, J.W.; Rubin, V.C. (Department of Terrestrial Magnetism, Carnegie Institution of Washington). Astrophys. J. 198: No. 3, 593-603 (15 June 1975).

Image-tube interference filter photographs and spectra are presented for NGC 7293, the "Helix" planetary nebula. Extinction values, and electron temperatures and densities, are derived for 12 points in the central region and in the bright SW filament. Temperatures derived from the $I_{5755}/I_{6548+6584}$ ratio are larger than expected if efficient cooling by forbidden radiation occurs in the nebula. This ratio is explained by assuming the existence of pockets of matter with high electron density ($10^5$–$10^6$ cm$^{-3}$) within the low-density ($\lesssim 300$ cm$^{-3}$) central zone. Such a hypothesis is perhaps consistent with the compact, presumably cold, neutral globules seen on high-resolution photographs of the object. Electron densities within the SW filamentary zone vary from a value of $\leq 300$ cm$^{-3}$, coinciding with the peak [O I] emission, to 1200 to 2000 cm$^{-3}$ on the outer and inner edges of the maximum [O I] surface brightness. Variable extinction is found across the face of the nebula, reaching nearly 2 mag at $H\beta$ at some points. The structure of the nebula probably consists of two or three rings of low-ionization material surrounding a higher ionization zone. The appearance of the object in the light of [O I] 6300 Å and the lack of adequate evidence from velocity data suggest that a true helical interpretation is not realistic. (auth)

**26562** THEORETICAL EMISSION LINE PROFILES IN QSOs AND SEYFERT GALAXIES. Blumenthal, G.R.; Mathews, W.G. (Lick Observatory, Board of Studies in Astronomy and Astrophysics, University of California, Santa Cruz). Astrophys. J. 198: No. 3, 517-526 (15 June 1975).

The gas responsible for the observed emission line spectra in QSOs and Seyfert galaxies is assumed to be in the form of small clouds which can be accelerated to high velocities by ultraviolet radiation from a small central source. The ionized clouds can be contained to very high densities ($n \gtrsim 10^8$ cm$^{-3}$) by high-pressure intercloud medium similar to those thought to exist in many compact radio sources. We show that for lines produced by recombination, the outward motion of the cloud system generates a logarithmic emission line profile which is independent of the mass distribution of the clouds, the change in the gas density and temperature in the clouds, and the initial location of the cloud-forming region. The logarithmic profile agrees very well with three symmetric profiles recently observed by Baldwin, except (as expected) in the cores of the lines and occasionally in the far wings. We discuss how the basic logarithmic line profile is influenced by drag, gravity, and chemical compositions, dust, and other effects, some of which may account for the deviations of the observed profiles from the logarithmic form. (auth)

**26563** AN H I STUDY OF Scd GALAXIES. Shostak, G.S. (National Radio Astronomy Observatory, Charlottesville, Virginia). Astrophys. J. 198: No. 3, 527-536 (15 June 1975).

H I line profiles, together with derived redshifts and integral properties, are presented for 46 Scd galaxies. The profile shapes are quite regular, with a double-peaked structure characteristic of galaxies with flat rotation curves. The ratios $M_{HI}/M_T$ and $M_{HI}/L_{pg}$, which are known to vary with Hubble type, have observed dispersions of ±80 percent within this classification, with intrinsic dispersions being probably less than ±50 percent. This establishes that integral property ratios are substantially homogeneous within the Scd classification. No indication of H I optical-depth effects with inclination is observed. Evidence is presented that distances derived solely from redshifts have an average uncertainty of $<0.8$ mag in the distance modulus. (auth)

**26564** FINE-SCALE STRUCTURE OF CARBON MONOXIDE EMISSION OBSERVED IN THE DIRECTION OF THE GALACTIC NUCLEUS. Liszt, H.S.; Sanders, R.H.; Burton, W.B. (National Radio Astronomy Observatory, Green Bank, West Virginia). Astrophys. J. 198: No. 3, 537-544 (15 June 1975).

Preliminary results are reported of a fine-scale survey of the Sgr A molecular cloud complex in the 2.6-mm line of carbon monoxide. Twenty-one spectra were observed on a 1′ grid over the velocity range $-250 < V < 250$ km s$^{-1}$, with a velocity resolution of 0.65 km s$^{-1}$ and an angular resolution of 1′. These observations contain no evidence that galactic rotation is the dominant factor in determining the kinematic characteristics of CO located within a few arcminutes of the galactic center; similarly no evidence is found here for a rapidly rotating disk of molecular gas in the core of the Galaxy. CO emission is weak in the direction of the thermal component Sgr A West relative to the emission from the direction of the nonthermal source Sgr A East. Thus the distribution of the major CO emission features correlates well with that of the 6-cm $H_2CO$ features observed by Whiteoak *et al.*; the structure of the Sgr A molecular cloud complex is discussed in terms of this correlation. Several of the CO spectra show a feature at zero velocity which we interpret as due to absorption by a cold (~2.7 K) molecular cloud situated between the Sun and the strongly emitting nuclear complex. (auth)

**26565** INVESTIGATION OF LOW-LATITUDE HYDROGEN EMISSION IN TERMS OF A TWO-COMPONENT INTERSTELLAR GAS MODEL. Baker, P.L. (Radio Astronomy Branch, Laboratory for Extraterrestrial Physics, Goddard Space Flight Center, Greenbelt, Maryland); Burton, W.B. Astrophys. J. 198: No. 2, 281-297 (1 June 1975).

The high-resolution 21-cm hydrogen line observations at low galactic latitude of Burton and Verschuur have been analyzed to determine the large-scale distribution of galactic hydrogen. The distribution parameters are found by model fitting; that is, a set of parameters is first assumed, synthetic line profiles are then generated, and finally a correction to the parameters is found by comparison of synthetic and observed profiles.

Optical depth effects, which should not be ignored at low galactic latitudes, have been computed using a two-component gas model suggested by 21-cm line observations of absorption features and of high-latitude emission features. Our analysis shows that a multiphase description of the medium is entirely consistent with and in fact essential to the interpretation of low-latitude emission observations. Where possible, the number of free parameters in the gas model has been reduced by the adoption of values obtained from other lines of evidence. Calculations were also performed for a one-component, uniform spin temperature, gas model in order to show the systematic departures between this model and the data caused by the incorrect treatment of the optical depth effect. In the two-component gas, radiative transfer is treated by a Monte Carlo calculation since the opacity of the gas arises in a randomly distributed, cold, optically thick, low velocity-dispersion, cloud medium. The emission arises in both the cloud medium and a smoothly distributed, optically thin, high velocity-dispersion, intercloud medium. The synthetic profiles computed from the two-component model reproduce both the large-scale trends of the observed emission profiles and the magnitude of the small-scale emission irregularities. The analysis permits the determination of values, corrected for optical depth effects, for the thickness of the galactic hydrogen disk between half density points—280 pc for the intercloud medium and 190 pc for the cloud medium for $R < 10$ kpc—the total observed neutral hydrogen mass of the Galaxy—$1.2 \times 10^9\ M_\odot$ of the background gas and $1.4 \times 10^9\ M_\odot$ of clouds—and the central number density of the intercloud hydrogen atoms—0.17 $cm^{-3}$. In addition, the analysis is sensitive to the size of clouds contributing to the observations. Typically, clouds must be greater than 1 pc in diameter but less than 13 pc; the best fit diameter is 5 pc. Computations also show that synthetic emission profiles based on the two-component model display both the zero-velocity and high-velocity ridges, indicative of optical thinness on a large scale, in spite of the presence of optically thick gas. In this and in other respects, the compatibility of emission and absorption hydrogen observations are emphasized. (auth)

**26566** ON THE NATURE OF THE INTERCLOUD MEDIUM. Hill, J.K.; Silk, J. (Department of Astronomy, University of California, Berkeley). Astrophys. J. 198: No. 2, 299-306 (1 June 1975).

Earlier interpretation of the *Copernicus* observations of interstellar absorption lines in the spectra of unreddened stars are reviewed in the context of steady-state ionization models of the low-density (intercloud) component of the interstellar medium. Except for the highest ionization states (which may be produced in the immediate vicinity of the central star), a simple homogeneous model is described that accounts satisfactorily for the interstellar lines of H, C, N, S, and Si observed in the spectrum of λ Sco in terms of an extensive low-density medium that is photoionized by Lyman continuum radiation from the II Sco OB association. Quantitative constraints are given on the maximum permissible flux of diffuse soft X-radiation. This model is generalized to provide an interpretation of the observed ion, electron, and hydrogen column densities in the low-density interstellar medium. It is that severe constraints on ionization models are imposed by the ratios Si III/Si, Si IV/Si, and S IV/S. We conclude that the observations can be adequately explained if between 10 and 30 percent of a representative line of sight passes through a photoionized medium of density 0.1—0.2 $cm^{-3}$; the bulk of the gas along the line of sight is H I, and can either be at a similar density, in which case the mean primary soft X-ray ionization rate cannot exceed $1 \times 10^{-18}\ s^{-1}$ (H atom)$^{-1}$, or else it must be in shielded clumps or clouds. (auth)

**26567** ON THE IONIZATION OF THE INTERCLOUD MEDIUM BY RUNAWAY O-B STARS. Thuan, T.X. (Princeton University Observatory). Astrophys. J. 198: No. 2, 307-329 (1 June 1975).

The H II regions around high-velocity stars of type O5 to B1 are studied, with "on the spot" reabsorption assumed for the diffuse ultraviolet radiation, but with time-dependent cooling and recombination behind the star considered. Ratios of column densities integrated through the H II regions are given for stationary and moving stars. For a star with $T_* = 35{,}000$ K, moving with $v_* = 50$ km $s^{-1}$ in a uniform medium in which the hydrogen is neutral, with $n$ (H) $= 0.1$ atom $cm^{-3}$, steady state is reached after $2.6 \times 10^6$ years. In front of the star the equality of photon and particle fluxes across the ionization front places this front at 140 pc compared with 190 pc when $v_* = 0$. The transition from completely ionized to completely neutral is sharp (~1 pc), the optical depth at the edge is small, and the ratio N I/N II is 11 times smaller than its value at $v_* = 0$. In back, the H II region is elongated (~265 pc), the optical depth is large, and, in the absence of ionizing photons, recombination produces a gradual transition from H II to H I (~100 pc); the ratio N I/N II is 2.3 times greater than its value with the star at rest. Shock waves are confined in the back, are of short duration ($\sim 5 \times 10^5$ years), and are not likely to affect the overall development of the H II region. The total volume ionized is practically independent of the velocity of the star. Global properties of the intercloud medium are discussed. It is found that the presence of clouds may reduce the volume ionized by runaway stars by as much as a factor of 7 and that as much as 30 percent of the total ionizing radiation from early-type stars may leak out of the Galaxy. The Copernicus observations are consistent with the lines of sight crossing only the H II regions around the observed stars and a neutral ICM and with the existence of a "hole" in the distribution of O—B5 stars in the vicinity of the Sun. (auth)

**26568** MOLECULE-DUST CORRELATIONS IN DARK CLOUD KHAVTASSI 3. Myers, P.C. (Research Laboratory of Electronic, Massachusetts Institute of Technology). Astrophys. J. 198: No. 2, 331-348 (1 June 1975).

Mapping observations of microwave spectral lines of $H_2CO$, OH, and H toward the dark cloud Kh 3 are reported. For each species, comparison is made between column density $N$, excitation temperature $T_{ex}$, and red extinction $A$, determined from star counts. Stars were counted in resolution elements which coincide with beam size and position for each microwave spectrum taken. It is found for $T_{ex}$ assumed independent of $A$, $N$ increases with $A$ strongly for $H_2CO$, increases moderately for H, and is independent of $A$ for OH. For $N$ assumed independent of $A$, $T_{ex}$ decreases strongly with $A$ for $H_2CO$, decreases moderately with $A$ for H, and is independent of $A$ for OH. The observed correlations are discussed in terms of "coupling parameters" $\chi(N) = (\partial N/\partial A)/N$ and $\chi(T_{ex}) = (\partial T/\partial A)/T_{ex}$. Models of abundance and collisional transition excitation are used to predict values of $\chi(N)$ and $\chi(T_{ex})$, which are compared for consistency with the present observations. For $H_2CO$, abundance prediction based on ion-molecule reactions gives better consistency than abundance predictions based on molecule formation on grain surfaces. For either abundance model, coupling of cloud temperature to extinction, $\chi(T)$, required for consistency between model predictions and observations, differs significantly from one species to the next. This may indicate variation in spatial extent from one species to the next, and/or model inaccuracies. Assumption of the same $\chi(T)$ for each species gives most plausible results when $\chi(T) \leq 0$, indicating either an isothermal or cool-core cloud. In that case, the observations imply strong coupling of $H_2CO$ to $A$, moderate to zero coupling of H to $A$, and zero to negative coupling of OH to $A$. (auth)

**26569** ON THE INTENSITIES OF DECIMETRIC-WAVELENGTH RADIO RECOMBINATION LINES. Parrish, A. (National Radio Astronomy Observatory, Green Bank, West Virginia); Pankonin, V. Astrophys. J. 198: No. 2, 349-354 (1 June 1975).

We summarize the intensity results of some of the 221 and 248α recombination-line observations taken with the Arecibo telescope, and report additional results including 166α observations from the NRAO 300-foot (91 m) telescope. The brightness temperatures of these lines increase sharply with wavelength. We show that these results require that the upper levels of the recombining atoms be overpopulated with respect to LTE conditions. The most reasonable interpretation of the results is that the line emission at these decimetric wavelengths is stimulated by a background source of continuum radiation. (auth)

**26570** CORE RADII AND CENTRAL DENSITIES OF 15 RICH CLUSTERS OF GALAXIES. Bahcall, N.A. (Princeton University Observatory). Astrophys. J. 198: No. 2, 249-254 (1 June 1975).

The projected galaxy distributions and centers are determined for 15 rich regular clusters of galaxies with redshifts up to about 0.1. The distributions are given for approximately the same fixed range of magnitudes. The galaxy distributions in all the clusters are similar and resemble the distribution of a projected, bounded, Emden isothermal gas sphere. The core radii obtained for the distributions exhibit a relatively small dispersion (±15%) around a constant linear value of $R_c = 0.25$ Mpc ($H_0 = 50$ km $s^{-1}$ $Mpc^{-1}$). This result suggests that the extension of the present study to high-redshift clusters, comparing their core radii with the low redshift values, will enable one to place some constraints on the cosmological deceleration parameter, $q_0$. The central densities, in galaxies per cubic Mpc, are also calculated and are found to be similar for the 15 cluster studied. Their values all lie in the range of 200±100 galaxies per $Mpc^3$, to the limit of 3 mag (±1 mag) below the third brightest galaxy of each cluster. (auth)

**26571** THE BROAD COMPONENT OF HYDROGEN EMISSION LINES IN NUCLEI OF SEYFERT GALAXIES: COMMENTS ON A CHARGE EXCHANGE MODEL. Katz, A. (Washburn Observatory, University of Wisconsin-Madison). Astrophys. J. 198: No. 2, 255-260 (1 June 1975).

A model to account for the broad hydrogen line emission from the nuclei of Seyfert galaxies based on charge exchange and collisional processes, as proposed by Ptak and Stoner is investigated. The model consists of a source of fast ($E \sim 10^3$ eV) protons streaming through a medium of quiescent gas. One of the major problems that results from such a model concerns the strong narrow hydrogen line core that would be produced, in direct conflict with the observations. The lines cannot arise from gas arranged throughout a spherical volume surrounding the source of the fast particles because the fast protons would produce far more ionizations than the possible number of recombinations. A very dense shell source of less than 1 AU in thickness and at least several tens of parsecs in radius must be invoked to reproduce the asymmetric broad profiles observed. There must be absorption throughout the center of the shell to account for the line profiles. The gas cannot be arranged in dense clumps throughout a large volume because momentum exchange of the gas with the primary particles would quickly accelerate any

clumps. The energy balance and energy requirements of such a model are investigated, and it is found that an energy equal to or greater than the total luminosity of most Seyfert galaxies is required to produce the hydrogen line alone. The gas must be mostly neutral and dense ($N \sim 10^7$) if a reasonable temperature is to be maintained. (auth)

**26572** NONTHERMAL CONTINUUM RADIATION IN THREE ELLIPTICAL GALAXIES. Ulrich, M. (Department of Astronomy, University of Texas at Austin); Kinman, T.D.; Lynds, C.R.; Rieke, G.H.; Ekers, R.D. Astrophys. J. 198: No. 2, 261-266 (1 June 1975).

Optical, infrared, and radio observations are presented for three elliptical galaxies (NGC 6454, B2 1652+39, and B2 1101+38) which have flat high-frequency radio spectra. Two of these galaxies emit optical nonthermal continuum radiation, as evidenced by linear polarization of the ultraviolet radiation of the nuclei. No emission lines were detected in the optical spectra of the galaxies, and in that respect they may be related to the BL Lacertae class. The redshifts were obtained from the Ca II H- and K-lines and the G-band in absorption. These galaxies appear to form a sequence by order of increasing contribution of a nonthermal source to the luminosity of the nuclear regions, and their optical properties appear to be intermediate between those of ordinary ellipticals and those of objects like BL Lacertae. (auth)

**26573** HYDROMAGNETIC WAVES AND SHOCK WAVES AS AN INTERSTELLAR HEAT SOURCE. Silk, J. (Department of Astronomy, University of California, Berkeley, CA 94720). Astrophys. J. Lett. 198: No. 2, L77-L80 (1 June 1975).

The dissipation of hydromagnetic waves in diffuse interstellar matter is investigated as a heat source that does not itself produce any significant nonthermal ionization. In the low-density interstellar medium, shock waves, both hydromagnetic and hydrodynamic, can provide appreciable heating and yield either a neutral intercloud medium ($T \sim 10^4$K) or a tenuous hot medium ($T \sim 10^6$K) that is in pressure equilibrium with interstellar clouds. Quantitative estimates are given of the heat input by these various mechanisms, and the predicted parameters and properties of the interstellar medium are discussed. (auth)

**26574** RADIO DETECTION OF INTERSTELLAR SULFUR DIOXIDE. Snyder, L.E.; Hollis, J.M. (University of Virginia); Ulich, B.L.; Lovas, F.J.; Johnson, D.R.; Buhl, D. Astrophys. J. Lett. 198: No. 2, L81-L84 (1 June 1975).

Interstellar sulfur dioxide ($SO_2$) has been detected in emission from the direction of the Orion Nebula molecular cloud and from Sgr B2.$SO_2$ is the heaviest interstellar molecule detected to date, and the only nonlinear triatomic molecule which does not contain hydrogen. The remarkable Orion emission profiles suggest that two components are supporting the $SO_2$ emission: a dense circumstellar-type envelope, which may be in maser emission, and a warm galactic cloud component. (auth)

**26575** EXCITATION OF INTERSTELLAR METHYLAMINE. Kaifu, N. (National Radio Astronomy Observatory, Green Bank, West Virginia); Takagi, K.; Kojima, T. Astrophys. J. Lett. 198: No. 2, L85-L88 (1 June 1975).

The $2_{02}$-$1_{01}$ transition of $CH_3NH_2$ (88.67 GHz) has been detected in Sgr B2. The observed intensity of the $2_{02}1_{01}$ line confirms an anomalously large population of the $2_{02}$ level as suggested by Fourikis *et al.* The collisional excitation of $CH_3NH_2$ is discussed, and it is concluded that an optically thin source with a particle density of $\sim 10^5$ cm$^{-3}$ can explain well the observed anomalies in intensity. (auth)

**26576** OBSERVATIONS OF M82 AND NGC 253 AT 8–13 MICRONS. Gillett, F.C. (Kitt Peak National Observatory); Kleinmann, D.E.; Wright, E.L.; Capps, R.W. Astrophys. J. Lett. 198: No. 2, L65-L68 (1 June 1975).

Observations of the 8–13 $\mu$ spectrum ($\Delta\lambda/\lambda = 0.02$) of the nuclear regions of M82 and NGC 253 are presented. The emission features seen in both spectra are very similar to those of the planetary nebula BD+30°3639, consisting of a continuum with a strong 12.8-$\mu$ $Ne^+$ line and emission features around 11.3 and 8.7 $\mu$. This similarity supports a thermal reradiation interpretation of the infrared sources in M82 and NGC 253. In addition, there is a strong, broad depression around 10 $\mu$. The bulk of this depression can be identified with "silicate" grain absorption of the type seen in the spectra of some heavily attenuated galactic objects. The neon abundance in M82 is at least a factor of 4 higher than normal. (auth)

**26577** ICE AGES AND THE GALAXY. McCrea, W. H. (Sussex Univ., Brighton, Eng.). Nature (London); 255: No. 5510, 607-609 (19 Jun 1975).

The passage of the solar system through a dust lane bordering a spiral arm of the Galaxy may cause a temporary variation of the sun's radiation and so lead to an 'ice' epoch on earth. (auth)

**26578** INTERSTELLAR MEDIUM. Gorenstein, P. (Center for Astrophysics, Cambridge, MA). pp 299-319 of X-ray Astronomy. Giacconi, R. (ed.). Dordrecht, Netherlands; Reidel (1974).

A discussion is given of the absorption of X-rays in interstellar space. Characteristics of the interstellar medium with respect to X-ray absorption are reviewed. (BJG)

**26579** WESTERBORK SURVEY OF CLUSTERS OF GALAXIES. I. 21 CM Observations of A1656, A2147, A2151, A2197 and A2199: Radio Data and Identifications. Jaffe, W. J.; Perola, G. C. (Huygens Lab., Leiden). Astron. Astrophys., Suppl. Ser.; 21: No. 2, 137-169(Aug 1975).

As a part of a programme of radio observations of rich clusters of galaxies, we have observed 5 nearby Abell clusters at 21 cm wavelength using the Westerbork Synthesis Radio Telescope. The angular resolution was $23'' \times 23'' \cos\delta$ and the ultimate detection limit was 2.4 mJy. Here we describe the observing and reduction techniques, and present a list of all detected radio sources, along with contour maps of the more extended sources. An identification search was carried out on the Palomar Sky Survey prints and on deep 48" IIIaJ Schmidt plates. For each identification we present optical data and include a finding chart. A total of 27 probable cluster members was detected. (auth)

**26580** THEORETICAL ISOCHRONES AND MAIN SEQUENCES FOR OLD DISK POPULATION STARS. DeMarque, P.; Gisler, G. R. (Yale Univ., New Haven). Astron. Astrophys., Suppl. Ser.; 20: No. 2, 237-253(May 1975).

Theoretical isochrones have been constructed for fourteen mixtures in the ranges of chemical compositions ($0.05 < Y < 0.45$) and ($0.01 < Z < 0.06$) and for ages relevant to the old disk population stars. The effects of autoionization absorption as computed by Watson were added to the Cox-Stewart radiative opacities. Comparison with the colour-magnitude diagram of M67 and NGC 188 does not favour supermetallicity, but rather normal abundances. Helium abundance by mass Y in the range of 0.25–0.35 is found. The distance of the Hyades cluster is discussed in terms of main sequence models extended to higher masses. The distance modulus is consistent with the models for a shift of 0.27 mag. from that given by the convergent point method. This shift would be smaller for lower interior opacities (i.e. if we have overestimated the heavy element abundance Z, or alternately if Watson's autoionization opacities are too large). (auth)

**26581** NEUTRAL HYDROGEN IN A MOLECULAR AND DUST CLOUD IN THE DIRECTION TOWARD THE NEBULA NGC 6618. Gosachinskii, I.V.; Rakhimov, I.A. (Special Astrophysical Observatory, Academy of Sciences of the USSR). Sov. Astron.—AJ 19: No. 1, 18-20 (July 1975).

The optical depth of the 21 cm H I absorption line is reduced by a factor of 2 in a dust cloud covering the western part of NGC 6618. This effect occurs at a mean radial velocity similar to that of the formaldehyde line detected in the same cloud. If one allows for the lower kinetic temperature, the density of H I atoms is diminished by a factor of about 10 in the cloud relative to the undisturbed regions. (auth)

**26582** ROLE OF THERMAL INSTABILITY IN THE FORMATION OF GALAXIES. Gurevich, L.É.; Chernin, A.D. (A. F. Ioffe Physicotechnical Institute, Academy of Sciences of the USSR). Sov. Astron.—AJ 19: No. 1, 1-3 (July 1975).

If large-scale hydrodynamic motions generating shock waves existed at the epoch of galaxy formation, the plasma heated behind the shock front would have cooled as a result of Compton scattering of the background blackbody photons and free-free transitions and would have cooled at approximately constant pressure. In the state when free-free transitions dominated, the plasma would have been unstable and the contracting layers would have fragmented. Estimates show that the mass of the fragments could be of the order of the mass of typical galaxies. Under certain conditions, a thermal instability of this type would have developed more rapidly than the gravitational instability. (auth)

**26583** INTERACTION OF PROTOCLUSTERS OF GALAXIES WITH THE INTERGALACTIC MEDIUM. Doroshkevich, A.G.; Shandarin, S.F. (Institute of Applied Mathematics, Academy of Sciences of the USSR). Sov. Astron.—AJ 19: No. 1, 4-7 (July 1975).

In the framework of the adiabatic theory of the formation of galaxies and clusters of galaxies a study is made of the interaction of protoclusters of galaxies with the intergalactic medium. It is shown that the emission of the protoclusters in the ultraviolet and soft x-ray range can ensure a high degree of ionization of the hydrogen that has not entered the clusters of galaxies, though it heats it only to a temperature $\sim 10^{4\circ}$K. The strongest restrictions on the parameters of the theory come from the estimate of the present background in the ultraviolet range based on the existence of neutral hydrogen at the periphery of galaxies. (auth)

**26584** BAR-LIKE OBJECTS IN THE CENTRAL REGIONS OF GALAXIES AS POSSIBLE GENERATORS OF SPIRAL DENSITY WAVES. I. Korchagin, V.I.; Marochnik, L.S. (Rostov State University). Sov. Astron.—AJ 19: No. 1, 8-13 (July 1975).

It is pointed out that a two-arm spiral pattern could be generated by

bar-like structures in a uniform, rigidly rotating gas disk. The sense of winding of the spirals is determined by the ratio of the angular velocities of the bar and the disk. A bar rotating faster than the disk generates a trailing two-arm spiral. A slow bar generates a leading spiral pattern. (auth)

**26585** THE UNIDENTIFIED HIGH GALACTIC LATITUDE X-RAY SOURCES: BRIGHT GALAXIES OR RICH CLUSTERS? Bahcall, J.N. (Institute for Advanced Study); Bahcall, N.A. Astrophys. J. Lett. 199: No. 2, L89-L92 (15 July 1975).

We analyze the positional correlations between the unidentified high galactic latitude 3*U* X-ray sources, as well as (1) all 2712 rich clusters of galaxies in the Abell catalog and (2) all bright galaxies ($m_p \leq 15.7$ mag) in the Zwicky catalog. Computer studies using simulated *Uhuru* catalogs are used to evaluate the chance coincidence rate and its dispersion. We confirm the validity of practically all of the identifications previously suggested by Kellogg *et al.* of 3*U* sources with nearby rich Abell clusters. One or two of the distance-group 4 Abell clusters ($z \sim 0.1$) may be associated with 3*U* sources. Very few, if any, of the *Uhuru* X-ray sources are associated with the most distant ($z = 0.12$–$0.2$) Abell clusters. This establishes an upper limit to the X-ray luminosity of $L_x \lesssim 6 \times 10^{45}$ ergs $s^{-1}$, in agreement with the highest X-ray luminosity observed for nearby clusters. About 50 percent of the high-latitude *Uhuru* error boxes contain a bright galaxy from the Zwicky catalog; but very few, if any, of these associations are expected to be valid identifications. (auth)

**26586** CARBON-HELIUM CHARGE TRANSFERS AND THE IONIZATION OF CARBON IN THE INTERCLOUD MEDIUM. Steigman, G. (Yale University Observatory). Astrophys. J. 199: No. 2, 336-339 (15 July 1975).

Charge transfer reactions are considered in collisions between carbon and helium ions: $C^{++} + He \rightleftharpoons C^{+} + He^{+}$. It is shown that, if these reactions proceed rapidly at high temperatures ($300 \lesssim T \lesssim 10^4$ K), as Brown (1972) suggested, then the degree of carbon ionization is directly tied to the degree of helium ionization: C III/C II $10^{-1}$ (He II/He I)$_{T=10^4}$. As a result, even if these charge transfer reactions are fast, it is impossible to account for the C III/C II ratios observed toward several unreddened stars (Rogerson *et al.* 1973) with a hot intercloud medium. More important, it is shown that the presence of the Coulomb barrier in $C^{+} + He^{+}$ collisions prevents the above reactions from proceeding rapidly (in either direction) at thermal energies ($T \lesssim 10^4$ K). (auth)

**26587** RADIATION TRANSPORT IN DENSE INTERSTELLAR DUST CLOUDS. I. GRAIN TEMPERATURE. Leung, C.M. (Astronomy Department, University of California, Berkeley). Astrophys. J. 199: No. 2, 340-360 (15 July 1975).

A numerical method is presented for solving the problem of radiation transport in dense interstellar dust clouds (DIDC) in spherical or planar geometry and for general anisotropic scattering. The method is used to determine the grain temperature distribution inside such dark clouds. Using laboratory-measured optical constants, silicon carbide, graphite, silicate, and the corresponding ice-coated core-mantle grain models are considered. It is found that pure silicate grains attain rather low temperatures ($T \lesssim 7$ k for $\tau \sim 5$). For most grain types, the grain temperatures vary by a factor of 4 to 5 from free space to the centers of very opaque clouds. The thermal role of grains in the thermodynamics and evolution of DIDC is discussed. In particular, the possible role of radiation pressure gradient in confining DIDC is examined. Also investigated are the effects on the grain temperature due to radiation field anisotropy, density inhomogeneity, and cloud geometry (slab versus sphere). It is found that the radiation field exhibits a sideward peaking effect (limb brightening) and that the radiation energy density is lower in slab clouds, resulting in a lower grain temperature. Finally our results are compared with those of Werner and Salpeter. (auth)

**26588** A COMPARATIVE STUDY OF $H_2CO$, OH, and H I IN THE DARK TAURUS DUST CLOUD. Heiles, C. (Astronomy Department, University of California, Berkeley); Gordon, M.A. Astrophys. J. 199: No. 2, 361-378 (15 July 1975).

High-sensitivity spectra of $H_2CO$, OH, and H I, all taken with the same angular resolution, were obtained in the dark dust cloud in Taurus. At some positions there exist three velocity components, instead of the two revealed by previous investigations. H I correlates rather well, but not perfectly, with the molecules, suggesting that much of it resides outside the region containing the molecules. We consider two extreme interpretations of the widely varying relative intensities of the molecular lines. The one, constant excitation temperature of $H_2CO$ within the cloud, leads to large variations of $N_{OH}/N_{H_2CO}$ from point to point within the cloud. The other, a constant value of $N_{OH}/N_{H_2CO} = 20$ deduced from independent observations of other dust clouds, leads to a correlation of OH and $H_2CO$ excitation temperatures —a natural result of collisional excitation of both molecules as previously suggested by others. We have carefully examined the OH principal line data in this cloud for the presence of anomalous ratios of line intensities. Only one case of an anomalous ratio is found, but various considerations suggest that the observational data are in error, or that the OH at this position is atypical of that usually found in dust clouds. (auth)

**26589** LINE SPECTRA IN INTERSTELLAR CLOUDS. II. CH AND $CH^+$ IN OPHIUCHUS. Chaffee, F.H. Jr. (Center for Astrophysics, Harvard College Observatory and Smithsonian Astrophysical Observatory). Astrophys. J. 199: No. 2, 379-382 (15 July 1975).

Observational evidence is presented that suggests that velocity differences of the order of 1 km $s^{-1}$ exist between interstellar CH and $CH^+$ in four stars on Ophiuchus. Such velocity stratification would be consistent with the formation mechanism proposed by Black and Dalgarno and by Watson in which CH is formed near the center of interstellar clouds where the density of molecular hydrogen, $n$ ($H_2$), is high, and $CH^+$ is formed in the outer regions where $n$ ($H_2$) is negligible. The velocity difference between $CH^+$ and Ca II in $\zeta$ Oph reported by Hobbs is corrobarated, but the interpretation that this implies separate clouds for interstellar molecular and atomic constituents is questioned. (auth)

**26590** INTERSTELLAR $H_2CO$. II. 2-CENTIMETER EMISSION FROM THE ORION MOLECULAR CLOUDS. Evans, N.J. II (University of California, Berkeley); Zuckerman, B.; Sato, T.; Morris, G. Astrophys. J. 199: No. 2, 383-397 (15 July 1975).

Emission in the $2_{11} \rightarrow 2_{12}$ line of formaldehyde at 2-cm wavelength has been mapped over a $3' \times 6'$ region in the Orion molecular cloud. The emission is elongated in the north-south direction, and peaks on the Kleinmann-Low nebula. Analysis of the excitation of this line, together with other lines from $H_2CO$, indicates hydrogen densities $n_{H_2} \simeq 10^5$ cm$^{-3}$ over a region $2' \times 5'$ in extent in addition to a denser, smaller core at the Kleinmann-Low nebula. The region emitting the 2-cm line displays a velocity gradient that is suggestive of rotation about an east-west axis —the direction of flattening. The total mass derived from considerations of excitation and, independently, from dynamical considerations is $\sim 500\ M_\odot$. (auth)

**26591** UNCERTAINTIES IN THE FAR-INFRARED ABSORPTION OF INTERSTELLAR CLOUDS. Harwit, M. (Center for Radiophysics and Space Research, Cornell University). Astrophys. J. 199: No. 2, 398-400 (15 July 1975).

The observed absorption of far-infrared radiation by an interstellar dust cloud is a complicated function of the material properties of grains, of their column density, and of the extent of stimulated emission. At long wavelengths, neglect of stimulated emission would lead to an underestimate of the amount of absorbing material observed along a line of sight. However, if the complex index of refraction for grains is measured at the low temperatures in question, a classical analysis will be correct since the measured refractive index correctly accounts for stimulated emission. Since the grain temperatures may strongly affect the refractive index of a grain, typical interstellar grain temperature fluctuations are analyzed in a final section. (auth)

**26592** G45.5+0.1 AND G45.1+0.1: COMPACT INFRARED SOURCES. Zeilik, M. II; Kleinmann, D.E.; Wright, E.L. (Center for Astrophysics, Harvard College Observatory). Astrophys. J. 199: No. 2, 401-405 (15 July 1975).

We have observed the compact H II regions G45.5+0.1 and G45.1+0.1 from 2.2-21 μ. The infrared emission from G45.5+0.1 appears to come from dust that is well mixed with ionized gas and heated by Lα radiation. For G45.1+0.1, the infrared luminosity cannot be accounted for by Lα heating alone. Compared with the conventional interstellar values, the gas-to-dust ratio in G45.5+0.1 is substantially depleted, but it is close to normal in G45.1+0.1. (auth)

**26593** SPECTROSCOPY OF R MONOCEROTIS AND NGC 2261. Stockton, A.; Chesley, D.; Chesley, S. (Institute for Astronomy, University of Hawaii). Astrophys. J. 199: No. 2, 406-410 (15 July 1975)

Spectrograms obtained in early 1974 of NGC 2261, the cometary nebula associated with R Mon, show a variation in the velocity of the reflected absorption spectrum as a function of distance from R Mon. The emission lines in the reflection spectrum show no significant variation; thus differential motions within the nebula cannot be responsible for the absorption-line variation. The effect is attributed instead to *time* variations in the absorption shell around R Mon, in conjunction with the differences in total light travel times for light scattered from different portions of the nebula. Over the course of approximately one year, the expansion velocity of the shell dropped from 260 km $s^{-1}$ to 135 km $s^{-1}$. The [O II] λ3727 doublet reported by Kazaryan and Khachikyan in the spectrum of NGC 2261 does not arise within the nebula, but results from the projection of the outer parts of the H II region surrounding the nearby O5 star, S Mon, onto NGC 2261. All of the differences observed between the spectra of R Mon and NGC 2261 can be interpreted in terms of (1) variations in the spectrum of R Mon and time delay in the light reaching us via NGC 2261, or (2) contamination of the spectrum of NGC 2261 by lines from the H II region around S Mon. Thus, the interpretation of NGC 2261 as a pure reflection nebula is reaffirmed. (auth)

**26594** PHOTOELECTRIC *UBV* PHOTOMETRY OF CEPHEIDS IN THE MAGELLANIC CLOUDS AND IN THE SOUTHERN MILKY WAY. Madore, B.F. (David Dunlap Observatory, University of Toronto, Richmond Hill, Ontario, Canada). Astrophys. J. Suppl. Ser. 29: No. 285, 219-284 (June 1975).

New photoelectric *UBV* photometry is presented for 46 long-period Cepheids in the southern Milky Way. Data are now essentially complete for Cepheids with $P>11$ days and $\langle B\rangle$ brighter than 14 mag. New *UBV* photometry is also given for 22 Cepheids in the Large Magellanic Cloud and for 15 Cepheids in the Small Magellanic Cloud. The implications of these observations will be discussed in subsequent papers. (auth)

**26595** SPECTROSCOPY OF THE ORION NEBULA FROM 80 TO 135 MICRONS. Brandshaft, D.; McLaren, R.A. (Department of Physics, University of California, Berkeley); Werner, M.W. Astrophys. J. Lett. 199: No. 2, L115-L117 (15 July 1975).

Airborne observations have been made of the spectrum of the Orion Nebula from 80 to 135 $\mu$ with 6-$\mu$ resolution and with a 7'.4 diameter beam. The spectrum is consistent with that of a smooth continuum source having a flux density which decreases linearly by approximately a factor of 1.7 from 80 to 135 $\mu$. (auth)

**26596** MOLECULAR CLOUDS IN THE GALAXY. Scoville, N.Z. (Owens Valley Radio Observatory, California Institute of Technology); Solomon, P.M. Astrophys. J. Lett. 199: No. 2, L105-L109 (15 July 1975).

The $J=1\rightarrow0$ emission of CO has been surveyed in the galactic plane between $l=-10°$ and $+90°$ with a 1' beam sampling every degree. Molecular clouds emitting in the CO line are plentiful over the inner region of the Galaxy. Their greatest number occurs in the galactic nucleus and at a radius of 5.5 kpc—a distribution similar to radio H II regions and galactic $\gamma$-ray emission but very different from that previously derived for atomic hydrogen. The total mass in molecular clouds is found to be $1\text{–}3\times10^9\ M_\odot$, and each typically has $10^5\ M_\odot$, an $H_2$ density of 700 cm$^{-3}$, and a temperature near 7 K. These results suggest that most of the interstellar medium in the interior of the Galaxy is molecular $H_2$. (auth)

**26597** COMPLEX INTERSTELLAR CALCIUM LINE STRUCTURE IN THE CARINA NEBULA. Walborn, N.R.; Hesser, J.E. (Cerro Tololo Inter-American Observatory). Astrophys. J. 199: No. 2, 535-543 (15 July 1975).

Exceedingly complex structure has been found in the interstellar Ca II lines on 9 Å mm$^{-1}$ coudé spectrograms of stars in the Carina Nebula. As many as six components have been observed in a single spectrum; moreover, the profiles show large variations over small angular distances, and a total velocity range of 330 km s$^{-1}$ has been measured. Stars in the outer part of the nebula have single calcium lines, which suggests that the additional components in the inner region are formed there. Measurements of the interstellar Ti II lines, which are double in a few cases, are also presented. These results probably represent a new kind of interstellar-line velocity structure, and some possible causes are summarized. The double nebular emission lines have been measured on a long-exposure spectrogram of HD 93204. There is good agreement with the previous interferometric results of Bohuski and Smith. In addition, the spectrograms of all stars in bright nebulosity show a *single* He I $\lambda$3889 nebular absorption line. Its velocity agrees with the negative component of the emission pairs, which suggests that the positive-velocity ionized material lies beyond the stars. A search for similar interstellar calcium-line structure at the center of the 30 Doradus Nebula in the Large Magellanic Cloud is briefly discussed. (auth)

**26598** SOUTHERN GALAXIES. VII. THE REMARKABLE LENTICULAR BARRED GALAXY NGC 1291. de Vaucouleurs, G. (McDonald Observatory and Department of Astronomy, The University of Texas). Astrophys. J. Suppl. Ser. 29: No. 284, 193-218 (June 1975).

The lenticular barred galaxy NGC 1291 is the largest example of revised type (R) SB(s)0/a at the transition stage between late lenticulars and early spirals. The central lens (12×10 kpc) is surrounded by a large, semidetached outer ring (21×19 kpc) from which emerge two faint spiral arms showing incipient resolution at $m_B\simeq20.5$. In the nuclear region at the center of the primary bar (10×2.5 kpc), a secondary bar (1.8×0.2 kpc) and secondary nucleus (0.5×0.4 kpc) have been detected, repeating the primary lens-bar-nucleus pattern on a smaller scale approximating the ratio of the Jeans lengths. Other examples suggest that this repetitive pattern may be typical. Detailed surface photometry from long- and short-exposure photographs with the Mount Stromlo 75-cm reflector and the McDonald 205-cm reflector is presented (isophotes, luminosity profiles, and photometric parameters). The total apparent magnitude $m\ (B)=9.37$ (photoelectrically calibrated) and maximum dimensions 20' × 18' (at the detection threshold $\mu_B\simeq28.2$ mag s$^{-2}$=0.3 $\mathfrak{L}_\odot$ pc$^{-2}$) correspond to $M_T(B)=-20.63$ and $D_n=52$ kpc, with $(B-V)_T=0.92$, $(U-B)_T=0.47$, if $m-M=30.0$ and $\Delta=8.9$ Mpc (estimated from brightest stars and redshift). The average surface brightness in the "dark" zone between the lens and the ring is about $\mu_B=24.5$ mag s$^{-2}$ $\simeq10\ \mathfrak{L}_\odot$ pc$^{-2}$ at an average radius $r\simeq8$ kpc from the center; the average maximum brightness in the ring is only slightly greater, about 24.0 mag s$^{-2}$. The effective equivalent radius of the isophote enclosing half the total flux is $r^e=1'.54=4.0$ kpc, the same as for M31, and indicating a giant system. The spheroidal component obeying the $r^{1/4}$ law dominates the light distribution within the lens and contributes 57 percent of the total luminosity; if it is valid up to $r=0$, the true central brightness may be as high as $\mu_B(0)=13.46$ mag s$^{-1}$=2.2×10$^5$ $\mathfrak{L}_\odot$ pc$^{-2}$. The flat component contributing to the lens and dominant in the ring does not obey the simple exponential distribution previously found in the disks of late-type spirals.

The nuclear spectrum observed in the blue region at medium resolution (Mount Stromlo) and in the red region at low resolution with an image-tube spectrograph (McDonald) is a typical K-type, approximating G5 at H and K and KO III at H$\gamma$ with weak $\lambda$3727 emission and no H$\alpha$. The mean heliocentric radial velocity from three optical and one radio observations is $V=+830$ km s$^{-1}$. The total mass, neutral hydrogen mass, and mass-luminosity ratio estimated from corrected values of the 21-cm line parameters given by Lewis and from an optical upper limit to the velocity dispersion ($\sigma<200$ km s$^{-1}$) are $\mathfrak{M}_T\simeq1\times10^{11}\ \mathfrak{M}_\odot$, with $\mathfrak{M}_H/\mathfrak{M}_T\simeq0.025$ and $\mathfrak{M}_T/\mathfrak{L}_B\simeq4$. These values are about normal for type S0/a ($t=0$). The frequency of outer ring structures around the main bodies of galaxies of different types is discussed in an Appendix; such structures are observed only around lenticulars and spirals earlier than Sc with a sharp maximum at S0/a. (auth)

**26599** DETECTION OF EXTRAGALACTIC CARBON MONOXIDE AT MILLIMETER WAVELENGTHS. Rickard, L.J; Palmer, P. (University of Chicago); Morris, M.; Zuckerman, B.; Turner, B.E. Astrophys. J. Lett. 199: No. 2, L75-L78 (15 July 1975).

We report the discovery of emission from the $J=1\rightarrow0$ transition of $^{12}C^{16}O$ toward the central regions of external galaxies. In this *Letter*, we present preliminary results for two galaxies with active nuclei, M82 and NGC 253, in which the observed emission features are surprisingly strong. In the directions of the nuclear continuum peaks, the velocity range of CO emission is roughly the same as that of 21-cm absorption. For each galaxy, the CO features are spatially extended, and the velocity shift of the emission centroid along the major axis is in the sense of the galactic rotation. (auth)

**26600** CARBON MONOXIDE IN EXTERNAL GALAXIES. Solomon, P.M. (Department of Earth and Space Sciences, State University of New York at Stony Brook); de Zafra, R. Astrophys. J. Lett. 199: No. 2, L79-L83 (15 July 1975).

We have observed emission lines from the $J=1\rightarrow0$ carbon monoxide rotational transition at 2.6 mm in the central regions of five external galaxies, including two at a distance of ~9 Mpc. We have also detected $^{13}CO$ emission in one of these (M82) with an observed $^{13}CO/^{12}CO$ intensity ratio of $\sim0.23\pm0.1$. Upper limits of $T_A^*\lesssim0.1$ K are established for six additional galaxies in $^{12}CO$. The total velocity widths of approximately 350 km s$^{-1}$ in M82, NGC 253, and M31 are similar to the dispersion observed in molecular clouds in the center of the Milky Way. Small velocity dispersions are observed for the nearly face-on system M51. The total mass in the form of molecular clouds is typically of order $2\times10^8\ M_\odot$ in the central 1' and probably a few times $10^9\ M_\odot$ for an entire galaxy. (auth)

**26601** PERMITTED IRON LINES IN NGC 7469. Shectman, S.A.; MacAlpine, G.M. (University of Michigan, Ann Arbor). Astrophys. J. Lett. 199: No. 2, L85-L87 (15 July 1975).

Using the Michigan multichannel spectrometer on the 1.3-meter telescope, relatively strong Fe II emission has been detected in the Seyfert galaxy NGC 7469. This object is different from the handful of others with permitted iron lines in that it also exhibits intense forbidden lines of oxygen. Our observations do not show the strong He II $\lambda$4686 reported by previous investigators. (auth)

# Cosmology

*Refer also to abstracts 26353, 26409, 26421, 26521, 26580, and 27207.*

**26602** AVERAGE EFFECT OF A HIGHLY TURBULENT GRAVITO-HYDRODYNAMIC FIELD IN THE HADRON ERA OF THE UNIVERSE. Nariai, H. (Hiroshima Univ., Takehara (Japan). Research Inst. for Theoretical Physics). Prog. Theor. Phys. (Kyoto); 52: 1539-1553(Nov 1974).

An attempt is made to give a physical basis for a modification of Einstein's gravitational equations, which has been proposed in a previous paper, to arrive at an isotropic model-universe that may bounce in the hadron era, tends rapidly to the Friedmann universe, and remains regular with respect to the excitation of gravitational and rotational waves. The basic idea lies in reinterpreting the modified field equations as those for the mean-value field of a highly turbulent gravito-hydrodynamic field (obeying Einstein's equations) whose substratum is dominated by the hadronic matter with large density fluctuation. In the case

where the mean-value metric represents the regular model-universe, it is shown that, so far as the bounce epoch of the universe is concerned, three characteristic mean-value quantities specifying metric velocity and density fluctuations are compatible with the basic idea. Several problems to be pursued further are also touched upon. (auth)

**26603** ON THE NON-LINEAR BEHAVIOR OF NONSPHERICAL PERTURBATIONS IN RELATIVISTIC GRAVITATIONAL COLLAPSE. Tomita, K. (Hiroshima Univ., Takehara (Japan). Research Inst. for Theoretical Physics). Prog. Theor. Phys. (Kyoto); 52: No. 4, 1188-1204(Oct 1974).

As a preparation for clarifying the final state of relativistic gravitational collapse, the way nonspherical perturbations behave in the neighbourhood of the Schwarzschild surface is examined by analyzing the second-order non-linear perturbations as well as the first-order linear ones. Through the self-interaction of the perturbations corresponding to incoming gravitational waves reflected by the potential barrier, the non-linear effect becomes important when the waves approach the Schwarzschild surface together with the surface of the collapsing object. Consequently, the conclusion derived in the linear approximation is questionable that the final gravitational state is expressed by the Schwarzschild or Kerr field. It is concluded that, however small the initial nonspherical perturbations are, full non-linearity must be considered, in order to analyze dynamical processes in the neighbourhood of the final state. (auth)

**26604** SOME REMARKS ON THE TWO-BODY-PROBLEM IN GEOMETRODYNAMICS. Čadež, A. (Observatoire de Paris, Groupe d'Astrophysique Fondamentale, 92190 Meudon, France). Ann. Phys. (N.Y.) 91: No. 1, 58-74 (May 1975).

The interest in the two body problem in geometrodynamics and its present status are discussed. Special consideration is given to time-symmetric initial data. An equation relating the "bare mass energy," the potential energy and the "vibrational energy" at the initial moment is proposed. The significance of coordinate conditions in dynamical equations is discussed next. Conditions implying maximal slicings of spacetime and harmonic coordinates in those slices are considered in detail, as they seem to be well suited for numerical calculations and for interpretation of the results of such calculations. (auth)

**26605** ECLIPSE INDUCED ATMOSPHERIC GRAVITY WAVES. Jones, B. W (Open Univ., Milton Keynes, Eng.); Bogart, R. S. J. Atmos. Terr. Phys.; 37: No. 9, 1223-1226(Sep 1975).

A null result is reported for eclipse induced atmospheric gravity waves along the center line of the total solar eclipse of 30 June 1973. This conflicts with the non-null result reported by others for the total solar eclipse of 7 March 1970. A means of reconciliation is suggested. (auth)

**26606** RGU THREE-COLOR PHOTOMETRY OF AN ANTI-CENTERFIELD NEAR M35. Topaktas, L. (Univ. of Basel). Astron. Astrophys., Suppl. Ser.; 20: No. 3, 269-288(Jun 1975).

A galactic anticenter field of 2.32 square degrees with 2400 stars near M35 has been studied photometrically in the RGU system down to a limiting magnitude of G = 15.5. The interstellar reddening function, the density functions for different groups of stars and luminosity functions have been determined. The reddening is caused by three interstellar clouds with distances of 360, 800 and 2560 pc. Two types of late-type giants have been identified forming branches at both sides of the main sequence of late-type dwarfs. The density functions reaching larger distances show almost a constant density from the sun to the outer border of the local spiral arm followed by a continuous decrease which is partly caused by incompleteness as revealed by a comparison with results found by Hersperger. For stars with M(G) > 5 the density gradients are affected by incompleteness already at distances smaller than 1 kpc. With few exceptions the density gradients of different groups extrapolated to zero distance conform with the space density as accepted for the solar neighbourhood. The luminosity function for distances smaller than 0.8 kpc shows an increase with decreasing luminosity similar to the solar neighbourhood. The function for distances between 0.8 and 1.2 kpc is almost constant for 0 < M(G) < 5. (auth)

**26607** HOMOGENEOUS RELATIVISTIC COSMOLOGIES. Ryan, M. P. Jr.; Shepley, L. C. Princeton, NJ; Princeton University Press (1975). 336p. $15.00.

The beginnings of modern cosmology are considered along with questions of geometry in the language of forms, aspects of spacetime and fluid flow, Friedmann-Robertson-Walker models, singularities in a spacetime, isometries of space and spacetime, universes homogeneous in space and time, and the T-NUT-M space. Other topics discussed are related to the general spatially homogeneous model in the synchronous system, singularities in spatially homogeneous models, Hamiltonian cosmology, type I models and type IX models, numerical techniques, and astrophysical studies in anisotropic type I models. (IAA)

**26608** UNIFORM MODEL UNIVERSES CONTAINING INTERACTING BLACKBODY RADIATION AND MATTER WITH INTERNAL ENERGY. May, T.L. (San Diego State University). Astrophys. J. 199: No. 2, 322-327 (15 July 1975).

Techniques previously developed for the production of general-relativistic models of the universe which contain interacting matter and blackbody radiation are extended to include models with internal energy and with nonzero cosmological constant. The material content of the model obeys a polytropic equation of state. The nature of the interaction between the matter and radiation is elucidated, and an alternate interpretation of the rate of interaction is presented. (auth)

**26609** SEARCH FOR GRAVITATIONAL RADIATION AT 145 Hz. Hirakawa, H.; Narihara, K. (Department of Physics, University of Tokyo, Bunkyo, Tokyo 113, Japan). Phys. Rev. Lett. 35: No. 6, 330-334 (11 Aug 1975).

We present the results of gravitational radiation experiments with two 1400-kg antennas at $\nu_0 = 145$ Hz. The square antennas, $1.65 \times 1.65 \times 0.19$ m$^3$, $Q_M \simeq 2.0 \times 10^5$, with electrostatic transducers of $\beta \simeq 1.8 \times 10^{-3}$, have mean effective noise energy $\bar{D} \simeq 0.034 kT_r$. The observed cross correlation of the outputs of the two detectors gives an upper limit for the relation between the mean energy spectrum density $F(\nu_0)$ and the daily occurrence rate $N_G$ of gravitational radiation pulses: $F(\nu_0)\, N_G^{1/2} \leqslant (3.6_{-1.4}{}^{+1.0}) \times 10^6$ J m$^{-2}$Hz$^{-1}$day$^{-1/2}$. (auth)

# Planetary Phenomena

*Refer also to abstract 26356.*

**26610** THERMODYNAMICS OF DENSE HYDROGEN-HELIUM FLUIDS. Graboske, H.C. Jr.; Olness, R.J. (Lawrence Livermore Laboratory, University of California, Livermore); Grossman, A.S. Astrophys. J. 199: No. 1, 255-264 (1 July 1975).

The equilibrium thermodynamic properties of hydrogen-helium fluids are studied in the density-temperature regime appropriate to the interiors of evolving very low mass stars and giant planets. The low-density molecular fluid is treated by a free energy minimization method, utilizing several theoretical models and recent high-pressure experimental results for hydrogen. The high-density metallic fluid is treated by an extension of Thomas-Fermi theory. These approaches are combined to yield a detailed thermodynamic description for two fluids: pure hydrogen ($X=1.$) and a solar mixture ($X=0.74$, $Y=0.24$, $Z=0.02$). Equations of state are given for the density range $10^{-4}$ g cm$^{-3}$ to 10 g cm$^{-3}$ and a temperature range 200–60,000 K. (auth)

**26611** THE STRUCTURE AND EVOLUTION OF JUPITER: THE FLUID CONTRACTION STAGE. Graboske, H.C. Jr. (Lawrence Livermore Laboratory, University of California); Pollack, J.B.; Grossman, A.S.; Olness, R.J. Astrophys. J. 199: No. 1, 265-281 (1 July 1975).

An evolutionary study of a 0.00095 $M_\odot$ star, composed of a convective, adiabatic, homogeneous fluid, has been performed using stellar structure methods. A new numerical technique is used to calculate model atmospheres in the form of time-average vertical temperatures structures, including all relevant opacity sources and a solar energy deposition component. Thermodynamic properties for pure hydrogen and a solar mixture ($X=0.74$, $Y=0.24$, $Z=0.02$) are developed for $-7 \leqslant \log \rho\ (\mathrm{g\ cm^{-3}}) \leqslant 1$ and $1.78 \leqslant \log T\ (K) \leqslant 4.78$, utilizing recent high-pressure experimental results and new theoretical methods. The resultant gravitationally contracting evolutionary models exhibit two phases. An early stellar phase, behaving like a typical low-mass pre-main-sequence object, has high luminosities which have left a record in the structure of the Galilean satellites. This phase also has high internal temperature, $(T_c)_{max}$ reaching 51,400, which ensures a long subsequent evolution as a fully mixed, convective structure. The second phase is an approach to a degenerate dwarf cooling curve, which gives excellent agreement with the observed radius and luminosity of Jupiter. A short time scale for the standard adiabatic fluid models ($2.6 \times 10^9$ years) is extended by combinations of several factors influencing the planetary evolution. An analysis of the sensitivity of evolution to chemical composition, solar energy deposition, equation of state, model atmospheres, and superadiabaticity demonstrates that the equation of state and superadiabaticity have the strongest influence over planetary time scales. (auth)

**26612** FORMATION OF COUPLED SPECTRAL LINES IN A PLANETARY ATMOSPHERE: II. NUMERICAL EVALUATION OF APPROXIMATE SOLUTIONS. Chamberlain, J.W. (Department of Space Physics and Astronomy, Rice University); Smith, G.R. Astrophys. J. 199: No. 1, 282-288 (1 July 1975).

Approximate solutions to the radiation-transfer problem of two or more resonance lines that share a common upper level have previously been obtained by Chamberlain and Wallace. Essentially exact solutions from a computer program are here compared with those approximate

solutions to evaluate the utility of the approximations in solving planetary radiation problems. Isotropic scattering and a semi-infinite atmosphere are adopted throughout. When the atmosphere is homogeneous with depth, the approximation is very good. When it is inhomogeneous, with scattering albedo $\tilde{\omega}$ $(t)$ gradually decreasing downward, the approximation is good only for single lines. The combined complication of multiple coupled transitions in an inhomogeneous atmosphere strains the presumption of a single effective albedo, $\tilde{\omega}_e$. Even in this case, however, the line ratios are satisfactory across the disk, even though the absolute center-to-limb variation and total reflected flux are not. The Appendix gives a simple technique for computing *H*-functions that is both reasonably accurate (always better than 1 percent) and easily adapted to programmable desk calculators. (auth)

**26613** OBSERVATIONS AND ANALYSIS OF THE JOVIAN SPECTRUM IN THE 10-MICRON $\nu_2$ BAND OF $NH_3$. Lacy, J.H.; Larrabee, A.I.; Wollman, E.R.; Geballe, T.R.; Townes, C.H. (Department of Physics, University of California, Berkeley); Bregman, J.D.; Rank, D.M. Astrophys. J. Lett. 198: No. 3, L145-L148 (15 June 1975).

Observations of the $\nu_2$ band of $NH_3$ in the Jovian atmosphere have been made at resolutions varying from 4 $cm^{-1}$ to 0.15 $cm^{-1}$. The observations have been interpreted by computation of synthetic atmospheric spectra. Derived atmospheric parameters include a pressure of 0.5 atm at 145 K and a minimum temperature of 118 K. (auth)

**26614** RADIO SEARCH FOR $HC_3N$, HCN, OH, AND DETECTION OF U8.19 IN COMET KOHOUTEK (1973f). Giguere, P.T. (NASA Goddard Space Flight Center); Clark, F.O. Astrophys. J. 198: No. 3, 761-764 (15 June 1975).

Comet Kohoutek (1973f) was observed with the NRAO 140-foot (43 m) telescope in the period 1974 January 4–7 in an attempt to detect the following molecular transitions: $HC_3N$, $J=1-0$, $v=0$; $HC_3N$, $J=1-0$, $2\nu_7$, $l=0$; HCN, $J=6$, $1\nu_2$; and OH, $^2\Pi_{1/2}$, $J=5/2$, $F=3-3$. All results for these lines were negative. An unidentified line was possibly detected at 8189 MHz. (auth)

**26615** SATURN RADIO EMISSION NEAR 1 MHz. Brown, L.W. (Radio Astronomy Branch, Laboratory for Extraterrestrial Physics, Goddard Space Flight Center, Greenbelt, Maryland). Astrophys. J. Lett. 198: No. 2, L89-L92 (1 June 1975).

Emission from the direction of the planet Saturn has been observed by the IMP-6 spacecraft at 15 frequencies between 375 and 2200 kHz during the period 1971 April–1972 October. The Saturnian radio bursts were identified in the IMP-6 data through an analysis of the phase of the observed modulated signal detected from the spinning dipole antenna. Initial data reduction has isolated approximately 12 storms whose occurrence corresponded to times in which the spacecraft had an unobstructed view in the direction of Saturn. These events persisted over periods between 1 and 10 minutes. Over the span of 500 days of data another 10–20 Saturnian events may exist, but positive identification is confused by the presence of terrestrial noise as well as a geometric ambiguity with Jupiter. A power spectral analysis of the storm occurrence times indicates a weak periodicity at $10^h30^m \pm 5^m$ at some of the observing frequencies. The spectral character of the radiation has been found analogous to that of Jupiter. The Saturnian emission most similar to the Jovian decametric source appears to be strongest at 1100 kHz with a bandwidth of approximately 1000 kHz. The spectrum hints also of a secondary spectral peak at 400 kHz similar to that recently observed for the Earth and Jupiter. The detection of this nonthermal radio emission is the first direct evidence for the existence of a Saturnian magnetic field containing energetic particles. (auth)

**26616** INTERPLANETARY SHOCK PAIR DISTURBANCES: COMPARISON OF THEORY WITH SPACE PROBE DATA. Steinolfson, R.S.; Dryer, M. (NOAA Space Environment Laboratory, Boulder, Colorado 80302); Nakagawa, Y. J. Geophys. Res. 80: No. 16, 1989-2000 (1 June 1975).

Three sets of data for shock pair disturbances, which are assumed to have been formed from stream-stream interactions, are modeled by using two time-dependent numerical codes. One code solves the fluid dynamic equations, and the other solves the magnetohydrodynamic equations. The observed disturbances are simulated by superimposing an initial interaction (a pulse in the dependent variables) onto the ambient solar wind and then following the time evolution of the resulting disturbance with the numerical codes. The magnitude of the initial interaction is such that the calculated solar wind agrees with the solar wind observed by the space probe both prior to the arrival of the forward shock at the space probe location and following passage of the reverse shock. The location of the initial interaction is iteratively chosen so that the simulated time interval between the forward and reverse shocks at the space probe location agrees with the measured value. The large-scale structure in the disturbance is reproduced if (1) the magnetic field and azimuthal velocity are included (that is, if the code which solves the magnetohydrodynamic equations is used), (2) the time dependence of the initial interaction is appropriately selected, and (3) the observed nonradial shock normals are accounted for in the modeling procedure. The relative importance of each of the above requirements varies for each set of data. The first and third requirements played the dominant roles in one data set, while for the other two data sets the second requirement was probably the most important. Hence it is recommended that all three requirements be met in attempting to simulate data for shock pair disturbances. (auth)

**26617** INTERPLANETARY SHOCK WAVES AND COMET BRIGHTNESS FLUCTUATIONS DURING JUNE-AUGUST 1972. Dryer, M. (Space Environment Laboratory, Environmental Research Laboratories, NOAA, Boulder, Colorado 80302); Eviatar, A.; Frohlich, A.; Jacobs, A.; Joseph, J.H.; Weber, E.J. J. Geophys. Res. 80: No. 16, 2001-2012 (1 June 1975).

A series of anomalous events associated with solar activity occurred in interplanetary space in June and August 1972. These events include non-Io-associated decametric emission from Jupiter; brightness variations of the periodic comets Schwassmann-Wachmann I and Giacobini-Zinner; interplanetary shock waves detected by Pioneer 9 and 10, Heos 2, and Prognoz and Prognoz 2; interplanetary scintillations; and sudden commencements of geomagnetic storms. Trajectories and deceleration characteristics for the shock waves are estimated primarily from observations using solar radio, in situ, and geomagnetic data. Generally, the trajectories indicate a piston-driven character to about 0.3–0.4 AU, after which the shocks decay to a blastlike motion with a shock velocity variation approximately inversely proportional to the heliocentric radius. Most of the shock waves apparently decayed into magnetoacoustic waves between 2 and 4 AU. In our opinion this decay explains the fact that no anomalous events occurred at either Jupiter or P/Schwassmann-Wachmann I at 5.2 and 5.6 AU, respectively, during August 1972. (auth)

**26618** COLLISIONLESS SHOCK WAVES IN SPACE: A VERY HIGH $\beta$ STRUCTURE. Formisano, V. (Laboratorio per il Plasma nello Spazio, Consiglio Nazionale delle Ricerche, Frascati, Italy); Russell, C.T.; Means, J.D.; Greenstadt, E.W.; Scarf, F.L.; Neugebauer, M. J. Geophys. Res. 80: No. 16, 2013-2022 (1 June 1975).

Measurements from six Ogo 5 particle and field experiments are used to examine the structure of the earth's bow shock during a period of extremely high $\beta$ (the ratio of plasma thermal to magnetic energy density), as determined from simultaneous measurements of the upstream plasma on Heos. Even though the interplanetary field is nearly perpendicular to the shock normal, the shock is extremely turbulent. Large field increases are observed up to a factor of 20 above the upstream values. Ahead of these large enhancements, smaller magnetic effects accompanied by electrostatic noise, electron heating, and ion deflection are observed for several minutes. These observations suggest that a steady state shock may not be able to form at very high $\beta$. Further, they show that while the magnetic energy density may be relatively unimportant in the upstream flow, it can become very significant within the shock structure, and hence the magnetic field should not be ignored in theoretical treatments of very high beta shocks. (auth)

**26619** NEWS FROM INTERPLANETARY DUST. Max-Planck-Institute of Nuclear Physics in Heidelberg Evaluates the Skylab Experiment. Koehler, H. W. Phys. Bl.; 31: No. 2, 65-68 (Feb 1975). (In German).

2 figs.; 1 tab.; 4 refs.

In the Skylab-experiment S-149 particle sizes, densities, and velocity distribution were measured in interplanetary dust in an average altitude of 430 km. These measurements were obtained from tracks of small injection craters and scrapers in gathering areas. (WL)

**26620** MOON IN THE POST-APOLLO ERA. Volume VII. Dordrecht, Netherlands; Reidel (1974). vp.

Separate abstracts are given for the four papers included. (BJG)

*For abstracts of individual papers see: 26356 and 26621–26623.*

**26621** INTERNAL STRUCTURE OF THE MOON. Kopal, Z. (Univ. of Manchester, Eng.). pp 96-110 of Moon in the Post-Apollo Era. Vol. VII. Dordrecht, Netherlands; Reidel (1974).

From considerations on mass, moment of inertia, hydrostatic equilibrium and seismic signals, conclusions are derived regarding the internal structure of the Moon which appears to be essentially different from the structure of the Earth Planet. Entirely new opinions derived from space flight research are presented in contrast to old ideas. (auth)

**26622** STRATIGRAPHY AND CHRONOLOGY OF THE LUNAR SURFACE. Kopal, Z. (Univ. of Manchester, Eng.). pp 171-184 of Moon in the Post-Apollo Era. Vol. VII. Dordrecht, Netherlands; Reidel (1974).

The method of isotopic age determination was used. The author speaks of nuclear or radiometric clocks and comes to the conclusion that it is possible for Nature to tamper with these clocks which, in fact, has happened several times in the history of the Moon. The radiometric ages show a systematic difference

in age between impact-generated breccias and mare basalts. (auth)

**26623** ORIGIN AND EVOLUTION OF THE MOON. Kopal, Z. (Univ. of Manchester, Eng.). pp 197-220 of Moon in the Post-Apollo Era. Vol. VII. Dordrecht, Netherlands; Reidel (1974).

Entirely new ideas on the origin and evolution of the Moon resulting from discoveries of space flight research are discussed. The Earth-Moon system receives thorough treatment. A separate section is devoted to the origin of the maria. (auth)

**26624** BERLAGE'S ACCRETION MODEL OF LUNAR ORIGIN AND ITS GEOCHEMICAL CONSEQUENCES. I. van Bemmelen, R. W. Proc. K. Ned. Adad. Wet. Ser. B.; 78: No. 3, 168-178(1975).

A critical examination is undertaken of the geochemical consequences of Berlage's model of lunar formation which starts from a proto-earth surrounded by a dust cloud. Theoretically, the cloud is supposed to differentiate into three rings: the inner one is attracted by the earth forming its sialic crust. The middle ring contracts forming the moon. Due to tidal torques, the moon is veered out and sweeps through the outer ring, absorbing it. (auth)

**26625** PHOTOGRAPHIC OBSERVATIONS OF MERCURY'S TRANSIT ACROSS THE SUN DISK ON NOVEMBER 10, 1973. Rizvanov, N.; Andrienko, D.; Ghezloun, A.; Svetchnikov, M.; Ourassine, L. (Kazan Univ., USSR). Astron. Astrophys., Suppl. Ser.; 21: No. 2, 171-175(Aug 1975). (In French).

The results of photographic observations of the Mercury transit across the Sun are given. These observations have been made with a normal astrograph at the Observatory of Algiers. The scale of the astrophotographs was defined by comparison with photographs of the star field in the Orion region. The orientation was made by using threads inserted on the photographs of the Sun and the star field. The negatives were measured with the coordinatometer "Ascorecord 2020". The calculations were carried out at ECCM "Nairi-K". (auth)

**26626** ESCAPE OF IONS FROM THE ATMOSPHERE OF VENUS. Nedyalkova, G.M.; Turchinovich, I.E. (A. I. Herzen Teachers' College, Leningrad). Sov. Astron.—AJ 19: No. 1, 81-85 (July 1975).

The equations of motion for ions in the plasma of Venus' ionosphere are formulated and solved, with allowance for interaction with the electric field and for deceleration of ions in the plasma. Values of the critical escape velocity are obtained for $H^+$ and $He^+$ ions and for electrons. The escape rates of these constituents from the ionosphere are calculated. The electric-field strength and total charge of Venus are estimated from the condition that the positive and negative particles have an equal flux. (auth)

**26627** HYDROGEN-ALPHA AURORAL ACTIVITY ON JUPITER. Clary, R.S.; Hunter, J.H. Jr. (Department of Astronomy, University of South Florida, Tampa). Astrophys. J. 199: No. 2, 517-529 (15 July 1975).

This paper deals with an attempt to observe Hα auroral activity on Jupiter. Photographs in Hα light were taken of the planet in the spring and summer of 1972 in Tampa, Florida, utilizing the University of South Florida's 26-inch Schmidt-Cassegrain telescope. This investigation and many others have been undertaken because Jupiter has been shown to have a strong magnetic field and to emit nonthermal radiation at various radio wavelengths which seems to be related to magnetic fields and solar activity. (auth)

**26628** MONTE CARLO TREATMENT OF LYMAN-ALPHA. II. RADIATION IN A SPHERICAL ATMOSPHERE. Modali, S.B. (Wolf Research and Development Corporation, Riverdale, Maryland); Brandt, J.C.; Kastner, S.O. Astrophys. J. 199: No. 2, 530-534 (15 July 1975).

Intensity and the state of polarization of solar Lα photons as they diffuse through an inhomogeneous, spherically symmetric, and isothermal geocorona are presented. The fine structure of Lα and Doppler redistribution of frequencies are taken into account. The calculations used the Monte Carlo technique involving Stokes vectors. Comparison of the results with OGO-4 and OSO-4 observed intensities at an altitude of 650 km shows good agreement. Calculations of the polarization versus solar zenith angle show a residual polarization at large zenith angles which is mainly due to multiply scattered photons. (auth)

# PHYSICS (ATMOSPHERIC)

## Auroral and Ionospheric Phenomena

*Refer also to abstract 26354.*

**26629** EFFECT OF PLASMA INSTABILITY ON *F* REGION PHOTOELECTRON DISTRIBUTIONS. Bloomberg, H.W. (Department of Physics, College of William and Mary, Williamsburg, Virginia 23185). J. Geophys. Res. 80: No. 19, 2851-2853 (1 July 1975).

Ionospheric suprathermal photoelectrons have relatively large cross sections for selected energies. In particular, electrons with energies of about 2.5 eV strongly excite nitrogen vibrational modes, while metastable states of oxygen are excited at about 5 eV. Thus an energy distribution based on chemical kinetic considerations gives rise to a maximum at around 4 eV in the *F* region below 250 km. However, rocket experiments have shown that the expected peaks in the flux spectrum are relatively weak. This discrepancy is explained by the development of a linear instability leading to a wave-particle interaction. The linear mode is driven by the photoelectrons near the $4\text{-}e^{-1}$ maximum in the presence of a magnetic field. The effect is shown to be ineffective at sufficiently low altitudes, where collisionless theory fails. (auth)

**26630** NEUTRAL WINDS AND ELECTROJET IRREGULARITIES. Sato, T. (Geophysics Research Laboratory, University of Tokyo, Tokyo, Japan). J. Geophys. Res. 80: No. 19, 2835-2838 (1 July 1975).

The influence of the neutral winds on charged particle motions in both the equatorial and the auroral electrojet region is studied as a causal mechanism of the phase velocity change of electrojet irregularities. It is found that although the way they are affected is quite different, both electrons and ions undergo the same velocity change in the equatorial region, which is equal to the neutral wind velocity. It is expected therefore that the velocity of any streaming irregularities is also subject to the same velocity change. On the other hand, electrons and ions in the auroral generally undergo different changes in velocity, so that without specifying the mechanism by which the irregularities are controlled, one cannot say how they are modified by neutral winds. For example, if the controlling mechanism is the quasi-linear retardation of the electron stream, the phase velocity of the two-stream irregularities would be changed in accord with the wind velocity variation. (auth)

**26631** ROCKET EXPERIMENT ON SPONTANEOUSLY AND ARTIFICIALLY STIMULATED VLF PLASMA WAVES IN THE IONOSPHERE. Matsumoto, H. (Ionosphere Research Laboratory, Kyoto University, Kyoto, Japan); Miyatake, S.; Kimura, I. J. Geophys. Res. 80: No. 19, 2829-2834 (1 July 1975).

In situ active experiments on the nonlinear wave-wave and wave-particle interactions in the ionospheric plasma were performed by a Japanese sounding rocket K−9M−41. Both spontaneously and artificially stimulated plasma waves in the VLF range were observed. When a large amplitude electron plasma wave was transmitted from the rocket, parametrically excited ion acoustic waves were observed in addition to natural emissions such as whistlers, LHR emissions, and hisslike emissions. It was also found that 'risers' were triggered by the LHR emissions, which seem to be very similar to a phenomenon of the so-called ASE (artificially stimulated emissions). When a slow electron beam with energy lower than 3 eV was ejected from the rocket, a new type of periodic U-shaped discrete emission was observed which was excited through a wave-particle interaction. The frequency of these emissions is lower than the LHR frequency and decreases as the beam energy is increased. Spectrograms of the observed plasma waves are presented, and some are analyzed theoretically. (auth)

**26632** INFLUENCE OF THERMAL PLASMA FLOW ON THE DAYTIME $F_2$ LAYER. Park, C.G. (Radioscience Laboratory, Stanford University, Stanford, California 94305); Banks, P.M. J. Geophys. Res. 80: No. 19, 2819-2823 (1 July 1975).

The coupling between the daytime ionosphere and the overlying magnetosphere is investigated theoretically. Steady state plasma densities and fluxes are computed in the height range 150–3000 km from continuity and momentum equations for $O^+$ and $H^+$ ions. It is found that $O^+$ densities near the $F_2$ layer peak are remarkably insensitive to plasma densities in the overlying magnetosphere, in sharp contrast to the nighttime results reported earlier (Park and Banks, 1974). Plasma flow out of the daytime ionosphere increases with decreasing pressure in the magnetosphere, but the upward $H^+$ flux reaches a well-known saturation limit before it can significantly reduce $O^+$ densities in the $F_2$ layer. Conversely, if the magnetospheric pressure is sufficiently high, plasma can flow downward into the sunlit ionosphere. However, in both cases the influence of such flow on ionospheric densities is not large owing to the dominating effect of photo-ionization within the *F* region. In the top side ionosphere is found that $H^+$ densities and the $H^+-O^+$ transition height depend strongly on plasma densities in the overlying magnetosphere. It is concluded that the daytime plasmapause should be associated with the $H^+$ trough in the top side ionosphere but not with the $O^+$ trough within the $F_2$ layer. In contrast, the nighttime plasmapause should produce a trough in both $H^+$ and $O^+$ densities. It is also concluded that plasma outflow cannot be responsbile for depressions in $N_mF_2$ observed in sunlit regions during ionospheric storms. However, it appears that changes in neutral gas composition or the $O^+ + N_2$ reaction rate can easily account for such depressions. (auth)

**26633** OBSERVATIONS OF EQUATORIAL EUV BANDS: EVIDENCE FOR LOW-ALTITUDE PRECIPITATION OF RING CURRENT HELIUM. Meier, R.R.; Weller, C.S. (E. O. Hulburt Center for Space Research, Naval Research Laboratory, Washington, D. C. 20375). J. Geophys. Res. 80: No. 19, 2813-2818 (1 July 1975).

A new extreme ultraviolet (EUV) emission in the 170− to 400−Å spectral range has been regularly observed at night when looking down over the magnetic dip equator from an earth orbiting satellite at 750−km altitude. The radiation is believed to be $\lambda \leq 304$ Å recombination emission from energetic helium ions and appears as a single arc, quite distinct in spatial form from the oxygen emission arcs. The magnitude of the EUV emission correlates with indices of geomagnetic activity, indicating that precipitating particles are the energy source. A mechanism is proposed in which alpha particles scatter downward from the ring current repeatedly recombine and strip as they enter the atmosphere and lose energy. As a result, numerous excited atomic states are created, and EUV emissions is produced. A computer-coded model of this process using Monte Carlo techniques has been developed. Comparison of the observations with models has yielded information on the altitude and scale height of the emitting region. (auth)

**26634** PROTON PRECIPITATION BY A WHISTLER-MODE WAVE FROM A VLF TRANSMITTER. Koons, H.C. (Space Physics Laboratory, The Aerospace Corporation, El Segundo, California 90245). Geophys. Res. Lett. 2: No. 7, 281-283 (July 1975).

Protons with 50 keV $< E <$ 530 keV were detected by sensors aboard satellite 1972-76B at an altitude of 700 km in the region conjugate to the transportable very-low-frequency (TVLF) transmitter which was being operated near Anchorage, Alaska ($L \sim 4$). Temporal maxima in the proton count rates can be identified on a one-to-one basis with short pulsed transmissions by the VLF transmitter. The observed time delay between the center of a transmitted pulse and the detection of the next maximum in the proton count rate at the sensor agrees well with the delay predicted from a simple plasmaspheric model. (auth)

**26635** ON THE RELATION OF THE 'SLANT E CONDITION' IN POLAR CAP IONOGRAMS TO THE SOLAR WIND SECTOR STRUCTURE. D'Angelo, N. (Danish Space Research Institute, Lyngby, Denmark); Olesen, J.K. J. Geophys. Res. 80: No. 19, 2866-2868 (1 July 1975).

The 'slant E condition' (SEC) in polar cap ionograms has been shown previously to indicate excitation of the Farley-Buneman instability in the *E* region. The SEC at Godhaven (Greenland) is shown here to correlate with the solar wind sector structure, the occurence rate of SEC being large a few days after passage of a sector boundary and declining in the trailing part of the sector. Analysis of SEC occurrence in terms of the solar wind velocity $V_{SW}$ measured on board Heos 2 indicates that no SEC occurs when $V_{SW} < 350$–400 km/s (in apparent agreement with the interpretation of SEC in terms of the Farley-Buneman instability). (auth)

**26636** SIMULTANEOUS INVESTIGATION OF PARENT ELECTRONS AND BREMSSTRAHLUNG X RAYS BY ROCKET-BORNE DETECTORS. Vij, K.K.; Venkatesan, D. (Department of Physics, University of Calgary, Calgary, Alberta, Canada); Sheldon, W.R.; Kern, J.W.; Benbrook, J.R.; Whalen, B.A. J. Geophys. Res. 80: No. 19, 2869-2875 (1 July 1975).

Simultaneous measurements of the energy spectrum of precipitating electrons and the resulting bremsstrahlung X ray spectrum were carried out during an auroral event on March 3, 1971, at the Churchill Research Range, Manitoba, Canada. The electron data were obtained with detectors on a Black Brant VB sounding rocket (275−km apogee), while the X ray flux was measured by an instrument package that was boosted to 60 km on an Arcas rocket. The X ray package was deployed on a parachute at apogee to provide a slow descent through the atmosphere. Thick target bremsstrahlung theory is used to calculate the X ray flux produced by the incident electrons, and a Monte Carlo method is used to predict the X ray spectrum at various altitudes appropriate for comparison with the measured X ray data. Satisfactory agreement between theory and experiment is obtained, and the value of the constant in the thick target theory has been estimated to be $(2 \pm 0.5) \times 10^{-5}$. (auth)

**26637** AURORAL $N_2$ VIBRATIONAL EXCITATION AND THE ELECTRON DENSITY TROUGH. Schunk, R.W.; Banks, P.M. (Department of Applied Physics and Information Science, University of California, San Diego, La Jolla, California 92037). Geophys. Res. Lett. 2: No. 6, 239-242 (June 1975).

Through various processes molecular nitrogen within the nocturnal auroral oval is vibrationally excited, substantially increasing the rate at which $O^+$ is lost via the reaction $O^+ + N^*_2 \rightarrow NO^+ + N$. Owing to the action of thermospheric winds and diffusion, $N^*_2$ does not remain at its point of origin but is transported to regions outside the auroral oval where it can act to substantially reduce the F-region electron density. For an equatorward transport speed of 100 m $sec^{-1}$, $N^*_2$ can travel 3° to 4° of latitude before quenching with atomic oxygen substantially reduces the $N^*_2$ density. This process may contribute significantly to the formation of the mid-latitude F-region electron density trough. (auth)

**26638** IN SITU MEASUREMENTS OF PLASMA DRIFT VELOCITY AND ENHANCED $NO^+$ IN THE AURORAL ELECTROJET BY THE BENNETT SPECTROMETER ON AE-C. Brinton, H.C. (Laboratory for Planetary Atmospheres, Goddard Space Flight Center, Greenbelt, Maryland 20771). Geophys. Res. Lett. 2: No. 6, 243-246 (June 1975).

Simultaneous measurements of ion composition and plasma drift velocity by the Bennett mass spectrometer on the Atmosphere Explorer-C satellite reveal a direct correlation between enhancements in $NO^+$ concentration and ion drift velocity in the southern auroral oval. Low altitude (137 to 250 km) data obtained between 1700 and 2400 hr magnetic local time on October 22, 1974 reveal a region of westward plasma flow at velocities up to 1.3 km/s between 62° and 68° invariant latitude, with corresponding $NO^+$ enhancements of up to a factor of 20. A narrow region of reverse flow at ~0.9 km/s was also measured. These drift observations are consistent with convective flow patterns derived from electric field measurements, and their correlation with $NO^+$ appears to support the suggestion that $NO^+$ enhancements would be expected in regions of drift owing to the dependence on ion energy of the reaction $O^+ + N_2 \rightarrow NO^+ + N$. (auth)

**26639** ELECTRON FLUXES AND CORRELATIONS WITH QUIET TIME AURORAL ARCS. Mizera, P.F.; Croley, D.R. Jr.; Morse, F.A.; Vampola, A.L. (Space Physics Laboratory, The Aerospace Corporation, El Segundo, California 90245). J. Geophys. Res. 80: No. 16, 2129-2136 (1 June 1975).

Primary electron fluxes, measured by two satellites as they crossed quiet time ($Kp=1$, $\Sigma Kp=11+$) auroral arcs, are presented for times near 1420 UT on November 12, 1972. The DMSP 30 satellite measured the optical intensity at 0.6—1.0 μm full width at half maximum (FWHM) and precipitated electrons with $0.22 \leqslant E \leqslant 19.7$ keV near 2100 MLT. The 72—1 satellite crossed the auroral arc system near 2200 MLT and measured 0.36— to 16.5-keV electrons at all pitch angles. A detailed description of the electron morphology that includes comparisons of electron fluxes with optical intensities is presented. We find that the optical intensities extending from 2100 to 2200 MLT correlate best with electrons with $E>1$ keV. The strongest emission bands at these near-infrared wavelengths are $N_2(1P)$ (first-positive band of $N_2$) and $N^+_2(M)$ (Meinel band of $N^+_2$). We estimate that between 4 and 10% of the primary electron energy input is converted to an optical intensity of 140 kR between 0.6 and 1.0 μm FWHM and is equivalent to a weak IBC 2 in the 5577-Å green line of atomic oxygen. (auth)

**26640** SIMULTANEOUS MEASUREMENTS OF AURORAL PARTICLES AND ELECTRIC CURRENTS BY A ROCKET-BORNE INSTRUMENT SYSTEM: INTRODUCTORY REMARKS. Anderson, H.R.; Cloutier, P.A. (Department of Space Physics and Astronomy, Rice University, Houston, Texas 77001). J. Geophys. Res. 80: No. 16, 2146-2151 (1 June 1975).

A rocket-borne experiment package has been designed to obtain simultaneous in situ measurements of the pitch angle distribution and energy spectra of primary auroral particles, the flux of neutral hydrogen at auroral energies, the electric currents flowing in the vicinity of the auroral arc as determined from vector magnetic data, and the modulation of precipitating electrons in the frequency range 0.5—10 MHz. The experiment package was launched by a Nike-Tomahawk rocket from Poker Flat, Alaska, at 0722 UT on February 25, 1972, over a bright auroral band. This paper is intended to serve as an introduction to the detailed discussion of results given in the companion papers. As such it includes a brief review of the general problem, a discussion of the rocket instrumentation, a delineation of the auroral and geomagnetic conditions at the time of launch, and comments on the overall payload performance. (auth)

**26641** ROCKET MEASUREMENT OF AURORAL ELECTRON FLUXES ASSOCIATED WITH FIELD-ALIGNED CURRENTS. Pazich, P.M.; Anderson, H.R. (Department of Space Physics and Astronomy, Rice University, Houston, Texas 77001). J. Geophys. Res. 80: No. 16, 2152-2160 (1 June 1975).

A Nike-Tomahawk rocket was instrumented with a vector magnetometer and an array of particle detectors including an electron and proton energy spectrometer covering the energy range 0.5—20 keV in seven fixed intervals and measuring the pitch angle distribution from 0° to 180° as the rocket spun. The payload was launched from Poker Flat, Alaska, at 0722 UT on February 25, 1972, over a bright auroral band that evidently was the poleward electron aurora, beyond the trapping boundary. An upper limit to the measured proton flux was $10^6$/cm² s sr keV. The energy spectrum of the electron flux measured during passage over the visible aurora always exhibited a peak within the measured energy range. During passage over the brighter auroral forms the peak shifted from ~3 to ~10 keV, the pitch angle distribution became peaked along B, and the intensity increased. Maximum fluxes of $\sim 3\times10^8$ el/cm² s sr keV were seen over the aurora, which reached ~60 kR of λ5577. The electron flux in regions of maximum flux tended to be the most field-aligned in the energy interval showing the highest intensity. (auth)

**26642** ELECTRON CURRENTS ASSOCIATED WITH AN AURORAL BAND. Spiger, R.J.; Anderson, H.R. (Department of Space Physics and Astronomy, Rice University, Houston, Texas 77001). J. Geophys. Res. 80: No. 16, 2161-2164 (1 June 1975).

Measurements of electron pitch angle distributions and energy spectra over a broad auroral band were used to calculate net electric current carried by auroral electrons in the vicinity of the band. The particle energy spectrometers were carried by a Nike-Tomahawk rocket launched from Poker Flat, Alaska, at 0722 UT on February 25, 1972. Data are presented which indicate the existence of upward field-aligned currents of electrons in the energy range 0.5—20 keV. The spatial relationship of these currents to visual structure of the auroral arc and the characteristics of the electrons carrying the currents are discussed. (auth)

**26643** ROCKET-BASED MAGNETIC OBSERVATIONS OF AURORAL BIRKELAND CURRENTS IN ASSOCIATION WITH A STRUCTURED AURORAL ARC. Casserly, R.T. Jr.; Cloutier, P.A. (Department of Space Physics and Astronomy, Rice University, Houston, Texas 77001). J. Geophys. Res. 80: No. 16, 2165-2168 (1 June 1975).

A rocket-borne experiment package containing a vector magnetometer and an array of charge particle detectors was launched over a structured auroral arc from Poker Flat, Alaska, at 0722 UT on February 25, 1972. This paper discusses the results of the magnetometer data which indicate the existence of a pair of oppositely directed Bireland current sheets with magnitudes of $\sim 2.7\times10^{-5}$ A/m² and a system of two eastward electrojets. The downward Birkeland current flowed to the south of the upward current which coincided with the location of the peak auroral luminosity and the region of maximum electron precipitation as measured by the on-board particle detectors. Some changes in the magnetic field profile during the flight are interpreted as being due to movement of the sheet currents in range and azimuth corresponding to the motion of two large folds in the arc as determined from the all-sky camera pictures. (auth)

**26644** NEUTRAL HYDROGEN FLUX MEASURED AT 100- TO 200-km ALTITUDE IN AN ELECTRON AURORA. Iglesias, G.E.; Anderson, H.R. (Department of Space Physics and Astronomy, Rice University, Houston, Texas 77001). J. Geophys. Res. 80: No. 16, 2169-2171 (1 June 1975).

Neutral hydrogen fluxes were measured at altitudes of 120—200 km by a rocket payload that also measured electron and proton fluxes and vector magnetic fields. An intense electron arc ($\sim 2\times10^8$ el/cm² s sr keV) was crossed, while an upper limit to the flux of 0.5— to 20—keV protons was $10^6$/cm² s sr keV. A neutral flux of $5\times10^7$/cm² s sr was observed, assuming hydrogen with >1—keV energy, with greater north-south extent than the electron flux. Its pitch angle distribution was peaked toward 90°, tending toward isotropy in the center. This is fitted to a model describing spreading of an initial proton arc above 500 km. (auth)

**26645** ON A CROSSED FIELD TWO-STREAM PLASMA INSTABILITY IN THE AURORAL PLASMA. Wang, T.N.C.; Tsunoda, R.T. (Stanford Research, Institute, Menlo Park, California 94025). J. Geophys. Res. 80: No. 16, 2172-2182 (1 June 1975).

This paper presents a detailed analysis of the Buneman-Farley two-stream plasma instability. We use a fluid plasma model appropriate for the $E$ region ionosphere, including the effects of the geomagnetic field and electron and ion temperatures and their collisions with neutrals. We derive a linearized dispersion equation for the coupled electron thermal wave and ion thermal wave. The results are compared with those derived from a kinetic theory. It is shown that in the long-wavelength limit the agreement between the above described fluid theory and kinetic theory is exact. The physical arguments for the agreement are clearly stated. From the dispersion equation we obtain closed form expressions for the phase velocities, frequencies, and growth rates describing the threshold condition and the unstable region. With these closed form results we are able to determine the physical behavior of the instability under a variety of ionospheric conditions. The closed form results show that unstable plasma waves having the maximum growth rate propagate at finite off-perpendicular angles with respect to the geomagnetic field. This property, together with the fact that the two-stream instability is a convective instability, is used to infer that radar auroral echoes scattered

from these waves should occur at finite off-perpendicular angles. Spatial maps of radar auroral echoes obtained with a 1210-MHz backscatter radar at Homer, Alaska, are presented as supporting evidence. By taking data during magnetic conditions, we were able to exclude magnetic field line distortion as a possible contributing factor. (auth)

**26646** ECHO 2: A STUDY OF ELECTRON BEAMS INJECTED INTO THE HIGH-LATITUDE IONOSPHERE FROM A LARGE SOUNDING ROCKET. Winckler, J.R.; Arnoldy, R.L.; Hendrickson, R.A. (School of Physics and Astronomy, University of Minnesota, Minneapolis, Minnesota 55455). J. Geophys. Res. 80: No. 16, 2083-2088 (1 June 1975).

The Black Brant V-C Echo 2 rocket was launched at Fort Churchill on September 25, 1972, and it injected 64-ms pulses of electron beams of 80-mA current and 45-keV voltage into the ionosphere. This paper studies the responses of on-board electrostatic deflection and solid state detectors to injected electrons after motion in the near ionosphere and atmosphere. It is shown that it was only through some form of scattering that the detectors could sense the injected beam electrons. By means of 'phase maps' of injection and detection pitch angles a number of distinct regions are found corresponding to a rocket scattering halo, an atmospheric scattering halo, a region of weak responses, and a source of strong scattering above the rocket. The atmospheric scattering has been compared with the theoretical and experimental results of the Echo 1 experiment, and it is found to be in reasonable agreement. The rocket halo is discussed qualitatively; but no explanation is found for the backscatter from above the rocket, which may be associated with an occasional violent beam instability. This analysis has been carried out to better understand the complexities of electron motion observed near large rockets carrying artifical electron accelerators as a guide in the planning of future experiments. (auth)

**26647** ENERGIZATION OF AURORAL ELECTRONS BY ELECTROSTATIC SHOCK WAVES. Kan, J.R. (Geophysical Institute, University of Alaska, Fairbanks, Alaska 99701). J. Geophys. Res. 80: No. 16, 2089-2095 (1 June 1975).

Electrostatic shock waves are proposed as a possible mechanism for energizing electrons which are responsible for discrete auroras. It is shown that electrostatic shock solutions can exist in a $T_i > T_e$ plasma carrying a field-aligned electron current if the plasma in the high-latitude plasma sheet has an earthward flow component. The model is formulated within the framework of the Vlasov-Poisson equations. The reflection of incident ions upstream, the trapping of electrons downstream, and the magnetic mirror of the earth's field are included in the present model. It is found that under the high-latitude plasma sheet conditions, a field-aligned potential jump of several kilovolts can be produced by the shock. Electrons passing through the shock are accelerated at the expense of the ion kinetic energy. (auth)

**26648** ON THE FORMATION OF AURORAL ARCS AND ACCELERATION OF AURORAL ELECTRONS. Swift, D.W. (Geophysical Institute, University of Alaska, Fairbanks, Alaska 99701). J. Geophys. Res. 80: No. 16, 2096-2108 (1 June 1975).

It is suggested that the highly structured auroral arc is caused by a current-driven laminar electrostatic shock oblique to the geomagnetic field. Electrons are accelerated by the potential jump associated with the shock. The shock is assumed to be confined to a plane. Self-consistent solutions to the Poisson-Vlasov systems are calculated for the electrostatic potential. Adiabatic theory is used to calculate the ion number density in terms of the electrostatic potential and its derivatives. The electrons are assumed to be highly magnetized so they can only move parallel to the magnetic field. Solutions are exhibited for two plasma models: (1) streaming electrons and a two-temperature distribution of ions and (2) streaming electrons and ions and thermal electrons and ions. In the latter model, solutions can be obtained for an arbitrary potential jump across the shock. The shock is identified with the linear electrostatic ion cyclotron wave, and stability of these waves is examined to determine conditions for the formation of oblique shocks. Finally, the theory is discussed in the context of the magnetosphere, and possible model shocks are exhibited and discussed in terms of auroral arc formation. (auth)

**26649** ECHO 2: OBSERVATIONS AT FORT CHURCHILL OF A 4-keV PEAK IN LOW-LEVEL ELECTRON PRECIPITATION. Arnoldy, R.L.; Hendrickson, R.A.; Winckler, J.R. (School of Physics and Astronomy, University of Minnesota, Minneapolis, Minnesota 55455). J. Geophys. Res. 80: No. 16, 2316-2318 (1 June 1975).

The Echo 2 rocket flight launched from Fort Churchill, Manitoba, offered the opportunity to observe high-latitude low-level electron precipitation during quiet magnetic conditions. Although no visual aurora was evident at the time of the flight, an auroral spectrum sharply peaked at a few keV was observed to have intensities from 1 to 2 orders of magnitude lower than peaked spectra typically associated with bright auroral forms. There is a growing body of evidence that relates peaked electron spectra to discrete aurora. The Echo 2 observations show that whatever the mechanism for peaking the electron spectrum in and above discrete forms, it operates over a range of precipitation intensities covering nearly 3 orders of magnitude down to subvisual or near subvisual events. (auth)

**26650** A RELATIONSHIP BETWEEN SYNCHRONOUS ALTITUDE ELECTRON FLUXES AND THE AURORAL ELECTROJET. Sharp, R.D.; Shelley, E.G. (Lockheed Palo Alto Research Laboratory, Palo Alto, California 94304); Rostoker, G. J. Geophys. Res. 80: No. 16, 2319-2324 (1 June 1975).

Simultaneous observations during four substorms are reported from the Lockheed auroral particle spectrometer on ATS 5 and the University of Alberta meridian magnetometer chain. During the four events studied there was a good correlation between the magnitude of the trapped electron fluxes in the energy range from 1.8 to 53 keV and the magnitude of the electrojet current as measured by a station in the magnetometer chain at a latitude close to that expected for the ATS conjugate point. A model electro-jet is constructed based on the work of Coroniti and Kennel (1972) which gives a good absolute agreement between the two measured quantities. The results are consistent with the convection electric field's remaining approximately constant during a substantial portion of each of the substorms studied. The temporal variations of the electrojet were apparently controlled by conductivity changes in the ionosphere as determined by the precipitating auroral electrons. (auth)

**26651** ON THE NONLINEAR INTERACTION BETWEEN WHISTLERS AND ALFVÉN WAVES. Larsson, J.; Stenflo, L. (Department of Plasma Physics, Umeå University, Umeå, Sweden). J. Geophys. Res. 80: No. 16, 2325-2326 (1 June 1975).

This paper reconsiders the theory for the generation of an Alfvén wave by nonlinear mixing of two whistler waves. The Alfvén wave is allowed to propagate at arbitrary angles to the geomagnetic field, and its frequency need not be much smaller than the ion gyrofrequency. In this way we can obtain coupling strengths which are larger than those of previous theory. (auth)

**26652** EXTRATERRESTRIAL PARTICLES AND PRECIPITATION. Rosinski, J. (National Center for Atmospheric Research, Boulder, CO); Nagamoto, C. T.; Bayard, M. J. Atmos. Terr. Phys.; 37: No. 9, 1231-1243 (Sep 1975).

Concentration peaks of magnetic spheroids appeared simultaneously at different latitudes in the northern and southern hemispheres, proving that the majority of spheroids is of extraterrestrial origin. Extraterrestrial particles present in a concentration peak are not from a single source but from many meteor streams. Sampling of magnetic particles at different latitudes can be used to detect meteor streams. Chemical composition of surfaces and interiors of magnetic particles is different due to selective fractionation of different chemical compounds between molten and solid phases and due to evaporation into the E- and D-regions during their entry into the atmosphere. The presence of the Bowen rainfall peaks in October and January coincides with the appearance of a high flux of 5- to 20-$\mu$m diameter magnetic particles of extraterrestrial origin. The link between certain Bowen rainfall peaks and particles of extraterrestrial origin is the modification of existing storm systems through worldwide interaction between low level clouds and cirrus ice crystals formed around particles of extraterrestrial origin. (auth)

**26653** CHANGE OF LOW IONOSPHERE CHARACTERISTICS WITH SOLAR CYCLE DEDUCED FROM SOLAR FLARE EFFECTS AT VLF. Piazza, L. R. (Universidade Mackenzie, Sao Paulo, Brazil); Kaufmann, P. J. Atmos. Terr. Phys.; 37: No. 9, 1281-1283 (Sep 1975).

Sudden ionospheric disturbances (SIDs) measured at very low frequencies (vlf) during the solar active years are compared with those occurring during solar quiet years. There is a solar cycle dependence of the low altitude ionosphere characteristics related to the behaviour of the ionospheric parameter L. (auth)

**26654** MODELS FOR THE RELATIONSHIP BETWEEN ELECTRON DENSITY AND TEMPERATURE IN THE UPPER IONOSPHERE. Bilitza, D. (Institut fuer Physikilische Weltraumforschung, Freiburg, i. B.). J. Atmos. Terr. Phys.; 37: No. 9, 1219-1222 (Sep 1975).

Relationships between electron density profiles and electron temperature profiles in the height range 300 to 500 km are determined, using incoherent scatter measurements taken at Millstone Hill (USA), at noon in the years 1965 to 1968. (auth)

**26655** CIRCULATION CHANGES IN THE FREE ATMOSPHERE DURING PROTON EVENTS ASSOCIATED WITH TYPE IV RADIO BURSTS. Zerefos, C. S. (National Hellenic Research Foundation, Athens). Planet. Space Sci.; 23: No. 7, 1035-1043 (Jul 1975).

New evidence of statistically significant circulation changes in the lower stratosphere and in the middle and upper troposphere following Type IV Proton and Ground Level Events confirms some earlier findings of a relationship between solar activity and weather. The maximum 24-hr circulation changes appear to occur in the North Pacific-Alaskan area. A comparison between the effects that followed the flare sample used in this study

with earlier results reported for less intense solar particle emission flare samples, implies that if these particles are responsible for triggering the atmospheric circulation in times of enhanced solar activity, their atmosphere effect is enhanced as one moves to the more energetic solar proton events. The physical explanation of the results may possibly be found in numerical-experimental models. Some possible causes of the results are discussed. (auth)

**26656** EFFECTIVE ELECTRON LOSS COEFFICIENT OF THE DISTURBED DAYTIME D REGION. Swider, W. (Air Force Cambridge Research Labs., Hanscom AFB, Bedford, MA); Dean, W. A. J. Geophys. Res.; 80: No. 13, 1815-1819(1 May 1975).

The effective electron loss coefficient of the D region is determined as a function of height for four daytime instances over a 49-hour time span during the November 2-5, 1969, solar proton event (SPE). The four altitude profiles of this coefficient are seen to be in very good agreement with one another, suggesting that at least for this SPE the average profile is a characteristic function of the disturbed D region over a considerable ionization production rate range. Our results are compared with the determinations of several other groups. The behavior of the loss coefficient at twilight and night is briefly discussed. (auth)

**26657** TWO-DIMENSIONAL NONLINEAR PROCESSES ASSOCIATED WITH "TYPE 1" IRREGULARITIES IN THE EQUATORIAL ELECTROJET. Rogister, A. (Kernforschungsanlage, Juelich, Germany); Jamin, E. J. Geophys. Res.; 80: No. 13, 1820-1828(1 May 1975).

It is suggested that the stabilization mechanism of type 1 irregularities in the equatorial electrojet has two aspects: the turbulence tends to inhibit the formation of large currents and to maintain the plasma in a state relatively "close" to linear marginal stability, and in this state, energy is transferred by two-dimensional nonlinear wave-coupling processes from the linearly growing modes to linearly damped ones propagating in other directions. Energy transfer processes can thus provide detailed stabilization over the entire spectrum. It is argued that the theory provides a plausible interpretation of the as yet puzzling experimental result that the irregularities appear more or less simultaneously over a substantial range of radar elevation angles and the fact that their phase velocities are close to the sound speed and often completely independent of the direction of propagation is perhaps a consequence of mode coupling, but definite prediction here requires numerical calculations. (auth)

**26658** SPECTROSCOPIC MEASUREMENT OF SODIUM DAYGLOW: ABSENCE OF A LARGE DIURNAL VARIATION. Burnett, C. R.; Lasher, R. W.; Miskin, A. S.; Sides, V. L. (Florida Atlantic Univ., Boca Raton, Florida). J. Geophys. Res.; 80: No. 13, 1837-1844(1 May 1975).

Measurements of the sodium dayglow were made with the Pepsios spectrometer at Fritz Peak Observatory, Colorado (40°N, 105°W), from July to November 1973. The average dayglow/twilight intensity ratio in October and November was 2.0 at noon and 1.8 at noon ±4 hours. These results are entirely consistent with solar flux changes due to absorption at twilight and to the daytime albedo contribution, and no diurnal variation of sodium is required. A Ring effect contribution at the $D_2$ line was observed with little diurnal or seasonal variation apparent. (auth)

**26659** IONOSPHERIC EFFECTS OF SOLAR FLARES. Mitra, A. P. Dordrecht, Netherlands; Reidel (1974). 304p.

After a review of the main radiowave and direct techniques for monitoring Sudden Ionospheric Disturbances (SIDs), X radiations in the bands from 1350 down to 1A, producing photoelectrons in the ionosphere are discussed and the X-ray spectrum below 8A is developed. Thresholds for the occurrence of SIDs and correlations in size and time of the different phenomena are dealt with and some analytical techniques are given using both those correlations and a time dependence based on photoionization rates and equations of continuity. A description of some outstanding solar flare events closes the phenomenological section of the book. Discussed also are electron density profiles derived from synoptic SIDs. Work is reviewed on ionization profiles and electron loss rates during flares; both profiles extend up to 90-100 km (d region). SIDs can be used both as a tool for the study of aeronomy and ionchemistry in d and f regions and for flare radiation monitoring. The ionchemistry in the d region falls apart in positive ion-chemistry in the upper d layer and negative ion-chemistry in the lower d layer. X-ray and UV fluxes are estimated. Finally, there is a short survey of Polar-cap absorption events and discussions on lower ionosphere chemistry data during those events. (auth)

**26660** AURORA. Jones, A. V. Dordrecht, Netherlands; Reidel (1974). 313p.

Over the past two decades, auroral science has developed from a somewhat mysterious and imprecise specialty into a discipline central to the study of the ionosphere and magnetosphere. In this handbook an attempt has been made to include those aspects of theory which are valuable in predicting the effects of auroral particle precipitation on the atmosphere. Treated in brief are the mechanisms by which particles are accelerated and precipitated into the atmosphere since this aspect can be found more abundantly in the literature on magnetospheric science. Topics covered on aurora and the ionosphere include the effects of ionization, electric fields and currents, heating effects, reflection of radiowaves, radioabsorption, X-ray production and propagation, radioemission, and infrasonic emission. The techniques of observation are described with particular emphasis on optical methods. Occurrence and morphology of aurorae are described, as well as optical emissions: optical transitions and the auroral spectrum, electron aurora, and proton aurora. A number of spectra are printed and interpreted and also energy level and transition schemes. (auth)

**26661** RELATIONSHIP BETWEEN THE OCCURRENCE OF SPORADIC-E AND SOLAR ACTIVITY. Saksena, R. C. (National Physical Lab., New Delhi). Indian J. Radio Space Phys.; 2: No. 3, 205-210(Sep 1973).

The relationship between the occurrence of sporadic-E and solar activity is not well established for all parts of the world. At high latitudes the negative and positive correlations in American and European zones respectively could be explained on the basis of movement of the north dip-pole. At temperate and equatorial latitudes, definite positive correlation could be shown by considering frequency distribution of occurrence of Es and taking the most probable value as the relevant parameter. (auth)

**26662** STATISTICAL ANALYSIS OF F-REGION ECHOES IN THE PRESENCE OF INTERVENING $E_s$ CLOUDS. Pradhan, S. M.; Singh, V.; Tripathi, A. N.; Tantry, B. A. P. (Banaras Hindu Univ., Varanasi, India). Indian J. Radio Space Phys.; 2: No. 3, 228-230(Sep 1973).

The amplitude fading records of F-region echoes in the presence of $E_s$ irregularities show statistical properties common to certain focussing processes in the ionosphere. This result is shown to support indirectly the hypothesis advanced by the authors that the $E_s$ clouds can focus the radiowaves, when the reflection is taking place from normal F-region. (auth)

**26663** EFFECT OF IONIZATION DRIFTS ON TID STATISTICS. Pradhan, S. M.; Singh, I. S.; Singh, B.; Tantry, B. A. P. (Banaras Hindu Univ., Varanasi, India). Indian J. Radio Space Phys.; 2: No. 3, 224-227(Sep 1973).

The effect of electromagnetic drifts of the ionospheric plasma on the amplitude of travelling ionospheric disturbances (TIDs) induced by gravity waves is studied. It is found that upward lifting of the F-layer causes the amplitude of the TIDs to increase in the evening hours. The other amplitude enhancement occasionally observed in the morning hours is attributed to spatial resonance mechanism, which is discussed in detail. Theoretical calculations show that horizontal drift rather than vertical drift is more important in controlling the diurnal variation of the TIDs at low latitudes by the spatial resonance mechanism. A reasonable agreement between the theoretical calculations and experimental observations is obtained within the limits of the approximations involved in the calculations. (auth)

**26664** WINTER ANOMALY IN THE F2 REGION OVER DELHI. Nalini Mohan Rao, M.; Malhotra, P. L. (National Physical Lab., New Delhi). Indian J. Radio Space Phys.; 2: No. 3, 199-204(Sep 1973).

The winter anomaly of $f$0F2 values on quiet and disturbed days around the lowest phase of solar activity (1962-65), has been studied using three techniques namely, (i) variation of noon $f$0F2, (ii) rates of change of $f$0F2 before and after noon, and (iii) analysis of the ionograms around the F1 maximum by overlay technique. The first two techniques have been used for making a morphological study of the anomaly and the third one yields a quantitative estimate of the factors affecting the anomaly. The winter anomaly in $f$0F2 shown to be accompanied by a stratification of the F-region into F1 and F2. The main cause of the anomaly seems to be a seasonal change in the rate of electron loss. Also, the ratio of linear loss coefficients from summer to winter seasons has been calculated for different solar activity years and for quiet and disturbed days, separately. Based upon this analysis it is confirmed that the increase in loss-rate during summer is responsible for the winter anomaly. (auth)

**26665** SOME STUDIES ON D-REGION ELECTRON DENSITY PROFILES. Chakrabarty, D. K.; Chakrabarty, P. (National Physical Lab., New Delhi). Indian J. Radio Space Phys.; 2: No. 3, 211-218(Sep 1973).

Model electron density profiles in the D-region have been prepared for various solar conditions and for mid-latitude and equatorial locations on the basis of production and loss rates of electrons established from the study of a large number of electron density profiles measured under various conditions. It is found that below 85 km, electron density variations follow a linear law of the type $q = \beta N_e$ and above this altitude a square law of the type $q = \alpha N_e^2$. The electron production rate for any condition of solar activity has been calculated after establishing variations connecting solar activity and solar $L_\alpha$ and X-ray intensities in various ranges as obtained from rocket and satellite observations made under various conditions since 1954. (auth)

**26666** WINTER ANOMALY IN IONOSPHERIC ABSORPTION OF RADIO WAVES OVER HALF A SUNSPOT CYCLE. Patel, B. M.; Patel, J. C.; Kotadia, K. M. (Gujarat Univ., Ahmedabad, India). Indian J. Radio Space Phys.; 2: No. 3, 219-223(Sep 1973).

The winter anomaly in ionospheric absorption is studied at a mid-latitude station over half a solar cycle. It is shown that the anomalous increases of absorption on some days in winter are better correlated with 10 mb-level geopotential height than with temperature at that level. The anomaly is most marked in the month of January. It was about 168% in 1964 and 79% in 1969. The present results along with those reported by others earlier are evidences to suggest that the possible cause of winter anomaly in ionospheric absorption may be an increase in ionization in the D and probably in the E regions of the ionosphere following disturbances in the pressure and wind circulation system at stratospheric and mesospheric levels. (auth)

**26667** LARGE SCALE FLUCTUATIONS IN F2 IONIZATION AT LOW AND TEMPERATE LATITUDES AS OBTAINED FROM TOPSIDE SOUNDER DATA. Dasgupta, A.; Chatterjee, S. K. (Univ., Calcutta). Indian J. Radio Space Phys.; 2: No. 3, 161-163(Sep 1973).

Alouette-I topside sounder data have been utilized to study the large scale irregularities of electron concentration in the F2 region ionization distribution. The nature and occurrence of these irregularities have been investigated at low and temperate latitudes in the American zone. (auth)

**26668** EFFECT OF MAGNETIC ACTIVITY ON IONOSPHERIC ABSORPTION AT WALTAIR. Madhusudhana Rao, D. N.; Jagan Mohana Rao, B.; Ramana, K. V. V. (Univ., Waltair, India). Indian J. Radio Space Phys.; 2: No. 3, 164-165(Sep 1973).

The effect of magnetic activity on the ionospheric absorption at Waltair (lat., 17°43'N) is studied by statistical methods. A positive and significant correlation is obtained between magnetic activity and nighttime absorption on 2 • 4 MHz. The noon time absorption on 2 • 4 MHz has no correlation with magnetic activity. It is also found that the noon time absorption on 5 • 6 MHz is influenced by magnetic activity. (auth)

**26669** OBSERVATIONS ON SPORADIC-E IONIZATION OVER TEMPERATE LATITUDES DURING SOLAR ECLIPSE. Datta, R. N. (University College of Science and Tech., Calcutta). Indian J. Radio Space Phys.; 2: No. 3, 180-182(Sep 1973).

Some further evidences are presented in support of earlier investigations [J. geophys. Res., 77 (1972), 260; 78 (1973),320] to establish a relation between the occurrence of sporadic-E ionization and internal gravity waves during a solar eclipse over temperate latitude stations. A qualitative explanation of sudden appearance of sporadic-E during the hours of eclipse maximum is also suggested. (auth)

**26670** LOCAL TIME VARIATION OF PC-PULSATION PERIOD AT CHOUTUPPAL (HYDERABAD), INDIA. Sarma, S. V. S.; Sarma, Y. S. (National Geophysical Research Inst., Hyderabad, India). Indian J. Radio Space Phys.; 2: No. 3, 183-184(Sep 1973).

From the Pc-micropulsation data recorded at the Choutuppal observatory (Hyderabad), power spectra for successive hours of Pc-regimes, over long intervals of time were obtained. Based on the variation of these spectra with progress of time, the nature of the local time dependence of the period of Pc-pulsations has been investigated. The results indicate that on magnetically quiet days, Pc-periods in the 35-45 and 55-65 sec ranges exhibit a U-type diurnal variation (period changing around local noon). The results presented here are relevant to the equatorial region, and have been further discussed in relation to those reported for middle and higher latitudes. (auth)

**26671** LATITUDINAL VARIATION OF TOTAL ELECTRON CONTENT OF THE IONOSPHERE. Prakash, S. (Regional College of Education., Phopal, India). Indian J. Radio Space Phys.; 2: No. 3, 185-187(Sep 1973).

Published total electron content data monitored from geostationary satellite at several locations have been used to study latitudinal variation of total electron content of the ionosphere (I). It has been found that I increases occasionally towards north in northern hemisphere and towards south in southern hemisphere, although higher values of magnetic activity have not been reported for such periods. It is conjectured that such enhancements are due to the larger influx of ionization from upper atmosphere. (auth)

**26672** HARMONIC ANALYSIS OF WORLD-WIDE $f_0F2$ DATA. Setty, C. S. G. K.; Lumb, H. M. (Univ., Delhi). Indian J. Radio Space Phys.; 2: No. 3, 188-192(Sep 1973).

The harmonic analysis of published $f_0F2$ data for the year 1969 is done for 36 stations distributed all over the world. The variations of the constant, the diurnal and the semi-diurnal components with the time of the day and season have been studied. It is found that the behaviour of the stations in the northern hemisphere differs markedly from those of the southern hemisphere. The diurnal component shows a maximum in local winter for the northern hemispheric stations, while in the southern hemisphere the maximum occurs in equinoxes. It is found that the diurnal component variation is more pronounced for the high latitude stations. The equatorial stations do not show significant seasonal variations. A marked diurnal variation of the ionization occurs for the polar stations in local winter, suggesting sources of ionization other than solar radiations which are under direct solar control. These findings have been discussed in the light of the available information. (auth)

**26673** SCL AND ITS ASSOCIATION WITH SOLAR AND GEOPHYSICAL ACTIVITY. Mitra, S. N. (All India Radio, New Delhi). Indian J. Radio Space Phys.; 2: No. 3, 193-195(Sep 1973).

Correlation is attempted between SCL (Sudden Change in Longwave field intensity) observed at Delhi on longwave transmissions from Radio Tashkent (164 kHz) and Radio Alma Ata (182 kHz) and corresponding solar and geophysical events observed at other places in the world during 5-8 March 1970. A special case studied is the correlation between time variation of X-ray flux during solar flares of 5th and 6th March and the corresponding SCLs. It has been concluded that SCL can be utilized as a reliable and effective means of flare patrol. (auth)

**26674** IONOSPHERIC DUCT PROPAGATION AND Pc 1 PULSATION SOURCES. Fraser[1], B.J. (Cooperative Institute for Research in Environmental Sciences, University of Colorado, Boulder, Colorado 80302). J. Geophys. Res. 80: No. 22, 2790-2796 (1 Aug 1975).

Detailed study of two Pc 1 hydromagnetic emission events observed at Great Whale River, Quebec: Boulder, Colorado; and College, Alaska, indicates that emission energy propagated westward in an ionospheric duct from an extended source region east of Great Whale River with duct velocities ranging from 500 to 2500 km $s^{-1}$. Sources located using both triangulation direction of arrival and polarization techniques were found to be generally consistent. Autocorrelation measurements of fine structure element spacing within the events show that dispersion increased with longitudinal distance from the source. (auth)

**26675** POLARIZATION OF Pc 1 PULSATIONS AT HIGH AND MIDDLE LATITUDES. Fraser[1], B.J. (Cooperative Institute for Research in Environmental Sciences, University of Colorado, Boulder, Colorado 80302). J. Geophys. Res. 80: No. 22, 2797-2807 (1 Aug 1975).

Polarization studies of hydromagnetic emission events have been undertaken over a 10-month period in 1971–1972 at Great Whale River, Quebec, Canada: Boulder, Colorado; and College, Alaska. The occurrence of events common to all three stations suggests that transverse ionospheric duct propagation of Pc 1 signals is possible at both high and middle latitudes. Polarization ellipse major axis azimuths, ellipticities, and perturbation vector rotation directions in the plane of the earth's surface often show consistent and related behavior at high and middle latitudes when statistical samples and individual events are considered. Erratic polarization associated with geomagnetic storm activity is observed at high latitudes but not at low latitudes. The results are interpreted in terms of the source location at ionospheric heights, ionospheric duct propagation, and ground induction effects. (auth)

**26676** AURORAL ELECTRONS AND THE OPTICAL EMISSIONS OF NITROGEN. Feldman, P.D.; Doering, J.P. (Johns Hopkins University, Baltimore, Maryland 21218). J. Geophys. Res. 80: No. 22, 2808-2812 (1 Aug 1975).

The differential flux of auroral primary and secondary electrons and the emission of the 1 PG and 2 PG (first and second positive) systems of $N_2$ and the 1 NG (first negative) system of $N_2^+$ were measured in a rocket experiment during a steady IBC II$^+$ aurora. The electron data indicate that the incident auroral electrons were nearly monoenergetic with energy of about 25 keV. A single power law of the form $F = F_0E^\alpha$ cannot accurately describe the secondary electron spectrum in the energy range of 3–85 eV. However, the spectrum may be approximated by using $\alpha = -3.2$ between 7 and 20 eV and $\alpha = -0.9$ between 25 and 85 eV. The measured intensity and altitude profile of the $N_2$ 1 PG (5, 2) band at 6685 Å agree well with the values

calculated by using the measured electron flux and laboratory cross-section data. About 40% of the $N_2^+$ 1 NG(0,0) band emission at 3914 Å is excited by electrons with energy below 85 eV. (auth)

**26677** INFLUENCE OF THERMAL PLASMA FLOW ON THE DAYTIME $F_2$ LAYER. Park, C.G. (Radioscience Laboratory, Stanford University, Stanford, California 94305); Banks, P.M. J. Geophys. Res. 80: No. 22, 2819-2823 (1 Aug 1975).

The coupling between the daytime ionosphere and the overlying magnetosphere is investigated theoretically. Steady state plasma densities and fluxes are computed in the height range 150–3000 km from continuity and momentum equations for $O^+$ and $H^+$ ions. It is found that $O^+$ densities near the $F_2$ layer peak are remarkably insensitive to plasma densities in the overlying magnetosphere, in sharp contrast to the nighttime results reported earlier (Park and Banks, 1974). Plasma flow out of the daytime ionosphere increases with decreasing pressure in the magnetosphere, but the upward $H^+$ flux reaches a well-known saturation limit before it can significantly reduce $O^+$ densities in the $F_2$ layer. Conversely, if the magnetospheric pressure is sufficiently high, plasma can flow downward into the sunlit ionosphere. However, in both cases the influence of such flows on ionospheric densities is not large owing to the dominating effect of photo-ionization within the $F$ region. In the top side ionosphere it is found that $H^+$ densities and the $H^+$-$O^+$ transition height depend strongly on plasma densities in the overlying magnetosphere. It is concluded that the daytime plasmapause should be associated with the $H^+$ trough in the top side ionosphere but not with the $O^+$ trough within the $F_2$ layer. In contrast, the nighttime plasmapause should produce a trough in both $H^+$ and $O^+$ densities. It is also concluded that plasma outflow cannot be responsible for depressions in $N_mF_2$ observed in sunlit regions during ionospheric storms. However, it appears that changes in neutral gas composition or the $O^+ + N_2$ reaction rate can easily account for such depressions. (auth)

**26678** ROCKET MEASUREMENT OF ION AND NEUTRAL TEMPERATURES IN THE LOWER IONOSPHERE. Sasaki, S.; Kawashima, N. (Institute of Space and Aeronautical Science, University of Tokyo, Tokyo, Japan). J. Geophys. Res. 80: No. 22, 2824-2828 (1 Aug 1975).

A direct measurement of ion and neutral temperatures simultaneously in the lower ionosphere was successfully carried out by a shadow method from a sounding rocket launched from Uchinoura, Kagoshima, Japan, on September 22, 1973. The apparatus based on this method and the obtained data of ion and neutral temperatures together with electron density simultaneously measured by a new direct display system of the electron density and temperature are described in detail. The data are consistent with the prediction that ion and neutral temperatures are nearly equal to each other in the lower ionosphere, and they show the existence of interesting gross structures in the temperature profiles of this region. (auth)

**26679** ROCKET EXPERIMENT ON SPONTANEOUSLY AND ARTIFICIALLY STIMULATED VLF PLASMA WAVES IN THE IONOSPHERE. Matsumoto, H. (Ionosphere Research Laboratory, Kyoto University, Kyoto, Japan); Miyatake[1], S.; Kimura, I. J. Geophys. Res. 80: No. 22, 2829-2834 (1 Aug 1975).

In situ active experiments on the nonlinear wave-wave and wave-particle interactions in the ionospheric plasma were performed by a Japanese sounding rocket K-9M-41. Both spontaneously and artificially stimulated plasma waves in the VLF range were observed. When a large amplitude electron plasma wave was transmitted from the rocket, parametrically excited ion acoustic waves were observed in addition to natural emissions such as whistlers, LHR emissions, and hisslike emissions. It was also found that 'risers' were triggered by the LHR emissions, which seem to be very similar to a phenomenon of the so-called ASE (artificially stimulated emissions). When a slow electron beam with energy lower than 3 eV was ejected from the rocket, a new type of periodic U-shaped discrete emission was observed which was excited through a wave-particle interaction. The frequency of these emissions is lower than the LHR frequency and decreases as the beam energy is increased. Spectrograms of the observed plasma waves are presented, and some are analyzed theoretically. (auth)

**26680** NEUTRAL WINDS AND ELECTROJET IRREGULARITIES. Sato, T. (Geophysics Research Laboratory, University of Tokyo, Tokyo, Japan). J. Geophys. Res. 80: No. 22, 2835-2838 (1 Aug 1975).

The influence of the neutral winds on charged particle motions in both the equatorial and the auroral electrojet region is studied as a causal mechanism of the phase velocity change of electrojet irregularities. It is found that although the way they are affected is quite different, both electrons and ions undergo the same velocity change in the equatorial region, which is equal to the neutral wind velocity. It is expected therefore that the velocity of any streaming irregularities is also subject to the same velocity change. On the other hand, electrons and ions in the auroral region generally undergo different changes in velocity, so that without specifying the mechanism by which the irregularities are controlled, one cannot say how they are modified by neutral winds. For example, if the controlling mechanism is the quasi-linear retardation of the electron stream, the phase velocity of the two-stream irregularities would be changed in accord with the wind velocity variation. (auth)

**26681** THERMOSPHERIC RESPONSE TO A MAGNETIC SUBSTORM. Richmond, A.D.; Matsushita, S. (High Altitude Observatory, National Center for Atmospheric Research, Boulder, Colorado 80303). J. Geophys. Res. 80: No. 22, 2839-2850 (1 Aug 1975).

A computer model is used to simulate the winds and temperature variations in the thermosphere which result from auroral region electric currents during a large isolated magnetic substorm. A disturbance propagates with a speed of 750 m/s poleward and equatorward, with an amplitude of about 200 m/s in the north-south velocity and about 100 K in the temperature at 400-km altitude. The amplitude decays relatively little before the disturbance reaches the equator. The time history of the disturbance is roughly that of a single sinusoid whose period increases with horizontal distance from the source and with decreasing altitude. East-west winds of over 400 m/s at 400-km altitude are created in the auroral region itself by the ion drag mechanism. The spatial distribution of these ion drag winds is significantly affected by momentum convection, so that a simple interpretation in terms of local ion drag forces is generally not sufficient. A residual electric field of about 5 mV/m remains after the substorm source is turned off, due to the dynamo effect of the ion drag winds. Vertical velocities up to about 40 m/s are produced inside the auroral region, primarily by the fact that the heated air is more buoyant than the air outside. Comparison of our simulation with numerous observations shows generally good agreement. (auth)

**26682** EFFECT OF PLASMA INSTABILITY ON $F$ REGION PHOTOELECTRON DISTRIBUTIONS. Bloomberg[1], H.W. (Department of Physics, College of William and Mary, Williamsburg, Virginia 23185). J. Geophys. Res. 80: No. 22, 2851-2853 (1 Aug 1975).

Ionospheric suprathermal photoelectrons have relatively large cross sections for selected energies. In particular, electrons with energies of about 2.5 eV strongly excite nitrogen vibrational modes, while metastable states of oxygen are excited at about 5 eV. Thus an energy distribution based on chemical kinetic considerations gives rise to a maximum at around 4 eV in the $F$ region below 250 km. However, rocket experiments have shown that they expected peaks in the flux spectrum are relatively weak. This discrepancy is explained by the development of a linear instability leading to a wave-particle interaction. The linear mode is driven by the photoelectrons near the 4-eV maximum in the presence of a magnetic field. The effect is shown to be ineffective at sufficiently low altitudes, where collisionless theory fails. (auth)

**26683** DIRECTION-FINDING MEASUREMENTS OF AURORAL KILOMETRIC RADIATION. Kurth, W.S.; Baumback, M.M.; Gurnett, D.A. (Department of Physics and Astronomy, University of Iowa, Iowa City, Iowa 52242). J. Geophys. Res. 80: No. 22, 2764-2770 (1 Aug 1975).

Direction-finding measurements with plasma wave experiments on the Hawkeye 1 and Imp 8 satellites are used to locate the source region of auroral kilometric radiation. This radiation has peak intensities between about 100 and 300 kHz and is emitted in intense sporadic bursts lasting for from half an hour to several hours. At peak intensity the total power emitted in this frequency range exceeds $10^9$ W. The occurrence of this radiation is known to be closely associated with bright auroral arcs which occur in the local evening auroral regions. Hawkeye 1 provides direction-finding measurements of kilometric radiation from observations at high latitudes (5–20 $R_E$) over the northern polar regions, and Imp 8 provides similar observations at large radial distances (23–46 $R_E$) near the equatorial plane. Results from both satellites place the source of the intense auroral kilometric radiation in the late local evening at about 22.0 hours LT and at a distance of about 0.75 $R_E$ from the polar axis of the earth. These direction-finding measurements, together with earlier results from the Imp 6 satellite, strongly indicate that the intense auroral kilometric radiation is generated by energetic auroral electrons at low altitudes in the evening auroral zone. The observed source location is in good quantitative agreement with the source position expected from simple propagation and ray path considerations. (auth)

**26684** ON THE RELATION OF THE 'SLANT E CONDITION' IN POLAR CAP IONOGRAMS TO THE SOLAR WIND SECTOR STRUCTURE. D'Angelo, N. (Danish Space Research Institute, Lyngby, Denmark); Olesen, J.K. J. Geophys. Res. 80: No. 22, 2866-2868 (1 Aug 1975).

The 'slant E condition' (SEC) in polar cap ionograms has been shown previously to indicate excitation of the Farley-Buneman instability in the $E$ region. The SEC at Godhavn (Greenland) is shown here to correlate with the solar wind sector structure, the occurrence rate of SEC being large a few days after passage of a sector boundary and declining in the trailing part of the sector. Analysis of SEC occurrence in terms of the solar wind velocity $V_{sw}$ measured on board Heos 2 indicates that no SEC occurs when $V_{sw} < 350$–$400$ km/s (in apparent agreement with the interpretation of SEC in terms of the Farley-Buneman instability). (auth)

**26685** SIMULTANEOUS INVESTIGATION OF PARENT ELECTRONS AND BREMSSTRAHLUNG X RAYS BY ROCKET-BORNE DETECTORS. Vij, K.K.; Venkatesan, D. (Department of Physics, University of Calgary, Calgary, Alberta, Canada); Sheldon, W.R.; Kern, J.W.; Benbrook, J.R.; Whalen, B.A. J. Geophys. Res. 80: No. 22, 2869-2875 (1 Aug 1975).

Simultaneous measurements of the energy spectrum of precipitating electrons and the resulting bremsstrahlung X ray spectrum were carried out during an auroral event on March 3, 1971, at the Churchill Research Range, Manitoba, Canada. The electron data were obtained with detectors on a Black Brant VB sounding rocket (275-km apogee), while the X ray flux was measured by an instrument package that was boosted to 60 km on an Arcas rocket. The X ray package was deployed on a parachute at apogee to provide a slow descent through the atmosphere. Thick target bremsstrahlung theory is used to calculate the X ray flux produced by the incident electrons, and a Monte Carlo method is used to predict the X ray spectrum at various altitudes appropriate for comparison with the measured X ray data. Satisfactory agreement between theory and experiment is obtained, and the value of the constant in the thick target theory has been estimated to be $(2\pm0.5)\times10^{-5}$. (auth)

**26686** ALTITUDE DEPENDENT NEUTRAL WIND EFFECTS ON THE NONLINEAR MOTION OF A SMALL BARIUM CLOUD. Book, D.L.; Ossakow, S.L. (Naval Research Laboratory, Washington, D. C. 20375); Goldman, S.R. J. Geophys. Res. 80: No. 22, 2879-2882 (1 Aug 1975).

The nonlinear motion of a small $F$ region barium release electrostatically coupled to the $E$ region is studied in the presence of a neutral wind with differing values for the $E$ and $F$ regions. In a reference frame moving with the $E$ region neutral wind an $F$ region neutral wind transverse to the background $E_0$ field is shown to retard or accelerate the evolution of the cloud without otherwise altering the development of the system. When the relative neutral wind has a component parallel to the background $E_0$ field, there is also a change in the direction of the axis of elongation of the cloud as a function of time, although the final direction is independent of the relative neutral wind. Barium cloud and image behavior are shown to be substantially identical for periodic and Dirichlet boundary conditions. (auth)

**26687** PARTICULATE EFFECTS ON THE LOW-LATITUDE $D$ REGION. Ganguly[1], S. (Institute of Radio Physics and Electronics, University of Calcutta, Calcutta, India). J. Geophys. Res. 80: No. 22, 2883-2886 (1 Aug 1975).

Radio wave absorption data for a number of stations have been utilized in studying the response of the low-latitude $D$ region toward solar particle events reported by Explorer 34. A large increase in ionization even at the equatorial latitude has been observed associated with the particle events; these increases in absorption are sometimes delayed by a few days in comparison with the corresponding increases in high-energy proton counts, though in general, the delay is less than that for the most intense events. These ionization increases could be due to precipitated electrons from the inner belt with a flux of less than $10^4$ el cm$^{-2}$ s$^{-1}$ for $E>40$ keV. (auth)

## Effects of Nuclear Detonations

**26688** MODELING OF ATMOSPHERIC NUCLEAR EXPLOSIONS OVER A MOUNTAINOUS REGION BY VERTICAL AND HORIZONTAL SINGLE FORCES. Ben-Menahem, A.; Vered, M. (Weizmann Inst. of Science, Rehovot, Israel). Bull. Seismol. Soc. Am.; 65: No. 4, 971-980(Aug 1975).

Observed P and S waves from the respective Soviet and Chinese atmospheric explosions of October 30, 1961 and October 30, 1970 are found to differ both in their S/P amplitude ratios and the form of the individual wavelets. This difference is attributed to the effect of the local topography on the ensuing ground motion at the source. Asymptotic ray theory indicates that an additional horizontal force component was acting at the source of the Chinese event while the Soviet event could be modeled by a vertical force only. Generalized ray theory is then applied to calculate the body wave forms in each case. The agreement between the theoretical results and the observations is excellent. (auth)

## Magnetospheric Phenomena

*Refer also to abstracts 26520, 26648, and 26660.*

**26689** USING THE MOON TO PROBE THE GEOMAGNETIC TAIL LOBE PLASMA. Schubert, G. (Department of Planetary and Space Science, University of California, Los Angeles, California 90024); Sonett, C.P.; Smith, B.F.; Schwartz, K.; Colburn, D.S. Geophys. Res. Lett. 2: No. 7, 277-280 (July 1975).

We have detected the presence of plasma in the lobes of the geomagnetic tail from observations of magnetic induction in the Moon forced by time variations of the Earth's magnetotail lobe field. The magnitude of the Moon's tangential electromagnetic transfer function when the Moon is in the lobes of the geomagnetic tail is less than that when the Moon is in the solar wind or geomagnetic tail plasma sheet. The tangential transfer function when the Moon is in the magnetotail lobes decreases at frequencies above about 8 milliHz due to finite wavelength effects. This shows that the waves in the magnetotail lobes which drive the lunar magnetic induction must have speeds far less than the speed of light and wavelengths comparable to the size of the Moon. (auth)

**26690** TWO BARIUM PLASMA INJECTIONS INTO THE NORTHERN MAGNETOSPHERIC CLEFT. Jeffries, R.A.; Roach, W.H.; Hones, E.W. Jr. (Los Alamos Scientific Laboratory, University of California, Los Alamos, New Mexico 87545); Wescott, E.M.; Stenbaek-Nielsen, H.C.; Davis, T.N.; Winningham, J.D. Geophys. Res. Lett. 2: No. 7, 285-288 (July 1975).

Barium plasma was injected into the northern magnetospheric cleft twice during January, 1975. Lofted by rockets launched after local magnetic noon from Cape Parry, NWT, Canada, high-explosive shaped charges compressed hollow barium cones to generate vapor jets moving upward with initial velocities near 13 km/s parallel to the geomagnetic field. Barium plasma streaks created by solar photoionization of the vapor were convected through the polar magnetosphere and were observed optically from airborne and ground-based sites until about 40 min after injection. Numerous indicators were monitored to determine the degree of magnetospheric disturbance; ionosondes at Cape Parry and Sachs Harbour, NWT, monitored latitudinal cleft motions preceding rocket launch. Spectrometers in the payloads recorded charged-particle fluxes during both flights. The first injection occurred poleward in the cleft with subsequent plasma convection antisunward across the polar cap; the second occurred centrally with plasma convection duskward at constant magnetic latitude. (auth)

**26691** THERMOSPHERIC RESPONSE TO A MAGNETIC SUBSTORM. Richmond, A.D.; Matsushita, S. (High Altitude Observatory, National Center for Atmospheric Research, Boulder, Colorado 80303). J. Geophys. Res. 80: No. 19, 2839-2850 (1 July 1975).

A computer is used to simulate the winds and temperature variations in the thermosphere which result from auroral region electric currents during a large isolated magnetic substorm. A disturbance propagates with a speed of 750 m/s poleward and equatorward, with an amplitude of about 200 m/s in the north-south velocity and about 100 K in the temperature at 400-km altitude. The amplitude decays relatively little before the disturbance reaches the equator. The time history of the disturbance is roughly that of a single sinusoid whose period increases with horizontal distance from the source and with decreasing altitude. East-west winds of over 400 m/s at 400-km altitude are created in the auroral region itself by the ion drag mechanism. The spatial distribution of these ion drag winds is significantly affected by momentum convection, so that a simple interpretation in terms of local ion drag forces is generally not sufficient. A residual electric field of about 5 mV/m remains after the substorm source is turned off, due to the dynamo effect of the drag winds. Vertical velocities up to about 40 m/s are produced inside the auroral region, primarily by the fact that the heated air is more buoyant than the air outside. Comparison of our simulation with numerous observations shows generally good agreement. (auth)

**26692** HEOS 2 PLASMA OBSERVATIONS IN THE DISTANT POLAR MAGNETOSPHERE: THE PLASMA MANTLE. Rosenbauer, H.; Grünwaldt, H.; Montgomery, M.D.; Paschmann, G.; Sckopke, N. (Max-Planck-Institut für Physik und Astrophysik, Institut für extraterrestrische Physik Garching, West Germany). J. Geophys. Res. 80: No. 19, 2723-2737 (1 July 1975).

Comprehensive plasma observations carried out on board the Hoes 2 satellite have provided the first systematic description of plasmas in the distant polar magnetosphere. These observations have revealed the presence of a persistent layer of tailward-flowing magnetosheathlike plasma inside of and adjacent to the magnetopause. This region has been termed the 'plasma mantle.' The mantle has been found to extend over the entire surface of the magnetosphere tailward of the polar cusp and northward of the plasma sheet. Vela observations of a 'magnetotail boundary layer' obtained in the vicinity of the plasma sheet by Hones and coworkers refer to the same phenomenon. The salient features of the plasma mantle as provided by Heos measurements from February to December 1972 can be summarized as follows: (1) The mantle was found to be present in over 70% of the passes through the polar magnetosphere in the region described above. (2) Its thickness varies greatly, ranging up to $\gtrsim 4\ R_E$, and does not appear to depend significantly on position or the state of the magnetosphere as measured by $Kp$. (3) A tailward-directed bulk flow parallel to the local terrestrial magnetic field was nearly always distinctly measurable. It was found to lie usually between 100 and 200 km s$^{-1}$ and was always less than the concurrent flow speed in the nearby magnetosheath. (4) The flow speed in the mantle is positively correlated with flow speeds in the magnetosheath and solar wind but depends only very weakly, if at all, on distance from the polar cusp, i.e., on $X_{OSM}$. (5) A narrow region of

low density and/or low flow speed plasma, i.e., a 'gap,' 0.1–0.2 $R_E$ thick, is frequently observed between the plasma mantle and the magnetopause. (6) The mantle protons are normally significantly cooler along $B$ than perpendicular, i.e., $T_\parallel < T_\perp$. (7) The proton density, temperature, and bulk speed all tend to decrease gradually with depth inside the magnetopause, but this trend can at times be obscured by fluctuations and magnetopause motions. At the inner edge of the mantle the proton distribution is often very narrow in both energy and angle, i.e., relatively cold, before it finally disappears below the 100–eV threshold of the instrument. It is concluded, after an appraisal of several possible mechanisms, that the most probable cause for the formation of the mantle is the day side merging of terrestrial and interplanetary field lines. (auth)

**26693** THE $L$=6.7 QUIET TIME BARIUM SHAPED CHARGE INJECTION EXPERIMENT 'CHACHALACA'. Wescott, E.M.; Rieger, E.P.; Stenbaek-Nielsen, H.C.; Davis, T.N. (Geophysical Institute, University of Alaska, Fairbanks, Alaska 99701); Peek, H.M.; Bottoms, P.J. J. Geophys. Res. 80: No. 19, 2738-2744 (1 July 1975).

Near dawn on October 9, 1972, UT, a barium plasma injection experiment was carried out from Poker Flat, Alaska, during quiet magnetic conditions (Kp=1+). The visible plasma flux tube produced was more diffuse than the flux tubes in previous experiments, but it could be tracked for 30 min out to an altitude of 2.5 $R_E$. The flux tube remained integral for about 20 min, when a single striation separated from the main streak. Comparisons of the observed flux tube orientation with theoretical field models show no significant deviations ascribable to field-aligned currents. Cross-field drift rates of the foot of the flux tube indicate an E field of approximately 7 mV/m at 200–km altitude. Although an attempt was made via a jet aircraft flight, barium ions were not detected in the southern conjugate region. No energetic particle precipitation phenomena were observed which could be ascribed to the barium plasma injection. (auth)

**26694** WEAK PITCH ANGLE SCATTERING OF ENERGETIC PROTONS IN THE MAGNETOSPHERE. Scholer, M.; Morfill, G.; Hovestadt, D. (Max-Planck-Institut für Physik und Astrophysik Institut für Extraterrestrische Physik, Garching, West Germany). J. Geophys. Res. 80: No. 19, 2745-2750 (1 July 1975).

During the solar particle event of April 12–14, 1973, a flux depression of solar protons in the dawn side pseudotrapping region relative to the flux in the dusk side pseudotrapping region was frequently observed with the low-altitude polar-orbiting satellite Esro 4. This flux decrease is interpreted as being due to weak pitch angle scattering of the solar protons during their drift from dusk to dawn. Treating the pitch angle diffusion as a simple initial value problem, we derive quantitative values of the equatorial bounce-averaged pitch angle diffusion coefficients at small pitch angles for different energies. These values represent lower limits for magnetospheric conditions at the time for the Esro 4 observations. Through the assumption that the pitch angle diffusion is a gyroresonant interaction process of the particles with either Alfvén or ion cyclotron waves, the necessary power of the waves at the resonant interaction frequency is calculated. (auth)

**26695** A CONTRIBUTION TO THE THEORY OF THE ELECTROSTATIC HALF-HARMONIC ELECTRON GYROFREQUENCY WAVES IN THE MAGNETOSPHERE. Ashour-Abdalla, M.; Chanteur, G. (Groupe de Recherches Ionosphériques, Centre National d'Etudes des Télécommunications Issy-les-Moulineaux, France); Pellat, R. J. Geophys. Res. 80: No. 19, 2775-2782 (1 July 1975).

The effect of different plasma parameters on the stability of the half-harmonic electron gyrofrequency waves is investigated. By making some simplifying assumptions about the cold plasma and using a ring distribution for the warm component the role of the different parameters is demonstrated. A maximum value of the ratio of the cold to hot plasma density above which we cannot get instability is derived, and this ratio increases with the temperature anisotropy. Calculations of the growth rates show that there is a sharp peak when $\theta = \tan^{-1} k_\perp/k_\parallel \sim 70° - 80°$. (auth)

**26696** PLASMA FLOW HYPOTHESIS IN THE MAGNETOSPHERE RELATING TO FREQUENCY SHIFT OF ELECTROSTATIC PLASMA WAVES. Oya, H. (Upper Atmosphere and Space Research Laboratory, Tohoku University, Sendai, Japan). J. Geophys. Res. 80: No. 19, 2783-2789 (1 July 1975).

The frequency dynamic spectrum indicating a monotonic frequency shift of the electrostatic electron cyclotron harmonic wave emissions in the data of VLF electric field observations by Ogo 5 has been detected in the midnight and dawn meridians outside the plasmapause; the emissions are produced from turbutent areas in the plasma states that include the temperature anisotropy, loss cone velocity distribution, or the double hump in the velocity distribution function. The frequency shift is also observed for the case of the emissions in the magnetosheath near the subsolar point. These frequency shifts are interpreted on a hypothesis of the Doppler effects of the plasma waves due to the plasma flow with respect to the satellite frame. The speeds of the plasma flow are obtained and have a range from 150 to 300 km/s. Disruption of the plasma flow due to the magnetic field bumps may produce the turbulent source generating the Harris type or beam type instabilities that generate the electrostatic electron cyclotron harmonic waves. (auth)

**26697** OBSERVATION OF THE FARLEY–BUNEMAN INSTABILITY IN LABORATORY PLASMA. John, P.I.; Saxena, Y.C. (Physical Research Laboratory, Ahmedabad 380 009, India). Geophys. Res. Lett. 2: No. 6, 251-254 (June 1975).

An experiment simulating certain characteristics of the equatorial electrojet plasma (viz. $\nu_e \ll \Omega_e \nu_i \gtrsim \Omega i$) is described. High frequency ($\omega \gtrsim \nu_i > \Omega_i$) instabilities are observed when electrons stream in the E × B direction past ions with a velocity exceeding the ion acoustic speed. The observed phase velocities and frequencies agree with the results of the Farley—Buneman instability theory, modified to take account of finite $k_\perp$. The measured instability spectrum for potential fluctuations goes as $k_\perp^{-n}$ with $n = 2 - 3.5$. (auth)

**26698** DYNAMIC SPECTRAL PATTERNS OF MAGNETIC PULSATIONS IN THE Pc 5 FREQUENCY RANGE AT CONJUGATE POINTS NEAR $L$=4. Fukunishi, H. (Bell Laboratories, Murray Hill, New Jersey 07974). J. Geophys. Res. 80: No. 16, 2199-2206 (1 June 1975).

Magnetic data observed at conjugate pair stations near L=4 have been used to compute dynamic power spectra in the frequency range 1–9 mHz ($T$ = 1000–110 s) for 15 days with various levels of magnetic activity. It is found that the dynamic spectral patterns at the conjugate points are quite similar to each other, often even in their fine structure. The dynamic spectra show a significant diurnal variation of the power intensity with a large power during the daytime hours, regardless of the level of magnetic activity. During the nightime hours on extremely quiet days the power intensity remains at much lower levels compared with the daytime intensity level, while on disturbed days the power amplitude during the nighttime hours is enhanced in association with the occurrences of substorms. It is also found that the conjugate power ratio has a well-defined local time dependence. The results suggest that the magnetic fluctuations in this frequency range arise principally from energy sources within the magnetosphere. The results also suggest that a main energy source in the Pc 5 frequency range comes from the day side of the magnetosphere, and the energy sources in the night side are closely related to the substorm mechanism. It is also suggested that the fluctuation of the $Sr_q$ current is important as an energy source in the Pc 5 frequency range. (auth)

**26699** A COMPARISON OF THERMOSPHERIC NEUTRAL GAS HEATING AND RELATED THERMAL AND ENERGETIC PLASMA PHENOMENA AT HIGH LATITUDES DURING GEOMAGNETIC DISTURBANCES. Raitt, W.J. (University College London, Mullard Space Science Laboratory, Holmbury St. Mary, Dorking, Surrey, England); von Zahn, U.; Christophersen, P. J. Geophys. Res. 80: No. 16, 2277-2288 (1 June 1975).

Simultaneous in situ measurements of energetic particle fluxes, ionospheric parameters, and neutral atmospheric parameters from the polar-orbiting satellite Esro 4 were made at altitudes in the range 250–500 km at middle and high latitudes. A study of changes in the parameters in both position and magnitude during geomagnetic disturbances in December 1972 and February 1973 showed three main regions of neutral atmosphere disturbance following the onset of magnetic activity indicated by the value of the Kp index. First, the largest effect was an enhancement of the $N_2$ and Ar densities and reduction of the He density over the whole polar cap. Second, on the night side middle- to high-altitude region an enhancement of $N_2$ density correlated with the zone of >44–keV-electron flux was observed, and this $N_2$ enhancement was correlated with the equatorward edge of the ionospheric plasma trough, the poleward edge of the latter being coincident with the equatorward edge of the 200–eV-electron flux zone. Third, on the day side a narrow region of enhanced $N_2$ density was frequently observed at invariant latitudes of 70°–80°. This heating region generally coincided with a narrow plasma trough and a region of enhanced electron temperature. (auth)

**26700** CHARACTERISTICS OF THE DEVELOPMENT OF THE WESTWARD ELECTROJET DURING THE EXPANSIVE PHASE OF MAGNETOSPHERIC SUBSTORMS. Wiens, R.G.; Rostoker, G. (Institute of Earth and Planetary Physics, University of Alberta, Edmonton, Alberta, Canada). J. Geophys. Res. 80: No. 16, 2109-2128 (1 June 1975).

By use of high-, mid-, and low-latitude magnetograms it is concluded that the westward expansion of the substorm westward electrojet is not continuous but takes place as a series of discrete steps or jumps. The substorm is pictured as consisting of the sequential development of a series of westward electrojets, which we have labeled a 'substorm sequence.' The westward electrojets develop in succession at intervals of about 10 min in such a way that each new electrojet appears to the northwest of the previous one. Associated with the westward jumps of substorm activity are enhancements in the growth rate of a ring or cross-tail current. These enhancements are concurrent with the onset of the westward electrojets and occur to the west of that sector which is

presently undergoing its initial onset of substorm activity. Each substorm intensification is accompanied by a response in the adjacent sector to the west, consistent with the signatures of growth suggested by McPherron (1972) and Iijima and Nagata (1972). We suggest that growth may be stimulated by the same mechanism which triggers the expansion phase and that the energy responsible for ensuing substorm intensifications in the evening sector is made available in this fashion. (auth)

**26701** LATITUDE-DEPENDENT NONLINEAR HIGH-SPEED SOLAR WIND STREAMS. Suess, S.T. (Space Environment Laboratory, National Oceanic and Atmospheric Administration, Boulder, Colorado 80302); Hundhausen, A.J.; Pizzo, V. J. Geophys. Res. 80: No. 16, 2023-2029 (1 June 1975).

The theory of the nonlinear interaction between high- and low-speed solar wind streams has been limited either to small amplitudes or to the equatorial plane. It is shown how both of these restrictions can be removed for flow more than a few solar radii away from the sun by employing a quasi-radial approximation to develop a perturbation expansion of the equations of motion. The lowest-order equations describe the radial flow in large-amplitude latitude-dependent streams. Higher-order equations describe the nonradial flow associated with the streams and can be used to test the validity of the quasi-radial approximation for any given set of boundary conditions. As an example, the theory is used to model a set of interplanetary scintillation observations indicating the disappearance, above 40°N latitude, of the scintillation associated with a specific set of streams. The analysis illustrates the relative nonlinear steepening and displacement in phase of the density and velocity peaks as a function of latitude and time. Results are given in terms of the range of possible latitudinal variations at the sun and 1 AU allowed by the observations. It is concluded that a disappearance of the streams above 40°N is not necessary to explain a weakening of stream interactions and thus the disappearance of scintillations at high solar latitudes. (auth)

**26702** CURRENT-DRIVEN PLASMA INSTABILITIES AT HIGH LATITUDES. Scarf, F.L.; Fredricks, R.W. (TRW Systems Group, Redondo Beach, California 90278); Russell, C.T.; Neugebauer, M.; Kivelson, M.; Chappell, C.R. J. Geophys. Res. 80: No. 16, 2030-2040 (1 June 1975).

Earlier Ogo 5 discussions of high-latitude magnetospheric wave-particle interation phenomena associated with field aligned current systems are extended by considering some September 7, 1968, out-bound measurements and corresponding March 11, 1969, observations, when the spacecraft was traversing auroral $L$ shells in midafternoon. It is shown that during moderate magnetospheric disturbances the most intense waves and currents were detected near sharp boundaries in the density of polar cleft electrons, and it is possible that local wave-particle interactions produced anomalous resistivity. Some observed changes in the electron distribution functions might be explained in terms of local acceleration, but significant causal questions about the dynamics remain open if one can use only local data from a single spacecraft in this region. (auth)

**26703** THE RESPONSE OF THE DAY SIDE MAGNETOSPHERE-IONOSPHERE SYSTEM TO TIME-VARYING FIELD LINE RECONNECTION AT THE MAGNETOPAUSE 1. THEORETICAL MODEL. Holzer, T.E. (NCAR High Altitude Observatory, Boulder, Colorado 80303); Reid, G.C. J. Geophys. Res. 80: No. 16, 2041-2049 (1 June 1975).

The process whereby magnetic flux is removed from the day side region of the magnetosphere and transferred to the magnetotail has been referred to as 'erosion' of the day side magnetosphere. Observations have suggested that the occurrence of this erosion process is related to increases in the southward component of the interplanetary magnetic field and hence by inference to increases in the rate of field line reconnection at the day side magnetopause. Similarly, the inverse of the erosion process (i.e., the net transfer of flux from the magnetotail to the day side magnetosphere) is associated with decreases in the southward component of the interplanetary magnetic field and hence to decreases in the magnetopause reconnection rate. A quantitative theory of the day side erosion process (and its inverse) is developed here in terms of an electrical circuit analogy, in which the ionosphere acts as a resistance with a voltage generator connected in parallel and the closed magnetosphere acts as a set of inductances and a capacitance. Changes in the rate of day side field line reconnection lead directly to changes in the potential drop across the magnetospheric capacitor and, after a characteristic time delay, to changes in the voltage applied by the generator. The response of the coupled ionosphere-magnetosphere circuit to such changes is studied in some detail, and a quantitative estimate for the rate of erosion is obtained. In addition to describing the mean motion of the magnetopause associated with erosion the theory predicts oscillations of the magnetopause about this mean with characteristic periods of several minutes. Such oscillations have frequently been observed by spacecraft. (auth)

**26704** THE RESPONSE OF THE DAY SIDE MAGNETOSPHERE-IONOSPHERE SYSTEM TO TIME-VARYING FIELD LINE RECONNECTION AT THE MAGNETOPAUSE 2. EROSION EVENT OF MARCH 27, 1968. Reid, G.C. (NOAA Aeronomy Laboratory, Boulder, Colorado 80302); Holzer, T.E. J. Geophys. Res. 80: No. 16, 2050-2056 (1 June 1975).

The circuit analogy for the response of the coupled magnetosphere-ionosphere system to changes in day side field line reconnection rate is applied to real conditions and is used to calculate the expected variation in magnetopause position during the erosion event described by Aubry et al. (1970). Generally good agreement between observation and theory is found. The role of the dawn-dusk electric field responsible for magnetospheric convection is examined in some detail and is treated in the circuit analogy as the field due to an external generator connected across the circuit. It is found that the erosion process requires two distinct time constants for a proper description: (1) the time needed for magnetosheath plamsa to travel down the freshly reconnected field lines to the ionosphere and (2) roughly, the time required for the foot of a reconnected field line to travel one quarter of the total noon-midnight dimension of the polar cap. The second time constant is the dominant one and is not related to the ionospheric conductivity, as has been suggested previously. Examination of high-latitude magnetograms obtained during the erosion event discussed shows that the electric field oscillations predicted by the theory and observed by the spacecraft in terms of oscillations in the magnetopause position are also reflected in oscillations in ionospheric current flow. (auth)

**26705** IDENTIFICATIONS OF THE POLAR CAP BOUNDARY AND THE AURORAL BELT IN THE HIGH-ALTITUDE MAGNETOSPHERE: A MODEL FOR FIELD-ALIGNED CURRENTS. Sugiura, M. (Laboratory for Planetary Atmospheres, NASA Goddard Space Flight, Center, Greenbelt, Maryland 20771). J. Geophys. Res. 80: No. 16, 2057-2068 (1 June 1975).

By means of the Ogo 5 Goddard Space Flight Center fluxgate magnetometer data the polar cap boundary is identified in the high-altitude magnetosphere by a sudden transition from a dipolar field to a more taillike configuration. It is inferred that there exists a field-aligned-current layer at the polar cap boundary. In the night side magnetosphere the polar cap boundary is identified as the high-latitude boundary of the plasma sheet. The field-aligned current flows downward to the ionosphere on the morning side of the magnetosphere and upward from the ionosphere on the afternoon side. Thus in the high-latitude boundary layer of the plasma sheet in the tail the current is toward the earth in the postmidnight region and away from the earth in the premidnight region. The basic pattern of the magnetic field variations observed during the satellite's traversal of the auroral belt is presented. This pattern shows the existence of a field-aligned-current layer on the low-latitude part of the auroral belt. Currents flow in opposite directions in the two field-aligned-current layers. The current directions in these layers as observed by Ogo 5 in the high-altitude magnetosphere are the same as those observed at low altitudes by the polar-orbiting Triad satellite (Armstrong and Zmuda, 1973). The magnetic field in the region where the lower-latitude field-aligned-current layer is situated is essentially meridional. Thus the equatorial current closure of this current system must be via the equatorial current sheet. A model is presented in which two field-aligned-current systems, one at the polar cap boundary and the other on the low-latitude part of the auroral belt, are mainly connected by ionospheric currents flowing across the auroral belt. The existence of field-aligned currents deduced from the Ogo 5 observations is a permanent feature of the magnetosphere. Even under disturbed conditions the basic pattern of the field variations in the critical regions of the auroral belt and the polar cap boundary is the same as it is at quiet times. Intensifications of the field-aligned currents and occurrences of multiple pairs of field-aligned-current layers characterize the disturbed conditions of these regions. (auth)

**26706** AN APPROXIMATE ANALYTIC DESCRIPTION OF PLASMA BULK PARAMETERS AND PITCH ANGLE ANISOTROPY UNDER ADIABATIC FLOW IN A DIPOLAR MAGNETOSPHERIC FIELD. Southwood, D.J. (Physics Department, Imperial College, London, England); Kivelson, M.G. J. Geophys. Res. 80: No. 16, 2069-2073 (1 June 1975).

An approximate expression for the variation with $L$ of the equatorial pitch angle of a particle undergoing adiabatic convection in a dipole magnetic field is obtained. The additional assumptions of no particle loss and the other usual conservation laws then are invoked to describe the variation of such bulk parameters as pressure and density for any assumed initial distribution function. Explicit solutions are obtained for initial distributions separable in energy and pitch angle with $\sin^k \alpha_0$ dependence on pitch angle and are shown to be weakly dependent on $k$. The expressions obtained are compared with the results predicted for the case of strong pitch angle diffusion to obtain bounds on the variation. The approximation for the $L$ dependence of the equatorial pitch angle is also used to show how pitch angle anisotropy is modified during inward convection, and the rapid development of anisotropy for sharply falling initial spectra is noted. (auth)

**26707** ENERGIZATION OF ELECTRONS AT SYNCHRONOUS ORBIT BY SUBSTORM-ASSOCIATED CROSS-MAGNETOSPHERE ELECTRIC FIELDS. Walker, R.J.; Kivelson, M.G. (Institute of

Geophysics and Planetary Physics, University of Califoria, Los Angeles, California 90024). J. Geophys. Res. 80: No. 16, 2074-2082 (1 June 1975).

The time variation of the flux of energetic electrons arriving at synchronous orbit subsequent to a sudden enhancement of a uniform cross-magnetosphere electric field has been calculated by using adiabatic theory and a model time-independent magnetic field. The initial ($t=0$) particle distribution was taken to be spatially uniform within the region from which particles are convected to synchronous orbit in 1 hour and was described by a power law in energy for high energies ($>50$ keV) and as a Maxwellian with a temperature of 1 keV for lower energies. The trajectories of particles of energy $W$ and pitch angle $\alpha$ observed at a given position at time $t$ were followed backward in time to determine their initial ($t=0$) energies and pitch angles. Liouville's theorem was then invoked to predict the flux at the desired position and time. As the model does not allow for a time-varying magnetic field, which is known to accompany substorm activity, the predictions have been compared with observations of substorm-associated particle injections during periods of relatively steady local magnetic fields. The model successfully reproduces many of the qualitative changes observed by ATS 1 in the >50-keV electrons during magnetospheric substorms. In particular, the predicted rapid flux increases in the midnight to dawn quadrant associated with a marked softening of the energy spectrum are observed. The observed energy-dependent delay in the onset of flux enhancements, which is an increasing function of local time, is also predicted. This delay has previously been adduced as evidence that newly accelerated particles are injected near local midnight and then drift in local time. However, the present calculation, which allows continuous acceleration along the particle trajectory, also predicts this delay, which results from the energy dependence of particle drift velocities. The pitch angle dependence of the particle energization depends on the magnetic field model used for the calculation. For a dipole field the model predicts a preferential enhancement of the flux of particles near 90° pitch angle in the morning hours. This may explain the correlation observed between energetic electrons at ATS 1 and precipitating electrons without requiring a local acceleration mechanism. For lower-energy (<20-keV) plasma a marked increase in energy flux accompanied by rapid heating of the plasma in the region near midnight is predicted. This result is consistent with ATS 5 observations. Thus many features of the model which assumes injection of particles in a spatially localized region at the onset of a substorm are present in a model in which a sudden increase in the cross-magnetosphere electric field affects a spatially uniform population of particles. This ambiguity must be considered in interpretation of substorm-associated particle measurements. A complete description of the response of particles to substorms must include the effect of time-varying magnetic fields and possible nonadiabatic acceleration and must also incorporate the response of the particles to the enhancement of large-scale electric fields. (auth)

**26708** SOME ASPECTS OF SSCs OBSERVED AT HYDERABAD DURING 1965-72. Srivastava, B. J.; Abbas, H. (National Geophysical Research Inst., Hyderabad, India). Indian J. Radio Space Phys.; 2: No. 3, 177-179(Sep 1973).

The rise-times of SSCs are found to range from 1 to 8 min and the amplitudes from 5 to 100 γ. An inverse relationship (negative correlation) has been obtained between the rise-time and the amplitude of SSCs at Hyderabad, similar to Alibag and Hermanus, but quite different from that observed for Budkov where a direct relationship (positive correlation) has been reported. SSC* events which are very rare at Hyderabad, are observed only during daytime and correspond to prominent events in the equatorial electrojet region. At high-latitude stations like Hartland, Eskdalemuir and Lerwick, SSC*s are observed both during day and night hours. The implications of these observations are examined. The observed association of micropulsations with SSCs and SSC*s is also discussed. (auth)

**26709** EARTH'S MAGNETOSPHERE. Zhulin, I. A. pp 193-297 of Solnechnyi Veter. Magnitosfere zemli. Tom 4. Moscow; Izdatel'stvo VINITI (1974). (In Russian).

Experimental data and theoretical models drawn from numerous sources and dealing with phenomena in the near-earth region of space are compiled and evaluated. This includes analyses based on satellite and ground observations of the radiation belts, the magnetotail and its current and plasma sheets, magnetosphere processes during storms, and various geophysical phenomena related to these storms. (IAA)

**26710** OBSERVATIONS OF A LOW-FREQUENCY CUTOFF IN MAGNETOSPHERIC RADIO NOISE RECEIVED ON IMP 6. Vesecky[1], J.F.; Frankel, M.S. (Stanford Center for Radar Astronomy, Stanford University, Stanford, California 94305). J. Geophys. Res. 80: No. 22, 2771-2774 (1 Aug 1975).

Observations of magnetospheric radio noise by the Goddard Space Flight Center radio experiment on the Imp 6 spacecraft have revealed a quasi-continuous component at frequencies between 30 and 110 kHz. When the spacecraft is in the interplanetary medium or the magnetosheath, a low-frequency cutoff often characterizes the otherwise power law ($f^{-a}$) spectrum of this noise. A positive correlation is observed between this cutoff frequency $f_{co}$ and the solar wind plasma frequency $f_{sw}$, deduced from the Los Alamos plasma experiment on the same spacecraft; on the average, $f_{co} \simeq 1.3 f_{sw}$. If one pictures the magnetosheath as a homogeneous layer of plasma lying between the radio noise source (at $L \sim 4$–7) and the spacecraft in the interplanetary medium and having an electron density 2–3 times that of the solar wind, then one will expect $f_{co} \gtrsim 2^{1/2} f_{sw} \sim 3^{1/2} f_{sw}$. Within the limits of experimental error this simple model correctly accounts for the observations. A rough calculation shows that radio wave scattering by electron density fluctuations in the magnetosheath plasma is likely to be important for frequencies below 200 kHz. However, the effects of such scattering cannot be detected in the Imp 6 observations considered here because neither concurrent measurements nor sufficiently accurate models of the necessary magnetosheath plasma parameters are presently available. (auth)

**26711** A CONTRIBUTION TO THE THEORY OF THE ELECTROSTATIC HALF-HARMONIC ELECTRON GYROFREQUENCY WAVES IN THE MAGNETOSPHERE. Ashour-Abdalla, M.; Chanteur, G. (Groupe de Recherches Ionosphériques, Centre National d'Etudes des Télécommunications, Issy-les-Moulineaux, France); Pellat, R. J. Geophys. Res. 80: No. 22, 2775-2782 (1 Aug 1975).

The effect of different plasma parameters on the stability of the half-harmonic electron gyrofrequency waves is investigated. By making some simplifying assumptions about the cold plasma and using a ring distribution for the warm component the role of the different parameters is demonstrated. A maximum value of the ratio of the cold to hot plasma density above which we cannot get instability is derived, and this ratio increases with the temperature anisotropy. Calculations of the growth rates show that there is a sharp peak when $\theta = \tan^{-1} \kappa_\perp/\kappa_\parallel \sim 70°$–80°. (auth)

**26712** PLASMA FLOW HYPOTHESIS IN THE MAGNETOSPHERE RELATING TO FREQUENCY SHIFT OF ELECTROSTATIC PLASMA WAVES. Oya, H. (Upper Atmosphere and Space Research Laboratory, Tohoku University, Sendai, Japan). J. Geophys. Res. 80: No. 22, 2783-2789 (1 Aug 1975).

The frequency dynamic spectrum indicating a monotonic frequency shift of the electrostatic electron cyclotron harmonic wave emissions in the data of VLF electric field observations by Ogo 5 has been detected in the midnight and dawn meridians outside the plasmapause: the emissions are produced from turbulent areas in the plasma states that include the temperature anisotropy, loss cone velocity distribution, or the double hump in the velocity distribution function. The frequency shift is also observed for the case of the emissions in the magnetosheath near the subsolar point. These frequency shifts are interpreted on a hypothesis of the Doppler effects of the plasma waves due to the plasma flow with respect to the satellite frame. The speeds of the plasma flow are obtained and have a range from 150 to 300 km/s. Disruption of the plasma flow due to the magnetic field bumps may produce the turbulent source generating the Harris type or beam type instabilities that generate the electrostatic electron cyclotron harmonic waves. (auth)

**26713** HEOS 2 PLASMA OBSERVATIONS IN THE DISTANT POLAR MAGNETOSPHERE: THE PLASMA MANTLE. Rosenbauer, H.; Grünwaldt, H.; Montgomery[1], M.D.; Paschmann, G.; Sckopke, N. (Max-Planck-Institut für Physik und Astrophysik, Institut für extraterrestrische Physik, Garching, West Germany). J. Geophys. Res. 80: No. 22, 2723-2737 (1 Aug 1975).

Comprehensive plasma observations carried out on board the Heos 2 satellite have provided the first systematic description of plasmas in the distant polar magnetosphere. These observations have revealed the presence of a persistent layer of tailward-flowing magnetosheathlike plasma inside of and adjacent to the magnetopause. This region has been termed the 'plasma mantle.' The mantle has been found to extend over the entire surface of the magnetosphere tailward of the polar cusp and northward of the plasma sheet. Vela observations of a 'magnetotail boundary layer' obtained in the vicinity of the plasma sheet by Hones and coworkers refer to the same phenomenon. The salient features of the plasma mantle as provided by Heos measurements from February to December 1972 can be summarized as follows: (1) The mantle was found to be present in over 70% of the passes through the polar magnetosphere in the region described above. (2) Its thickness varies greatly, ranging up to $\gtrsim 4\ R_E$, and does not appear to depend significantly on position or the state of the magnetosphere as measured by $K_p$. (3) A tailward-directed bulk flow parallel to the local terrestrial magnetic field was nearly always distinctly measurable. It was found to lie usually between 100 and 200 km $s^{-2}$ and was always less than the concurrent flow speed in the nearby magnetosheath. (4) The flow speed in the mantle is positively correlated with the flow speeds in the magnetosheath and solar wind but depends only very weakly, if at all, on distance from the polar cusp, i.e., on $X_{GSM}$. (5) A narrow region of low density and/or low flow speed plasma, i.e., a 'gap,' 0.1–0.2 $R_E$

thick, is frequently observed between the plasma mantle and the magnetopause. (6) The mantle protons are normally significantly cooler along $B$ than perpendicular, i.e., $T_{\|} < T_{\perp}$. (7) The proton density, temperature, and bulk speed all tend to decrease gradually with depth inside the magnetopause, but this trend can at times be obscured by fluctuations and magnetopause motions. At the inner edge of the mantle the proton distribution is often very narrow in both energy and angle, i.e., relatively cold, before it finally disappears below the 100-eV threshold of the instrument. It is concluded, after an appraisal of several possible mechanisms, that the most probable cause for the formation of the mantle is the day side merging of terrestrial and interplanetary field lines. (auth)

**26714 WEAK PITCH ANGLE SCATTERING OF ENERGETIC PROTONS IN THE MAGNETOSPHERE.** Scholer, M.; Morfill, G.; Hovestadt, D. (Max-Planck-Institut für Physik und Astrophysik, Institut für Extraterrestrische Physik, Garching, West Germany). J. Geophys. Res. 80: No. 22, 2745-2750 (1 Aug 1975).

During the solar particle event of April 12–14, 1973, a flux depression of solar protons in the dawn side pseudotrapping region relative to the flux in the dusk side pseudotrapping region was frequently observed with the low-altitude polar-orbiting satellite Esro 4. This flux decrease is interpreted as being due to weak pitch angle scattering of the solar protons during their drift from dusk to dawn. Treating the pitch angle diffusion as a simple initial value problem, we derive quantitative values of the equatorial bounce-averaged pitch angle diffusion coefficients at small pitch angles for different energies. These values represent lower limits for magnetospheric conditions at the time of the Esro 4 observations. Through the assumption that the pitch angle diffusion is a gyroresonant interaction process of the particles with either Alfvén or ion cyclotron waves, the necessary power of the waves at the resonant interaction frequency is calculated. (auth)

# PHYSICS (ATOMIC AND MOLECULAR)

**26715** SCATTERING THEORY FOR QUANTUM ELECTRODYNAMICS. II. REDUCTION AND CROSS-SECTION FORMULAS. Zwanziger, D. (Department of Physics, New York University, New York, New York 10003). Phys. Rev. D 11: No. 12, 3504-3530 (15 June 1975).

The quantum-electrodynamical $S$ matrix is obtained as the set of on-mass-shell values of the renormalized momentum-space Green's functions multiplied by $C_i(m^2{}_i - p_i^2)^{1+}{}_{\xi_i}$ for each particle $i$, where $\xi_i$ is proportional to the fine-structure constant and $C_i$ is a constant. A photon mass is not needed to eliminate virtual infrared divergences. Instead the parameters $\delta_i = m^2{}_i - p_i^2$ regularize Feynman integrals in the infrared region, and the dependence on the $\delta_i$ is canceled against the expansion of $(m_i^2 - p_i^2)_{\xi_i}$ multiplying lower-order Green's functions. Exact cross-section formulas are developed which express transition rates in terms of this $S$ matrix. They account for radiation damping nonperturbatively, whereas the $S$ matrix must be calculated perturbatively as a power series in $\alpha$. It is seen that in processes with very small energy loss to unobserved photons individual elements of the quantum-electrodynamical $S$ matrix are directly observable. Rules for practical calculations are summarized. (auth)

## Beams and Their Reactions

**26716** THE KAPITZA-DIRAC EFFECT FOR ATOMS IN A STRONG RESONANT FIELD. Kazantsev, A.P.; Surdutovich, G.I. (L. D. Landau Institute of Theoretical Physics, USSR Academy of Sciences). JETP Lett. 21: No. 6, 158-159 (20 Mar 1975).

It is shown that the scattering of atoms in a strong resonant field of a standing wave proceeds more effectively than scattering of electrons. A resonant field of power 0.1–$10^2$ W is needed to deflect Na atoms through an angle 0.01–0.1 rad. (auth)

**26717** SECONDARY ELECTRON EJECTION FROM CONTAMINATED METAL SURFACE BY He AND Ar ATOMS. Kadota, K.; Kaneko, Y. (Tokyo Metropolitan Univ. (Japan). Faculty of Science). Jpn. J. Appl. Phys.; 13: No. 10, 1554-1561(Oct 1974).

Secondary electron yields $r_0$ on a contaminated Cu-Be surface for neutral He and Ar atoms of 19 eV to 500 eV have been measured. The neutral beams are produced from the ground state ion beams by charge transfer with the same kind of atoms. The yields $r_0$ obtained are confirmed to be of the ground state atoms. The values of $r_0$ are 0.58 for He and 0.24 for Ar at 500 eV, and rapidly decrease to $6 \times 10^{-6}$ for He and $2 \times 10^{-6}$ for Ar at 19 eV. The ejection mechanism is discussed. In the case of Ar, the secondary electron yield increases notably when the electron energy producing the primary ion beam is increased above 32 eV. This indicates that metastable atoms $Ar^m$ are produced from metastable ions $Ar^{+m}$ by the charge transfer process $Ar^{+m} + Ar \rightarrow Ar^m + Ar^+$. This fact can be used as a new technique of detecting metastable ions. An example of its application is presented. (auth)

**26718** CORRECTIONS FOR THE BEAM POLARIZATION FROM POLARIZED ION SOURCES. Hasuyama, H.; Sonoda, M. (Kyushu Univ., Fukuoka (Japan). Faculty of Engineering). Kyushu Daigaku Kogaku Shuho; 47: No. 4, 389-395(Sep 1974). (In Japanese).

It is effective to make uniform the spin direction of incident particles in the study of the polarized phenomenon of atomic nuclei. The apparatus for this purpose is called polarized ion source. It is desirable that in this apparatus, beam polarization can be controlled and is intense. The prototype of this apparatus has been constructed in the laboratory for the first time in Japan. To improve the performance of this prototype, various improvements are in progress now. When the beam polarization from the polarized ion sources is measured, if the ion is a deuteron, the T(d, n)$^4$He reaction is often utilized as an analyzer. At that time, if the beam contains useless particles such as unpolarized deuterons or deuterium besides polarized deuterons, the beam polarization determined from the anistropy of released particles by reaction appears smaller than that of the intrinsic polarized ion sources. A method to acquire the intrinsic beam polarization of polarized ion sources by making correction for useless particles without using a beam polarizer, which usually utilizes magnetic field or electric field, is reported. (Tai, I)

**26719** BEAM FOCUSING BY APERTURE DISPLACEMENT IN MULTIAMPERE ION SOURCES. Stewart, L.D.; Kim, J.; Matsuda, S. (Oak Ridge National Laboratory, Oak Ridge, Tennessee 37830). Rev. Sci. Instrum. 46: No. 9, 1193-1196 (Sept 1975).

Results are given of an experimental study of beam focusing by aperture displacement ($\Delta x$) in duoPIGatron ion sources. Measurements with a single aperture, accel–decel electrode geometry show that the beam deflection angle is linear with $\Delta x/z$ for the round aperture and with $\Delta x/z^{*2}$ for the slit aperture, where $z$ and $z^*$ are, respectively, the extraction gap distance and the effective gap distance. Applying the result of the single aperture study to the multiaperture duoPIGatron sources, it was possible to increase the neutral beam injection power to the Oak Ridge Tokamak (ORMAK) plasma by $\simeq$40%. Also presented are a discussion and comparison of other work on the effect of aperture displacement on beam deflection. (auth)

**26720** THE SCATTERING OF NOBLE GAS ATOMS (He, Ne, Ar) FROM (100) COPPER. (SPACE AND VELOCITY DISTRIBUTION). Lapujoulade, J.; Lejay, Y. (CEN. Saclay, Service de Physique Atomique, Section d'Etudes des Interactions Gaz-Solides, B.P. N° 2, 91190—Gif-sur-Yvette, France). J. Chem. Phys. 63: No. 4, 1389-1400 (15 Aug 1975).

The scattering of He, Ne, and Ar from (100) copper has been studied experimentally. Both space and velocity distributions were measured. Special attention was paid to the cleanliness of the surface and to the effect of possible surface contamination. The influence of the beam incidence, the crystal azimuth, and the temperature are discussed. The behavior of the reflection lobe is in agreement with the phenomenological description of Merrill. The velocity distribution suggests that there is always superposition of elastic and inelastic scattering. Many-phonon processes predominate in the scattering of Ne and Ar, while the helium case may be described by an elastic, single-phonon process. A comparison of these experimental data with existing theoretical calculations (many-phonon by G. Armand, single-phonon by F. O. Goodman) is given. (auth)

**26721** EVIDENCE OF RESIDUAL *K*-SHELL EXCITATION IN CHLORINE IONS PENETRATING CARBON. Hopkins, F. (Department of Physics, State University of New York at Stony Brook, Stony Brook, New York 11794). Phys. Rev. Lett. 35: No. 5, 270-274 (4 Aug 1975).

Chlorine ions at 70 and 140 MeV energy impinge upon $\sim$1-$\mu$g/cm$^2$ Cu targets, in one case after emerging from a carbon prefoil and in the second striking Cu on the back side of a carbon foil. The latter approach leads to an appreciable increase in the Cu $K$ x-ray yield, an effect which is explained in terms of residual Cl $K$-shell excitation and which is in accord with a simple model of competing rearrangement processes. (auth)

**26722** *L*-SHELL X–RAY PRODUCTION CROSS SECTIONS OF Pd, Ag, AND Sn FOR INCIDENT PROTON ENERGIES IN THE RANGE 3–12 MeV AND OXYGEN IONS IN THE RANGE 15–40 MeV. Chaturvedi, R.P.; Wheeler, R.M.; Liebert, R.B.; Miljanic, D.J.; Zabel, T.; Phillips, G.C. (T. W. Bonner Nuclear Laboratories, Rice University, Houston, Texas 77001). Phys. Rev. A 12: No. 1, 52-56 (July 1975).

Absolute $L$-shell x-ray production cross sections have been measured for thin targets of Pd, Ag, and Sn at 1-MeV increments for incident protons in the range from 3 to 12 MeV and in 5-MeV increments for oxygen ions in the range from 15 to 40 MeV. $L$-shell ionization cross sections are calculated from theoretical average $L$-shell fluorescence yields and then compared to both plane-wave Born-approximation (PWBA) and binary-encounter-approximation (BEA) theories. The data are found to be higher than the theoretical predictions except at the lowest projectile energies. (auth)

**26723** METHOD OF GENERATING VERY INTENSE POSITIVE-ION BEAMS. Creedon, J.M.; Smith, I.D.; Prono, D.S. (Physics International Company, San Leandro, California 94577). Phys. Rev. Lett. 35: No. 2, 91-94 (14 July 1975).

The combination of multiply reflected electrons and positive ion flow in a reflex triode arrangement is analyzed. Under certain conditions it is possible to generate very intense beams of positive ions with this device. The analysis demonstrates that the energy loss and scattering of the electrons as they pass through the anode have a major effect on the ion and electron currents. Solid fractional-range anodes are shown to produce more intense ion beams than semitransparent mesh anodes. (auth)

**26724** CURRENT-PRESSURE TRANSITIONS IN A MAGNETICALLY SUPPORTED DC SPUTTERING SYSTEM. Green, F.A.; Chapman, B.N. (Materials Section, Department of Electrical Engineering, Imperial College, London, SW7 2BT, England). Appl. Phys. Lett. 27: No. 4, 189-190 (15 Aug 1975).

Sputtering in a cylindrical magnetron configuration, current-pressure characteristics show an unexpected discontinuity and current–magnetic field curves exhibit a maximum. These characteristics seem to be closely related to the ratio of the height from the target of the secondary electron initial trajectory compared to the cathode dark space distance. (auth)

**26725** ELECTRON-BEAM-DRIVEN INSTABILITY IN A SOLID. Perry, F.C.; Mix, L.P. (Sandia Laboratories, Albuquerque, New Mexico 87115). Appl. Phys. Lett. 27: No. 4, 194-196 (15 Aug 1975).

A relativistic electron beam (REB) accelerator was used to generate a shock wave (6–10 kbar) in a solid aluminum plate, and the tensile wave following the compressive wave produced an instability of the back surface of the plate. The wavelength of the instability, observed by holographic interferometry, and the measured negative acceleration of the solid-gas interface were used in a modified theory of Taylor instability to determine a value of $1.7\times10^3$ P for the viscosity of aluminum which was in reasonable agreement with a previously reported value. It is suggested that the mechanism of Taylor instability can qualitatively explain the observation in a previous experiment of a distribution of particle velocities at a surface of a solid upon arrival of a very high-amplitude ($\sim$1 Mbar) shock wave. (auth)

**26726** HOT ELECTRONS ON LIQUID HELIUM. Crandall, R.S. (RCA Laboratories, Princeton, New Jersey 08540). Phys. Rev. B 12: No. 1, 119-124 (1 July 1975).

Using a model of electrons trapped in image-potential-induced surface states, I have calculated the mobility of electrons moving parallel to the liquid surface in high electric fields. To obtain agreement with experiment, it is necessary to include a large number of quantum levels of the electron motion perpendicular to the liquid surface. As the electrons are heated by the electric field they populate these higher states. (auth)

**26727** MECHANISM OF RF REACTIVE SPUTTERING. Shinoki, F.; Itoh, A. (Electrotechnical Laboratory, Tanashi, Tokyo, Japan). J. Appl. Phys. 46: No. 8, 3381-3384 (Aug 1975).

The reactive mechanism of rf reactive sputtering has been investigated by mass spectrometry in an rf diode sputtering system. The result indicates that the gettering action of the sputtered active atom deposits influences the progress of reactive sputtering in addition to the target reaction. A model, taking the gettering action into consideration, is presented for the reactive sputtering of a metal. This model shows that an abrupt steplike decrease in the sputtering rate may occur at a definite partial pressure of a reactive gas $p^*$ in the plasma. The pressure $p^*$ is determined from the gettering rate of the sputtered deposits relative to the throughput of the reactive gas. The value of the pressure $p^*$ calculated on this model is in good agreement with the experimental results. (auth)

**26728** RECOIL CONTRIBUTION TO ION-IMPLANTATION ENERGY-DEPOSITION DISTRIBUTIONS. Brice, D.K. (Sandia Laboratories, Albuquerque, New Mexico 87115). J. Appl. Phys. 46: No. 8, 3385-3394 (Aug 1975).

A previous method for directly calculating the spatial distribution of energy deposition into damage or ionization for ions implanted into solid targets is extended to account for energy transport by recoiling target atoms. The new calculations extend the applicability of the method to lower incident ion energies. In addition, an intermediate step in the calculations provides information on the spectrum of target recoil atoms. Good agreement is obtained between experiment and theory using the improved procedure. Calculated damage energy distributions are presented for 10-keV–1-MeV B, P, As, and Sb ions incident on silicon. (auth)

**26729** ORIGIN OF SECONDARY-ELECTRON-EMISSION YIELD-CURVE PARAMETERS. Dionne, G.F. (Massachusetts Institute of Technology, Lincoln Laboratory, Lexington, Massachusetts 02173). J. Appl. Phys. 46: No. 8, 3347-3351 (Aug 1975).

From an analysis of the one-dimensional constant-loss theory of secondary electron emission, maximum yield ($\delta_m$), primary electron energy at maximum yield ($E_{mm}$), and both crossover energies $E'_{oc}$ and $E^{II}_{oc}$ are shown to depend on the surface and bulk properties of the emitting material through simple relations. In particular, the results strongly suggest that the first crossover energy can be very dependent on surface properties, whereas the energy at maximum yield is entirely controlled by bulk properties. Refinement of the low-energy part of the reduced yield curve by means of the results of the more realistic three-dimensional theory leads to the development of the expression $E'_{oc}=0.51\,E_{mm}\delta_m^{-1.32}$. Comparison between theory and experiment for several secondary-emitting materials is presented to demonstrate the accuracy of this useful relation. Finally, the implications of these results for different classes of materials are discussed in terms of basic physical properties, such as density, electrical conductivity, work function, and band gap. (auth)

**26730** MULTIPLE REFLECTIONS OF ELECTRONS AND THE POSSIBILITY OF INTENSE POSITIVE-ION FLOW IN HIGH $\nu/\gamma$ DIODES. Prono, D.S.; Creedon, J.M.; Smith, I.; Bergstrom, N. (Physics International Company, San Leandro, California 94577). J. Appl. Phys. 46: No. 8, 3310-3319 (Aug 1975).

Variations of the nature and pressure of the background gas used for neutralizing the charge of a relativistic electron beam have been observed to alter the current waveform of the propagating beam, the time delay before propagation begins, and the voltage and current waveforms of the diode which accelerates the beam. This interaction between the beam region and the diode occurs during the delay phase before beam propagation begins and can be explained by (1) the reflection of electrons back into the diode from a virtual cathode which exists in the beam region during the delay phase and (2) the flow of a significant positive-ion current in the diode during this same period. A theory describing positive-ion flow in the presence of multiply reflected electrons is developed and compared to experimental observations. (auth)

**26731** PRODUCTION OF POLARIZED ELECTRONS. Ladish, J. S. New Haven; Yale Univ. (1974). 288p. University Microfilms Order No. 75-15,324.

Thesis (Ph. D.).

Two sources of polarized electrons which were developed for use in experiments planned at Yale are described. The first is a pulsed source of polarized electrons based on the photoionization of an intense polarized lithium-6 atomic beam by uv light produced by a pulsed high pressure xenon flash lamp. The second source is a dc source of polarized electrons based on the photoionization of an unpolarized cesium atomic beam by a circularly polarized beam of uv light in the spectral range near the cesium photoionization threshold. (JFP)

## Atomic and Molecular Properties

*Refer also to abstracts 26765, 26775, and 26787.*

**26732** (LBL-3476) RELAXATION AND FINAL-STATE STRUCTURE IN XPS OF ATOMS, MOLECULES, AND METALS. Shirley, D. A.; Martin, R. L.; McFeely, F. R.; Kowalczyk, S. P.; Ley, L. (California Univ., Berkeley (USA). Lawrence Berkeley Lab.). Mar 1975. Contract W-7405-ENG-48. 26p. (CONF-750702-2). Dep. NTIS $4.50.

From conference of the Faraday Society on electron spectroscopy of solids and surfaces; Vancouver, B.C., Canada (15 Jul 1975).

Photoemission from a many-electron system is a many-electron process, even though the transition operator may affect only one electron directly. Relaxation and "shake-up" structure are related by a sum rule. When one is present, the other must be also. Shake-up structure is shown to be accurately predictable in atomic neon and molecular HF if the CI calculations are done carefully. In metals the sum rule also applies but final-state effects usually appear as relaxation energy, which is large even for valence electrons. Finally, in rare-earth metals discrete shake-up structure is observable in the 4p region. (7 figs, 30 refs) (auth)

**26733** ASYMPTOTIC BEHAVIOR OF THE CROSS SECTION FOR TWO-PHOTON IONIZATION OF A HYDROGEN ATOM NEAR THE THRESHOLD FOR ONE-PHOTON IONIZATION. Khristenko, C.V.; Vetchinkin, S.I. Opt. Spectrosc. (USSR) 38: No. 3, 237-239 (Mar 1975).

Two-photon ionization of the hydrogen atom in its ground state has been examined for radiation frequencies $\omega$ close to the threshold for single-photon ionization I. Simple asymptotic expressions have been found for the two-photon ionization cross section as $\omega\rightarrow$I. The results from the asymptotic estimates are compared with the exact calculations. It is shown that the asymptotic expressions derived hold good in the general case of $N$-photon ionization of the hydrogen atom at frequencies close to the threshold for ($N$–1) -photon ionization. (auth)

**26734** DISPERSION INTERACTION OF ATOMS OF ALKALI METALS. Shestakov, A.F.; Khristenko, S.V.; Vetchinkin, S.I. Opt. Spectrosc. (USSR) 38: No. 3, 261-262 (Mar 1975).

The dispersion interaction constants $C_6(AB)$ between the atoms H, Li, Na, K, Rb, and Cs (in the ground states) are calculated in the quantum defect approximation for atoms of the alkali metals. (auth)

**26735** KINETIC PROCESSES DETERMINING THE TIME DEPENDENCE OF VUV EMISSION IN He. Payne, M.G.; Klots, C.E.; Hurst, G.S. (Health Physics Division, Oak Ridge National Laboratory, Oak Ridge, Tennessee 37830). J. Chem. Phys. 63: No. 4, 1422-1428 (15 Aug 1975).

We present an interpretation of the data by Bartell, Hurst, and Wagner (BHW) on the time resolved vuv emission from He excited by pulses of fast charged particles. Here we argue that the very large term, linear in pressure, observed in the decay rate of the He($2\,^1P$) population represents He($2\,^1P$) + He($1\,^1S$) $\rightarrow$He($2\,^1S$) + He($1\,^1S$) and that the dominant mechanism for this reaction is strong rotational coupling of the adiabatic states $^1\Pi_g(1\,^1S+2\,^1P)$ and $^1\Sigma^+_g(1\,^1S+2\,^1S)$ in the region of internuclear separation near the potential curve crossing at $R\simeq2.04$ Å. The accurate prediction of the reaction rate, together with the fact that no other singlet states appear accessible at room temperature, leads to the conclusion that in nearly pure He most of the large He($2\,^1P$) population is converted to He($2\,^1S$) either by radiative transitions, the two-body process described above, or by the related predissociation of $B\,^1\Pi_g(1\,^1S+2\,^1P)$ when the molecule is formed in a

high vibrational state. Thus, most of the continuum radiation comes from the $A\,^1\Sigma^+_u$ and possibly the $D\,^1\Sigma^+_u$ molecules, and the time dependence of radiation from the $A\,^1\Sigma^+_u$ molecule is rate-limited by decay of He(2 $^1S$) by various collisional processes. (auth)

**26736** A RANDOM-WALK SIMULATION OF THE SCHRÖDINGER EQUATION: $H^+_3$. Anderson, J.B. (Department of Chemistry, The Pennsylvania State University, University Park, Pennsylvania 16802). J. Chem. Phys. 63: No. 4, 1499-1503 (15 Aug 1975).

A simple random-walk method for obtaining *ab initio* solutions of the Schrödinger equation is examined in its application to the case of the molecular ion $H^+_3$ in the equilateral triangle configuration with side length $R=1.66$ bohr. The method, which is based on the similarity of the Schrödinger equation and the diffusion equation, involves the random movement of imaginary particles (psips) in electron configuration space subject to a variable chance of multiplication or disappearance. The computation requirements for high accuracy in determining energies of $H^+_3$ are greater than those of existing LCAO–MO–SCF–CI methods. For more complex molecular systems the method may be competitive. (auth)

**26737** MOLECULAR INTERACTIONS IN THE CONDENSED PHASES OF ORTHO-PARA HYDROGEN MIXTURES. Fleury, P.A. (Bell Laboratories, Murray Hill, New Jersey 07974); McTague, J.P. Phys. Rev. A 12: No. 1, 317-326 (July 1975).

Because mixtures containing arbitrary ratios of ortho ($J = 1$) and para ($J = 0$) concentrations can be prepared, the condensed phases of hydrogen afford a unique opportunity to study interactions between isotropic and anisotropic molecules which are chemically identical. Detailed measurements are reported here of the rotational Raman spectra in the liquid and solid phases of ortho-para hydrogen mixtures, with para concentrations between 25% and 96% at temperatures between 10 and 23 °K. Changes in the configuration and dynamics of the molecular environment with temperature and ortho concentration are clearly reflected in the rotational Raman line shapes. Logarithmically recorded spectra, covering an intensity dynamic range of typically $10^4$, reveal two relatively independent types of interaction which respectively govern the near ($<30$ cm$^{-1}$) and far ($>30$ cm$^{-1}$) wings. Quantum calculations of the low-frequency mechanism, electric quadrupole-quadrupole molecular pair interactions, are presented. They are found to produce values for the second frequency moments for all three ($J = 1 \rightarrow 1$, $J = 1 \rightarrow 3$, and $J = 0 \rightarrow 2$) rotational transitions which agree well both in absolute magnitude and in concentration dependence with experimental observations. The far wings in the solid spectra consist of phonon sidebands whose structure is in good agreement with the phonon density of states previously observed by neutron scattering. In the liquid mixtures the far-wing line shapes are insensitive to temperature or concentration variation and are very similar to the solid wings. (auth)

**26738** SYSTEMATICS OF MOMENTS OF DIPOLE OSCILLATOR-STRENGTH DISTRIBUTIONS FOR ATOMS OF THE FIRST AND SECOND ROW. Dehmer, J.L.; Inokuti, M.; Saxon, R.P. (Argonne National Laboratory, Argonne, Illinois 60439). Phys. Rev. A 12: No. 1, 102-121 (July 1975).

The moments $S(\mu)$ and $L(\mu) = dS(\mu)/d\mu$ for $-6 \leqslant \mu \leqslant 1$ are derived from comprehensive Hartree-Slater oscillator-stength distributions for He through Ar. For $\mu \leqslant -2$, these moments are governed by valence excitations only, and therefore exhibit a pronounced periodic variation that repeats in each row. Inner shells begin to contribute appreciably to $S(-1)$, which retains a periodic variation superimposed upon an over-all increase with increasing atomic number $Z$. For $\mu \geq 0$, the $Z$ dependence of the moments becomes dominated by inner-shell contributions; as $\mu$ increases, the over-all increase with $Z$ becomes more rapid. Another perspective of the voluminous data is gained by plotting $\log S(\mu)$ vs $\mu$. The plot reveals three classes of behavior—"tight," "intermediate," and "loose" atoms. Comparisons with experiment and more detailed calculations are made where possible. (auth)

**26739** VARIATIONAL PRINCIPLE FOR QUASIBOUND STATES. Froelich, P.; Brändas, E. (Quantum Chemistry Group, University of Uppsala, Box 518, S-751 20 Uppsala 1, Sweden and Quantum Theory Project, Departments of Chemistry and Physics, Williamson Hall, University of Florida, Gainesville, Florida 32611). Phys. Rev. A 12: No. 1, 1-5 (July 1975).

A minimum-variance principle for quasibound states is defined and utilized to investigate the corresponding energy resonances. The variational principle yields simultaneously a resonance energy $E$ and a square-integrable wave function $\varphi$, such that minimum variance is obtained for arbitrary variations of a restricted class of square-integrable functions as well as with respect to variations of $E$. It is further shown that the optimum energy $\mathcal{E}_0$ obtained from this method can simultaneously be written as an expectation value of the actual Hamiltonian with respect to $\varphi = \varphi(E_0)$. The example of the Stark effect in the hydrogen atom is studied. It is shown that the variationally obtained resonance energy coincides with the real part of the complex pole of the $m$ function of Weyl, related to the Green's function of the system under consideration. It is also shown that the corresponding numerical application of the Rayleigh-Ritz variational method only gives meaningful results for field intensities below 0.06 a.u., as compared with the "exact" results of Hehenberger, McIntosh, and Brändas. (auth)

**26740** RESONANCES IN THE DIFFERENTIAL EXCITATION FUNCTIONS OF FIVE ELECTRONIC STATES OF Ne IN THE AUTOIONIZATION REGION. Roy, D.; Delage, A.; Carette, J. (Laboratoire de Physique atomique et moléculaire, Département de Physique, et Centre de Recherches sur les Atomes et les Molécules, Université Laval, Québec, Canada G1K 7P4). Phys. Rev. A 12: No. 1, 45-51 (July 1975).

We have observed many resonances by electron spectrometry in the differential excitation functions of the states $3s$, $3s'$, $3p$, and $3d$ of neon in the autoionization region. These measurements are compared to the data obtained by other spectroscopic methods and their interpretation is discussed. For the main resonances, the energies and natural widths are determined. Moreover, their effective strengths and profile indices are presented for the various decay channels in comparison with the data obtained in the ionization channel. (auth)

**26741** SATURATED TWO-PHOTON RESONANCE IONIZATION OF He(2$^1S$). Hurst, G.S.; Payne, M.G.; Nayfeh, M.H.; Judish, J.P.; Wagner, E.B. (Oak Ridge National Laboratory, Oak Ridge, Tennessee 37830). Phys. Rev. Lett. 35: No. 2, 82-85 (14 July 1975).

We have developed a photoionization method for complete conversion of a quantum-selected population to ionization, making possible sensitive and absolute measurement of the selected populations in a gas. Each photoionization involves the absorption of two photons (from a pulsed dye laser), one of which is resonant with an intermediate state. In this demonstration we measured the absolute number of He(2$^1S$) states per ion pair following interaction of pulses of 2-MeV protons with He. (auth)

**26742** OBSERVATIONS OF DIATOMIC AND TRIATOMIC HYDROGEN NEGATIVE IONS. Aberth, W.; Schnitzer, R.; Anbar, M. (Mass Spectrometry Research Center, Stanford Research Institute, Menlo Park, California 94025). Phys. Rev. Lett. 34: No. 26, 1600-1603 (30 June 1975).

Mass-spectrometric observations have been made of $HD^-$, $D^-_2$, $H^-_3$, $H_2D^-$, $HD^-_2$, and $D^-_3$, using a hollow-cathode duoplasmatron negative-ion source operating between 0.1 and 2 Torr. Both the diatomic and triatomic hydrogen negative ions appear stable, with half-lives greater than $10^{-5}$ sec. Attenuation-cross-section measurements of $D^-_2$ and $D^-_3$ with helium between 3 and 5 keV yield average values of (5.5 and 7.0) $\times 10^{-15}$ cm$^2$, respectively. (auth)

**26743** CONFIGURATION INTERACTION WAVEFUNCTIONS FOR $^3S$ EXCITED STATES OF HELIUM. Birss, F.W.; Senn, P. (Department of Chemistry, University of Alberta, Edmonton, Alberta, Canada T6G 2E1). J. Chem. Phys. 63: No. 3, 1276-1279 (1 Aug 1975).

The method of configuration interaction is used to determine accurate upper bounds of the $2^3S$ to $23^3S$ states of helium by minimization of the eigenvalues corresponding to one state or a group of states without concern as to the fate of other eigenvalues. The relative importance of radial and angular correlation in triplet state is discussed. (auth)

**26744** RATIONAL ORBITALS FOR $^3S$ STATES OF TWO-ELECTRON SYSTEMS. Birss, F.W.; Choi, J.H. (Department of Chemistry, University of Alberta, Edmonton, Alberta, Canada T6G 2E1). J. Chem. Phys. 63: No. 3, 1280-1284 (1 Aug 1975).

The concept of rational orbitals for $^3S$ states of two-electron systems is introduced, based upon finding that pair of orbitals which yield that single configuration function which maximally overlaps with a configuration interaction wavefunction. Methods for obtaining these orbitals are discussed and applied to a number of $^3S$ states of helium. (auth)

**26745** HYPERFINE STRUCTURE OF $2s$ $^3He^+$ BY AN ION-STORAGE TECHNIQUE. Prior, M.H.; Wang, E.C. (Department of Physics and Lawrence Berkeley Laboratory, University of California, Berkeley, California 94720). Phys. Rev. Lett. 35: No. 1, 29-32 (7 July 1975).

An electrostatic confinement device has provided resonance linewidths $\simeq$1 kHz for the hyperfine transition $F=1$, $m_F=0$ to $F=0$, in metastable $2s$ $^3He^+$. The state-selection and resonance-detection scheme is the same used in an earlier ion-beam experiment; however, ion storage has yielded a resonance linewidth narrower by a factor of 100. Our result for the $2s$ hyperfine structure is $\Delta\nu_2 = 1083.354969(30)$ MHz. Comparison with the $1s$ hyperfine structure yields a test of state-dependent terms in the theory. (auth)

**26746** LEVEL CROSSING INVESTIGATION OF THE HYPERFINE SPLITTING IN THE $Z^6\,P_{\frac{5}{2}}$-LEVEL OF Eu I. Lange, W. (Technische Univ. Hannover (F. R. Germany). Inst. A fuer Experimentalphysik). Z. Phys., A; 272: No. 3, 223-226 (Mar 1975).

1 fig.; 3 tabs.; 15 refs.

By means of a level crossing experiment the hyperfine structure constants of the $Z^8\,P_{\frac{5}{2}}$-level of Eu were determined. The results are A = −6.51(6) MHz and B = 131.2(1.0) MHz in the isotope $^{151}$Eu and A = −2.84(3) MHz and B = 327.5(1.5) MHz in the isotope $^{153}$Eu. Experimental data on the hyperfine splitting are available now for 11 of the 12 levels of the configuration $4f^7(^8S)6s6p$ of EuI. These data are compared with the theoretical interpretation given by Bordarier et al. which was based on only 7 A-factors and B-factors. It is shown that the agreement between theory and experiment can be improved by taking into account configuration interactions. (auth)

**26747** EVALUATION OF THE DIPOLE–DIPOLE INTERACTION COEFFICIENT AND COMPARISON OF POTENTIAL ENERGY OF TWO NEUTRAL HELIUM ATOMS. Prasad, N. (Kisan College, Bihar, India). Indian J. Pure Appl. Phys.; 13: No. 3, 201-203(Mar 1975).

The coefficient of the dipole-dipole interaction ($A_1$) of two neutral helium atoms has been numerically evaluated. This independent calculation of the numerical value of $A_1$ gives the same value as reported earlier by Nageshwar Prasad. Using this value of $A_1$ and that of $A_2$, the coefficient of dipole-quadrupole interaction reported by C. H. Page, the total energy has been computed at different values of R and compared with those obtained by different procedures used by other workers. (auth)

**26748** DECAY KINETICS FOR THE $5^1D_2$ HELIUM LEVEL. Kvater, G.S.; Oginets, O.V.; Smirnov, V.B.; Tolmachev, Yu.A.; Bagaev, S.A. Opt. Spectrosc. (USSR) 38: No. 4, 468-469 (Apr 1975).

The decay kinetics of the $5^1D_2$ level of helium atoms was studied experimentally, by exciting helium gas with a pulsed electron beam. The resulting emission was monitored by means of a multichannel apparatus. (AIP)

## Positronium, Muonium, and Muonic and Mesic Atoms and Molecules

**26749** (JINR-P14-8937) CONNECTION OF MECHANISM OF NEGATIVE PION CAPTURE BY BOUND HYDROGEN AND THAT OF RADIATION–CHEMICAL REACTIONS. Petrukhin, V. I.; Suvorov, V. M.; Yutlandov, I. A. (Joint Inst. for Nuclear Research, Dubna (USSR)). 1975. 9p. (In Russian). Dep. NTIS (US Sales Only) $4.00.

A critical analysis is presented of the paper by V. I. Goldansky, N. N. Zatsepina, I. F. Tupitsin and N. I. Kholodov (DAN SSSR, 216, 1250 (1974) deducing analogy between the mechanism of negative pion capture by bound hydrogen and that of radiation-chemical reactions. The groundlessness of this analogy is supported by the following remarks. The correlation between the coefficients $\alpha$ and the radiation-chemical parameters $G(H_2)$ and J indicate not the identity of the pion capture and radiation-chemical reaction mechanism but the dependence of both $\alpha$ and $G(H_2)$, J on the chemical bond energy E. The inadditivity in the pion capture probability "at the accumulation hydrogen in the molecules of aromatic and saturated compounds" observed by the authors results from the incorrect use of the literature data. The inadditive decrease in the pion capture probability at replacing $H_2O$ and $NH_3$ by $H_2O_2$ and $N_2H_4$, respectively, is explained by the induction effect and not by the attachment of $\pi^-H^+$ mesic atoms to multiple bonds (in the above compounds there is no one). The data showing some "external isotope transfer" in the mixture $C_6H_6 + C_6D_6$ and in $C_6H_xD_{6-x}$ are statistically unreasoned. (auth)

**26750** DOUBLE-VERTEX CONTRIBUTION TO THE DECAY RATE OF ORTHOPOSITRONIUM. Stroscio, M.A. (Energetic Particles Branch, Space Physics Laboratory, Air Force Cambridge Research Laboratories, Bedford, Massachusetts 01731). Phys. Rev. A 12: No. 1, 338-339 (July 1975).

The recently calculated decay rate of orthopositronium differs with the experimental value by 2 1/2 standard deviations. This communication reports a 100-fold improvement in the numerical error estimate for the double-vertex diagram contribution to the decay rate. This improvement reduces the numerical error estimate of the previously calculated decay rate of orthopositronium by 20%. This improvement of the double-vertex diagrams alone does not bring the experimental and calculated values into good agreement; however, the discrepancy is reduced. (auth)

**26751** CHEMIIONIZATION INVOLVING RARE GAS METASTABLE ATOMS. West, W.P.; Cook, T.B.; Dunning, F.B.; Rundel, R.D.; Stebbings, R.F. (Department of Space Physics and Astronomy, Rice University, Houston, Texas 77001). J. Chem. Phys. 63: No. 3, 1237-1242 (1 Aug 1975).

Crossed beams studies of chemiionization in thermal energy collisions of helium, neon, argon, and krypton metastable atoms with ground state atoms and molecules (Ar, Kr, Xe, $N_2$, $H_2$, $O_2$, NO, CO, $CO_2$, and $N_2O$) are described. Branching ratios are presented and in some cases absolute total ion production cross sections have been measured. (auth)

**26752** $\alpha^2(Z\alpha)^2$ VACUUM-POLARIZATION CORRECTION IN MUONIC ATOMS. Fujimoto, D.H. (Physics Department, University of Washington, Seattle, Washington 98195). Phys. Rev. Lett. 35: No. 6, 341-344 (11 Aug 1975).

The order-$\alpha^2(Z\,\alpha)^2$ vacuum-polarization correction for transition energies in muonic atoms is calculated in the static-muon, massless-electron limit. Conventional Feynman–parametric-integral techniques are utilized. The correction is found to be negligibly small, contrary to a previous claim appearing in the literature. (auth)

## Collision Phenomena

*Refer also to abstract 27154.*

**26753** CALCULATION OF THE FAST ELECTRON SCATTERING CROSS SECTIONS FROM THE HYDROGEN MOLECULE. Ishi, S.; Tanaka, K. (Hokkaido Univ., Sapporo (Japan). Faculty of Science). J. Phys. Soc. Jpn.; 37: No. 4, 1073-1076(Oct 1974).

The electron scattering cross sections of the hydrogen molecule in its ground state are calculated with three types of configuration interaction wavefunctions based on the one-center expansion method. A wavefunction involving left-right and angular correlations is found to give good agreement with experiment. A table of calculated scattering factors is given. (auth)

**26754** ELECTRON IMPACT EXCITATION OF POTASSIUM AND CESIUM ATOMS INTO IONIC STATES. Postoi, E.N.; Aleksakhin, I.S.; Ivanchov, P.G. Opt. Spectrosc. (USSR) 38: No. 3, 263-265 (Mar 1975).

The results of investigating the process of excitation of discrete ionic states of potassium and cesium during electron-atom collisions are presented. The investigations were carried out by the method of intersection of electron and atomic beams, and a vapor-filled cell was used in the case of low intensity transitions. (auth)

**26755** CALCULATION OF INELASTIC CROSS SECTIONS FOR $H^+ + Cs \rightarrow H(n=2) + Cs^+$. Valance, A.; Spiess, G. (Service de Physique Atomique, Centre d'Etudes Nucléaires de Saclay, BP N° 2-91190, Gif-sur-Yvette, France). J. Chem. Phys. 63: No. 4, 1487-1489 (15 Aug 1975).

The cross sections for the processes $H^+ + Cs \rightarrow H(2p \text{ and } 2s) + Cs^+$ were calculated in the center of mass energy range 250–2400 eV using a simple pseudopotential formalism for the potential curves and coupling matrix elements and a perturbed stationary state (pss) formulation for the calculation of the cross sections. The results are found to be in reasonable agreement with experiment. (auth)

**26756** DIRECT VIBRATIONAL EXCITATION VIA CHARGE EXCHANGE IN SYMMETRIC ION–MOLECULE COLLISIONS. Flannery, M.R.; McCann, K.J.; Moran, T.F. (Georgia Institute of Technology, Atlanta, Georgia 30332). J. Chem. Phys. 63: No. 4, 1462-1468 (15 Aug 1975).

Integral and differential cross sections for vibrational excitation in symmetric $H^+_2(X\,^2\Sigma^+_g, v_0) + H_2(X\,^1\Sigma^+_g, v_0)$ collisions have been determined for incident kinetic energies $E$ (keV) in the range $0.01 < E < 2.0$. A multistate impact parameter description of the collision was used. At low kinetic energies, the inclusion of a relatively small number of states in the wavefunction expansion of the system achieves converged cross sections while at high energies a large number of product states are needed. The inelastic channels in this symmetric system are strongly coupled to each other and to the energy resonant charge exchange channels. Differential cross sections for excitation of individual product channels have been computed as a function of scattering angle within the multistate impact parameter approach. Small angle scattering within several degrees is dominant with forward inelastic scattering becoming more pronounced as the ion kinetic energy is increased. Integral cross sections for individual channels and integral cross sections summed over all product channels are presented as a function of both ion kinetic energy and reactant internal energy. (auth)

**26757** A HARTREE–FOCK INTERACTION POTENTIAL BETWEEN A RIGID ASYMMETRIC TOP AND A SPHERICAL ATOM: ($H_2CO$,He). Garrison, B.J. (Department of Chemistry and Inorganic Materials Research Division, Lawrence Berkeley Laboratory, University of California, Berkeley, California 94720); Lester, W.A. Jr.; Schaefer, H.F. III. J. Chem. Phys. 63: No. 4, 1449-1454 (15 Aug 1975).

A basis set of better than "triple zeta plus polarization" quality is used to compute the interaction potential between a rigid $H_2CO(^1A_1)$ and $He(^1S)$. The highly anisotropic energy surface has a slight attraction arising from induction effects at intermolecular separations around 9 a.u. It is fitted to a spherical harmonic expansion to facilitate scattering applications. (auth)

**26758** ON THE DISPLAY OF BASIC PROPERTIES OF THE MOLECULAR ELECTRONIC WAVEFUNCTIONS IN THE

(e,2e) QUASIELASTIC KNOCKOUT EXPERIMENTS. Levin, V.G. (Institute of Nuclear Physics, Moscow State University, Moscow, USSR); Neudatchin, V.G.; Pavlitchenkov, A.V.; Smirnov, Yu.F. J. Chem. Phys. 63: No. 4, 1541-1546 (15 Aug 1975).

Some theoretical aspects of quasielastic knockout of an electron by a fast electron from molecules are discussed and a few general formulas are given. Angular correlation curves of two final electrons are calculated for loosely bound electron orbitals in molecules $Li_2$, $N_2$, $F_2$, BH, CH, LiH, and HF to illuminate the influence of both hybridization and kind of bonding (ionic, covalent) on $(e,2e)$ form factors. (auth)

**26759** THE ABSOLUTE GENERALIZED OSCILLATOR STRENGTH FOR THE LYMAN-BIRGE-HOPFIELD BAND OF $N_2$ AS DETERMINED BY HIGH ENERGY ELECTRON IMPACT SPECTROSCOPY. Wong, T.C.; Lee, J.S.; Wellenstein, H.F.; Bonham, R.A. (Department of Chemistry, Indiana University, Bloomington, Indiana 47401). J. Chem. Phys. 63: No. 4, 1538-1540 (15 Aug 1975).

The absolute generalized oscillator strength for the dipole forbidden quadrupole allowed Lyman–Birge–Hopfield band $[a\,^1\Pi_g \leftarrow X\,^1\Sigma^+_g]$ in molecular nitrogen at an energy loss of 9.35 eV is observed by electron impact spectroscopy using 25 keV electrons over the momentum transfer range $0.04 \leqslant K^2 \leqslant 10$ a.u. The results agree in the zero angle (zero momentum transfer) limit with the previous observations of Skerbele and Lassettre, but are in disagreement with previous theoretical and experimental results for $K^2 > 0.5$. (auth)

**26760** DISSOCIATION OF $CH_4$ AND $CD_4$ BY ELECTRON IMPACT: PRODUCTION OF METASTABLE AND HIGH-RYDBERG HYDROGEN AND CARBON FRAGMENTS. Finn, T.G.; Carnahan, B.L.; Wells, W.C.; Zipf, E.C. (Department of Physics, University of Pittsburgh, Pittsburgh, Pennsylvania 15260). J. Chem. Phys. 63: No. 4, 1596-1604 (15 Aug 1975).

The production of hydrogen and carbon atoms in metastable and high-lying Rydberg states due to electron-impact dissociation of $CH_4$ and $CD_4$ has been investigated for incident electron energies from threshold to 300 eV. Onset energies for the production of metastable hydrogen atoms were observed at electron impact energies of $22.0 \pm 0.5$, $25.5 \pm 0.6$, $36.7 \pm 0.6$, and $66 \pm 3$ eV, and at $26.6 \pm 0.6$ eV for the production of metastable carbon atoms. Most of the excited H fragments appear to have been formed initially in high-lying Rydberg states with the metastable H(2S) state populated principally by cascade. The differential cross section, $(d\sigma/d\Omega)_{90}$, for the dissociative excitation of H atoms to metastable and high-lying Rydberg states reached a maximum value of approximately $1 \times 10^{-19}$ cm²/sr at 100 eV. At the same energy, the metastable carbon differential cross section is $2 \times 10^{-20}$ cm²/sr. (auth)

**26761** CHEMI–IONIZATION AND SECONDARY ION REACTIONS IN MOLECULAR HYDROGEN AND ITS ISOTOPES ON IMPACT OF METASTABLE HELIUM ATOMS. Specht, L.T.; Foster, K.D.; Muschlitz, E.E. Jr. (Department of Chemistry, University of Florida, Gainesville, Florida 32611). J. Chem. Phys. 63: No. 4, 1582-1585 (15 Aug 1975).

Relative cross sections for the following reactions are reported:

$$\begin{aligned} He^*(2^1S, 2^3S) + X_2 &\rightarrow X_2^* + He + e \\ &\rightarrow HeX^+ + X + e \\ &\rightarrow HeX_2^+ + e \end{aligned}$$

in which $X_2$ is (a) $H_2$, (b) $D_2$, and (c) HD. The isotope effect in the production of $HeH^+$ and $HeD^+$ in Reaction (2c) was determined and relative measurements were made of the kinetic energy of the ion product in Reaction (1). The cross section for the secondary reaction

$$H_2^+ + H_2 \rightarrow H_3^+ + H$$

was also determined as a function of the relative kinetic energy of the reactants. This energy-dependent cross section was determined for $H_3^+$ formed both by helium metastable atom collisions and by electron impact. The cross section for $H^+_2$ formed by metastable helium was found to be greater than for $H^+_2$ formed by electron impact. This may be evidence for an additional reaction producing $H^+_3$ involving highly excited Rydberg states of $H_2$ as reactants. (auth)

**26762** VIBRATION–TRANSLATION ENERGY TRANSFER IN ANHARMONIC DIATOMIC MOLECULES. I. A COMPARATIVE EVALUATION OF THE SEMICLASSICAL APPROXIMATION. McKenzie, R.L. (Ames Research Center, NASA, Moffett Field, California 94035). J. Chem. Phys. 63: No. 4, 1655-1662 (15 Aug 1975).

The semiclassical approximation (quantum oscillator, classical path) is applied to anharmonic diatomic oscillators in excited initial states. Multistate numerical solutions giving the vibrational transition probabilities for collinear collisions with an inert atom are compared with equivalent, exact quantum-mechanical calculations. Several symmetrization methods are shown to correlate accurately the predictions of both theories for all initial states, transitions, and molecular types tested, but only if coupling of the oscillator motion and the classical trajectory of the incident particle is considered. In anharmonic heteronuclear molecules, the customary semiclassical method of computing the classical trajectory independently leads to transition probabilities with anomalous low-energy resonances. Proper accounting of the effects of oscillator compression and recoil on the incident particle trajectory removes the anomalies and restores the applicability of the semiclassical approximation. (auth)

**26763** OBSERVATION OF A NEW ELECTRONIC TRANSITION IN $N_2$ AT 31.4 eV BY MEANS OF HIGH ENERGY ELECTRON IMPACT SPECTROSCOPY. Lee, J.S.; Wong, T.C.; Bonham, R.A. (Department of Chemistry, Indiana University, Bloomington, Indiana 47401). J. Chem. Phys. 63: No. 4, 1643-1645 (15 Aug 1975).

A new transition in molecular nitrogen at an energy loss of $31.4 \pm 0.5$ eV has been observed by high energy electron impact spectroscopy at momentum transfers larger than 2 a.u. The absolute generalized oscillator strength was measured over the momentum transfer range $0.5 \leqslant K^2 \leqslant 5.08$ a.u. using 25 and 33 keV electrons. The observed angular behavior of this line suggests that it may be due to a dipole forbidden quadrupole allowed process. The term symbol $^1\Pi_g$ with the electronic configuration $(2s\sigma_g)^{-1}\,(2p\pi_g)^1$ is tentatively assigned to this transition and it is suggested that this state may decay into the $D\,^2\Pi_g$ state of $N^+_2$ by Auger cascade. (auth)

**26764** A SEARCH FOR COHERENT FEATURES IN THE ANGULAR DEPENDENCE OF THE 10 eV AND 14 eV ENERGY LOSS LINES IN $CCl_4$ USING 25 keV ELECTRONS. Lee, J.S.; Wong, T.C.; Bonham, R.A. (Department of Chemistry, Indiana University, Bloomington, Indiana 47401). J. Chem. Phys. 63: No. 4, 1609-1611 (15 Aug 1975).

A reinvestigation of the angular dependence of the 10 eV and 14 eV energy loss lines in $CCl_4$ has shown that the coherent features most easily observed are due to intermolecular multiple scattering. The high sensitivity of these lines to multiple scattering and their observed angular dependence strongly argues that both transitions must be dipole allowed. From this study it is concluded that previously predicted coherent structure in the angular dependence must be of a smaller magnitude than heretofore suspected. (auth)

**26765** CLOSE COUPLED CALCULATIONS OF ELECTRON–HYDROGEN ATOM SCATTERING USING A NONITERATIVE INTEGRAL EQUATION TECHNIQUE [J. Chem. Phys. 57, 4770 (1972)]. Knirk, D.L. (Department of Chemistry, University of California at Berkeley, Berkeley, California 94720); Hayes, E.F. J. Chem. Phys. 63: No. 4, 1699-1699 (15 Aug 1975).

Some comments are made upon the origin and implementation of the equations for electron–hydrogen atom scattering presented in the earlier paper by Kirk and Hayes, J. Chem. Phys. 57, 4770 (1972). (AIP) (auth)

**26766** OBSERVATION OF AUTOIONIZING TRANSITIONS IN HELIUM USING THE $(e,2e)$ TECHNIQUE. Weigold, E.; Ugbabe, A.; Teubner, P.J.O. (School of Physical Sciences, The Flinders University of South Australia, Bedford Park, South Australia, 5042, Australia). Phys. Rev. Lett. 35: No. 4, 209-212 (28 July 1975).

Resonance ionization from the $(2s2p)^1P$ and $(2p^2)^1D$ levels of helium has been observed in an $(e,2e)$ experiment, in which the kinematics of all electrons is fully determined, at incident energies of 200 and 400 eV and a scattering angle of 10°. The results show that as the angle of emission approaches the direction $-\vec{Q}$, where $\vec{Q}$ is the momentum transfer to the helium atom, the resonance profile becomes more symmetric and the resonance cross section increases sharply. (auth)

**26767** CHEMICAL EFFECT ON $K\alpha$ X-RAY SATELLITES: NEW EVIDENCE FOR INTERATOMIC TRANSITIONS. Watson, R.L.; Chiao, T.; Jenson, F.E. (Cyclotron Institute and Department of Chemistry, Texas A&M University, College Station, Texas 77843). Phys. Rev. Lett. 35: No. 4, 254-257 (28 July 1975).

$K\,\alpha$ x-ray satellite spectra produced by bombardment with 2.0-MeV/nucleon oxygen and neon ions have been measured for several sulfur compounds. Comparison of the satellite-peak relative-intensity distributions has revealed a dependence on chemical environment. We interpret this effect to be caused by variations in the lifetimes of $L$-shell vacancies and find evidence that transitions from ligand valence levels play an important role. (auth)

**26768** VAN HOVE SINGULARITIES OF THE SURFACE PHONON DENSITY FROM INELASTIC REFLECTION OF ATOMS. Benedek, G. (Gruppo Nazionale de Struttura della Matteria del Consiglio Nazionale delle Ricerche, Instituto di Fisica dell'Università, Milan, Italy). Phys. Rev. Lett. 35: No. 4, 234-237 (28 July 1975).

The main peaks of the angular distribution of atoms inelastically reflected from a crystal surface are shown to be associated with analytical critical points of the surface phonon dispersion curves, particularly those of Rayleigh and Lucas modes. Because of such a relation, the frequencies and wave vectors of these modes could be measured by analyzing the shift of the peaks under a change of the angle of incidence. (auth)

**26769** FESHBACH RESONANCES IN POSITRON-HYDROGEN SCATTERING. Drachman, R.J. (Theoretical Studies Group, Goddard Space Flight Center, Greenbelt, Maryland 20771). Phys. Rev. A 12: No. 1, 340-344 (July 1975).

Seiler, Oberoi, and Callaway first located resonances in the positron-hydrogen system below the $n = 2$ inelastic threshold, using the algebraic close-coupling method without including the open positronium channel. Several other calculations including both open channels have failed to find any resonances. In an attempt to clarify the situation, a calculation has been performed which is an extension of the work of Seiler, Oberoi, and Callaway. A wave function including the 1s, 2s, and 2p eigenstates of hydrogen and the $\overline{1}\overline{3}$ ground state of positronium was used in a calculation that is a simplification of the usual close-coupling technique and that resembles the optical-potential method. In this approximation it is found that the lowest resonance of Seiler, Oberoi, and Callaway is destroyed by opening the $\overline{1}\overline{3}$ channel. It is concluded that any resonances which may occur in this system must lie closer to the $n = 2$ threshold than do the corresponding electron-hydrogen resonances. (auth)

**26770** ELECTRON IMPACT EXCITATION OF ZINC VAPOR AT 40 eV. Williams, W. (Jet Propulsion Laboratory, California Institute of Technology, Pasadena, California 91103); Bozinis, D. Phys. Rev. A 12: No. 1, 57-59 (July 1975).

Differential and integral electron impact cross sections for elastic scattering and for the excitation of the $4p\,^3P$, $4p\,^1P$, $5s\,^1S$, and $5p\,^1P$ states of zinc have been determined for the first time at 40 eV impact energy. The measurements were normalized to the absolute scale by utilizing the optical $f$ value of the $4p\,^1P$ transition. We find that the integral cross section for the $4p\,^1P$ excitation is quite large ($1.0 \times 10^{-15}$ cm$^2$) and exceeds that for elastic scattering ($2.1 \times 10^{-16}$ cm$^2$) by a factor of nearly 5. (auth)

**26771** ENERGY AND ANGULAR DISTRIBUTION OF ELECTRONS EJECTED FROM HELIUM BY FAST PROTONS AND ELECTRONS: THEORY AND EXPERIMENT. Manson, S.T. (Department of Physics, Georgia State University, Atlanta, Georgia 30303); Toburen, L.H.; Madison, D.H.; Stolterfoht, N. Phys. Rev. A 12: No. 1, 60-79 (July 1975).

A comprehensive study of the angular and energy distributions of electrons ejected in collisions of fast electrons and protons with He is presented. New experimental results for 300-keV, 1-MeV, and 5-MeV proton impact are reported along with theoretical results for 2-keV electron impact and 100-keV, 300-keV, 1-MeV, and 5-MeV proton impact. The theoretical results, based upon Born approximation with Hartree-Slater initial discrete and final continuum wave functions, show excellent agreement with experimental electron-impact results. Serious discrepancies are found between theory and experiment in the angular distribution of ejected electrons for forward angles for 100- and 300-keV proton impact; the discrepancies decrease markedly for 1-MeV proton impact and are absent for 5-MeV protons. The agreement between theory and experiment for intermediate and backward angles of electron ejection, on the other hand, is uniformly good for all proton impact energies. The reasons for this behavior in terms of a charge-exchange process to a continuum state contributing to electron ejection at forward angles is discussed, and the energy dependence of the data is shown to be consistent with this explanation. (auth)

**26772** INTEGRAL REPRESENTATION FOR THE GLAUBER SCATTERING AMPLITUDE FOR DIRECT COULOMB IONIZATION BY CHARGED PARTICLES. Golden, J.E.; McGuire, J.H. (Theoretical Studies Group, Goddard Space Flight Center, Greenbelt, Maryland 20771 and Department of Physics, Kansas State University, Manhattan, Kansas 66506). Phys. Rev. A 12: No. 1, 80-84 (July 1975).

An integral representation is developed for the scattering amplitude for ionization by charged particles in the Glauber approximation. Unlike previous results based on a series expansion in the momentum of the ejected electron, $\vec{k}_e$, the present results are rigorously convergent for all physical values of $\vec{k}_e$. Results calculated by this method agree with earlier results for ionization of atomic hydrogen by electron impact using Padé approximants to approximately sum the series. Total cross sections for the ionization of atomic hydrogen by proton impact are presented and compared to experimental data. This technique is applicable to the ionization of neutral atoms whose participating electron is represented by a hydrogenic wave function, and the remaining electrons are ignored. (auth)

**26773** COMMENTS ON Ar $L_{23}$ -SHELL FLUORESCENCE YIELDS AND ARGON-CHARGE-STATE FRACTIONS. Oona, H. (Department of Physics, University of Arizona, Tucson, Arizona 85721). Phys. Rev. Lett. 34: No. 26, 1649-1650 (30 June 1975).

New theoretical numbers for fluorescence yields are used to calculate charge states of argon produced by bombardment with $H^+$ and $He^+$ ions. High-resolution x-ray-spectrometer data are used to determine charge-state fractions. Average fluorescence yields determined using this new data still show discrepancies with Auger-electron data. (auth)

**26774** ELASTIC AND ROTATIONALLY INELASTIC H–$H_2$ AND H–$D_2$ COLLISIONS. McGuire, P.; Krüger, H. (Fachbereich Physik, Universität Kaiserslautern, 675 Kaiserslauterr., Germany). J. Chem. Phys. 63: No. 3, 1090-1094 (1 Aug 1975).

The coupled-states approximation in the body-fixed coordinate system is applied to the study of elastic and rotationally inelastic H–$H_2$ and H–$D_2$ collisions. For both systems, integral and differential cross sections are computed in the collision energy range 0.5–1.5 eV. The isotope effect in the integral cross sections for $j{=}0{\rightarrow}j'$ ($j'{=}0,2,4,6$) is found to be more pronounced for increasing $j'$. In addition, as the ratio of rotational energy transferred to kinetic energy, i.e., $\Delta E/E$, decreases, the differential cross sections shift from backward to forward peaked. (auth)

**26775** DISSOCIATIVE EXCITATION OF $H_2$ BY ELECTRON IMPACT: TRANSLATIONAL SPECTROSCOPY OF LONG LIVED HIGH RYDBERG FRAGMENT ATOMS. Schiavone, J.A.; Smyth, K.C.; Freund, R.S. (Bell Laboratories, Murray Hill, New Jersey 07974). J. Chem. Phys. 63: No. 3, 1043-1051 (1 Aug 1975).

Electron impact excitation of $H_2$ leads to three distinguishable groups of high Rydberg fragment atoms. High Rydberg molecules are also detected. The measurements consist of (1) excitation functions and (2) time of flight distributions which are transformed to fragment translational energy distributions. For high Rydberg fragments from molecular high Rydberg states converging to the repulsive wall of the $H^+{}_2$ ground state, the measured and calculated kinetic energy distributions agree, in accordance with the prediction of the core ion model of high Rydberg dissociation. The remaining high Rydberg fragments result from dissociation of states of $H_2$ with both electrons excited to low principal quantum numbers rather than from dissociation of molecular high Rydberg states. (auth)

**26776** MEASURED CROSS SECTION FOR THE FORMATION OF $H^+{}_2$ BY FAST PROTON IMPACT ON METHANE. Cook, C.J. (Stanford Research Institute, Menlo Park, California 94025); Smyth, N.R.A.; Heinz, O. J. Chem. Phys. 63: No. 3, 1218-1223 (1 Aug 1975).

The classical theory of ion–molecule rearrangement collisions proposed by Bates, Cook, and Smith for the capture cross section for the formation of $\underline{H}^+{}_2$ in the reaction $H^+ + CH_4 \rightarrow CH_3 + \underline{H}^+{}_2$ was confirmed. Measurements at incident proton energies of 70, 85, 100, and 150 eV gave cross sections peaking sharply at scattering angles (laboratory coordinates) of about 46° as predicted. Typical values of the total cross section are $2.0{\times}10^{-21}$ cm$^2$ at 70 eV and $7.6{\times}10^{-22}$ cm$^2$ at 100 eV, a factor of 30 less than the theoretical values, which are believed to represent upper limits to the cross section. The asymmetrical shape of the differential cross section is consistent with that predicted by a classical construction method described by Gillen, Mahan, and Winn. (auth)

**26777** HARTREE-FOCK AND GORDON-KIM INTERACTION POTENTIALS FOR SCATTERING OF CLOSED-SHELL MOLECULES BY ATOMS: ($H_2CO$,He) AND ($H_2$,$Li^+$). Green, S. (Department of Chemistry, Columbia University, New York, New York 10027); Garrison, B.J.; Lester, W.A. Jr. J. Chem. Phys. 63: No. 3, 1154-1161 (1 Aug 1975).

The Gordon–Kim (GK) electron gas model for calculating the forces between closed-shell atoms and molecules is applied to the He–$H_2CO$ and $Li^+$–$H_2$ systems. GK interaction energies are computed following the original theory and also including the self-energy correction suggested by Rae. GK interaction energies, neglecting correlation, are found to be in qualitative accord with Hartree–Fock (HF) interaction energies for the two systems. However, quantitative discrepancies are noted which are possible sources of error if GK potential energy surfaces are used to compute accurate scattering cross sections. (auth)

**26778** EXCITATION OF THE $C\,^3\Pi_u$ STATE OF $N_2$ BY ELECTRON IMPACT. Chen, S.T.; Anderson, R.J. (Department of Physics, University of Arkansas, Fayetteville, Arkansas 72701). J. Chem. Phys. 63: No. 3, 1250-1254 (1 Aug 1975).

The $\lambda{=}3371$ Å spectral band of the $C\,^3\Pi_u{\rightarrow}B\,^3\Pi_g$ ($v{=}0$, $v'{=}0$) second positive system is investigated using time-resolved spectroscopy with electron beam pulse widths of 100 nsec, 260 nsec, and 5 μsec. Lifetime data for the $v{=}0$ vibrational level of the $C\,^3\Pi_u$ electronic state are obtained for incident electron energies and $N_2$ gas pressures in the range 25–200 eV and 2–380 mtorr, respectively. In the case of the 260 nsec electron pulse, a single radiative decay component is observed which exhibits a dependence upon electron impact energy. However, in the case of a 5 μsec excitation pulse the resulting radiative decay is observed to consist of two decay components. The short-lived component is identified as the primary $C\,^3\Pi_u$ state excitation, while the long-lived component is identified as the radiative cascade contribution from higher electronic states, including possibly the metastable $E\,^3\Sigma^+{}_g$ state. When the long-lived cascade contribution is subtracted from the total $C\,^3\Pi_u$ population, the $C$ state natural radiative lifetime becomes independent of energy. In addition, the lifetime is observed to be independent of $N_2$ gas pressure over the pressure range ~2–380 mtorr. (auth)

**26779** ION PAIR PRODUCTION BY ELECTRON IMPACT ON $H_2$ AND CO: KINETIC ENERGY DISTRIBUTIONS AND THRESHOLD BEHAVIOR. Köllmann, K. (Institut für Experimentalphysik Universität Hamburg, Jungiusstr. 9, D 2000

Hamburg, West Germany). J. Chem. Phys. 63: No. 3, 1314-1316 (1 Aug 1975).

Kinetic energy distributions and ion efficiency curves are obtained for ion pair production by electron impact on $H_2$ and CO. The results are used to test the hypothesis that, if the threshold behavior of the cross section can be described by a step function, the first derivative of the ion efficiency curve should reflect the total kinetic energy distribution of the ion pairs. (AIP)

**26780** CHEMICAL REACTION KINEMATICS. XVII. Crossed Beam Study of the Reaction $CH^+ + H_2 + H$. Eisele, G.; Henglein, A. (Meitner-Institut fuer Kernforschung, Berlin). Int. J. Radiat. Phys. Chem.; 7: No. 2/3, 293-303 (Apr 1975).

The reactions $CH^+ + H_2 \rightarrow CH_2^+ + H$, $CH^+ + D_2 \rightarrow \{CHD^+ + D, CD_2^+ + H, CD^+ + HD\}$ have been investigated with respect to energy and angular distribution of the product ions at various collision energies [0.39 to 14 eV, in the center of mass (C. M.) system]. An intermediate complex $CH_3^+$ (or $CHD_2^+$) is formed at low energies with a high cross-section, which decays into the reactants and products in a ratio of about 1:2.3. The $CH_2^+$ ion is often formed in a rotationally excited state. Only at the lowest collision energy used was a small part of the reaction enthalpy transformed into translational energy of the products. With increasing energy, a transition to an impulsive mechanism (stripping) takes place. This transition also explains the marked changes observed in the relative abundances of the product ions $CHD^+$, $CD_2^+$ and $CD^+$ from the $CH^+ + D_2$ reaction. (auth)

**26781** PROPERTIES OF ENERGY SPECTRA OF ELECTRONS RELEASED DURING SLOW COLLISIONS OF ATOMIC SYSTEMS. Dalidchik, F.I.; Ivanov, G.K. Opt. Spectrosc. (USSR) 38: No. 4, 359-361 (Apr 1975).

In the framework of the nonstationary model of degenerate perturbation, the properties of the interaction of electrons released during slow collisions of atomic systems with a quasimolecule at the moment of detachment were investigated. The influence of this interaction on the energy spectra of released electrons is studied. The spectrum of one-channel ionization is determined by the electron penetrability factor whose energy dependence has a resonance character when fine levels or quasistationary electron states are present in the field of an unexcited quasimolecule. It is shown that the possibility of excitation of autoionization states of a quasimolecule along with the resonance peaks leads to the appearance of characteristic jumps and kinks in the energy spectra. Their existence is confirmed by available experimental data. (auth)

## Atomic Theory

*Refer also to abstracts 26732 and 26744.*

**26782** (DESY-L-UEB-201) ANALYSIS OF THE EFFECTIVE POTENTIAL BARRIER. The Case of an Isoelectronic Line. Kariosiene, A.; Kisieliovas, A.; Karazija, R. (AN Litovskoj SSR, Vilnyus. Inst. Fiziki i Matematiki). Apr 1975. 12p. (In German). INIS.

4 figs.; 3 refs.; 14 refs. Translated from Liet. Fiz. Rinkinys (1973) v. 13(3). Available from ZAED.

The formation of atomic potential barriers with the aid of wave function measurements by the Hartree-Fock method is discussed. The influence of a nonlocal potential on the statistical approximation is shown, along with the influence of the integral functions $Y(nl, n'l'/r)$ and the effective charge on the effective potential. (auth)

**26783** ONE-DIMENSIONAL MODELS FOR TWO-ELECTRON SYSTEMS. Lapidus, I.R. (Department of Physics, Stevens Institute of Technology, Hoboken, New Jersey 07030). Am. J. Phys. 43: No. 9, 790-792 (Sept 1975).

One-dimensional models for two-electron systems resembling the helium atom and hydrogen molecule are studied using $\delta$-function potentials between all particles. It is noted that the essential features of the helium atom and hydrogen molecule ground states are exhibited by these models. The calculations are simple and useful pedagogical tools for illustrating the techniques used in more complicated and realistic calculations of energy eigenvalues and eigenfunctions. (auth)

**26784** QUANTUM THEORY OF A ONE-DIMENSIONAL OPTICAL CAVITY WITH OUTPUT COUPLING. FIELD QUANTIZATION. Ujihara, K. (The University of Electro-Communications, Chofugaoka, Chofu-shi, Tokyo, Japan). Phys. Rev. A 12: No. 1, 148-158 (July 1975).

The quantum theory of a one-dimensional optical cavity is developed with emphasis on the presence of output coupling. First the resonant mode is defined and calculated classically. Then the field is decomposed into a sequence of modes by introducing an imaginary boundary at a large distance. The mode functions are proved to be orthogonal with respect to an integration with the dielectric constant as a weighting factor. The Hamiltonian of the field is shown to be equivalent to that of a collection of independent harmonic oscillators, the mass of which is a function of the frequency of oscillation. This equivalent of mass appears on normalizing the mode functions and proves to carry information on the structure of the cavity. Quantization of the field is carried out, and the commutation relation for the electric fields inside and outside the cavity is derived. The commutator is composed of an infinite set of derivatives of $\delta$ functions, which discloses the effect of the presence of output coupling and that of the small size of the cavity on the radiation field. Also, the commutator is shown to have some properties common with the classical resonant mode, i.e., the property of exponential decay and its rate. (auth)

**26785** TEST OF THE NEOCLASSICAL THEORY OF RADIATION IN A WEAKLY EXCITED ATOMIC SYSTEM. Brink, G.O. (State University of New York at Buffalo, Buffalo, New York 14214). Phys. Rev. A 12: No. 1, 99-101 (July 1975).

The neoclassical theory of radiation predicts that the decay rate of an excited atomic state depends on the population density of the lower state. Experimental evidence is presented here which shows that in the case of $^{39}K$ the decay rate is in agreement with the predictions of quantum electrodynamics and definitely in disagreement with the neoclassical theory. (auth)

**26786** VARIATIONAL PRINCIPLES WHICH ARE FUNCTIONALS OF ELECTRON DENSITY. Nakatsuji, H.; Parr, R.G. (Department of Chemistry, University of North Carolina, Chapel Hill, North Carolina 27514). J. Chem. Phys. 63: No. 3, 1112-1117 (1 Aug 1975).

The Ritz variational principle, ordinarily written as a functional of the ground-state wavefunction, is rewritten in such a way that only one-electron functions are included as variables. Three different such variational formulas are derived explicitly based on the formula given by Hohenberg and Kohn. They constitute variational expressions of the integrated Hellmann–Feynman theorem, integral Hellmann–Feynman theorem, and virial theorem. These variational formulas are exact within the Born–Oppenheimer approximation, and when applied, they give the same results as does the conventional Ritz variational principle. However, they still have the defect that they require knowledge of the correct density function associated with a suitably chosen reference potential. Some applications are given for one-electron systems. A new formula for the kinetic energy plus electron–electron repulsion energy is obtained from the integrated Hellmann–Feynman theorem. (auth)

**26787** APPROXIMATION OF TFD MOLECULAR DENSITIES BY THE SUM OF SEPARATED ATOM TFD DENSITIES. Junker, B.R.; Menendez, M.G. (Department of Physics and Astronomy, University of Georgia, Athens, Georgia 30602). J. Chem. Phys. 63: No. 3, 1243-1249 (1 Aug 1975).

It is shown analytically that the "bounds" on the approximate TFD potential obtained when the molecular TFD density is approximated by the sum of the separated atom densities must cross. This is in agreement with the result of Gunther that the lower "bound" is not a true bound. (auth)

**26788** BROKEN ORBITAL SYMMETRY IN EXCITED AND IONIZED STATES OF MOLECULES. Jonkman, H. T. Groningen, Netherlands; Rijksuniversiteit(4 Jul 1975). 88p.

Thesis.

Hartree-Fock calculations in which one requires the molecular orbitals to transform according to the irreducible representations of the molecular point-group can yield poor results for those states which involve the removal of an electron from a molecular orbit whose amplitude is mainly localized on a set of atoms which are equivalent by symmetry and which are relatively far apart. By relaxing the symmetry constraints, the remaining electron hole can become localized on one of the equivalent sites which may be a better description of the physical situation. The conditions under which these improvements are relevant are discussed. After a survey of the formalisms involved, the competition between a delocalized (restricted) and localized (unrestricted) description is discussed for a simple one-particle, two-site system and $He_2^+$. For the last molecule ion, first the molecular orbital and the Heitler-London results are derived using Slater-type orbitals and then the restricted and unrestricted Hartree-Fock calculations are carried out using a Gaussian type basis set. A full configuration interaction calculation on the symmetry restricted Hartree-Fock results for $He_2^+$ shows that an important part of the correlation energy can be formally identified with the localization energy gain obtained by relaxing the inversion symmetry constraint in a Hartree-Fock calculation. (NL)

# PHYSICS (ELECTROFLUID AND MAGNETOFLUID)

**26789** (N-71-37295) EXISTENCE CONDITIONS FOR COLLISIONLESS HYDROMAGNETIC SHOCK WAVES ALONG THE MAGNETIC FIELD. Kato, Y.; Tajiri, M.; Taniuti, T. (Nagoya Univ. (Japan). Inst. of Plasma Physics). Mar 1971. 61p. (IPPJ-106). NTIS $3.00.

**26790** (N-71-38453) INVESTIGATION OF PULSED QUASI-STEADY MPD ARC JETS. Technical Report, 26 June 1970--26 June 1971. Ducati, A. C.; Jahn, R. G. (Plasmadyne Corp., Santa Ana, Calif. (USA)). Jun 1971. Contract NAS1-10140. 112p. (NASA-CR-111970; FR-061-10140). NTIS $3.00.

**26791** (N-72-31710) LAMINAR WAVE TRAIN STRUCTURE OF COLLISIONLESS MAGNETIC SLOW SHOCKS. Coroniti, F. V. (California Univ., Los Angeles (USA). Plasma Physics Group). Sep 1970. 59p. (NASA-CR-122475). NTIS $5.00.

The laminar wave train structure of collisionless magnetic slow shocks is investigated using two fluid hydromagnetics with ion cyclotron radius dispersion. For shock strengths less than the maximally strong switch-off shock, in the shock leading edge dispersive steepening forms a magnetic field gradient, while in the downstream flow dispersive propagation forms a trailing wave train; dispersion scale lengths are the ion inertial length if beta is smaller than 1 and the ion cyclotron radius if beta is greater than 1. In the switch-off slow shock leading edge, dispersion only produced rotations of the magnetic field direction; the gradient of the magnetic field magnitude, and hence the shock steepening length, is determined solely by resistive diffusion. The switch-off shock structure consists of a long trailing of magnetic rotations which are gradually damped by resistivity. (auth)

**26792** (N-73-24701) ION STREAMING INSTABILITIES WITH APPLICATION TO COLLISIONLESS SHOCK WAVE STRUCTURE. Golden, K. I.; Linson, L. M.; Mani, S. A. (Avco-Everett Research Lab., Everett, Mass. (USA)). Mar 1973. 27p. (NASA-CR-132953). NTIS $3.50.

The electromagnetic dispersion relation for two counterstreaming ion beams of arbitrary relative strength flowing parallel to a dc magnetic field is derived. The beams flow through a stationary electron background and the dispersion relation in the fluid approximation is unaffected by the electron thermal pressure. The dispersion relation is solved with a zero net current condition applied and the regions of instability in the k-U space (U is the relative velocity between the two ion beams) are presented. The parameters are then chosen to be applicable for parallel shocks. It was found that unstable waves with zero group velocity in the shock frame can exist near the leading edge of the shock for upstream Alfven Mach numbers greater than 5.5. It is suggested that this mechanism could generate sufficient turbulence within the shock layer to scatter the incoming ions and create the required dissipation for intermediate strength shocks. (auth)

**26793** (N-73-28180) RESEARCH IN ELECTROHYDRODYNAMICS. Final Report. (Massachusetts Inst. of Tech., Cambridge (USA)). 1 Jun 1973. Contract NGL-22-009-014. 17p. (NASA-CR-133456). NTIS $3.00.

An overview is presented in the form of publications for NASA research in electrohydrodynamics. Data cover basic electrohydrodynamics, management of liquids in zero gravity, continuum feedback control, and magnetohydrodynamics and ferrohydrodynamics. (GRA)

**26794** LONGITUDINAL NUCLEAR MAGNETIC RESONANCE IN SUPERFLUID $^3$He AS INTERNAL JOSEPHSON EFFECT. Maki, K. (Tohoku Univ., Sendai (Japan). Dept. of Physics); Tsuneto, T. Prog. Theor. Phys. (Kyoto); 52: No. 3, 773-776(Sep 1974).

We discuss the longitudinal nuclear magnetic resonance in the A phase of the superfluid $^3$He as the internal Josephson effect between the up and down spin pairs. An interesting transient behavior after a sudden application of a magnetic field is predicted. (auth)

**26795** PHONON MEDIATED ROTON–ROTON INTERACTION IN SUPERFLUID He$^4$. Ishikawa, K.; Yamada, K. (Nagoya Univ. (Japan). Dept. of Physics). Prog. Theor. Phys. (Kyoto); 52: No. 3, 777-785(Sep 1974).

Roton-roton interaction mediated by phonons in superfluid helium is derived with use of the canonical transformation to eliminate the phonon-roton interaction introduced phenomenologically by Landau and Khalatnikov. The d-partial wave of this roton-roton interaction is examined which is relevant to the possibility of roton bound pairs, observed in the experiment of Raman scattering. It is found that the coupling of d-waves may be attractive and be on the order of $10^{-19}$ erg · cm$^{-3}$, for the roton minimum momentum. These results accord semi-quantitatively with the observed ones. (auth)

**26796** CORRELATIONS IN BOSE FLUIDS, 1. An Elementary Excitation and Its Effective Hamiltonian; Sunakawa's Collective Description. Tsuzuki, T. (Kyushu Univ., Fukuoka (Japan). Dept. of Physics). Prog. Theor. Phys. (Kyoto); 52: No. 3, 793-810(Sep 1974).

An elementary excitation which is evolved from the unperturbed Bogoljubov excitation adiabatically is constructed for Sunakawa's Hamiltonian of the collective description. By introducing the Feynman excitation into the theory we get a method to calculate the excitation energy perturbationally. It is shown that Sunakawa's excitation energy is nothing but the present one in the lowest order. The excitation energy at finite temperatures is shown to be almost independent of temperature, failing to explain the experimental temperature variation of the phonon-roton spectrum in liquid helium II. The effective interaction among the present excitations is made up in the lowest approximation in order to attack the possibility of forming a new type of correlation below the transition temperature, which is able to explain the experiment. Very rough discussion is presented on the above possibility. (auth)

**26797** QUANTUM EFFECT, CRITICAL DYNAMICS AND ONE-PARTICLE EXCITATION IN 1/n EXPANSION, 1. Abe, R. (Tokyo Univ. (Japan). Faculty of Science). Prog. Theor. Phys. (Kyoto); 52: No. 4, 1135-1145(Oct 1974).

The classical 1/n expansion for critical phenomena is extended to a quantum system by introducing the Bose field with m(= n/2) independent components. The case just at the critical point is considered. It is shown that there is no quantum effect on $\eta$ up to 0(1/m). The energy spectrum $E_q$ of one-particle excitation is expressed as $E_q \propto q^{2-\zeta}$ and $\zeta$ is calculated exactly up to 0(1/m). The result turns out to be in accordance with the one obtained recently by Kondor and Szépfalusy. (auth)

**26798** PAIR THEORY FOR INDIVIDUAL PARTICLES IN LIQUID HELIUM II. Nishiyama, T.; Watanabe, Y. (Osaka Univ., Toyonaka (Japan). Coll. of General Education). Prog. Theor. Phys. (Kyoto); 52: No. 4, 1161-1173(Oct 1974).

For liquid helium at the absolute zero temperature, a systematic calculation is performed so as to elucidate the inherences associated with the excitations in the roton region by solving the Girardeau-Arnowitt integral equation by the aid of a kind of Monte Carlo method in the scheme of the collective description. The whole frame work of the previous theory is kept unchanged, even if the Bogoliubov approximation is replaced by the present pair approximation. For a suitable effective potential, the pair theory yields the negative chemical potential and the peak of the form factor in accord with the experimental result. (auth)

**26799** SUPERFLUID FILM ON THE SURFACE OF A SOLID IMMERSED IN A NONSUPERFLUID SOLUTION OF He$^4$ IN He$^3$. Peshkov, V.P. (Institute of Physics Problems, USSR Academy of Sciences). JETP Lett. 21: No. 6, 162-164 (20 Mar 1975).

It is established that a film of the superfluid lower phase is produced on the wall in the upper phase of laminating He$^3$–He$^4$. (auth)

**26800** MOTION OF IONS TRAPPED ON VORTICES IN He II. Ostermeier, R.M.; Glaberson, W.I. (Department of Physics, Rutgers University, New Brunswick, New Jersey 08903). Phys. Rev. Lett. 35: No. 4, 241-244 (28 July 1975).

We have measured the drift velocity of ions trapped on vortex lines at temperatures down to 0.35 K. We observe several effects which cannot easily be explained in terms of existing theories, including the broadening of an ion pulse, a limiting velocity in high electric fields, and a zero-field mobility which increases, at lower temperatures, much more rapidly than expected. An attempt is made to explain qualitatively some of these effects. (auth)

**26801** EFFECT OF $^3$He IMPURITIES ON THE LIFETIME OF IONS TRAPPED ON QUANTIZED VORTEX LINES. Williams, G.A.; Packard, R.E. (University of California, Berkeley, California 94720). Phys. Rev. Lett. 35: No. 4, 237-240 (28 July 1975).

The lifetimes of both positive and negative ions trapped on quantized vortex lines in rotating $^3$He-$^4$He mixtures have been measured at temperatures down to 0.1 K. Evidence is found that the $^3$He condenses at the vortex core, and possibly at the surface of the electron bubble. (auth)

**26802** RENORMALIZED DENSITY-FUNCTIONAL THEORY OF NONUNIFORM SUPERFLUID $^4$He AT ZERO TEMPERATURE. Ebner, C. (Department of Physics, The Ohio State University,

Columbus, Ohio 43210 and Battelle Memorial Institute, Columbus, Ohio 43201); Saam, W.F. Phys. Rev. B 12: No. 3, 923-939 (1 Aug 1975).

A density-functional theory is constructed for nonuniform systems of superfluid $^4$He at zero temperature. In calculations of the free-surface shape and tension it is found necessary to self-consistently renormalize the theory in order to account for the important effects of the zero-point motion of the long-wavelength (wave number $q \ll q_m$) surface modes. Use of a cutoff $q_m = 0.99$ Å$^{-1}$, self-consistently determined within the theory, yields a surface tension of 0.384 erg/cm$^2$, which compares well with the experimental results of 0.378 erg/cm$^2$. Detailed liquid-structure effects are included, but no static density oscillations near the free surface result, in contrast to a theory of Regge. When the theory is applied to the case of $^4$He bounded by a single hard wall, density oscillations near the wall are obtained. For a much simplified version of the density functional, an analytic solution for a planar free surface, vortex-line structure, and various properties of $^4$He droplets, including the curvature dependences of the surface tension and Gibbs surface mass, are obtained. (auth)

**26803** PROPAGATION OF SURFACE SOUND IN SUPERFLUID $^3$He-$^4$He. Edwards, D.O.; Shen, S.Y.; Eckardt, J.R.; Fatouros, P.P.; Gasparini, F.M. (Department of Physics, The Ohio State University, Columbus, Ohio 43210). Phys. Rev. B 12: No. 3, 892-904 (1 Aug 1975).

"Surface sound," a longitudinal compressional wave in $^3$He adsorbed on the surface of superfluid $^4$He, has been propagated in the temperature range from 20 to 120 mK. Measurements of the surface-sound velocity and of the surface tension are compared to a model of interacting surface $^3$He quasiparticles. A least-squares fit to the model is used to obtain the $^3$He binding energy, $\epsilon_b/k_B = 2.28 \pm 0.03$ K, the $^3$He effective mass, $M/m_3 = 1.3 \pm 0.1$, and some limits on the sign and magnitude of the effective interaction between the quasiparticles. The interaction is found to be very weak and predominantly repulsive at large distances. (auth)

**26804** SPECIFIC HEAT OF $^4$He AND $^3$He-$^4$He MIXTURES AT THEIR λ TRANSITION. Gasparini, F.M. (Department of Physics and Astronomy, State University of New York at Buffalo, Buffalo, New York 14214); Moldover, M.R. Phys. Rev. B 12: No. 1, 93-113 (1 July 1975).

We have measured the specific heat near the λ transition of pure $^4$He and of five $^3$He-$^4$He mixtures up to a mole fraction of 0.39 $^3$He in $^4$He. Our data for $^4$He confirm the results of Ahlers revealing an asymmetry in the exponents above and below $T_\lambda$ when the specific heat is represented by a simple-power-law temperature dependence. Our results for these exponents ($\alpha = 0.012 \pm 0.002$ and $\alpha' = -0.012 \pm 0.004$) differ somewhat from Ahlers's. Our results can be reconciled with the requirement of scaling ($\alpha = \alpha'$) only by supposing substantial contributions to $C_p$ are made by singular correction terms to a simple power law. The measured specific heat of the mixtures richest in $^3$He appears to be finite, continuous, and cusped at the λ line. These qualitative features have been termed "renormalization" by Fisher. An analysis of our mixture data with a power-law temperature dependence does not yield a fully renormalized exponent, but rather an effective exponent. We have calculated the following derivatives at the λ line: $(\partial x/\partial T)_{\phi,\lambda}$, $(\partial\phi/\partial T)_{\phi,\lambda}$, and $(\partial x/\partial T)_{\mu,\lambda}$. We have used these derivatives to calculate the specific heat along paths of constant pressure and constant relative chemical potential $C_{p\phi}$. This specific heat behaves very much like $C_p$ of pure $^4$He supporting the idea of universality for the specific-heat exponents. It is also true that the same asymmetry in the branches above and below $T_\lambda$ which is observed in pure $^4$He is retained in the mixtures. The persistence of the asymmetry of $C_{p\phi}$ as one moves along the λ line towards increasing $^3$He concentration (at the saturated vapor pressure of the mixtures) is analogous to the persistence of the asymmetry of $C_p$ as one moves along the λ line towards increasing pressure in pure $^4$He. In both cases a unique reconciliation of the asymmetry with scaling must await better predictions of the form of the corrections to scaling. We have used our calculated $C_{p\phi}$ to construct the derivative $(\partial x/\partial T)_{p,\phi}$ hence paths of constant $\phi$ on the $x$-$T$ plane, as well as the derivative $(\partial x/\partial\phi)_{p,T}$. (auth)

**26805** PHENOMENOLOGICAL TWO-BRANCH MODEL FOR THE LONG-WAVELENGTH EXCITATION SPECTRUM OF SUPERFLUID $^4$He. Hastings, R.; Halley, J.W. (School of Physics and Astronomy, University of Minnesota, Minneapolis, Minnesota 55455). Phys. Rev. B 12: No. 1, 267-275 (1 July 1975).

It is suggested that the long-wavelength spectrum of superfluid $^4$He may consist of a branch of quasiparticle excitations which has a gap at zero momenta in addition to a branch of hydrodynamic phonons. A phenomenological two-branch spectrum is constructed. The model is suggested by the structure of a theory of boson pairing similar to the BCS theory of fermions. The low-temperature specific heat of $^4$He is calculated within the model and compared with experimental data. It is found that a two-branch-model excitation spectrum can describe the low-temperature anomaly in the specific heat without contradicting existing direct measurement of the excitation spectrum. Some features of a possible microscopic theory of the two-branch spectrum are discussed, and the possibilities of making direct measurements testing the idea of a two-branch excitation spectrum are considered. (auth)

**26806** EFFECTIVE-INTERACTION APPROACH TO LIQUID HELIUM. Iachello, F. (Kernfysisch Versneller Instituut, University of Groningen, Groningen, The Netherlands); Rasetti, M. Phys. Rev. B 12: No. 1, 134-146 (1 July 1975).

It is shown that a semiquantitative understanding of the properties liquid helium is possible in terms of a simple parametrization of the effective helium-helium interaction and of its temperature and density dependence. Some properties of the effective interaction are discussed within the framework of the temperature-dependent Green's-function formalism and the difficulties connected with the extension of the approach to more elaborate situations are briefly indicated. (auth)

**26807** EVIDENCE AGAINST $f$-WAVE PAIRING IN SUPERFLUID $^3$He. Mermin, N.D. (Laboratory of Atomic and Solid State Physics, Cornell University, Ithaca, New York 14850). Phys. Rev. Lett. 34: No. 26, 1651-1652 (30 June 1975).

It is shown that unless strong-coupling corrections to the BCS free energy are very large, the observation by Osheroff and Anderson of a Leggett NMR shift in the $A_1$ phase of superfluid $^3$He is incompatible with the hypothesis of $f$-wave pairing. (auth)

**26808** ELECTROHYDRODYNAMICS OF A CHARGE-SEPARATED PLASMA. Heintzmann, H. (Institut für theoretische Physik der Universität zu Köln, D5 Köln 41, West Germany); Kundt, W.; Lasota, J.P. Phys. Rev. A 12: No. 1, 204-210 (July 1975).

We derive and discuss the dispersion relation and polarization of waves in a one-component, cold, homogeneous plasma moving at arbitrary speed. The relevance to wave propagation (both low frequency and radio) through the pulsar magnetosphere is briefly discussed. (auth)

**26809** LOW TEMPERATURE PHASES OF HELIUM. Leggett, A. J. (Sussex Univ., Brighton, Eng.). Phys. Bull. (London); 26: 311-312 (Jul 1975).

Low temperature physics provides the testing ground for the effects of quantum mechanics on a large scale. The two stable isotopes of liquid helium, $^4$He and $^3$He, provide a readymade laboratory for the investigation of the indistinguishable effects in quantum mechanics on a macroscopic scale. The phenomena associated with lambda transition in $^4$He are considered. In 1972 experiments below $3 \times 10^{-3}$K revealed the existence of two new and quite anomalous phases in $^3$He, $^3$He A and $^3$He B which have been the subject of intensive research over the last three years. It is generally believed that both new phases are qualitatively similar to the superconducting state of electrons in metals, in that pairs of particles in states at or near the Fermi surface form a type of bound state known as a Cooper pair. The properties of these pairs are considered. (UK)

**26810** APPROXIMATE METHOD FOR TREATING THE LAMINAR MAGNETOHYDRODYNAMIC BOUNDARY LAYER IN THE UNSTEADY REGIME. Askovic, R. (Univ., Belgrade). Bull. Cl. Sci., Acad. R. Belg.; 40: 1261-1273 (9 Nov 1974). (In French).

The unsteady laminar magnetohydrodynamic boundary layer on a body in nonuniform motion in the presence of some given magnetic field is discussed. An universalization of the unsteady magnetohydrodynamic boundary layer equations is first made in the sense that neither equations nor boundary conditions depend on particular problem conditions. The universality is achieved by transferring sets of parameters which express the influence of time and external conditions, as well as of the given magnetic induction, characteristic for each particular problem, into the independent variables. Subsequently, the solution of the obtained universal equation is found in the form of series expansions in mentioned parameters. (2 figures) (auth)

**26811** STABILITY OF THE HELIUM FILM TO A CHEMICAL POTENTIAL PERTURBATION. Blair, D. G.; Matheson, C. C. (East Anglia Univ., Norwich, Eng.). J. Low Temp. Phys.; 20: No. 5/6, 585-591 (Sep 1975).

A negative result for a highly sensitive measurement to detect changes in the helium film thickness profile induced by torsional oscillation of the film substrate is reported. The results are in agreement with Keller's failure to detect film thinning, but are in disagreement with recent results of Williams and Packard, Graham and Vittoratos, and Hallock. (2 figures) (auth)

**26812** CAPTURE OF IONS BY VORTEX LINES IN PURE $^4$He AND $^3$He-$^4$He SOLUTIONS. Ostermeier, R. M.; Glaberson, W. I. (Rutgers--the State Univ., New Brunswick, NJ). J. Low Temp. Phys.; 20: No. 1/2, 159-179 (Jul 1975).

Measurements of the capture cross section for the negative ion by vortex lines in pure $^4$He and a 0.94 percent solution of $^3$He in $^4$He are presented. A measurable capture of positive ions was not observed in either system. In pure $^4$He the departure of the experimental data from the predictions of stochastic theory at lower

temperatures is explained in terms of a simple breakdown in that theory, and lifetime effects are shown to be of only secondary importance. The decrease in cross section with decreasing temperature, due essentially to a reduced number density of rotons, is predicted by the results of a Monte Carlo calculation. The cross section in the solution follows stochastic theory to significantly lower temperatures, but at about 1 K there again occurs a marked discrepancy. Measurements of the ion trapping lifetime at low temperatures indicate that it is the finite lifetime that accounts for this discrepancy. Elimination of lifetime effects results in fair agreement between the cross section data in the solution and the predictions of stochastic theory. (11 figures) (auth)

# PHYSICS (HIGH-ENERGY)

## Particle Interactions and Properties (Experimental)

*Refer also to abstract 26976.*

**26813** (NP-20565) WORK OF THE RUTHERFORD LABORATORY IN 1974. Smith, J. R.; Telling, F. M. (eds.). (Science Research Council, Chilton (UK). Rutherford Lab.). May 1975. 207p. Dep. NTIS (US Sales Only) $13.50.

Work carried out at the Rutherford Laboratory (UK) of the Science Research Council in 1974 is described under the following headings: high energy physics, accelerator operations and development, instrumentation and data handling, applied research, neutron beam research, computing services, and technical services and administration. A list of publications is included. (UK)

**26814** HIGH ENERGY PHYSICS INDEX, VOLUME 13, NO. 17, AUGUST 21, 1975. Leopoldshafen, Ger.; Zentralstelle fuer Atomkernenergie-Dokumentation (1975). 104p.

**26815** HIGH ENERGY PHYSICS INDEX, VOLUME 12, NO. 26, DECEMBER 27, 1974. Leopoldshafen, Ger.; Zentralstelle fuer Atomkernenergie-Dokumentation (1974). 86p.

**26816** HIGH ENERGY PHYSICS INDEX, VOLUME 13, NO. 16, AUGUST 7, 1975. Leopoldshafen, Ger.; Zentralstelle fuer Atomkernenergie-Dokumentation (1975). 119p.

**26817** HIGH ENERGY PHYSICS INDEX, VOLUME 13, NO. 15, JULY 24, 1975. Leopoldshafen, Ger.; Zentralstelle fuer Atomkernenergie- Dokumentation (1975). 127p.

### *Electromagnetic*

*Refer also to abstract 27176.*

**26818** (DESY-75/17) SOME RECENT RESULTS ON PHOTOPRODUCTION AND ELECTROPRODUCTION OF HADRONS. Weber, G. (Deutsches Elektronen-Synchrotron (DESY), Hamburg (F. R. Germany)). Jul 1975. 34p. (CONF-750654-11). Dep. NTIS (US Sales Only) $4.75.

From international conference on high energy physics; Palermo, Italy(Jun 1975).

The review is restricted to contributions submitted to the conference and to some important developments of the past two years. The coverage includes photo- and electroproduction of $\pi^-$ and $\eta$ mesons, vector meson production and Compton scattering with real photons, and hadronic final states in electro- and muoproduction. (JFP)

**26819** EVIDENCE AT THE $10^{-38}$ PROBABILITY LEVEL AGAINST THE PRODUCTION OF MAGNETIC MONOPOLES IN PROTON INTERACTIONS AT 300 GeV/c. Eberhard, P.H.; Ross, R.R.; Taylor, J.D.; Alvarez, L.W. (Lawrence Berkeley Laboratory, University of California, Berkeley, California 94720); Oberlack, H. Phys. Rev. D 11: No. 11, 3099-3104 (1 June 1975).

An electromagnetic search for magnetic monopoles that requires very few assumptions about their properties has been performed in material exposed to protons accelerated at Fermilab, to electrons at SLAC, and to $pp$ interactions at the CERN ISR. The most significant irradiation (Fermilab, 300 GeV/c) produced $2.5\times10^{13}$ primary proton-aluminum interactions. No monopoles were found. If monopoles exist with masses less than 12 GeV, the probability of pair production in a proton-nucleon collision is of the order of $10^{-38}$ or less with 95% confidence. (auth)

**26820** ANALYSIS OF THE REACTIONS $\gamma p \rightarrow p\pi^+\pi^-\pi^0$ AND $\gamma p \rightarrow n\pi^+\pi^+\pi^-$ IN A STREAMER CHAMBER WITH AN ENERGY MARKED PHOTON BEAM IN THE RANGE OF 3-4 GeV. Pollmann, D. Heidelberg; Heidelberg Univ. (1973). 48p. (In German). INIS.

Thesis.

In the experiment described the photoproduction of protons in an energy region of 1.3 GeV is investigated with energy-marked photons in a streamer chamber. The whole experiment is subdivided into four energy regions whose photos were taken at different times. Reactions with three charged and one neutral leaving particle are examined in the energy region of 3 to 4 GeV energy in laboratory system. As in this experiment the energy marking and the trigger electronics of the chamber together with the photometrical plotting exhibits a connection of hitherto methodically separate experimental technique. This point was especially dealt with. (auth)

### *Weak*

**26821** (UCI-10-P19-95) PROGRESS REPORT FOR A RESEARCH PROGRAM IN NEUTRINO PHYSICS, COSMIC RAYS, AND ELEMENTARY PARTICLES, 1 OCTOBER 1974--30 SEPTEMBER 1975. Reines, F. (California Univ., Irvine (USA)). Aug 1975. Contract AT(11-1)-Gen-10. 7p. Dep. NTIS $4.00.

The elastic scattering reaction anti nu/sub e/ + $e^-$ yields anti nu/sub e/ + $e^-$ under continuing study at the Savannah River Reactor has now yielded a 3.1 standard deviation signal, a result obtained in approximately $\frac{1}{9}$ the time previously required to obtain a 2.3 standard deviation effect. Operation for several more months can be expected to yield a definitive answer to the question of the existence of this fundamental interaction, providing it is at the V-A level. An improved limit of sigma/sub expt//sigma/sub theory/ less than 4 at 3 standard deviations was obtained for the neutral current reaction anti nu/sub e/ + d yields n + p + anti nu/sub e/. Further analysis and consideration of detector designs reaffirms the feasibility of a measurement to test the theoretical predictions of Weinberg-Salam. The double beta decay detector was turned on using $^{82}$Se as emitter. It appears to be operating very satisfactorily indeed and initial test runs have yielded a half-life for the 2 neutrino mode of tau/sub 1/2/ greater than $10^{19}$ yrs. In 20 hours of operation no events were seen. Providing the background meets our expectations the system should yield a signal of 1/20 days for a tau/sub 1/2/ equals $3 \times 10^{20}$ yrs, the geochemical value. Early data from the advanced electromagnetic potential search has established an upper limit for the admixture of advanced to retarded components of $10^{-6}$. Considerable improvement is contemplated in these results. (auth)

### *Strong (Baryon-induced)*

*Refer also to abstract 26986, 26987, and 27043.*

**26822** (CONF-750654-16) PROTON DIFFRACTION DISSOCIATION IN THE REACTION p + p yields LAMBDA$^0$ + $K^+$ + p AT THE CERN ISR. Webb, R.; Trilling, G.; Telegdi, V. (California Univ., Los Angeles (USA). Dept. of Physics; California Univ., Riverside (USA). Dept. of Physics; Technische Hochschule Aachen (F. R. Germany). 3. Physikalisches Inst.; European Organization for Nuclear Research, Geneva (Switzerland)). 1975. 13p. Dep. NTIS $4.00.

From eighth biennial conference on elementary particles; Palermo, Italy (Jun 1975).

The exclusive reaction pp yields LAMBDA$^0K^+$p has been studied at 0.1 less than - t/sub pp/ less than 0.6 GeV$^2$ and energies root s equals 45 GeV and 53 GeV at the CERN ISR. Diffractive excitation p yields LAMBDA$^0K^+$ occurs predominantly in the mass range M(LAMBDA$^0K^+$) less than 2.0 GeV. The cross section for pp yields LAMBDA$^0K^+$p is 10 +- 3mu b for M(LAMBDA$^0K^+$) less than 3.0 GeV, and the t dependence is exp(bt) with b equals 8.0 + - 1.0 GeV$^2$. (5 figures) (auth)

**26823** (LA-UR-75-1624) TESTS OF PARITY CONSERVATION IN p-p AND p-NUCLEUS SCATTERING. Potter, J. M. (Los Alamos Scientific Lab., N. Mex. (USA)). 1975. Contract W-7405-ENG-36. 7p. (CONF-750829-1). Dep. NTIS $4.00.

From fourth international symposium on polarization phenomena in nuclear reactions; Zurich, Switzerland (25 Aug 1975).

Two experiments are described which look for parity violation in proton-proton scattering at 15 MeV and p-nucleus scattering at 6 GeV. Details of the experimental set-ups and error contributions are discussed. (3 figures) (SDF)

**26824** (LBL-3882) MEASUREMENT OF THE ANTI pp YIELDS ANTI nn AND NEUTRAL ANNIHILATION CROSS SECTIONS FROM 300 TO 1000 MeV/c. Tripp, R.; Alston-Garnjost, M.; Kenney, R.; Pollard, D.; Ross, R.; Nicholson, H. (California Univ., Berkeley (USA). Lawrence Berkeley Lab.). May 1975. Contract W-7405-eng-48. 11p. (CONF-750547-11). Dep. NTIS $4.00.

From 4th international symposium on nucleon-antinucleon interactions; Syracuse, New York, USA (2 May 1975).

The results of a counter experiment in which the partial cross sections for anti pp charge exchange and neutral annihilation were measured at 20 momenta from 300 to 1000 MeV/c with a typical point-to-point precision of about 1 percent. (JFP)

**26825** INVARIANT CROSS SECTION FOR THE INCLUSIVE REACTION $p + p \rightarrow p + X$ AT 205 GeV/c. Whitmore, J. (Fermi National Accelerator Laboratory, Batavia, Illinois 60510); Barish, S.J.; Colley, D.C.; Schultz, P.F. Phys. Rev. D 11: No. 11, 3124-3133 (1 June 1975).

Inclusive proton production in $pp$ interactions at 205 GeV/$c$ is studied using the Fermi National Accelerator Laboratory (Fermilab) 30-in. bubble chamber. The invariant cross section is presented in terms of several kinematic variables and compared with similar data obtained from counter experiments at Fermilab and at the CERN Intersecting Storage Rings (ISR). An important feature of this experiment is that it provides data for much wider ranges of the four-momentum transfer than have been attained in the counter experiments. It also gives full information on the associated charged-particle multiplicity of every event, thus permitting a detailed investigation of how various kinematic quantities depend on this parameter. (auth)

**26826** PRODUCTION OF HADRONS AT LARGE TRANSVERSE MOMENTUM AT 200, 300, AND 400 GeV. Cronin, J.W.; Frisch, H.J.; Shochet, M.J. (The Enrico Fermi Institute, University of Chicago, Chicago, Illinois 60637); Boymond, J.P.; Piroué, P.A.; Sumner, R.L. Phys. Rev. D 11: No. 11, 3105-3123 (1 June 1975).

We have measured, as a function of transverse momentum ($p_\perp$), the invariant cross section $E\,d\sigma/d^3p$ for the production of $\pi^+$, $K^+$, $p$ $\bar{p}$, $d$, and $\bar{d}$ in proton collisions with a tungsten (W) target at incident proton energies of 200, 300, and 400 GeV. The measurements were made in the region of 90° in the c.m. system of the incident proton and a single nucleon at rest. Measurements were also made with 300-GeV protons incident on Be, Ti, and W targets of equal interaction length. These $p$-nucleus measurements, which show a strong dependence on atomic number at high $p_\perp$, were used to extract effective proton-nucleon cross sections by extrapolation to atomic number unity. At large values of the scaling variable $x_\perp = 2p_\perp/\sqrt{s}$, where $s$ is the square of the c.m. energy, the pion data are found to be well represented by the expression $(\sqrt{s})^{-n}e^{-ax_\perp}$, with $n = 11.0 \pm 0.4$ and $a = 36.0 \pm 0.4$. At $x_\perp < 0.35$, where similar measurements have been made at the CERN, our data are in good agreement with the ISR data. (auth) agreement with the ISR data. (auth)

**26827** PRODUCTION OF HIGH-ENERGY DEUTERONS IN THE $^3He + {}^3He$ REACTION AND THE SOLAR NEUTRINO PROBLEM. Slobodrian, R.J.; Pigeon, R.; Irshad, M. (Laboratoire de Physique Nucleáire, Département de Physique, Université Laval, Québec, G1K 7P4 Canada). Phys. Rev. Lett. 35: No. 1, 19-22 (7 July 1975).

A spectrum of deuterons consistent with the reaction $^3He + {}^3He \rightarrow {}^2H + {}^4He + e^+ + \nu$ has been detected with a system sensitive to cross sections of 300 pb sr$^{-1}$ MeV$^{-1}$. The measured cross section is too high for a weak-interaction process: 3.4 nb MeV$^{-1}$ sr$^{-1}$. It might be due to an interaction of intermediate strength and it could explain the low flux of high-energy solar neutrinos. (auth)

**26828** SEARCH FOR $\varphi$ MESONS PRODUCED AT HIGH $p_\perp$ IN $p$-Be COLLISIONS AT 300 GeV. Appel, J.A.; Bourquin, M.H.; Gaines, I.; Hom, D.C.; Lederman, L.M.; Paar, H.P.; Repellin, J.; Snyder, H.D.; Weiss, J.M.; Yoh, J.K. (Columbia University, New York, New York 10027); Brown, B.C.; Brown, C.N.; Gaillard, J.; Sauer, J.R.; Yamanouchi, T. Phys. Rev. Lett. 35: No. 1, 9-12 (7 July 1975).

We have searched for production of $\phi$ mesons at high transverse momenta. Upper limits with a 95% confidence level on the ratio $\phi/\pi^-$ ranging from 0.055 at $p_\perp$=2.48 GeV/$c$ to 0.103 at $p_\perp$=3.33 GeV/$c$ are given, ruling out the $\phi$ meson as a significant source of the high-$p_\perp$ leptons observed to be produced directly in hadron collisions. (auth)

**26829** NEUTRAL PARTICLE PRODUCTION IN $\pi^+p$ AND $pp$ COLLISIONS AT 100 GeV/c. Alston-Garnjost, M. (Lawrence Berkeley Laboratory, University of California, Berkeley, California 94720); Erwin, J.; Klems, J.H.; Ko, W.; Lander, R.L.; Pellett, D.E.; Yager, P.M. Phys. Rev. Lett. 35: No. 3, 142-145 (21 July 1975).

We have measured the inclusive cross sections for $\gamma$, $K_1{}^0$, $\Lambda$, and $\bar{\Lambda}$ production in $\pi^+p$ and $pp$ interactions at 100 GeV/$c$ and compared various inclusive distributions of the produced $\gamma$ and $K_1{}^0$. (auth)

**26830** REACTION ANTI PN YIELDS $pi^+pi^-pi^-$ FROM 1.09 TO 1.43 GeV/c. Mountz, J. M. East Lansing, MI; Michigan State Univ. (1974). 164p. University Microfilms Order No. 75-14,794.

Thesis (Ph. D.).

In a deuterium bubble chamber experiment 3, 4, 5, and 6 prong topological cross sections were obtained for an incident anti-proton momenta from 1.09 to 1.43 GeV/c. Also determined were cross sections for the reactions anti pn yields $pi^+pi^-pi^-$, anti pn yields $rho^0pi^-$ and anti pn yields $f^0pi^-$. The differential cross sections for anti pn yields $rho^0pi^-$ and anti pn yields $f^0pi^-$ were obtained. A test of the crossing symmetry principle was made by comparing the differential cross sections for the reaction anti pn yields $rho^0pi^-$ with those of its line reversed reaction $pi^-p$ yields $nrho^0$. Within experimental error the crossing symmetry principle was found to be valid for these reactions. In an analysis of the c.m. angular distributions for the $rho^0$ and $f^0$ mesons the spin state composition of the anti pn system was found to be predominately in a s equals 2 state. The Dalitz plot was used to compare the predictions of the Veneziano model with the data. The overall agreement is good, but the areas of discrepancies become more prominent when the model is compared to data from 1.6 to 2.0 GeV/c. (Diss. Abstr. Int., B)

**26831** ANTIPROTON--PROTON CHARGE EXCHANGE AND ANTINEUTRON--PROTON (CHARGED PRONG) ANNIHILATION IN THE LOW MOMENTUM RANGE. Scherer, V. R. Madison, WI; Univ. of Wisconsin (1974). 174p. University Microfilms Order No. 75-10,000.

Thesis (Ph. D.).

Results of the study of the anti pp yields anti nn charge-exchange reaction in the low anti p momentum range from 800 MeV/c down to about 250 MeV/c (laboratory kinetic energy region 35 to 290 MeV) are presented. The data arise from the analysis of some 220,000 pictures taken in a series of exposures of the 30-inch Brookhaven liquid hydrogen bubble chamber to a low momentum separated anti p beam at the AGS. The measurement is based on a final filtered sample of 2,016 events in which the annihilation star of the antineutron is observed. Angular distributions for the charge-exchange process are obtained, and results are given for the total and differential cross sections. The experimental results are analyzed and compared with some existing theoretical model predictions. The results of an independent measurement of total anti pp cross sections down to low anti p momentum are also given, as well as results for the total anti pp cross sections into neutrals and the neutral annihilation cross sections. Also examined are several aspects of the anti np annihilation reaction. Results of absorption-fitting technique measurements of total anti np cross sections (the first direct measurements of sigma/sub t/(anti np) in the low anti n momentum region) are presented, together with relative rates for anti np annihilation into charged prongs, and the data compared wherever possible to those of other anti np and anti pn (anti pd) experiments. (Diss. Abstr. Int., B)

**26832** MEASUREMENT OF $\psi$ (3.1) MESON PRODUCTION BY PIONS AND PROTONS. Blanar, G.J.; Boyer, C.F.; Faissler, W.L.; Garelick, D.A.; Gettner, M.W.; Glaubman, M.J.; Johnson, J.R.; Johnstad, H.; Mallary, M.L.; Pothier, E.L.; Potter, D.M.; Ronan, M.T.; Tautz, M.F.; von Goeler, E.; Weinstein, R. (Northeastern University at Boston, Boston, Massachusetts 02115). Phys. Rev. Lett. 35: No. 6, 346-349 (11 Aug 1975).

The production of $\psi$ (3.1) mesons is reported for the reactions $\pi^- + Fe \rightarrow \mu^+ + \mu^- +$ anything, at 200 GeV, and $p + Fe \rightarrow \mu^+ + \mu^- +$ anything, at 240 GeV. For $\psi$ production, distributions in $x \equiv P_\parallel/P_{\text{beam}}$ and $P_\perp$ are given. For $x \geq 0.5$, the ratio of the $\psi$ production cross sections in iron for pions to that for protons is found to be 7.4±2.0. (auth)

## *Strong (Meson-induced)*

*Refer also to abstract 26927, 26973, 26989, and 27066.*

**26833** (DESY-75/20) OBSERVATION OF THE TWO PHOTON CASCADE $3.7 \rightarrow 3.1 + \gamma\gamma$ VIA AN INTERMEDIATE STATE $P_c$. Braunschweig, W.; Martyn, H. U.; Sander, H. G.; Schmitz, D.; Sturm, W.; Wallraff, W. (Deutsches Elektronen-Synchrotron (DESY), Hamburg (F. R. Germany)). Jul 1975. 14p. Dep. NTIS (US Sales Only) $4.00.

The two-photon cascade decay of the 3.7-GeV resonance into the 3.1-GeV resonance was observed in two nearly independent experiments. The clustering of the photon energies around 160 and 420 MeV observed in the channel $3.7 \rightarrow (3.1 \rightarrow \mu^+\mu^-) + \gamma\gamma$ indicates the existence of at least one intermediate state with even charge conjugation at a mass around 3.52 or 3.26 GeV. (auth)

**26834** (JINR-P1-9021) STUDY OF THE INCLUSIVE REACTION $\pi\text{-}C^{12} \rightarrow pX$ at PC = 40 GeV. Azimov, S. A.; Inogamov, Sh. V.; Igamberdyev, K. R. (Joint Inst. for Nuclear Research, Dubna (USSR)). 1975. 20p. (In Russian). Dep. NTIS (US Sales Only) $4.00.

The experimental data are presented on studying the inclusive reaction $\pi^-C^{12} \rightarrow pX$ at 40 GeV/c. The proton momenta were limited in the range of 140 to 700 MeV/c. The proton characteristics depend weakly on their multiplicity. Associative multiplicities of the relativistic charged particles do not depend on the total and transverse proton momentum. It is shown that in the reaction $\pi^-C^{12} \rightarrow mp + X$ ($m \geq 2$) the angular and momentum distributions of the protons are invariant with respect to the energy of the primary $\pi^-$-meson. (auth)

**26835** (JINR-P1-9032) FURTHER INVESTIGATION OF FORM FACTORS IN K/sub $\mu 3$/$^0$ DECAYS. Genchev, V. I.; Kekelidze, V. D.; Krivokhizhi, V. G.; Kukhtin, V. V.; Likhachev, M F.; Manno, I.; Ryzek, Kh. E.; Savin, I. A.; Silvestrov, L. B. (Joint Inst. for Nuclear Research, Dubna (USSR)). 1975. 20p. (In Russian). Dep. NTIS (US Sales Only) $4.00.

An analysis was performed of 67839 $K^0_{\mu 3}$-decays recorded in the experiments on transmission regeneration of neutral kaons. Two solutions which agree with the linear approximation were found for vector and scalar form factors. In the assumption of $\mu$-e-universality it was found that $\lambda_+ = 0.045 \pm 0.004$ and $\lambda_0 = 0.025 \pm 0.006$. It is shown that in $K^0_{\mu 3}$-decays the vector coupling in matrix element dominates. (auth)

**26836** ELECTRON-ION RECOMBINATION IN TRIPLE COLLISIONS. Borodin, V.M. Opt. Spectrosc. (USSR) 38: No. 3, 266-269 (Mar 1975).

The resonance mechanism of the elementary reaction of electron-ion recombination during a triple collision $A^+ + B + e \rightarrow A^* + B$ ($A^+$ and $B$ are the ion and neutral atom, respectively) is considered within the framework of the model proposed in Ref. 3 for describing ionization during collisions of two atoms. It is noted that for studying the mechanism of the reaction, it is necessary to describe the electron recombination process in the plasma as the diffusion of a bound electron with respect to energy levels under the effect of collisions with atoms $B$. By means of the principle of detailed balance an expression is found for the constants of the electron recombination rate at any Rydberg level of the atom. A numerical calculation for the rate constants of the reaction $K^+ + e + Ne \rightarrow K + Ne$ in an isothermal plasma with a temperature $\theta \sim 3000$ °K was performed. The critical density of Ne atoms at which the recombination rate of the electron and $K^+$ during a triple collision is greater than the rate of the corresponding photorecombination is given. (auth)

**26837** BACKWARD ELASTIC $\pi^+ p$ SCATTERING AT 3.7 AND 7.1 GeV/c. Michael, W.; Abrams, G.S.; Alston-Garnjost, M.; Barbaro-Galtieri, A.; Daugeras, B.Y.; Gidal, G.; Johnson, A.D.; Lynch, G.R.; Solmitz, F.T.; Winkelmann, F.C. (Lawrence Berkeley Laboratory, University of California, Berkeley, California 94720). Phys. Rev. Lett. 35: No. 4, 193-195 (28 July 1975).

The differential cross section of $\pi^+ p$ elastic scattering has been measured in two high-statistics bubble-chamber exposures at laboratory beam momenta of 3.7 and 7.1 Gev/c. A new feature suggested by these data is a dip in $d\sigma/du$ at $-u \simeq 3$ GeV$^2$. This dip corresponds well to the third zero of $J_0(b\sqrt{-u})$, where $\hbar c/b = 1$ fm. The effective $u$-channel Regge trajectory computed for these two energies has a slope of $0.22 \pm 0.26$. (auth)

**26838** MEASUREMENT OF THE REACTIONS $K^- p \rightarrow \Sigma^+ \pi^-$ AND $\pi^- p \rightarrow p \pi^-$ NEAR THE BACKWARD DIRECTION AT 3.0 AND 5.1 GeV/c. Hoffman, E.W. (Argonne National Laboratory, Argonne, Illinois 60439); Dixon, R.L.; Fletcher, J.M.; Garfinkel, A.F.; Loeffler, F.J.; Mudrak, S.; Shibata, E.I.; Stanfield, K.C.; Tang, Y.W. Phys. Rev. Lett. 35: No. 3, 138-141 (21 July 1975).

We have measured differential cross sections for $K^- p \rightarrow \Sigma^+ \pi^-$ and $\pi^- p \rightarrow p \pi^-$ at 3.0 and 5.1 GeV/$c$ near the backward direction. At 3.0 GeV/$c$ both have a dip near $-u \sim 0.1$ (GeV/$c$)$^2$. At 5.1 GeV/$c$, $d\sigma/du$ for $\pi^- p \rightarrow p \pi^-$ falls exponentially with slope $3.8 \pm 0.1$ (GeV/$c$)$^{-2}$ whereas $du/d\sigma$ for $K^- p \rightarrow \Sigma^+ \pi^-$ exhibits a decreasing slope for larger $|u|$. These data are discussed in terms of SU(3), and the relative importance of the helicity-flip and -non-flip amplitudes is investigated. (auth)

**26839** COMMENT ON THE BROAD $p\pi$ ENHANCEMENT IN THE REACTION $K^+ n \rightarrow K^+ p \pi^-$. Carmony, D.D.; Garfinkel, A.F.; Rangan, L.K. (Purdue University, Lafayette, Indiana 47907); Yen, W.L. Phys. Rev. D 11: No. 11, 3331-3333 (1 June 1975).

We show that the $Y_1^*$ moments of the $p\pi^-$ low-mass enhancement in the reaction $K^+ n \rightarrow K^+ p \pi^-$ at 9 GeV/$c$ can be interpreted in terms of a double-Regge-pole exchange model. (auth)

**26840** STUDY OF $\Sigma^\pm \pi^\mp$ PRODUCTION FROM NEGATIVE KAONS STOPPED IN He$^4$. Riley, B.; Wang, I.; Fetkovich, J.G.; McKenzie, J.M. (Carnegie-Mellon University, Pittsburgh, Pennsylvania 15213). Phys. Rev. D 11: No. 11, 3065-3077 (1 June 1975).

We have measured the $\Sigma^\pm \pi^\mp$ invariant mass distributions produced when $K^-$ mesons stop in liquid He$^4$. The Kim and Martin-Sakitt parameterizations of the low-energy $\bar{K}N$ scattering data were used in various impulse models to calculate $\Sigma\pi$ invariant-mass distributions which were compared with the data. Neither parameterization fit the data well. Nevertheless, the evidence appears to support definite conclusions concerning the orbital atomic state from which the $K^-$ undergoes nuclear absorption. It is found that $S$-state capture dominates, while there is very little $D$-state capture. (auth)

**26841** REACTIONS $K^- p \rightarrow \Sigma^0 \pi^0$ AND $K^- p \rightarrow \Lambda \pi^0$ IN THE MOMENTUM RANGE 240 TO 450 MeV/c. Mast, T.S.; Alston-Garnjost, M.; Bangerter, R.O.; Barbaro-Galtieri, A.S.; Solmitz, F.T.; Tripp, R.D. (Lawrence Berkeley Laboratory, University of California, Berkeley, California 94720). Phys. Rev. D 11: No. 11, 3078-3091 (1 June 1975).

An analysis has been made of 57 600 events of the type $K^- p \rightarrow \Lambda +$ missing neutrals obtained in the Berkeley 25-in. hydrogen bubble chamber. The data were divided into intervals of 10 MeV/$c$ in incident momentum and fits were made to the distribution in missing neutral mass, the production cosine, and the polarization of the $\Lambda$ These fits yielded Legendre coefficients describing the cross sections and polarizations for $K^- p \rightarrow \Sigma^0 \pi^0$ and $K^- \rightarrow \Lambda \pi^0$ in the momentum range 240 to 450 MeV/$c$. The cross sections and polarization in the $\Sigma^0 \pi^0$ final state show marked structure coming from the production and decay of $\Lambda$ (1520). The cross sections and polarizations for the $\Lambda \pi^0$ final state vary slowly. No new structure is observed. (auth)

**26842** PRODUCTION OF POSITIVE PARTICLES IN 8-GeV/$c$ $\pi^- p$ AND 18.5-GeV/$c$ $\pi^+ p$ SINGLE-PARTICLE INCLUSIVE REACTIONS. Go, P.T.; Shephard, W.D.; Kenney, V.P.; Bishop, J.M.; Biswas, N.N.; Cason, N.M. (Department of Physics, University of Notre Dame, Notre Dame, Indiana 46556). Phys. Rev. D 11: No. 11, 3092-3098 (1 June 1975).

Inclusive cross sections and invariant single-particle distributions are presented for positive pions and protons produced in 8.05-GeV/$c$ $\pi^- p$ and 18.5-GeV/$c$ $\pi^+ p$ inclusive reactions. Distributions in $p_T{}^2$ and in the longitudinal variables $x$,$y$ (c.m.) and $p_l$ (lab) are shown. Comparisons are made with inclusive distributions for other particles produced in the same reactions. (auth)

**26843** FOUR CHARGED PARTICLE FINAL STATES FROM THE REACTION PI$^+$D AT 15 GeV/c. Pewitt, N. D. Tallahassee, FL; Florida State Univ. (1975). 181p. University Microfilms Order No. 75-15,505.

Thesis (Ph. D.).

The data from 387,000 stereotriplet photographs of the deuterium filled Stanford Linear Accelerator Center 82-inch bubble chamber exposed to a 15-GeV/c pi$^+$ separated beam are presented. The film was measured on a Flying Spot Digitizer with an accuracy of one micron. The final states pi$^+$pi$^-$pp, pi$^+$pi$^-$pi$^0$pp, pi$^+$pi$^+$pi$^-$np, pi$^+$pi$^+$pi$^-$d and pi$^+$pi$^+$pi$^-$pi$^0$d are discussed. With an experimental sensitivity of 4.75 +- .09 events/mu b there is no new boson resonance structure in these data. The one-pion-exchange process dominates the breakup reactions. A rising (3 pi) coherent cross section established by these data is explained in terms of a kinematical effect. The data were used in a search for direct evidence for nuclear isobar (DELTA DELTA) component of the deuteron and established an upper limit at about one per cent. Details of the experimental procedure and the data reduction are described as well as an alternate data processing system, RESURX, which allows human intervention in the pattern recognition process to save over half the events failed by the normal data reduction system. (Diss. Abstr. Int., B)

# Particle Interactions and Properties (Theoretical)

## General

*Refer also to abstracts 26814–26817.*

**26844** QUARK STRUCTURE OF RESONANCES AS A CONSEQUENCE OF SPONTANEOUS VACUUM TRANSITIONS IN DUAL MODELS. Volkov, D.V.; Zheltukhin, A.A.; Pashnev, A.I. (Physico-technical Institute, Ukrainian Academy of Sciences). JETP Lett. 21: No. 7, 207-208 (5 Apr 1975).

It is shown that spontaneous vacuum transitions in the dual Veneziano model lead to the appearance of internal quantum numbers and, depending on the intercept of the Regge trajectories $\alpha_0$, to one group of internal symmetries or another. (auth)

**26845** TWO-PARTICLE NONLEPTONIC DECAYS OF $D$ AND $F$ MESONS, AND STRUCTURE OF WEAK INTERACTIONS. Voloshin, M.B.; Zakharov, V.I.; Okun', L.B. (Institute of Theoretical and Experimental Physics). JETP Lett. 21: No. 6, 183-185 (20 Mar 1975).

We consider nonleptonic decays of the hypercharged (charmed) $D$ and $F$ mesons. Relations are obtained between the amplitudes of different decays, which follow from unitary symmetry and from the assumption that the Hamiltonian of the weak interactions takes the form of the product of a current by a current. We consider the consequences of the $T$-, $U$-, and $V$-spin selection rules. (auth)

**26846** ELECTROPRODUCTION AT SMALL $Q^2$ IN THE PARTON MODEL. Volkonskiĭ, N.Yu.; Prokhorov, L.V. (Leningrad State University). JETP Lett. 21: No. 6, 177-178 (20 Mar 1975).

It is shown that allowance for the coherent contribution to the cross section for the scattering of a virtual photon by partons leads to suprisingly good description of the electroproduction process also outside the scaling region (small $Q^2$), and that the recently observed violation of scaling [5] can be attributed to the fact that the partons have a mass distribution. (auth)

**26847** QUASISTABLE STATES IN THE PHYSICAL SPECTRUM OF THE DUAL MODEL AT LARGE MASSES. Gerasyuta, S.M.; Kudryavtsev, V.A. (Leningrad Institute of Nuclear Physics, USSR Academy of Sciences). JETP Lett. 21: No. 6, 179-180 (20 Mar 1975).

Physical states (PS) of a vertex, the connections of which with arbitrary other states are anomalously small if their mass is large enough, were observed in the dual spectrum. Such PS should therefore have small partial and total widths in comparison with the usual ones. We shall henceforth call these quasistable (QS) states. (auth)

**26848** THE NUMBER OF PHYSICAL STATES SATISFYING SUPERGAUGE CONDITIONS IN DUAL RESONANCE MODELS. Konisi, G. (Kwansei Gakuin Univ., Nishinomiya, Hyogo (Japan). Dept. of Physics); Saito, T. Prog. Theor. Phys. (Kyoto); 52: No. 6, 1902-1909(Dec 1974).

In the dual resonance models we give generating functions to calculate the number of positive-norm on-shell states which are simultaneous eigenstates of the mass-squared operator R and the angular momentum J and satisfy the supergauge conditions. It is found that there are a few missing states and there occurs a saturation of the degeneracy of the states along each trajectory. It is pointed out that all the states on the odd-daughter trajectories in the dual pion model cannot couple to the $2\pi$-channel, but to the other channels. (auth)

**26849** TWO-BODY REACTIONS AT ALL ANGLES AS THE EXCLUSIVE LIMIT OF INCLUSIVE REACTIONS. Kinoshita, K. (Kyushu Univ., Fukuoka (Japan). Dept. of Physics); Myozyo, Y. Prog. Theor. Phys. (Kyoto); 52: No. 6, 1873-1882(Dec 1974).

Differential cross section for ab → cd is obtained from the whole-region formula for ab → cX by taking the exclusive limit X → d. The resultant formula exhibits a Regge-like behaviour at small absolute t or absolute u, and $s^{-n}$ fall-off at high energy fixed angles. At large s, absolute t and absolute u, the differential cross section is written as a product of inverse powers of s, t and u, where the power is determined by the number of valence urbaryon bonds connecting a, b, c and d. The formula explains gross features of the all-angle data of $K^{\pm}p$, pp, $\bar{p}p$ and other processes. (auth)

**26850** WHOLE-REGION FORMULA FOR SINGLE-PARTICLE DISTRIBUTIONS AND TWO-BODY REACTIONS AT ALL ANGLES. Kinoshita, K. (Kyushu Univ., Fukuoka (Japan). Dept. of Physics); Noda, H. Prog. Theor. Phys. (Kyoto); 52: No. 5, 1622-1639(Nov 1974).

A formula for inclusive distributions ab → cX is proposed, which incorporates the large pr scaling with power fall-off in pr, the limiting behaviour in the fragmentation region and the approach from below to the Feynman scaling in the central region. By taking the exclusive limit X = d of the formula, the differential cross section for ab → cd at all angles is obtained, which exhibits both the fixed-angle scaling at large angles and the Regge-like behaviour at small angles. The parameters in the formula are determined by the bond numbers of urbaryon lines connecting a, b, c and X (or d). The formula is closely related to the structure functions of the colliding hadrons. Construction of the formula from certain factors assigned to urbaryon lines is suggested. (auth)

**26851** SCALING BEHAVIOUR OF HADRON INTERACTIONS AND URBARYON BOND MODEL. Noda, H. (Ibaraki Univ., Mito (Japan). Dept. of Physics); Kinoshita, K. Prog. Theor. Phys. (Kyoto); 53: No. 1, 185-199(Jan 1975).

A model is given which treats the exclusive and inclusive reactions uniformly and is applicable to both the peripheral and large transverse momentum reactions; inclusive amplitudes are constructed by assignment of certain factors to urbaryon lines, and the corresponding exclusive amplitudes are obtained by taking the exclusive limit of specifying the anything state to be a hadron. The model incorporates various types of scaling properties, i. e., the Bjorken scaling, the Feynman scaling, the large transverse momentum scaling and the large angle scaling, and also the Regge-like behavior of exclusive and inclusive reactions. (auth)

**26852** A POLE-CUT DUAL REPRESENTATION AND PHOTOPRODUCTION AMPLITUDE WITH FIXED CUT. Imoto, M. (Nihon Univ., Funabashi, Chiba. Physical Science Lab.). Prog. Theor. Phys. (Kyoto); 53: No. 1, 152-160(Jan 1975).

A method is proposed by which a fixed cut model is introduced in a photoproduction amplitude. The photoproduction amplitude is constructed from the scattering amplitude of hadrons with an external current. This hadronic current amplitude is extracted from the pole-cut dual lepton-hadron scattering amplitude with the lepton-antilepton pair. It is shown that the appearance of constant cut trajectories in the photoproduction amplitude is attributed to the pole-cut duality in this lepton-hadron amplitude. (auth)

**26853** CLUSTER SIZE AND THE RAPIDITY GAP-LENGTH DISTRIBUTION. Ludlam, T. (Physics Department, Yale University, New Haven, Connecticut 06520); Slansky, R. Phys. Rev. Lett. 35: No. 2, 127-128 (14 July 1975).

The sensitivity of the rapidity gap-length distribution to the kinematical effects caused by clustering, but with the multiplicity distribution constrained to reproduce the data, does not adequately distinguish among models with widely varying cluster sizes. (auth)

**26854** POMERON DECOUPLING THEOREMS. Brower, R.C. (Physics Department, University of California-Santa Cruz, Santa-Cruz, California 95060); Weis, J.H. Rev. Mod. Phys. 47: No. 3, 605-635 (July 1975).

We investigate the hypothesis that diffractive scattering is dominated (as $s \to \infty$) by a Pomeron Regge pole $[\alpha_P(t)]$. This hypothesis is particularly attractive since a Regge pole and its attendant cuts satisfy $t$-channel unitarity. For a complete theory the constraints of $s$-channel unitarity must also be satisfied. In addition to Froissart's bound and its well-known consequence, $\alpha_P(0) \leqslant 1$, $s$-channel unitarity implies a large number of decoupling theorems for an isolated Pomeron pole with $\alpha_P(0) = 1$. Here we systematically review these decoupling theorems. The theorems are treated in order of increasing strength so as to clearly distinguish the "strong theorems" which can be used to prove the complete decoupling of the Pomeron (e.g., $\sigma_{\text{Tot}} \to 0$) from the "weak theorems" which cannot. This review is undertaken with two goals in view: (1) To focus attention on possible points of departure for more realistic treatments of diffractive scattering, and (2) to emphasize the importance of $s$-channel unitarity which is expected to strongly constrain diffractive production in certain regions of phase space regardless of the exact nature of the Pomeron singularity. (auth)

**26855** OPERATOR ALGEBRA OF DUAL RESONANCE MODELS. Arik, M.; Coon, D.D.; Lam, Y. (Department of Physics, University of Pittsburgh, Pittsburgh, Pennsylvania 15260). J. Math. Phys. (N.Y.) 16: No. 9, 1776-1779 (Sept 1975).

Properties of a set of operators introduced by Baker, Coon, and Yu are discussed. The operators involve generalizations of harmonic oscillator operators and facilitate the construction of a family of dual resonance models which includes the Veneziano model as a limiting case. Matrix representations of the operators are constructed, and it is shown that the operators have finite norm in contrast with the unboundedness of creation and annihilation operators of the Veneziano model. (auth)

**26856** GENERALIZED ISOBAR MODEL FORMALISM. Herndon, D.J.; Söding, P. (Lawrence Berkeley Laboratory, University of California, Berkeley, California 94720); Cashmore, R.J. Phys. Rev. D 11: No. 11, 3165-3182 (1 June 1975).

We present an isobar model formalism for analyzing the reaction $a + b \to 1 + 2 + 3$. Arbitrary spins are allowed for all the particles. Polarized particles and weak decays of an outgoing particle are discussed. We also show how to extend the formalism to allow an isobar analysis of a three-body subsystem of an $n$-particle final state. (auth)

**26857** INTERACTING DUAL RESONANCE MODEL IN TERMS OF DIRECT INTER-STRING ACTION. Kalb, M. New Haven; Yale Univ. (1974). 151p. University Microfilms Order No. 75-15,315.

Thesis (Ph. D.).

The interactions of the bosonic sector of dual resonance models using the strong formalism and the possible couplings generated by an action-at-a-distance theory are considered. The anti-symmetric tensor coupling which exhibits an appealing similarity to electrodynamics is mainly discussed. (JFP)

**26858** GENERAL SCHEME FOR MICROSCOPIC THEORIES. Toller, M. (Univ., Bologna). Int. J. Theor. Phys.; 12: No. 6, 349-381(Apr 1975).

A discussion is given of a general scheme of physical theory, which was developed as a preliminary to an investigation of the space-time structure, at the microscopic level of elementary particles. The discussion covers sections on measurement procedures and transformation procedures, an order relation between measurement procedures of $\xi_2$, the mathematical structure of measurements, the mathematical structure of transformations, compatibility of measurements, and extended structures of measurements. (UK)

**26859** HAS $\psi_s$ ALREADY BEEN OBSERVED AT STANFORD LINEAR ACCELERATOR CENTER? Feldman, G.; Matthews, P.T.

(Physics Department, Imperial College, London SW7, England). Phys. Rev. Lett. 35: No. 6, 344-346 (11 Aug 1975).

Okubo mass splitting is generalized to Han-Nambu color theory and used to predict a fourth $\psi$ particle with mass about 4.8 GeV/$c^2$ and partial width into $e^+e^-$ of 0.8 keV. (auth)

**26860** ON-SHELL ASYMPTOTICS OF NON-ABELIAN GAUGE THEORIES. Cornwall, J.M.; Tiktopoulos, G. (Department of Physics, University of California, Los Angeles, California 90024). Phys. Rev. Lett. 35: No. 6, 338-341 (11 Aug 1975).

In the leading-logarithm approximation, the high-energy fixed-angle elastic fermion-fermion amplitude and the asymptotic form factor have been calculated to sixth order for a Yang-Mills theory; some other processes have been calculated to fourth order. The results suggest properties of exponentiation and factorization which can be described in terms of momentum-dependent anomalous dimensions in the renormalization-group equations. We discuss the possible relation of the zero-mass limit of our results to particle confinement. (auth)

## *Electromagnetic*

*Refer also to abstracts 26934, 27154, and 27210.*

**26861** (HD-THEP-75-5) GAUGE THEORIES OF WEAK AND ELECTROMAGNETIC INTERACTIONS (MAINLY HADRONS). Gromes, D. (Heidelberg Univ. (F. R. Germany). Inst. fuer Theoretische Physik). Apr 1975. 22p. (AED-CONF-75-041-003). INIS.

From spring meeting of the Fachausschuss Kernphysik und Hochenergiephysik of the DPG; Muenchen, F. R. Germany (5 Mar 1975).

1 fig.; 2 tabs.; 26 refs. With abstract.

It is intended to explain some of the main ideas in an elementary way without going into details of calculations. (auth)

**26862** (JINR-E2-8984) NON-GALILEAN PARTON MODEL OF DEEP INELASTIC SCATTERING. Toth, K. (Joint Inst. for Nuclear Research, Dubna (USSR)). 1975. 13p. Dep. NTIS (US Sales Only) $4.00.

An extension of parton models is proposed to calculate deep-inelastic structure functions. As a result, an approximate formula $W(q^2,pq) = f(pq/2q^2) + \{[(m^2/M^2)(pq/q^2)]f'(pq/2q^2)\} - \{[(pq/M^2)(pq/q^2)]f'(pq/2q^2)\} + \ldots$, is obtained, in which the scaling term is only the zeroth order approximation in the phenomenological parameter $m^2/M^2$. (auth)

**26863** (JINR-P2-8776) UNITARITY RELATION AND RHO$^0$–$\omega$ MIXING. Lyuboshits, V. L. (Joint Inst. for Nuclear Research Dubna (USSR)). 1975. 17p. (In Russian). Dep. NTIS (US Sales Only) $4.00.

The Bell–Steinberger unitarity sum rule is applied to the $\rho^0$–$\omega$ system. Due to T invariance of the theory and the unitarity condition, the imaginary part of the parameter $\epsilon$ that characterizes electromagnetic mixing of the states of isotopic spin 0 and 1 is expressed by the amplitudes of $\rho^0$ and $\omega$ resonance decay into the same channels. Analysis of the experimental data of $\rho^0$- and $\omega$-meson partial widths shows that two-pion decay contributes the dominant part to the sum $\Sigma_n A^*_{\rho^0\to n} A_{\omega\to n}$. On this basis quantitative estimates for the imaginary part of the mixing parameter and for the relative phase of the amplitudes $A_{\rho^0\to\pi^+\pi^-}$ and $A_{\omega\to\pi^+\pi^-}$ were obtained. (auth)

**26864** ELECTROMAGNETIC CORRECTIONS TO THE PRODUCTION OF NARROW RESONANCES IN COLLIDING $e^+e^-$ BEAMS. Azimov, Ya.I.; Vainshtein[1]; A.I.; Lipatov, L.N.; Khoze, V.A. (Leningrad Institute of Nuclear Physics, USSR Academy of Sciences). JETP Lett. 21: No. 6, 172-174 (20 Mar 1975).

Formulas that are exact in the parameter $(4\alpha/\pi)\ln(W/m_e)\ln(W/\Delta E)$ were obtained for the radiative corrections to the cross sections for the production of narrow resonances in colliding $e^+e^-$ beam experiments. Phenomena connected with the interference of the resonance with the nonresonant background are discussed. (auth)

**26865** COHERENT INTERACTION OF LEPTONS WITH QUARKS IN DEEP INELASTIC PROCESSES. Anisovich, V.V. (Institute of High Energy Physics). JETP Lett. 21: No. 6, 174-175 (20 Mar 1975).

Coherent interaction processes with two or with three quarks are considered. It is shown that allowance for these processes leads to $W^{3/2}_{ep}/W^{1/2}_{ep} \simeq 1/3$ at $x \simeq 2/3$ and $W^{3/2}_{ep}/W^{1/2}_{ep} \simeq 0$ at $x \simeq 1$. (auth)

**26866** NEW RESONANCES IN $e^+e^-$ ANNIHILATIONS AS THE DAUGHTERS OF $\phi$(1019). Chen, C.K. (Department of Natural Philosophy, University of Glasgow, Glasgow G12 8QQ, Scotland). Phys. Rev. Lett. 35: No. 1, 4-6 (7 July 1975).

The experimental consequences of a scheme to identify the newly discovered resonances in $e^+e^-$ annihilation as the daughters of the $\phi$(1019) meson are discussed. The two narrow-width resonances with masses at 3105 and 3695 MeV are proposed to be described by closely located zero-pole systems instead of simple poles. (auth)

**26867** COMMENTS ON GAUGE INVARIANCE IN COMPTON SCATTERING. Weaver, D.L. (Department of Physics, Tufts University, Medford, Massachusetts 02155). Phys. Rev. D 11: No. 12, 3635-3636 (15 June 1975).

The scattering of neutral vector mesons from a pseudoscalar-meson target is considered. It is shown that using the $SL(2,C)$ description for the vector particles, one obtains a clear understanding of gauge invariance in the limit of vanishing vector-meson mass, i.e., there are no gauge-invariance conditions on the invariant amplitudes. Some related properties of the description are also given. (auth)

**26868** COMMENT ON A RECENT CALCULATION OF THE ANOMALOUS MAGNETIC MOMENT OF THE ELECTRON TO ORDER $\alpha$. Mikaelian, K.O. (Department of Physics, The Pennsylvania State University, University Park, Pennsylvania 16802). Phys. Rev. D 11: No. 12, 3626-3627 (15 June 1975).

We evaluate analytically the results given in integral form by Lai *et al.* for the anomalous magnetic moment of the electron to order $\alpha$. We point out that for small cutoff energies ($\omega_c \lesssim \frac{1}{2}m_e$) the result is negative. A short critique of the nonrelativistic approximation is included. (auth)

**26869** THEOREM FOR THE PHOTON ASYMMETRY IN RADIATIVE MUON CAPTURE. Fearing, H.W. (Nuclear Research Centre, Department of Physics, University of Alberta, Edmonton, Alberta, Canada). Phys. Rev. Lett. 35: No. 2, 79-82 (14 July 1975).

I show, for the standard theory of radiative muon capture including all couplings except $g_s$ and all usual diagrams, that the photon asymmetry $\alpha$ and circular polarization $\beta$ satisfy $\alpha = +1 + O(1/m^2)$ and $\beta = +1 + O(1/m^2)$, where $m$ is the nucleon mass. This may bear on current disagreement between $\alpha^{\text{theor}}$ and $\alpha^{\text{expt}}$ since $O(1/m^2)$ terms have never been calculated consistently and since other uncalculated corrections, some of which are discussed, may contribute in the same order. (auth)

**26870** STELLAR ROTATION, AND VIOLATIONS OF THE ODD-EVEN EFFECT IN THE MANGANESE STARS. Cowley, C.R. (Dominion Astrophysical Observatory). Astrophys. J. 198: No. 2, 379-382 (1 June 1975).

Abundances of phosphorus and yttrium are examined in a number of slowly rotating Ap stars. It is argued that slow rotation is not a sufficient condition to establish the odd-$Z$ abundance anomalies that are frequently observed for these elements. Implications for the diffusion hypothesis are discussed. (auth)

**26871** COMMENT ON "DIFFERENCE BETWEEN $e^+$ AND $e^-$ DEEP-INELASTIC SCATTERING." Bodwin, G.T.; Stockham, C.D. (Laboratory of Nuclear Studies, Cornell University, Ithaca, New York 14853). Phys. Rev. D 11: No. 11, 3324-3327 (1 June 1975).

On the basis of a parton model, Fishbane and Kingsley have investigated the difference between $e^-p$ and $e^+p$ deep-inelastic scattering in the backward direction and found it to be of relative order $\alpha \ln^2(Q^2/\mu^2)$, where $\mu$ is a typical hadronic mass. We have reexamined this problem in the more general kinematic region $E_1 \gg E_3$ ($E_1$ and $E_3$ are the initial and final electron energies, respectively) and have taken care to distinguish between hard- and soft-photon radiative corrections. The noninfrared part of the virtual photon correction has been found to be of relative order $\alpha \ln^2(E_1/E_3)$. It is hard to conceive of a situation where such a contribution to the cross section would be observable. (auth)

**26872** ROTATIONAL INVARIANCE AND THE MAGNETIC MONOPOLE FIELD. Leinaas, J. M. (Oslo Univ.). Phys. Norv.; 8: No. 1, 41-45 (1975).

A general expression for the generator of rotations of a spinless particle is found. It is shown to correspond to the total angular momentum of the system of a charged particle in a magnetic monopole field. Dirac's charge quantization rule is contained in the possible forms of the transformation equation. An expression for possible forms of the singular vector potential of the monopole field is found. The possibility of accepting multiple valued wave functions is discussed. (auth)

**26873** SIMULTANEOUS EXPANSION FOR THE ELECTROMAGNETIC FIELD OF A RELATIVISTIC CHARGED PARTICLE. Gordeyev, A. N. (Ife Univ., Nigeria). J. Phys., A (London); 8: No. 7, 1048-1059(Jul 1975).

The expressions for electromagnetic potentials and fields of a charged particle in arbitrary motion in terms of simultaneous characteristics of the motion were derived with the help of the Lagrange expansion for a retarded function. The expressions do not contain expansions in powers of the ratio v/c, and hence they are effective for particles with arbitrarily high velocities. The derived expressions may be useful in classical field theory and

may serve as a starting point for development of a nonquantal relativistic statistical mechanics. (auth)

**26874** RADIATION FIELD OF A SENDER PLACED IN AN ANISOTROPIC MEDIUM. Sellner, J. (Technische Hochschule, Graz). Acta Phys. Austriaca; 39: No. 1, 76–82(1974). (In German).

The radiation field of a sender placed in an anisotropic medium which borders an isotropic medium is considered. Two different directions of the source current must therefore be considered. In spite of differing expressions, the amplitudes of the irradiated and reflected partial waves are almost equal for both cases. The calculation of these amplitudes is the purpose, and it is shown that they assume a very complicated appearance. (tr-auth)

## Weak

*Refer also to abstract 27113.*

**26875** (IFKKI-75/3) NEW THEORY OF THE $\beta$-DECAY OF NEUTRONS. Bagge, E. (Kiel Univ. (F. R. Germany). Inst. fuer Reine und Angewandte Kernphysik). Feb 1975. 20p. (In German). INIS.

2 figs. 10 refs. Available from ZAED. Shortened version published in Atomkernenergie 25(4) 1975 p. 251–256.

If the law of energy conservation will be extended in such a way that besides the positive energy states also the transitions in the region of Dirac's negative energy states will be taken into account, then the $\beta$-decay of nuclei can be interpreted as a special form of electron pair production or annihilation without any engagement of neutrinos. The $\beta$-decay of the neutron in this case is the pair production with the emission of an electron and the capture of the positron by the nucleon, which becomes a proton in this way. Within the scheme of these ideas one receives a formula for the $\beta$-spectrum identical with Fermi's energy distribution. The extended law of energy conservation and the conservation law for the momenta are fulfilled exactly. (auth)

**26876** NEUTRAL CURRENT INTERACTIONS BASED ON A GENERAL BARYON-LEPTON SYMMETRY MODEL. Nakagawa, M. (Meijo Univ., Nagoya (Japan)). Prog. Theor. Phys. (Kyoto); 52: No. 6, 1883–1889(Dec 1974).

A baryon-lepton symmetry, which was first discovered in charged weak current by Gamba, Marshak and Okubo in 1959 and extended to the two-neutrino scheme in 1962, is applied to neutral weak current. We generalize the symmetry, hitherto only based on a real rotation of one angle (the so-called Cabibbo angle), to a general rotation, double SU(2), including three angles. The neutral hadronic current with $\Delta S = 1$ is automatically forbidden as a consequence of muon number conservation and electron-muon universality in neutral leptonic current. A possible model is suggested from our symmetry that strengths of the $\Delta S = 1$ neutral current and of the CP violation are of the same order as that of violation of electron-muon universality in the leptonic current. Other physical effects are discussed in detail. (auth)

**26877** WEAK NEUTRAL CURRENTS AND THE HIROSHIMA MODEL. Koide, Y. (Shizuoka Women's Coll. (Japan)). Prog. Theor. Phys. (Kyoto); 52: No. 5, 1640–1646(Nov 1974).

A possible feature of weak neutral currents is investigated on the basis of the Hiroshima model, in which neutral hadron currents follow from lepton currents without assuming existence of neutral lepton currents. Neutral hadron currents depend not only on the models of urbaryon (the Hiroshima model and the new Nagoya model) but also on the models of hadron (the quark model and the quartet model). Moreover, those depend on the choice of forms of pure leptonic weak interaction. Cross sections for elastic $\nu N$ scattering are predicted. (auth)

**26878** CHARMED-QUARK MODEL FOR NARROW RESONANCES. Barnett, R.M. (Lyman Laboratory of Physics, Harvard University, Cambridge, Massachusetts 02138). Phys. Rev. D 11: No. 11, 3246-3252 (1 June 1975).

An isospin suppression is used as a possible explanation of the narrow width of the 3.1-GeV resonance in a model with three charmed quarks. This follows from an analogy with $\rho$-$\omega$ mixing and the $\omega \to 2\pi$ decay. The decays and widths of radial excitations of the 3.1-GeV resonance are discussed. The weak couplings of the model predict different decays for charmed particles than other models with charm; in particular, $K$ mesons are not always found in the decays. An experimental test which clearly distinguishes this model from other models is given. (auth)

**26879** WEINBERG ANGLE IN THE QUARK-PARTON MODEL WITH CHARM FOR HIGH-ENERGY NEUTRINO-NUCLEON COLLISIONS. Kang, K.; Rizvi, S.M.A.H. (Department of Physics, Brown University, Providence, Rhode Island 02912). Phys. Rev. D 11: No. 11, 3305-3308 (1 June 1975).

General expressions for $\sin^2\theta_w$, $R \equiv \sigma^{\nu N}_{nc}/\sigma^{\nu N}_{cc}$, and $\bar{R} \equiv \sigma^{\bar{\nu}N}_{nc}/\sigma^{\bar{\nu}N}_{cc}$ are given in the quark-parton model with the charmed quark. Convenient parametrizations of the experimental results for the charged and neutral $(\nu,\bar{\nu})$ $N$ interactions, in the scaling limit, are introduced and their implications on $\theta_w$ are discussed. In particular, we study the effect of the charmed quark in the neutral current processes explicitly by analyzing the available experimental data. Constraints on the relative contributions of the antiquarks, strange quarks, and charmed quarks are obtained. (auth)

**26880** LEPTON-LEPTON SCATTERING IN A SPONTANEOUSLY BROKEN GAUGE THEORY SATISFYING STRONG-INTERACTION DUALITY. Dicus, D.A.; Teplitz, V.L.; Young, J.E. (Laboratory for Nuclear Science and Department of Physics, Massachusetts Institute of Technology, Cambridge, Massachusetts 02139). Phys. Rev. D 11: No. 11, 3295-3304 (1 June 1975).

We construct a spontaneously broken gauge theory of leptons ($e$, $\mu$, $\nu_e$, $\nu_\mu$) in which the two-body scattering amplitudes are dual. The resultant model leads to suppression of $\nu_\mu e \to \nu_\mu e$ and predictions for $\nu_e e \to \nu_e e$ and $e^+e^- \to \mu^+\mu^-$ that are distinctly different from both the conventional $V-A$ theory and the Weinberg-Salam model. (auth)

**26881** MODELS FOR WEAK CURRENTS WITH HAN-NAMBU THREE-TRIPLETS. Sacliogiu, C. (The Enrico Fermi Institute, and the Department of Physics, The University of Chicago, Chicago, Illinois 60637). Phys. Rev. D 11: No. 11, 3284-3294 (1 June 1975).

A mechanism introduced by Stech to suppress $\Delta S = 1$ neutral currents is adapted to the Han-Nambu model. Consequences of different schemes arising from the freedom in baryon number assignment are investigated. Though first order processes are eliminated in all of these models, only two of them give sufficiently small second-order rates for $K_L^0 \to \mu^+\mu^-$. In these cases, it is possible to obtain $\sin\theta_C = 1/3\sqrt{2} \simeq 0.235$ in a rather natural manner. These two models and one of the others can be extended to SU(2) ⊗ U(1) gauge theories of weak and electromagnetic interactions which are anomaly-free in the quark sector and thus require heavy leptons to cancel leptonic anomalies. The rates for neutral events in inclusive neutrino-nucleon reactions predicted by these gauge theories are compatible with experimental results when $\sin^2\theta_w \simeq 1/3$. The models giving acceptable $K_L^0 \to \mu^+\mu^-$ rates do not predict any enhancement of neutrino-nucleon total cross sections associated with the production of SU(3)$'$ nonsinglet states. None of the above schemes helps explain the $\Delta T = 1/2$ rule. (auth)

**26882** NEUTRAL-CURRENT EFFECTS IN THE DECAY $\psi \to \mu^+\mu^-$. Isgur, N. (Department of Physics, University of Toronto, Toronto, Canada). Phys. Rev. D 11: No. 11, 3236-3239 (1 June 1975).

We calculate the angular distribution and polarization of muon pairs from the decay of a $\psi$ particle produced in $e^+e^-$ collisions. We show, among other things, that weak neutral-current effects do not produce a forward-backward asymmetry but do give the muons a net helicity which is a sensitive test of both neutral current theories and models of the $\psi$ particles. The possibility of measuring the resulting net helicity in the near future is briefly discussed. (auth)

**26883** BOUNDS ON WEAK RADIATIVE DECAYS OF CHARGED PIONS. Koul, B.L.; Pandita, P.N.; Singh, Y. (Department of Physics, Kashmir University, Srinagar 190006, India). Phys. Rev. D 11: No. 11, 3355-3358 (1 June 1975).

Using the Schwarz inequality we obtain bounds on the form factors for the weak radiative decays $\pi^+ \to l\nu\gamma$ in terms of the structure functions describing deep-inelastic neutrino scattering from charged pions and the photon spectral function. As a by-product we obtain positivity conditions for the neutrino-pion structure functions. (auth)

**26884** POLARIZED MØLLER SCATTERING. DeRaad, L.L. Jr. (Department of Physics, University of California, Los Angeles, California 90024). Phys. Rev. D 11: No. 11, 3328-3330 (1 June 1975).

The differential cross section is calculated through order $\alpha^3$ for transversely polarized incident electrons using the helicity amplitudes presented in a previous paper. The high-energy limit is compared with a recent calculation of Gastmans and Van Ham and certain errors are pointed out. (auth)

**26885** SUPERWEAK MODEL OF *CP* VIOLATION IN UNIFIED GAUGE THEORIES. Mohapatra, R.N. (Department of Physics, The City College of the City University of New York, New York, New York 10031); Pati, J.C.; Wolfenstein, L. Phys. Rev. D 11: No. 11, 3319-3323 (1 June 1975).

Superweak *CP* violation may be incorporated into the neutral current interactions of unified gauge theories by assuming there exists a stage in the hierarchy of spontaneous symmetry breaking characterized by large *CP* violation and gauge boson masses of the order of $10^6$ GeV. Two specific models are presented. (auth)

**26886** DIMUON PAIRS AS A SIGNAL FOR NEUTRAL HEAVY-LEPTON PRODUCTION. Chang, L.N.; Derman, E.; Ng,

J.N. (Department of Physics, University of Pennsylvania, Philadelphia, Pennsylvania 19174). Phys. Rev. Lett. 35: No. 1, 6-9 (7 July 1975).

The possibility that dimuons observed in $\nu$ ($\bar{\nu}$) -$N$ scattering are due to the production of a neutral heavy lepton is considered. Various distributions are presented. (auth)

**26887** CHANGING THE CHARMED CURRENT. De Rújula, A.; Georgi, H.; Glashow, S.L. (Lyman Laboratory of Physics, Harvard University, Cambridge, Massachusetts 02138). Phys. Rev. Lett. 35: No. 2, 69-72 (14 July 1975).

We propose as an addition to the conventional charm-changing charged current the $V+A$ current $\bar{\beta}\gamma_\mu(1-\gamma_5)\mathfrak{M}$ It explains the observed enhancement of nonleptonic $\Delta I=1/2$ weak decays, allows low-lying charmed hadrons to decay comparably into strange and non-strange final states, predicts the appearance of $\mu^- l^-$ (as well as $\mu^- l^+$) dilepton events in neutrino interactions, and leads to copious quasielastic charm production by neutrinos. (auth)

**26888** DYNAMICS OF THE ZWEIG-IIZUKA RULE AND A NEW VECTOR MESON BELOW 2 GeV/$c^2$. Freund, P.G.O.; Nambu, Y. (Enrico Fermi Institute, Department of Physics, University of Chicago, Chicago, Illinois 60637). Phys. Rev. Lett. 34: No. 26, 1645-1649 (30 June 1975).

The breaking of the Zweig-Iizuka rule in vector-meson decays is explained by mixing the $\omega$, $\varphi$, and $\psi$ mesons with a new SU(4) -singlet meson $O$ (a Pomeron daughter), expected to lie between 1.4 and 1.8 GeV/$c^2$. We predict rates for many $\psi$-decay modes. The $O$ meson itself is predicted to decay copiously into $\rho\pi$, but its branching ratios into the $K\bar{K}$, $e^-e^+$, and $\mu^-\mu^+$ modes are severely suppressed. (auth)

**26889** COMMENTS ON $K_L \to \mu+\bar{\mu}$ IN THE WEINBERG-SALAM MODEL. Marciano, W.J. (Department of Physics, The Rockefeller University, New York, New York 10021). Phys. Rev. D 11: No. 11, 3334-3336 (1 June 1975).

The highly suppressed decay mode $K_L \to \mu + \bar{\mu}$ is reexamined in the Weinberg-Salam SU(2) $\times$ U(1) gauge model after dropping the constraint $M_Z \cos\theta_W = M_W$. Comparing our result with the experimental data, we find the bound $M_Z$ — 18 GeV for this enlarged class of quartet charm models. (auth)

**26890** THEORY OF LEPTON–HADRON PROCESSES AT HIGH ENERGIES. Partons, Scale Invariance, and Light-cone Physics. Roy, P. Oxford; Clarendon Press (1975). 182p.

The subject is dealt with in chapters entitled: the kindergarten parton model (including inelastic ep scattering, inelastic ($\nu$,$\bar{\nu}$)p scattering, quark-partons); the theoretical basis of the parton picture; fundamentals of scale invariance; short-distance scale invariance; rudiments of light-cone physics; applications of light-cone physics (including spin-averaged deep inelastic lN scattering, spin-dependent deep inelastic scattering). (UK)

## Strong (General)

*Refer also to abstracts 27181 and 27184.*

**26891** SCATTERING OF ONE-DIMENSIONAL BAGS IN THE INTERACTING STRING FORMALISM. Thorn, C.B.; Ulehla, M.V.K. (Laboratory for Nuclear Science and Department of Physics, Massachusetts Institute of Technology, Cambridge, Massachusetts 02139). Phys. Rev. D 11: No. 12, 3531-3536 (15 June 1975).

We apply the interacting string formalism of Mandelstam to the scattering problem of one-dimensional bags. We obtain the usual conditions $\alpha_0 = g/24$ and $\alpha_0 = 1$, with the result that the $n$-point scattering amplitudes are those of the dual resonance model. However, we also write the four-point scattering amplitudes for arbitrary $\alpha_0$. Then these still possess crossing symmetry but are not Lorentz-covariant unless $\alpha_0 = 1$. (auth)

**26892** TRANSITION AMPLITUDE FOR EXCITED PARTICLES IN THE DUAL-STRING MODEL. Torres-Hernández, J.L. (University of California, Physics Department, Berkeley, California 94720). Phys. Rev. D 11: No. 12, 3565-3571 (15 June 1975).

In the context of the string description for dual resonance models, the Fourier coefficients of a general function (Neumann function) are determined. These are needed in the calculation of the amplitude for the scattering of excited hadrons. (auth)

**26893** HOW QUARK CONFINEMENT SOLVES THE $\eta \to 3\pi$ PROBLEM. Kogut, J. (Laboratory for Nuclear Studies, Cornell University, Ithaca, New York 14853); Susskind, L. Phys. Rev. D 11: No. 12, 3594-3610 (15 June 1975).

Gauge theories of quarks which have chiral SU(3) $\times$ SU(3) symmetries necessarily also have a ninth axial-vector symmetry. Empirically this symmetry is not manifest in the particle spectrum in either the conventional or Goldstone form. We argue on the basis of an exactly solvable model that the apparent lack of the ninth axial-vector symmetry is due to the same long-range forces which confine quarks in infrared-unstable Yang-Mills theories. A related problem is the violation of Sutherland's low-energy theorem for the decay $\eta \to \pi^+\pi^-\pi^0$. We show how the same phenomenon naturally ruins the validity of Sutherland's conclusion for soft neutral pions. In the course of this work we discuss the Schwinger model with massive fermions. On the basis of mass perturbation theory and simple energy considerations, it appears that this is a well-behaved theory of confinement. (auth)

## Strong (Baryon No. = 0)

*Refer also to abstracts 26937 and 26938.*

**26894** (DESY-75/21) HEAVY VECTOR MESON DOMINANCE. Walsh, T. F. (Deutsches Elektronen-Synchrotron (DESY), Hamburg (F. R. Germany)). Jul 1975. 11p. Dep. NTIS (US Sales Only) $4.00.

It is suggested that current amplitudes involving known (light) hadrons are dominated solely by light vector mesons $\rho$, $\omega$, $\phi$, $\rho^1$, ... and that current amplitudes where one or more new heavy particles are present are dominated solely by new heavy vector mesons $J/\psi$, $\psi^1$, ... The consequences of this are discussed for radiative decays of the new heavy mesons and for photo and lepto-production of new particles. (auth)

**26895** (HU-TFT-74-30) MESON MASS RELATIONS AND MIXING IN U(4) $\times$ U(4). Montonen, C.; Roos, M.; Toernqvist, N. (Helsinki Univ. (Finland). Research Inst. for Theoretical Physics). 1975. 15p. Dep. NTIS (US Sales Only) $4.00.

The consequences of assigning the $\psi(3105)$ or both the $\psi(3105)$ and the $\psi(3695)$ to the vector meson 16-plet are investigated under the assumption of a simple breaking of U(4) $\otimes$ U(4). The multiplet is found to be nearly ideally mixed, with the $\psi(3105)$ as a $c\bar{c}$ state. New mass relations are found between known mesons, valid in the case of near ideal mixing, and satisfied by the $1^-$, $2^+$ nonets. Using them some missing states are predicted in complete nonets. (auth)

**26896** ESTIMATION OF TWO GAMMA-RAY INVARIANT MASS BY USING THE CHAMBER-15. Miyashita, T. (Waseda Univ., Tokyo (Japan). Science and Engineering Research Lab.). Uchusen Kenkyu; 18: No. 4, 313-324(Jun 1974). (In Japanese).

An analysis was performed on $\pi^0$ events with two $\gamma$-ray invariant mass observed in the chamber 15. Observed $\Sigma E\gamma$-spectra are shown in a figure. Data used for the analysis were in the total energy range more than 10 TeV. The gamma-ray used was in the energy range more than 1 TeV. As the origins of experimental error, the height of producer, spread of core, and estimation of energy were considered. The invariant mass distribution of gamma-ray pairs was obtained. The background was estimated from phase space and is shown in the same mass distribution. In the analysis of the data, 93 pairs, that is 186 gamma-rays, were identified as $\pi^0$ decay, while 128 gamma-rays were noncoupling ones. Among the noncoupling gamma-rays, 109 gamma-rays may couple with the gamma-rays with energy less than 1 TeV. It was concluded that $\pi^0$ events existed statistically significantly in the chamber. It was also shown that the energy determination by the track counting method was able to be made with an error within 20%, since the coincidence of background and the significant peak around the stationary mass of $\pi^0$ was seen. (JA)

**26897** CORRECTIONS TO THE NUCLEAR GOLDBERGER-TREIMAN RELATION AND PIONIC FORM FACTOR. II. FORBIDDEN TRANSITION. Kim, C.W. (Department of Physics, The Johns Hopkins University, Baltimore, Maryland 21218); Kim, J. Phys. Rev. D 11: No. 11, 3347-3351 (1 June 1975).

Corrections to the nuclear Goldberger-Treiman relation and the pionic nuclear form factor are investigated using the $\Delta J = 0$ transition with parity change as an example of forbidden transitions. It is shown that (1) the corrections are as large as the main term, implying that the original Goldberger-Treiman relation with pion-pole dominance is no longer valid, (2) the pionic form factor $f_{\pi\beta}(q^2)$ is a very rapidly varying function of $q^2$ for $|q^2| < m_\pi{}^2$, and (3) the ratio $[f_{\pi\beta}(0) / f_{\pi\beta}(-m_\pi{}^2)]$ is essentially zero. (auth)

**26898** MATTER DISTRIBUTION IN $\pi^*$ AND $K^*$ AND POSSIBLE UNIVERSALITY OF MESON FORM FACTORS. Chou, T.T. (Department of Physics and Astronomy, University of Georgia, Athens, Georgia 30602 and Institute for Theoretical Physics, State University of New York, Stony Brook, New York 11790). Phys. Rev. D 11: No. 11, 3145-3147 (1 June 1975).

Analysis of the Fermi National Accelerator Laboratory 200—GeV meson-proton elastic scattering data based on the geometrical picture leads to predictions for the matter distribution in $\pi^*$ and $K^*$. The result suggests that form factors for these particles are essentially identical. At higher incident energies, form factors calculated from the model will remain fixed, while the effective blackness for the particles increases. (auth)

## Strong (Baryon No. = 1)

**26899** (JINR-E2-8865) STRINGENT ISOSPIN CONSTRAINTS ON EXPERIMENTAL OBSERVABLES OF $(0\ 1/2 \to 0'0'\ 1/2)$. Ion, D. B. (Joint Inst. for Nuclear Research, Dubna (USSR)). 1975. 28p. NTIS (US Sales Only) $4.50.

The stringent constraints implied by the isospin invariance on the experimental observables of $(0\frac{1}{2} \to 0'0'\frac{1}{2})$ reactions are investigated. These results are useful to obtain certain tests of the isospin invariance when the experimental data on differential cross sections and spin density matrices of $(0\frac{1}{2} \to 0'0'\frac{1}{2})$ reactions are available. (auth)

**26900** $\pi N \to \pi\Delta_\delta$ PRODUCTION BY SINGLE QUARK TRANSITION IN SU(6) × O(3) STRUCTURE. Hirano, M. (Hokkaido Univ. of Education, Sapporo (Japan)). Prog. Theor. Phys. (Kyoto); 52: No. 6, 1841-1854(Dec 1974).

We analyze $\pi N \to \pi\Delta_\delta$ production based upon the SU(6) × O(3) structure of N and $\Delta_\delta$ in the symmetric quark model. On the assumption of additivity and factorizability, we investigate the general properties of $N \to \Delta_\delta$ transition mechanism by a single quark transition. We calculate the differential cross section of the Δ (1236) production in the forward region at high energies and its Δ (1236) spin density matrix. The results agree fairly well with experimental data although there is a difference by a factor $\lesssim 2$ between the results and data in the forward region at $-t \lesssim 0.2$. We also predict both quantities of the Δ(1950) production. (auth)

**26901** MESON-BARYON BACKWARD SCATTERING AND RESONANCE CORRELATION. Ghoroku, K.; Imachi, M.; Otsuki, S. (Kyushu Univ., Fukuoka (Japan). Dept. of Physics); Toyoda, F. Prog. Theor. Phys. (Kyoto); 53: No. 1, 125-139(Jan 1975).

Backward meson-baryon scattering is studied by taking the urbaryon rearrangement diagram (URD) into consideration. Analysis of $\pi N$ backward scattering at 6 GeV/c shows that the resonant part of the helicity amplitude, which corresponds to the Z type URD, has a Hankel function dependence similar to the forward case. Considering that many s-channel resonances with different parities and signatures cancel out with one another leading to a rapid decrease with s in the backward region, it may be rather surprising that the Hankel type structure is observed. In other words, this suggests again importance of the peripheral interaction to form correlated resonances. The non-resonant amplitude corresponding to the X type URD is real and smooth. It is found that natural parity baryon resonances are much more suppressed than unnatural ones, as compared with the prediction of the SU(6) models. A possible scheme of SU(6) breaking is discussed. (auth)

**26902** ELASTIC DIFFRACTION SLOPES OF MESON-BARYON SCATTERING. Yoshida, T. (Fukushima Univ. (Japan). Faculty of Education). Prog. Theor. Phys. (Kyoto); 53: No. 1, 140-151 (Jan 1975).

The diffraction slope parameters B for $\pi^+p$ and $K^+p$ at 25.2 and 40.1 GeV/c are calculated by the use of experimental values of B for $\pi^-p$ and $K^-p$ and of the total cross sections for $\pi^-p$, $\pi^+p$, $K^-p$ and $K^+p$. Various inelastic processes are grouped into several relatives associated with quark-line diagrams of D-, H-, X- and Z-types. Overlap functions due to D and H (Z is neglected and X is set equivalent to H) are taken as Gaussian types in the impact-parameter space, and helicities are neglected. Decomposition of the final baryonic states into 1, 8 and 10 is made. A damping factor is introduced for strangeness-exchange amplitudes. The predicted values of the diffraction slope parameters B are essentially independent of the free parameter (seven parameters against six input data). The results are, in the unit of $(GeV/c)^{-2}$, $8.97 \pm 0.41$ and $8.25 \pm 0.46$ at 25.2 GeV/c and $9.42 \pm 0.51$ and $8.17 \pm 0.43$ at 40.1 GeV/c for $\pi^+p$ and $K^+p$, respectively. These values are in agreement with those extrapolated from low energy data. For $K^-n$ and $K^+n$, B and total cross sections are calculated; the results comparatively depend on the free parameter. The predicted values of total cross sections cover the experimental ones with minor ambiguity. (auth)

**26903** GENERALIZED DUALITY, π-REGGEON EXCHANGE AND RESONANCE DECAY EFFECTS IN INCLUSIVE REACTIONS. Hidaka, K. (Tokyo Univ. (Japan). Dept. of Physics). Prog. Theor. Phys. (Kyoto); 53: No. 1, 175-184(Jan 1975).

Inclusive processes $pp \to \Delta^{++}X$, $\pi^-p \to \Delta^{++}X$, $pp \to pX$ and $\pi^-p \to pX$ are investigated in the proton fragmentation region and at small momentum transfer on the basis of Reggeon exchange. For the first two reactions a simple π-exchange mechanism explains the observed cross section successfully both in shape and in absolute magnitude in $-1.0 \lesssim x \lesssim -0.6$. For the other reactions some resonance decay effects, such as $pp \to \Delta X$, $(\Delta \to p\pi)$ as well as π exchange are significant at high energies and the observed cross sections are well saturated by their sum in $-0.85 \lesssim x \lesssim -0.5$. Double counting in a "duality" scheme is never committed in adding these effects because of G-parity conservation. The reason for the significance of π exchange in these processes is also explained in this scheme. (auth)

**26904** ANALYSIS OF $P_{11}N \to VN$ REACTIONS THROUGH s-CHANNEL PICTURE. Inoue, K.; Kawabe, T.; Uehara, M. (Kyushu Univ., Fukuoka (Japan). Dept. of Physics). Prog. Theor. Phys. (Kyoto); 52: No. 5, 1567-1582(Nov 1974).

Four neutral vector meson production processes initiated by $\pi^+N$ and $K^+N$ are analysed through s-channel picture. Amplitudes for $\pi^-p \to \rho^0n$ are constructed by Hankel functions of the first kind under the assumption that imaginary parts of pion exchange amplitudes, too, are saturated by s-channel resonances with a common impact parameter $b_0 \simeq 5\ GeV^{-1}$, while for real parts the long tail in the impact parameter space is very important. It is shown that partial cross sections, density matrices and the phase coherence between unnatural parity exchange amplitudes are well reproduced. Through SU(3) counting, ω production is analysed and using $\rho^0$ and ω production amplitudes, we investigate $K^{*0}$ and $K^{*0}$-bar productions. Experimental features are qualitatively reproduced. Strong exchange degeneracy between π and B is shown to be broken. (auth)

**26905** COMMENT ON A SCALING LAW FOR PION-NUCLEON SCATTERING. Eichmann, G.; Kaiser, F. (Institut für Theoretische Kernphysik, Universität Karlsruhe, Karlsruhe, Germany). Phys. Rev. D 11: No. 11, 3352-3354 (1 June 1975).

A recently proposed scaling law for meson-baryon scattering is shown to be in disagreement with important features of $\pi N$ data. (auth)

**26906** INCLUSIVE ρ EFFECTS ON TWO-PION PRODUCTION. Randa, J. (Physics Department, Texas A & M University, College Station, Texas 77843). Phys. Rev. D 11: No. 11, 3232-3235 (1 June 1975).

The effects of inclusive ρ production on two-pion distributions are investigated. The differential cross section, correlation function, and azimuthal asymmetry are calculated for decay-product pions. Two cases of ρ polarization are considered. (auth)

**26907** SYSTEMATICS OF CROSSOVER EFFECTS IN INELASTIC DIFFRACTION DISSOCIATION. Berger, E.L. (High Energy Physics Division, Argonne National Laboratory, Argonne, Illinois 60439). Phys. Rev. D 11: No. 11, 3214-3231 (1 June 1975).

The behavior in momentum transfer of the differential cross sections for (exclusive) inelastic diffraction dissociation processes is examined. Cross sections for pairs of reactions related to each other by $t$-channel charge conjugation (line reversal) may exhibit crossover phenomena near $t = -0.2\ (GeV/c)^2$ similar to elastic scattering. Detailed predictions for crossovers are developed based on the pion-exchange Deck model and are contrasted with expectations obtained from an analogy with the Regge phenomenology of elastic scattering. The two sets are not always in agreement. Experimental checks are proposed. Quantitative values of slopes and integrated cross sections are derived from the Reggeized Deck model for $Kp \to K^*\pi p$, and for the charge-exchange reaction $Kp \to K^*\pi n$; these are presented as a function of energy. Selections on decay angles in the rest frame of the low-mass excited system are described as a method for isolating the π-exchange Deck graph. (auth)

**26908** EVEN-WAVE HARMONIC OSCILLATOR THEORY OF BARYONIC STATES: A NEW CLASSIFICATION. Mitra, A.N. (International Centre for Theoretical Physics, Miramare, Trieste, Italy and Department of Physics, University of Delhi, Delhi-7, India). Phys. Rev. D 11: No. 11, 3270-3283 (1 June 1975).

An even-wave harmonic oscillator (h.o.) model for the quark-quark interaction proposed recently for the baryon spectrum is described with a detailed mathematical formulation. The mechanism, which formally admits of a relativistic extension of the Feynman-Kislinger-Ravndal type, leaves unchanged the usual h.o. predictions for 56 states (symmetric) for all $L$ values even and odd, but totally keeps out the 20 states (antisymmetric). It changes the structure of the 70 states considerably, while retaining the principal feature of linear rise of $(mass)^2$ with $J$ through the interplay of two reduced slopes of magnitudes $\alpha/2$ and $\sqrt{3}\alpha/2$, compared to $\alpha$ for the 56 spectrum. The new features of the 70 states are (i) a dual spectrum leading to considerable mass splitting compared to the usual h.o. model without SU(6) -breaking effects, (ii) prediction of a unique $(70, 0^+)$ supermultiplet *lower* than the $(70, 1^-)$, and (iii) the prediction of low radial excitations because of the reduced slopes. The immediate experimental successes are (i) an understanding of $P_{11}(1470)$ together with possible Δ,Σ,Λ counterparts, (ii) two distinct mass groupings manifest in $(70, 1^-)$ states, and (iii) plausible explanation of $P'_{11}(1750)$ as a radial excitation of $P_{11}(1470)$. The mass splittings of Δ,Σ,Λ from their $N$ counterparts, as between 56 and 70 states, conform extremely well to the ratio of the *average* slope $\delta = \alpha(1+\sqrt{3})/4 \approx 0.68\,\alpha$ for 70 states to that $(\alpha)$ for the 56, thus facilitating the prediction of Δ,Σ,Λ positions from those of $N$ states for different quantum numbers. Extra predictions of states are discussed in terms of an extended classification scheme given by an ordered set of four quantum numbers $(n_s l_s n_l l_l)$ defined in the text. (auth)

**26909** GALILEAN INVARIANCE OF THE PION-NUCLEON INTERACTION. Ho, H.W.; Alberg, M.; Henley, E.M. (Physics Department, University of Washington, Seattle, Washington 98195). Phys. Rev. C 12: No. 1, 217-224 (July 1975).

We examine the role of Galilean invariance in a nonrelativistic theory of pions and nucleons. We define a nonrelativistic pion-nucleon interaction $h$ as one which in perturbation theory gives the same matrix for a physical reaction as the limit of small nucleon velocities of the relativistic matrix. The latter matrices are always Galilean invariant, but this does not require that $h$ be Galilean invariant. If pion emission or absorption occurs from a nucleon moving in a potential, then the Galilean correction term can be shown to be ambiguously of order $v/c$ or of order $v^2/c^2$. We show that $h$ cannot always reproduce the nonrelativistic limit of a relativistic matrix. Finally, we suggest that pion production by nucleons on nuclei with excitation of giant dipole and quadrupole states may be particularly sensitive to the presence of a Galilean correction term in the production matrix. (auth)

**26910** PATH-INTEGRAL EVALUATION OF THE TIME-EVOLUTION PROPAGATOR FOR QUADRATIC HAMILTONIAN SYSTEMS WITH APPLICATION TO THE LEE MODEL. Pell, J. L. Baton Rouge, LA; Louisiana State Univ. (1974). 72p. University Microfilms Order No. 75-14,275.

Thesis (Ph. D.).

Path-integral methods are used to derive an exact expression for the time-evolution propagator for a broad class of systems with quadratic Hamiltonians. For a certain sub-class of such systems, the result is reduced to a simplified closed form. The propagators are exhibited for several illustrative elementary cases and for the Lee model for a single heavy particle, with two isotopic states of equal mass, interacting with a bosonic field. The propagator for the latter is used to calculate the survival probability of the unstable state of the heavy particle with no bosons present. (Diss. Abstr. Int., B)

## *Strong (Baryon No. ≥ 2)*

*Refer also to abstract 26992.*

**26911** (CONF-750654-6) COHERENT DISSOCIATION AND TOTAL CROSS SECTIONS OF NEUTRONS IN THEIR COLLISIONS WITH NUCLEAR TARGETS AT FERMILAB ENERGIES. Biel, J.; Bromberg, C.; Blesser, E. J. (Rochester Univ., N.Y. (USA); Fermi National Accelerator Lab., Batavia, Ill. (USA); Stanford Linear Accelerator Center, Calif. (USA); Northwestern Univ., Evanston, Ill. (USA)). Jun 1975. 14p. Dep. NTIS $4.00.

From international conference on high energy physics; Palermo, Italy (Jun 1975).

Preliminary results from an investigation of the coherent dissociation of neutrons into (p $\pi^-$) systems in the 120 GeV/c-300 GeV/c range of neutron momenta are presented. Using a variety of nuclear targets, for light elements the dominance of diffraction dissociation over the electromagnetic excitation of neutrons is observed. Conversely, for the heaviest elements coherent dissociation of neutrons is dominated by production in the nuclear coulomb field. Cross sections for diffraction dissociation on nuclei change by less than 10 percent in this neutron-momentum range. The experiment was performed at the Meson Detector Laboratory of Fermilab. (6 figures) (auth)

**26912** (JINR-P1-9018) CORRELATIONS IN THE REACTION DP → PPN AT SMALL MOMENTA TRANSFERRED. Aladashvili, B. S.; Badelek, B.; Glagolev, V. V. (Joint Inst. for Nuclear Research, Dubna (USSR)). 1975. 12p. (In Russian). Dep. NTIS (US Sales Only) $4.00.

It is shown that the strong correlation of the break up planes and of the quasielastic scattering in the dp → ppn charge retention at small transferred momenta can be qualitatively explained in the framework of the simple Glauber model without taking into account the rescattering. (auth)

**26913** (JINR-P2-8906) BREMSSTRAHLUNG APPROXIMATION FOR INCLUSIVE PROCESSES. Nesterenko, V. V.; Nguyen, S. H. (Joint Inst. for Nuclear Research, Dubna (USSR)). 1975. 15p. (In Russian). Dep. NTIS (US Sales Only) $4.00.

In the framework of the quantum field theory model $L_{int} = -ig\psi^{+}\overleftrightarrow{\partial_\mu}\psi A^\mu$ there has been considered the inclusive reaction a + b → c +..., where a and b are scalar "nucleons" $\psi$, c is a detected meson A. By using the bremsstrahlung approximation the cross section of this reaction has been found in the pionization region. It is shown that a simple model of the bremsstrahlung production of secondaries cannot pretend to describe the inclusive processes in the central region ($x \sim 0$). (3 figures) (auth)

**26914** KNOCKOUT OF AN ISOBAR FROM A DEUTERON. Markushin, V.E. (Institute of Theoretical and Experimental Physics). JETP Lett. 21: No. 7, 211-213 (5 Apr 1975).

It is shown that the probability of observing the configuration Δ-Δ (1236) when an isobar is knocked out from a deuteron is larger than the probability that determines the contribution of the Δ component to the magnetic moment of the deuteron. Theoretical predictions are obtained for the momentum and energy distributions of the Δ isobars knocked out from a deuteron. (auth)

**26915** PROPERTIES OF THE SAITO NONLOCAL POTENTIAL. Englefield, M. J.; Shoukry, H. S. M. (Monash Univ., Clayton (Australia). Dept. of Mathematics). Prog. Theor. Phys. (Kyoto); 52: No. 5, 1554-1566(Nov 1974).

We consider a Schrödinger radial equation containing a local potential and a Saito non-local term which constrains the wave function to be orthogonal to a redundant state. A formula is obtained for the extra phase shift due to the nonlocal term, and conditions for bound states are derived. The extra phase shift is positive, and its low energy behaviour indicates whether a bound state of the local potential is removed, demonstrating the generalized Levinson theorem. For the $\alpha$-$\alpha$ and n-p interactions, we consider the possibility of a local potential which could fit the experimental data with the addition of a Saito term. A strong short-ranged attraction is necessary in the n-p case. (auth)

**26916** ON THE MULTIPLICITY DISTRIBUTION IN SEMI-INCLUSIVE REACTIONS. Nakamura, R.; Hori, S. (Kanazawa Univ. (Japan). Dept. of Physics). Prog. Theor. Phys. (Kyoto); 52: No. 5, 1610-1621(Nov 1974).

It has been observed that the correlation coefficients $f_2^-$ and $f_3^-$ for the negative-prong multiplicity distribution in proton-proton collision, change sign around the incident momentum $P_L \sim 50$ GeV/c. On the other hand, the scaling limits of the specific moments $\langle n \rangle / \langle n \rangle^q$ for the charged-prong multiplicity distribution have been found to increase rapidly with order q. It turned out that existing models cannot explain the above behavior. We present here a formula for the grand-partition function, which contains two functions F(ζ) and g(x) to be determined empirically. The function F(ζ) has turned out to be expressed most likely in terms of the hypergeometric function. The available data were not enough to determine the function g(x) in any reliable degree of accuracy. The experimental data of the correlation coefficients $f_k^-$ for the charged-prong multiplicity distribution, can be used to check the proposed formula. The same formula can be applied to processes other than proton-proton collision. (auth)

**26917** THE FIXED SCATTERER APPROXIMATION AND NUCLEON DEUTERON SCATTERING. Sparrow, D.A. (Department of Physics, Massachusetts Institute of Technology, Cambridge, Massachusetts 02139). Ann. Phys. (N.Y.) 91: No. 1, 157-193 (May 1975).

A method of solving the Schroedinger Equation for the scattering from two fixed local potentials is presented. The solutions are used within the framework of the fixed scatterer approximation to perform model calculations of *N-D* scattering using both effective range theory potentials and a "semi-realistic" potential with a strong repulsive core. For smooth potentials approximate solutions to the fixed scatterer problem are proposed and found to be quite accurate. Other procedures for calculating elastic scattering were compared with the exact fixed scatterer approximation. The results show that the neglect of longitudinal momentum transfer in the Glauber multiple diffraction theory is a severe effect except in the forward direction. For small angle scattering the Glauber prediction for the double scattering amplitude is quite accurate, and does not depend strongly upon either the extent of potential overlap, or the ratio *V/E*. Comparisons with the Agassi and Gal results for nonoverlapping potentials indicate that the effects of potential overlap are important, at least for the lowest partial waves. Conclusions about the overall importance of off-energy shell effects in nucleon-deuteron scattering, and about the interference of these effects with the determination of the correlation structure of nuclei are not free from ambiguities. (auth)

**26918** SCATTERING FROM NONOVERLAPPING POTENTIALS II. EXTENSION AND COMPARISON WITH GLAUBER MULTIPLE SCATTERING THEORY FOR DEUTERIUM. Agassi, D. (Max Planck Institut für Kernphysik, Heidelberg, W. Germany); Gal, A.; Mandelzweig, V. Ann. Phys. (N.Y.) 91: No. 1, 194-225 (May 1975).

Scattering on a two-body nuclear target is considered in the nonoverlapping potentials model. The double scattering terms are discussed and it is suggested that their off-shell propagation part is not cancelled by higher-order terms of the multiple scattering series. The effect of reflections is discussed and practical ways to sum up their effect are offered. Finally, spin degrees of freedom are introduced within the nonoverlap formalism. (auth)

**26919** ANALYSIS OF THE $\psi p$ TOTAL CROSS SECTION. Finkelstein, J. (Department of Physics, Columbia University, New York, New York 10027). Phys. Rev. D 11: No. 11, 3337-3339 (1 June 1975).

It is pointed out that the assumption that the $\psi$ is composed of charmed quarks, when taken together with the assumption of conventional dynamics of the states produced in $\psi p$ collisions, does not account for the value of the $\psi p$ total cross section. (auth)

**26920** RADIAL SCALING IN INCLUSIVE AND SEMI-INCLUSIVE DISTRIBUTIONS. Pratap, M.; Schlesinger, J. (Faculté des Sciences, Université de l'Etat, 7000 Mons, Belgique). Phys. Rev. D 11: No. 11, 3340-3343 (1 June 1975).

It has recently been shown that data from 10 GeV/$c$ to 1500 GeV/$c$ lab momenta for the inclusive reactions $pp \rightarrow cX$ ($c = \pi^+$, $K^+$, $p$, $\bar{p}$) are consistent with scaling in terms of $x_R$ ($\equiv 2E/\sqrt{s}$) and $P_T$. In this note, we discuss some elementary consequences of this observation. A straightforward extension of the above scaling property to the semi-inclusive distributions is suggested. (auth)

**26921** POSSIBLE PRODUCTION OF CHARMED HADRONS IN CONJUNCTION WITH THE $\psi$ (3100). Sivers, D. (Stanford Linear Accelerator Center, Stanford University, Stanford, California 94305). Phys. Rev. D 11: No. 11, 3253-3260 (1 June 1975).

If the $\psi$ (3100) is interpreted as bound state of a $c\bar{c}$ pair, then the dynamical mechanism which suppresses its strong decays should also imply that it is produced copiously in association with charmed hadrons. Model calculations indicate the feasibility of looking for charmed particles in events where there is a $\psi$. (auth)

**26922** MULTIPERIPHERAL MODEL OF DIRECT MUON PRODUCTION. Chu, G. (Lawrence Berkeley Laboratory, University of California, Berkeley, California 94720); Koplik, J. Phys. Rev. D 11: No. 11, 3134-3144 (1 June 1975).

We discuss the production of massive $\mu\mu^-$ pairs in $pp$ collisions at high energy using the pion-exchange multiperipheral model. The reaction is assumed to proceed through the sequence (virtual $\pi^+\pi^-$) $\rightarrow \gamma \rightarrow \mu\mu^-$, with a pion form factor included at the first stage. We present both numerical results for various cross sections of interest and some general results following from a Regge expansion. In particular, we find a scaling law for $d\sigma/dq^2$ easily distinguishable from the parton-model analog. The numerical results are in rough agreement with presently available data, and we conclude that the bulk of muon-pair production can be attributed to familiar hadronic mechanisms. (auth)

**26923** SOME CONSIDERATIONS ON THE PRODUCTION MECHANISMS FOR THE $J$ AND $\psi$ PARTICLES AND CHARMED PARTICLES. Pilachowski, L.; Tuan, S.F. (Department of Physics and Astronomy, University of Hawaii, Honolulu, Hawaii 96822). Phys. Rev. D 11: No. 11, 3148-3156 (1 June 1975).

The recent discovery of $J$ and $\psi$ particles with anomalous properties, together with the theoretical expectation of charm related particles with predicted mass values accessible to the Fermilab range of energy, suggests that a reasonably systematic discussion of production mechanisms for these particles might be appropriate. We discuss here (a) hadron-initiated, (b) photon-initiated, and (c) lepton-initiated ($l = e,\mu$) mechanisms for the production of these objects. (auth)

**26924** PHENOMENOLOGY OF PRODUCTION OF MASSIVE AND NEW PARTICLES IN HADRONIC INTERACTIONS. Gaisser, T.K. (Bartol Research Foundation of The Franklin Institute, Swarthmore, Pennsylvania 19081); Halzen, F. Phys. Rev. D 11: No. 11, 3157-3164 (1 June 1975).

We develop a general framework relating cross sections for production of different massive final states in hadronic interactions. The $p\bar{p}$ total inclusive cross section is correctly calculated up to 1500 GeV from the observed $K^-$ inclusive cross section. Predictions for $\Lambda$ production have been confirmed by recent Fermilab measurements. The same framework strongly suggests that $\psi$ ($J$) particles are predominantly produced in association with another massive particle. Production of a $\psi\psi$ pair on a nuclear target at (or below) threshold, where Fermi momentum of the nulceons in the nucleus is important, is calculated and compared to the recent BNL experiment. Production of heavier $\psi$ ($J$) resonances is strongly suppressed at BNL energies. The total cross section (integrated over Feyman $x$) for $pp \rightarrow \psi$ ($\rightarrow \mu^+\mu^-$) in the Fermilab energy range is (100-400 GeV/$c$) is expected to be substantially (2-3 orders of magnitude) above the BNL measurement and should roughly be $10^{-32}$-$10^{-31}$ cm$^2$. Excitation curves for associated production of the $\psi$ (3.105) are calculated for various associated masses. We also calculate cross sections that are large for production of possible massive states of charmed hadrons through the Fermilab and CERN-ISR energy range. (auth)

**26925** KINEMATICAL ASPECTS OF SINGLE-PARTICLE DISTRIBUTIONS. Nyborg, P.; Frodesen, A. G. Phys. Norv.; 8: No. 1, 1-12 (1975).

A survey is given of various two-dimensional distributions which can be used to characterize individual particles from multi-particle final states. For the chosen example with 19-GeV/c proton-proton reactions the purely kinematical distributions (LIPS - Lorentz-invariant phase space) were studied as well as the fairly experiment-like distributions according to the PERPS (peripheral phase space) model. It can be seen that the gross dissimilarities between LIPS and PERPS decrease with increasing multiplicity, and also that some of the variable sets will be more efficient than others in displaying important dynamical effects. (auth)

**26926** THEORETICAL PROTON--PROTON PAIR PRODUCTION CROSS-SECTION CALCULATION. Phippen, J. W. Logan, UT; Utah State Univ. (1974). 129p. University Microfilms Order No. 75-14,464.

Thesis (Ph. D.).

The calculation of both electron-pair and muon-pair production cross sections was made using Feynman's quantum electrodynamics. Pseudoscalar coupling was used between the nucleons and vector coupling was used between the photon and the fermions. The protons were considered as Dirac particles and radiative corrections were omitted. Eight fourth-order Feynman-Dyson diagrams were used. The subsequent sixty-four TRACES were reduced to seven basic topologically different TRACES. From the seven basic TRACES, it was possible to generate the sixty-four TRACES by the proper permutations of the variables. With the mathematics and the corresponding computer programs written down, data (energies and momenta which represent the kinematics of the reaction) were needed. Using a Monte Carlo method, random relativistically invariant data were generated and then substituted into the computer programs from which pair production cross sections were calculated. Using the random nature of the data, it was possible to compare the theoretical treatment of the muon-pair production process with the experimental results of Christenson (1970). The comparison was very favorable. (Diss. Abstr. Int., B)

**26927** MEASUREMENT OF THE RADIATIVE DECAY WIDTH $\Gamma(\bar{K}^{*0}(890) \rightarrow \bar{K}^0\gamma)$. Carithers, W.C.; Mühlemann, P.; Underwood, D. (University of Rochester, Rochester, New York 14627); Ryan, D.G. Phys. Rev. Lett. 35: No. 6, 349-352 (11 Aug 1975).

The differential cross sections for coherent production of $\bar{K}^{*0}(890)$ were measured with nuclear targets. These measurements are interpreted using a two-component model which accounts for Coulomb production and $\omega$ exchange. The radiative decay width is determined to be $\Gamma(\bar{K}^{*0}(890) \rightarrow \bar{K}^0\gamma) = 75 \pm 35$ keV, which is 3 times lower than expected from a simple quark model. (auth)

# Particle Invariance Principles and Symmetries

## General

**26928** FEYNMAN DIAGRAM APPROACH TO DUAL-PARTON MODEL, 2. Spontaneous Symmetry Breaking Due to Collective Partons. Kanki, T. (Osaka Univ., Toyonaka (Japan). Coll. of General Education). Prog. Theor. Phys. (Kyoto); 53: No. 1, 247-260(Jan 1975).

An exploration is made on how the spontaneous symmetry breaking occurs as a collective phenomenon of many partons. The fishing-net Feynman diagram is calculated by means of the functional integral method. This method gives rise to a constraint, as a reflection of the symmetry, on the fields defined on the two-dimensional world sheet. This constraint shows non-independence among the components of the fields and is just the two-dimensional analogue of that proposed in the nonlinear $\sigma$ model. The full symmetry is realized non-linearly and the Goldstone mechanism appears, after elimination of the dependent components. (auth)

**26929** GRADED LIE ALGEBRAS IN MATHEMATICS AND PHYSICS (BOSE-FERMI SYMMETRY). Corwin, L. (Department of Mathematics, Yale University, New Haven, Connecticut 06520); Ne'eman, Y.; Sternberg, S. Rev. Mod. Phys. 47: No. 3, 573-603 (July 1975).

Graded Lie algebras have recently become a topic of interest in physics in the context of "supersymmetries," relating particles of differing statistics. In mathematics, graded Lie algebras have been known for some time in the context of deformation theory. In this paper we discuss basic properties of graded Lie algebras and present various new constructs for producing examples of such algebras. In addition we present a short survey of the role played by graded Lie algebras in mathematics and review in some detail the recent applications of supersymmetry in the physics of particles and fields. (auth)

**26930** DYNAMICS OF SYMMETRY BREAKING. Eliezer, S. (Department of Physics and Astronomy, University of Massachusetts, Amherst, Massachusetts 01002). Phys. Rev. D 11: No. 12, 3611-3615 (15 June 1975).

We show that the SU($n$) -symmetry breaking is obtained from $d_{ijk}x_jx_k = \lambda x_i$. Two derivations of this equation are given: (a) using a bootstrap approach, and (b) minimizing an SU($n$) -invariant potential, leading to spontaneous breakdown of the symmetry. We discuss the implementation of the second approach for the groups SU(3) and SU(4). (auth)

## Applications (Electromagnetic and Weak)

*Refer also to abstract 26881.*

**26931** CHIRAL SYMMETRY AND $\psi \to \psi\pi\pi$ DECAY. Brown, L.S. (Fermi National Accelerator Laboratory, Batavia, Illinois 60510); Cahn, R.N. Phys. Rev. Lett. 35: No. 1, 1-4 (7 July 1975).

Unbroken chiral symmetry (with a vanishing $\sigma$ term) relates the $\psi \to \psi\pi\pi$ decay amplitude to three basic parameters. Two of these parameters put strong angular correlations in the amplitude which, apparently, are not observed. Taking these two parameters to vanish, we obtain an isotropic decay which is strongly peaked in the region where the invariant mass of the $\pi\pi$ system is large. (auth)

**26932** RENORMALIZATION CONSTANTS FOR SCALAR, PSEUDOSCALAR, AND TENSOR CURRENTS. Adler, S.L.; Colglazier, E.W. Jr.; Healy, J.B.; Karliner, I.; Lieberman, J.; Ng, Y.J.; Tsao, H. (Institute for Advanced Study, Princeton, New Jersey 08540). Phys. Rev. D 11: No. 11, 3309-3318 (1 June 1975).

We calculate the renormalization constants describing nucleon and pion matrix elements of scalar, pseudoscalar, and tensor ($S$, $P$, $T$) current densities. For certain of the constants, expressions can be obtained using standard $SU_3$ and chiral $SU_3 \otimes SU_3$ methods. To get the remaining constants, we employ the quark model with spherically symmetric quark wave functions to relate the $S$, $P$, $T$ renormalization constants to known parameters of the usual vector and axial-vector ($V$, $A$) currents. We also evaluate the renormalization constants using the MIT "bag" model quark wave functions. We summarize our results in tabular form, compare the results of the various calculational methods used, and attempt to estimate the accuracy of our predictions. (auth)

**26933** SU(4) AND SU(8) MASS FORMULAS AND WEAK INTERACTIONS. Okubo, S. (Department of Physics and Astronomy, University of Rochester, Rochester, New York 14627). Phys. Rev. D 11: No. 11, 3261-3269 (1 June 1975).

Mass formulas for SU(4) and SU(8) groups have been obtained and are especially simple for degenerate representations. Also, tensor representations of baryon multiplets are discussed together with some applications to weak decay processes. (auth)

**26934** ON-MASS-SHELL CURRENT ALGEBRA AND THE $\pi^0 \to 2\gamma$ DECAY AND PARTIAL CONSERVATION OF AXIAL-VECTOR CURRENT ANOMALY. Golestaneh, A.A. (International Centre for Theoretical Physics, Trieste, Italy, and The Center for Particle Theory, Department of Physics, The University of Texas, Austin, Texas). Phys. Rev. D 11: No. 11, 3240-3245 (1 June 1975).

Using the algebra of the axial-vector current which is defined as a source for the pion field, we study the $\pi^0 \to 2\gamma$ decay rate and the Adler anomaly. Our treatment is identical to the one previously applied to other interactions which are mentioned in the text. It consists of expressing the reduction formula in terms of the above current and evaluating it directly on the mass shell. In the process, we have a set of intermediate states from which we choose the one- and two-meson states. The $3\pi$ continuum is taken into account effectively by a pion isobar, $\pi'$. Hence the $\pi^0$ amplitude is expressed in terms of the parameters of the $\rho$, $\omega$, $\phi$, and $\pi'$ and a coefficient $\beta$ which represents the momentum dependence of the coupling constants of these mesons at the $\pi\gamma$ vertex. A feature of our method is that it does not explicitly depend on the anomaly operator. However, by writing our current in terms of the modified PCAC (partial conservation of axial-vector current) operator, the $\pi^0$ lifetime is linked with the anomaly via these meson data and two unknown parameters, in addition to the $\beta$, which represent the $\pi'$ contributions in the $\pi^0$ lifetime and in the chiral-symmetry-breaking terms underlying the PCAC relation. We give the most appropriate combinations of these parameters for obtaining the observed $\pi^0$ lifetime in accord with the anomaly given by either of the existing quark-theoretical models. We find the correction to the Adler anomaly, in terms of the $\pi'$ parameters and according to the quark model we choose. Assuming that the $\pi'$ contribution to the decay amplitude is small, our results favor the integral charge quark schemes. (auth)

### *Applications (Strong)*

*Refer also to abstracts 26823 and 26893.*

**26935** (FERMILAB-Conf-75/60-THY) $A_1$ PROBLEM, AND SHOULD SU(3) MULTIPLETS BE COMPLETE. Kane, G. L. (Fermi National Accelerator Lab., Batavia, Ill. (USA); Michigan Univ., Ann Arbor (USA)). Jul 1975. 12p. (CONF-750729-1). Dep. NTIS $4.00.

From new directions in hadron spectroscopy meeting; Argonne, Illinois, USA (7 Jul 1975).

The reasons for expecting certain axial vector states to exist (chiral symmetry, the quark model, exchange degeneracy, . . .) are briefly reviewed. The compelling evidence against the existence of the A1 is discussed, some implications of the absence of the A1 for sum rules, the quark model, neutrino reactions, etc. are tentatively explored, SU(3) related axial vector states (Q, D, H), the possibility that SU(3) multiplets will not be complete because of symmetry breaking effects and dynamics, and a possible direction to look to understand which higher mass resonances are considered briefly. (JFP)

**26936** THE U(1) PROBLEM. Weinberg, S. (Lyman Laboratory of Physics, Harvard University, Cambridge, Massachusetts 02138). Phys. Rev. D 11: No. 12, 3583-3593 (15 June 1975).

A detailed analysis of the problems associated with the conserved U(1) axial-vector current in quark-gluon models is presented. It is shown that such models involve a light isoscalar pseudoscalar boson, with a mass less than $(\sqrt{3})\, m_\pi$. The existence of this boson would produce a strong off-shell variation in the $\eta \to 3\pi$ matrix element, thus invalidating the usual conclusions about the rate and energy dependence of this decay. Following Kogut and Susskind, it is proposed that the light Goldstone boson is actually a dipole, with positive- and negative-metric parts, which cancel in matrix elements of gluon-gauge-invariant operators but not in operators such as the U(1) current. It is shown that the masses of the observable pseudoscalar bosons and the $\eta$ decay rate are then just as they would be in a theory without the U(1) symmetry, and in fair agreement with experiment. The application of current algebra to theories with charmed quarks is briefly discussed. (auth)

**26937** $\psi$ (3105) AND SU(8) SYMMETRY. Eliezer, S.; Holstein, B.R. (Department of Physics and Astronomy, University of Massachusetts, Amherst, Massachusetts 01002). Phys. Rev. D 11: No. 11, 3344-3346 (1 June 1975).

We attempt to include $\psi$ (3105) within a simple model of SU(8) symmetry. This is workable only if the pseudoscalar singlet representation mixes with the 63-dimensional representation. Charmed-particle masses are predicted, as well as the mass of paracharmonium. (auth)

## Scattering Theory

*Refer also to abstracts 26715, 26856, and 27185.*

**26938** REGGE AMPLITUDES THROUGH SOLUTION OF $S$-MATRIX EQUATIONS. Frederiksen, J.S. (Research School of Physical Sciences, The Australian National University, Canberra, Australia 2600); Johnson, P.W.; Warnock, R.L. J. Math. Phys. (N.Y.) 16: No. 9, 1886-1900 (Sept 1975).

This work is a first step in a program for construction of meson–meson scattering amplitudes with analyticity, crossing symmetry, and unitarity. The construction is to be carried out by solving a nonlinear integral equation for the partial wave amplitude $a(l,s)$ at complex $l$ and physical $s$. The program is intended to overcome the difficulties encountered in the traditional approach based on the Mandelstam iteration of double-spectral functions. An important initial step is to analyze nonrelativistic potential scattering from this autonomous $S$-matrix viewpoint, in which the Schrödinger equation is replaced by a nonlinear equation for the partial wave amplitude. In the present paper, it is demonstrated that the partial-wave equation has a locally unique solution, provided the potential is of a suitably restricted Yukawa type. This result indicates the feasibility of a pure $S$-matrix approach to dynamics. In the present report, the potential is so restricted in strength as to preclude bound states or resonances. The extension of the method to the case of strong potentials will be pursued in a later publication. (auth)

**26939** EQUIVALENCE BETWEEN TIME-DEPENDENT AND TIME-INDEPENDENT FORMULATIONS OF TIME DELAY. Bollé, D. (Department of Physics and Astronomy, University of Maryland, College Park, Maryland 20742); Osborn, T.A. Phys. Rev. D 11: No. 12, 3417-3423 (15 June 1975).

The time-dependent and time-independent treatments of time delay in two-body scattering are discussed and shown to be completely equivalent. Further, we provide a careful discussion of the definition of time delay in both approaches. We are able to establish that the customary method of using an average limiting process is unnecessary if the time delay is evaluated between normalizable wave packets. (auth)

**26940** UNITARY REPRESENTATION OPERATORS. Ramanujam, G. A. (Nallamuthu Gounder Mahalingam Coll., Pollachi, India). Int. J. Theor. Phys.; 12: No. 6, 407-415(Apr 1975).

A representation (called the U-representation) which remains unitary for all spins and for all ranges of velocities was obtained recently (Alagar Rämanujam, G. Nuovo Cimento: 20A; 27 (1974)). Relevant expressions are obtained for the boosts operator and the observables in such a representation. (auth)

# PHYSICS (LOW-TEMPERATURE)

## Superconductivity

*Refer also to abstracts 26167, 26180, 26196, 26228–26231, 26233, 26235, 26239, 26241, 26242, 26247–26249, 26252, 26253, 26255, 26258, 26277–26280, 26282, 26283, 26292, 26302, 26309, and 26515.*

**26941** SUPERCONDUCTIVITY OF BISMUTH TELLURIDE AT HIGH PRESSURES. Il'ina, M.A.; Itskevich, E.S. (Institute of High-Pressure Physics, Academy of Sciences of the USSR, Akademgorodok, Moscow Province). Sov. Phys.—Solid State 17: No. 1, 89-91 (July 1975).

The effect of hydrostatic pressures up to $\simeq$100 kbar on the superconducting transition temperature $T_c$ of p— and *n*-type bismuth telluride samples of different initial carrier density was investigated. The critical temperature $T_c$ of phase I($Bi_2Te_3$I) was found to depend on the type of conduction and on the initial carrier density. The results obtained are discussed in terms of the band structure of bismuth telluride and its change under pressure. (auth)

**26942** PROBLEM OF THE SUPERCONDUCTIVITY IN LAYERED SEMICONDUCTOR STRUCTURES. Gabovich, A.M.; Moiseev, D.P. (Institute of Physics, Academy of Sciences of the Ukrainian SSR, Kiev). Sov. Phys.—Solid State 17: No. 1, 160-162 (July 1975).

Calculations were made of the critical temperature $T_c$ of the superconducting transition in layered sandwich-type semiconductor (semimetal) structures. The optimum conditions for obtaining high values of $T_c$ were analyzed and the dependences of the critical temperature on the carrier density were determined for an ideal quantized film and for an inhomogeneous film with a rough surface which reflected electrons diffusely. (auth)

**26943** DENSITY OF STATES IN THE ENERGY GAP IN THE SUPERCONDUCTING TRANSITION METAL ALLOY. Tankei, K.; Takano, F. (Tokyo Univ. of Education (Japan). Dept. of Physics). Prog. Theor. Phys. (Kyoto); 52: No. 3, 760-772(Sep 1974).

For a model introduced in a preceding paper for the binary alloy of superconducting transition metals, the density of states is investigated. In the case of single impurity, the bound state is shown to appear in the energy gap if and only if the intraatomic Coulomb repulsion is stronger in the impurity atom than in the host atom. In the case of the finite concentration, it is shown both in the c-linear and the coherent potential approximations that this bound state broadens and constitutes the impurity band in the energy gap if the Coulomb repulsion is stronger in the impurity atom. If the Coulomb repulsion is weaker in the impurity, on the other hand, the impurity band is shown not to appear in the energy gap. (auth)

**26944** RELATION BETWEEN $2\Delta_0/T_C$ AND THE PHONON SPECTRUM OF SUPERCONDUCTORS. Belogolovskii, M.A.; Galkin, A.A.; Svistunov, V.M. (Donets Physicotechnical Institute, Academy of Sciences of the Ukrainian SSR). Sov. Phys.—Solid State 17: No. 1, 83-85 (July 1975).

An approximate solution of the Éliashberg equations at zero temperature is obtained approximating the gap by a step function. An analytic relation between the ratio of the energy gap $\Delta_0$ to the critical temperature $T_C$ and the actual phonon spectrum of a superconductor is derived. The numerical results for many metals and alloys are in good agreement with the experimental values of $2\Delta_0/T_C$. The dependence of $2\Delta_0/T_C$ on the position of the low-frequency singularity in the phonon spectrum is studied for a model phonon density of states consisting of two Einstein peaks. It is found that this ratio can represent a useful criterion of the strength of the electron-electron coupling. (auth)

**26945** PHONON-INDUCED ENHANCEMENT OF THE SUPERCONDUCTING ENERGY GAP. Tredwell, T.J.; Jacobsen, E.H. (Department of Physics and Astronomy, University of Rochester, Rochester, New York 14627). Phys. Rev. Lett. 35: No. 4, 244-247 (28 July 1975).

We have observed large increases of the critical current in Josephson junctions under 10-GHz phonon excitation. Eliashberg has predicted that absorption of microwaves in a superconducting film will increase the energy gap by creating a nonthermal quasiparticle distribution. By modifying this theory to account for phonon absorption we obtain a good agreement with our results on the phonon-induced enhancement of the critical current. We conclude that absorption of phonons of frequency $\omega < 2\Delta$ (T)/ħ increases the superconducting energy gap. (auth)

**26946** SUPERCONDUCTIVITY IN TRANSITION METALS AND COMPOUNDS. Stern, H. (Faculté des Sciences, Université Libre de Bruxelles, Brussels, Belgium). Phys. Rev. B 12: No. 3, 951-960 (1 Aug 1975).

A qualitative account of the $T_c$ systematics of transition metals and compounds is presented from a novel point of view. The suggestion is that the *d* density of states at the Fermi surface is zero near the center of the series. The idea unifies the $T_c$ systematics with other physical properties, and includes the relationship betwen high $T_c$ and lattice instability. The superconductivity of rare earths and neighboring elements is considered with special emphasis on the role of the 4*f* core. (auth)

**26947** MULTIPLE QUANTUM FLUX PENETRATION IN SUPERCONDUCTING LOOPS. Smith, H.J.T. (Physics Department, University of Waterloo, Waterloo, Ontario, Canada); Blackburn, J.A. Phys. Rev. B 12: No. 3, 940-942 (1 Aug 1975).

The dynamics of flux entry into a superconducting loop interrupted by a thin-film Josephson junction have been studied experimentally. A computer simulation of the system yields excellent agreement with these data. It is found that a specific number of flux quanta will bubble into a loop, and that this number depends only on the relative damping which is present. (auth)

**26948** TRANSITION TEMPERATURE OF STRONG-COUPLED SUPERCONDUCTORS REANALYZED. Allen, P.B. (Department of Physics, State University of New York, Stony Brook, New York 11790); Dynes, R.C. Phys. Rev. B 12: No. 3, 905-922 (1 Aug 1975).

A thorough analysis is made of the dependence of the superconducting transition temperature $T_c$ on material properties ($\lambda$, $\mu^*$, phonon spectrum) as contained in Eliashberg theory. The most striking new feature of the analysis is in the asymptotic regime of very large $\lambda$ where $T_c$ is found to equal 0.15 $(\lambda\langle\omega^2\rangle)^{1/2}$ (assuming $\mu^* = 0.1$). This result implies the surprising conclusion that within Eliashberg theory $T_c$ is not limited by the phonon frequencies, and also shows that McMillan's "$\lambda = 2$ limit" is spurious. The McMillan equation (with a prefactor altered from $\Theta_D/1.45$ to $\omega_{\log}/1.2$) is found to be highly accurate for all known materials with $\lambda < 1.5$ but in error for large values of $\lambda$. Correction factors to McMillan's equation are found in terms of $\lambda$, $\mu^*$, and one additional parameter, $(\langle\omega^2\rangle)^{1/2}/\omega_{\log}$. The frequency $\omega_{\log}$ is defined as $\exp\langle\ln\omega\rangle$ where the averages $\langle\ln\omega\rangle$ and $\langle\omega^2\rangle$ are defined using $(2/\lambda\omega)\,\alpha^2F(\omega)$ as a weight factor. These conclusions are based on a combination of analytic and numerical solutions of the Eliashberg equations, and are supported by a comparison with tunneling data. Especially strong support comes from a new experimental result for amorphous $Pb_{0.45}Bi_{0.55}$ reported herein. This material has parameters $\lambda = 2.59$ and $T_c/\omega_{\log} = 0.284$, in serious disagreement with McMillan's formula but in good agreement when the correction factors are included. The McMillan-Hopfield parameter $\eta$ [or $N(0)\langle I^2\rangle$] is extracted from tunneling measurements or from a combination of empirical values of $\lambda$ and neutron-scattering measurements of phonon dispersion. It is proposed that $\eta$ (which is now known not to be accurately constant) is the most significant single parameter in understanding the origin of high $T_c$ and the limitation of $T_c$ by colvalent instabilities. (auth)

**26949** THEORY OF THE UPPER CRITICAL FIELD IN LAYERED SUPERCONDUCTORS. Klemm, R.A.; Luther, A. (Department of Physics, Harvard University, Cambridge, Massachusetts 02138); Beasley, M.R. Phys. Rev. B 12: No. 3, 877-891 (1 Aug 1975).

The upper critical field $H_{c2}$ in layered superconductors is calculated from a microscopic theory in which the electrons are assumed to propagate freely within the individual layers subject to scattering off impurities and to propagate via tunneling between the layers. For the magnetic field parallel to the layers, there is a temperature $T^* < T_c$ below which the normal cores of the vortices fit between the metallic layers, removing the orbital effects as a mechanism for the quenching of superconductivity in the individual layers. In this temperature regime, $H_{c2\parallel}$ is thus determined by the combined effects of Pauli paramagnetism and spin-orbit scattering, and for sufficiently strong spin-orbit scattering rates, $H_{c2\parallel}(T=0)$ can greatly exceed the Chandrasekhar-Clogston Pauli limiting field $H_P$. This unusual behavior is found to be most pronounced in the dirty limit for the electron propagation within the layers and when the electrons scatter many times in a given layer before tunneling to an adjacent layer. Our results are also discussed in light of the available experimental data. (auth)

**26950** THEORY OF THE ARREST OF ELASTIC SOFTENING IN SUPERCONDUCTING $\beta$-W COMPOUNDS. Ting, C.; Birman, J.L. (Department of Physics, Brown University, Providence, Rhode Island 02912). Phys. Rev. B 12: No. 3, 1093-1097 (1 Aug 1975).

Gorkov's model is employed to investigate the temperature dependence of the elastic shear modulus $C_t$ for nontransforming $\beta$-W compounds. By applying the BCS theory to describe the superconducting phase of the system, we show analytically that the onset of superconductivity stops the softening of $C_t$. This result is in agreement with experimental measurements of $C_t$ for both $V_3Si$ and $Nb_3Sn$. (auth)

**26951** CURRENT FLOW IN LARGE JOSEPHSON JUNCTIONS. Barone, A. (Laboratorio di Cibernetica del Consiglio Nazionale delle Ricerche, Arco Felice, Napoli, Italy); Johnson, W.J.; Vaglio, R. J. Appl. Phys. 46: No. 8, 3628-3632 (Aug 1975).

Some aspects of current flow in large Josephson junctions are discussed within the approximation of a linear current-phase relationship. The behavior of various geometrical junction configurations, widely employed in practice, has been investigated. (auth)

**26952** SUPERCONDUCTIVITY IN THE PALLADIUM-HYDROGEN SYSTEM. Papaconstantopoulos, D.A.; Klein, B.M. (George Mason University, Fairfax, Virginia 22030). Phys. Rev. Lett. 35: No. 2, 110-113 (14 July 1975).

Band theory and phonon measurments are used to calculate the electron-phonon coupling constant $\lambda$ for Pd and PdD. The results indicate that superconductivity is absent in Pd metal because of the large value of the Coulomb pseudopotential $\mu^*$, and that superconductivity occurs in PdD primarily because of coupling with the optic phonons. These results are consistent with superconducting transition-temperature measurements for these systems. (auth)

**26953** STRUCTURAL INSTABILITY AND SUPERCONDUCTIVITY IN A-15 COMPOUNDS. Testardi, L.R. (Bell Laboratories, Murray Hill, New Jersey 07974). Rev. Mod. Phys. 47: No. 3, 637-648 (July 1975).

Structural instabilities are now being found in many high-temperature superconductors. Compounds with the A-15 ($\beta$-W) structure comprise the most important group of these materials, and their properties have been extensively studied for over 15 years. A review is given of some of these results, particularly those relating to the elastic behavior. The empirical relation of the structural instability and the anharmonicity to the high superconducting transition temperature is discussed. (auth)

**26954** SINGLE AND MULTIPLE SUPERCONDUCTING WEAK-LINK SYSTEMS. Blackburn, J. A. (Wilfrid Laurier Univ., Waterloo, Ontario); Schwartz, B. B.; Baratoff, A. J. Low Temp. Phys.; 20: No. 5/6, 523-545 (Sep 1975).

Using the one-dimensional Ginzburg–Landau equation and the boundary conditions of Zaitsev, we have evaluated the order parameters in single and multiple weak-link systems. From this information the current-phase characteristics were computed and it was found that Josephson-type behavior occurs for an intermediate range of link parameters. Other pertinent data, including associated thermodynamic free energies of the various solutions, have been obtained. (2 tables, 9 figures, 38 references) (auth)

**26955** SOLUTION OF THE EQUATION FOR THE ENERGY-GAP PARAMETER IN SUPERCONDUCTORS. Ivanchenko, Yu. M.; Medvedev, Yu. V. (Donets Physical-Technical Inst., Kiev). Sov. Phys.-Solid State (Engl. Transl.); 16: No. 8, 1606-1607(Feb 1975).

Translated from Fiz. Tverd. Tela; 16: No. 8, 2457-2459(Aug 1974).

The energy gap equation for anomalous superconductors is solved for the frequency dependent energy gap parameter. The solution is of the form $\Delta = \Sigma/Z$ where $\Sigma$ is the anomalous self-energy and Z is a renormalization factor. (SDF)

**26956** QUASIPARTICLE CONCEPT IN SUPERCONDUCTIVITY. Hittmair, O. (Technische Hochschule, Vienna). Acta Phys. Austriaca; 39: No. 2, 157-171(1974). (In German).

The quasiparticle concept is the key to the understanding of superconductor properties in the BCS theory. If this concept is developed using thermodynamic Green function, a dynamic phonon approximation is then possible. This is possible by an adaptation of the electronphonon coupling strength. The behavior of strongly coupled superconductors deviating from the BCS theory can also be described by the dynamic phonon approximation as comparison with experiment shows. (tr-auth)

# PHYSICS (NUCLEAR)

**26957** (RISO-320) PHYSICS DEPARTMENT ANNUAL PROGRESS REPORT, 1 JANUARY–31 DECEMBER 1974. Moeller, H. B.; Lebech, B. (eds.). (Danish Atomic Energy Commission, Risoe. Research Establishment). Dec 1974. 108p. Dep. NTIS (US Sales Only) $8.50.

Separate abstracts were prepared for 3 of the included sections. Two abstracts were prepared for Nuclear Science Abstracts and one abstract was prepared for ERDA Research Abstracts. (MOW)

*For abstracts of individual sections see: 25696 and 26151.*

## Neutron Interactions with Matter

*Refer also to abstracts 25753 and 27416.*

**26958** (IFA-DNBR-14-1975) SET OF PROGRAMS FOR THE STORAGE AND SELECTIVE RETRIEVAL OF EXPERIMENTAL NEUTRON NUCLEAR DATA FOR THE DANEX LIBRARY. (INDEX, SINTEX, REDEX). Mateescu, S.; Vasiliu, G. (Institutul de Fizica Atomica, Bucharest (Romania)). 1975. 26p. (In Rumanian). Dep. NTIS (US Sales Only) $4.50.

The programs presented permit the storage and selective retrieval of nuclear neutron experimental data for the computerised library DANEX. The data stored are the typical cross sections necessary for reactor calculations. They are stored on magnetic tapes, and the retrieval can be offered on listings or tapes. (auth)

**26959** (ORNL-TM-5018) MEASUREMENT OF SECONDARY NEUTRONS AND GAMMA RAYS PRODUCED BY NEUTRON BOMBARDMENT OF WATER OVER THE INCIDENT ENERGY RANGE 1 TO 20 MeV. Morgan, G. L. (Oak Ridge National Lab., Tenn. (USA)). Aug. 1975. Contract W-7405-Eng-26. 46p. Dep. NTIS $5.50.

The spectra of secondary neutrons and gamma rays produced by neutron bombardment of a thick (approx. 1 mean free path) sample of water have been measured as a function of the incident neutron energy over the range 1 to 20 MeV. Data were taken for angles of $90^0$ and $140^0$. A linac (ORELA) was used as a neutron source with a 47-m flight path. Incident energy was determined by time-of-flight, while secondary spectra were determined by pulse-height unfolding techniques. The results of the measurements are presented in forms suitable for comparison to calculations based on the evaluated data files. (6 figures, 9 tables) (auth)

**26960** (VTT-YDI-5) ETOF: PROGRAM TO PROCESS DATA FROM ENDF/B TO FORM. Patrakka, E.; Teraesvirta, R. (Valtion Teknillinen Tutkimuskeskus, Helsinki (Finland)). Jun 1973. 61p. Dep. NTIS (US Sales Only) $6.25.

Program ETOF processes basic nuclear data in the ENDF/B format and produces the data required for the generation of FORM library. ETOF is mainly based on the ETOM-1 program. However, a number of modifications have been made in the processing procedures, e.g. an improved treatment of the resolved resonance region has been incorporated. In addition, some auxiliary routines have been added. ETOF is written in FORTRAN V for the Univac 1108 and is designed to be computer independent as far as possible. In addition to printed results, the output includes punched cards in the format appropriate for the generation of the FORM library. (auth)

**26961** APPARATUS FOR HIGH-PRESSURE, LOW-TEMPERATURE, NEUTRON-SCATTERING MEASUREMENTS. Kleb, R.; Copley, J.R.D. (Solid State Science Division, Argonne National Laboratory, Argonne, Illinois 60439). Rev. Sci. Instrum. 46: No. 9, 1190-1192 (Sept 1975).

We describe an apparatus which is designed for neutron-scattering studies of single crystals under hydrostatic pressures up to 5 kilobar and at temperatures between 77 and ~300 K. The safety features of the system are emphasized. (auth)

**26962** A THREE-DIMENSIONAL NEUTRON TRANSPORT PROBLEM. Mangiarotti, L. (Istituto Matematico "U. Dini," Università di Firenze, Viale Morgani 67/A, 50134 Firenze, Italy). J. Math. Phys. (N.Y.) 16: No. 9, 1840-1843 (Sept 1975).

We study the stationary neutron transport Boltzmann equation as applied to a three-dimensional system $D$, made by a rectangular multiplying core surrounded by a finite reflector, in both the Lebesgue space $L_2(D)$ and the space $C(D)$ (with the sup norm). As a result of this analysis, we prove some basic properties, such as the continuous dependence of the neutron flux on the parameters characterizing both the geometrical and the material properties of the system and the continuous and monotonic dependence of the average number of secondary neutrons per collision in the core on these parameters. (auth)

**26963** A TOROIDAL SOLUTION OF THE VACUUM EINSTEIN FIELD EQUATIONS. Thorne, K.S. (Kellogg Radiation Laboratory, California Institute of Technology, Pasadena, California 91125). J. Math. Phys. (N.Y.) 16: No. 9, 1860-1865 (Sept 1975).

This paper presents a new solution to the vacuum Einstein field equations for the static external gravitational field of a toroidal singularity. This solution is unique among known toroidal solutions in that the singularity is locally cylindrically symmetric; near it the spacetime geometry becomes that of an infinite line mass ("Levi-Civita metric"). (auth)

## Nuclear Properties and Reactions, $A \leq 5$

*Refer also to abstracts 26827 and 27136.*

**26964** COULOMB CORRECTIONS FOR EXTRACTING SPECTROSCOPIC FACTORS USING ANALYTICITY. Kisslinger, L.S.; Nichols, K. (Department of Physics, Carnegie-Mellon University, Pittsburgh, Pennsylvania 15213). Phys. Rev. C 12: No. 1, 36-41 (July 1975).

The Coulomb scattering and Coulomb distortions are included in the optimal expansion technique in the $\cos\theta$ plane. From $p$-$^3$He elastic scattering from 4–20 MeV an energy independent spectroscopic factor for $^3\mathrm{H}_e \rightarrow p+d$ is found, with an accuracy of a few percent. The method seems most promising for transfer reactions. (auth)

**26965** COMPARISON OF REALISTIC LOCAL AND ONE-BOSON-EXCHANGE POTENTIALS IN THE THREE-NUCLEON SYSTEM. Afnan, I.R.; Read, J.M. (School of Physical Sciences, The Flinders Unversity of South Australia, Bedford Park, South Australia, 5042). Phys. Rev. C 12: No. 1, 293-305 (July 1975).

The disagreement that currently exists regarding the calculated and experimental values of the triton binding energy ($E_T$) and the doublet scattering length ($^2a$) is analyzed in considerable detail. Using the unitary pole approximation, which has previously been tested with great success, we have calculated $E_T$ and $^2a$ for a large class of realistic potentials. The results show that the one-boson-exchange potentials (OBEP) give in general ~1 MeV more binding for $^3$H and correspondingly smaller $^2a$ than the local hard- and soft-core potentials. This difference is shown to be partly due to the fact that the OBEP have in general smaller deuteron $D$-state probability, and partly due to the fact that they fit the $^1S_0$ $n$-$p$ rather than the $p$-$p$ data. Finally, we demonstrate that the correlation between $E_T$ and $^2a$, predicted by Phillips on the basis of separable potential calculations, has validity for the more realistic interactions. (auth)

**26966** COULOMB EFFECTS IN HADRON-NUCLEUS AND NUCLEUS-NUCLEUS COLLISIONS AND THE HADRON-NEUTRON AMPLITUDE. Franco, V.; Varma, G.K. (Physics Department and Institute for Nuclear Theory, Brooklyn College of the City University of New York, Brooklyn, New York 11210). Phys. Rev. C 12: No. 1, 225-242 (July 1975).

Coulomb effects in high energy charged hadron-nucleus collisions are studied in a formalism which is exact within the framework of multiple diffraction theory and takes into account the extended charge effects of the incident hadron and the bound protons. Several more approximate but simpler formulas are also considered and their accuracy discussed. Results are extended to include heavy-ion collisions in the optical limit of the Glauber theory and in the Chou-Yang model. Applications are made to the proton-deuteron elastic and elastic plus quasielastic scattering measurements below 70 GeV to extract the ratio of real to imaginary part and the slope parameter of the proton-neutron elastic scattering amplitude. The results are compared with those from dispersion relation calculations and from earlier analyses. Approximate analytic formulas derived for $p$-$d$ scattering give results almost identical to the more exact expressions. For nucleus-nucleus collisions the Coulomb effects are found to be important over a rather wide range of momentum transfers. (auth)

**26967** $^4$He($p$, $2p$)$^3$H AND $^4$He($p$, $pd$)$^2$H REACTIONS AT 156 MeV. Frascaria, R.; Roos, P.G.; Morlet, M.; Marty, N.; Willis, A.; Comparat, V.; Fujiwara, N. (Institut de Physique Nucléaire, Orsay, France). Phys. Rev. C 12: No. 1, 243-250 (July 1975).

Quasifree proton-proton and proton-deuteron scattering cross sections on $^4$He have been measured and compared with theoretical calculations in the distorted wave impulse approximation. Information on the low

components for the proton and deuteron momentum distributions in $^4$He are deduced. (auth)

**26968** ELASTIC PROTON SCATTERING ON $^4$He AT 156 MeV. Comparat, V.; Frascaria, R.; Fujiwara, N.; Marty, N.; Morlet, M.; Roos, P.G.; Willis, A. (Institut de Physique Nucléaire 91406, Orsay, France). Phys. Rev. C 12: No. 1, 251-255 (July 1975).

The differential cross section for the proton $^4$He elastic scattering at 156 MeV was measured in the angular range from 10° to 168°. An optical potential analysis with an exchange term is performed and extended to the 100 and 85 MeV data. Some of the impulse approximations are tested and a comparison is performed with a Glauber calculation. (auth)

**26969** PION-$^4$He SCATTERING AROUND THE 3/2, 3/2 RESONANCE. Binon, F.; Duteil, P.; Gouanère, M.; Hugon, L.; Jansen, J.; Lagnaux, J.; Palevsky, H.; Peigneux, J.; Spighel, M.; Stroot, J. (Institut Interuniversitaire des Sciences Nucléaires, Belgium). Phys. Rev. Lett. 35: No. 3, 145-148 (21 July 1975).

We present $\pi^- - ^4$He differential cross sections at 110, 150, 180, 220, and 260 MeV, as well as total cross sections at eleven energies between 67 and 285 MeV. (auth)

**26970** ON THE UNITARY POLE EXPANSION OF THE POTENTIALS I AND III OF MALFLIET AND TJON. Bakker, B. L. G. (Amsterdam Univ. (Netherlands). Natuurkundig Lab.). Z. Phys., A; 272: No. 3, 335-340(Mar 1975).

4 figs.; 8 tabs.; 3 refs.

The unitary pole expansion for the local soft-core potentials I and III of Malfliet and Tjon is obtained, and the Faddeev-Lovelace equations are solved for the separable potentials. The energy E of the triton and the doublet scattering length a were obtained. The results are $-8.59$ MeV $\leq E \leq -8.57$ MeV and 0.89 fm $\leq a \leq$ 0.91 fm. For the quartet scattering length a value $a = 6.39$ fm was found. (auth)

**26971** REACTION $^3$He($d$, $t$)2$p$ AT 23.5 MeV CENTER OF MASS. Rutkowski, R.W.; Gross, E.E. (Oak Ridge National Laboratory, Oak Ridge, Tennessee 37830). Phys. Rev. C 12: No. 2, 362-369 (Aug 1975).

We have measured the absolute spectra for the yield of high-energy tritons for the process $^3$He($d$, $t$)2$p$ at 24 MeV c.m. Elastic scattering of deuterons from $^3$He has also been measured at the same c.m. energy. The reaction data are characterized by forward and backward peaking and by a deep minimum near 90° c.m. The forward-angle triton spectrum is consistent with a simple pickup process. A comparison of the forward-angle triton yield to the cross section for elastic scattering at back angles provides strong evidence both for the dominance of the pickup process at small angles in the reaction and for the importance of this process to back-angle elastic scattering. (auth)

## Nuclear Properties and Reactions, 6 ≤ A ≤ 19

*Refer also to abstracts 26826, 27066, 27101, and 27116.*

**26972** (JAERI-1231, pp 69-70) POLARIZATION-ASYMMETRY DIFFERENCE IN THE INELASTIC SCATTERING OF 50 MeV PROTONS FROM CARBON-12. Nakamura, M. (Kyoto Univ.). 13 Dec 1972.

From symposium on nuclear reaction and nuclear structure; Tokai, Ibaraki, Japan (13 Dec 1972).

In proceedings of a symposium on nuclear reaction and nuclear structure. (Japan Atomic Energy Research Inst., Tokyo).

Polarization of protons in the reaction $^{12}$C(p,p')$^{12}$C(4.44 MeV) has been observed. It is compared with the asymmetry of a completely polarized beam in the same reaction. Considerable differences are found. The DWBA calculation indicates that the adiabatic condition is reasonably well satisfied in the present case. It is likely that a simple macroscopic model does not explain such large differences. (auth)

**26973** INVESTIGATION OF THE SPECTRUM OF PROTONS EMITTED BY THE C$^{12}$ NUCLEUS AT 90° WHEN BOMBARDED By 1-GeV/$c$ NEGATIVE PIONS. Bayukov, Yu.D.; Vorob'ev, L.S.; Leksin, G.A.; Pivnyuk, N.A.; Stolin, V.L.; Fedorov, V.B. (Institute of Theoretical and Experimental Physics). JETP Lett. 21: No. 7, 210-211 (5 Apr 1975).

A spark chamber with thin electrodes, in which the particles were stopped, was used to measure the spectrum of the protons emitted from a C$^{12}$ nucleus in the angle range 95°±20° under the influence of $\pi^-$ mesons with momentum 1.06 GeV/$c$. (auth)

**26974** ROLE OF PARTICLE-HOLE INTERACTION IN THE FOUR-PARTICLE-FOUR-HOLE STATES IN $^{16}$O. Takada, K.; Tazaki, S. (Kyushu Univ., Fukuoka (Japan). Dept. of Physics). Prog. Theor. Phys. (Kyoto); 52: No. 4, 1205-1213(Oct 1974).

Role of the particle-hole interaction in the four-particle-four-hole states in $^{16}$O is investigated with relation to the alpha-cluster-like spatial correlations by using the vertically-truncated-subspace shell model which was proposed by Kamimura, Matsuse and Takada. It is concluded that the coupling between the two kinds of modes (spatially correlated four-particle mode and four-hole mode) is nearly independent of the spatial localization of the four particles outside the $^{16}$O core and the particle-hole interaction does not strongly mix the states of the two "rotors" (the ground band of $^{20}$Ne and that of $^{12}$C,). (auth)

**26975** MIRROR $\gamma$ DECAYS IN $^{13}$C AND $^{13}$N. Marrs, R.E.; Adelberger, E.G.; Snover, K.A.; Cooper, M.D. (Department of Physics, University of Washington, Seattle, Washington 98195). Phys. Rev. Lett. 35: No. 4, 202-205 (28 July 1975).

We have measured the $\gamma$-ray branching ratios of the lowest $T=3/2$ levels in $^{13}$C and $^{13}$N, and the absolute strength of the $\gamma_0$ transition in $^{13}$N. The mirror electromagnetic selection rule is obeyed by the M1 ($\gamma_0$ and $\gamma_2$) transitions. However the E1($\gamma_1$) transitions exhibit a surprisingly large charge asymmetry. Charge-dependent differences in the radial wave functions do not account for a similar asymmetry in strong $T=1/2 \rightarrow T=1/2$ E1 transitions in mass 13. (auth)

**26976** COMMENT ON LARGE-MOMENTUM-TRANSFER PHOTOPRODUCTION OF $J$ (3.1). Pilachowski, L.; Simmons, W.A.; Tuan, S.F. (Department of Physics and Astronomy, University of Hawaii at Manoa, Honolulu, Hawaii 96822). Phys. Rev. Lett. 35: No. 4, 261-263 (28 July 1975).

Recent data on photoproduction of $J^0$(3.1) suggest that the fraction of events produced with large momentum transfer $t$ is surprisingly large. Here we comment on a mechanism involving diffractive $\rho^0$ photoproduction in conjunction with large-$t$ $J^0$(3.1) production as a possible way of understanding some aspects of the anomaly. (auth)

**26977** C + $^{19}$F REACTIONS AT $E_{lab}$ = 25–72 MeV. Zeller, A.F.; Choppin, G.R. (Department of Chemistry, The Florida State University, Tallahasse, Florida 32306); Plendl, H.S.; Delaune, C.I. Phys. Rev. C 12: No. 1, 124-127 (July 1975).

Thick targets of natural carbon were bombarded with $^{19}$F ions at $E_{lab}$ = 25–72 MeV. Residual activities were counted off-line with a Ge(Li) detector. $\gamma$ rays from the decay of $^7$Be, $^{22}$Na, $^{24}$Na, $^{27}$Mg, $^{28}$Mg, $^{28}$Al, and $^{29}$Al were observed, and yield curves were determined. Yield curves calculated with the Blann-Plasil statistical evaporation code were compared with the experimental results and found to agree well in most cases. (auth)

**26978** 5.534 MeV LEVEL IN $^{23}$Na. Jones, G.D.; Green, P.W.; Kelly, D.T.; Frank, G.G.; Kuehner, J.A. (Tandem Accelerator Laboratory, McMaster University, Hamilton, Ontario, Canada). Phys. Rev. C 12: No. 1, 132-135 (July 1975).

The $^{12}$C($^{12}$C,$p\gamma$)$^{23}$Na reaction has been used at an incident energy of 28.2 MeV to populate the 5.534 MeV level in $^{23}$Na. A particle $\gamma$-ray linear polarization measurement carried out simultaneously with a particle $\gamma$-ray angular correlation measurement for the 3.457 MeV transition between the 5.534 MeV and 2.077 MeV ($7/2^+$) levels allows an unambiguous $J^\pi = 11/2^+$ assignment to be made to the 5.534 MeV level. The multipole mixing ratio of the 2.829 MeV transition between the 5.534 MeV and 2.705 MeV ($9/2^+$) levels has been obtained and confirms previous measurements, as does the measured branching ratio for the two observed decay modes from the 5.534 MeV level. (auth)

**26979** PION-NUCLEUS ELASTIC SCATTERING AT INTERMEDIATE ENERGIES. Julius, D.I.; Rogers, C. (Institut für Theoretische Kernphysik, Universität Karlsruhe, Germany). Phys. Rev. C 12: No. 1, 206-216 (July 1975).

Dynamical modifications of the pion-nucleus optical potential due to binding effects on the target nucleons are calculated for pions of energies in the range 120–600 MeV. Calculations are performed using an independent particle model for the nucleus; however, a prescription for incorporation of the Pauli pinciple is given and its effects are studied. Resulting corrections to the potential are of the order of 50–100% near (3,3) resonance and fall to negligible values at energies less than 120 MeV and greater than 450 MeV. Our correction is such as to increase the nuclear opacity. Pion-nucleus total cross sections and angular distributions are modified by binding effects by 10–20%. Comparison with $\pi^-$$^{12}$C total cross section data shows that our theory reproduces well the energy dependence of the correction required to reconcile theory and experiment, and produces about 50% of the necessary increase in the magnitude of the theoretical cross section. (auth)

**26980** MEASUREMENT OF THE BRANCHING RATIO FOR THE $\beta$ DECAY OF $^{19}$Ne TO THE 1554 keV STATE IN $^{19}$F AND ITS IMPLICATIONS FOR A STUDY OF THE NEUTRAL WEAK CURRENT. Freedman, S.J.; Del Vecchio, R.M.; Callias, C. (Joseph Henry Laboratories, Princeton University, Princeton, New Jersey 08540). Phys. Rev. C 12: No. 1, 315-317 (July 1975).

The branching ratio $[^{19}Ne \rightarrow {}^{19}F^{*}$ (1554 keV) + $e^{+} + \nu]$ / $[^{19}Ne \rightarrow {}^{19}F + e^{+} + \nu]$ as inferred from observing a subsequent $\gamma$ transition in $^{19}F$ is found to be $(8.2 \pm 2.0) \times 10^{-6}$. Uncertainties about possible $^{19}O$ contamination lead to the conservative interpretation of this result as an upper limit for the branching ratio. The implications for a recently suggested study of inelastic neutrino scattering from $^{19}F$ are discussed. (auth)

**26981** ($\pi, \pi N$) PUZZLE: EFFECTS OF PION CHARGE EXCHANGE. Silbar, R.R. (Theoretical Division, Los Alamos Scientific Laboratory, University of California, Los Alamos, New Mexico 87544). Phys. Rev. C 12: No. 1, 341-342 (July 1975).

The ratio of cross sections for nucleon knockout by pions, e.g. $\sigma[^{12}C(\pi^{-}, \pi N)^{11}C] / \sigma[^{12}C(\pi^{+}, \pi N)\ ^{11}C]$, is shown to be insensitive to pion charge either before or after the knockout collision. (auth)

**26982** STUDY OF UNBOUND LEVELS IN $^{10}C$ VIA $^{10}B(^{3}He, t)$. Schneider, M.J.; Ridley, B.W.; Rickey, M.E.; Kraushaar, J.J.; Zimmerman, W.R. (Nuclear Physics Laboratory, Department of Physics and Astrophysics, University of Colorado, Boulder, Colorado 80302). Phys. Rev. C 12: No. 1, 335-337 (July 1975).

The unbound level structure of $^{10}C$ has been studied using the $^{10}B(^{3}He,t)^{10}C$ reaction. Bombarding energy was 38.2 MeV and tritons were detected in an energy-loss spectrometer. In the seven spectra taken, at lab angles from 2.5° to 30°, the broad 6.60 MeV prominence was well fitted by a single Lorentzian-shaped peak, while the 5.28 MeV region was well fitted by two peaks. The excitation energies of these peaks were obtained using known levels in $^{11}C$, populated from the $^{11}B$ impurity in the $^{10}B$ target. (auth)

**26983** INFLUENCE OF SHORT RANGE CORRELATIONS ON $(e, e'p)$ CROSS SECTIONS. Royer, D.; Mougey, J.; Priou, M.; Bernheim, M.; Bussière, A.; Gillebert, A. (Centre d'Etudes Nucleaires de Saclay, 91190 Gif-sur-Yvette, France); Wagner, G.J. Phys. Rev. C 12: No. 1, 327-329 (July 1975).

Distorted wave impulse approximation calculations of $^{12}C(e,e'p)$ cross sections show no sensitivity to short range correlations in the range of recoil momenta covered by the data. For this result, which is in contrast to previous calculations, it is crucial to use correlated wave functions of correct rms radii on which the quality of the fit depends critically. (auth)

**26984** MOMENTUM DISTRIBUTIONS OF ISOTOPES PRODUCED BY FRAGMENTATION OF RELATIVISTIC $^{12}C$ AND $^{16}O$ PROJECTILES. Greiner, D.E.; Lindstrom, P.J.; Heckman, H.H.; Cork, B.; Bieser, F.S. (Lawrence Berkeley Laboratory and Space Sciences Laboratory, University of California, Berkeley, California 94720). Phys. Rev. Lett. 35: No. 3, 152-155 (21 July 1975).

The fragment momentum distributions in the projectile rest frame are, typically, Gaussian shaped, narrow, consistent with isotropy, depend on fragment and projectile, and have no significant correlation with target mass or beam energy. The nuclear temperature is inferred from the momentum distributions of the fragments and is approximately equal to the projectile nuclear binding energy, indicative of small energy transfer between target and fragment. (auth)

**26985** PRODUCTION CROSS SECTIONS OF Be ISOTOPES IN C AND O TARGETS BOMBARDED BY 2.8-GeV $\alpha$ PARTICLES: IMPLICATIONS FOR FACTORIZATION. Raisbeck, G.M.; Yiou, F. (Laboratoire René Bernas du Centre de Spectrométrie Nucléaire et de Spectrométrie de Masse, 91406 Orsay, France). Phys. Rev. Lett. 35: No. 3, 155-159 (21 July 1975).

We have measured the production cross sections of $^{7}Be$ in C and O targets, and $^{9}Be$ and $^{10}Be$ in C targets irradiated by 2.8-GeV $\alpha$ particles. The results are discussed in terms of the applicability of a factorization relationship proposed for high-energy nuclear cross sections. (auth)

**26986** MEASUREMENT OF PROMPT-MUON PRODUCTION IN NUCLEON-NUCLEUS COLLISIONS. Bintinger, D.; Curry, J.; Pilcher, J. (The Enrico Fermi Institute, University of Chicago, Chicago, Illinois 60637); Rubbia, C.; Sulak, L.; Ford, W.; Mann, A.K.; Cline, D.; Imlay, R.; Wanderer, P. Phys. Rev. Lett. 35: No. 2, 72-75 (14 July 1975).

We have measured the production cross section for prompt muons relative to pions, produced in nucleon-nucleus interactions at incident energies from 30 to 300 GeV and for muon transverse momenta from 1 to 2.3 GeV/c. Upper limits on the production and leptonic decay of heavy particles are presented. (auth)

**26987** SEARCH FOR NARROW RESONANCES PRODUCED BY NEUTRON DISSOCIATION. Bleser, E.J. (Fermi National Accelerator Laboratory, Batavia, Illinois 60510); Gobbi, B.; Kenah, L.; Keren, J.; Rosen, J.; Ruchti, R.; Scott, H.; Spelbring, D.; Biel, J.; Bromberg, C.; Ferbel, T.; Slattery, P.; Underwood, D.; Freytag, D. Phys. Rev. Lett. 35: No. 2, 76-79 (14 July 1975).

We present the results of a search for charged two-body decays of neutral high-mass resonances produced via neutron dissociation. The spectrometer, located in the *M*-3 beam at Fermilab, was sensitive to final states produced forward ($x > 0.3$) with charged multiplicity $\lesssim 4$. We find no significant enhancement in the high-mass $K^{+}\pi^{+}$ or $pK^{-}$ systems. The cross section times branching ratio is $\lesssim 50$ nb/nucleon for $K\pi$ masses between 2 and 3 GeV. (auth)

**26988** ASYMMETRY OF BETA-RAY ANGULAR DISTRIBUTION IN POLARIZED NUCLEI AND *G*-PARITY NONCONSERVATION. Morita, M.; Tanihata, I. (Department of Physics, Osaka University, Toyonaka, Osaka 560, Japan). Phys. Rev. Lett. 35: No. 1, 26-29 (7 July 1975).

We have derived an equation for the $\beta$-ray angular distribution including Coulomb corrections, radiative corrections, induced effect, and higher-order nuclear matrices. With this equation and the experimental data on $\beta$-ray asymmetries in polarized $^{12}B$ and $^{12}N$, we conclude that the strength of the second-class induced tensor is $f_T/f_A = -(0.96 \pm 0.35) \times 10^{-3}$ in the limit of the impulse approximation. A possible modification of this value due to mesonic corrections is discussed. (auth)

**26989** MEASUREMENT OF THE $\alpha$-PARTICLE SPECTRUM RESULTING FROM $\pi^{-}$ CAPTURE IN $^{12}C$. Comiso, J.; Meyer, T.; Schlepuetz, F.; Ziock, K.O.H. (Physics Department, University of Virginia, Charlottesville, Virginia 22901). Phys. Rev. Lett. 35: No. 1, 13-15 (7 July 1975).

We have detected and identifed charged particles with an energy of more than 0.5 MeV that were emitted by a carbon target following the absorption of stopped negative pions. Particles of mass 1, 2, 3, 4, 6, and 7 were found. The energy spectrum of the $\alpha$ particles was measured from 0.5 to 30 MeV. The rate for the emission of $\alpha$'s integrated over all energies above 0.5 MeV was found to be $1.00 \pm 0.07$ $\alpha$/pion. (auth)

**26990** TRANSIENT FIELD MEASUREMENT FOR $^{18}O$ IN Fe. van Hienen, J. F. A. Utrecht, Netherlands; Rijksuniversiteit (1975). 14p.

The integral precession of $^{18}O$ recoiling into magnetized Fe has been measured at a recoil velocity of $v/c = 0.021$. The measured effect, $\Delta\theta = -2.7 \pm 0.2$ mrad, yields a negative sign for the g-factor of the first-excited $2^{+}$ state. The magnitude of this effect is $2.2 \pm 0.4$ mrad larger than calculated with the Lindhard-Winther theory and the known value of the g-factor. This enhancement is ascribed to contributions from unpaired polarized 1s and 2s electrons. (auth)

**26991** REALISTIC NUCLEAR CHARGE DISTRIBUTION AND THE PROTON OPTICAL POTENTIAL. Marwadi, P. R.; Shastry, C. S. (Birla Inst. of Tech. and Science, Pilani, India). Indian J. Pure Appl. Phys.; 13: No. 169-174(Mar 1975).

Electrostatic potentials due to the realistic charge distributions are calculated for $^{13}C$, $^{16}O$, $^{40}Ca$, $^{58}Ni$, $^{197}Au$ and $^{209}Bi$ and are compared with the corresponding potentials due to uniform charge distribution. The effect of the realistic charge distribution on the proton-nucleus optical potential is discussed. An estimate of change in differential cross-section expected, if one replaces the electrostatic potential due to uniform nuclear charge distribution by a realistic electrostatic potential, is given. Differential cross-sections obtained by using (i) the realistic electrostatic potential, $V_p$ (r), and (ii) the electrostatic potential $V_c$ (r), corresponding to the uniform charge distributions in the proton-nucleus optical model are compared. (auth)

**26992** SIMPLE QUARK-COUNTING PREDICTIONS FOR BAND STRUCTURE IN $p + Be^{9} \rightarrow (h^{+} + h^{-} + X,$ $h^{+} + h^{+} + X, h^{-} + h^{-} + X)$. Chodos, A.; Willemsen, J.F. (Laboratory for Nuclear Science and Department of Physics, Massachusetts Institute of Technology, Cambridge, Massachusetts 02139). Phys. Rev. Lett. 35: No. 6, 334-338 (11 Aug 1975).

A model based on simple quark counting is presented, which describes the inclusive production of charged hadron pairs at large transverse momenta. Predictions are given for the ratios of cross sections for $p + Be^{9} \rightarrow h_1 + h_2 + X$, where $H_1$ and $h_2$ are any of $p$, $\bar{p}$, $\pi^{+}$, $\pi^{-}$, $K^{+}$, and $K^{-}$. The essential feature of the model is that the valence quarks of the initial particles must be included in the counting. (auth)

**26993** RADIATIVE WIDTH OF THE 2.31-MeV LEVEL IN $^{14}N$. Rasmussen, V.K.; Metzger, F.R. (Bartol Research Foundation of The Franklin Institute, Swarthmore, Pennsylvania 19081). Phys. Rev. C 12: No. 2, 706-707 (Aug 1975).

By observation of the resonant scattering of bremsstrahlung, the width of the 2.31-MeV level of $^{14}N$ has been measured as $6.2 \pm 0.6$ meV. This is somewhat smaller than previous values and in disagreement with inelastic electron scattering results and the prediction of the conserved vector current theory from the shape of the $^{14}O \rightarrow {}^{14}N$ $\beta^{+}$ spectrum. (auth)

**26994** TWO-STEP ANALYSIS OF THE $^{18}O(p, t)^{16}O$ $2^{-}$ EXCITATION AND PHASE RELATIONS IN THE NONORTHOGONAL TERM. Segawa, H.; Kubo, K.; Arima, A. (Department of Physics, University of Tokyo, Tokyo, Japan). Phys. Rev. Lett. 35: No. 6, 357-360 (11 Aug 1975).

We perform second-order distorted-wave Born-approximation analyses of the $^{18}O(p,t)^{16}O$ $2^-$ excitation. The experimental angular distribution can be well reproduced by the simultaneous consideration of $(p,t,t)$, $(p,p',t)$, and $(p,d,t)$ processes and the last two processes are found to be comparably important. The phase relations in the nonorthogonal term are also discussed and it is shown that this term gives a negligibly small contribution to such unnatural-parity-state excitation processes. (auth)

**26995** PION PHOTOPRODUCTION AT THRESHOLD ON $^6$Li AND LOW-ENERGY THEOREMS. Moreno, M.; Pestieau, J.; Urias, J. (Institut de Physique Théorique, Université de Louvain, Louvain-la-Neuve, Belgique). Phys. Rev. C 12: No. 2, 514-522 (Aug 1975).

The Low, Kroll-Ruderman, and Fubini-Furlan-Rossetti theorems are derived in the case of pion photoproduction on $^6$Li. Particular care has been taken to be consistent with electromagnetic current conservation and Low's theorem in the extrapolation from soft to real pions. This is new compared to previous treatments of soft pion theorems in nuclear processes where one photon is present. Difficulties due to the spin−1 nature of $^6$Li have been put forward. (auth)

**26996** MASS AND ENERGY DISTRIBUTIONS OF FUSION PRODUCTS FROM $^{32}$S ON $^{12}$C, $^{25}$Mg, AND $^{40}$Ca. Garrett, J.D.; Wegner, H.E. (Brookhaven National Laboratory, Upton, New York 11973); Cormier, T.M.; Cosman, E.R.; Lazzarini, A.J. Phys. Rev. C 12: No. 2, 481-488 (Aug 1975).

The mass and energy distributions for fusion products corresponding to 128.9 MeV $^{32}$S on $^{12}$C, $^{25}$Mg, and $^{40}$Ca targets has been measured at 8° (lab) using a time-of-flight spectrometer. The heaviest product observed with significant cross section for each system has a mass five units less than that of the corresponding compound system. Lighter dominant mass groups are separated by approximately three mass units. Such mass systematics can be understood in terms of neutron, proton, and α-particle competition in the deexcitation of the compound system and are reproduced qualitatively by particle evaporation calculations. (auth)

**26997** HALF-LIVES OF SOME $T = 1/2$ MIRROR DECAYS. Azuelos, G.; Kitching, J.E. (Foster Radiation Laboratory, McGill University, Montreal, P. Q., Canada). Phys. Rev. C 12: No. 2, 563-566 (Aug 1975).

Precision measurements of the half-lives of the decay of some $T=1/2$ mirror nuclei have been determined. The results are $^{11}$C (1222.9 ± 1.2 sec), $^{19}$Ne (17.219 ± 0.017 sec), $^{21}$Na (22.47 ± 0.03 sec), $^{23}$Mg (11.327 ± 0.014 sec), $^{25}$Al (7.174 ± 0.007 sec), $^{27}$Si (4.109 ± 0.004 sec), and $^{29}$P (4.083 ± 0.012 sec). In addition, the half-life of $^{26}$Al$^m$, which proceeds by a pure Fermi decay, has been determined to be 6.346 ± 0.005 sec. (auth)

**26998** $^{17}O(\alpha, d)^{19}F$ TO THE 7/2$^+$ AND 11/2$^+$ STATES. Fortune, H.T.; Medsker, L.R. (Physics Department, University of Pennsylvania, Philadelphia, Pennsylvania 19174); Chien, W.S.; Nann, H.; Wildenthal, B.H. Phys. Rev. C 12: No. 2, 359-361 (Aug 1975).

The pertinence of the observed features of the $^{17}O(\alpha,d)^{19}F$ transitions to the first two 7/2$^+$ and first two 11/2$^+$ states in $^{19}$F to rotational-model and shell-model descriptions of this nucleus is outlined. (auth)

**26999** MICROSCOPIC MODEL STUDY OF NUCLEON ELASTIC SCATTERING FROM $^{16}$O. George, J.; Philpott, R.J. (Department of Physics, The Florida State University, Tallahassee, Florida 32306). Phys. Rev. C 12: No. 2, 658-665 (Aug 1975).

The compound resonances and the bound states observed in the $^{16}$O+ nucleon system are studied using the continuum shell model. The method of solution involves a division of configuration space as in the $R$-matrix theory. Shell model basis states which are eigenfunctions of the spherical harmonic oscillator potential are employed in the construction of trial wave functions for the internal region. The basis states contain active $1p_{1/2}$, $1d_{5/2}$, and $2s_{1/2}$ orbits as well as higher orbits into which at most a single nucleon is placed. Excitations of up to four particles from the spherical closed core are included. The two-body interaction used in our model was taken from a shell model calculation for $^{18}$O and $^{18}$F by Zuker, supplemented by a two-body central Gaussian interaction from True and a one-body interaction of Woods-Saxon form. Calculated neutron total cross sections, neutron and proton phase shifts as well as differential cross sections and polarizations are presented and compared with experiment. Calculated spectroscopic factors of $^{17}$O states are also given. The results show excellent qualitative and fair quantitative agreement with experiment. An investigation of the discrepancies between calculated and experimental resonance widths point to our lack of knowledge of the effective interaction. (auth)

**27000** DIRECT MEASUREMENT OF THE MASSES OF $^{11}$Li AND $^{26-32}$Na WITH AN ON-LINE MASS SPECTROMETER. Thibault, C.; Klapisch, R.; Rigaud, C.; Poskanzer, A.M.; Prieels, R.; Lessard, L.; Reisdorf, W. (Laboratoire René Bernas du Centre de Spectrométrie Nucléaire et de Spectrométrie de Masse, 91406 Orsay, France). Phys. Rev. C 12: No. 2, 644-657 (Aug 1975).

The use of an on-line mass spectrometer to make direct mass measurements of short-lived isotopes far from the stability line has been improved to yield more accurate mass measurements for $^{27-30}$Na, new mass measurements for $^{11}$Li, $^{31,32}$Na, and to remove a discrepancy between existing mass measurements of $^{26}$Na. The mass excesses (keV) measured are: $^{11}$Li, 40940 ± 80; $^{26}$Na, −6901 ± 25; $^{27}$Na, −5620 ± 60; $^{28}$Na, −1140 ± 80; $^{29}$Na, 2650 ± 100; $^{30}$Na, 8370 ± 200; $^{31}$Na, 10600 ± 800; $^{32}$Na, 16400 ± 1100. The $^{11}$Li value indicates that it is bound by only 170 ± 80 keV. The masses of $^{31}$Na and $^{32}$Na imply that these nuclei are more tightly bound than expected from theoretical predictions. (auth)

**27001** EVAPORATION TRACKS FROM $\pi^-$ CAPTURE IN LOADED NUCLEAR EMULSIONS. Carruth, R.T.; Larson, D.A.; Gangotena, S.; French, J.D. (Auburn University, Auburn, Alabama 36830). Phys. Rev. C 12: No. 2, 374-377 (Aug 1975).

Some features of evaporation tracks following $\pi^-$ capture in carbon are reported. These include angles between tracks, ranges by track pairs for two track events, and degree of collimation of tracks for three track events, from which some conclusions are drawn. Kinematical analysis is used to find evidence for nuclear structure effects in the breakup of the residual nucleus. (auth)

# Nuclear Properties and Reactions, 20 ≤ A ≤ 38

*Refer also to abstracts 26819, 26978, 26984, 26996, 26997, and 27000.*

**27002** (JAERI-1231, pp 123-133) $F_{\frac{1}{2}}$ SHELL NUCLEI. Horie, H. (Tokyo Inst. of Tech.). 13 Dec 1972.

From symposium on nuclear reaction and nuclear structure; Tokai, Ibaraki, Japan (13 Dec 1972).

In proceedings of a symposium on nuclear reaction and nuclear structure. (Japan Atomic Energy Research Inst., Tokyo).

Properties of $1f_{\frac{1}{2}}$ and N = 29 and 30 nuclei are reviewed from the standpoint of the nuclear shell model. Energy levels of $1f_{\frac{1}{2}}$ nuclei and N = 29 and 30 nuclei and the electromagnetic properties are discussed. (auth)

**27003** (JAERI−1231, pp 137-141) NEW TAMM−DANCOFF CALCULATIONS OF FOUR-BODY MODES IN $^{20}$Ne. Tazaki, S. (Kyushu Univ., Fukuoka). 13 Dec 1972.

From symposium on nuclear reaction and nuclear structure; Tokai, Ibaraki, Japan (13 Dec 1972).

In proceedings of a symposium on nuclear reaction and nuclear structure. (Japan Atomic Energy Research Inst., Tokyo).

Effects of ground-state correlations induced by the four-body modes are discussed in detail. It is found that the effect on energy-level systematics is comparable to that of the higher level mixing which is related to spatial localization (spatial correlations) and that the ground-state correlations enhance the spatial correlations. Then it is concluded that the ground-state correlations are as important as the higher level mixing. (auth)

**27004** EVIDENCE FOR A $^{12}$C+$^{12}$C COLLECTIVE BAND IN $^{24}$Mg. Cosman, E.R.; Cormier, T.M.; Van Bibber, K.; Sperduto, A.; Young, G. (Massachusetts Institute of Technology, Cambridge, Massachusetts 02139); Erskine, J.; Greenwood, L.R.; Hansen, O. Phys. Rev. Lett. 35: No. 5, 265-268 (4 Aug 1975).

Excitation functions of the reaction $^{12}C(^{12}C,p)^{23}Na$ reveal a distinct set of resonances in the 11/2$^+$, 13/2$^+$, (15/2$^+$), and (17/2$^+$) members of the $^{23}$Na $K^\pi = 3/2^+$ ground-state band near $E_x(^{24}Mg)$ =25.2, 28.2, and 33.3 MeV. These plus earlier data suggest the possible existence of an excited collective band in $^{24}$Mg with very high deformation and large $^{12}$C + $^{12}$C width. (auth)

**27005** ELASTIC AND INELASTIC PROTON SCATTERING FROM $^{21}$Ne AND $T = 1$ ENERGY LEVELS IN $^{22}$Na. Chambon, B.; Desgrolard, P.; Drain, D.; Lambert, M.; Perschaye, N. (Institut de Physique Nucléaire, Université Claude Bernard Lyon-I and *IN2P3*, 43, Bd du 11 November 1918, 69621 Villeurbanne, France). Phys. Rev. C 12: No. 1, 1-13 (July 1975).

Excitation functions for the reactions $^{21}Ne(p,p)$ and $^{21}Ne(p,p')$ were studied at eight angles for bombarding energies in the range $E_p$ = 0.6 - 2.0 MeV. A total of 21 resonances were observed corresponding to $^{22}$Na levels between 7.3 and 8.6 MeV excitation energy. The proton angular momenta are determined and spin and parity assignments are presented. Several new isobaric analog pairs in $^{22}$Na and $^{22}$Ne are also presented. Previous experimental and nuclear structure information is discussed. (auth)

**27006** SPECTROSCOPIC STUDIES INVOLVING TWO-STEP PROCESSES IN THE REACTION $^{28}Si(d,p)^{29}Si(5/2^+)$. Boyd, R.N.; Kaminstein, J.; Arking, R.; Clement, H. (Nuclear Structure Research

Laboratory, University of Rochester, Rochester, New York 14627). Phys. Rev. C 12: No. 1, 14-20 (July 1975).

Particle-$\gamma$-ray angular correlations have been studied in the $^{28}$Si($d,p$)$^{29}$Si(5/2$^+$, 203 MeV) reaction and subsequent $\gamma$-ray decay to the $^{29}$Si ground state. The calculated correlations represent the data well near the stripping peak, and show appreciable sensitivity to the details of the two-step reaction processes. This sensitivity allows the determination of structure information about excited core components of the nuclear wave function. (auth)

**27007** MASSES OF $T_z = -1/2$ NUCLEI IN THE $1f_{7/2}$ SHELL. Mueller, D.; Kashy, E.; Benenson, W.; Nann, H. (Cyclotron Laboratory and Department of Physics, Michigan State University, East Lansing, Michigan 48824). Phys. Rev. C 12: No. 1, 51-55 (July 1975).

The ($p$,$^6$He) reaction was used to observed and measure the masses of the proton-rich nuclei $^{45}$V, $^{49}$Mn, and $^{53}$Co, thus completing all mirror pairs in the $f_{7/2}$ shell. New measurements of the masses of $^{43}$Ti, $^{47}$Cr, $^{51}$Fe, and $^{55}$Ni were made using the ($^3$He, $^6$He) reaction. Coulomb energy differences of the $T = 1/2$ mirror pairs are extracted, and the new masses are used to predict the masses of proton-rich nuclei with $23 \leq Z \leq 28$. (auth)

**27008** $^{12}$C($^{12}$C, $\alpha$)$^{20}$Ne EXCITATION FUNCTIONS AND ANGULAR DISTRIBUTIONS. Greenwood, L.R.; Segel, R.E.; Raghunathan, K.; Lee, M.A. (Northwestern University, Evanston, Illinois 60201 and Argonne National Laboratory, Argonne, Illinois 60439); Fortune, H.T.; Erskine, J.R. Phys. Rev. C 12: No. 1, 156-178 (July 1975).

Excitation functions have been measured at a laboratory angle of 5° over an incident energy range of 18–25.5 MeV (c.m.) for the $^{12}$C($^{12}$C,$\alpha$) reaction leading to about 30 levels in $^{20}$Ne ($E_x$ = 0–20 MeV). Angular distributions were measured at five energies. An Ericson fluctuation analysis yields the result that most levels are populated by a large nonstatistical reaction component. A significant compound-nuclear component is also present, with correlation widths on the order of 150–250 keV (c.m.). The energy-averaged cross sections have been compared with statistical compound-nuclear (Hauser-Feshbach) calculations. This comparison indicates the presence of a strong direct-reaction mechanism, especially for the members of the proposed 8p-4h band (at 7.196, 7.834, 9.040, and 12.16 MeV). A pronounced minimum in the excitation functions is evident at $E_{c.m.}$ = 19.2 MeV, near the recently reported strong resonance in the $^{12}$C($^{12}$C,$p$)$^{23}$Na channel. Other correlated effects also appear to be present at specific energies, but the cross correlations, calculated for the entire energy range, are largely statistical. (auth)

**27009** UNNATURAL PARITY TRANSITIONS IN $^{22}$Ne($p$, $t$)$^{20}$Ne. Chien, W.S.; King, C.H.; Nolen, J.A. Jr.; Shahabuddin, M.A.M. (Cyclotron Laboratory, Michigan State University, East Lansing, Michigan 48824). Phys. Rev. C 12: No. 1, 332-334 (July 1975).

New measurements have been made with the $^{22}$Ne($p$,$t$) reaction to excite the $K^\pi = 2^-$ rotational band in $^{20}$Ne. Coupled-channel Born approximation calculations fail to account for the angular distribution of the transition to the $4^-$ member of this band, although they describe well that for the transition to the $2^-$ member. Particularly significant is the failure of the cross section for the $4^-$ transition to decrease at forward angles. This behavior is in disagreement with that expected for unnatural parity transitions in ($p$,$t$) reactions which proceed through multistep processes involving inelastic excitations. The implications of these results for the reaction mechanism are discussed. (auth)

**27010** IDENTIFICATION OF THE 6$^+$ AND 8$^+$ YRAST STATES IN $^{40}$Ca. Simpson, J.J.; Wilson, S.J. (Department of Physics, University of Guelph, Guelph, Ontario N1G 2W1, Canada); Green, P.W.; Kuehner, J.A.; Dixon, W.R.; Storey, R.S. Phys. Rev. Lett. 35: No. 1, 23-26 (7 July 1975).

The reaction $^{28}$Si($^{14}N$,$p\pi\gamma$)$^{40}$Ca has been used to populate high-spin states in $^{40}$Ca, and levels at 6930 and 8098 keV are identified as the 6$^+$ and 8$^+$ yrast states. The results suggest the termination at spin 8 of the band based on the 3.35-MeV state. The previously identified level at 6930 keV is found to be a doublet. (auth)

**27011** INVESTIGATIONS OF (n,t) CROSS SECTIONS AT 14.7 MeV. Biro, T.; Sudar, S.; Miligy, A.; Dezsoe, Z.; Csikai, J. (Kossuth Lajos Tudomanyegyetem, Debrecen, Hungary). J. Inorg. Nucl. Chem.; 37: No. 7/8, 1583-1585 (Jul 1975).

The (n,t) reaction cross sections have been measured at $E_n$ = 14.7 MeV for 5 isotopes ($^9$Be, $^{27}$Al, $^{39}$K, $^{59}$Co, $^{103}$Rh) and 7 elements (B, K, Tl, Fe, Ni, Cu, Zn), between A = 9 and 103 using the tritium beta counting technique. The (n,t) reaction cross sections show a general trend to decrease with increasing atomic number. Results are compared with statistical model predictions. (auth)

**27012** SHELL-MODEL CALCULATIONS IN A = 23 TO 28 NUCLEI. van Hienen, J. F. A. Utrecht, Netherlands; Rijksuniversiteit (1975). 15p.

Thesis.

Energy levels, electromagnetic transition rates and multipole moments have been calculated for positive parity states in A = 23–28 nuclei in an untruncated $1d_{\frac{5}{2}}2s_{\frac{1}{2}}$ configuration space. The results obtained by considering all two-body matrix elements as free parameters (FP) are compared with those obtained with matrix elements from a realistic Hamada-Johnston interaction (HJ). The binding and excitation energies as well as strong B(E2) values calculated with RP and MSDI are found to be rather similar and in good agreement with experiment, in contrast to the B(M1) values. Poor agreement with experiment is obtained for JH matrix elements. (auth)

**27013** SHELL-MODEL INVESTIGATION OF NEGATIVE-PARITY STATES IN THE A = 30 TO 35 MASS REGION. van Hienen, J. F. A. Utrecht, Netherlands; Rijksuniversiteit (1975). 24p.

A shell-model calculation has been performed for negative-parity states with $T \leq 3/2$ in A = 30 – 35 nuclei. A $2s_{\frac{1}{2}}1d_{\frac{3}{2}}1f_{\frac{7}{2}}2p_{\frac{3}{2}}$ configuration space was used, restricted by allowing only one nucleon to occupy either the $1f_{\frac{7}{2}}$ or the $2p_{\frac{3}{2}}$ orbit. The parameters of the MSDI effective interaction were determined from a fit to 24 experimental energies. The spectroscopic factors calculated are in excellent agreement with experiment except for A = 30. Analogue-to-antianalogue M1 transitions are also well reproduced. Not all E1 and M2 transitions, however, agree with experiment. (auth)

**27014** ELASTIC SCATTERING AND TRANSFER REACTIONS INDUCED BY 100 MeV $^{32}$S ON $^{27}$Al. Garrett, J.D.; Wegner, H.E. (Brookhaven National Laboratory, Upton, New York 11973); Cormier, T.M.; Cosman, E.R.; Hansen, O.; Lazzarini, A.J. Phys. Rev. C 12: No. 2, 489-498 (Aug 1975).

Angular distributions have been obtained at an incident energy of 100 MeV corresponding to $^{32}$S elastic scattering on $^{27}$Al, $^{27}$Al($^{32}$S,$^{31}$P) transitions to the ground and first-excited states of $^{28}$Si and $^{27}$Al($^{32}$S,$^{33}$S) transitions to an unresolved group of low-lying states in $^{26}$Al. An optical model analysis of the elastic data shows that the "best fit" potentials with constant diffusivity follow the $Ve^{R/a}$=constant ambiguity extremely well. It appears that the elastic data is most sensitive to the ion-ion potential near a radius of $\simeq$10.1 fm. The absolute cross sections of the $^{27}$Al($^{32}$S,$^{31}$P) transitions to the ground and first-excited states of $^{28}$Si are well reproduced in a distorted-wave Born-approximation analysis using optical model parameters which reproduce elastic scattering. The angular positions of the ($^{32}$S, $^{31}$P) grazing peaks, however, are observed a few degrees forward of their predicted position, and the measured cross sections forward of the grazing peaks are considerably larger than predicted. The agreement between measured and predicted angular shape apparently is better for the $^{27}$Al($^{32}$S,$^{33}$S)$^{26}$Al neutron transfer than for the proton transfer data. From this limited first data for $^{32}$S induced reactions it appears that such reactions can be explained to the extent that "lighter heavy-ion" induced reactions are understood. (auth)

**27015** YRAST LEVELS IN $^{44}$Ti. Simpson, J.J. (Max-Planck-Institut für Kernphysik, Heidelberg, Germany and University of Guelph, Guelph, Ontario, Canada); Dünnweber, W.; Wurm, J.P.; Green, P.W.; Kuehner, J.A.; Dixon, W.R.; Storey, R.S. Phys. Rev. C 12: No. 2, 468-473 (Aug 1975).

The reaction $^{32}$S($^{14}$N, $p\pi\gamma$)$^{44}$Ti has been studied with a view to populating high spin states in $^{44}$Ti. In singles and $\gamma$-$\gamma$ coincidence experiments $\gamma$-ray transitions in the ground state band and a negative parity band are seen and three levels connected to the ground state band, at 6508, 7671, and 8040 keV, are inferred. Angular distributions are consistent with stretched cascades. The lifetime of the 7671-keV level, presumed 10$^+$, has been determined by the attenuated Doppler-shift method to be 2.7 ± 0.5 ps. A comparison of the present reaction with the recently reported $^{28}$Si($^{19}$F, $p2\pi\gamma$)$^{44}$Ti reaction is made and a method for predicting the propensity of these types of reaction to feed high spin states is proposed. An $(fp)^4$ shell model calculation of yrast levels up to $J$ = 12 has been made. (auth)

# Nuclear Properties and Reactions, 39 ≤ A ≤ 58

*Refer also to abstracts 26826, 26984, 26991, 26996, 27007, 27008, 27010, 27011, 27015, and 27101.*

**27016** (JAERI–1231, pp 27-42) HEAVY ION REACTION. Kohno, I. (Institute of Physical and Chemical Research, Wako, Saitama, Japan). 13 Dec 1972.

From symposium on nuclear reaction and nuclear structure; Tokai, Ibaraki, Japan (13 Dec 1972).

In proceedings of a symposium on nuclear reaction and nuclear structure. (Japan Atomic Energy Research Inst., Tokyo).

Recent experimental results of one and multi-nucleon transfer reactions induced by $^{16}$O, $^{14}$N and $^{12}$C projectiles on the target

of nuclei (A ≥ 40) are described. As the energy range of projectiles is between 40 and 120 MeV, the Sommerfeld parameter, $\eta$, is above 10. In the case of these combinations of projectiles and targets, two mechanisms of transfer reaction are found, the one is a direct reaction which occurrs at the narrow surface region of nuclei and the other is a grazing collision or quasi-inelastic process which occurs at the more overlapping distance of two nuclei. The latter process is only found at the reactions induced by heavy ions. One- and multi-nucleon transfer reactions induced by heavy ions not only contribute to the study of nuclear structure from analyses of the angular distributions, but also can give valuable information for nuclear structure and reaction mechanisms by their selectivity of excited levels, which seems to be explained by, for example, j dependence, two step reaction process or special character of residual levels as quartet state, etc. (auth)

**27017** (JAERI-1231, pp 71-77) MECHANISM OF THE ($^3$He,t) REACTION. Toyama, M. (Institute of Physical and Chemical Research, Wako, Saitama, Japan). 13 Dec 1972.

From symposium on nuclear reaction and nuclear structure; Tokai, Ibaraki, Japan (13 Dec 1972).

In proceedings of a symposium on nuclear reaction and nuclear structure. (Japan Atomic Energy Research Inst., Tokyo).

The ($^3$He, t) reactions are investigated by means of the second order perturbation method with ($^3$He-$\alpha$-t) process and the ordinary DWBA term. The analyses are performed on the data of $^{48}$Ca($^3$He,t) $^{48}$Sc ($0^+$, $2^+$, $4^+$, $6^+$), $^{90}$Zr($^3$He, t)$^{90}$Nb ($2^+$,$4^+$, $6^+$, $8^+$) and $^{48,49,50}$Ti ($^3$He,t) $^{48,49,50}$V($0^+$). The results show that the ($^3$He-$\alpha$-t) process is a main process in these reactions and a very good agreement between observed and calculated cross sections is obtained. Some attempts are made to explain analytically the relation between the cross sections obtained by each of the ($^3$He-$\alpha$-t) processes and the ordinary DWBA term. (auth)

**27018** (JAERI-1231, pp 112-116) 1 $g_{\frac{9}{2}}$ NEUTRON STATE IN NUCLEI WITH NEUTRON NUMBERS BETWEEN 52 AND 82. Ishimatsu, T. (Tohoku Univ., Sendai, Japan). 13 Dec 1972.

From symposium on nuclear reaction and nuclear structure; Tokai, Ibaraki, Japan (13 Dec 1972).

In proceedings of a symposium on nuclear reaction and nuclear structure. (Japan Atomic Energy Research Inst., Tokyo).

Deuteron spectra from (p, d) reactions on 18 nuclei with neutron numbers between 52 and 82 were measured at an angle of 20° with 52 MeV incident protons. In every spectrum a broad bump with the distinct top is observed at excitation energies higher than several MeV. From the systematic behaviour of the bump it is inferred that the top of the bump stands for an approximate position of the 1 $g_{\frac{9}{2}}$ neutron orbit, and energies of the orbit are deduced from the observed spectra. The symmetry effect on the 1 $g_{\frac{9}{2}}$ neutron orbit is seen for Mo and Sn isotopes; the energy of the orbit rises regularly with increasing neutron number. The ground-state single-quasiparticle energy with respect to the 1 $g_{\frac{9}{2}}$ orbit shows rather an abrupt change by about 2 MeV around the neutron number of 64. (auth)

**27019** FOUR-HOLE STRUCTURE IN Fe ISOTOPES. Itonaga, K. (Osaka Univ., Toyonaka (Japan). Faculty of Engineering Science). Prog. Theor. Phys. (Kyoto); 52: No. 2, 487-508(Aug 1974).

Four-hole correlations seen in the Fe isotopes (A = 52, 53, 54) are systematically investigated in the framework of the shell model. The structure of the correlated four-holes in the $1f_{\frac{7}{2}}$ orbit is understood as the cooperative interplay of the important pairing plus T = 0, $J^\pi_{max} = 7^+$ correlations and T = 1, $J^\pi = 2^+$ correlations. The coupling scheme is very similar to the stretch-coupling one. Correlated four-hole changes its structure gradually when a few particles are added to it. However the weak-coupling-like features are seen for the lowest series of 4-hole n particle states. The states of other types of configurations in the Fe isotopes are well reproduced. Renormalization techniques are employed for such physical quantities as the single particle energy, the hole-hole interaction and the particle-hole interaction. (auth)

**27020** EFFECTIVE INTERACTIONS IN FINITE NUCLEI BASED ON REACTION MATRIX THEORY, 1. Reaction Matrix Consistent With Model Space. Ando, K.; Nagata, S. (Kyoto Univ. (Japan). Dept. of Physics); Bando, H. Prog. Theor. Phys. (Kyoto); 52: No. 2, 509-520(Aug 1974).

Reaction matrix is calculated in rigorous ways, special attentions being paid to the consistency with the chosen model space. In our treatment of the reaction matrix, there occurs no ambiguity concerning the double counting. Core-polarization corrections to the effective interactions are considered in second order. The energy spectra of $^{42}$Sc are calculated from two types of free nucleon-nucleon potentials, H-J and OBEP-K, with a model space chosen as $(fp)^2$-configurations, at first, and then extended to $((fp)^2 + (sdg)^2)$-configurations. This extension of the model space is found to be important to push down the lowest $(J^\pi T) = (1^+0)$ state and $(0^+1)$ state; the former has the strongest correlation in bare G and the correlation of the latter is most enhanced through the core-polarization. For the lowest $(1^+0)$ state, however, the binding is still weaker compared with the experimental result, even for the OBEP-K potential which is more favourable for the deuteron-like correlation in nuclei. (auth)

**27021** OCCUPATION NUMBER DEPENDENCE OF INTERFERENCE IN TWO-NEUTRON TRANSFER REACTIONS. Izumoto, T. (Tokyo Univ., Tanashi (Japan). Inst. for Nuclear Study). Prog. Theor. Phys. (Kyoto); 52: No. 4, 1214-1231(Oct 1974).

A study is made on the mass number dependence of the form factors for two-neutron transfer reactions leading to the $0^+_{\frac{1}{2}}$ and $2^+_{\frac{1}{2}}$ states of spherical vibrational nuclei. The calculations are performed for nuclei with the neutron number N from 50 to 82 on the basis of the quasi-particle RPA and the Tamm-Dancoff method. The results predict that the nature of interference between a direct process and inelastic processes exciting the collective $2^+_{\frac{1}{2}}$ state depends on the mass number within a framework of the coupled channel Born approximation. This fact originates dynamically from the role of ground state correlations. The blocking effects arising from the presence of quasi-particles reduces the L = 0 transfer amplitude between excited states by a factor 0.7 ~ 0.8. The effect of number non-conservation inherent in BCS wave functions is found to be rather small. (auth)

**27022** SPIN-FLIP PROBABILITIES VIA ISOBARIC ANALOGUE RESONANCES IN $^{50}$Ti(p,p')$^{50}$Ti* INELASTIC SCATTERING. Nojiri, T. (Tokyo Univ. of Education (Japan). Dept. of Physics); Toyama, H. J. Phys. Soc. Jpn.; 37: No. 6, 1479-1484(Dec 1974).

Proton spin-flip probabilities ($S(\theta)$) and differential cross sections in inelastic scattering of $^{50}$Ti(p,p')$^{50}$Ti* (1.55 MeV, $2^+$) were measured on isobaric analogue resonances at $E_p$ = 3.606 MeV and 3.588 MeV. Both differential cross sections and $S(\theta)$ showed nearly symmetric angular distributions about 90° and were analyzed with a single resonance formula. Good fits were obtained. Especially $S(\theta)$ was found to be important in the investigation of the ratio of partial widths and the relative phase between partial widths in the exit channel. (auth)

**27023** $^{37}$Cl($p$, $n$)$^{37}$Ar EXCITATION FUNCTION UP TO 24 MeV: STUDY OF ($p$,$n$) REACTIONS. Kishore, R.; Collé, R.; Katcoff, S.; Cumming, J.B. (Chemistry Department, Brookhaven National Laboratory, Upton, New York 11973). Phys. Rev. C 12: No. 1, 21-27 (July 1975).

Cross sections for the $^{37}$Cl($p$,$n$)$^{37}$Ar reaction were determined from 2 to 24 MeV by the activation method. NaCl targets of natural isotopic composition were irradiated inside of Al cells having thin Havar windows. Beam intensities were determined with a Faraday cup and the $^{37}$Ar disintegration rates were measured with internal gas proportional counters. The cross sections (±6% uncertainty) increase from threshold (1.64 MeV) to a broad maximum of 365 mb at 10 Mev and then decrease to 34 mb at 23.5 MeV. These results and five other recently measured ($p$,$n$) excitation functions are compared with each other and with various cascade-evaporation calculations. Reasonable agreement was attained between experiment and calculation, and possible sources of remaining discrepancies are discussed. The $^{37}$Ar half-life is observed to be 35.02 ± 0.05 day, in good agreement with previously reported values. (auth)

**27024** HEAVY-ION OPTICAL POTENTIALS FROM FEW-NUCLEON TRANSFER REACTIONS. Baltz, A.J.; Bond, P.D.; Garrett, J.D.; Kahana, S. (Brookhaven National, Laboratory, Upton, New York 11973). Phys. Rev. C 12: No. 1, 136-148 (July 1975).

The sensitivity of forward angle heavy-ion transfer calculations to the details of the imaginary optical potential in the region of the nuclear surface is demonstrated. A phenomenological imaginary potential, consisting of a deep volume term of sharp diffusivity and a shallow surface term of standard diffusivity, is proposed and used in distorted-wave Born-approximation calculations to reproduce a variety of angular distribution shapes. The proposed parametrization of the imaginary potential allows the region of the nuclear surface to be transparent enough to produce large forward angle cross sections, seen experimentally, and yet remain strongly enough absorbing in the nuclear interior to suppress unphysical contributions from this region. Bound state configuration dependence of angular shapes, produced in two-particle transfer calculations with weakly absorbing volume potentials, is shown to be removed by the use of the proposed surface transparent potentials. (auth)

**27025** CALCULATION OF $B$ ($E2$) TRANSITION RATES IN $1f_{7/2}$-shell NUCLEI WITH REALISTIC EFFECTIVE INTERACTION AND CHARGES. Kuo, T.T.S.; Osnes, E. (Institute of Physics, University of Oslo, Oslo 3 Norway). Phys. Rev. C 12: No. 1, 309-311 (July 1975).

$B$ ($E2$) transition rates in $A$ = 42 and $A$ = 43 nuclei have been calculated in $(pf)^n$ model spaces using an effective interaction and

effective charges obtained by summing the diagrams of the Tamm-Dancoff approximation for screened particle-hole vertices. Good agreement with measured $B$ ($E2$) rates is obtained for transitions between high-spin states. The results are further very similar to those obtained by parametrizing the effective charges. (auth)

**27026** LIFETIMES OF LEVELS IN $^{45}$Sc. Metzger, F.R. (Bartol Research Foundation of The Franklin Institute, Swarthmore, Pennsylvania 19081). Phys. Rev. C 12: No. 1, 312-314 (July 1975).

In an attempt to clear up discrepancies between lifetimes measured by the nuclear resonance fluorescence method and by the Doppler shift attenuation method, the results of a further resonance fluorescence experiment are reported for the 720, 1237, 1409, 1662, and 2092 keV levels in $^{45}$Sc. (auth)

**27027** SEARCH FOR AN $l$-FORBIDDEN $M1$ TRANSITION IN $^{39}$K BY ELECTROEXCITATION. Webb, D.V.; Peterson, G.A. (Department of Physics and Astronomy, University of Masssachusetts, Amherst, Massachusetts 01002); Bendel, W.L.; Jones, E.C. Jr.; Fagg, L.W. Phys. Rev. C 12: No. 1, 330-331 (July 1975).

Inelastic electron scattering 180° cross sections for the excitation of the 2.523 MeV $1/2^+$ first excited state in $^{39}$K have been determined to be predominantly $E2$, and from them an upper limit of $\Gamma_\gamma(M1) \leq 0.1$ meV for an $l$-forbidden $M$ component has been extracted. This disagrees with other results for this state that imply an $M1$ width comparable to the $E2$ width. (auth)

**27028** INELASTIC PROTON SCATTERING AS A TEST OF SURFACE-DELTA WAVE FUNCTIONS. Throop, M.J.; Cheng, Y.T.; McDaniels, D.K. (University of Oregon, Eugene, Oregon 97403); Stupin, D.M.; Swenson, L.W.; Jarmie, N.; Jett, J.H.; Lovoi, P.A.; Ohlsen, G.G.; Salzman, G.C. Phys. Rev. Lett. 35: No. 1, 16-19 (7 July 1975).

Analyzing power and differential cross sections for the inelastic scattering of protons to the collective states of $^{58,60}$Ni and $^{64}$Zn have been measured with 15-MeV polarized protons. The success in fitting the experimental data with a microscopic reaction analysis strikingly points out the usefulness of nuclear-structure calculations with a spin-dependent surface-delta interaction. (auth)

**27029** CROSS SECTIONS FOR ($n$, $xn$) REACTIONS BETWEEN 7.5 AND 28 MeV. Bayhurst, B.P.; Gilmore, J.S.; Prestwood, R.J.; Wilhelmy, J.B.; Jarmie, N.; Erkkila, B.H.; Hardekopf, R.A. (University of California, Los Alamos Scientific Laboratory, Los Alamos, New Mexico 87544). Phys. Rev. C 12: No. 2, 451-467 (Aug 1975).

A total of 236 cross sections for ($n$, $xn$) reactions have been measured at neutron energies between 7.5 and 28 MeV, using radiochemical techniques. Cross sections for ($n$, $n'$) and ($n$, $2n$) reactions are reported on $^{193}$Ir; ($n$, $2n$) cross sections on $^{45}$Sc and $^{58}$Ni; ($n$, $2n$) and ($n$, $3n$) cross sections on $^{89}$Y, $^{90}$Zr, and $^{107}$Ag; ($n$,$2n$), ($n$,$3n$), and ($n$,$4n$) cross sections on $^{169}$Tm, $^{175}$Lu, $^{191}$Ir, $^{197}$Au, and $^{203}$Tl; ($n$,$3n$) and ($n$,$4n$) cross sections on $^{151}$Eu; and ($n$,$4n$) cross sections on $^{205}$Tl. Neutron fluences were determined by either the $^{27}$Al($n$,$\alpha$)$^{24}$Na or the $^{90}$Zr($n$,$2n$)$^{89}$Zr reactions appropriately combined with proton-recoil telescope measurements. The excitation functions are compared with calculations based on a model incorporating both compound-nucleus and preequilibrium decay modes. Cross sections for the $^{27}$Al($n$,$\alpha$)$^{24}$Na reaction between 21 and 26 MeV are also reported. (auth)

**27030** $\beta$ DECAY OF $^{43}$Sc. Young, K.C. Jr.; Tabor, S.L.; Fifield, L.K.; Zurmühle, R.W. (Physics Department, University of Pennsylvania, Philadelphia, Pennsylvania 19174). Phys. Rev. C 12: No. 2, 567-571 (Aug 1975).

The spectrum of $\gamma$ rays following the $\beta$ decay of $^{43}$Sc has been measured with a 65 cm$^3$ Ge(Li) detector. $\beta$-decay branches to the following states in $^{43}$Ca were observed (log$ft$ values in parentheses); ground state (5.03), 373 keV (4.97), and 1931 keV (5.66). The last $\beta$-decay branch has not been previously reported. In contrast to earlier works, $\beta$ branches to the 593 ($J^\pi=3/2^-$) and 990 keV ($J^\pi=3/2^+$) levels were not observed and upper limits on these dec branches were obtained. (auth)

**27031** HARTREE-FOCK-BOGOLIUBOV CALCULATIONS FOR ODD-MASS NUCLEI IN THE 0$f$-1$p$ SHELL. Sandhu, T.S. (Physics Department, State University of New York, Buffalo, New York 14214); Rustgi, M.L. Phys. Rev. C 12: No. 2, 666-675 (Aug 1975).

Employing the Hartree-Fock-Bogoliubov approximation and the Kuo-Brown interaction, results for odd-mass nuclei in the 0$f$-1$p$ shell are reported. A $^{40}$Ca core has been assumed. The blocking effect due to the presence of the odd nucleon has been taken into account. The ground-state energies, the intrinsic and ground-state quadrupole moments, reduced transition rates, and the pickup strengths are calculated and compared with the corresponding available experimental values. (auth)

**27032** PROTON-UNBOUND STATES IN $^{41}$K. Medsker, L.R.; Fortune, H.T.; Headley, S.C. (Physics Department, University of Pennsylvania, Philadelphia, Pennsylvania 19174). Phys. Rev. C 12: No. 2, 401-406 (Aug 1975).

The $^{40}$Ar($^3$He,$d$) reaction, at 18 MeV $^3$He energy, has been used to study states in $^{41}$K that are unbound to proton emission. The $^{40}$Ar target was contained in a gas cell with no entrance window. Excitation energies and angular distributions were obtained for levels from $E_x$=7.836 to 10.239 MeV. A distorted-wave analysis was used to determine $l$ values and to extract widths $\Gamma_p$ for comparison with the results of previous $^{40}$Ar($p$,$p$) work. The analog of the ground state of $^{41}$Ar, at 8.349 MeV excitation in $^{41}$K, and six excited-state analogs were observed. (auth)

**27033** MICROSCOPIC DESCRIPTION OF ISOBARIC-ANALOG-STATE TRANSITIONS INDUCED BY 25-, 35-, AND 45-MeV PROTONS. Doering, R.R.; Patterson, D.M.; Galonsky, A. (Cyclotron Laboratory, Department of Physics, Michigan State University, East Lansing, Michigan 48824). Phys. Rev. C 12: No. 2, 378-389 (Aug 1975).

Differential cross sections have been measured for ($p$, $n$) reactions to the isobaric analogs of the targets $^{48}$Ca, $^{90}$Zr, $^{120}$Sn, and $^{208}$Pb at proton bombarding energies of 25, 35, and 45 MeV. The isospin-flip strength of a phenomenological nucleon-nucleon force has been determined with microscopic distorted-wave calculations including the "knock-on" exchange amplitude. A realistic $G$-matrix effective interaction also provides a reasonable account of the observed cross sections, particularly at the higher proton energies. (auth)

# Nuclear Properties and Reactions, 59 ≤ A ≤ 89

*Refer also to abstracts 27011, 27018, 27021, 27024, 27028, 27031, and 27064.*

**27034** ENERGY LEVELS IN $^{77}$Br. Motal, B.W.; Lueders, D.H.; Daley, J.M.; Durham, F.E.; Buccino, S.G. (Tulane University, New Orleans, Louisiana 70118); Hollandsworth, C.E.; Bucher, W.P.; Jones, H.D. Phys. Rev. C 12: No. 1, 63-68 (July 1975).

$\gamma$ transitions in the reaction $^{72}$Se($p$,$n\gamma$)$^{77}$Br have been studied at proton energies between 2.150 and 2.850 MeV. Sixteen $\gamma$ rays were assigned to transitions in $^{77}$Br below an excitation energy of ~625 keV. Ten of these had not previously been reported. A previously reported 77 keV $\gamma$ ray was not observed. A level scheme was determined from threshold measurements, energy sums, and $\gamma$-$\gamma$ coincidence studies. This scheme includes five new levels located at energies of 167.0, 226.6, 336.9, 425.1, and 471.1 keV. (auth)

**27035** NUCLEAR DATA SHEETS FOR A EQUALS 61. Auble, R. L. (Oak Ridge National Lab., TN). Nucl. Data Sheets; 16: No. 1, 1-24(Sep 1975).

Nuclear structure data for A equals 61 nuclei are compiled, and adopted level properties and decay schemes are presented. The compilation includes data available through April 1975. The compilation contains two sections: level schemes which include the bulk of the data plus adopted level energies and half-lives; and sheets which include more details about individual measurements, additional adopted level properties, and comments regarding inconsistencies found in the literature. (auth)

**27036** NUCLEAR DATA SHEETS FOR A EQUALS 75. Horen, D. J.; Lewis, M. B. (Oak Ridge National Lab., TN). Nucl. Data Sheets; 16: No. 1, 25-54(Sep 1975).

The literature pertaining to nuclei with A equals 75 was reviewed, and a summary of the nuclear structure properties is presented here. This compilation marks a departure from the Nuclear Data Sheets style in that emphasis is placed upon summaries of the nuclear structure information rather than compilation of all the data; complete data sets for each type of reaction are stored in the Evaluated Nuclear Structure Data File (ENSDF) at the Nuclear Data Project, but only portions of the data are included here; the complete compilation, i.e., drawings, data sheets, and references, was produced from computer files; comments have been kept to a minimum, thus leaving it to the reader to refer to the original work for fine details; and the compilers have not included all nuclear quantities that could be deduced from the data, e.g., transition matrix elements, parameters for suggested rotational bands, etc. The $^{74}$Se(n, gamma) data were reinterpreted by the compilers, and a neutron separation energy of 8027.4 keV is suggested for $^{75}$Se. All Q values were adopted from the compilation of Wapstra et al., except as noted. Literature received prior to March 1975 was considered. (auth)

**27037** HALF-LIFE OF $^{77}$Br. Waters, S. L. (Hammersmith Hospital, London); Woods, M. J. Int. J. Appl. Radiat. Isot.; 26: No. 8, 484-485(Aug 1975).

The measurement of the half-life of $^{77}$Br using a sealed liquid source and a re-entrant ionisation chamber, over a period of approximately 5 half-lives, is described. Using a weighted mean of two sets of readings gives a half-life value of 57.036 hr with a standard error of the mean of 0.01%. The total random uncertainty

at a 99% confidence level is ±0.05% and the overall systematic uncertainty is ± 0.2%. (UK)

**27038** $^{66}$Zn(*d*, *p*)$^{67}$Zn REACTION AT 7.5 MeV. Ismail, H.A.; Hallock, J.N.; Moore, W.H.; Enge, H.A. (Department of Physics and Laboratory for Nuclear Science, Massachusetts Institute of Technology, Cambridge, Massachusetts 02139). Phys. Rev. C 12: No. 2, 708-709 (Aug 1975).

The $^{66}$Zn(*d*,*p*)$^{67}$Zn reaction has been studied with an incident deuteron bombarding energy of 7.5 MeV. A total of 48 levels below $E_x$=4.8 MeV have been identified in $^{67}$Zn. (auth)

**27039** VARIOUS PROCESSES OCCURRING IN STRONG INTERACTIONS BETWEEN HEAVY IONS: COMPOUND NUCLEUS FORMATION, INCOMPLETE FUSION, AND QUASIFISSION. Lefort, M. (Chimie Nucléaire, Institut Physique Nucléaire, 91406 Orsay, France). Phys. Rev. C 12: No. 2, 686-690 (Aug 1975).

This paper deals with the problem of various deep processes occurring when two complex nuclei enter in collision. It is suggested that very deep inelastic processes may lead to either a compound nucleus or a composite system which shortly decays into two fission fragments (quasifission process). Particularly for heavy projectiles and targets, the predominant Coulomb potential inhibits the compound nucleus formation *for low l waves*. Then a critical angular momentum can be defined as the limit below which both processes (quasifission and compound nucleus formation) occur. For the heaviest nuclei, nearly all *l* waves below $l_c$ contribute to the quasifission phenomenon. (auth)

**27040** STRUCTURE OF $^{7}$Be AND $^{63}$Cu DETERMINED FROM THE $^{63}$Cu($^{6}$Li, $^{7}$Be)$^{62}$Ni REACTION. Hudson, G.M.; Kemper, K.W.; Moore, G.E.; Williams, M.E. (Department of Physics, The Florida State University, Tallahassee, Florida 32306). Phys. Rev. C 12: No. 2, 474-480 (Aug 1975).

Angular distributions have been measured for the reaction $^{63}$Cu($^{6}$Li, $^{7}$Be$_{0,1}$)$^{62}$Ni$_{0,1}$ at $E$ ($^{6}$Li) =34 MeV in the angular range 2–52.5° (lab). Exact finite-range distorted-wave-Born-approximation (DWBA) calculations were not able to reproduce the shape of the angular distributions even though similar calculations with the same optical model parameters were able to describe the $^{62}$Ni($^{7}$Li, $^{6}$He)$^{63}$Cu reaction. Elastic scattering data for $^{7}$Li+$^{62}$Ni and $^{6}$Li+$^{63}$Cu were reanalyzed with the optical model assuming a real radius given by $R=1.2A_T^{1/3}$ instead of the previously used $R=1.2(A_T^{1/3}+A_P^{1/3})$. The optical model fits to the elastic scattering data and the finite-range DWBA calculations for the $^{62}$Ni($^{7}$Li,$^{6}$He) reaction data were equivalent with both optical parameter sets while the $^{63}$Cu($^{6}$Li,$^{7}$Be) fit was greatly improved. The shape of the forward angle $^{63}$Cu($^{6}$Li,$^{7}$Be$_{0,1}$)$^{62}$Ni$_{0}$ data indicates that $^{7}$Be$_1$ has a larger $1p_{3/2}/1p_{1/2}$ ratio than found in the ground state of $^{7}$Be. Ratios of $1p_{3/2}/1p_{1/2}$ strengths in $^{7}$Be$_{0,1}$ extracted by fitting the shape of the forward angle data with finite-range DWBA calculations of the cross sections are in excellent agreement with the calculations of Cohen and Kurath. In addition, the spectroscopic factor for $^{63}$Cu is in good agreement with values found from other reactions when the Cohen and Kurath results for $^{7}$Be are assumed. The spectroscopic factor for the component in the $^{63}$Cu ground state wave function which corresponds to $^{62}$Ni(2$^+$) $\otimes$ $2p_{3/2}$ has been extracted. An upper limit for the magnitude of the cross section for the reaction $^{63}$Cu($^{6}$Li,$^{9}$Be) has been determined. (auth)

**27041** DECAY OF THE NEW ISOTOPE $^{62}$Fe. Franz, E.; Katcoff, S. (Brookhaven National Laboratory, Upton, New York 11973); Smith, H.A. Jr.; Ward, T.E. Phys. Rev. C 12: No. 2, 616-618 (Aug 1975).

The neutron-rich isotope $^{62}$Fe was discovered in a $^{64}$Ni metal foil irradiated in a new medium energy intense neutron beam at the Brookhaven 200-MeV linac. A flux in the energy range 25–200 MeV of $\sim 1.3 \times 10^{11}$ *n*/cm$^2$ sec is obtained on target at this unique facility. The $^{62}$Fe decays with a half-life of 68 ± 2 sec primarily by emission of 2.5-MeV $\beta$ rays to a $J^\pi$=1$^+$ level in $^{62}$Co at 506.1 ±0.1 keV. (auth)

**27042** Li, Be, AND B PRODUCTION IN THE 3-GeV PROTON BOMBARDMENT OF Ni. Raisbeck, G.M.; Boerstling, P.; Klapisch, R.; Thomas, T.D. (Princeton-Pennsylvania Accelerator, Princeton, New Jersey 08540). Phys. Rev. C 12: No. 2, 527-532 (Aug 1975).

Measurements have been made of the energy spectra and angular distributions of Li, Be, and B nuclei emitted from a Ni target bombarded with 3-GeV protons, using a counter telescope technique. By integrating the spectra and normalizing to the radiochemically determined cross section of $^{7}$Be, total isotopic cross sections have been determined, and these are discussed in terms of the cosmic ray production of Li, Be, and B. The experimental cross sections are compared with a recent semiempirical formula; within the uncertainties the agreement between experiment and prediction is satisfactory. (auth)

**27043** COULOMB DISSOCIATION OF RELATIVISTIC HADRONS ON NUCLEI AND GIANT DIPOLE RESONANCES. Adamovich, M.I.; Kharlamov, S.P.; Larionova, V.G.; Yagudina, F.R. (P. N. Lebedev Physics Institute, USSR Academy of Sciences). JETP Lett. 21: No. 7, 209-210 (5 Apr 1975).

Dissociation of 9.4-GeV/*c* deuterons and 200-GeV/*c* protons on nuclei, due to the Coulomb momentum of the target nucleus and accompanied by excitation of giant dipole resonance, was observed. The possibilities of using the observed phenomenon to study electromagnetic interactions with mesons and hyperons as targets is discussed. (auth)

# Nuclear Properties and Reactions, 90 ≤ A ≤ 149

*Refer also to abstracts 26984, 27011, 27017, 27029, 27033, and 27043.*

**27044** (JINR-P4-8922) SPIN–ORBIT VIBRATIONS OF SPHERICAL NUCLEI. Telitsyn, V. B.; Stoyano, C.; Vdovin, A. I. (Joint Inst. for Nuclear Research, Dubna (USSR)). 1975. 16p. (In Russian). Dep. NTIS (US Sales Only) $4.00.

One-phonon 0$^+$ states of Zr and Mo nuclei were studied. The state structure was calculated while taking into account the coupling interaction in the particle–particle channel and spin–orbit interaction in the particle–hole channel. The spin–orbit forces are taken in a non-factorized form. In most cases the states turned out to be strongly collective; the first 0$^+$ state appears below the energy gap. The relative spectroscopic factors of (p,t) and (t,p) reactions were calculated as well as the E0 transition probabilities. (2 tables) (auth)

**27045** QUASIELASTIC ELECTRON SCATTERING AND GIANT MULTIPOLE RESONANCES IN $^{116}$Sn. Hosoyama, K.; Torizuka, Y. (Laboratory of Nuclear Sciences, Tohoku University, Tomizawa, Sendai, Japan). Phys. Rev. Lett. 35: No. 4, 199-202 (28 July 1975).

Electron-$^{116}$Sn scattering spectra were obtained over an excitation energy range of about 100 MeV. The experimental transverse spectrum is in good agreement with the Fermi-gas model, but not the longitudinal spectrum. The quasielastic contribution was then obtained from the shape of the transverse spectrum. The residual amount interpreted to be the resonance part was divided into many multipoles. (auth)

**27046** NEUTRON BLOCKING IN α-PARTICLE-TRANSFER REACTIONS. Becchetti, F.D.; Jänecke, J. (Cyclotron Laboratory, Department of Physics, The University of Michigan, Ann Arbor, Michigan 48105). Phys. Rev. Lett. 35: No. 5, 268-270 (4 Aug 1975).

The (*d*,$^{6}$Li) α-transfer reaction on several even-*A* and odd-*A* tin isotopes has been investigated at $E_d$ = 35 MeV. A significant reduction (~factor 2) in transition strength is observed for the odd-*A* target nuclei. This reduction is attributed to the "blocking" effect of unpaired nucleons and is comparable to that observed in (*p*,*t*) reactions. (auth)

**27047** SHAPE TRANSITIONAL ASPECTS OF ODD-*A* Eu ISOTOPES STUDIED BY THE (*p*, *t*) REACTION. Taketani, H.; Sharma, H.L. ; Hintz, N.M. (J. H. Williams Laboratory of Nuclear Physics, University of Minnesota, Minneapolis, Minnesota 55455). Phys. Rev. C 12: No. 1, 108-123 (July 1975).

The abrupt shape transition as is observed around $N \simeq 88$–90 in even nuclei has been examined for the odd-*A* Eu isotopes $^{151}$Eu$_{88}$ and $^{149}$Eu$_{86}$ by the (*p*,*t*) reaction at 18.5 and 19.0 MeV with an average resolution of 10 keV. Angular distributions, taken from 10 to 70°, enabled unambiguous indentification of many $L$ = 0 ($J^\pi$ = 5/2$^+$) transitions in both residual nuclei; seven for $^{151}$Eu and seven or eight for $^{149}$Eu. The summed $L$ = 0 cross sections are close to those of the (*p*,*t*) reactions for the neighboring even-*A* Sm isotopes connecting the same neutron numbers. A number of new levels have been found in both isotopes. We have obtained markedly different level structures for the two neighboring isoptopes. In $^{151}$Eu, whose ground state and low-lying states below 200 keV can be described in terms of spherical shell-model configurations, two deformed bands have been tentativeiy identified. One of these is a 5/2$^+$[413] band with members at 261 keV, 5/2$^+$; 414 keV, (7/2$^+$); and possible a 597 keV, (9/2$^+$) member. In addition a 5/2$^+$[413] $\beta$ band is postulated with members at 654 keV, 5/2$^+$; 801 keV, (7/2$^+$). These deformed states, coexisting with the spherical states, have been strongly excited while the spherical low-lying states have shown vanishingly small (*p*,*t*) cross sections. The (*p*,*t*) cross sections to the $^{151}$Eu states were found to be in strong anticorrelation with $B$ (*E*2) values from Coulomb excitation and (*d*,*d*′) cross sections leading to the same final states. On the other hand, $^{149}$Eu has shown the usual (*p*,*t*) pattern of a strong ground state transition and weak excited state transitions, showing similar coupling schemes are involed in the ground states of $^{151}$Eu and $^{149}$Eu. The detailed experimental results up to 1.6 MeV excitation in both nuclei and their interpretation for some of the levels are presented. (auth)

**27048** STATES IN $^{121}$Sn FROM THE $^{120}$Sn(*d*, *p*)$^{121}$Sn REACTION AT 17 MeV. Bechara, M.J. (Instituto de Física, Universidade de São Paulo, São Paulo, Brasil); Dietzsch, O. Phys. Rev. C 12: No. 1, 90-101 (July 1975).

The $^{120}Sn(d,p)^{121}Sn$ reaction has been investigated at a bombarding energy of 17 MeV. The proton groups were analyzed by a magnetic spectrograph and detected in nuclear emulsions with a resolution of ~10 keV. Excitation energies and angular distributions were obtained for levels below $E_x = 4.9$ MeV in $^{121}Sn$. A distorted-wave analysis was used to determine $l$ values and spectroscopic strengths. The results are compared to previous data from transfer reactions. Centers of gravity and sums of spectroscopic factors are presented for the detected levels and are compared with the results of pairing theory. (auth)

**27049** STUDY OF $^{101}Rh$ WITH THE $(p, t)$ REACTION. Del Vecchio, R.M.; Naumann, R.A.; Duray, J.R.; Hübel, H. (Joseph Henry Laboratories, Princeton University, Princeton, New Jersey 08540); Daehnick, W.W. Phys. Rev. C 12: No. 1, 69-78 (July 1975).

The $^{103}Rh(p,t)^{101}Rh$ reaction has been studied at bombarding energies of 17, 30, and 42 MeV. The 30 MeV data, which was taken with a quadrupole-dipole-dipole-dipole magnet QDDD, provided the most information on the $^{101}Rh$ spectrum. The $(p,t)$ reaction is is apparently exciting $^{101}Rh$ states which look like a $2p_{1/2}$ proton weakly coupled to states of the $^{100}Ru$ core. This is suggested by the multiplet structure observed up to about 1 MeV of excitation. Considerable $(p,t)$ strength is observed above 2 MeV of excitation but multiplet structure is not so apparent. Although two of the strong states above 2 MeV may carry expected $L = 3$ $(p,t)$ strength, the others are more surprising. (auth)

**27050** EVIDENCE FOR AN $M1$ GIANT RESONANCE IN $^{138}Ba$. Holt, R.J.; Jackson, H.E. (Argonne National Laboratory, Argonne, Illinois 60439). Phys. Rev. C 12: No. 1, 56-62 (July 1975).

The $M1$ strength function was measured in $^{138}Ba$ at an excitation energy of approximately 8.6 MeV throughout the neutron energy region 9–60 keV using the threshold photoneutron technique. A method was developed for extracting the dipole strength even though the first excited state of the daughter nucleus, $^{137}Ba$, is only 281 keV above the ground state. The photoneutron spectrum was measured at laboratory angles of 90° and 135° with high resolution (0.5 ns/m) using the time-of-flight spectrometer associated with the Argonne high current linac. The $M1$ strength function for $^{138}Ba$ was found to be anomalously large at 8.6 MeV. In addition, the $E1$ dipole strength function was estimated at this excitation energy. (auth)

**27051** 723 keV BETA TRANSITION IN THE NEGATRON DECAY OF $^{122}Sb$. Reddy, B.V.; Narasimha Raju, M.L.; Sastry, D.L. (Laboratories for Nuclear Research, Andhra University, Waltair, Visakhapatnam, India). Phys. Rev. C 12: No. 1, 256-259 (July 1975).

The energy dependence of the angular correlation of the cascade $2^-$(723 keV $\beta$ particle) $2^+$(1260 keV $\gamma$ ray)$0^+$ in the decay of $^{122}Sb$ is measured and found to agree with the reports of Raghavan *et al.* and Yamada *et al.* Nuclear matrix elements governing the 723 keV $\beta$ transition are extracted using the available experimental data on this transition. Buhring's formulas that are simplified by Simms are used in the analysis. It is observed that the contribution of the nondiagonal elements to the Coulomb Hamiltonian is significant. (auth)

**27052** NUCLEAR SPECTROSCOPY OF $^{145}Nd$. Hillis, D.L.; Bingham, C.R. (Department of Physics and Astronomy, University of Tennessee, Knoxville, Tennessee 37916 and Oak Ridge National Laboratory, Oak Ridge, Tennessee 37830); McClure, D.A.; Kendrick, N.S. Jr.; Hill, J.C.; Raman, S.; Ball, J.B.; Harvey, J.A. Phys. Rev. C 12: No. 1, 260-278 (July 1975).

The nuclear spectroscopy of $^{145}Nd$ has been studied by means of $\gamma$-ray and charged-particle spectroscopy. Information on $^{145}Nd$ levels was obtained via the decay of $^{145}Pr$ and the $^{144}Nd$ $(n, \gamma)$ reaction with thermal neutrons. From the $\gamma$-ray spectroscopy $\simeq$ 20 energy levels were assigned to $^{145}Nd$, and 43 $\gamma$ rays could be placed in the decay scheme. The charged-particle spectroscopy of $^{145}Nd$ consists of the $^{144}Nd(d, p)$ reaction at $E_d$=33.3 MeV, the $^{144}Nd(\alpha, {}^3He)$ reaction at $E_\alpha$=66.2 MeV, and the $^{144}Nd(p, d)$ reaction at $E_p$=31 MeV. Differential cross sections for the charged particle reactions were measured over the range of ~ 7° to ~ 37° lab for ≃40 excited states. These angular distributions are compared with distorted-wave Born approximation calculations to extract $l$ values and spectroscopic factors. (auth)

**27053** NUCLEAR PROPERTIES OF THE LOW-LYING STATES IN $^{99}Mo$. Barman Roy, B. (Department of Physics, Herbert H. Lehman College of the City University of New York, Bronx, New York 10468); Choudhury, D.C. Phys. Rev. C 12: No. 1, 323-326 (July 1975).

Energy levels and spectroscopic factors for the low-lying levels in $^{99}Mo$ are calculated within the framework of the quasiparticle-vibration coupling approach in the unified nuclear model. The calculated results are in very good agreement with the experimental data. Nuclear moments for the ground and first excited states are also predicted. (auth)

**27054** INTERPLAY OF CLASSICAL AND QUANTAL DESCRIPTIONS OF HEAVY-ION INTERACTIONS. Glendenning, N.K. (Lawrence Berkeley Laboratory, University of California, Berkeley, California 94720). Rev. Mod. Phys. 47: No. 3, 659-682 (July 1975).

Quasielastic collisions between complex nuclei, elastic, inelastic, and few-nucleon transfer are discussed both as a classical and quantal process. The classical trajectories can be used to illuminate the dependence of the quantal calculations on the physical parameters, and indeed can be used in a predictive way to suggest under what circumstances ambiguities can be resolved. The $S$-matrices for various quasielastic processes are exhibited and the quantal analog of the classical deflection function is compared with the classical one. The smooth behavior of the $S$-matrix for large angular momentum $l$ suggests the possibility of a two-part approach where the lower $l$ region is computed quantum mechanically, and the high-$l$ region is either parametrized, treated semiclassically, or interpolated between widely spaced $l$'s. The much greater sensitivity of several-nucleon transfer reactions to the interior region compared to elastic and inelastic scattering is stressed. Various aspects of two-nucleon transfer are discussed, including multiple-step processes, their dependence upon collectivity of the intermediate states, and the opposite sense of the interference involved in pickup and stripping reactions to vibrational states. (auth)

**27055** ENHANCEMENT OF FORWARD-ANGLE CROSS SECTIONS IN HEAVY-ION REACTIONS BECAUSE OF PROJECTILE EXCITATION. Glendenning, N.K.; Wolschin, G. (Lawrence Berkeley Laboratory, University of California, Berkeley, California 94720). Phys. Rev. Lett. 34: No. 26, 1642-1645 (30 June 1975).

It is shown that the forward-angle cross section in heavy-ion reactions can be strongly enhanced by indirect processes in the projectile or outgoing nucleus. This is demonstrated specifically for the reaction $^{122}Sn(^{16}O,^{18}O)^{120}Sn$ at 100 MeV, where data for the relevant transitions exist. At the lower energy of 60 MeV, which is just above the barrier, the effect on the forward cross section vanishes but at large angles beyond the peak the cross section is reduced in agreement with experiment. (auth)

**27056** DISINTEGRATION OF /SUP 103m/Rh. Czock, K. H.; Haselberger, N.; Reichel, F. (International Atomic Energy Agency, Vienna). Int. J. Appl. Radiat. Isot.; 26: No. 6-7, 417-421 (Jun 1975).

A technique for determination of the disintegration rate of /sup 103m/Rh in thick foils is described. In addition, the following parameters for the 39.75 keV isomeric transition were redetermined: total internal conversion coefficient $\alpha = 1531 + 30$; K shell internal conversion coefficient $\alpha_K = 127 + 6$; number of K x-rays per disintegration: $0.0676 \pm 0.0005$. (auth)

**27057** NUCLEAR DATA SHEETS FOR A EQUALS 90. Kocher, D. C. (Oak Ridge National Lab., TN). Nucl. Data Sheets; 16: No. 1, 55-105(Sep 1975).

The 1961 version of Nuclear Data Sheets for A equals 90 and the 1970 Midstream Evaluation, A equals 90 were revised on the basis of experimental data received prior to May 1, 1975. Results from approximately 225 papers and communications chosen from the extensive literature for this A–chain were included in the present evaluation. Numerous additional references dealing with reaction mechanism studies and nuclear structure theory are not included in this compilation, but are available upon request from the Nuclear Data Project. Data on nine A equals 90 nuclei are presented. The decay of $^{90}Br$ has been observed, but the decay scheme has not been established. Recent unpublished results on $^{90}Kr$ and $^{90}Rb$ decays are presented. These results are not yet complete, but appear to be considerably more extensive than previously published work. The particularly simple decay schemes for $^{90}Sr$ and $^{90}Y$ are well known. A few spin assignments have been proposed for levels in $^{90}Sr$, but additional reaction studies would be useful. Many spin assignments have been made for levels in $^{90}Y$, $^{90}Zr$, $^{90}Nb$, and $^{90}Mo$ from a variety of decay and reaction studies. The results for $^{90}Zr$ are particularly extensive. The decay schemes for $^{90}Nb$ and $^{90}Mo$ appear reasonably well established. Recent results on the decay of two $^{90}Tc$ isomers are presented, but the decay schemes have not been established and the energy ordering of the two isomers is not known. (auth)

**27058** NUCLEAR DATA SHEETS FOR A EQUALS 114. Kim, H. J. (Oak Ridge National Lab., TN). Nucl. Data Sheets; 16: No. 1, 107-133(Sep 1975).

Experimental nuclear structure information available through February 1975 are compiled, and adopted properties are presented. Where possible, the data are presented in comparative level diagrams, thereby eliminating many tabular listings, which resulted in substantial reduction in the size of the compilation. (auth)

**27059** HALF-LIFE OF $^{133}Xe$ AND ITS CALIBRATION FACTOR FOR THE 1383A IONIZATION CHAMBER. Woods, M. J.; Goodier, I. W.; Lucas, S. E. M. (National Physical Lab., Teddington, Eng.). Int. J. Appl. Radiat. Isot.; 26: No. 8, 485–487 (Aug 1975).

Measurement of the half-life of $^{133}$Xe using a high pressure ionisation chamber and a sealed gas ampoule is reported. The calibration of a simple jig designed to be used in conjunction with 1 ml single dose cartridges for $^{133}$Xe as supplied by the Radiochemical Centre, Amersham and the 1383A ionization chamber to facilitate the assaying of the $^{133}$Xe in solution is described. The manufacturing tolerances of the jigs are such that the same calibration factor would be obtained for all jigs used in one 1383A ionisation chamber to within ±3%. (UK)

**27060** DECAY SCHEME OF CESIUM-137. Goodier, I. W.; Makepeace, J. L.; Stuart, L. E. H. Int. J. Appl. Radiat. Isot.; 26: No. 8, 490-492(Aug 1975).

The decay of $^{137}$Cs has been reinvestigated with a view to determining more accurate decay scheme parameters necessary in the absolute standardisation and routine assay of this radionuclide. This necessitated the measurement of the absolute disintegration rate together with the γ-quantum emission rate of a $^{137}$Cs solution, and the total internal conversion coefficient of the 662 keV level in $^{137m}$Ba. (UK)

**27061** ABSOLUTE MEASUREMENTS OF ANOMALOUS $\epsilon/\beta^+$-DECAY BRANCHING RATIOS. Firestone, R.B.; Warner, R.A.; McHarris, W.C. (Department of Chemistry, Cyclotron Laboratory, and Dept of Physics, Michigan State University, East Lansing, Michigan 48824); Kelly, W.H. Phys. Rev. Lett. 35: No. 6, 401-403 (11 Aug 1975).

Absolute values of $\epsilon/\beta^+$-decay branching ratios for decay of $^{145}$Gd to twelve levels in $^{145}$Eu have been measured. These measurements are all shown to deviate substantially from the calculated $\epsilon/\beta^+$ ratios of Gove and Martin. Skew ratios (exp/theor) are found to range from 1.5 to 40. These "anomalies" are ascribed to second-order corrections to allowed decay which have not been included in the calculations. (auth)

**27062** HALF-LIVES OF $^{92-97}$Rb AND $^{142-145}$Cs. Reeder, P.L.; Wright, J.F. (Battelle, Pacific Northwest Laboratories, Richland, Washington 99352). Phys. Rev. C 12: No. 2, 718-720 (Aug 1975).

Half-lives of $^{92-97}$Rb and $^{142-145}$Cs have been measured by counting $\beta$ particles emitted from sources deposited on the first dynode of an electron multiplier at the collector end of an on-line mass spectrometer. Decay curve analysis included corrections for growth and decay of daughter and granddaughter activities as well as for growth and decay of delayed-neutron products. These results differ from some earlier measurements at masses 93, 94, and 145. They confirm with equal or smaller uncertainties the recent half-life measurements done by direct counting of neutrons from those nuclides which are delayed neutron precursors. (auth)

**27063** SPECTROSCOPY OF $^{146}$Sm VIA THE ($d$, $t$) AND OF $^{148}$Sm VIA THE ($d$, $t$) AND ($d$, $p$) REACTIONS. Oelert, W.; Maher, J.V.; Sink, D.A.; Spisak, M.J. (Nuclear Physics Laboratory, University of Pittsburgh, Pittsburgh, Pennsylvania 15260). Phys. Rev. C 12: No. 2, 417-441 (Aug 1975).

The ($d$, $t$) reaction on the isotopes $^{147}$Sm and $^{149}$Sm has been investigated at a deuteron energy of 17 MeV; the ($d$, $p$) reaction on the isotope $^{147}$Sm at a deuteron energy of 12.5 MeV. Angular distributions were taken in 2.5° steps in the range of $7.5 \leqslant \theta_{lab} \leqslant 35°$ and in 5° steps for $\theta_{lab} > 35°$. The experimental energy resolution is 9–11 keV for the pickup reactions and 10–12 keV for the stripping case. Spectroscopic factors and $l$ transfers were extracted by distorted wave Born approximation analysis. Eighty-three states in $^{146}$Sm are observed; $l$ transfer and $J^\pi$ limits are given for 36 of them. For the nucleus $^{148}$Sm 97 states are observed; $l$ transfers and $J^\pi$ limits are given for 63 of them. Reasonable $l=3$, $l=1$, and $l=0$ summed strengths have been found. Comparison with ($p$,$t$) and ($t$,$p$) studies of the same final nuclei investigated here is made in a phenomenological collective picture. (auth)

**27064** DIFFERENCES BETWEEN ARGON- AND KRYPTON-INDUCED REACTIONS LEADING TO THE SAME COMPOUND NUCLEI $^{158}$Er AND $^{156}$Er. Seglie, E. (Rensselaer Polytechnic Institute, Troy, New York 12181). Phys. Rev. C 12: No. 2, 683-685 (Aug 1975).

The observed differences in the neutron-evaporation excitation functions for argon- and krypton-induced reactions may be due to the strong friction in the classical dynamic model. In order to reproduce the complete fusion cross sections, a large energy loss in the Kr entrance channel is needed. This large energy loss may be associated with the preequilibrium emission of neutrons in the Kr channel. Neither the large energy loss nor the preequilibrium emission is expected in the Ar channel. (auth)

**27065** GAMMA-RAY LINEAR POLARIZATION MEASUREMENTS FOLLOWING HEAVY-ION BOMBARDMENT OF ODD ISOTOPES OF Pd. Kim, J.S.; Lee, Y.K. (The Johns Hopkins University, Baltimore, Maryland 21218); Hardy, K.A.; Simms, P.C.; Grau, J.A.; Smith, G.J.; Rickey, F.A. Phys. Rev. C 12: No. 2, 499-506 (Aug 1975).

γ-ray linear polarization measurements have been used to locate negative parity states in the even-odd isotopes $^{99,101,103}$Pd. A Compton polarimeter based on two Ge(Li) coaxial detectors was used. Collective bands ($I=11^-/2$, $15^-/2$, $19^-/2$, ...) built on $11^-/2$ states were observed in $^{101}$Pd and $^{103}$Pd. Many negative parity states were also observed in $^{99}$Pd, but they do not appear to be part of a similar collective band. These polarization measurements also confirm many angular momentum assignments which previously had been made using systematic arguments. (auth)

**27066** $\pi^+$ + NUCLEUS → $K^+$ + HYPERNUCLEUS IN THE IMPULSE APPROXIMATION. Calzavara, S.; Schick, L.H. (Department of Physics and Astronomy, University of Wyoming, Laramie, Wyoming 82071). Phys. Rev. C 12: No. 2, 507-513 (Aug 1975).

The impulse approximation and some crude nuclear and hypernuclear wave functions are used to calculate cross sections for some reactions of the type $\pi^+$ + nucleus → $K^+$ + hypernucleus for incident $\pi^+$ laboratory energies in the range 0.55–1.0 GeV. Target nuclei considered were $^4$He, $^7$Li, and $^{119}$Sn. Cross sections (or cross sections per nucleon) were calculated for production of the ground states and some possible excited states of the resultant hypernuclei. Although some results are marginal, on the whole the calculated cross sections appear to be too small for this to be a useful production method for hypernuclei at the pion energies available at present meson factories. (auth)

**27067** DECAYS OF $^{101}$Mo AND $^{101}$Tc. Wright, J.F.; Talbert, W.L. Jr.; Voigt, A.F. (Ames Laboratory-ERDA and Departments of Physics and Chemistry, Iowa State University, Ames, Iowa 50010). Phys. Rev. C 12: No. 2, 572-581 (Aug 1975).

The activities $^{101}$Mo and $^{101}$Tc produced from neutron capture by natural Mo were chemically separated and studied using Ge(Li) γ-ray detectors. Out of 185 transitions observed in the decay of $^{101}$Mo, 170 were assigned to 44 excited levels in $^{101}$Tc. For the decay of $^{101}$Tc, 26 of 27 transitions were placed among 10 excited levels in $^{101}$Ru. The interpretation of the $^{101}$Tc level scheme using the shell-model approach is not satisfactory even for a five-particle calculation. Systematics of odd-$A$ level structures in the region of $A=101$ indicate that the level structure of $^{101}$Tc could be due partly to the onset of collective effects. (auth)

**27068** LEVEL STRUCTURE OF $^{106}$Pd FROM THE DECAY OF $^{106}$Rh$^g$. Hsue, S.T.; Hsu, H.H. (Department of Physics, University of Northern Iowa, Cedar Falls, Iowa 50613); Wohn, F.K.; Western, W.R.; Williams, S.A. Phys. Rev. C 12: No. 2, 582-594 (Aug 1975).

The low-spin level structure of $^{106}$Pd was studied using high-resolution large volume Ge(Li) detectors for γ-ray singles, coincidence and angular correlation measurements. The measurements allowed the resolution of most of the discrepancies found among previous studies. In particular, the use of two Ge(Li) detectors for coincidences and angular correlations allowed unambiguous placement of previously multiply placed γ rays and resolved discrepancies in energy level of $J^\pi$ assignments. The experimental level structure and $B$ ($E2$) ratios are compared with predictions of an anharmonic spherical vibrator model and a rotor-vibrator model; we find that the evidence strongly supports the latter of the two models. (auth)

**27069** IDENTIFICATION OF AN ISOMER IN $^{110}$Ag AT 1-keV EXCITATION ENERGY. Clark, D.D.; Kostroun, V.O.; Siems, N.E. (Ward Laboratory of Nuclear Engineering, Department of Applied and Engineering Physics, Cornell University, Ithaca, New York 14853). Phys. Rev. C 12: No. 2, 595-608 (Aug 1975).

The existence of a new isomeric state in $^{110}$Ag at ~ 1 keV excitation has been established in two experiments using a new instrument, the inner-shell-vacancy (ISV) detector. In the first experiment, a transition with a half-life of 660 ± 40 ns was observed to follow the well-known 116-keV $M4$ transition that depopulates the $6^+$ 250-day isomeric level in $^{110}$Ag; the energy of the new transition was deduced to be $<3.3$ keV. In the second experiment, a half-life consistent with 660 ns was observed in the $^{109}$Ag($n$, γ)$^{110}$Ag reaction to follow γ transitions previously assigned by others to populate a 1-keV excited state. In combination the two results indicate the existence of a $2^-$ 660-ns isomer at 1.11 keV, although the (remote) possibility of more than one state near 1 keV cannot be excluded by direct experimental evidence. Under the assumption that the newly observed transition is from a $2^-$ 1.11-keV state to the $1^+$ ground state, its hindrance factor with respect to the Moszkowski estimate is $\sim 2.6 \times 10^3$, within the range expected from systematics. Possible chemical-state perturbations of the measured half-life are estimated to be much smaller than the measurement error. In both experiments the ~ 1-keV transition was detected with the ISV detector, a new device based on the well-established atomic effect that within $\sim 10^{-14}$ s after the formation of an inner shell vacancy an atom will undergo a multiple loss of electrons ranging from several to 20 or more, the number being a function of Z and subshell. The emitted electrons, which are very soft, are collected with an accelerating and focusing electrostatic lens and detected with a plastic scintillator and a photomultiplier tube. Nuclear transitions that cause ISVs can thus be sensed. Experiments are described that show the detector is fast,

sensitive, selective, and efficient in responding to ISVs. It is primarily a timing device with very restricted suitability for determining the energy of an initiating nuclear transition. (auth)

**27070** ANGULAR CORRELATION AND NUCLEAR ORIENTATION STUDY OF $^{131}$I POPULATED IN THE DECAY OF $^{131}$Te$^{m}$. Lhersonneau, G.; De Raedt, J.; Van de Voorde, H.; Ooms, H.; Haroutunian, R.; Schoeters, E.; Silverans, R.E.; Vanneste, L. (Katholieke Universiteit Leuven, Departement Natuurkunde, Celestijnenlaan 200 D, 3030 Heverlee, Belgium). Phys. Rev. C 12: No. 2, 609-615 (Aug 1975).

Some additional levels are proposed in the decay scheme of $^{131}$Te$^{m}$. From angular correlation and nuclear orientation measurements the spin and parity of several levels are determined uniquely: 774 keV ($11/2^+$), 852 keV ($9/2^+$), 1060 keV ($9/2^+$), 1315 keV ($9/2^+$), 1556 keV ($15/2^+$), 1596 keV ($13/2^+$), 1646 keV ($11/2^-$), 1797 keV ($15/2^-$), 1899 keV ($13/2^-$), 1980 keV ($11/2^-$), and 2001 keV ($9/2^+$ or $11/2^+$). The $\delta$ ($E2/M1$) ratios for the different transitions are obtained. The magnetic moment of the $^{131}$Te isomeric state is derived: $\mu = (-1.04 \pm 0.04)\ \mu_N$. (auth)

**27071** PERTURBED-ANGULAR-CORRELATION STUDIES OF $2^+$ LEVELS OF EVEN XENON ISOTOPES. Gordon, D.M.; Eytel, L.S. (Rutgers University, New Brunswick, New Jersey 08903); deWaard, H.; Murnick, D.E. Phys. Rev. C 12: No. 2, 628-636 (Aug 1975).

Thin solid xenon targets were prepared by condensing xenon gas on iron at 4.2 K. First $2^+$ levels of $^{124\text{-}132}$Xe were Coulomb excited and recoil implanted into the polarized iron foils. $B$ ($E2\uparrow$) values and g factors were determined from excitation and perturbed angular correlation data, respectively, and are in reasonable agreement with collective model calculations. A value for the average hyperfine field on xenon implanted into iron under these experimental conditions was determined to be $H_{\text{eff}} = 1.40 \pm 0.37$ MOe. (auth)

**27072** STRUCTURE OF $^{142}$Sm FROM THE DECAY OF $^{142}$Eu. Kennedy, G.G.; Gujrathi, S.C.; Mark, S.K. (Foster Radiation Laboratory, McGill University, Montreal, Canada). Phys. Rev. C 12: No. 2, 553-562 (Aug 1975).

$^{142}$Eu has been observed to have two isomers with half-lives $1.22 \pm 0.22$ min ($^{142}$Eu$^{m}$) and $2.4 \pm 0.2$ sec ($^{142}$Eu$^{g}$), both of which decay by $\beta^+$ emission to states in $^{142}$Sm, resulting in 32 and 8 $\gamma$ transitions, respectively. On the basis of $\beta^+$ and $\gamma$ ray singles and coincidence as well as conversion electron measurements, a level scheme comprising 20 excited states with deduced $J^\pi$ assignments has been constructed. Among the levels, a 5- and a 7-state at 2347.9 and 2372.0 keV, respectively, have been identified as two-quasiparticle neutron states. The half-life of the 2372.0 keV level has been measured to be $170 \pm 2$ ns using the $\beta^+$-$\gamma$ delayed coincidence technique. The $\beta^+$ end-point energy measurements yielded decay energies $Q_{EC} = 8.0 \pm 0.3$ MeV and $8.15 \pm 0.10$ MeV for $^{142}$Eu$^{g}$ and $^{142}$Eu$^{m}$, respectively. (auth)

**27073** $^{98}$Mo($p$, $d$)$^{97}$Mo REACTION AND CORE COUPLING IN $^{97}$Mo AND $^{97}$Nb. Bindal, P.K.; Youngblood, D.H.; Kozub, R.L. (Cyclotron Institute and Physics Department, Texas A&M University, College Station, Texas 77843); Hoffmann-Pinther, P.H. Phys. Rev. C 12: No. 2, 390-400 (Aug 1975).

The $^{98}$Mo($p$,$d$)$^{97}$Mo reaction has been used at a bombarding energy of 38.6 MeV to populate neutron hole states of $^{97}$Mo. Excitation energies and angular distributions were measured for levels up to 4.5 MeV in excitation. A distorted-wave-Born-approximation analysis was used to make $l$ assignments and to obtain spectroscopic factors. Three distinct groups of weakly excited levels, one corresponding to $l=4$ and two corresponding to $l = 1$, were observed lying above 2.7 MeV excitation. A hole-core-coupling model is used to predict the properties of $^{97}$Mo and $^{97}$Nb and good agreement with the experiment is obtained. (auth)

# Nuclear Properties and Reactions, 150 ≤ A ≤ 189

*Refer also to abstracts 26826, 27029, 27039, 27047, and 27081.*

**27074** (ANL/NDM-15) RADIATIVE CAPTURE OF FAST NEUTRONS IN $^{165}$Ho AND $^{181}$Ta. Poenitz, W. P. (Argonne National Lab., Ill. (USA)). Jun 1975. 31p. Dep. NTIS $4.75.

The fast neutron capture cross sections of $^{165}$Ho and $^{181}$Ta were measured from 0.3 to 3.0 MeV. A 1300 l large liquid scintillator with a time-resolution of 3-4 nsec was used for the detection of capture events. The time-of-flight technique was utilized for background suppression. A Grey Neutron Detector was used as a neutron flux monitor. The data were normalized at 500 keV to the standard capture cross section of gold. The resulting cross sections had an uncertainty of about 7 percent. The present capture cross sections and activation cross sections reported in the literature were interpreted in terms of the statistical model, using the Hauser-Feshback formalism and the gamma-cascade model. (6 figures, 2 tables) (auth)

**27075** EXCITATION OF HIGH-SPIN METASTABLE STATES FOLLOWING CAPTURE OF NEGATIVE PIONS BY NUCLEI. Buttsev, V.S.; Gavrilov, Yu.K.; Ganzorig, Zh.; Polikanov, S.M.; Chultém, D. (Joint Institute for Nuclear Research). JETP Lett. 21: No. 6, 182-183 (20 Mar 1975).

Formation of metastable states with high spin was observed following the capture of stopped negative pions by nuclei. (auth)

**27076** INELASTIC SCATTERING OF 14 MeV NEUTRONS BY HEAVY NUCLEI. Akiyoshi, T.; Katase, A.; Wakuta, Y.; Sonoda, M. (Kyushu Univ., Fukuoka (Japan). Faculty of Engineering). J. Nucl. Sci. Technol. (Tokyo); 11: No. 12, 523-534(Dec 1974).

Energy spectra of neutrons scattered inelastically from natural samples of Ta, W, Au, Hg, Tl, Pb and Bi have been studied at an incident energy of 14 MeV, using time-of-flight technique. Angular distributions were also measured for Ta and Bi. The energy spectra from 2 MeV to 4 MeV were found to be qualitatively consistent with the prediction from statistical theory taking account of effects of nuclear pairing and shell structure. The Fermi gas level density parameter and the nuclear temperature were obtained by considering the contribution of the (n, 2n) reaction. The variation of level density parameter plotted against mass number was found to agree with the trend predicted theoretically by Newton. Angular distributions proved to be symmetric about 90° and the spin cut-off parameter was estimated to be about 5.8 for Ta and 4.3 for Bi. Cross sections for the (n,n') and (n,2n) reactions were obtained. (auth)

**27077** PROTON-HOLE STATES OBSERVED IN THE $^{166}$Er($d$, $^3$He)$^{165}$Ho REACTION AT 34.5 MeV. Lewis, D.A.; Gray, W.S. (Cyclotron Laboratory, Physics Department, The University of Michigan, Ann Arbor, Michigan 48105). Phys. Rev. C 12: No. 1, 79-86 (July 1975).

The ($d$,$^3$He) pickup reaction at 34.5 MeV has been used to populate proton-hole states in $^{165}$Ho. No previous studies of this reaction on targets in the $A \sim 150$–$190$ region have been reported. At 34.5 MeV the angular distributions, measured over the range 15–35°, have sufficient structure to permit determination of $l$ transfers, although the detailed agreement with distorted-wave Born approximation (DWBA) predictions is not very good. The ($d$,$^3$He) spectra were examined up to 2 MeV of excitation in $^{165}$Ho, using nuclear emulsions and position-sensitive detectors in conjunction with a magnetic spectrometer. the $7/2^-$[523], $1/2^+$[411], $3/2^+$[411], $1/2^-$[541], and $5/2^+$[413] bands, which had previously been identified in decay or stripping studies, were also populated in the pickup reaction. In addition, new assignments were made for members of the $5/2^-$[532] and $1/2^+$[420] bands. Spectroscopic information determined from a DWBA analysis of the ($d$,$^3$He) reaction was compared with previously published ($^3$He,$d$) results to obtain separate values of the pairing occupation probabilities $U^2$ and $V^2$, and tne Nilsson coefficients $C_{lj}$ for levels populated in both reactions. The values of $U^2$ and $V^2$ obtained from this analysis agree remarkably well with predictions based on the BCS approximation, but the values of $C_{lj}$ are generally larger than Nilsson-model predictions, in some cases by a factor of two or more. These results, together with the poor agreement between some of the measured angular distributions and DWBA predictions, suggest the importance of multistep processes induced by inelastic scattering. We conclude that while the ($d$,$^3$He) reaction at $E \sim 35$ MeV is a useful tool for investigating proton-hole states in the rare-earth region, spectroscopic strengths, deduced from a conventional DWBA analysis should be regarded with caution. (auth)

**27078** NUCLEAR-ORIENTATION MEASUREMENT OF PARITY ADMIXTURE IN THE 501-keV GAMMA TRANSITION IN $^{180}$Hf$^{m}$. Chou, T.S.; Krane, K.S.; Shirley, D.A. (Department of Chemistry and Lawrence Berkeley Laboratory, University of California, Berkeley, California 94720). Phys. Rev. C 12: No. 1, 286-292 (July 1975).

The effect of the parity nonconserving nuclear force on the 501-keV $\gamma$ transition of $^{180}$Hf has been confirmed by a remeasurement of the angular distribution asymmetry of the radiation emitted by $^{180}$Hf$^{m}$ polarized at temperatures down to 16 mK. A difference of 1% was observed between the $\gamma$-ray intensities parallel and antiparallel to the nuclear polarization direction. When the results of the present study are averaged with previous nuclear polarization experiments and compared with the results of circular polarization experiments, it is deduced that the parity mixing can be uniquely assigned to an irregular $\tilde{E}2$ multiple, rather than to a higher order irregular multiple, such as $\tilde{M}3$. Assuming a vanishing $\tilde{M}3$ component, the present study yields $\epsilon = \langle \tilde{E}2 \rangle / \langle M2 \rangle = -0.026 \pm 0.002$, and the global average from all measurements is $\epsilon = -0.030 \pm 0.002$. (auth)

**27079** HIGH-SPIN STATES IN ODD-MASS DYSPROSIUM ISOTOPES STUDIED BY MEANS OF THE $\tau$, $\alpha$ REACTION. Grotdal, T.; Nyboe, K.; Straume, O.; Thorsteinsen, T. (Univ., Bergen). Phys. Norv.; 8: No. 1, 23-31 (1975).

High spin states in $^{157}$Dy, $^{159}$Dy, $^{161}$Dy, and $^{163}$Dy were studied by means of the ($\tau$, $\alpha$) reaction, with the main emphasis on localizing the lowest $13/2^+$ state and the 11/2 505↑ state. The identification of these states is based on the absolute cross sections and the comparison of the ($\tau$, $\alpha$) and the (d, t) cross sections. In $^{157}$Dy, $^{159}$Dy, and $^{161}$Dy, previous assignments are confirmed, whereas in $^{163}$Dy new assignments are given for the 11/2 505↑ state at 849 keV and for the lowest $13/2^+$ state at 495 keV excitation energy. (auth)

**27080** MIXING OF POSITIVE PARITY STATES IN ODD-MASS DYSPROSIUM NUCLEI. Grotdal, T.; Nyboe, K.; Straume, O.; Thorsteinsen, T. (Univ., Bergen). Phys. Norv.; 8: No. 1, 33-39 (1975).

The influence of the Coriolis coupling, the $\Delta N = 2$ coupling, and the particle-phonon coupling on the positive parity states in the odd-mass dysprosium nuclei was investigated. The particle-phonon coupling is shown to describe the splitting of the 400↑ orbital in $^{161}$Dy and $^{163}$Dy. The result of the calculations is compared with experimental data from (d, t) and ($\tau$, $\alpha$) reactions. (auth)

**27081** DECAY OF $^{152m1}$Eu AND $^{152m2}$Eu AND REACTION CROSS SECTIONS OF $^{153}$Eu AND 14 MeV NEUTRONS. Pruys, H. S.; Hermes, E. A.; von Gunten, H. R. (Eidgenoessisches Inst. fuer Reaktorforschung, Wuerenlingen, Switzerland). J. Inorg. Nucl. Chem.; 37: No. 7/8, 1587-1589(Jul 1975).

Energies and intensities of the $\gamma$-rays in the decay of Eu/sup 152m 1/ Eu and Eu/sup 152m 2/Eu have been measured using Ge-detectors. A new transition of 77.23 keV has been observed in the decay of /sup 152m 2/Eu. The half-lives of /sup 152m 1/Eu and /sup 152m 2/Eu have been measured to be 9.30 + 0.05 hr and 96 + 1 min, respectively. The reaction cross sections of $^{153}$Eu(n,$\alpha$)$^{150}$Pm, $^{153}$Eu(n, p)$^{153}$Sm and $^{153}$Eu(n, 2n) /sup 152m 2/Eu for 14 MeV neutrons were found to be 2.2 + 0.3 m.b., 8.9 + 0.8 m.b. and 116 + 11 m.b., respectively. (auth)

**27082** ENERGY LEVELS OF $Pt^{197}$. Calzavara Alves, S. (Centro Brasileiro de Pesquisas Fisicas, Rio de Janeiro); Barros, S. de; Goncalves, A. (Sao Paulo Univ. (Brazil). Instituto de Fisica). Z. Naturforsch., A; 29: No. 12, 1917-1918(Dec 1974).

7 refs.; 2 figs.; 3 tabs.

Spectra of $\gamma$ rays (higher than 0.3 MeV) following the $\beta$ decay of $Ir^{197}$ are measured with a Ge-Li detector (30 $cm^3$). The existence of four new branches to the $Pt^{197}$ levels at 877.6 ± 0.3; 939.7 ± 0.3; 1,049.6 ± 0.3; 1,341.8 ± 0.3 keV is proposed and lower limit log f t values are determined. Spin and parity $(\frac{1}{2}, \frac{3}{2})^+$ are assigned to the ground state of $Ir^{197}$. A new transition of 299.5 ± 0.2 keV was observed following the $Pt^{197}$ (80 min) decay. (auth)

**27083** NUCLEAR DATA SHEETS FOR A EQUALS 177. Ellis, Y. A.; Harmatz, B. (Oak Ridge National Lab., TN). Nucl. Data Sheets; 16: No. 1, 135-194(Sep 1975).

Nuclear structure information for all nuclei with mass number A equals 177 is summarized. Data from various decay and reaction experiments are compared. Evaluated data and the adopted spin, parity, and Nilsson-state assignments are given. Deviations from the regional trend of Nilsson ground-state assignments are noted for $^{177}$W and $^{177}$Re. Similar shifts have been observed in this region for nuclei 8 to 10 neutrons removed from the beta-stability line. In all cases, low-lying K/sup pi/ equals 1/2/sup +-/ orbitals move to ground. Data received prior to February 1975 were included. (auth)

**27084** *K*-CAPTURE PROBABILITY ($P_K$) IN THE DECAY OF $^{152}$Eu (12.4 yr) AND $^{192}$Ir (74 day). Dasmahapatra, B.K. (Saha Institute of Nuclear Physics, Calcutta-9, India). Phys. Rev. C 12: No. 2, 702-705 (Aug 1975).

From the analysis of the *K* x-ray–$\gamma$-ray sum peaks observed with a Ge(Li) detector the *K*-capture probability ($P_K$) for the 1529.8 keV and 1233.8 keV states of $^{152}$Sm in the decay of $^{152}$Eu(12.4 yr) and 690.5 keV state of $^{192}$Os in the decay of $^{192}$Ir(74 day) have been determined. The observed values are: $P_K^{1529.8}$=0.76 ± 0.09, $P_K^{1233.8}$=0.88 ± 0.10 and $P_K^{690.5}$=0.70 ± 0.06. (auth)

**27085** PRODUCTION AND INVESTIGATION OF TUNGSTEN $\alpha$ EMITTERS INCLUDING THE NEW ISOTOPES, $^{165}$W AND $^{166}$W. Toth, K.S. (Oak Ridge National Laboratory, Oak Ridge, Tennessee 37830); Schmidt-Ott, W.; Bingham, C.R.; Ijaz, M.A. Phys. Rev. C 12: No. 2, 533-540 (Aug 1975).

Neutron-deficient tungsten isotopes were produced by bombarding an enriched $^{156}$Dy target with $^{16}$O ions accelerated in the Oak Ridge isochronous cyclotron. A gas-jet-capillary system was used to transport product nuclei to an area where their $\alpha$-decay properties could be investigated. The data of Eastham and Grant concerning $^{162,163,164}$W were confirmed. In addition, two new weak $\alpha$ groups were observed. On the basis of excitation functions, $^{16}$N + $^{156}$Dy cross bombardments, and $\alpha$-decay energy systematics they were assigned to the new isotopes $^{165}$W and $^{166}$W. Their decay properties are as follows: (1) $^{165}$W, $E_\alpha$ = 4.909 ± 0.005 MeV, $T_{1/2}$ = 5.1 ± 0.5 sec, and (2) $^{166}$W, $E_\alpha$ = 4.739 ± 0.005 MeV, $T_{1/2}$ = 16 ± 3 sec. (auth)

# Nuclear Properties and Reactions, 190 ≤ A ≤ 219

*Refer also to abstracts 26984, 26991, 27029, 27033, 27039, 27075, 27076, and 27084.*

**27086** (CONF-750829-3) POLARIZATION OF PHOTONEUTRONS FROM THE THRESHOLD REGION OF $^{208}$Pb. Holt, R. J.; Jackson, H. E. (Argonne National Lab., Ill. (USA)). 1975. 3p. Dep. NTIS $4.00.

From fourth international symposium on polarization phenomena in nuclear reactions; Zurich, Switzerland(25 Aug 1975).

In order to determine the parities of several resonances in $^{208}$Pb, the polarization of photoneutrons from the $^{208}$Pb(gamma,n(pol)) $^{207}$Pb reaction was measured. This represents the first measurement of the polarization of photoneutrons from resonances near threshold. The observations are tabulated. (SDF)

**27087** (JAERI–1231, pp 107-111) EFFECT OF DEUTERON BREAKUP CHANNELS ON THE $^{208}$Pb(p,d)$^{207}$Pb REACTION AT Eq = 52 MeV. Aoki, Y.; Yagi, K. (Osaka Univ., Toyonaka, Japan). 13 Dec 1972.

From symposium on nuclear reaction and nuclear structure; Tokai, Ibaraki, Japan (13 Dec 1972).

In proceedings of a symposium on nuclear reaction and nuclear structure. (Japan Atomic Energy Research Inst., Tokyo).

"Deuteron breakup effect" on the $^{208}$Pb(p, d)$^{207}$Pb reaction is investigated for neutron-hole states $p_{\frac{1}{2}}^{-1}$, $f_{\frac{5}{2}}^{-1}$, $p_{\frac{3}{2}}^{-1}$, $f_{\frac{7}{2}}^{-1}$, $i_{\frac{13}{2}}^{-1}$ and $h_{\frac{9}{2}}^{-1}$. When the angular momentum transferred does not span the orbital-angular momentum difference of the incident and exit channels in a classical sense, this affects the differential cross sections by suppressing the contributions from lower partial waves. A greatly improved fit to the differential cross sections of the angular-momentum mismatched transfers is obtained, when compared with the usual DWBA. (auth)

**27088** DIRECT NEUTRON DECAY OF ISOBARIC ANALOG RESONANCES. Guba, V.G.; Zaretskii, D.F.; Urin, M.G. (Moscow Engineering Physics Institute). JETP Lett. 21: No. 6, 176-177 (20 Mar 1975).

An interpretation of the isospin-forbidden direct neutron decay of isobaric analog resonances (IAR) is proposed on the basis of the shell model. A formula is obtained for the elastic IAR neutron width. The concrete calculations were performed for the case of neutron scattering by the nuclei $^{90}$Zr and $^{206}$Pb. (auth)

**27089** GAMMA–GAMMA ANGULAR CORRELATIONS IN THE DECAY OF $^{192}$Ir. Yamada, S.; Hayashi, T. (Kyoto Univ., Kumatori, Osaka (Japan). Research Reactor Inst.); Aoki, K. Annu. Rep. Res. Reactor Inst., Kyoto Univ.; 7: 1-9(Oct 1974).

Angular correlation measurements of the $\gamma$-rays in $^{192}$Pt and $^{192}$Os following the decay of 74.2 day $^{192}$Ir have been made using two coaxial Ge(Li) detectors in conjunction with the two-dimensional multi-channel coincidence method. The analysis of the data on fourteen cascades has elucidated the spins and multipolarities of the levels and $\gamma$-ray transitions. Ratios of the multipolarities $\delta$ = (E2/M1) have been determined to be $\delta$ (296) = −7.4 ± 0.2, $\delta$ (308) = −8.0 ± 0.6, $\delta$ (416) = −3.1 ± 1.4 and $\delta$ (604) = 1.2 ± 0.1 in $^{192}$Pt and $\delta$ (283) = $1.6^{+\infty}_{-1.1}$ and $\delta$ (485) = 5.1 ± 0.5 in $^{192}$Os. The obtained results are discussed in comparison with those by other workers and with theoretical calculations. (auth)

**27090** NEUTRON RESONANCE SPECTROSCOPY: $^{203,205}$Tl. Liou, H.I.; Rainwater, J.; Hacken, G.; Singh, U.N. (Columbia University, New York, New York 10027). Phys. Rev. C 12: No. 1, 102-107 (July 1975).

Results are presented for high resolution time of flight neutron spectroscopy measurements of samples of natural Tl metal and of samples enriched in $^{203}$Tl and in $^{205}$Tl. Plots of $\sigma_t$ vs $E$ are given to 160 keV. Below 20 keV all observed levels are identified by isoptope, and as *s* or *p*, the orbital angular momentum of the interacting neutron. Values of $E_0$ and $g\Gamma_n$ are given for all observed levels, comprised of 25 *s* and 11 *p* levels in $^{203}$Tl and 5 *s* and 6 *p* levels in $^{205}$Tl. Favored *J* is given in many cases. Values of $\Gamma_\gamma$ for 6 *s* levels in $^{203}$Tl and 2 *s* levels in $^{205}$Tl give $\langle\Gamma_\gamma\rangle$ = 0.65 eV for $^{203}$Tl and 0.80 eV for $^{205}$Tl. Above 20 keV, values of $E_0$ and $\Gamma$ ($\simeq \Gamma_n$) are given for 29 *s* levels to 104 keV, with favored *A* for 20 levels and favored *J* for 16 levels. Values of $E_0$ and ($ag\Gamma_n$) are given for 44 *p* levels above 20 keV. Intermediate structure effects seem to be present for $^{203}$Tl to give $\Sigma g\Gamma_n^0/\Delta E$ below 6.6 keV much larger than 6.6 keV < $E$ < 20 keV. Ignoring that effect,

a usual analysis for the results below 20 keV gives $10^4 S_0 = (1.28_{-0.31}{}^{+0.45})$ for $^{207}$Tl and $(0.38_{-0.18}{}^{+0.44})$ for $^{205}$Tl, with $10^4 S_1$ $(0.25_{-0.09}{}^{+0.16})$ for $^{207}$Tl and $(0.15_{-0.07}{}^{+0.14})$ for $^{205}$Tl. (auth)

**27091** $^3$He ELASTIC SCATTERING FROM $^{208}$Pb AND $^{209}$Bi AT 71 MeV. Fulmer, C.B. (Oak Ridge National Laboratory, Oak Ridge, Tennessee 37830); Hafele, J.C.; Clarke, N.M. Phys. Rev. C 12: No. 1, 87-89 (July 1975).

Angular distributions of elastic scattering of 71 MeV $^3$He ions from $^{208}$Pb and $^{209}$Bi were measured over the range 18°–116°. Pronounced structure is observed at the larger angles. Optical-model analyses yield good fits to the data with $V \sim 120$ MeV and $J_R \sim 270$ MeV fm$^3$. The diffuseness term for the absorption well is larger and the radius smaller than for the real well. A grid-type analysis yielded evidence for discrete families of potentials similar to those observed for medium mass targets. (auth)

**27092** HALF-LIFE MEASUREMENT OF THE $^{212}$Po GROUND STATE. Sanyal, S.; Garg, R.K.; Chauhan, S.D.; Gupta, S.L.; Pancholi, S.C. (Department of Physics and Astrophysics, University of Delhi, Delhi-110007, India). Phys. Rev. C 12: No. 1, 318-319 (July 1975).

The half-life of the ground state of $^{212}$Po in the decay of $^{212}$Bi has been measured by recording $\beta\alpha$-delayed coincidences. The decay curve analyzed by the slope method gave the half-life $T_{1/2}(^{212}\text{Po ground state}) = 296 \pm 2$ ns. (auth)

**27093** OBSERVATION OF AN ENHANCED $4_1^+ \rightarrow 0^+$ CROSSOVER TRANSITION IN $^{202}$Pb BY CONVERSION ELECTRON SPECTROSCOPY. Hanser, A.; Wisshak, K.; Klewe-Nebenius, H.; Rebel, H. (Institut für Angewandte Kernphysik des Kernforschungszentrums Karlsruhe and II. Physikalisches Institut der Universität Heidelberg). Phys. Rev. C 12: No. 1, 338-340 (July 1975).

An enhanced $E4$ crossover transition ($4_1^+ \rightarrow 0^+$) in $^{202}$Pb has been observed by means of conversion electron spectroscopy using a Si(Li) detector with a special filter of permanent magnets. This method has shown to be much more sensitive in this case than the measurement of the $E4$ $\gamma$ rays. The branching ratio $E4(4_1^+ \rightarrow 0+)$ / $E2(4_1^+ \rightarrow 2_1^+)$ was found to be $(3.8 \pm 0.6)10^{-6}$, resulting in a partial half-life of $(4.6 \pm 0.8)$ Weisskopf units for the $E4$ transition. (auth)

**27094** DETERMINATION OF THE NUMBER OF INTERACTING NUCLEONS IN NITROGEN-EMULSION NUCLEUS COLLISIONS. Tomaszewski, A.; Wdowczyk, J. (Lodz Univ., Poland). J. Phys., A (London); 8: No. 7, 1189-1192 (Jul 1975).

An experimental study has been made of the interaction of nitrogen nuclei in nuclear emulsions. Particular attention has been paid to the determination of the number of incident nucleons which participate in the interaction. It is found that on average 75% of the nucleons emerging as free particles have interacted and produced pions. This number is close to what would be expected on the assumption that the incident nucleons in the nitrogen nucleus behave independently. The relevance of the measurements to the important case of extensive air showers initiated by heavy nuclei is considered and it is shown that the commonly used superposition model is sufficiently accurate for many applications. (auth)

**27095** FISSION OF LEAD INDUCED BY 600 MeV PROTONS. Hageboe, E. (Oslo Univ.); Lund, T. J. Inorg. Nucl. Chem.; 37: No. 7/8, 1569-1582 (Jul 1975).

Absolute radiochemical fission yields have been measured for 12 nuclides of Rb, Ag, Cd and Cs and relative fission yields measured for seven Kr isotopes and eight Xe isotopes produced by fission of natural lead induced by 600 MeV protons. The relative Kr and Xe yields have been determined using the ISOLDE facility at CERN. It is suggested that the production rate of a nuclide per m.b. of nuclear reaction cross section should be used as a figure of merit for on-line facilities like Isolde. During the present experiment $3.4 \times 10^6$ nuclei/sec m.b. and $2.0 \times 10^6$ nuclei/sec, m.b. were obtained for Kr and Xe isotopes, respectively. Charge and mass distributions and charge dispersion for fission of lead with 600 MeV protons are determined using the measured fission yields and some yields measured by other groups. The most probable charge $Z_p$, for a given mass and the width (FWHM) of the charge dispersion, both increase linearly with mass number. The integrated mass distribution curve gives a fission cross section of 149 ± 6 m.b. Elemental yield distribution is constructed and shows a most probable atomic number of 40.0, giving Mercury as the most probable fissioning element. Assuming no proton evaporation from fission fragments, it is suggested that elemental yield distributions and isotopic yield distribution and charge distribution and dispersion for the purpose of obtaining information on the fissioning nuclei. The elemental yield distribution is discussed on the basis of the liquid drop model for fission giving an average nuclear temperature at saddle point of 2.09 MeV, and a total number of neutrons evaporated after fission of about 13. Estimates of most probable cascade residuals for each residual element based on Monte Carlo intranuclear cascade calculations at 380 MeV together with presently observed most probable isotopes for each product Z are used to predict average cascade deposition energies for events leading to specific products. The agreement with literature values from recoil experiments is good. (auth)

**27096** TWO INNER $\beta$-TRANSITIONS IN THE DECAY OF $^{199}$Au. Reddy, B. V.; Narasimha Raju, M. L.; Sastry, D. L. (Andhra Univ., Waltair, India). Indian J. Pure Appl. Phys.; 13: No. 3, 166-168(Mar 1975).

The directional correlations of the $\beta$ (302 keV)$-\gamma$ (158 keV) and $\beta$ (251 keV)$-\gamma$ (208 keV) cascades in $^{199}$Au decay are measured and found to be isotropic, consistent with the validity of $\xi$-approximation for both the $\beta$-transitions. These results are also in accordance with the core-excitation model. (2 figures) (auth)

**27097** SEARCH FOR ANISOTROPY IN THE $L$ X—GAMMA ANGULAR CORRELATIONS FOLLOWING THE DECAY OF $^{207}$Bi. Cambiaggio, M.C.; Davidson, J.; Silbergleit, V.; Behar, M. (Laboratorio de Fisica Nuclear, Departamento de Fisica, Facultad de Ciencias Exactas y Naturales, Universidad de Buenos Aires, Buenos Aires, Argentina). Phys. Rev. C 12: No. 2, 699-701 (Aug 1975).

An investigation of the $Ll$ x-$\gamma$ angular correlations following the decay of $^{207}$Bi is done by using a Si(Li) semiconductor counter as $L$ x-ray detector. Coincidence measurements at five different angles were made between the 570-keV $\gamma$ ray (gated in the movable counter) and the $Ll$ x spectrum (displayed in a multichannel analyzer). (auth)

**27098** PARTICLE-VIBRATION RESONANCES IN NEUTRON SCATTERING FROM $^{208}$Pb. Ferguson, J.M. (Lawrence Livermore Laboratory, University of California, Livermore, California 94550). Phys. Rev. C 12: No. 2, 713-715 (Aug 1975).

The $^{208}$Pb total cross section below 600 keV is calculated by the coupled channel method. In this model the incident neutron is coupled to several $^{208}$Pb vibrational levels. The $s$-wave cross section including the resonance near 500 keV is well reproduced by the calculation. The model also predicts serveral narrow resonances with higher angular momentum. (auth)

**27099** 32.1 ms ISOMER IN $^{198}$Tl. Sen, P.; Cue, N.; Bakhru, H. (Physics Department, State University of New York at Albany, Albany New York 12222). Phys. Rev. C 12: No. 2, 716-717 (Aug 1975).

An isomer of $^{198}$Tl with a half-life of 32.1 ± 1.0 ms and transition energy of 198.8 ± 0.2 keV has been observed in the reaction $^{197}$Au($\alpha$,3$n$)$^{198}$Tl$^m$. (auth)

**27100** APPEARANCE OF NOVEL SIDEWAYS PEAKING IN LIGHT-FRAGMENT ANGULAR DISTRIBUTIONS FROM 28-GeV PROTON IRRADIATION OF U AND Au. Remsberg, L.P.; Perry, D.G. (Chemistry Department, Brookhaven National Laboratory, Upton, New York 11973). Phys. Rev. Lett. 35: No. 6, 361-363 (11 Aug 1975).

Energy spectra of fragments with $6 \leq Z \leq 12$ produced by the interactions of 28-BeV protons with uranium and gold were measured at several angles with a ($dE/dX$) -$E$ counter telescope. The angular distributions exhibit broad peaks at ~70° which tend to become more prominent with increasing fragment $Z$. The presence of these peaks may be evidence for the generation of nuclear shock waves. (auth)

**27101** FINITE RANGE CALCULATIONS OF LIGHT-ION TWO-NEUTRON TRANSFER REACTIONS. Charlton, L.A. (Department of Physics, The Florida State University, Tallahassee, Florida 32306). Phys. Rev. C 12: No. 2, 351-358 (Aug 1975).

A full finite-range distorted-wave Born-approximation formalism is used to calculate the two-neutron transfer reactions $^{18}$O($p,t$)$^{16}$O(g.s.), $^{40}$Ca($t,p$)$^{42}$Ca(g.s.), and $^{208}$Pb($p,t$)$^{206}$Pb(g.s.). It is found that the shape of the differential cross section is well predicted in the forward direction for all nuclei studied, but the normalization is given correctly only for $^{18}$O. (auth)

## Nuclear Properties and Reactions, A ≥ 220

*Refer also to abstracts 25924 and 27100.*

**27102** (COO-2176-27) FRAGMENT ENERGY DEPENDENT BIASES IN IONIZATION CHAMBER MEASUREMENTS OF FISSION CROSS SECTIONS. Cohensedgh, F.; Felvinci, J. P.; Melkonian, E. (Columbia Univ., New York (USA). Div. of Nuclear Science and Engineering). 1974. 3p. (CONF-751019-1). Dep. NTIS $4.00.

From ANS winter meeting; Washington, District of Columbia, USA (27 Oct 1975).

By using accepted fragment energy loss data, pulse height responses were calculated for fragments in the 50–110 MeV emission

energy range as a function of fissile target thickness, target chemical composition, chamber plate spacing and gas pressure. Usually a low discriminator level is set on the chamber to reject natural alpha particles. Subsequently, the effects of such a discriminator on chamber detection efficiency were calculated. The results are summarized. (auth)

**27103** (UCID-16885(Rev.1)) NEUTRON REACTIONS ON U-237. Gardner, D. G. (California Univ., Livermore (USA). Lawrence Livermore Lab.). 25 Aug 1975. Contract W-7405-Eng-48. 35p. Dep. NTIS $4.00.

Calculations were made of the major reactions induced by neutrons in the energy range of 10 eV to 2.5 MeV incident on $^{237}$U. The ground state as well as two isomeric states were considered as targets. The isomers treated were the 3.1 ns $^{5}/_{2}^{+}$ state at 0.160 MeV and the 0.15 mu s $^{7}/_{2}^{-}$ state at 0.274 MeV. Using the COMNUC and UHL statistical model codes and Moldauer's optical-model parameters, the total, shape elastic, compound elastic, inelastic, capture, and fission cross sections were calculated, and are presented in tabular and graphic form. The fission calculations are compared with cross sections inferred from (t,p fission) measurements on $^{236}$U, with cross sections measured on the Pommard underground nuclear explosion, and with recent calculations of Jary for neutrons above 2 MeV. The production of the ground state and the isomers of $^{237}$U was estimated from a consideration of the (n,2n) reaction on $^{238}$U and the inelastic scattering reactions among the $^{237}$U levels. (10 tables, 11 figures) (auth)

**27104** (ZJE-158) FISSION PRODUCT DATA LIBRARY. Hep, J.; Valenta, V. (Skoda, Plzen (Czechoslovakia)). 1975. 306p.

The library includes data for 584 isotopes of fission products. There are presented decay constants, branching ratios (both burn-up and decay), emitted radiation, relative and absolute yields, capture cross section for thermal neutrons, and resonance integrals. If a detailed decay scheme is not known, average energies of beta particles, neutrino and gamma radiation are presented. In the ZVJE SKODA system the library is named BIBFP and is stored on the film No 49 of the NE 803 B computer. It is used for calculations of inventory of fission products in fuel elements, further for determination of absorption cross sections for burn-up calculations, gamma ray sources, heat generation, and for a solution of transport of activities in primary circuits. It can be also used in a spectrometric method for determination of burn-up of fuel elements. The library has been set up by compilation of the last accessible literary data. From this, the library BIBGRFP of group constants of fission products with independent yields of isotopes from fission has been worked out. By the choice from the last one the BIBDN library has been obtained, where data for predecessors of delayed neutron emitters are collected. (auth)

**27105** STATISTICAL ESTIMATION OF DISTRIBUTIONS OF PHYSICAL QUANTITIES IN NUCLEAR FISSION. Yamamoto, T.; Sugiyama, K. (Tohoku Univ., Sendai (Japan). Faculty of Engineering). J. Nucl. Sci. Technol. (Tokyo); 11: No. 11, 461-470(Nov 1974).

Making use of a model based on the statistical theory, calculations were performed to obtain the mass yields, the most probable charges, the kinetic energies and the prompt neutron yields of fission fragments, and the mass yields of fission products from thermal-neutron-induced fission of $^{233}$U, $^{235}$U, $^{239}$Pu, $^{241}$Pu and from the spontaneous fission of $^{252}$Cf. The calculations are further extended to fast-neutron-induced fission. The scission-point distance is treated as a parameter varying with the mass number of the heavy fragments of fission. This proved successful in approaching the calculated curves closer to the observed values. It is possible to predict unknown physical quantities in nuclear fission with use made of the method developed in the present work. (auth)

**27106** $^{6}$Li AND $^{7}$Li INDUCED FISSION OF $^{232}$Th AND $^{238}$U. Freiesleben, H.; Rizzo, G.T.; Huizenga, J.R. (Nuclear Structure Research Laboratorys and Department of Chemistry and Physics, University of Rochester, Rochester, New York 14627). Phys. Rev. C 12: No. 1, 42-50 (July 1975).

The energy dependence of the total fission cross section, the fragment angular distribution, and the fragment correlation angles were measured for $^{6}$Li and $^{7}$LI induced fission of $^{232}$Th and $^{238}$U at bombarding energies of 24–38.4 MeV. Angular distributions of elastically scattering projectiles for the four systems were measured at 37.2 MeV. Characteristic differences were found for $^{6}$Li and $^{7}$Li projectiles which are independent of the target. These differences include (1) the $^{7}$Li induced fission has a larger anisotropy, (2) the energy dependence of the fragement anisoptropy shows more structure for $^{7}$Li, and (3) at low bombarding energy the cross section for $^{6}$Li induced fission is considerably larger. These factors are discussed in terms of (1) competition between compound nucleus fission and fission following transfer reactions and (2) the deexcitation branching ratios between neutron emission and fission. (auth)

**27107** CALCULATION OF THE NEUTRON-CAPTURE CROSS SECTIONS OF $Th^{232}$ AND $U^{238}$. De-ji, F.; Yan-huang, C.; Ke-ding, X. (The Nuclear Institute, Shanghai). Chin. J. Phys. 23: No. 3, 127-131 (Nov 1974).

The neutron-capture cross sections of $Th^{232}$ and $U^{238}$ before the opening of the fission channels are calculated with the use of statistical theory. The effects of optical-potential parameters, such as the gamma radiation widths, the nuclear temperature, and the statistical width-fluctuation correction factor, are illustrated and discussed. (auth)

**27108** THEORY OF CHARGE DISPERSION IN NUCLEAR FISSION. Gupta, R.K.; Scheid, W.; Greiner, W. (Institut für Theoretische Physik der Johann Wolfgang Goethe Universität, Frankfurt am Main, Germany). Phys. Rev. Lett. 35: No. 6, 353-356 (11 Aug 1975).

By introducing charge asymmetry as a new dynamical collective coordinate in the asymmetric two-center shell model, the nuclear charge dispersion in the fission of $^{236}$U is calculated without using any free parameter. The agreement between theory and experiment is quite good. (auth)

**27109** INDEPENDENT FISSION YIELDS OF Rb AND Cs FROM THERMAL-NEUTRON-INDUCED FISSION OF $^{239}$Pu. Balestrini, S.J.; Forman, L. (Los Alamos Scientific Laboratory, University of California, Los Alamos, New Mexico 87544). Phys. Rev. C 12: No. 2, 413-416 (Aug 1975).

The relative independent fission yields of Rb and Cs from thermal-neutron-induced fission of $^{239}$Pu have been measured on line using a mass spectrograph and thermalized neutrons from a burst reactor. Independent yields were derived by normalizing the measurements to products of chain yields and fractional independent yields, estimating the latter from measured cumulative yields of Kr and Xe. Comparing the independent yields with those from $^{238}$U fission, the $^{239}$Pu results show shifts in isotopic yield distribution toward lower mass for both Rb and Cs and also toward the production of more Cs and less Rb when $^{239}$Pu is fissioned. (auth)

**27110** PARTICLE-PHONON INTERACTIONS IN $^{248}$Cf AND $^{249}$Cf. Yates, S.W.; Chasman, R.R.; Friedman, A.M.; Ahmad, I.; Katori, K. (Chemistry Division, Argonne National Laboratory, Argonne, Illinois 60439). Phys. Rev. C 12: No. 2, 442-450 (Aug 1975).

The extent of particle-phonon mixing in $^{248}$Cf and $^{249}$Cf has been determined using the $^{249}$Cf($d,t$) and $^{249}$Cf($d,d'$) reactions. $K^{\pi}=2^{-}$ bands were identified at 593 and 1477 keV in $^{248}$Cf. Since the only $K^{\pi}=2^{-}$ neutron two quasiparticle configuration expected below 2 MeV in $^{248}$Cf is $\{9/2^{-}[734];5/2^{+}\ [622]\}_{2^{-}}$, the second $K^{\pi}=2^{-}$ band is considered to be predominantly of phonon character. In $^{249}$Cf a $K^{\pi}=5/2^{+}$ band at 145 keV, known from decay scheme studies, receives a measurable population in the ($d,d'$) reaction. The phonon admixture in the $5/2^{+}$ state which results from the $\{9/2^{-}[734]\otimes 2^{-}$ phonon$\}$ configuration was determined to be (29±5) %. The collective admixture in the $5/2^{+}$ state was also calculated from an octupole particle-hole interaction and was found to be 35%, in good agreement with the experimental value. The anomalously low energy of the $5/2^{+}$ state could not be entirely reproduced by this calculation. (auth)

**27111** LEVELS IN $^{237}$Pu POPULATED BY $^{237}$Am (ELECTRON CAPTURE) AND $^{241}$Cm($\alpha$) DECAYS. Ahmad, I.; Porter, F.T.; Freedman, M.S.; Sjoblom, R.K.; Lerner, J.; Barnes, R.F.; Milsted, J.; Fields, P.R. (Chemistry Division, Argonne National Laboratory, Argonne, Illinois 60439). Phys. Rev. C 12: No. 2, 541-552 (Aug 1975).

The electron capture decay scheme of $^{237}$Am (73 min) has been investigated by measuring the $\gamma$-ray and conversion-electron spectra of mass-separated $^{237}$Am samples. The $\gamma$-ray spectra were measured with a Ge(Li) spectrometer and the conversion-electron spectra were measured with a cooled Si(Li) detector and a magnetic $\beta$-ray spectrometer. Thirty-five $\gamma$ rays were identified and the multipolarities of most of the transitions were deduced. The half-life of $^{237}$Am was determined by following the decay of the 280.2 keV photopeak and was found to be 73.0 ± 1.0 min. The $\alpha$-particle energy and $\alpha$ branching were measured to be 6.042 ± 0.005 MeV and $[(2.5 \pm 0.3) \times 10^{-2}]$%, respectively. On the basis of the present investigation the following single-particle states have been identified in $^{237}$Pu: 7/2-[743], 0; 1/2+[631], 145.5; 5/2+[622], 280.2; 3/2+[631], 370.4; 5/2+[633], 407.8; 7/2+[624], 473.5; 5/2-[752], 655.3; and 7/2+[613], 908.8 keV. The ground state of $^{237}$Am has been deduced to be the 5/2-[523] Nilsson orbital. The log$ft$ values for electron capture transitions to the observed states were derived. The $\alpha$-particle spectrum of a mass-separated $^{241}$Cm sample was measured with the Argonne double focusing magnetic spectrometer. Eleven $\alpha$ groups identified in this spectrum populate the members of the ground state, 1/2+[631], and 3/2+[631] bands. The $\alpha$-decay hindrance factors are consistent with the Nilsson-state assignments deduced from $^{237}$Am electron capture decay. (auth)

# Nuclear Theory

*Refer also to abstracts 26860, 26875, 26897, 26965, 26988, 27002, 27020, and 27168.*

**27112** (CONF-750663-1) COMPUTATION OF THE REACTION MATRIX, G. Becker, R. L. (Oak Ridge National Lab., Tenn. (USA)). 1975. 20p. Dep. NTIS $4.00.

From international solvent extraction conference; The Hague, Netherlands (19 Aug 1971).

Properties of the reaction operator for the interaction of two identical fermions in a medium of the same kind of fermions are described. Unlike the bare interaction, the reaction operator is dependent on the medium through Q (density dependence) and through the self-energy U, and is energy (or momentum) dependent. Two ways of representing G in terms of Hermitian projection operators are considered. The integral equation relating two reaction operators is derived and simple approximations providing insight into the interaction are discussed. For finite nuclei, one would like to calculate a G matrix for which Q and U correspond to the self-consistent orbitals. To this end, two common choices of approximate Hamiltonian are discussed along with nearly exact methods for calculating G with a propagator diagonal in N and L where NLM are relative center of mass coordinates. Finally the case is examined in which a propagator defined in terms of individual particles is used. (5 figures, 53 references) (SDF)

**27113** (IFKKI-75/4) PHYSICAL CONSERVATION LAWS AND THE $\beta$-DECAY OF NUCLEI. Bagge, E. (Kiel Univ. (F. R. Germany). Inst. fuer Reine und Angewandte Kernphysik). Apr 1975. 16p. (In German). INIS.

3 figs.

The law of conservation of energy is extended to the region of the Dirac states of negative energy. When particles are produced or disappear, energy changes occur in the negative energy region which can be seen in the positive energy region. The law of conservation of energy then says that the total change in energy is equal to naught. The same is valid for translations and angular momentum. The way in which completely occupied states change energy and momentum is not shown. The $\beta$-decay of the neutron is considered as pair production in which an electron is emitted and a positron is bonded to the neutron. Neutrinos are not produced. The latest results on neutrino experiments on accelerators are not discussed. (auth)

**27114** (JAERI-1231, pp 1-18) THEORETICAL TREATMENT OF DIRECT REACTIONS INDUCED BY HEAVY IONS. Imanishi, B. (Nihon Univ., Tokyo). 13 Dec 1972.

From symposium on nuclear reaction and nuclear structure; Tokai, Ibaraki, Japan (13 Dec 1972).

In proceedings of a symposium on nuclear reaction and nuclear structure. (Japan Atomic Energy Research Inst., Tokyo).

The theoretical treatments of the direct reactions induced by heavy ions are reviewed. First, the DWBA treatment of the inelastic scattering and the transfer reactions are considered. Some questions in the heavy-ion approximation which is sometimes introduced into the DWBA-form factors are discussed in some detail. In order to treat more exactly the motion of the valence nucleons in heavy-ion reactions, the PSS-method (adiabatic treatment) and coupled channel method are investigated. The effective interactions for the wave functions of the relative motions are discussed. It is also shown that the semi-classical treatment of the relative motion between heavy-ions considerably simplifies the theoretical treatment of the reaction amplitude in some cases. (auth)

**27115** (JAERI-1231, pp 19-23) PARITY-DEPENDENT INTERACTION IN ALPHA-NUCLEUS ELASTIC SCATTERING. Tanimure, O. (Kyoto Univ.). 13 Dec 1972.

From symposium on nuclear reaction and nuclear structure; Tokai, Ibaraki, Japan (13 Dec 1972).

In proceedings of a symposium on nuclear reaction and nuclear structure. (Japan Atomic Energy Research Inst., Tokyo).

The extended optical potential model with parity-dependent real potential is presented to analyse phenomenologically elastic $\alpha$-particle scatterings from sd-shell nuclei. The parity-dependent potential is derived from the $\alpha$-particle model through the $\alpha$-exchange process between incident $\alpha$-particle and target nucleus, and is shown to have the attraction of the surface-type. This model explains experimental cross-sections, especially, the backward rise and pattern of angular distributions at the $\alpha$-particle energies between 20 and 50 MeV. (auth)

**27116** (JAERI-1231, pp 24-26) EXCHANGE EFFECTS AND NONLOCALITY OF A POTENTIAL. Yoshida, H. (Osaka Univ., Toyonaka, Japan). 13 Dec 1972.

From symposium on nuclear reactions and nuclear structure; Tokai, Ibaraki, Japan (13 Dec 1972).

In proceedings of a symposium on nuclear reaction and nuclear structure. (Japan Atomic Energy Research Inst., Tokyo).

The Schrödinger equation with a non-local potential is solved by an iterative method. The non-local potential is obtained by taking account of exchange effects in the elastic scattering. In a nucleon scattering, the solution of the equation in the phenomenological non-local potential shows the well known damping in the nuclear interior compared to the solution in the equivalent local potential. In $^{16}O-^{12}C$ elastic scattering where the exchange of two $^{12}C$ cores is taken into account explicitly, the potential shows parity dependence. The solutions with even partial waves are pulled in and those with odd partial waves are pushed out due to the parity dependent non-local potential. (auth)

**27117** (JAERI-1231, pp 43-48) NEW MECHANISM IN HEAVY ION REACTIONS. Kamitsubo, H. (Institute of Physical and Chemical Research, Wako, Saitama, Japan). 13 Dec 1972.

From symposium on nuclear reaction and nuclear structure; Tokai, Ibaraki, Japan (13 Dec 1972).

In proceedings of a symposium on nuclear reaction and nuclear structure. (Japan Atomic Energy Research Inst., Tokyo).

At sufficiently high bombarding energies above Coulomb barrier, broad bumps of about 15 MeV width are observed in the spectrum of multi-nucleon transfer reactions. Angular distributions are monotonically increasing at forward angles. The shape and position of a bump are well reproduced with level density analysis. In the analysis, angular momentum matching condition and angular momentum cut off are included. Level density parameter, a, is about one third of the usual value. The possibility of direct process which causes the multi-particle multi-hole states is discussed. (auth)

**27118** (JAERI-1231, pp 49-68) TOPICS IN DIRECT NUCLEAR REACTION THEORIES. Kawai, M. (Tokyo Inst. of Tech.). 13 Dec 1972.

From symposium on nuclear reaction and nuclear structure; Tokai, Ibaraki, Japan (13 Dec 1972).

In proceedings of a symposium on nuclear reaction and nuclear structure. (Japan Atomic Energy Research Inst., Tokyo).

Some recent developments in direct nuclear reaction theories are reviewed. The subjects discussed are: (1) microscopic theories of nuclear inelastic scattering and effective nucleon-nucleon interaction, (2) excitation of "giant resonance states" below dipole giant resonance, (3) form factor of one-nucleon transfer reactions, and (4) multi-step processes in direct nuclear reactions. (auth)

**27119** (JAERI-1231, pp 78-106) TWO-NEUTRON TRANSFER REACTIONS AND NUCLEAR STRUCTURE. Yagi, K. (Osaka Univ., Toyonaka, Japan). 13 Dec 1972.

From symposium on nuclear reaction and nuclear structure; Tokai, Ibaraki, Japan (13 Dec 1972).

In proceedings of a symposium on nuclear reaction and nuclear structure. (Japan Atomic Energy Research Inst., Tokyo).

Two-neutron transfer reactions produced by (p, t) or (t, p) reactions provide a powerful tool for investigating the pairing correlation of neutrons in nuclei. The following subjects are described: (1) Introduction. (2) DWBA theory (one-step process) of two-neutron transfer reactions. (3) Collective enhancement of two-neutron transfer reactions between levels of the BCS state. (4) Pairing vibrations. (5) The pairing phase transition. (6) Quadrupole pairing correlations. (6-1) Nuclei around N = 82. (6-2) Actinide Nuclei (7) Effect of inelastic scattering processes on (p, t) reactions. (auth)

**27120** (JAERI-1231, pp 117-121) DETERMINATION OF THE ABSOLUTE CROSS SECTION OF THE (p,t) AND (t,p) REACTIONS WITH THE ZERO-RANGE DWBA CALCULATION. Suehireo, T. (Tohoku Inst. of Tech., Sendai). 13 Dec 1972.

From symposium on nuclear reaction and nuclear structure; Tokai, Ibaraki, Japan (13 Dec 1972).

In proceedings of a symposium on nuclear reaction and nuclear structure. (Japan Atomic Energy Research Inst., Tokyo).

Equations are summarized for the derivation of zero-range form factors and absolute cross sections for (p, t) and (t, p) reactions with common DWBA computer codes. Results of empirical determination of the absolute normalization factor $D_0^2$ are briefly reviewed. The value is estimated to be $20^{+5}_{-10}$. A theoretical method for evaluating $D_0^2$ is discussed which is based on the Schroedinger equation of the triton. (auth)

**27121** (JAERI-1231, pp 142-145) MICROSCOPIC THEORY OF EVEN-EVEN SPHERICAL NUCLEI. Sakata, F. (Kyushu Univ., Fukuoka). 13 Dec 1972.

From symposium on nuclear reaction and nuclear structure; Tokai, Ibaraki, Japan (13 Dec 1972).

In proceedings of a symposium on nuclear reaction and nuclear structure. (Japan Atomic Energy Research Inst., Tokyo).

A new systematic approximation method beyond the random phase approximation to describe the first excited state and higher collective excited states of spherical even-even nuclei has been proposed by N. Kanesaki, T. Marumori, K. Takada and the author. In our method, the collective excitations of spherical even-even nuclei are described by a set of various elementary excitation modes with small anharmonicities. The theory is recapitulated, and the structure of the so-called "two phonon" states is investigated. (auth)

**27122** (JINR-P4-8774) COMMENT ON THE STRENGTH FUNCTION CALCULATION. Ochirbat, G. (Joint Inst. for Nuclear Research, Dubna (USSR)). 1975. 14p. (In Russian). Dep. NTIS (US Sales Only) $4.00.

Expressions are obtained which allow one to calculate the strength function in increasing powers of the interaction. (auth)

**27123** (LA-UR-75-1643) MECHANISM OF HEAVY-ION REACTIONS AND THE PRODUCTION OF SUPERHEAVY NUCLEI. Nix, J. R.; Sierk, A. J. (Los Alamos Scientific Lab., N. Mex. (USA)). 1 Sep 1975. Contract W-7405-ENG-36. 11p. (CONF-750938-1). Dep. NTIS $4.00.

From seminar on reactions of heavy ions with nuclei and synthesis of new elements; Dubna, USSR (23 Sep 1975).

The statics and dynamics of very-heavy-ion reactions are discussed, with special emphasis on those aspects associated with the production of superheavy nuclei. Cross sections for forming compound nuclei in symmetric heavy-ion collisions are calculated by use of the criterion that the dynamical trajectory for the fusing system must pass inside the fission saddle point in a multidimensional space in order to form a compound nucleus. (5 figures) (auth)

**27124** (ORO-4856-23) QUASIPARTICLE POLE STRENGTH IN NUCLEAR MATTER. Poggioli, R. S.; Jackson, A. D. (Maryland Univ., College Park (USA). Dept. of Physics and Astronomy). 1975. 7p. Dep. NTIS $4.00.

It is argued that single-particle-like behavior in nuclear matter is much less probable than Brueckner theory suggests. In particular, the quasiparticle pole strength is evaluated for nuclear matter and it is shown that, contrary to the spirit of Brueckner theory, low momentum states play a crucial role in determining the magnitude of z/sub k/sub F/. (auth)

**27125** EFFECTIVE INTERACTIONS IN FINITE NUCLEI BASED ON REACTION MATRIX THEORY, 2. Properties of Reaction Matrix and Core-Phonon-Exchange Interaction. Ando, K.; Nagata, S. (Kyoto Univ. (Japan). Dept. of Physics); Bando, H. Prog. Theor. Phys. (Kyoto); 52: No. 3, 928-951(Sep 1974).

The calculated reaction matrix and core-phonon-exchange interaction in second order are decomposed into various interaction components; central, 1-s, vector and tensor. Spin-isospin-multipole dependence is analyzed and the effective strengths are given for each component. Comparisons are made with schematic multipole and multipole-pairing interactions. (auth)

**27126** CORRELATION EFFECTS AND ENERGY SPECTRA IN ODD NUCLEI. Yokoi, T. (Nagoya Univ. (Japan). Dept. of Physics). Prog. Theor. Phys. (Kyoto); 52: No. 4, 1232-1247(Oct 1974).

The energy-spectra of the three-quasi-particle states in odd nuclei are discussed in relation to various types of correlation effects such as particle-particle ones and the particle-hole ones, and formulas representing qualitative aspects of them are obtained. (auth)

**27127** TWO-BODY OFF-SHELL T AND S MATRICES. Takemiya, T.; Nakamura, H. (Kumamoto Univ. (Japan). Dept. of Physics). Prog. Theor. Phys. (Kyoto); 52: No. 4, 1248-1263(Oct 1974).

The two-body off-shell T matrix elements with complex energy parameter for uncoupled and coupled states of the orbital angular momenta are investigated in a numerical method. The off-shell T matrix has a branch cut from the origin along the positive energy axis on the complex energy plane. If a two-body potential has several bound states, the poles of the off-shell T matrix appear only on the negative energy axis and correspond to the bound states of the potential. Redundant poles never appear. Once the off-shell T matrix is determined, an off-shell S matrix with two complex energy parameters can be made of the off-shell T matrix. The scattering amplitude on the energy shell can be derived from the on-shell limit of the off-shell S matrix. The above approach can be extended to the case of the Coulomb plus nuclear potential. In this case, the Coulomb potential must be included into the unperturbed Hamiltonian, because of the long range property of the potential. (auth)

**27128** PROPERTIES OF NUCLEAR MATTER FOR THE PROPOSED NN ONE-BOSON-EXCHANGE POTENTIAL WITH FULL NONSTATIC EFFECTS. Hoshizaki, N.; Kadota, T. (Kyoto Univ. (Japan). Faculty of Engineering); Kasahara, T. Prog. Theor. Phys. (Kyoto); 52: No. 4, 1264-1273(Oct 1974).

The properties of nuclear matter have been calculated to first order of the reaction matrix G. The Brueckner-Bethe-Goldstone equation for G has been solved in momentum space, with the single-particle potential energy being taken to be zero for particle states above the Fermi surface. The two-body interaction assumed is the proposed one-boson-exchange type potential represented in momentum space. It is found that the binding energy is −12.3 MeV/particle at a saturation density corresponding to the Fermi momentum of 1.57 $fm^{-1}$, the compressibility is 148 MeV and the defect parameter is 0.133 at the saturation density. The saturation comes about essentially from tensor force. Influence of the experimental uncertainty in the $^3S_1$-$^3D_1$ mixing parameter on nuclear matter is discussed. The results are compared with corresponding ones of other potentials. (auth)

**27129** THEORY OF COLLECTIVE EXCITATIONS IN SPHERICAL ODD-MASS NUCLEI, 4. Formulation in the General Many-J-Shell Model. Kuriyama, A.; Okamoto, R. (Kyushu Univ., Fukuoka (Japan). Dept. of Physics); Marumori, T.; Matsuyanagi, K. Prog. Theor. Phys. (Kyoto); 52: No. 6, 1819-1840(Dec 1974).

The aim of this paper is to give a systematic formulation of a microscopic description of the collective excitations in spherical odd-mass nuclei. The theory can be regarded as a natural extension of the conventional quasi-particle-random-phase approximation for spherical even-mass nuclei to the case of spherical odd-mass nuclei. In the same manner as the conventional random-phase approximation for even-mass nuclei leads us to the concept of "phonon", the theory necessarily leads us to the concept of a new kind of fermion-type collective excitation mode. Recent rapid accumulation of experimental data seems to be revealing the systematic presence of this kind of collective mode in many odd-mass nuclei. (auth)

**27130** RELATIVISTIC SINGLE-PARTICLE POTENTIALS FOR NUCLEI. Miller, L.D. (Department of Physics, University of Maryland, College Park, Maryland 20742). Ann. Phys. (N.Y.) 91: No. 1, 40-57 (May 1975).

The Dirac equation with general local, Lorentz covariant, interactions is investigated as the appropriate wave equation for the description of single-nucleon motion inside nuclei. Four of the original 16 potential components are shown to satisfy the requirements of angular momentum and parity conservation. Only three of these four components are capable of satisfying simultaneously the requirements of hermiticity and time reversal invariance. Nevertheless, state-dependent potentials involving all four components are found which are completely equivalent to nonlocal state-independent potentials satisfying all of the above requirements. Using the three well behaved state-independent potentials, only two local qualitatively distinct models are capable of producing an eigenvalue spectra similar to the experimental single-nucleon removal energies which show strong spin-orbit splittings. All such models are shown to predict large relativistic corrections to the single-particle Dirac magnetic moments unless a strong contribution to the unusual fourth component of the potentials is also included. The success of the nonrelativistic Schmidt estimates in predicting the magnetic moments of light, odd $Z$-even $N$ nuclei leads one to conclude that any internally consistent shell model of nuclear single-particle states must be strongly nonlocal. Any equivalent local representations of this model must be state-dependent in order to satisfy the usual conservation requirements of the shell model. (auth)

**27131** SPECTRAL DISTRIBUTION METHOD IN THE $J$-SCHEME. Nomura, M. (Service de Physique Théorique, Centre d'Etudes Nucléaires de Saclay, BP n° 2—91190 Gif-sur-Yvette, France). Ann. Phys. (N.Y.) 91: No. 1, 83-105 (May 1975).

Techniques of the usual shell model in the $J$-scheme are used to formulate a spectral distribution method. The particle-hole relation for the matrix element of a general $k$-body operator is derived. With the help of this, the $k$-body operator can be reexpressed as a sum of operators each of which has a definite symmetry under the particle-hole transformation. A reduction relation for the average of the product of two operators is derived, with and without use of the particle-hole relation, as a reformulation of the work by Chang, French, and Thio. The analog of the reduction relation in the boson system is also given. As a simple application of the present work, we estimate the "correlation" between effective two-body and three-body interactions in the configuration $(0f\ 7/2)^n$. The reduction relation is given for the configuration moment of the product of two operators. (auth)

**27132** ELECTROEXCITATION OF NUCLEAR MAGNETIC DIPOLE TRANSITIONS. Fagg, L.W. (Naval Research Laboratory, Washington, D.C. 20375). Rev. Mod. Phys. 47: No. 3, 683-711 (July 1975).

The field of electroexcitation of nuclear M1 transitions is reviewed. The subject is introduced with an elementary description of the relationship between backward-angle electron scattering and M1 excitation. Data analysis methods as well as 180° electron scattering techniques are also treated. The discussion of experimental results emphasizes the strength of the spin–flip transition, the concentration of M1 strength in self-conjugate nuclei, the degree of fragmentation of this strength in other nuclei, the response of odd-$A$ rotational nuclei to 180° electron scattering, and the possible existence of an M1 giant resonance among the nuclides, especially the heavy nuclei. (auth)

**27133** MEASUREMENTS OF THE GIANT DIPOLE RESONANCE WITH MONOENERGETIC PHOTONS. Berman, B.L.; Fultz, S.C. (Lawrence Livermore Laboratory, University of California, Livermore, California 94550). Rev. Mod. Phys. 47: No. 3, 713-761 (July 1975).

Photoneutron cross-section data obtained with monoenergetic photon beams are presented, many of them in graphical form in a uniform format. Tables of values for quantities derived directly from the data, such as integrated cross sections, and for quantities derived indirectly from the data, such as parameters of Lorentz curves fitted to the data, are presented as well. Average properties of the giant dipole resonance obtained from the data are compared with theory, as are more general nuclear quantities, such as symmetry energies, deformations, and level-density parameters. Structure in the cross sections and various other special topics are discussed, and a survey and a critique of the experimental techniques used to obtain the data are included. (auth)

**27134** EFFECTS OF ISOSCALAR AND ISOVECTOR MAGNETIC MULTIPOLE POLARIZATIONS ON SINGLE-PARTICLE MAGNETIC TRANSITIONS. Ejiri, H.; Shibata, T. (Department of Physics, Osaka University, Toyonaka, Osaka, Japan). Phys. Rev. Lett. 35: No. 3, 148-151 (21 July 1975).

Isoscalar and isovector components of M2 and M4 transition matrix elements are obtained by comparing stretched single- (quasi)proton transitions with stretched single- (quasi)neutron transitions. Both the isoscalar and the isovector components are found to be smaller by factors $g^{eff}/g \simeq 0.2$–$0.3$ than the single-quasiparticle values. The reductions are accounted for, respectively, in terms of destructive effects of the isoscalar magnetic (spin) and the isovector magnetic (isospin-spin) core polarizations. (auth)

**27135** NUCLEAR SHOCK WAVES IN RELATIVISTIC HEAVY-ION COLLISIONS. Abul-Magd, A.Y. (Institut für Theoretische Physik der Johann Wolfgang Goethe-Universität, Frankfurt am Main, Germany). Phys. Rev. C 12: No. 1, 343-345 (July 1975).

A simplified relativistic-hydrodynamic calculation of shock waves occurring during the encounter of two complex nuclei shows the nuclear density in the compressed region does not exceed an upper limit whose value depends on the ansatz for the nuclear equation of state, and differs from the upper limit of the density of the compressed region predicted by an analogous nonrelativistic calculation. (auth)

**27136** CONVERGENCE OF A NEUTRON-DEUTERON MULTIPLE-SCATTERING SERIES. Whiting, J. (Department of Physics and Astronomy, State University of New York, Buffalo, New York 14214); Fuda, M.G. Phys. Rev. C 12: No. 1, 320-322 (July 1975).

It is shown by means of an example, that a multiple-scattering series for neutron-deuteron scattering, based on the Alt-Grassberger-Sandhas version of the Faddeev equations, can be made to converge by subtracting out the deuteron pole in the two-nucleon $T$ matrix. The subtraction is carried out by means of Kowalski's generalized Sasakawa method. The interactions between the nucleons are rank one separable potentials with Gaussian form factors. (auth)

**27137** RECOIL CORRECTIONS IN ELECTRON SCATTERING. de Forest, T. Jr. (Instituut voor Kernphysisch Onderzoek (IKO), Oosterringdijk 18, Amsterdam, The Netherlands). Phys. Rev. C 12: No. 1, 306-308 (July 1975).

A method recently proposed for treating recoil effects in electron scattering is shown to be incorrect. The appropriate recoil correction factors are given for the extraction for both radiative decay widths and integrated photoabsorption cross sections from electron scattering. (auth)

**27138** NUCLEAR REARRANGEMENT ENERGY. Friedman, W.A. (University of Wisconsin, Physics Department, Madison, Wisconsin 53706). Phys. Rev. C 12: No. 1, 279-285 (July 1975).

The concept of rearrangement energy in nuclear particle removal is carefully defined by specifying several energies associated with the process and its analysis. Connection is made between definition and closely related concepts apt to be confused with "rearrangement energy" so defined. Remarks are made concerning the implications of rearrangement to analysis and interpretation of experimental data. (auth)

**27139** HIGH-ENERGY EXPANSION FOR NUCLEAR MULTIPLE SCATTERING. Wallace, S.J. (Department of Physics, Harvard University, Cambridge, Massachusetts 02138 and Department of Physics and Astronomy, University of Maryland, College Park, Maryland 20742). Phys. Rev. C 12: No. 1, 179-193 (July 1975).

The Watson multiple scattering series is expanded to develop the Glauber approximation plus systematic corrections arising from three (1) effects: (1) deviations from eikonal propagation between scatterings, (2) Fermi motion of struck nucleons, and (3) the kinematic transformation which relates the many-body scattering operators of the Watson series to the physical two-body scattering amplitude. Operators which express effects ignored at the outset to obtain the Glauber approximation are subsequently reintroduced via perturbation expansions. Hence a particular set of approximations is developed which renders the sum of the Watson series to the Glauber form in the center of mass system, and an expansion is carried out to find leading order corrections to that summation. Although their physical origins are quite distinct, the eikonal, Fermi motion, and kinematic corrections produce strikingly similar contributions to the scattering amplitude. It is shown that there is substantial cancellation between their effects and hence the Glauber approximation is more accurate than the individual approximations used in its derivation. It is shown that the leading corrections produce effects of order $(2kR_c)^{-1}$ relative to the *double scattering* term in the uncorrected Glauber amplitude, $\hbar k$ being momentum and $R_c$ the nuclear charge radius. The leading order corrections are found to be small enough to validate quatitative analyses of experimental data for many intermediate to high energy cases and for scattering angles not limited to the very forward region. In a Gaussian model, the leading corrections to the Glauber amplitude are given as convenient analytic expressions. (auth)

**27140** CROSSING, UNITARITY, AND THE IMPULSE APPROXIMATION IN PION-NUCLEUS SCATTERING. Celenza, L.; Liu, L.C.; Shakin, C.M. (Department of Physics and Institute of Nuclear Theory, Brooklyn College, Brooklyn, New York 11210). Phys. Rev. C 12: No. 1, 194-205 (July 1975).

We present a theory of pion-nucleus scattering which incorporates crossing symmetry. The resulting nonlinear $T$ matrix equation is a generalization of the Low equation to the case of complex targets. If one neglects crossing symmetry in the formalism, the theory reduces to the linear theory of pion-nucleus scattering discussed previously. Our method requires the introduction of a non-Hermitian effective Hamiltonian (for the description of elastic scattering) whose definition is based on a projection operator technique. It is pointed out that one great advantage of our theory over other approaches which incorporate crossing symmetry lies in the fact (in the simplest approximation) the driving term in our equation may be identified with the "triangle diagram," that is, the leading term in a covariant multiple scattering series for the relativistic optical potential. The approximations which are necessary to obtain familiar expressions for the driving term are made explicit in the context of this theory. (auth)

**27141** ESTIMATION OF TOTAL REACTION CROSS SECTIONS FROM ELASTIC SCATTERING DATA. Alexander, J.M.; Delagrange, H.; Fleury, A. (Centre d'Etudes Nucléaires de Bordeaux-Gradignan, Laboratoire de Chimie Nucléaire ERA No. 144, Le Haut-Vigneau, 33170-Gradignan, France and Department of Chemistry, State University of New York at Stony Brook, Stony Brook, New York 11794). Phys. Rev. C 12: No. 1, 149-155 (July 1975).

A study is made of the interaction distance parameters from sharp and smooth cutoff analysis of elastic scattering data. These distance parameters are compared to interaction barrier parameters from analysis of total-reaction-cross-section data. A simple method is proposed for calculation of total reaction cross sections from the empirical parameters. (auth)

**27142** WAVE-PACKET ASPECTS OF HIGH-MOMENTUM STRONGLY ABSORBING NUCLEAR REACTIONS. Austern, N. (Los Alamos Scientific Laboratory, Los Alamos, New Mexico 87544 and University of Pittsburgh, Pittsburgh, Pennsylvania 15260). Phys. Rev. C 12: No. 1, 128-131 (July 1975).

Properties of the wave function associated with a simple parametrized expression for the transfer amplitude are discussed. Near the nuclear surface the wave function is localized in angle, but is not appreciably localized in radius. These results seem to contradict descriptions of reactions in terms of classical trajectories. (auth)

**27143** MULTIPOLE EXCITATIONS IN NUCLEAR MUON CAPTURE AND MEAN NUCLEAR EXCITATION ENERGIES. Duplain, D.; Goulard, B. (Laboratoire de Physique Nucléaire, Université de Montréal, Montréal, Canada); Joseph, J. Phys. Rev. C 12: No. 1, 28-35 (July 1975).

The various transitions induced by muon capture are described and classified in the framework of the shell model. The influence of the muon amplitude overlap with the initial nucleus on the distribution of the multipole transitions is considered, after which the interplay of those various excitations is analyzed to obtain information on the over-all trend of the mean excitation energy of the final nucleus. (auth)

**27144** OFF-SHELL BORN APPROXIMATION FOR LOCAL POTENTIALS. Warburton, A. E. A. (Hull Univ., Eng.). J. Phys., A (London); 8: No. 7, 1060-1066(Jul 1975).

Assuming the existence of a (possibly energy-dependent) local potential, the off-shell partial-wave amplitudes in the Born approximation, $V_l(p_1, p_2)$, are expressed explicitly in terms of the on-shell $V_l(k,k)$ provided that $p_1 + p_2 > 2k$. (auth)

**27145** SOME REMARKS ON MAGNETIC DIPOLE MOMENTS IN LIGHT NUCLEI. van Hienen, J. F. A. Utrecht, Netherlands; Rijksuniversiteit (1975). 3p.

Multi-shell mixed-configuration calculations employing various effective interactions show that for low-lying states the g-factor in $T_z = 0$ nuclei as well as the average of g-factors of corresponding states in mirror nuclei varies between +0.4 and +0.9 n.m. in rather good agreement with a pure $j^n$ description; for excited states in even-even T = 0 nuclei, one finds $g \simeq +0.50$ n.m. The results agree well with present experimental data on magnetic dipole moments of ground states and excited states. (auth)

**27146** NUCLEAR EXCITATION ENERGY IN MUON CAPTURE: A REPLY. Christillin, P.; Dellafiore, A.; Rosa-Clot, M. (Scuola Normale Superiore, Istituto Nazionale di Fisica Nucleare, Sezione di Pisa, Pisa, Italy). Phys. Rev. C 12: No. 2, 691-694 (Aug 1975).

The parametrization of total muon capture rates in terms of a mean nuclear excitation energy $\bar{E}$, recently proposed by Christillin, Dellafiore and Rosa-Clot, is reexamined in view of recent criticisms. The previously obtained results are reconfirmed. (auth)

**27147** RESPONSE TO DILATATION AND SOME SOLUBLE "SQUASHING" MODELS OF INTERACTING MANY-FERMION SYSTEMS. Rockmore, R. (Physics Department, Rutgers, The State University, New Brunswick, New Jersey 08903). Phys. Rev. C 12: No. 2, 676-682 (Aug 1975).

The response of a many-fermion system to dilatation is studied through the introduction, in close analogy with the "cranking" and "pushing" models, of a "squashing" model characterized by the Hamiltonian, $H = H_0 - \dot{\epsilon} D_x$, where $D_x$ is the generator of dilatations in the $x$ direction. The evaluation of the "rigid" dilatational moment of such a noninteracting system is carried out for both standing wave and periodic boundary conditions in a cubic box of side $L$. As in the pushing model, the dilatation moment can be evaluated formally using the relation between $D_x$ and the commutator $[x^2, H_0]$. For independent fermions moving in a harmonic oscillator one-body potential, this relation is shown to lead to further simplification after the introduction of perturbed one-body wave functions. In the case of periodic boundary conditions, it is shown that the rigid dilatational moment is not altered by an interparticle interaction to first order in the interaction strength; by comparison with the analogous cranking moment problem, this result extends to all orders in the interaction strength. The response to a symmetric dilatation, $D = D_x + D_y + D_z$, is studied in a soluble Hartree model of "nuclear" correlations wherein a separable monopole-monopole interaction acts between "nucleons." In this model the dilatation moment in the presence of pair correlations is found to be the rigid moment, with the kinetic energy of dilatation $\propto \dot{\epsilon}^2$, there being no higher order corrections. (auth)

**27148** NO-RESONANCE CONDITION FOR A $^1S_0$ SEPARABLE $AN$ POTENTIAL WITH SUPPRESSION EFFECTS. Schick, L.H. (University of Wyoming, Laramie, Wyoming 82071). Phys. Rev. C 12: No. 2, 523-526 (Aug 1975).

Two-channel $AN$ potentials each of whose matrix elements is a single nonlocal separable are discussed. A simpler condition than obtained previously is derived for the $\Lambda$-channel shape such that the $AN$ scattering length and effective range agree with the values obtained from a meson-theoretic potential both with the $\Sigma$ channel unsuppressed and fully suppressed and which at the same time guarantees the absence of an unwanted $AN$ resonance below the $\Sigma$-channel threshold due to a bound state in the uncoupled $\Sigma$ channel. A specific nonlocal separable shape is exhibited which obeys this condition for a range of values of its parameters when the most recent $^1S_0$ meson-theoretic potential scattering lengths and effective ranges of Brown, Downs, and Iddings are used as input. (auth)

**27149** OFF-SHELL JOST FUNCTION AND $T$ MATRIX FOR THE MORSE POTENTIAL. Talukdar, B.; Roy, M.N.S.; Mallick, N.; Nayek, D.K. (Department of Physics, Bolpur College, Bolpur 731204, West Bengal, India). Phys. Rev. C 12: No. 2, 370-373 (Aug 1975).

Analytic expressions for the $s$-wave part of the off-shell Jost solution and Jost function are obtained for the Morse potential. The results are used to compute the off-shell $T$ matrix. (auth)

**27150** EXCHANGE EFFECTS AND $n$-BODY FORCES IN NUCLEAR MATTER. Blatt, D.W.E. (Department of Theoretical Physics, University of Sydney, Sydney, New South Wales, 2006, Australia and School of Computing Science, New South Wales Institute of Technology, Sydney, New South Wales, 2007, Australia); McKellar, B.H.J. Phys. Rev. C 12: No. 2, 637-643 (Aug 1975).

The $n$-pion-exchange $(n+1)$ -body force is written explicitly in coordinate space and separated into its central and tensor parts. Exchanges of the spectator nucleons are shown to cause large cancellations. The ratio of $n$-body forces to $(n+1)$ -body forces is estimated and compared with recent three- and four-body calculations. (auth)

**27151** COMPARISON OF HARTREE-FOCK AND ENERGY-DENSITY FORMALISM CALCULATIONS FOR SOME SPHERICAL NUCLEI. Dworzecka, M. (University of Massachusetts, Amherst, Massachusetts 01002 and University of Maryland, College Park, Maryland 20742); Moszkowski, S. Phys. Rev. C 12: No. 2, 619-627 (Aug 1975).

The purpose of this paper is twofold. We calculate the parameters of the nuclear droplet model introduced by Myers and Swiatecki (an extension of the conventional liquid drop model) to higher powers $A^{-1/3}$. We do Hartree-Fock (HF) calculations for a large number of spherical nuclei, using the modified $\delta$ interaction version of the Skyrme interaction and average over shell structure by making a least squares fit to the Hartree-Fock energies. We also compare the shell-averaged HF results with those obtained by using a simple version of the energy density formalism developed by Brueckner, Lombard, and others. We assume the simple form of the energy density first introduced by Skyrme for $N = Z$ nuclei, and minimize the total energy with respect to the actual density and diffuseness, subject to the constraint of fixed number of particles. Detailed comparison with the HF results was made for two $A = 100$ nuclei with $Z = 50$ and 40. We find that the droplet model energies calculated either exactly (numerically) or analytically by expansion of the radial integrals in powers of $(a/R)$ ($a$ = diffuseness, $R$ = half density radius for a Fermi density) are in good agreement with the shell averaged HF results although there is some uncertainty in the latter. However, the central density is too small by about 10% for the cases considered. Yet, for the case $Z = 40$, $A \simeq 100$, the ratio of neutron and proton densities is close to the Hartree-Fock value. Thus, we find the energy density formalism can reproduce quite closely the results of more complicated Hartree-Fock calculations. (auth)

# PHYSICS (RADIATION AND SHIELDING)

## Radiation Physics

*Refer also to abstract 26742.*

**27152** HYDRODYNAMIC EFFECT IN THE PASSAGE OF FISSION FRAGMENTS THROUGH CONDENSED MATTER. Gol'danskii, V.I.; Lantsburg, E.Ya.; Yampol'skii, P.A. (Institute of Chemical Physics, USSR Academy of Sciences). JETP Lett. 21: No. 6, 166-167 (20 Mar 1975).

When fission fragments pass through condensed matter, the hydrodynamic mechanism of energy transfer causes a short-duration compression of the matter in the vicinity of the fragment track; this, in turn, can increase the concentration of the active particles that stimulate the course of various chemical processes. (auth)

**27153** DETERMINATION OF EXPOSURE TIME IN RADIOGRAPHY. Soenarmo (National Atomic Energy Agency (Indonesia). Bandung Reactor Centre). Proc. Jap. Conf. Radioisotop.; No. 11, 307-310 (Aug 1974).

From 11th Japan conference on radioisotopes; Tokyo, Japan (13 Nov 1973).

Determination of exposure time by means of putting a detector underneath an object to be examined was discussed. Total dose required by the film to get a good contrast is based on the dose rate received by the detector. By comparing the dose and the dose rate, exposure time can be determined, and the knowledge of activity, thickness of the object, distance between source and film are considered to be unnecessary. (auth)

**27154** ENERGY SPECTRUM OF GAMMA-PHOTONS SCATTERED BY HOT-ELECTRON PLASMAS. Yamamoto, T.; Kawanishi, M. (Osaka Univ., Suita (Japan). Inst. of Scientific and Industrial Research). Mem. Inst. Sci. Ind. Res., Osaka Univ.; No. 31, 25-36 (Mar 1974).

The energy distribution of Compton-scattered $\gamma$-photons was calculated with Monte Carlo method under a situation that the hot electron plasmas which contain many relativistic electrons were irradiated with $\gamma$-ray of a monochromatic energy. The characteristic feature of the relativistic Compton phenomena is that the energy of some scattered photons can exceed that of the incident photons as a result of the energy exchange with relativistic electrons. The simulation was performed with the assumption that $Co^{60}$ was used as a $\gamma$-ray source considering the practical experiment. (auth)

**27155** EXPERIMENTAL THICK-TARGET BREMSSTRAHLUNG SPECTRA FROM ELECTRONS IN THE RANGE 10 TO 30 keV. Chervenak, J.G.; Liuzzi, A. (Lowell Technological Institute, Lowell, Massachusetts 01854). Phys. Rev. A 12: No. 1, 26-33 (July 1975).

The x-ray spectra produced by the bombardment of thick targets with monoenergetic electrons between 10 and 30 keV have been determined as a function of the incident and emission angles. Spectra have been obtained for Al, Cu, Mo, and W using a Si(Li) detector. The electron current absorbed in the target was measured and corrected for backscattering, allowing a determination of absolute x-ray emission. A modified least-squares procedure was used to represent the spectra as analytical functions while taking into account the efficiency and resolution of the detector. The spectra show the effects of both target absorption and angular distribution of the thin-target bremsstrahlung production. Agreement with the Kramers formula is only moderate. (auth)

**27156** CALCULATIONS ON THE SLOWING DOWN OF 0.4-4.0-MeV He IONS IN SOLIDS. Latta, B.M.; Scanlon, P.J. (Queen's University, Kingston, Ontario, Canada K7L 3N6). Phys. Rev. A 12: No. 1, 34-39 (July 1975).

The localization of atoms in solids leads, in principle, to changes in the electron distribution compared with the free-atom state. The effect of such changes on the calculation of the He-ion stopping cross section $S_e$ in solids has been investigated for an energy range 0.4–4.0 MeV. It is found that at low energies with free-atom wave functions, a large part of the calculated $S_e$ arises from regions at large distances from the target atom where the electron density is low compared to that in solids. The experimentally observed oscillations in $S_e$ as a function of target atomic numbers, which have been calculated from stopping-power theory by other authors, are also obtained in the present work with simple modifications of the electron density distributions. However, the detail of the structure of the stopping curves is altered. In addition, the use of an effective charge to account for electron capture by the He ion at low velocities, without a corresponding modification of the basic stopping-power theory to take into account the departure from point-charge behavior, leads to discrepancies from the experimental data. (auth)

**27157** STRIPPING OF HIGH-ENERGY KRYPTON IONS BY VARIOUS SOLID MATERIALS. Baron, E. (Institut de Physique Nucléaire, B.P. No.1, Orsay, France); Delaunay, B. Phys. Rev. A 12: No. 1, 40-44 (July 1975).

The charge-state distributions of 373-, 444-, and 552-MeV krypton ions passing through carbon foils of different thicknesses were measured; they were found to agree within about one charge state with the existing semiempirical predictions. Measurements of equilibrium distributions produced by Cu, Ag, and Au foils showed differences of two to three charge states when compared to C-foil results. Evidence is also given that the distributions are not significantly modified when the angle of observation is different from 0°. (auth)

**27158** QUASI-SCALING OF ELECTRON DEGRADATION SPECTRA. Fano, U.; Spencer, L. V. (Univ. of Chicago). Int. J. Radiat. Phys. Chem.; 7: No. 2/3, 63-76 (Apr 1975).

Douthat (Ph.D Thesis, University of Chicago, 1974, submitted to Radiat. Res.) has found that plots of electron spectra calculated for different initial energies nearly coincide if a suitable choice of scaled variables is adopted for abscissas and ordinates. This paper provides a rationale for this choice of variables, reformulates the degradation equation in terms of the new variables, and shows how the trend of the solution of the transformed equation can be predicted semi-quantitatively by inspection. (auth)

**27159** ABSORPTION OF $\beta$-PARTICLES IN Cu, Ag, Sn, and Pb TARGETS. Mudhole, T. S. (Karnatak Univ., Dharwar, India). Indian J. Pure Appl. Phys.; 13: No. 3, 199-200(Mar 1975).

The mass absorption coefficients, $(\mu/\rho)$, for $^{32}P$, $^{91}Y$, $^{89}Sr$, and $^{204}Tl$ $\beta$-sources have been determined using Cu, Ag, Sn and Pb targets. It is shown that the fraction $f_A$ of the incident $\beta$-particles that is completely absorbed within a foil follows an empirical relation of the type $t \exp(-\Sigma_A t)$, where $\Sigma_A$ is a constant. The ratio of $(\mu/\rho)/\Sigma_A$ is found to be about 4 for all these $\beta$-sources and the targets used. (auth)

## Radiation Protection Standards

**27160** (BNWL-B-351) SUBDOSA: A COMPUTER PROGRAM FOR CALCULATING EXTERNAL DOSES FROM ACCIDENTAL ATMOSPHERIC RELEASES OF RADIONUCLIDES. Strenge, D. L.; Watson, E. C.; Houston, J. R. (Battelle Pacific Northwest Labs., Richland, Wash. (USA)). Jun 1975. Contract AT(45-1)-1830. 186p. Dep. NTIS $7.60.

A computer program, SUBDOSA, was developed for calculating external gamma and beta doses to individuals from the accidental release of radionuclides to the atmosphere. Characteristics of SUBDOSA are: doses from both gamma and beta radiation are calculated as a function of depth in tissue, summed and reported as skin, eye, gonadal, and total body dose; doses are calculated for releases within each of several release time intervals and nuclide inventories and atmospheric dispersion conditions are considered for each time interval; radioactive decay is considered during the release and/or transit using a chain decay scheme with branching to account for transitions to and from isomeric states; the dose from gamma radiation is calculated using a numerical integration technique to account for the finite size of the plume; and the program computes and lists the normalized air concentrations at ground level as a function of distance from the point of release. (auth)

## Radiation Source Calibration and Standardization

*Refer also to abstracts 25932 and 27153.*

**27161** (AED-CONF-75-141-002) MONTE-CARLO CALCULATIONS FOR ENERGY AND ANGULAR DEPENDENCE OF FAST ELECTRONS BEHIND SCATTERING LEAD FOILS. Abou Mandour, M.; Harder, D. (Goettingen Univ. (F. R. Germany). Inst. fuer Medizinische Physik und Biophysik). 1975. 17p. (In German). INIS.

From 6th scientific symposium of the Deutsche Gesellschaft fuer Medizinische Physik; Berlin, F. R. Germany (28 Apr 1975).

11 figs.; 6 refs.

Possibilities of improving the homogeneity of the dose distribution in the irradiation field of electron accelerators in medical use by additional measures in order to reduce the thickness of the scattering foil are considered. (GE)

# PHYSICS (THEORETICAL)

**27162** MARGINALLY SINGULAR INTEGRAL EQUATION WITH DIVIDED-DIFFERENCE KERNEL: A PROBLEM IN N/D THEORY. Johnson, P.W.; Warnock, R.L. (Department of Physics, Illinois Institute of Technology, Chicago, Illinois 60616). J. Math. Phys. (N.Y.) 16: No. 9, 1880-1885 (Sept 1975).

We describe a method for solution of a linear integral equation of the form $\phi(s) = f(s) + (1/\pi)\int_{s_4}^{\infty} [B(s) - B(t)]/(s-t)^{-1}\, q(t)\phi(t)dt$, where $q(t) = (1-4/t)^{1/2}$. The specified functions $f(s)$ and $B(s)$ have the asymptotic behaviors $f(s) \sim f_0 (\ln s)^{-\alpha}$, $\alpha > 1$, $B(s) \sim b (\ln s)^{-1}$, $s \to \infty$; in addition, $B$ is subject to smoothness conditions. The equation is analyzed on a Banach space $S$ of continuous functions $\phi(s)$ which have asymptotes of the form $\phi_0(\ln s)^{-\alpha}$. It is found that the integral operator $K$ is bounded but not compact on the space $S$, so that the equation is not of Fredholm type on $S$. We separate $K$ into a noncompact part $K_1$ and a compact part $K_2$, and construct explicitly the inverse of $1-K_1$ by solving an associated differential equation. We then convert the original equation $\phi = f + K\phi$ into an equivalent Fredholm equation $\phi = (1-K_1)^{-1}(f + K_2\phi)$. (auth)

**27163** CLASSIFICATION OF WAVE FUNCTIONS IN A MANY-NUCLEON SYSTEM BY A ROTATION GROUP METHOD. Geng-wei, R. Chin. J. Phys. 23: No. 3, 101-108 (Nov 1974).

In this paper, we have given a projection operator method for classifying wave functions in a many-nucleon system. We have also given the results of the classification coefficients for A=1 to 3. (auth)

**27164** STATE-DEPENDENT EQUIVALENT LOCAL POTENTIALS FOR THE DIRAC EQUATION. Miller, L.D. (Laboratory for Nuclear Science and Department of Physics, Massachusetts Institute of Technology, Cambridge, Massachusetts 02139). Phys. Rev. C 12: No. 2, 710-712 (Aug 1975).

It is pointed out that previously published equivalent local representations of the relativistic Hartree-Fock exchange potentials are too small by a factor of 2. The implications of this error for the relativistic Hartree-Fock calculations of closed shell nuclei are discussed. (auth)

**27165** RELATIVISTIC EFFECTS ON THE WAVE FUNCTION OF A MOVING SYSTEM. Friar, J.L. (Department of Physics, Brown University, Providence, Rhode Island 02912). Phys. Rev. C 12: No. 2, 695-698 (Aug 1975).

An alternative approach to the recent results of Krajcik and Foldy is presented which stresses a different point of view, but is completely equivalent to their results. (auth)

## General

*Refer also to abstract 26739.*

**27166** (ITP-75-63E) REPRESENTATIONS OF LIE GROUPS U(n,1), IU(n) AND THEIR ALGEBRAS. III. Gavrilik, A. M.; Klimyk, A. U. (AN Ukrainskoj SSR, Kiev. Inst. Teoreticheskoj Fiziki). 1975. 23p. Dep. NTIS (US Sales Only) $4.25.

All nonzero intertwining operators for the elementary representations of the group U(n,1) are found. The explicit matrix form of these operators is given. (auth)

**27167** (ITP-75-65E) HAMILTONIAN OF A SYSTEM OF N PARTICLES WITH SEPARATED COLLECTIVE MOTION. Ovcharenko, V. I. (AN Ukrainskoj SSR, Kiev. Inst. Teoreticheskoj Fiziki). 1975. 61p. NTIS (US Sales Only) $6.25.

The kinetic energy operator $\hat{T}$ of the motion of a system of N particles relative to the center of mass is transformed to 3N-3 variables: six of these (a, b, c, $\theta_1^{(q)}$, $\theta_2^{(q)}$, $\theta_3^{(p)}$) are collective and characterize the form, the dimension, and the rotations of the system, and 3N-9 ($\theta_1^{(\gamma)}$) define the orientation of three mutually orthogonal vectors in (N-1)-dimensional space. The matrix $|\gamma|$ of the metric tensor, which defines the operator $\hat{T}$ in the new variables, has the form of a product $|\gamma| = |\Gamma| = |\tilde{\gamma}| = |\Gamma^t|$ so that the variables a, b, c are contained only in the elements of the quasi-diagonal matrix $|\tilde{\gamma}|$ and the dependence on the sets $\{\theta_1^{(\gamma)}\}$ and $\{\theta_1^{(p)}\}$ is given by two separate blocks of the quasi-diagonal matrix $|\Gamma|$ (and the transposed matrix $|\Gamma^t|$). The relation between the differential operators in the variables $\theta_0^{(\gamma)}$ and $\theta_0^{(p)}$ (which parametrize the homogeneous spaces SO(3) and O(N-4)/O(N-1) and the infinitesimal operators of left translations on the groups SO(3) and O(N-1) is established. (auth)

**27168** (LA-UR-75-1119) FOLDED DIAGRAM THEORY, TIME-DEPENDENT APPROACH OF JOHNSON AND BARANGER. Johnson, M. B. (Los Alamos Scientific Lab., N. Mex. (USA)). 1975. Contract W-7405-ENG-36. 17p. (CONF-750663-5). Dep. NTIS $4.00.

From international topical conference on effective interactions and operators in nuclei; Tucson, Arizona, USA (2 Jun 1975).

The folded diagram expansion of Brandow and extensively developed by Johnson and Baranger is discussed in detail. The time-dependent approach is reviewed through Feynman-Goldstone diagrams to establish the conventions used. The problem of calculating the effective interaction for nuclei beyond $^{208}$Pb is then considered as an example. Finally, examples are given which show how to do the time integrations. (17 figures) (SDF)

**27169** GENERALIZED FREE STATES OF THE GAUGE INVARIANT ALGEBRA OF THE CANONICAL ANTICOMMUTATION RELATIONS. Stamatopoulos, G. P. Philadelphia; Univ. of Pennsylvania (1974). 131p. University Microfilms Order No. 75-14,628.

Thesis (Ph. D.).

Generalized free (quasi-free according to previous work) states of the gauge invariant algebra of the canonical anticommutation relations (GICAR algebra) are discussed. This algebra is believed to be the appropriate algebra of observables for any physical system of fermions, possibly with infinite degrees of freedom. (JFP)

## Quantum Field Theories

*Refer also to abstracts 26752, 26848, 26913, 26929, 27203–27205, and 27209.*

**27170** (IFA-FT-111-1975) DEDUCTION OF LORENTZ AND EINSTEIN TRANSFORMATIONS USING CONCEPTS OF DISTANCE AND DURATION. Hafner, H.; Ionesco-Pallas, N. (Institutul de Fizica Atomica, Bucharest (Romania)). 1975. 10p. (In French). Dep NTIS (US Sales Only) $4.00.

Inertial transformations in vectorial form are established proceeding with Einstein's definitions of distance and duration. Linearity of the transformations along an axis goes by itself, as being involved in the definitions of distance and duration. Invariance of the transverse coordinate—for the displacement along an axis—is demonstrated by asserting that space is Cartesian in any frame of inertia. The adoption of distance and duration definitions as well as of the Euclidean structure of space, leads to the vectorial form of the transformations and consequently to the conclusion about homogeneity and isotropy of the space-time. (auth)

**27171** (JINR-E2-8925) CLASSIFICATION OF DOMAINS OF CLOSED OPERATORS. Lassner, G.; Timmermann, W. (Joint Inst. for Nuclear Research, Dubna (USSR)). 1975. 22p. NTIS (US Sales Only) $4.25.

The structure of domains of closed operators in Hilbert space is investigated by means of sequence spaces. A complete classification leads to three classes of domains. Necessary and sufficient conditions for the unitary equivalence of domains expressed by the equivalence of appropriate sequences of naturals. A connection with perturbation theory is mentioned. (auth)

**27172** (JINR-E2-8974) SINGULAR SOLUTIONS OF RENORMALIZATION GROUP EQUATIONS AND THE SYMMETRY OF THE LAGRANGIAN. Kazakov, D. I.; Shirkov, D. V. (Joint Inst. for Nuclear Research, Dubna (USSR)). 1975. 24p. NTIS (US Sales Only) $4.25.

On the basis of the solution of the differential renormalization group equations a method is proposed for finding out the Lagrangians possessing some kind of internal symmetry. It is shown that in the phase space of the invariant charges the internal symmetry corresponds to the straight-line singular solution of these equations remaining straight-line when taking into account the higher order corrections. The model of scalar fields with quartic couplings, as well as the set of models containing scalar, pseudoscalar, and spinor fields with Yukawa and quartic interactions were studied. Straight-line singular solutions in the first case correspond to isotopical symmetry only. For the second case they correspond to supersymmetry. No other symmetries have been discovered. For the model containing the gauge fields the solution corresponding to supersymmetry is obtained, and it is shown that this is also the only symmetry that can be realized in the given set of fields. (auth)

**27173** (JINR-P4-8695) ONE-DIMENSIONAL INTEGRAL EQUATIONS FOR A SYSTEM OF THREE IDENTICAL PARTICLES

IN THE BOUNDARY CONDITION MODEL AND THE POSSIBILITY OF TAKING INTO ACCOUNT THREE-PARTICLE FORCES. Efimov, V. N.; Shul'ts, G. (Joint Inst. for Nuclear Research, Dubna (USSR)). 1975. 37p. (In Russian). Dep. NTIS (US Sales Only) $5.00.

It is shown that, in the framework of the boundary condition model (BCM) for the two-particle interaction, the Schrödinger equation for the system of three identical bosons can be reduced to the one-dimensional integral equation in an exact way. The method used for obtaining such an equation is based on a special consideration of the two-particle off-shell wave functions. The binding energy of the simple three-particle system is calculated. It is indicated that by means of the equation obtained it is possible to take into account three-particle effects. (1 figure, 2 tables) (auth)

**27174** MODEL OF ASYMPTOTICALLY FREE MASSIVE PARTICLES. Voronov, V.L.; Tyutin, I.V. (P. N. Lebedev Physics Institute, USSR Academy of Sciences). JETP Lett. 21: No. 6, 180-182 (20 Mar 1975).

A procedure is proposed for constructing theories of asymptotically free massive particles. The general scheme is illustrated with a concrete example. (auth)

**27175** NONLINEAR REALIZATION OF CONFORMAL SYMMETRY. Hori, S.; Sakamoto, J.; Sato, A. (Osaka Univ., Toyonaka (Japan). Dept. of Physics). Prog. Theor. Phys. (Kyoto); 52: No. 5, 1647-1651 (Nov 1974).

A nonlinear realization of conformal symmetry which is linear under scale and Lorentz transformations is derived with the aid of the technique developed by Coleman, Wess and Zumino in connection with chiral symmetry. (auth)

**27176** LAGRANGIAN AND MINIMAL CURRENTS FOR MULTI-LOCAL HADRON FIELDS IN THE UR-CITON SCHEME. Ishida, S.; Otokozawa, J. (Nihon Univ., Tokyo. Dept. of Physics). Prog. Theor. Phys. (Kyoto); 53: No. 1, 217-236 (Jan 1975).

A general prescription to introduce conserved currents is given for multi-local hadron fields in the ur-citon scheme, which is a relativistic extension of the quark model. First, Lagrangian formalism is developed. The characteristic feature of our multi-local fields, independence of the external coordinates of the internal ones, facilitates the correspondence of our theory to the usual local theory, and we can proceed almost straightly along the line of the usual theory. Secondly, the "minimal" electromagnetic interaction is introduced through replacement of the usual derivatives by properly defined covariant derivatives. Then the e.m. form factors of nucleons for the current thus obtained are examined. Finally, similar consideration is given for the usual type of multi-local fields whose center-of-mass coordinate is determined from the coordinates of constituent points. (auth)

**27177** ON QUANTUM FIELD THEORY, 1. Quantum Field Theory as Quantum Mechanics. Kambe, R. (Kwansei Gakuin Univ., Nishinomia, Hyogo (Japan). Dept. of Physics). Prog. Theor. Phys. (Kyoto); 52: No. 2, 688-706 (Aug 1974).

A new approach to finding a steady foundation of quantum field theory is investigated with the help of the so-called non-standard mathematics. We construct a model of the quantum field theory as a quantum mechanical system with many degrees of freedom. The importance of the notion of the models incidental to the formally given quantum field theory and the notion of their physical equivalence are strongly emphasized. (auth)

**27178** GAUGE DEPENDENCE OF GREEN'S FUNCTIONS IN QUANTUM ELECTRODYNAMICS FROM PARALLEL TRANSLATION. Meetz, K. (Physikalisches Institut der Universität Bonn, Germany). J. Math. Phys. (N.Y.) 16: No. 9, 1765-1771 (Sept 1975).

The classical concept of parallel translation is extended to scalar quantum electrodynamics in order to give a gauge-independent definition of differentiation. This is achieved by a suitable definition of time ordering for operator products. However, due to some essentially nonlocal commutation relations, the differential equations for the Green's functions are still gauge-dependent. The gauge dependence of the commutators can be removed by parallelism at large. Since this is not considered to be a physically reasonable concept, the gauge dependence of the Green's functions is discussed for general linear gauges in space-time. (auth)

**27179** PSEUDOSCALAR MESODYNAMICS IN $4-\epsilon$ DIMENSIONS. Hu, B. (Laboratory of Nuclear Studies, Cornell University, Ithaca, New York 14850 and Service de Physique Théorique, Centre d'Etudes Nucléaires de Saclay, BP No.2-91190-Gif-sur-Yvette, France). Phys. Rev. D 11: No. 12, 3630-3634 (15 June 1975).

The pseudoscalar Yukawa interaction $-ig\bar{\psi}\gamma_5\psi\phi$ is studied in $4-\epsilon$ dimensions. Following Wilson's prescription for coupling-constant renormalization we find a nontrivial infrared-stable fixed point for the Callan-Symanzik $\beta$ function, and the theory is scale-invariant with anomalous dimensions at short distances. The anomalous dimensions of the tensor operators that govern the Callan-Gross and Cornwall-Norton sum rules for the deep-inelastic structure functions are calculated to first order in $\epsilon$. The deviation from their canonical value is considerable, consistent with Nachtmann's recent reassessment of experimental data. (auth)

**27180** HIGH-ENERGY BEHAVIOR IN ABELIAN GAUGE THEORY, APPLICATION TO $\gamma^*$ DECAY, AND HIGH-ENERGY ESTIMATES FOR FORM FACTORS. Manoukian, E.B. (Dublin Institute for Advanced Studies, Dublin 4, Ireland). Phys. Rev. D 11: No. 12, 3616-3625 (15 June 1975).

Previously, we have made a study of the high-energy behavior of quantum electrodynamics in the presence of neutral-meson theory with pseudoscalar-pseudoscalar coupling proceeding loopwise. We have seen, by an elementary summation procedure, that the Adler-Baker-Johnson eigenvalue condition for the fine-structure constant $\alpha$ remains stable (unaltered) in the presence of the strong dynamics and that the photon self-energy part in the multi-fermion-loop contribution is asymptotically finite at $x = \alpha$ independently of the strong-coupling value. We have also learned that the strong dynamics damps out at high energies and no $\phi^4$ counterterm was required. Conversely, in the present work, we study this dynamics at high energies when the Callan-Symanzik function occurring in *pure* electrodynamics vanishes at $\alpha$ at the outset (with an infinite-order zero) by adding the $-\frac{1}{4}\lambda_0\phi^4$ term to our dynamics. We argue that the effective $\gamma_5$ and $\phi^4$ couplings in this Abelian gauge theory may become very small at high energies and that then they finally vanish even faster than the presently estimated non-Abelian gauge-theory ones. As an application, the ratio $R(Q^2)$ of the cross section associated with the reaction $\gamma^*(Q^2) \to$ anything to the corresponding one with the strong couplings set equal to zero is studied when the momentum squared of the virtual photon $Q^2 \to \infty$. $R(Q^2)$ is shown to have a linear increase with $Q^2$ (broken possibly by logarithmic terms) at truly asymptotic energies, and, contrary to common belief, the leading contribution to it comes from the strong interaction. Some of the statements made in this work are also in pure electrodynamics. For example, the explicit asymptotic form of the photon spectral function in finite quantum electrodynamics *at* the eigenvalue $\alpha$ is given here for the first time. Finally, explicit high-energy estimates are obtained for elastic form factors in quantum electrodynamics in isolation and in the present correlated dynamics. At very large momenta for the external photon, the former are bounded by a power-law behavior. Some interesting aspects of this Abelian gauge theory are also mentioned. (auth)

**27181** CHIRAL CONFINEMENT: AN EXACT SOLUTION OF THE MASSIVE THIRRING MODEL. Chang, S.; Ellis, S.D.; Lee, B.W. (Fermi National Accelerator Laboratory, Batavia, Illinois 60510). Phys. Rev. D 11: No. 12, 3572-3582 (15 June 1975).

We investigate the possibility of fermion confinement in a manifestly chiral-invariant theory. In particular we study the nonlinear $\sigma$ model in one time and one space dimension, and demonstrate that it is equivalent to the massive Thirring model plus a free massless scalar field. We find an exact, time-independent, classical solution to the massive Thirring model. This solution is characterized by a fermion confined in a self-generated potential. In the $\sigma$-model analog of this solution, the chiral phase changes rapidly in the region of the confined fermion, and has two different constant limits on either side of this region. We also consider the case in which the mass of the pseudoscalar meson is small but finite, and find an approximate solution which displays both partial conservation of axial-vector current and fermion confinement. (auth)

**27182** VERIFICATION OF VIRTUAL COMPTON-SCATTERING SUM RULES IN QUANTUM ELECTRODYNAMICS. Tsai, W.; DeRaad, L.L. Jr.; Milton, K.A. (Department of Physics, University of California, Los Angeles, California 90024). Phys. Rev. D 11: No. 12, 3537-3540 (15 June 1975).

Two new sum rules for virtual-photon forward Compton scattering derived by Schwinger are shown to be satisfied in the case of quantum electrodynamics by explicit calculation of the lowest-order contributions. (auth)

**27183** FERMIONS IN YANG-MILLS ELECTRIC AND MAGNETIC POLE POTENTIALS. Dereli, T.; Swank, J.H.; Swank, L.J. (Department of Physics, Yale University, New Haven, Connecticut 06520). Phys. Rev. D 11: No. 12, 3541-3544 (15 June 1975).

Solutions are given for the Dirac equation with a Yang-Mills magnetic monopole potential and with combined Yang-Mills electric and magnetic pole potentials. (auth)

**27184** QUANTIZATION OF THE BAG IN TWO DIMENSIONS BY DIRAC'S METHOD. Shalloway, D. (Laboratory for Nuclear Science and Department of Physics, Massachusetts Institute of Technology, Cambridge, Massachusetts 02139). Phys. Rev. D 11: No. 12, 3545-3564 (15 June 1975).

We apply Dirac's method of quantization in the presence of

constraints to the two-dimensional scalar bag. The earlier results of Chodos, Jaffe, Johnson, Thorn, and Weisskopf are reproduced and a new parametrization of relevance to the construction of a local field operator in the bag model is presented. The generally parametrized form of the theory and the difficulties encountered in the approach to equal-time quantization are discussed. (auth)

**27185** SCATTERING THEORY FOR QUANTUM ELECTRODYNAMICS. I. INFRARED RENORMALIZATION AND ASYMPTOTIC FIELDS. Zwanziger, D. (Department of Physics, New York University, New York, New York 10003). Phys. Rev. D 11: No. 12, 3481-3503 (15 June 1975).

The present article lays the theoretical foundation for a scattering theory of quantum electrodynamics, which is completed into a practical calculational scheme in the accompanying article. In order to circumvent infrared divergences, an infrared renormalization procedure is instituted whereby a Lorentz-invariant, but indefinite, inner product is defined for a class of photon test functions defined on the future light cone $k^\mu = \omega\,(1, \hat{k})$, $\omega \geq 0$. This class includes test functions whose low-frequency behavior is given by $\phi^\mu(k) \sim \epsilon p^\mu/p \cdot k$, for which the usual inner product $\int d^3k(2\omega)^{-1}\ \phi_a^*\ (k)(-g^{\mu\nu})\ \phi_\nu(k)$ is infrared-divergent. The Fock space of such test functions provides a representation space for the asymptotic fields of quantum electrodynamics. It contains subspaces in which the indefinite metric is non-negative which, when completed in the norm, yield physical Hilbert spaces. This Fock space of test functions thereby replaces the nonphysical Hilbert space of the usual Gupta-Bleuler method and its positive-definite but noncovariant metric. As an application the $S$ matrix and finite transition probabilities are found for the bremsstrahlung emitted by the classical external current of a scattered charged particle. A final result is a simple weak asymptotic limit of the charged field $\psi$. It is used as a starting point in the accompanying article, for the derivation of reduction formulas for the quantum electrodynamical $S$ matrix. (auth)

**27186** PARTICLE SPECTRUM IN MODEL FIELD THEORIES FROM SEMICLASSICAL FUNCTIONAL INTEGRAL TECHNIQUES. Dashen, R.F.; Hasslacher, B.; Neveu, A. (Institute for Advanced Study, Princeton, New Jersey 08540). Phys. Rev. D 11: No. 12, 3424-3450 (15 June 1975).

We have used a semiclassical method developed earlier to compute the particle spectrum of a field theory in two-dimensional space-time defined by the (sine-Gordon) Lagrangian $1/2(\partial_\mu\phi)^2 + (m^4/\lambda)$ $\{\cos[(\sqrt{\lambda}/m)\phi] - 1\}$. For weak coupling we find a heavy particle, the soliton, corresponding to a peculiar classical field configuration and an antisoliton. Below the soliton-antisoliton threshold there are a large number of further states. They can be viewed either as soliton-antisoliton bound states or as bound states of $n$ of the usual quanta of the theory. The "elementary particle" $\phi$ is the lowest of these. As the coupling increases, the higher states successively unbind, decaying into soliton-antisoliton pairs. At $\lambda/m^2 = 4\pi$, the "elementary particle" unbinds leaving only solitons and antisolitons for $\lambda/m^2 > 4\pi$. Comparing our semiclassical results with recent exact results of Coleman and with perturbation theory, we find that the semiclassical calculations are *exact*. This field theory seems similar to the hydrogen atom for which the Bohr-Sommerfeld quantization rules give the energy levels exactly. We also treat a $\phi^4$ theory in weak coupling and carry out a number of calculations which provide nontrivial illustrations of the semiclassical method. (auth)

**27187** REDUCTION OF THE EIGENVALUE EQUATION IN FINITE QUANTUM ELECTRODYNAMICS. Eilam, G. (Physics Department, Technion–Israel Institute of Technology, Haifa, Israel). Phys. Rev. D 11: No. 12, 3451-3457 (15 June 1975).

We prove that the eigenvalue equation in finite quantum electrodynamics $F_1(y_0) = 0$, where $F_1$ is the coefficient of the logarithmically divergent part of the single-fermion-loop vacuum-polarization diagrams, simplifies to $H_1(y_0) = 0$. $H_1$ includes all the diagrams with at least one photon exchanged between the upper and the lower parts of the fermion loop. It is shown that the zero of $H_1$ is, like the zero of $F_1$, of infinite order (essential singularity), and both zeros are at the same value of the coupling constant. (auth)

**27188** ALGEBRA OF CAUSALITY. Scharfstein, H. (International Centre for Theoretical Physics, Trieste, Italy). Phys. Rev. D 11: No. 12, 3458-3471 (15 June 1975).

A set of trilinear equal-time commutation relations is proposed as a generalized second-quantization scheme for fields satisfying conventional statistics. The scheme specifies the bilinear equal-time commutation relations between distinct fields (a finite number for each spin for the representations considered) in addition to the commutation relations of fields with themselves. Multiplet schemes for a particular representation of "generalized fields" satisfying the trilinear equal-time commutation relations are studied. It is shown that generalized vacuum expectation values can be defined, and that the $S$-matrix formalism can be developed for generalized fields. Differences with the conventional $S$-matrix expansions are examined, in particular in connection with possible applications to renormalization procedures. A novel regularization method, based on the bilinear equal-time commutation relations between distinct fields, is considered. (auth)

**27189** STRUCTURE OF THE VERTEX FUNCTION IN FINITE QUANTUM ELECTRODYNAMICS. Mannheim, P.D. (Lawrence Berkeley Laboratory, University of California, Berkeley, California 94720). Phys. Rev. D 11: No. 12, 3472-3480 (15 June 1975).

We study the structure of the renormalized electromagnetic current vertex, $\tilde{\Gamma}_\mu(p,p+q,q)$, in finite quantum electrodynamics. Using conformal invariance we find that $\tilde{\Gamma}_\mu(p,p,0)$ takes the simple form of $Z_1\gamma_\mu$ when the external fermions are far off the mass shell. We interpret this result as an old theorem on the structure of the vertex function due to Gell-Mann and Zachariasen. We give the general structure of the vertex for arbitrary momentum transfer parametrically, and discuss how the Bethe-Salpeter equation and the Federbush-Johnson theorem are satisfied. We contrast the meaning of pointlike in a finite field theory with the meaning understood in the parton model. We discuss to what extent the condition $Z_1 = 0$, which may hold in conformal theories other than finite quantum electrodynamics, may be interpreted as a bootstrap condition. We show that the vanishing of $Z_1$ prevents there being bound states in the Migdal-Polyakov bootstrap. (auth)

**27190** VARIATIONAL METHOD FOR SOLENOIDAL EXCITATION OF YANG-MILLS FIELD. Suura, H. (Department of Physics and Astronomy, University of Minnesota, Minneapolis, Minnesota 55455). Phys. Rev. D 11: No. 12, 3398-3404 (15 June 1975).

A solenoidal excitation mode of the massless Yang-Mills field coupled to fixed classical $I$-spin sources is investigated by the variational method. The lattice point quantization is introduced as an intermediate step to evaluate the variational integral of the field Hamiltonian. We obtain Ginzburg-Landau-type equations (without the mass term) for the electric field, with the magnitude of the vector potential playing the role of the order parameter. It is shown that induced field $I$-spin densities associated with fluctuating magnetic fields could shield the Coulomb interaction, thus lowering the self-energy relative to the static classical limit where no magnetic field exists. (auth)

**27191** 16-COMPONENT THEORY OF THE SPIN-1 PARTICLE AND ITS GENERALIZATION TO ARBITRARY SPIN. Durand, E. (Université Paul Sabatier, Physique Théorique, 31077-Toulouse Cedex, France). Phys. Rev. D 11: No. 12, 3405-3416 (15 June 1975).

The criteria of validity of this theory are, among others, the nonrelativistic approximation, the classical approximation which gives the Thomas spin theory, and the values of the energy in a homogeneous magnetic field. In the tensorial form, this theory is more complicated than the 10-component Proca theory, but, in the matrix form, it is more convenient than the preceding theory using the Petiau-Duffin-Kemmer matrices, because only matrices obeying the Dirac conditions intervene. When the mass term is equal to zero ($k=0$) one can recover the Maxwell equations, as a particular case. Finally, the theory may be easily generalized for an arbitrary spin of value $J=n/2$. (auth)

**27192** COVARIANT PROPAGATORS FROM THE SINGH-HAGEN LAGRANGIAN. Kobayashi, M.; Mori, Y. (Department of Physics, Gifu University, Gifu 502, Japan). Phys. Rev. D 11: No. 12, 3637-3643 (15 June 1975).

Prescriptions for constructing covariant propagators from the Singh-Hagen Lagrangian are presented. Propagators are derived explicitly for spin $J \leq 5$ ($J$ an integer) according to this prescription. They agree with the propagators proposed by Harnad and Snoke in connection with the O(4) propagator. They do not depend on arbitrary parameters contained in the free Lagrangian. Some comments on daughter fields associated with contact-interaction fields are given. (auth)

**27193** ZEROTH ORDER APPROXIMATION OF A STEP FUNCTION PERTURBATIVE NUMERICAL METHOD FOR THE SOLUTION OF THE SCHROEDINGER EQUATION. Adam, G.; Ixaru, L. G. (Inst. of Atomic Physics, Bucharest). Rev. Roum. Phys.; 20: No. 1, 17-28 (1975).

The Schroedinger-like equation $y''(x) = f(x)y(x)$ is solved by a perturbative numerical method which starts with a step function approximation for f(x). The best algorithm for the zeroth order approximation is given and an error analysis is reported which yields: sharp error bounds for the numerical solution, the optimal step function approximation, and a correction to the algorithm of the zeroth order, which, while leaving the computation time practically the same, raises the rate of convergence from $\varphi(h^2)$ to $\varphi(h^4)$. This $\varphi(h^4)$ algorithm shows several advantages over those produced by the methods of Fox-Goodwin, Numerov, Runge-Kutta, and Hulme. (auth)

**27194** INEQUALITIES FOR ISING MODELS AND FIELD THEORIES WHICH OBEY THE LEE-YANG THEOREM. Newman, C. M. (Indiana Univ., Bloomington (USA). Dept. of Mathematics). Commun. Math. Phys.; 41: No. 1, 1-9(Mar 1975).

20 refs.

A series of inequalities for partition, correlation, and Ursell functions are derived as consequences of the Lee-Yang theorem. In particular, the n-point Schwinger functions of even phi$^4$ models are bounded in terms of the 2-point function as strongly as is

the case for Gaussian fields; this strengthens recent results of Glimm and Jaffe and shows that renormalizability of the 2-point function by fourth degree counter-terms implies existence of a phi[4] field theory with a moment generating function which is entire of exponential order at most two. (auth)

**27195** BOUND-STATE PAIRING SINGULARITIES IN THE $^3$He GALITSKII–FEYNMAN T-MATRIX: TEMPERATURE DEPENDENCE. Bishop, R. F.; Strayer, M. R.; Irvine, J. M. (Manchester, Univ., England). J. Low Temp. Phys.; 20: No. 5/6, 573-584 (Sep 1975).

The temperature-dependent Galitskii–Feynman T-matrix, which sums the two-body scattering series, allowing any number of pairs of either particles outside or holes inside the Fermi sea in intermediate states, for a two-body potential appropriate to liquid $^3$He, is shown to exhibit a bound-state singularity. The two-body binding energy within the $^3$He background is shown to be highly sensitive to both the temperature and the density of the system. A critical density below which the binding disappears is observed to be a function of the temperature and of the total momentum of the interacting pair. Detailed numerical computations of this structure are presented using the modified Frost–Musulin potential. To our knowledge, these computations represent the first attempt at a temperature-dependent many-body calculation based on a realistic $^3$He potential. Possible consequences are drawn for more detailed and realistic calculations of the properties of liquid $^3$He. (2 figures) (auth)

**27196** UNIQUENESS OF PHI[4] INTERACTIONS IN TWO- AND THREE-COMPONENT SPIN SYSTEMS. Zia, R. K. P.; Wallace, D. J. (Southampton Univ., Eng.). J. Phys., A (London); 8: No. 7, 1089-1096 (Jul 1975).

The constraints imposed on the $\phi^4$ interactions of a two- or three-component spin system are examined by the demand that the spin-spin correlation function is isotropic. The phase transition behavior of such systems is considered and proves to be essentially unique. The two-component model provides a very clean example of a redundant operator in the renormalization group formalism. (auth)

# Gravitation and General Relativity

*Refer also to abstracts 26425 and 26604.*

**27197** (HU-TFT-74-31) GRAVITATIONAL THREE-BODY SCATTERING EXPERIMENT. Valtonen, M. J. (Helsinki Univ. (Finland). Research Inst. for Theoretical Physics). 1975. 33p. Dep. NTIS (US Sales Only) $4.75.

The gravitational interaction between an equal component circular binary and a third particle of equal mass was studied in detail for nearly parabolic planar orbits. An approximate analytical model for energy transfer was constructed by harmonic analysis. (auth)

**27198** YANG'S GRAVITATIONAL FIELD EQUATIONS. Ni, W. (Institute of Physics, National Tsing Hua University, Hsinchu, Taiwan, Republic of China). Phys. Rev. Lett. 35: No. 5, 319-320 (4 Aug 1975).

Yang's gravitational field equations *in vacuo* can be regarded as "derivative" equations of both Einstein's equations and Nordström's equations, and embrace all their solutions. Yang's equations admit monopole gravitational radiations; therefore no analog of the Birkhoff theorem can be valid. The most general static spherical-symmetric solution contains four arbitrary parameters. In particular, $ds^2 = -dt + (1 + c_1/r + c_2r^2)^{-1}dr^2 + r^2(d\theta^2 + \sin^2\theta \times d\varphi^2)$ is a two-parameter exact solution. This metric prossesses no gravitational red shifts. (auth)

**27199** GEOMETRICALLY DEGENERATE SOLUTIONS OF THE KILMISTER-YANG EQUATIONS. Thompson, A.H. (Department of Mathematics, University of Pittsburgh, Pittsburgh, Pennsylvania 14260). Phys. Rev. Lett. 35: No. 5, 320-322 (4 Aug 1975).

I solve, in principle, the Kilmister-Yang equations for the degenerate cases of conformal flatness and decomposability of space-time. The unphysical metrics discussed by Pavelle belong to these degenerate classes. Perhaps using the methods outlined here it will be possible to determine if these "unphysical" metrics are isolated examples or if they are typical of such "geometric-degenerate" classes. (auth)

**27200** NULL GEODESIC DEVIATION I. CONFORMALLY FLAT SPACE-TIMES. Peters, P.C. (Department of Physics, University of Washington, Seattle, Washington 98195). J. Math. Phys. (N.Y.) 16: No. 9, 1780-1785 (Sept 1975).

The equation of geodesic deviation is solved in conformally flat space-time in a covariant manner. The solution is given as an integral equation for general geodesics. The solution is then used to evaluate second derivatives of the world function and derivatives of the parallel propagator, which need to be known in order to find the Green's function for wave equations in curved space-time. A method of null geodesic limits of two-point functions is discussed, and used to find the scalar Green's function as an iterative series. (auth)

**27201** ALL STATIONARY AXISYMMETRIC ROTATING DUST METRICS. Winicour, J. (Department of Physics, University of Pittsburgh, Pittsburgh, Pennsylvania 15260). J. Math. Phys. (N.Y.) 16: No. 9, 1806-1808 (Sept 1975).

The Einstein equations for stationary axisymmetric space-times with a rotating dust source are systematically reduced to quadratures. The general solution depends upon an arbitrary axisymmetric solution of the flat three-dimensional Laplace equation and upon an arbitrary function of one variable. (auth)

**27202** NONMETRICAL DYNAMICS. I. Pereira, C.M. (Department of Physics and Astronomy, University of Maryland, College Park, Maryland 20742). J. Math. Phys. (N.Y.) 16: No. 9, 1939-1944 (Sept 1975).

Einstein's nonvacuum gravitational field equations are examined. The following nonmetrical existence theorem is proved. It is shown that given any analytic symmetric contravariant energy–momentum tensor density as a function of the space–time coordinates, a solution to the gravitational field equations always exists. Furthermore, this solution is such that the law of conservation of energy–momentum is satisfied. The new proof of the present paper makes no use of the coordinate transformation method used in a previous paper. The Cauchy–Kowalewsky existence theorem is used in the proof, and the literature on the Cauchy–Kowalewsky existence theorem is briefly reviewed. (Riquier's existence theorem is avoided except for a brief discussion in the Appendix.) The initial value problem of Einstein's equations is examined as part of the proof. The physical and mathematical meaning of this new proof is discussed. It is noted that the nonmetrical existence theorem disappears when Einstein's equations are linearized whereas the familiar Lichnerowicz-type existence theorems survive linearization. This suggests that the nonmetrical existence theorem may add a new dimension to our understanding of the physical meaning of nonlinearity in Einstein's equations. (auth)

**27203** QUANTUM VACUUM ENERGY IN GENERAL RELATIVITY. Ford, L.H. (Department of Physics, University of Wisconsin-Milwaukee, Milwaukee, Wisconsin 53201). Phys. Rev. D 11: No. 12, 3370-3377 (15 June 1975).

The vacuum energy of a quantized field in a non-Minkowskian spacetime is discussed. The approach taken emphasizes the analogy between this vacuum energy and the energy of the vacuum state of the quantized electromagnetic field in the presence of a pair of parallel conducting plates, the Casimir energy. The energy of the vacuum state of a quantized scalar field in a one-dimensional box of length $L$ (the spacetime manifold $S^1 \times R$) is shown to be $\pi\hbar c/6L$. A massless, conformal scalar field in the Einstein universe ($S^3 \times R$) also possesses a nonzero vacuum energy. The vacuum energy density in this case is $\rho = \hbar c\ (480\pi^2 a_0^4)^{-1}$, where $a_0$ is the radius of the universe. The pressure $P$ is $1/3\ \rho$, so the energy-momentum tensor associated with these zero-point fluctuations is of the same form as that for classical radiation. It is shown that a closed Robertson-Walker universe has the same vacuum energy density and pressure as a static universe of instantaneously equal radius. The electromagnetic, neutrino, and minimally coupled scalar fields in the Einstein universe cannot be treated successfully by these techniques. Finally, the vacuum energy of a scalar field in the presence of a linearized plane gravitational wave is discussed. It is shown that for a certain choice of vacuum state, which is an eigenstate of the Hamiltonian so no pair production occurs, the vacuum energy and pressue vanish. This result holds for both the conformal and nonconformal energy-momentum tensors. (auth)

**27204** VACUUM FLUCTUATIONS OF A QUANTIZED SCALAR FIELD IN A ROBERTSON-WALKER UNIVERSE. Streeruwitz, E. (Institut für Theoretische Physik der Universität Wien A-1090 Wien, Boltzmanngasse 5, Austria). Phys. Rev. D 11: No. 12, 3378-3383 (15 June 1975).

The vacuum expectation value of the energy-momentum tensor of a quantized scalar field is calculated in a Robertson-Walker universe. The resulting divergences are regularized by averaging over an appropriate mass spectrum, which fulfills the same regularization conditions as needed for regularization of the vacuum energy-momentum tensor in Minkowski space. Up to higher orders in time derivatives and inverse radius of universe, there result three contributions to the vacuum energy-momentum density: a cosmological term, a term proportional to the Einstein tensor, and a term derivable by variation of a gravitational Lagrangian containing quadratic expressions of the curvature quantities $R$, $R_{\mu\nu}$, $R_{\mu\nu\rho\sigma}$. These contributions are estimated with the following result: There is no direct evidence that the collapse of a Robertson-Walker universe is averted at some realistic dimensions of the universe, or that gravitation is described in a natural way by the elastic properties of the vacuum of some particles. On the other hand, there is

given some evidence that quantum corrections of the type shown must be taken into account in general relativity and are important at least for highly collapsed states of the early universe. (auth)

**27205** GRAVITATION AND POSITIVE-ENERGY WAVE EQUATIONS. Ahner, H.F. (Adelphi University, Garden City, New York 11530). Phys. Rev. D 11: No. 12, 3384-3387 (15 June 1975).

Relativistic equations that describe massive particles with only positive-energy eigenvalues are generalized to include gravitational interactions. The method developed, using a *vierbein* field, is applied specifically to Staunton's spin-½ equation. All consistency conditions are satisfied. A second-rank symmetric tensor whose covariant divergence is zero is found. (auth)

**27206** EXACT SOLUTION TO THE EINSTEIN-MAXWELL FIELD EQUATIONS FOR A CHARGE AND MASS DISTRIBUTION WITH A QUADRUPOLE MOMENT. Young, J.H.; Bentley, S.L. (Department of Physics, University of Alabama in Birmingham, Birmingham, Alabama 35294). Phys. Rev. D 11: No. 12, 3388-3391 (15 June 1975).

The method introduced by Erez and Rosen to obtain exact multipole-type solutions to the static axially symmetric Einstein field equations is generalized to the Einstein-Maxwell system for the case of a static axially symmetric distribution of mass and charge. This is accomplished by defining an auxiliary function which, when assumed to be related to the electrostatic potential through certain derivative conditions, reduces the Einstein-Maxwell equations for this case to the Weyl form of the pure gravitational field equations. A general expression is then given for the electrostatic potential in terms of the auxiliary function. We interpret the solutions, which contain the Reissner-Nordström solution as a special case, as fields produced by mass and charge distributions possessing multipole structure, and we give the explicit form of the metric for the monopole plus quadrupole case. (auth)

**27207** BLACK HOLES WITH SCALAR CHARGE. Bekenstein, J.D. (Center for Relativity Theory, Department of Physics, University of Texas at Austin, Austin, Texas 78712). Ann. Phys. (N.Y.) 91: No. 1, 75-82 (May 1975).

Previously it had been thought that a stationary black hole with an exterior devoid of matter can be parametrized only by mass, angular momentum, and electric charge. We show here that scalar charge is also an admissible parameter. Our starting point is a new solution of Einstein's equations with stress-energy of electromagnetic and conformal scalar fields which we presented earlier. It has a black-hole geometry, and is parametrized by electric and scalar charges. Its conformal scalar field is unbounded at the event horizon, and we originally regarded this feature as incompatible with a black hole interpretation. However, following a suggestion of B. DeWitt, we show here that the infinity in the scalar field need not be physically pathological: it is not associated with an infinite potential barrier for test scalar charges; it does not cause the termination of any trajectories of these test particles at finite proper time; and it is not connected with unbounded tidal accelerations between neighboring trajectories. In view of these facts, we now regard the new solution as a genuine black hole solution. (auth)

**27208** COMMENT ON THE MODIFICATIONS OF MAXWELL'S EQUATIONS PROPOSED BY TRIMMER AND BAIERLEIN. Duncan, G.C.; Fulcher, L.P. (Department of Physics, Bowling Green State University, Bowling Green, Ohio 43403). Phys. Rev. D 11: No. 12, 3628-3629 (15 June 1975).

It is shown that the recent modifications of Maxwell's equations proposed by Trimmer and Baierlein do not allow one to discuss energy conservation of the electromagnetic field from the point of view of a generalization of Poynting's theorem. (auth)

**27209** HAMILTONIAN PROPAGATION OFF CHARACTERISTIC SURFACES. Motill, R. A. Syracuse, NY; Syracuse Univ. (1974). 133p. University Microfilms Order No. 75-14,006.

Thesis (Ph. D.).

In the usual Hamiltonian formalism of general relativity there are constraints due to the covariance of the theory. If one introduces null coordinate hypersurfaces and also imposes for their description conditions of the Bondi type into the Lagrangian, additional constraints appear, and the system is now completely second class. Contrary to some statements in the literature, no linear combination of the null surface constraints themselves can exist which would generate a subgroup of the canonical group. This result precludes the role of such constraints as generators of the Bondi news function. The presence of second class constraints is known to be undesirable for a number of reasons. Accordingly, in this treatment an algebra is constructed that eliminates all null surface constraints as generators of canonical transformations. Only massless fields are considered, and in the absence of sources: First, the massless scalar field, then electrodynamics in terms of potentials, followed in turn by linearized gravitation, and finally, by general relativity. (JFP)

**27210** ELECTROMAGNETIC AND NEUTRINO FIELDS IN GENERAL RELATIVITY: A CONSTRUCTIVE PROCEDURE. Kegeles, L. S. Philadelphia; Univ. of Pennsylvania (1974). 112p. University Microfilms Order No. 75-14,580.

Thesis (Ph. D.).

A new procedure for constructing electromagnetic and neutrino fields in curved space-times is formulated. The basic method consists of a covariant generalization of the Debye–or two-component Hertz–potential formalism of flat space. The formulation replaces the strongly coupled first-order Maxwell or Dirac system by a fully decoupled second-order differential equation. The problem of computing these fields is thus reduced to solving a single complex linear second-order scalar wave equation; the fully covariant physical spinor or tensor field is derived from the scalar solution of this wave equation by prescribed and straightforward differentiation. The Hertz formalism is extended to all curved space-times; the Debye two-component (or one-complex-component) formalism is extended to those space-times conformally related to vacuum space-times with algebraically specialized Weyl tensor. This ("generalized Goldberg-Sachs") class of space-times covers most known astrophysically important solutions to Einstein's field equations, including black-hole and neutron-star spaces and cosmological models. Since the extended Debye formalism provides a practical new computational tool in these space-times, it is hoped that future applications of the method developed may assist in a better theoretical understanding of electromagnetic and neutrino phenomena in relativistic astrophysics. (Diss. Abstr. Int., B)

**27211** GENERAL RELATIVITY DERIVED FROM AN AFFINE VARIATION OF A QUADRATIC LAGRANGIAN. Roxburgh, I. W. (Queen Mary Coll., London). J. Phys., A (London); 8: No. 7, 1075-1080(Jul 1975).

An alternative derivation of general relativity is presented in which the field equations are derived from a gauge invariant quadratic Lagrangian by varying the affine field $\Gamma^a_{bc}$ and keeping the geometry fixed. The field equations show that the $\Gamma^a_{bc}$ can be considered as a Christoffel connection of a tensor $g^{ab}$ and if, after the variation, the metric tensor is chosen to be this tensor, the field equations of general relativity with a cosmical constant are recovered. (auth)

# REACTOR TECHNOLOGY AND REGULATION

**27212** (CONF-701074-P2) PROCEEDINGS OF THE SCIENTIFIC-TECHNICAL CONFERENCE "ATOMIC POWER, FUEL CYCLES, RADIATION STUDY OF MATERIALS", ULYAOVSK, 5–10 OCTOBER 1970. Vol. 2. 1970. Translation of Trudy Nauchno-Tekhnicheskoi Konferentsii "Atomnaya Energetika, Toplivnye Tsikly, Radiatsionnoe Materialovedenie", Ul'yanovsk, 5–10 Oktyabrya 1970 G. Vol. II. (TT-73-53042/02). 624p. Dep. NTIS $13.60.

From conference on atomic power, fuel cycles, and radiation study of materials; Ul'yanovsk, USSR (5 Oct 1970).

Thirty-two papers are presented on studies related to power reactor technology. Each paper has been separately abstracted and indexed. (DG)

*For abstracts of individual papers see: 26152, 27213–27216, 27221–27226, 27232–27235, 27263–27265, 27271–27274, 27372, 27418, 27419, 27423, 27424, and 27432–27436.*

## Power Reactors, Non-Breeding, BWR-Type

*Refer also to abstracts 27375, 27379, 27383, 27440, 27442, and 27444–27446.*

**27213** (CONF-701074-P2, pp 35-47) DISTRIBUTION OF DEPOSITS AND THEIR ACTIVITY: ON THE SURFACES OF EQUIPMENT AND COMMUNICATIONS OF A SINGLE-CIRCUIT ATOMIC ELECTRIC POWER PLANT. Chechetkin, U. V.; Zabelin, A. I.; Rozdestvenskaya, L. N.; Kizin, V. D.; Syvatesheva, T. S. 1970. Translated from Trudy Nauchno-Tekhnicheskoi Konferentsii "Atomnaya Energetika, Toplivnye Tsikly, Radiatsionnoe Materialovedenie", Ul'yanovsk, 5–10 Oktyabrya 1970 G. Vol. II.

From conference on atomic power, fuel cycles, and radiation study of materials; Ul'yanovsk, USSR (5 Oct 1970).

In proceedings of the scientific-technical conference "atomic power, fuel cycles, radiation study of materials".

The data on the content of admixtures in the coolant, their dispersity, and the activity of the coolant are discussed; the data on the studies of deposits and their activity on the surface of the equipment and communications of the atomic electric power plant VK-50 are given for the period of operation of the station from 1965 to 1970; an estimation of the activity absorbed by the surface of pipes and turbogenerators has been carried out. Conclusions have been made, namely, that there is no marked growth of activity in deposits despite lengthy operation of the station with non-hermetic fuel elements (with daily fume-off at approx. 2000 Curies). The experimental data obtained could be used for studying the dynamics of activity in deposits of similar stations. (auth)

**27214** (CONF-701074-P2, pp 89-106) QUESTION OF EXPLOITATION OF ION-EXCHANGE FILTERS FOR SINGLE CIRCUIT ATOMIC ELECTRIC POWER PLANTS. Chechetkin, U. V.; Zabelin, A. I.; Rozjdestvensakaya, L. N.; Kizin, V. D.; Yashin, E. K.; Masnaya, L. N. 1970. Translated from Trudy Nauchno-Tekhnicheskoi Konferentsii "Atomnaya Energetika, Toplivnye Tsikly, Radiatsionnoe Materialovedenie", Ul'yanovsk, 5–10 Oktyabrya 1970 G. Vol. II.

From conference on atomic power, fuel cycles, and radiation study of materials; Ul'yanovsk, USSR (5 Oct 1970).

In proceedings of the scientific-technical conference "atomic power, fuel cycles, radiation study of materials".

A design diagram is proposed and an estimation of the integral dose of radiation is carried out in order to determine the working ability of the ion-exchange resins in systems for purification of turbine condensate for various situations of leakage in fuel element of single circuit boiling type atomic electric power plants. The radiation fields, close to the ion-exchange filters, have been studied. The respective data, calculated and experimental, are recorded. (auth)

**27215** (CONF-701074-P2, pp 241-269) METHOD OF ESTIMATION OF FISSION-FRAGMENT ACTIVITY IN THE COOLANT, DISCHARGE FROM INDUSTRIAL ATOMIC ELECTRIC POWER PLANTS HAVING ROD-TYPE FUEL ELEMENTS, COOLED BY BOILING WATER. Guseinov, A. G.; Kobozov, M. G.; Kharizomenov, U. V. 1970. Translated from Trudy Nauchno-Tekhnicheskoi Konferentsii "Atomnaya Energetika, Toplivnye Tsikly, Radiatsionnoe Materialovedenie", Ul'yanovsk, 5–10 Oktyabrya 1970 G. Vol. II.

From conference on atomic power, fuel cycles, and radiation study of materials; Ul'yanovsk, USSR (5 Oct 1970).

In proceedings of the scientific-technical conference "atomic power, fuel cycles, radiation study of materials".

A method of calculation of fission-fragment activity in the coolant of the primary circuit is discussed for the case of partial leakage in power reactors with rod-type fuel elements cooled by boiling water. The migration of fragments along the circuit and determination of the radioactive effluents were studied with an improved and modified model, which is normally used for observing the transfer of deposits and washing-out of products of corrosion in water cooled reactors. (auth)

**27216** (CONF-701074-P2, 346-361 ANALYSIS OF FUEL ELEMENTS OF A CASSETTE THAT HAS OPERATED FOR 17000 HOURS IN THE REACTOR CORE OF VK-50. Belokopitov, B. S.; Votinov, S. N.; Sarichev, V. M.; Demyanovitch, M. A.; Pletin, B. P.; Andreeva, A. B.; Derbizov, M. D.; Schepetilnikov, V. A. 1970. Translated from Trudy Nauchno-Tekhnicheskoi Konferentsii "Atomnaya Energetika, Toplivnye Tsikly, Radiatsionnoe Materialovedenie", Ul'yanovsk, 5–10 Oktyabrya 1970 G. Vol. II.

From conference on atomic power, fuel cycles, and radiation study of materials; Ul'yanovsk, USSR (5 Oct 1970).

In proceedings of the scientific-technical conference "atomic power, fuel cycles, radiation study of materials".

Results of analysis of a rod-type fuel element of a cassette that has operated for 17,000 hours in the reactor core of VK-50 are presented. Working conditions in the reactor core and data of preliminary results are discussed. Results of tests of construction materials, structure of zirconium shells and fuel of assemblies are analyzed. Data of mechanical tests of samples, cut out from the fuel element shells, are discussed. (auth)

**27217** (CONF-750822-7) TECHNOLOGY FOR DISMANTLING LARGE RADIOACTIVE STRUCTURAL COMPONENTS. Blumberg, R. (Oak Ridge National Lab., Tenn. (USA)). 1974. 12p. Dep. NTIS $4.00.

From conference on decontamination and decommissioning of ERDA facilities; Idaho Falls, Idaho, USA (19 Aug 1975).

The dismantling of the ERR (Elk River Reactor) was completed successfully and safely in September, 1974. The 58 MW(t), boiling water reactor was removed down to its foundations, and all of the radioactive material was shipped in suitable containers to licensed burial grounds. The most difficult and the unique part of this effort was the cutting up and removal of the radioactive structural parts, namely the inner thermal shield, the pressure vessel, and the outer thermal shield. The tools and techniques for this operation were designed, developed, and fabricated at the Oak Ridge National Laboratory. This development provides the nuclear industry with a viable alternative to entombment and surveillance for decommissioning reactors. The technology used is described, and comments are made on its application to larger, more highly radioactive systems. (auth)

**27218** (NP-20527) GENERAL ELECTRIC NUCLEAR POWER PLANT SIMULATOR TRAINING MANUAL. (General Electric Co., San Jose, Calif. (USA). Atomic Power Equipment Dept.). [nd]. 81p. General Electric Co., San Jose, CA.

The nuclear power plant simulator adjacent to the Dresden plant site is presented. The program that a reactor operator trainee will follow while he attends is presented. This training program breakdown must be considered as preliminary even though it is certain that no major changes will be made in the subjects to be studied or in the simulator exercises. General Electric's reactor operator training experience at both VBWR and EVESR have shown this approximate subject study schedule to be effective in preparing the trainees to safely operate a nuclear power plant. (auth)

**27219** NON-DESTRUCTIVE GAMMA-RAY SPECTROMETRY ON SPENT FUELS OF A BOILING WATER REACTOR. Matsuura, S.; Tsuruta, H.; Suzaki, T.; Okashita, H.; Umezawa, H. (Japan Atomic Energy Research Inst., Tokai, Ibaraki. Tokai Research Establishment). J. Nucl. Sci. Technol. (Tokyo); 12: No. 1, 24-34 (Jan 1975).

The spent fules from the JPDR-I reactor were measured by means of a $\gamma$-scanning facility installed in the fuel storage pool. The spatial distributions of the fission products ($^{134}Cs$ and $^{137}Cs$) were measured and analyzed in reference to the effects of control rod patterns. The ratios holding between the products of neutron capture and of direct fission ($^{134}Cs/^{137}Cs$ and $^{154}Eu/^{137}Cs$) were also examined for its relevance to non-destructive burnup determination. The activity ratios of the fission products can be expressed by a linear function of burnup, provided that corrections are made to account for differences in irradiation history and for spatial variations in the neutron spectrum. (auth)

**27220** PUMPS FOR NUCLEAR POWER PLANTS. Suzuki, A. (Hitachi Ltd., Tokyo (Japan)). Haikan Gijutsu; 16: No. 12, 164-170 (Oct 1974). (In Japanese).

The pumps used in BWR nuclear power stations are described. The problems encountered in pumps for nuclear power generation and features of major pumps are examined. There are a number of special requirements including high reliability, radioactivity countermeasures, shaft sealing, etc. Among the major pumps, there are those for recirculation, purification, core spray, and feed water. (JA)

## Power Reactors, Non-Breeding, PWR-Type

*Refer also to abstracts 27364–27372, 27375, 27379–27383, 27394–27402, 27408, 27441, 27443, and 27447–27451.*

**27221** (CONF-701074-P2, pp 117-127) ANALYSIS OF THE PROCESSES OF ACCUMULATION OF FISSION PRODUCTS IN THE PRELIMINARY CIRCUIT OF THE WATER-MODERATED WATER-COOLED POWER REACTOR. Mironov, V. N.; Teplov, P. V.; Kazakov, V. A. 1970. Translated from Trudy Nauchno-Tekhnicheskoi Konferentsii "Atomnaya Energetika, Toplivnye Tsikly, Radiatsionnoe Materialovedenie", Ul'yanovsk, 5–10 Oktyabrya 1970 G. Vol. II.

From conference on atomic power, fuel cycles, and radiation study of materials; Ul'yanovsk, USSR (5 Oct 1970).

In proceedings of the scientific-technical conference "atomic power, fuel cycles, radiation study of materials".

An attempt has been made to present a mathematical model which will permit calculation of fission product accumulation in the fuel and water of the primary circuit and on the surfaces of the cooling circuit and to compare the calculated results with experimental data obtained from the first block of the Novo Voronezh atomic electric power plant. (auth)

**27222** (CONF-701074-P2, pp 128-148) PERIODIC INSPECTION OF THE STATE OF THE METAL OF EQUIPMENT OF UNITS I AND II OF THE NOVO VORONEZH AES. Shabanov, N. N.; Mentsov, V. A. 1970. Translated from Trudy Nauchno-Tekhnicheskoi Konferentsii "Atomnaya Energetika, Toplivnye Tsikly, Radiatsionnoe Materialovedenie", Ul'yanovsk, 5–10 Oktyabrya 1970 G. Vol. II.

From conference on atomic power, fuel cycles, and radiation study of materials; Ul'yanovsk, USSR (5 Oct 1970).

In proceedings of the scientific-technical conference "atomic power, fuel cycles, radiation study of materials".

Methods and results are presented for inspection of cooling system components of the WWER-1 and WWER-2 reactors. (DG)

**27223** (CONF-701074-P2, 149-176) WATER SYSTEM FOR BORON REGULATED VVER REACTORS. Chernorotov, E. S. 1970. Translated from Trudy Nauchno-Tekhnicheskoi Konferentsii "Atomnaya Energetika, Toplivnye Tsikly, Radiatsionnoe Materialovedenie", Ul'yanovsk, 5–10 Oktyabrya 1970 G. Vol. II.

From conference on atomic power, fuel cycles, and radiation study of materials; Ul'yanovsk, USSR (5 Oct 1970).

In proceedings of the scientific-technical conference "atomic power, fuel cycles, radiation study of materials".

The properties of a mixed ammonia-potassium water system for the primary circuit of an atomic electric power plant with reactor type VVER, which is the most favorable for operation of the reactor core and the reactor on the whole, are studied. Experimental data from a mixed ammonia-potassium system with boric acid are given. (auth)

**27224** (CONF-701074-P2, pp 177-197) EXPERIMENTAL TESTS OF THE PHYSICAL CHARACTERISTICS OF THE REACTOR OF THE SECOND BLOCK OF NOVO VORONEZB ATOMIC ELECTRIC POWER PLANT. Kamishan, A. N.; Andrianov, G. Ya.; Kostushin, V. A.; Kurilchik, S. S. 1970. Translated from Trudy Nauchno-Tekhnicheskoi Konferentsii "Atomnaya Energetika, Toplivnye Tsikly, Radiatsionnoe Materialovedenie", Ul'yanovsk, 5–10 Oktyabrya 1970 G. Vol. II.

From conference on atomic power, fuel cycles, and radiation study of materials; Ul'yanovsk, USSR (5 Oct 1970).

In proceedings of the scientific-technical conference "atomic power, fuel cycles, radiation study of materials".

Results of experiments for determining core physical characteristics of the second unit of the Novo Voronezb atomic electric power plant are discussed. The analyses of the dependence of the geometrical buckling parameter in the critical assembly on the concentration of the boric acid have been carried out. In a full scale fuel assembly, the flux of thermal neutrons has been measured. The results of calculations and experimental data have been compared. The results of experiments in determining the temperature coefficient of reactivity, temperature effect and effectiveness of boric acid solutions introduced into the moderator are discussed. The experiments were carried out during the start-up of the second unit of Novo Voronezh atomic electric power plant. (auth)

**27225** (CONF-701074-P2, pp 319-336) POST-RADIATIONAL ANALYSES OF THE HEAT RELEASING ELEMENTS, THAT HAVE OPERATED FOR 262 EFFECTIVE DAYS IN THE REACTOR CORE OF VVER-1 OF THE NOVO VORONEZH ATOMIC ELECTRIC POWER PLANT. Belokopitov, V. S.; Votinov, S. N.; Pakhomov, Z. I.; Deribizov, M. D.; Gabeskrya, V. Ya.; Portnov, V. F. 1970. Translated from Trudy Nauchno-Tekhnicheskoi Konferentsii "Atomnaya Energetika, Toplivnye Tsikly, Radiatsionnoe Materialovedenie", Ul'yanovsk, 5–10 Oktyabrya 1970 G. Vol. II.

From conference on atomic power, fuel cycles, and radiation study of materials; Ul'yanovsk, USSR (5 Oct 1970).

In proceedings of the scientific-technical conference "atomic power, fuel cycles, radiation study of materials".

The results of the analyses of rod-type fuel elements, with fuel of sintered 2% enriched uranium dioxide in shells made of Zr + 1% Nb alloy, which have remained in operation for 626 effective days in VVER-type reactor of the Novo Voronezh atomic electric power plant are presented. Fuel elements that had reached maximum burn-up of 22000 MW day/t.U. were analyzed. The data of construction materials of zirconium shells of fuel elements are discussed. The results of a mechanical analysis of samples, cut out from fuel element shells at varying thermal stress and testing temperature, are described. (auth)

**27226** (CONF-701074-P2, pp 337-345) CONSTRUCTION AND BASIC CHARACTERISTICS OF FUEL ELEMENTS TYPE VVER-1000. Zaimovskii, A. S.; Kalashnikov, V. V.; Kostrov, V. N.; Malanchenko, L. L.; Nikulina, A. V.; Yamnikov, V. S. 1970. Translated from Trudy Nauchno-Tekhnicheskoi Konferentsii "Atomnaya Energetika, Toplivnye Tsikly, Radiatsionnoe Materialovedenie", Ul'yanovsk, 5–10 Oktyabrya 1970 G. Vol. II.

From conference on atomic power, fuel cycles, and radiation study of materials; Ul'yanovsk, USSR (5 Oct 1970).

In proceedings of the scientific-technical conference "atomic power, fuel cycles, radiation study of materials".

A fuel element is described which is intended for the water-cooled, water moderated VVER-1000 reactor. The fuel is in the shape of $UO_2$ tablets, 7.56 mm in diameter and 12 mm height with holes at both ends. A zirconium alloy tube with 1 percent Nb and measuring phi 9.1 × 0.65 mm serves as the shell. The height of the fuel element is 3860 mm. The fuel element is planned for maximum thermal flux of $1.35 \cdot 10^6$ kcal/m$^2$ hour, maximum neutron flux (with an energy of over 0.4 MeV) $2.8 \cdot 10^{14}$ n/cm$^2$ sec and average burn-up for the reactor core of 40000 MW dat/tU. (auth)

**27227** (WCAP-7685-A) TEST REPORT ON ISOLATION AMPLIFIERS. Garber, I. (Westinghouse Electric Corp., Pittsburgh, Pa. (USA). Nuclear Energy Systems Div.). May 1975. 10p. Westinghouse Electric Corp., Pittsburgh, PA.

A description is provided for two types of Foxboro isolation amplifiers which are used with protection instrument channels. Test results were obtained on these isolation amplifiers to determine that there would be no effect on their input side (Protection Channel Side), when their outputs were subjected to opens, shorts and the application of voltages commonly available in the control room. (auth)

**27228** (WCAP-7755-A) TOPICAL REPORT: INTERCHANNEL THERMAL MIXING WITH MIXING VANE GRIDS. (Westinghouse Electric Corp., Pittsburgh, Pa. (USA). Nuclear Energy Systems Div.). Jan 1975. 46p. Westinghouse Electric Corp., Pittsburgh.

Experimental results and data analysis are presented for a series of mixing tests using top, split mixing vane grids on 20 inch axial spacing. These tests were conducted in pressurized water loops at Reynolds numbers similar to that of a PWR core under single and two phase (subcooled boiling) flow conditions. The thermal diffusion coefficient, TDC, is determined by comparing the THINC code predictions with the measured subchannel exit temperatures. The mean value of TDC for these data is $\overline{TDC}$ equals .066. TDC is found to be independent of Reynolds number, mass velocity, pressure and quality over the ranges tested. The two phase runs (local, subcooled boiling) fell within the scatter of the single phase runs. A conservative value of TDC equals .038 is recommended for current design use. This represents a lower limit value of all the test runs. (11 references) (auth)

**27229** (WCAP-7757-A) PANDA CODE. Altomare, S.; Minton, G. (Westinghouse Electric Corp., Pittsburgh, Pa. (USA).

Nuclear Energy Systems Div.). Feb 1975. 47p. Westinghouse Electric Corp., Pittsburgh.

PANDA is a new two-group one-dimensional (slab/cylinder) neutron diffusion code designed to replace and extend the FAB series. PANDA allows for the nonlinear effects of xenon, enthalpy and Doppler. Fuel depletion is allowed. PANDA has a completely general search facility which will seek criticality, maximize reactivity, or minimize peaking. Any single parameter may be varied in a search. PANDA is written in FORTRAN IV, and as such is nearly machine independent. However, PANDA has been written with the present limitations of the Westinghouse CDC-6600 system in mind. Most computation loops are very short, and the code is less than half the useful 6600 memory size so that two jobs can reside in the core at once. (auth)

**27230** (WCAP-7758-A) TURTLE 24.0 DIFFUSION DEPLETION CODE. Altomare, S.; Barry, R. F. (Westinghouse Electric Corp., Pittsburgh, Pa. (USA). Nuclear Energy Systems Div.). Sep 1971. 45p. Westinghouse Electric Corp., Pittsburgh, PA.

TURTLE is a two-group, two-dimensional (x-y, x-z, r-z) neutron diffusion code featuring a direct treatment of the nonlinear effects of xenon, enthalpy, and Doppler. Fuel depletion is allowed. TURTLE was written for the study of azimuthal xenon oscillations, but the code is useful for general analysis. The input is simple, fuel management is handled directly, and a boron criticality search is allowed. Ten thousand space points are allowed (over 20,000 with diagonal symmetry). TURTLE is written in FORTRAN IV and is tailored for the present CDC-6600. The program is core-contained. Provision is made to save data on tape for future reference. (auth)

**27231** (WCAP-7819-A(Rev.1)) NUCLEAR INSTRUMENTATION SYSTEM ISOLATION AMPLIFIER. Lipchak, J. B.; Bartholomew, R. R. (Westinghouse Electric Corp., Pittsburgh, Pa. (USA). Nuclear Energy Systems Div.). Apr 1975. 34p. Westinghouse Electric Corp., Pittsburgh, PA.

A description is presented of the isolation amplifier used in the nuclear instrumentation system. The results of in-circuit testing of the isolation capabilities of the prototype amplifier are included. The test results demonstrate that the unit will provide the required isolation - there being no significant effect on the input (protection) circuit when the output (non-protection) circuit is subjected to shorts or the application of 120 VAC or ±150 VDC. (auth)

## Power Reactors, Non-Breeding, Graphite Moderated

*Refer also to abstracts 26153, 27290, 27374, 27383, and 27437.*

**27232** (CONF-701074-P2, pp 1-14) MEASUREMENT OF THE CONCENTRATION OF FISSION FRAGMENTS IN THE PRIMARY LOOP BY THE DELAYED-NEUTRON METHOD. 1970. Translated from Trudy Nauchno-Tekhnicheskoi Konferentsii "Atomnaya Energetika, Toplivnye Tsikly, Radiatsionnoe Materialovedenie", "Ul'yanovsk, 5–10 Oktyabrya 1970 G. Vol. II.

From conference on atomic power, fuel cycles, and radiation study of materials; Ul'yanovsk, USSR (5 Oct 1970).

In proceedings of the scientific-technical conference "atomic power, fuel cycles, radiation study of materials".

A description is given of a method of measurement of delayed neutrons from the point of view of use for monitoring fission fragments in the primary circuit of a nuclear reactor with gas coolant. An algorithm is derived for calculation of the sensitivity of detection of fission fragments, and the results of calculation of the dependence of sensitivity on the principal parameters of the reactor and detector are presented. On the basis of the calculation a theoretical optimization is made of the principal parameters of the detector, and a design of the detector is proposed. An evaluation is given of the method from the point of view of the chemical state and behavior of radioactive iodine in the primary circuit and in the piping, its sampling, and the possibilities of using it as a supplementary control for the system of monitoring the hermetic seal of the fuel elements. (auth)

**27233** (CONF-701074-P2, pp 15-34) DETECTION OF DAMAGE TO FUEL ELEMENT SHELLS IN REACTORS USING GAS COOLANT. Gladki, E.; Melikhar, E.; Kubik, I.; Kapishovakii, 1970. Translated from Trudy Nauchno-Tekhnicheskoi Konferentsii "Atomnaya Energetika, Toplivnye Tsikly, Radiatsionnoe Materialovedenie", Ul'yanovsk, 5–10 Oktyabrya 1970 G. Vol. II.

From conference on atomic power, fuel cycles, and radiation study of materials; Ul'yanovsk, USSR (5 Oct 1970).

In proceedings of the scientific-technical conference "atomic power, fuel cycles, radiation study of materials".

On the basis of experiments carried out on gas cooled foreign reactors, a critical review of the various methods was carried out and possible solutions were proposed for detection of damage in heat releasing elements. Attention has also been given to the additional control for the coolant and methods of processing the given system. General criteria have been formulated for optimum selection of systems and possibilities of theoretical optimization of the system with concrete results of calculations and illustrations. In connection with the calculation of sensitivity detection, the relationship between the time dependence of the signal of damage to the detector and the type of damage to heat releasing element is discussed. (auth)

**27234** (CONF-701074-P2, pp 66-88) SOME PROBLEMS ON THE WATER SYSTEM IN ATOMIC ELECTRIC POWER PLANTS WITH BOILING TYPE REACTORS AND SELECTION OF CONSTRUCTION MATERIALS FOR THE SAME. Alexseev, B. A.; Ermakov, V. A.; Kozlova, V. F. 1970. Translated from Trudy Nauchno-Tekhnicheskoi Konferentsii "Atomnaya Energetika, Toplivnye Tsikly, Radiatsionnoe Materialovedenie", Ul'yanovsk, 5–10 Oktyabrya 1970 G. Vol. II.

From conference on atomic power, fuel cycles, and radiation study of materials; Ul'yanovsk, USSR (5 Oct 1970).

In proceedings of the scientific-technical conference "atomic power, fuel cycles, radiation study of materials".

The basis for selection of the water system for the atomic electric power plant with water-boiling reactors is discussed briefly. The so called "neutral, unadulterated" water system, where, judging by the data so far obtained, it is possible to use carbon steel in the reactor circuit, is quite acceptable. The problem of purification of the drainage and make-up water is highlighted. (auth)

**27235** (CONF-701074-P2, pp 107-116) WATER-CHEMICAL SYSTEM FOR ATOMIC ELECTRIC POWER PLANT WITH CHANNEL-TYPE REACTORS AND NUCLEAR SUPERHEATING OF STEAM. Konovalova, O. T.; Kosheleva, T. I.; Gerasimov, V. V.; Zjuravlev, L. S.; Schapov, G. A. 1970. Translated from Trudy Nauchno-Tekhnicheskoi Konferentsii "Atomnaya Energetika, Toplivnye Tsikly, Radiatsionnoe Materialovedenie", Ul'yanovsk, 5–10 Oktyabrya 1970 G. Vol. II.

From conference on atomic power, fuel cycles, and radiation study of materials; Ul'yanovsk, USSR (5 Oct 1970).

In proceedings of the scientific-technical conference "atomic power, fuel cycles, radiation study of materials".

The water system of the second block of the Beloyarsk atomic electric power plant was selected on the basis of the minimum speed of corrosion in the material used for the construction of the working channels of the reactor and main circuits of communication. A weak ammonia-water system has been used, where the pH value varies from 8 to 9.5. The concentration of ammonia is such that radiolysis is practically nil, ensuring at the same time, a notable lowering of the recorded pH value as a result of formation of nitrogen oxides. (auth)

**27236** (DP-REPORT-612) PRACTICAL DETAILS OF THE ULTRASONIC THERMOMETERS BEING INSTALLED IN THE DRAGON REACTOR. Dragon Project. Mobsby, E. G. (UKAEA Reactor Group, Winfrith. Atomic Energy Establishment). Nov 1968. 20p. Dep. NTIS (US Sales Only) $4.00.

The ultrasonic thermometers, three of which are currently being fitted into one fuel element of the Dragon Third Fuel Charge, employ resonant sensors connected by a wire transmission line to a magneto-strictive transducer. The basic principle was described in D. P. Report 950; we have now had a considerable and satisfactory out-of-pile experience from which we have made the assessment set out in this report. Two possible modes of operation of resonant ultrasonic and sonic temperature measuring devices present themselves, continuous excitation or pulsed excitation. For continuous excitation two separate connecting channels to the oscillator are needed, one to introduce the exciting energy; one to connect the receiver to the resonator (the energy may be applied directly to the oscillator, in which case one connection may be electrical). The chief drawback to continuous excitation is the poor sensitivity; the indication of resonance being the frequency of maximum amplitude of the received signal. With pulsed excitation the indication of resonance is both characteristic and sharp, resulting in a good reading sensitivity. Accordingly the resonant system described is a pulsed one. (auth)

**27237** (DP-Report-625) STABILITY BEHAVIOUR OF STEAM GENERATORS WITH UPWARD FLOW OF HELIUM. Final Report. Dragon Project Report. Fritz, K.; Gilli, P. V. (UKAEA Reactor Group, Winfrith. Atomic Energy Establishment). Apr 1969. 33p. Dep. NTIS (US Sales Only) $4.75.

For a new design proposal for a 660 MW(e) High Temperature Gas Cooled Reactor with downward gas flow in the core and up-

ward gas flow, downward $H_2O$ flow in the pod type steam generators, the question of $H_2O$ flow stability was investigated. A preliminary design with 6 steam generator units has been developed on the basis of the former steam generator studies of a 1,250 MW(t) HTGR with downward flow of helium, employing 18 steam generator units. Heat transfer and pressure drop calculations as well as an estimation of the stability behavior have been performed by means of the Waagner–Biro Computer Codes ADURHELIX, ISENT, VAMUTH, ODYN-2 and PULS. Stability calculations indicate that the high static and sufficient dynamic stability of the arrangement with downward gas flow is also obtained in an arrangement with upward helium flow. (auth)

**27238** (DP-REPORT-628) DESCRIPTION OF THE COMPUTER CODE FIPDIG. Dragon Project. Preinreich, G. (UKAEA Reactor Group, Winfrith. Atomic Energy Establishment). Feb 1969. 49p. Dep. NTIS (US Sales Only) $5.50.

The FIPDIG code is a one-dimensional time-dependent fission product diffusion code. It is written in EGTRAN for the KDF-9 computer. The mathematical model, method of solution, and modes of application are described. An input listing is appended. (JMR)

**27239** (DP-Report-739) XEBASS-2: EQUILIBRIUM FUEL CYCLE PROGRAMME FOR CONTINUOUSLY ON-LOAD REFUELLED HIGH TEMPERATURE REACTORS. Dragon Project Report. Pedersen, J.; Schoeber, H. R. (UKAEA Reactor Group, Winfrith. Atomic Energy Establishment). Dec 1970. 26p. Dep. NTIS (US Sales Only) $4.50.

Code in FORTRAN IV is provided to calculate equilibrium HTGR fuel cycles with any desired degree of xenon override and for parameters which are of immediate interest to the designer using a zero-dimensional reactor model and allowing for a variety of recycling schemes both for U-238 and TH-232. The spectrum calculations are performed in 43 energy groups. The burn-up is calculated in one condensed group. (auth)

**27240** (DP-Report-741) CORE CORROSION FOLLOWING A LARGE WATER INLEAKAGE INTO THE DRAGON PRIMARY CIRCUIT. Dragon Project Report. Forsyth, N.; Gray, P. S. (UKAEA Reactor Group, Winfrith. Atomic Energy Establishment). Dec 1970. 13p. Dep. NTIS (US Sales Only) $4.00.

The study of fuel element corrosion by water emanating from leaking boilers is of primary importance in considerations of commercial high temperature gas cooled reactor design. A large body of basic data has been assembled and computer codes developed for evaluating the corrosion process within a reactor at power. Should a large leak develop, the reactor would be shutdown. It would then be necessary to remove as much of the water as possible from the primary circuit coolant and core components in the shutdown state to reduce the loss of graphite on start-up to a minimum. Some basic work has been carried out on the degassing of graphite and this was related to the dewatering of the Dragon Reactor core following construction. However in November 1969 a primary heat exchanger began to leak during shutdown releasing several kilograms of secondary coolant, i.e., approximately 1.6% aqueous lithium sulphate solution into the reactor. This resulted in very high concentrations of water vapor in the helium coolant. This incident simulated quite closely the ingress of large amounts of water into a power reactor core. It was possible to estimate the amount of water (7.8 kg) that leaked in, by the lithium sulphate recovered (which was all deposited close to the site of the leak) and to balance this against the quantity of water removed by the purification plant prior to start-up (98 percent) and subsequently as water or oxides of carbon during the degassing phase of the reactor operation. (auth)

**27241** (DP-REPORT-759) BASIC DESIGN OF A MOLECULAR SIEVE PURIFICATION PLANT FOR THE REMOVAL OF WATER VAPOR AND CARBON DIOXIDE AT LOW PARTIAL PRESSURES FROM THE HELIUM COOLANT USED IN A HIGH TEMPERATURE GAS COOLED NUCLEAR REACTOR. Dragon Project. Harper, C.; Mourareau, R. (UKAEA Reactor Group, Winfrith. Atomic Energy Establishment). Jul 1971. 42p. Dep. NTIS (US Sales Only) $5.25.

Molecular sieve beds for use in purifying the helium coolant in HTGR-type reactors are described. The beds were designed for water and carbon dioxide removal. (JWR)

**27242** (DP-Report-762) CREAM-7: ONE-DIMENSIONAL FEW GROUP BURN-UP PROGRAMME WITH SPECTRUM CALCULATIONS. Schober, H. R. (UKAEA Reactor Group, Winfrith. Atomic Energy Establishment). Aug 1971. 56p. Dep. NTIS (US Sales Only) $6.00.

The program CREAM-7 (Combination of RELOAD FEVER and MUPO) was developed from the one-dimensional multi-group code burn-up FEVER-D and the spectrum code MUPO. FEVER-D was developed from the GGA few group burn-up code RELOAD FEVER and the GGA diffusion routine DCALC. CREAM-7 is similar to the MAFIA code which was developed by L. Massimo and J. Schlösser from FEVER and MUPO. It uses a nuclear data tape, the format of which is described in a reference. The code consists of a spectrum part working in 43 energy groups and a diffusion and burn-up part working in up to 7 energy groups. The logic of the diffusion routine DCALC has not been changed and the reader is therefore referred to a reference for details. The philosophy of the control search and burn-up parts follows closely the one of the RELOAD FEVER program, and large parts have been taken from this source with only minor modifications. For the sake of completeness, these parts of the program are described. CREAM-7 may be used for one-dimensional diffusion or burn-up calculations. (auth)

**27243** (DP-Report-766) BUPO: A ONE-DIMENSIONAL NEUTRON TRANSPORT PROGRAMME FOR BURNABLE POISON AND CELL BURNUP CALCULATIONS. Dragon Project Report. Pedersen, J. (UKAEA Reactor Group, Winfrith. Atomic Energy Establishment). Sep 1971. 17p. Dep. NTIS (US Sales Only) $4.00.

BUPO is a fast transport program with built-in burn-up, originally intended for use in calculating burnable poison sticks in a High Temperature Reactor. The program is, however, coded in such a general way that it can be used for the calculation of burn-up in any annular cell of any type of reactor. In the transport part, the program uses collision probability theory, and in the burn-up part, the program can treat the burn-up of up to 60 individual isotopes in each zone of the cell. Concentration dependent self-shielding factors for the burnable poisons may be calculated in broad energy groups for use in overall (1-D, 2-D or 3-D) reactor calculations. (auth)

**27244** (DP-Report-769) STUDIES ON THE BEHAVIOR OF GRAPHITE STRUCTURES IRRADIATED IN THE DRAGON REACTOR. Dragon Project Report. Everett, M. R.; Graham, L. W.; Ridealgh, F. (UKAEA Reactor Group, Winfrith. Atomic Energy Establishment). Nov 1971. 28p. Dep. NTIS (US Sales Only) $4.50.

Design data for the physical and mechanical property changes which occur in graphite structural and fuel body components irradiated in an HTR are largely obtained from small specimens tested in the laboratory and in materials test reactors. A brief data summary is given. This graphite physics data can be used to predict dimensional changes, internal stress generation and strength changes in the graphite materials of HTR fuel elements irradiated in the Dragon Reactor. The results which have been obtained from post-irradiation examination of a number of fuel pins are compared with predicted values. (auth)

**27245** (DP-Report-773) STEREOSCAN EXAMINATION OF COATINGS FROM DRAGON IRRADIATED FUEL PARTICLES. Wadley, H. N. G.; Bainbridge, J. E.; Rose, K. S. B. (UKAEA Reactor Group, Winfrith. Atomic Energy Establishment). Aug 1972. 25p. Dep. NTIS (US Sales Only) $4.25.

Coated particle fuels were selected from a number of irradiations so that the effects of a wide range of burnup, fast neutron dose, and temperature conditions on their coating materials could be studied. The temperatures were in the range 600–1500°C, and the burnups and DNE fast neutron doses up to 12.3% and $4.9 \times 10^{21}$ n $cm^{-2}$. The unirradiated buffer layer consisted of two regions, only the outer of which was porous. The inner region, adjacent to the kernel, appeared to have a high density and a vitreous appearance; its thickness varied between 2–8 μm. Fission fragment bombardment caused pitting and cracking of the inner vitreous buffer layer surface and in most cases increased the thickness of the inner region. Fast neutron bombardment does not cause any observable damage to either the pyrocarbon or the silicon carbide coating layers – no significant clusters of porosity or incipient cracks were seen. The pyrocarbon platelets tended to align themselves parallel to the substrate in all pyrocarbons irradiated to high fast neutron doses at temperatures above 600°C. 7 references. (auth)

**27246** (DP-REPORT-774) CARBON DIOXIDE ADSORPTION ON FIXED BEDS OF MOLECULAR SIEVES. Dragon Project. Barrett, D. J.; Capp, P. D.; Carter, J. W.; Husain, H. (UKAEA Reactor Group, Winfrith. Atomic Energy Establishment). Dec 1971. 86p. Dep. NTIS (US Sales Only) $7.50.

Two 6 ft deep × 2 in diameter adsorber beds were used to measure breakthrough curves of carbon dioxide in flows of dry helium (and nitrogen) at 25°C (and 35°C) at 1.25 atmospheres absolute through molecular sieve adsorbents. Regeneration was done at 310–350°C with heated, evaporated liquid nitrogen passing through in the reverse direction to adsorption. During adsorption the temperature was controlled by a water coil wound on each column. The inlet carbon dioxide partial pressure was approximately 0.37 mm Hg maximum. Lower values were also used to obtain

isotherm data. Concentration/time profiles at 1 ft. bed intervals (and less) enabled mass transfer (MTZ) zone data to be obtained. Bed velocities of 8-50 fpm were used. The MTZ lengths (u = 0.5 to 0.85) increased with bed length position in all cases and were least at the lowest velocities (expansion = 0.03 to 0.06 ft./ft.). The equilibrium capacity and isotherm shape of the 4A sieve was better than the 5A. Prediction of breakthrough curves to better than ±7% accuracy was possible using computer programme ISOBED 2 and the isotherm data. A simple graphical method enabled the calculated curves to be extrapolated to larger bed lengths, thus saving computing time. Rate, and equilibrium data, should be determined under the actual conditions of operation since their calculation cannot be relied on. Accurate isotherm shape, particularly at low partial pressures, is also important. More than one combination of diffusion coefficient ($D_{pe}$) and isotherm shape (R) was found to give substantially the same outlet prediction. ISOBED 2 was also used to study the breakthrough curves on carbon dioxide adsorption by Linde 4A sieve from helium at 40 atm at 15°C. This and the 1,25 atm $N_2$ and He work suggest that the rate controlling mechanism is inter-crystallite diffusion in the granular macro-pores. The MTZ expansion rate at 40 atm (0.19 ft./ft.) is greater than the equivalent velocity experiment at 1.25 atm, presumably due to the lower values of $D_{pe}$ at high pressure. The length of the bed required for development of a stable MTZ can be calculated approximately from Rosen's asymptotic solution. This length is decreased by the use of lower bed velocities but is increased by high pressure operation because of decreased inter-granular (inter-crystallite) $CO_2$ pore diffusion coefficients. (auth)

**27247** (DP-REPORT-778) DRAGON OPERATIONS BRANCH TWENTY-SECOND QUARTERLY PROGRESS REPORT, SEPTEMBER 1970–NOVEMBER 1970. Dragon Project. Capp, P. D. (UKAEA Reactor Group, Winfrith. Atomic Energy Establishment). Jan 1972. 23p. Dep. NTIS (US Sales Only) $4.25.

**27248** (DP-REPORT-779) DRAGON OPERATIONS BRANCH TWENTY-THIRD QUARTERLY PROGRESS REPORT, DECEMBER 1970–MARCH 1971. Dragon Project. Mason, I. K. (UKAEA Reactor Group, Winfrith. Atomic Energy Establishment). Feb 1972. 35p. Dep. NTIS (US Sales Only) $4.75.

**27249** (DP-REPORT-783) HTR SYSTEM AND THE CHANGING MARKET FOR ENRICHED URANIUM. Dragon Project. Hansen, U. (UKAEA Reactor Group, Winfrith. Atomic Energy Establishment). Mar 1972. 19p. Dep. NTIS (US Sales Only) $4.00.

Separation costs and tail enrichment have undergone major changes during the last year. The uranium ore price is expected to rise significantly during the next two decades, coinciding with the introduction and operation of HTR power plants. The more expensive separation work has increased the fuel cycle costs by approximately 0.1 mills/kWh(e) and the higher tail enrichment has raised the demand of natural uranium by 20-25%. The expected economic scene in the future seems to favour Th-U-235 and Th-Pu as alternative fuel cycles to the low enriched uranium system. (auth)

**27250** (DP-REPORT-784) DESIGNER'S APPROACH TO THE CONSERVATION OF HELIUM IN HIGH TEMPERATURE POWER REACTORS. Dragon Project. Lockett, G. E.; Hosegood, S. B.; Harper, C. (UKAEA Reactor Group, Winfrith. Atomic Energy Establishment). Mar 1972. 31p. Dep. NTIS (US Sales Only) $4.75.

Helium losses from an HTR must be kept within the limits set by economic, safety and technical criteria. A brief examination shows that designers should have little difficulty in providing for considerably higher standards of helium conservation than any currently required. Assessment of the losses to be expected in a 630 MW(e) HTR, leads to the conclusion that the dominant ones will be those occurring during major maintenance work, due to accidents, maloperation or occasional large temporary leaks. Normal leakage should be a negligible proportion of the total. Since such major non-routine losses must be of infrequent occurrences, if a satisfactory station availability is to be achieved, it is concluded that average annual helium wastage will be correspondingly low. As a result of this, a tenfold increase in the price of helium, such as might occur if underground reserves became exhausted after the end of the current century, should not penalize the economics of the HTR significantly. (auth)

**27251** (DP-Report-786) GRAPHITE FUEL ELEMENT SLEEVES FOR HIGH TEMPERATURE GAS COOLED REACTORS. Dragon Project Report. Head, J. L.; Kinkead, A. N. (UKAEA Reactor Group, Winfrith. Atomic Energy Establishment). Mar 1972. 19p. (CONF-720339-2). Dep. NTIS (US Sales Only) $4.00.

From conference on graphite structures for nuclear reactors; London, UK (7 Mar 1972).

Methods used for the structural analysis of fuel sleeves for High Temperature Gas Cooled Reactors are described. Representative results are given from analyses of several types of fuel sleeve. (auth)

**27252** (DP-Report-787) TECHNIQUES USED IN THE DRAGON PROJECT TO MEASURE THE FISSION PRODUCT RELEASE PERFORMANCE OF HIGH TEMPERATURE REACTOR FUEL. Dragon Project Report. York, J.; Good, P. D.; Hick, H.; Nabielek, H.; Neubauer, J.; Ohman, H. (UKAEA Reactor Group, Winfrith. Atomic Energy Establishment). Mar 1972. 48p. Dep. NTIS (US Sales Only) $5.50.

High temperature gas-cooled reactor fuel elements have no hermetic metal cans surrounding the fissile material to prevent fission products escaping into the primary coolant. Instead, the fissile material is divided into microspheres which are coated with pyrocarbon and silicon carbide to prevent the release of fission products. In any development program on such fuel its fission product retention performance is of paramount importance, and for this reason a variety of techniques have been developed and are used during post-irradiation examination of fuel elements which have been irradiated in the Dragon Reactor. The techniques are described for assaying the release of: Gamma-ray emitting solid fission products using high resolution gamma-spectrometry, beta emitting fission products by autoradiography and beta-counting, and fission gas release by annealing. (auth)

**27253** (DP-Report-792) REACTIVITY CALIBRATION OF CONTROL RODS. Dragon Project Report. Hunt, C.; Stillwell, J. C. (UKAEA Reactor Group, Winfrith. Atomic Energy Establishment). Apr 1972. 22p. Dep. NTIS (US Sales Only) $4.25.

The excess multiplication or reactivity of the DRAGON Reactor is determined from the critical rod configuration and from a reactivity calibration of a small section of a rod. To interpret the results it is necessary to know the shape characteristic of the rod worth as a function of axial position. The methods used for this purpose are outlined and the computer programme CONROD used to analyse the measurements and present the results both graphically and in tabular form for application by the reactor operators is described. (auth)

**27254** (DP-Report-798) BEHAVIOR OF SMALL LEAKS IN MILD STEEL BOILER TUBES WHEN SUBJECT TO WATER AT 2,500 PSIG AND 350°C. Dragon Project Report. Harper, C.; Coe, I. M.; Stringer, A. L. F. (UKAEA Reactor Group, Winfrith. Atomic Energy Establishment). Jul 1972. 40p. Dep. NTIS (US Sales Only) $5.00.

In the Dragon Reactor there is a small excess pressure of helium in the primary coolant circuit which passes over the secondary water/steam circuit tubes and leaks are indicated by the presence of helium in the water circuit. In a power HTGCR the water/steam circuit will be at a considerably higher pressure than the helium primary circuit coolant, and a tube failure or a small crack or pin hole penetrating the tube wall will result in a leak with water passing into the helium, possibly in significant quantities. With conventional boiler and heat exchanger installations small amounts of water inleakage from the high pressure to the low pressure sides of the equipment is accepted as more or less inevitable, although considerable efforts are made on the part of the manufacturers to keep this water ingress to the lowest practical level. In a power HTGCR the magnitude of this water inleakage and its rate of increase or decrease will be of considerable importance both with regard to the amount of graphite corrosion within the core and to the design of the helium purification plants. In tests of boiler tube leaks, water leaks less than $10^{-1}$ g/min have sealed themselves while water leaks greater than 10 g/min have increased in size. It should be noted that these results are for only one boiler tube material, one tube wall thickness, and one water treatment procedure. Another important factor is that all the tubes tested to date have only been subjected to steam/water at pressures up to 2,500 psig and temperatures up to about 350°C. Leaks of almost dry steam or superheated steam may react in a different manner. It should also be noted that the leaks studied were subjected to stresses due to pressure effects only. (auth)

**27255** (DP-REPORT-805) DIFFUSION OF STRONTIUM AND CAESIUM IN PYROLYTIC SILICON CARBIDE. Dragon Project. Chinaglia, B.; Corte, T.; Costanzo, G.; Mosca, G.; Novario, P. (UKAEA Reactor Group, Winfrith. Atomic Energy Establishment). Jul 1972. 82p. Dep. NTIS (US Sales Only) $7.25.

The diffusion of strontium and cesium through the pyrolytic polycrystalline silicon carbide layer on a fuel particle is shown to be highly dependent upon the deposition conditions. Techniques are described for establishing and measuring concentration pro-

files in the layers and a mathematical model is evolved to explain the results, which are not in accord with simple diffusion theory. Partition, evaporation and diffusion coefficients are deduced and the model transferred to a computer programme for calculation of the release from a triplex particle. For silicon carbide formed under optimum conditions the diffusion coefficient at 1400°C for cesium is found to be less than $10^{-15}$-$10^{-16}$ cm $s^{-1}$, and for strontium at 1400°C, less than $10^{-12}$-$10^{-13}$ cm $s^{-1}$. As the layers depart from the optimum structure the diffusion coefficients increase by up to five orders of magnitude. The silicon carbide layers deposited under optimum conditions on graphite discs simultaneously fluidised with the particles are greatly inferior to those on the particles. (auth)

**27256** (DP-Report-809) TWO PHASE DIFFUSION MODEL. Dragon Project Report. Walther, H.; Novario, P. G. (UKAEA Reactor Group, Winfrith, Atomic Energy Establishment). Sep 1972. 49p. Dep. NTIS (US Sales Only) $5.50.

A two phase diffusion model has been developed, whose formulation is described. This model is suitable for describing fission product transport along grain boundaries with transition into or from the grains, as well as transport in a matrix with trapping. The formulation is compared with the conventional one phase formulation and it is shown that it can explain anomalies in concentration profiles which cannot be explained conventionally. A computer programme in FORTRAN IV, based on a finite difference formulation of the model, is outlined schematically. Examples are given, where the results from the finite difference procedure are compared with an analytical solution. Further examples concern concentration profiles of fission products according to a pure grain boundary transport process during irradiation and during post-irradiation annealing. It is shown, that an increase of the grain boundary volume near a coating boundary can produce a concentration gradient in the direction of the mass transport. (auth)

**27257** (DP-Report-811) KPD PRESENT WORTH FUEL CYCLE CALCULATION METHODS AND CODES. Dragon Project Report. Hansen, U. (UKAEA Reactor Group, Winfrith, Atomic Energy Establishment). Sep 1972. 42p. Dep. NTIS (US Sales Only) $5.25.

The methods used for fuel cycle evaluations are described. The calculations are based on present worth theory and all relevant equations are given to enable a detailed comparison with other codes in use. For each operational period all expenditures and revenues are calculated and discounted to the beginning of the period yielding the fuel cycle costs for that particular period. The method gives time dependent costs starting with the initial core and ending with the equilibrium phase. Each fuel charge handled in the in-pile and out-of-pile fuel management is treated separately. Cost calculations for a typical Dragon Power Reactor Design are included to show some of the features characterising running-in and equilibrium operating conditions. (auth)

**27258** (GA-A-13229) FINAL TASK REPORT ON FORT ST. VRAIN TEMPERATURE SCANNER SYSTEM. Duffy, R. W. (General Atomic Co., San Diego, Calif. (USA)). 16 Dec 1974. Contract AT(04-3)-633. 223p. Dep. NTIS $7.60.

A Fort St. Vrain temperature scanner system was designed. Its primary use is to display in graphic format the thermal distribution of the helium, the feedwater, and the steam temperatures on the 12 steam generators during rise-to-power testing at the Fort St. Vrain High-Temperature Gas-Cooled Reactor. The graphic information allows an operator to immediately access hot spots, thermal imbalance, and any thermal information that indicates impending trouble. The system, including the software written for it, is described. (auth)

**27259** (GA-A-13444) HTGR FUELS AND CORE DEVELOPMENT PROGRAM. Quarterly Progress Report for the Period Ending May 31, 1975. (General Atomic Co., San Diego, Calif. (USA)). 30 Jun 1975. Contract AT(04-3)-167. 262p. Dep. NTIS $7.60.

The work reported includes studies of reactions between core materials and coolant impurities, basic fission product transport mechanisms, core graphite development and testing, the development and testing of recyclable fuel systems, and physics and fuel management studies. Materials studies include irradiation capsule tests of both fuel and graphite. Experimental procedures and results are discussed and, where appropriate, the data are presented in tables, graphs, and photographs. (auth)

**27260** (SM-200/85) OVERVIEW OF GAS-COOLED REACTOR SYSTEMS, THEIR IMPORTANCE AND THEIR INTERACTIONS. Kasten, P. R.; Spiewak, I.; Tobias, M. L. (Oak Ridge National Lab., Tenn. (USA)). 1975. 32p. (CONF-751007-3). Dep. NTIS $4.75.

From IAEA international meeting on gas-cooled reactors; Julich, F. R. Germany (13 Oct 1975).

The economic interactions between fueling, separative work, and capital requirements are illustrated for HTGR, GCFR, HTGR-GT, VHTR, LWRs and LMFBRs. The influence of finite low-cost uranium resources and of extensive LWR application within the next two decades on reactor use is also discussed. Technological developments required for the practical application of HTGRs, GCFRs, HTGR-GT and VHTRs are presented, along with the importance and environmental effects features of these applications. The technical advantages and disadvantages associated with use of the uranium and the thorium fuel cycles in HTGRs are given, including the implications a given fuel cycle has on fuel recycle and mined-fuel requirements. The influence of core design on HTGR fuel and coolant temperatures and on associated performance features are illustrated by considering prismatic and pebble-bed type cores. Finally, several scenarios relative to the development of the HTGR, GCFR, HTGR-GT and VHTR are presented. (auth)

**27261** INTEGRAL-FUEL BLOCKS. Cunningham, C.; Simpkin, S. D. (to British Nuclear Design of Construction Ltd.). US Patent 3,888,735. 10 Jun 1975. Priority date 30 Jun 1972, United Kingdom of Great Britain and Northern Ireland. 4p.

A prismatic moderator block is described which has fuel-containing channels and coolant channels disposed parallel to each other and to edge faces of the block. The coolant channels are arranged in rows on an equilateral triangular lattice pattern and the fuel-containing channels are disposed in a regular lattice pattern with one fuel-containing channel between and equidistant from each of the coolant channels in each group of three mutually adjacent coolant channels. The edge faces of the block are parallel to the rows of coolant channels and the channels nearest to each edge face are disposed in two rows parallel thereto, with one of the rows containing only coolant channels and the other row containing only fuel-containing channels. (Official Gazette)

## Power Reactors, Non-Breeding, Otherwise Moderated

*Refer also to abstract 27430.*

**27262** (AECL-5119) IRRADIATION OF $UO_2$-ZIRCALOY FUEL ELEMENTS WITH FREE-STANDING CLADDING AND LARGE DIAMETRAL CLEARANCES. MacDonald, R. D.; Card, D. C. (Atomic Energy of Canada Ltd., Chalk River, Ontario. Chalk River Nuclear Labs.). Apr 1975. 50p. Dep. NTIS (US Sales Only) $5.50. AECL $1.50.

Fuel elements fabricated from free-standing cladding with large diametral clearances between fuel and sheath may experience less sheath strain during irradiation than elements with collapsible cladding and small clearances. The irradiation behaviour of free-standing fuel elements was studied with $UO_2$ fuelled elements with 0.69 mm thick Zircaloy-4 sheaths and diametral clearances of 0.10, 0.20 and 0.28 mm. The elements were irradiated in pressurized water coolant to a peak burnup of 151 MWh/kg U at linear heat outputs between 43 and 86 kW/m. Although overall sheath expansions were reduced by the large clearances, fuel relocation in the sheath-pellet gap produced high localized strains in the cladding. Gap heat transfer coefficients for the high-clearance elements varied from 6.6 to 7.0 kW/$m^2$K at a linear output of 86 kW/m and were sufficiently low to cause central melting of the fuel at this power output. 21 references. (auth)

**27263** (CONF-701074-P2, pp 270-291) DEVELOPMENT OF ROD-TYPE FUEL ELEMENT TECHNOLOGY BASED ON URANIUM METAL, USED IN CONSTRUCTION OF THE CRITICAL ASSEMBLY OF REACTOR A-2. Vatzlavik, E.; Kain, S. 1970. Translated from Trudy Nauchno-Tekhnicheskoi Konferentsii "Atomnaya Energetika, Toplivnye Tsikly, Radiatsionnoe Materialovedenie", Ul'yanovsk, 5-10 Oktyabrya 1970 G. Vol. II.

From conference on atomic power, fuel cycles, and radiation study of materials; Ul'yanovsk, USSR (5 Oct 1970).

In proceedings of the scientific-technical conference "atomic power, fuel cycles, radiation study of materials".

The various methods of producing low-uranium alloys, type U-Fe-Al-Si and the influence on the uniform distribution of Si are discussed. The technology of extrusion of uranium rods in the upper range of temperature $\alpha$-modification, the flow of uranium during extrusion along with the results of the behavior of dissolved salts, lubricating grease and the effect of surface defects in billets on the defective uranium rods are discussed. (auth)

**27264** (CONF-701074-P2, pp 436-470) DEGREE OF STABILITY OF ROD-TYPE URANIUM HEAT RELEASING ELEMENTS WHEN SUBJECTED TO RADIATION. Ivanov, V. E.; Zelensky,

V. F. 1970. Translated from Trudy Nauchno-Tekhnicheskoi Konferentsii "Atomnaya Energetika, Toplivnye Tsikly, Radiatsionnoe Materialovedenie", Ul'yanovsk, 5–10 Oktyabrya 1970 G. Vol. II.

From conference on atomic power, fuel cycles, and radiation study of materials; Ul'yanovsk, USSR (5 Oct 1970).

In proceedings of the scientific-technical conference "atomic power, fuel cycles, radiation study of materials".

The influence of various factors of radiational growth, swelling, and creeping on the life span of the rod-type uranium fuel element when the latter is exposed to radiation is analyzed. Studies carried out are applicable to working conditions of fuel elements of reactor KC-150. The results obtained on the basis of analysis compare favorably with results obtained experimentally during radiation tests of rod-type fuel elements. Conclusions are drawn regarding the future of this type of fuel element for use in reactors, up to 1.5 to 2 percent burnup. (auth)

**27265** (CONF-701074-P2, pp 488-522) ANALYSIS OF THE ROD-TYPE FUEL ELEMENTS OF REACTOR KC-150. Golovchenko, U. M.; Vorobev, M. A.; Bishkov, B. A.; Davidenko, A. C.; Votinova, V. V.; Deripasko, V. T.; Zagorodnii, A. Ya.; Sich, A. P. 1970. Translated from Trudy Nauchno-Tekhnicheskoi Konferentsii "Atomnaya Energetika, Toplivnye Tsikly, Radiatsionnoe Materialovedenie", Ul'yanovsk, 5–10 Oktyabrya 1970 G. Vol. II.

From conference on atomic power, fuel cycles, and radiation study of materials; Ul'yanovsk, USSR (5 Oct 1970).

In proceedings of the scientific-technical conference "atomic power, fuel cycles, radiation study of materials".

The results of radiation tests and post-reactor analysis of full-sized heavy water fuel elements of the gas cooled reactor KC-150 are analyzed. The results of complex analysis of rod-type fuel element assemblies with magnesium-beryllium coating spacers of zirconium alloy Tz2M, used in reactor KC-150 are described. The analysis of the data obtained and conclusions drawn about the correct selection of the construction materials for heat releasing elements and fuel elements in particular are discussed. The technology, the construction and the heat treatment of these elements, as well as, the effectiveness of these fuel elements in conditions of reactor KC-150 are discussed. (auth)

**27266** SOME ASPECTS OF CHEMICAL AND RADIOCHEMICAL ANALYSIS FOR THE CANDU REACTOR SYSTEM. Guest, A. Ont. Hydro Res. Q.; 26: No. 3, 19-24 (1974).

To monitor corrosion product formation in the heat transport system, samples of particulates and heavy water are analysed to determine the radioisotopes present and the elemental composition of corrosion products. The sources of active isotopes and apparatus for quantitative measurement of radioisotopes are discussed. (auth)

**27267** CORROSION AND RADIOACTIVITY DEPOSITION ON METAL COUPONS EXPOSED IN A REACTOR SYSTEM. Vekris, S. L. Ont. Hydro Res. Q.; 26: No. 3, 12-17 (1974).

Knowledge of the condition of the internal surfaces of the heat transport system within a nuclear reactor is important both as a check of the physical integrity of the system and for gaining insight into activity transport. Because of the difficulties associated with examining actual surfaces, a set of coupons of various metals mounted on rigid stainless holders was designed. These holders are in bypass lines of the heat transport system which can be isolated. The design was made by Hydro's Central Nuclear Services and was based on similar systems used by Atomic Energy of Canada Limited. (auth)

**27268** SOURCE AND NATURE OF RADIOACTIVITY IN NUCLEAR REACTOR SYSTEMS. Neil, B. C. J. Ont. Hydro Res. Q.; 26: No. 3, 3-11 (1974).

Minimization of radiation exposure to operators and maintenance staff of nuclear power generating stations is important for both economic and health reasons. Research is being carried out to identify the sources and nature of radiation fields in Ontario Hydro's CANDU reactors, the manner in which radioactive materials move within reactor systems, and the influence of reactor operating conditions on radiation fields. (auth)

**27269** AUTORADIOGRAPHY AND SCANNING ELECTRON MICROSCOPY OF HEAT TRANSPORT PARTICULATES. Vekris, S. L. Ont. Hydro Res. Q.; 26: No. 3, 25-29 (1974).

Autoradiography was used to locate the positions of radioactive sources on filters containing heat transport particles. Size distributions and radioactivities of particles from the four units of Pickering GS were compared, and selected particles were examined and analysed in a scanning electron microscope. Considerable inhomogeneity in the samples is evident. (auth)

**27270** SUMMER DISTRIBUTION OF THE NEARSHORE FISH COMMUNITY NEAR A THERMAL GENERATING STATION AS DETERMINED BY ACOUSTIC CENSUS. Kelso, J. R. M.; Minns, C. K. (Canada Center for Inland Waters, Burlington, Ont.). J. Fish. Res. Board Can.; 32: No. 8, 1409-1418(Aug 1975).

The relation between thermal plumes and fish abundance and distribution was studied at the Pickering Nuclear Generating Station, Lake Ontario, using simultaneous digital echo counting and temperature monitoring systems during summer thermal stratification of the lake. Fish relative abundance varied from 20.8/10,000 $m^3$ to 1,037/10,000 $m^3$ and both these extreme density estimates occurred in the 7.5-12.5-m depth shell. Also, changes in distribution of the nearshore community were apparent during the July-October study period. The fish community in July was pelagic and selected 10-11 C and 14-16 C. That same community later appeared to become segregated into benthic and pelagic communities. Thermal plumes, either well defined or diffuse, appeared to have little effect on the pelagic community either because fish were not available to elevated temperatures by habitat selection or because fish failed to respond to increased surface temperatures. (auth)

## Power Reactors, Breeding

*Refer also to abstracts 25991, 27260, 27377, 27378, 27383, 27405, and 27407.*

**27271** (CONF-701074-P2, pp 1[illegible]8-218) CERTAIN QUESTIONS ON THE DEVELOPMENT OF FAST REACTOR FUEL ELEMENTS. Golovnin, I. S.; Bibilashvili, U. K.; Menshikova, T. S.; Medvedev, A. V.; Kalashnik, G. V. 1970. Translated from Trudy Nauchno-Tekhnicheskoi Konferentsii "Atomnaya Energetika, Toplivnye Tsikly, Radiatsionnoe Materialovedenie", Ul'yanovsk, 5–10 Oktyabrya 1970 G. Vol. II.

From conference on atomic power, fuel cycles, and radiation study of materials; Ul'yanovsk, USSR (5 Oct 1970).

In proceedings of the scientific-technical conference "atomic power, fuel cycles, radiation study of materials".

Results of work carried out during the development of fuel elements for fast power reactors are given. The examples given for reactors BOR-60 and BN-350 show the approach to selecting the effective density of fuel and density of baked core tablets. The methods of estimating the temperature system for the working of the core are described, taking into consideration the change in its geometry in the process of fuel element operation. A comparison of fuel elements filled with oxide and carbide fuels is given. Recommendations are made for selection of the optimum core diameter with carbide fuel elements. (auth)

**27272** (CONF-701074-P2, 381-414) RESULTS OF ANALYSIS OF USED HEAT RELEASING ELEMENTS OF OPERATING PACKAGES OF REACTOR BR-5 WITH MONOCARBIDE URANIUM FUEL. Ladkin, A. Ya.; Likhachev, U. I.; Alexandrov, U. I. 1970. Translated from Trudy Nauchno-Tekhnicheskoi Konferentsii "Atomnaya Energetika, Toplivnye Tsikly, Radiatsionnoe Materialovedenie", Ul'yanovsk, 5–10 Oktyabrya 1970 G. Vol. II.

From conference on atomic power, fuel cycles, and radiation study of materials; Ul'yanovsk, USSR (5 Oct 1970).

In proceedings of the scientific-technical conference "atomic power, fuel cycles, radiation study of materials".

Post-irradiation determinations of fuel swelling and fission gas production are described together with mechanical tests of fuel can materials. (DG)

**27273** (CONF-701074-P2, pp 415-435) ANALYSIS OF PERSPECTIVE FUEL COMPOSITION BASED ON CARBIDES, URANIUM AND PLUTONIUM NITRIDES FOR FAST REACTORS. Golonin, I. S.; Menshikova, T. S.; Geshetnikov, G. G. 1970. Translated from Trudy Nauchno-Tekhnicheskoi Konferentsii "Atomnaya Energetika, Toplivnye Tsikly, Radiatsionnoe Materialovedenie", Ul'yanovsk, 5–10 Oktyabrya 1970 G. Vol. II.

From conference on atomic power, fuel cycles, and radiation study of materials; Ul'yanovsk, USSR (5 Oct 1970).

In proceedings of the scientific-technical conference "atomic power, fuel cycles, radiation study of materials".

Methods of obtaining stoichiometric composition of uranium nitride by direct synthesis and of uranium and plutonium carbides by carbonization of dioxide and gaseous carbonization of metals are discussed, as well as methods of preparing fuel element cores from the above compounds. The results of compatibility studies of fuel composition with clearances filled with sodium and helium are given. (auth)

**27274** (CONF-701074-P2, pp 471-487) ANALYSIS OF THE INTERACTION OF SODIUM WITH WATER. Kulpin, B. V.; Masanov, A. S.; Petukhov, P. V. 1970. Translated from Trudy Nauchno-Tekhnicheskoi Konferentsii "Atomnaya Energetika, Toplivnye Tsikly, Radiatsionnoe Materialovedenie", Ul'yanovsk, 5–10 Oktyabrya 1970 G. Vol. II.

From conference on atomic power, fuel cycles, and radiation study of materials; Ul'yanovsk, USSR (5 Oct 1970).

In proceedings of the scientific-technical conference "atomic power, fuel cycles, radiation study of materials".

A study is described of the fracture speeds of austenic steel 1818N9T in the region where sodium comes in contact with water and water exchange is slow. The results of measurements of the target loss of weight of steel in the region of interaction are discussed, and curves are illustrated giving the target burning-through time at sodium temperatures of 350 to 600°C and various distances to the place of leakage. Results of the analysis of temperature target field, which are within the range of reaction, and the results of the relationship between the burn-through time and the target thickness are given. (auth)

**27275** (CONF-750478-1) CRBR REACTOR STRUCTURES DESIGN. BRC Meeting Presentation. Pennell, W. E. (Westinghouse Electric Corp., Madison, Pa. (USA). Advanced Reactors Div.). 16 Apr 1975. 48p. Dep. NTIS $5.50.

From proceedings of the Breeder Reactor Corporation; Los Angeles, California, USA (15 Apr 1975).

Some of the more important developments in LMFBR structures design technology are described and the application of the technology to design of the CRBR reactor components is illustrated. The LMFBR is both a high-temperature and a high-DELTAT machine. Both characteristics affect the structural design of the components. High-temperature operation (up to 1100°F) requires that the designer consider the effects of thermal creep as a deformation mechanism and stress rupture as a failure mode. The large DELTAT across the core coupled with a low core thermal inertia and the high conductivity of the sodium coolant combine to produce severe temperature gradients during a reactor scram, particularly in the region immediately above the core. Thermal strains and residual thermal stresses generated within the structure as a result of the scram transient temperature gradients must be evaluated on a cumulative damage basis, with full consideration of the effect of creep/fatigue interaction. Structures designed to operate in this environment must be both light and stiff to minimize transient thermal stresses and prevent unacceptable flow-induced vibrations. Thermal shields may be required to protect the load-bearing structure in regions where the transients are particularly severe, or where core effluent at widely differing temperatures mixes adjacent to structural components. At CRBR core-component goal fluence levels, the predicted magnitude of core-component dimensional changes due to irradiation swelling and creep is very large compared with the more familiar dimensional changes associated with thermal expansion and thermal creep. The design of the core components, and in particular the core restraint system, is dominated by the need to accommodate the effects of irradiation swelling, creep and ductility loss considerations. (auth)

**27276** (CONF-750478-3) REACTOR ENCLOSURE. BRC Meeting Presentation. Fisch, J. W. (Westinghouse Electric Corp., Madison, Pa. (USA). Advanced Reactors Div.). 16 Apr 1975. 28p. Dep. NTIS $4.50.

From proceedings of the Breeder Reactor Corporation; Los Angeles, California, USA (15 Apr 1975).

The latest status of key components of the Reactor Enclosure System of the Clinch River Breeder Reactor Plant is described. Areas where there have been notable design changes or significant design detail maturity in the six months since the last BRC presentation are highlighted. (auth)

**27277** (CONF-750908-4) STRUCTURAL ANALYSIS TECHNOLOGY FOR HIGH-TEMPERATURE DESIGN. Greenstreet, W. L. (Oak Ridge National Lab., Tenn. (USA)). 1974. 17p. Dep. NTIS $4.00.

From third international conference on structural mechanics in reactor technology; London, UK (1 Sep 1975).

The procedures associated with inelastic analyses for predicting deformation behaviors and the technology currently available and in use by LMFBR design analysts are described. These analyses utilize mechanical behavior information on the materials of construction, constitutive equations to mathematically describe these behaviors, and certified structural analysis methods and tools. (auth)

**27278** (CONF-750911-5) FABRICATION AND INSPECTION DEVELOPMENT FOR CRBRP STEAM GENERATORS. McClung, R. W.; Slaughter, G. M.; Spalaris, C. N.; Lillie, A. F. (Oak Ridge National Lab., Tenn. (USA); General Electric Co., San Jose, Calif. (USA). Breeder Reactor Dept.; Atomics International Div., Canoga Park, Calif. (USA)). Sep 1975. 31p. Dep. NTIS $4.75.

From international conference on materials for nuclear steam generators; Gatlinburg, Tennessee, USA (9 Sep 1975).

One of the critical nonnuclear elements of the CRBRP is the steam generator that transfers the heat from the sodium system to the high-pressure steam system but must maintain integrity and separation of the two fluids. The construction material is 2¼ Cr–1 Mo alloy steel with high-purity (e.g. vacuum arc remelt) material being used for the tubing and tubesheets. For confidence in successful manufacturing of the several evaporator and superheater modules, key development activities are under way (1) for procurement of high-quality components, (2) to assure proper assembly (with emphasis on welding), and (3) to assure that adequate nondestructive testing methods are available to examine the units. (auth)

**27279** (EURFNR-1217) LAYOUT, IRRADIATION, AND POST-IRRADIATION EXAMINATION OF THE SHORT-TIME MIXED CARBIDE IRRADIATION EXPERIMENT LOOP TEST GROUP 4a. Weimar, P.; Fiedler, H. (Kernforschungszentrum Karlsruhe (F.R. Germany). Inst. fuer Material- und Festkoerperforschung). Jul 1974. Translation of KFK-1919. 173p. Dep. NTIS $7.60.

Work performed under United States--Euratom Fast Reactor Exchange Program.

The irradiation was carried out in the helium-loop in the central channel of FR 2. Pins each with an active length of 150 mm were irradiated for 3 or 15 days. The whole series consisted of 8 specimens. The plutonium content was some 15 wt percent (rest natural uranium) and the density of pellets was some 86 percent T.D. The cladding was an austenitic steel (No. 1.4988). The O.D. of cladding was 10.0 mm with a wall thickness of 0.55 mm. Besides the thermocouples on the cladding, the specimen possessed a central thermocouple. The rod power was some 1100 W/cm, the outer cladding temperature 500°C, and the burnup only some 0.2 percent. Three pins melted near the central thermocouple by a peritectic reaction between thermocouples, cladding, and fuel. Results of non-destructive and destructive post irradiation examinations are represented. (auth)

**27280** (GBRA-R-37) 1200 MWe GAS-COOLED BREEDER REACTOR (GBR-4). (Gas Breeder Reactor Association, Brussels (Belgium)). Jul 1973. 4p. INIS.

A brief description is given of the design of a 1200 MW(e) gas-cooled breeder reactor, and main parameters are listed. The reactor, boilers, gas circulators and coolant purification plant are integrated into a prestressed concrete pressure vessel. The He coolant flows upward through the core. Fuel pins are similar to those in the sodium cooled breeder reactor but the steel cladding is roughened to improve heat transfer. Other differences include a marginally higher clad temperature and the use of fission product venting. (UK)

**27281** (HEDL-TME-7584) PROTOTYPE APPLICATIONS LOOP: STATUS OF DEVELOPMENT AND TEST RESULTS. Mettler, G. W.; McCown, J. J. (Hanford Engineering Development Lab., Richland, Wash. (USA)). Aug 1975. Contract AT-(45-1)-2170. 17p. AT.

The Prototype Application Loop (PAL) has now been in service for over three years. The proof testing of FFTF prototype hardware for sodium and cover gas sampling and purity monitoring has been completed. Further evaluations of cold trap and vapor trap performance have been done. The field testing of analytical methods for measuring oxygen, hydrogen and carbon in sodium by metal equilibration techniques has also been completed. The facility has been expanded a second time by the addition of a side loop for the study of Flow Impedance Phenomena (FIP). The PAL/SCS is presently being used to service the needs of the FIP program and to test new on-line meter concepts. Details of the test work performed during the past year are described. (9 references) (auth)

**27282** (KFK-2088) SOME CONSIDERATIONS ON NEUTRON INSTRUMENTATION REQUIREMENTS FOR MALFUNCTION DIAGNOSIS IN POWER REACTORS USING NOISE ANALYSIS TECHNIQUES. Edelmann, M. (Kernforschungszentrum Karlsruhe (F. R. Germany). Inst. fuer Neutronenphysik und Reaktortechnik; Kernforschungszentrum Karlsruhe (F. R. Germany). Projekt Schneller Brueter). Oct 1974. 16p. (AED-CONF-74-492-024). INIS.

From special meeting on reactor noise; From critical assemblies to power reactors; Casaccia, Italy (21 Oct 1974).

9 figs.; 1 tab.; 12 refs. With abstract.

To determine the response of a neutron detector to local perturbations in a typical fast breeder reactor detailed numerical calculations of space-dependent source transfer functions were performed for the German prototype reactor SNR-300. The detector materials B-10, U-235 and Pu-239 were chosen for comparison. The positions of source and detector were independently varied within the core and blanket of the reactor. It was found that in the present class of fast breeder prototype reactors no incore neutron detectors will be needed for a continuous inspection using noise analysis techniques to detect local perturbations. (GE)

**27283** (KFK-2200, pp 193-234) DEVELOPMENT OF THE GAS COOLED FAST BREEDER REACTOR. Dalle Donne, M. Apr 1975.

In contributions to nuclear engineering. Dedicated to Karl Wirtz on the occassion of his 65th birthday. (Kernforschungszentrum Karlsruhe (F. R. Germany)).

A survey of the present technological state is given on the basis of the developments made so far. Some milestones of development—e.g., the German gas breeder memorandum, the Gas Breeder Reactor Association, the results of the BR-2 radiation experiments and of GfK-KWU design and safety studies—are described. The problems connected with a large store of plutonium are also discussed. (GE)

**27284** (UCLA-ENG-7527) LAMINAR NATURAL CONVECTION FROM BLUNT BODIES WITH ARBITRARY SURFACE HEAT FLUX OR SURFACE TEMPERATURE. Harpole, G. M. (California Univ., Los Angeles (USA). School of Engineering and Applied Science). Apr 1975. Contract AT(04-3)-34. 82p. Univ. of California, Los Angeles.

The laminar boundary layer equations for free convection over bodies of arbitrary shape and with arbitrary surface heat flux or surface temperature are solved in local Cartesian coordinates. Both two-dimensional axisymmetric bodies (e.g., horizontal cylinders) and three-dimensional axisymmetric bodies (e.g., spheres) with finite radii of curvature at their stagnation points are considered. A Blasius series expansion is applied to convert from partial to ordinary differential equations. An additional transformation removes the surface shape dependence and the surface heat flux or surface temperature dependence of the equations. A second-order-correct, finite-difference method is used to solve the resulting equations. Tables of results for low Prandtl numbers are presented, from which local Nusselt numbers can be computed. The equations are also solved in cylindrical coordinates for horizontal cylinders. This solution includes curvature terms neglected in using local Cartesian coordinates. Solutions are presented for low Prandtl numbers and a range of Grashof numbers. 33 references. (auth)

**27285** EXPERIMENTAL STUDY OF STEADY-STATE BOILING OF SODIUM FLOWING IN A SINGLE-PIN ANNULAR CHANNEL. Kikuchi, Y.; Haga, K.; Takahashi, T. (Power Reactor and Nuclear Fuel Development Corp., Oarai, Ibaraki (Japan). Oarai Engineering Center). J. Nucl. Sci. Technol. (Tokyo); 12: No. 2, 83-91 (Feb 1975).

An experimental study was carried out on steady-state boiling of sodium flowing in the annular channel formed around an electrically heated simulation of a fuel pin. The inlet temperature and flow rate were held constant, and the heat flux was gradually increased up to the inception of boiling. Thereafter, the heat flux was further increased step by step until the surface temperature of the heater pin marked a sharp rise, indicating the occurrence of dry-out. Records were obtained of the changes brought by the increasing heat flux to boiling phenomena, with particular reference to the behavior of the two-phase flow pattern and to the characteristics of boiling noise, as well as of the frequency of bubble formation. It was made clear that there exists a region in which steady-state boiling will be established, and under these conditions the two-phase flow pattern changes sequentially from bubbly flow to slug flow and then to annular flow. This behavior of sodium boiling in a narrow channel is quite similar to the case of water. With rising heat flux, the level of noise intensity associated with boiling first increased sharply to attain a maximum point, then decreased somewhat and remained constant thereafter until dry-out. The frequency of bubble formation depended on the size of the bubble. The product of bubble frequency and equivalent diameter was found to be constant. (auth)

**27286** EFFICIENCY OF THE REACTIVITY CONTROL ELEMENTS IN A FAST REACTOR AS A FUNCTION OF CERTAIN FACTORS. Shibaev, V. A.; Dubrovin, A. M. Tr. Gor'k. Politekh. Inst.; 29: No. 16, 51-54(1973). (In Russian).

By using precision calculation programs a mathematical model was constructed which describes the efficiency of the shim rods as a function of selected factors and can be used in general nuclear reactor optimization studies. The methods of mathematical theory of planning and the planning of extremal experiments are used. A study was made of finding the efficiency of the rods from the selected factors using a multigroup neutron-physical calculation. A cylindrical nuclear reactor symmetric with respect to the central and the diametral planes with a sodium heat exchange agent and oxide fuel is investigated. It is planned for an atomic electric power plant with an individual unit electric power from 1,000 to 2,000 megawatts. A study was made of the efficiency of the reactivity control rods made of fuel, boron carbide (natural enrichment) and tantalum as a function of four parameters with different arrangement of the rods: in the center of the core, uniformly with respect to the small enrichment zone, uniformly with respect to the entire core, uniformly in the layer at the boundary of the small and large enrichment zones. The results obtained can be recommended for estimating the efficiency of the shim rod system in a large fast reactor. (auth)

**27287** EFFICIENCY OF THE SHIM ROD SYSTEM OF A FAST POWER REACTOR CONSIDERING INTERFERENCE. Samoylov, O. B.; Evse'ev, V. I. Tr. Gor'k. Politekh. Inst.; 29: No. 16, 45-50(1973). (In Russian).

It is proposed that a somewhat varied small-group diffusion method be used to calculate the efficiency of the rods in the control and safety rod system and the heat release fields used ordinarily when calculating the thermal nuclear reactor. The calculation is performed in a two-group approximation with statement of the effective boundary conditions on the surface of the rods. For simplification the following assumptions are made which are usually used in practice: the rods are sufficiently removed from the core boundary; the spacing between them is much greater than the rod radius. The procedure was checked by comparing the calculated and experimental results obtained when investigating the efficiency of boron rods in the BFS-17 critical assembly simulating the BN-350 core. Ten versions were assembled and investigated. These versions differed by the number and the location of the boron rods. The diameters of the assemblies were 123.3–156 cm and the height was 106 cm. The measurements demonstrated that for close arrangement of the rods, just as in the BN-350, there is quite strong interference expressed in a decrease in efficiency of the rods by 20-30 percent. Satisfactory agreement (within the limits of 10 percent) was obtained for the calculated and experimental values of the efficiency for both single rods and groups of rods. (auth)

## Research, Test, and Experimental Reactors

*Refer also to abstracts 27367, 27386, 27392, and 27452.*

**27288** (DP-REPORT-780) DRAGON OPERATIONS BRANCH TWENTY FOURTH QUARTERLY PROGRESS REPORT, APRIL 1971–JUNE 1971. Dragon Project. Mason, I. K. (UKAEA Reactor Group, Winfrith. Atomic Energy Establishment). Feb 1972. 30p. Dep. NTIS (US Sales Only) $4.50.

Activities described include reactor operation and maintenance, chemical plant operation and maintenance, core and primary circuit performance, chemistry and fission product studies, and unusual occurrences. (JWR)

**27289** (DP-REPORT-799) TRITIUM PRODUCTION AND DISTRIBUTION IN HIGH TEMPERATURE GAS COOLED REACTORS. Part I. Tritium Production, Migration and Removal in the Dragon Reactor Between Core 5 Charge III and Core 1 Charge IV. Dragon Project. Forsyth, N. (UKAEA Reactor Group, Winfrith. Atomic Energy Establishment). Jun 1972. 55p. Dep. NTIS (US Sales Only) $5.75.

A detailed study on tritium production, migration, and removal in the Dragon Reactor is presented. (JWR)

**27290** (DP-REPORT-801) DRAGON OPERATIONS BRANCH TWENTY-FIFTH QUARTERLY PROGRESS REPORT, JULY–SEPTEMBER 1971. Dragon Project. Mason, I. K. (UKAEA Reactor Group, Winfrith. Atomic Energy Establishment). Jul 1972. 32p. Dep. NTIS (US Sales Only) $4.75.

Reactor plant operations and maintenance, chemical plant operations and maintenance, core and primary circuit performance, and chemistry and fission product studies are summarized for the period. (JWR)

**27291** (ERDA-tr-60) ACOUSTIC DETECTION OF BUBBLE EMISSION IN THE RAPSODIE REACTOR. Bret, A.; Gaillard, M.; Lechel, V. 1975. Translation of French Report. (CONF-750411-39). 15p. Dep. NTIS $4.00.

From European nuclear conference; Paris, France (21 Apr 1975).

The acoustic detection instrumentation of the RAPSODIE reactor is described and the results of acoustic measurements obtained during the study of the operational parameters are presented. Finally, it is shown how phenomena such as argon entrainments can be detected with a great sensitivity. (auth)

**27292** (HEDL-TME-75-58) FFTF/IVHM LIQUID METAL MAINTENANCE SEAL TEST. Carlson, B. A. (Hanford Engineering Development Lab., Richland, Wash. (USA)). Jul 1975. Contract AT(45-1)-2170. 35p. AT.

The operation and effectiveness of the In-Vessel Handling Machine (IVHM) liquid metal maintenance seal are tested. Operation in the Fast Flux Test Facility (FFTF) of the IVHM mainte-

nance seal is expected for only short periods of time during maintenance on the main IVHM elastomer seals. Successful operation of one complete maintenance seal cycle was demonstrated during the test. This cycle included (1) installation of maintenance seal hardware on the IVHM, (2) annulus heat up and fill with alloy, (3) annulus cool down and check of seal effectiveness, and (4) heat up and drain. (auth)

**27293** (JINR-P13-8711) CORRELATION SPECTROMETRY AT PULSED REACTOR. Vizi, I.; Zsigmond, D.; Zhukov, G. P.; Kroo, H.; Nagy, D.; Pelionisz, P.; Cser, L. (Joint Inst. for Nuclear Research, Dubna (USSR)). 1975. 19p. (In Russian). Dep. NTIS (US Sales Only) $4.00.

It is shown that the correlation technique can be applied to pulsed reactors so that a white ingoing neutron beam can be used and the whole two-dimensional scattering spectrum can be evaluated by data processing of correlation type. The principles of the method and the description of the electronic device are given. Results of a simple test-run at the IBR-30 pulsed reactor are shown. The investigation has been performed at the Neutron Physics Laboratory, JINR. (auth)

**27294** (SAND-74-5861) ANALYSIS OF AN IN-PILE REACTOR TUBE. Von Riesemann, W. A.; Gubbels, M. H. (Sandia Labs., Albuquerque, N. Mex. (USA)). 1974. 18p. (CONF-750933-1). Dep. NTIS $4.00.

From 5th national conference on mechanical vibrations; Washington, District of Columbia, USA (17 Sep 1975).

The results are presented of an analysis of an in-pile pressure tube and its components which are subjected to a severe dynamic overpressure pulse. The in-pile tube is part of a closed loop used in the Power Burst Facility at The National Reactor Testing Station, Idaho. This facility is used to test power reactor fuels. The hardware, loading conditions and modeling techniques are described. A two dimensional dynamic nonlinear finite element computer program HONDO was used in the analysis. 7 references. (auth)

**27295** (WANL-TME-749) ANALYSIS IN SUPPORT OF THE FLEXIBLE CRITICAL EXPERIMENT. Mowery, A. L. (Westinghouse Electric Corp., Pittsburgh, Pa. (USA). Astronuclear Lab.). 15 Apr 1964. 107p. Dep. NTIS $8.50.

Declassified 14 Jul 1975.

The FCX experimental program is designed to provide data with which systematic nuclear investigations may be carried out to verify and improve the standard design methods used for NERVA nuclear calculations. The purpose is to reduce the uncertainty in the prediction of such factors as critical mass, power distribution, reactivity coefficients, radiation heating, and kinetic parameters in NERVA systems. The primary design criterion of FCX is minimization of in-core structural material and impurities so that the cleanest possible critical experiments can be performed. The results of an investigation of the nuclear characteristics, especially static nuclear parameters, of the Flexible Critical Experiment (FCX) are described. The critical radius and mass were determined for a wide range of loadings, void fractions, and reflector types and thicknesses. Control rod worths, reactivity coefficients of important materials, temperature coefficients, and average neutron lifetimes were obtained for arrays spanning the range of FCX configurations. In planning experiments these results are useful both in designing the reactor physical composition and in evaluating the potential hazards. Specification of the fueled and unfueled graphite elements was investigated to ensure sufficiently low experimental uncertainties. An uncertainty analysis derived from the results of the static nuclear calculations is included. A short history of graphite-uranium systems shows the range of earlier studies. The potential extension of this range by the FCX program and its relation to the NERVA program is indicated. (auth)

**27296** (WANL-TME-1442) PROPOSED NR-1 CRITICALS EXPERIMENT PROGRAM. Kovacik, W. P. (Westinghouse Electric Corp., Pittsburgh, Pa. (USA). Astronuclear Lab.). 10 Jun 1966. 26p. Dep. NTIS $4.50.

Declassified 22 Jul 1975.

A program of reactor critical experiments in support of the NR-1 test article has been prepared. This program has been designed to provide the NERVA program with experimental criticals data for nuclear design, shielding analysis, analytical methods development and for the Nevada operations. This criticals program will also provide the basic facility and capability for continuing support throughout the succeeding NR and NE series. The criticals experiments in support of the NR-1 will be performed on two WANEF assemblies—the present Flexible Critical Experiment (FCX) and the NERVA Critical Experiment (NCX), which is presently being designed. The first nuclear mockup of the NR-1 will be assembled and operated in the FCX. Experimental information obtained from the FCX mockup experiments will be used to fix the NR-1 fuel specification, and provide preliminary dosimetry, drum worth, core reactivity, and material worth data. The NCX will have the flexibility and capability to provide final and precise in-reactor criticals data similar to the PAX-NRX tests (orificing and shimming data) as well as external radiation environment data such as shielding, leakage flux, and dosimetry data. These latter data will be obtained using realistic mockups of the reactor configurations to be used at Nevada. The FCX will also be used for basic physics studies for the NR-1 program, including criticality, reactivity worth, and flux and power distribution measurements, on bare and reflected cores using the basic NERVA type fuel module. (auth)

**27297** DYNAMIC OPERATION OF THE UNIVERSITY OF TOKYO REACTOR YAYOI. Tamura, T.; An, S.; Furuhashi, A.; Wakabayashi, H. (Tokyo Univ. (Japan). Nuclear Engineering Research Lab.). J. Fac. Eng., Univ. Tokyo, Ser. B; 32: No. 3, 519-534 (Sep 1974).

University of Tokyo research reactor YAYOI is intended as a dynamic fast source reactor as well as a stationary one like AFSR and HARMONIE. It is equipped with reactivity adding devices with both slow and quick action, and a PNS (pulsed neutron source) operating in conjunction with the reactivity devices. The unique idea of fly-through type reactivity addition lends itself to minimizing background neutrons due to delayed neutrons. Some explanation of the dynamic operation of YAYOI and preliminary experimental and calculational results are presented. (auth)

**27298** EVOLUTION OF GAS FROM STRUCTURAL MATERIALS OF THE HIGH TEMPERATURE HELIUM GAS LOOP. Tone, H.; Yokouchi, K.; Baba, O. (Japan Atomic Energy Research Inst., Ourai, Ibaraki. Oarai Research Establishment). Shitsuryo Bunseki; 22: No. 4, 275-280 (Jan 1975). (In Japanese).

The high temperature helium gas loop, which is used for irradiation tests of the nuclear fuels of the gas cooled reactors, is constructed in JAERI (Japan Atomic Energy Research Institute). Since the maximum temperature of the helium gas coolant in the gas loop is 1000°C, it is necessary that the concentration of impurities present in the helium gas coolant is held less than 10 ppm to prevent the corrosion of structural materials. To obtain the design data of the helium coolant purification system, the outgassing behavior of the structural materials such as graphite and ceramic thermal insulator was measured by mass spectrometer and gas chromatograph. It is found that the outgassing rate from graphite and ceramic thermal insulator can be expressed by the following equation, $s(t) = Ge^{-kt}t^2$. (auth)

**27299** AMERICAN NATIONAL STANDARD REVIEW OF EXPERIMENTS FOR RESEARCH REACTORS. ANS-15.6; ANSI N401-1974. Hinsdale, IL; American Nuclear Society (1975). 5p. $8.50.

Safe and reliable operation of a research reactor includes strict control over the use of experiment facilities, the experiments performed in those facilities, and the persons using those facilities. This standard identifies the major areas that shall be reviewed for each experiment to ensure that it (a) falls within the limits delineated in the Technical Specifications, (b) does not present an unreviewed safety question as defined in 10 CFR Section 50.59, (c) does not constitute a threat to the health and safety of any individual or groups of individuals, and (d) does not constitute a hazard to the reactor facility or other equipment. In addition, this standard recommends a system for classifying experiments to establish levels of review and approval commensurate with the level of risk inherent in the experiment. (auth)

## Production and Materials Testing and Processing Reactors

**27300** (UNI-351) N REACTOR 1974 STEAM GENERATOR OPERATING EXPERIENCE. Kratzer, W. K. (United Nuclear Industries, Inc., Richland, Wash. (USA)). 14 Mar 1975. Contract AT(45-1)-1857. 4p. Dep. NTIS $4.00.

## Propulsion and Package Reactors

*Refer also to abstracts 27295, 27296, 27384, 27385, 27387–27391, 27293, and 27431.*

**27301** (AED-CONF-74-720-000, pp 250-253) AN INTEGRATED NUCLEAR ELECTRO-THERMAL ENGINE CONCEPT FOR GEOSTATIONARY MISSIONS. Bond, A. 1974.

From 3rd European conference on electric propulsion; Hinterzarten, F. R. Germany (14 Oct 1974).

2 figs.; 8 tabs.; 6 refs. With abstract. Available from ZAED.

In proceedings of the 3rd European electric propulsion conference, Hinterzarten, October 14-18, 1974. (Deutsche Gesellschaft fuer Luft- und Raumfahrt e. V., Koeln (F. R. Germany)).

A preliminary design for a nuclear electric "Space Tug" is proposed for use in conjunction with the American Space Shuttle for high energy missions. The vehicle would employ a SNAP 10A/2 or SNAP 8 nuclear reactor derivative for its power supply and slush hydrogen as the working fluid for the electrothermal thrusters. A thermodynamic conversion cycle would be employed for electrical power generation, for which the hydrogen working fluid would perform the duty of the heat sink. The cycle would eliminate the need for heavy waste heat radiators and improve the overall thermal efficiency. The vehicle promises a considerable payload advantage over a chemical recoverable Tug for geostationary missions. (auth)

**27302** (RN-S-0268) FINAL TEST REPORT FOR PHASE I-D (KIWI-TNT) OF THE COUNTERMEASURES RADIATION EFFECTS PROGRAM. (Aerojet-General Corp., Sacramento, Calif. (USA)). Nov 1965. 31p. Dep. NTIS $4.75.

Declassified 10 Sep 1973.

A KIWI reactor excursion experiment was conducted by the Los Alamos Scientific Laboratory and the REON Division was granted permission to place explosion-proof irradiation capsules containing selected pseudo-stable materials identified in the report on the reactor pressure vessel and support structure. The high rate of pulsed neutron and gamma flux encountered there was used to evaluate transient effects on these materials by measuring changes in weight loss, vacuum stability, differential thermal analysis, explosion temperature, and detonation velocity. The excursion resulted in high flux exposures of $1.5 \times 10^7$R gamma, combined with $3.5 \times 10^{14}$ n/cm$^2$ fast neutrons (E >0.18 MeV) and $1.6 \times 10^{15}$ thermal neutrons (E < 0.17 eV) at the pressure vessel. None of the nine materials tested were significantly damaged by the lower flux pulse at the support structure which resulted in exposures of $3 \times 10^6$R gamma, combined with $7.3 \times 10^{13}$ n/cm$^2$ fast neutrons and $2.2 \times 10^{14}$ n/cm$^2$ thermal neutrons. The AGY-5 sample of lead styphnate (exposed on the pressure vessel) appeared to have detonated, but none of the eight other materials tested appeared to have been significantly damaged by the transient pulse. No samples showed evidence of significant weight loss (more than ± 0.2%) except AGP-5 and AGP-6. All of the materials analyzed passed the 200°C vacuum stability test. Nevertheless, a measurable radiation damage was produced on these samples as evidenced by an increase in gas release. None of the materials showed significant changes in explosion temperature or differential thermal analysis. A high-pressure shock wave passed through the samples, shattering the quartz ampoules which contained flux and temperature monitors, and broke the pressed explosive pellets, making it impossible to conduct detonation velocity tests. The temperature of the samples attached to the reactor exceeded 124°C (both temperature monitors melted), while the temperatures of the samples on the reactor support structure never exceeded 70°C (neither monitor melted). (auth)

**27303** (TID/SNA-2265) ENGINE-SYSTEM EVALUATION FOR ALTERNATIVE SOURCES FOR TURBINE DRIVE GAS, HOT-BLEED ENGINE. (Aerojet-General Corp., Sacramento, Calif. (USA)). Mar 1970. 161p. Dep. NTIS $11.25.

Declassified 10 Sep 1975.

The object of this trade study was to determine the feasibility of extracting turbine drive fluid from sources other than the present hot-bleed design. It was not feasible to extract turbine drive fluid from the supersonic portion of the nozzle because of insufficient pressure to drive the turbine. Methods of extracting turbine drive fluid from the reactor peripheral-flow area were determined to be impractical because of major changes required in the nuclear subsystem. The concept of using multiports from the subsonic region of the nozzle was found to be practical but did not provide improved reliability over that of the single-bleed-port concept. (auth)

**27304** (WANL-PR(J)-001) NERVA NUCLEAR SUBSYSTEM, PHASE I. Progress Report, July 10—July 30, 1961. (Westinghouse Electric Corp., Pittsburgh, Pa. (USA). Astronuclear Lab.). 10 Aug 1961. 22p. Dep. NTIS $4.25.

Declassified 29 Jul 1975.

The effort in this period was directed primarily at planning, organizing and initiating the Phase I work program. A planning and technical information exchange meeting was held at Azusa on July 26, 27 and 28 with discussions in the areas of control, general reactor arrangement and shielding. These were discussed from the viewpoint of areas requiring immediate attention to establish the reactor-engine interface. The KIWI-A1, A-3 and B1A reactor component tests and test program were reviewed with LASL at Los Alamos on June 26, 27 and 28. A technical information meeting was held at Los Alamos on July 10 and 11. The technical aspects of reactor design, fuel fabrication and reactor control were discussed following the formal portions of this meeting. A number of documents dealing with the KIWI design were received from LASL and are being reviewed by Westinghouse technical personnel. Design work has been confined to modifications of the LASL KIWI B-1 and B-4 concepts. An extensive review of the physical and mechanical properties of reactor materials has been initiated. Consideration is being given to structural graphite, fueled graphite and to metal alloys required for other reactor components. It has been found that most of the required materials property data are not available from the literature or from graphite suppliers, particularly the change in a property as a function of temperature. (auth)

**27305** (WANL-PR(J)-002) NERVA NUCLEAR SUBSYSTEM, PHASE I. Progress Report, July 31—August 31, 1961. (Westinghouse Electric Corp., Pittsburgh, Pa. (USA). Astronuclear Lab.). 10 Sep 1961. 27p. Dep. NTIS $4.50.

Declassified 29 Jul 1975.

Significant work has been initiated in the basic technical areas covered by the Phase I Program. Initial results are providing guidance for increased effort in the basic areas and for extension of the work. Preliminary layouts of the reactor have been initiated and, in conjunction with detailed review of the LASL information, are being studied to provide a basis for the flight reactor design. Extensive effort was devoted to continued coordination and information exchange. (auth)

**27306** (WANL-PR(J)-003) NERVA PROGRAM NUCLEAR SUBSYSTEM, PHASE 1. Progress Report, 1 September—30 September 1961. (Westinghouse Electric Corp., Pittsburgh, Pa. (USA). Astronuclear Lab.). 10 Oct 1961. 49p. Dep. NTIS $5.50.

Declassified 29 Jul 1975.

The initial definition of the flight environmental conditions has permitted the extension of the technical investigation of the reactor into the specific component designs required to meet the flight environmental requirements. Modifications to components not suitable for flight environment are being investigated. A number of core support schemes designed to provide lateral support and damping have been completed. Preliminary materials design properties and hydrogen characteristics have been compiled for use in analytical studies. The radiation environment in the vicinity of the unshielded reactor has been determined. Two shield concepts are being considered to reduce the hydrogen tank heat input. Initial design work on the PHOEBUS concept has indicated the possibility of design problems in connection with the support tube cooling. Draft plans for fuel procurement have been completed. Progress is being made in compiling specifications for core fuel elements. In the safety studies several experiments are planned. A beryllium burnup experiment will be conducted at Edwards in connection with SATURN spill studies. Progress is being made in planning for reentry burnup studies. The transient experiments in TREAT are going well. A failure mode analysis of the KIWI B-1 design has been completed. A scheme of reliability apportionment has been devised for the nuclear subsystem. (auth)

**27307** (WANL-PR(J)-005) NERVA PROGRAM NUCLEAR SUBSYSTEM PROGRESS REPORT, NOVEMBER 1—NOVEMBER 30, 1961. (Westinghouse Electric Corp., Pittsburgh, Pa. (USA). Astronuclear Lab.). 10 Dec 1961. 53p. Dep. NTIS $5.75.

Declassified 29 Jul 1975.

Progress continued in the technical and program control areas in accordance with the planned Phase I program. Preliminary mechanical design studies of the reactor and shield are continuing. Shock loading and the results of coolant flow studies in the shield have been taken into account and incorporated in the mechanical design. The shielded tank heat input calculations have been completed using as the shield material 63 percent lithium hydride, 27 percent stainless steel and 10 percent void. This composition was determined to give minimum shield weight. A controls system schematic was prepared, preliminary circuits for many of the components were considered and a preliminary description has been written to correspond with the controls system schematic. A combined failure mode analysis and design review was completed on the Bendix Acutator. Recommendations were made to improve reliability. A failure mode analysis of the KIWI B-4 reactor is 95% complete. The details of the equipment to be used to irradiate electronic circuits and components at WTR are being worked out. Present plans are to use helium gas for cooling and as an inert atmosphere in the reactor test loop. Review of various electro-pneumatic and electro-mechanical regulating and shim actuator designs was continued to determine limitations and potential development problems associated with each type. The Bendix, GE and LASL electro-pneumatic designs were analyzed

to establish possible applicability to flight specifications. Four autoclave assemblies were loaded with $UC_2$ fuel specimens and irradiated in the TREAT Reactor. Visual examination of the specimens indicated that reactor transients of 386, 645 and 887 MW/sec respectively caused disintegration of the fuel. Static hystersis curves were obtained on a single cantilevered module of the KIWI B-1A type. Tests were made with and without a gasket to determine the flexibility due to the gasket. The vibration study and testing of graphite is continuing. (auth)

**27308** (WANL-PR(J)-016) NERVA NUCLEAR SUBSYSTEM PROGRESS REPORT, OCTOBER 1-OCTOBER 30, 1962. (Westinghouse Electric Corp., Pittsburgh, Pa. (USA). Astronuclear Lab.). 10 Nov 1962. 47p. Dep. NTIS $5.50.

Declassified 29 Jul 1975.

Primary effort was concentrated on the completion of layouts and continuation of detail design for the NRX-A1 reactor, shipping container and assembly stand. The shipping container subcontract has been placed. The layout of the Hot-Bleed Shield for NRX-A1 has been released. The basis for setting the NRX-A loading has been established. Sufficient nuclear information has been developed to permit completion of detail design of the NRX-A1 Reactor and Shield. Testing of the Bendix pneumatic actuator has been initiated in the WANL Laboratory. The General Electric pneumatic actuator has undergone a complete set of performance tests using helium at ambient temperatures. Initial deliveries of pyro-coated fuel particles will be delayed approximately one month. The rescheduled delivery rate is higher than originally planned so that the total quantity of fuel will be delivered as required. Experiments to assess reentry problems of the fragmented reactor after an explosive destruct have been initiated. Plasmajet tests have been run on fueled graphite samples which had been subjected to an explosive destruct test. These samples which were irregular in shape following the explosion were machined to $\frac{1}{4}$ inch diameter hemispheres. Mass loss rates were compared with those for graphite samples which had not been subjected to explosion. No difference in mass loss rate was observed. (auth)

**27309** (WANL-PR(J)-021) NERVA NUCLEAR SUBSYSTEM. Progress Report, 1 March-31 March 1963. (Westinghouse Electric Corp., Pittsburgh, Pa. (USA). Astronuclear Lab.). 10 Apr 1963. 60p. Dep. NTIS $6.00.

A detail study layout has been started of a metal band which surrounds the core inlet end. This band should improve inlet end bundling and decrease the leakage of cold gas past the lateral support plungers. Non-interlocking peripheral support blocks have been released as backup for the interlocking support blocks. Drawings were issued to define unloaded fueled elements, central elements and multi hole central elements to be obtained from Oak Ridge for the NRX-A1 and Phase I and II vibration test programs. Drawings defining aluminum cluster plates, control drum cylinders, reflector sectors and graphite insulating tiles were released for the Phase I vibration test reactor. Revisions to the NRX-A lithium hydride shield drawings were completed. The KIWI-B5 shield final stress and vibration report is being published. The first edition of the WANL Materials Manual was completed and distributed. Analysis indicates that the NRX-A core pressure drop has increased from 125 psi to 129 psi because design changes in the core periphery have decreased the number of coolant channels. Reactor analysis instrumentation requirements for NRX-A1 were modified in accordance with the data acquisition system capacity. A computer analysis of normal and emergency cooldown from full power was completed. Coolant requirements following shutdown for equivalent full power operating times of from two to five minutes were completed. Heat generation rates in the NRX aluminum pressure vessel and support stand with the NRX shield replaced by an aluminum simulated shield were calculated. The power supply for the NRX control amplifiers was tested and noise level reduced to acceptable levels. The report "NERVA Engine Reactor Control System: Preliminary Synthesis and Analysis" was completed. Actuator vibration tests were conducted on the gear motor and piston prototypes. A one g vibration revealed no major detrimental effect. Cooldown tests were started on the horizontal multiple-pass test section set up. (auth)

**27310** (WANL-PR(J)-023) NERVA NUCLEAR SUBSYSTEM. Progress Report, 1 May-31 May 1963. (Westinghouse Electric Corp., Pittsburgh, Pa. (USA). Astronuclear Lab.). 10 Jun 1963. 79p. Dep. NTIS $7.00.

Assembly drawings and assembly procedure manuals have been issued for the vibration reactor. Instrumentation schematics for NRX-A1 were released, and a preliminary instrumentation list for NRX-A2 was defined. Three reports analyzing NRX-A core statics were completed. The shipping container for NRX-A1 was completed and is undergoing proof tests. The shield replacement unit drawings are released and a revised program for shield component testing has been defined. The irradiation phase of the shield materials program is complete. Analysis has continued on reactor structural materials, thermal capsules and control materials. Stress analysis of the NRX-B graphite support plate has continued and designs utilizing fuel elements clustered in graphite modules are being investigated. Studies have continued on counterflow tie rod designs and a segmented girdle lateral support system. The functional design analysis of the present KIWI-B4 control system as applied to the NRX-A reactor has been completed. The NRX control system fabrication is in progress. The design and development of the second-generation electro-pneumatic actuator prototypes has been initiated by General Electric. Developmental type neutron detectors were tested and construction work is in progress for full range detectors. Irradiation tests of candidate transducers has been completed. Text fixtures for the July tests at GTR are being constructed. Production of fuel elements for NRX-A2 is in process. Procurement has continued for all reactors including component testing. First unloaded core elements for NRX-A1 reached final production stages at Oak Ridge. The initial entry of the monthly instrumentation procurement report has been completed. Initial assembly of the vibration reactor has commenced. (auth)

**27311** (WANL-TME-008) WANL RECOMMENDATIONS AND COMMENTS ON PRELIMINARY MODEL SPECIFICATIONS. AGC 10097 (Heated Bleed). Retallick, F. D. (Westinghouse Electric Corp., Pittsburgh, Pa. (USA). Astronuclear Lab.). 31 Jan 1962. 52p. Dep. NTIS $5.75.

Declassified 22 Jul 1975.

The AJ 31-6 Rocket Engine is a liquid propellant, turbopump-fed nuclear engine rated at 57700 lb nominal vacuum thrust. The engine consists of a thrust chamber assembly, a turbopump assembly, connectings lines and fittings and components required for engine operation, all supported by a mount structure. The thrust chamber consists of a pressure vessel enclosing a beryllium reflected graphite core reactor with a primary shield, a nozzle assembly, and a gimbal mechanism. The propellant utilized is liquid hydrogen. The turbine drive gas shall be bled from the upper reactor plenum and heated in the radiation shield and nozzle skirt. In addition, the engine includes vector control and restart capability systems. The turbopump is accelerated during start using a portion of the gas generated from the heat energy stored, and avaliable for use, in the nozzle, reflector, shield, and nozzle skirt. The tank pressure causes the initial flow of propellant through the engine, and this pressure is supplemented by the pump pressure rise as the turbopump accelerates. This listing of preliminary specifications includes comments and WANL'S recommendations for changes. (auth)

**27312** (WANL-TME-016) WANL RECOMMENDATIONS AND COMMENTS ON PRELIMINARY MODEL SPECIFICATIONS. AGC 10095 A (Hot Bleed). Retallick, F. D. (Westinghouse Electric Corp., Pittsburgh, Pa. (USA). Astronuclear Lab.). 31 Jan 1962. 54p. Dep. NTIS $5.75.

Declassified 22 Jul 1975.

The AJ 30-5 Rocket Engine is a liquid propellant, turbopump-fed nuclear engine rated at 56,790 lb nominal vacuum thrust. The engine consists of a thrust chamber assembly, a turbopump assembly, connecting lines and fittings and components required for engine operation, all supported by a mount structure. The thrust chamber consists of a pressure vessel enclosing a beryllium reflector graphite core reactor with a primary shield, a nozzle assembly, and a gimbal mechanism. The propellant utilized is liquid hydrogen. The turbine drive gas shall be bled off ahead of the main nozzle throat and diluent added for temperature reduction. In addition, the engine includes vector control and restart capability systems. The turbopump is accelerated during start using a portion of the gas generated from the heat energy stored, and available for use, in the nozzle, reflector, shield, and reactor core. The tank pressure causes the initial flow of propellant through the engine, and this pressure is supplemented by the pump pressure rise as the turbopump accelerates. WANL'S comments and recommendations for changes are included. (auth)

**27313** (WANL-TME-067) INFORMATION REQUIREMENTS: FUEL ELEMENT INSPECTION. Thomas, G. R. (Westinghouse Electric Corp., Pittsburgh, Pa. (USA). Astronuclear Lab.). 6 Aug 1962. 15p. Dep. NTIS $4.00.

A preliminary attempt to outline the information required by the Reactor Analysis Department from Fuel Element Inspection is provided. In general, the data needed would fall into two categories: 1. Data needed to predict the effects of deviations from nominal specifications. In these cases, enough data are needed to allow a statistical treatment to be made where necessary. 2. Data needed for the Orifice Selection Computer Program. These data are needed on every element (or channel where indicated) in order to select the proper orifice sizes for the core. For convenience, the tests required are listed: Coolant channel

location, reamed channel diameter, axial fuel concentration, cross section radiograph, density, weight, miscellaneous dimensions, chemical analysis, fuel particle size, total fuel loading, air flow impedance, etc. (auth)

**27314** (WANL-TME-082) HYDROGEN REACTIVITY WORTH IN NRX-A-1. Ortenberg, L. I. (Westinghouse Electric Corp., Pittsburgh, Pa. (USA). Astronuclear Lab.). 3 Jul 1962. 1p. Dep. NTIS $4.00.
Declassified 22 Jul 1975.

**27315** (WANL-TME-094) PRELIMINARY DESCRIPTION OF NRX-A-1 REACTOR REGIONS FOR NEUTRONIC CALCULATIONS. Ortenberg, L. I. (Westinghouse Electric Corp., Pittsburgh, Pa. (USA). Astronuclear Lab.). 3 Aug 1962. 10p. Dep. NTIS $4.00.
Declassified 22 Jul 1975.
An analytical description of the NRX-A1 reactor includes radial and axial geometries and atomic densities. (LTN)

**27316** (WANL-TME-291(Add. 1)) NRX-A CONFIGURATION FOR RADIATION ANALYSES. Capo, M. A.; Nassano, R. N.; Soltesz, R. G. (Westinghouse Electric Corp., Pittsburgh, Pa. (USA). Astronuclear Lab.). 10 Jul 1963. 8p. Dep. NTIS $4.00.
Declassified 21 Jul 1975.

**27317** (WANL-TME-291(Add. 2)) NRX-A CONFIGURATION FOR RADIATION ANALYSIS. Capo, M. A.; Nassano, R. N.; Soltesz, R. G. (Westinghouse Electric Corp., Pittsburgh, Pa. (USA). Astronuclear Lab.). 29 Nov 1963. 8p. Dep. NTIS $4.00.
Declassified 21 Jul 1975.

**27318** (WANL-TME-369(Rev. 0)(No. 38)) POWER TESTING OF NRX-A-2. Project NERVA: Reactor Analysis Test Request. Vetere, A. M. (Westinghouse Electric Corp., Pittsburgh, Pa. (USA). Astronuclear Lab.). 31 May 1963. 12p. Dep. NTIS $4.00.
Declassified 22 Jul 1975.
The power tests planned for the NRX-A-2 reactor are intended to prove the capability of the reactor at a power level which, depending upon the results, could be below 100% power. Transient operation up to this level and steady-state operation at the selected level, must produce engineering data that will permit a valid evaluation of the reactor performance and point the way to any necessary design changes. Successful operation of the NRX-A-2 is a necessary prerequisite before tests related more closely to engine conditions can be performed. The test shall be considered successful only if the primary objectives have been accomplished. Failure to meet these objectives would indicate a need for further design and development. The additional engineering information desired in addition to successful operation is listed. (auth)

**27319** (WANL-TME-381) NRX-A-2 CYCLE SCHEMATIC DIAGRAM. Thomas, G. R. (Westinghouse Electric Corp., Pittsburgh, Pa. (USA). Astronuclear Lab.). 4 Jun 1963. 2p. Dep. NTIS $4.00.
Declassified 16 Jul 1975.
The principal revisions to the NRX-A-2 Cycle Schematic Diagram have been the correction of shield pressure drops and temperature rises to those consistent with the use of an aluminum shield replacement and revision of reflector and pressure vessel annulus conditions to be consistent with the latest available information. Other very minor changes such as a slight increase in core pressure drop and a small tie-rod coolant flow change are also incorporated. The values shown are for full power, full flow conditions with liquid hydrogen feed. While it is anticipated that NRX-A-2 may be tested using a mixing chamber to supply cold hydrogen gas (~ 90°R), it is likely that the feed will be adjusted to liquid should full power conditions be approached. (auth)

**27320** (WANL-TME-540) MECHANICAL PROOF TESTS ON NERVA FUEL MATERIAL. Andersson, C. A. (Westinghouse Electric Corp., Pittsburgh, Pa. (USA). Astronuclear Lab.). Sep 1963. 23p. Dep. NTIS $4.25.
Declassified 29 Jul 1975.
The feasibility of mechanically proof testing NERVA graphite fuel elements by prestressing each element in flexure was investigated. No reduction in flexure strength occurred after prestressing full-sized elements to 50 and 75 per cent of their rupture stress. It was found possible to reduce permanent set introduced during prestressing cycles by continuing the cycles at subsequently lower loads. The flexural fatigue characteristics also appear to be unaffected by prestressing to 50 and 75 per cent of the static rupture load. (auth)

**27321** (WANL-TME-607) THERMAL, FLUID FLOW, AND NUCLEAR CHARACTERISTICS OF CORES WITH COOLED INTERNAL STRUCTURES. Boman, L. H.; Dickson, P. W. Jr.; Doncals, R. A.; Lescisin, J. J.; Zemanick, P. P. (Westinghouse Electric Corp., Pittsburgh, Pa. (USA). Astronuclear Lab.). 16 Dec 1963. 186p. Dep. NTIS $12.25.
Declassified 22 Jul 1975.
The performance of six core cage reactor designs is evaluated under a variety of conditions. Fuel loading density requirements are developed, control spans calculated, and hydrogen reactivities estimated. It is concluded that a core with a one-pass metal structure can be designed with a peak fuel loading density of 500 mg/cc, and with a more than adequate control range. Propellant reactivity ranges are from $3 to $5. Power peaking will probably be somewhat higher than in NRX-A, even with fuel zoning. The thermal performance of the metal structure is evaluated at full power, part power, and with allowance for tolerances and variations. It is concluded to have substantial thermal margin under all conditions. Propellant requirements during decay heat removal are found to be slightly higher (3%) than in NRX-A. Variations in the hot channel fuel element temperature which result from the use of metal structures are examined. It is found that module to module variations in the inlet hydrogen temperature to the fuel elements may cause increases in local fuel temperatures; the magnitude of this increase may be controlled through orificing. The startup characteristics of the core structures are examined, and all modules are found to startup smoothly, simultaneously, and without significant reactivity overshoot. It is concluded that the design of a core cage reactor is fully feasible, but that it may entail additional complexities and/or a slight reduction in performance. (auth)

**27322** (WANL-TME-673) EXPERIMENTAL DETERMINATION OF LOSS COEFFICIENTS FOR THE MODEL OF THE BERYLLIUM REFLECTOR ASSEMBLY USING AIR AND HYDROGEN. Bouille, J. R. (Westinghouse Electric Corp., Pittsburgh, Pa. (USA). Astronuclear Lab.). 31 Jan 1964. 60p. Dep. NTIS $6.00.
Declassified 22 Jul 1975.
The results of flow tests on the model of a segment of the beryllium reflector assembly are summarized. Three distinct series of tests were conducted. The first series was conducted using air as the test fluid. Various sizes of flow holes and plenum heights were used within the model. These test results were used to establish the design and were reported in WANL-TME-333. The second series of tests were conducted on the design configuration using hydrogen gas and were reported in WANL-TME-543. These tests were to be used to confirm the design established by the air data. However, these tests were combined with the initial use of a new test loop. Control problems in the loop resulted in time variable flow rates and considerable scatter was encountered. As a consequence, the correlation of hydrogen data with the original air data was not considered adequate. The third series of tests were a repeat of the second series and were conducted after modifications were made to the flow loop. The results were more consistent and the correlation with the first series of tests on air was excellent. Loss coefficients and data obtained from the first and third series of tests are presented for the design configuration and from the first series of tests for off-design geometries. (auth)

**27323** (WANL-TME-697(Add.1)) ANALYSIS OF THE ALTERNATE STARTUP SYSTEM FOR NRX REACTORS. Jones, D. H.; Junker, D. W. (Westinghouse Electric Corp., Pittsburgh, Pa. (USA). Astronuclear Lab.). 17 Jul 1964. 25p. Dep. NTIS $4.25.
Declassified 22 Jul 1975.
Since the writing of WANL-TME-697, "Analysis of Alternate Startup Method for NRX-Reactors", the predicted control-drum worth function for the NRX-A2 test has been changed considerably. Because of this change the curves which present the correlation between the control-drum-position profile and the resulting reactor power profile are no longer accurate, so an additional study was performed to update the curves, using the latest predictions of the control-drum worth. Also, it was learned, from the experience of the Los Alamos group with the automatic single-range startup tests during the recent KIWI-B4D test, that the reactor power level prior to initiating the startup was considerably higher than initially anticipated. For that reason, the predictions for the minimum reactor period corresponding to specific ramp rates were in error. To eliminate this problem in the NRX-A2 test, analog-computer studies were performed to determine the effect of startup source level (or range of power variation during startup) on the dependency of minimum period and total startup time upon ramp rate in the control-drum-position profile. The curves contained in this addendum are presented for startups over power ranges from 2 decades through 9 decades, permitting choice of the ramp rate of the control-drum-position profile to be made just prior to the startup when the initial reactor power level is known. (auth)

**27324** (WANL-TME-712) EXPERIMENTAL DETERMINATION OF THE PRESSURE LOSS COEFFICIENT FOR THE PRODUCTION TIE ROD CENTERING BUSHING. Fix, H. J. (Westinghouse Electric Corp., Pittsburgh, Pa. (USA). Astronuclear Lab.). 6 Mar 1964. 32p. Dep. NTIS $4.75.

Declassified 12 Sep 1973.

Flow tests were conducted on a production-type centering bushing using hydrogen gas at inlet pressures of 670 and 330 psig and at ambient and cryogenic temperature. Tie rods having diameters of 0.110 inches and 0.122 inches were tested at the above conditions with the centering bushing leakage paths sealed and unsealed. For similar leakage paths varying the tie rod diameter from 0.110 to 0.122 inch diameter has no effect on the flow rate pressure drop characteristics. The nominal pressure loss coefficient based on orifice flow area for the 0.110 and 0.122 inch diameter tie rods for the unsealed case was found to be 1.4 and for the sealed case to be 1.8. The loss coefficient is relatively independent of Reynolds number and dependent on Mach number. (auth)

**27325** (WANL-TME-720) INDUCED VIBRATIONS DIGITAL PROGRAM FOR ANALYSIS OF KIWI AND NERVA REACTOR CORES. Pierce, B. L. (Westinghouse Electric Corp., Pittsburgh, Pa. (USA). Astronuclear Lab.). Mar 1964. 47p. Dep. NTIS $5.50.

Declassified 22 Jul 1975.

A flow induced vibration (VIB) digital code was written to analyze the KIWI and NERVA reactor cores. To establish the validity of the code, calculation comparisons were made between the codes results and both analytical and experimental (KIWI B-4A) data. The agreement was quite good. The conclusions for KIWI and NERVA reactor cores based on digital results are consistent with conclusions based on results from previous work done on an analog computer. The NRX-A1 configuration did not vibrate for any of the flow rates investigated and the resulting VIB code calculated pressure distribution is shown for a pressure drop of 36 psi and with ambient hydrogen gas flowing. The reflector cylinder core annulus pressures are greater than the internal core pressures except around the 17th seal which is ineffective. (auth)

**27326** (WANL-TME-744(SUPPL. 2) THERMAL ANALYSIS OF HIGH TEMPERATURE FUEL ELEMENT CORROSION TESTS. Guzek, J. C.; Bournia, A. (Westinghouse Electric Corp., Pittsburgh, Pa. (USA). Astronuclear Lab.). 31 May 1966. 37p. Dep. NTIS $5.00

Declassified 14 Jul 1975.

Results of a thermal analysis made in the light of modifications to the quality control single element furnace test are reported. The objective of these modifications was to achieve comparable bore conditions in the electrical test as exists in local pertinent regions of the reactor, i.e. the area of mid-band corrosion in the coolant channels and the hot end region. The major modification consists of using a molybdenum thermal radiation shield to reduce excessive radiation heat loss at the hot end of the element. This moly shield covers the last 15 inches to the hot end of the element. It has reduced the maximum radial temperature difference (maximum material less surface temperature) from 500°R occurring with a graphite shield to approximately 300°R. The axial temperature profile has remained basically unchanged. Other improvements which have been made but have only indirect thermal implications include: (1) a longer hot-end chuck exposing the exterior surface areas of the element at the hot end to corrosive conditions and thus providing a better evaluation for reactor conditions, and (2) an improved seal at the cold end of the element. The latter improvement in addition to providing better sealing reliability, also provides flexibility of varying the helium atmosphere pressure in the exterior region of the element during corrosion testing. This flexibility is useful to investigate the influence of pressure differential on the tendency of fuel elements to form pin holes. For a detailed discussion of the hardware modifications see WANL-TME-1381. Also, the analytical model used in this analysis have been enlarged to obtain a temperature distribution across the element face at each axial station analyzed. The maximum temperature difference calculated across the face (between channel less corner temperature), at the hot end is 157°R. (auth)

**27327** (WANL-TME-746) SEVEN CLUSTER TRANSPORTATION TEST. Gesinski, L. T. (Westinghouse Electric Corp., Pittsburgh, Pa. (USA). Astronuclear Lab.). Apr 1964. 21p. Dep. NTIS $4.25.

Declassified 14 Jul 1975.

A seven cluster assembly, simulating a section of the inner core, was subjected to a series of shipping environment tests to evaluate the integrity of the niobium carbide coatings on both unfueled elements and NRX-A2 enriched elements. The test specimen was simultaneously excited vertically and laterally within a load envelope simulating the data reported in WANL-TME-458 and WANL-TME-680. This data was recorded on actual trips to the test site using dummy and NRX-A1 reactors. The load envelopes for the two unfueled coated cluster tests are given. The load envelope for the fueled coated cluster is also given and is 50 percent higher in order to provide a more severe test environment. There were no indications of any detrimental damage to the coatings on the fuel elements after completion of test. (auth)

**27328** (WANL-TME-755) EVALUATION OF THORIA DISPERSION-HARDENED NICKEL FOR NERVA APPLICATIONS. Levine, P. J. (Westinghouse Electric Corp., Pittsburgh, Pa. (USA). Astronuclear Lab.). 27 Apr 1964. 29p. Dep. NTIS $4.50.

Declassified 14 Jul 1975.

TD Nickel, a thoria dispersion hardened nickel alloy, maintains excellent mechanical properties up to 2400°F and possesses desirable physical properties of pure nickel. Although the room temperature strength is low, the material should be considered for structural applications in the NERVA reactors where high temperatures limit the selection of other materials. This report presents a preliminary evaluation of TD Nickel based on test results and published information, including the nuclear characteristics, mechanical properties, joining techniques and oxidation resistance. (auth)

**27329** (WANL-TME-770) VIBRATIONAL STABILITY OF NRX-A1 INNER REFLECTOR AND CORE. Persin, W. J.; Warner, P. C.; Maguire, A. F. (Westinghouse Electric Corp., Pittsburgh, Pa. (USA). Astronuclear Lab.). May 1964. 29p. Dep. NTIS $4.50.

Declassified 11 Sep 1973.

A study was made to investigate the vibrational stability of the inner reflector when subjected to various displacement perturbations. These perturbations allow leakage flow between the nozzle pressure-vessel plenum and the core exit plenum which may provide proper conditions for self-excited vibrations of the inner reflector and core system. Of prime importance was the finding that the frictional force between the inner reflector and core plays a key and necessary role in determining stability. In the present NRX-A1 design normal friction is sufficient to hold the system stable even with large changes in the relevant physical quantities. (auth)

**27330** (WANL-TME-849) EVALUATION OF THE NRX-A1 OUTER REFLECTOR SECTOR CRACKS. Pianka, E. W. (Westinghouse Electric Corp., Pittsburgh, Pa. (USA). Astronuclear Lab.). Aug 1964. 21p. Dep. NTIS $4.25.

Declassified 11 Sep 1973.

Upon disassembly of the NRX-A1 reactor, it was found that all 12 of the outer reflector sectors were cracked at the nozzle end spigot. All of the sectors were cracked in substantially the same manner with circumferential fractures starting at the outside of the spigot and extending through the wall into the control drum bore. The fractures appeared primarily in the heavy portion of the sector, extending over a minimum of approximately 45 degrees in some sectors to a maximum of approximately 260 degrees of the perimeter in others. The conditions which could have caused these cracks can be summarized as follows: (1) A severe temperature difference between the thin spigot section and the massive sector. (2) Interference between the sector spigot and the nozzle end support ring caused by differential thermal expansion between the beryllium sector and the titanium support ring. (3) Interference between the sector spigot and the nozzle end support ring caused by the thermally induced interference between the aluminum pressure vessel and the titanium support ring. An analysis of these possibilities led to the conclusion that the third condition is the most probable cause. The analysis showed that a 0.015 radial interference between the pressure vessel and the support ring could cause cracking of the sector spigot, whereas the estimated interference based on thermocouple readings during the NRX-A1 tests was at least 0.022 inch. (auth)

**27331** (WANL-TME-869) EXPERIMENTAL DETERMINATION OF ORIFICE COEFFICIENTS FOR PRODUCTION TYPE FUEL ELEMENT ORIFICES FOR NRX-A2. Chronis, W. C.; Fix, H. J. (Westinghouse Electric Corp., Pittsburgh, Pa. (USA). Astronuclear Lab.). 30 Jun 1964. 58p. Dep. NTIS $6.00.

Declassified 14 Jul 1975.

The results of tests on production type fuel element orifices are summarized. The areas investigated were: The variation in loss coefficient as a function of Reynolds number for a particular diameter orifice; and the variation in loss coefficient as a function of orifice diameter for the operating Reynolds number range. Tests were conducted on production fuel element orifices

using hydrogen gas at an inlet pressure of 675 psia and at cryogenic temperature. Twelve (12) nominal sizes ranging from 22.5 to 70.0 mils diameter were tested. Three (3) orifices (maximum, master, minimum) were tested for each of the twelve (12) nominal sizes. In the design range (in most cases) the loss coefficient is relatively independent of Reynolds number. A curve is given for the loss coefficient versus orifice diameter for NRX-A2 design Reynolds numbers. (auth)

**27332** (WANL-TME-887(Suppl.4)) NRX-A2 TEST PREDICTIONS REPORT: STARTUP WITH FLOW LAG AND 50%, 83% POWER POINTS. Knecht, W. L. (Westinghouse Electric Corp., Pittsburgh, Pa. (USA). Astronuclear Lab.). 13 Oct 1964. 8p. Dep. NTIS $4.00.

Declassified 14 Jul 1975.

Based on NRX-A1 test data, a flow lag was estimated for the NRX-A2 startup, and was used to calculate the programmed power schedule and reactor performance data. The flow lag extends up to approximately 30 lb/sec flow. Therefore, only the startup to the first hold is affected. Steady state data at 50 and 83% power are tabulated. (auth)

**27333** (WANL-TME-1001) DIRE: A DIGITAL REACTOR MODEL FOR EXCURSION STUDIES. Riese, J. W.; Collier, G. (Westinghouse Electric Corp., Pittsburgh, Pa. (USA). Astronuclear Lab.). Oct 1964. 45p. Dep. NTIS $5.25.

Declassified 10 Sep 1973.

The code described was written to analyze the nuclear excursions resulting from some postulated flow rate and/or control drum accidents in NRX-A2 cold flow tests. The usefulness of the TNT code for this type of problem was limited because: the very rapid neutronics changes occurring required the use of very small time-steps, otherwise the code became unstable; and each time step required a fair amount of computing time because of the very detailed heat transfer and fluid flow model. Hence computer running times became excessive. It was proposed to remedy this situation by: (1) using a much simplified heat transfer-fluid flow model, hence reducing the computation per time-step; and (2) using many small neutronic time-steps for each single fluid flow and heat transfer step, thus reducing the number of time-steps for the nonneutronic part of the calculation. A completely new code was tailored to the needs of the cold-flow accident problem. The neutronics was kept very simple—1 energy group, 6 precursors, point kinetics—since this is adequate for the accuracy needed in an accident calculation. The fluid flow treatment was of necessity fairly detailed, however, since the low temperatures involved in cold flow are far indeed from the "ideal gas" conditions present in a power test. The ability of this model to accurately represent a NERVA reactor may perhaps be improved by changing some of the input data or by modifying the code to include details which have been neglected. As a useful tool for transient analysis, the code provides a one-pass program to replace the iterative procedure (previously used in accident calculations) which was carried out between such codes as TNT and RTS, and which involved intermediate hand calculations besides. (auth)

**27334** (WANL-TME-1665) CLUSTER CORROSION PROOF TESTS FOR NRX-A6. Salvador, L. A.; Stahl, B. H. (Westinghouse Electric Corp., Pittsburgh, Pa. (USA). Astronuclear Lab.). 29 Sep 1967. 86p. Dep. NTIS $7.50.

Declassified 12 Sep 1973.

The results of the proof-tests of axial support components for the NRX-A6 core design are summarized. Twenty-five cluster corrosion tests were conducted in the cluster corrosion furnace at WANL. Four basic configurations were tested and each configuration was made up of several candidate components. These configurations included: regular skirtless block with the exit gas thermocouple asembly and related hardware; composite protection cup with a modified skirtless block; and LASL cluster with composite pedestal and protection cup. The purpose of the tests was to evaluate the ability of the reactor components to endure 60 minutes operation at a nominal NRX-A6 exit gas temperature of 4325°R with a hydrogen flow of about 50 per cent of the NRX-A6 cluster flow rate. All components were qualified for 60 minutes at these conditions on the basis of these tests and, with the exception of the LASL cluster, were included in the NRX-A6 assembly. (auth)

**27335** (WANL-TME-1678) METAL TUBE BORE INSERTS. Kochka, E. (Westinghouse Electric Corp., Pittsburgh, Pa. (USA). Astronuclear Lab.). Sep 1967. 23p. Dep. NTIS $4.25.

Declassified 22 Jul 1975.

"Mid-band" corrosion is a prime reason for the failure of NERVA fuel elements to meet design specifications. This type of corrosion signifies the attack of bare graphite by hydrogen in the 100-1500°C temperature region. Although the fuel elements are protected by niobium carbide coatings, differences between coating temperatures and actual test temperatures together with thermal expansion differences between the coating and the graphite produce a region of open cracks where graphite-hydrogen reactions occur. This region defines the area of "mid-band" corrosion. A barrier placed between the hydrogen coolant flow and the open cracks should improve the corrosion performance of fuel elements. To determine the feasibility of using metal tube liners in coolant channels to improve the corrosion performance of fuel elements, an experimental program was outlined with the objectives of: 1. Establishing the feasibility of fabricating fuel elements with tube liners; and 2. Determining the corrosion performance of tube-lined elements. The work completed under the A-6 program and plans for the continuation of this project are presented. (auth)

**27336** (WANL-TME-1719) NRX-A6 INSTRUMENTATION INSTALLATION REPORT. McCullough, C. (Westinghouse Electric Corp., Pittsburgh, Pa. (USA). Astronuclear Lab.). 5 Dec 1967. 41p. Dep. NTIS $5.25.

Declassified 22 Jul 1975.

The installation history of the NRX-A6 internal instrumentation has been documented, inclusive from the receipt of transducers by Reactor Assembly Lab (RAL) to WANL final electrical checkout. A total of 177 sensors were installed. Of these, 2 became non-operational during the reactor assembly and the measurements were deleted. An additional 4 sensors experienced electrical problems at the final electrical checkout and were scheduled for cable retransitioning at NRDS. Thus 171 sensors were completely operative as the reactor was shipped. (auth)

**27337** (WANL-TME-1773) HIGH TEMPERATURE THERMOCOUPLE QUALIFICATION AND DEVELOPMENT TESTING. Progress Report, January 1, 1967—March 31, 1968. Zellner, G. J. (Westinghouse Electric Corp., Pittsburgh, Pa. (USA). Astronuclear Lab.). Mar 1969. 458p. Dep. NTIS $26.00.

Declassified 11 Sep 1973.

The high temperature thermocouple development effort for NERVA made substantial advances. An exit gas thermocouple was qualified for NRX-A6, two new sources were qualified for NRX in-core thermocouples, and several new materials and designs achieved reactor qualification levels. Progress was made in sheath and insulator development and in the preliminary evaluation of new designs. The improvements in sheath materials included the development and qualification of high purity molybdenum tubes made by chemical vapor deposition, the continued improvement in chemically vapor deposited (CVD) tungsten 25 percent rhenium alloy tubing, and the initial progress with wrought tungsten tubes containing thoria as a grain growth inhibitor. The tungsten rhenium sheath development still is limited to temperatures below the W-Re-C eutectic temperature. CVD molybdenum has proved to be a satisfactory replacement for the wrought material in present designs. Insulator developments were primarily in the improvement of the consistency of quality of BeO and MgO insulators by imposing certain limitations on processes and handling of insulators during manufacture. The combination of the best available insulators, sheaths, and design features into a single thermocouple has been the overall goal of the thermocouple development program. At the lower end of the high temperature scale, CVD molybdenum sheaths coated with CVD tungsten and with BeO conforming to the WANL PDS specification as insulation best accomplished this goal for temperature measurements below 4200°R. Between 4200°R and 4600°R, the sheath is changed to CVD tungsten 25 per cent rhenium coated with CVD tungsten, and a spaced floating junction plug is employed in lieu of the grounded junction. Above 4600°R thoriated tungsten is used for the sheath along with the spaced floating plug and the PDS specification grade of BeO insulators. Tantalum inner sheath liners are also suggested for carbonaceous environments to extend thermoelement life. BeO is limited to a useful maximum temperature of approximately 4900°R. At present, thermoelement materials are the weakest link in the reliability chain. Recrystallization and grain growth occurs in thermoelements in the same manner as in sheaths and, therefore, some of the techniques applied in improving sheath materials are considered applicable to improvement of thermoelements. The test program and the development work associated with it resulted in a number of innovations and improvements in high temperature technology. (auth)

**27338** (WANL-TME-1832) NRX-A6 REACTOR STRUCTURAL PERFORMANCE. (Westinghouse Electric Corp., Pittsburgh, Pa. (USA). Astronuclear Lab.). Mar 1969. 48p. Dep. NTIS $5.50.

Declassified 11 Sep 1973.

The structural performance of the NRX-A6 reactor is evaluated and the implications on future NERVA design are discussed. Component structural performance and test data analysis are described separately. The general structural performance of the NRX-A6

reactor was excellent. The reactor surpassed its objectives of a full hour run without being limited by the structural performance of any of the components. Disassembly and post test evaluation confirmed that the design met all of the NRX-A6 reactor performance and design objectives. In the test data analysis the measurements from the displacement, strain, and vibration transducers are examined and compared with values calculated from other measured reactor parameters, such as temperatures and pressures. (auth)

**27339** (WANL-TME-1841(Rev.1)) FIRST REVISION TO R-1 COMMON ANALOG MODEL. (Westinghouse Electric Corp., Pittsburgh, Pa. (USA). Astronuclear Lab.). 28 Mar 1969. 74p. Dep. NTIS $6.75.

Declassified 14 Jul 1975.

**27340** (WANL-TME-1852(Vol.2)(App.)) R-1 PARAMETRIC SHIELD MEASUREMENTS CONDUCTED ON THE NERVA PERMANENT ASSEMBLY EXPERIMENT (PAX) REACTOR. Volume II. Oblock, V. S. (Westinghouse Electric Corp., Pittsburgh, Pa. (USA). Astronuclear Lab.). May 1969. 531p. Dep. NTIS $29.75.

Declassified 11 Sep 1973.

The PAX-E5 zero power reactor core is described. Then the calibration of the eleven different means of neutron dosimetry is discussed. Data reduction techniques and the uncertainties in the measurements are considered. (LTN)

**27341** (WANL-TME-1856) NOTES OF MONTHLY DEVELOPMENT TEST PROGRAM REVIEW MEETING HELD WITH SNPO AT WANL ON AUGUST 27, 1968. (Westinghouse Electric Corp., Pittsburgh, Pa. (USA). Astronuclear Lab.). [nd]. 59p. Dep. NTIS $6.00.

Declassified 11 Sep 1973.

Tests were mainly in support of NRX-A6, PEWEE-1, R-1 and XE-2 reactors and involved mostly tests of fuel elements and fuel element clusters. Various other tests of supports, seals, reflectors, instrumentation parts, vibration tests, etc. are mentioned briefly. Procedures for the operation of WANL liquid hydrogen facilities have been completed. (LTN)

**27342** (WANL-TME-1858) FUEL DEVELOPMENT TEST ON SPECIFICATION IV-3 "HI-EXPANSION GRAPHITE". Final Report. Anderson, R. E. (Westinghouse Electric Corp., Pittsburgh, Pa. (USA). Astronuclear Lab.). Dec 1968. 44p. Dep. NTIS $5.25.

Declassified 11 Sep 1973.

The primary objective of this experiment was to test the effect of increased thermal expansion on the corrosion test performance of NERVA fuel elements. Fueled elements were manufactured using 25, 50, and 75 percent Robinson Coke mixed with Great Lakes flour as the graphite coke constituent. These elements were processed along with standards through coating and corrosion testing. The results of the corrosion testing were not conclusive for a number of reasons. However, it was found that the highest-expansion elements had far fewer coating cracks and better coating adherence than did the standard elements. Un-overcoated high-expansion elements outperformed un-overcoated standard elements, especially in the midband region, in corrosion testing. The high-expansion elements appeared to withstand cycling in the corrosion test better than the standard elements. (auth)

**27343** (WANL-TME-1859) WFDD-TS-3005 PERMEABILITY STUDIES. Final Report. Anderson, R. E. (Westinghouse Electric Corp., Pittsburgh, Pa. (USA). Astronuclear Lab.). 23 Sep 1968. 29p. Dep. NTIS $4.50.

Declassified 11 Sep 1973.

An experiment was designed to test methods for lowering the leak rate of high-loaded elements. Three different methods were tried: (1) processing variations, such as extended green mix state holds, (2) atmosphere cure variations, and (3) matrix particle size variations. All three methods were effective to various degrees in lowering the leak rate of NERVA fuel elements. (auth)

**27344** (WANL-TME-1911) PAX-GO POWER DISTRIBUTION MEASUREMENTS. Final Test Report. Magaw, J. R.; Sipush, P. J. (Westinghouse Electric Corp., Pittsburgh, Pa. (USA). Astronuclear Lab.). Jan 1970. 52p. Dep. NTIS $5.75.

Declassified 14 Jul 1975.

An experiment performed to assist in prescribing the R-1 fuel loading distribution provided two types (gross and detailed) of measured radial fission density distributions in the PAX-GO reactor for use in power analysis calculations. The PAX-GO reactor has a large core (larger than the NRX-A/PAX-E series and no inner reflector) and a 12 control drum configuration in the beryllium reflector. The experimental procedure utilized U-Al wires located at the core midplane to determine the measured radial fission density distributions and included self-shielding effects of the U-Al wires. Comparisons of the calculated and measured radial fission density distributions show generally good agreement except at the core periphery where differences are larger due to fuel element hererogeneity and irregular core periphery. These comparisons, along with similar comparisons of fission density distributions for PAX-G1 and PAX-G2 reactors, will be utilized in the analytical calculations used to prescribe the R-1 fuel loading distribution. (auth)

**27345** (WANL-TME-1917) PAX-G1 GROSS POWER MEASUREMENTS. Final Test Report. Magaw, J. R.; Sipush, P. J. (Westinghouse Electric Corp., Pittsburgh, Pa. (USA). Astronuclear Lab.). Jan 1970. 40p. Dep. NTIS $5.25.

Declassified 14 Jul 1975.

An experiment performed to assist in prescribing the R-1 fuel loading distribution provided a measured radial fission density (gross) distribution in the PAX-G1A reactor for use in power analysis calculations. The PAX-G1A reactor has a large core (larger than NRX-A/PAX-E series and no inner reflector) and a 60 degree mockup of the R-1, 18 control drum configuration in the beryllium reflector. The experimental procedure utilized U-Al wires located at the core midplane to determine the measured radial fission density distributions and included the self-shielding effects of the U-Al wires previously measured and reported in WANL-TME-1911. Comparisons of the calculated and measured radial fission density distributions show generally good agreement except at the core periphery where differences are larger due to fuel element heterogeneity and irregular core periphery. These comparisons, along with similar comparisons of fission density distributions for the PAX G2 reactor, will be utilized in the analytical calculations to prescribe the R-1 fuel loading specification. (auth)

**27346** (WANL-TME-1925) POST-TEST CALIBRATION OF NRX-A6 CLUSTER EXIT GAS THERMOCOUPLES. Burlas, T. C. (Westinghouse Electric Corp., Pittsburgh, Pa. (USA). Astronuclear Lab.). 30 Apr 1969. 18p. Dep. NTIS $4.00.

Declassified 10 Jul 1975.

Twenty-one cluster exit gas thermocouples were installed in the NRX-A6 reactor and all indicated successful performance throughout the test series. Seven of these thermocouples were salvaged intact after the NRX-A6 disassembly and post operative inspection. They were returned to WANL to determine the extent of any physical degradation caused by the NRX-A6 test and for recalibration. Two of the seven thermocouples returned to WANL were damaged and could not be tested. Of the five that were tested, four indicated accurate temperature measurements as high as 4640°R. One thermocouple (AT 706) was found to have shorted wires behind the junction and hence calibrated low. The preinstallation radiographs did not indicate this condition. However, enough information was obtained from the post calibration of the four good thermocouples to demonstrate the accuracy of the data obtained by the cluster exit gas thermocouples during the NRX-A6 test series was well within the predicted error band. Even with evidence of eutectic melting at the junctions of AT 696 and AT 700, the integrity of the thermocouples to give true temperature indications did not appear to be impaired. They continued to calibrate accurately throughout three runs above 4200°R during the post calibration tests. (auth)

**27347** (WANL-TME-1947) INITIAL CHARACTERIZATION OF BATH SHIELDING MATERIAL. Seaman, F. D. (Westinghouse Electric Corp., Pittsburgh, Pa. (USA). Astronuclear Lab.). Aug 1969. 53p. Dep. NTIS $5.75.

Declassified 10 Sep 1973.

A quantity of extruded boron carbide, aluminum, and titanium hydride (BATH) bar has been produced and subjected to an extensive characterization program. A DRM has been prepared which presents the experimentally determined mechanical and thermophysical properties. The mechanical and chemical and density results exceed all specified program requirements. The thermophysical properties were not specified. Machinability is improved by controlling carbide particle size. The cost is $6–7 per pound. (auth)

**27348** (WANL-TME-1950) EFFECTS OF COMPOSITION AND PROCESSING ON THE PROPERTIES OF NIOBIUM CARBIDE–GRAPHITE COMPOSITE MATERIAL. Singleton, R. H. (Westinghouse Electric Corp., Pittsburgh, Pa. (USA). Astronuclear Lab.). Nov 1969. 178p. Dep. NTIS $12.00.

Declassified 10 Sep 1973.

A process was developed for the hot press fabrication, from powder, of crack-free, strong billets of NbC-graphite using acicular calcined petroleum coke as the graphite source. Thermal expansion measurements showed a reduction in expansion coefficient in the with-grain (WG) direction compared with material

of similar composition made with isotropic graphite flour. The reduction was greater (15%) at the lower NbC content (65 w/o) than at the higher (75 w/o) content (5%). The reduction in expansion coefficient was accompanied by a substantial (35 to 40%) reduction in the across-grain (AG) room temperature flexural strength. AG creep deformation rates at 2500°C and WG room temperature flexural strength were not affected significantly. Post pressing the billets at 2700°C did not affect properties. Post pressing at 2500°C lowered the AG creep deformation rate at 2500°C. Lowering the composition from 75 w/o to 65 w/o decreased the WG expansion coefficient, decreased the AG compressive creep rate, and decreased the room temperature flexural strength, particularly in the AG direction. The composition effect was more pronounced with calcined petroleum coke composites than with flour composites. The averaged data is shown. An analysis of quality control data including creep deformation rate, expansion coefficient and flexural strength performed on 49 vendor-fabricated 75/25 post pressed calcined petroleum coke billets supported the conclusions reached in the experimental program. (auth)

**27349** (WANL-TME-1983) PEWEE-2 HIGH EXPANSION MATRIX DEVELOPMENT PROGRAM. Final Report. (Westinghouse Electric Corp., Pittsburgh, Pa. (USA). Astronuclear Lab.). 1 Dec 1969. 81p. Dep. NTIS $7.25.

Declassified 10 Sep 1973.

The developmental work required to produce and characterize a high expansion matrix for use in the Pewee 2 reactor is described. Information is included on both fabrication and matrix performance. It was found that basic NERVA fabrication technology could be applied directly to the fabrication of high expansion element with only minor difficulties. However, the major problem with the high expansion element is thermal stress. Irrespective of this problem, the AXM based fuel element developed in this study is sufficiently good to be used in Pewee 2. (auth)

**27350** (WANL-TME-1987) PARTIAL CORE VIBRATION TEST RESULTS. Final Report. (Westinghouse Electric Corp., Pittsburgh, Pa. (USA). Astronuclear Lab.). Apr 1970. 29p. Dep. NTIS $4.50.

Declassified 10 Sep 1973.

Current lateral support system designs have resulted in a system which has a core natural frequency of 10 Hz or lower. Previous testing of these designs have been frequency-limited to 10 Hz and above due to displacement limitations of the vibration exciter equipment, even though the critical "G" loads are expected to occur in practice at lower frequencies. The purpose of this test was to investigate the low frequency characteristics of the lateral support system. A flat seal design was tested for simplicity of test and analysis of friction damping phenomena. The results from this development test can be applied to the current lateral support system utilizing angled seals since both systems employ friction damping in the same manner. The analytical model used for predicting the system response was verified as a suitable tool for design purposes. The test has also demonstrated that large core motion can occur at resonance when the input "G" is sufficient to "break friction" between the core and reflector. (auth)

**27351** (WANL-TME-2016) ENGINEERING CRITICAL COMPONENT SPECIFICATION. Part I. Performance/Design and Qualification Requirements. Fuel Elements for NERVA Nuclear Subsystem. (Westinghouse Electric Corp., Pittsburgh, Pa. (USA). Astronuclear Lab.). 15 May 1968. 19p. Dep. NTIS $4.00.

Declassified 29 Jul 1975.

This part of this specification establishes the requirements for performance, design, test and qualification of the component identified as the Fuel Elements (FE). This component includes the fuel elements of various nuclear loadings which make up the reactor. (auth)

**27352** (WANL-TME-2751) RADIATION EFFECTS ANALYSIS REPORT. Nuclear Subsystem. (Westinghouse Electric Corp., Pittsburgh, Pa. (USA). Astronuclear Lab.). Feb 1971. 247p. Dep. NTIS $15.50.

Declassified 11 Sep 1973.

The purpose of this program is to investigate and document the effects of nuclear radiation on the materials and components of the Nuclear Subsystem. The materials used in the NSS Engineering Critical Components (ECC) are evaluated to determine if significant mechanical/physical property changes can be expected to occur when subjected to the anticipated thermal and radiation environments for the specific ECC applications. This evaluation is conducted by rigorously examining data from the NERVA program and other nuclear programs and correlating the findings with the expected NERVA ECC environmental conditions. This correlation then provides a basis for determining whether the material may be employed without radiation-induced performance degradation. In those instances where there is insufficient data available to make the proper correlation, Radiation Effects Information Requests (REIRs) are developed and define what data is needed to support the design and analysis effort. The Radiation Effects Analysis Report represents an integration of existing knowledge on radiation effects on ECC components and materials which have been considered in the design selection process. The analysis integrates the documentation and rationale provided by Materials, Design Engineering and Radiation Effects people into a central document. Either the design is substantiated or REIRs are issued. These REIRs form the basis for a Radiation Effects testing/analysis program which feeds data, through the Materials Department, back into the design process. As the program matures, it will provide justification for each material and component in the NSS to meet the projected radiation environment. (auth)

**27353** (WANL-TME-2761) NERVA CLUSTER AND HOT END HARDWARE. Trade Study No. 774. Polinak, D. (Westinghouse Electric Corp., Pittsburgh, Pa. (USA). Astronuclear Lab.). Jan 1971. 65p. Dep. NTIS $6.25.

Declassified 11 Sep 1973.

A trade study of design concepts for the Cluster Hardware of the NERVA Nuclear Subsystem (NSS) is presented. Previously, Trade Study 751 compared basic core support configurations and resulted in the selection of the counterflow tie tubes with pedestals concept for continued development, and Trade Study 761 resulted in a selection of Inconel 718 stem material, Inconel 625 liner tube material, and two standoff hot end designs using tungsten and composite hot end hardware. Subsequently, a technical directive was issued to incorporate A-286 material for the stems and liner tubes. The purpose of this study is to evaluate and select the most favorable of four variations of the counterflow tie tube concepts. These design approaches differ in the method of primary support and in type of material used for the hot end hardware. The evaluation and selection are based on the construction of a comparison matrix. Detail Specification for Cluster Hardware, and each design approach is evaluated against the requirements. The selection is based on an objective approach which identifies the design approach having the maximum likelihood of meeting the functional, technical, and programmatic requirements. The prime hot end support and tungsten hot end hardware design, Design Approach 1, is selected for the R-1 design. Also, the additional design approach that removes tungsten from the load path is selected for further evaluation. This approach will be handled as a modification of the selected design approach. The designs utilizing cold end prime supports are not selected but are to be retained for possible evaluation at some future date. Recommendations are made to develop application of a carbide barrier coating for tungsten and to continue the bonding development program for bonding coated tungsten to NbC coated composite. (auth)

**27354** (WANL-TME-2762) CORE PERIPHERY. Trade Study No. 778. Davidson, A. (Westinghouse Electric Corp., Pittsburgh, Pa. (USA). Astronuclear Lab.). Jan 1971. 61p. Dep. NTIS $6.25.

Declassified 11 Sep 1973.

A trade study of design approaches for the Core Periphery, a component of the NERVA Nuclear Subsystem, NSS, is presented. The primary purpose is to identify the R-1 candidate periphery design approach for continued detail design and development of this component consistent with the programmatic and technical requirements for the ten hour, full-flow-cycle engine as defined in the NERVA Program Requirements Document. In addition, this study is to provide recommendations for longer range backup areas of development for possibly enhancing the confidence in the periphery in post R-1 reactors. The evaluation and selection was based on the construction of a comparison matrix. Each alternate was evaluated against the requirements and the final selection based on an objective approach which identified the concept having the maximum likelihood of meeting the functional, technical, and programmatic requirements. A corrosion resistant core periphery design is recommended for the R-1 NERVA reactor utilizing the basic concepts of Design Approach 1 (Corrosion Resistant, Double Metal Wrapper, Forward End Supported Filler Strips). Some areas of design modification and material investigation for this approach are also identified as a result of the analysis accomplished in support of this trade study. In addition it is recommended that a backup longer range study of alternate, corrosion-resistant, insulator materials be pursued to assure that no material possibility is missed that could enhance the confidence in the periphery if the material was incorporated in the R-2 reactor which has a more ambitious endurance goal. (auth)

**27355** (WANL-TME-2763) LATERAL SUPPORT. Data Item S-54, Trade Study No. 782. (Westinghouse Electric Corp., Pittsburgh, Pa. (USA). Astronuclear Lab.). Jan 1971. 69p. Dep. NTIS $6.50.

Declassified 11 Sep 1973.

A Trade Study was conducted to select a lateral support design approach that can be further developed for the NERVA Nuclear Subsystem (NSS) reflector assembly. Five design approaches were evaluated by the various technical disciplines and their individual inputs condensed into a comparison matrix that was used to select the more desirable design approach. The evaluation of the design approaches was primarily based on meeting the functional, technical, and non-technical requirements identified in the Reflector Assembly Specification, No. EC-677559. Design Approach 5 (wedged seal with end-guided plungers) was selected as the design to be further developed into a lateral support system for the NSS reflector assembly. This design approach was selected because it provides the most flexibility for satisfying the launch, boost and space operational requirements defined in ECC Specification No. EC-677559. This is primarily due to the fact that it can function at high coefficients of friction (approaching 1.0) than any of the other design approaches. An early test of a partial length lateral support system test was recommended to provide data for input to the detailed design. A full-length vibration test accurately simulating the core restraints was recommended prior to R-1 assembly. (auth)

**27356** (WANL-TME-2780) ORIFICE JET BRAZING PROCESS DEVELOPMENT, QUALIFICATION, AND INITIAL APPLICATION. (Westinghouse Electric Corp., Pittsburgh, Pa. (USA). Astronuclear Lab.). May 1971. 102p. Dep. NTIS $8.25.

Experiments were carried out to develop acceptable procedures for brazing molybdenum alloy orifices to fuel element channel inlets of the NERVA R-1 reactor core. Results achieved with various procedures are described, and qualification tests of the selected process are documented. The recommended procedure includes preplacing of Au-Ni-Cr alloy washers and induction heating to 1600°F, holding two minutes, heating further to 2400°F, holding one minute, and allowing to cool. Inert atmosphere is used, and fixturing maintains proper positioning of the orifices. Leak testing of the joints has demonstrated reproducibly satisfactory sealing. Repair brazing is feasible if needed. (auth)

**27357** (WANL-TNR-060) ARGONNE NUCLEAR ROCKET STUDY. Sege, G. (Westinghouse Electric Corp., Pittsburgh, Pa. (USA). Astronuclear Lab.). 11 Jul 1962. 12p. Dep. NTIS $4.00.

Declassified 11 Jul 1975.

Argonne National Laboratory's study of a nuclear rocket reactor (considered as a backup for the NERVA-ROVER development) is described briefly (a few other possible developments are treated even more briefly). The Argonne program has been narrowed to consideration of a 1000 to 20,000 MW fast reactor with a tungsten fuel matrix. A ground rule of the study was that only fuel materials other than fueled graphite be considered. Tentative reactor core designs are presented involving three possible fuels (uranium dioxide, uranium sulfide or uranium phosphide) in a tungsten matrix. Tungsten-rhenium alloys were considered for the unfueled structures. Other reactors mentioned were a GE fast reactor, the Lewis tungsten-184 thermal reactor, DUMBO (a LASL zirconium-hydride-moderated thermal reactor) and a LASL tungsten fast reactor. (LTN)

**27358** (WANL-TNR-172) NRX-A TEST PROGRAM. (Westinghouse Electric Corp., Pittsburgh, Pa. (USA). Astronuclear Lab.). 30 Nov 1962. 34p. Dep. NTIS $4.75.

Declassified 14 Jul 1975.

A reactor test program is defined leading to a reactor suitable for incorporation in the NERVA engine. A general description of the individual tests which are tentatively planned for the NRX-A test program are given. The NERVA reactor development effort is an extension of a reactor development program being conducted for the Atomic Energy Commission by Los Alamos Scientific Laboratories. The prime objective is to produce a nuclear reactor which, when assembled into a complete nuclear rocket engine system, will be suitable for practical propulsion service. To provide the NERVA reactor test program with the reliability required of the reactor, specific nuclear characteristics for each NRX series reactor will be experimentally verified in a proof test experiment, PTX, prior to shipment of the reactor to the Nevada Test Site, (NTS). The prime objective of the NRX test program is to evaluate the performance of candidate reactor designs for incorporation in the NERVA engine. These tests will be conducted primarily to determine reactor performance since non-NERVA control and propellant feed systems will be used during the NRX-A tests. The reactor must be shown to be capable of startup, shutdown, restart and cooldown at specified rates and steady-state operation of specified duration and power levels without structural deterioration beyond established limits. Presuming achievement of adequate performance capabilities, reliability will be the most important consideration in the application of the reactor to the NERVA engine. Details of the various planned tests are given. (auth)

**27359** (WANL-TR-6548) NERVA FUEL DEVELOPMENT STATUS (MEETING REPORT). Zemanick, P. P. (Westinghouse Electric Corp., Pittsburgh, Pa. (USA). Astronuclear Lab.). 2 Nov 1970. 8p. Dep. NTIS $4.00.

Declassified 22 Jul 1975.

The meeting program is given. Only one paper is discussed in detail: LASL has developed a thermal stress test rig for testing fuel elements. Test results are given for several production lots for which the matrix materials are given. Poor lots ruptured at 80 Btu/sec.in. whereas good lots could not be broken with the rig at 150 Btu/sec.in. (LTN)

**27360** (WANL-TR-6575) [TRIP TO AEC TO PRESENT AS PART OF THE PEWEE-2 READINESS REVIEW THE WANL NON-FUELED COMPONENT ANALYSIS TEST AND PERFORMANCE PREDICTIONS]. Smith, R. A. (Westinghouse Electric Corp., Pittsburgh, Pa. (USA). Astronuclear Lab.). 24 Dec 1970. 22p. Dep. NTIS $4.25.

Declassified 22 Jul 1975.

The agenda of the PEWEE-2 review is given. Viewgraphs used by WANL during the presentation on non-fueled components are attached. (LTN)

**27361** (WANL-TR-6669) [TRIP TO LASL TO DISCUSS FUEL STRUCTURAL BEHAVIOR, STRUCTURAL MODELING, AND THERMAL STRESS TESTING]. Tobin, J. M.; Stancompiano, P. A. (Westinghouse Electric Corp., Pittsburgh, Pa. (USA). Astronuclear Lab.). 1 Sep 1971. 10p. Dep. NTIS $4.00.

Declassified 22 Jul 1975.

At a meeting between WANL and LASL representatives, NERVA fuel element testing methods were discussed: Thermal stress tests, corrosion performance of the coating-matrix combination, stress-strain tests, etc. Interpretational methods, the value of some models or theories, the significance of cracks of various types and computer programs were discussed. (LTN)

**27362** STUDY ON THE THERMOHYDRAULIC CHARACTERISTICS OF MARINE NUCLEAR REACTOR, 1. Bibliographical Investigation and Description of the Experimental Loop. Kurosawa, A.; Otsuji, T. (Kobe Univ. of Mercantile Marine (Japan)). Kobe Shosen Daigaku Kiyo. Dai-2-rui. Kokai, Kikan, Rigaku-hen; No. 22, 253-278 (Aug 1974). (In Japanese).

91 refs.

The effect of ship motion on the characteristics of marine nuclear reactors is examined. The effect of ship motion is important for the assurance of reactor safety and understanding the dynamic behavior of reactors. Previous work relating to this theme is summarized, and problems to be solved are described. A review of recent progress in the field of forced convection boiling heat transfer and two-phase flow dynamics which constitute the basis of the problem are presented. The experimental facility consists of a refrigerant-113 loop and the apparatus which moves the loop vertically to simulate ship's motion. The maximum operating pressure of the loop is 5kg/cm$^2$ abs., and the maximum power input is 20kW. Both conditions of natural and forced circulation are available by means of adjusting valves. The amplitude (peak-to-peak) of the moving apparatus is 5.4m, and the frequency can be varied continuously from 0 to 0.3Hz. Previous experimental results are presented, and the future plan of the study are described. (auth)

## Reactor Safety and Environmental Aspects

*Refer also to abstracts 25901–25905 and 26035.*

**27363** (AED-CONF-74-712-002) RELIABILITY DATA ACQUIRED IN OPERATING EXPERIENCE. II. Hoertner, H.; Wohak, B. (Technische Univ. Muenchen, Garching (F. R. Germany). Lab. fuer Reaktorregelung und Anlagensicherung). 1974. 10p. (In German). INIS.

From KTG special seminar on statistical methods; Berlin, F. R. Germany (5 Mar 1974).

Failure statistics are used to establish failure parameters of power plant units and systems with the aid of a data bank system where the collected data are classified, stored, and processed in accordance with established criteria. The information system which is under construction at LRA (Laboratorium fuer Anlagen-

sicherung und Reaktorregelung—Laboratory for Plant Safety and Reactor Control in Garching/Muenchen) is tested by a model case. (GE)

**27364** (AED-CONF-75-003-013) EFFECT OF THE BBR REACTOR VENTING SYSTEM ON THE THERMOHYDRAULIC BEHAVIOR OF THE OVERALL SYSTEM DURING BLOWDOWN. Klenke, H. (Babcock—Brown Boveri Reaktor G.m.b.H., Mannheim (F. R. Germany)). 1975. 8p. (In German). INIS.

From special meeting on thermo and fluid dynamic problems related to reactor incidents; Stuttgart, F. R. Germany (28 Jan 1975).

8 figs. With abstract.

It was shown that the venting systems used in the PWR reactor facilities are very effective in meeting the problems of "steam binding" which arise in connection with ruptures on the cold side. In double-end ruptures, their influence is insignificant during the blowdown phase whereas in the reflood phase the core flooding rate is considerably increased. In small ruptures, the water volume in the core is already increased by the venting systems during the "pool boiling" phase, i.e. after interruption of the forced circulation. (GE)

**27365** (ANCR-1229) EVALUATION OF PIPING HEAT TRANSFER, PIPING FLOW REGIMES, AND STEAM GENERATOR HEAT TRANSFER FOR THE SEMISCALE MOD-1 ISOTHERMAL TESTS. French, R. T. (Aerojet Nuclear Co., Idaho Falls, Idaho (USA). Idaho National Engineering Lab.). Aug 1975. Contract E(10-1)-1375. 59p. (NRC-2). Dep. NTIS $5.45.

Selected experimental data pertinent to piping heat transfer, transient fluid flow regimes, and steam generator heat transfer obtained during the Semiscale Mod-1 isothermal blowdown test series (Test Series 1) are analyzed. The tests in this first test series were designed to provide counterparts to the LOFT nonnuclear experiments. The data from the Semiscale Mod-1 intact and broken loop piping are evaluated to determine the surface heat flux and average heat transfer coefficients effective during the blowdown transient and compared with well known heat transfer correlations used in the RELAP4 computer program. Flow regimes in horizontal pipe sections are calculated and compared with data obtained from horizontal and vertical densitometers and with an existing steady state flow map. Effects of steam generator heat transfer are evaluated quantitatively and qualitatively. The Semiscale Mod-1 data and the analysis presented in this report are valuable for evaluating the adequacy and improving the predictive capability of analytical models developed to predict system response to piping heat transfer, piping flow regimes, and steam generator heat transfer during a postulated loss-of-coolant accident (LOCA) in a pressurized water reactor (PWR). 16 references. (auth)

**27366** (ANCR-1231) EXPERIMENTAL DATA REPORT FOR SEMISCALE MOD-1 TEST S-02-1 (BLOWDOWN HEAT TRANSFER TEST) Crapo, H. S.; Jensen, M. F.; Sackett, K. E. (Aerojet Nuclear Co., Idaho Falls, Idaho (USA)). Jul 1975. Contract E(10-1)-1375. 90p. Dep. NTIS $5.45.

Recorded test data are presented for Test S-02-1 of the Semiscale Mod-1 blowdown heat transfer test series. Test S-02-1 is one of several Semiscale Mod-1 experiments conducted to investigate the thermal and hydraulic phenomena accompanying a hypothesized loss-of-coolant accident (LOCA) in a water-cooled nuclear reactor system and to provide data for the assessment of the Loss-of-Fluid Test (LOFT) design basis. Test S-02-1 was conducted from an initial temperature of 546$^0$F (cold leg) and an initial pressure of 2,253 psig. A simulated double-ended offset shear of the hot leg initiated the test to investigate the system response to a depressurization transient with a moderately heated core (75 percent design power level). An electrically heated core was used in the pressure vessel to simulate the effects of a nuclear core. The flow resistance of the intact loop was based on core area scaling. During system depressurization, core power was reduced from the initial level of 1.2 MW in such a manner as to simulate the surface heat flux response of the LOFT nuclear fuel rods until such time that departure from nucleate boiling (DNB) occurs. Blowdown to the pressure suppression system was accomplished without simulated emergency core cooling injection or pressure suppression system coolant spray. (auth)

**27367** (ANCR-1251) LOFT DATA REDUCTION. Norman, N. L. (Aerojet Nuclear Co., Idaho Falls, Idaho (USA)). Aug 1975. Contract E(10-1)-1375. 25p. Dep. NTIS $4.00.

The Loss-of-Fluid Test (LOFT) Facility is an experimental facility built around a "scaled" version of a large pressurized water reactor (LPWR). LOFT will be used to run loss-of-coolant experiments (LOCEs) and to acquire the necessary data required "to evaluate the adequacy and improve the analytical methods currently used to predict the loss-of-coolant accident (LOCA) response of LPWRs" and "to identify and investigate any unexpected event(s) or threshold(s) in the response of either the plant or the engineered safety features and develop analytical techniques that adequately describe and account for the unexpected behavior(s)". During the LOCE this required data will be acquired and recorded in both analog and digital modes. Subsequent to the test the analog data will also be converted to the raw digital mode. This raw digital data will be converted to the desired engineering units using the LOFT Data Reduction System. This system is implemented on the IBM 360/75 and is a part of a commercially available data processing program called MAC/RAN III. The theory of reducing LOFT data to engineering units and the application of the MAC/RAN III system to accomplish this reduction is given. (auth)

**27368** (CENPD-107) ATWS MODEL MODIFICATIONS TO CESEC, Supplement 3. (Combustion Engineering, Inc., Windsor, Conn. (USA)). Aug 1975. 200p. Combustion Engineering, Inc., Windsor, CT.

Supplement 3 to CENPD-107 augments the information contained in CENPD-107 Supplement 1, and is provided in response to the following questions of the March 4 letter on ATWS: 240.1, 240.2, 240.8, 240.9, 240.10, 240.11, 240.20, 240.21, 240.22, 240.23, 240.24, 240.26, and 240.27. (auth)

**27369** (CENPD-132(Suppl.2)) CALCULATIONAL METHODS FOR THE C-E LARGE BREAK LOCA EVALUATION MODEL, Supplement 2. (Combustion Engineering, Inc., New York (USA)). Jul 1975. 68p. Combustion Engineering, Inc., Windsor, CT

This document presents descriptive material which represents a modification or addition to the Combustion Engineering (C-E) Large Break Loss-of-Coolant Accident analysis methodology and, as such, is a supplement to Reference 1. The specific modifications or additions to the evaluation model are summarized below: the containment wall noding technique has been revised in order to provide a converged wall temperature solution; based on a recent review of steam-water mixing data, the resistance across the ECCS injection section, during the period after the safety injection tanks have emptied, has been revised; and reflood heat transfer coefficients for 16 x 16 fuel assemblies have been selected according to a conservative, empirical model. The effect of these modifications or additions to the C-E evaluation model results are exemplified by parameter studies presented in Appendix A. (auth)

**27370** (CENPD-158(Suppl.2)) ANTICIPATED TRANSIENTS WITHOUT REACTOR TRIP. Topical Report, Supplement 2. (Combustion Engineering, Inc., Windsor, Conn. (USA)). Aug 1975. 12pp Combustion Engineering, Inc., Windsor, CT.

CENPD-158, "Anticipated Transients Without Reactor Trip" was submitted to the NRC in September 1974. A request for additional information on ATWS was issued by the NRC in a letter of March 4, 1975. This supplement provides C-E's response to the following questions of the March 4 letter: 210.3, 210.8, 210.9, 210.10, 310.1, 310.9, and 310.10. (auth)

**27371** (CENPD-183) C-E METHODS FOR LOSS OF FLOW ANALYSIS. (Combustion Engineering, Inc., Windsor, Conn. (USA)). Jul 1975. 80p. Combustion Engineering, Inc., Windsor, CT.

A method is described for analyzing loss of reactor coolant forced flow in licensing submittals. The method, which is referred to as the dynamic method, includes transient hydraulic effects in the reactor coolant channels in the calculation of the minimum Departure from Nucleate Boiling Ratio (DNBR) in the hot channel. Also included as an appendix is a discussion of the method of loss of flow analysis used for C-E licensing submittals to date. This method, which is referred to as the static method, neglects transient hydraulic effects in the reactor coolant channels. Example calculations are presented and the results of the dynamic method of analysis are compared to those from the static method. It is concluded that the dynamic method of analysis provides an adequately conservative means of determining the consequences of LOF transients. 9 references. (auth)

**27372** (CONF-701074-P2, pp 219-240) SOME PROBLEMS OF COOLING THE VVER-1000 REACTOR CORE. Naleton, V. I.; Spaskov, V. P.; Podshibyakin, A. K.; Kulikov, E. V.; Abramov, V. I.; Sarigin, A. P.; Denisov, V. P.; Vikhorev, U. V.; Birukov, G. I. 1970. Translated from Trudy Nauchno-Tekhnicheskoi Konferentsii "Atomnaya Energetika, Toplivnye Tsikly, Radiatsionnoe Materialovedenie", Ul'yanovsk, 5—10 Oktyabrya 1970 G. Vol. II.

From conference on atomic power, fuel cycles, and radiation study of materials; Ul'yanovsk, USSR (5 Oct 1970).

In proceedings of the scientific-technical conference "atomic power, fuel cycles, radiation study of materials".

A description is presented of the WWER-1000 reactor cooling system. Operation under steady state and also in more dangerous emergency conditions in case of loss of the coolant is discussed together with the protection of the reactor core during emergency conditions. (auth)

**27373** (DEU-75-2) BURN-OUT MEASUREMENTS IN THE COURSE OF STUDIES OF SAFETY. P. 2. Studies of the Critical Heat Flux Under Stationary and In-Stationary Conditions in Frigen 12 and Water. Hein, D.; Kastner, W. (Maschinenfabrik Augsburg-Nuernberg (M. A. N.) A. G., Nuernberg (F. R. Germany); Zentralstelle fuer Atomkernenergie-Dokumentation, Leopoldshafen (F. R. Germany)). Jan 1972. 64p. (In German). INIS.

The research programme included burnout tests on annular space geometries as well as 4-rod and 9-rod clusters under steady state and transient conditions using Frigen 12 and water. Roughly 520 burnout points, of which about 90 were obtained in water and 430 in Frigen 12, permit essential conclusions to be drawn regarding the mechanism of film boiling inception during transient events. The information obtained forms a basis for considerations directed at establishing similarity relationships for transient events, such as fast power and mass flow excursions. (GE)

**27374** (DP-Report-700) MODEL OF DEPRESSURISATION OF A STEAM-CYCLE HTR. Dragon Project Report. Soubelet, G. (UKAEA Reactor Group, Winfrith. Atomic Energy Establishment). May 1970. 50p. Dep. NTIS (US Sales Only) $5.50.

The sudden development of a breach in the primary circuit of a steam-cycle HTR may cause abnormal gas flows and pressures. From the point of view of safety, it is of interest to know whether these could: damage any of the components in the primary circuit (such as the blowers or the insulation), or cause fission products to be released into the gas which are normally held on surfaces, e.g., plated-out or on stagnant dust. A method of representing a steam-cycle HTR by a model particularly suited to an analog computer is described which can be used to calculate the gas flows and pressures during the transient following a burst in a typical system. It then considers one particular design, and gives results of analog computer tests. For this design it was found that the behavior of system pressure depended on the size and resistance of the discharge hole rather than its position. Only with holes of manhole size, or, e.g., an ejected blower, were the gas velocities significantly higher (2 to 6 times) in the core or heat exchangers. There never was a reversal of flow or pressure drop. The largest increase in previous drop across the blowers was about 22 percent, so they probably would not be damaged and would be available for decay heat removal. (auth)

**27375** (EQL-9) ASSESSMENT OF EMERGENCY CORE COOLING SYSTEM EFFECTIVENESS FOR LIGHT WATER NUCLEAR POWER REACTORS. Finlayson, F. C. (California Inst. of Tech., Pasadena (USA)). May 1975. 346p. Dep. NTIS $20.50.

The effectiveness of Emergency Core Cooling Systems (ECCS) for light water nuclear power reactors was the subject of hearings conducted by the AEC over the two years from 1971 through 1973. An independent, objective review and assessment of the technical issues associated with ECCS effectiveness was conducted in a study performed at the Environmental Quality Laboratory of the California Institute of Technology. From the review, the critical technical parameters influencing ECCS performance are identified. Of fifteen parameters cited by the Advisory Committee on Reactor Safety in the hearings as being of unproved conservatism, essentially all are reviewed in detail. The relative influence of uncertainties in the performance criteria associated with these parameters is assessed. Alternative responses to resolution of the ECCS problem are analyzed. The importance of the core reflooding rate in resolving the technical issues of the problem is emphasized. The conservatism of the proposed criteria (current and past) is reviewed. Recommendations are made for improvements in criteria conservatism, especially in the establishment of minimum reflood heat transfer rates (or alternatively, reflooding rates). Several new and/or accelerated research programs and additional large scale testing programs are also recommended. (67 references) (auth)

**27376** (ETR-1003) VELOCITIES OF TORNADO GENERATED MISSILES. Iotti, R. C. (Ebasco Services, Inc., New York (USA)). Feb 1975. vp. Ebasco Services, Inc., New York, NY

A rational procedure of calculating the velocities of tornado generated missiles is presented. A tornado model has been developed to compute velocities reached by missiles injected in tornadic wind field, in order that their hazards to nuclear installations be properly assessed. A spectrum of typical missiles has been selected and their behavior has been evaluated in tornadic wind fields of four different intensities ranging from 200 mph to 360 mph. The results of the study indicate that for any given tornado each missile can achieve any given velocity within the spectrum of attainable velocities and that the most probable velocity is reasonably represented by that calculated employing a constant random tumbling mode drag coefficient to simulate the different drag forces acting on a missile through its trajectory. In order to establish a design basis missile spectrum to be used in assessing the hazards to the nuclear plant, the criterion chosen to select a design basis velocity for each missile is that the overall probability of having any tornado striking the plant site, coupled with the probability of that tornado attaining winds of a given intensity, and further multiplied by the probability of generating a missile of the design basis velocity equal to or less than $10^{-7}$, considering the possibility of having multiple missiles. This value of probability for a design basis event provides an acceptable conservative criterion for design evaluation when one conservatively assumes that the combined probability of the generated missile impacting a critical component, of impacting at the "worst" angle for most damaging penetration, and the probability that, if struck, loss of system function occurs together with a single failure in the damaged system's redundant counterpart, if any, is unity. (auth)

**27377** (EURFNR-1200) MODEL TESTS FOR THE EMERGENCY COOLING SYSTEM OF THE PROTOTYPE REACTOR SNR 300. Hain, H.; Hofmann, F.; Kirsch, D.; Kleefeldt, K.; Kramer, W.; Meyder, R. (Kernforschungszentrum Karlsruhe (F.R. Germany)). Jun 1974. Translation of KFK-1895. 214p. Dep. NTIS $7.60.

Work performed under United States--Euratom Fast Reactor Exchange Program.

The accident considered is a pipe rupture of the pump pressure pipe coupled with a failure of the pump shutdown system. The emergency cooling concept is based upon natural convection inside the tank generated by heat added in the core and a heat sink consisting of immersion coolers attached to the inside of the tank. This cooling circuit within the tank is covered by a computer program (NOTUNG) drafted by the Interatom Company for a theoretical model describing the thermodynamic behavior of the circuit. Model tests to support the analytical calculations are outlined. Comparison between calculation and experiment was made. (auth)

**27378** (EURFNR-1242) PROBLEM OF PIN-TO-PIN FAILURE PROPAGATION IN SODIUM-COOLED FAST BREEDER REACTORS. Jacobi, S.; Kramer, W.; Schleisiek, K. (Kernforschungszentrum Karlsruhe (F.R. Germany)). Feb 1975. Translation of KFK-2047. 37p. Dep. NTIS $4.00.

Work performed under United States--Euratom Fast Reactor Exchange Program.

The possibility of a pin-to-pin failure propagation is an important question in connection with LMFBR safety analysis. A brief review is given of the present state of knowledge. Conceivable mechanisms of an accident sequence are discussed, and the possibilities for a fast failure propagation are demonstrated. A pin-to-pin failure propagation is concluded to be rather unlikely but it may not be excluded completely under certain accident conditions. (auth)

**27379** (KFK-2176) COMPARISON OF METHODS FOR CALCULATION OF LARGE CLADDING DEFORMATION IN THE CASE OF A LOSS-OF-COOLANT ACCIDENT. Fabian, H.; Krugmann, U.; Lassmann, K.; Schwarz, R. (Kernforschungszentrum Karlsruhe (F. R. Germany). Projekt Nukleare Sicherheit; Technische Univ. Darmstadt (F. R. Germany). Fachgebiet Reaktortechnik). Jun 1975. 73p. (In German). Dep. NTIS (US Sales Only) $6.75.

Some results of mechanical computations of cladding deformation are discussed in the case of a loss-of-coolant accident. The models for data-creation realize isothermal and transient conditions. The creep-deformation of the cladding is caused by significant temperature and pressure profiles. In all cases the constitutive creep-law of Norton is used. The computations are based on three methods: analytical solution (one-dimensional); finite element solution (two-dimensional); and theory of creeping shells (two-dimensional). The influence of large deflection theory is discussed. In comparing the results it is evident that the differences in the methods are covered by a small variation of the creep-parameters. 12 references. (auth)

**27380** (NP-20554) CORROSION EFFECTS OF CHEMICAL ENVIRONMENTS (SHORT TERM) RESULTING FROM POSTULATED ACCIDENTS ON REQUIRED SAFETY RELATED TRANSMITTERS. (Westinghouse Electric Corp., Pittsburgh, Pa. (USA). PWR Systems Div.). 25 Jul 1975. 14p. Westinghouse Electric Corp.; Pittsburgh, PA.

The capability of the safety related transmitters located inside PWR containments to withstand the chemical environment resulting from postulated accidents thereby allowing the transmitters to complete their assigned protection and safeguards initiation functions is analyzed. The analysis is applicable to current Westinghouse plants seeking operating licenses. The analysis includes a study of the transmitters required for pro-

tection and safeguards actuation, their materials of construction, and the resistance of the material to the potentially corrosive environment associated with the accident. (auth)

**27381** (NP-20562) ENVIRONMENTAL QUALIFICATION OF LIMITORQUE SMB-O MOV OPERATORS UTILIZING CLASS H INSULATED PEERLESS ELECTRIC MOTORS. Eicheldinger, C. (Westinghouse Electric Corp., East Pittsburgh, Pa. (USA)). 10 Jul 1975. 5p. Westinghouse Electric Corp., Pennsylvania.

A technical basis is presented for the environmental qualification of valve operators in PWR engineered safety systems. (JWR)

**27382** (NP-20563) FAILURE MODE ANALYSIS FOR SAFETY RELATED SOLENOID VALVES IN AN ACCIDENT ENVIRONMENT. Eicheldinger, C. (Westinghouse Electric Corp., East Pittsburgh, Pa. (USA)). 15 Aug 1975. 5p. Westinghouse Electric Corp., Pittsburgh.

It is shown that the containment isolation system solenoid valves, which regulate the air supply to safety related air operators, will close (its safe position) in a postulated accident environment for all potential modes of failure in Westinghouse PWR plants. (auth)

**27383** (ORNL-TM-5086) MONTHLY HIGHLIGHTS FOR OFFICE OF NUCLEAR REGULATORY RESEARCH PROGRAMS AT OAK RIDGE NATIONAL LABORATORY. Fee, G. G. (comp.). (Oak Ridge National Lab., Tenn. (USA)). Aug 1975. 27p. Dep. NTIS $4.00.

Brief highlights are presented for the following programs: heavy section steel technology; fission product beta and gamma energy release; LOCA release from LWR fuel; multirod burst tests; NSIC; PWR blowdown heat transfer; zircaloy fuel cladding collapse studies; zirconium metal-water oxidation kinetics; transient release from LMFBR fuel; HTGR safety analysis; and design criteria for piping and nozzles. (JWR)

**27384** (TID/SNW-128) NUCLEAR SAFETY ANALYSIS FOR WANL BUILDING 9. Nuclear Safety Manual. Appendix II of IL-020, Revision III. (Westinghouse Electric Corp., Pittsburgh, Pa. (USA). Astronuclear Lab.). Aug 1969. 37p. Dep. NTIS $5.00.

Declassified 16 Jul 1975.

Procedures are established to assure that criticality control is maintained to prevent a nuclear incident in the handling of enriched uranium bearing materials in Building 9. The control system detailed limits the quantity and/or geometry of $^{235}U$ in clearly marked locations by limiting and monitoring the movement of fuel material from location to location and maintaining the fuel in safe spatial relationships within the locations. The General Regulations apply to all activities and locations in the building which are involved with $^{235}U$-bearing materials. The lines of personnel responsibility for assuring that a nuclear incident does not occur are laid down. Specific regulations applicable to particular areas are listed: work area; the drum storage and scrapping area; the two- and four-suitcase racks and drum area; and the vault. (auth)

**27385** (TID/SNW-129) NUCLEAR SAFETY ANALYSIS FOR WANHES. Salvador, L. A. (Westinghouse Electric Corp., Pittsburgh, Pa. (USA). Astronuclear Lab.). 1968. 25p. Dep. NTIS $4.25.

Declassified 16 Jul 1975.

To maintain adequate criticality control within the (WANHES) Westinghouse Astronuclear Hydrogen Experimental Site, Waltz Mills Site, criticality control procedures have been established with reference to the Criticality Hazards Control Guide (WANL-TME-185, November 1962), and the "Thermo-Flow Criticality Hazards Control Procedure, HC-100". The control procedures will insure safety from criticality hazards by either limiting mass, establishing the geometry, or restricting the handling of enriched uranium within and between designated work areas and their internal criticality zones. The WANHES facility has been divided into work areas and some work areas are designated as criticality zones. The basic control area is the criticality zone. The boundaries of these zones are designated by special tape where there is no wall or barrier to provide a physical separation. Where walls serve as boundaires of a criticality zone, the entrances are marked by sign or special tape to designate the criticality zone. In addition, signs designating element or cluster limits are displayed. A detailed listing of the criticality zones is given. Both mass and geometry are used as control parameters. The control in some zones is based on mass; in others, on geometry. However, the specific parameter of control and applicable rules, limitations, and restrictions are posted in each work area or criticality zone. The supervisor of WANHES is responsible for the enforcement of nuclear safety. This responsibility is not delegated, but for implementation and control reasons, certain duties with respect to criticality hazards control are assigned to specific individuals. To strengthen the criticality hazards control procedures, all forms and categories of uranium-bearing material entering or leaving the WANHES site or the individual criticality zones must be cleared through the WANHES Fuel Custodian or his alternate. In addition, a Nuclear Safety Engineer will make periodic inspections of the facilities. (auth)

**27386** (UCID-16893) SAFETY ANALYSIS FOR NEUTRON RADIOGRAPHY OF HIGH EXPLOSIVES AT THE LPTR. Sutton, S. B.; McCauley, E. W. (California Univ., Livermore (USA). Lawrence Livermore Lab.). Aug 1974. 53p. Dep. NTIS $5.45.

Hazards associated with neutron radiography of high explosive samples at the Livermore Pool Type Reactor (LPTR) were assessed. Preliminary discussions recognized the possibility of accidental detonation of the high explosive sample. Thus efforts centered upon definition of the environment resulting from a high explosive burn and assessment of the effect of this environment on surrounding reactor structures. (auth)

**27387** (WANL-TME-064) SHIPMENT OF THE INTEGRAL REACTOR. Ortenberg, L. I. (Westinghouse Electric Corp., Pittsburgh, Pa. (USA). Astronuclear Lab.). 30 Apr 1962. 17p. Dep. NTIS $4.00.

Declassified 22 Jul 1975.

Various accidents during shipment are described and the maximum credible incident is concluded to be that of water immersion and flooding. Possible methods of protection against criticality resulting from these accidents are investigated and a final design for a safing system is defined. It incorporates two major subsystems: A sealed shipping structure to prevent water penetration to the core and poisoning in the event of breakdown of the sealing subsystem. The preliminary conceptual design of a shipping container is described. The design consists of a structure with an enclosing sealed vessel for the reactor which in turn is shock mounted in a larger watertight container. A poisoning system is defined in which natural boron carbide encased in a suitable tabular structure is inserted in 6360 coolant channels. It is estimated that this will result in a $k_{eff}$ of 0.8 in the event of water immersion and flooding. In view of the chain of improbable events necessary for the breakdown of the total system it is felt that the integral reactor may be shipped with confidence and criticality control maintained. (auth)

**27388** (WANL-TME-071) DOSE RATES AND RADIOLOGICAL EFFECTS FROM A FRAGMENTED CORE. Grandy, G. L. (Westinghouse Electric Corp., Pittsburgh, Pa. (USA). Astronuclear Lab.). 13 Apr 1962. 10p. Dep. NTIS $4.00.

**27389** (WANL-TME-761(Suppl.3)). SUPPLEMENT TO NRX-A2 SAFETY EVALUATION REPORT. (Westinghouse Electric Corp., Pittsburgh, Pa. (USA). Astronuclear Lab.). 5 Aug 1964. 42p. Dep. NTIS $5.25.

Declassified 10 Jul 1975.

Additional details on safety aspects of the NRX-A2 power test are presented. Information is included on: NRX-A1 and KIWI-B4D test results, test facilities control, thermal design of the NRX-A2 power test, emergency shutdown, test operations, and fission product release and radiation doses for the power run. (HDR)

**27390** (WANL-TNR-099(Add.2)) ADDENDUM NO. 2 TO WANL-TNR-099. Hemmerle, E. H. (Westinghouse Electric Corp., Pittsburgh, Pa. (USA). Astronuclear Lab.). 2 Jan 1964. 9p. Dep. NTIS $4.00.

Declassified 11 Jul 1975.

Reviewers of a report on criticality design of WANEF storage vault requested additional information and suggested the use of a better analytical model to determine the reactivity shutdown of the flooded array of fuel element shipping suitcases placed on a shelf of the fuel storage vault. Results of these additional calculations are given and indicate that the array is safe flooded. (auth)

**27391** (WANL-TNR-099(App.B)(Rev.)) NUCLEAR SAFETY ANALYSIS. WANEF Test Cell Fuel Storage Rack. Revised Appendix B. (Westingbouse Electric Corp., Pittsburgh, Pa. (USA). Astronuclear Lab.). 8 Nov 1965. 13p. Dep. NTIS $4.00.

Declassified 11 Jul 1975.

This revision describes fuel element storage racks at WANEF and presents the nuclear safety analysis of the cluster storage array on the racks. Radiation monitoring and criticality alarm systems are discussed briefly. (LTN)

**27392** (WANL-TNR-099(Rev.C)) SAFETY REPORT FOR THE WESTINGHOUSE ASTRONUCLEAR EXPERIMENTAL FACILITY (PAX AND FCX). (Westinghouse Electric Corp., Pittsburgh, Pa. (USA). Astronuclear Lab.). [nd]. 74p. Dep. NTIS $6.75.

Declassified 11 Jul 1975.

Revisions to take care of planned modifications in PAX-E in support of NRX-A6 and R-1 reactors were the main cause of changes in the Safety Report. These modifications involve changes in the reflectors, supports, fuel element loading and control drums. Provisions for additional poisons during manual changes to the mockup (reflector segment, control drums, etc.) are specified in greater detail. Possible hazards due to additional neutron reflection from materials or people close to the reactor are treated in more detail. The design features of the PAX assembly and the administrative controls and engineered safeguards that have been incorporated in the WANEF operating procedures are considered to be most adequate in preventing a criticality accident in the course of the NERVA experimental program. The consequences of those accidents which have been judged to be credible fall within the limitations imposed by control vane melting and the threshold for fission product diffusion. Operation of the PAX reactor within the constraints specified in this safety analysis can therefore be accomplished without undue risk to either operating personnel or the general public. (auth)

**27393** (WANL-TNR-206(Vol.3)(Pt.A)) PROGRAM REPORT ON THE ANTI-CRITICALITY POISON WIRE SYSTEM. Volume III, Part A. (Westinghouse Electric Corp., Pittsburgh, Pa. (USA). Astronuclear Lab.). 30 Sep 1965. 146p. Dep. NTIS $10.50. Declassified 11 Jul 1975.

The status of the development program for the Anti-Criticality Poison Wire System (ACPS) is documented. The need for an in-flight poison wire system for maintaining the NERVA reactor sub-critical from assembly to operation in space was realized early in the NERVA program. At the present time, a shipping type of poison wire is in use. However, its use for space operation is limited due to material rigidity, excessive weight and neutronic values. It was therefore necessary to develop a flexible poison wire capable of being extracted from the reactor core through the nozzle throat for system storage or ejection. The system design is based on criteria derived from normal and accidental environmental conditions which might conceivably be encountered during assembly and space flight. In addition to listing the criteria upon which the ACPS system is based, a description of the entire system, operational sequences, and control features is provided. Reliability has been stressed and is reflected in the conceptual design of each component. Problems of hardware availability, manufacturing technique, and material selection have been substantially resolved. Fabrication and successful testing of key sections of the ACPS have been accomplished. (auth)

**27394** (WCAP-8566) WESTINGHOUSE ECCS: FOUR LOOP PLANT (17x17) SENSITIVITY STUDIES. Johnson, W. J.; Massie, H. W. Jr.; Thompson, C. M. (Westinghouse Electric Corp., Pittsburgh, Pa. (USA). Nuclear Energy Systems Div.). Jul 1975. 56p. Westinghouse Electric Corp., Pittsburgh.

Presented in this report are results of 4 loop plant (with 17 x 17 fuel) sensitivity studies using the 3/15/75 version of the Westinghouse ECCS Evaluation Model. These studies will be referenced by applicable individual plant Safety Analysis Reports to aid in demonstrating compliance with the ECCS Acceptance Criteria, 10CFR50.46. (auth)

**27395** (WCAP-8573-NP) WESTINGHOUSE ECCS: THREE LOOP PLANT (17x17) SENSITIVITY STUDIES. Buterbaugh, T. L.; Julian, H. V.; Tome, A. E. (Westinghouse Electric Corp., Pittsburgh, Pa. (USA). Nuclear Energy Systems Div.). Jul 1975. 58p. Westinghouse Electric Corp., Pittsburgh.

Presented in this report are results of 3 loop plant (with 17 x 17 fuel) sensitivity studies using the 3/15/75 version of the Westinghouse ECCS Evaluation Model. These studies will be referenced by applicable individual plant Safety Analysis Reports to aid in demonstrating compliance with the ECCS Acceptance Criteria, 10CFR50.46. (auth)

**27396** (XN-75-4(Supp.1)) EXXON NUCLEAR COMPANY WREM-BASED GENERIC PWR ECCS EVALUATION MODEL. Supplement 1. Further Definitions and Justifications to Reflood Heat Transfer Models. (Exxon Nuclear Co., Richland, Wash. (USA)). 14 Aug 1975. 79p. Exxon Nuclear Co., Inc., Richland, WA.

Conformance to the 10 CFR 50 Appendix K requirement for heat transfer at reflood rates greater or equal to one inch per second is accomplished by modification of the FLECHT heat transfer coefficient correlation given in WCAP-7931. The modification is accomplished by multiplication factors which are defined such that the time integrals of heat transfer coefficients for the experimental and predicted values are equal for each of the three FLECHT correlation time periods. Revised multiplication factors have been developed. The new multipliers correspond to five (5) axial and nine (9) temporal zones for a total of 45 multipliers, referred to as ENC-2 FLECHT multipliers. The W FLECHT correlation with the ENC-2 multipliers is referred to as FLECHT/ENC-2 correlation. (auth)

**27397** (XN-75-4(Vol.3)(Rev.2)) EXXON NUCLEAR COMPANY WREM-BASED GENERIC PWR ECCS EVALUATION MODEL. Volume III. Small Break Model. Revision 2. (Exxon Nuclear Co., Richland, Wash. (USA)). 20 Aug 1975. vp. Exxon Nuclear Co., Inc., Richland, WA.

A description and the justification of the Exxon Nuclear Company (ENC) Small Break-Generic PWR-ECCS Evaluation Model are presented. This model compliments the ENC Generic PWR-ECCS Evaluation Model, for large and intermediate break size analyses, used for licensing of fuel reloads for PWR plants, in accordance with criteria in Appendix K of 10 CFR 50. The small break model is comprised of three digital computer codes (RELAP4-EM, RELAP4-EM HOT CHANNEL and TOODEE2) developed by the Nuclear Regulatory Commission (NRC) and these codes are described in the Water Reactor Evaluation Model documentation. RELAP4-EM was modified to include the capability of predicting small break phenomena. These modifications only affect small break analysis results and have no impact on large or intermediate break analysis results. Modifications to the ENC version of the TOODEE2 code were not required for small break ECC analysis. A sample calculation for a typical 3-loop Westinghouse PWR plant small pipe break (0.5 $ft^2$) located in the cold leg or the primary coolant system between the vessel nozzle and the pump discharge. (auth)

**27398** (XN-75-41(Suppl.2)) EXXON NUCLEAR COMPANY WREM-BASED GENERIC PWR ECCS EVALUATION MODEL. Supplement 2. Supplementary Information Related to Blowdown and Reflood Analysis. (Exxon Nuclear Co., Richland, Wash. (USA)). 14 Aug 1975. 68p. Exxon Nuclear Co., Inc., Richland, WA.

During the course of review of the ENC-WREM ECCS model as documented in XN-75-41, Volumes I, II and III, a number of items were identified that required further elaboration and analysis. This supplement addresses a portion of the items mostly related to the blowdown analysis. However, description of containment backpressure and pump rotational conditions for the ENC-WREM model during reflood are also included. (auth)

**27399** (XN-75-41(Supp.3)) EXXON NUCLEAR COMPANY WREM-BASED GENERIC PWR ECCS EVALUATION MODEL. Supplement 3. Supplementary Information Relating to Blowdown and Heatup Analysis. (Exxon Nuclear Co., Richland, Wash. (USA)). 16 Aug 1975. 56p. Exxon Nuclear Co., Inc., Richland, WA.

During the course of review of the ENC WREM-based ECCS model as documented in XN-75-41, Volumes I, II and III, a number of items have been identified which required further elaboration and analysis. Supplement 3 addresses items relating to the entire ENC model. These items are divided into five sections pertaining to blowdown, hot channel, reflood, TOODEE2, and small break analysis, respectively. (auth)

**27400** (XN-75-41(Supp.4)) EXXON NUCLEAR COMPANY WREM-BASED GENERIC PWR ECCS EVALUATION MODEL. Supplement 4. Supplementary Information Relating to Blowdown and Heatup Analysis. (Exxon Nuclear Co., Richland, Wash. (USA)). 20 Aug 1975. 48p. Exxon Nuclear Co., Inc., Richland, WA.

During the course of review of the ENC WREM-based ECCS Model as demonstrated in XN-75-41, Volumes I, II and III, a number of items were identified which required further elaboration and analysis. Supplement 4 continues the expansion of information on the items relating to the entire ENC model. It is divided into five sections pertaining to blowdown, hot channel, reflood, TOODEE2, and small break analysis, respectively. Also included under each section is an index and source check list describing sensitivity studies performed with the ENC Evaluation Model and with the WREM package. (auth)

**27401** (XN-75-41(Vol.2)(App)) EXXON NUCLEAR COMPANY WREM-BASED GENERIC PWR ECCS EVALUATION. Appendix to Volume II. Model 3-Loop Westinghouse Sample Problem. (Exxon Nuclear Co., Richland, Wash. (USA)). 1 Aug 1975. vp. Exxon Nuclear Co., Inc.; Richland, WA.

An example large break LOCA analysis for a typical 3-loop PWR plant is presented. (JWR)

**27402** (XN-75-41(Vol.3)) EXXON NUCLEAR COMPANY WREM-BASED GENERIC PWR ECCS EVALUATION MODEL. Volume III. Small Break Model. (Exxon Nuclear Co., Richland, Wash. (USA)). 1 Aug 1975. 25p. Exxon Nuclear Co., Inc.; Richland, WA.

An Exxon small break evaluation model was developed using RELAP4-EM HOT CHANNEL, and TOODEE2 as base computer codes. The significant development effort was directed at modi-

fying the RELAP4-EM mixture level calculation to obtain an appropriate core mixture level to be input in TOODEE2 as required for small break hydraulic behavior. The heat transfer model in RELAP4-EM was also modified to determine the heat transfer regimes above and below the mixture level prevalent during a small break. The ENC small break evaluation model is also shown to conform with the required and acceptable features described in Appendix K of 10 CFR 50. (auth)

**27403** FRAGMENTATION OF URANIUM DIOXIDE AFTER MOLTEN URANIUM DIOXIDE-SODIUM INTERACTION. Mizuta, H. (Power Reactor and Nuclear Fuel Development Corp., Tokai, Ibaraki (Japan). Tokai Works). J. Nucl. Sci. Technol. (Tokyo); 11: No. 11, 480-487 (Nov 1974).

A series of 30 runs were performed to gain information on the fragmentation of molten $UO_2$ when dropped into a bath of liquid sodium. Hollow cylindrical $UO_2$ pellets were heated with electric current fed to a tungsten rod, passed through to center hole. The resulting molten $UO_2$ dripped down its fall into the sodium bath. High-speed cinematography (500~2,000 frames/sec) was utilized to observe the fragmentation of the $UO_2$ droplets on its impact with the sodium surface. Records were taken of the changes in pressure and temperature induced in the sodium bath by the impact of the $UO_2$ droplets. The physical characteristics of the solid $UO_2$ particles resulting from the quench were examined for particle size distributions, particle shape, and surface condition, as well as microstructure, to gain an insight into the mechanism of fragmentation. For the purpose of Fuel Coolant Interaction (FCI) analysis, the $UO_2$ particles can be assumed to be spherical in shape and to have log-normal particle-size distribution. The density function in terms of particle weight, representing the finest particle-size distribution, can be expressed on the basis of presently available empirical data, by $f(\log D) = 58.1 \exp [-(\log D - 2.27)^2/0.944]$, D: Diameter of $UO_2$ particle in microns. (auth)

**27404** PRESENT STATUS OF COUNTERPLAN ON THERMAL POLLUTION AND FUTURE RESEARCH. Senshu, S. (Central Research Inst. of Electric Power Industry, Abiko, Chiba (Japan). Technical Lab. No. 2). Genshiryoku Kogyo; 20: No. 7, 12-22 (Jul 1974). (In Japanese).

Thermal pollution due to the warm water from nuclear power plants is now a serious environmental problem. The government is going to regulate water temperature by law. At present, it is necessary to establish the standards for the regulation. The Water Quality Act in the U.S.A. was the first law, and applied to all rivers, lakes and coastal water in the U.S.A. According to the recommendation by National Technical Advisory Committee, NTAC, the temperature of water is controlled by the allowable limit for temperature rise. Problems of thermal pollution must be investigated from two aspects. One is to evaluate the physical effect of warm water diffusion, and the other is the resulting effect on fish and other organisms. The diffusion of warm water in the sea has been studied with analytical models. Study with hydrographical models has also been made. The purposes of these studies are to estimate temperature rise and the area of diffusion. The results of these studies should be combined with the results of biological studies. The most important problem is to reduce the effect of thermal pollution. Various methods of reduction are introduced and discussed. (auth)

**27405** FAULT TREE AND SAFETY DESIGN. Kondo, S. (Tokyo Univ. (Japan). Faculty of Engineering). Nippon Genshiryoku Gakkaishi; 16: No. 6, 298-305 (Jun 1974). (In Japanese).

A method of the drawing-up and utilization of fault trees is explained, and four examples of application are briefly presented from the standpoint of safety design. The drawing-up procedure, the drawing-up of logical diagrams and the fundamental use of the fault tree are illustrated. The fundamental uses of the fault tree are: (1) classification of the mode of occurrence of top events by minimal cut set; (2) finding of critical path by the evaluation of occurrence probability of each mode; and (3) calculation of the occurrence probability of top events. The fault tree is employed in the fields of design, fabrication, safety assessment, and operation control in industries, and particularly in the atomic industry. Its applications extend to the assessment of safety control systems. In one example, the undesired events of failure of a reactor by pressure in the core of an LMFBR was found by using several hundred events. In another example, the fault tree was utilized in the course of the design of a reactor control system for a chemical plant. In another example, common mode failure is explained. In the final example, the management oriented risk tree (MORT) as the application to safety control is described. (JA)

**27406** REMOVAL OF AIRBORNE RADIOIODINE IN A LOSS-OF-COOLANT ACCIDENT IN LIGHT WATER REACTOR. Kitani, S.; Ikezawa, Y. (Japan Atomic Energy Reseach Inst., Tokai, Ibaraki. Tokai Research Establishment). Hoken Butsuri; 9: No. 4, 223-231 (Dec 1974). (In Japanese).

The chemical form and removal of airborne radioiodine released in a loss-of-coolant accident in a light water reactor are described. The chemical form of the iodine is considered to be elemental and partially organic as methyl iodide. The airborne iodine is removed in the reactor containment by spray and air-filter systems, and the iodine leaked from the containment by another air-filter system. Those air-filter systems consist of impregnated charcoal, HEPA filter, and additional installations. The materials impregnated on charcoal for removal of methyl iodide are triethylenediamine, KI and $SnI_2$. Those charcoals, however, should be operated under the condition of relative humidity less than 97%. In order to use the charcoals with good performance, it is necessary to have information on the deterioration due to adsorption of impurities in the environmental atmosphere. (auth)

**27407** CONTAINABILITY OF MOLTEN FUEL RELEASE IN FAST REACTOR FUEL-SUBASSEMBLIES. Kondo, S. (Tokyo Univ. (Japan). Faculty of Engineering). J. Nucl. Sci. Technol. (Tokyo); 12: No. 1, 12-23 (Jan 1975).

Various safety implications relevant to local faults in a LMFBR and the basic factors affecting the ability of the subassembly wrapper wall to contain the effects of molten fuel release are discussed. The response of the wrapper tube is evaluated by the method proposed by Youngdahl. An equation is derived for calculating the energy repartition between the portions consumed in wall deformation and sodium slug acceleration. Then, using this equation, analyses are performed covering various situations where molten fuel coolant interaction (FCI) significantly affects the surrounding matter. This analysis shows that the degree of coherence in fuel mixing process alters substantially the severity of the FCI. The peak pressure generated by the FCI depends on the volume of the mixing zone, which is closely related to the spatial randomness of fuel failure. For the case of a MONJU-type core design, if the height of the mixing zone is greater than 2 cm, the effects of the release of 200 g of molten fuel can be contained within the subassembly without damaging the unaffected wrapper tube. Melt-through of the wrapper tube is also analyzed, and it is found that the integrity of the adjacent wrapper tube is lost about 16 sec after deposition of the molten fuel, and that the melt-through process would differ substantially according to whether forced convection is present or absent in the subassembly gap. (auth)

**27408** TEST FACILITY ENHANCES REACTOR SAFETY. McIntyre, B.; Vijuk, R. P.; Cermak, J. O.; Young, M. Y. (Westinghouse Electric Corp., Pittsburgh). Electr. World.; 184: No. 6, 60-63 (15 Sep 1975).

Tests were performed in the G-loop test facility at Westinghouse's Forest Hills Laboratory to obtain basic data on the thermal/hydraulic performance of the PWR under LOCA conditions. The loss-of-coolant accident as a result of the rupture of the main coolant pipe is the most severe postulated accident that could occur in a PWR. As stipulated by Article 10CFR50.46 of the Nuclear Regulatory Commission's regulations, the peak allowable temperature that the sheathing surrounding the nuclear fuel can reach during this accident is 2,200 F. Tests were performed with and without upper-head injection. The tests provide data for defining core cooling in plant with UHI. The data have been developed into heat-transfer correlations and applied in analysis of PWR performance during a postulated LOCA. The effect of UHI gives a hot-rod/hot-spot temperature during the depressurization phase much lower than the case without UHI. The net effect of UHI on the calculated hot-spot temperature is a valve lower by 500 F compared to the case without UHI. (MCW)

**27409** GAMMA SPECTROMETRY OF NUCLEAR REACTOR SYSTEM COMPONENTS. Neil, B. C. J. Ont. Hydro Res. Q.; 26: No. 3, 30-33 (1974).

A technique is described for directly determining individual radionuclide contributions to radiation fields at on-site nuclear reactor locations. A small portable germanium-lithium gamma ray detector with its own power supplies and pre-amplifier is used in conjunction with fixed laboratory spectrum analyzing and computing facilities. A coaxial cable connects the portable detector to the analyzer. Semi-quantitative data obtained on the radionuclide percentage contributions to radiation fields provides not only research and development information but is also useful in planning work to minimize radiation dosages and in determining the radiological characteristics of reactor systems. (auth)

**27410** WHAT DO YOU WANT TO KNOW ABOUT NUCLEAR POWER. Kauffman, J. T. The Nuclear Controversy. Allentown, PA; Pacific Power and Light Company (Jul 1975). 29p.

A booklet is presented in which various aspects of the nuclear controversy are examined. Included are comments on energy economics, reliability, safety, nuclear materials management and safeguards, and radiation hazards. (DG)

**27411** ASSURING STATION-SERVICE AND EMERGENCY POWER SUPPLIES IN NUCLEAR POWER PLANTS. Borst, A. (Kraftwerk Union A. G., Erlangen (F. R. Germany)). Elektrotech. Z., A; 96: No. 2, 76-83(Feb 1975). (In German).

From ETG discussion meeting "station service power supplies in nuclear power plants"; Frankfurt am Main, F. R. Germany (11 Jun 1974).

Stricter safety requirements have led to the further development of emergency power supplies for nuclear power plants. Redundancy and spatial separation are achieved by means of sectionalized diesel plants. Draft Standard DIN 25417, Sheet 5, provides guidelines on the layout of the diesel engine, generator, supply and auxiliaries, erection and servicing, and also on reliability. D. C. installations and conversions plant also tend towards sectionalized design. The requirements relating to aseismic layout of electrical components are described together with the self-sufficient electrical systems essential for LWR emergency arrangements. (auth)

**27412** THE SAFETY OF AND THE RISKS FROM NUCLEAR POWER STATIONS. Baust, E. (Hochtemperatur-Reaktorbau G.m.b.H., Mannheim (F. R. Germany). Hauptabteilung Sicherheit und Genehmigungsverfahren); Bugl, J. (Brown, Boveri und Cie A. G., Mannheim (F. R. Germany). Stabsabteilung Kerntechnik); Stuermer, W. (Babcock-Brown Boverie Reaktor G.m.b.H., Mannheim (F. R. Germany). Abt. Genehmigung und Sicherheit). Elektrotech. Z., A; 96: No. 1, 35-38(1975). (In German).

4 refs.

The requirement that power stations should be built so that even in case of hypothetical breakdown no person shall be injured, cannot be achieved absolutely. A slight risk remains. In order to carry out the Federal energy program the licensing procedure must, among other things, be made more clear and efficient. This can be achieved only by appropriate efforts for definition of rules and specifications, the standardisation of nuclear power stations and the rationalization of all procedures involved. (GE)

**27413** IEEE STANDARD CRITERIA FOR THE PERIODIC TESTING OF NUCLEAR POWER GENERATING STATION CLASS 1E POWER AND PROTECTION SYSTEMS. IEEE Std 338-1975. New York; Inst. of Electrical and Electronics Engineers, Inc. (1975). 15p. (ICONS-00512).

Design and operational criteria for the performance of periodic testing of nuclear power generating station Class 1E power and protection systems are presented. The scope of testing covered consists of functional tests, checks, calibration verification, and time response measurements. Criteria are also provided for determining system operational availability, status, and necessary documentation; and for establishing test intervals, shutdown test procedures, and test procedures during operation. (auth)

## Reactor Theory and Calculation

**27414** (IFA-NT-1-1975) CODE FOR COUPLED REACTOR PARAMETER ANALYSIS. Druta, E.; Cuculeanu, V.; Mocioiu, D.; Martin, V.; Constantinescu, D. (Comitetul de Stat pentru Energia Nucleara, Bucharest (Romania)). 1975. 5p. Dep. NTIS (US Sales Only) $4.00.

ASTERA is a multigroup one-dimensional diffusion approximation code, devoted to the analysis of the coupled reactor neutronic parameters. Using the partial neutron flux concept, the code optionally calculates: coupling coefficients between reactor regions; mean neutron lifetime; delayed neutron effective fraction; and the power fraction of each reactor zone. (auth)

**27415** (LA-6023-MS) PROPRIETARY, STANDARD, AND GOVERNMENT-SUPPORTED NUCLEAR DATA BASES. Poncelet, C. G.; Ozer, O.; Harris, D. R. (Los Alamos Scientific Lab., N. Mex. (USA)). Jul 1975. Contract W-7405-Eng-36. 23p. Dep. NTIS $4.00.

This study presents an assessment of the complex situation surrounding nuclear data bases for nuclear power technology. Requirements for nuclear data bases are identified as regards engineering functions and system applications for the many and various user groups that rely on nuclear data bases. Current practices in the development and generation of nuclear data sets are described, and the competitive aspect of design nuclear data set development is noted. The past and current role of the federal government in nuclear data base development is reviewed, and the relative merits of continued government involvement are explored. National policies of the United States and other industrial countries regarding the availability of nationally supported nuclear data information are reviewed. Current proprietary policies of reactor vendors regarding design library data sets are discussed along with the basis for such proprietary policies. The legal aspects of protective policies are explored as are their impacts on the nuclear power industry as a whole. The effect of the regulatory process on the availability and documentation of nuclear data bases is examined. Current nuclear data standard developments are reviewed, including a discussion of the standard preparation process. Standards currently proposed or in preparation that directly relate to nuclear data bases are discussed in some detail. (auth)

**27416** (RISO-M-1809) SOLUTION OF THE MULTIGROUP NEUTRON DIFFUSION EQUATIONS BY THE FINITE ELEMENT METHOD. Misfeldt, I. (Danish Atomic Energy Commission, Risoe. Research Establishment). 29 Jul 1975. 35p. Dep. NTIS (US Sales Only) $4.75.

The finite element method is applied to the multigroup neutron diffusion equations. General formulas are given for Lagrange type elements. Description of some 2D- and one 3D computer code is given. Several investigations are described and the results are presented. The capability of the 3D code is demonstrated on the 3D IAEA Benchmark problem. Suggestions for further work are given. (auth)

**27417** TIME BEHAVIOR OF COLD NEUTRON PULSES IN THE COLD MODERATORS. Otomo, N.; Inoue, K. (Hokkaido Univ., Sapporo (Japan). Faculty of Engineering). Hokkaido Daigaku Kogakubu Kenkyu Hokoku; No. 73, 105-114 (Dec 1974). (In Japanese).

Theoretical calculations of a time-dependent neutron spectra were carried out in detail in water at room temperature, in ice and condensed methane at extremely low temperatures, and a comparison of the results of several experiments was run. The pulsed neutron method, measurement of the monochromatic neutron pulses by the neutron reflections of a single crystal, and the time-dependent neutron spectra were examined. The neutron pulse width can be obtained from the monochromatic neutron pulse characteristics and the mean emission time of the cold neutrons at 0.001 eV was more than 200 micro-sec. in ice and solid methane at 20°K. The effect of the time resolution in the experiment on the cold neutron spectroscopy cannot be disregarded. (auth)

## Reactor Components and Accessories

**27418** (CONF-701074-P2, pp 48-65) PROSPECTS OF THE USE OF COMPLEXONES IN NUCLEAR POWER ENGINEERING. 1970. Translated from Trudy Nauchno-Tekhnicheskoi Konferentsii "Atomnaya Energetika, Toplivnye Tsikly, Radiatsionnoe Materialovedenie", Ul'yanovsk, 5-10 Oktyabrya 1970 G. Vol. II.

From conference on atomic power, fuel cycles, and radiation study of materials; Ul'yanovsk, USSR (5 Oct 1970).

In proceedings of the scientific-technical conference "atomic power, fuel cycles, radiation study of materials".

The following are discussed: the application of complexones and compositions based on them for pre-start and operational cleaning, their advantages, and the results of industrial application, increase of the corrosion resistance of materials of construction as a result of treatment with complexones (perlite steels and the materials of shells), the results of investigations on loops and in autoclaves in industry (operating and standing conditions), (3) the influence of complexone treatment on the hydrogen absorption of steels, (4) the use of complexones for correction of the water conditions, and the results of investigations on loops and in sealed tubes, and (5) the further development of scientific research work in the area of the application of complexones in nuclear power engineering. (auth)

**27419** (CONF-701074-P2, pp 523-534) INFLUENCE OF REACTOR RADIATION ON THE SURFACE STRUCTURE OF IRON AND STAINLESS STEEL. Teodersku, I. A.; Vasiliu, F. 1970. Translated from Trudy Nauchno-Tekhnicheskoi Konferentsii "Atomnaya Energetika, Toplivnye Tsikly, Radiatsionnoe Materialovedenie", Ul'yanovsk, 5--10 Oktyabrya 1970 G. Vol. II.

From conference on atomic power, fuel cycles, and radiation study of materials; Ul'yanovsk, USSR (5 Oct 1970).

In proceedings of the scientific-technical conference "atomic power, fuel cycles, radiation study of materials".

The effects of neutrons and gamma-radiation were studied to obtain more accurate data on the mechanism of metal-gas reaction caused by gamma-radiation. Similarly treated samples were exposed to radiation at identical temperatures and pressures in a reactor, in the remnant gamma-flux of the reactor, and from a $^{60}$Co source. The change in the micro-relief structure was recorded. (auth)

**27420** (KFK-EXT-13/75-2) PROPOSAL OF PROGRAMMING STANDARDS FOR A COMPUTERIZED PROTECTION SYSTEM. Voges, U.; Ehrenberger, W. (Kernforschungszentrum Karlsruhe (F. R. Germany). Inst. fuer Datenverarbeitung in der Technik). May 1975. 41p. (In German). Dep. NTIS (US Sales Only) $5.25.

In process computer systems with high safety and reliability requirements, correctness of the software has to be proven. During the development of a program, specific guidelines should be met in order to facilitate the verification of its correctness. A collection of relevant proposals is presented. 19 references. (auth)

**27421** METHOD AND SYSTEM FOR NUCLEAR POWER PLANT SYNCHROSCOPE SIMULATION FOR OPERATOR TRAINING. Alliston, W. H.; Johnson, S. J. (to Westinghouse Electric Corporation). US Patent 3,889,106. 10 Jun 1975. Filed date 14 Mar 1973. 26p.

A method and system are described for the real-time simulation of the dynamic operation of a nuclear power plant in which a synchroscope is provided for determining the frequency and phase difference of two voltage sources for informing the operator of the proper conditions for connecting the two voltage sources to a common electrical distribution line. A digital computer means is used for calculating data relating to the frequency difference between combinations of two voltage sources in accordance with predetermined simulated conditions including the operation of control panel devices. A digital to analogue converter utilizes the selected frequency difference and a bias factor to operate a voltage controlled generator for producing an AC voltage which operates a synchroscope dial in accordance with its frequency and the frequency of a constant reference voltage. (Official Gazette)

**27422** METHOD OF CONTROLLING THE BORON CONTENT IN THE COOLANT OF A NUCLEAR REACTOR PLANT AND CONSTRUCTIONAL LAYOUT FOR THE REALIZATION OF THIS METHOD. Grogan, D. B.; D'Amaddio, E. R.; Miller, D. A. (to Combustion Engineering, Inc., Windsor, Conn. (USA)). German (FRG) Patent 2326152/A/. 30 Jan 1975. 13p. (In German). 1 fig.

A method of controlling the boron content in the coolant of a reactor facility is described. Because of the low concentration of the accumulated boron acid, it is unnecessary to keep the boric acid at a higher temperature. (GE)

## Reactor Fuels

*Refer also to abstracts 25645 and 25646.*

**27423** (CONF-701074-P2, pp 308-318) PROBLEMS OF DISTRIBUTION OF FISSION FRAGMENTS AND OXYGEN IN URANIUM DIOXIDE. Viskubov, V. P.; Kosenkov, V. M.; Lebedev, I. G. 1970. Translated from Trudy Nauchno-Tekhnicheskoi Konferentsii "Atomnaya Energetika, Toplivnye Tsikly, Radiatsionnoe Materialovedenie", Ul'yanovsk, 5-10 Oktyabrya 1970 G. Vol. II.

From conference on atomic power, fuel cycles, and radiation study of materials; Ul'yanovsk, USSR (5 Oct 1970).

In proceedings of the scientific-technical conference "atomic power, fuel cycles, radiation study of materials".

Using the roentgenographical method, the condition of the crystal lattice of $UO_2$ of rod-type fuel elements, after exposure to high temperature radiation up to 9 atm.% of uranium burn-up, was analyzed. From the relationship of the structural factors of diffractional lines having even and odd semi-number interference indices, it is assumed that part of the fission fragments penetrate into the octahedron voids in the $UO_2$ lattice. An irregular change of parameters of the crystal lattice and width of diffraction lines along the radius of fuel elements has been established. The results are discussed from the point of view of distribution of fission fragments and oxygen in the $UO_2$ lattice. The analytical equation of diffusion of oxygen ions along the section of fuel elements confirms the presence of an extreme point in the distribution of oxygen along the radius of the core. (auth)

**27424** (CONF-701074-P2, pp 362-380) STUDY OF MIGRATION OF FISSION FRAGMENTS IN HEAT RELEASING ELEMENTS USING THE GAMMA-SPECTROMETRY. Sukhikh, A. V.; Davidov, E. F.; Shashurin, V. K.; Suzev, V. I.; Krapivn, M. N. 1970. Translated from Trudy Nauchno-Tekhnicheskoi Konferentsii "Atomnaya Energetika, Toplivnye Tsikly, Radiatsionnoe Materialovedenie", Ul'yanovsk, 5-10 Oktyabrya 1970 G. Vol. II.

From conference on atomic power, fuel cycles, and radiation study of materials; Ul'yanovsk, USSR (5 Oct 1970).

In proceedings of the scientific-technical conference "atomic power, fuel cycles, radiation study of materials".

The results of measurements of concentration of fission fragments $^{137}Cs$, $^{144}Ce$, $^{95}Zr$, $^{95}Nb$ and $^{106}Ru$ along the height of the experimental heat releasing elements based on ceramic fuel, various types of fuel, their densities, duration and temperature of radiation, the number of changing power cycles of a reactor, and the method of filling fuel are discussed. Analysis of the redistribution of fragments is carried out as a function of these parameters. The relationship between finding the daughter fission products and the chemical nature of the parent fragments and their thermodynamic properties is discussed. The anomalous behavior of less volatile fragments as a result of the formation and breaking up of compounds is explained. (auth)

**27425** (RCN-229) ON THE EFFECTIVE TEMPERATURE OF AN EXPANDING TUBE WITH A RADIAL TEMPERATURE GRADIENT OVER THE WALL. van Witzenbueg, W.; Janssen, L. G. J.; Prij, J. (Stichting Reactor Centrum Nederland, Petten). Jul 1975. 19p. Dep. NTIS (US Sales Only) $4.00.

Using the finite-strain theory an effective temperature of a thick-walled internally pressurized closed-end tube having a radial temperature gradient over the wall, is expressed in terms of the original tube geometry, the strain, the temperature distribution and the creep properties of the tube material. It is shown that for the case of a stainless steel cladding tube of a fission reactor fuel pin, with a temperature gradient of 50 degrees centigrade over the wall, the effective temperature equals the average of the instantaneous inner and outer surface temperatures to within one degree. (auth)

**27426** OUT-OF-REACTOR STUDY ON EXTERNAL-PRESSURE CREEP OF ZIRCALOY-2 FUEL CLADDING TUBES. Maki, H.; Hara, T. (Hitachi Ltd., Ibaraki (Japan). Hitachi Research Lab.). J. Nucl. Sci. Technol. (Tokyo); 12: No. 1, 43-52 (Jan 1975).

In Zircaloy-2 fuel cladding tubes the hour-glass shape of $UO_2$ pellets acquired by thermal distortion was simulated by flanges machined out at both ends of stainless steel pellets 21 mm long. The mock-up specimens thus formed were pressurized externally in a furnace, and the changes brought upon the tube diameter were measured at intervals. The external-pressure creep deformation was observed to proceed in a three-step diametral decrease, elliptical deformation, and final collapse. In the case of hollow tubes tested without pellets, elliptical deformation was observed, which accelerated with time until abrupt final collapse. Elliptical deformation was not observed on the pellet-filled tubes. Empirical equations were derived from the experimental results as functions of time, of hoop stress, and of temperature, to express the external-pressure creep strain behavior of the stress-relieved tube, pellet-filled and thus internally supported at intervals of 20 mm. No difference in the external-pressure creep deformation was observed between stress-relieved and recrystallized tubes under the condition of 350°C and 72.5 kg/cm$^2$. The pellet-filled specimens showed larger deformation than the hollow tubes in the process of diameter reduction. A certain length of unsupported distance in the range of 0~20 mm appeared to maximize the external-pressure creep deformation at the pellet center, under conditions similar to that of the present experiment. (auth)

**27427** DIFFUSION AND EVAPORATION OF FISSION PRODUCTS IN COATED FUEL PARTICLES. Fukuda, K.; Iwamoto, K. (Japan Atomic Energy Research Inst., Tokai, Ibaraki. Tokai Research Establishment). J. Nucl. Sci. Technol. (Tokyo); 12: No. 3, 181-189 (Mar 1975).

Fractional releases of $^{133}Xe$, $^{140}Ba$ and $^{89}Sr$ from slightly-irradiated pyrolytic-carbon-coated and SiC-coated particles were measured over a temperature range of 1,200° to 1,750°C. The results are analyzed mathematically in order to obtain the diffusion and evaporation coefficients relevant to PyC and SiC. The resulting expressions for the coefficient of diffusion in PyC are $2.9 \times 10^{-7} \exp(-61 \times 10^3/RT)$ for $^{133}Xe$ and $4.7 \times 10^{-2} \exp(-51 \times 10^3/RT)$ for $^{140}Ba$. For the coefficient of evaporation of $^{140}Ba$ from PyC, the expression is $3.5 \times 10^{-3} \exp(-42 \times 10^3/RT)$. As for SiC, the diffusion and evaporation coefficients of these nuclides are given for a temperature of 1,750°C. A high diffusivity path for the diffusion of $^{140}Ba$ is postulated to explain the difference in diffusion behavior between $^{133}Xe$ and $^{140}Ba$ in PyC. (auth)

**27428** STUDY OF DENSIFICATION OF NUCLEAR FUEL FOR LIGHT-WATER TYPE POWER REACTOR. Morishima, A.; Harayama, Y.; Uchida, M. (Japan Atomic Energy Research Inst., Tokai, Ibaraki. Tokai Research Establishment); Tobioka, T. Genshiryoku Kogyo; 20: No. 6, 19-25 (Jun 1974). (In Japanese).

Densification of fuel pellets was discovered in the Beznau Reactor of Switzerland in 1971. It is important to study this phenom-

enon from the viewpoint of reactor safety. The final density and axial contraction of fuel pellets were analyzed statistically by using experimental data on fuel irradiation. The increase of linear power density due to the densification of pellets was estimated, and the lowering of heat transfer of the gap and hang-up of pellets due to creep were also studied. The considered mechanisms of the densification were the mechanism in relation to resolution and the mechanism in relation to spike due to nuclear fission. Various experiments on densification are in progress. The experiment performed with the Halden reactor, Norway, is described. Contraction of all fuel rods were observed, and quantitative data on the contraction are presented. (JA)

**27429** NUCLEAR REACTOR FUEL ELEMENT ASSEMBLIES. Raven, L. F. (to British Nuclear Fuels Ltd.). US Patent 3,886,038. 27 May 1975. Priority date 13 Jan 1972, United Kingdom of Great Britain and Northern Ireland. 6p.

A spacer grid for a nuclear fuel element comprises a plurality of cojointed cylindrical ferrules adapted to receive a nuclear fuel pin. Each ferrule has a pair of circumferentially spaced rigid stop members extending inside the ferrule and a spring locating member attached to the ferrule and also extending from the ferrule wall inwardly thereof at such a circumferential spacing relative to the rigid stop members that the line of action of the spring locating member passes in opposition to and between the rigid stop members which lie in the same diametric plane. At least some of the cylindrical ferrules have one rim shaped to promote turbulence in fluid flowing through the grid. (Official Gazette)

## Reactor Control Systems

**27430** (AED-CONF-73-434-003) MODAL SPATIAL CONTROL. Kendall, J. D. (Kendall (James D.) Consultants Ltd., Mississauga, Ontario (Canada)). 1973. 17p. (CONF-731233-4). INIS.

From conference on automatic control; Fredericton, New Brunswick, Canada (24 Sep 1973).

Modal spatial control for spatially distributed systems combines the weighted signals from a number of detectors to drive each control element. The weighting factors are derived from the nominal distribution and the modes of the controlled variable, associated with each control element. This control technique reduces the effects of instruments errors, noise and the loss of an instrument and minimizes the errors in the distribution of the controlled variable at a specified number of points. The propagation of instrument errors is a function of the placement of detectors and of the method used to invert the characteristic matrix. Modal spatial control was developed for, and applied to the control of neutron flux in the nuclear reactor Gentilly-1 under a contract to AECL. This control system is described. (auth)

**27431** (AGC-2212) DYNAMIC ANALYSIS AND ANALOG COMPUTER SIMULATION OF THE NERVA ENGINE. (Aerojet-General Corp., Azusa, Calif. (USA)). May 1962. 132p. Dep. NTIS $9.75.

Declassified 11 Sep 1973.

The NERVA power plant has been shown to be controllable from subpower nuclear operation, through engine startup, at design thrust conditions, and during shut-down. A nonlinear analog simulation of the overall engine was developed and used. A representative control system with expected nonlinearities has been analyzed, including the interaction between control loops, and transfer function block diagrams have been prepared. (auth)

**27432** (CONF-701074-P2, pp 535-559) EFFECT OF RADIATION ON THE PROPERTIES OF BORON-CONTAINING ABSORBING MATERIALS. Goltzev, V. P.; Guseevy, T. M.; Nevorotin, V. K.; Ponomarenko, V. B.; Krasnoyarov, N. V.; Kuznetzev, S. A.; Kozlov, V. G.; Arabey, B. G. 1970. Translated from Trudy Nauchno-Tekhnicheskoi Konferentsii "Atomnaya Energetika, Toplivnye Tsikly, Radiatsionnoe Materialovedenie", Ul'yanovsk, 5--10 Oktyabrya 1970 G. Vol. II.

From conference on atomic power, fuel cycles, and radiation study of materials; Ul'yanovsk, USSR (5 Oct 1970).

In proceedings of the scientific-technical conference "atomic power, fuel cycles, radiation study of materials".

The behavior of boron-containing absorbing materials, namely, pure boride of intermediate metals, boride with additions of molybdenum, chromium, etc., is discussed; and the composition of pure borides and absorbers of the dispersion type after exposure to radiation in the SM-2 reactor in a thermal neutron flux of $5.10^{-14}$ n/cm$^2$ sec and in a fast flux of $1.10^{14}$ n/cm$^2$ sec, during 150 effective days is examined. On the basis of analysis of the change in density, structure, and ability to retain gas, conclusions have been drawn about the radiation stability of these or other absorbing materials and the possibility of utilizing these materials for manufacturing safety rod elements in nuclear assemblies. (auth)

**27433** (CONF-701074-P2, pp 560-576) RADIATION STABILITY OF ABSORBING MATERIALS BASED ON RARE-EARTH ELEMENTS. Goltzev, V. P.; Guseva, T. M.; Krasnoyarov, N. V.; Ponomarenko, V. B.; Kuznetzov, C. A.; Nevorotin, V. K.; Kozlov, V. G.; Arabey, B. G. 1970. Translated from Trudy Nauchno-Tekhnicheskoi Konferentsii "Atomnaya Energetika, Toplivnye Tsikly, Radiatsionnoe Materialovedenie", Ul'yanovsk, 5--10 Oktyabrya 1970 G. Vol. II.

From conference on atomic power, fuel cycles, and radiation study of materials; Ul'yanovsk, USSR (5 Oct 1970).

In proceedings of the scientific-technical conference "atomic power, fuel cycles, radiation study of materials".

The behavior of absorbing materials of pure oxidized rare earth elements (Eu, Sm, Dy, Gd), metal-ceramic compositions based on pure oxidized rare elements with additions of intermediate metals (W, Ta, Mo, Cr and others), compounds of the dispersion type, and tantalum and hafnium was studied in reactor SM-2 in a flux of thermal neutrons of $5 \cdot 10^{14}$ n/cm$^2$ sec during 150 effective days. The influence of radiation on the size and structural stability of these absorbing materials has been studied in detail. On the basis of the results obtained, recommendations have been made with regard to the use of tested and analyzed neutron absorbers as material for the control and safety rods for nuclear reactors. (auth)

**27434** (CONF-701074-P2, pp 577-593) RADIATION STABILITY AND EFFECTIVENESS OF DYSPROSIUM BASED ABSORBING MATERIALS. Emelyanov, I. Ya.; Grebennikov, R. V.; Tabachenkov, L. F. 1970. Translated from Trudy Nauchno-Tekhnicheskoi Konferentsii "Atomnaya Energetika, Toplivnye Tsikly, Radiatsionnoe Materialovedenie", Ul'yanovsk, 5--10 Oktyabrya 1970 G. Vol. II.

From conference on atomic power, fuel cycles, and radiation study of materials; Ul'yanovsk, USSR (5 Oct 1970).

In proceedings of the scientific-technical conference "atomic power, fuel cycles, radiation study of materials".

The calculated results of burnup of dysprosium with additions of gadolinium, erbium, and holmium oxides are given. The results of the effects of extended irradiation are discussed, and the stability and sizes of baked ceramic samples based on dysprosium oxides in a reactor at temperatures of 550 to 650°C and 750 to 850°C are studied. It is shown that the ceramic materials based on dysprosium oxides have a very high radiation stability. (auth)

**27435** (CONF-701074-P2, pp 594-607) INFLUENCE OF WOLFRAM AND MOLYBDENUM ON THE RADIATION STABILITY OF THE BORON CHROMIUM-IRON ALLOY. Emelyanov, I. Ya.; Grebennikov, R. V.; Sergeev, B. S.; Pereverzeva, R. K.; Bukolova, V. N. 1970. Translated from Trudy Nauchno-Tekhnicheskoi Konferentsii "Atomnaya Energetika, Toplivnye Tsikly, Radiatsionnoe Materialovedenie", Ul'yanovsk, 5--10 Oktyabrya 1970 G. Vol. II.

From conference on atomic power, fuel cycles, and radiation study of materials; Ul'yanovsk, USSR (5 Oct 1970).

In proceedings of the scientific-technical conference "atomic power, fuel cycles, radiation study of materials".

**27436** (CONF-701074-P2, pp 608-616) INFLUENCE OF ALLOYING WITH ELEMENTS OF IV-A AND VII-A GROUPS ON THE RADIATION STABILITY OF BORON CARBIDE. Goltzev, V. P.; Guseeva, T. M.; Krasnoyarov, N. V.; Kuznetzov, C. A.; Ponomarenko, V. B.; Nevorotin, V. K.; Chesanov, V. V. 1970. Translated from Trudy Nauchno-Tekhnicheskoi Konferentsii "Atomnaya Energetika, Toplivnye Tsikly, Radiatsionnoe Materialovedenie", Ul'yanovsk, 5--10 Oktyabrya 1970 G. Vol. II.

From conference on atomic power, fuel cycles, and radiation study of materials; Ul'yanovsk, USSR (5 Oct 1970).

In proceedings of the scientific-technical conference "atomic power, fuel cycles, radiation study of materials".

The behavior of the pure and alloyed boron carbide with elements of IV-A and VII-A groups under reactor radiation was analyzed. Samples were exposed to radiation in the reactor SM-2 with a thermal neutron flux $5 \cdot 10^{14}$ n/cm$^2$ sec during 150 effective days. A substantial emission of helium was noted during radiation dependent on the presence of alloying additions and preliminary density of boron carbide. According to the results of the analysis, certain conclusions and recommendations have been drawn for the use of boron carbide as neutron absorbers in nuclear reactors (auth)

**27437** (DP-Report-712) CONTROL AND SAFETY STUDIES FOR AN HTR GAS TURBINE SYSTEM. Dragon Project Report. Dean, J. R.; Preinreich, G.; Soubelet, G. C. (UKAEA Reactor Group, Winfrith, Atomic Energy Establishment). Feb 1970. 70p. Dep. NTIS (US Sales Only) $6.50.

In order to assess sensibly the influences in HTR-GT systems of various system arrangements on reactor design, physics and economics, the steady-state and kinetic behaviour of these arrangements must be studied. Unlike steam systems, gas turbine systems do not lend themselves to division into fairly independent parts, of which the reactor is one. The means of study which have been developed are digital computer codes for steady-states and analog models for kinetics. The steady-state code has been written so that various machine and heat exchanger routes and some design parameters can be specified. At present only the design parameters of the recuperator can be varied. Due to the difficulties of synthesising from theoretical transfer functions a kinetics system which can be represented on a digital computer using finite time-step kinetics are studied by analog computer. Models have been limited by the capacity of the economies are expected from synthesising the models, not theoretically, but by running separate analog (or eventually digital) models of the elements, (e.g., heat exchangers, reactor) to derive transfer functions valid over the range of interest. The digital codes have been used to establish a reference cycle based on selected design parameters and part-load steady-state performances determined with two types of control, one in which only the reactor control rods are manipulated and the other in which the helium circuit inventory is altered and the control rods are assumed to hold the reactor outlet gas temperature constant. With the same reference cycle and control systems, the analog models have been used to study the transient response to changes in power demand, reactivity perturbations, sudden loss of alternator load, and accidental depressurisation. (auth)

## Nuclear Power Plant Economics

**27438** CIVIL ENGINEERING WORKS IN THE CONSTRUCTION OF NUCLEAR POWER PLANTS. Myoi, T. (Kajima Construction Co. Ltd., Tokyo (Japan)). Haikan Gijutsu; 16: No. 13, 153-159 (Nov 1974). (In Japanese).

The civil engineering and construction for nuclear power plants differ from those in thermal power plants, as well as ordinary civil engineering works. Nuclear power stations are a complex of thick ferroconcrete structures. It is not possible to install some large machinery and pipings after the completion of such structures, therefore both works have to proceed together. With emphasis on the differences from ordinary civil engineering and construction, the works for nuclear power stations are described: features of nuclear power stations such as siting, radioactivity and aseismatic design; construction of station buildings, including excavation, base work in assembling of containment vessels, above-ground structures, reactor pressure vessels, etc. (JA)

**27439** NUCLEAR ELECTRICITY GENERATION STATISTICS BASED ON UNIT NUCLEAR FUEL LOADED (MWh/MTU). Matsumura, M. (Nuclear Power Training Center Ltd. (Japan)). Nippon Genshiryoku Gakkaishi; 17: No. 3, 115-121 (Mar 1975). (In Japanese).

For assessing the performance of power plants, a quantity called "capacity factor" (average power/nominal capacity) has been widely used. It is proposed to adopt for the denominator the weight of the nuclear fuel (MTU). The resulting values of MWh/MTU (annual and cumulative totals) are presented in tabulated and graphic forms for gas-cooled (GCR) and light-water (LWR) reactors, based on actual operating data from nuclear power stations in various parts of the world. The values of MWh/MTU (annual and cumulative) provide good indicators representing the economy and reliability of a reactor, being closely related to the capacity factor, the linear power density (kW/ft), and core life (cumulative fuel burn-up (MWD/MTU) or fast neutron exposure (nvt) of core structure), and formulae for deriving these values are given. Some observations are also presented with regard to the GCR. The relation between output performance (MWh) and fuel weight (MTU) is presented graphically, in which areas are indicated that represent regions pertaining to proven types of reactor and other zones that remain to be covered by future improvements aimed at realizing higher output performance (MWh) with a given amount of nuclear fuel (MTU), even with proven types of GCR and LWR. (auth)

## Reactor Licensing and Regulation

**27440** (DOCKET-50010-417) DRESDEN NUCLEAR POWER STATION, UNITS 1, 2, AND 3. Semiannual Operating Report, January--June 1975. (Commonwealth Edison Co., Chicago, Ill. (USA)). 21 Aug 1975. 279p. (DOCKET-50237-837; DOCKET-50249-663). Dep. NTIS $17.00.

Information is presented concerning operations, power generation, shutdowns, maintenance, changes, tests, experiments, and primary coolant chemistry for Dresden Units 1, 2, and 3. (FS)

**27441** (DOCKET-50029-479) YANKEE NUCLEAR POWER STATION. Semiannual Operating Report, January--June 1975. (Yankee Atomic Electric Co., Westboro, Mass. (USA)). 21 Aug 1975. 52p. Dep. NTIS $5.75.

The plant operated at power with brief shutdowns and load reductions during this period. Net electrical power generated was 741,551,035 MWh with the generator on line 4,271.30 hrs. Data is presented concerning power generation, shutdowns, corrective maintenance, chemistry and radiochemistry, occupational personnel radiation exposures, release of radioactive materials, and abnormal occurrences. (FS)

**27442** (DOCKET-50254-625) QUAD-CITIES STATION, UNITS 1 AND 2. Semiannual Operating Report, January–June 1975. (Commonwealth Edison Co., Chicago, Ill. (USA)). 1975. 94p. (DOCKET-50265-600). Dep. NTIS $7.75.

Unit 1 generated 2,024,125 net electrical MWH and the generator was on line 3162.6 hours. Unit 2 generated 746,184 net electrical MWH and was on line 1475.3 hrs. Data is included concerning operations, power generation, shutdowns, maintenance, changes, and tests. (FS)

**27443** (DOCKET-50269-427) OCONEE NUCLEAR STATION, UNITS 1, 2, AND 3. Semiannual Operating Report, January–June 1975. (Duke Power Co., Charlotte, N. C. (USA)). 29 Aug 1975. 686p. (DOCKET-50270-393; DOCKET-50287-315). Dep. NTIS $37.50.

Information is presented concerning operations, performance characteristics, changes, tests, inspections, containment leak tests, maintenance, primary coolant chemistry, station staff changes, reservoir investigations, plume mapping, and operational environmental radioactivity monitoring data for Oconee Units 1, 2, and 3. The non-radiological environmental surveillance program is also described. (FS)

**27444** (DOCKET-50298-398) COOPER NUCLEAR STATION. Semiannual Operating Report, January–June 1975. (Nebraska Public Power District, Columbus (USA)). Sep 1975. 113p. Dep. NTIS $8.75.

Net electrical power generated was 2,357,710 (MWH) with the generator on line 4081.3 hours. Information is presented concerning power generation, shutdowns, corrective maintenance, chemistry and radiochemistry, occupational radiation exposure, release of radioactive materials, and abnormal occurrences. (FS)

**27445** (DOCKET-50331-498) DUANE ARNOLD ENERGY CENTER, UNIT 1. Semiannual Operating Report, January--June 1975. (Iowa Electric Light and Power Co., Cedar Rapids (USA)). 29 Aug 1975. 202p. Dep. NTIS $13.25.

Net electrical power generated was 1,000,903 (MWh) with the generator on line 3,193.7 hours. Information is presented concerning power generation, shutdowns, corrective maintenance, chemistry and radiochemistry, occupational radiation exposure, release of radioactive materials, and abnormal occurrences. (FS)

**27446** (DOCKET-50333-382) JAMES A. FITZPATRICK NUCLEAR POWER PLANT. Semiannual Operating Report, January–June 1975. (Power Authority of the State of New York (USA)). 28 Aug 1975. 109p. Dep. NTIS $8.50.

The reactor, which was licensed for operation on October 17, 1974, has been in the start-up testing phase and has successfully completed the 50% testing plateau. Information is presented concerning operations, maintenance, instrumentation and control, radiochemistry and radiation protection, fuel loading, and abnormal occurrences. Two supplements are included. Supplement A is the environmental report and Supplement B describes effluents and waste disposal. (FS)

**27447** (DOCKET-STN-50545-1) RESAR-3S. Reference Safety Analysis Report. Volume I. (Westinghouse Electric Corp., Pittsburgh, Pa. (USA)). 27 Jun 1975. 411p. Dep. NTIS $23.75.

The nuclear steam supply system consists of a Westinghouse pressurized water reactor and closed reactor coolant loops connected in parallel to the reactor vessel. Each loop contains a reactor coolant pump and a steam generator. Also described are an electrically heated pressurizer and certain auxiliary systems. The thermal output of the system is 3425 MW(t) and the thermal output of the core is 3411 MW(t). (FS)

**27448** (FIND-50496/7) FIND: MONTAGUE NUCLEAR POWER STATION, UNITS 1 AND 2. Hendricks, P. L. (ed.). Nuclear Regulatory Commission, Washington, D. C. (USA). Sep 1975. 21p. Dep. NTIS $4.00.

An index is presented for the docket report material submitted in conjunction with the application for a nuclear power plant construction permit and operating license. The index citations are to the beginnings of major headings, sections, responses, etc., and refer to grid coordinates on microfiche sheets prepared for each docket report. (DCC)

**27449** (FIND-50514) FIND: PEBBLE SPRINGS NUCLEAR PLANT, UNITS 1 AND 2. Hendricks, P. L. (ed.). Nuclear Regulatory Commission, Washington, D. C. (USA). Sep 1975. 19p. (FIND-50515). Dep. NTIS $4.00.

An index is presented for the docket report material submitted in conjunction with the application for a nuclear power plant construction permit and operating license. The index citations are to the beginnings of major headings, sections, responses, etc., and refer to grid coordinates on microfiche sheets prepared for each docket report. (DCC)

**27450** (FIND-STN-50528) FIND: PALO VERDE NUCLEAR GENERATING STATION, UNITS 1–3. Williams, W. H. (ed.). (Energy Research and Development Administration, Oak Ridge, Tenn. (USA). Technical Information Center). Sep 1975. 20p. NTIS $4.00.

This index is presented for microfiche items of Dockets STN-50528–30, Palo Verde Nuclear Generating Station, Units 1–3. The material covers correspondence from the Applicant, the Nuclear Regulatory Commission and various agencies concerning the application to construct the proposed nuclear facility. Information from July 1974–June 1975 is included and all microfiche are of 24:1 reduction. The application is submitted by Arizona Public Service Company for itself and five other utilities. (auth)

**27451** (NP-20528) QUALITY ASSURANCE PROGRAM: OPERATIONS PHASE. Topical Report, VEP-1. (Virginia Electric and Power Co., Richmond (USA)). 1 Jul 1975. 56p. Virginia Electric and Power Co., Richmond.

This topical report describes the Virginia Electric and Power Company's quality assurance program for the operational phase of its nuclear power plants. The report is organized as, and is generically used for, Chapter 17, Part 2--Quality Assurance (Operations) of Vepco's Safety Analysis Reports. The Vepco quality assurance program conforms to applicable regulatory requirements such as 10CFR50, Appendix B and to approved industry standards such as ANSI N45.2-1971 and ANSI N18.7-1972 and corresponding daughter standards, or to equivalent alternatives. The program also follows additional guidance developed by the Nuclear Regulatory Commission. This report describes the quality assurance program beginning with preoperational testing and continuing through all phases of startup and operation. Included are organizational charts and a point-by-point comparison of the program with the 18 criteria of 10CFR50, Appendix B. (auth)

**27452** (REG/G-2.3(9-75)) QUALITY VERIFICATION FOR PLATE-TYPE URANIUM–ALUMINUM FUEL ELEMENTS FOR USE IN RESEARCH REACTORS. (Nuclear Regulatory Commission, Washington, D. C. (USA). Office of Standards Development). Sep 1975. 1p. DRS.

A method acceptable to the NRC staff for establishing and executing a quality assurance program for verifying the quality of plate-type uranium-aluminum fuel elements used in research reactors is described. (auth)

# GENERAL AND MISCELLANEOUS

## Information Handling

**27453** (JINR-P2-8785) PRINCIPLES OF CONSTRUCTION OF THE INFORMATION RETRIEVAL SYSTEM OF JINR. Govorun, N. N.; Arnaudov, D. D. (Joint Inst. for Nuclear Research, Dubna (USSR)). 1975. 19p. (In Russian). Dep. NTIS (US Sales Only) $4.00.

The principles of the construction of the information retrieval system of JINR are considered. A great deal of attention is paid to the organization of the system files, allowing one to minimize the response time in the batch mode and retrieval in real time. (auth)

## Management

**27454** (ERDA-1542(Vol.1)(Draft)) U. S. NUCLEAR POWER EXPORT ACTIVITIES. Volume I. Environmental Statement. (Energy Research and Development Administration, Washington, D. C. (USA)). Aug 1975. 253p. W. H. Pennington, USERDA, Washington, D. C. (Free).

The nuclear power export process includes U. S. activities related to the export of commercial nuclear steam supply systems and related components and of source and special nuclear material for commercial use in foreign power reactors. This statement analyzes generally the incremental environmental impact of such activities. The scope of the statement encompasses the potential environmental impacts on the U. S. and high seas from U. S. nuclear power export activities conducted within the U. S. and on the high seas. Also included within the scope are the potential impacts on the U. S. and high seas from the possible diversion, theft, or sabotage abroad of U. S.-supplied materials or facilities. (auth)

**27455** (ERDA-1542) (Vol.2)(App.)(Draft)) U. S. NUCLEAR POWER EXPORT ACTIVITIES. Volume II. Appendices. Environment Statement. (Energy Research and Development Administration, Washington, D. C. (USA)). Aug 1975. 303p. W. H. Pennington, USERDA, Washington, D. C. (Free).

Agreements between the USA and Austria and the Argentine Republic for safeguards during the export of nuclear materials from the USA are presented. Safeguards proposed by the International Atomic Energy Agency are discussed. (CH)

**27456** RADIATION SCIENCE AT THE NATIONAL PHYSICAL LABORATORY 1912-1955. Smith, E. E. London; Her Majesty's Stationery Office (1975). 114p.

This book on ionizing radiations and radioactive materials records chronologically the work at National Physical Laboratory. The following subjects are included in the account: the events which led, in 1912, to the British national radium standard; radioactivity measurements; absorption and scattering of gamma rays and X-rays; measurement of gamma ray and X-ray intensity and dosage; radiography and fluoroscopy; X-ray crystallography (diffraction); radiation protection; dosimetry; standardization of radioisotopes. (UK)

**27457** KERNFORSCHUNGSPOLITIK IN DER BUNDESREPUBLIK DEUTSCHLAND. Projekt Wissenschaftsplanung. (Nuclear Research Policy in the Federal Republic of Germany. Project Science Planning). Pruess, K. Frankfurt am Main, F. R. Germany; Suhrkamp (1974). 374p. (In German).

With tabs. and refs.

A report is given on atomic policy and heavy ion research, on the nuclear research policy in the FRG, on the development of heavy ion research and the origination of the GSI, as well as on problems of scientific development. (GE)

## Mathematics and Computers

*Refer also to abstracts 26035, 26048, 26097, and 26960.*

# COMPLETE OR PARTIAL COLLECTIONS OF ERDA REPORTS IN COUNTRIES OTHER THAN THE UNITED STATES

**ARGENTINA**
Buenos Aires, Comisión Nacional de Energía Atómica

**AUSTRALIA**
Canberra, National Library of Australia
Sutherland, New South Wales Atomic Energy Research Establishment

**AUSTRIA**
Vienna, International Atomic Energy Agency (IAEA)
Vienna, Zentralbibliothek der Physikalischen Institute der Universität

**BELGIUM**
Brussels, European Atomic Energy Community (Euratom)
Mol-Donk, Centre d'Etude de l'Energie Nucléaire

**BRAZIL**
Rio de Janeiro, Comissão Nacional de Energia Nuclear
São Paulo, Instituto de Energia Atómica

**CANADA**
Chalk River, Ontario, Atomic Energy of Canada, Ltd.
Hamilton, Ontario, McMaster University
Ottawa, National Research Council

**CONGO, REPUBLIC OF**
Kinshasa, Trico Nuclear Center

**DENMARK**
Risö, Danish Atomic Energy Commission

**FINLAND**
Otaniemi, Teknillinen Korkeakoulu

**FRANCE**
Saclay, Gif-sur-Yvette, Centre d'Etudes Nucléaires de Saclay

**GERMANY, WEST**
Karlsruhe, Zentralstelle für Atomkernenergie Dokumentation
Munich, Technische Universität

**GREECE**
Athens, Nuclear Research Center, Democritus Library

**INDIA**
Bombay, Trombay, Bhabha Atomic Research Center Library

**IRAQ, REPUBLIC OF**
Baghdad, Atomic Energy Commission, Nuclear Research Institute

**IRELAND**
Dublin, University College

**ISRAEL**
Yavne, Israel Atomic Energy Commission, Soreq Nuclear Research Centre

**ITALY**
Ispra, Cetis Library
Rome, Centro di Studi Nucleari della Casaccia

**JAPAN**
Tokyo, National Diet Library
Tokai-Mura, Naka-gun, Ibaraki-ken, Japan Atomic Energy Research Institute

**KOREA, REPUBLIC OF**
Seoul, Atomic Energy Research Institute

**MEXICO**
Mexico, D. F., Comisión Nacional de Energía Nuclear

**NETHERLANDS, THE**
Petten, Reactor Centrum Nederland
The Hague, Bibliothek Octrooiraad

**NORWAY**
Kjeller, Institutt for Atomenergi

**PORTUGAL**
Sacavem, Junta de Energia Nuclear

**SOUTH AFRICA, REPUBLIC OF**
Pretoria, Atomic Energy Board Library

**SPAIN**
Madrid, Junta de Energía Nuclear, Ciudad Universitaria

**SWEDEN**
Nyköping, Aktiebolaget Atomenergi Library

**SWITZERLAND**
Zürich, Swiss Federal Institute of Technology

**UNITED KINGDOM**
Boston Spa, Wetherby, Yorkshire, British Library Lending Division
Harwell, Didcot, Berkshire, Atomic Energy Research Establishment

# IN INTERNATIONAL AGENCIES

**EUROPEAN ATOMIC ENERGY COMMUNITY (EURATOM)**
Brussels, Belgium
Ispra, Varese, Italy, Cetis Library

**OECD NUCLEAR ENERGY AGENCY (NEA)**
British Library Lending Division
Boston Spa, Wetherby, Yorkshire, England

**INTERNATIONAL ATOMIC ENERGY AGENCY (IAEA)**
Vienna, Austria

UNITED STATES
ATOMIC ENERGY COMMISSION
P. O. BOX 62
OAK RIDGE, TENNESSEE 37830
OFFICIAL BUSINESS

POSTAGE AND FEES PAID
U. S. ATOMIC ENERGY COMMISSION

U.S.MAIL

POSTAGE AND FEES PAID
GOVERNMENT PRINTING OFFICE

U.S.MAIL

XEROX UNIVERSITY MICROFILMS 1
SERIALS DEPT.
300 N. ZEEB ROAD
ANN ARBOR, MI 48106

# NUCLEAR POWER PLANT DESIGN ANALYSIS

**Alexander Sesonske**
Purdue University

Published by
Technical Information Center,
Office of Information Services,
U. S. Atomic Energy Commission

November 1973

495 pages, 151 illustrations, 6 by 9 inches
Library of Congress Catalog Card
Number 73-600245

Available as TID-26241 for $10.60 from
National Technical Information Service
U. S. Department of Commerce
Springfield, Virginia 22161

**CONTENTS**

Introduction
Electric Utility Economics
Nuclear-Plant Economics
Thermal-Transport Systems and Core Design
Nuclear Analysis Methods
Safety and Related Design Requirements
Fuel-System Analysis
Design Considerations
Some Optimization Approaches
Index

*Nuclear Power Plant Design Analysis* provides background in two basic areas: (1) design of nuclear power plants with emphasis on the reactor system and (2) design analysis, the systematic consideration of important individual parameters that affect the design in an interrelated way. It is a text for design-oriented courses for nuclear engineering students who have already had an introduction to the field but require additional perspective of interacting engineering areas important to reactor design. Emphasis is given to such areas as engineering economics, thermal-hydraulics, safety analysis, and fuel systems, which in an introductory course are often not covered with sufficient breadth to enable a student to participate in a meaningful group-design effort. The book is also intended for the practicing engineer interested in improving his background in reactor design.

Areas covered are principles of engineering design as they apply to nuclear projects; economics affecting nuclear power plants; thermal transport (thermal-hydraulics) in developing core specifications; computer methods for nuclear analysis; safety analysis, licensing, and environmental considerations; the fuel system and fuel-management strategies; the synthesis of all these design considerations; and modern optimization approaches and their potential usefulness in nuclear systems.

The author has taken full advantage of the report literature and other sources to obtain a unified treatment of topics not previously covered in a single book. An extensive bibliography is given to aid in additional study.